TT 74-52006
NASA TT F-765

AERODYNAMICS

[AERODINAMIKA]

Authorised by the Ministry of Higher and Secondary Specialized Education, USSR as a Textbook for the Students of Polytechnics

N.F. Krasnov

Vysshaya Shkola Publishers
Moscow 1971

TRANSLATED FROM RUSSIAN

Published for the National Aeronautics and Space Administration and the National Science Foundation, Washington, D.C. by Amerind Publishing Co. Pvt. Ltd., New Delhi
1978

© 1978 Amerind Publishing Co. Pvt. Ltd., New Delhi

Translated and published for the National Aeronautics and Space Administration, pursuant to an agreement with the National Science Foundation, Washington, D.C. by Amerind Publishing Co. Pvt. Ltd., 66 Janpath, New Delhi

Translator: Dr. T.S. Patel
General Editor: Dr. V.S. Kothekar

Available from the U.S. Department of Commerce National Technical Information Service Springfield, Virginia 22161

Printed at Oxonian Press Pvt. Ltd., Faridabad, India

UDC 533.6

In this book the basic concepts of modern aerodynamics are discussed. The question of the kinematics of a fluid medium and the basic equations of hydrodynamics for a complicated, chemically reactive, viscous, compressible model of fluid flow are discussed in detail. These questions are applicable to the problems of hypersonic flight, wing theories in subsonic and supersonic flows, supersonic flow past rotating bodies, aerodynamic interference, determination of frictional force, heat transfer and heat-resistant sheaths. The basic concepts of the aerodynamics of dissociating gases are also treated.

The book is recommended as a textbook for students in higher technical institutions and will also be useful to engineers and scientists.

PREFACE

Aerodynamics forms the theoretical basis of space-rocket and artillery technology and the foundation of aerodynamic calculations for modern flight vehicles. The basic concepts of aerodynamics are used in the investigation of an outer flow over different bodies and the motion of air (gas) past some of these structures. Therefore it is difficult to be a good engineer in the field of aviation, artillery, rocketry, automobile transport, internal combustion engines, etc. without a thorough knowledge of aerodynamics. To be a specialist one must acquire knowledge of aerodynamics where air or gas flow phenomena occur in some form.

In this book the applications of aerodynamics particularly in rocket technology and modern high-speed aviation are studied along with the general laws of motion of a gas medium. In following any course embracing aerodynamics a deep understanding of its theoretical principles is very important. Without it the actual solution of practical problems, scientific investigations and research work become impossible. Therefore special attention must be devoted to mastering the material in the first six chapters of this book. These cover the following: basic concepts and definitions of aerodynamics, kinematics of a fluid medium, equations of motion of a gas in the general case, where variations in its physico-chemical properties are considered, the theory of shock waves, the method of characteristics, which is very widely used in the investigation of supersonic flows, and finally the general theory of the motion of a gas in two-dimensional space (known as the theory of two-dimensional motion).

The scientific information given in the remaining chapters of this book shows the practical applications or connections with the formulation of methods of aerodynamic calculations for flight vehicles and their individual elements. This is also useful if we are to achieve a deep understanding of the theoretical foundations of aerodynamics. This structuring of a course corresponds to the important principle of presenting scientific information according to a deep, thorough approach for the use of students as an active means of obtaining solutions of some practical problems. This method of study is based on the multipurpose approach of managing scientific information for easy retrieval and cross-reference to the logical connections obtaining among different items of knowledge.

It is worth noting here that the presentation of the methods of aerodynamic

calculations has a significant value in itself. It enriches the students' knowledge and steers them along the road of establishing the interrelation between the theoretical and practical solutions of specific problems besides acquainting them with the new phenomena related to the processes of the interactions of bodies.

Here the aerodynamics of isolated wings (lifting surfaces) and rotating bodies (cones) are first considered and then the aerodynamic calculations of flight vehicles in the form of various combinations of wings, control surfaces and rotating bodies including mutual interference are taken up. This layout is quite normal for a textbook aimed at a complete and up-to-date understanding of the problems of applied aerodynamics.

In this book particular attention is given to the highlights of important problems of theoretical and applied modern aerodynamics of high speeds associated with the investigation of friction, heat transfer, mass ablation, force and heat interactions under the condition of motion of a body in a dissociating medium. The thermodynamic and kinematic parameters of a dissociating gas and the basic physical properties of a highly dissociating medium are also discussed as applied to the above problems.

Obviously not all the problems pertaining to aerodynamics can be covered in a textbook. The scientific information presented in this book is what is necessary for any specialist engaged in scientific and engineering activities in the field of aviation and space-rocket technology. The content and volume of this information will be enough for the understanding of other problems of aerodynamics faced by young specialists in practice. Among the problems not treated in this book are, in particular, magnetoaerodynamic investigations, determination of an unsteady flow over bodies, the problems of experimental aerodynamics and the optimum shapes of flight vehicles.

The author will be very satisfied if the mastery of the material presented in this book serves as an aid for individual work and detailed study of modern aerodynamics. The book is written on the basis of teaching experience in aerodynamics following the teaching program in the N.E. Bauman Moscow Higher Technical Institute. It is recommended for students of higher educational institutes and of faculties for special training in the field of flight vehicles. It may also be useful to workers in the affiliated scientific research institutes, design bureaus and production plants.

A special conversion table is provided at the end of this book for convenience in converting the units of measurement of physical quantities used here to the corresponding new units accepted in the International System (SI).

The leading scientists and technologists of the RSFSR, Prof. N.S. Arzanikov and Prof. I.P. Ginzburg, and colleagues of their section carefully went through the manuscript of this book. They made many useful comments and came up with valuable suggestions for the improvement of the contents and presentation of the manuscript, which were highly appreciated during

preparation of this book. The author acknowledges his deep indebtedness to all of them.

The author appreciates that this book is not necessarily free from defects and will gratefully accept all comments and suggestions from readers.

THE BASIC NOTATIONS USED IN THE USSR AND THE USA

The following list gives the basic notations popularly used in the field of aerodynamics in the Soviet Union and the United States of America. This will help readers who are used to American and English notations to understand the material in this book. The typical coordinate systems used in these countries are reproduced in Figs. 1 and 2.

In the USA and England	*In the USSR*	
AR	λ	aspect ratio
a	a	sound velocity
a^*	a^*	critical sound velocity
b	l	wing span
C	F	cross sectional area
C_L	C_y	lift coefficient
C_y	C_z	side wind force coefficient
C_D	C_x	drag coefficient
C_m	m_z	pitching moment coefficient
C_l	m_x	rolling moment coefficient
C_n	m_y	yawing moment coefficient
C_p	C_p	specific heat at constant pressure
C_v	C_v	specific heat at constant volume
c	b	chord
g	g	acceleration due to gravity
h	H	altitude
i	i	enthalpy
L	M_x	rolling moment
M	M_z	pitching moment
N	M_y	yawing moment
m	m	mass
n	n	load factor
p	ω_x	angular velocity about X axis
q	ω_z	angular velocity about Y axis (Z axis in the USSR)
r	ω_y	angular velocity about Z axis (Y axis in the USSR)

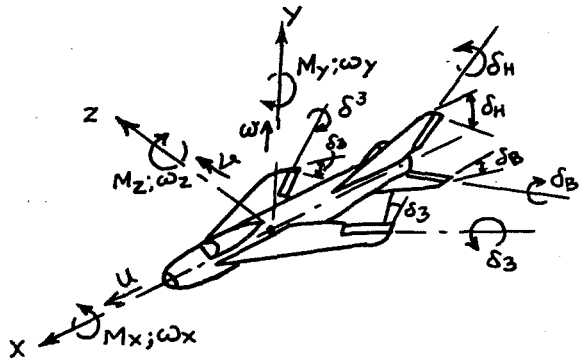

FIXED SYSTEM OF COORDINATES

ACCEPTED IN THE U S S R

Fig. 1

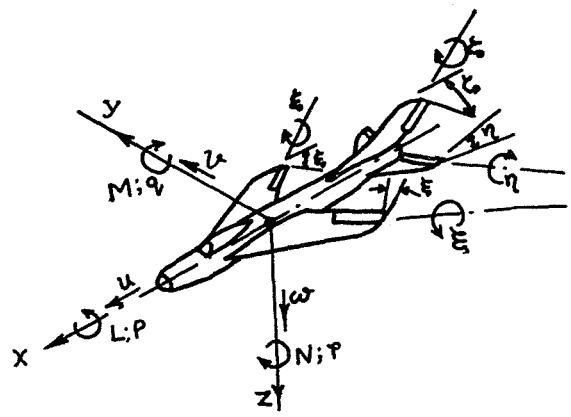

FIXED SYSTEM OF COORDINATES

ACCEPTED IN THE U S A AND GREAT BRITAIN

Fig. 2

S	S	wing planform area
S	S	entropy
s	$l/2$	semispan
T	T	absolute temperature
T	P	thrust of propeller or engine
t	c	maximum thickness of wing
U	V	velocity
u	V_x	component of velocity along X axis
v	V_z	component of velocity along Y axis (Z axis in the USSR)
w	V_y	component of velocity along Z axis (Y axis in the USSR)
W	G	weight of airplane
L	Y	lift
D	X	drag
Y	Z	cross-wing force
α	α	angle of attack
β	β	angle of side slip
γ	k	ratio of specific heats
Γ	Γ	circulation
δ	δ	boundary layer thickness
δ	Δ	relative density
ε	ε	downwash angle
η	δ_B	angle of elevator deflection
θ	θ	angle of pitch
Λ	χ	sweepback angle
μ	μ	coefficient of viscosity
ν	ν	kinematic coefficient of viscosity
ρ	ρ	mass density
τ	τ	time ratio
ψ	ψ	stream function
Φ	Φ	velocity potential

TRANSLATOR

CONTENTS

Preface v

The Basic Notations Used in the USSR and the USA ix

Introduction 1

Chapter 1. Basic Concepts in Aerodynamics 11
1. Force-interaction of the Medium on a Moving Body . . . 11
   1.1 Surface force 11
   1.2 Properties of pressure in an ideal fluid 12
   1.3 Effect of viscosity on fluid motion 14
2. Resultant Force-interaction 19
3. Determination of Aerodynamic Forces and Moments from a Given Distribution of Normal Pressure and Shear Stress. Concept of Aerodynamic Coefficients 22
4. Basic Properties of High-Speed Gas Flow 31
   4.1 Compressibility of gas 31
   4.2 Heating of gas 32
   4.3 Condition of air at high temperatures 37
5. Basic Relations for a Diatomic Dissociating Gas 41
   5.1 Degree of dissociation 41
   5.2 Equation of state 43
   5.3 Thermodynamic relations 45
   5.4 Coefficient of dynamic viscosity 47
   5.5 Mixture of diatomic gases 47

Chapter 2. Kinematics of a Fluid Medium 51
1. Methods of Kinematic Investigation of a Fluid 51
   1.1 Lagrangian method 51
   1.2 Eulerian method 52
   1.3 Stream line and streak line 53
2. Analysis of Motion of Fluid Particles 54
3. Irrotational Motion of a Fluid 58
4. Equation of Continuity 59
   4.1 General form of equation of continuity 59
   4.2 Cartesian system of coordinates 60
   4.3 System of curvilinear coordinates 62

4.4 Equation of continuity for gas flow over curvilinear surface 66
4.5 Equation of mass flow 68
5. Stream Function 69
6. Vortex Lines 70
7. Circulation of Velocity 71
7.1 Concept of the circulation of velocity 71
7.2 Stokes' theorem 72
7.3 Velocities induced by vortices 74
8. Complex Potential 76
9. Typical Fluid Flows 77
9.1 Uniform flow 77
9.2 Plane source and sink 78
9.3 Three-dimensional source (sink) 79
9.4 Dipole 79
9.5 Flow with circulation (vortex) 82

Chapter 3. Foundations of Fluid and Gas Dynamics 84
1. Equations of Motion of a Viscous Fluid 84
1.1 Cartesian coordinates 84
1.2 Equation of motion in vector form 91
1.3 Curvilinear coordinates 92
2. Equation of Energy and Diffusion of Gas 99
2.1 Equation of diffusion 99
2.2 Equation of energy 101
3. System of Gas Dynamic Equations. Initial and Boundary Conditions 106
4. Integrals of Equations of Motion in an Ideal Fluid 111
5. Aerodynamic Similarity 115
5.1 Concept of similarity 115
5.2 Similarity criteria to account for viscosity and heat conductivity effects 118
6. Isentropic Gas Flows 125
6.1 Form of gas jet 125
6.2 Flow velocity 127
6.3 Pressure, density and temperature 129
6.4 Gas flow from reservoir 131
6.5 Motion of incompressible gas (fluid) 134
6.6 Dissociating gas flow from reservoir (one-dimensional problem) 134

Chapter 4. Theory of Shock Waves 137
1. Physical Process of Appearance of Shock Waves 137
2. General Equations for Shock Waves 140

2.1 Oblique shock 140
2.2 Normal shock 146
3. Oblique Shock in a Gas Flow with Constant Specific Heats . 146
3.1 System of equations 147
3.2 Formulas for calculation of gas parameters behind shock . 148
3.3 Angle of inclination of oblique shock 153
4. Hodograph of Velocity 156
5. Normal Shock in Gas Flow with Constant Specific Heats . . 161
6. Shock at Very High Supersonic Speeds and Constant Specific Heats of Gas 162
7. Solution of Problem of Shock in a Gas Flow with Variable Specific Heats taking into Account Dissociation and Ionization . 165
8. Shock Wave in Pure Dissociating Diatomic Gas 169
9. Relaxation Phenomena 170
9.1 Concept of nonequilibrium flows 170
9.2 Equation of rate of chemical reactions 172
9.3 Time of relaxation 175
9.4 Equilibrium processes 177
9.5 Effects of relaxation in shock waves 178

Chapter 5. Method of Characteristics 182
1. Equations for Velocity Potential and Stream Function . . . 182
2. Cauchy's Problem 187
3. Characteristics 191
3.1 Conditions of existence 191
3.2 Existence of characteristics 192
3.3 Property of orthogonal conjugate characteristics . . . 195
3.4 Transformation of equations of characteristics in hodograph plane of velocity 196
3.5 Equations of characteristics in the hodograph plane for particular cases of gas motion 202
4. Scheme of Solving Gas Dynamic Problems by Method of Characteristics 205
5. Application of Method of Characteristics to Solution of the Problem of Contour Design of Nozzle of a Supersonic Aerodynamic Wind Tunnel 214

Chapter 6. An Airfoil and a Finite Wing in an Incompressible Fluid Flow 218
1. Thin Airfoil in Incompressible Flow 218
2. Cross Flow over Thin Plate 225
3. Thin Plate at an Angle of Attack 227
4. Finite Wing in Incompressible Fluid 234

Chapter 7. Wing Profile in a Compressible Gas Flow 240
1. Subsonic Compressible Flow over Thin Airfoil 240

1.1 Linearization of equation of velocity potential 240
1.2 Relationship between compressible gas flow and incompressible fluid flow over thin airfoil 242
2. Academician S.A. Khristianovich's Method 244
2.1 Description of method 244
2.2 Conversion of pressure coefficient from incompressible fluid flow to Mach number $M_\infty > 0$ 247
2.3 Conversion of pressure coefficient from Mach number $M_{\infty 1} > 0$ to Mach number $M_{\infty 2} > 0$ ($M_{\infty 1} \neq M_{\infty 2}$) 248
2.4 Determination of critical Mach number M 248
3. Wing Profile in Flow having Supercritical Velocity ($M_\infty > M_{\infty cr}$) 249
4. Flat Plate in Supersonic Flow of Gas having Constant Heat Coefficients 253
5. Supersonic Flow Past Airfoil of Arbitrary Form 260
5.1 Application of method of characteristics 260
5.2 Hypersonic flow over thin profile 266
5.3 Thin profile in small perturbation flow 267
5.4 Aerodynamic coefficients 268
6. Swept Wing of Infinite Span 272
7. Airfoil in Supersonic Gas Flow with Variable Heat Coefficients 277

Chapter 8. A Wing in a Supersonic Flow 279
1. Linearized Theory of Finite Wing in Supersonic Flow . . . 279
1.1 Linearization of equation for a potential function . . . 279
1.2 Boundary conditions 281
1.3 Components of resultant velocity potential and aerodynamic coefficients 284
1.4 Characteristics of supersonic flow-interaction of wings . . 286
2. Method of Sources 288
3. Delta Wing with Symmetrical Profile ($a=0$, $c_y=0$) 292
3.1 Semi-wing with subsonic leading edge 292
3.2 Delta wing symmetrical about x axis with subsonic leading edge 298
3.3 Infinite semi-wing with supersonic edge 300
3.4 Delta wing symmetrical about x axis with supersonic leading edge 304
4. Flow-interaction of Swept Wing with Four Corners having Symmetrical Profile and Subsonic Edges at Zero Angle of Attack 305
5. Flow-interaction of Wing with Four Corners, Symmetrical Airfoil and Edges of Different Types (Subsonic and Supersonic) . 319
5.1 Leading edge and middle edge subsonic, trailing edge supersonic 319

5.2 Leading edge subsonic, middle edge and trailing edge supersonic 320
5.3 All edges of wing supersonic 322
5.4 Delta wing 323
6. Zone of Application of Method of Sources 324
7. Method of Dipoles 326
8. Flow-interaction of Delta Wing with Subsonic Leading Edge . 328
9. Wing with Six Corners having Subsonic Leading Edges and Supersonic Trailing Edges 340
10. Wing with Six Corners having Supersonic Leading and Trailing Edges 345
11. Drag of Wings with Subsonic Leading Edges 360
11.1 Suction force 361
11.2 Induced drag 362
12. Aerodynamic Characteristics of Wing of Rectangular Plan . . 363
13. Method of Reversal 369

Chapter 9. Cone in a Supersonic Flow 373
1. System of Equations of Axisymmetrical Flow-interaction of Sharp-Nosed Cone 373
2. Flow-interaction of Cone at Constant Specific Heats 376
3. Effect of Balanced Dissociation and Ionization of Gas on Flow-interaction of Cone 386
4. Blunt Cone 391
4.1 Form of blunt noses 391
4.2 Special features of supersonic flow 394
4.3 Flow-interaction of cone with spherical blunt nose . . . 396
5. Special Cases of Flow-interaction 420
5.1 Unbalanced gas flows 420
5.2 Flows with radiation 424

Chapter 10. Sharp-Nosed Body of Revolution in a Supersonic Flow . . 425
1. Application of Method of Characteristics 425
2. Linearization of Equations of Flow-interaction for Thin Bodies of Revolution 438
3. Axisymmetrical Flow-interaction 444
4. Nonaxisymmetrical Flow-interaction 456
5. Calculation of Aerodynamic Coefficients 461

Chapter 11. Aerodynamic Interference 471
1. Nature of Aerodynamic Interference 471
1.1 Interference of wing-body combination 471
1.2 Interference between wing and tail 474
2. Lift for Combination of Fuselage and Plane Wing 476

2.1 Concept of coefficients of interference 476
2.2 Determination of velocity potential 478
2.3 Velocity and pressure on fuselage with wing 480
2.4 Velocity and pressure on wing in presence of fuselage . . 483
2.5 Determination of interference coefficients 486
2.6 Center of pressure 492
2.7 Lift force of wing-fuselage combination 495
3. Effect of Angle of Banking on Interference between Fuselage and Plane Wing 495
3.1 General relation for coefficient of pressure 495
3.2 Pressure over fuselage 498
3.3 Pressure over wing 500
3.4 Lift force and center of pressure 502
3.5 General relations of forces and moments for plain combination with banking 505
4. Cruciform Combination 506
4.1 Pressure and lift force 506
4.2 Coefficients of interference and center of pressure . . . 511
4.3 General relations for forces and moments 513
4.4 Calculation of interference of flight vehicles consisting of "thick" bodies and wings 516
5. Interference between Wing and Tail 520
5.1 General definitions 520
5.2 Subsonic speeds 522
5.3 Supersonic speeds 523
5.4 Coefficient of interference 529
6. Control Elements 536
6.1 Basic types of control elements 536
6.2 Aerodynamic analysis of controls 538

Chapter 12. Friction 547
1. Boundary Layer Equations 547
2. Generalized Equation of Boundary Layer 554
2.1 Generalized equation of boundary layer in differential form 554
2.2 Integral relation of boundary layer 556
2.3 Characteristic thicknesses of boundary layer 559
3. Laminar Boundary Layer over Flat Plate 561
4. Turbulent Boundary Layer over Flat Plate 569
4.1 Application of logarithmic velocity distribution 569
4.2 Index law for velocity distribution 579
5. Temperature and Enthalpy in Boundary Layer in Presence of Heat Transfer 583
5.1 Distribution of temperature and enthalpy 583

5.2 Characteristic temperature 589
6. Application of Characteristic Parameters for Boundary Layer Calculations over Flat Plate at High Speeds of Flow-interaction 592
6.1 Laminar boundary layer 592
6.2 Turbulent boundary layer 595
6.3 Friction on cone at supersonic speeds of flow-interaction . 597
7. Effect of Axial Pressure Gradient on Friction 602
8. Mixed Boundary Layer. Critical Reynolds Number 617

Chapter 13. Heat Transfer 625
1. Aerodynamic Heating 625
1.1 Equation of heat balance 625
1.2 Heat inflow from heated gas 626
1.3 Solar and earth radiation 634
1.4 Radial heat flow from wall surface 636
2. Relation between Friction and Heat Transfer 636
3. Heat Transfer in Laminar Boundary Layer over Curved Surface 644
3.1 Arbitrary form of surface 644
3.2 Hemisphere 656
3.3 Blunt cone 657
4. Heat Transfer by Diffusion 660
5. Wall Temperature 669
5.1 Radiational equilibrium temperature 669
5.2 Equilibrium temperature in presence of additional sources of input and output of heat 673

Chapter 14. Thermal Protection for Flight Vehicles 675
1. Methods of Thermal Protection 675
2. Determination of Heat of Ablation 680
2.1 Sublimation, complete evaporation or carbonization (pyrolysis) 680
2.2 Simultaneous melting and sublimation (evaporation) . . 683
2.3 Melting 686
3. Mass Transfer and Effectiveness of Thermal Protection Shield . 687
4. Example for Calculation of Thickness of Heat-Protection Shield 689

Chapter 15. Aerodynamics of Rarefied Medium 694
1. Limits of Applicability of Theory of Motion of a Continuous Medium 694
1.1 Molecular free path length 694
1.2 Regimes of gas flow 695
2. Pressure and Friction in Free Molecular Flow 699
2.1 Scheme of interaction of molecules with wall 699
2.2 Mass transfer 700
2.3 Pressure 706

2.4 Frictional stress 710
2.5 Transfer of kinetic energy 711
3. Adaptability 713
3.1 Exchange of momentum 713
3.2 Exchange of energy 715
4. Aerodynamic Forces 716
4.1 General expression for drag forces 716
4.2 Cone 719
4.3 Cylinder 723
4.4 Flat plate 725
5. Heat Transfer 727
5.1 Temperature of reflected molecules 727
5.2 Calculation of heat transfer and wall temperature . . . 730

Conversion Table for Units of Measurement Used in Aerodynamics from MKS System to International System (SI), GOST 9867-61 . . . 735

Bibliography 737

INTRODUCTION

Aerodynamics is a complicated word. It comes from the Greek words $\alpha\eta\rho$ (air) and $\delta\upsilon\nu\alpha\mu\iota\sigma$ (related to force). The science known by these terms happens to be a part of mechanics, which is a science about the motion of bodies in general. It studies the laws of motion of air in relation to applied forces and on the basis of these forces establishes particular laws of interaction between the air and the body.

The practical problems confronting man in connection with the flight of machines heavier than air served as a stimulus to the development of aerodynamics as a science. These problems were connected with the determination of forces and moments (known as aerodynamic forces and moments) acting on moving bodies. During this process the calculation of so-called supporting lift force was the main concern in the investigation of force-interaction.

In the early days of the history of aerodynamics it dealt only with low wind velocities as flight vehicles had low flight speeds. It is obvious that hydrodynamics—the science of the motion of liquid (incompressible) particles—was the theoretical basis of aerodynamics. The foundation of this science was laid in the 18th century by L. Euler (1707–1783) and D. Bernoulli (1700–1783), members of the Academy of Science of Russia. In the scientific conference on "General Principles of Fluid Motion" (1755) L. Euler for the first time produced basic differential equations of motion of so-called ideal (inviscid) fluids and gases. Investigation of the fundamental law of hydrodynamics which establishes the relation between the pressure and velocity in an incompressible fluid goes to the credit of D. Bernoulli. He published this law in 1738 in his work *Hydrodynamics.*

At relatively low flight speeds the effect of important properties of air, like compressibility, is infinitesimally small. However, the development of artillery and high-speed airplanes raised the problem of study of the laws of motion of air or, in general, of gas, at high speeds. It is found that if the forces acting on a body moving at high speed are calculated on the basis of the laws of motion of air at low speeds, these forces may be considerably different from the real values. The explanation of such phenomena was supplied by the investigation of the motion of air (gas) at high speeds resulting in changes in density with pressure. This change in density can often be

very appreciable. Along with this change in density there appears the property of compressibility of air.

The compressibility of a gas is related to its internal energy which is to be taken into account when calculating the flow parameters determining the motion of the medium. The change in internal energy of the gaseous state and the total derivative of work done by the compressible gas during expansion are determined by the first law of thermodynamics. Thus thermodynamic relations must be applied in the aerodynamics of a compressible medium.

If the gas medium moves at low speeds the heat content will be higher than the kinetic energy. In this case it is practically speaking unnecessary to calculate the change in heat energy with a change in speed (i.e. with a change in the kinetic energy of a fluid). Therefore it is not necessary to apply thermodynamic concepts and thermodynamic relations in the aerodynamics (hydrodynamics) of low speeds.

Very high flight speeds, sometimes known as hypersonic speeds, are represented by the motion of rockets and space vehicles entering the dense layer of the atmosphere. At such speeds the surrounding gas or air not only undergoes a change in density but also a rise in temperature leading to various physico-chemical changes in it. A considerable part of the kinetic energy due to the flight speed is transformed into heat and chemical energy.

All these peculiarities in the motion of a gas medium resulted in the development of high-speed aerodynamics or gas dynamics as a special part of aerodynamics. Here we will be studying the laws of air (gas) motion at high subsonic and supersonic speeds and also the laws of interaction between the gas medium and the body moving through it at these speeds.

Academician S.A. Chaplygin (1869–1942), one of the founders of gas dynamics, published the seminal work *About Gas Jets* in 1902. In this work he presented equations which form the theoretical basis of modern gas dynamics. These equations are known in science as "Chaplygin's equations."

With the development of theoretical aerodynamics experimental aerodynamics came into existence. It deals with the experimental investigation of the flow interaction between a body and a gas flowing around it with the help of various technical aids like wind tunnels and other equipment simulating the flow around an aircraft.

The very first aerodynamic laboratories were built under the guidance of N.E. Zhukovskii (1847–1921) in Russia (at Moscow State University, the Moscow Higher Technical Institute and at Kuchin in the outskirts of Moscow). The N.E. Zhukovskii Central Aerohydrodynamic Institute (TsAGI) was organized in 1918 with the help of V.I. Lenin on the initiative of N.E. Zhukovskii. This institute is now one of the most important centers in the world in the field of aerodynamics and has been named after N.E. Zhukovskii.

With the development of aviation, artillery and rocket techniques the

perfection of the theoretical basis of aerodynamics altered the nature of aerodynamic experimental techniques. The early comparatively small, low-speed wind tunnels were superseded and the gigantic high-speed wind tunnel of TsAGI (1940), the modern hypersonic wind tunnels and the special tunnels with an artificially created supersonic flow of dissociating gas (namely wind tunnels with heated air and shock tubes, the plasmatunnel and others) came into being.

The nature of the interaction between the gas medium and the body moving through it can be different for different conditions. The interaction at low speeds of motion is by nature basically of forces. With an increase in speed this force-interaction is associated with surface heating due to the heat flow from the gas to the body, giving rise to heat interaction. At very high speeds the aerodynamic heating becomes so intense that it may lead to the destruction of the material of the walls of flight vehicles as a result of melting or sublimation. Consequently an ablation of the material and a change in the nature of the wall heating take place. Aerodynamic heating also leads to a chemical reaction between the solid wall and the gaseous medium around it as a result of which there appears the same effect, ablation of the body.

High flight speeds can be the cause of ablation of the mass. The erosion of the material of the wall and damage to its structures can occur as a consequence of the mechanical interaction of the gas medium and the moving body.

Investigation of all types of interactions between the gas medium and flight vehicles allows us to carry out aerodynamic analysis in relation to the quantitative estimations of criteria for a given interaction, in particular, to determine aerodynamic forces and moments, heat transfer and mass erosion (known as mass ablation). The given problem in modern conditions leads not only to the determination of total aerodynamic quantities such as resultant lift and drag forces, heat flow from dissociated gas to the surface, etc. but also to the estimation of distribution of aerodynamic quantities (both forces and heat) over the surface of the flying vehicle (e.g. normal pressure, frictional stress, local heat flows, local mass ablation).

The solution of such problems requires a deeper investigation of gas motion than is necessary just to determine total aerodynamic interactions. This investigation includes determination of the gas parameters that characterize the motion at each point of the space it occupies and at every moment of time.

Modern methods of investigation of the motion of a gaseous medium are based on a number of principles and hypotheses established in aerodynamics. One of them is the hypothesis of continuity of the moving gaseous medium, according to which the inter-molecular spaces and molecular motions may be neglected and continuous variation of the basic gas parameters in space and time may be assumed. This hypothesis is derived from the condition that the free path lengths of molecules and amplitudes of their vibrational motion are

negligibly small in comparison to the linear characteristic dimensions of flow, for example, wing span, diameter or length of cone, etc.

The introduction of the hypothesis of continuity (solidity) should not contradict the concept of a gas medium even though it would seem that the medium must be incompressible in the absence of free molecular spaces. The postulation of a compressible continuous medium is based on the fact that the existence of molecular free spaces need not be taken into account in many investigations but the possibility of different degrees of concentration (density) may be assumed as a consequence of changes in these free spaces.

In aerodynamic investigations the interaction between the gas medium and the body moving through it is determined on the basis of the principle of reversed motion. Thereby the interacting system of "stationary gas (air) medium and moving body" is replaced by the system of "moving gas medium and stationary body." In replacing one system with the other we have to observe the condition of the equality of the speed of the oncoming gas flow vis-a-vis the stationary body and the speed of this body in a stationary medium. This principle of reversed motion follows from the basic law of mechanics according to which the forces of interaction are independent of the circumstance which of the two interacting bodies (in this case gas and flight vehicle) is stationary and which in rectilinear uniform motion (law of relativity).

From the practical point of view the principle of superposition is very helpful in calculation of the resultant aerodynamic characteristics (pressure, forces, heat flows, etc.). By the principle of superposition these characteristics can be resolved into their individual components. The calculation of each of the components requires the solution of an independent, simpler problem than the determination of the resultant values. In this way the total aerodynamic characteristics will take the form of superposed quantities, i.e. they will be obtained by the addition of respective components.

The system of differential equations that forms the basis of the solution of flow-interaction problems in modern aerodynamics is treated separately as two main types of motions: one is free (external) inviscid flow and the other, flow in thin layers of gas, i.e. boundary layer flow where fluid motion is studied along with frictional effects. These divisions of flow are based on the hypothesis of the absence of adverse effects of the boundary layer on free flow. Then the parameters of the inviscid flow (i.e. at the external limit of the boundary layer) will be the same as those at the wall in the absence of this layer.

Physical similarity conditions of flow interaction problems should be kept in mind when conducting aerodynamic experiments and calculations. The aerodynamic calculations of flying objects (rockets, airplanes) are generally based on preliminary investigations (theoretical and experimental) of flow over models.

Aerodynamic similarity conditions must be observed in such investigations on models. These conditions are based on the characteristic, simple parameters determining the basic regimes of processes of investigation known as similarity parameters or criteria. The modern similarity problems and dimensional analysis widely used in aerodynamics are formulated in the fundamental work of Academician L.I. Sedov on *Methods of Similarity and Dimensional Analysis in Mechanics.*

Aerodynamics is a many-faceted science with a typical structure. The basic scientific directions and sections are more or less distinctly established in line with the fast developing aviation and space rocket technology. They are connected with the aerodynamic investigation of flight vehicles, individual structural elements and specific types of gas flows and the processes associated with them. It is natural that the whole classification of aerodynamics will to some extent be conditional because all these directions and sections or subsections are interrelated. But still, this "branch-wise" specialization in aerodynamic science is of practical relevance.

Let us study some typical directions and sections of modern aerodynamics. Two basic directions in which modern aerodynamics is developing can be distinguished. The first represents the so-called aerodynamics of forces associated with the solution of problems that deal with the force-interaction of a medium. In other words this section of aerodynamics deals with the distribution of normal pressure and frictional stresses over the surface of flight apparatus and also the calculation of resultant forces and moments. The data so obtained are used in strength calculations for the structure of the bodies and individual elements and also in determination of its flight characteristics. The second direction includes the problems of science covering aerodynamics, thermodynamics and heat transfer and the flow-interaction with the heat effects being investigated. The heat flows from a heated gas to the wall are obtained and the wall temperature is determined. These data are necessary in strength calculations and in designing cooling systems for flight vehicles. In addition, the consideration of changes in the properties of a gas at high temperature facilitates the understanding of the quantitative criteria of the force-interactions of the external flow as well as of the boundary layer.

All these problems are of great significance in very high-speed flight during which the heat processes take place fairly intensively. However, the solution of such problems becomes very complicated because they are related to the chemical processes taking place in the gas and also to the chemical interactions between the gaseous medium and the wall material.

Keeping in mind the speed range of flight vehicles from low subsonic to very high supersonic flight, the science of the investigation of flow, as indicated in the preface, can be divided into the following fundamental sections: aerodynamics of an incompressible fluid or hydrodynamics (Mach number

$M=0$); and aerodynamics of high speeds. The latter is further subdivided into the aerodynamics of subsonic ($M<1$), nearly sonic (transonic $M\approx1$), supersonic ($M>1$) and hypersonic ($M\gg1$) flows. It must be pointed out that in each of these sections the flow interaction processes have some different specific peculiarities. As a result the investigation of each of these flows may be based on different mathematical foundations.

Aerodynamic investigations, as already mentioned, are based on the types of flow motions over a body—the free (external) inviscid flow and the boundary layer flow. The individual sections of aerodynamics deal with each of the types of motions. The aerodynamics of an inviscid (ideal) fluid is attributed to free flows and the aerodynamics of a boundary layer, to boundary layer flows.

The aerodynamics of an ideal medium investigates the distribution of inviscid parameters of flow-interaction at the outer limit of the boundary layer. Consequently they are the boundary conditions for the solution of the differential equation in the boundary layer. Normal pressure is related to the inviscid parameters. The resultant forces and moments due to this pressure can be derived from the distribution of these parameters. The aerodynamics of an ideal medium is mainly based on Euler's fundamental equations.

Boundary layer science is one of the most widely developed sections of the science of fluid and gas motion. The solution of problems of motion in the boundary layer allows us to determine the distribution of tangential stresses and hence the total aerodynamic forces and moments due to friction. It also helps in estimating heat transfer from a heated gas flow around a surface to the wall of the body.

Modern boundary layer theory is based on the fundamental investigations of L. Navier, D. Stokes, O. Reynolds, L. Prandtl and T. Karman. Soviet scientists contributed significantly to the development of boundary layer theory. Academician A.A. Dorodnitsyn worked out the basic theory of a boundary layer in a compressible gas. Professor L.G. Loitsyanskii developed the effective method of calculation of the boundary layer on a curvilinear surface. In the aerodynamic investigations of high-speed flight it is necessary to consider heat processes in the boundary layer in spite of their low intensities. Here the aerodynamics of forces is kept to the fore even though the heat transfer and effect of temperature on the boundary layer should be taken into account at high flight speeds. It is natural that much attention is being paid to the solution of such problems, particularly in these days. In the Soviet Union Professors L.Ye. Kalikhman, I.A. Kibel', V.I. Ievlyev and others are working out gas dynamic theory for heat transfer by investigating viscous flow in a boundary layer over different types of bodies at high temperatures. Similar problems are under investigation by many scientists in other countries.

Aerodynamic heating is not the only problem of flow-interactions at hypersonic speeds. The fact that at such speeds an ionization of gas takes place due to the high temperatures and the gas becomes a conductor of electricity raises new problems associated with the control of plasma flow by use of magnetic poles. In the formulation of problems of interactions between the moving body and the plasma the corresponding aerodynamic calculations must consider electromagnetic forces along with gas dynamic forces. These problems are studied in magnetoaerodynamics.

A special section of aerodynamics, namely the aerodynamics of a continuous medium, deals with the investigation of fluid and gas motion on the basis of the hypothesis of continuity stated earlier. However, it must be noted that this hypothesis is valid only for the conditions of low-altitude flight, i.e. in sufficiently dense layers of atmosphere where the length of the mean free paths of molecules of air is small. In the condition of highly rarefied atmosphere at high altitudes this length of the free path of molecules becomes quite appreciable and air cannot be treated as a continuous medium. Hence the conclusions of the aerodynamics of a continuous medium will not remain valid under such conditions.

The interaction between the rarefied medium and the body moving through it is studied in a special section of aerodynamics known as aerodynamics of a rarefied medium. The rapid development of this science during the last few years was called for by space research with the help of artificial earth satellites and space rocket vehicles and rocket systems of different types (intercontinental ballistic missiles, global rockets and others) which circle the earth at very high altitudes.

The conditions of flow-interaction and consequently the aerodynamic characteristics of an aircraft will vary according to the nature of the variation in the flow parameters at given points in space. The major class of problems of flow-interactions in practice can be solved within the framework of steady aerodynamics, assuming that the flow parameters at given points are independent of time. However, it becomes necessary to account for the unsteady nature of flow-interactions when investigating the stability of flow due to nonuniform flight velocity, oscillations or rotation of flight vehicles, etc. This is due to the fact that under such conditions the surrounding flow will be characterized by the local variation of its parameters with time. Study of this type of flow-interactions is related to unsteady aerodynamics.

We have considered the classification of modern aerodynamics on the basis of types of gas flows. It is obvious that in each of the sections of aerodynamics the investigation of flow-interaction leads in general to different shapes of aircraft or components. Hence it is interesting to consider the classification of modern aerodynamics according to the form of the aircraft or of its individual structural elements.

The modern airplane in its aerodynamic scheme basically represents a

combination of the main body (fuselage), wing and stabilizer and control surfaces. The effects of aerodynamic interference—the aerodynamic interaction between given elements of the flight vehicle—must be taken into account in the aerodynamic calculation of such bodies. Accordingly the resultant aerodynamic characteristics of lift, drag and moment may be calculated as a summation of similar characteristics of isolated fuselage, wings, stabilizers and controls with corrections introduced as a result of given interactions. Thus a given scheme of aerodynamic calculations requires knowledge of the aerodynamic characteristics of the individual components of the flight vehicle.

The aerodynamic calculation of the lifting surface of wings occupies a special section in aerodynamic science known as the aerodynamics of wings. The great Russian engineer-scientists N.E. Zhukovskii and S.A. Chaplygin are considered to be the founders of the aerodynamic theory of the wing. The beginning of the 20th century saw N.E. Zhukovskii's discovery of the nature of the lift force on a wing. He invented the formula for calculating it which is commonly known as the Zhukovskii formula. The work of N.E. Zhukovskii on bound vortices representing a hydrodynamic model of the wing is considered to be a very valuable contribution. The series of wing profiles he worked out (Zhukovskii profiles) is widely used in the design of airplanes.

Academician S.A. Chaplygin is the author of several pioneer works on the aerodynamics of wings. In the work *On Pressure Distribution over Bodies in Rectilinear Flow* of 1910 S.A. Chaplygin laid the foundation of the theory of the infinite wing. In 1922 he published a scientific work, *Theory of the Monoplane* in which he gave the theory of a series of profiles (Chaplygin's profiles) and also worked out the theory of the stability of a monoplane wing. S.A. Chaplygin is the originator of the theory of a wing of finite span.

The Soviet scientists, Academician A.I. Nekrasov (1883–1954) and Corresponding Member of the Academy of Sciences of the USSR V.V. Golubev (1884–1954), contributed greatly to the aerodynamics of wings. A.I. Nekrasov worked out basic wing theory in an unsteady flow. V.V. Golubev invented various kinds of high lift devices for a wing, methods of controlling the boundary layer and flow-interaction of small-aspect ratio wings.

In his work *Interaction of Bodies and Gas at High Subsonic Speeds*, Academician S.A. Khristianovich developed an original and very effective method of accounting for compressibility effects in the interaction of profiles of arbitrary shapes.

Abroad, Professor L. Prandtl (Germany) and G. Glauert (England), who also contributed to the approximate theory of thin airfoils in a subsonic flow at small angles of attack, worked on the problems of compressibility effects on the flow-interaction of wings. The results they obtained can be treated as particular cases of the general theory of flow-interaction worked out by S.A. Khristianovich.

The theory of thin wings of various plans in a supersonic flow was developed in the works of Professors Ye.A. Krasil'shchikova and S.V. Fal'kovich.

The results of aerodynamic research on wings are applied to the calculation of the aerodynamic characteristics of the stabilizer and also of some control surfaces having plans similar to those of wings. The specific peculiarities of flow-interactions of various types of aerodynamic controls and the presence of other types of components for controls led to the growth of a special section in modern aerodynamics known as the aerodynamics of components of control surfaces.

Modern flight vehicles of the rocket type in many cases have the form of rotating bodies or something like them. The combined rocket system of fuselage-wing-stabilizer has a fuselage (rotating body) as the basic component of the aerodynamic system. As a result the aerodynamics of conical shapes (rotating bodies) in recent years underwent very rapid development as one of the important parts of modern aerodynamic science.

Soviet scientists Professors F.I. Frankl' and E.I. Karpovich, authors of an interesting scientific work, *Gas Dynamics of Thin Bodies*, contributed greatly to the development of the aerodynamics of rotating bodies. A group of scientific workers (K.I. Babenko, G.P. Voskresenskii and others) of the Mathematical Institute of the Academy of Sciences, USSR, worked out the method of three-dimensional supersonic flow past sharp bodies, particularly when chemical reactions are taken into account in the flow field surrounding the body. Aerodynamic specialists abroad—D. Taylor (England) and Z. Kopal (USA)—found the solution of a very important problem in a supersonic flow past a sharp cone.

The rapid development of modern mathematics and number techniques in the direction of perfecting the methods of aerodynamic investigations facilitates the solution of many difficult problems of aerodynamics including the problems of aerodynamic interference and corresponding corrections to the aerodynamic characteristics of flight vehicles. The special section of aerodynamic science called the aerodynamics of interference has developed rapidly in recent years.

At low supersonic flight speeds aerodynamic heating is comparatively low and cannot cause damage to flight vehicle structures. The basic problem here relates to the selection of the technique of cooling which maintains the required temperature of the wall surface. More complicated problems arise at very high flight velocities of bodies having high kinetic energy. For example, if the flight vehicle has cosmic speed the conversion of even 25 to 30% of this energy into heat is enough to evaporate the vehicle completely. The main problem that arises in the safe launching of space vehicles in dense layers of the atmosphere is the dissipation of this energy so that the minimum amount is absorbed by the body in the form of heat. It was found that bodies with a

blunt nose have such properties. This brought about the development of aerodynamic research on blunt bodies.

The Soviet scientists, Academician A.A. Dorodnitsyn, Corresponding Member of the Academy of Sciences, USSR, G.G. Chernii, Professor O.M. Belotserkovskii and others greatly contributed to the study of the problems of the aerodynamics of blunt bodies. Similar investigations were carried out by M. Lighthill (England), P. Garabedyan (USA) and other scientists abroad.

The provision of a blunt nose to the body surface can always be treated as an aid in the heat protection of a flight vehicle. In this process the blunt nose itself undergoes the most intensive heat interaction. Therefore this part needs more heat protection than the peripheral part of the apparatus. The most effective heat protection may be obtained by the use of various sheaths of a material that gradually erodes at such temperatures and is carried away bit by bit. In this process a considerable part of the energy imparted to the flight vehicle by the heated air is absorbed. The analysis of theoretical and practical methods for calculating the separated mass (ablation) is related to the modern section of aerodynamic science called aerodynamics of the ablation of surfaces.

The wide range of problems of aerodynamics deals in general with the determination of the flow-interaction of the medium with flight vehicles of arbitrary shapes. The forms of flight vehicle surfaces can be selected with the particular aim of fulfilling this or that aerodynamic effect. The form of blunt bodies minimizes the heat transfer to the rest of the body. Consequently the blunt surface is taken to be the optimum from the heat exchange point of view. In designing flight vehicles the problem arises of the selection of shapes producing the least interaction of forces. One such problem is specifically related to the determination of the form of the nose of the flight vehicle that offers least drag at given flight speeds. Similar types of problems are studied in the section of aerodynamics known as aerodynamics of optimum shapes.

Such are the contents, basic problems and corresponding classification of modern aerodynamics.

1

BASIC CONCEPTS IN AERODYNAMICS

1. Force-Interaction of the Medium on a Moving Body

1.1 Surface force

Let us examine the force-interaction of the medium on a body moving in it, assuming that the medium is a viscous gas (real fluid) and fairly dense. The gas is then taken as a continuous medium, i.e. there is no empty space between gas molecules. The force-interaction of such a fluid leads to a continuous distribution of forces $\bar{P}_n$, due to normal stress, and also to the distribution of forces $\bar{P}_\tau$ as a result of tangential stresses (Fig. 1.1.1). The resultant force, known as the *surface force*, acts on the elemental surface dS that we are considering. The vector $\bar{P}$ of this force is determined by the rule of addition of two vectors: $\bar{P}=\bar{P}_n+\bar{P}_\tau$. Here the force $\bar{P}_n$ also includes the additional component derived from frictional force along with the force due to normal pressure.

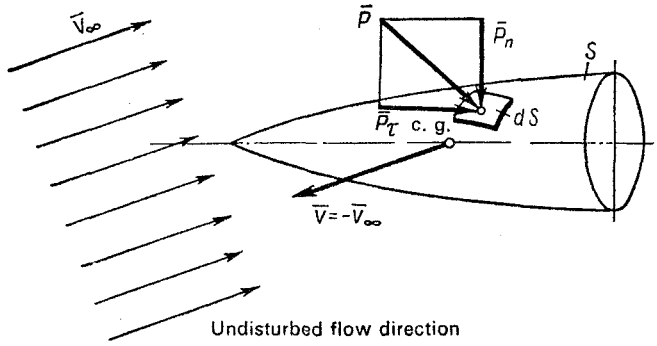

Fig. 1.1.1. Forces acting on element of surface of moving body.

In the case of an ideal fluid it is assumed that viscous forces are absent and that the force-interaction on the surface of a body produces only the forces that arise from normal pressure. This is quite clear, since the projec-

tion of a force on this surface exists if the force vector is inclined to the normal at a point on the elemental surface, i.e. a shear stress exists which is however absent in an ideal fluid.

The force-interaction will be the same if a uniform fluid flow over a steady body with the velocity at an infinite distance from the body is equal to the velocity of the body in the above case. The velocity is moreover called the *velocity at infinity or velocity of oncoming (undisturbed) flow* and is represented by the vector $-\bar{V}_\infty$ in place of $\bar{V}$ (velocity vector of the flight). It is obvious that $\bar{V} = -\bar{V}_\infty$.

The oncoming flow is characterized by the undisturbed parameters—pressure p_∞, density ρ_∞, temperature T_∞ in place of the corresponding parameters p, ρ, T of the disturbed flow that exists during the interaction of the body (Fig. 1.1.2). The physical properties of a gas (air) are also characterized by the kinetic parameters: coefficient of viscosity μ and coefficient of thermal conductivity λ (the corresponding undisturbed parameters will be μ_∞ and λ_∞), and also by the thermodynamic parameters: specific heats at constant pressure c_p (c_{p_∞}) and at constant volume c_v (c_{v_∞}) and the ratio of specific heats (index of isentropic flow) $k = c_p/c_v$ ($k_\infty = c_{p_\infty}/c_{v_\infty}$).

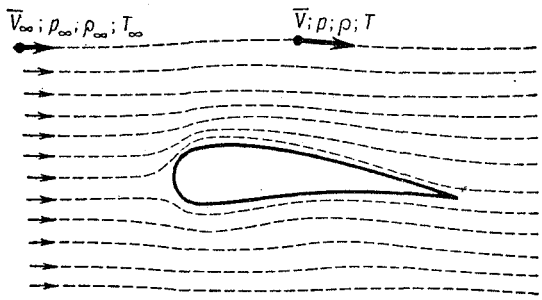

Fig. 1.1.2. Notation of parameters of disturbed and undisturbed flows.

1.2 Properties of pressure in an ideal fluid

Let us examine the properties of pressure in an ideal fluid. Let us first write down the equations of motion of the elementary tetroid $M_1M_0M_2M_3$ of a fluid of sides Δx, Δy, Δz along the x, y, z axes respectively (Fig. 1.1.3) by equating the product of the elemental mass and its acceleration to the summation of forces acting on it. These equations can be written down in terms of the components of forces along the axes of coordinates. Let us restrict ourselves to the formulation of these equations of motion of a tetroid along the x axis, assuming that the other two components will have similar forms. The product of the elemental mass and its acceleration along the x axis is equal to

$$\rho_{av} \Delta W \, (dV_x/dt),$$

where ρ_{av} is the average density of fluid in the elementary volume ΔW; dV_x/dt is the component of acceleration of motion of this mass along the x axis.

The forces acting on the mass of fluid are determined in the following way: As already mentioned, these forces consist of so-called surface forces. In a given case they are determined by the action of normal pressure on the sides of an elementary fluid mass with projection on the x axis being equal to

$$p_x \Delta S_x - p_n \Delta S_n \cos(\widehat{nx}).$$

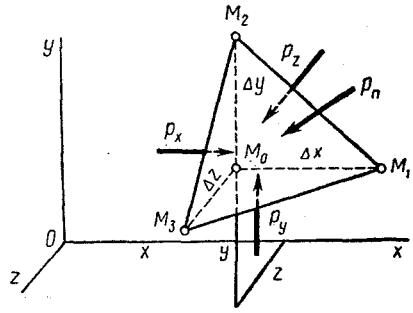

Fig. 1.1.3. Normal stresses acting on sides of elemental fluid particle in form of tetroid.

The other force, acting on the separated elementary volume of fluid, is volume (or mass) force which is proportional to the mass of fluid particles in this volume. The universal gravitational forces and, in particular, centrifugal forces are examples of volume forces. The mass force acting on an electrified (ionized) gas in an electromagnetic field is also an example of volume forces due to electromagnetic action. Here the motion of gas under such forces will not be studied (see special course in magneto-hydrodynamics).

For the case in question the component of mass force along the x axis can be expressed by $X\rho_{av}\Delta W$ with X as the component of volume force per unit mass. Considering these values of components of surface and volume forces, the equation of motion will be

$$\rho_{av}\Delta W \frac{dV_x}{dt} = X\rho_{av}\Delta W + p_x \Delta S_x - p_n \Delta S_n \cos(\widehat{nx}),$$

where X is the x-component of volume forces per unit mass; ΔS_x and ΔS_n are the corresponding values of areas $M_0M_2M_3$ and $M_1M_2M_3$; $\cos(\widehat{nx})$ is the cosine of the angle between the normal n to surface $M_1M_2M_3$ and the x axis; p_x, p_n are normal pressures acting on the surfaces $M_0M_2M_3$ and $M_1M_2M_3$ respectively.

Divide the equation so obtained by ΔS_x and, keeping in mind that $\Delta S_x = \Delta S_n \cos(\widehat{nx})$, take the limits of Δx, Δy, Δz tending to zero. Then terms containing $\Delta W/\Delta S_x$ will also tend to zero as ΔW will have a small value of the third order and ΔS_x is a small quantity of the second order in comparison of the sides of the elements. As a result $(p_x - p_n) = 0$ and consequently $p_x = p_n$.

Study of the equations of motion along the y and z axes gives $p_y = p_n$ and $p_z = p_n$.

As elementary volume is arbitrarily oriented the following conclusion can be drawn from the results so obtained: the pressure at any point in the ideal fluid flow is the same on all the surfaces passing through that point. Consequently, it can be considered as a scalar quantity which depends only on the coordinates of the point and time.

1.3 Effect of viscosity on fluid motion

Laminar and turbulent motion: Observations show that a viscous fluid is characterized by two types of motion. The first, laminar or layer-wise motion, is characterized by orderly positioned streams that do not intermix. In a laminar flow the transfer of momentum, heat and fluid particles takes place by processes of friction, heat conduction and diffusion of molecules. Such motion is found and is usually steady at small velocities of fluid flow.

If the magnitude of the velocities of fluid flow exceeds its critical value at given conditions of interaction of the surface, the laminar motion does not remain steady and becomes a new type of motion characterized by movement of fluid particles from one layer to another. As a result the orderly layer-wise flow vanishes. This type of flow is called a turbulent flow. In a turbulent flow the mixing of microscopic particles is superposed on the molecular orderly motion which is typical of a laminar flow. This flow has an unsteady character because the velocity and other parameters at a given point depend on time.

In analyzing turbulent flow it is convenient not to deal with instantaneous velocity but with its average value for some interval of time (t_2). For example, the component of velocity along the x axis will be $\overline{V}_x=(1/t_2)\int_{t_1}^{t_1+t_2} V_x\,dt$, where V_x is a component of instantaneous velocity at a given point as a function of time t. In the same way, the components $\overline{V}_y$ and $\overline{V}_z$ along axes y and z can be written down. Taking the usual meaning of average velocity, the instantaneous velocity can be expressed in the form $V_x=\overline{V}_x+V_x'$, where V_x' is an additional variable component of velocity known as fluctuating velocity. The perturbation components of velocity along the y and z axes are denoted by V_y' and V_z' respectively.

The fluctuating component of velocity can be measured by positioning a measuring instrument with small inertia (for example, a thermoanemometer has such properties) at a required point in the flow. The instrument indicates deviation of velocity from the average velocity (i.e. it indicates perturbation velocity) in a turbulent flow.

The kinetic energy of the turbulent flow can be determined by summation of kinetic energies, calculated for average and fluctuating velocities. Kinetic energy of the pulsating flow at a point being considered can be obtained as the value proportional to the mean square of the perturbation velocity. If the pulsating flow is resolved into components along the axes of coordinates the kinetic energies of each of the components of such a flow will be proportional

to the respective mean square of the fluctuating components designated by $\overline{\Delta V_x'^2}$, $\overline{\Delta V_y'^2}$, $\overline{\Delta V_z'^2}$, which may be determined by

$$\overline{\Delta V_{x\,(y,\,z)}'^2}=\frac{1}{t_2}\int_{t_1}^{t_1+t_2} V_{x\,(y,\,z)}'^2\,dt.$$

If the equality

$$\overline{\Delta V_x'^2}=\overline{\Delta V_y'^2}=\overline{\Delta V_z'^2}$$

is satisfied at a point being considered the turbulence is called isotropic at that point. If this condition is fulfilled at all points it is called a homogenous isotropic turbulent flow.

The meaning of average and perturbation values can be extended to pressure and other physical variables. The existence of the perturbing velocities leads to additional normal and shear stresses and to more intensive heat and mass transfer.

Frictional stress: Let us examine the formula for frictional force in a laminar flow. In such case the friction appears as a result of diffusion of molecules associated with the transfer of momentum from one layer to another that results in variation of flow velocity, i.e. it leads to the appearance of relative motion of particles of gas in layers. The frictional force, according to the hypothesis first put forward by Newton, is proportional to the value of the variation of the velocity between the mixing particles situated in layers which are unit distance apart from each other. If the distance between the layers is Δn and the relative velocity of particles Δv, the ratio $\Delta v/\Delta n$ in the limit $\Delta n\to 0$, for adjacent layers, is equal to the derivative $\partial v/\partial n$, known as normal velocity gradient. On the basis of the above hypothesis Newton's formula for frictional stress can be written as

$$\tau=\mu\,(\partial V/\partial n), \tag{1.1.1}$$

where μ is the coefficient of proportionality depending on the properties of the fluid, its temperature and pressure. It is also known as the coefficient of dynamic viscosity.

The value of this coefficient for gas, by the kinetic theory formula, at a given density ρ is

$$\mu=0.499\,\rho\bar{c}l \tag{1.1.2}$$

and depends on the kinetic properties of gas, like mean free path l and average velocity of motion of molecule $\bar{c}$. This value of μ is also called the coefficient of kinetic viscosity.

Consider friction in a turbulent flow. Take the simplified model for the presence of additional frictional force in a turbulent regime suggested by

Prandtl for an incompressible medium and the semiempirical relations introduced for it. Now take two layers in a uniform flow characterized by variation of mean velocity only in one direction. Further assume that in one of the layers the velocity $\overline{V}_x \neq 0$ and $\overline{V}_y = \overline{V}_z = 0$. Then for an adjacent layer situated at a distance $\Delta y = l'$ the mean velocity is equal to $\overline{V}_x + (d\overline{V}_x/dy)\, l'$. The particle moving from the first layer to the second, by Prandtl's hypothesis, maintains its velocity $\overline{V}_x$. Consequently at the time of appearance of this particle in the second layer the pulsating velocity component will be $V'_x = (d\overline{V}_x/dy)\, l'$.

It has been found experimentally that away from a solid surface a fluid has properties of isotropic turbulence. So by Prandtl's hypothesis it can be assumed that the absolute value of component V'_y is proportional to the absolute value of V'_x:

$$V'_y = aV'_x = al'(d\overline{V}_x/dy),$$

where a is some constant of proportionality.

The absolute value of momentum due to motion of fluid mass $\rho V'_y\, dS$ through elementary area dS will be equal to $\rho V'_y\, (\overline{V}_x + V'_x)\, dS$. This momentum determines the additional force due to stress created by the perturbation components of velocities. From this the absolute value of shear stress is

$$|\tau_T| = \rho V'_y\, (\overline{V}_x + V'_x).$$

Taking the mean value of this expression we get

$$|\overline{\tau_T}| = \frac{\rho \overline{V}_x}{t_2} \int_{t_1}^{t_1+t_2} V'_y\, dt + \frac{\rho}{t_2} \int_{t_1}^{t_1+t_2} V'_y\, V'_x\, dt = \rho \overline{V}_x\, \overline{V}'_y + \rho \overline{V'_x\, V'_y},$$

where $\overline{V'_x\, V'_y}$ is the mean value of the product of perturbation velocities and $\overline{V}'_y$ is the average value of perturbation velocity. It can be shown that the last one is equal to zero. Integrating the derived quantity $V_y = \overline{V}_y + V'_y$ with respect to t in the interval from t_1 to $(t_1 + t_2)$ and then dividing it by t_2, we get

$$\frac{1}{t_2} \int_{t_1}^{t_1+t_2} V_y\, dt = \frac{1}{t_2} \int_{t_1}^{t_1+t_2} \overline{V}_y\, dt + \frac{1}{t_2} \int_{t_1}^{t_1+t_2} V'_y\, dt = \overline{V}_y + \frac{1}{t_2} \int_{t_1}^{t_1+t_2} V'_y\, dt.$$

But $\overline{V}_y = (1/t_2) \int_{t_1}^{t_1+t_2} V_y dt$ by definition. Therefore it is obvious that $\overline{V}'_y = (1/t_2) \int_{t_1}^{t_1+t_2} V'_y\, dt = 0$. Then the mean value of frictional stress

$$|\bar{\tau}_T| = \rho\overline{V_x' V_y'} = \frac{\rho}{t_2}\left(\frac{d\bar{V}_x}{dy}\right)^2 \int_{t_1}^{t_1+t_2} l'^2\, a\, dt = \rho l^2 \left(\frac{d\bar{V}_x}{dy}\right)^2, \qquad (1.1.3)$$

where coefficient of proportionality a is absorbed in the average value of l' and denoted by l. The magnitude of l is called mixing path length and is, in its own way, an analog of the length of the mean free path of molecules in the kinetic theory of gases. The sign of frictional stress is determined by the sign of velocity gradient; consequently

$$\tau_T = \rho l^2 \,|\, d\bar{V}_x/dy \,|\, (d\bar{V}_x/dy). \qquad (1.1.3')$$

The complete value of frictional stress can be obtained by direct addition of the frictional stresses τ_T due to viscosity and due to interchange of molecules, i.e. where the value $\tau_b = \mu\,(d\bar{V}_x/dy)$ is added to the value of τ_T which is obtained from the energy loss of particles in their collision and irregular mixing. Thus

$$\tau = \tau_b + \tau_T = \mu\,(d\bar{V}_x/dy) + \rho l^2 \,|\, d\bar{V}_x/dy \,|\, (d\bar{V}_x/dy). \qquad (1.1.4)$$

The investigations conducted by Prandtl showed that the path length of intermixing $l = \kappa y$, where κ is some constant value. Consequently near the wall

$$\tau_{y=0} = \tau_b = |\, \mu\,(d\bar{V}_x\,/dy)\,|_{\,y=0}\,. \qquad (1.1.5)$$

From experimental data it follows that turbulent flow cannot occur in the direct vicinity of a wall, where a very small rate of mixing occurs. Here the flow remains laminar and for that relation (1.1.5) is valid. Under these conditions the stress τ_b is very small and hence it can be assumed that the frictional stress is determined by (1.1.3').

Concept of boundary layer: From equations (1.1.1), (1.1.3) it follows that the frictional stress in the different parts of a fluid is not the same for one and the same medium-interacting body and it is determined by the value of the local velocity gradient.

Investigations have proved that the velocity gradient has its highest value near a wall because the viscous medium undergoes stagnation due to adhesion to the surface of the body under interaction. The flow velocity changes from zero at the wall (Fig. 1.1.4) and gradually increases with the increase in the distance from the surface. The frictional stress changes accordingly, i.e. near the wall it is significantly higher than away from the surface. The thin layer of fluid over a surface, characterized by high velocity gradients along normals to the surface and consequently by significantly high frictional stresses, is called the boundary layer. The physical representation of the boundary layer can be understood by covering the surface of a body with colored material soluble in fluid. It is obvious that the paint will diffuse in a layer of fluid and simultaneously will be carried away downstream along with the flow. This colored

zone will represent in itself a layer with gradually increasing thickness along the flow direction. This colored zone of fluid approximately coincides with the boundary layer. It breaks away from the surface in the form of a colored eddy stream (or aerodynamic wake, see Fig. 1.1.4). It is known that with an increase in flow velocity the thickness of the layer diminishes and the wake becomes narrower.

The nature of velocity distribution across the section of the boundary layer depends on whether it is laminar or turbulent. The above-mentioned distribution of velocity or its mean values with respect to time seems more uniform for a turbulent flow than for a laminar flow (see Fig. 1.1.4) as a result of the cross flow of particles and their collisions. From the distribution of velocities in a flow field near the surface of the body it is found that higher frictional stress exists in a turbulent boundary layer which is usually governed by the increased value of velocity gradients.

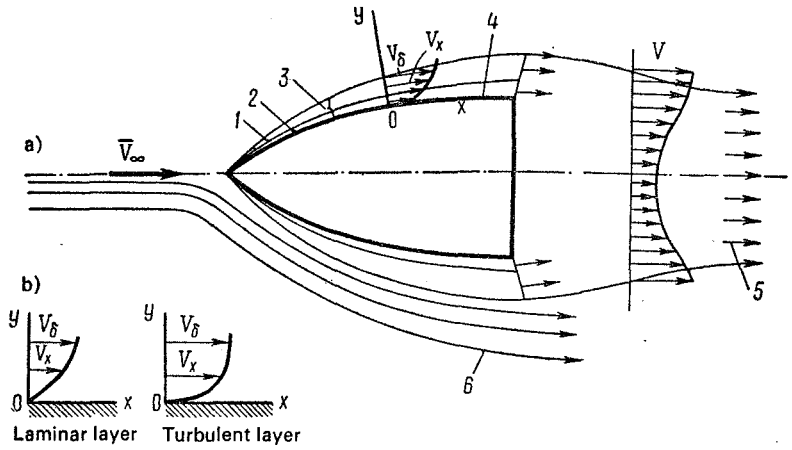

Fig. 1.1.4. Scheme of interaction of body and viscous fluid flow:
a—general flow pattern: *1*—turbulent core; *2*—laminar sublayer; *3*—boundary layer; *4*—surface in flow; *5*—slip stream (wake); *6*—free flow; *b*—velocity profile in boundary layer.

There exists a region of flow within the boundary layer where velocity gradients and hence frictional forces are small. This part of the flow is called the external free flow. This type of flow is also called inviscid. The velocity across the thickness of the boundary layer varies from zero at the wall to a value equal to that in the external free flow.

Fluctuating flows, as mentioned earlier, are prevented near the wall and this helps to reduce the fluctuating velocity components. Therefore part of the boundary layer is always laminar. This thin section of boundary layer is called the laminar sublayer. The basic part of the boundary layer outside the laminar sublayer can be either laminar or turbulent depending on the intensity

of cross flows in the boundary layer. Thus study of motion in the region of a turbulent boundary layer, called the turbulent core (see Fig. 1.1.4), is at the same time connected with the investigation of fluid flow in the laminar sublayer.

The variation in speed across the section of the boundary layer is characterized by the fact that after gradually increasing with the distance from the wall it asymptotically approaches the value of the velocity of the external flow.

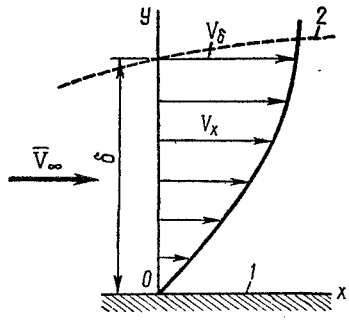

Fig. 1.1.5. Boundary layer scheme: *1*—wall; *2*—outer limit of layer.

However, for all practical purposes it is convenient to separate the part of the boundary layer where changes in velocity take place quite fast from the upper boundary where the velocity differs negligibly from its value in the outer free flow. The distance from the wall to this boundary limit is termed the boundary layer thickness δ (Fig. 1.1.5). Usually this thickness determines the point in the boundary layer section where the velocity differs from its value in the outer flow by about one per cent.

The introduction of the concept of the boundary layer made it easier to investigate friction and heat transfer because its smaller thickness compared to the size of the body allows us to simplify the differential equations of the fluid flow and hence makes their integration easier.

2. Resultant Force-Interaction

Components of aerodynamic forces and moments: The forces due to normal and shear stresses are continuously distributed over the surface of a body in a fluid flow. They can be expressed by one main vector $\overline{F}$ of aerodynamic forces and vector $\overline{M}$ of moment due to these forces about some reference point (Fig. 1.2.1). This point may be an arbitrary point on the body, for example its center of gravity, the nose of a rocket cone, a point on the leading edge of a wing, etc.

In practice we do not deal with vectors $\overline{F}$ and $\overline{M}$ but with their projections on the axes of some system of coordinates. Let us consider two popular systems of coordinates in aerodynamics, namely the velocity and the fixed systems of coordinates (see Fig. 1.2.1). In the velocity system of coordinates the longitudinal axis Ox is always directed along the velocity vector of motion of the center of gravity of the apparatus; the vertical axis Oy lies in the plane of symmetry and directed upward (positive direction) and the axis Oz along the span of the right wing (right system of coordinates). For reversed motion the

longitudinal axis coincides with the flow direction and the axis Oz points along the span of the left wing so that the right system of coordinates is maintained. In this case the velocity system of coordinates is also called the flow system of coordinates.

In the fixed system of coordinates, rigidly connected with the flight vehicle, the axis Ox_1 is directed along the principal axis of inertia, the vertical axis Oy_1 lies in the plane of symmetry and the horizontal axis Oz_1 is directed along the span of the right wing and forms the right system of coordinates. The positive direction of axis Ox_1 from tail to nose corresponds to the case of the positive direction of motion of the vehicle (see Fig. 1.2.1). In both systems of coordinates—the velocity (flow) and the fixed—the origin of a system coincides with the center of gravity of the flight vehicle.

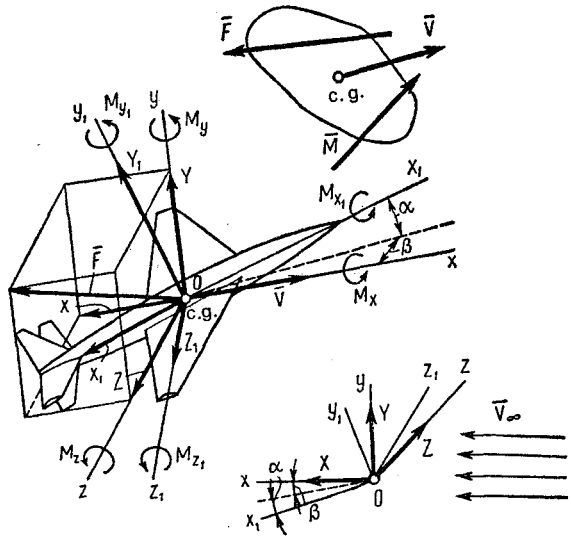

Fig. 1.2.1. System of aerodynamic forces and moments acting on aircraft in velocity system (x, y, z) and fixed system (x_1, y_1, z_1) of coordinates.

The projections of vector $\overline{F}$ on the axes x, y, z in the velocity system of coordinates are known as the drag force X, side force Z and lift Y. The corresponding projections of the same vector on axes x_1, y_1, z_1 of the fixed system of coordinates are called the axial force (X_1 or R), the side force Z_1 and the normal force (Y_1 or N).

The projections of vector $\overline{M}$ in both systems of coordinates carry the same names. The component of $\overline{M}$ about the longitudinal axis is called rolling moment (the corresponding symbols in the velocity and fixed systems of coordinates are M_x and M_{x_1} respectively), the component about the vertical axis is called yawing moment (M_y, M_{y_1}) and the component about the lateral axis is called pitching moment (M_z, M_{z_1}).

The vectors of aerodynamic forces and moments in the velocity and fixed systems of coordinates are then:

$$\overline{F}=Xi+Yj+Zk=X_1i_1+Y_1j_1+Z_1k_1; \tag{1.2.1}$$

$$\overline{M}=M_xi+M_yj+M_zk=Mx_1i_1+My_1j_1+Mz_1k_1, \tag{1.2.2}$$

respectively, where i, j, k and i_1, j_1, k_1 are unit vectors along axes corresponding to the velocity and fixed systems of coordinates. The positive moment about an axis is considered to be the moment which tends to rotate the flight vehicle in a clockwise direction (if the observations are made from the origin of a moment vector). With the accepted systems of coordinates in Fig. 1.2.1 positive pitching moment, for example, increases the angle of attack and negative moment reduces it.

The magnitude and direction of action of the forces and moments depend on the orientation of the body with respect to the velocity vector $\overline{V}$ (or if the reverse motion is considered it is relative to the direction of oncoming flow $\overline{V}_\infty$) at given flight speed and altitude. This orientation of the body is determined by an angle of attack α—an angle between the axis Ox_1 and the projection of vector $\overline{V}$ in plane x_1Oy_1—and by an angle of side slip β—an angle between vector $\overline{V}$ and the plane x_1Oy_1.

Transformation of the aerodynamic forces and moments from one system of coordinates to the other: Knowing the angles α and β it is possible to transform, with the help of concepts of analytical geometry, the components of force and moment in one system of coordinates to the corresponding components in the other system of coordinates. The components of aerodynamic forces and moments in the fixed system of coordinates, for example, can be changed to the drag and rolling moment in the velocity system of coordinates by the formulas:

$$X=X_1\cos(\widehat{x_1x})+Y_1\cos(\widehat{y_1x})+Z_1\cos(\widehat{z_1x}); \tag{1.2.3}$$

$$M_x=M_{x_1}\cos(\widehat{x_1x})+M_{y_1}\cos(\widehat{y_1x})+M_{z_1}\cos(\widehat{z_1x}), \tag{1.2.3'}$$

where $\cos(\widehat{x_1x})$, $\cos(\widehat{y_1x})$, $\cos(\widehat{z_1x})$ are cosines of angles between the axis Ox and the axes Ox_1, Oy_1, Oz_1, respectively.

TABLE 1.2.1

Fixed system	Velocity system		
	Ox	Oy	Oz
Ox_1	$\cos\alpha\cos\beta$	$\sin\alpha$	$-\cos\alpha\sin\beta$
Oy_1	$-\sin\alpha\cos\beta$	$\cos\alpha$	$\sin\alpha\sin\beta$
Oz_1	$\sin\beta$	0	$\cos\beta$

Similar expressions can be written for the other components of the force and moment vectors. The values of sines and cosines used for the transformation of forces and moments from one system of coordinates to the other are shown in Table 1.2.1.

Using the necessary quantities from Table 1.2.1 in formulas (1.2.3) and (1.2.3′) we get

$$X = X_1 \cos\alpha \cos\beta - Y_1 \sin\alpha \cos\beta + Z_1 \sin\beta; \tag{1.2.4}$$

$$M_x = M_{x_1} \cos\alpha \cos\beta - M_{y_1} \sin\alpha \cos\beta + M_{z_1} \sin\beta. \tag{1.2.4′}$$

For example, in the case of motion of the flight vehicle shown in Fig. 1.2.1, equation (1.2.4) gives

$$-X = -X_1 \cos\alpha \cos\beta - Y_1 \sin\alpha \cos\beta + Z_1 \sin\beta.$$

Similarly the forces and moments can be transformed from the velocity system to the fixed system of coordinates. For example, the data from Table 1.2.1 lead to the following formulas for longitudinal force and rolling moment:

$$X_1 = X \cos\alpha \cos\beta + Y \sin\alpha - Z \cos\alpha \sin\beta; \tag{1.2.5}$$

$$M_{x_1} = M_x \cos\alpha \cos\beta + M_y \sin\alpha - M_z \cos\alpha \sin\beta. \tag{1.2.5′}$$

3. Determination of Aerodynamic Forces and Moments from a Given Distribution of Normal Pressure and Shear Stress. Concept of Aerodynamic Coefficients

Aerodynamic forces, moments and their coefficients: Let us examine the following problems: Assume that the distribution of the normal pressure p and the tangential stress τ are known on the surface of a body in a flow at a given angle of attack and sideslip under given conditions of undisturbed flow parameters (velocity V_∞, static pressure p_∞, density ρ_∞ and temperature T_∞). It is required to find the resultant values of the aerodynamic forces and moments.

The normal force $(p - p_\infty)\, dS$ and the tangential force τdS due to differential pressure and tangential stresses respectively act on an isolated elementary area dS of the body surface. The summation of the projections of these forces on the x axis in the velocity system of coordinates is given by

$$[(p - p_\infty) \cos(\widehat{\overline{P}_n x}) + \tau \cos(\widehat{\overline{P}_\tau x})]\, dS. \tag{1.3.1}$$

The other two projections of these forces on y and z axes can be obtained similarly by appropriate changes in cosines. To get the resultant of the forces it is necessary to integrate (1.3.1) over the complete surface S. Introducing terminology for the pressure coefficient $\bar{p} = (p - p_\infty)/q_\infty$ and the local friction coefficient $c_{fx} = \tau/q_\infty$ in the above relations, where $q_\infty = \rho_\infty V^2_\infty/2$ is the velocity head, we get the following expressions for drag, lift and side forces:

$$X=q_\infty S_0 \int_{(S)} [\bar{p}\cos(\widehat{\bar{P}_n x})+c_{fx}\cos(\widehat{\bar{P}_\tau x})]\frac{dS}{S_0}; \tag{1.3.2}$$

$$Y=q_\infty S_0 \int_{(S)} [\bar{p}\cos(\widehat{\bar{P}_n y})+c_{fx}\cos(\widehat{\bar{P}_\tau y})]\frac{dS}{S_0}; \tag{1.3.3}$$

$$Z=q_\infty S_0 \int_{(S)} [\bar{p}\cos(\widehat{\bar{P}_n z})+c_{fx}\cos(\widehat{\bar{P}_\tau z})]\frac{dS}{S_0}. \tag{1.3.4}$$

The characteristic area S_0 in the above formulas may be replaced by any given surface like the wing plan area, the maximum cross sectional area of the body, etc. The integrals in (1.3.2) to (1.3.4) are nondimensional quantities comprising the effects of types of interaction of a body of a given geometrical form and the distribution of nondimensional pressure coefficients and friction coefficients of aerodynamic forces.

In formula (1.3.2) for the drag force X the nondimensional quantity is usually denoted by c_x. It is called an aerodynamic coefficient of drag. In the remaining two formulas the corresponding notations for nondimensional quantities c_y and c_z are introduced: the first is the coefficient of lift and the second the coefficient of side force. Thus

$$X=c_x q_\infty S_0, \qquad Y=c_y q_\infty S_0, \qquad Z=c_z q_\infty S_0. \tag{1.3.5}$$

The general relations for moments can be obtained in a similar way. For example, consider relations for rolling moment M_x. Obviously the elementary moment dM_x is determined by summing all the moments about the x axis arising out of the forces acting on the elementary surface area dS in a direction perpendicular to the x axis. If the coordinates of an elementary surface area dS are y and z from the x axis then the elementary moment will be

$$dM_x=q_\infty S_0 \{[\bar{p}\cos(\widehat{\bar{P}_n z})+c_{fx}\cos(\widehat{\bar{P}_\tau z})]\, y-[\bar{p}\cos(\widehat{\bar{P}_n y}) + c_{fx}\cos(\widehat{\bar{P}_\tau y})]\, z\}\frac{dS}{S_0}.$$

Integrating this expression over surface S and introducing the nondimensional parameter

$$m_x=\int_{(S)} \{[\bar{p}\cos(\widehat{\bar{P}_n z})+c_{fx}\cos(\widehat{\bar{P}_\tau z})]\, y-[\bar{p}\cos(\widehat{\bar{P}_n y}) + c_{fx}\cos(\widehat{\bar{P}_\tau y})]\, z\}\frac{dS}{S_0 L}, \tag{1.3.6}$$

where L is some characteristic length, we get the formula for total rolling moment,

$$M_x=m_x q_\infty S_0 L. \tag{1.3.7}$$

The parameter m_x is called the aerodynamic coefficient moment.

Similarly the formulas for the other components of moment:

$$M_y = m_y q_\infty S_o L, \qquad M_z = m_z q_\infty S_o L. \tag{1.3.8}$$

The nondimensional parameters m_y and m_z are called the coefficients of pitching and yawing moments respectively.

The corresponding aerodynamic coefficients of forces and moments can also be introduced in the fixed system of coordinates. With the help of these coefficients the forces and moments may be expressed in the following way:

$$\left.\begin{aligned} &X_1 = R = c_{x_1} q_\infty S_o = c_R q_\infty S_o,\ M_{x_1} = m_{x_1} q_\infty S_o L; \\ &Y_1 = N = c_{y_1} q_\infty S_o = c_N q_\infty S_o,\ M_{y_1} = m_{y_1} q_\infty S_o L; \\ &Z_1 = c_{z_1} q_\infty S_o,\ M_{z_1} = m_{z_1} q_\infty S_o L. \end{aligned}\right\} \tag{1.3.9}$$

The quantities c_{x_1} (c_R), c_{y_1} (c_N), c_{z_1} are called the corresponding coefficients of axial (longitudinal), normal and cross forces and the parameters m_{x_1}, m_{y_1}, m_{z_1}, are the coefficients of rolling, pitching and yawing moments. In some cases the above coefficients of moments in the fixed system of coordinates may be represented by

$$c_{m_x} = m_{x_1},\ c_{m_y} = m_{y_1},\ c_{m_z} = m_{z_1}.$$

Typical geometrical dimensions: The absolute values of the aerodynamic coefficients, though they happen to be arbitrary to some extent, depend on the choice of the characteristic geometrical dimensions S_o and L. However, for the sake of convenience in practical calculations the characteristic geometrical sizes are fixed on in advance in some form or other. Usually in rocket technology the area of maximum cross section of cone $S_o = S_m$ and the length of rocket L are taken as the characteristic area and characteristic length respectively.

For the aerodynamic calculations of an airplane system it is customary to use $S_o = S_w$, the wing plan area, and the wing span l (or the chord b) as the characteristic area and characteristic length respectively. The line joining the two farthest points of the wing profile is called the chord of the wing. For rectangular wing plan forms the chord is equal to the width of the wing. Usually in practice we find wings with variable chord distribution along the span. For such wings usually the mean geometric chord $b = b_{av}$ or the mean aerodynamic chord $b = b_{mac}$ are chosen as the characteristic length, where $b_{av} = S_w/l$ and b_{mac} is the chord of the equivalent rectangular wing with the same area and aerodynamic characteristics.

In calculating the forces and moments from the known aerodynamic coefficients one must confine oneself to the geometrical lengths from which these coefficients were derived. If it is desired to carry out calculations on the basis of other geometrical parameters one has to recalculate in advance all the aerodynamic coefficients on the basis of the respective new geometrical parameters.

The condition of constant values of forces and moments acting on one and the same flight vehicle, while using different geometrical lengths, leads to the relations $c_1S_1=c_2S_2$ (for force coefficients) and $m_1S_1L_1=m_2S_2L_2$ (for moment coefficients). Here c_1, c_2 and m_1, m_2 are the force and moment coefficients respectively for two different geometrical parameters S_1, L_1 and S_2, L_2. The respective coefficients c_2 and m_2 recalculated for the new characteristic parameters S_2 and L_2 can therefore be found, since

$$c_2=c_1\,(S_1/S_2), \quad m_2=m_1\,(S_1L_1/S_2L_2),$$

where the earlier dimensions S_1, L_1 and the aerodynamic coefficients c_1, m_1 and also the new dimensions S_2, L_2 are supposed to be known quantities.

Drag polar of an aircraft: Let us examine the so-called drag polar of a flight vehicle as a practical example of use of the aerodynamic coefficients. It relates lift force to drag or the lift coefficient to the drag coefficients in the velocity system of coordinates. This curve, known as the drag polar of the first type (Fig. 1.3.1, c), represents the geometrical position of the vectors of total aerodynamic force $\bar{F}$ acting on a flight vehicle at various angles of attack (or the vector coefficient c_F for this force obtained from the relation $c_F=F/S_0q_\infty$).

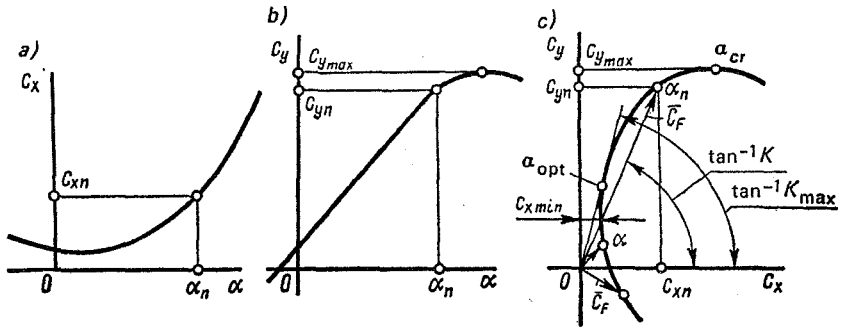

Fig. 1.3.1. Construction of drag polar of first type for flight apparatus:
a—graph of function $c_x=c_x(\alpha)$; *b*—graph of function $c_y=c_y(\alpha)$; *c*—drag polar of first type.

The drag polar of the first type can be constructed from the graphs $c_x=c_x(\alpha)$ and $c_y=c_y(\alpha)$ in such a way that the values of the drag and lift coefficients c_x and c_y are plotted along abscissa and ordinate respectively. Thus each point of this curve corresponds to a particular value of the angle of attack as a parameter of the drag polar. Therefore the indication of angles of attack is shown on the curve $c_y=f(c_x)$.

The drag polar of the first type is convenient in practice as it easily determines, for any angle of attack, an important characteristic of the *aerodynamic efficiency factor.*

$$K = c_y/c_x = Y/X. \tag{1.3.10}$$

If the scales for $c_y(Y)$ and $c_x(X)$ are the same K is equal to the tangent of the angle of inclination between the abscissa and the vector drawn from the origin of the coordinates to the point on the drag polar diagram corresponding to the given angle of attack.

From the drag polar it is possible to determine the *optimum angle of attack* α_{opt} for the maximum value of the Y/X ratio

$$K_{max} = \tan \alpha_{opt}, \tag{1.3.10'}$$

if the tangent is drawn from the origin to the drag polar curve.

The point $c_{y\,max}$ on a drag polar curve indicates the maximum lift that can be achieved at critical angle of attack α_{cr}.

It is possible to find the point on the drag polar curve showing minimum drag coefficient $c_{x\,min}$ and the respective values of angle of attack and lift coefficient.

The drag polar is symmetrical about abscissa if the flight vehicle is symmetrical about the horizontal axis. For such a flight vehicle the value of $c_{x\,min}$ occurs at zero lift $c_y = 0$.

The drag polar of the second type is also used in place of the above. This drag polar is connected with the fixed system of coordinates. The coefficients of axial force c_R and of normal force c_N are plotted along the abscissa and ordinates of this drag polar respectively (Fig. 1.3.2). This curve is used, in particular, in strength calculations for flight vehicles.

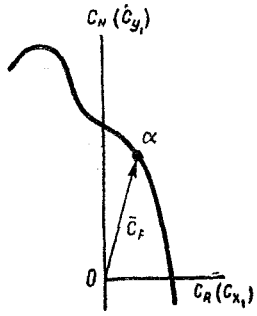

Fig. 1.3.2. Drag polar of second type.

Theoretical and experimental investigations show that in most cases the aerodynamic coefficients for the given body shape and angle of attack depend on such nondimensional parameters as the Mach number $\mathbf{M}_\infty = V_\infty/a_\infty$ & Reynolds number $\mathbf{Re}_\infty = V_\infty L \rho_\infty/\mu_\infty$. Here a_∞ is the speed of sound in an undisturbed flow; ρ_∞ and μ_∞ are the corresponding density and coefficient of dynamic viscosity of gas; L is the length of the body. Therefore many drag polar curves exist for each flight vehicle. For example, it is possible to draw a family of curves for the given Reynolds number $\mathbf{Re}_\infty$. Each one of these curves corresponds to its own value of velocity $\mathbf{M}_\infty$. The curves on Figs. 1.3.1 and 1.3.2 correspond to the fixed value of $\mathbf{Re}_\infty$ and determine the relation of c_y and c_x in a case where flight takes place at low speeds (of the order of 100 m/sec) at which the aerodynamic coefficients are independent of $\mathbf{M}_\infty$.

Center of pressure and aerodynamic center: The point of action of the resultant of distributed aerodynamic forces is called the *center of pressure of the aircraft*. It represents some conditional point because the interaction of

a fluid medium in reality does not lead to a concentrated force but to forces distributed over the surface of a moving body. Usually it is understood that this conditional point lies on one of the main axes of the body, for example the longitudinal axis of the aircraft passing through its c.g., the axis of symmetry of the rotating body or chord of the wing profile.

The position of the center of pressure is usually determined by the coordinate $x_{c.p}$ measured from the nose of the body in a fluid flow. If the moment M_z about this point and the normal force N (Fig. 1.3.3, a) are known the coordinate of the center of pressure is given as

$$x_{c.p} = -M_z/N. \tag{1.3.11}$$

If the moment M_z tending to decrease the angle of attack is considered negative (see Fig. 1.3.3, a) the coordinate $x_{c.p}$ is positive. Keeping in mind that

$$M_z = m_z q_\infty S_0 b \quad \text{and} \quad N = c_N q_\infty S_0,$$

we have

$$x_{c.p} = -m_z b/c_N,$$

and hence

$$x_{c.p}/b = c_{c.p} = -m_z/c_N. \tag{1.3.11'}$$

The nondimensional value of $x_{c.p}$, determined as the ratio of the distance of the center of pressure from the nose to the characteristic length of body (in this case, to the wing chord b), is called the coefficient of the center of pressure. At low angles of attack when the coefficients of lift and normal force are approximately equal ($c_y \approx c_N$) we get

$$c_{c.p} = -m_z/c_y. \tag{1.3.12}$$

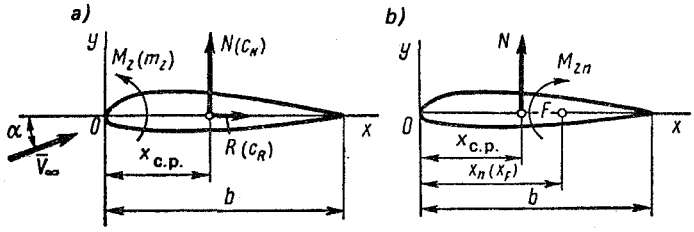

Fig. 1.3.3. Determination of center of pressure (*a*) and aerodynamic center (*b*).

The center of pressure, as seen from Fig. 1.3.4, changes its position with the change in angle of attack. This effect is significant at low angles of attack. In such conditions the coefficient $c_{c.p}$ of a cambered profile increases considerably with a decrease in α and becomes infinitely high at the angle of attack corresponding to zero lift. This directly follows from the formula (1.3.12) in which at $c_y \to 0$ the coefficient of moment m_z can have some finite value $m_z = m_{z0}$.

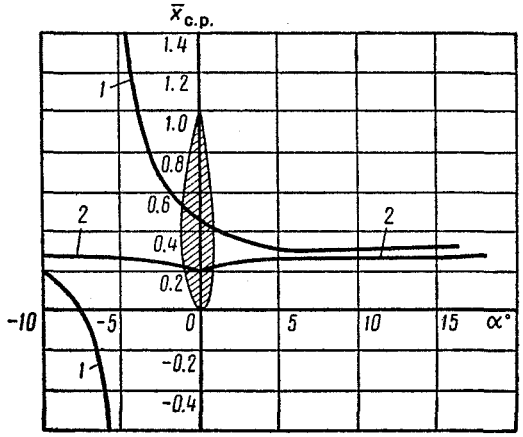

Fig. 1.3.4. Variation in coefficient of center of pressure as a function of angle of attack:
1—cambered profile; *2*—symmetrical profile.

The position of the center of pressure of both types of profiles (cambered and symmetrical), as shown in Fig. 1.3.4, is roughly constant in a fairly large range of angles of attack (from 5 to 20°).

The values of c_y and m_z are simultaneously zero at $\alpha \to 0$ for a symmetrical airfoil. The following expressions

$$c_y = (\partial c_y/\partial a)\, a, \quad m_z = (\partial m_z/\partial a)\, a \tag{1.3.13}$$

are valid at low angles of attack (here the derivatives $\partial c_y/\partial a$ and $\partial m_z/\partial a$ are constant values which may be obtained at about a zero angle of attack $a \approx 0$) and the coefficient $c_{c.p}$ will be equal to some constant value

$$c_{c.p} = -\frac{\partial m_z/\partial a}{\partial c_y/\partial a},$$

or

$$c_{c.p} = -\partial m_z/\partial c_y. \tag{1.3.14}$$

For flight machines not having horizontal symmetry the flight parameters can be easily understood from the position of the aerodynamic center and not from the position of the center of pressure. To understand the meaning of this take an unsymmetrical profile and calculate moment M_{zn} about an arbitrary point F with coordinate x_n lying on the chord of this profile. It is directly seen from Fig. 1.3.3, b that

$$M_{zn} = N\,(x_n - x_{c.p}),$$

or, since

$$-N \cdot x_{c.p} = M_z \text{ about leading edge point } O,$$

we get

$$M_{zn}=Nx_n+M_z.$$

Keeping in mind the concepts of aerodynamic coefficients and assuming small angles of attack for which $c_N\approx c_y$, we get

$$m_{zn}=c_y\,(x_n/b)+m_z. \tag{1.3.15}$$

The relation $m_z=f(c_y)$ assumes a linear form at small angles of attack (Fig. 1.3.5), i.e.

$$m_z=m_{z0}+(\partial m_z/\partial c_y)\,c_y. \tag{1.3.16}$$

Then

$$m_{zn}=c_y\,(x_n/b)+m_{z0}+(\partial m_z/\partial c_y)\,c_y,$$

or

$$m_{zn}=m_{z0}+c_y\,(\partial m_z/\partial c_y+x_n/b), \tag{1.3.17}$$

where m_{z0} is the coefficient of moment about the leading edge point at $c_y=0$.

The second term in (1.3.17) determines the variation in that part of the moment that is connected with the variation in lift coefficient. If a point F on the chord is selected so that the coordinate $x_n=x_F$ is obtained from the condition (see Fig. 1.3.3, b)

$$x_n/b=x_F/b=\bar{x}_F=-\partial m_z/\partial c_y, \tag{1.3.18}$$

then the coefficient of moment about this point will not depend on c_y and at all (small) angles of attack it will have a constant value. This point is called the aerodynamic center or simply the focus of a given body. Obviously the aerodynamic center represents the point of action of all uniformly distributed forces due to the angle of attack.

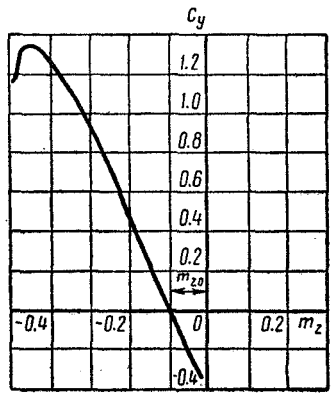

Fig. 1.3.5. Dependence of moment coefficient on coefficient of lift for unsymmetrical configuration of flight vehicle.

The relation between the center of pressure and the aerodynamic center is given by

$$c_{c\cdot p}=-\frac{m_z}{c_y}=-\frac{m_{z0}+(\partial m_z/\partial c_y)\,c_y}{c_y}$$
$$=c_{c\cdot p0}+\bar{x}_F, \tag{1.3.19}$$

where

$$c_{c\cdot p0}=-m_{z0}/c_y.$$

For symmetrical profiles $m_{z0}=0$ and consequently the center of pressure coincides with the aerodynamic center.

Static stability: A chance disturbance (initial throb on starting, a gust of wind, a change in engine functioning from the previous condition, etc.) may change the angles of attack and yaw for a body in motion. After the disturbance disappears the moment arising as a result of this leads to further variations in those angles. If during the subsequent motion the changes in the angles α and β tend to the initial values the flight will be *statically stable*. If the deviation continues to increase the flight will be *statically unstable.*

Static stability of a flight vehicle is subdivided into longitudinal, directional and lateral static stability.

In the case of *longitudinal static stability* the general longitudinal moment will be stabilized, i.e. will tend to bring back the angle of attack to its initial value. In this case the direction of change of moment M_z (and the corresponding coefficient m_z) is against the direction of change of the angle α. Thus the condition of longitudinal static stability can be expressed by the inequality $\partial M_z/\partial\alpha<0$ or $\partial m_z/\partial\alpha=m_z^\alpha<0$.

A *positive destabilizing moment* which, if it exists, tends to increase the angle of attack is responsible for longitudinal static instability. Therefore the condition of *longitudinal static instability* will be given by the inequality $\partial M_z/\partial\alpha>0$, i.e. $\partial m_z/\partial\alpha=m_z^\alpha>0$.

Static directional stability is characterized by the inequality $\partial M_y/\partial\beta<0$ or $\partial m_y/\partial\beta=m_y^\beta<0$; *static directional instability* by the inequality $\partial M_y/\partial\beta>0$ or $\partial m_y/\partial\beta=m_y^\beta>0$. In the first case the directions of changes of yawing moment and the angle of yaw are different and in the second case they are equal. Consequently the yawing moments will be stabilizing and destabilizing in the first and the second case respectively.

Lateral static stability (or static stability in bank) is represented by the derivative $\partial M_x/\partial\beta$ or $\partial m_x/\partial\beta=m_x^\beta$. If the derivative $m_x^\beta<0$ the flight apparatus has lateral static stability. If $m_x^\beta>0$ it has *lateral static instability.*

The flight apparatus is neutral in the sense of longitudinal, directional and lateral static stability if it has the properties of $m_z^\alpha=0$, $m_y^\beta=0$, $m_x^\beta=0$ respectively.

Use of the concepts of the coefficient of center of pressure and the aerodynamic center in evaluation of longitudinal static stability: The distance between the center of pressure $x_{c.p}$ and the center of gravity $x_{c.g}$, i.e. the difference $x_{c.p}-x_{c.g}$, or in nondimensional form

$$(x_{c.p}/b)-(x_{c.g}/b)=c_{c.p}-\bar{x}_{c.g},$$

can be taken as the criterion for longitudinal static stability of a flight vehicle. If the coefficient of center of pressure $c_{c.p}$ is more than the relative value of the coordinate of the center of gravity $x_{c.g}$, i.e. if the center of pressure lies behind the center of gravity, then the flight will be *statically*

stable. If the center of pressure is in a forward position (the difference $c_{c.p}-\bar{x}_{c.g}$ being negative) there exists static longitudinal instability. The criterion $c_{c.p}-\bar{x}_{c.g}$ is called the static stability margin. It can be positive, negative or equal to zero depending on static longitudinal instability or neutral longitudinal stability respectively.

The concept of the aerodynamic center is used for evaluation of the static stability of unsymmetrical machines or symmetrical flight machines with controls deflected. The coordinate of this point is determined by the formula (1.3.18). Then, assuming the value of x_n equal to the coordinate of center of gravity $x_{c.g}$ in (1.3.17), we get

$$m_{zc.g}=m_{z0}+c_y\,[(-x_F/b)+(x_{c.g}/b)],$$

from which

$$m_{zc.g}-m_{z0}=-(\bar{x}_F-\bar{x}_{c.g})\,c_y. \tag{1.3.20}$$

Differentiating (1.3.20) with respect to c_y, we obtain

$$\partial m_{zc.g}/\partial c_y=-(\bar{x}_F-\bar{x}_{c.g}). \tag{1.3.21}$$

This shows that longitudinal static stability depends on the position of the aerodynamic center relating to the center of gravity of the flight vehicle. For a rearward position of the aerodynamic center with respect to the center of gravity (the difference $\bar{x}_F-\bar{x}_{c.g}$ being positive) the derivative $\partial m_z/\partial c_y<0$ and the flight will be statically stable. On the other hand if the aerodynamic center is ahead of the center of gravity (the difference $\bar{x}_F-\bar{x}_{c.g}$ being negative), then $\partial m_z/\partial c_y>0$ and consequently the flight will be statically unstable.

4. Basic Properties of High-Speed Gas Flow

4.1 Compressibility of gas

One of the important properties of gas is its compressibility, i.e. the capacity to change density under the action of pressure. All the processes connected with a gas flow are characterized by variation in pressure and, consequently, to some extent by the effect of compressibility on these processes. Research has shown that the variations in density arising out of small changes in pressure are insignificant at low speeds and hence the compressibility effect can be neglected. The equations of hydrodynamics for the study of the laws of motion in an incompressible flow may be considered valid in pursuing investigations on a body in a fluid at low speeds.

In practice the effect of compressibility can be neglected at speeds of air flow ranging from a few meters per second through 100 to 150 meters per second. This range of speeds, in actual conditions, corresponds to the Mach

numbers from $\mathbf{M}_\infty = V_\infty/a_\infty \approx 0$ to $\mathbf{M}_\infty = 0.3$ to 0.45 (a_∞ is the speed of sound in an undisturbed flow). This idealization of the flow processes assumes that in the given range of speeds the Mach number is taken to be zero because the small disturbances (sonic vibrations) in an incompressible medium propagate at an infinitely high speed and hence the ratio of the flight speed to the sound speed tends to zero.

Modern flight vehicles fly at high speeds for which the flow-interaction is associated with a significant change in pressure and hence there exist considerable variations in density and temperature. In high-speed flight conditions it is necessary to take into account the compressibility effect on the flow-interaction with the body as it may be quite appreciable. The compressibility effect of a gas on the aerodynamic characteristics of a body at high speed is one of the important features of high-speed aerodynamics.

4.2 Heating of gas

The rise in flight speeds resulted in the need to investigate the special characteristics of gas flows in aerodynamic research. These characteristics are connected with the physico-chemical properties of air. Compressibility is taken as the most important characteristic of high-speed gas flows in "usual" supersonic aerodynamics; the effect of high temperatures on thermodynamic parameters, the kinetic coefficients of air and the physico-chemical processes occurring in it are neglected. On the other hand at very high (hypersonic) speeds the properties of air related to the effects of high temperatures are given first place.

The high temperature appears as a result of stagnation of a gas flow during which the systematic undisturbed flow of gas particles changes to a chaotic motion of the molecules. The kinetic energy of a uniform undisturbed flow is transformed into internal energy of the gas.

The excitation of the vibrational modes of the internal energy of the molecules of oxygen and nitrogen in air begins to play an important role at a temperature of about 1,500°K. The free vibrational modes of oxygen molecules are found to be completely excited at a temperature of about 3,000°K and pressure of 1 atmosphere. A further increase in temperature makes the atoms break their intra-molecular bonds as a result of which, for example, a diatomic molecule breaks into two separate bonds. This process is known as dissociation. Along with dissociation there occurs the phenomenon of recombination, i.e. formation of a new molecule during the collision of two atoms ($O_2 \rightleftharpoons 2O$). This reaction is accompanied by the generation of heat which encourages the collision of the two atoms with a third particle, which carries with it a part of the energy generated and thus helps to create a more stable molecule. Besides this, the chemical reactions taking place in air result in the formation of a certain quantity of nitrogen oxide NO. Further heating leads to the formation of atomized nitrogen and oxygen and the

dissociation takes place according to the equations

$$N_2+O_2 \rightleftarrows 2NO, \quad N_2+O \rightleftarrows NO+N \quad \text{or} \quad N+O_2 \rightleftarrows NO+O.$$

The molecules of oxygen are almost completely dissociated at temperatures of the order of 5,000–6,000°K and pressure of 1 atmosphere. In addition the dissociation of a major part of the nitrogen along with the recombination of atoms in molecules takes place at such temperatures. This process continues according to the equation $N_2 \rightleftarrows 2N$. The degree of dissociation is determined by the intensity of dissociation, which is equal to the ratio of the number of air particles breaking up during dissociation to the total number of molecules. The degree of dissociation depends on the temperature and pressure.

The intensity of dissociation increases with a rise in temperature because the speed and energy of the moving molecules increases with the temperature. This enhances the probability of their collision and disintegration. During this process the rate of dissociation increases with any reduction in pressure (density) as a result of the decrease in the probability of triple collisions of particles leading to the formation of molecules out of atoms. For example, oxygen starts dissociating at $T=2{,}000$°K if the pressure is equal to 0.001 atmosphere but at normal atmospheric pressure the dissociation of O_2 begins at $T=3{,}000$°K. The temperature at which the dissociation of nitrogen starts has a tendency to fall from 6,000°K at a pressure of 1 atmosphere to 4,000°K at a pressure of 0.001 atmosphere.

One more process begins at temperatures of 5,000–6,000°K as a result of the excitation of electrons due to the large energy flow, which induces the separation of electrons from the atoms of nitrogen and oxygen and also from the molecules of nitrogen oxide. This process is called ionization. Primarily it takes place as a result of the collision of air particles during movements in a heated condition. Hence this kind of ionization is called thermo-ionization. The process of ionization takes place more intensively with a rise in temperature and it is naturally associated with an increase in the concentration of free electrons. The intensiveness of this process is characterized by the degree of ionization, which is equal to the ratio of ionized atoms (molecules) to their total number. Experiments have shown that nitrogen, for example, is fully thermodynamically ionized (degree of ionization is one) at a temperature of 17,000°K and pressure of 1 atmosphere.

Variation of specific heats: At high enough temperatures the heat added to air is dissipated not only in terms of an increase in the energy of irrotational and rotational flows of molecules but also in some other processes. These processes are the rise in the vibrational energy of atoms and molecules, the work done to overcome the forces of interactions between the atoms during dissociation of molecules and the separation of electrons from atoms

during ionization. As a result the specific heats increase.

The change in the specific heats of air is determined by its temperature until dissociation sets in. For an approximate estimate of the effect of temperature on specific heat at constant pressure the formula

$$c_p/c_{p\infty}=(T/T_\infty)^\varphi \tag{1.4.1}$$

is used, where φ in its turn depends on temperature (Fig. 1.4.1). For $T>1{,}000$°K this index may be assumed constant and equal to 0.1. At $T_\infty=288$°K the specific heat $c_{p\infty}=0.24$ k·cal/kg·degree (in the SI system it is 1,000 J/kg·degree). Formula (1.4.1) is applicable up to $T=2{,}000$ to 2,500°K, during which the intensity of free vibration reaches the state of excitation.

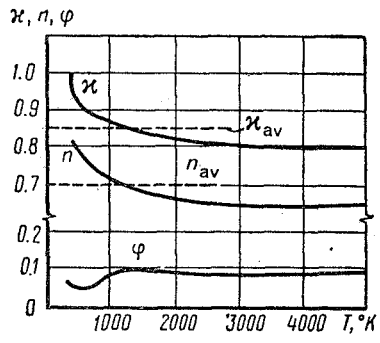

Fig. 1.4.1. Variation of indices φ, n, κ in respective formulas for determination of specific heats, coefficient of dynamic viscosity and coefficient of heat transfer.

In the first phase of dissociation the specific heat depends not only on temperature but also on pressure. The calculations of specific heats and also of the ratio of specific heats $k=c_p/c_v$ under conditions of thermodynamic equilibrium at high temperatures were carried out on electronic computers by a group of Soviet scientists under the guidance of the member of the Soviet Academy of Sciences, Prof. A.S. Pryedvodityelyev [17], [18]. These calculations were conducted for the temperature range from 1,000 through 6,000°K without consideration of ionization since its effect in this interval of temperatures is infinitesimally small. At very high temperatures the effect of simple ionization in equilibrium was considered. This was assumed to be complete at $T=12{,}000$°K and pressure $p=0.001$ atmosphere.

The data of $k=c_p/c_v$ at temperatures up to 2,000°K and pressures of 1 atmosphere or more are governed by temperature and are practically independent of pressure. The curves drawn from the data of works [17] and [18] characterizing the variation of c_p and k at high temperatures are given in Figs. 1.4.2 and 1.4.3 [7].

Kinetic coefficients: The processes of friction and heat transfer occurring in a viscous heat-conducting gas depend on the kinetic coefficients of the gas, such as the coefficients of dynamic viscosity μ and heat conductivity λ. It is found that in the absence of dissociation the coefficient μ depends on temperature only and can be determined by the formula

$$\mu/\mu_\infty=(T/T_\infty)^n, \tag{1.4.2}$$

where index n depends on temperature (see Fig. 1.4.1). In approximate calculations the average value of $n_{av}\approx 0.7$ can be used for quite a wide range of

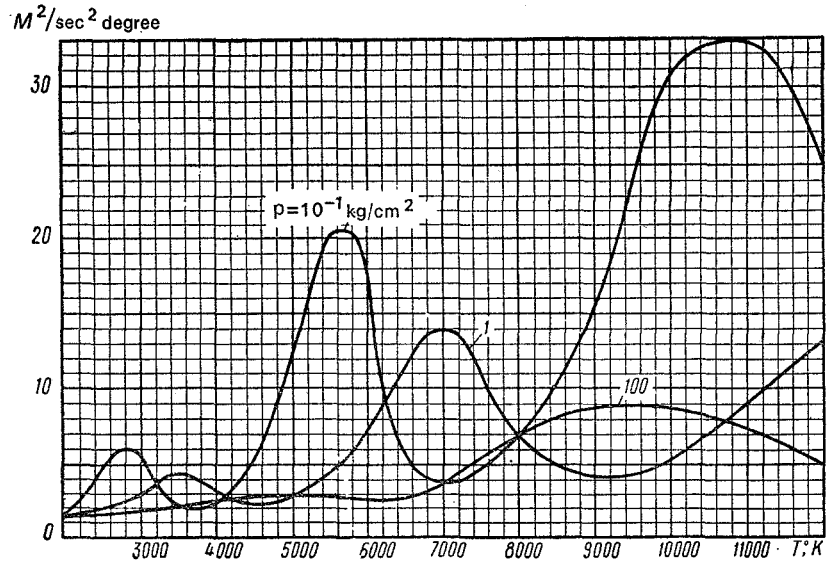

Fig. 1.4.2. Variation of specific heat c_p of air at high temperatures.

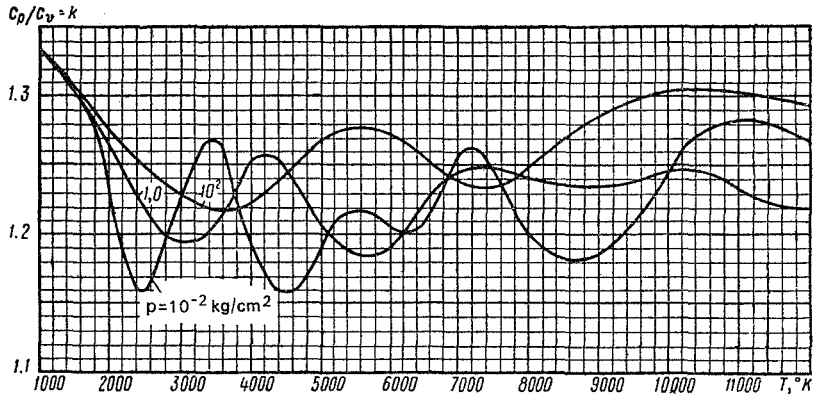

Fig. 1.4.3. Variation of ratio of specific heats at constant pressure and volume ($k=c_p/c_v$) for air at high temperatures.

temperatures where the initial value of μ may be assumed to be $\mu_\infty = 1.82 \times 10^{-6}$ kg·sec/m² (1.79×10^{-5} N·sec/m²) at $T_\infty = 288°$K. Formula (1.4.2) is applicable up to temperatures of the order of 2,000 through 2,500°K. With the rise in temperature the error in this formula increases significantly. Experiments show that at high temperatures up to 9,000°K the coefficient of dynamic viscosity of air under a steady state of dissociation can be estimated within an accuracy of 10% by Sutherland's formula

$$\frac{\mu}{\mu_\infty}=\left(\frac{T}{T_\infty}\right)^{\frac{1}{2}}\frac{1+(111/T_\infty)}{1+(111/T)}. \tag{1.4.3}$$

At temperatures less then 1,500°K this formula gives somewhat better results than (1.4.2).

More accurate calculations proved that the coefficient of dynamic viscosity at high temperatures also depends on pressure. Fig. 1.4.4 shows the graph [7] characterizing the variation in coefficient μ at temperatures up to 12,000°K in the pressure range from 0.01 through 100 atmospheres.

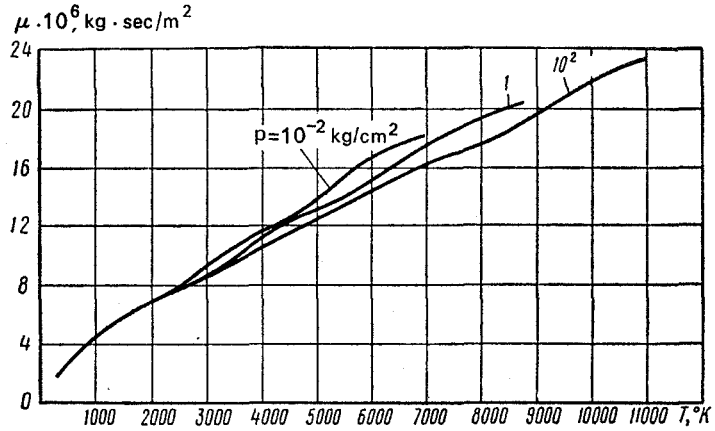

Fig. 1.4.4. Variation of coefficient of dynamic viscosity of air at high temperatures.

Heat conductivity, in the same way as viscosity, does not depend on pressure at temperatures up to about 2,000°K and can be estimated by the formula

$$\lambda/\lambda_\infty=(T/T_\infty)^\kappa, \tag{1.4.4}$$

where the index κ in its turn depends on temperature, as seen from Fig. 1.4.1. The average values $\kappa_{av}=0.85$ and $\lambda_\infty=5.53\times10^{-3}$ k·cal/m·sec·degree (23.2 watt/m·degree) at $T_\infty=261$°K may be assumed for approximate calculations. The relation of the coefficient of heat conductivity to the temperature and pressure is typical for dissociating air. The corresponding diagram is given in Fig. 1.4.5.

The existence of viscous forces, like the process of heat conductivity in gas, is connected with the molecular structure of the substance. During their movements the gas molecules transfer energy and momentum from one place to another. The result of the change of momentum is the viscous force and the transfer of energy leads to the process of heat transfer. From this discussion it is clear that the coefficients of heat conductivity and the dynamic viscosity in gas increase with an increase in temperature. At the inception of dissociation the nature of variation of λ and μ will be very complicated. Their

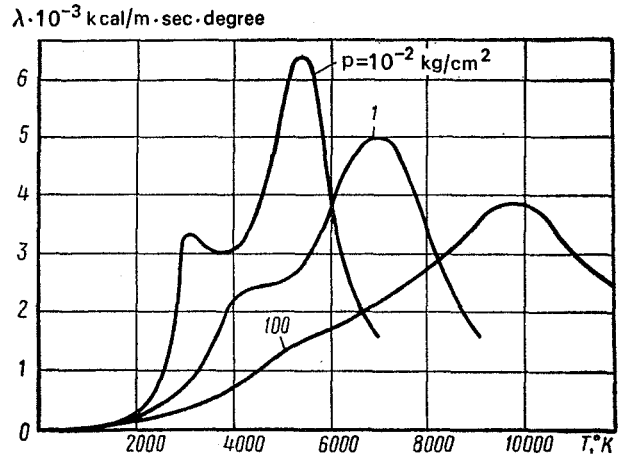

Fig. 1.4.5. Variation of coefficient of heat conductivity of air at high temperatures.

values diminish at a low degree of dissociation, which is called for by the losses in internal energy during the process of breaking of molecular bonds and the consequent reduction in the temperature of the gas. With a rise in the degree of dissociation the more intensive breaking up of molecules into atoms leads to an increase in the number of particles that take part in transferring energy and momentum, and thereby elevates the kinetic coefficients.

4.3 Condition of air at high temperatures

Equation of state: Experiments on the interaction between an air flow and a body showed that the relations of conventional aerodynamics are quite reliable as long as the air remains comparatively "cold." These relations assume constant thermodynamic characteristics and constant physico-chemical structures. "Cold" air is confined within the limits of the hypothesis of constant specific heats and the possibility of applying the thermal equation of state for a perfect gas:

$$p=R\rho T \quad \text{or} \quad p=R_0\rho T/(\mu_{av})_0, \tag{1.4.5}$$

where R and R_0 are absolute and universal gas constants respectively ($R_0=848$ kg·m/mol· degree); ρ and T are density and temperature; $(\mu_{av})_0$ is the average molecular weight of air with constant ingredients; $(\mu_{av})_0$ is constant.

Any gas satisfying equation (1.4.5) is called thermodynamically perfect. The calorical equation of state $i=pc_p/\rho R$ which determines the enthalpy of a gas corresponds to equation (1.4.5). If $c_p/R=k/(k-1)$ is assumed this equation is transformed to

$$i=\frac{k}{k-1}\cdot\frac{p}{\rho}\cdot \tag{1.4.6}$$

The gas is called calorically perfect if its state is defined by equation (1.4.6) following the condition that c_p and c_v are constant and independent of temperature.

It should be borne in mind that the necessity of considering the variation of specific heats with temperature comes into the picture before the equation of state is applied, this being different from that for a perfect gas. For example, the variation of specific heats with temperature, as shown by calculations, begins at the Mach number of undisturbed flow $\mathbf{M}_\infty=3$ through 4

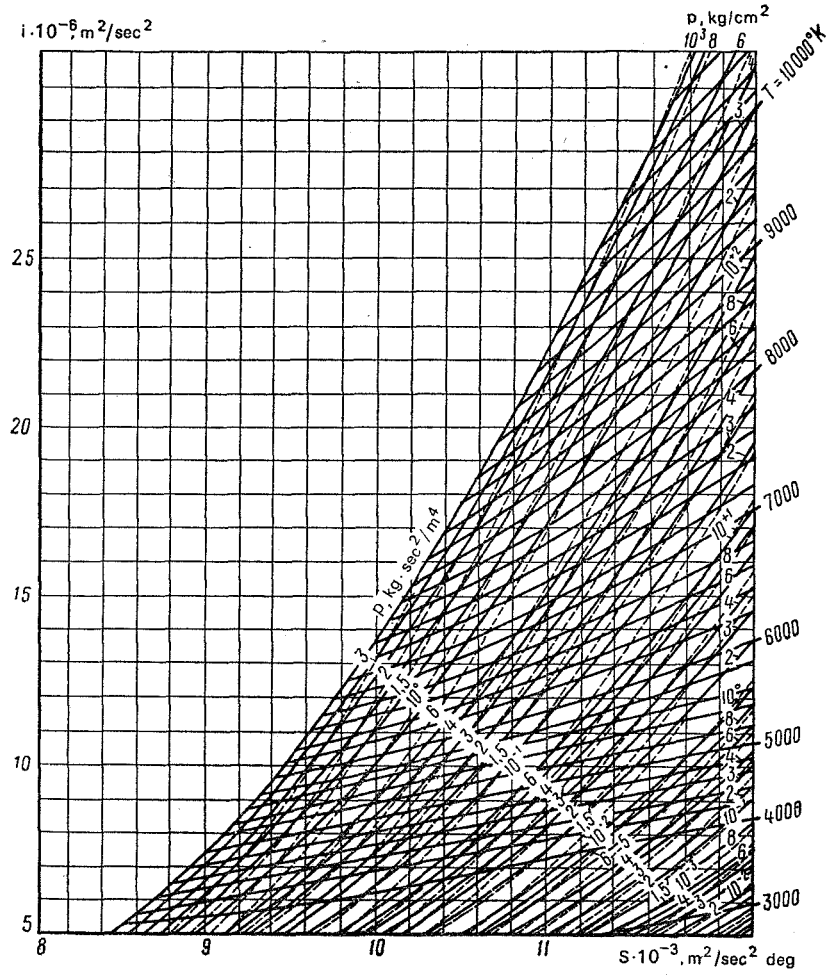

Fig. 1.4.6. i–S diagram for dissociating air.

during motion across a normal shock wave. At $\mathbf{M}_\infty = 6$ through 7 the equation of state for a perfect gas and also the equation of sound speed

$$a^2 = kRT, \tag{1.4.7}$$

are valid because the components of the heated gas behind the shock wave remain unchanged.

Thus a gas is calorically not perfect in this case but it will have the properties of a thermally perfect gas.

For a gas with varying heat coefficients the calorical equation of state (1.4.6) gives large errors. The actual relation between the enthalpy and temperature is determined by the more complicated function $f_1(T)$ in place of (1.4.6).

The equation

$$p = (R_0/\mu_{av})\,\rho T, \tag{1.4.8}$$

where $\mu_{av} = f_2(p, T)$ is valid for dissociating air having specific heats and molecular weight as the functions of its state.

The calorical equation of a dissociating gas medium also has a more complicated nature; in general it can be expressed by $i = f_3(p, T)$. Such a medium does not have the properties of a perfect gas for which an enthalpy depends only on temperature.

The nature of thermal and calorical equations of state for a dissociating (real) gas, not following equation (1.4.5), is still more complicated. This is because these equations also take into account the forces of interaction between molecules and the volume of the molecules themselves. These equations can be solved by numerical methods with the help of electronic digital computers and are usually expressed in the form of tables and diagrams of state.

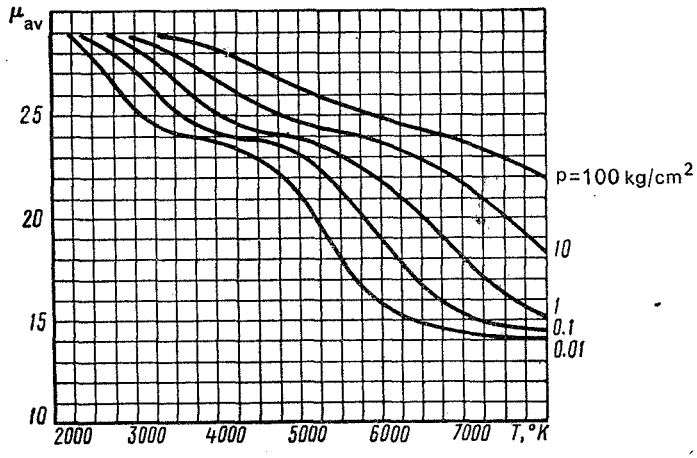

Fig. 1.4.7. Average molecular weight of air at high temperatures.

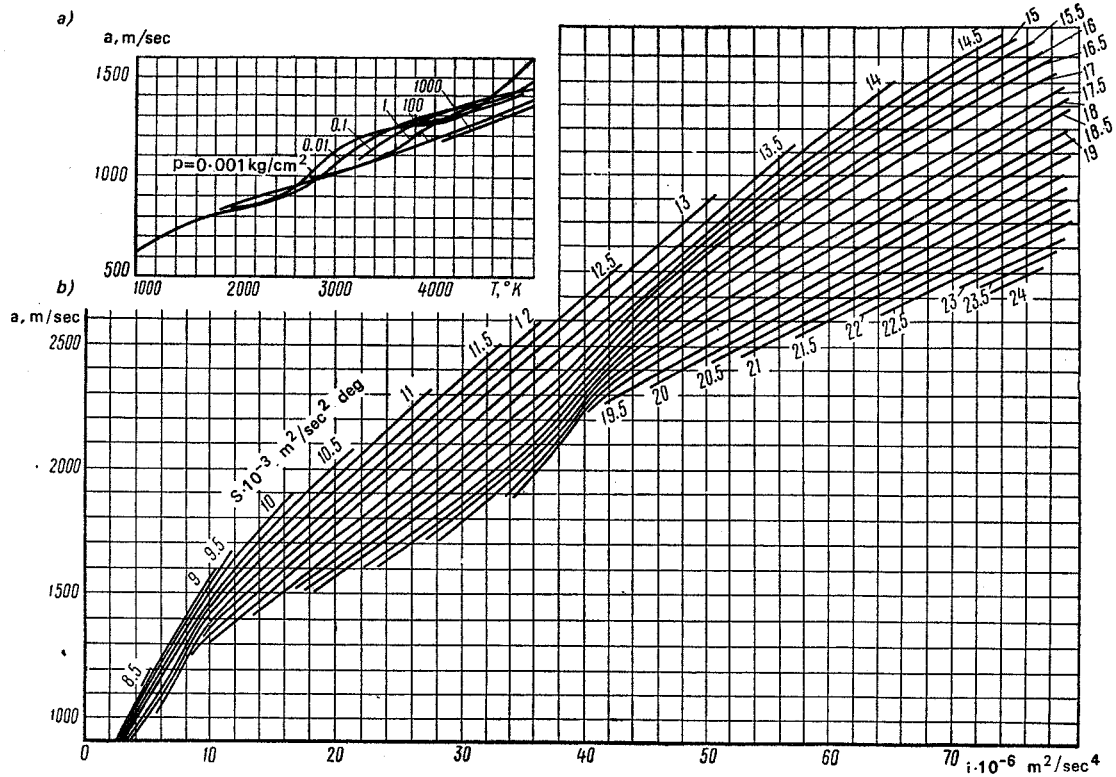

Fig. 1.4.8. Dependence of sound velocity in air at high temperatures:
a—on temperature and pressure; *b*—on enthalpy and entropy.

The results of the calculations of parameters for the state of air under thermodynamic equilibrium at high temperatures and under pressures of 0.001 through 1,000 atmospheres are given in the works [17], [18]. On the basis of these results the atlas of diagrams of state was composed by a group of scientists [7]. The famous i–S diagram (diagram of enthalpy-entropy) of dissociating air for heat calculations in aerodynamics is reproduced in Fig. 1.4.6. In this diagram, showing the calorical equation of state in graphic form, the curves of $p=\text{const}$ (isobars), $T=\text{const}$ (isothermal) and $\rho=\text{const}$ (isochor—dotted lines) are drawn.

In some cases the diagram of calorical state expressed by the relation of i–p with the curves of $T=\text{const}$, $\rho=\text{const}$ and $S=\text{const}$ may be more convenient for calculations. This diagram, prepared on the basis of data from the i–S diagram, is to be found in work [7]. In the same work there are diagrams of different variants graphically representing thermal equations of state.

These graphs, helpful in determining an average molecular weight μ_{av} for dissociating and ionizing air (Fig. 1.4.7) and also the speed of sound (Fig. 1.4.8) as a function of p and T [18] or i and S [7], are important for practical calculations. In studying these graphs it may be noted that the speed of sound changes considerably with temperature and to a lesser extent with pressure. This is explained by the insignificant effect of the composition of air on the nature of the propagation of small disturbances. At the same time any change in the constituents of air during its dissociation considerably affects its molecular weight, which has its own expression in the powerful effects of pressure on the value of μ_{av}. The three characteristics of the section on reduction in μ_{av} depending on temperature may be noted from the curves plotted in Fig. 1.4.7. The first of them is decided by dissociation of oxygen, the second by dissociation of nitrogen and the third by ionization of air components.

5. Basic Relations for a Diatomic Dissociating Gas

5.1 Degree of dissociation

Almost always the working medium in aerodynamics is a mixture of gases. Such a mixture in itself is a homogeneous system if the values of all parameters at all points of the system are equal under conditions of thermodynamic equilibrium. At the same time this mixture is not a simple system if the mass components of the different gases, in addition to the usual parameters of state of gas, are taken into account.

The mixture of gases can be taken as a simple perfect gas if its components are inert gases and will not react among themselves. Air under normal atmospheric conditions is such a mixture of N_2 and O_2 with some admixture of Ar, CO_2, etc.

At high temperatures air behaves as a reacting mixture because the

diatomic gases become dissociated and atoms so formed take part in recombination. To simplify each project in terms of models of working medium air is assumed to be a mixture of dissociating components N_2 and O_2, not reacting with one another. Then each component is assumed to be some conditional diatomic gas consisting of symmetrical molecules of the same type which dissociate into two atoms as a result of double collisions. The atoms can also recombine into molecules by triple collisions. This system helps in the study of the mechanism of dissociation of pure dissociating diatomic gas ([46], 1957, No.1). The dissociation is assumed to be uniform. This indicates that during chemical reactions determined, for example by the simple equation for the binary process,

$$A_2 \underset{r_R}{\overset{r_D}{\rightleftarrows}} A+A, \tag{1.5.1}$$

the rates of reaction from left to right r_D and right to left r_R (corresponding to the rate of dissociation and recombination) are equal.

Investigations of all flows of dissociating medium are connected with the definition of degree of uniform dissociation α. In chemical thermodynamics its value for pure dissociating diatomic gas is given by the relation

$$\alpha^2/(1-\alpha)=(\rho_d/\rho)\, e^{-T_d/T}. \tag{1.5.2}$$

An interpretation of this equation is found in the work ([44], 1957, No.5).

In equation (1.5.2) the degree of dissociation α is found by the expression

$$\alpha=n_A/(n_A+2n_{A_2}), \tag{1.5.2'}$$

where n_A is the number of atoms of element A in a given volume;

n_{A_2} is the number of molecules of gas A_2 in the same volume.

In equation (1.5.2) the quantities ρ_d, T_d represent characteristic density and temperature of dissociation respectively. The characteristic temperature T_d is determined by the ratio D/k, where D is the energy of dissociation of one molecule of A_2; k is the gas constant for a single molecule (Boltzmann's constant). Calculations show that the value of T_d does not depend on the temperature of the gas. It is equal to 59,000 and 113,000°K for oxygen and nitrogen respectively. The characteristic density of dissociation in general depends on the temperature of the gas. However, the variation of ρ_d in the range of temperatures from 1,000°K through 7,000°K for oxygen as well as nitrogen is very small compared to the very high changes in the values of $e^{-T_d/T}$ in the same range. Therefore it is in practice accepted that the characteristic density ρ_d in this interval can be replaced by its average constant value. Calculations show that in approximate estimates the values of $\rho_d=150$ g/cm^3 for oxygen and $\rho_d=130$ g/cm^3 for nitrogen may be accepted.

With the help of the diagram (Fig. 1.5.1) prepared on the basis of equation (1.5.2) the degree of dissociation for any nondimensional values of T/T_d and

ρ/ρ_d can be determined. From an analysis of equation (1.5.2) we arrive at the conclusion that dissociation starts at temperatures much lower than the characteristic temperature. If $\rho/\rho_d = 10^{-5}$ is assumed as the most probable value in the vicinity of the ground then from (1.5.2) or from the graph in Fig. 1.5.1 it follows that the values of $\alpha = 0.05$ (5%) at $T/T_d = 0.057$ and the degree of dissociation $\alpha = 0.92$ (92%) at $T/T_d = 0.105$. For the values of density typical of the upper layers of the atmosphere, for example $\rho_d/\rho = 10^7$, the ratio of T/T_d corresponding to the values of $\alpha = 0.05$ and 0.92 comes down to 0.045 and 0.071.

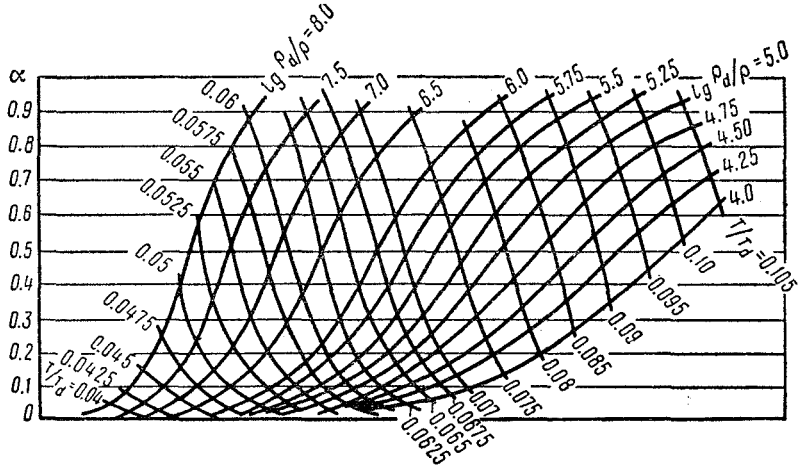

Fig. 1.5.1. Relation of degree of dissociation of diatomic gas with density and temperature.

5.2 Equation of state

Let us consider an equation of state for a gas mixture appearing as a result of the dissociation of diatomic molecules. This equation can be obtained by using the relations for determining pressure p and gas constant R of the mixture of gases, and also the partial pressure component p_i:

$$\left.\begin{aligned} p = \sum_i p_i,\ R = \sum_i c_i R_i, \\ p_i = \rho_i T R_i = \rho_i T (k/m_i) = (x_i/V) T (k/m_i), \end{aligned}\right\} \tag{1.5.3}$$

where ρ_i is the density of component, m_i is the mass of the atom or molecule, R_i is the gas constant of component; V is the volume of mixture of gases.

Equations (1.5.3) are popularly known as Dalton's law. Now let the component of atom ($i=1$) be denoted by an index 'A' and the molecular component ($i=2$) by an index 'M'. Since concentration of component $c_i = \rho_i/\rho$, where ρ is the density of the mixture, we get

$$c_1 = c_A = a = \rho_A/\rho, \quad c_2 = c_M = \rho_M/\rho = 1 - a$$

for atomic and molecular components respectively.

Now from (1.5.3), if the condition $m_M = 2m_A$ and the relation between the masses of x_i components ρ_i, ρ and a are fixed by the usual expressions

$$\rho_A = \rho a = x_A/V, \quad \rho_M = \rho(1-a) = x_M/V,$$

we get equation of state in the following form:

$$p = \rho Tk\left(\frac{\rho_A}{\rho}\cdot\frac{1}{m_A} + \frac{\rho_M}{\rho}\cdot\frac{1}{m_M}\right) = \frac{k}{2m_A}\rho T(1+a), \tag{1.5.4}$$

where $k/(2m_A)$ is the gas constant for 1 gram of component of A_2 in the mixture. Multiplying by $(1+a)$ this formula gives the value of gas constant R (absolute gas constant) for 1 gram of mixture of components A and A_2, the ratio of their masses being expressed as $a/(1-a)$.

Let us assume some conditional value which is determined by characteristic values of density and temperature following the expression

$$p_d = \frac{k}{2m_A}\rho_d T_d. \tag{1.5.5}$$

This value is known as the characteristic pressure. Numerical values of p_d are shown in Table 1.5.1. With the help of expression (1.5.5) the equation of state (1.5.4) can be written in more convenient nondimensional form:

$$\bar{p} = \bar{\rho}\bar{T}(1+a), \tag{1.5.4'}$$

where

$$\bar{p} = p/p_d, \quad \bar{\rho} = \rho/\rho_d, \quad \bar{T} = T/T_d.$$

TABLE 1.5.1

Element	Characteristic parameters of dissociation					
	$p_d \cdot 10^{-7}$, kg/cm²	ρ_d, g/cm³	$T_d \cdot 10^{-3}$, °K	$u_d \cdot 10^{-3}$, k·cal/kg	$u_d \cdot 10^{-7}$, m²/sec²	$V_d \cdot 10^{-3}$, m/sec
Oxygen	2.3	150	59	3.7	1.5	3.9
Nitrogen	4.1	130	113	8.0	3.4	5.8
Air	3.7	135	100	7.1	3.0	5.4

Mean molecular weight: As is known from thermodynamics, the mean molecular weight of the mixture of gases

$$\mu_{av} = \frac{1}{\sum\limits_i c_i/\mu_i}, \tag{1.5.6}$$

where c_i is the mass concentration of an arbitrary component; μ_i is its molecular weight; the summation sign determines the number of molecules in the mixture. For diatomic dissociating gas

$$\sum_i c_i = c_1 + c_2 = c_A + c_M = 1.$$

Since

$$c_A = a, \quad c_M = 1 - a, \quad 2\mu_A = \mu_M = (\mu_{av})_0,$$

we have

$$\mu_{av} = \left(\frac{c_A}{\mu_A} + \frac{c_M}{\mu_M}\right)^{-1} = \frac{(\mu_{av})_0}{1+a}. \tag{1.5.7}$$

5.3 Thermodynamic relations

Let us examine the thermodynamic relations used in the investigation of a diatomic dissociating gas flow. One is the equation of internal energy. It can be obtained from the condition that the internal energy is determined as the sum of the average translational energy of atoms and molecules $(3/2)\, kTn_A$, and also from the rotational and vibrational energy $2(3/2)kTn_{A_2}$ that the molecules possess additionally. Here the energy of electrons can be neglected. Besides this if the chemical energy of dissociation, equal to $(1/2)\, Dn_A$, is taken into account we get an equation for internal energy

$$U = (3/2)\, kT\,(n_A + 2n_{A_2}) + (1/2)\, Dn_A.$$

The value of internal energy per unit mass of gas is

$$u = U/\rho V = (3k/2m_A)\, T + (D/2m_A)\, a, \tag{1.5.8}$$

where $V = m_A\,(n_A + 2n_{A_2})/\rho$ is the volume occupied by the gas.

Introducing the characteristic energy of dissociation per unit mass (per 1 g of A_2)

$$u_d = D/2m_A, \tag{1.5.9}$$

equation (1.5.8) can be written in nondimensional form

$$\bar{u} = 3\bar{T} + a, \tag{1.5.8'}$$

where $\bar{u} = u/u_d$; values of u_d are given in Table 1.5.1. In the same table are shown the values of parameter $V_d = \sqrt{u_d}$, representing characteristic velocity of dissociation. Physically this parameter represents the velocity that provides kinetic energy to the flow which is equal to half of the energy necessary for complete dissociation of the gas.

Comparing (1.5.5) and (1.5.9) and bearing in mind that $T_d = D/k$, we get the formula

$$p_d = \rho_d\, V_d^2, \tag{1.5.10}$$

from which it follows that p_d characterizes pressure developing during stagnation of the flow, with velocity and density represented by V_d and ρ_d respectively.

Now let us examine an equation of enthalpy. It is well known that

$$i=u+(p/\rho). \tag{1.5.11}$$

Dividing terms of this equation by u_d, we get the relation for enthalpy in nondimensional form

$$\bar{i}=\bar{u}+(\bar{p}/\bar{\rho}), \tag{1.5.12}$$

where $\bar{i}=i/u_d$. Substituting expression (1.5.8′) from $\bar{u}$ in (1.5.12) and using equation (1.5.4′), we get the enthalpy relation

$$\bar{i}=a+\bar{T}(4+a), \tag{1.5.13}$$

or

$$\bar{i}=a+\frac{4+a}{1+a}\cdot\frac{\bar{p}}{\bar{\rho}}\cdot \tag{1.5.13′}$$

If the value of $\bar{T}=T/T_d$ in equation (1.5.2) is replaced by an expression

$$\bar{T}=(\bar{i}-a)/(4+a), \tag{1.5.14}$$

based on (1.5.13) we get the relation for the degree of dissociation a as a function of enthalpy $\bar{i}$ and the ratio of densities ρ_d/ρ. This relation is graphically shown in Fig. 1.5.2.

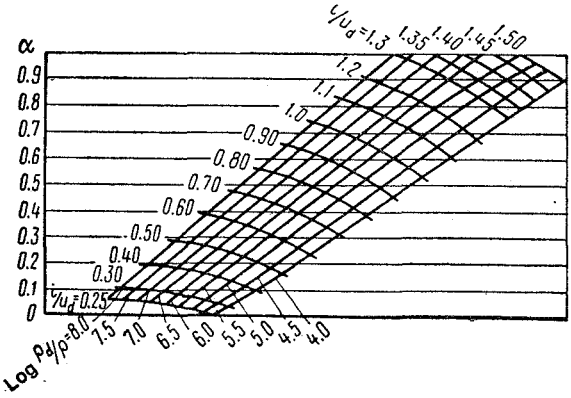

Fig. 1.5.2. Relation of degree of dissociation of diatomic gas with density and enthalpy.

Let us find the enthalpy of dissociation, i.e. quantity of heat necessary for dissociation of a unit mass of gas component at constant p and T. To do this we use the second law of thermodynamics, i.e.

$$dq=di-(dp/\rho),$$

which can be rewritten in the form

$$dq=\frac{\partial i}{\partial T}\,dT+\left(\frac{\partial i}{\partial p}-\frac{1}{\rho}\right)dp+\frac{\partial i}{\partial a}\,da.$$

Then under constant p and T conditions we get an equality

$$(dq/da)_{p,T}=\partial i/\partial a.$$

This quantity also determines the heat of dissociation $i_R=\partial i/\partial a$. Differentiating (1.5.13) with respect to a, we get $\partial\bar{i}/\partial a=\bar{T}+1$. For the real temperatures at which dissociation takes place the relative temperature $\bar{T}\ll 1$. Consequently the enthalpy of dissociation of the gas component will be

$$i_R=u_d. \tag{1.5.15}$$

5.4 Coefficient of dynamic viscosity

Experiments show that Sutherland's modified formula can be used for calculation of the coefficient of dynamic viscosity for a dissociating diatomic gas

$$\frac{\mu}{\mu_\infty}=\left(\frac{T}{T_\infty}\right)^{\frac{1}{2}}\frac{1+(111/T_\infty)}{1+(111/T)}\left[\frac{1}{1+(0.89c_A/c_M)}+\frac{1.42}{1+(1.26c_M/c_A)}\right]. \tag{1.5.16}$$

Here the concentrations of atomic and molecular gas components are $c_A=a$, $c_M=(1-a)$ respectively. In the absence of dissociation ($c_A=a=0$) the relation (1.5.16) changes to the usual Sutherland formula. At complete dissociation ($a=1$) the quantity in the square brackets in (1.5.16) is equal to 1.42, which shows that the coefficient of viscosity increases by 42% in comparison with an undissociated gas.

5.5 Mixture of diatomic gases

Degree of balanced dissociation: So far we have been considering pure dissociating diatomic gas. Strictly speaking these relations are not accurate for calculations of the parameters of gas dynamics and thermodynamics for a mixture of diatomic gases and in particular for estimation of the degree of dissociation. However, since the values of the molecular weight of nitrogen and oxygen are known fairly accurately a modified gas model postulating a mixture of diatomic gases can be reasonably correct. In this context the difference in the characteristic temperatures of nitrogen and oxygen has to be taken into account. Oxygen, with the smaller energy of the atomic bond in its molecules, starts dissociating at comparatively lower temperatures than nitrogen and is found to be completely dissociated when nitrogen is only entering the dissociation phase.

If the temperature at the beginning of dissociation of N_2 is 3,500°K the degree of resulting dissociation of a diatomic model of air at this temperature

will be determined by the relative mass of oxygen in the mixture, i.e. by its value of 0.235. At $T<3{,}500°K$ the degree of dissociation of the air model is

$$a=0.235\,a_{O_2}, \tag{1.5.17}$$

where a_{O_2} is the degree of dissociation of pure oxygen. After completion of dissociation of O_2 (at temperature $T=3{,}500°K$) the value of $a_{O_2}=1$ and degree of dissociation of air at $T>3{,}500°K$ will be determined by the expression

$$a=0.235+0.765\,a_{N_2}, \tag{1.5.18}$$

where a_{N_2} is the degree of dissociation of pure nitrogen and the quantity 0.765 determines the volume of N_2 in air. For completely dissociated air $a_{O_2}=a_{N_2}=1$ and thus the degree of dissociation of mixture $a=1$.

For approximate calculations of the degree of dissociation a simplified mass composition of undissociated air is taken as 76.5% of N_2 and 23.5% of O_2, where the 1% of inert gases in the atmosphere is included in the nitrogen.

Effective characteristic parameters: The effective characteristic parameters for the dissociation of air model can be determined from the above-mentioned mass components of undissociated air. For example, effective characteristic pressure for dissociation

$$p_d=0.765\,p_{dN_2}+0.235\,p_{dO_2}, \tag{1.5.19}$$

where p_{dN_2} p_{dO_2} are characteristic pressures for dissociation of nitrogen and oxygen respectively. Similarly the effective values of other characteristic parameters can be calculated. Values of p_d, ρ_d, T_d, u_d and V_d for a given air model calculated in this way are shown in Table 1.5.1.

Enthalpy for uniform dissociation: In the case of the air model in the form of a mixture of nitrogen and oxygen the enthalpy for uniform dissociation is

$$i_D=c_N\,i_{RN_2}+c_O\,i_{RO_2}, \tag{1.5.20}$$

where the enthalpy of dissociation of component for nitrogen $i_{RN_2}=u_{dN_2}=(D/2m_A)_{N_2}$ and for oxygen $i_{RO_2}=u_{dO_2}=(D/2m_A)_{O_2}$ (see Table 1.5.1); c_N and c_O are the atomic concentrations of nitrogen and oxygen in air respectively (values of concentration can be found in the work [17]).

If air is considered as a diatomic model of gases

$$i_D=au_d, \tag{1.5.21}$$

where $u_d=7.1\times10^3$ k·cal/kg according to the data of Table 1.5.1. For a more complicated model of air, representing in itself the mixture of diatomic oxygen and nitrogen, the enthalpy of dissociation can be calculated in the following way: We assume that the whole of the oxygen is dissociated by the time the nitrogen begins to dissociate. Consequently atomic concentra-

tion is decided only by the breakdown of oxygen, the value of $a_{O_2}=1$ and $a_{N_2}=0$. According to this

$$i_D=0.235\, u_{dO_2}. \tag{1.5.22}$$

If conditions are such that the dissociation of oxygen takes place partially, the degree of dissociation of the mixture is $a<0.235$ and

$$i_D=0.235\, a_{O_2}\, u_{dO_2}. \tag{1.5.22'}$$

At high temperatures nitrogen, like oxygen, starts dissociating and enthalpy of dissociation of the mixture will be

$$i_D=0.765\, a_{N_2}\, u_{dN_2}+0.235\, u_{dO_2}. \tag{1.5.23}$$

For an approximate estimation of the values of i_D we can use tables or diagrams of the state of air at high temperatures. In this case the enthalpy i_α at temperature T and pressure p can be found with consideration of dissociation and i_D can be determined as a difference

$$i_D=i_\alpha-i_{\alpha=0},$$

where $i_{\alpha=0}$ is enthalpy at the same temperature T but without taking into consideration dissociation. Its value can be calculated by the formula

$$i_{\alpha=0}=c_{p\infty}\,(T/T_\infty)^\varphi\, T, \tag{1.5.24}$$

in which for $T>1{,}000°K$, the index $\varphi=0.1$, and at $T_\infty=273°K$ specific heat $c_{p\infty}=0.24$ k·cal/kg·deg.

The determination of the thermodynamic parameters of air as a model of a pure dissociating gas in the form of a mixture of N_2 and O_2 is limited to the condition that the given gas medium seems to be heated in advance in the initial (undissociated) phase. The adiabatic index $k=1.33$ corresponds to the condition of excited vibrational mode of energy.

Strictly speaking such a medium does not seem to occur under normal flight conditions. Even then the relations shown above have practical importance. The transition through a shock wave appearing ahead of the body represents itself as an unbalanced process. In practice, it is found that even at very high velocities and temperatures the extent of dissociation is zero immediately behind the wave front but vibrational levels of energy are excited. Thus behind the shock wave the properties of a real and a hypothetical gas coincide. Therefore the accuracy of thermodynamic and gas dynamic calculations improves with increase in flight speed when the gas behind the shock wave is heated to very high temperatures.

Average heat coefficient of mixture: The average heat coefficient of a mixture is given by

$$(c_p)_{av}=\sum_i c_{p_i}\, c_i. \tag{1.5.25}$$

For the mixture of monoatomic and diatomic gases

$$(c_p)_{av} = c_{pA}\, c_A + c_{pM}\, c_M,$$

or, because $c_A = a$, $c_M = 1 - a$,

$$(c_p)_{av} = c_{pA}\, a + (1-a)\, c_{pM}, \tag{1.5.26}$$

where the first term on the right side represents the atomized component of average heat coefficient and the second term represents the molecular component of average heat coefficient.

Enthalpy of gas: Enthalpy of the mixture of gas is given by

$$i = \sum_i i_i\, c_i, \tag{1.5.27}$$

where c_i and i_i are the concentration and enthalpy of the i-th component of the mixture respectively. The value of i_i is equal to the total energy including heat energy $\left(\int_0^T c_p\, dT\right)_i$ of the i-th component of the gas and the chemical energy $(i_{chem})_i$ of its formation, i.e.

$$i_i = \left(\int_0^T c_p\, dT\right)_i + (i_{chem})_i. \tag{1.5.28}$$

Enthalpy i_i is called the total enthalpy of the i-th component and enthalpy i in (1.5.27) is the total enthalpy of the mixture of gases.

If the mixture of interacting atom-molecules is considered, keeping in mind that $(i_{chem})_M = 0$ for molecules, we get

$$i_A = \int_0^T c_{pA} dT + (i_{chem})_A, \quad i_M = \int_0^T c_{pM} dT. \tag{1.5.28'}$$

During the flow of a mixture of gases the enthalpy of some of the total volume may be changed as a result of heat flow into or out of it due to heat exchange, transfer of energy directly during inflow and outflow of gas and transfer of energy due to diffusion. The heat of formation $(i_{chem})_i$ for each component has a constant value. This value for atomized components of nitrogen and oxygen, which occurs as a result of dissociation of air, is equal to the corresponding values of enthalpy of dissociation, i.e.

$$(i_{chem})_O = u_{dO} = i_{RO}$$

and

$$(i_{chem})_N = u_{dN} = i_{RN} \qquad \text{(see Table 1.5.1).}$$

2

KINEMATICS OF A FLUID MEDIUM

1. Methods of Kinematic Investigation of a Fluid

The main problem of aerodynamic research is the determination of the force of interaction and heat exchange between the fluid medium and the body under interaction. Solution of this problem involves study of the motion of the fluid medium adjacent to the body. From this the variables entering into the governing motion, namely velocity, pressure, density, temperature, etc., are determined for every point in the flow field.

Under certain assumptions the investigation can be reduced to the determination of a flow field representing a close link with the velocities of the particles of a fluid, i.e. to the solution of the kinematic problem. Then, from a known velocity distribution the remaining parameters as well as the resultant forces, moments and heat flows are obtained.

There are two methods of kinematic investigation of a fluid medium. One is called Lagrange's method and the other Euler's method.

1.1 Lagrangian method

The Lagrangian method deals with the motion of the individual particles of a fluid and determines the trajectory for each of them, i.e. their coordinates, as a function of time.

Since there are an infinite number of particles it is necessary for this purpose to characterize in a given way the particle which has this trajectory. Thus the coordinates of a particle a, b, c at a given moment $t=t_0$ designate the particle. This indicates that from an infinite number of trajectories the one that passes through the point with coordinates a, b, c belongs to the given particle. Therefore the equation of the trajectory in a functional form will be as follows:

$$\left.\begin{aligned} x&=f_1(a, b, c, t);\\ y&=f_2(a, b, c, t);\\ z&=f_3(a, b, c, t), \end{aligned}\right\} \tag{2.1.1}$$

where a, b, c, t are called Lagrangian parameters. The quantities a, b, c are parameters determining the trajectory. The components of the velocity vector at any point on the trajectory are equal to the partial derivatives $V_x=\partial x/\partial t$, $V_y=\partial y/\partial t$, $V_z=\partial z/\partial t$, and components of the acceleration vector are equal to the corresponding second partial derivatives $W_x=\partial^2 x/\partial t^2$, $W_y=\partial^2 y/\partial t^2$, $W_z=\partial^2 z/\partial t^2$.

1.2 Eulerian method

The Eulerian method is often used in aerodynamic research. Unlike in Lagrange's method, not the particle of the fluid but a point in space with coordinates x, y, z is considered to be fixed and the variations of velocity with time at this point are investigated. The Eulerian method consists of expressions for velocities of particles of fluid as functions of time t and coordinates x, y, z of a point in space, i.e. in a field of velocities, which are determined by the vector $\overline{V}=V_x i+V_y j+V_z k$, where i, j, k are unit vectors along axes of coordinates and $V_x=dx/dt$, $V_y=dy/dt$, $V_z=dz/dt$ are components of velocity vectors described by the equations

$$\left.\begin{aligned} V_x&=f_1(x, y, z, t);\\ V_y&=f_2(x, y, z, t);\\ V_z&=f_3(x, y, z, t). \end{aligned}\right\} \tag{2.1.2}$$

The quantities x, y, z, t are called Euler's variables. Solving the system of differential equations,

$$\left.\begin{aligned} \frac{dx}{dt}&=f_1(x, y, z, t);\\ \frac{dy}{dt}&=f_2(x, y, z, t);\\ \frac{dz}{dt}&=f_3(x, y, z, t), \end{aligned}\right\} \tag{2.1.3}$$

the equations of the family of trajectories in a parametric form coinciding with equations (2.1.1) can be obtained. Here a, b, c are constants of integrations. Taking the complete derivative of the velocity vector with respect to time we get the acceleration vector,

$$\overline{W}=\frac{d\overline{V}}{dt}=\frac{\partial \overline{V}}{\partial t}+V_x\frac{\partial \overline{V}}{\partial x}+V_y\frac{\partial \overline{V}}{\partial y}+V_z\frac{\partial \overline{V}}{\partial z}\cdot \tag{2.1.4}$$

In this expression $\partial\overline{V}/\partial t$ indicates local acceleration and the remaining three terms give convective acceleration. Projecting vector $\overline{W}$ on axes of coordinates we get the components of total acceleration as follows:

$$\left.\begin{aligned} W_x &= \frac{\partial V_x}{\partial t} + V_x \frac{\partial V_x}{\partial x} + V_y \frac{\partial V_x}{\partial y} + V_z \frac{\partial V_x}{\partial z}; \\ W_y &= \frac{\partial V_y}{\partial t} + V_x \frac{\partial V_y}{\partial x} + V_y \frac{\partial V_y}{\partial y} + V_z \frac{\partial V_y}{\partial z}; \\ W_z &= \frac{\partial V_z}{\partial t} + V_x \frac{\partial V_z}{\partial x} + V_y \frac{\partial V_z}{\partial y} + V_z \frac{\partial V_z}{\partial z}. \end{aligned}\right\} \quad (2.1.5)$$

The relation (2.1.5) for acceleration corresponds to the flow which is characterized by the variation in velocity with time at a given point and hence the inequality $\partial \overline{V}/\partial t \neq 0$. This kind of fluid flow is called an unsteady flow. A fluid flow in which velocity and other parameters at a given point are independent of time ($\partial \overline{V}/\partial t = 0$) is called a steady flow.

1.3 Stream line and streak line

At the moment $t = t_0$ a line can be drawn in a fluid flow so that at every point it coincides with the direction of velocity. This line is known as a stream line.

To get a stream line we have to proceed as follows: Let us take some point A_1 in a flow at a moment $t = t_0$ (Fig. 2.1.1, a) and express the velocity of a particle at this point by vector $\overline{V}_1$. Then take another point A_2 in the neighborhood of point A_1 and lying on vector $\overline{V}_1$. Let the velocity vector at this point at time $t = t_0$ be $\overline{V}_2$. Similarly we examine point A_3 on vector $\overline{V}_2$, the velocity at which is determined at the same moment by vector $\overline{V}_3$, and so on. As a result of these constructions we get a stepped line consisting of segments of velocity vectors. Reducing these segments to zero and simultaneously increasing their number to infinity we get, at the limit, the line that follows the complete set of velocity vectors. This is the stream line.

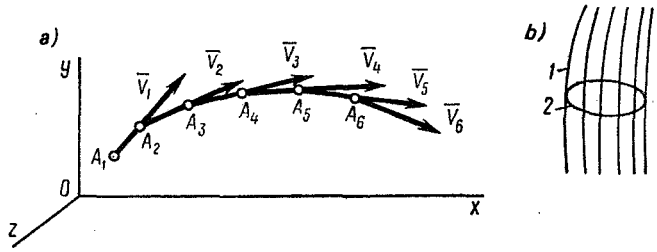

Fig. 2.1.1. Construction of stream line (*a*) and stream tube (*b*):
1—stream lines; *2*—contour.

To get the equation of the stream line we make use of the property that at every point on the line the direction of velocity vector $\overline{V}$ must coincide with the vector $d\bar{s} = dx\,i + dy\,j + dz\,k$, where dx, dy, dz, are projections of the element of an arc $d\bar{s}$ on a stream line. Consequently vector product $d\bar{s} \times \overline{V} = 0$, i.e.

$$\begin{vmatrix} i & j & k \\ dx & dy & dz \\ V_x & V_y & V_z \end{vmatrix} = i(V_z\,dy - V_y\,dz) - j(V_z\,dx - V_x\,dz) + k(V_y\,dx - V_x\,dy) = 0.$$

Since, for example $V_z dy - V_y dz = 0$, etc. we obtain a system of differential equations:

$$dx/V_x = dy/V_y = dz/V_z. \tag{2.1.6}$$

So the problem of determining the stream line reduces to the integration of a system of equations (2.1.6). Each of the integrals $F_1(x, y, z, C_1) = 0$ and $F_2(x, y, z, C_2) = 0$ of this equation represents a family of surfaces which depend on one parameter C_1 or C_2. An intersection of these surfaces gives a family of stream lines.

In contrast to the stream line, whose formation is calculated for a fixed moment of time, the concept of a streak line is connected with some interval of time during which the particle follows a certain path. From this it follows that the stream line and streak line are the particle-paths of one and the same particle and in a steady flow case they coincide. If the fluid motion is unsteady the stream line and streak line will not coincide.

In aerodynamics the concepts of a stream tube and jet of fluid or gas are used. If stream lines are drawn through the points on an elementary closed contour (see Fig. 2.1.1, b) they form a surface which is known as the surface of a stream tube. If streak lines are drawn through points on an elementary closed contour the surface so formed by restricting part of the fluid is called the fluid jet. The stream tube and gas jet, constructed through a point on one and the same closed contour in a steady flow, coincide with each other.

2. Analysis of Motion of Fluid Particles

Investigation of a fluid flow is based on the application of the Lagrangian method with the help of which the motion of a given particle of fluid can be studied and the correct analysis of this motion established. The motion of a solid body is determined by its translational motion or shift and its rotation about an instantaneous axis passing through its center of gravity. Unlike a solid body, the motion of a fluid particle is characterized, in addition, by the presence of deforming motion changing the form of this particle.

Let us examine a fluid particle in the form of an elemental parallelepiped with its sides dx, dy, dz. Let us analyze the motion of its side $ABCD$ (Fig. 2.2.1). Since the coordinates of corners of this side are different, the velocities determined at a given moment of time $t = t_0$ will also be different:

$$\left.\begin{aligned} &V_{xA} = V_x(x, y), \quad V_{xB} = V_x(x+dx, y); \\ &V_{yA} = V_y(x, y), \quad V_{yB} = V_y(x+dx, y); \\ &V_{xC} = V_x(x+dx, y+dy), \quad V_{xD} = V_x(x, y+dy); \\ &V_{yC} = V_y(x+dx, y+dy), \quad V_{yD} = V_y(x, y+dy), \end{aligned}\right\} \tag{2.2.1}$$

where x, y are coordinates of point A.

Let us resolve the expressions for velocities in Taylor's series by retaining values of only the first order, i.e. the terms containing dx, dy, dz of the first order. Denoting that velocity $V_{xA}=V_x$ and $V_{yA}=V_y$ at a point A, we get

$$\left.\begin{aligned} &V_{xB}=V_x+(\partial V_x/\partial x)\,dx+\cdots,\quad V_{xD}=V_x+(\partial V_x/\partial y)\,dy+\cdots;\\ &V_{yB}=V_y+(\partial V_y/\partial x)\,dx+\cdots,\quad V_{yD}=V_y+(\partial V_y/\partial y)\,dy+\cdots;\\ &V_{xC}=V_x+(\partial V_x/\partial x)\,dx+(\partial V_x/\partial y)\,dy+\cdots;\\ &V_{yC}=V_y+(\partial V_y/\partial x)\,dx+(\partial V_y/\partial y)\,dy+\cdots. \end{aligned}\right\} \quad (2.2.2)$$

From these expressions it follows, for example that the velocity component along the x axis at point B differs from its value at point A by the amount $(\partial V_x/\partial x)\,dx$. This indicates that the point B, undergoing gradual change in velocity V_x in the direction of the x axis, has the velocity $(\partial V_x/\partial x)\,dx$

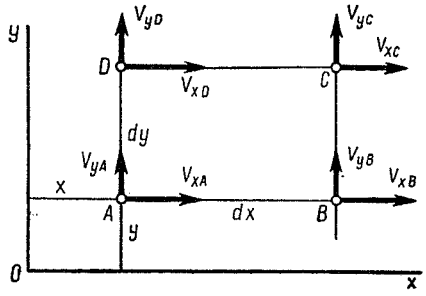

Fig. 2.2.1. Scheme of motion of fluid particle.

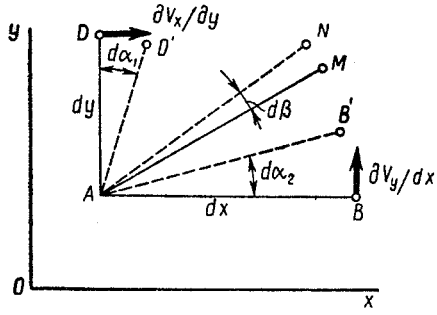

Fig. 2.2.2. Angular deformation of fluid particle.

with respect to velocity at point A along the x axis. As a result linear deformation of the segment AB takes place. The rate of this deformation is $\theta_x=\partial V_x/\partial x$.

Point B also moves in the direction of the y axis with velocity V_y together with point A and simultaneously rotates about it with velocity $\partial V_y/\partial x$.

Similarly it can be established for point D that the relative linear velocity of this point along the y axis is $(\partial V_y/\partial y)\,dy$ and hence the rate of linear deformation of segment AD will be $\theta_y=\partial V_y/\partial y$. The angular velocity of rotation of this segment about point A is equal to $-\partial V_x/\partial y$ (the minus sign indicates that point D rotates about point A in a direction opposite to the rotation of point B). As a result of rotation of the element AD and AB a change in angle DAB (Fig. 2.2.2) takes place, i.e. angular deformation of the particle occurs. Simultaneously, the bisector AM of angle DAB rotates and hence some angle $d\beta$ comes into the picture between it and the bisector AN of deformed angle $D'AB'$. Thus the particle will undergo rotation along with deformation.

Now, the angle of rotation of the bisector (see Fig. 2.2.2) is

$$d\beta=\gamma-\tau,$$

where

$$\gamma=\frac{1}{2}\left[\frac{\pi}{2}-(da_2-da_1)\right];\ \tau=\frac{\pi}{4}-da_1.$$

The angles da_2 and da_1 shown in Fig. 2.2.2 are equal to $(\partial V_y/\partial x)\,dt$ and $(\partial V_x/\partial y)\,dt$ respectively. Hence

$$d\beta=\frac{1}{2}(da_2-da_1)=\frac{1}{2}\left(\frac{\partial V_y}{\partial x}-\frac{\partial V_x}{\partial y}\right)dt.$$

Therefore the angular velocity $d\beta/dt$ of the rotation of a fluid particle about the z axis can be obtained. Denoting it by ω_z, we can write

$$\omega_z=\frac{d\beta}{dt}=\frac{1}{2}\left(\frac{\partial V_y}{\partial x}-\frac{\partial V_x}{\partial y}\right). \tag{2.2.3}$$

If the motion of an edge AD relative to segment AB is considered it is clear that the angular velocity of this sector is

$$2\varepsilon_z=(\partial V_x/\partial y)+(\partial V_y/\partial x). \tag{2.2.4}$$

The quantity

$$\varepsilon_z=\frac{1}{2}\left(\frac{\partial V_x}{\partial y}+\frac{\partial V_y}{\partial x}\right) \tag{2.2.4'}$$

is known as the semi-rate of deformation of the right angle DAB.

Let us extend all these results to a three-dimensional flow and examine point C, occupying a particle in the form of an elemental parallelepiped with lengths of sides dx, dy, dz. The velocity at this point at time $t=t_0$ is a function of coordinates $x+dx$, $y+dy$, $z+dz$. Expressing velocity components in the form of Taylor's series and retaining terms only of the first order we get:

$$\left.\begin{aligned}
V_{xC}&=V_x+\frac{\partial V_x}{\partial x}\,dx+\frac{\partial V_x}{\partial y}\,dy+\frac{\partial V_x}{\partial z}\,dz;\\
V_{yC}&=V_y+\frac{\partial V_y}{\partial x}\,dx+\frac{\partial V_y}{\partial y}\,dy+\frac{\partial V_y}{\partial z}\,dz;\\
V_{zC}&=V_z+\frac{\partial V_z}{\partial x}\,dx+\frac{\partial V_z}{\partial y}\,dy+\frac{\partial V_z}{\partial z}\,dz.
\end{aligned}\right\} \tag{2.2.5}$$

We introduce notations similar to those in the analysis of the motion of a plane particle. Assume that $\theta_z=\partial V_z/\partial z$. This value determines the rate of linear deformation of a three-dimensional particle along the z axis. Now we introduce the notations:

$$\omega_x=\frac{1}{2}\left(\frac{\partial V_z}{\partial y}-\frac{\partial V_y}{\partial z}\right),\quad \omega_y=\frac{1}{2}\left(\frac{\partial V_x}{\partial z}-\frac{\partial V_z}{\partial x}\right). \tag{2.2.6}$$

The quantities ω_x and ω_y represent the components of angular velocities of

this particle about the x and y axes. The components of angular velocity ω_x, ω_y, ω_z of a particle are taken as positive if rotation takes place from the x axis to the y axis, from the y axis to the z axis and from the z axis to the x axis respectively. Accordingly, the signs of derivatives $\partial V_y/\partial x$, $\partial V_z/\partial y$, $\partial V_x/\partial z$ will coincide with signs of angular velocities and the signs of derivatives $\partial V_x/\partial y$, $\partial V_y/\partial z$, $\partial V_z/\partial x$ will be opposite to those of the angular velocities.

By analogy to (2.2.4') we write the expressions:

$$\varepsilon_x=\frac{1}{2}\left(\frac{\partial V_z}{\partial y}+\frac{\partial V_y}{\partial z}\right),\quad \varepsilon_y=\frac{1}{2}\left(\frac{\partial V_x}{\partial z}+\frac{\partial V_z}{\partial x}\right), \tag{2.2.7}$$

which are equal to the semi-rate of deformation of two right angles of a parallelepiped in planes yOz and xOz respectively.

With the help of simple manipulations it can be shown that

$$\partial V_z/\partial y=\varepsilon_x+\omega_x;\ \partial V_x/\partial z=\varepsilon_y+\omega_y;\ \partial V_y/\partial x=\varepsilon_z+\omega_z;$$
$$\partial V_y/\partial z=\varepsilon_x-\omega_x;\ \partial V_z/\partial x=\varepsilon_y-\omega_y;\ \partial V_x/\partial y=\varepsilon_z-\omega_z.$$

Considering these expressions, the components of velocity at a point C (2.2.5) can be written as follows:

$$\left.\begin{aligned} V_{xC}&=V_x+\theta_x\,dx+\varepsilon_y\,dz+\varepsilon_z\,dy+\omega_y\,dz-\omega_z\,dy;\\ V_{yC}&=V_y+\theta_y\,dy+\varepsilon_z\,dx+\varepsilon_x\,dz+\omega_z\,dx-\omega_x\,dz;\\ V_{zC}&=V_z+\theta_z\,dz+\varepsilon_x\,dy+\varepsilon_y\,dx+\omega_x\,dy-\omega_y\,dx. \end{aligned}\right\} \tag{2.2.8}$$

Thus the motion of point C can be taken as the result of summation of three types of motion: translational motion along the trajectory together with point A at a velocity $\overline{V}(V_x, V_y, V_z)$, rotation about it with an angular velocity

$$\overline{\omega}=\omega_x\,i+\omega_y\,j+\omega_z\,k \tag{2.2.9}$$

and deforming motion. This concludes the essence of Helmholtz's theorem.

Deforming motion, in its way, is built up from linear deformation characterized by coefficients θ_x, θ_y, θ_z and angular deformation which is represented in terms of ε_x, ε_y, ε_z.

The linear deformation of the edges of an element limits the variation of its volume $\tau=dxdydz$, which is determined by the difference

$$d\tau=dx_1\,dy_1\,dz_1-dx\,dy\,dz,$$

where dx_1, dy_1, dz_1 are lengths of sides of the element at time $t+dt$.

Substituting the values of side lengths, we get

$$d\tau=(dx+\theta_x\,dx\,dt)\,(dy+\theta_y\,dy\,dt)\,(dz+\theta_z\,dz\,dt)-dxdydz.$$

Neglecting terms higher than of the fourth order in this expression, we have

$$d\tau=(\theta_x+\theta_y+\theta_z)\,dxdydzdt.$$

From this, the rate of change of relative volume or rate of deformation of specific volume $\theta=(1/\tau)\, d\tau/dt$ can be determined as

$$\theta=\theta_x+\theta_y+\theta_z\,, \tag{2.2.10}$$

which is equal to the sum of rates of linear deformation along any three mutually perpendicular directions at every point in the flow. The quantity θ is also known as the divergence of the velocity vector at a given point, i.e.

$$\text{div}\ \overline{V}=\theta=\theta_x+\theta_y+\theta_z\,. \tag{2.2.11}$$

So it is clear that the motion of a fluid particle is of a complex nature and that it can be expressed as the summation of three types of motion: translational, rotational and deforming.

A flow in which the fluid undergoes rotation is called a rotational flow and the components of the angular velocity of rotations ω_x, ω_y, ω_z are called the vortex components. To identify rotational flow the concept of rotation of velocity rot $\overline{V}$, represented by rot $\overline{V}=2\overline{\omega}$, is used. The rotation of velocity represents by itself a vector

$$\text{rot}\ \overline{V}=(\text{rot}\ \overline{V})_x\, i+(\text{rot}\ \overline{V})_y\, j+(\text{rot}\ \overline{V})_z\, k, \tag{2.2.12}$$

and the components

$$(\text{rot}\ \overline{V})_x=2\omega_x,\ (\text{rot}\ \overline{V})_y=2\omega_y \text{ and } (\text{rot}\ \overline{V})_z=2\omega_z$$

are equal to twice the corresponding values of the vortex components.

3. Irrotational Motion of a Fluid

In investigating fluid motion its rotation is often not taken into account due to the infinitesimally small angular velocities of the particles. This kind of motion is called irrotational motion.

For irrotational flow $\overline{\omega}=0$ (or curl $\overline{V}=0$) and hence the vortex components ω_x, ω_y, ω_z are zero. Accordingly, formulas (2.2.3), (2.2.6) give

$$\partial V_x/\partial y=\partial V_y/\partial x,\ \partial V_z/\partial y=\partial V_y/\partial z,\ \partial V_x/\partial z=\partial V_z/\partial x. \tag{2.3.1}$$

These equalities are the necessary and sufficient conditions for the sum of the three terms $(V_x dx+V_y dy+V_z dz)$ to be a total derivative of some function which characterizes fluid flow in the same way as the velocities V_x, V_y, V_z. Denoting this function as $\varphi\ (x, y, z, t)$ at any time t, it can be written as

$$d\varphi=V_x\, dx+V_y\, dy+V_z\, dz.$$

On the other hand the same differential will also be

$$d\varphi=(\partial\varphi/\partial x)\, dx+(\partial\varphi/\partial y)\, dy+(\partial\varphi/\partial z)\, dz.$$

Equating the last two expressions we get

$$V_x=\partial\varphi/\partial x,\ V_y=\partial\varphi/\partial y\,,\ V_z=\partial\varphi/\partial z. \tag{2.3.2}$$

This function φ is called the velocity potential or potential function of an irrotational flow. The existence of this function characterizes the flow as a potential flow. It follows from the relation (2.3.2) that the partial derivative of function φ with respect to any coordinate is equal to the projection of velocity on the respective axis of coordinates. This property of potential function is maintained even for any arbitrary direction. In particular, the tangential component of velocity at any point on an arbitrary curve s will be equal to the partial derivative $V_s = \partial\varphi/\partial s$ and the normal component will be $V_n = \partial\varphi/\partial n$, where n is normal to the arc s at the point being considered. The projections of velocity vector $\overline{V}$ in polar coordinates r and θ at some point in the directions of the polar radius vector and the perpendicular to this radius vector will be the partial derivatives

$$V_r = \partial\varphi/\partial r \text{ and } V_s = \partial\varphi/\partial s = (1/r)\,\partial\varphi/\partial\theta.$$

respectively.

It is obvious that the magnitude of velocity in any given direction is determined by the rate of change of potential φ in the same direction. The rate of change of potential along direction s is equal to the partial derivative of potential function along this direction, i.e. $\partial\varphi/\partial s$. The quantity $\partial\varphi/\partial s$ is the projection of some vector along the directions, while the gradient of φ is the direction of the highest rate of increase of this function. Obviously this vector is equal to the velocity vector $\overline{V}$. Expressing the gradient of the function in the form of grad φ, we can write

$$\overline{V} = \text{grad } \varphi, \tag{2.3.3}$$

or the same thing in the form

$$\overline{V} = \text{grad } \varphi = (\text{grad } \varphi)_x\, i + (\text{grad } \varphi)_y\, j + (\text{grad } \varphi)_z\, k, \tag{2.3.4}$$

where the coefficients in brackets on the right side indicate the projections of the vector of the velocity gradient on the coordinate axes:

$$(\text{grad } \varphi)_x = V_x = \partial\varphi/\partial x,\ (\text{grad } \varphi)_y = V_y = \partial\varphi/\partial y,$$
$$(\text{grad } \varphi)_z = V_z = \partial\varphi/\partial z. \tag{2.3.5}$$

The use of a potential function considerably simplifies the study of fluid motion because in place of investigating three unknowns such as the components of velocity V_x, V_y, V_z, it is enough to find one unknown function φ. Then, with the help of this function, the velocity field can be fully determined.

4. Equation of Continuity

4.1 General form of equation of continuity

The equation of continuity of motion in mathematical form represents by itself the law of conservation of mass—one of the fundamental laws of

physics. This equation is related to a number of basic equations in aerodynamics which are used to find the parameters governing the motion of a gas medium.

Let us take some moving volume of fluid and obtain the equation of continuity. This volume, consisting of the same particles, varies with time. According to the law of conservation of mass it can be written that $\rho_{av}\tau = \text{const}$ for this volume, where ρ_{av} is the average density of the fluid contained in the volume τ. Hence the derivative $d(\rho_{av}\tau)/dt = 0$ or, seeing that the density and volume are both variable quantities,

$$\frac{1}{\rho_{av}} \cdot \frac{d\rho_{av}}{dt} + \frac{1}{\tau} \cdot \frac{d\tau}{dt} = 0.$$

This equation deals with any arbitrary finite volume. To get the relation characterizing fluid motion at a point we take the limit of $\tau \to 0$ in the above equation. This indicates contraction of the volume τ to some inner point. If it is assumed that the moving fluid completely fills the volume we are considering, i.e. if there is no vacuum or discontinuity, then density ρ at a given point will be completely determined and can be expressed by the equation

$$\frac{1}{\rho} \cdot \frac{d\rho}{dt} + \operatorname{div} \bar{V} = 0, \tag{2.4.1}$$

where the quantity $\lim_{\tau \to 0} (1/\tau)\, d\tau/dt$ is replaced by divergence of a vector as indicated in (2.2.10) and (2.2.11).

The equation (2.4.1) represents the equation of continuity in general form.

4.2 Cartesian system of coordinates

Let us study the equation of continuity in the Cartesian system of coordinates. This could be done by finding the derivative $d\rho\ (x, y, z, t)/dt$ and replacing div $\bar{V}$ in (2.4.1) by (2.2.11). The continuity equation will then be obtained in the following form:

$$\frac{\partial \rho}{\partial t} + \frac{\partial (\rho V_x)}{\partial x} + \frac{\partial (\rho V_y)}{\partial y} + \frac{\partial (\rho V_z)}{\partial z} = 0. \tag{2.4.2}$$

Introducing the usual meaning of divergence of vector $\rho\bar{V}$

$$\operatorname{div}(\rho \bar{V}) = \frac{\partial (\rho V_x)}{\partial x} + \frac{\partial (\rho V_y)}{\partial y} + \frac{\partial (\rho V_z)}{\partial z},$$

we get

$$(\partial \rho/\partial t) + \operatorname{div}(\rho \bar{V}) = 0 \tag{2.4.3}$$

in place of equation (2.4.2).

The equation of continuity was obtained by assuming that the moving volume is filled with the same fluid particles. In a given case we studied fluid motion using Lagrange's method. The same equation could be obtained from

the analysis of the flow of different fluid particles through some fixed volume by the application of Euler's method.

The difference between the fluid flow rate from the control volume and the momentum of the fluid entering this volume during a given interval of time, on the assumption of continuity of medium, is equal to the change in momentum of the fluid in the given volume in the same interval of time. Let us put this condition in mathematical form. Take a control volume in the form of an elementary parallelepiped having sides dx, dy, dz. Let the fluid mass $f_x = \rho V_x dydzdt$ flow from the left side of the volume in time dt. The mass efflux during this time through the right side is equal to $f_x + (\partial f_x/\partial x)\, dx$. Consequently the difference between the mass efflux and the influx along the x axis will be

$$\frac{\partial f_x}{\partial x}\, dx = \frac{\partial (\rho V_x\, dydzdt)}{\partial x}\, dx = \frac{\partial (\rho V_x)}{\partial x}\, \tau dt.$$

Similarly the expressions for the difference between the mass outflow and inflow along the y and z axes could be written as

$$\frac{\partial f_y}{\partial y}\, dy = \frac{\partial (\rho V_y)}{\partial y}\, \tau dt\,, \quad \frac{\partial f_z}{\partial z}\, dz = \frac{\partial (\rho V_z)}{\partial z}\, \tau dt.$$

The change in mass of the fluid in the control volume occurs due to the change in density of the fluid. At time t the mass of fluid in control volume is $\rho\tau$ and at time $t+dt$ is equal to $\rho\tau + (\partial\rho/\partial t)\, \tau dt$. That is, change in mass is equal to $-(\partial\rho/\partial t)\tau dt$. By the condition of continuity this quantity is equal to the sum $(\partial f_x/\partial x)\, dx + (\partial f_y/\partial y)\, dy + (\partial f_z/\partial z)\, dz$, which leads to equation (2.4.2) obtained above.

The continuity equation (2.4.2) describes an unsteady flow. For a steady flow we have $\partial\rho/\partial t = 0$ and hence

$$\frac{\partial (\rho V_x)}{\partial x} + \frac{\partial (\rho V_y)}{\partial y} + \frac{\partial (\rho V_z)}{\partial z} = 0, \tag{2.4.4}$$

or

$$\operatorname{div} (\rho \bar{V}) = 0. \tag{2.4.4'}$$

The equation of continuity in a two-dimensional flow will be

$$\frac{\partial (\rho V_x)}{\partial x} + \frac{\partial (\rho V_y)}{\partial y} = 0. \tag{2.4.5}$$

For an incompressible flow $\rho = \text{constant}$; therefore

$$\frac{\partial V_x}{\partial x} + \frac{\partial V_y}{\partial y} + \frac{\partial V_z}{\partial z} = 0, \tag{2.4.6}$$

or

$$\operatorname{div} \bar{V} = 0. \tag{2.4.7}$$

The continuity equation for potential flow, taking into account (2.3.2), can be put in the following form:

$$\frac{1}{\rho}\cdot\frac{d\rho}{dt}+\frac{\partial^2\varphi}{\partial x^2}+\frac{\partial^2\varphi}{\partial y^2}+\frac{\partial^2\varphi}{\partial z^2}=0. \tag{2.4.8}$$

For an incompressible flow $\rho=$constant; hence

$$\frac{\partial^2\varphi}{\partial x^2}+\frac{\partial^2\varphi}{\partial y^2}+\frac{\partial^2\varphi}{\partial z^2}=0. \tag{2.4.8'}$$

The equation so obtained is known as Laplace's equation. It is known that any harmonic function could be the solution of this equation. Therefore the velocity potential φ in an incompressible flow represents such a harmonic function.

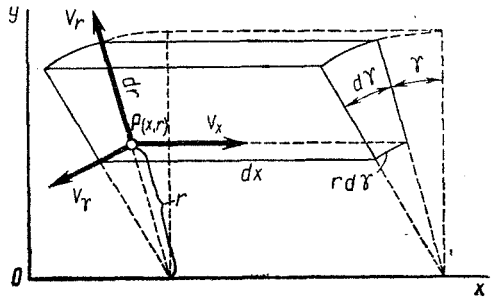

Fig. 2.4.1. Elementary particle of fluid in cylindrical system of coordinates.

4.3 System of curvilinear coordinates

Formulas of transformation: Some aerodynamic problems can be conveniently solved by using a system of orthogonal curvilinear coordinates. The cylindrical and the spherical systems of coordinates, in particular, are such curvilinear systems of coordinates.

In the cylindrical system of coordinates the position of any point P in space (Fig. 2.4.1) is determined by angle γ between the reference plane and the plane passing through point P and coordinate axis Ox, and the rectangular coordinates x and r in this plane. The formulas of transformation from the Cartesian coordinates to the cylindrical ones take the following form:

$$x=x; \qquad y=r\cos\gamma; \qquad z=r\sin\gamma. \tag{2.4.9}$$

In a spherical system of coordinates the position of point P (Fig. 2.4.2) is determined by the angular coordinates θ (polar distance), ψ (azimuthal angle) and the polar radius r.

The relation between rectangular and spherical coordinates is given by the following relations:

$$x=r\cos\theta, \quad y=r\sin\theta\cos\psi, \quad z=r\sin\theta\sin\psi. \tag{2.4.10}$$

The corresponding transformations of the above aerodynamic equations from Cartesian coordinates to one or other system of orthogonal curvilinear coordinates may be achieved in two ways:

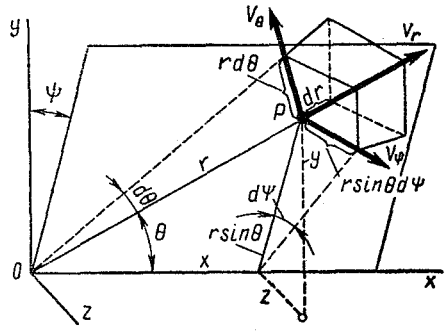

Fig. 2.4.2. Elementary particle of fluid in spherical system of coordinates.

either by direct substitution of (2.4.9), (2.4.10) in these equations or by application of a more general method based on the concepts of generalized coordinate curves [8]. Let us examine the latter method.

The elementary arc-lengths of coordinate-curves about a point P can be written in the following general form:

$$ds_1 = h_1\, dq_1\,, \quad ds_2 = h_2\, dq_2, \quad ds_3 = h_3\, dq_3, \tag{2.4.11}$$

where q_n $(n = 1, 2, 3)$ are curvilinear coordinates;

h_i coefficients are known as Lame's parameters.

Then we have for cylindrical coordinates

$$q_1 = x, \quad q_2 = r, \quad q_3 = \gamma, \tag{2.4.12}$$

and for spherical coordinates

$$q_1 = r, \quad q_2 = \theta, \quad q_3 = \psi. \tag{2.4.13}$$

From Fig. 2.4.1 it directly follows that for cylindrical coordinates

$$ds_1 = dx, \quad ds_2 = dr, \quad ds_3 = r d\gamma. \tag{2.4.14}$$

From Fig. 2.4.2 the arc-lengths of corresponding coordinate lines in a spherical system of coordinates will be

$$ds_1 = dr, \quad ds_2 = r d\theta, \quad ds_3 = r \sin\theta\, d\psi. \tag{2.4.15}$$

Lame's parameters in cylindrical coordinates will then be:

$$h_1 = 1, \quad h_2 = 1, \quad h_3 = r, \tag{2.4.16}$$

and for spherical coordinates they will be:

$$h_1 = 1, \quad h_2 = r, \quad h_3 = r \sin\theta. \tag{2.4.17}$$

Let us examine some expressions for vector and scalar quantities in curvilinear coordinates which will be necessary for transformation of the continuity equation in these systems of coordinates. The gradient of some scalar function Φ is

$$\operatorname{grad} \Phi = \frac{\partial \Phi}{\partial s_1} i_1 + \frac{\partial \Phi}{\partial s_2} i_2 + \frac{\partial \Phi}{\partial s_3} i_3,$$

where i_1, i_2, i_3 are unit vectors along the corresponding coordinate lines. From formulas (2.4.11) it follows that

$$\operatorname{grad} \Phi = \frac{1}{h_1} \cdot \frac{\partial \Phi}{\partial q_1} i_1 + \frac{1}{h_2} \cdot \frac{\partial \Phi}{\partial q_2} i_2 + \frac{1}{h_3} \cdot \frac{\partial \Phi}{\partial q_3} i_3. \tag{2.4.18}$$

For further transformations the material of a course in mathematics on vector analysis may be used. The divergence of the velocity vector can be obtained by expressing it as a sum of components along coordinate lines

$$\overline{V}=V_1\,i_1+V_2\,i_2+V_3\,i_3=\sum_{n=1}^{3}V_n\,i_n. \tag{2.4.19}$$

Taking the divergence of both sides of this equation, we get

$$\operatorname{div}\overline{V}=\sum_{n=1}^{3}(V_n\operatorname{div}i_n+i_n\operatorname{grad}V_n). \tag{2.4.20}$$

The following well-known relation of vector analysis is used in determination of div i_n,

$$\operatorname{div}i_n=\operatorname{div}(i_m\times i_j)=i_j\operatorname{rot}i_m-i_m\operatorname{rot}i_j, \tag{2.4.21}$$

where n takes the successive values of $n=1, 2, 3$ corresponding to the values of $m=2, 3, 1$ and $j=3, 1, 2$. In this relation there appear the vectors rot i_m and rot i_j for which the general representation of rot i_n can be introduced. Keeping (2.4.18) in mind and using general methods of transformation of vector quantities, we find

$$\operatorname{rot}i_n=\frac{1}{h_n}\left(\frac{1}{h_j}\cdot\frac{\partial h_n}{\partial q_j}\,i_m-\frac{1}{h_m}\cdot\frac{\partial h_n}{\partial q_m}\,i_j\right). \tag{2.4.22}$$

Now we substitute (2.4.22) in (2.4.21). Naturally, for this substitution it is necessary to change index n in rot i_n to indices m and j and also to effect corresponding changes of indices on the right side of (2.4.22). Then we arrive at

$$\operatorname{div}i_n=\frac{1}{h_n}\left(\frac{1}{h_m}\cdot\frac{\partial h_m}{\partial q_n}+\frac{1}{h_j}\cdot\frac{\partial h_j}{\partial q_n}\right). \tag{2.4.23}$$

Now it is possible to substitute these equations in (2.4.20). Considering

$$i_n\operatorname{grad}V_n=\frac{1}{h_n}\cdot\frac{\partial V_n}{\partial q_n},$$

from (2.4.18) and using it in the above expressions, we get the following relation for divergence:

$$\operatorname{div}\overline{V}=\frac{1}{h_1\,h_2\,h_3}\left[\frac{\partial(V_1\,h_2\,h_3)}{\partial q_1}+\frac{\partial(V_2\,h_3\,h_1)}{\partial q_2}+\frac{\partial(V_3\,h_2\,h_1)}{\partial q_3}\right]. \tag{2.4.24}$$

Keeping this expression in mind, the transformation of continuity equation (2.4.1) to different forms of orthogonal curvilinear coordinates can be discussed.

Equation of continuity in cylindrical coordinates: In cylindrical coordinates Lame's parameters are given by the relations (2.4.16) and the values of q_n ($n=1, 2, 3$) are given by relations (2.4.12). The velocity components along the axes of cylindrical coordinates are:

$$V_1 = V_x = dx/dt,\ V_2 = V_r = dr/dt,\ V_3 = V_\gamma = r\,(d\gamma/dt). \tag{2.4.25}$$

Taking this into consideration, the divergence of the velocity vector in (2.4.24) will be

$$\operatorname{div} \overline{V} = \frac{\partial V_x}{\partial x} + \frac{\partial V_r}{\partial r} + \frac{1}{r} \cdot \frac{\partial V_\gamma}{\partial \gamma} + \frac{V_r}{r}. \tag{2.4.26}$$

The transformation formula

$$\frac{df}{dt} = \frac{\partial f}{\partial q_1} \cdot \frac{dq_1}{dt} + \frac{\partial f}{\partial q_2} \cdot \frac{dq_2}{dt} + \frac{\partial f}{\partial q_3} \cdot \frac{dq_3}{dt} + \frac{\partial f}{\partial t}, \tag{2.4.27}$$

where $f(x, y, z, t)$ is a function in Cartesian coordinates and may be used for transformation of derivative $d\rho/dt$ in equation of continuity (2.4.1) to the cylindrical coordinates. Then

$$\frac{d\rho}{dt} = \frac{\partial \rho}{\partial t} + \frac{dx}{dt} \cdot \frac{\partial \rho}{\partial x} + \frac{dr}{dt} \cdot \frac{\partial \rho}{\partial r} + \frac{d\gamma}{dt} \cdot \frac{\partial \rho}{\partial \gamma} = \frac{\partial \rho}{\partial t} + V_x \frac{\partial \rho}{\partial x} + V_r \frac{\partial \rho}{\partial r} + \frac{V_\gamma}{r} \cdot \frac{\partial \rho}{\partial \gamma}. \tag{2.4.28}$$

Introducing values of div V and $d\rho/dt$ in equation (2.4.1), one gets

$$\frac{\partial \rho}{\partial t} + \frac{\partial (\rho V_x)}{\partial x} + \frac{\partial (\rho V_r)}{\partial r} + \frac{1}{r} \cdot \frac{\partial (\rho V_\gamma)}{\partial \gamma} + \frac{\rho V_r}{r} = 0. \tag{2.4.29}$$

This equation could be written in somewhat different form:

$$r \frac{\partial \rho}{\partial t} + \frac{\partial (\rho r V_x)}{\partial x} + \frac{\partial (\rho r V_r)}{\partial r} + \frac{1}{r} \cdot \frac{\partial (\rho r V_\gamma)}{\partial \gamma} = 0. \tag{2.4.30}$$

For the particular case of a steady flow it will be

$$\frac{\partial (\rho r V_x)}{\partial x} + \frac{\partial (\rho r V_r)}{\partial r} + \frac{1}{r} \cdot \frac{\partial (\rho r V_\gamma)}{\partial \gamma} = 0. \tag{2.4.31}$$

For potential flow, the following relations could be substituted in the equation of continuity:

$$V_x = \partial\varphi/\partial x,\ V_r = \partial\varphi/\partial r,\ V_\gamma = (1/r) \cdot (\partial\varphi/\partial\gamma). \tag{2.4.25'}$$

If the motion of the gas is axisymmetric, like the flow past a rotating body at zero angle of attack, the flow parameters do not depend on the angular coordinates γ. The continuity equation will then have a still simpler form:

$$\frac{\partial (\rho r V_x)}{\partial x} + \frac{\partial (\rho r V_r)}{\partial r} = 0. \tag{2.4.32}$$

Equations (2.4.5) and (2.4.32) can be combined into one equation by writing

$$\frac{\partial (\rho y^\varepsilon V_x)}{\partial x} + \frac{\partial (\rho y^\varepsilon V_y)}{\partial y} = 0, \tag{2.4.32'}$$

where $\varepsilon = 0$ for two-dimensional plane motion and $\varepsilon = 1$, $y = r$ for two-dimensional axisymmetric flow.

Spherical coordinates: Using relation (2.4.24) and taking into account formulas (2.4.13) for spherical coordinates, relation (2.4.17) for Lame's parameters and the expressions for velocity components

$$V_1=V_r=\frac{dr}{dt},\quad V_2=V_\theta=\frac{1}{r}\cdot\frac{d\theta}{dt},\quad V_3=V_\psi=r\sin\theta\frac{d\psi}{dt}, \tag{2.4.33}$$

the divergence of velocity can be written as

$$\operatorname{div}\overline{V}=\frac{1}{r^2}\cdot\frac{\partial(V_r r^2)}{\partial r}+\frac{1}{r\sin\theta}\cdot\frac{\partial(V_\theta\sin\theta)}{\partial\theta}+\frac{1}{r\sin\theta}\cdot\frac{\partial V_\psi}{\partial\psi}. \tag{2.4.34}$$

The total derivative of density $d\rho/dt$, taking into account equation (2.4.27), could be represented in the following form:

$$\begin{aligned}\frac{d\rho}{dt}&=\frac{\partial\rho}{\partial t}+\frac{\partial\rho}{\partial r}\cdot\frac{dr}{dt}+\frac{\partial\rho}{\partial\theta}\cdot\frac{d\theta}{dt}+\frac{\partial\rho}{\partial\psi}\cdot\frac{d\psi}{dt}\\&=\frac{\partial\rho}{\partial t}+V_r\frac{\partial\rho}{\partial r}+\frac{V_\theta}{r}\cdot\frac{\partial\rho}{\partial\theta}+\frac{V_\psi}{r\sin\theta}\cdot\frac{\partial\rho}{\partial\psi}.\end{aligned} \tag{2.4.35}$$

Using values of div $\overline{V}$ from (2.4.34) and the derivative $d\rho/dt$ from (2.4.35) into (2.4.1) and grouping the terms properly, we will have

$$\frac{\partial\rho}{dt}+\frac{1}{r^2}\cdot\frac{\partial(\rho V_r r^2)}{\partial r}+\frac{1}{r\sin\theta}\cdot\frac{\partial(\rho V_\theta\sin\theta)}{\partial\theta}+\frac{1}{r\sin\theta}\cdot\frac{\partial(\rho V_\psi)}{\partial\psi}=0. \tag{2.4.36}$$

For a steady flow the partial derivative $\partial\rho/\partial t=0$. Consequently,

$$\frac{1}{r}\cdot\frac{\partial(\rho r^2 V_r)}{\partial r}+\frac{1}{\sin\theta}\cdot\frac{\partial(\rho V_\theta\sin\theta)}{\partial\theta}+\frac{1}{\sin\theta}\cdot\frac{\partial(\rho V_\psi)}{\partial\psi}=0. \tag{2.4.37}$$

In the case of an incompressible fluid ($\rho=$const) the above expression reduces to

$$\frac{1}{r}\cdot\frac{\partial(V_r r^2)}{\partial r}+\frac{1}{\sin\theta}\cdot\frac{\partial(V_\theta\sin\theta)}{\partial\theta}+\frac{1}{\sin\theta}\cdot\frac{\partial V_\psi}{\partial\psi}=0. \tag{2.4.38}$$

The following changes are used for transforming the continuity equation for the case of potential motion:

$$V_r=\frac{\partial\varphi}{\partial r},\quad V_\theta=\frac{1}{r}\cdot\frac{\partial\varphi}{\partial\theta},\quad V_\psi=\frac{1}{r\sin\theta}\cdot\frac{\partial\varphi}{\partial\psi}. \tag{2.4.39}$$

4.4 Equation of continuity for gas flow over curvilinear surface

Let us examine the particular form of continuity equation in orthogonal curvilinear coordinates that is applied in the study of a flow over a curvilinear wall. The x axis, in this system, coincides with the wall contour and the y axis is directed along the normal to this wall at a selected point. The coordinates of point P in a plane (Fig. 2.4.3) are equal to length x measured along

the wall and distance y along the normal to the wall respectively. Assume that the wall is a surface of rotation interacted by an axisymmetric flow of gas. The curvilinear coordinates of point P will be

$$q_1=x,\quad q_2=y,\quad q_3=\gamma. \tag{2.4.40}$$

The elemental arc-lengths of coordinate lines are

$$ds_1=[1+(y/R)]\,dx,\quad ds_2=dy,\quad ds_3=r\,d\gamma. \tag{2.4.41}$$

where r is the radial coordinate of point P measured along the normal to the axis of the rotating surface; R is the radius of curvature of the surface at a given cross section.

Then Lame's parameters will be

$$h_1=1+(y/R),\quad h_2=1,\quad h_3=r. \tag{2.4.42}$$

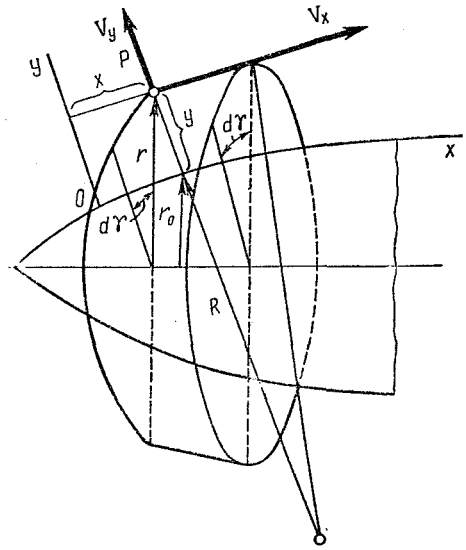

Fig. 2.4.3. Equation of continuity in curvilinear coordinates.

Now we use formula (2.4.24) for div $\overline{V}$, where the velocity components are

$$V_1=V_x=ds_1/dt=[1+(y/R)]\,dx/dt,\quad V_2=V_y=dy/dt,\quad V_3=0. \tag{2.4.43}$$

Substituting these values of velocity components in (2.4.24), we get

$$\operatorname{div}\overline{V}=\frac{1}{\left(1+\frac{y}{R}\right)r}\left\{\frac{\partial(V_x r)}{\partial x}+\frac{\partial\left[V_y r\left(1+\frac{y}{R}\right)\right]}{\partial y}\right\}. \tag{2.4.44}$$

The total derivative of density can be obtained by

$$\frac{d\rho}{dt}=\frac{\partial\rho}{\partial t}+\frac{\partial\rho}{\partial x}\cdot\frac{dx}{dt}+\frac{\partial\rho}{\partial y}\cdot\frac{dy}{dt}=\frac{\partial\rho}{\partial t}+\frac{V_x}{1+\frac{y}{R}}\cdot\frac{\partial\rho}{\partial x}+V_y\frac{\partial\rho}{\partial y}. \tag{2.4.45}$$

Incorporating expressions (2.4.44) and (2.4.45) in (2.4.1), the equation of continuity, after some modifications, will be obtained in the following form:

$$\frac{\partial\rho}{\partial t}r\left(1+\frac{y}{R}\right)+\frac{\partial(\rho r V_x)}{\partial x}+\frac{\partial\left[\rho r\left(1+\frac{y}{R}\right)V_y\right]}{\partial y}=0. \tag{2.4.46}$$

In investigating a gas flow near a wall with curvature in a thin layer on the surface (for example, in the boundary layer), the coordinate $y \ll R$. Consequently we have

$$\frac{\partial \rho}{\partial t} r + \frac{\partial (\rho r V_x)}{\partial x} + \frac{\partial (\rho r V_y)}{\partial y} = 0. \tag{2.4.47}$$

The equation so obtained is similar to that for a surface with no curvature. In the case of a steady flow we get

$$\frac{\partial (\rho r V_x)}{\partial x} + \frac{\partial (\rho r V_y)}{\partial y} = 0. \tag{2.4.48}$$

For a flow near a plane curvilinear surface the continuity equation will have the following form:

$$\frac{\partial \rho}{\partial t}\left(1 + \frac{y}{R}\right) + \frac{\partial (\rho V_x)}{\partial x} + \frac{\partial \{\rho V_y [1 + (y/R)]\}}{\partial y} = 0. \tag{2.4.49}$$

For $y \ll R$ it will be approximately given by

$$\frac{\partial \rho}{\partial t} + \frac{\partial (\rho V_x)}{\partial x} + \frac{\partial (\rho V_y)}{\partial y} = 0. \tag{2.4.50}$$

Thus for a flow near a wall the continuity equation in curvilinear coordinates will be the same as in the case of Cartesian coordinates.

For a steady flow $\partial \rho / \partial t = 0$, so the equation of continuity will be

$$\frac{\partial (\rho V_x)}{\partial x} + \frac{\partial (\rho V_y)}{\partial y} = 0. \tag{2.4.50'}$$

Equations (2.4.48), (2.4.50') can be combined into one equation as below:

$$\frac{\partial (\rho V_x r^\varepsilon)}{\partial x} + \frac{\partial (\rho V_y r^\varepsilon)}{\partial y} = 0, \tag{2.4.48'}$$

where $\varepsilon = 0$ for two-dimensional plane motion and $\varepsilon = 1$ for two-dimensional axisymmetric flow.

4.5 Equation of mass flow

Consider the particular form of continuity equation for a steady fluid flow in the form of a jet. The mass of fluid in some fixed volume enclosed by the jet surface and the plane cross sections does not change with time because at each point in the flow the condition of $\partial \rho / \partial t = 0$ is satisfied. Then the quantity of fluid entering the volume across a plane cross section of area S_1 per unit time will be equal to $\rho_1 V_1 S_1$. This is the same as the mass of fluid $\rho_2 V_2 S_2$ flowing out through the opposite section with area S_2 (ρ_1, ρ_2 are densities and V_1, V_2 are velocities at the first and second cross sections of the jet respectively). Thus $\rho_1 V_1 S_1 = \rho_2 V_2 S_2$. As this equality can be applied to any section it

can be written in general form as

$$\rho VS = \text{const.} \tag{2.4.51}$$

This equation is known as an equation of mass flow.

5. Stream Function

The study of irrotational gas flow can be simplified if it is connected with the solution of only one unknown potential function which fully determines this flow (see Section 3). It will be shown that for certain types of rotational flow there exists a function that also determines its kinetic characteristics.

Let us take a two-dimensional (plane or axisymmetric) steady rotational flow of fluid. From continuity equation (2.4.32′) it can be shown that some function ψ of coordinates x, y exists that can be determined by the relations:

$$\partial\psi/\partial y = \rho y^{\epsilon} V_x, \quad \partial\psi/\partial x = -\rho y^{\epsilon} V_y. \tag{2.5.1}$$

Then from (2.4.32′) it follows that $\partial^2\psi/\partial y\partial x = \partial^2\psi/\partial x\partial y$, i.e. this identity is obtained. Substituting (2.5.1) in the equation of stream line $V_y/dy = V_x/dx$, which can be expressed in the form

$$\rho y^{\epsilon} V_y\, dx - \rho y^{\epsilon} V_x\, dy = 0, \tag{2.5.2}$$

we get

$$\frac{\partial\psi}{\partial x}\, dx + \frac{\partial\psi}{\partial y}\, dy = 0.$$

From this it follows that equation (2.5.2) represents the differential of function ψ and hence

$$d\psi = 0. \tag{2.5.3}$$

Integrating (2.5.3), the equation of stream line is obtained in the form:

$$\psi(x, y) = \text{const.} \tag{2.5.4}$$

The function ψ, known as a stream function, completely determines the velocity of rotational flow by the relations

$$V_x = \frac{1}{\rho y^{\epsilon}} \cdot \frac{\partial\psi}{\partial y}, \quad V_y = -\frac{1}{\rho y^{\epsilon}} \cdot \frac{\partial\psi}{\partial x}. \tag{2.5.5}$$

It should be noted that it is necessary to take $\varepsilon = 0$ for a plane flow and $\varepsilon = 1$, $y = r$ for a three-dimensional axisymmetric flow.

The family of stream lines for a potential flow can also be characterized by a function $\psi = \text{const}$, which is related to velocity potential by relations

$$\frac{\partial\varphi}{\partial x} = \frac{1}{\rho y^{\epsilon}} \cdot \frac{\partial\psi}{\partial y}, \quad \frac{\partial\varphi}{\partial y} = -\frac{1}{\rho y^{\epsilon}} \cdot \frac{\partial\psi}{\partial x}. \tag{2.5.6}$$

Assuming $\rho=\text{const}$, in (2.5.5) and (2.5.6), we get the corresponding expressions for an incompressible flow:

$$V_x=\frac{1}{y^\epsilon}\cdot\frac{\partial\psi}{\partial y},\quad V_y=-\frac{1}{y^\epsilon}\cdot\frac{\partial\psi}{\partial x}; \tag{2.5.7}$$

$$\frac{\partial\varphi}{\partial x}=\frac{1}{y^\epsilon}\cdot\frac{\partial\psi}{\partial y},\quad \frac{\partial\varphi}{\partial y}=-\frac{1}{y^\epsilon}\cdot\frac{\partial\psi}{\partial x}. \tag{2.5.8}$$

Assuming $\varepsilon=0$ in these last equations we get equations for an incompressible plane flow:

$$\partial\varphi/\partial x=\partial\psi/\partial y,\quad \partial\varphi/\partial y=-\partial\psi/\partial x. \tag{2.5.9}$$

Knowing the velocity potential, the stream function can be determined from these equations with an accuracy to the arbitrary constant and vice versa.

In a potential flow the family of equipotential lines (in a plane flow) or equipotential surfaces (in an axisymmetric flow) can be drawn besides the stream lines. This family of lines or surfaces can be determined by the equation $\varphi=\text{const}$.

Let us examine the vectors

$$\text{grad}\,\varphi=\frac{\partial\varphi}{\partial x}i+\frac{\partial\varphi}{\partial y}j \text{ and } \text{grad}\,\psi=\frac{\partial\psi}{\partial x}i+\frac{\partial\psi}{\partial y}j,$$

whose directions coincide with the directions of normals to the curves $\varphi=\text{const}$ and $\psi=\text{const}$ respectively. The scalar product of these vectors is

$$\text{grad}\,\varphi\cdot\text{grad}\,\psi=\frac{\partial\varphi}{\partial x}\cdot\frac{\partial\psi}{\partial x}+\frac{\partial\varphi}{\partial y}\cdot\frac{\partial\psi}{\partial y}.$$

Taking into account formulas (2.3.2) and (2.5.5), it can be shown that this scalar product is equal to zero. It follows that stream lines will be orthogonal to equipotential lines (in a plane flow) or to equipotential surfaces (in an axisymmetric flow).

6. Vortex Lines

A curve S drawn in a flow field at a given moment of time such that at each point the angular velocity vector $\bar{\omega}$ coincides with the tangent to this curve at that point is called a vortex line.

A vortex line is developed in a similar way to a stream line (see Fig. 2.1.1). The difference between them is that in place of uniform velocity vectors the angular velocity vectors ($\bar{\omega}_1$, $\bar{\omega}_2$, etc.) for rotation of particles are considered for vortex lines. So now the vector product $\bar{\omega}\times d\bar{S}=0$, i.e.

$$\begin{vmatrix} i & j & k \\ \omega_x & \omega_y & \omega_z \\ dx & dy & dz \end{vmatrix}=i(\omega_y\,dz-\omega_z\,dy)-j(\omega_x\,dz-\omega_z\,dx)+k(\omega_x\,dy-\omega_y\,dx)=0.$$

Keeping in mind that, for example, $\omega_y\,dz-\omega_z dy=0$, etc., we get the equation of the vortex line from the above condition

$$dx/\omega_x=dy/\omega_y=dz/\omega_z. \tag{2.6.1}$$

A vortex tube can be obtained by drawing vortex lines through the points on an elementary contour with cross sectional area σ. The product of $\omega\sigma$ is called the intensity or strength of the vortex tube or of the vortex.

We will now prove that the intensity of the vortex tube is constant at all its sections. For this purpose we will use the analogy of an incompressible fluid flow. For the case of incompressible fluid motion it was shown that div $\overline{V}=0$. The mass flow rate of jet $V_1S_1=V_2S_2=\ldots=VS=$constant is an example of this equation.

Let us study the vortex motion and the expression for divergence of the angular velocity vector,

$$\operatorname{div}\overline{\omega}=\frac{\partial\omega_x}{\partial x}+\frac{\partial\omega_y}{\partial y}+\frac{\partial\omega_z}{\partial z}.$$

Substituting here the values of components of $\overline{\omega}$ from (2.2.3), (2.2.6) we get the expression div $\overline{\omega}=0$ under the condition that the second derivatives of of V_x, V_y, V_z should be continuous. Using the analogy of the equation of mass flow rate $VS=$const, we get the equation of flow for vector $\overline{\omega}$ along a vortex tube in the form

$$\omega_1\sigma_1=\omega_2\sigma_2=\ldots=\omega\sigma=\text{const}. \tag{2.6.2}$$

This equation represents Helmholtz's theorem that the vortex strength remains constant along the vortex tube. From this theorem there follows the property of a vortex tube that it cannot suddenly terminate or end in a point. The latter is based on the fact that as the area of the cross section of a vortex tube $\sigma\to 0$ the angular velocity ω tends to infinity by Helmholtz's theorem, which is physically impossible.

7. Circulation of Velocity

7.1 Concept of the circulation of velocity

The concept of the circulation of velocity is very important in aerodynamics. It is used to investigate the flow interaction of an aircraft and, in particular, to determine the lift force acting on a wing.

Let us consider some known closed contour K in a fluid flow. Assume that the velocity $\overline{V}$ at each point on this contour is known. Let us now find the integral along this contour

$$\Gamma=\int_{(K)}\overline{V}\,d\overline{s}, \tag{2.7.1}$$

where $\bar{V}.\ d\bar{s}$ is the scalar product of two vectors $\bar{V}$ and $d\bar{s}$. The quantity Γ calculated in this way is known as circulation of velocity around a closed contour. As $\bar{V}=V_x i+V_y j+V_z k$ and $d\bar{s}=dxi+dyj+dzk$, the above integral may be written as

$$\Gamma=\int_{(K)} V_x\,dx+V_y\,dy+V_z\,dz. \tag{2.7.2}$$

Now, taking into account that the scalar product $\bar{V}d\bar{s}=V\cos(\widehat{\bar{V}d\bar{s}})\,ds=V_s ds$, where V_s is the projection of velocity on the tangent to the given contour at a given point, then

$$\Gamma=\int_{(K)} V_s\,ds. \tag{2.7.3}$$

If the contour coincides with the stream line of circular form of radius r, at each point of which the velocity V_s is constant in magnitude and direction, then

$$\Gamma=2\pi r V_s. \tag{2.7.4}$$

The circulation of velocity in an irrotational flow can be expressed in terms of velocity potential. Assuming that $V_x dx+V_y dy+V_z dz=d\varphi$, we get, for an open contour L,

$$\Gamma=\int_{(L)} d\varphi=\varphi_A-\varphi_B, \tag{2.7.5}$$

where φ_A and φ_B are the values of the potential function at the ends of the contour. For a closed contour φ_A and φ_B represent the values of velocity potential at points A and B on the contour which coincide with one another. If the potential function is single-valued $\varphi_A=\varphi_B$ and the circulation of velocity around the closed contour is equal to zero; a multi-valued velocity potential ($\varphi_A\neq\varphi_B$) gives a value of circulation different from zero.

7.2 Stokes' theorem

Let us consider an elementary contour $ABCD$ (see Fig. 2.2.1) and find the circulation around this contour. Assume that the velocities are constant along each side and are given by the following values:

$$V_x\,(AB),\ V_y+\frac{\partial V_y}{\partial x}dx\,(BC),\ V_x+\frac{\partial V_x}{\partial y}dy\,(CD),\ V_y\,(AD).$$

Taking anticlockwise circumvention of the contour as positive (from the x axis toward the y axis), we get for circulation

$$d\Gamma_z=V_x\,dx+\left(V_y+\frac{\partial V_y}{\partial x}dx\right)dy-\left(V_x+\frac{\partial V_x}{\partial y}dy\right)dx-V_y\,dy,$$

or

$$d\Gamma_z=\left(\frac{\partial V_y}{\partial x}-\frac{\partial V_x}{\partial y}\right)dxdy.$$

According to (2.2.3) the value in brackets is equal to double the value of the component of angular velocity about the z axis, i.e. $2\omega_z$. Consequently

$$d\Gamma_z=2\,\omega_z\,dxdy. \tag{2.7.6}$$

Similarly it can be shown that

$$d\Gamma_x=2\omega_x\,dydz, \quad d\Gamma_y=2\omega_y\,dxdz.$$

The products of differentials in these expressions represent areas contained in the corresponding elementary contours. Taking into account the results obtained above for an area $d\sigma$ arbitrarily oriented in space and restricted within an elementary contour, the circulation may be given by

$$d\Gamma_n=2\,\omega_n d\sigma, \tag{2.7.7}$$

where ω_n is the component of the angular velocity about the direction of normal n to the elementary area $d\sigma$. From (2.7.7) it can be seen that the circulation of velocity around any closed contour is equal to twice the value of the intensity of vorticity lying inside the contour.

The relation (2.7.7) can be extended to the case of contour L of finite size having some surface area S for which the value ω_n is known at each point. Then the circulation of velocity around the contour is

$$\Gamma=2\iint\limits_{(S)}\omega_n\,d\sigma. \tag{2.7.8}$$

Formula (2.7.8) represents Stokes' theorem: the circulation of velocity around a given closed contour L is equal to twice the value of the integral of intensities of vortices through the surface enclosed in the contour. The quantity on the right-hand side is called the vortex strength and is designated by

$$\kappa=2\iint\limits_{(S)}\omega_n\,d\sigma. \tag{2.7.8'}$$

If the circulation Γ in (2.7.8) is replaced by the formula (2.7.3) we get a relation representing the integral along the contour K by an integral over the surface S enclosed by the same contour K,

$$\int\limits_{(K)}V_s\,ds=2\iint\limits_{(S)}\omega_n\,d\sigma. \tag{2.7.8''}$$

The above relations are given for a singly connected contour (the region being considered is limited by one contour, Fig. 2.7.1, a). However, Stokes' theorem can also be extended to multi-connected contours (the region is surrounded by one external and some internal contours). Here equation (2.7.8'')

is applicable under the conditions that the external contour is connected with the internal contours by auxiliary lines (section) so that the singly-connected region may be obtained. Then the double integral in (2.7.8′) can be extended to the shaded region (Fig. 2.7.1, b) and the line integral is taken around the singly-connected region so obtained, i.e. around the external contour along all sections and also along all internal contours. In accordance with this and by formula (2.7.8″) and also from Fig. 2.7.1, b, where a triply-connected region is shown, we get

$$\Gamma_K - \Gamma_{K_1} - \Gamma_{K_2} = 2 \iint\limits_{(S)} \omega_n \, ds,$$

from which the circulation around contour K for the given region will be

$$\Gamma_K = \Gamma_{K_1} + \Gamma_{K_2} + 2 \iint\limits_{(S)} \omega_n \, ds.$$

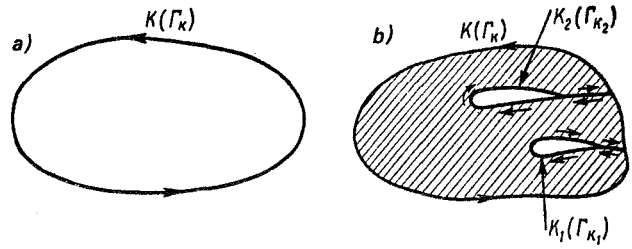

Fig. 2.7.1. Singly connected and triply-connected regions in plane:
a—singly-connected region (Γ_K—circulation along contour K);
b—triply-connected region (Γ_K—circulation along external contour; Γ_{K1} and Γ_{K2}–circulations along internal contour K_1 and K_2 respectively).

Extending this formula to the case of n internal contours, we find

$$\Gamma_K = \sum_{i}^{i=n} \Gamma_{K_i} + 2 \iint\limits_{(S)} \omega_n \, ds.$$

7.3 Velocities induced by vortices

The vortices appearing in a fluid create velocities in the surrounding space. This effect is similar to the electromagnetic effect of a conductor carrying electric current. Velocities created by a vortex are called induced velocities.

The electromagnetic analogy above acknowledges the fact that the Biot-Savart formula, used to determine velocity induced by a vortex, is similar to that representing the law of electromagnetic induction established by Biot-Savart.

Let us consider a curvilinear vortex of arbitrary form (Fig. 2.7.2). The velocity vector $d\bar{w}$ induced at a point A by an element of vortex $d\bar{L}$ is determined by the radius vector $\bar{r}$ and coincides with the direction of vector product $\bar{r}\times d\bar{L}$, i.e. the vector $d\bar{w}$ is perpendicular to the plane containing vectors $\bar{r}$ and $d\bar{L}$. The value of $d\bar{w}$ is determined by means of the Biot-Savart formula which has the following form in vector notations:

$$d\bar{w}=\frac{\Gamma}{4\pi}\cdot\frac{\bar{r}\times d\bar{L}}{r^3}, \tag{2.7.9}$$

where Γ is circulation of velocity, equal to double the value of the intensity of the vortex. Conclusions of formula (2.7.9) can be found in the book [23].

Since $\bar{r}\times d\bar{L}=r\sin a\ dL$, where a is the angle between the direction of an element of the vortex and the radius vector $\bar{r}$, the value of induced velocity at a point A is given by

$$dw=\frac{\Gamma}{4\pi}\cdot\frac{\sin a\ dL}{r^2}\cdot \tag{2.7.10}$$

Let us apply the Biot-Savart formula for calculation of the velocity induced by the section of line vortex (Fig. 2.7.3).

Since $r=h/\sin a$, $dL=rda/\sin a=hda/\sin^2 a$, we have

$$w=\frac{\Gamma}{4\pi h}\int_{a_1}^{a_2}\sin a\ da=\frac{\Gamma}{4\pi h}(\cos a_1-\cos a_2). \tag{2.7.11}$$

For a vortex with both ends extending to infinity (infinite vortex) $a_1=0$, $a_2=\pi$ and consequently

$$w=\frac{\Gamma}{2\pi h}\cdot \tag{2.7.12}$$

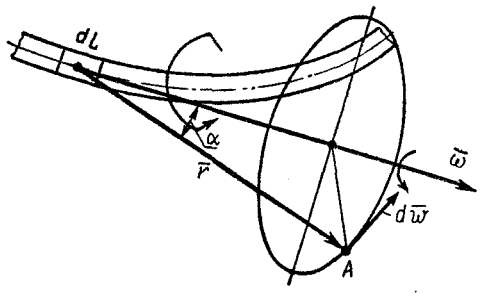

Fig. 2.7.2. Scheme of vortex-interaction.

For a vortex with one end extending to infinity and the other at the origin point A (semi-infinite vortex) $a_1=0$, $a_2=\pi/2$. Therefore

$$w=\Gamma/4\pi h. \tag{2.7.13}$$

If there are two or more vortices in a fluid they interact with each other. As a result the vortex system will be in motion. The velocities of this motion are determined with the help of the Biot-Savart formula. Consider, as an

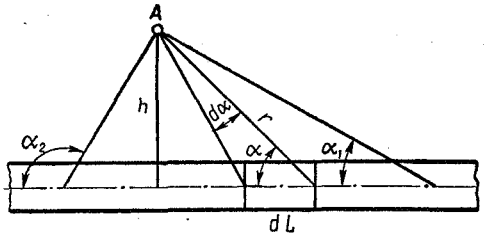

Fig. 2.7.3. Effect of line vortex on fluid particle situated at point A.

example, two infinite vortices having equal intensity and direction of rotation (Fig. 2.7.4, a). These vortices impart velocities $V_2 = -(\Gamma/2\pi h)$ and $V_1 = \Gamma/2\pi h$ to each other, which are equal in magnitude and opposite in direction. As a result of this both vortices will rotate about an axis passing through the midpoint between them. If one of the two vortices has an intensity of vortex opposite in sign (Fig. 2.7.4, b) the induced velocities will be in the same direction and consequently the system of vortices will be displaced uniformly with velocity $V = \Gamma/2\pi h$ in a direction perpendicular to the line joining these vortices.

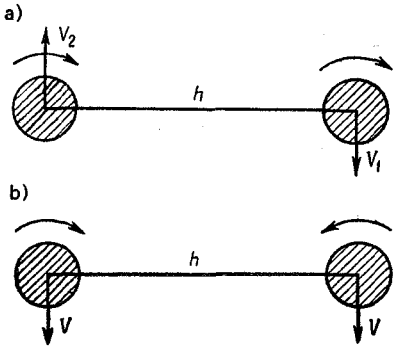

Fig. 2.7.4. Interaction between vortices: *a*—vortices with same direction of rotation; *b*—with opposite directions of rotation.

8. Complex Potential

The motion of an incompressible potential flow can be completely determined if the potential function φ or stream function ψ is known. The relation between these two functions is given by equations (2.5.9), which are known as the Cauchy-Riemann equations in the theory of functions of complex variables. These equations represent the necessary and sufficient conditions such that the combination of the two functions $\varphi + i\psi$ happens to be the analytical function of complex variable $z = x + iy$, i.e. the functions can be differentiated at all points of the given domain. Let us introduce the symbol for this function:

$$W(z) = \varphi + i\psi. \tag{2.8.1}$$

The function $W(z)$, which can be determined if the functions of the two real variables $\varphi = \varphi(x, y)$ and $\psi = \psi(x, y)$ satisfy the differential equations (2.5.9), is called the complex potential. If the values of the function $\varphi(x, y)$ or $\psi(x, y)$ are known uniquely in the flow field the complete two-dimensional plane flow

can be obtained by the complex potential. Hence the problem of estimating such a flow can be reduced to the determination of function $W(z)$.

Let us find the derivative of function $W(z)$ with respect to the complex variable z:

$$\frac{dW}{dz}=\frac{\partial\varphi}{\partial x}+i\frac{\partial\psi}{\partial x}\,. \tag{2.8.2}$$

Since $\partial\varphi/\partial x=V_x$, $\partial\psi/\partial x=-V_y$,

$$dW/dz=V_x-iV_y. \tag{2.8.3}$$

This expression is known as the complex velocity, the modulus of which gives the velocity itself, i.e. $|dW/dz|=\sqrt{V_x^2+V_y^2}=V$. It is obvious that the actual velocity vector $\overline{V}=V_x+iV_y$ happens to be the reflection about the x axis of the vector of complex velocity.

Denoting the angle between the vector dW/dz and the x axis by θ, the velocity components will be $V_x=V\cos\theta$ and $V_y=V\sin\theta$.

Using Euler's formula

$$\cos\theta-i\sin\theta=e^{-i\theta},$$

we get

$$dW/dz=Ve^{-i\theta}. \tag{2.8.4}$$

9. Typical Fluid Flows

Let us consider simple incompressible fluid flows, their geometrical pattern (aerodynamic specter), expressions for complex potentials and the corresponding potential functions and stream functions.

9.1 Uniform flow

Let the fluid motion be given by a complex potential

$$W(z)=V(\cos\theta-i\sin\theta)\,z, \tag{2.9.1}$$

where V and θ are some quantities constant under given conditions. In accordance with (2.8.1)

$$\varphi+i\psi=V(\cos\theta-i\sin\theta)\,(x+iy),$$

from which the velocity potential and stream function are obtained:

$$\varphi=V(x\cos\theta+y\sin\theta); \tag{2.9.2}$$

$$\psi=V(y\cos\theta-x\sin\theta). \tag{2.9.3}$$

It follows from the expressions for φ and ψ that the given flow is plane and steady because time does not appear here as a parameter. The stream lines and the streak lines coincide in such a flow.

The velocity components of flow can be found from (2.9.2):

$$\partial\varphi/\partial x=V_x=V\cos\theta,\quad \partial\varphi/\partial y=V_y=V\sin\theta,\quad \partial\varphi/\partial z=V_z=0. \tag{2.9.4}$$

Here V is the resultant velocity of flow and θ is the angle between its direction and the x axis. Equating stream function ψ (2.9.3) with constant, including in it the velocity V, we get the equation

$$y \cos \theta - x \sin \theta = \text{const}, \tag{2.9.5}$$

from which it can be seen that the stream lines themselves represent the parallel lines inclined to the x axis by an angle θ (Fig. 2.9.1). Since the velocity components V_x and V_y are positive the flow direction will be that shown in Fig. 2.9.1. This kind of flow is known as plane uniform flow.

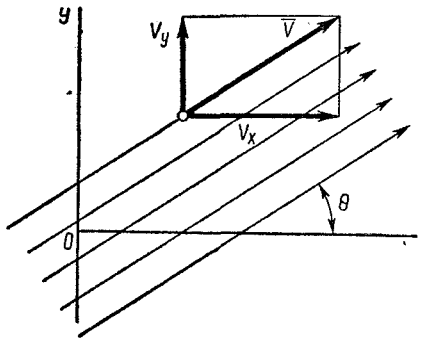

Fig. 2.9.1. Steady uniform flow.

In a particular case where the flow is parallel to the x axis ($\theta = 0$, $V_x = V$, $V_y = 0$) the complex potential will be

$$W(z) = V_z. \tag{2.9.6}$$

9.2 Plane source and sink

Consider the complex potential

$$W(z) = (q/2\pi) \ln z, \tag{2.9.7}$$

where q is a constant quantity. This equation can be rewritten in the form

$$\varphi + i\psi = (q/2\pi) \ln (re^{i\theta}) = (q/2\pi)(\ln r + i\theta),$$

where r is the distance to the point with coordinates x, y (polar radius), θ is the polar angle. From the equation obtained above it follows that

$$\varphi = (q/2\pi) \ln r = \frac{q}{2\pi} \ln \sqrt{x^2 + y^2}; \tag{2.9.8}$$

$$\psi = (q/2\pi)\theta. \tag{2.9.9}$$

From (2.9.8) we find that the radial component of velocity (along radius r) is

$$\partial\varphi/\partial r = V_r = q/2\pi r, \tag{2.9.10}$$

and the component along the normal to this radius

$$V_s = 0.$$

The flow so obtained consists of stream lines (trajectories) representing a family of straight lines passing through the origin of coordinates (this follows from the equation of stream line $\psi =$ const). This radial flow starting from

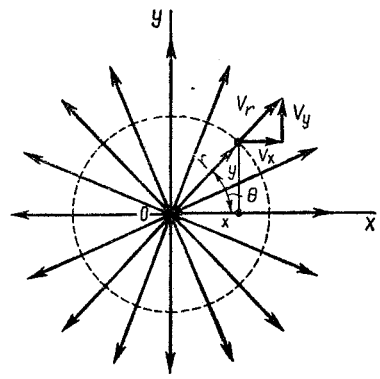

Fig. 2.9.2. Plane point source.

the origin of coordinates is called the plane source (Fig. 2.9.2).

The fluid flow rate across a contour of radius r will be equal to $2\pi r V_r = Q$. Substituting here the value of V_r from (2.9.10), we get $Q = q$. Consequently the constant q is determined by the fluid flow rate of the source. This quantity q is known as the strength or intensity of source.

There exists a fluid flow, along with the source, called the plane sink. The complex potential of sink is

$$W(z) = -(q/2\pi) \ln z. \tag{2.9.11}$$

The minus sign indicates that unlike a source flow the fluid flow for sink will be toward the center. Sink, in the same way as source, is characterized by strength or intensity q (flow rate in unit time).

9.3 Three-dimensional source (sink)

Three-dimensional source (sink) occurs in a similar way to plane source (sink). The flow from such a source (sink) is given by the following conditions:

$$V_x = \frac{q}{4\pi} \cdot \frac{\pm x}{R^3}, \quad V_y = \frac{q}{4\pi} \cdot \frac{\pm y}{R^3}, \quad V_z = \frac{q}{4\pi} \cdot \frac{\pm z}{R^3}, \tag{2.9.12}$$

where $R = \sqrt{x^2+y^2+z^2}$; q is the intensity of source (plus sign) or sink (minus sign). The intensity of source (sink) is equal to the quantity q determined as the flow rate per second through a spherical surface of radius R. The total velocity is

$$V = \sqrt{V_x^2 + V_y^2 + V_z^2} = \pm q/4\pi R^2 \tag{2.9.13}$$

and it coincides with the direction of radius vector R. Therefore the velocity potential depends only on R and can be written as

$$\frac{\partial \varphi}{\partial R} = \frac{\pm q}{4\pi R^2}.$$

After integration it leads to

$$\varphi = \mp q/4\pi R, \tag{2.9.14}$$

where the minus sign is for source and plus sign for sink.

9.4 Dipole

Consider a flow for which the complex potential is

$$W(z) = \frac{M}{2\pi} \cdot \frac{1}{z}, \tag{2.9.15}$$

where M is a constant quantity. From this equation we can write

$$\varphi + i\psi = \frac{M}{2\pi} \cdot \frac{1}{re^{i\theta}}.$$

Transform the right side of this equation. Bearing in mind that

$$\frac{1}{re^{i\theta}}=\frac{1}{r(\cos\theta+i\sin\theta)}=\frac{1}{r}(\cos\theta-i\sin\theta),$$

one gets

$$\varphi+i\psi=(M/2\pi r)(\cos\theta-i\sin\theta).$$

From this it is found that

$$\varphi=\frac{M}{2\pi}\cdot\frac{\cos\theta}{r}, \tag{2.9.16}$$

$$\psi=-\frac{M}{2\pi}\cdot\frac{\sin\theta}{r}. \tag{2.9.17}$$

Assuming $\psi=\text{const}$ and taking into account that $r=\sqrt{x^2+y^2}$ and $\sin\theta=y/r=y/\sqrt{x^2+y^2}$, the equation of the family of stream lines for a given flow will be

$$y/(x^2+y^2)=\text{const}. \tag{2.9.18}$$

The family of stream lines represents an infinite series of circles each passing through the origin of coordinates with centers on the y axis (Fig. 2.9.3, a).

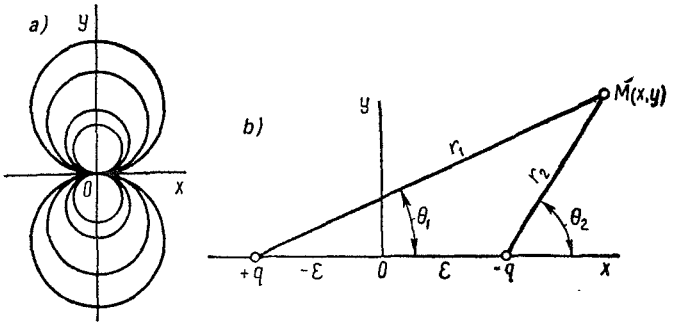

Fig. 2.9.3. Determination of dipole:
a—stream lines of dipole; *b*—scheme of formation of dipole.

To get the physical picture we assume a flow resulting from the superposition of flows from a source and a sink of equal strength situated on the x axis at a very small distance ε from the origin of coordinates (Fig. 2.9.3, b). The velocity potential at a point $M(x, y)$ due to flow from source at a distance r_1 will be $\varphi_{\text{source}}=(q/2\pi)\ln r_1$. Similarly the velocity potential at point M due to sink at a distance r_2 from this point will be $\varphi_{\text{sink}}=(-q/2\pi)\ln r_2$.

The principle of superposition of incompressible flows can be used to determine the resultant flow from a source and a sink. The velocity potential of the resultant flow by this principle $\varphi=\varphi_{\text{source}}+\varphi_{\text{sink}}$. In line with the

equation of continuity (Laplace equation) the following relation is obtained from (2.4.8′):

$$\frac{\partial^2\varphi}{\partial x^2}+\frac{\partial^2\varphi}{\partial y^2}=\frac{\partial^2(\varphi_{\text{source}}+\varphi_{\text{sink}})}{\partial x^2}+\frac{\partial^2(\varphi_{\text{source}}+\varphi_{\text{sink}})}{\partial y^2}=0.$$

Since the functions φ_{source} and φ_{sink} satisfy the equations

$$\frac{\partial^2\varphi_{\text{source}}}{\partial x^2}+\frac{\partial^2\varphi_{\text{source}}}{\partial y^2}=0 \text{ and } \frac{\partial^2\varphi_{\text{sink}}}{\partial x^2}+\frac{\partial^2\varphi_{\text{sink}}}{\partial y^2}=0,$$

the value of $\partial^2\varphi/\partial x^2+\partial^2\varphi/\partial y^2$ is also uniformly equal to zero. Consequently the resultant function φ satisfies the equation of continuity. The resultant potential due to source and sink, then, is

$$\varphi=\frac{q}{2\pi}\ln\frac{r_1}{r_2}\cdot$$

As $r_1=\sqrt{(x+\varepsilon)^2+y^2}$, $r_2=\sqrt{(x-\varepsilon)^2+y^2}$, we get

$$\ln\frac{r_1}{r_2}=\frac{1}{2}\ln\frac{(x+\varepsilon)^2+y^2}{(x-\varepsilon)^2+y^2} \text{ or } \ln\frac{r_1}{r_2}=\frac{1}{2}\ln\left[1+\frac{4x\varepsilon}{(x-\varepsilon)^2+y^2}\right].$$

The value of ε can be selected so that the second term in brackets will be small compared to unity. Applying the formula for expansion of a logarithmic series and neglecting terms of higher order, we get

$$\varphi=\frac{q}{2\pi}\cdot\frac{x\varepsilon}{(x-\varepsilon)^2+y^2}\cdot \tag{2.9.19}$$

Let the source and sink come closer ($\varepsilon\to 0$) and at the same time their intensities increase in such a way that the product $q\cdot 2\varepsilon$, in the limit of source and sink approaching each other, tends to some finite quantity M. The combined flow appearing as a result of this is called the dipole. The quantity M characterizing this flow is called the strength of the dipole and the x axis, the axis of the dipole. In equation (2.9.19), for φ using the limit of $\varepsilon\to 0$ and $2q\varepsilon\to M$, one can get the expression for the dipole,

$$\varphi=\frac{M}{2\pi}\cdot\frac{x}{x^2+y^2}=\frac{M}{2\pi}\cdot\frac{\cos\theta}{r},$$

which coincides with (2.9.16). So the flow under study, characterized by the complex potential (2.9.15), happens to be for dipole. The same thing can be shown if we consider the stream function of a mixed flow that coincides with (2.9.17). It can easily be seen that the formulas (2.9.16) and (2.9.17) can also be expressed in the form:

$$\varphi=\frac{M}{2\pi}\cdot\frac{\partial}{\partial x}(\ln\sqrt{x^2+y^2})=\frac{M}{2\pi}\cdot\frac{\partial\ln r}{\partial r}\cos\theta; \tag{2.9.16′}$$

$$\psi = -\frac{M}{2\pi} \cdot \frac{\partial}{\partial y}(\ln \sqrt{x^2+y^2}) = -\frac{M}{2\pi} \cdot \frac{\partial \ln r}{\partial r} \sin\theta. \qquad (2.9.17')$$

Performing differentiation of (2.9.16), we determine the velocity components of dipole:

$$\frac{\partial \varphi}{\partial r} = V_r = -\frac{M}{2\pi} \cdot \frac{\cos\theta}{r^2}, \quad \frac{1}{r} \cdot \frac{\partial \varphi}{\partial \theta} = V_s = -\frac{M}{2\pi} \cdot \frac{\sin\theta}{r^2}. \qquad (2.9.20)$$

Let us take a three-dimensional case. As in (2.9.14), the potential function for the flow created by the source and sink of equal strength q, which are placed on axis Or ($r=\sqrt{y^2+z^2}$) at points $r=-\varepsilon$ and $r=+\varepsilon$, will be

$$\varphi = \frac{q}{4\pi}\left(\frac{1}{R_2} - \frac{1}{R_1}\right) = \frac{q}{4\pi}\left[\frac{1}{\sqrt{(r-\varepsilon)^2+x^2}} - \frac{1}{\sqrt{(r+\varepsilon)^2+x^2}}\right]. \qquad (2.9.20')$$

For small values of ε we have

$$(r \mp \varepsilon)^2 + x^2 \approx x^2 + r^2 \mp 2r\varepsilon,$$

and the quantity

$$\frac{1}{\sqrt{(r\mp\varepsilon)^2+x^2}} = \frac{1}{\sqrt{x^2+r^2}} \cdot \frac{1}{\sqrt{1 \mp \frac{2r\varepsilon}{x^2+r^2}}} \approx \frac{1 \pm \frac{r\varepsilon}{x^2+r^2}}{\sqrt{x^2+r^2}}.$$

By substituting these in (2.9.20') we get

$$\varphi = \frac{q}{4\pi} \cdot \frac{2r\varepsilon}{(x^2+r^2)^{3/2}}.$$

If we take the limit of $\varepsilon \to 0$ and assume that the product $q \cdot 2\varepsilon$ tends to a finite quantity M, the velocity potential from the above expression for a flow created by dipole with strength M will be

$$\varphi = \frac{M}{4\pi} \cdot \frac{r}{(x^2+r^2)^{3/2}}, \qquad (2.9.21)$$

or

$$\varphi = -\frac{M}{4\pi} \cdot \frac{\partial}{\partial r}\left(\frac{1}{R}\right). \qquad (2.9.21')$$

If the source and sink of equal strength q are located on axis Ox at the points $x=-\varepsilon$ and $x=+\varepsilon$, then at $\varepsilon \to 0$ the velocity potential of dipole is

$$\varphi = \frac{M}{4\pi} \cdot \frac{x}{(x^2+r^2)^{3/2}} = -\frac{M}{4\pi} \cdot \frac{\partial}{\partial x}\left(\frac{1}{R}\right). \qquad (2.9.21'')$$

9.5 Flow with circulation (vortex)

Let us study the flow given by a complex potential

$$W(z) = -ai \ln z, \tag{2.9.22}$$

where a is a constant quantity. Rewriting this equation in the form

$$\varphi + i\psi = -ai \ln (re^{i\theta}) = a(\theta - i \ln r).$$

we find

$$\varphi = a\theta; \tag{2.9.23}$$

$$\psi = -a \ln r. \tag{2.9.24}$$

From (2.9.23) it is found that radial component of velocity $V_r = \partial\varphi/\partial r = 0$ and the normal component V_s perpendicular to the radius is equal to the derivative of φ with respect to arc length s along the stream line, i.e.

$$\partial\varphi/\partial s = (1/r)(\partial\varphi/\partial\theta) = V_s = a/r. \tag{2.9.25}$$

The equation of stream line can be obtained from the condition of $\psi =$ const which, according to (2.9.24), gives the equation $r =$ const. This equation itself represents a family of stream lines in the form of concentric circles. Along these circles the direction of motion is positive if it is anticlockwise (from axis x to y), in which case the coefficient a in (2.9.25) will have the plus sign.

This kind of flow with particles moving (circulating) along concentric circles is called a flow with circulation or vortex flow (Fig. 2.9.4).

The circulation of velocity in the flow being considered has $\Gamma = 2\pi r(\partial\varphi/\partial s)$. Since $\partial\varphi/\partial s = (1/r)\partial\varphi/\partial\theta = a/r$ the circulation $\Gamma = 2\pi a$ or $a = \Gamma/2\pi$. Thus the physical meaning of the constant a lies in the fact that its value is determined by the circulation of flow which, as established earlier, is equal to the strength of the vortex. The flow created by a vortex lying at the origin of coordinates where $V_s = a/r \to \infty$ is called the plane vortex source or simply the vortex.

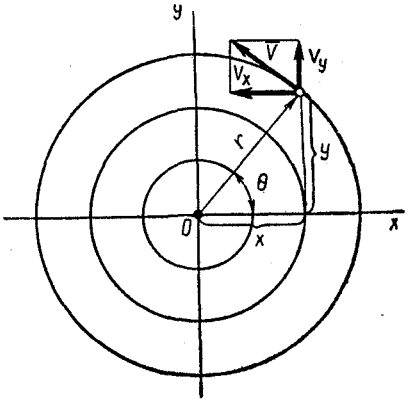

Fig. 2.9.4. Circulating flow (vortex).

We have examined most simple cases of flow for which the velocity potential and stream function are exactly determined. Combining these flows it is possible, under given conditions, to determine more complicated potential flows equivalent to those arising during a flow past bodies of given shapes.

3

FOUNDATIONS OF FLUID AND GAS DYNAMICS

1. Equations of Motion of a Viscous Fluid

The equations of motion constituting the theoretical foundations of aerodynamics form part of the group of basic equations of aerodynamics. They connect the variables determining motion such as speed, normal and tangential stresses, etc. The solution of equations of motion helps to determine these unknown quantities.

Let us examine the different types of equations of motion useful in the study of gas flows.

1.1 Cartesian coordinates

Let us study the motion of fluid particles having the form of elementary parallelepipeds of sides dx, dy, dz about a point A with coordinates x, y, z. The velocity components at this point are given by V_x, V_y, V_z. The motion of fluid particles with mass $\rho\tau$ ($\tau = dxdydz$, elemental volume) takes place under the action of the mass and surface forces. The components of mass force are represented by $X\rho\tau$, $Y\rho\tau$, $Z\rho\tau$, and the components of surface force by $P_x\tau$, $P_y\tau$, $P_z\tau$. The values of P_x, P_y, P_z themselves represent the projections of vectors of surface force counted per unit volume of body.

Equations of particle motion in projection on the x axis will have the form

$$\rho\tau\, dV_x/dt = X\rho\tau + P_x\,\tau,$$

from which

$$dV_x/dt = X + (1/\rho)\, P_x, \tag{3.1.1}$$

where dV_x/dt is total acceleration along the x axis. Similarly, two more equations for projections on axes y and z can be obtained:

$$dV_y/dt = Y + (1/\rho)\, P_y; \tag{3.1.2}$$

$$dV_z/dt = Z + (1/\rho)\, P_z. \tag{3.1.3}$$

The surface force can be expressed in terms of stresses acting on the sides

of an elemental parallelepiped. The peculiarity of the surface forces in comparison with the ideal (inviscid) medium lies in the fact that not only normal but also tangential stresses will be acting on the surface.

Every surface force acting on the side will have three components along coordinate axes (Fig. 3.1.1). The projections of surface forces acting on unit area of the left-hand side are p_{xx}, τ_{xz}, τ_{xy}. The quantity p_{xx} represents normal stress and τ_{xz}, τ_{xy} are tangential stresses. It is obvious that the first index shows the axis perpendicular to the side being considered and the second index indicates the axis along which the given stress is projected. The components of stress p_{zz}, τ_{zx} τ_{zy}, act on the given side perpendicular to the z axis and the components p_{yx}, τ_{yz}, τ_{zy} act on the lower side perpendicular to the y axis.

Here the normal stresses are assumed to be positive if they are directed away from the separated element and place the body under stress as shown in Fig. 3.1.1. The tangential stresses will have the plus sign if these stresses are oriented along directions opposite to the positive directions of the axes of coordinates for three sides intersecting at the starting point A. For the other three sides they are positive if directed toward the positive directions of these axes. Having noted this we will study the components of surface forces along the x axis. The force due to normal stress $p_{xx}\,dydz$ acts on the left side and the force $[p_{xx}+(\partial p_{xx}/\partial x)\,dx]\cdot dydz$ due to normal stress acts on the right side. Consequently the resultant of these forces is equal to $(\partial p_{xx}/\partial x)dydzdx$. The components of forces as a result of tangential stresses acting on these sides will be equal to zero.

It is, however, necessary to consider the tangential stresses τ_{zx} and τ_{yx}. Force $\tau_{zx}\,dydx$ acts on the rear face and force $[\tau_{zx}+(\partial\tau_{zx}/\partial z)dz]\,dxdy$ on the front face. The resultant of these forces is equal to $(\partial\tau_{zx}/\partial z)\,dxdydz$. Similarly the resultant of the forces acting on the lower and upper faces will be equal to $(\partial\tau_{yx}/\partial y)\,dxdydz$.

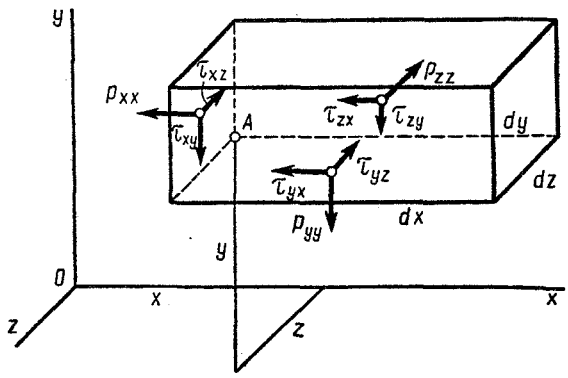

Fig. 3.1.1. Surface forces acting on fluid particle.

In this way the projection of surface force on the x axis taken for unit volume is

$$P_x=\partial p_{xx}/\partial x+\partial\tau_{yx}/\partial y+\partial\tau_{zx}/\partial z. \tag{3.1.4}$$

Similarly the projections of surface force on other coordinate axes per unit volume are:

$$\left.\begin{aligned} P_y&=\partial\tau_{xy}/\partial x+\partial p_{yy}/\partial y+\partial\tau_{zy}/\partial z\,;\\ P_z&=\partial\tau_{xz}/\partial x+\partial\tau_{yz}/\partial y+\partial p_{zz}/\partial z\ .\end{aligned}\right\} \tag{3.1.4'}$$

Tangential stresses acting over orthogonal sides are equal to each other, i.e. $\tau_{zx}=\tau_{xz}$, $\tau_{zy}=\tau_{yz}$ and $\tau_{yx}=\tau_{xy}$. This can be proved by writing the equations of moments about the axes acting on the particle as a result of forces which are perpendicular to the sides and passing through the center of the parallelepiped. For example, the equation of moments of forces about an axis perpendicular to the front and rear faces will be as following:

$$\begin{aligned}-\tau_{yx}\,dxdz\,(dy/2)-[\tau_{yx}+(\partial\tau_{yx}/\partial y)\,dy]\,dxdz\,(dy/2)+\tau_{xy}\,dydz\,(dx/2)\\ +[\tau_{xy}+(\partial\tau_{xy}/\partial x)\,dx]\,dydz\,(dx/2)=\Delta M_z,\end{aligned}$$

where ΔM_z is the moment of inertial forces during relative motion of the element about this axis. In this equation, the moments of gravitational forces and normal components of surface forces do not exist because it is assumed that the resultant of these forces passes through the center of the parallelepiped.

It is worth noting that the inertial force, by nature, is the volume force proportional to the elemental volume $\tau=dxdydz$ and is consequently in this context a small quantity of the third order. Therefore the inertial moment obtained by multiplication of this force by an infinitesimally small arm will be a small quantity of the fourth order and hence can be neglected. Neglecting other small values of the fourth order in the equation we get an equality $\tau_{xy}=\tau_{yx}$. Similarly the other two equalities of tangential stresses can be proved. In this equality of tangential stresses, lying in two mutually perpendicular elemental areas passing through some point and acting in the plane normal to both the elemental areas, the property of mutual dependence of tangential stresses is included. Thus only three tangential stresses will be unknown out of the six.

The law of proportionality of stresses to strains is used to determine the values of tangential stresses. Newton's formula for determination of friction arising during motion of a viscous fluid relative to a solid wall is an illustration of the application of this law. According to this formula $\tau_{yx}=\mu(\partial V_y/\partial x)$, i.e. the stress proportional to semi-speed $\varepsilon_z=(1/2)\,(\partial V_y/\partial x)$ of angular deformation in the direction of the z axis, from which we may write $\tau_{yx}=2\mu\varepsilon_z$. This relation can be extended for the general case of spatial motion in which the angular deformation in the direction of the z axis is

determined by semi-speed of deformation $\varepsilon_z=(1/2)\,(\partial V_y/\partial x+\partial V_x/\partial y)$. The other two values of frictional stresses can be written in the form $\tau_{yz}=2\mu\varepsilon_x$, $\tau_{zx}=2\mu\varepsilon_y$. In this way:

$$\left.\begin{aligned}\tau_{yx}&=2\mu\varepsilon_z=\mu\,(\partial V_y/\partial x+\partial V_x/\partial y);\\ \tau_{yz}&=2\mu\varepsilon_x=\mu\,(\partial V_y/\partial z+\partial V_z/\partial y);\\ \tau_{zx}&=2\mu\varepsilon_y=\mu\,(\partial V_z/\partial x+\partial V_x/\partial z).\end{aligned}\right\}\tag{3.1.5}$$

The above-mentioned law of proportionality can be used to establish the relation for normal stresses p_{xx}, p_{yy}, p_{zz}. Under the action of stress p_{xx} the fluid particle experiences linear deformation along the x axis. If $\bar{\theta}'_x$ represents the value of linear strain, it can be stated that $p_{xx}=E\bar{\theta}'_x$, where E is the coefficient of proportionality or modulus of elasticity of the fluid. The particle will also be deformed in the directions of axes y and z under the action of stresses p_{yy} and p_{zz}, which reduces the deformation along x axis.

It will be recalled from courses on the strength of materials that the reduction of this strain for elastic bodies, i.e. the quantity $\Delta\theta_x$, is proportional to the sum of strains along the y and z axes under the action of given stresses. Accordingly

$$\Delta\bar{\theta}_x=-(1/m)\,(p_{yy}/E+p_{zz}/E),$$

where m is a constant quantity, known as the coefficient of transverse linear deformation. The complete strain along x axis will therefore be

$$\bar{\theta}_x=\bar{\theta}'_x+\Delta\bar{\theta}_x=(p_{xx}/E)-(1/m)\,(p_{yy}/E+p_{zz}/E).\tag{3.1.6}$$

Similarly the strains $\bar{\theta}_y$ and $\bar{\theta}_z$ along axes y and z can be calculated. The normal stresses can be found from the expressions so obtained:

$$\left.\begin{aligned}p_{xx}&=E\,\bar{\theta}_x+(1/m)\,(p_{yy}+p_{zz});\\ p_{yy}&=E\,\bar{\theta}_y+(1/m)\,(p_{zz}+p_{xx});\\ p_{zz}&=E\,\bar{\theta}_z+(1/m)\,(p_{xx}+p_{yy}).\end{aligned}\right\}\tag{3.1.7}$$

The relative linear deformations of a particle along the directions of coordinate axes determine its relative volumetric deformation. Expressing the value of this deformation by $\bar{\theta}$, we can write

$$\bar{\theta}=\bar{\theta}_x+\bar{\theta}_y+\bar{\theta}_z.\tag{3.1.8}$$

Performing summation of (3.1.7) and considering an expression for $\bar{\theta}$, we get

$$p_{xx}+p_{yy}+p_{zz}=\frac{mE}{m-2}\,\bar{\theta}.\tag{3.1.9}$$

Determining the sum of $p_{yy}+p_{zz}$ from this expression and substituting it in (3.1.6), we find

$$p_{xx}=\frac{m}{m+1}\,E\,\bar{\theta}_x+\frac{m}{m+1}\cdot\frac{E}{m-2}\,\bar{\theta}.\tag{3.1.10}$$

The known relation between the modulus of rigidity G, the modulus of linear elasticity E and the coefficient of transverse deformation can be used for the last derivations. This relation is valid for elastic media, including compressible fluids:

$$G=mE/2\,(m+1). \tag{3.1.11}$$

Transferring this relation to equation (3.1.10), we get

$$p_{xx}=2G\,\bar{\theta}_x+\frac{2G}{m-2}\,\bar{\theta}\,. \tag{3.1.12}$$

Introduce the notation

$$\bar{\sigma}=(1/3)\,(p_{xx}+p_{yy}+p_{zz}). \tag{3.1.13}$$

Addition and subtraction of the quantity $\bar{\sigma}$ on the right side of (3.1.12) gives

$$p_{xx}=\bar{\sigma}+2G\bar{\theta}_x+\frac{2G}{m-2}\,\bar{\theta}-\frac{1}{3}\,(p_{xx}+p_{yy}+p_{zz}).$$

Using (3.1.9) and (3.1.11), we write

$$p_{xx}=\bar{\sigma}+G\,[2\bar{\theta}_x-(2/3)\,\bar{\theta}]. \tag{3.1.14}$$

Similarly the expressions for p_{yy} and p_{zz} will be

$$\left.\begin{aligned} p_{yy}&=\bar{\sigma}+G\,[2\bar{\theta}_y-(2/3)\,\bar{\theta}];\\ p_{zz}&=\bar{\sigma}+G\,[2\bar{\theta}_z-(2/3)\,\bar{\theta}]. \end{aligned}\right\} \tag{3.1.14'}$$

It has been established that for an inviscid fluid the pressure p at any point in the flow (see Chapter 1, Section 1) is equal for all the elemental areas passing through this point, i.e. in terms of established notations $p_{xx}=p_{yy}=p_{zz}=-p$. Consequently, $p=(-1/3)\,(p_{xx}+p_{yy}+p_{zz})$. So in investigating the motion of a viscous fluid the pressure can be determined as the arithmetic mean, with negative sign, of the three normal stresses corresponding to three mutually perpendicular planes. Accordingly $\bar{\sigma}=-p$.

The following relations for shear (tangential) stresses acting on a solid body are established in the theory of elasticity:

$$\tau_{yx}=G\gamma_{yx},\ \tau_{yz}=G\gamma_{yz},\ \tau_{zx}=G\gamma_{zx}, \tag{3.1.15}$$

where γ_{yx}, γ_{yz}, γ_{zx} are angular strains about axes z, x, y respectively. It can be seen from a comparison of formula (3.1.15) with the corresponding relations for a viscous fluid (3.1.5) that they can be obtained from each other if the modulus of rigidity G is replaced by coefficient of dynamic viscosity μ and angular strains γ by the corresponding values of angular deformation

rates ε. Accordingly, in replacing G by μ in formulas (3.1.14), (3.1.14') the linear strains $\overline{\theta_x}$, $\overline{\theta_y}$, $\overline{\theta_z}$ must be replaced by the corresponding values of the rates of linear deformation $\theta_x=\partial V_x/\partial x$, $\theta_y=\partial V_y/\partial y$, $\theta_z=\partial V_z/\partial z$ (see Section 2 of Chapter 2) and the rate of volumetric deformation

$$\theta=(\partial V_x/\partial x)+(\partial V_y/\partial y)+(\partial V_z/\partial z)=\operatorname{div}\overline{V}.$$

After these substitutions in (3.1.14), (3.1.14') we get

$$\left.\begin{aligned} p_{xx}&=-p+\mu\left(2\frac{\partial V_x}{\partial x}-\frac{2}{3}\operatorname{div}\overline{V}\right);\\ p_{yy}&=-p+\mu\left(2\frac{\partial V_y}{\partial y}-\frac{2}{3}\operatorname{div}\overline{V}\right);\\ p_{zz}&=-p+\mu\left(2\frac{\partial V_z}{\partial z}-\frac{2}{3}\operatorname{div}\overline{V}\right). \end{aligned}\right\} \tag{3.1.16}$$

The second terms on the right side of expressions (3.1.16) give additional stresses due to viscosity.

Using the relations (3.1.4), (3.1.4'), (3.1.5) and (3.1.16), one can find P_x, P_y and P_z. For example, from (3.1.4) the value of P_x will be

$$\begin{aligned} P_x&=-\frac{\partial p}{\partial x}+\frac{\partial}{\partial x}\left[\mu\left(2\frac{\partial V_x}{\partial x}-\frac{2}{3}\operatorname{div}\overline{V}\right)\right]\\ &+\frac{\partial}{\partial y}\left[\mu\left(\frac{\partial V_y}{\partial x}+\frac{\partial V_x}{\partial y}\right)\right]+\frac{\partial}{\partial z}\left[\mu\left(\frac{\partial V_z}{\partial x}+\frac{\partial V_x}{\partial z}\right)\right]\\ &=-\frac{\partial p}{\partial x}+\mu\Delta V_x+\frac{\mu}{3}\cdot\frac{\partial}{\partial x}\operatorname{div}\overline{V}+\frac{\partial\mu}{\partial x}\left(2\frac{\partial V_x}{\partial x}-\frac{2}{3}\operatorname{div}\overline{V}\right)\\ &+\frac{\partial\mu}{\partial y}\left(\frac{\partial V_x}{\partial y}+\frac{\partial V_y}{\partial x}\right)+\frac{\partial\mu}{\partial z}\left(\frac{\partial V_x}{\partial z}+\frac{\partial V_z}{\partial x}\right), \end{aligned}$$

where Δ is the Laplace operator:

$$\Delta=\partial^2/\partial x^2+\partial^2/\partial y^2+\partial^2/\partial z^2.$$

In particular,

$$\Delta V_x=\partial^2 V_x/\partial x^2+\partial^2 V_x/\partial y^2+\partial^2 V_x/\partial z^2.$$

Similarly the relations for P_y and P_z can be obtained.

The relations for the stresses due to surface forces in a fluid were obtained here by applying the generalized rules connecting stresses and deformations in solid bodies to the case of a fluid medium having the properties of elasticity and viscosity. The same relations can be obtained from the series of hypothetical statements about molecular forces acting in the fluid itself (see [2], [8]).

Writing the components of total acceleration by the law of calculating the derivative of multi-variable function $f(x, y, z, t)$ (x, y, z are also functions of

time t), the equations of motion (3.1.1) to (3.1.3) can be obtained in the following form, taking into account the above expressions for P_x, P_y, P_z:

$$\left.\begin{aligned}
&\frac{\partial V_x}{\partial t}+V_x\frac{\partial V_x}{\partial x}+V_y\frac{\partial V_x}{\partial y}+V_z\frac{\partial V_x}{\partial z}=X-\frac{1}{\rho}\cdot\frac{\partial p}{\partial x}+\nu\Delta V_x\\
&\quad+\frac{\nu}{3}\cdot\frac{\partial}{\partial x}\operatorname{div}\overline{V}+\frac{1}{\rho}\left[\frac{\partial\mu}{\partial x}\left(2\frac{\partial V_x}{\partial x}-\frac{2}{3}\operatorname{div}\overline{V}\right)\right.\\
&\quad\left.+\frac{\partial\mu}{\partial y}\left(\frac{\partial V_x}{\partial y}+\frac{\partial V_y}{\partial x}\right)+\frac{\partial\mu}{\partial z}\left(\frac{\partial V_x}{\partial z}+\frac{\partial V_z}{\partial x}\right)\right];\\
&\frac{\partial V_y}{\partial t}+V_x\frac{\partial V_y}{\partial x}+V_y\frac{\partial V_y}{\partial y}+V_z\frac{\partial V_y}{\partial z}=Y-\frac{1}{\rho}\cdot\frac{\partial p}{\partial y}+\nu\Delta V_y\\
&\quad+\frac{\nu}{3}\cdot\frac{\partial}{\partial y}\operatorname{div}\overline{V}+\frac{1}{\rho}\left[\frac{\partial\mu}{\partial y}\left(2\frac{\partial V_y}{\partial y}-\frac{2}{3}\operatorname{div}\overline{V}\right)\right.\\
&\quad\left.+\frac{\partial\mu}{\partial z}\left(\frac{\partial V_y}{\partial z}+\frac{\partial V_z}{\partial y}\right)+\frac{\partial\mu}{\partial x}\left(\frac{\partial V_y}{\partial x}+\frac{\partial V_x}{\partial y}\right)\right];\\
&\frac{\partial V_z}{\partial t}+V_x\frac{\partial V_z}{\partial x}+V_y\frac{\partial V_z}{\partial y}+V_z\frac{\partial V_z}{\partial z}=Z-\frac{1}{\rho}\cdot\frac{\partial p}{\partial z}+\nu\Delta V_z\\
&\quad+\frac{\nu}{3}\cdot\frac{\partial}{\partial z}\operatorname{div}\overline{V}+\frac{1}{\rho}\left[\frac{\partial\mu}{\partial z}\left(2\frac{\partial V_z}{\partial z}-\frac{2}{3}\operatorname{div}\overline{V}\right)\right.\\
&\quad\left.+\frac{\partial\mu}{\partial x}\left(\frac{\partial V_z}{\partial x}+\frac{\partial V_x}{\partial z}\right)+\frac{\partial\mu}{\partial y}\left(\frac{\partial V_z}{\partial y}+\frac{\partial V_y}{\partial z}\right)\right],
\end{aligned}\right\}\quad(3.1.17)$$

where $\nu=\mu/\rho$, coefficient of kinematic viscosity.

The differential equations (3.1.17) form the theoretical basis for the gas dynamics of a viscous compressible fluid medium and are known as the Navier-Stokes equations. It is assumed in these equations that the coefficient of viscosity μ is a function of coordinates x, y, z, i.e. $\mu=f(x, y, z)$. Assuming that $\mu=\text{const}$, the Navier-Stokes equations can be written in the following form:

$$\left.\begin{aligned}
&\frac{dV_x}{dt}=X-\frac{1}{\rho}\cdot\frac{\partial p}{\partial x}+\nu\,\Delta V_x+\frac{\nu}{3}\cdot\frac{\partial}{\partial x}\operatorname{div}\overline{V};\\
&\frac{dV_y}{dt}=Y-\frac{1}{\rho}\cdot\frac{\partial p}{\partial y}+\nu\,\Delta V_y+\frac{\nu}{3}\cdot\frac{\partial}{\partial y}\operatorname{div}\overline{V};\\
&\frac{dV_z}{dt}=Z-\frac{1}{\rho}\cdot\frac{\partial p}{\partial z}+\nu\,\Delta V_z+\frac{\nu}{3}\cdot\frac{\partial}{\partial z}\operatorname{div}\overline{V}.
\end{aligned}\right\}\quad(3.1.18)$$

The effect of mass forces need not be taken into account in the investigation of gas flows. Consequently, we take $X=Y=Z=0$. In that case

$$\left.\begin{aligned}
&\frac{dV_x}{dt}=-\frac{1}{\rho}\cdot\frac{\partial p}{\partial x}+\nu\,\Delta V_x+\frac{\nu}{3}\cdot\frac{\partial}{\partial x}\operatorname{div}\overline{V};\\
&\frac{dV_y}{dt}=-\frac{1}{\rho}\cdot\frac{\partial p}{\partial y}+\nu\,\Delta V_y+\frac{\nu}{3}\cdot\frac{\partial}{\partial y}\operatorname{div}\overline{V};\\
&\frac{dV_z}{dt}=-\frac{1}{\rho}\cdot\frac{\partial p}{\partial z}+\nu\,\Delta V_z+\frac{\nu}{3}\cdot\frac{\partial}{\partial z}\operatorname{div}\overline{V}.
\end{aligned}\right\}\quad(3.1.19)$$

For two-dimensional plane motion with variable values of coefficient of dynamic viscosity ($\mu \neq \text{const}$):

$$\left.\begin{aligned}
\frac{dV_x}{dt} &= -\frac{1}{\rho}\cdot\frac{\partial p}{\partial x}+\frac{1}{\rho}\cdot\frac{\partial}{\partial x}\left[\mu\left(2\frac{\partial V_x}{\partial x}-\frac{2}{3}\operatorname{div}\overline{V}\right)\right] \\
&\quad +\frac{2}{\rho}\cdot\frac{\partial}{\partial y}(\mu\varepsilon_z); \\
\frac{dV_y}{dt} &= -\frac{1}{\rho}\cdot\frac{\partial p}{\partial y}+\frac{1}{\rho}\cdot\frac{\partial}{\partial y}\left[\mu\left(2\frac{\partial V_y}{\partial y}-\frac{2}{3}\operatorname{div}\overline{V}\right)\right] \\
&\quad +\frac{2}{\rho}\cdot\frac{\partial}{\partial x}(\mu\varepsilon_z).
\end{aligned}\right\} \qquad (3.1.20)$$

If $\operatorname{div}\overline{V}=0$ and $\mu=\text{const}$ these equations lead to the equations of a viscous incompressible fluid.

Let us examine the equation of motion of an ideal (inviscid) compressible fluid. Taking the coefficients μ an ν as equal to zero in (3.1.17), we get

$$\left.\begin{aligned}
&\frac{\partial V_x}{\partial t}+V_x\frac{\partial V_x}{\partial x}+V_y\frac{\partial V_x}{\partial y}+V_z\frac{\partial V_x}{\partial z}=X-\frac{1}{\rho}\cdot\frac{\partial p}{\partial x}; \\
&\frac{\partial V_y}{\partial t}+V_x\frac{\partial V_y}{\partial x}+V_y\frac{\partial V_y}{\partial y}+V_z\frac{\partial V_y}{\partial z}=Y-\frac{1}{\rho}\cdot\frac{\partial p}{\partial y}; \\
&\frac{\partial V_z}{\partial t}+V_x\frac{\partial V_z}{\partial x}+V_y\frac{\partial V_z}{\partial y}+V_z\frac{\partial V_z}{\partial z}=Z-\frac{1}{\rho}\cdot\frac{\partial p}{\partial z}.
\end{aligned}\right\} \qquad (3.1.17')$$

These equations were first obtained by Leonard Euler and are known as Euler's equations. They form the theoretical foundation of the science of the motion of an ideal gas, the hypothetical properties of which are determined by absence or negligibly small effect of tangential stresses.

1.2 Equation of motion in vector form

Multiplying equations (3.1.18) by unit i, j, k, respectively and summing them, we get the equation of motion in vector form:

$$\frac{d\overline{V}}{dt}=\overline{G}-\frac{1}{\rho}\operatorname{grad}p+\nu\,\Delta\overline{V}+\frac{\nu}{3}\operatorname{grad}\operatorname{div}\overline{V}, \qquad (3.1.21)$$

where the vector of mass forces in Cartesian coordinates

$$\overline{G}=Xi+Yj+Zk;$$

gradient of pressure

$$\operatorname{grad}p=(\partial p/\partial x)\,i+(\partial p/\partial y)\,j+(\partial p/\partial z)\,k;$$

vectors

$$\Delta\overline{V}=\Delta V_x\,i+\Delta V_y\,j+\Delta V_z\,k;$$

$$\operatorname{grad}\operatorname{div}\overline{V}=\frac{\partial\operatorname{div}\overline{V}}{\partial x}\,i+\frac{\partial\operatorname{div}\overline{V}}{\partial y}\,j+\frac{\partial\operatorname{div}\overline{V}}{\partial z}\,k.$$

If the fluid is incompressible, div $\overline{V}=0$ and consequently

$$d\overline{V}/dt=\overline{G}-(1/\rho)\ \text{grad}\ p+\nu\ \Delta\overline{V}. \tag{3.1.21'}$$

In the absence of mass forces $\overline{G}=0$ and therefore

$$d\overline{V}/dt=-(1/\rho)\ \text{grad}\ p+\nu\ \Delta\overline{V}+(\nu/3)\ \text{grad div}\ \overline{V}. \tag{3.1.21''}$$

The complete acceleration vector can be expressed in the following form:

$$d\overline{V}/dt=\partial\overline{V}/\partial t+\text{grad}\ (V^2/2)+\text{rot}\ \overline{V}\times\overline{V}. \tag{3.1.22}$$

Taking (3.1.21'') and (3.1.22) together, the equation of motion can be written in the form

$$\frac{\partial\overline{V}}{\partial t}+\text{grad}\ \frac{V^2}{2}+\text{rot}\ \overline{V}\times\overline{V}=-\frac{1}{\rho}\ \text{grad}\ p+\nu\Delta\overline{V}+\frac{\nu}{3}\ \text{grad div}\ \overline{V}. \tag{3.1.22'}$$

1.3 Curvilinear coordinates

Let us transform equation (3.1.22') with the help of the concept of generalized curvilinear coordinates q_n discussed in Section 4 of Chapter 2. This helps us to carry out changes comparatively easily in the equation of motion pertaining to the particular form of curvilinear orthogonal coordinates in the same way as in the equation of continuity.

Let us consider the transformation of individual terms in (3.1.22'). The following expressions, bearing in mind (2.4.18), represent the second term on the left side and also the first and third term on the right side of (3.1.22'):

$$\text{grad}\ \frac{V^2}{2}=\sum_{n=1}^{3}\left(\text{grad}\ \frac{V^2}{2}\right)_n i_n=\sum_{n=1}^{3}\frac{1}{h_n}\cdot\frac{\partial\,(V^2/2)}{\partial q_n}\,i_n; \tag{3.1.23}$$

$$\text{grad}\ p=\sum_{n=1}^{3}(\text{grad}\ p)_n\ i_n=\sum_{n=1}^{3}\frac{1}{h_n}\cdot\frac{\partial p}{\partial q_n}\,i_n; \tag{3.1.24}$$

$$\text{grad div}\ \overline{V}=\sum_{n=1}^{3}(\text{grad div}\ \overline{V})_n\ i_n=\sum_{n=1}^{3}\frac{1}{h_n}\cdot\frac{\partial\ \text{div}\ \overline{V}}{\partial q_n}\,i_n. \tag{3.1.25}$$

For the transformation of vector product rot $\overline{V}\times\overline{V}$ it is necessary to find the formula for vector rot $\overline{V}$ in generalized coordinates. To do this, find the rotation of both parts of equation (2.4.19):

$$\text{rot}\ \overline{V}=\sum_{n=1}^{3}(V_n\ \text{rot}\ i_n+\text{grad}\ V_n\times i_n), \tag{3.1.26}$$

where

$$\text{grad}\ V_n\times i_n=(\text{grad}\ V_n)_j\ i_m-(\text{grad}\ V_n)_m\ i_j. \tag{3.1.27}$$

Here the components of vector grad V_n in the corresponding coordinates are determined from expression (2.4.18), where Φ is replaced by V_n. Inserting the values of (3.1.27) and the expressions for rot i_n from (2.4.22) in (3.1.26), the rotation of velocity will be

$$\left.\begin{aligned}\operatorname{rot}\overline{V} = &\frac{1}{h_2 h_3}\left[\frac{\partial (h_3 V_3)}{\partial q_2} - \frac{\partial (h_2 V_2)}{\partial q_3}\right] i_1 + \frac{1}{h_3 h_1}\left[\frac{\partial (h_1 V_1)}{\partial q_3}\right. \\ &\left. - \frac{\partial (h_3 V_3)}{\partial q_1}\right] i_2 + \frac{1}{h_1 h_2}\left[\frac{\partial (h_2 V_2)}{\partial q_1} - \frac{\partial (h_1 V_1)}{\partial q_2}\right] i_3.\end{aligned}\right\} \tag{3.1.28}$$

Now the vector product can be determined by

$$\operatorname{rot}\overline{V} \times \overline{V} = \sum_{n=1}^{3} (\operatorname{rot}\overline{V} \times \overline{V})_n \, i_n, \tag{3.1.29}$$

where the component of this vector on a tangent to the corresponding coordinate line is

$$\begin{aligned}(\operatorname{rot}\overline{V} \times \overline{V})_n = &\frac{V_j}{h_j h_n}\left[\frac{\partial (h_n V_n)}{\partial q_j} - \frac{\partial (h_j V_j)}{\partial q_n}\right] \\ &- \frac{V_m}{h_n h_m}\left[\frac{\partial (h_m V_m)}{\partial q_n} - \frac{\partial (h_n V_n)}{\partial q_m}\right].\end{aligned} \tag{3.1.30}$$

Note that the indices $m=2, 3, 1$ and $j=3, 1, 2$ correspond to the values of $n=1, 2, 3$.

The left side of equation (3.1.22) represents vector of total acceleration $\overline{W}=d\overline{V}/dt$ which can be written as

$$\overline{W} = \sum_{n=1}^{3} W_n \, i_n, \tag{3.1.31}$$

where W_n is a component of the acceleration vector along the direction tangential to the coordinate lines q_n. It is obvious that each value of W_n can be taken as the sum of the corresponding components of vectors $\partial\overline{V}/\partial t$ and of vectors (3.1.23) and (3.1.29) along the given directions. Accordingly

$$\begin{aligned}W_n = &\frac{\partial V_n}{\partial t} + \frac{V_n}{h_n} \cdot \frac{\partial V_n}{\partial q_n} + \frac{V_m}{h_n h_m} \cdot \frac{\partial (h_n V_n)}{\partial q_m} + \frac{V_j}{h_j h_n} \cdot \frac{\partial (h_n V_n)}{\partial q_j} \\ &- \frac{V_m^2}{h_n h_m} \cdot \frac{\partial h_m}{\partial q_n} - \frac{V_j^2}{h_j h_n} \cdot \frac{\partial h_j}{\partial q_n}.\end{aligned} \tag{3.1.32}$$

To transform the Laplacian operator which is given in the form of vector $\Delta\overline{V}$ the following identity can be used:

$$\Delta\overline{V} = \sum_{n=1}^{3} \Delta V_n \, i_n = \operatorname{grad}\operatorname{div}\overline{V} - \operatorname{rot}\operatorname{rot}\overline{V}, \tag{3.1.33}$$

where ΔV_n is the component of velocity vector along coordinate lines q_n. The first vector on the right side of (3.1.33) has already been determined in (3.1.25) and the second vector can be obtained with the help of equation (3.1.28). Performing rotation of both parts of this equality, we get

$$\text{rot rot } \bar{V} = \sum_{n=1}^{3} (\text{rot rot } \bar{V})_n \, i_n$$

$$= \sum_{n=1}^{3} \frac{1}{h_m h_j} \left\{ \frac{\partial [h_j (\text{rot } \bar{V})_j]}{\partial q_m} - \frac{\partial [h_m (\text{rot } \bar{V})_m]}{\partial q_j} \right\} i_n , \qquad (3.1.34)$$

where the corresponding components of the vector of rot $\bar{V}$ are found from (3.1.28). With these data the transformation of the equation can be studied with respect to the particular form of curvilinear orthogonal coordinates.

Cylindrical coordinates: Using (2.4.12), (2.4.16) and (2.4.25), we get

$$q_1 = x, \quad q_2 = r, \quad q_3 = \gamma, \quad h_1 = 1, \quad h_2 = 1, \quad h_3 = r,$$
$$V_1 = V_x, \quad V_2 = V_r, \quad V_3 = V_\gamma.$$

Hence

$$W_1 = \frac{\partial V_x}{\partial t} + V_x \frac{\partial V_x}{\partial x} + V_r \frac{\partial V_x}{\partial r} + \frac{V_\gamma}{r} \cdot \frac{\partial V_x}{\partial \gamma};$$
$$(\text{grad } p)_1 = \partial p / \partial x.$$

Moreover we find that

$$(\text{grad div } \bar{V})_1 = \partial \text{ div } \bar{V} / \partial x.$$

Keeping in mind that div $\bar{V}$ is determined by the formula (2.4.26), we get

$$\frac{\partial \text{ div } \bar{V}}{\partial x} = \frac{\partial}{\partial x} \left(\frac{\partial V_x}{\partial x} + \frac{\partial V_r}{\partial r} + \frac{1}{r} \cdot \frac{\partial V_\gamma}{\partial \gamma} + \frac{V_r}{r} \right).$$

Equation (3.1.28) results in

$$(\text{rot } \bar{V})_3 = \frac{\partial V_r}{\partial x} - \frac{\partial V_x}{\partial r}, \quad (\text{rot } \bar{V})_2 = \frac{1}{r} \left(\frac{\partial V_x}{\partial \gamma} - r \frac{\partial V_\gamma}{\partial x} \right).$$

Substitution of these expressions in (3.1.34) gives

$$(\text{rot rot } \bar{V})_1 = \frac{1}{r} \left\{ \frac{\partial \left[r \left(\frac{\partial V_r}{\partial x} - \frac{\partial V_x}{\partial r} \right) \right]}{\partial r} - \frac{\partial \left[\frac{1}{r} \left(\frac{\partial V_x}{\partial \gamma} - r \frac{\partial V_\gamma}{\partial x} \right) \right]}{\partial \gamma} \right\}$$
$$= \frac{\partial^2 V_r}{\partial x \, \partial r} - \frac{\partial^2 V_x}{\partial r^2} + \frac{1}{r} \left(\frac{\partial V_r}{\partial x} - \frac{\partial V_x}{\partial r} \right) - \frac{1}{r^2} \left(\frac{\partial^2 V_x}{\partial \gamma^2} - r \frac{\partial^2 V_\gamma}{\partial x \, \partial \gamma} \right).$$

Further, since $(\text{grad div } \bar{V})_1 = \partial \text{ div } \bar{V} / \partial x$, the equation (3.1.33) leads to

$$(\Delta\overline{V})_1=(\text{grad div }\overline{V})_1-(\text{rot rot } V)_1=\frac{\partial^2 V_x}{\partial x^2}+\frac{\partial^2 V_x}{\partial r^2}$$
$$+\frac{1}{r^2}\cdot\frac{\partial^2 V_x}{\partial\gamma^2}+\frac{1}{r}\cdot\frac{\partial V_x}{\partial r}\,.$$

So the equation of motion for the component along the x axis in a cylindrical system of coordinates will be

$$\frac{\partial V_x}{\partial t}+V_x\frac{\partial V_x}{\partial x}+V_r\frac{\partial V_x}{\partial r}+\frac{V_\gamma}{r}\cdot\frac{\partial V_x}{\partial\gamma}$$
$$=-\frac{1}{\rho}\cdot\frac{\partial p}{\partial x}+\nu\,\Delta V_x+\frac{\nu}{3}\cdot\frac{\partial\,\text{div}\,\overline{V}}{\partial x}\,. \tag{3.1.35}$$

In the same way the other two equations for the components along coordinate lines r and γ will be:

$$\left.\begin{aligned}&\frac{\partial V_r}{\partial t}+V_x\frac{\partial V_r}{\partial x}+V_r\frac{\partial V_r}{\partial r}+\frac{V_\gamma}{r}\cdot\frac{\partial V_r}{\partial\gamma}-\frac{V_\gamma^2}{r}=-\frac{1}{\rho}\cdot\frac{\partial p}{\partial r}+\\&+\nu\left(\Delta V_r-\frac{2}{r^2}\cdot\frac{\partial V_\gamma}{\partial\gamma}-\frac{V_r}{r^2}\right)+\frac{\nu}{3}\cdot\frac{\partial\,\text{div}\,\overline{V}}{\partial r};\\&\frac{\partial V_\gamma}{\partial t}+V_x\frac{\partial V_\gamma}{\partial x}+V_r\frac{\partial V_\gamma}{\partial r}+\frac{V_\gamma}{r}\cdot\frac{\partial V_\gamma}{\partial\gamma}+\frac{V_r V_\gamma}{r}\\&=-\frac{1}{\rho r}\cdot\frac{\partial p}{\partial\gamma}+\nu\left(\Delta V_\gamma+\frac{2}{r^2}\cdot\frac{\partial V_r}{\partial\gamma}-\frac{V_\gamma}{r^2}\right)+\frac{\nu}{3r}\cdot\frac{\partial\,\text{div}\,\overline{V}}{\partial\gamma}\,.\end{aligned}\right\} \tag{3.1.35'}$$

The following convention for Δ is observed in these equations:

$$\Delta=\frac{\partial^2}{\partial x^2}+\frac{\partial^2}{\partial r^2}+\frac{1}{r^2}\cdot\frac{\partial^2}{\partial\gamma^2}+\frac{1}{r}\cdot\frac{\partial}{\partial r}\,.$$

Divergence of velocity is obtained by formula (2.4.26).

For an axisymmetric flow the equations of motion are simplified so that

$$\left.\begin{aligned}&\frac{\partial V_x}{\partial t}+V_x\frac{\partial V_x}{\partial x}+V_r\frac{\partial V_x}{\partial r}=-\frac{1}{\rho}\cdot\frac{\partial p}{\partial x}+\nu\,\Delta V_x+\frac{\nu}{3}\cdot\frac{\partial\,\text{div}\,\overline{V}}{\partial x};\\&\frac{\partial V_r}{\partial t}+V_x\frac{\partial V_r}{\partial x}+V_r\frac{\partial V_r}{\partial r}=-\frac{1}{\rho}\cdot\frac{\partial p}{\partial r}+\nu\,\Delta V_r+\frac{\nu}{3}\cdot\frac{\partial\,\text{div}\,\overline{V}}{\partial r}\,,\end{aligned}\right\} \tag{3.1.36}$$

where

$$\text{div}\,\overline{V}=\frac{\partial V_x}{\partial x}+\frac{\partial V_r}{\partial r}+\frac{V_r}{r},$$
$$\Delta=\frac{\partial^2}{\partial x^2}+\frac{\partial^2}{\partial r^2}+\frac{1}{r}\cdot\frac{\partial}{\partial r}\,.$$

In the case of a steady flow it is necessary to take

$$\partial V_x/\partial t=\partial V_r/\partial t=\partial V_y/\partial t=0.$$

in these equations.

Spherical coordinates: Spherical coordinates, Lame's parameters and components of velocity vectors along the directions of coordinate lines are related by the formulas (2.4.13), (2.4.17) and (2.4.33):

$$q_1=r,\quad q_2=\theta,\quad q_3=\psi,\quad h_1=1,\quad h_2=r,\quad h_3=r\sin\theta,$$
$$V_1=V_r,\quad V_2=V_\theta,\quad V_3=V_\psi.$$

Using these details, equation (3.1.32) gives the component of acceleration in the direction of coordinate line r:

$$W_1=\frac{\partial V_r}{\partial t}+V_r\frac{\partial V_r}{\partial r}+\frac{V_\theta}{r}\cdot\frac{\partial V_r}{\partial\theta}+\frac{V_\psi}{r\sin\theta}\cdot\frac{\partial V_r}{\partial\psi}-\frac{V_\theta^2+V_\psi^2}{r}. \tag{3.1.37}$$

The pressure gradient component will be

$$(\text{grad } p)_1=\partial p/\partial r. \tag{3.1.38}$$

Further, using (2.4.34) for div $\overline{V}$ we get the relations

$$(\text{grad div }\overline{V})_1=\frac{\partial\,\text{div}\,\overline{V}}{\partial r}=\frac{\partial}{\partial r}\left[\frac{1}{r^2}\cdot\frac{\partial(V_r r^2)}{\partial r}\right.$$
$$\left.+\frac{1}{r\sin\theta}\cdot\frac{\partial(V_\theta\sin\theta)}{\partial\theta}+\frac{1}{r\sin\theta}\cdot\frac{\partial V_\psi}{\partial\psi}\right]. \tag{3.1.39}$$

This relation is used to determine the component $(\Delta V)_1$ of vector $\Delta\overline{V}$ by formula (3.1.33). Before doing this we find the value of $(\text{rot rot }\overline{V})_1$ from (3.1.34) which occurs in (3.1.33). From (3.1.28) we have:

$$(\text{rot }\overline{V})_3=\frac{1}{r}\left[\frac{\partial(V_\theta r)}{\partial r}-\frac{\partial V_r}{\partial\theta}\right],$$
$$(\text{rot }\overline{V})_2=\frac{1}{r\sin\theta}\left[\frac{\partial V_r}{\partial\psi}-\frac{\partial(r\sin\theta\,V_\psi)}{\partial r}\right].$$

Substitution of these relations in (3.1.34) gives

$$\left.\begin{aligned}(\text{rot rot }\overline{V})_1=&\frac{1}{r^2\sin\theta}\left\{\frac{\partial\left\{\sin\theta\left[\frac{\partial(V_\theta r)}{\partial r}-\frac{\partial V_r}{\partial\theta}\right]\right\}}{\partial\theta}\right.\\&\left.-\frac{\partial\left\{\frac{1}{\sin\theta}\left[\frac{\partial V_r}{\partial\psi}-\frac{\partial(r\sin\theta\,V_\psi)}{\partial r}\right]\right\}}{\partial\psi}\right\}\\=&\frac{1}{r^2\sin\theta}\left[\left(V_\theta+r\frac{\partial V_\theta}{\partial r}-\frac{\partial V_r}{\partial\theta}\right)\cos\theta\right.\\&+\sin\theta\left(\frac{\partial V_\theta}{\partial\theta}+r\frac{\partial^2 V_\theta}{\partial r\,\partial\theta}-\frac{\partial^2 V_r}{\partial\theta^2}\right)\\&\left.-\frac{1}{\sin\theta}\left(\frac{\partial^2 V_r}{\partial\psi^2}-r\sin\theta\frac{\partial^2 V_\psi}{\partial r\,\partial\psi}-\sin\theta\frac{\partial V_\psi}{\partial\psi}\right)\right].\end{aligned}\right\} \tag{3.1.40}$$

Considering relations (3.1.39) and (3.1.40), we get

$$\left.\begin{aligned}(\Delta V)_1=(\text{grad div }\bar V)_1-(\text{rot rot }\bar V)_1=\frac{\partial^2 V_r}{\partial r^2}+\frac{1}{r^2}\cdot\frac{\partial^2 V_r}{\partial\theta^2}\\ +\frac{1}{r^2\sin^2\theta}\cdot\frac{\partial^2 V_r}{\partial\psi^2}+\frac{2}{r}\cdot\frac{\partial V_r}{\partial r}+\frac{\cot\theta}{r^2}\cdot\frac{\partial V_r}{\partial\theta}-\frac{2}{r^2}\cdot\frac{\partial V_\theta}{\partial\theta}\\ -\frac{2}{r^2\sin\theta}\cdot\frac{\partial V_\psi}{\partial\psi}-\frac{2}{r^2}V_r-\frac{2\cot\theta}{r^2}V_\theta,\end{aligned}\right\}\quad(3.1.41)$$

or

$$(\Delta V)_1=\Delta V_r-\frac{2V_r}{r^2}-\frac{2}{r^2}\cdot\frac{\partial V_\theta}{\partial\theta}-\frac{2V_\theta\cot\theta}{r^2}-\frac{2}{r^2\sin\theta}\cdot\frac{\partial V_\psi}{\partial\psi},\quad(3.1.41')$$

where

$$\left.\begin{aligned}\Delta V_r=\frac{1}{r^2}\cdot\frac{\partial}{\partial r}\left(r^2\frac{\partial V_r}{\partial r}\right)+\frac{1}{r^2\sin\theta}\cdot\frac{\partial}{\partial\theta}\left(\sin\theta\frac{\partial V_r}{\partial\theta}\right)\\ +\frac{1}{r^2\sin^2\theta}\cdot\frac{\partial^2 V_r}{\partial\psi^2}.\end{aligned}\right\}\quad(3.1.42)$$

Using relations (3.1.37) to (3.1.39) and (3.1.41'), the equation of motion for the component along coordinate line r will be

$$\frac{\partial V_r}{\partial t}+V_r\frac{\partial V_r}{\partial r}+\frac{V_\theta}{r}\cdot\frac{\partial V_r}{\partial\theta}+\frac{V_\psi}{r\sin\theta}\cdot\frac{\partial V_r}{\partial\psi}-\frac{V_\theta^2+V_\psi^2}{r}=-\frac{1}{\rho}\cdot\frac{\partial p}{\partial r}$$
$$+\nu\left(\Delta V_r-\frac{2}{r^2}\cdot\frac{\partial V_\theta}{\partial\theta}-\frac{2}{r^2\sin\theta}\cdot\frac{\partial V_\psi}{\partial\psi}-\frac{2V_r}{r^2}-\frac{2V_\theta\cot\theta}{r^2}\right)+\frac{\nu}{3}\cdot\frac{\partial\,\text{div}\,\bar V}{\partial r}.\quad(3.1.43)$$

The other two equations, in the same way, will be:

$$\left.\begin{aligned}\frac{\partial V_\theta}{\partial t}+V_r\frac{\partial V_\theta}{\partial r}+\frac{V_\theta}{r}\cdot\frac{\partial V_\theta}{\partial\theta}+\frac{V_\psi}{r\sin\theta}\cdot\frac{\partial V_\theta}{\partial\psi}+\frac{V_rV_\theta-V_\psi^2\cot\theta}{r}=-\frac{1}{r\rho}\cdot\frac{\partial p}{\partial\theta}\\ +\nu\left(\Delta V_\theta+\frac{2}{r^2}\cdot\frac{\partial V_r}{\partial\theta}-\frac{V_\theta}{r^2\sin^2\theta}-\frac{2\cos\theta}{r^2\sin^2\theta}\cdot\frac{\partial V_\psi}{\partial\psi}\right)+\frac{\nu}{3}\cdot\frac{1}{r}\cdot\frac{\partial\,\text{div}\,\bar V}{\partial\theta};\\ \frac{\partial V_\psi}{\partial t}+V_r\frac{\partial V_\psi}{\partial r}+\frac{V_\theta}{r}\cdot\frac{\partial V_\psi}{\partial\theta}+\frac{V_\psi}{r\sin\theta}\cdot\frac{\partial V_\psi}{\partial\psi}+\frac{V_\psi(V_r+V_\theta\cot\theta)}{r}\\ =-\frac{1}{\rho r\sin\theta}\cdot\frac{\partial p}{\partial\psi}+\nu\left(\Delta V_\psi-\frac{V_\psi}{r^2\sin^2\theta}+\frac{2}{r^2\sin\theta}\cdot\frac{\partial V_r}{\partial\psi}\right.\\ \left.+\frac{2\cos\theta}{r^2\sin^2\theta}\cdot\frac{\partial V_\theta}{\partial\psi}\right)+\frac{\nu}{3r\sin\theta}\cdot\frac{\partial\,\text{div}\,\bar V}{\partial\psi},\end{aligned}\right\}\quad(3.1.43')$$

where the operator

$$\Delta=\frac{1}{r^2}\cdot\frac{\partial}{\partial r}\left(r^2\frac{\partial}{\partial r}\right)+\frac{1}{r^2\sin\theta}\cdot\frac{\partial}{\partial\theta}\left(\sin\theta\frac{\partial}{\partial\theta}\right)+\frac{1}{r^2\sin^2\theta}\cdot\frac{\partial^2}{\partial\psi^2}.\quad(3.1.44)$$

The equations of motion can be written in still simpler form in the case of two-dimensional gas flows with variations in variables (velocity, pressure, density, etc.) along two coordinate lines only:

$$\left.\begin{aligned}
&\frac{\partial V_r}{\partial t}+V_r\frac{\partial V_r}{\partial r}+\frac{V_\theta}{r}\cdot\frac{\partial V_r}{\partial\theta}-\frac{V_\theta^2}{r}=-\frac{1}{\rho}\cdot\frac{\partial p}{\partial r}\\
&+\nu\left(\Delta V_r-\frac{2}{r^2}\cdot\frac{\partial V_\theta}{\partial\theta}-\frac{2V_r}{r^2}-\frac{2\,V_\theta\cot\theta}{r^2}\right)+\frac{\nu}{3}\cdot\frac{\partial\,\mathrm{div}\,\bar{V}}{\partial r};\\
&\frac{\partial V_\theta}{\partial t}+V_r\frac{\partial V_\theta}{\partial r}+\frac{V_\theta}{r}\cdot\frac{\partial V_\theta}{\partial\theta}+\frac{V_r\,V_\theta}{r}\\
&=-\frac{1}{r\rho}\cdot\frac{\partial p}{\partial\theta}+\nu\left(\Delta V_\theta+\frac{2}{r^2}\cdot\frac{\partial V_r}{\partial\theta}-\frac{V_\theta}{r^2\sin^2\theta}\right)+\frac{\nu}{3r}\cdot\frac{\partial\,\mathrm{div}\,\bar{V}}{\partial\theta},
\end{aligned}\right\}\quad(3.1.45)$$

where

$$\Delta=\frac{1}{r^2}\cdot\frac{\partial}{\partial r}\left(r^2\frac{\partial}{\partial r}\right)+\frac{1}{r^2\sin\theta}\cdot\frac{\partial}{\partial\theta}\left(\sin\theta\frac{\partial}{\partial\theta}\right);\qquad(3.1.46)$$

$$\mathrm{div}\,\bar{V}=\frac{1}{r^2}\cdot\frac{\partial\,(V_r r^2)}{\partial r}+\frac{1}{r\sin\theta}\cdot\frac{\partial\,(V_\theta\sin\theta)}{\partial\theta}.\qquad(3.1.47)$$

Equations of two-dimensional motion of gas along curved surface: For the case we are considering the curvilinear coordinates, Lame's parameters and velocity components are determined by equations (2.4.40), (2.4.42) and (2.4.43) respectively. Consider a further condition, that the motion takes place near a wall and consequently $y\ll R$. Then

$$q_1=x,\ q_2=y,\ q_3=\gamma,\ h_1=1,\ h_2=1,\ h_3=r,$$
$$V_1=dx/dt=V_x,\ V_2=V_y,\ V_3=0.$$

The acceleration component from these data will be

$$W_1=(\partial V_x/\partial t)+V_x\,(\partial V_x/\partial x)+V_y\,(\partial V_x/\partial y),\qquad(3.1.48)$$

and the pressure gradient component

$$(\mathrm{grad}\,p)_1=\partial p/\partial x.\qquad(3.1.49)$$

Besides, we have

$$(\mathrm{grad\ div}\,\bar{V})_1=\partial\,\mathrm{div}\,\bar{V}/\partial x,\qquad(3.1.50)$$

where divergence of velocity is determined by the relation (2.4.44). So

$$(\mathrm{grad\ div}\,\bar{V})_1=\frac{\partial}{\partial x}\left\{\frac{1}{r}\left[\frac{\partial\,(V_x r)}{\partial x}+\frac{\partial\,(V_y r)}{\partial y}\right]\right\}.\qquad(3.1.51)$$

The rotation of velocity component can be found with the help of (3.1.28):

$$(\mathrm{rot}\,\bar{V})_3=\partial V_y/\partial x-\partial V_x/\partial y,\quad(\mathrm{rot}\,\bar{V})_2=0.\qquad(3.1.52)$$

Substituting these expressions in (3.1.34), we get

$$(\text{rot rot } \bar{V})_1 = \frac{1}{r} \cdot \frac{\partial}{\partial y}\left[r\left(\frac{\partial V_y}{\partial x} - \frac{\partial V_x}{\partial y}\right)\right]. \tag{3.1.53}$$

From (3.1.51) and (3.1.53) we have

$$(\Delta V)_1 = (\text{grad div } \bar{V})_1 - (\text{rot rot } \bar{V})_1$$
$$= \frac{\partial}{\partial x}\left\{\frac{1}{r}\left[\frac{\partial (V_x r)}{\partial x} + \frac{\partial (V_y r)}{\partial y}\right]\right\} - \frac{1}{r} \cdot \frac{\partial}{\partial y}\left[r\left(\frac{\partial V_y}{\partial x} - \frac{\partial V_x}{\partial y}\right)\right]. \tag{3.1.54}$$

Similarly, the following expressions can be obtained for components along coordinate line q_2:

$$W_2 = \partial V_y/\partial t + V_x\,(\partial V_y/\partial x) + V_y\,(\partial V_y/\partial y); \tag{3.1.55}$$

$$(\text{grad } p)_2 = \partial p/\partial y, \tag{3.1.56}$$

$$(\text{grad div } \bar{V})_2 = \partial \text{ div } \bar{V}/\partial y; \tag{3.1.57}$$

$$\left.\begin{aligned}(\Delta V)_2 &= (\text{grad div } \bar{V})_2 - (\text{rot rot } \bar{V})_2 \\ &= \frac{\partial}{\partial y}\left\{\frac{1}{r}\left[\frac{\partial (V_x r)}{\partial x} + \frac{\partial (V_y r)}{\partial y}\right]\right\} - \frac{1}{r} \cdot \frac{\partial}{\partial x}\left[r\left(\frac{\partial V_y}{\partial x} - \frac{\partial V_x}{\partial y}\right)\right].\end{aligned}\right\} \tag{3.1.58}$$

Using the relations so obtained, the equations of motion can be written as:

$$\left.\begin{aligned}\frac{\partial V_x}{\partial t} + V_x \frac{\partial V_x}{\partial x} + V_y \frac{\partial V_x}{\partial y} &= -\frac{1}{\rho} \cdot \frac{\partial p}{\partial x} + \nu\,(\Delta V)_1 + \frac{\nu}{3} \cdot \frac{\partial \text{ div } \bar{V}}{\partial x}; \\ \frac{\partial V_y}{\partial t} + V_x \frac{\partial V_y}{\partial x} + V_y \frac{\partial V_y}{\partial y} &= -\frac{1}{\rho} \cdot \frac{\partial p}{\partial y} + \nu\,(\Delta V)_2 + \frac{\nu}{3} \cdot \frac{\partial \text{ div } \bar{V}}{\partial y},\end{aligned}\right\} \tag{3.1.59}$$

where $(\Delta V)_1$ and $(\Delta V)_2$ are given by formulas (3.1.54) and (3.1.58) respectively.

This way we get different forms of equations of motion of a viscous fluid. This was done because experience in research shows that in some cases it is convenient to use one form of equation, in other cases another form. The analysis of particular types of fluid motion using the most suitable form of equation will be discussed in the following chapters.

2. Equation of Energy and Diffusion of Gas

2.1 Equation of diffusion

Investigation of the motion of a dissociating viscous gas is related to the effect of diffusion of gas on this motion. This is due to the fact that diffusion is considered to be one of the basic equations of gas dynamics occurring in the study of an energy equation.

The process of dispersion of concentration as a result of molecular transfer is called diffusion. This is a thermodynamically irreversible process which acts as one of the sources of loss of mechanical energy on the part of a moving gas medium.

An equation of diffusion represents an equation of transfer of the i-th

component of a gas mixture (this equation will be the equation of continuity for the same component).

For simplification of research we assume that the difference between thermodiffusion and barodiffusion is infinitesimally small and the diffusion rate of the i-th component in any direction n is determined by the equation

$$Q_{idn} = -\rho D_i \, (\partial c_i / \partial n), \tag{3.2.1}$$

where c_i is concentration of the i-th component; D_i is the coefficient of diffusion determined by the diffusion flow in the presence of a concentration gradient.

For a mixture of gas components it is necessary to keep in mind the coefficients of binary diffusion corresponding to each pair of components, for example, for each pair of atoms and molecules of oxygen or nitrogen. The coefficient of binary diffusion in approximate calculations may be taken to be of a unique value $\overline{D}$ for each pair of components. Then $Q_{idn} = -\rho \overline{D}$ $(\partial c_i / \partial n)$. Assuming that diffusion takes place along x, y and z directions, we have:

$$Q_{idx} = -\rho \, \overline{D} \, (\partial c_i / \partial x), \; Q_{idy} = -\rho \, \overline{D} \, (\partial c_i / \partial y), \; Q_{idz} = -\rho \, \overline{D} \, (\partial c_i / \partial z), \tag{3.2.2}$$

or in vector form

$$\overline{Q}_{id} = -\rho \, \overline{D} \, \text{grad} \, c_i. \tag{3.2.3}$$

Diffusion of a substance takes place in a region of low concentration. Consequently, $\partial c_i / \partial n$ has a negative sign. Hence Q_{id} will be positive. The equation of diffusion can be examined on the assumption that motion is steady and takes place with respect to the cylindrical system of coordinates. Here the flow is supposed to be three-dimensional and symmetrical about the x axis, i.e. the component of velocity $V_y = 0$.

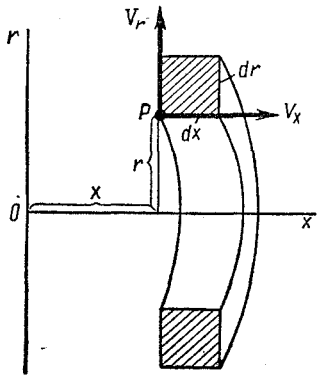

Fig. 3.2.1. Elementary gas particle in axisymmetrical three-dimensional flow.

Let us separate out an elemental volume of gas in the form of a ring with thickness dr and length dx (Fig. 3.2.1). Let the components of velocity be V_x and V_r at a point P having coordinates x and r. Assume that the diffusion flow occurs in a radial direction only. Hence the flow rate of the i-th component through an internal surface of the element is $m_r = 2\pi r \rho \; V_r c_i \; dx + Q_{id} 2\pi r dx$, where c_i and Q_{id} are the concentration and diffusion flow rate of the i-th component, calculated per unit area.

The flow rate of the i-th component through the external surface is

$$m_r + \frac{\partial m_r}{\partial r} dr = m_r + \frac{\partial (\rho V_r r c_i)}{\partial r} \; 2\pi dr dx + \frac{\partial (Q_{id} r)}{\partial r} \; 2\pi \, dr dx.$$

Ignoring the diffusion flow rate of the substance along the x axis, the gas flow rate through a left-hand element area perpendicular to this axis will be

$$m_x = \rho V_x c_i \, 2\pi r dr,$$

and through a right-hand elemental area

$$m_x + \frac{\partial m_x}{\partial x} dx = m_x + \frac{\partial (\rho V_x r c_i)}{\partial x} 2\pi dr dx.$$

Thus the flow rate of the i-th component in a given volume will be equal to

$$[\partial (\rho V_x r c_i)/\partial x] \, 2\pi dr dx.$$

As the quantity of gas in a given volume must not change the general inflow of the i-th component will be equal to its consumption in chemical reactions. If the rate of transformation of the i-th component in unit volume of gas due to chemical reactions is $(W_{\text{chem}})_i$ [kg/m^3·sec] the consumption rate of the i-th component in a given elemental volume will be $(W_{\text{chem}})_i \, 2\pi r dr dx$. Then the balance of mass of the i-th component in a given volume can be written in the following way:

$$\frac{\partial (\rho V_x r c_i)}{\partial x} + \frac{\partial (\rho V_r r c_i)}{\partial r} = -\frac{\partial (Q_{id} r)}{\partial r} + (W_{\text{chem}})_i \, r. \tag{3.2.4}$$

This equation is known as the equation of diffusion in cylindrical coordinates. Similarly the equation of diffusion for a plane flow can be obtained in the Cartesian system of coordinates x and y:

$$\frac{\partial (\rho V_x c_i)}{\partial x} + \frac{\partial (\rho V_y c_i)}{\partial y} = -\frac{\partial Q_{id}}{\partial y} + (W_{\text{chem}})_i, \tag{3.2.5}$$

where Q_{id} is found from (3.2.3).

If a binary mixture of atoms and molecules is taken $\Sigma c_i = c_A + c_M = 1$ and hence $Q_{Ad} = -Q_{Md}$. The value of $(W_{\text{chem}})_i$ for a given reaction in a dissociating gas is determined by the formula of chemical kinetics (4.9.7′).

2.2 Equation of energy

An equation of energy comes into the picture along with the equations of state, motion and continuity in the system of differential equations. The solution of these equations completely determines the motion of a gas.

Consider a system of Cartesian coordinates and formulate the equation of energy for a fluid particle in the form of an elemental parallelepiped. This equation represents the law of conservation of energy according to which the change in total energy consisting of the kinetic and internal energy of particles in time dt is equal to the work done on an elemental particle by external forces plus the heat flow to it from outside.

The kinetic energy of a particle having volume $\tau = dxdydz$ is equal to $(\rho V^2/2)\tau$ and its internal energy is $U\rho\tau$ (U is the internal energy of unit mass of fluid). Consequently the change in total energy for the time dt will be

$$\frac{d}{dt}\left[\left(\frac{\rho V^2}{2}+\rho U\right)\tau\right]dt=\rho\tau\frac{d}{dt}\left(\frac{V^2}{2}+U\right)dt.$$

The work done by external mass (volume) forces during the motion of a particle in time dt can be expressed by the scalar product $\overline{G}\cdot\overline{V}$, multiplied by the mass of particle $\rho\tau$ and time dt. The vector of mass force is $\overline{G}=Xi+Yj+Zk$ and hence

$$(\overline{G}.\overline{V})\,\rho\tau\,dt=(XV_x+YV_y+ZV_z)\,\rho\tau\,dt.$$

Let us now calculate the work done by surface forces. First we will consider the work done in time dt by the forces set up by stresses acting on the right and left sides. The work done by such forces on the left side is equal to the scalar product $\overline{\sigma}_x\cdot\overline{V}$ multiplied by area $dydz$ and time dt. In a scalar product the vector of surface forces is

$$\overline{\sigma}_x=p_{xx}\,i+\tau_{xy}\,j+\tau_{xz}\,k.$$

The work done by the surface forces acting on the right side is equal to

$$\left[\overline{\sigma}_x\cdot\overline{V}+\frac{\partial\,(\overline{\sigma}_x\cdot\overline{V})}{\partial x}\,dx\right]dydzdt.$$

This expression has a positive sign because the forces on the right side are directed to the opposite side.

Summation of the work done by all surface forces acting on the left and right sides gives:

$$\frac{\partial\,(\overline{\sigma}_x\cdot\overline{V})}{\partial x}\,\tau\,dt=\left[\frac{\partial}{\partial x}\,(p_{xx}\,V_x+\tau_{xy}\,V_y+\tau_{xz}\,V_z)\right]\tau dt. \tag{3.2.6}$$

Similarly the expressions for work done by the surface forces acting on the lower and upper faces and on the rear and front faces of the element can respectively be obtained by:

$$[\partial\,(\overline{\sigma}_y\cdot\overline{V})/\partial y]\;\tau dt \quad\text{and}\quad [\partial\,(\overline{\sigma}_z\cdot\overline{V})/\partial z]\,\tau dt.$$

As the vectors of surface forces acting on the lower and rear faces are respectively equal to

$$\overline{\sigma}_y=\tau_{yx}\,i+p_{yy}\,i+\tau_{yz}\,k;$$

$$\overline{\sigma}_z=\tau_{zx}\,i+\tau_{zy}\,j+p_{zz}\,k,$$

the expressions for work done will be:

$$\frac{\partial\,(\overline{\sigma}_y\cdot\overline{V})}{\partial y}\,\tau\,dt=\left[\frac{\partial}{\partial y}\,(\tau_{yx}\,V_x+p_{yy}\,V_y+\tau_{yz}\,V_z)\right]\tau dt, \tag{3.2.6'}$$

$$\frac{\partial\,(\overline{\sigma}_z\cdot\overline{V})}{\partial z}\,\tau\,dt=\left[\frac{\partial}{\partial z}\,(\tau_{zx}\,V_x+\tau_{zy}\,V_y+p_{zz}\,V_z)\right]\tau dt. \tag{3.2.6''}$$

The stresses in expressions (3.2.6), (3.2.6′) and (3.2.6″) are determined by the relations (3.1.5) and (3.1.16) respectively.

The heat flow to a particle takes place through heat conduction, diffusion and radiation. Let $q_x dydz$ (where q_x is the specific heat flow rate) represent heat flow due to heat conduction or diffusion to the particle through its left side in unit time. The amount of heat flow rate to the particle is $q_x dydzdt$ in time dt. Heat flow through the right side is equal to $-[q_x+(\partial q_x/\partial x)dx]$ $dydzdt$. The amount of heat flow to the particle across both these sides is $-(\partial q_x/\partial x)\,\tau dt$. Similar expressions can be obtained for sides perpendicular to axes y and z. The resultant total heat flow to the particle will then be equal to

$$-[(\partial q_x/\partial x)+(\partial q_y/\partial y)+(\partial q_z/\partial z)]\,\tau dt.$$

If heat transfer due to heat conduction is examined the heat flow rates, equal to the flow of heat along corresponding coordinate directions through unit area in unit time, can be expressed by Fourier's rule:

$$q_{Tx}=-\lambda\,(\partial T/\partial x),\quad q_{Ty}=-\lambda\,(\partial T/\partial y),\quad q_{Tz}=-\lambda\,(\partial T/\partial z). \tag{3.2.7}$$

Taking this into account, we get

$$-[(\partial q_{Tx}/\partial x)+(\partial q_{Ty}/\partial y)+(\partial q_{Tz}/\partial z)]\,\tau\,dt=\operatorname{div}(\lambda\,\operatorname{grad}T)\,\tau dt, \tag{3.2.8}$$

where

$$\operatorname{grad}T=(\partial T/\partial x)\,i+(\partial T/\partial y)\,j+(\partial T/\partial z)\,k.$$

The energy flow to the particle of gas as a result of diffusion can be written in the following way:

$$q_{dx}=\sum_i Q_{idx}\,i_i,\quad q_{dy}=\sum_i Q_{idy}\,i_i,\quad q_{dz}=\sum_i Q_{idz}\,i_i,$$

where i_i is the total enthalpy of the component of gas mixture.
Consequently

$$-\left(\frac{\partial q_{dx}}{\partial x}+\frac{\partial q_{dy}}{\partial y}+\frac{\partial q_{dz}}{\partial z}\right)\tau dt=-\left(\sum_i i_i\frac{\partial Q_{idx}}{\partial x}\right.$$

$$\left.+\sum_i i_i\frac{\partial Q_{idy}}{\partial y}+\sum_i i_i\frac{\partial Q_{idz}}{\partial z}\right)\tau dt=\left(-\sum_i i_i\operatorname{div}\overline{Q}_{id}\right)\tau dt.$$

Inserting the value of $\overline{Q}_{id}$ from (3.2.3) in this, we get

$$-[(\partial q_{dx}/\partial x)+(\partial q_{dy}/\partial y)+(\partial q_{dz}/\partial z)]\,\tau dt=\sum_i i_i\operatorname{div}(\rho\,\overline{D}\,\operatorname{grad}c_i)\,\tau dt. \tag{3.2.9}$$

Besides the energy brought to the particle by means of heat conductivity

and diffusion the heat due to radiation equal to $\varepsilon\tau dt$ (ε is the heat flow rate due to radiation in unit time per unit volume) also flows to it.

Equating the change in energy of this particle in time dt to the summation of work done by mass and surface forces and the heat flow due to heat conductivity, diffusion and radiation, we get the equation of energy:

$$\left.\begin{aligned}\rho\frac{d}{dt}\left(\frac{V^2}{2}+U\right)&=\rho\,(XV_x+YV_y+ZV_z)+\frac{\partial}{\partial x}(p_{xx}\,V_x+\tau_{xy}\,V_y\\&+\tau_{xz}\,V_z)+\frac{\partial}{\partial y}(\tau_{yx}\,V_x+p_{yy}\,V_y+\tau_{yz}\,V_z)+\frac{\partial}{\partial z}(\tau_{zx}\,V_x+\tau_{zy}\,V_y\\&+p_{zz}\,V_z)+\operatorname{div}(\lambda\operatorname{grad}T)+\sum_i i_i\operatorname{div}(\rho\,\overline{D}\operatorname{grad}c_i)+\varepsilon.\end{aligned}\right\}\quad(3.2.10)$$

During the motion of a chemically reacting mixture of gases the equation of energy must show the condition of heat balance, which includes heat appearing as a result of chemical reactions. However if we assume that the resultant enthalpy of gas mixture $\Sigma c_i i_i$ during reactions remains unaltered, we need not separately consider in equation (3.2.10) the liberation or absorption of heat due to chemical reactions.

Substituting expressions for stresses from (3.1.5), (3.1.16) to (3.2.10) and ignoring the term for the work done by mass forces, we get, after suitable changes, an equation of energy for gas in the following form:

$$\left.\begin{aligned}\rho\frac{d}{dt}\left(\frac{V^2}{2}+U\right)&=-\operatorname{div}(p\overline{V})-\frac{2}{3}\operatorname{div}(\mu\overline{V}\operatorname{div}\overline{V})+\frac{\partial}{\partial x}\left(\mu\frac{\partial V_x^2}{\partial x}\right)\\&+\frac{\partial}{\partial y}\left(\mu\frac{\partial V_y^2}{\partial y}\right)+\frac{\partial}{\partial z}\left(\mu\frac{\partial V_z^2}{\partial z}\right)+2\frac{\partial}{\partial x}[\mu\,(V_y\,\varepsilon_z+V_z\,\varepsilon_y)]\\&+2\frac{\partial}{\partial y}[\mu(V_x\varepsilon_z+V_z\varepsilon_x)]+2\frac{\partial}{\partial z}[\mu\,(V_x\varepsilon_y+V_y\,\varepsilon_x)]\\&+\operatorname{div}(\lambda\operatorname{grad}T)+\sum_i i_i\operatorname{div}(\rho\,\overline{D}\operatorname{grad}c_i)+\varepsilon.\end{aligned}\right\}\quad(3.2.11)$$

Equation (3.2.11) shows the reason for change in the kinetic energy of a fluid. Besides heat conduction, diffusion and radiation, this energy varies due to the work done through compression div $(p\overline{V})$ and work done by frictional force (terms containing the coefficient of dynamic viscosity μ). The dissipation (from Latin *dissipare*—"disperse") of energy is related to the losses of mechanical energy in overcoming frictional forces. Dissipation of energy occurs due to the fact that part of the mechanical energy will be unidirectionally transformed into heat. Therefore frictional forces are known as dissipating forces. The terms on the right side of equation (3.2.11) containing μ form the dissipating function.

For a two-dimensional plane motion of a viscous medium the energy equation will be:

$$\left.\begin{aligned}\rho\frac{d}{dt}\left(\frac{V^2}{2}+U\right)&=-\operatorname{div}(p\overline{V})-\frac{2}{3}\operatorname{div}(\mu\,\overline{V}\operatorname{div}\overline{V})\\+\frac{\partial}{\partial x}\left(\mu\frac{\partial V_x^2}{\partial x}\right)&+\frac{\partial}{\partial y}\left(\mu\frac{\partial V_y^2}{\partial y}\right)+2\frac{\partial}{\partial x}(\mu V_y\varepsilon_z)+2\frac{\partial}{\partial y}(\mu V_x\varepsilon_z)\\&+\operatorname{div}(\lambda\operatorname{grad}T)+\sum_i i_i\operatorname{div}(\rho\bar{D}\operatorname{grad}c_i)+\varepsilon,\end{aligned}\right\}\quad(3.2.12)$$

where

$$\overline{V}=V_x i+V_y j,\quad \operatorname{div}\overline{V}=\partial V_x/\partial x+\partial V_y/\partial y,$$

$$\operatorname{grad}T=(\partial T/\partial x)\,i+(\partial T/\partial y)\,j,\quad \operatorname{grad}c_i=(\partial c_i/\partial x)i+(\partial c_i/\partial y)\,j.$$

Let us transform the equation of energy (3.2.12). Multiply the first equation of (3.1.20) by V_x, the second by V_y and add. Then

$$\left.\begin{aligned}\rho\frac{d}{dt}\left(\frac{V^2}{2}\right)&=-\left(V_x\frac{\partial p}{\partial x}+V_y\frac{\partial p}{\partial y}\right)+V_x\frac{\partial}{\partial x}\left[\mu\left(2\frac{\partial V_x}{\partial x}-\frac{2}{3}\operatorname{div}\overline{V}\right)\right]\\+V_y\frac{\partial}{\partial y}&\left[\mu\left(2\frac{\partial V_y}{\partial y}-\frac{2}{3}\operatorname{div}\overline{V}\right)\right]+2\left[V_x\frac{\partial}{\partial y}(\mu\varepsilon_z)+V_y\frac{\partial}{\partial x}(\mu\varepsilon_z)\right].\end{aligned}\right\}\quad(3.2.13)$$

Using simple transformations, it can be shown that

$$V_x(\partial p/\partial x)+V_y(\partial p/\partial y)=\operatorname{div}(p\overline{V})-p\operatorname{div}\overline{V},$$

where $p\operatorname{div}\overline{V}$ can be found from the equation of continuity

$$p\operatorname{div}\overline{V}=-(p/\rho)(d\rho/dT),$$

or

$$p\operatorname{div}\overline{V}=\rho(d/dt)(p/\rho)-(dp/dt).$$

Two other terms on the right side of the equation can be transformed into the following form:

$$\begin{aligned}V_x\frac{\partial}{\partial x}&\left[\mu\left(2\frac{\partial V_x}{\partial x}-\frac{2}{3}\operatorname{div}\overline{V}\right)\right]+V_y\frac{\partial}{\partial y}\left[\mu\left(2\frac{\partial V_y}{\partial y}-\frac{2}{3}\operatorname{div}\overline{V}\right)\right]\\&=\frac{\partial}{\partial x}\left(\mu\frac{\partial V_x^2}{\partial x}\right)+\frac{\partial}{\partial y}\left(\mu\frac{\partial V_y^2}{\partial y}\right)-\mu\left[\left(\frac{\partial V_x}{\partial x}\right)^2+\left(\frac{\partial V_y}{\partial y}\right)^2\right]\\&\quad-\frac{2}{3}\operatorname{div}(\mu\overline{V}\operatorname{div}\overline{V})+\frac{2}{3}\mu(\operatorname{div}\overline{V})^2.\end{aligned}$$

For the last term of (3.2.13) we get the expression

$$\begin{aligned}2\left[V_x\frac{\partial}{\partial y}(\mu\varepsilon_z)+V_y\frac{\partial}{\partial x}(\mu\varepsilon_z)\right]&=2\frac{\partial}{\partial x}(\mu V_y\varepsilon_z)\\&+2\frac{\partial}{\partial y}(\mu V_x\varepsilon_z)-4\mu\varepsilon_z^2.\end{aligned}$$

Introducing a corresponding change in (3.2.13) and subtracting the equation so obtained from (3.2.12), we get

$$\left.\begin{aligned}\rho\frac{di}{dt}=\frac{dp}{dt}+\mu\left\{\left[\left(\frac{\partial V_x}{\partial x}\right)^2+\left(\frac{\partial V_y}{\partial y}\right)^2\right]-\frac{2}{3}(\operatorname{div}\overline{V})^2+4\varepsilon_z^2\right\}\\ +\operatorname{div}(\lambda\operatorname{grad}T)+\sum_i i_i\operatorname{div}(\rho\,\overline{D}\operatorname{grad}c_i)+\varepsilon.\end{aligned}\right\}\quad(3.2.14)$$

where enthalpy $i=U+(p/\rho)$.

In the absence of the heat transfer due to diffusion and radiation the equation of energy can be written in the form

$$\left.\begin{aligned}\rho\frac{di}{dt}=\frac{dp}{dt}+\mu\left\{\left[\left(\frac{\partial V_x}{\partial x}\right)^2+\left(\frac{\partial V_y}{\partial y}\right)^2\right]-\frac{2}{3}(\operatorname{div}\overline{V})^2\right.\\ \left.+4\varepsilon_z^2\right\}+\operatorname{div}(\lambda\operatorname{grad}T).\end{aligned}\right\}\quad(3.2.15)$$

At low speeds of gas flow, i.e. when the work done by frictional forces is small, the dissipating terms can be neglected. Moreover the work done by pressure forces ($dp/dt\approx 0$) under such conditions is also small. In this case, in place of equation (3.2.15) we will have

$$(dT/dt)=(\lambda/\rho\,c_p)\operatorname{div}(\operatorname{grad}T).\qquad(3.2.16)$$

The quantity $\lambda/(\rho c_p)=a$, known as the coefficient of temperature flow, characterizes the intensity of molecular heat exchange.

3. System of Gas Dynamic Equations. Initial and Boundary Conditions

Study of the motion of a gaseous medium, i.e. determination of the parameters at each point in space that characterize this motion, consists of solution of the appropriate equations connecting these parameters. All these equations are independent and together they form the system of gas dynamic equations. The number of such independent equations in the system is determined by the number of unknown gas parameters that we wish to know.

Let us consider the case of the motion of an ideal compressible gas. If the flow velocity is not high the variation of specific heats with temperature can be ignored and the radiation of energy can also be ignored. In this case the gas flow represents itself as a thermodynamically isolated system and will be treated as an adiabatic flow. The unknown quantities for the case we are considering will be the three velocity components V_x, V_y, V_z, pressure p, density ρ and temperature T. Hence the system of gas dynamic equations must consist of six independent equations. The equations of motion, continuity, state and energy, known as the basic equations of gas dynamics, are included in this system.

Before writing down this system of equations we will study the equation of energy independently. According to the assumption of adiabatic flow the energy equation (3.2.14) can be transformed into

$$di=dp/\rho. \tag{3.3.1}$$

Keeping in mind that $di=c_p dT$ and taking into account the expressions $c_p-c_v=R$ and $p=R\rho T$, it can be shown that

$$c_p=\frac{(c_p/c_v)\,R}{c_p/c_v-1}=\frac{k}{k-1}R, \quad dT=\frac{1}{R}d\left(\frac{p}{\rho}\right).$$

Then equation (3.3.1) leads to

$$dp/p=k\,(d\rho/\rho).$$

Hence we get an expression for pressure in the form

$$p=A\rho^k, \tag{3.3.2}$$

where A is a constant quantity typical for given conditions of gas flow.

As we know, equation (3.3.2) is called an adiabatic (isentropic) equation. So in the present case the equation of energy coincides with an adiabatic equation. Then all the equations of the system can be written as follows:

$$\left.\begin{array}{ll} \dfrac{dV_x}{dt}=-\dfrac{1}{\rho}\cdot\dfrac{\partial p}{\partial x}, & \dfrac{dV_y}{dt}=-\dfrac{1}{\rho}\cdot\dfrac{\partial p}{\partial y}; \\ \dfrac{dV_z}{dt}=-\dfrac{1}{\rho}\cdot\dfrac{\partial p}{\partial z}, & \dfrac{d\rho}{dt}+\rho\,\mathrm{div}\,\overline{V}=0; \\ p=R\rho T, & p=A\rho^k. \end{array}\right\} \tag{3.3.3}$$

Let us now study the system of equations for a more general case of motion of an inviscid gas at high speeds during which the specific heat changes with the temperature and the processes of dissociation and ionization may occur in the gas. Here, for the sake of generality, we acknowledge the possibility of radiation of energy by the heated gas. Then the thermodynamic process in the gas flow will no longer be adiabatic. Accordingly, the quantity ε determining the radiating heat flow remains on the right side of the energy equation (3.2.14). Further, the equation of state should be taken in the form of (1.4.8) where the variation of average molecular weight μ_{av} with temperature and pressure is considered. Assuming that the equations of motion and state do not change in form, the basic equations of the system will have the following form:

$$\left.\begin{array}{ll} \dfrac{dV_x}{dt}=-\dfrac{1}{\rho}\cdot\dfrac{\partial p}{\partial x}, & \dfrac{dV_y}{dt}=-\dfrac{1}{\rho}\cdot\dfrac{\partial p}{\partial y}; \\ \dfrac{dV_z}{dt}=-\dfrac{1}{\rho}\cdot\dfrac{\partial p}{\partial z}, & \dfrac{d\rho}{dt}+\rho\,\mathrm{div}\,\overline{V}=0; \\ p=\dfrac{R_0}{\mu_{av}}\rho T, & \rho\dfrac{di}{dt}=\dfrac{dp}{dt}+\varepsilon. \end{array}\right\} \tag{3.3.4}$$

It can easily be seen that three more quantities, i.e, enthalpy i, average molecular weight of gas μ_{av} and heat flow due to radiation ε, appear in this system in addition to the above-mentioned six unknown quantities (V_x, V_y, V_z, p, ρ, T). Along with these quantities it is necessary to determine entropy S and also speed of sound a in studying the behavior of the gas flow. So the total number of unknown parameters figuring in the gas flow problem becomes five. Therefore it is necessary to add the same number of independent relations for these additional unknowns to the system of basic equations. These relations can be written in the form of general equations determining unknown quantities as functions of pressure and temperature:

$$i=f_1(p, T); \tag{3.3.5}$$

$$S=f_2(p, T); \tag{3.3.6}$$

$$\mu_{av}=f_3(p, T); \tag{3.3.7}$$

$$a=f_4(p, T); \tag{3.3.8}$$

$$\varepsilon=f_5(p, T). \tag{3.3.9}$$

Investigation of these functions is the subject of special departments of physics and thermodynamics.

The solution of equations (3.3.4) to (3.3.9) determines the parameters of motion of an inviscid, dissociating and ionizing gas with consideration of radiation effects. Study of such motion is dealt with in the aerodynamics of radiating gas.

Finally we will consider a still more general case of flow, taking in the effects of frictional forces and heat transfer. We assume here that chemical reactions take place in the gas. The main equations of this system will therefore be written in the following way (for brevity only a plane two-dimensional flow will be considered):

$$\left.\begin{aligned}
&\frac{dV_x}{dt}=-\frac{1}{\rho}\cdot\frac{\partial p}{\partial x}+\frac{1}{\rho}\cdot\frac{\partial}{\partial x}\left[\mu\left(2\frac{\partial V_x}{\partial x}-\frac{2}{3}\operatorname{div}\overline{V}\right)\right]\\
&\qquad+\frac{2}{3}\cdot\frac{\partial}{\partial y}(\mu\varepsilon_z);\\
&\frac{dV_y}{dt}=-\frac{1}{\rho}\cdot\frac{\partial p}{\partial y}+\frac{1}{\rho}\cdot\frac{\partial}{\partial y}\left[\mu\left(2\frac{\partial V_y}{\partial y}-\frac{2}{3}\operatorname{div}\overline{V}\right)\right]\\
&\qquad+\frac{2}{3}\cdot\frac{\partial}{\partial x}(\mu\varepsilon_z);\\
&\frac{d\rho}{dt}+\rho\operatorname{div}\overline{V}=0;\quad p=\frac{R_0}{\mu_{av}}\rho T;\\
&\rho\frac{di}{dt}=\frac{dp}{dt}+\mu\left\{\left[\left(\frac{\partial V_x}{\partial x}\right)^2+\left(\frac{\partial V_y}{\partial y}\right)^2\right]-\frac{2}{3}(\operatorname{div}\overline{V})^2+4\varepsilon_z^2\right\}\\
&\qquad+\operatorname{div}(\lambda\operatorname{grad}T)+\sum_i i_i\operatorname{div}(\rho\overline{D}\operatorname{grad}c_i)+\varepsilon.
\end{aligned}\right\} \tag{3.3.10}$$

This system is to be completed by the relations (3.3.5) to (3.3.9) and by the general relations for the coefficient of heat transfer

$$\lambda = f_6(p, T); \tag{3.3.11}$$

coefficient of dynamic viscosity

$$\mu = f_7(p, T) \tag{3.3.12}$$

and specific heats

$$\left.\begin{aligned} c_p &= f_8(p, T); \\ c_v &= f_9(p, T). \end{aligned}\right\} \tag{3.3.13}$$

The last two quantities do not enter directly into equations (3.3.10). However, they are used in their solution so far as the determination of the thermodynamic characteristics of the gas is concerned. In addition, it is necessary to use the equation of diffusion (3.2.5) because the heat exchange due to diffusion is taken into account in the energy equation. At the same time it should be borne in mind that the concentration c_i appearing in the equations of energy and diffusion is a function of pressure and temperature and may be expressed by the general relation

$$c_i = f_{10}(p, T). \tag{3.3.14}$$

The system of equations given above, consisting of the basic equations of gas dynamics and the corresponding number (depending on the number of unknown quantities to be found) of additional relations, is studied in the aerodynamics of viscous gas. This system, in principle, helps in the determination of the distribution of normal and tangential stresses and also the aerodynamic heat flows from a heated gas to the wall under interaction. The given system is simplified in some particular cases for which determination of the scheme of interaction processes is possible. This makes the solution of differential equations easy.

In the process of solving these equations the necessity arises for additional relations for determination of the characteristic parameters of motion. These include, for example, relations for determining specific heats and the degree of dissociation as functions of pressure and temperature, formulas for calculation of frictional stress depending on velocity, etc.

The solution of a system of gas dynamic equations, describing a flow over a given surface, must satisfy the given initial and boundary conditions of this flow-interaction.

The initial conditions are determined by the values of the gas parameters for a given moment of time and obviously they have significance only for unsteady motion.

The boundary conditions are imposed on the solution of the problem for both steady and unsteady flows and they must be fulfilled at every moment of time for this motion. The solution under this condition must be such that

the parameters so determined at the boundary dividing disturbed and undisturbed regions of flow are equal to the values of the undisturbed parameters.

The second boundary condition is obtained by the nature of the gas flow on the surface being studied. If the gas is viscous and the surface is impermeable the flow is characterized by motion adhering to the surface (no separation). According to this condition of flow the component of velocity normal to the surface at any point over it is equal to zero and the resultant velocity vector coincides with the direction of the tangent to the surface at that point.

It is known that the vector grad F [$F(q_1, q_2, q_3)=0$ is the equation of the surface in a flow, q_1, q_2, q_3 being the generalized curvilinear coordinates] coincides with the direction of a normal to the surface. Then a smooth flow over the surface leads to the condition that the scalar product of this vector and the velocity vector $\overline{V}$ will be equal to zero. So the condition of smooth flow over a body can be expressed in mathematical form as

$$\overline{V}\cdot\operatorname{grad} F=0.$$

Bearing in mind that

$$\operatorname{grad} F=\frac{1}{h_1}\cdot\frac{\partial F}{\partial q_1}i_1+\frac{1}{h_2}\cdot\frac{\partial F}{\partial q_2}i_2+\frac{1}{h_3}\cdot\frac{\partial F}{\partial q_3}i_3, \tag{3.3.15}$$

the condition of flow without separation can be written as

$$\frac{1}{h_1}\cdot\frac{\partial F}{\partial q_1}V_1+\frac{1}{h_2}\cdot\frac{\partial F}{\partial q_2}V_2+\frac{1}{h_3}\cdot\frac{\partial F}{\partial q_3}V_3=0. \tag{3.3.16}$$

In Cartesian coordinates

$$\operatorname{grad} F=\frac{\partial F}{\partial x}i_1+\frac{\partial F}{\partial y}i_2+\frac{\partial F}{\partial z}i_3.$$

Consequently equation (3.3.16) will be

$$V_x\frac{\partial F}{\partial x}+V_y\frac{\partial F}{\partial y}+V_z\frac{\partial F}{\partial z}=0. \tag{3.3.17}$$

In the case of a two-dimensional plane flow

$$V_y/V_x=-\frac{\partial F/\partial x}{\partial F/\partial y}. \tag{3.3.17'}$$

If the equation of surface is given in cylindrical coordinates,

$$\operatorname{grad} F=\frac{\partial F}{\partial x}i_1+\frac{\partial F}{\partial r}i_2+\frac{1}{r}\cdot\frac{\partial F}{\partial \gamma}i_3;$$

hence the condition of zero normal velocity will be

$$\frac{\partial F}{\partial x}V_x+\frac{\partial F}{\partial r}V_r+\frac{1}{r}\cdot\frac{\partial F}{\partial \gamma}V_\gamma=0. \tag{3.3.18}$$

In the case of a rotating surface in a gas flow we get

$$\frac{\partial F}{\partial x} V_x + \frac{\partial F}{\partial r} V_r = 0, \tag{3.3.18'}$$

from which the ratio of velocities will be given by

$$\frac{V_r}{V_x} = -\frac{\partial F/\partial x}{\partial F/\partial r}. \tag{3.3.19}$$

Other boundary conditions determined for any particular body can also be formulated. Here, boundary conditions for a viscous gas differ from those of an ideal medium. In particular, the solution of the corresponding equations in the case of motion of a viscous gas in the boundary layer must satisfy the conditions on the surface and on the external limit of the boundary layer. Experimentally it is found that the gas particles seem to adhere to the surface and hence the velocity over the surface is equal to zero. At the external limit of the boundary layer the velocity will be the same as in the free (inviscid) flow and the frictional stress will be equal to zero.

4. Integrals of Equations of Motion in an Ideal Fluid

The differential equations written for the general case of motion cannot be integrated in their final form. But the integrals of these equations can at least be obtained for a particular case of ideal (inviscid) gas flow.

The equation of motion of an ideal gas is written in vector form as:

$$\frac{\partial \overline{V}}{\partial t} + \operatorname{grad} \frac{V^2}{2} + \operatorname{rot} \overline{V} \times \overline{V} = -\frac{1}{\rho} \operatorname{grad} p. \tag{3.4.1}$$

This equation can be obtained from the vector relation (3.1.22') in which the terms on the right side, accounting for the viscous effect, are supposed to be zero.

The equation of motion in the form (3.4.1) was first obtained by the Russian scientist Prof. I.S. Gromyeko. In the presence of mass forces Gromyeko's equation takes the following form:

$$\frac{\partial \overline{V}}{\partial t} + \operatorname{grad} \frac{V^2}{2} + \operatorname{rot} \overline{V} \times \overline{V} = \overline{G} - \frac{1}{\rho} \operatorname{grad} p. \tag{3.4.2}$$

Assuming the unsteady flow to be potential, we get $\operatorname{rot} \overline{V} = 0$, $\overline{V} = \operatorname{grad} \varphi$. Besides, we assume that the mass forces have potential U and therefore $\overline{G} = -\operatorname{grad} U$, where

$$\operatorname{grad} U = \frac{\partial U}{\partial x} i + \frac{\partial U}{\partial y} j + \frac{\partial U}{\partial z} k.$$

If the medium is barotropic, characterizing a single-valued relation between pressure and density (this takes place, for example, in the case of an adiabatic flow for which $p = A\rho^k$) the ratio dp/ρ is equal to a differential for some func-

tion P and hence

$$(1/\rho)\,\text{grad}\,p=\text{grad}\,P.$$

Taking this into account, equation (3.4.2) can be written in the following form:

$$(\partial/\partial t)\,\text{grad}\,\varphi+\text{grad}\,(V^2/2)=-\text{grad}\,U-\text{grad}\,P.$$

Replacing the derivative $(\partial/\partial t)\,\text{grad}\,\varphi$ by the quantity $\text{grad}\,(\partial\varphi/\partial t)$, we get

$$\text{grad}\,(\partial\varphi/\partial t)+\text{grad}\,(V^2/2)=-\text{grad}\,U-\text{grad}\,P. \tag{3.4.3}$$

Transferring this relation of gradients to the relation of corresponding scalar functions we get

$$(\partial\varphi/\partial t)+(V^2/2)+P+U=C\,(t), \tag{3.4.4}$$

where

$$P=\int dp/\rho. \tag{3.4.5}$$

Equation (3.4.4) is called Lagrange's equation or Lagrange's integral. The right side of equation (3.4.4) represents the function of time independent of coordinates, i.e. it is unique for any point in a given potential flow. The terms on the right side have a simple physical meaning: $V^2/2$ is kinetic energy per unit mass and $P=\int dp/\rho$ is potential energy due to pressure per unit mass; U is potential energy due to the position of fluid particle per unit mass. We recall the relation for potential function $\partial\varphi/\partial s=V_s$ to understand the physical meaning of the first term, where V_s is the projection of a velocity vector along some direction s. Function φ can be determined from the condition $\varphi=\int_{s_0}^{s} V_s ds$ (where s_0 and s are coordinates of fixed and arbitrary points respectively). The derivative $\partial\varphi/\partial t=\int_{s_0}^{s}(\partial V_s/\partial t)ds$. Local acceleration $\partial V_s/\partial t$ can be taken as the projection of inertial force due to the presence of local acceleration per unit mass and the product $(\partial V_s/\partial t)\,ds$ is the work done by this force on segment ds. Then the derivative $\partial\varphi/\partial t$ is equal to the work done by inertial force on the segment between points s_0 and s. It can be considered as the energy per unit mass due to the rate of change of velocity at a given point and due to the pressure in that condition.

Then the expression on the left side of (3.4.4) represents energy per unit mass of gas. Thus Lagrange's equation establishes the fact that the total energy per unit mass of gas at a given time in potential flow is the quantity that is constant for all points in the flow.

For an incompressible fluid, whose motion takes place under the action of pressure force and weight, the integral (3.4.4) is given by

$$(\partial\varphi/\partial t)+(V^2/2)+(p/\rho)+U=C\,(t). \tag{3.4.6}$$

If, in particular, the y axis is directed vertically upward $U=gy$ and

$$(\partial\varphi/\partial t)+(V^2/2)+(p/\rho)+gy=C(t). \tag{3.4.6'}$$

The particular case of steady potential flow, for which $\partial\varphi/\partial t=0$ and function $C(t)=\text{const}$, i.e. φ independent of time, is of great practical value. In this case equation (3.4.4) reduces to

$$V^2/2+\int(dp/\rho)+U=\text{const}. \tag{3.4.7}$$

This particular form of Lagrange's equation is known as Euler's equation. It represents the limitation of steady potential motion of a gas, indicating that the total energy per unit mass of gas has constant value at all points in the flow. In this way the constant in Euler's equation is not only unique for the whole region of flow but, unlike the function $C(t)$ of Lagrange's integral, it is independent of time.

Euler's equation for an incompressible fluid ($\rho=\text{const}$) will be the same as (3.4.7) in form with the difference that the ratio p/ρ replaces $\int dp/\rho$.

Let us consider the more general case of a steady potential flow of gas. The equation of this type of motion will be given as

$$\text{grad}\,(V^2/2)+\text{rot}\,\overline{V}\times\overline{V}=-\text{grad}\,P-\text{grad}\,U \tag{3.4.8}$$

or

$$\text{grad}\,[V^2/2+\int(dp/\rho)+U]=-\text{rot}\,\overline{V}\times\overline{V}. \tag{3.4.8'}$$

The right side of equation (3.4.8') is equal to zero if the vectors rot $\overline{V}$ and $\overline{V}$ are parallel, i.e. under the condition that the vortex line and stream line coincide with each other. In that case

$$V^2/2+\int(dp/\rho)+U=C_1. \tag{3.4.9}$$

This equation was first obtained by I.S. Gromyeko. The constant C_1 will be the same over the whole region in which the condition of coincidence of the vortex line and stream line is satisfied. This flow-interaction is characterized by formation of vortices practically coinciding with the direction of stream lines near a wing. However, such regions are not always found in a flow. A flow is usually characterized by the presence of vortex lines and stream lines not coinciding with each other. In such condition the family of vortex lines is given by equation (2.6.1) and the family of stream lines is given by equation (2.1.6). The flow we are considering can be described by equation (3.4.8').

Let us take the vector of an arc in the form $d\bar{s}=dx\cdot i+dy\cdot j+dz\cdot k$ belonging to a stream line or vortex line and determine the scalar product

$$d\bar{s}\cdot\text{grad}\,[V^2/2+\int(dp/\rho)+U]=-d\bar{s}(\text{rot}\,\overline{V}\times\overline{V}).$$

The left side of this equation shows the total differential of the three terms in square brackets. Consequently

$$d[V^2/2+\int (dp/\rho)+U]=-d\bar{s}(\text{rot}\,\bar{V}\times\bar{V}). \tag{3.4.10}$$

The vector product rot $\bar{V}\times\bar{V}$ represents the vector perpendicular to the vectors rot $\bar{V}$ and $\bar{V}$. The scalar product of this vector and vector $d\bar{s}$ will be zero in two cases: when vector $d\bar{s}$ coincides with the direction of the stream line (trajectory) and when this vector coincides with the direction of vortex. In these two cases the equation

$$V^2/2+\int (dp/\rho)+U=C_2, \tag{3.4.11}$$

is valid, where C_2 will vary depending on the type of stream line or vortex line.

Integral (3.4.11) is known as Bernoulli's equation. It is obvious that the constant for different vortex lines, passing through points on given stream lines, will be the same as for the stream line. In the same way the constants will be the same for the family of stream lines (trajectories) and for the vortex through the points in which the stream lines pass.

It is necessary to explain clearly the difference between these equations of Gromyeko's and Bernoulli's. Both of them are worked out for rotational (not potential) flow. However, the first equation shows the constant total energy per unit mass of gas in the whole region where vortex lines and stream lines coincide. The second equation establishes the limitation about the constant value of this energy along a given stream line or along a given vortex line. Then the constant in Gromyeko's equation will be the same for the whole region of flow. In Bernoulli's equation the constant is related only to a given stream line or a given vortex line. It is obvious that the two constants C_1 and C_2 in a general case are not the same. From the above discussion the difference between these equations follows. At the same time the difference between Lagrange's and Euler's equations also becomes clear, namely that they are related to unsteady and steady vortex-free (potential) flow respectively. The difference between any two of the equations considered above is clear from the above discussion.

Bernoulli's equation, related to the conditions along stream lines (trajectories), is very widely used in the study of the flow of a fluid or gas. It is known that the constant C_2 of this equation (3.4.11) is determined for each of the stream lines being considered. If the steady flow is vortex-free (potential) Bernoulli's equation coincides with Euler's equation and therefore the constant will be the same for all stream lines, i.e. for the whole region of flow.

Let us study some particular forms of Bernoulli's equation. For an incompressible flow under the condition that the function $U=gy$ this equation can be written in the form

$$(V^2/2)+(p/\rho)+yg=C_2. \tag{3.4.12}$$

The effect of weight can be neglected in the case of a gas flow. Consequently we can assume $U=0$ in equation (3.4.11) and in other integrals. In this particular case equation (3.4.12) is replaced by

$$(V^2/2)+(p/\rho)=C_2. \tag{3.4.13}$$

Let us consider the motion of an ideal compressible gas. The heat transfer processes connected with the property of viscosity (heat conduction, diffusion) are absent in such a gas. Assuming that the gas does not radiate energy we will be dealing with the adiabatic (isentropic) motion of a gas. From equation of energy (3.2.14) it follows that equation (3.3.1) represents the motion of this inviscid gas without radiation ($\varepsilon=0$). Hence Bernoulli's integral is

$$(V^2/2)+i=C. \tag{3.4.14}$$

Bernoulli's integral in this form represents the equation of energy for isentropic flow. According to this equation the sum of kinetic energy and enthalpy of a gas particle has constant value. Assuming that $i=c_pT=c_p\ p/(\rho R)$, $c_p-c_v=R$ and $k=c_p/c_v$, we get

$$i=\frac{k}{k-1}\cdot\frac{p}{\rho}. \tag{3.4.15}$$

Hence

$$\frac{V^2}{2}+\frac{k}{k-1}\cdot\frac{p}{\rho}=C \tag{3.4.16}$$

or

$$\frac{V^2}{2}+\frac{k}{k-1}RT=C. \tag{3.4.16'}$$

Bernoulli's equation for an ideal compressible gas happens to be the theoretical basis for investigation of the limitations of isentropic flows of a gaseous medium. This is examined in Section 6.

5. Aerodynamic Similarity

5.1 Concept of similarity

The aerodynamic characteristics of flight vehicles or of their individual elements can be determined theoretically as well as with the help of experimental research. Theoretical methods are based on the application of a system of gas dynamic equations which are solved with respect to a flow over a body of a given form having in general arbitrary values of absolute sizes.

In running experiments to obtain the aerodynamic parameters, which can be directly used for further research and for confirmation of theoretical findings, the actual body cannot always be used due to its large size. It is often

necessary to use a model of the body on a reduced scale. There the problem arises of transferring the experimental findings to the real body. Dimensional analysis and the theory of similarity take care of this problem. They establish the conditions that must be observed in experimental work with models and indicate the characteristic, convenient parameters determining basic effects and flow regimes.

Let us assume that the drag force, measured on a model in an aerodynamic wind tunnel, is equal to $X_m = c_{x_m} q_m S_m$ according to equation (1.3.5). We will now determine how the result so obtained can be used to estimate the drag force on the prototype body which is given by the formula $X_p = c_{x_p} q_p S_p$ where c_{x_p} is the unknown coefficient of drag for the actual body and q_p and S_p are the given velocity head and characteristic area respectively. Dividing X_p by X_m, we get

$$X_p = X_m \frac{c_{x_p}}{c_{x_m}} \cdot \frac{q_p S_p}{q_m S_m}. \tag{3.5.1}$$

It can be seen from this expression that estimation of the force on the real body X_p from the experimental value of X_m can be achieved only on the basis of equality of aerodynamic coefficients c_{x_m} and c_{x_p} because the values of $q_m S_m$ and $q_p S_p$ are uniquely determined by the given values of velocity heads and characteristic areas.

In this case the flows over model and prototype will have the property of aerodynamic similarity which, in this case, yields force characteristics of one flow (force X_p) from the given force characteristics of the other flow (force X_m) by simple calculation involving transfer of one system of measurable quantities to the other.

The requirements that bring about the equality $c_{x_m} = c_{x_p}$ in a given case, and in the general case for other aerodynamic coefficients, are established by the theory of similarity and dimensional analysis. They follow either from the physical nature of the problem being investigated or from the corresponding differential equations of aerodynamics.

Examining the expression for aerodynamic coefficient

$$c_x = \int_{(S)} [\bar{p} \cos(\widehat{\bar{P}_n x}) + c_{f_x} (\widehat{\bar{P}_\tau x})] \frac{dS}{S_p}, \tag{3.5.2}$$

obtained from (1.3.2), it may be noted that this coefficient depends on nondimensional geometric parameters and on nondimensional quantities like the coefficients of pressure and local friction. It follows from this that the aerodynamic coefficients for the real body and for an experimental model of different absolute sizes are maintained constant if these bodies are geometrically similar and the distribution of coefficients $\bar{p}$ and c_{f_x} is kept the same over their surfaces.

Consider a steady uniform flow of compressible gas over a body without heat transfer. It follows from physical considerations that the coefficients $\bar{p}$ and c_{f_x} for the given form of body and known values of angles of attack and banking will be functions of velocity V_∞, pressure p_∞, density ρ_∞, coefficients of dynamic viscosity μ_∞, specific heats of gas $c_{p\infty}$ and $c_{v\infty}$ in an undisturbed flow and some linear characteristic dimension of body L. Hence the coefficient of drag force will also depend on these parameters, for which the functional relation can be written in the form

$$c_x = f(V_\infty, p_\infty, \rho_\infty, \mu_\infty, c_{p\infty}, c_{v\infty}, L).$$

Since this coefficient is a nondimensional quantity the parameters of this function in the above expression must be nondimensional. From the general discussion on dimensional analysis it follows that the seven dimensional variables of function c_x can be reduced to three parameters which represent nondimensional combinations of $V_\infty, p_\infty, \rho_\infty, \mu_\infty, c_{p\infty}, c_{v\infty}, L$. This is because there are four independent measurable quantities; mass, length, time and temperature. These nondimensional combinations can be expressed in the following form: $V_\infty/\sqrt{k_\infty p_\infty/\rho_\infty} = V_\infty/a_\infty = \mathbf{M}_\infty$, Mach number of an undisturbed flow; $V_\infty \rho_\infty L/\mu_\infty = \mathbf{Re}_\infty$, Reynold's number calculated on the basis of undisturbed flow parameters and the characteristic linear dimension L; $c_{p\infty}/c_{v\infty} = k_\infty$, index of adiabatic process.

In the expression for $\mathbf{M}_\infty$ it is assumed that $\sqrt{k_\infty p_\infty/\rho_\infty} = a_\infty$, the speed of sound in an undisturbed flow. According to the general expression for speed of sound $a^2 = dp/d\rho$. Assuming the adiabatic nature of the propagation of sonic disturbances in a gas so that $p = A\rho^k$ (where A is a constant to be determined by initial conditions), we have

$$a^2 = (d/d\rho)\ (A\rho^k) = k\,(p/\rho).$$

For the propagation of sound in an undisturbed flow it will be given by

$$a_\infty^2 = k_\infty\,(p_\infty/\rho_\infty).$$

In this way the ratio $V_\infty/\sqrt{k_\infty p_\infty/\rho_\infty} = V_\infty/a_\infty$. All the other nondimensional combinations except $\mathbf{M}_\infty$, $\mathbf{Re}_\infty$, k_∞ composed of the given seven parameters or, in general, of any other quantities determining them will be functions of combinations of $\mathbf{M}_\infty$, $\mathbf{Re}_\infty$ and k_∞. The coefficient of drag can therefore be written as

$$c_x = f(\mathbf{M}_\infty, \mathbf{Re}_\infty, k_\infty). \tag{3.5.3}$$

Similar expressions can be formulated for other aerodynamic coefficients. It follows from these expressions that in equating $\mathbf{M}_\infty$, $\mathbf{Re}_\infty$ and the parameter k_∞ of the model with those of the prototype the aerodynamic coefficients of geometrically similar bodies are taken as identical. So we arrive at the important conclusion of the theory of similarity and dimensional analysis according

to which the necessary and sufficient condition of aerodynamic similarity is identical values of the nondimensional parameters forming the so-called basis of analysis, i.e. the system of nondimensional quantities determining all remaining flow parameters. These nondimensional combinations are known as the similarity parameters.

The similarity criteria given above have a particular physical meaning. The expression $a^2=dp/d\rho$ shows that the speed of sound can be taken as a parameter depending on the compressibility of a gas, i.e. depending on the property of gas whereby it changes its density with any change in pressure. Therefore the Mach number happens to be that nondimensional similarity criterion that characterizes the relative value of the compressibility effect on a gas flow. Reynold's number represents by itself a criterion to account for the relative value of viscous force on a moving gas and the parameter $k_\infty = c_{p\infty}/c_{v\infty}$ determines the peculiarities of flow that are based on the thermodynamic properties of a gas.

5.2 Similarity criteria to account for viscosity and heat conductivity effects

In more general cases of flow-interaction, characterized by the effect of a series of other physical parameters on the aerodynamic and thermodynamic properties of the flight vehicle, the criteria of dynamic similarity are more complicated and of various types. The other method of the theory of similarity and dimensional analysis can be applied to establish these criteria. This method is based on the use of the equation of motion of a viscous heat-conducting gas.

Let us write down these equations in nondimensional form, i.e. in a form such that the parameters entering into the equations (velocity, pressure, temperature, etc.) are expressed in terms of some characteristic parameters. For a given flow these parameters are constant quantities and they represent the characteristic quantities of the flow. In the name of characteristic quantities we select the flow parameters of undisturbed flow: velocity V_∞, pressure p_∞, density ρ_∞, temperature T_∞, coefficient of dynamic viscosity μ_∞ (or corresponding value of ν_∞), etc. It is necessary to bear in mind that only two of the three parameters p_∞, ρ_∞, T_∞ may be given and that the third can be calculated from the equation of state. The characteristic time indicating a period of unsteady flow will be quantity t_∞, the characteristic length will be the characteristic linear size L (for example, length of the body in a flow). Gravitational acceleration g can be taken as the characteristic acceleration of mass forces. The nondimensional parameters of length and time may be given by

$$\bar{x}=x/L,\quad \bar{y}=y/L,\quad \bar{z}=z/L,\quad \bar{t}=t/t_\infty, \tag{3.5.4}$$

and the nondimensional coefficients of speed, pressure, density, viscosity and mass forces can be written in the following form:

$$\left.\begin{aligned}\overline{V}_x=V_x/V_\infty,\ \overline{V}_y=V_y/V_\infty,\ \overline{V}_z=V_z/V_\infty,\ \overline{p}=p/p_\infty,\ \overline{\rho}=\rho/\rho_\infty,\\ \overline{\mu}=\mu/\mu_\infty,\ \overline{\nu}=\nu/\nu_\infty,\ \overline{X}=X/g,\ \overline{Y}=Y/g,\ \overline{Z}=Z/g.\end{aligned}\right\} \tag{3.5.5}$$

Let us introduce nondimensional quantities in the equation of motion (3.1.17) and the continuity equation (2.4.2). In this process of transformation we take the first equation of the system (3.1.17) because the remaining two equations can be written similarly. The above-mentioned equations in nondimensional form will have the form:

$$\begin{aligned}&\frac{V_\infty}{t_\infty}\cdot\frac{\partial\overline{V}_x}{\partial\overline{t}}+\frac{V_\infty^2}{L}\left(\overline{V}_x\frac{\partial\overline{V}_x}{\partial\overline{x}}+\overline{V}_y\frac{\partial\overline{V}_x}{\partial\overline{y}}+\overline{V}_z\frac{\partial\overline{V}_x}{\partial\overline{z}}\right)\\ &=g\overline{X}-\frac{p_\infty}{\rho_\infty L}\cdot\frac{1}{\overline{\rho}}\cdot\frac{\partial\overline{p}}{\partial\overline{x}}+\frac{\nu_\infty V_\infty}{L^2}\left\{\overline{\nu}\Delta\overline{V}_x+\frac{\overline{\nu}}{3}\cdot\frac{\partial}{\partial\overline{x}}\operatorname{div}\overline{V}\right.\\ &\quad+\frac{1}{\overline{\rho}}\left[\frac{\partial\overline{\mu}}{\partial\overline{x}}\left(2\frac{\partial\overline{V}_x}{\partial\overline{x}}-\frac{2}{3}\operatorname{div}\overline{V}\right)\right.\\ &\quad\left.\left.+\frac{\partial\overline{\mu}}{\partial\overline{y}}\left(\frac{\partial\overline{V}_x}{\partial\overline{y}}+\frac{\partial\overline{V}_y}{\partial\overline{x}}\right)+\frac{\partial\overline{\mu}}{\partial\overline{z}}\left(\frac{\partial\overline{V}_x}{\partial\overline{z}}+\frac{\partial\overline{V}_z}{\partial\overline{x}}\right)\right]\right\};\\ &\frac{\rho_\infty}{t_\infty}\cdot\frac{\partial\overline{\rho}}{\partial\overline{t}}+\frac{\rho_\infty V_\infty}{L}\left[\frac{\partial(\overline{\rho}\overline{V}_x)}{\partial\overline{x}}+\frac{\partial(\overline{\rho}\overline{V}_y)}{\partial\overline{y}}+\frac{\partial(\rho\overline{V}_z)}{\partial\overline{z}}\right]=0.\end{aligned}$$

From the characteristic quantities entering into these equations it is possible to form a series of nondimensional numbers characterizing the similarity of gas flows. These numbers are known by the names of the scientists who first conceived them and are written in the following form:

$$\left.\begin{aligned}&\mathbf{Sh}=V_\infty t_\infty/L,\ \text{Strouhal number;}\\ &\mathbf{Fr}=V_\infty^2/gL,\ \text{Froude number;}\\ &\mathbf{M}=V_\infty/a_\infty,\ \text{Mach number;}\\ &\mathbf{Re}=(V_\infty L\rho_\infty/\mu_\infty)=V_\infty L/\nu_\infty,\ \text{Reynolds number}\\ &\text{(index ``}\infty\text{'' for }\mathbf{M}\text{ and }\mathbf{Re}\text{ is dropped).}\end{aligned}\right\} \tag{3.5.6}$$

Here $a_\infty=\sqrt{k_\infty RT_\infty}$ is the speed of sound in an undisturbed flow (k_∞ and T_∞ are respectively the adiabatic index and gas temperature in an undisturbed flow). Introducing these numbers in the equations of motion and continuity, we get:

$$\begin{aligned}&\mathbf{Sh}^{-1}\frac{\partial\overline{V}_x}{\partial\overline{t}}+\overline{V}_x\frac{\partial\overline{V}_x}{\partial\overline{x}}+\overline{V}_y\frac{\partial\overline{V}_x}{\partial\overline{y}}+\overline{V}_z\frac{\partial\overline{V}_x}{\partial\overline{z}}=\frac{1}{\mathbf{Fr}}\overline{X}\\ &-\frac{1}{k_\infty\mathbf{M}}\cdot\frac{1}{\overline{\rho}}\cdot\frac{\partial\overline{p}}{\partial\overline{x}}+\frac{1}{\mathbf{Re}}\left\{\overline{\nu}\Delta\overline{V}_x+\frac{\overline{\nu}}{3}\cdot\frac{\partial}{\partial\overline{x}}\operatorname{div}\overline{V}\right.\\ &+\frac{1}{\overline{\rho}}\left[\frac{\partial\overline{\mu}}{\partial\overline{x}}\left(2\frac{\partial\overline{V}_x}{\partial\overline{x}}-\frac{2}{3}\operatorname{div}\overline{V}\right)+\frac{\partial\overline{\mu}}{\partial\overline{y}}\left(\frac{\partial\overline{V}_x}{\partial\overline{y}}+\frac{\partial\overline{V}_y}{\partial\overline{x}}\right)\right.\\ &\left.\left.\left.+\frac{\partial\overline{\mu}}{\partial\overline{z}}\left(\frac{\partial\overline{V}_x}{\partial\overline{z}}+\frac{\partial\overline{V}_z}{\partial\overline{x}}\right)\right]\right\};\end{aligned} \tag{3.5.7}$$

$$\mathbf{Sh}\frac{\partial\bar{\rho}}{\partial\bar{t}}+\frac{\partial(\bar{\rho}\bar{V}_x)}{\partial\bar{x}}+\frac{\partial(\bar{\rho}\bar{V}_y)}{\partial\bar{y}}+\frac{\partial(\bar{\rho}\bar{V}_z)}{\partial\bar{z}}=0. \tag{3.5.8}$$

Let us now represent the equation of energy (3.2.14) in nondimensional form, neglecting the terms for radiation and diffusion. The following nondimensional parameters

$$\bar{T}=T/T_\infty,\ \bar{c}_p=c_p/c_{p\infty},\ \bar{\lambda}=\lambda/\lambda_\infty, \tag{3.5.9}$$

will be introduced, where $c_{p\infty}$ and λ_∞ are respectively the specific heat and coefficient of heat conductivity of the gas in an undisturbed flow. Recalling that $di=c_p dT$ and expanding the total derivative dT/dt, after necessary substitutions we get

$$\begin{aligned}\frac{\rho_\infty c_{p\infty}T_\infty}{t_\infty}\bar{\rho}\,\bar{c}_p\frac{\partial\bar{T}}{\partial\bar{t}}+\frac{\rho_\infty c_{p\infty}V_\infty T_\infty}{L}\bar{\rho}\,\bar{c}_p\left(\bar{V}_x\frac{\partial\bar{T}}{\partial\bar{x}}+\bar{V}_y\frac{\partial\bar{T}}{\partial\bar{y}}+\bar{V}_z\frac{\partial\bar{T}}{\partial\bar{z}}\right)\\ =\frac{p_\infty}{t_\infty}\cdot\frac{d\bar{p}}{d\bar{t}}+\frac{\mu_\infty V_\infty^2}{L^2}\bar{\mu}\left\{\left[\left(\frac{\partial\bar{V}_x}{\partial\bar{x}}\right)^2+\left(\frac{\partial\bar{V}_y}{\partial\bar{y}}\right)^2\right]\right.\\ \left.-\frac{2}{3}\bar{\mu}(\operatorname{div}\bar{V})^2+4\bar{\mu}\bar{\varepsilon}_z^2\right\}+\frac{\lambda_\infty T_\infty}{L^2}\operatorname{div}(\bar{\lambda}\operatorname{grad}\bar{T}).\end{aligned} \tag{3.5.10}$$

Let us introduce the Prandtl number

$$\mathbf{Pr}=\mu_\infty c_{p\infty}/\lambda_\infty, \tag{3.5.11}$$

which helps us in comparing the relative values of interaction of viscosity and heat conductivity or, in other words, in establishing the relation between heat flow due to friction and molecular heat transfer. Then, taking into account that $p_\infty/\rho_\infty=RT_\infty=c_{p\infty}(1-1/k_\infty)T_\infty$, one can write

$$\begin{aligned}\bar{\rho}\,\bar{c}_p\left(\mathbf{Sh}^{-1}\frac{\partial\bar{T}}{\partial\bar{t}}+\bar{V}_x\frac{\partial\bar{T}}{\partial\bar{x}}+\bar{V}_y\frac{\partial\bar{T}}{\partial\bar{y}}+\bar{V}_z\frac{\partial\bar{T}}{\partial\bar{z}}\right)\\ =\mathbf{Sh}^{-1}\frac{k_\infty-1}{k_\infty}\cdot\frac{d\bar{p}}{d\bar{t}}+\frac{\mathbf{M}^2(k_\infty-1)}{\mathbf{Re}}\left\{\left[\left(\frac{\partial\bar{V}_x}{\partial\bar{x}}\right)^2+\left(\frac{\partial\bar{V}_y}{\partial\bar{y}}\right)^2\right]\right.\\ \left.-\frac{2}{3}\bar{\mu}(\operatorname{div}\bar{V})^2+4\bar{\mu}\bar{\varepsilon}_z^2\right\}+\frac{1}{\mathbf{Re}\,\mathbf{Pr}}\operatorname{div}(\bar{\lambda}\operatorname{grad}\bar{T}).\end{aligned} \tag{3.5.10'}$$

Now we perform the transformation of some additional relations from the system of gas dynamic equations to the nondimensional form (see Section 3):

$$(p_\infty/\rho_\infty T_\infty)\bar{p}=\bar{\rho}\,\bar{T} \tag{3.5.12}$$

$$\bar{\mu}_{\mathrm{av}}=f_3(p_\infty\bar{p},T_\infty\bar{T})(1/\mu_{\mathrm{av}\infty}); \tag{3.5.13}$$

$$\bar{\lambda}=f_6(p_\infty\bar{p},T_\infty\bar{T})(1/\lambda_\infty); \tag{3.5.14}$$

$$\bar{\mu}=f_7(p_\infty\bar{p},T_\infty\bar{T})(1/\mu_\infty); \tag{3.5.15}$$

$$\bar{c}_p = f_8(p_\infty \bar{p}, T_\infty \bar{T})(1/c_{p\infty}). \tag{3.5.16}$$

Let us suppose that two flows over two geometrically similar surfaces are being investigated. For such surfaces the nondimensional coordinates of respective points are the same. This is actually the necessary condition of aerodynamic similarity of flows. To satisfy the sufficient condition of similarity the equality of nondimensional quantities of gas dynamic parameters (velocity, pressure, density, etc.) must be observed at similar points in the two flows. Since the nondimensional parameters occur simultaneously as the solutions of the system of equations (3.5.7), (3.5.8), (3.5.10′), (3.5.12) to (3.5.16) it is obvious that the above-mentioned equality will be observed on condition that the systems of nondimensional equations and the nondimensional initial and boundary conditions for each of the flows be identical.

Examination of the systems of nondimensional equations for the two flows shows that these systems will be identical if:

1) similarity parameters are equal:

$$\mathbf{Fr}_1 = \mathbf{Fr}_2,\ \mathbf{Re}_1 = \mathbf{Re}_2,\ \mathbf{M}_1 = \mathbf{M}_2,\ \mathbf{Sh}_1 = \mathbf{Sh}_2; \tag{3.5.17}$$

2) the equality of Prandtl numbers

$\mathbf{Pr}_1 = \mathbf{Pr}_2$ is fulfilled, i.e.

$$(c_{p\infty}\mu_\infty/\lambda_\infty)_1 = (c_{p\infty}\mu_\infty/\lambda_\infty)_2, \tag{3.5.18}$$

and the equality of adiabatic indices for gas in the two flows is satisfied:

$$k_{\infty 1} = k_{\infty 2}; \tag{3.5.19}$$

3) each of the equations (3.5.13) through (3.5.16) determines the dependence of the nondimensional quantities $\bar{\mu}_{av}$, $\bar{\lambda}$, $\bar{\mu}$ or $\bar{c}_p$ on the nondimensional quantities $\bar{p}$ and $\bar{T}$ and on the parameters in (3.5.17) through (3.5.19). However, in the case of a dissociating gas such relations do not hold because the nondimensional criteria of the type (3.5.17) through (3.5.19) or of any other form cannot be separated. Therefore the corresponding nondimensional equations (3.5.13) through (3.5.16) for the real flow and for the flow over the model will not be identical and complete dynamic similarity cannot be obtained.

Two particular cases may be mentioned where this similarity is satisfied. The first is the case of a nondissociating gas flow for which the average molecular weight remains constant ($\mu_{av_1} = \mu_{av_2}$) and the heat content, coefficient of heat conductivity and viscosity change with the temperature according to a law of the type $y = aT^x$. In this case equations (3.5.14) through (3.5.16) for quantities $\bar{\lambda}$, $\bar{\mu}$ and $\bar{c}_p$ are replaced by the corresponding relations of nondimensional temperature $\bar{T} = T/T_\infty$. The second case is connected with a gas flow at comparatively low speeds when parameters λ, μ and c_p do not depend on temperature. The corresponding values of these parameters will be identi-

cal for the actual flow and the flow over the model. In this case the system of equations consists of the Navier-Stokes nondimensional equations of continuity and energy and also an equation of state.

The boundary conditions imposed for the solution of nondimensional equations may introduce some additional similarity criteria. This is not connected with the condition of unseparated flow, which does not carry any new similarity criteria. In reality this boundary condition in nondimensional terms has the form

$$\overline{V}_x \frac{\partial \overline{F}}{\partial \overline{x}} + \overline{V}_y \frac{\partial \overline{F}}{\partial \overline{y}} + \overline{V}_z \frac{\partial \overline{F}}{\partial \overline{z}} = 0$$

and will be one and the same for both the actual flow and the flow over the model as a consequence of the geometrical similarity of the surface in the flow. However, the boundary condition for temperature, indicating that the solution for temperature must satisfy the condition that $T = T_{su}$ (T_{su} is the temperature of the surface), poses additional criteria for similarity. In practice it follows from the boundary conditions for actual and model surfaces with the corresponding forms $T_1 = (T_{su})_1$ and $T_2 = (T_{su})_2$ that the nondimensional temperatures $\overline{T}_1 = (\overline{T}_{su})_1$ and $\overline{T}_2 = (\overline{T}_{su})_2$. By the similarity condition we have $\overline{T}_1 = \overline{T}_2$ and hence the equality $(\overline{T}_{su})_1 = (\overline{T}_{su})_2$ must be observed. Thus the boundary condition for wall temperature leads to an additional similarity criterion

$$(T_{su}/T_\infty)_1 = (T_{su}/T_\infty)_2. \tag{3.5.20}$$

The nondimensional gas dynamic parameters on the surface of a body in a flow, as seen from the system of nondimensional equations [under the condition that equations (3.5.13)–(3.5.16) determine $\overline{\mu}_{av}$, $\overline{\lambda}$, $\overline{\mu}$ and c_p as functions of $\overline{T}$], depend on the nondimensional coordinates and time and on the similarity criteria (3.5.17)–(3.5.19). In particular, nondimensional pressure can be expressed as a function

$$(p/p_\infty) = \varphi_1 (\mathbf{Fr}, \mathbf{Re}, \mathbf{M}, \mathbf{Sh}, \mathbf{Pr}, k_\infty, \overline{T}_{su}, \bar{x}, \bar{y}, \bar{z}, \bar{t}). \tag{3.5.21}$$

At a given moment of time the nondimensional coefficient of drag force can be determined from the known distribution of pressure

$$c_x = X/q_\infty S = \varphi_2 (\mathbf{Fr}, \mathbf{Re}, \mathbf{M}, \mathbf{Sh}, \mathbf{Pr}, k_\infty, \overline{T}_{su}). \tag{3.5.22}$$

This expression, being more complete than (3.5.3), determines the relation of the aerodynamic drag coefficient to the nondimensional similarity criteria. However, the relation (3.5.22) does not reflect all the peculiarities of a dissociating gas flow because it is derived from the simplified equations (3.5.13) to (3.5.16). Therefore formula (3.5.22) is less accurate for such a flow than for a nondissociating gas flow but it at least represents partial similarity.

Similarity criteria, which determine the nondimensional aerodynamic coefficient, have a particular physical meaning and characterize the real factors affecting aerodynamic forces.

The Froude number happens to be the similarity criterion accounting for the effect of the weight of a fluid on its resistance. From the equation of motion in nondimensional form it can be seen that **Fr** is equal to the ratio of quantity V_∞^2/L, based on the effect of inertial forces, to the characteristic mass force g. Equality of Froude numbers for the real body and a geometrically similar model indicates that they will have identical drag coefficients, which are based on the effect of the weight of a fluid. This similarity criterion does not have any significant value in the study of gas flows because the effect of the weight of a gas on motion is negligibly small. However, this criterion may have considerable value in hydrodynamics, in particular in experimental research on the wave drag of different types of ships.

For the motion of bodies in a real fluid aerodynamic forces depend on viscosity. The viscous force is characterized by the Reynolds number, which can be obtained as the ratio of quantity V_∞^2/L, which takes into account the effect of inertial forces, to the quantity $\nu_\infty V_\infty/L^2$, accounting for viscous effect. If the Reynolds number for two geometrically similar flows is kept equal the condition of partial aerodynamic similarity accounting for viscous effects is fulfilled. The coefficients of frictional drag for the real body and the model will be equal under this condition.

The similarity criterion based on the Mach number is obtained from the ratio of quantity V_∞^2/L to the parameter $p_\infty/\rho_\infty L$, which takes care of the effect of pressure forces on the compressibility of gas. The partial similarity of two flows of compressible gas over geometrically similar bodies will be observed if the Mach number for both flows is identical.

In the study of the problems of an unsteady flow the Strouhal number has an important role. This number is obtained by comparing inertial forces to the forces due to unsteady effect, i.e. it is obtained from the ratio of quantities V_∞^2/L and V_∞/t_∞. Two unsteady flows over the actual body and the model will have partial aerodynamic similarity if the Strouhal numbers are identical for both.

Similarity criteria based on the Prandtl number and the ratio of specific heats are determined for given requirements of the physical properties of gases in the real flow and in the flow past the model. The gases used for these two flows may be different but their physical characteristics must be such that the equalities $\mathbf{Pr}_1 = \mathbf{Pr}_2$ and $k_{\infty 1} = k_{\infty 2}$ are satisfied. The Prandtl number depends on the coefficients of dynamic viscosity and heat conductivity. The coefficient of viscosity represents gas properties related to molecular momentum transfer and the coefficient of heat conductivity characterizes the intensity of molecular heat transfer. Prandtl's criterion $\mathbf{Pr} = \mu_\infty c_{p\infty}/\lambda_\infty$ determines the mode of transfer of the energy of molecular exchange to heat energy. For gas, we have $\mathbf{Pr} < 1$.

The nondimensional coefficient of aerodynamic force or heat transfer is the complicated function of a series of similarity criteria, each of which reflects

the effect of some given physical process. Complete similarity between the real flow and the flow over the model can be satisfied only if all the similarity criteria are fulfilled. In practice, however, this cannot be observed because some of these criteria are of incompatible nature.

Let us take, for example, the Reynolds number, Froude number and Mach number. To satisfy similarity of frictional forces it is necessary that $V_1L_1/\nu_1 = V_2L_2/\nu_2$. If the coefficients are assumed equal, i.e. $\nu_1 = \nu_2$ for flows over the real body and the model the velocity of flow over model $V_2 = V_1(L_1/L_2)$, i.e. the velocity of flow over the prototype is higher than the velocity of flow over the model in the same ratio as the size of the prototype to the model.

To satisfy the similarity of forces based on gravitational weight it is necessary to observe equality of Froude numbers, i.e. $V_1^2/(L_1g_1) = V_2^2/(L_2g_2)$, from which it follows that if the experiments are conducted at identical g, velocity of model flow $V_2 = V_1\sqrt{L_2/L_1}$. Obviously the velocity V_2 for the scaled-down model must be appropriately lower, not higher than V_1.

Finally, in observing equality of Mach numbers we will have $V_1/a_1 = V_2/a_2$. Assuming, for simplicity, that $a_2 = a_1$, we get the condition of equality of velocities in the flows over the model and the prototype.

It is obvious that all these criteria cannot be satisfied at one time and hence only partial similarity can be observed. It should, however, be noted that there is no necessity in practice to satisfy all similarity criteria because their effects in some or other specific case of motion are not identical. For example, the effect of frictional forces and pressure on the interaction of body and gas flow will be more appropriate than weight forces. Therefore the criteria of **Re** and **M** have more significance in such cases than **Fr**. That is why the Froude number is not considered as a similarity criterion in such cases.

If, at the same time, the velocity of motion is not high the effect of pressure forces related to the compressibility of gas is negligibly small. Then it is possible to ignore the similarity criterion of the Mach number and assume that the aerodynamic coefficients depend on the Reynolds number.

Aerodynamic force, moment and heat flow from gas to the surface are the result of interaction between the moving gas and the body where different processes like friction, compression (or expansion), heating, variation in physical properties, etc. take place simultaneously. Therefore it is necessary to try to satisfy the maximum number of important similarity criteria. For example, it is desirable that equalities of the Reynolds numbers and Mach numbers as between the actual flow and the model flow be fulfilled simultaneously, i.e. $\mathbf{Re}_1 = \mathbf{Re}_2$ and $\mathbf{M}_1 = \mathbf{M}_2$. This is particularly important during the investigation of aerodynamic forces for bodies with large surfaces, which could be made up of various types of components depending on friction and normal pressure related to compressibility. The fulfillment of the above conditions can be observed in running experiments in aerodynamic wind

tunnels of variable density. If the experiments are carried out in a gas flow in which the speed of sound is the same as in the actual flow ($a_2=a_1$) the condition of equality of Mach numbers results in $V_2=V_1$. Then, using equality $\mathbf{Re}_1=\mathbf{Re}_2$ or, in other words,

$$V_2 L_2 \rho_2/\mu_2=V_1 L_1 \rho_1/\mu_1,$$

we get the condition of $L_2\rho_2/\mu_2=L_1\rho_1/\mu_1$. Since $\mu_2=\mu_1$ it can be established that the gas density of flow in an aerodynamic wind tunnel should be $\rho_2=\rho_1(L_1/L_2)$. Assuming that temperatures in the actual and model flows are equal ($T_2=T_1$) we get, using the equation of state, the condition of $p_2=p_1(L_1/L_2)$. Hence for simultaneous fulfillment of similarity in frictional forces and pressure forces accounting for compressibility, i.e. to satisfy equalities $\mathbf{Re}_1=\mathbf{Re}_2$ and $\mathbf{M}_1=\mathbf{M}_2$, it is necessary that the static pressure in the gas flow in the wind tunnel exceeds the pressure in the actual flow by the same ratio as the size of the prototype to the size of the model. Wind tunnel design allows us to regulate static pressure in the model gas flow in a certain range depending on the size of the model in the flow.

The effect of heat transfer may be neglected as an approximation in certain known cases of determination of force-interaction. Here the aerodynamic coefficients will depend on **Re, M** and **Sh**. If the experiments are conducted in a gaseous medium for which $k_{\infty 2}=k_{\infty 1}$, then

$$c_x=f(\mathbf{Re, M, Sh}). \tag{3.5.23}$$

For steady flow-interaction

$$c_x=f(\mathbf{Re, M}). \tag{3.5.24}$$

6. Isentropic Gas Flows

In this section we will examine one-dimensional steady isentropic flows of compressible gas. The study of such flows is of great practical significance because it allows us to establish the connection between the jet cross section and variations in gas parameters and at the same time helps us to find how to control the flow by changing the form of the jet (or canal). We will also examine the wide range of gas dynamic relations consisting of the basic mathematics for calculation of isentropic gas flows with constant heat coefficients.

6.1 Form of gas jet

Let us consider a steady flow of ideal (inviscid) gas in a jet with low expansion and small curvature. The flow in this jet can be taken as one-dimensional, characterizing the variation of parameters depending on one linear coordinate of a point along the jet axis. For a steady flow the parameters determining this flow at every point will be constant at any moment of time. If the width of the jet is small compared to the radius of curvature of the

axial line the pressure gradient across the section can be neglected and the pressure at any two points of the jet cross section can be considered equal.

Study of this one-dimensional steady flow of compressible gas leads to the most simple approximate solution of gas dynamic equations. Along the jet axis the condition (2.4.51) of constant mass flow is satisfied, i.e. $\rho_1 V_1 S_1 = \rho_2 V_2 S_2 = \rho_3 V_3 S_3 = \ldots$, or $\rho VS = \text{const}$, where indices "1", "2", "3" correspond to the gas parameters over the control surfaces in terms of cross sectional areas S_1, S_2, $S_3 \ldots$. Taking the logarithm of both sides, we get $\ln \rho + \ln V + \ln S = \text{const}$. Differentiation of this expression gives

$$d\rho/\rho + dV/V + dS/S = 0,$$

where

$$\frac{dS}{dV} = -S\left(\frac{1}{V} + \frac{1}{\rho} \cdot \frac{d\rho}{dV}\right). \tag{3.6.1}$$

Now we take relation (3.4.14). Differentiating it, we get

$$VdV = -di. \tag{3.6.2}$$

Replacing di by dp/ρ, we have

$$VdV = -dp/\rho. \tag{3.6.3}$$

Recalling the formula for the speed of sound $a = \sqrt{dp/d\rho}$ and using relation (3.6.3), we transform (3.6.1) into the form

$$dS/dV = (S/V)(\mathbf{M}^2 - 1), \tag{3.6.4}$$

where $\mathbf{M} = V/a$ is the Mach number at a given cross section of the jet. Let us assume that speed increases along the jet ($dV > 0$) but that it remains subsonic and hence $\mathbf{M} < 1$. From (3.6.4) it can be seen that for this case the derivative $dS/dV < 0$. This shows that downstream of the flow the jet diminishes in cross section. Conversely, for a subsonic flow of decreasing velocity ($\mathbf{M} < 1$, $dV < 0$) the cross section of the jet increases, which is indicated by the inequality $dS > 0$ as seen from (3.6.4).

Let us now examine a supersonic flow ($\mathbf{M} > 1$). If the velocity diminishes along the jet axis it can be seen from (3.6.4) that differential $dS < 0$ and hence the jet decreases in cross sectional area. In the opposite case of increasing jet velocity the value of $dS > 0$, i.e. the jet expands.

Consider a nozzle of diminishing cross section, opening out again at the tail end: a subsonic flow, under given conditions, will be accelerated in the initial section and reach sonic velocity at the narrowest point [here, $dS = 0$ and hence from (3.6.4) we have $\mathbf{M} = 1$]. Thereafter it will be supersonic. Nozzles in rocket engines, gas turbines and aerodynamic wind tunnels are designed in this way to obtain supersonic flows.

6.2 Flow velocity

Let us consider a gas jet passing over some surface (Fig. 3.6.1). The parameters for the undisturbed flow region in a jet are denoted by V_∞, p_∞, ρ_∞, T_∞, i_∞, a_∞, etc. and those for the disturbed flow region by V, p, ρ, T, i, a, etc.

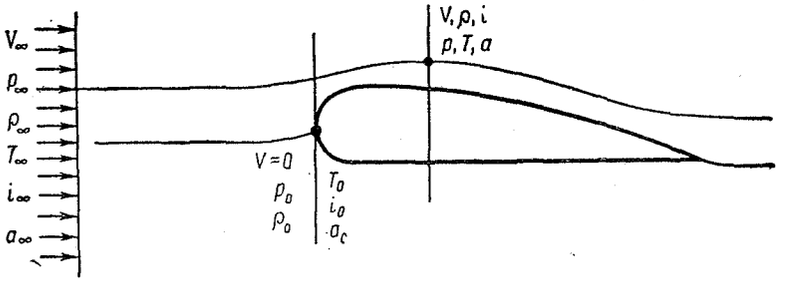

Fig. 3.6.1. Parameters of gas flow under interaction.

Equation (3.4.14) can be used to find the velocity at any arbitrary section of the jet and constant C can be determined from the condition of the undisturbed flow parameters:

$$C=(V_\infty^2/2)+i_\infty. \tag{3.6.5}$$

Then we have

$$(V^2/2)+i=(V_\infty^2/2)+i_\infty,$$

from which

$$V=\sqrt{V_\infty^2+2(i_\infty-i)}. \tag{3.6.6}$$

At stagnation point $V=0$. Consequently, enthalpy

$$i=i_0=(V_\infty^2/2)+i_\infty. \tag{3.6.7}$$

Thus constant C, in the physical sense, can be regarded as the stagnation enthalpy. Taking this value of C, the velocity in the jet will be

$$V=\sqrt{2(i_0-i)}. \tag{3.6.8}$$

Enthalpy i_0 corresponds to pressure p_0 and density ρ_0 for stagnation conditions and can be determined from the condition

$$i_0=\frac{k}{k-1}\cdot\frac{p_0}{\rho_0}=\frac{V_\infty^2}{2}+i_\infty=\frac{V_\infty^2}{2}+\frac{k}{k-1}\cdot\frac{p_\infty}{\rho_\infty}. \tag{3.6.9}$$

Expressing i_0 in terms of p_0 and ρ_0, we get

$$\frac{V^2}{2}+\frac{k}{k-1}\cdot\frac{p}{\rho}=\frac{k}{k-1}\cdot\frac{p_0}{\rho_0}. \tag{3.6.10}$$

As the flow is isentropic,

$$p/\rho^k = p_0/\rho_0^k, \tag{3.6.11}$$

hence

$$V = \sqrt{\frac{2k}{(k-1)} \cdot \frac{p_0}{\rho_0}\left[1-\left(\frac{p}{p_0}\right)^{(k-1)/k}\right]}. \tag{3.6.12}$$

Keeping in view that the speed of sound $a_0 = \sqrt{kp_0/\rho_0}$, for the condition of complete stagnation we find

$$V = a_0\sqrt{\frac{2}{k-1}\left[1-\left(\frac{p}{p_0}\right)^{(k-1)/k}\right]}. \tag{3.6.13}$$

From (3.6.8) it follows that velocity along the jet increases as enthalpy decreases and hence more heat is converted into kinetic energy. Maximum velocity is achieved when enthalpy $i=0$, i.e. when the whole of the heat is spent on accelerating the gas flow. The value of this velocity is

$$V_{\max} = \sqrt{2\,i_0}\ , \tag{3.6.14}$$

or, recalling (3.6.9),

$$V_{\max} = \sqrt{\frac{2k}{k-1} \cdot \frac{p_0}{\rho_0}} = a_0\sqrt{\frac{2}{k-1}}. \tag{3.6.15}$$

Using the concept of maximum velocity, the relation of velocity at any arbitrary section can be written in the following way:

$$V = V_{\max}\sqrt{1-(i/i_0)}, \tag{3.6.16}$$

or

$$V = V_{\max}\sqrt{1-(p/p_0)^{(k-1)/k}}. \tag{3.6.17}$$

At the narrowest critical section of the jet a speed equal to the speed of sound is achieved. This speed is called the critical speed and is denoted by a^*. This critical speed corresponds to the critical pressure p^* and density ρ^*. From Bernoulli's equation it follows for the critical section that

$$\frac{a^{*2}}{2} + \frac{k}{k-1} \cdot \frac{p^*}{\rho^*} = \frac{k}{k-1} \cdot \frac{p_0}{\rho_0}.$$

Since $kp^*/\rho^* = a^{*2}$ we get for critical speed

$$a^* = \sqrt{\frac{2k}{k+1} \cdot \frac{p_0}{\rho_0}} = a_0\sqrt{\frac{2}{k+1}}, \tag{3.6.18}$$

or, using (3.6.15),

$$a^* = V_{\max}\sqrt{(k-1)/(k+1)}. \tag{3.6.19}$$

Equation (3.6.10) may be used to determine the local velocity of speed of sound a. Introducing into it the quantities $a^2=kp/\rho$ and $a_0^2=kp_0/\rho_0$, we get

$$a^2=a_0^2-\frac{k-1}{2}V^2, \tag{3.6.20}$$

or

$$a^2=\frac{k+1}{2}a^{*2}-\frac{k-1}{2}V^2; \tag{3.6.21}$$

$$a^2=\frac{k-1}{2}(V_{\max}^2-V^2). \tag{3.6.22}$$

Let us introduce notation $\lambda=V/a^*$ for relative velocity. Dividing equation (3.6.21) by V^2 and keeping in mind the ratio $V/a=\mathbf{M}$, we get the relation between λ and $\mathbf{M}$:

$$\lambda^2=\frac{[(k+1)/2]\,\mathbf{M}^2}{1+[(k-1)/2]\,\mathbf{M}^2}. \tag{3.6.23}$$

From this it follows that at that section of the jet where velocity $V_{\max}$ is reached the Mach number $\mathbf{M}=\infty$. The corresponding value of $\lambda=\lambda_{\max}$ can be found from (3.6.23) under the condition of $\mathbf{M}\to\infty$

$$\lambda_{\max}=\sqrt{(k+1)/(k-1)}. \tag{3.6.24}$$

It is obvious that at the critical section, where $\mathbf{M}=1$, we have $\lambda=1$. At any arbitrary section characterized by the value $1\leqslant\mathbf{M}\leqslant\infty$ the relative speed

$$1\leqslant\lambda\leqslant\sqrt{(k+1)/(k-1)}. \tag{3.6.25}$$

6.3 Pressure, density and temperature

It follows from (3.6.17) that pressure at any arbitrary section of the jet will be

$$p=p_0\left(1-\frac{V^2}{V_{\max}^2}\right)^{k/(k-1)}. \tag{3.6.26}$$

According to (3.6.22) the quantity

$$1-\frac{V^2}{V_{\max}^2}=\left(1+\frac{k-1}{2}\mathbf{M}^2\right)^{-1}, \tag{3.6.27}$$

and therefore

$$p=p_0\left(1+\frac{k-1}{2}\mathbf{M}^2\right)^{-k/(k-1)}=p_0\,\pi\,(\mathbf{M}), \tag{3.6.28}$$

where function π of Mach number $\mathbf{M}$ is determined by the pressure ratio p/p_0.

Applying the conditions of undisturbed flow to formula (3.6.28), we have

$$p_0=p_\infty\left(1+\frac{k-1}{2}\mathbf{M}_\infty^2\right)^{k/(k-1)}=\frac{p_\infty}{\pi(\mathbf{M}_\infty)}. \tag{3.6.29}$$

Consequently we get

$$p=p_\infty\left\{\frac{1+[(k-1)/2]\,\mathbf{M}_\infty^2}{1+[(k-1)/2]\,\mathbf{M}^2}\right\}^{k/(k-1)}=p_\infty\frac{\pi(\mathbf{M})}{\pi(\mathbf{M}_\infty)}. \tag{3.6.30}$$

From the adiabatic equation $p/\rho^k=p_0/\rho_0^k$ in which p is replaced by formulas (3.6.26) and (3.6.28) the relation for density will be

$$\rho=\rho_0\left(1-\frac{V^2}{V_{\max}^2}\right)^{1/(k-1)}=\rho_0\left(1+\frac{k-1}{2}\mathbf{M}^2\right)^{-1/(k-1)}=\rho_0\,\varepsilon(\mathbf{M}), \tag{3.6.31}$$

where function ε of Mach number $\mathbf{M}$ can be determined by density ratio ρ/ρ_0.

Using the equation of state

$$p/p_0=(\rho/\rho_0)\,(T/T_0), \tag{3.6.32}$$

and the relations for pressure (3.6.26), (3.6.28) and for density (3.6.31), we get the formula for temperature:

$$T=T_0\left(1-\frac{V^2}{V_{\max}^2}\right)=T_0\left(1+\frac{k-1}{2}\mathbf{M}\right)^{-1}=T_0\,\tau(\mathbf{M}), \tag{3.6.33}$$

where function $\tau(\mathbf{M})$ is determined from the temperature ratio T/T_0.

The tables of gas dynamic functions $\pi(\mathbf{M})$, $\varepsilon(\mathbf{M})$ and $\tau(\mathbf{M})$ for various values of index k from 1.1 through 1.67 are shown in [53].

For density ρ_0 and temperature T_0 the corresponding relations can be obtained with the help of equations (3.6.31) and (3.6.33). Applying the conditions of undisturbed flow to these relations, we get

$$\rho_0=\rho_\infty\left(1+\frac{k-1}{2}\mathbf{M}_\infty^2\right)^{1/(k-1)}=\frac{\rho_\infty}{\varepsilon(\mathbf{M}_\infty)}; \tag{3.6.34}$$

$$T_0=T_\infty\left(1+\frac{k-1}{2}\mathbf{M}_\infty^2\right)=\frac{T_\infty}{\tau(\mathbf{M}_\infty)}. \tag{3.6.35}$$

At the critical section of the jet $\mathbf{M}=1$ and hence, from (3.6.28), (3.6.31) and (3.6.33) we get the following formulas for critical values of pressure p^*, density ρ^* and temperature T^*:

$$p^*=p_0\left(\frac{2}{k+1}\right)^{k/(k-1)}=p_0\,\pi(1); \tag{3.6.36}$$

$$\rho^*=\rho_0\left(\frac{2}{k+1}\right)^{1/(k-1)}=\rho_0\,\varepsilon(1); \tag{3.6.37}$$

$$T^*=T_0\left(\frac{2}{k+1}\right)=T_0\,\tau(1), \tag{3.6.38}$$

where π (1), ε (1), τ (1) are values of gas dynamic functions at $\mathbf{M}=1$.

From the above formulas applicable for any speeds approximate relations can be obtained for cases where Mach numbers $\mathbf{M}$ are very high. From (3.6.30) it follows that at $\mathbf{M}_\infty \gg 1$ and $\mathbf{M} \gg 1$ it can be written that

$$p/p_\infty = (\mathbf{M}_\infty/\mathbf{M})^{2k/(k-1)}. \tag{3.6.39}$$

Similar relations for density and temperature have the form:

$$\rho/\rho_\infty = (\mathbf{M}_\infty/\mathbf{M})^{2/(k-1)}; \tag{3.6.40}$$

$$T/T_\infty = (\mathbf{M}_\infty/\mathbf{M})^2. \tag{3.6.41}$$

Using relation (3.6.27) for undisturbed flow conditions

$$1-\frac{V_\infty^2}{V_{\max}^2} = \left(1+\frac{k-1}{2}\mathbf{M}_\infty^2\right)^{-1}, \tag{3.6.27'}$$

we get the following approximate formula of local velocity under the conditions of $\mathbf{M}_\infty \gg 1$ and $\mathbf{M} \gg 1$:

$$\frac{V}{V_\infty} = 1+\frac{1}{k-1}\left(\frac{1}{\mathbf{M}_\infty^2}-\frac{1}{\mathbf{M}^2}\right). \tag{3.6.42}$$

6.4 Gas flow from reservoir

Formula (3.6.12) helps to determine the velocity of a gas flow through a nozzle from a reservoir (Fig. 3.6.2), where the flow parameters are determined by the stagnation conditions corresponding to the speed of gas flow in reservoir $V \approx 0$. Such conditions are practically satisfied if the critical cross section of the nozzle is fairly small compared to the cross section of the reservoir. At the critical section of the nozzle, where the value of derivative $dS/dV=0$, the Mach number $\mathbf{M}$, as seen from (3.6.4), is equal to unity, i.e. the speed at this section is equal to the local speed of sound:

$$V = a^* = \sqrt{\frac{2k}{k+1}\cdot\frac{p_0}{\rho_0}} = a_0\sqrt{\frac{2}{k+1}} = \sqrt{\frac{2kRT_0}{k+1}}.$$

This velocity relation is satisfied under the condition where the pressure in the reservoir, according to (3.6.36), is not below the value

$$p_0 = p^*\left(\frac{k+1}{2}\right)^{k/(k-1)}. \tag{3.6.43}$$

If the nozzle opens to atmospheric conditions with pressure $p_a=1$ atmosphere (this pressure is called adverse pressure) motion of gas along the nozzle is possible under the condition that $p^* \geqslant 1$ atmosphere. With $p^*=1$ atmosphere and $k=1.4$ the pressure necessary at the reservoir to achieve sonic speed at the end of a converging nozzle will be

$$p_0 = 1\left(\frac{1.4+1}{2}\right)^{1.4/(1.4-1)} \approx 1.9 \text{ atm.}$$

After achieving critical parameters in the narrowest section of the nozzle the further reduction of adverse pressure ($p_a < p^*$) has no effect on the values of a^* and p^* and these values depend on reservoir conditions only. However, conditions for occurrence of a supersonic speed of gas flow in the divergent part of the nozzle may arise during this process. This regime of isentropic flow is

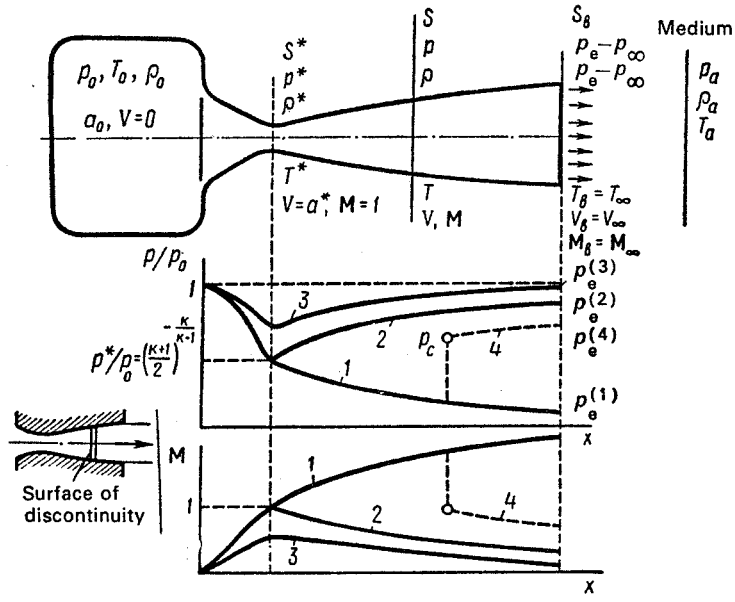

Fig. 3.6.2. Gas parameters for flow from reservoir.

characterized by the curves 1 in Fig. 3.6.2, indicating variation of ratio p/p_0 and Mach number **M** along the nozzle. This regime of flow is found where adverse pressure p_a is equal to pressure $p_e^{(1)}$ or less than this at the exit of the divergent part of the nozzle. Then changes in the adverse atmospheric pressure have no effect on gas parameters at the exit of the nozzle.

Let us look at one more important regime of isentropic flow along a nozzle. Assume that the adverse pressure increases to the value $p_a^{(2)} > p_e^{(1)}$ at which pressure at exit $p_e^{(2)}$ reaches the same value as $p_a^{(2)}$. The subsonic flow so formed can be characterized by lines 2 shown in Fig. 3.6.2. The relative velocity λ (**M**) of this section can be found from equation (3.6.23) by selecting one of the two solutions having value $\lambda < 1$.

A further increase in adverse atmospheric pressure to $p_a^{(3)}$ creates conditions where the pressure at the exit will be the same as atmospheric $p_e^{(3)} = p_a^{(3)}$. At the throat section the pressure increases beyond critical value p^*; the

corresponding velocity at this section will be subsonic ($V<a^*$). Therefore the speed in the divergent part of the nozzle will diminish and remain subsonic (curve 3 in Fig. 3.6.2).

For values of pressure at exit less than $p_e^{(2)}$ and more than $p_e^{(1)}$ the flow does not remain isentropic. Discontinuity of flow appears at some section of the nozzle, associated with sudden stagnation of the flow across it. Because this stagnation has an irreversible adiabatic character the supersonic flow changes to a subsonic flow through shock. Variations in pressure and Mach number **M** along the nozzle in this region of flow are characterized by curves 4 in Fig. 3.6.2. The separation surface (shock wave) must lie at the section with the Mach number that could have given pressure p_c behind this surface, providing pressure $p_e^{(4)}$ ($p_e^{(1)}<p_e^{(4)}<p_e^{(2)}$) at the exit as a result of further expansion of the gas. Thus analysis of the gas flow in this case must be carried out in light of shock wave theory. The basic concepts of this theory will be discussed in Chapter 4.

At any arbitrary section of the nozzle including its exit section the supersonic speed can be determined by formula (3.6.12). For a given Mach number $\mathbf{M}_e=\mathbf{M}_\infty$ and pressure $p_e=p_\infty$ at the exit cross section the required reservoir pressure p_0 can be determined by (3.6.29).

Let us write the equation of mass flow

$$\rho SV=\rho^*S^*a^*, \tag{3.6.44}$$

from which we find that the ratio of specific mass flow $q=\rho V$ through section S to the specific mass flow $q^*=\rho^*a^*$ through the throat section S^* is

$$\bar{q}=q/q^*=\rho V/\rho^*a^*=S^*/S. \tag{3.6.45}$$

Keeping in view equations (3.6.19) and (3.6.31), we get

$$\rho=\rho_0\left(1-\frac{V^2}{V_{\max}^2}\right)^{1/(k-1)}=\rho_0\left(1-\frac{k-1}{k+1}\cdot\frac{V^2}{a^{*2}}\right)^{1/(k-1)}$$
$$=\rho_0\left(1-\frac{k-1}{k+1}\lambda^2\right)^{1/(k-1)}.$$

After determining the ratio of ρ_0/ρ^* from (3.6.37) we get relation (3.6.45) in the following form:

$$\bar{q}(\lambda)=\lambda\left(1-\frac{k-1}{k+1}\lambda^2\right)^{1/(k-1)}\left(\frac{k+1}{2}\right)^{1/(k-1)}=\frac{S^*}{S}. \tag{3.6.46}$$

The function $\bar{q}(\lambda)$ is called the mass flow density. According to formula (3.6.23) it is possible to determine this function in terms of Mach number **M**:

$$\bar{q}(\mathbf{M})=\mathbf{M}\left[\frac{2}{k+1}\left(1+\frac{k-1}{2}\mathbf{M}^2\right)\right]^{-(k+1)/[2(k-1)]}=\frac{S^*}{S}. \tag{3.6.46'}$$

The tabulated values of function $\bar{q}$ in the range of k from 1.1 through 1.67 are shown in the work [53]. From these relations it follows that number

λ (or **M**) at some section S of the nozzle happens to be a function of the ratio of areas S^*/S and does not depend only on the gas parameters in the reservoir.

The variation of the specific flow $\bar{q}$ (or ratio of areas S^*/S) as a function of λ is shown in Fig. 3.6.3. At a given critical section of the nozzle in the subsonic region of flow ($\lambda < 1$) the increase in velocity is achieved by reduction of area S. On the other hand, in the supersonic region it can be achieved by reduction of the nozzle section area S. Therefore a reduction in reservoir pressure does not affect the value of λ or **M** at the nozzle exit. In the case being considered, as can be seen from (3.6.29), the pressure at exit $p_e = p_\infty$ will change in accordance with the variation in pressure p_0.

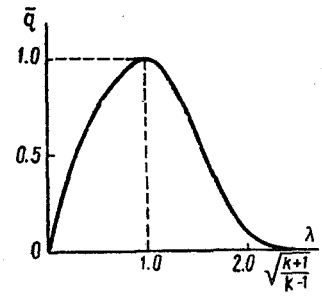

Fig. 3.6.3. Variation of specific flow rate for gas flow.

The weight flow rate of gas from the reservoir can be determined by the formula

$$W_{sec} = \rho^* g a^* S^*.$$

Determining values of ρ^* and a^* by the formulas (3.6.37) and (3.6.18) respectively, we get

$$W_{sec} = S^* \left(\frac{2}{k+1}\right)^{1/(k-1)} \sqrt{\frac{2k}{k+1} p_0 \gamma_0 g}, \tag{3.6.47}$$

where $\gamma_0 = g\rho_0$ is the specific weight of gas in the reservoir.

6.5 Motion of incompressible gas (fluid)

The equation of mass flow for an incompressible gas (fluid) flow, according to (2.4.51) and under the condition $\rho = \text{const}$, will take the form

$$VS = \text{const}. \tag{3.6.48}$$

This kinematic equation (3.6.48) contains all the information on the one-dimensional motion of an incompressible fluid. According to this equation flow velocity V is inversely proportional to the area of the cross section of the canal. The pressure for a Bernoulli's equation steady flow case can be obtained from (3.4.12) or (3.4.13).

6.6 Dissociating gas flow from reservoir (one-dimensional problem)

Let us consider the flow calculations for a nozzle connected to a reservoir of gas at a high enough temperature for balanced dissociation to take place. We will assume that the distribution of velocities and pressure at every cross

section of the nozzle is uniform and depends only on the location of the section, i.e. the flow is considered to be one-dimensional. We will also assume that there is no frictional loss in flow and no shock wave, i.e. the flow is isentropic.

The given parameters usually consist of the parameters for the stagnation condition: pressure, temperature in the reservoir (the density, enthalpy or entropy are usually calculated from this), velocity (Mach number) at the exit section of the jet and the area of this section.

The aim of this flow analysis is to determine the gas parameters at each section of the nozzle and the corresponding cross sectional area from the above data. In tackling this task it is necessary to account for the thermodynamic relations of flow parameters, not only with temperature but also with pressure. To do this the diagram of "enthalpy–entropy" developed for the condition of balanced dissociation or the relevant thermodynamic tables can be used. Equation (3.6.7) complements the tables and the diagram inasmuch as it helps us to determine the local velocity of isentropic flow from a known value of enthalpy and vice versa.

The following sequence may be observed in this calculation: Enthalpy i_0 and entropy S_0 are obtained with the help of the i–S diagram (see Fig. 1.4.6) or from tables of thermodynamic functions, using known values of p_0 and T_0 at the reservoir. For a given velocity V_A at the exit the corresponding value of enthalpy can be obtained from the equation $i_0 = i_A + (V_A^2/2)$ in the following form:

$$i_A = i_0 - (V_A^2/2). \qquad (3.6.49)$$

Then we assign a series of values to enthalpy i_K ($i_A < i_K < i_0$) and, based on these values, we find velocities

$$V_K = \sqrt{2(i_0 - i_K)}. \qquad (3.6.50)$$

As the flow is isentropic and consequently $S_0 = \text{const}$ for all sections the corresponding gas parameters (pressure p_K, temperature T_K, density ρ_K and specific mass flow rate $\rho_K V_K$) can be obtained for different values of i_K from the i–S diagram using the above value of S_0. To determine the flow parameters at the critical section it is necessary to draw the curves of variation of velocity $V_K = f_1(i_K)$ from equation (3.6.50) and the curves of variation in the speed of sound $a_K = f_2(i_K)$ from the a–i diagram (see Fig. 1.4.8). The point of intersection

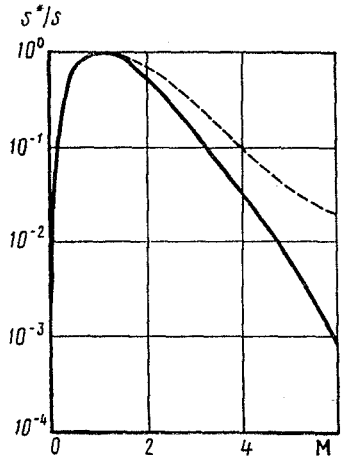

Fig. 3.6.4. Variation in area of cross sections of nozzle during flow of dissociating air:

—— dissociating air; - - - perfect gas at $k = 1.4$.

of these curves gives the values $V^*=a^*$ and i^*. After determining density ρ^* from i^* and S_0 the specific flow rate through the critical section can be calculated.

The area of the critical section can be found by the formula

$$S^*=\rho_A V_A S_A/\rho^* a^*, \tag{3.6.51}$$

and areas of other sections can be determined by the corresponding expression

$$S_K=\rho_A V_A S_A/\rho_K V_K. \tag{3.6.52}$$

Mach numbers at corresponding sections are determined by the relation $M_K=V_K/a_K$.

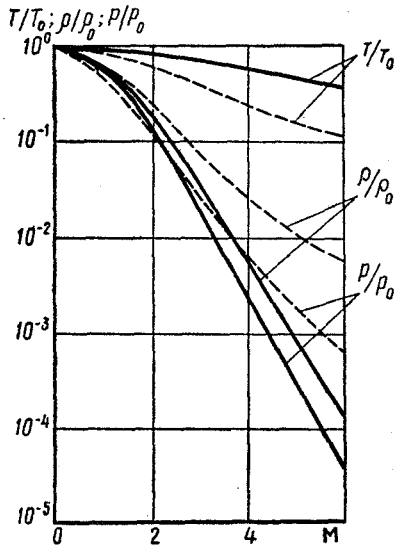

Fig. 3.6.5. Variation in gas parameters in flow through nozzle:

—— dissociating air; - - - perfect air at $k=1.4$.

The results of this calculation show that with an increase in Mach number the temperature along the nozzle diminishes at a lower rate than for an undissociated gas. This is explained by the fact that with the increase in velocity and consequent cooling liberation of energy of recombination, making for additional heating, takes place in the dissociating gas flow. This rise in temperature leads to a reduction in density, which has an effect on the reduction in pressure by comparison with the pressure in an undissociating gas. So in the presence of dissociation it is necessary to have a considerably higher degree of expansion to achieve a given velocity (Mach number) than without dissociation. The cross sectional areas of the nozzle are also found to be bigger with a dissociating gas flow.

The results obtained for a particular case of flow from the reservoir with pressure $p_0=100$ kg/cm^2 and temperature $T_0=12{,}000$°K are shown on Figs. 3.6.4 and 3.6.5.

4

THEORY OF SHOCK WAVES

1. Physical Process of Appearance of Shock Waves

The distinguishing feature of supersonic gas flows is the formation of discontinuity surfaces in face of obstacles. Across such surfaces the gas parameters change suddenly: velocity is suddenly decreased and density, pressure and temperature are suddenly increased. Discontinuity surfaces moving with respect to the gas medium are sometimes known as moving waves and steady discontinuity surfaces are called stationary shock waves. In this chapter we will consider the conditions of gas flow behind stationary shock waves. We will use the term "shock" for such surfaces.

In the most general case the shock has a curvilinear form. Fig. 4.4.1, a shows the scheme of an attached curvilinear shock formed during interaction with a sharp body. Fig. 4.1.1, b shows the scheme of a detached curvilinear shock that appears before a blunt surface in a supersonic flow. An attached plane shock (Fig. 4.1.1, c) may appear during the interaction of a sharp body with plane faces.

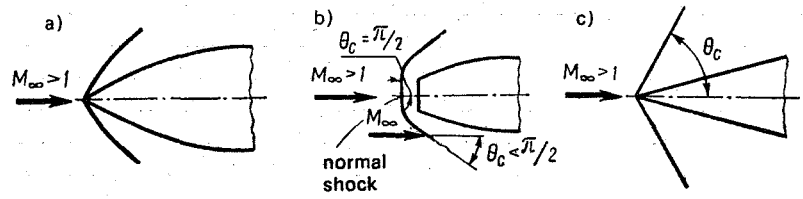

Fig. 4.1.1. Types of shock waves:

a—attached curvilinear shock; *b*—detached curvilinear shock; *c*—attached linear shock.

From Fig. 4.1.1, b it can be seen that the surfaces of a shock may be oriented along the normal to the undisturbed velocity vector (angle of inclination $\theta_c = \pi/2$) or may be inclined at some angle θ, diverging from the right angle ($\theta_c < \pi/2$). In the first case it is known as a normal shock and in the second as an oblique shock. It is obvious that an attached curvilinear shock

can be regarded as a collection of a number of oblique shocks and a detached shock may be regarded as one consisting of a normal shock and a system of oblique shocks.

The formation of shock waves is based on the particular characteristic of the propagation of disturbances in a supersonic gas flow. By "disturbance" we understand the local irregularity associated with a rise in pressure. Such an increase in pressure appears in a flow during interaction with some obstacle known as the source of disturbance.

Let us consider a source of infinitesimally small disturbances situated at a point O (Fig. 4.1.2). Such disturbances spread through the stationary gas ($V=0$) in all directions at the speed of sound a in the form of spherical waves in space and circular waves in a plane (Fig. 4.1.2, a). At time t the radius of wave $r=a\cdot t$. If a subsonic gas flow ($V<a$; Fig. 4.1.2, b) moves over the source the waves will be carried away downstream with the flow; during this the center of the waves moves with velocity $V<a$ and the wave itself propagates at the speed of sound. After some time t the center of the waves will have moved by a distance $V\cdot t$ and the radius of the wave will be $r=a\cdot t$, where $a\cdot t>V\cdot t$. Thus in a subsonic flow the disturbance spreads even upstream vis-a-vis the flow.

In the special case of sonic speed ($V=a$) the leading front of the spherical or circular waves of the disturbance is restricted to the vertical surface or straight line tangent to the sphere or circle through point O respectively. This is because the distance by which the center of the waves moves in time t is equal to its radius at the same moment of time t.

Assume that the oncoming flow has a supersonic speed ($V>a$). The center of the waves moves by the distance $V\cdot t$ in time t and the sonic wave propagates by distance $a\cdot t$. Since $a\cdot t< V\cdot t$ it is possible to draw a moving conical surface as an envelope of all the spherical sound waves (Fig. 4.1.2, c). This is called the cone of disturbance (Mach cone). On the plane of the moving circular waves we have lines of disturbance (Mach lines). On the Mach cone or Mach lines acting as the boundary separating the flow of the disturbed and undisturbed regions the disturbances are grouped more tightly because all sonic waves lie on this cone in the same phase of vibrations or phase of concentration. Such regions of disturbance, conical or plane waves determined by straight Mach lines are known as plane compression waves or Mach waves.

The angle of inclination μ for a conical wave or line of disturbance is determined from the condition (see Fig. 4.1.2, c) that $\sin\mu=a\,t/Vt$; hence

$$\sin\mu=1/\mathbf{M}. \tag{4.1.1}$$

The angle μ is called an angle of disturbance or Mach angle. Supersonic flow carries all sonic disturbances downstream with the flow and hence limits their propagation by a cone or lines of disturbance inclined by the angle μ.

The front of the plane wave propagates with the same sonic speed as the spherical (or circular) wave. Therefore the projection of the velocity vector of the undisturbed flow on the normal to the wave front is equal to the speed of sound (see Fig. 4.1.2, c).

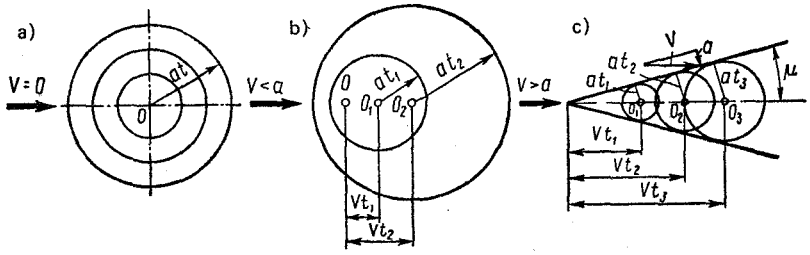

Fig. 4.1.2. Nature of propagation of disturbances in a gas:
a—gas at standstill; *b*—subsonic flow; *c*—supersonic flow.

In a plane compression wave, as in a sonic wave, the gas parameters (pressure, density, etc.) change by an infinitesimally small value which, specifically, indicates the famous relation of physics for sonic speed $a=\sqrt{dp/d\rho}$. In a disturbed region of flow the velocity remains practically the same as in an undisturbed flow. Therefore the plane compression wave is regarded as a shock wave of infinitesimally small intensity and in practice it can be assumed that the flow parameters across a plane compression wave remain unchanged. That is why this kind of shock wave is known as a weak shock and its leading front (Mach line) is known as a line of weak disturbances.

It is natural to assume that the formation of a shock of finite intensity is connected with the superposition of plane compression waves which mutually strengthen the shock. Let us consider the process of generation of oblique shock wave. Assume that a supersonic flow initially moves over a smooth surface (Fig. 4.1.3). We will create a local increase in pressure at point A artificially by turning the flow through an infinitely small angle $d\beta$. This produces a plane compression wave AB starting from point A as from the source of disturbance. It is inclined to the surface by an angle μ. If an additional inclination by a small angle $\delta\beta$ is to be made, a new plane wave AC is formed which begins from the same point A but is situated to the left of the first wave. However, in a supersonic flow, as shown earlier, the wave cannot propagate upstream. Therefore the wave AC will be carried away downstream until it coincides with the first wave. In this process a more powerful wave is formed which is con-

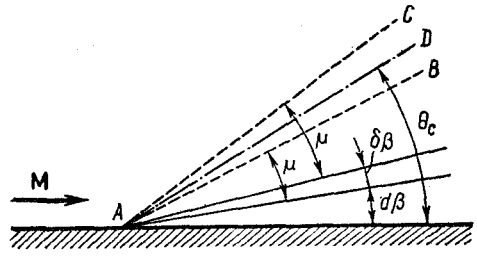

Fig. 4.1.3. Formation of shock wave.

siderably strengthened if the flow is turned some more. The shock wave of finite intensity formed in this way has a propagation speed higher than the speed of sound at which the plane wave of disturbance propagates. Therefore this shock of finite strength must be inclined to the left of the plane wave AB and must occupy the position AD where it remains in equilibrium because its velocity of propagation will be equal to the velocity component of the undisturbed free flow velocity along the normal to wave front $V \sin \theta_c$, where θ_c is the angle of inclination of shock. From the above discussion it follows that the angle of inclination of a shock of finite strength is more than the angle of inclination of the line of (cone) disturbance, i.e. $\theta_c > \mu$.

2. General Equations for Shock Waves

Let us consider a more general case in which gas experiences physico-chemical changes behind a shock wave due to considerable heating which changes its heat coefficients. In the investigation of shocks of this kind which bring in their train vibrational excitation, dissociation, ionization and chemical reactions the problem of the speed of physico-chemical changes assumes great importance.

The processes behind shock waves are characterized by the fact that a part of the kinetic energy of a moving gas almost instantaneously changes into internal energy of the gas. In such conditions, in general, it should not be forgotten that thermodynamic equilibrium is achieved after a lapse of time and it is only under such conditions of equilibrium that all macroscopically measured parameters (pressure, density, temperature) become independent of time. The analysis of these phenomena represents a still more complicated problem and is connected, first of all, with the study of the mechanism of unbalanced processes and in particular with the knowledge of rates of chemical reactions in air.

The simplest case is characterized by an infinitely high rate of physico-chemical transformation and consequently by instantaneous reversion to thermodynamic equilibrium. Such processes are physically possible behind a shock wave. This has been proved by experimental research.

Let us study the basic theoretical relations that help in analyzing gas parameters in the equilibrium behind a shock wave.

2.1 Oblique shock

The shock appearing in real situations is characterized by some thickness: strictly speaking, the variations in gas parameters in such flows will not occur instantaneously but will take some time. However, as shown by theoretical and experimental research, the thickness of a shock is very small: it is of the order of the free path length of molecules. Therefore in studying shock in an ideal medium this thickness can be neglected and the shock can be repre-

sented in the form of a discontinuity surface for gas parameters, assuming that variations in these parameters take place abruptly.

The problem of the shock lies in determination of the unknown gas parameters behind it from the given parameters characterizing the motion of the gas in front of it.

For an oblique shock appearing in dissociating and ionizing gas there are nine unknown parameters: pressure p_2, density ρ_2, temperature T_2, velocity V_2, enthalpy i_2, entropy S_2, speed of sound a_2, average molecular weight μ_{av2}, and angle of inclination of shock θ_c (or angle of flow inclination β_c). Consequently it is necessary to construct a system out of nine equations. In these equations the parameters in front of the shock will be known parameters: pressure p_1, density ρ_1, velocity V_1, etc. In place of velocity V_2 behind the shock it is possible to determine its components V_{n2} and $V_{\tau 2}$, normal and tangential to the shock respectively. As a result the number of equations needed goes up to ten. This system of equations will include the basic gas dynamic equations (equations of motion, continuity, energy and state), a series of kinematic relations for velocities and the thermodynamic relations characterizing the properties of the gas. Let us study each of the equations of this system.

Figure 4.2.1 shows triangles of flow-velocities in front of the shock (parameters with index "1") and behind it (parameters with index "2"). The following relations for given components can be determined from this figure:

$$V_{\tau 2} = V_2 \cos(\theta_c - \beta_c),\ V_{n2} = V_2 \sin(\theta_c - \beta_c). \tag{4.2.1}$$

The first equation of the system is determined from this:

$$V_{n2}/V_{\tau 2} = \tan(\theta_c - \beta_c). \tag{4.2.2}$$

The second equation will be the equation of mass flow (continuity) which determines the amount of the fluid flow rate through unit surface area of shock per unit time:

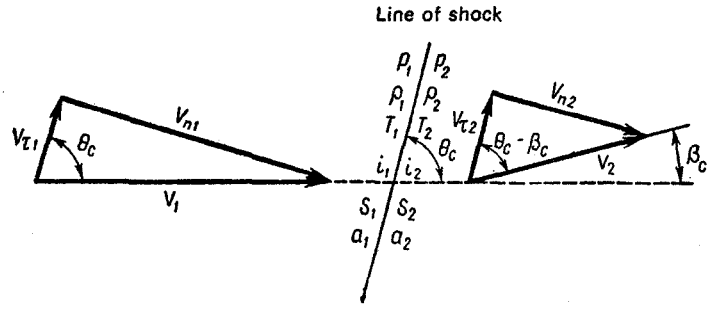

Fig. 4.2.1. Schematic diagram of oblique shock.

$$\rho_1 V_{n1} = \rho_2 V_{n2}\,; \tag{4.2.3}$$

where normal component of velocity in front of the shock (see Fig. 4.2.1) $V_{n1} = V_1 \sin \theta_c$.

The equation of momentum can be used for transformations of parameters across the shock. This will be the third equation of the system. It can be obtained by equating the variation in momentum of a fluid flowing in unit time through unit surface area of shock in the direction normal to it, to the pressure force:

$$\rho_1 V_{n1}^2 - \rho_2 V_{n2}^2 = p_2 - p_1\,. \tag{4.2.4}$$

With the help of equation (4.2.3) this equation can be written in the following way:

$$\rho_1 V_{n1} (V_{n1} - V_{n2}) = p_2 - p_1. \tag{4.2.4'}$$

Equation (4.2.4) could be expressed in the form

$$p_1 + \rho_1 V_{n1}^2 = p_2 + \rho_2 V_{n2}^2\,. \tag{4.2.4''}$$

The equation in this form represents the law of conservation of momentum during flow across the shock. If the change in the momentum of the fluid along a direction tangential to the surface is taken into account along with the zero value of the pressure gradient in this direction we get the relation

$$\rho_1 V_{n1} V_{\tau 1} - \rho_2 V_{n2} V_{\tau 2} = 0,$$

whence, using $\rho_1 V_{n1} = \rho_2 V_{n2}$, we have

$$V_{\tau 1} = V_{\tau 2}. \tag{4.2.5}$$

This fourth equation of the system indicates that tangential components of velocity across the shock do not change. From Fig. 4.2.1 it can be seen that $V_{\tau 1} = V_1 \cos \theta_c$; consequently equation (4.2.5) can be written in the form

$$V_{\tau 2} = V_1 \cos \theta_c = V_{n1}/\tan \theta_c. \tag{4.2.5'}$$

The equation of conservation of energy may be written in the form:

$$i_1 + (V_1^2/2) = i_2 + (V_2^2/2).$$

Under the condition that

$$V_1^2 = V_{n1}^2 + V_{\tau 1}^2\,,\quad V_2^2 = V_{n2}^2 + V_{\tau 2}^2 \text{ and } V_{\tau 1} = V_{\tau 2}\,,$$

this equation can be modified to

$$i_1 + (V_{n1}^2/2) = i_2 + (V_{n2}^2/2). \tag{4.2.6}$$

Combining the equation of state before and after the shock we get the relation

$$p_2 - p_1 = R_2 \rho_2 T_2 - R_1 \rho_1 T_1\,;$$

or recalling that $R=R_0/\mu_{av}$, it will be given by

$$p_2-p_1=R_0\left(\frac{\rho_2T_2}{\mu_{av2}}-\frac{\rho_1T_1}{\mu_{av1}}\right). \tag{4.2.7}$$

The four equations useful in determination of enthalpy, entropy, average molecular weight and speed of sound in the dissociating gas of the system we are considering can be represented in the form of general relations of these parameters as functions of pressure and temperature:

$$i_2=f_1(p_2, T_2); \tag{4.2.8}$$

$$S_2=f_2(p_2, T_2); \tag{4.2.9}$$

$$\mu_{av2}=f_3(p_2, T_2); \tag{4.2.10}$$

$$a_2=f_4(p_2, T_2). \tag{4.2.11}$$

These functions are analytically not expressed in the usual form but they are determined by means of experimental research or with the help of fairly complicated calculations from the solution of the corresponding thermodynamic equations. The relations for the above functions are usually prepared in graphic form and their values are tabulated in special tables of the thermodynamic functions of air at high temperatures (see [7], [17], [18]).

Let us express the basic parameters behind the shock in terms of relative change in normal components of velocity, i.e. by the quantity

$$\Delta\bar{V}_n=\Delta V_n/V_{n1}=(V_{n1}-V_{n2})/V_{n1}. \tag{4.2.12}$$

From (4.2.3) the density ratio will be

$$\rho_2/\rho_1=1/(1-\Delta\bar{V}_n), \tag{4.2.13}$$

and from (4.2.4′) the pressure ratio will be

$$\frac{p_2}{p_1}=1+\frac{\rho_1V_{n1}^2}{p_1}\Delta\bar{V}_n. \tag{4.2.14}$$

Introducing the concept of a "normal component" of Mach number $\mathbf{M}_1$ in the above condition so that $\mathbf{M}_{n1}=V_{n1}/a_1$ or $\mathbf{M}_{n1}=\mathbf{M}_1\sin\theta_c$ and assuming that the gas remains undissociated before the shock with sound velocity $a_1=\sqrt{k_1p_1/\rho_1}$, we get

$$p_2/p_1=1+k_1\mathbf{M}_{1n}^2\Delta\bar{V}_n \tag{4.2.15}$$

in place of (4.2.14).

The enthalpy ratio i_2/i_1 can be determined from (4.2.6):

$$i_2/i_1=1+(1/2\,i_1)(V_{n1}^2-V_{n2}^2).$$

The difference between the squares of the velocities will be

$$V_{n1}^2-V_{n2}^2=V_{n1}^2\left(1-\frac{V_{n2}}{V_{n1}}\right)\left(1+\frac{V_{n2}}{V_{n1}}\right)=V_{n1}^2\Delta\bar{V}_n(2-\Delta\bar{V}_n).$$

Hence

$$\frac{i_2}{i_1}=1+\frac{V_{n1}^2}{2}\cdot\frac{\Delta\bar{V}_n}{i_1}(2-\Delta\bar{V}_n). \tag{4.2.16}$$

To determine the temperature ratio T_2/T_1 we use the equations of state for the flows in front of and behind the shock. This leads to

$$\frac{T_2}{T_1}=\frac{p_2}{p_1}\cdot\frac{\mu_{av2}}{\mu_{av1}}\cdot\frac{\rho_1}{\rho_2}. \tag{4.2.17}$$

Replacing the ratios of densities and pressures by equations (4.2.13) and (4.2.15) respectively, we get

$$T_2/T_1=(1+k_1\,\mathbf{M}_{n1}^2\,\Delta\bar{V}_n)\,(1-\Delta\bar{V}_n)\,(\mu_{av2}/\mu_{av1}). \tag{4.2.17'}$$

To determine the velocity behind the shock the relations

$$V_2^2=V_\tau^2+V_{n2}^2 \quad \text{and} \quad V_1^2=V_\tau^2+V_{n1}^2,$$

are used, from which

$$V_2^2/V_1^2=1-\left(\frac{V_{n1}^2}{V_1^2}\right)\Delta\bar{V}_n(2-\Delta\bar{V}_n). \tag{4.2.18}$$

Since $V_{n1}/V_1=\sin\theta_c$ we get

$$V_2^2/V_1^2=1-\sin^2\theta_c\,\Delta\bar{V}_n\,(2-\Delta\bar{V}_n). \tag{4.2.18'}$$

Let us determine the relation for the angle of inclination of flow behind the shock. From (4.2.2) and (4.2.5') we have

$$\Delta\bar{V}_n=1-[\tan(\theta_c-\beta_c)]/\tan\theta_c. \tag{4.2.19}$$

Hence, taking into account that

$$\tan(\theta_c-\beta_c)=(\tan\theta_c-\tan\beta_c)/(1+\tan\theta_c\tan\beta_c),$$

the relation for β_c will be

$$\tan\beta_c=\tan\theta_c\,\frac{\Delta\bar{V}_n}{1-\Delta\bar{V}_n}\left(\frac{1}{1-\Delta\bar{V}_n}+\tan^2\theta_c\right)^{-1}. \tag{4.2.20}$$

The change in velocity $\Delta\bar{V}_n$ is determined from (4.2.13) in terms of nondimensional density:

$$\Delta\bar{V}_n=1-(\rho_1/\rho_2). \tag{4.2.21}$$

From this it follows that the pressure ratio, temperature ratio, enthalpy ratio and angle of inclination β_c can be expressed as functions of density ratio ρ_2/ρ_1. Besides, the quantities V_{n1} and $\mathbf{M}_{n1}$ can be replaced by the values $V_{n1}=V_1\sin\theta_c$ and $\mathbf{M}_{n1}=\mathbf{M}_1\sin\theta_c$.

So the solution of the problem of an oblique shock with a known angle of inclination θ_c leads to the determination of density ratio ρ_2/ρ_1 or function

$\Delta\bar{V}_n$. This function can be determined with the help of relations (4.2.16) and (4.2.17′), each of which can be rewritten in the form of a quadratic equation of $\Delta\bar{V}_n$. From the first quadratic equation we find

$$\Delta\bar{V}_n = 1 - \sqrt{1 - \frac{2(i_2 - i_1)}{V_{n1}^2}}, \tag{4.2.22}$$

and from the second we get

$$\Delta\bar{V}_n = A + \sqrt{A^2 - B}, \tag{4.2.23}$$

where

$$A = \frac{k_1 \mathbf{M}_{n1}^2 - 1}{2k_1 \mathbf{M}_{n1}^2}, \quad B = \frac{1}{k_1 \mathbf{M}_{n1}^2}\left(\frac{T_2}{T_1} \cdot \frac{\mu_{av1}}{\mu_{av2}} - 1\right). \tag{4.2.24}$$

The signs before the quantities under the square root, minus in (4.2.22) and plus in (4.2.23), reflect the condition that velocity is always less behind the shock than in front of it and hence $\Delta\bar{V}_n < 1$ must be observed. Here the plus sign in (4.2.23) also accounts for the physically possible value of $\Delta\bar{V}_n < 1$.

Equations (4.2.22) and (4.2.23) are solved by the method of successive iterations. The problem of an oblique shock can be solved if angle β_c is given. Then, the calculation of angle θ_c is carried out with the help of relation (4.2.20), from which

$$\tan^2 \theta_c - \frac{\tan \theta_c}{\tan \beta_c} \cdot \frac{\Delta\bar{V}_n}{1 - \Delta\bar{V}_n} + \frac{1}{1 - \Delta\bar{V}_n} = 0.$$

The solution of this equation gives

$$\tan \theta_c = \cot \beta_c \left[\frac{1}{2} \cdot \frac{\Delta\bar{V}_n}{1 - \Delta\bar{V}_n} \pm \sqrt{\frac{1}{4} \cdot \frac{\Delta\bar{V}_n^2}{(1 - \Delta\bar{V}_n)^2} - \frac{\tan^2 \beta_c}{1 - \Delta\bar{V}_n}}\right]. \tag{4.2.25}$$

One solution (plus sign before the square root) gives a higher value of angle θ_c, which occurs in a detached curvilinear shock, and the other (minus sign before the square root) gives a lower value of θ_c, which is observed in an attached shock of fairly weak strength.

For ease of calculation it is desirable to calculate θ_c in advance on the basis of given values of β_c and to prepare the corresponding table or graph. With the help of this table or graph for some value of $\Delta\bar{V}_n$ corresponding to the values of ratios p_2/p_1, ρ_2/ρ_1, etc. obtained earlier it is possible to find angle θ_c or β_c with one of them as a known quantity.

The calculation of velocity V_1 and Mach number $\mathbf{M}_1$ of the flow upstream of the shock, where the parameters in the shock are observed for given values of angle θ_c (or β_c) and V_{n1} (or $\mathbf{M}_{n1}$), is performed with the help of the formulas

$$V_1 = V_{n1}/\sin\theta_c, \quad \mathbf{M}_1 = \mathbf{M}_{n1}/\sin\theta_c. \tag{4.2.26}$$

2.2 Normal shock

Formulas for calculation of flow parameters across a normal shock can be obtained from the above relations for an oblique shock by taking $\theta_c = \pi/2$ and $\beta_c = 0$. Then we get velocity $V_{n1} = V_1$ and Mach number $\mathbf{M}_{n1} = \mathbf{M}_1$. In switching from oblique shock to normal shock it is required to exclude index "n" in the above relations for oblique shock. Then the basic relations take the following form:

$$p_2/p_1 = 1 + k_1\mathbf{M}_1^2\Delta\bar{V}; \tag{4.2.27}$$

$$i_2/i_1 = 1 + (V_1^2/2)\,(\Delta\bar{V}/i_1)\,(2-\Delta\bar{V}); \tag{4.2.28}$$

$$T_2/T_1 = (1 + k_1\mathbf{M}_1^2\Delta\bar{V})\,(1-\Delta\bar{V})\,(\mu_{av2}/\mu_{av1}); \tag{4.2.29}$$

$$V_2^2/V_1^2 = 1 - \Delta\bar{V}\,(2-\Delta\bar{V}), \tag{4.2.30}$$

where the change in relative velocity

$$\Delta\bar{V} = \Delta V/V_1 = (V_1 - V_2)/V_1 \tag{4.2.31}$$

is determined with the help of relations (4.2.22)–(4.2.24):

$$\Delta\bar{V} = 1 - \sqrt{1 - [2\,(i_2 - i_1)/V_1^2]}; \tag{4.2.32}$$

$$\Delta\bar{V} = A + \sqrt{A^2 - B}; \tag{4.2.33}$$

$$A = \frac{k_1\mathbf{M}_1^2 - 1}{2k_1\mathbf{M}_1^2}, \quad B = \frac{1}{k_1\mathbf{M}_1^2}\left(\frac{T_2}{T_1}\cdot\frac{\mu_{av1}}{\mu_{av2}} - 1\right). \tag{4.2.34}$$

The relation between $\Delta\bar{V}$ and the relative density is determined by the formula

$$\Delta\bar{V} = 1 - (\rho_1/\rho_2). \tag{4.2.35}$$

These are the general relations for shock waves. Let us now analyze the nature of motion with the help of these relations and study the methods of calculation of gas parameters behind shocks in the case of constant specific heats. Then we will discuss in detail the practical methods of calculation of similar parameters for a dissociating medium, i.e. in the more general case of variable specific heats.

3. Oblique Shock in a Gas Flow with Constant Specific Heats

One problem concerning a gas flow behind a shock wave with constant specific heats (c_p, c_v) happens to be of great theoretical and practical interest. Although such a flow is seen as a particular (ideal) case of the motion of gas, whose physico-chemical properties change to a greater or lesser extent during transition through a shock, the solution of this problem allows us to establish

a qualitative picture of flow through a shock. The results to be obtained in the form of the usual relations characterizing the variations in gas parameters during motion through a shock can be used for an approximate estimation of these parameters when the more general case of heat flow parameters is considered. Finally, the problem we are examining has its own significance because its solution is directly applicable in the determination of the gas parameters behind a shock occurring in a flow of comparatively low supersonic speed at which variations in specific heats in a compressed gas are negligibly small. These velocities of flow, to be determined for the most intensive—normal—shock, correspond approximately to Mach number $\mathbf{M}_\infty < 5$ to 6.

3.1 System of equations

The method of calculation of an oblique shock to be considered here is based on application of a system of equations which happens to be the particular case of the system of equations (4.2.2) through (4.2.11).

If the specific heats remain constant during the flow of gas through the shock it follows that average molecular weight remains unchanged and the speed of sound and enthalpy depend only on temperature. Accordingly the equations (4.2.8), (4.2.10) and (4.2.11) take the following form:

$$i_2 = c_p T_2 ; \tag{4.3.1}$$

$$\mu_{av2} = \mu_{av1} = \mu_{av} = \text{const}; \tag{4.3.2}$$

$$a_2^2 = kRT_2 . \tag{4.3.3}$$

In place of equation (4.2.9) it is necessary to use the thermodynamic equation for entropy of an undissociating perfect gas:

$$dS = (di/T) - (dp/\rho T).$$

Recalling the equations

$$di = c_p\, dT \text{ and } dp = d(R\rho T) = R\rho dT + RTd\rho ,$$

we get

$$dS = c_p d \ln T - Rd \ln T - Rd \ln \rho .$$

But

$$c_p - R = c_v \text{ and } R/c_v = (c_p - c_v)/c_v = k - 1.$$

Consequently

$$dS = c_v [d \ln T - (k-1)\, d \ln \rho].$$

Integrating this equation with $k = \text{const}$, we find

$$S = c_v \ln (T/\rho^{k-1}) + \text{const}. \tag{4.3.4}$$

Replacement of T by its value from the equation of state $p = R\rho T$ leads to

$$T/\rho^{k-1} = p/\rho^k R \text{ and } \ln (p/\rho^k R) = \ln (p/\rho^k) - \ln R.$$

Absorbing ln R in the constant on the right side of equation (4.3.4), we get the relation for entropy in the following way:

$$S=c_v \ln (p/\rho^k)+\text{const.} \tag{4.3.5}$$

Transferring this equation to the flow conditions before and after the shock and determining the difference in entropy on either side of the shock, equation (4.2.9) can be replaced by the equation used in the theory of oblique shock:

$$S_2-S_1=c_v \ln [(p_2/p_1)(\rho_1^k/\rho_2^k)]. \tag{4.3.6}$$

The entropy behind the shock within the accuracy of the constant can be determined by an expression

$$S_2=c_v \ln (p_2/\rho_2^k). \tag{4.3.7}$$

The equation of state (4.2.7) in the case of constant specific heats can be simplified to

$$p_2-p_1=R(\rho_2 T_2-\rho_1 T_1). \tag{4.3.8}$$

The system of equations (4.2.2) through (4.2.6) remains unchanged.

3.2 Formulas for calculation of gas parameters behind shock

To determine density, pressure and enthalpy it is necessary to use the formulas (4.2.13), (4.2.15) and (4.2.16) respectively. To determine temperature the equation (4.2.17′) can be used, in which it is assumed that $\mu_{av2}=\mu_{av1}$, i.e.

$$T_2/T_1=(1+k\,\mathbf{M}_{n1}^2\,\Delta\bar{V}_n)(1-\Delta\bar{V}_n). \tag{4.3.9}$$

In all these expressions the variation in relative velocity $\Delta\bar{V}_n$ is the known quantity. Let us determine this quantity assuming that the angle of inclination of shock θ_c and the Mach number of oncoming flow $\mathbf{M}_1$ are known quantities. To do this we use equation (4.2.4′). Dividing this by $\rho_1 V_{n1}=\rho_2 V_{n2}$, we get

$$(p_2/\rho_2 V_{n2})-(p_1/\rho_1 V_{n1})=V_{n1}-V_{n2}.$$

Introducing here substitution of p_2/ρ_2 and p_1/ρ_1 by a_1^2/k and a_2^2/k respectively and using equation (3.6.21) for the speed of sound, we find

$$\frac{1}{kV_{n2}}\left(\frac{k+1}{2}a^{*2}-\frac{k-1}{2}V_2^2\right)-\frac{1}{kV_{n1}}\left(\frac{k+1}{2}a^{*2}-\frac{k-1}{2}V_1^2\right)=V_{n1}-V_{n2}.$$

Substituting here the values of $V_2^2=V_{n2}^2+V_\tau^2$ and $V_1^2=V_{n1}^2+V_\tau^2$ and multiplying both sides by $V_{n1}V_{n2}$, we obtain after some simplifications the following expression:

$$\frac{k+1}{2k}\,a^{*2}\,(V_{n1}-V_{n2})-\frac{k-1}{2k}\,V_\tau^2\,(V_{n1}-V_{n2})$$

$$+\frac{k-1}{2k}\,V_{n1}\,V_{n2}\,(V_{n1}-V_{n2})=V_{n1}V_{n2}\,(V_{n1}-V_{n2}).$$

Excluding here the trivial solution of $V_{n1}-V_{n2}=0$ that corresponds to the case of absence of shock, we get an equation

$$V_{n1}V_{n2}=a^{*2}-\frac{k-1}{k+1}\,V_\tau^2, \tag{4.3.10}$$

which helps in the determination of the velocity of flow behind the shock. Equation (4.3.10) is known as the basic equation for an oblique shock. From this equation the relative variation in velocity $\Delta\bar{V}_n=(V_{n1}-V_{n2})/V_{n1}$ can be found. For this purpose we express $V_{n1}V_{n2}$ in the form

$$V_{n1}V_{n2}=V_{n1}^2\,(V_{n2}/V_{n1})$$

and use the relations

$$V_{n1}=V_1\sin\theta_c,\quad V_\tau=V_1\cos\theta_c.$$

Adequate simplifications in (4.3.10) result in

$$\sin^2\theta_c\,(1-\Delta\bar{V}_n)=\frac{1}{\lambda_1^2}-\frac{k-1}{k+1}\,(1-\sin^2\theta_c),$$

where $\lambda_1=V_1/a^*$. Replacing λ_1 by the formula (3.6.23) and performing further transformations, we get

$$\Delta\bar{V}_n=\frac{2}{k+1}\left(1-\frac{1}{\mathbf{M}_1^2\sin^2\theta_c}\right). \tag{4.3.11}$$

Let us introduce the notation

$$\delta=(k-1)/(k+1). \tag{4.3.12}$$

Then formula (4.3.11) will be

$$\Delta\bar{V}_n=(1-\delta)\left(1-\frac{1}{\mathbf{M}_1^2\sin^2\theta_c}\right). \tag{4.3.11'}$$

Substituting this quantity in (4.2.13), the density ratio can be determined as

$$\rho_2/\rho_1=\mathbf{M}_1^2\sin^2\theta_c/(1-\delta+\delta\,\mathbf{M}_1^2\sin^2\theta_c). \tag{4.3.13}$$

Formula (4.2.15) can be used to find the pressure ratio p_2/p_1. Let us take $\mathbf{M}_{n1}=\mathbf{M}_1\sin\theta_c$ here and in place of $\Delta\bar{V}_n$ the relation (4.3.11'). Further, we replace quantity k by

$$k=(1+\delta)/(1-\delta) \tag{4.3.14}$$

according to (4.3.12).

As a result we get

$$p_2/p_1=(1+\delta)\,\mathbf{M}_1^2\sin^2\theta_c-\delta. \tag{4.3.15}$$

The intensity of shock is characterized by this quantity. For this purpose it is also possible to use the relation

$$(p_2-p_1)/p_1=\Delta p/p_1=(1+\delta)\,(\mathbf{M}_1^2\sin^2\theta_c-1). \tag{4.3.15'}$$

One more parameter characterizing the strength of the shock and, in particular, the coefficient of pressure $\bar{p}_2=(p_2-p_1)/q_1$, where $q_1=[(1+\delta)/(1-\delta)]$ $p_1\,\mathbf{M}_1^2/2$, can be obtained with the help of formula (4.3.15'). Representation of (4.3.15') in the form of $\bar{p}_2$ with respect to quantity q_1 gives

$$\bar{p}_2=[2\,(1-\delta)/\mathbf{M}_1^2]\,(\mathbf{M}_1^2\sin^2\theta_c-1). \tag{4.3.15''}$$

Eliminating the quantity $\mathbf{M}_1^2\sin^2\theta_c$ from equations (4.3.15) and (4.3.13), we get the relation between expressions for pressure and density, i.e. a Hugoniot equation:

$$\frac{p_2}{p_1}=\left(\frac{\rho_2}{\rho_1}-\delta\right)\Big/\left(1-\delta\,\frac{\rho_2}{\rho_1}\right). \tag{4.3.13'}$$

This relation is also known as the adiabatic shock relation which, unlike the usual adiabatic (isentropic) equation of the type $p=A\rho^k$, determines the variation in flow parameters across the shock wave. This process of transition through the shock is accompanied by a rise in entropy which can be determined by equation (4.3.6).

In this way the process of gas flow through the shock is nonisentropic. With the change in the above parameters the temperature behind the shock will increase. Its value is calculated by the equation of state:

$$\frac{T_2}{T_1}=\frac{p_2}{p_1}\cdot\frac{\rho_1}{\rho_2}=\frac{(1+\delta)\,\mathbf{M}_1^2\sin^2\theta_c-\delta]\,(1-\delta+\delta\,\mathbf{M}_1^2\sin^2\theta_c)}{\mathbf{M}_1^2\sin^2\theta_c}. \tag{4.3.16}$$

The peculiarity of flow across the shock, unlike isentropic flow, consists in the different character of the variations in the gas parameters. From (4.3.15) and (4.3.16) it follows that as $\mathbf{M}_1\to\infty$ the pressure and temperature rise indefinitely. At the same time equation (4.3.13) shows that under the same condition of $\mathbf{M}_1\to\infty$ the density tends to some finite value which is equal to $(\rho_2/\rho_1)_{\mathbf{M}_1\to\infty}=1/\delta$. At $k=1.4$ this gives the value of $1/\delta=6$. From formula $p=A\rho^k$ or $T=B\rho^{k-1}$ (A and B are constants) it follows that an infinite rise in density and temperature corresponds to an infinite increase in pressure in the case of an isentropic (adiabatic) process. From this it may be concluded that for the same variation in pressure in a flow across a shock and an adiabatic process the first is characterized by more intensive heating of the gas, which leads to some reduction in density.

Formula (4.3.16) determines the ratio of the squares of sound velocities in front of and behind the shock in the following way:

$$a_2^2/a_1^2=T_2/T_1. \tag{4.3.17}$$

Using this relation and an expression (4.2.18′) it is possible to determine Mach number $\mathbf{M}_2$ behind the shock. Substituting the expression (4.2.21) for $\Delta\bar{V}_n$ in (4.2.18′), we get

$$V_2^2/V_1^2=\cos^2\theta_c+(\rho_1/\rho_2)^2\sin^2\theta_c. \tag{4.3.18}$$

Taking (4.3.18) and (4.3.17), the ratio of the left sides and right sides gives the ratios of the squares of the Mach numbers

$$\frac{\mathbf{M}_2^2}{\mathbf{M}_1^2}=\frac{T_1}{T_2}\left[\cos^2\theta_c+\left(\frac{\rho_1}{\rho_2}\right)^2\sin^2\theta_c\right], \tag{4.3.19}$$

where T_1/T_2 and ρ_1/ρ_2 are found from the formulas (4.3.16) and (4.3.13) respectively.

The formula for calculating $\mathbf{M}_2$ could be obtained in somewhat different form, with the help of the equation of momentum (4.2.4″). Let us write this equation in the form:

$$\frac{p_1}{p_2}\left(1+\frac{\rho_1}{p_1}V_1^2\sin^2\theta_c\right)=1+\frac{\rho_2}{p_2}V_2^2\sin^2(\theta_c-\beta_c).$$

Recalling that $kp/\rho=[(1+\delta)/(1-\delta)]\,p/\rho$ and determining p_2/p_1 by the Hugoniot equation (4.3.13′), we get

$$\frac{1-\delta(\rho_2/\rho_1)}{(\rho_2/\rho_1)-\delta}\left(1+\frac{1+\delta}{1-\delta}\mathbf{M}_1^2\sin^2\theta_c\right)=1+\frac{1+\delta}{1-\delta}\mathbf{M}_2^2\sin^2(\theta_c-\beta_c).$$

The quantity $\mathbf{M}_1^2\cdot\sin^2\theta_c$ can be replaced by equation (4.3.13), so that

$$\mathbf{M}_2^2\sin^2(\theta_c-\beta_c)=(1-\delta)\,[(\rho_2/\rho_1)-\delta]^{-1}. \tag{4.3.19′}$$

Let us determine the stagnation pressure for flow conditions behind the shock. Taking the gas flow behind and in front of the shock as isentropic, the thermodynamic relations

$$p_2/\rho_2^k=p_0'/(\rho_0')^k,\quad p_1/\rho_1^k=p_0/\rho_0^k,$$

where p_0 and p_0', ρ_0 and ρ_0' are stagnation pressure and density in the regions of flow in front of and behind the shock respectively. From these relations the coefficient of established pressure in the shock will be

$$\nu_0=p_0'/p_0=(p_2/p_1)\,(\rho_1/\rho_2)^k\,(\rho_0'/\rho_0)^k.$$

Multiplying both sides of this equation by $(p_0/p_0')^k$, we get

$$\nu_0^{1-k}=\left(\frac{p_0'}{p_0}\right)^{1-k}=\frac{p_2}{p_1}\left(\frac{\rho_1}{\rho_2}\right)^k\left(\frac{\rho_0'}{p_0'}\cdot\frac{p_0}{\rho_0}\right).$$

We recall the equation of energy $(V^2/2)+c_p \cdot T=\text{const}$ and write it down for the conditions in front of and behind the shock:

$$(V_1^2/2)+c_pT_1=(V_2^2/2)+c_pT_2.$$

At points of complete stagnation $V_1=V_2=0$. From the equation of energy it follows that the temperatures at the two points are equal, i.e. $T_0=T_0'$, or in other words $p_0/\rho_0=p_0'/\rho_0'$. Hence,

$$\nu_0=p_0'/p_0=(p_1/p_2)^{1/(k-1)}\,(\rho_2/\rho_1)^{k/(k-1)} \tag{4.3.20}$$

or

$$\nu_0=p_0'/p_0=(p_1/p_2)^{(1-\delta)/2\delta}\,(\rho_2/\rho_1)^{(1+\delta)/2\delta}, \tag{4.3.20'}$$

where p_1/p_2 and ρ_2/ρ_1 are obtained from formulas (4.3.15) and (4.3.13) respectively. According to (3.6.28) the stagnation pressure will be

$$p_0=p_1\left(1+\frac{\delta}{1-\delta}\mathbf{M}_1^2\right)^{(1+\delta)/2\delta}; \tag{4.3.21}$$

hence

$$\frac{p_0'}{p_1}=[(1+\delta)\,\mathbf{M}_1^2\sin^2\theta_c-\delta]^{(\delta-1)/2\delta}\,(\mathbf{M}_1\sin\theta_c)^{(1+\delta)/\delta}$$
$$\times(1-\delta)^{-(1+\delta)/2\delta}\,\frac{\left(1+\frac{\delta}{1-\delta}\mathbf{M}_1^2\right)^{(1+\delta)/2\delta}}{\left(1+\frac{\delta}{1-\delta}\mathbf{M}_1^2\sin^2\theta_c\right)^{(1+\delta)/2\delta}}. \tag{4.3.22}$$

Then the coefficient of stagnation pressure behind an oblique shock will be:

$$\bar{p}_0=\frac{p_0'-p_1}{q_1}=\frac{2(1-\delta)}{(1+\delta)\,\mathbf{M}_1^2}\left\{[(1+\delta)\,\mathbf{M}_1^2\sin^2\theta_c-\delta]^{(\delta-1)/2\delta}\right.$$
$$\left.\times(\mathbf{M}_1\sin\theta_c)^{(1+\delta)/\delta}(1-\delta)^{-(1+\delta)/2\delta}\,\frac{\left(1+\frac{\delta}{1-\delta}\mathbf{M}_1^2\right)^{(1+\delta)/2\delta}}{\left(1+\frac{\delta}{1-\delta}\mathbf{M}_1^2\sin^2\theta_c\right)^{(1+\delta)/2\delta}}-1\right\}. \tag{4.3.23}$$

Analysis of relation (4.3.20) shows that the pressure ratio p_0'/p_0 behind a shock of finite strength is always less than unity. A more intensive shock results in higher loss of stagnation pressure and hence the ratio p_0'/p_0 diminishes more sharply.

Let us take a stream line and two points on it such that one is situated before the shock and the other behind it (in the general case at some distance from the wave front). Let the velocities at these points be the same and

equal to V. As can be seen from (3.6.26), the pressure at the points before and after the shock will be

$$p^{(1)}=p_0\left(1-\frac{V^2}{V_{\max}^2}\right)^{k/(k-1)} \quad \text{and} \quad p^{(2)}=p_0'\left(1-\frac{V^2}{V_{\max}^2}\right)^{k/(k-1)}$$

respectively. From expression (3.6.15) it follows that, since $p_0/\rho_0=p_0'/\rho_0'$, the values of maximum velocity are equal, i.e. $V_{\max 1}=V_{\max 2}=V_{\max}$. Thus in the two formulas for $p^{(1)}$ and $p^{(2)}$ the quantities in brackets are equal. Therefore pressure $p^{(1)}$ before the shock will be more than pressure $p^{(2)}$ behind the shock because $p_0'<p_0$. This is how the static pressure loss comes about.

In explaining the physical nature of these losses the shock should not be regarded as a discontinuity surface. It is necessary to assume that the real process of compression takes place in a layer of small thickness of the order of the mean free path length of the gas molecules. Only this kind of flow process through a shock is possible: physically it is incorrect to posit the juxtaposition of two regions exhibiting finite differences in temperature, pressure and density. This is no more than a mathematical abstraction.

The process of flow across a shock of small thickness is characterized by such large gradients of velocity and temperature that there will be considerable friction and heat transfer effects in the compression zone. From this it follows that the irreversible losses of kinetic energy by the gas during flow across the shock are connected with frictional forces and also with heat conduction. The effect of these dissipating forces and the heat flow inside the compression zone is an increase in entropy and consequent decrease in static pressure in the flow behind the shock in comparison with the isentropic process of compression.

3.3 Angle of inclination of oblique shock

Parameters behind an oblique shock are determined not only by Mach number $\mathbf{M}_1$ but also by angle of inclination θ_c of the shock. Its value, which depends on Mach number $\mathbf{M}_1$ and angle of inclination β_c of the flow, can be determined with the help of equation (4.2.19). In this equation the replacement of quantity $\Delta\overline{V}_n$ by its value from (4.2.21) gives relation

$$\tan\theta_c/\tan(\theta_c-\beta_c)=\rho_2/\rho_1. \tag{4.3.24}$$

Determining ρ_1/ρ_2 from (4.3.13), we find

$$\frac{\tan\theta_c}{\tan(\theta_c-\beta_c)}=\frac{\mathbf{M}_1^2\sin^2\theta_c}{1-\delta+\delta\mathbf{M}_1^2\sin^2\theta_c}. \tag{4.3.25}$$

On the other hand this relation helps us to find angle of inclination β_c of the flow behind the shock from the known inclination of shock. The connection between angles θ_c and β_c for various values of Mach number $\mathbf{M}_1$ is shown graphically on Fig. 4.3.1. As can be seen from the graph the value of angle β_c

changes with the decrease in angle θ_c. In the region to the left of the dotted line indicating the maximum value of angle β_c ($\beta_{c\,max}$) the value of angle θ_c diminishes. Conversely, on the right side of this dotted line θ_c increases. This type of relation is based on a different form of shock. In the first case the variation in angle θ_c corresponds to the attached shock of curvilinear form in front of a sharp body. With greater bluntness (angle of leading edge) the angle of flow inclination increases and hence the angle of inclination of the shock increases. The maximum angle of flow inclination $\beta_c = \beta_{c\,max}$ is determined only by the given Mach number M_1. This angle is also known as the critical angle β_{cr} of inclination (or turning) of flow. The points corresponding to the values of this angle are connected by the dotted line in Fig. 4.3.1. Experiments show that the flow behind an attached shock is steady in the sense that its form is maintained as long as the angle of flow inclination in the whole region remains less than critical. Accordingly this kind of flow is called a subcritical flow.

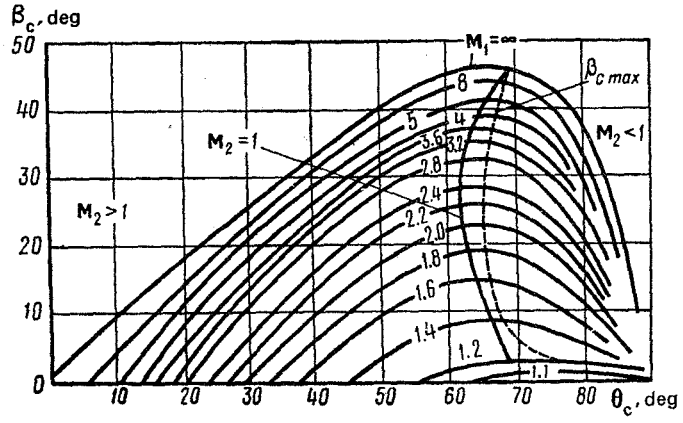

Fig. 4.3.1. Variation of angle of flow inclination β_c with angle of shock θ_c for different Mach numbers M_1.

With any further increase in the angle of the leading edge the angle β_c could be critical. With a still higher angle of leading edge steady flow behind an attached flow cannot be realized. The shock moves ahead from the nose of a body. A steady flow region, characterized by inclination through an angle less than the critical value, comes into being behind this detached shock. However, as distinct from a subcritical flow, this flow is called supercritical. This definition corresponds to the fact that the angle of the nose part of a body in a flow surpasses the value at which an attached flow may still be observed.

A detached shock completely changes form, which is clearly seen in the example of a flow past a sharp cone or wedge (Fig. 4.3.2). As long as the flow is subcritical the shock remains attached to the body and the surface so form-

ed is rectilinear. A flow around thick wedges or cones may be supercritical and then the shock separates from the body and adopts a curvilinear form. At the point of cross section of surface of the shock to the axis of flow the angle of shock inclination is $\theta_c=\pi/2$ and hence the flow parameters change their value by the rule of normal shock. There exists a region near the axis where some part of the shock is practically normal.

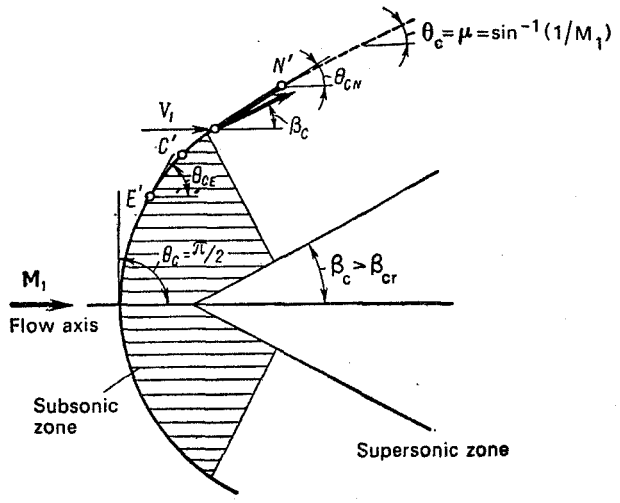

Fig. 4.3.2. Detached shock in front of sharp-edged body.

As we move away from the axis the angle of inclination θ_c decreases, as shown in the graph in Fig. 4.3.2. But it maintains higher values in some places, corresponding to subcritical flow. The variation in the angle of flow inclination has the opposite character. At the peak of the detached wave behind the straight part the value of angle $\beta_c=0$ and then it increases. At some point on the wave surface the angle β_c becomes critical and then it decreases again along with the angle of inclination of the wave. Here, as can be seen from (4.3.25), the angle θ_c tends to a value $\theta_c=\mu=\sin^{-1}(1/M_1)$ with the limit of $\beta_c\to 0$. So the angles of inclination of shock for given values of Mach number M_1 vary in the range of $\mu\leqslant\theta_c\leqslant\pi/2$. The value of $\theta_c=\mu$ corresponds to a weak shock representing a simple disturbance wave.

For a curvilinear shock (see Fig. 4.3.1) it is possible to find two points corresponding to the two values of θ_c which determine the single value of β_c at a given M_1. This angle is calculated by formula (4.2.20) which, after substitution for the value of $\Delta\bar{V}_n$ from (4.3.11), takes the form

$$\tan\beta_c=\cot\theta_c\,(M_1^2\sin^2\theta_c-1)\left[1+\left(\frac{1}{1-\delta}-\sin^2\theta_c\right)M_1^2\right]^{-1}. \quad (4.3.26)$$

Here the strong shock corresponds to the higher value of angle θ_c and the weak shock with supersonic flow behind it (if we exclude the region around the shock with angle β_c near its critical value, where the flow can be subsonic) corresponds to the lower value of angle θ_c.

Calculation of the angle of inclination of an oblique shock can be carried out with the help of formula (4.2.25). Replacing $\Delta\overline{V}_n$ by the density ratio according to (4.2.21), we get

$$\tan\theta_c=\cot\beta_c\left[\frac{1}{2}\left(\frac{\rho_2}{\rho_1}-1\right)\pm\sqrt{\frac{1}{4}\left(\frac{\rho_2}{\rho_1}-1\right)^2-\tan^2\beta_c\frac{\rho_2}{\rho_1}}\right]. \quad (4.3.27)$$

On each of the curves in Fig. 4.3.1 there is a point where the value of Mach number $M_2=1$ behind the curvilinear shock. Joining these points with a continuous curve, we get the boundary of two regimes of flow behind the shock: on the left side of this curve the flow is supersonic ($M_2>1$) and on the right side subsonic ($M_2<1$).

4. Hodograph of Velocity

An analytic solution of the problem of determining flow parameters behind an oblique shock was set forth in the preceding section. There exists a graphic method along with this analysis which is based on the principle of the hodograph of velocity.

A hodograph of velocity is a curve representing the geometrical position of the ends of velocity vectors behind a shock. Let us study the equation of a hodograph of velocity. Let point A (Fig. 4.4.1) be the end of velocity vector $\overline{V}_2$ and be located accordingly on a hodograph velocity that is constructed in the system of coordinates with its horizontal axis coinciding with the direction of velocity $\overline{V}_1$ in front of the shock. Hence an inclination of velocity vector $\overline{V}_2$ is determined by angle β_c. Let the horizontal and vertical components of velocity behind the shock be denoted by u_2 and w_2 respectively. From Fig. 4.4.1 it can be seen that u_2 and w_2 can be expressed by the components V_{n2} and V_τ of velocity V_2 normal and tangential to the plane of shock in the following way:

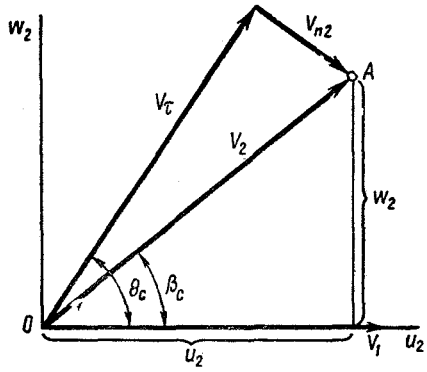

Fig. 4.4.1. Formulation of equation of hodograph of velocity.

$$u_2=V_\tau\cos\theta_c+V_{n2}\sin\theta_c,$$
$$w_2=V_\tau\sin\theta_c-V_{n2}\cos\theta_c. \quad (4.4.1)$$

The component V_{n2} is determined from formula (4.3.10), where $V_{n1}=V_1\sin\theta_c$, $V_\tau=V_1\cos\theta_c$. Accordingly

$$u_2=V_1\cos^2\theta_c+\left(a^{*2}-\frac{k-1}{k+1}V_1^2\cos^2\theta_c\right)\Big/V_1. \tag{4.4.2}$$

To eliminate angle θ_c we use equations (4.4.1). Multiplying the first equation of (4.4.1) by $\cos\theta_c$ and the second by $\sin\theta_c$ and summing them, we have

$$u_2\cos\theta_c+w_2\sin\theta_c=V_\tau.$$

Since $V_\tau=V_1\cos\theta_c$, it leads to

$$\tan\theta_c=(V_1-u_2)/w_2. \tag{4.4.3}$$

Then

$$\cos^2\theta_c=(1+\tan^2\theta_c)^{-1}=[1+(V_1-u_2)^2(1/w_2^2)]^{-1}.$$

Substitution of this in (4.4.2) results in the following equation:

$$u_2=\frac{V_1}{1+\left(\dfrac{V_1-u_2}{w_2}\right)^2}+\frac{a^{*2}-\dfrac{k-1}{k+1}V_1^2\left[1+\left(\dfrac{V_1-u_2}{w_2}\right)^2\right]^{-1}}{V_1}.$$

This equation, connecting the variables w_2 and u_2, represents the equation of a hodograph of velocity. Usually it is written in the form

$$\frac{w_2^2}{(V_1-u_2)^2}=\frac{u_2-\dfrac{a^{*2}}{V_1}}{\dfrac{2}{k+1}V_1+\dfrac{a^{*2}}{V_1}-u_2}. \tag{4.4.4}$$

Let us introduce nondimensional parameters $\lambda_u=u_2/a^*$, $\lambda_w=w_2/a^*$, $\lambda_1=V_1/a^*$ and $\delta=(k-1)/(k+1)$. Then the hodograph equation can be written in the following way:

$$\frac{\lambda_w^2}{(\lambda_1-\lambda_u)^2}=\frac{\lambda_u\lambda_1-1}{(1-\delta)\lambda_1^2+1-\lambda_1\lambda_u}. \tag{4.4.4'}$$

Equation (4.4.4') is reproduced on plane λ_w, λ_u graphically by the curve known as the strofoid (Fig. 4.4.2). Let us determine some characteristic points of the strofoid. Specifically, let us find the coordinates of points of intersection A and D of the strofoid and axis λ_u. From (4.4.4') it can be seen that the condition of $\lambda_w=0$ is fulfilled if $\lambda_u=\lambda_1$ or $\lambda_u=1/\lambda_1$. The value $\lambda_u=\lambda_1$ determines the coordinates of point A and gives the solution for an infinitesimally weak shock across which the velocity does not change. The other value $\lambda_u=1/\lambda_1$ determines the coordinate of point D nearest to the origin and happens to be the solution for normal shock (see Section 5).

From the construction of the strofoid it follows that its two branches on the right side of point A extend to infinity asymptotically to the line passing through point B and parallel to the vertical axis. The coordinate of this point

can be obtained from (4.4.4'), recalling the limit of $\lambda_w \to \infty$. As a result we get the condition $(1-\delta)\lambda_1^2+1-\lambda_1\lambda_u=0$ from which the coordinate of point B can be obtained:

$$\lambda_u=\lambda_1(1-\delta)+(1/\lambda_1).$$

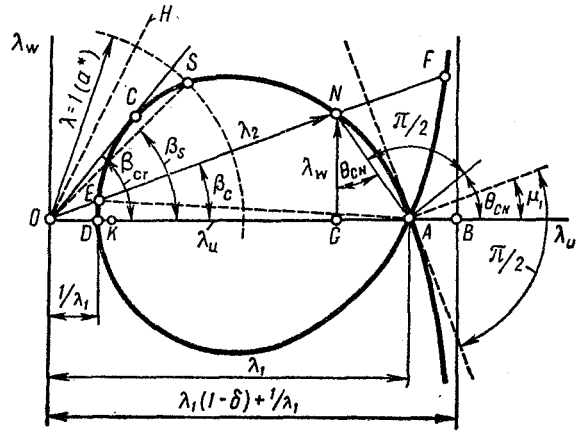

Fig. 4.4.2. Strofoid (shock polar).

Any point on the branch of the strofoid extending to infinity in principle gives the solution for compression shock. For example, let us examine point F in Fig. 4.4.2. It may be assumed that for a shock behind which the velocity direction changes by the given amount of angle β_c the velocity increases due to shock to the value λ_2 determined by the length of line OF. Meantime the density and pressure can be reduced due to shock. In other words, in a given case there can exist expansion shock in place of compression shock. However, formation of such a shock is physically impossible. To prove this we use formula (4.3.6) for variation in entropy. Applying the relations $p_2/\rho_2^k=p_0'/(\rho_0')^k$, $p_1/\rho_1^k=p_0/\rho_0^k$ and recalling that $p_0'/p_0=\rho_0'/\rho_0$, from formula (4.3.6) we get

$$S_2-S_1=R\ln(p_0/p_0')=-R\ln\nu_0. \tag{4.4.5}$$

In the case of a compression shock $p_0>p_0'$ and hence, $S_2-S_1>0$. This conclusion corresponds to the second law of thermodynamics, according to which the entropy of an isolated system of gas having jumps must increase.

Let us now consider a reverse flow where a gas in condition (2), characterized by stagnation pressure p_0', moves to the condition (1) with stagnation pressure p_0 by means of an expansion shock. In this case, by analogy with (4.4.5), the change in entropy

$$S_1-S_2=R\ln(p_0'/p_0)=R\ln\nu_0.$$

So by maintaining the condition $p_0'<p_0$ an enthalpy must be reduced, which

is against the second law of thermodynamics. From this it follows that an expansion shock cannot appear.

From the above discussion it can be seen that the process of motion through a shock, which happens to be adiabatic by nature, as it occurs in a thermally isolated system, will represent by itself an irreversible adiabatic nonisentropic process.

It can easily be checked with the help of (4.3.6) that the real process of rise in entropy ($S_2-S_1>0$) corresponds to the case of a supersonic flow [$\mathbf{M}_1>1$ (normal shock), $\mathbf{M}_1 \sin\theta_c>1$ (oblique shock)] and the physically impossible phenomenon of reduction in entropy ($S_2-S_1<0$) corresponds to the subsonic flow ($\mathbf{M}_1<1$ and $\mathbf{M}_1 \sin\theta_c<1$). Thus compression shocks can take place only in a supersonic flow. It should be emphasized that the relations obtained for variation in entropy $|S_2-S_1|$ are valid for the case of an irreversible process of motion through a shock accompanied by an isentropic gas flow up to the shock and also behind it.

From the above discussion it follows that the branches of the strofoid proceeding to infinity have no physical meaning. The remaining part of the strofoid (left side of point A) has physical significance: it is called the shock polar. This kind of curve is drawn for given λ_1 (or Mach number $\mathbf{M}_1$). Some such curves drawn for different values of λ_1 represent a family of shock polars which help to find the velocity of flow behind a shock and its angle of inclination graphically.

Take an attached shock at a wedge-shaped surface with semi-angle β_c (see Fig. 4.1.1, c). To determine the velocity behind this shock for a given value of λ_1 (or $\mathbf{M}_1$) a shock polar can be constructed and a line can be drawn through point O at an angle β_c (see Fig. 4.4.2). The point of intersection N of this line with the shock polar determines vector $\overline{ON}$, whose modulus gives the value of relative velocity λ_2 behind the shock. According to formula (4.4.3), which can be expressed by

$$\tan\theta_c=(\lambda_1-\lambda_u)/\lambda_w, \tag{4.4.3'}$$

the angle ANG on a shock polar is equal to the angle of inclination θ_c of the shock wave. It is easy to see that this angle can also be determined as an angle between the horizontal axis and the normal to a line joining the ends of the velocity vectors before and after the shock (in Fig. 4.4.2 the corresponding points are A and N).

From the shock polar we arrive at the conclusion that with a reduction in angle β_c (point N moves along the curve toward point A) the angle of inclination θ_c of the shock decreases. In the limit of $\beta_c\to 0$ the point N approaches point A, which physically corresponds to the transformation of a shock wave into a shock of very low strength, i.e. into a line of weak disturbance. The angle of inclination of this shock $\theta_c=\mu$ is determined as an angle between the horizontal axis and the line perpendicular to the tangent of a shock

polar at a point A (see Fig. 4.4.2).

An increase in the angle of inclination of the flow (in Fig. 4.4.2 this corresponds to a shift of point N away from A) leads to an increase in the angle of shock and a rise in its intensity. On the shock polar it can be seen that at some value of angle β_c the line drawn through point O touches the curve at a point C. The angle of inclination of this tangent line determines the maximum angle of flow inclination, which we earlier designated the critical angle ($\beta_c = \beta_{cr}$). Let the angle $\beta_c > \beta_{cr}$. On the curve this angle corresponds to the dotted line drawn from point A and does not intersect the shock polar. Thus at $\beta_c > \beta_{cr}$ it is not possible to find a solution for shock graphically with the help of the shock polar. This is because the condition $\beta_c > \beta_{cr}$ does not correspond to the assumptions of the rectilinear type of shock attached to the nose of a surface, on the basis of which the shock equations were derived. Physically speaking, the case of an angle of wedge β_c producing a more than critical angle of turning β_{cr} results in a detached curvilinear shock.

The determination of the shape of this curvilinear shock in front of a body is material for a special problem of aerodynamics related, in particular, to the conditions of the supersonic flow-interaction of wedge-type bodies. If this problem is not solved it is possible at least to give a qualitative estimation of the variation in parameters in some region ahead of the body with the help of the shock polar from point D to A. When the form of a shock is determined for given conditions of flow-interaction (apart from calculations this can be done with the help of the aerodynamic wind tunnel) it is possible to establish the quantitative relation between the points of the shock polar and the shock surface.

For example, let angle β_c be given and the points E and N lie on the shock polar. The angle of shock $\theta_{CN} = \angle ANG$ corresponds to point N and angle $\theta_{CE} = \angle AEK$ ($EK \perp OB$) corresponds to point E. If the configuration of the wave front is known it is possible to find on it point N' with an angle of inclination of wave θ_{CN} and point E' with angle θ_{CE} (see Fig. 4.3.2) by direct measurement. In the same way point C' corresponding to the critical (maximum) angle of turning β_{cr} can be found.

Point D on the shock polar corresponds to the peak on the given surface of the detached shock (normal shock) and the end point A of the polar corresponds to the farthest part of shock, which transforms into a line of weak disturbance.

For an attached shock ($\beta_c < \beta_{cr}$) two solutions can be obtained, as seen from the shock polar. One of them is point E, which corresponds to a lower velocity behind the shock. The other, point N, refers to a higher velocity behind the shock. It is found experimentally that attached shocks with higher speeds behind them are realized physically, i.e. shocks of low intensity occur.

If the arc of a circle of radius equal to unity (in dimensional axes w_2, u_2 this refers to a radius equal to the critical speed of sound a^*) is drawn on the

graph regions of flow can be determined—subsonic and supersonic—that are related to the points lying on the shock polar to the left and right of the arc. The part of the flow representing subsonic speed is shown shaded in Fig. 4.3.2. From the shock polar it can be seen that the flow velocity behind a normal shock is always subsonic. At the same time the flow velocity behind an oblique (curvilinear) shock can be supersonic (corresponding points on the shock polar lie on the right side of point S) as well as subsonic (the points on the shock polar lie on the left side of point S). Further, the points lying between S and C correspond to an attached shock behind which the velocities are subsonic. Experimental research shows that the shock remains attached for wedge angles β_c less than the critical angle β_{cr} or more than $\angle SOB$. However, in the latter case it becomes curved. Here the theoretical values for angle θ_c and gas velocity λ_2 in the whole region behind this curvilinear shock, obtained from the shock polar on the basis of angle β_c do not correspond to the real values.

5. Normal Shock in Gas Flow with Constant Specific Heats

The appropriate relations for a normal shock are obtained from the condition that $\theta_c=\pi/2$ and hence $V_{n1}=V_1$ and $V_{n2}=V_2$. The basic equation (4.3.10) takes the form

$$V_1V_2=a^{*2} \tag{4.5.1}$$

or

$$\lambda_1\lambda_2=1, \tag{4.5.1'}$$

where $\lambda_1=V_1/a^*$, $\lambda_2=V_2/a^*$.

The relative change in velocity is found from (4.3.11'):

$$\overline{\Delta V}=\frac{V_1-V_2}{V_1}=(1-\delta)\left(1-\frac{1}{\mathbf{M}_1^2}\right). \tag{4.5.2}$$

For the ratios of densities, pressures and temperatures, the corresponding relations can be found from (4.3.13), (4.3.15), (4.3.16):

$$\rho_2/\rho_1=\mathbf{M}_1^2/(1-\delta+\delta\,\mathbf{M}_1^2); \tag{4.5.3}$$

$$p_2/p_1=(1+\delta)\,\mathbf{M}_1^2-\delta; \tag{4.5.4}$$

$$\frac{T_2}{T_1}=\frac{[(1+\delta)\,\mathbf{M}_1^2-\delta]\,(1-\delta+\delta\,\mathbf{M}_1^2)}{\mathbf{M}^2}. \tag{4.5.5}$$

Eliminating $\mathbf{M}_1^2$ from (4.5.3) and (4.5.4), we get an equation of adiabatic flow for normal shock which does not differ in external form the equation for oblique shock [see (4.3.13')].

Taking $\theta_c=\pi/2$ in (4.3.19), the relation for the Mach number behind a normal shock can be obtained:

$$\mathbf{M}_2^2/\mathbf{M}_1^2=(T_1/T_2)\,(\rho_1/\rho_2)^2. \tag{4.5.6}$$

Let us examine the gas parameters at a stagnation point (at a critical point) of a blunt surface situated behind a normal shock (Fig. 4.5.1). Pressure p_0' at this point is determined by the formula (4.3.20′) in which the ratios ρ_2/ρ_1 and p_2/p_1 are found from (4.5.3) and (4.5.4) respectively. Incorporating this, we have

$$\frac{p_0'}{p_0}=[(1+\delta)\mathbf{M}_1^2-\delta]^{(\delta-1)/2\delta}\left(\frac{\mathbf{M}_1^2}{1-\delta+\delta\mathbf{M}_1^2}\right)^{(1+\delta)/2\delta} \tag{4.5.7}$$

Determining p_0 from (4.3.21), we get

$$p_0'/p_1=[(1+\delta)\mathbf{M}_1^2-\delta]^{(\delta-1)/2\delta}\ \mathbf{M}_1^{(1+\delta)/\delta}\,(1-\delta)^{-(1+\delta)/2\delta}. \tag{4.5.8}$$

Knowing absolute pressure p_0' the nondimensional quantity $\bar{p}_0=(p_0'-p_1)/q_1$, i.e. the coefficient of pressure at the point of complete stagnation, can be determined.

Recalling that the velocity head

$$q_1=\frac{kp_1\mathbf{M}_1^2}{2}=\frac{1+\delta}{2(1-\delta)}p_1\mathbf{M}_1^2,$$

we have

$$\bar{p}_0=\frac{2(1-\delta)}{(1+\delta)\mathbf{M}_1^2}\{[(1+\delta)\,\mathbf{M}_1^2-\delta]^{(\delta-1)/2\delta}\,\mathbf{M}_1^{(1+\delta)/\delta}\,(1-\delta)^{-(1+\delta)/2\delta}-1\}. \tag{4.5.9}$$

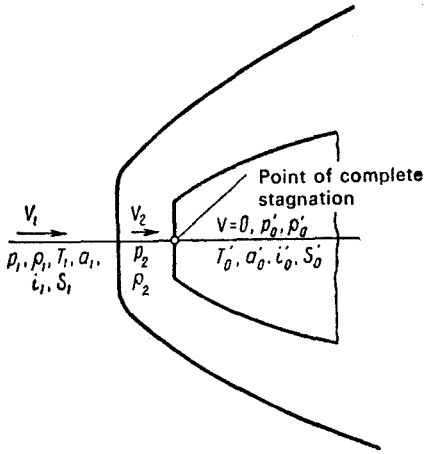

Fig. 4.5.1. Gas parameters at point of complete stagnation behind normal shock.

In Section 3 it was proved that the stagnation temperature behind the shock does not change, i.e. $T_0'=T_0$. Consequently at a point of complete stagnation

$$T_0'=T_1\left(1+\frac{\delta}{1-\delta}\mathbf{M}_1^2\right). \tag{4.5.10}$$

The expression $i_0'=c_pT_0'$ and $i_1=c_pT_1$ can be used to determine enthalpy. Accordingly, at the point of complete stagnation

$$i_0'=i_1\left(1+\frac{\delta}{1-\delta}\mathbf{M}_1^2\right). \tag{4.5.11}$$

6. Shock at Very High Supersonic Speeds and Constant Specific Heats of Gas

At very high (supersonic) speeds with values of $\mathbf{M}_1 \sin\theta_c \gg 1$ the nondimensional gas parameters behind the shock are close to their limiting values

obtained at $\mathbf{M}_1 \sin\theta_c \to \infty$. From (4.3.11') it follows that under this condition

$$\Delta\overline{V}_n = 1-\delta. \tag{4.6.1}$$

Consequently the limiting density ratio, according to (4.2.13), will be

$$\rho_1/\rho_2 = 1-\Delta\overline{V}_n = \delta. \tag{4.6.2}$$

Inserting this value in (4.3.27) in the limit of $\mathbf{M}_1 \sin\theta_c \to \infty$, we get

$$\tan\theta_c = (\cot\beta_c/2\delta)\ [1-\delta \pm \sqrt{(1-\delta)^2 - 4\delta\tan^2\beta_c}]. \tag{4.6.3}$$

Let us find the limiting value of the coefficient of pressure. For the conditions immediately behind the shock it follows from (4.3.15'') that at $\mathbf{M}_1 \sin\theta_c \to \infty$ and $\mathbf{M}_1 \to \infty$

$$\bar{p}_2 = 2(1-\delta)\sin^2\theta_c\,. \tag{4.6.4}$$

For the stagnation point the corresponding value is obtained from (4.3.23):

$$\bar{p}_0 = 2(1-\delta)^{(\delta-1)/2\delta}(1+\delta)^{-(1+\delta)/2\delta}\sin^2\theta_c. \tag{4.6.5}$$

The ratio of coefficients of pressure will be

$$\bar{p}_0/\bar{p}_2 = (1-\delta^2)^{-(1+\delta)/2\delta}. \tag{4.6.6}$$

In a particular case when $\delta = 1/6$ ($k = 1.4$) the ratio $\bar{p}_0/\bar{p}_2 = 1.09$. The limiting value of Mach number $\mathbf{M}_2$ may be found from (4.3.19), taking into account the relation (4.3.16) for T_2/T_1. Going back to the limit, at $\mathbf{M}_1 \sin\theta_c \to \infty$ and $\mathbf{M}_1 \to \infty$ we get

$$\mathbf{M}_2^2 = [1/\delta(1+\delta)](\cot^2\theta_c + \delta^2). \tag{4.6.7}$$

To find the limiting parameters behind a normal shock by the above relations it is necessary to take $\theta_c = \pi/2$. Then from (4.6.4) and (4.6.5) we get

$$\bar{p}_2 = 2(1-\delta); \tag{4.6.4'}$$

$$\bar{p}_0 = 2(1-\delta)^{(\delta-1)/2\delta}(1+\delta)^{-(1+\delta)/2\delta}. \tag{4.6.5'}$$

It is clear that the ratio $\bar{p}_0/\bar{p}_2$ will be the same as for an oblique shock. The limiting Mach number behind a normal shock

$$\mathbf{M}_2 = \sqrt{\delta/(1+\delta)}. \tag{4.6.7'}$$

For $\delta = 1/6$ ($k = 1.4$) the Mach number $\mathbf{M}_2 = \sqrt{1/7} \approx 0.38$. The actual values of nondimensional parameters behind a shock with finite but very high Mach numbers will depend on $\mathbf{M}_1$.

Let us study the relations for the case where attached shocks appear before thin wedges and are therefore inclined at low angles. Assuming that $\tan\theta_c \approx \theta_c$ and $\tan(\theta_c - \beta_c) \approx \theta_c - \beta_c$ in (4.3.25), we get

$$\frac{\theta_c-\beta_c}{\theta_c}=\frac{1-\delta+\delta M_1^2\theta_c^2}{M_1^2\theta_c^2}.$$

Introducing the notation $K=M_1\beta_c$, after simplification we get

$$\frac{\theta_c^2}{\beta_c^2}-\frac{1}{1-\delta}\cdot\frac{\theta_c}{\beta_c}-\frac{1}{K^2}=0. \tag{4.6.8}$$

Solving this equation for θ_c/β_c and assuming that the physically possible condition will be $\theta_c/\beta_c>1$, we find

$$\frac{\theta_c}{\beta_c}=\frac{1}{2(1-\delta)}+\sqrt{\frac{1}{4(1-\delta)^2}+\frac{1}{K^2}}. \tag{4.6.9}$$

Examining equation (4.6.9), it can be seen that the parameters determining flow for a shock at very high speeds are combined in functional groups that describe the solution of the problem of shock in a wide range of Mach numbers M_∞ and of values of β_c. Equation (4.6.9) is an example of a similarity relation. From this equation for the ratio θ_c/β_c it is found that the quantity $K=M_1\beta_c$ happens to be the similarity parameter. This similarity is to be understood in the sense that the ratios of angles θ_c/β_c will be the same for flows with identical parameters K independent of the absolute value of the quantities that characterize hypersonic flows. As $K\to\infty$ the ratio θ_c/β_c tends to the limit equal to

$$\theta_c/\beta_c=1/(1-\delta). \tag{4.6.10}$$

Let us now take the relation for the coefficient of pressure. At small values of θ_c the formula (4.3.15″) takes the form

$$\bar{p}_2=2(1-\delta)\left(\theta_c^2-\frac{1}{M_1^2}\right)$$

or

$$\bar{p}_2=2(1-\delta)\,\beta_c^2\left(\frac{\theta_c^2}{\beta_c^2}-\frac{1}{K^2}\right). \tag{4.6.11}$$

Substituting the value of $1/K^2$ from (4.6.8), we get

$$\bar{p}_2=2\beta_c\theta_c. \tag{4.6.11′}$$

Substituting the value of θ_c from (4.6.9) here, we get

$$\frac{\bar{p}_2}{\beta_c^2}=\frac{1}{1-\delta}\left[1+\sqrt{1+\frac{4(1-\delta)^2}{K^2}}\right]. \tag{4.6.12}$$

This formula shows that K also happens to be the similarity parameter for the ratio $\bar{p}_2/\beta_c^2$. As $K\to\infty$ the value of this ratio will be

$$\bar{p}_2/\beta_c^2=2(1-\delta). \tag{4.6.13}$$

According to (4.3.13) the density ratio at small values of θ_c could be expressed by

$$\rho_2/\rho_1=\mathbf{K}_c^2/(1-\delta+\delta\,\mathbf{K}_c^2), \tag{4.6.14}$$

where the parameter $\mathbf{K}_c=\mathbf{M}_1\theta_c$ is determined by (4.6.9) in the following form:

$$\mathbf{K}_c=\frac{\mathbf{K}}{2(1-\delta)}\left[1+\sqrt{1+\frac{4(1-\delta)^2}{\mathbf{K}^2}}\right]. \tag{4.6.15}$$

From (4.3.18) it follows that the second term on the right side can be neglected at small θ_c ($\sin\theta_c\approx\theta_c$); hence $V_2\approx V_1$. Bearing this in mind, the ratio of the squares of Mach numbers using (4.3.19) will be

$$\mathbf{M}_2^2/\mathbf{M}_1^2=T_1/T_2.$$

Substituting the ratio T_1/T_2 here by formula (4.3.16) and taking $\sin\theta_c\approx\theta_c$, we get

$$\theta_c^2\mathbf{M}_2^2=\frac{\mathbf{K}_c^4}{[(1-\delta)\,\mathbf{K}_c^2-\delta](1-\delta+\delta\,\mathbf{K}_c^2)}. \tag{4.6.16}$$

As $\mathbf{K}_c\to\infty$

$$\theta_c^2\mathbf{M}_2^2\to 1/\delta\ (1+\delta). \tag{4.6.16'}$$

7. Solution of Problem of Shock in a Gas Flow with Variable Specific Heats Taking into Account Dissociation and Ionization

The parameters of air at some altitude H (pressure p_1, temperature T_1, density ρ_1, etc.) and the value of normal velocity component V_{n1} are selected as the initial data in solving the problem of a shock wave in dissociated and ionized gas. In this instance an oblique shock, in a given case, is regarded as

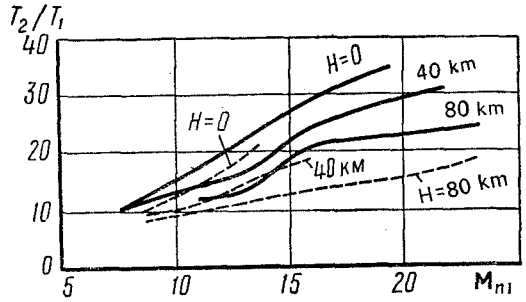

Fig. 4.7.1. Ratio of air temperatures behind and ahead of shock taking into account dissociation and ionization:

thick line—$T_1=220°K$; *dotted line*—$T_1=350°K$.

a normal shock. Assuming the value of $\Delta\overline{V}_n \approx 0.9$ to 0.95 as a first approximation, which refers to the density ratio across the shock

$$\rho_2/\rho_1 = (1-\Delta\overline{V}_n)^{-1} \approx 10 \text{ to } 20,$$

we find pressure p_2 from formula (4.2.15) and enthalpy i_2 from expression (4.2.16) which is, obviously, near the stagnation enthalpy i_0'. Then, from the i–S diagram [7, 17] temperature T_2 and from Fig. 1.4.7 average molecular weight μ_{av2} can be determined. In place of these diagrams appropriate tables of thermodynamic functions of air [18] can be used. This increases the accuracy of calculations.

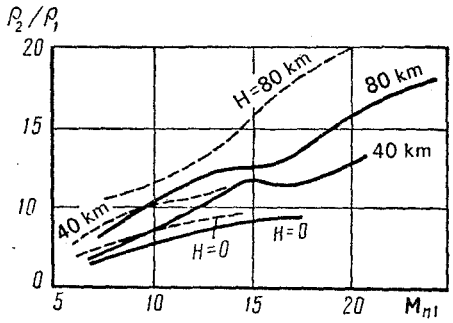

Fig. 4.7.2. Ratio of air densities behind and ahead of shock taking into account dissociation and ionization:

thick line $-T_1 = 220°K$; *dotted line*— $T_1 = 350°K$.

The density ρ_2 can be found from the values of p_2, T_2, μ_{av2} obtained and the equation of state (1.4.8). The value of $\Delta\overline{V}_n$ can be improved by formula (4.2.21). Then with this value the pressure and enthalpy can be obtained by formulas (4.2.15) and (4.2.16) respectively as a second approximation. With the help of these more accurate values of temperature and average molecular weight can be obtained from tables and graphs. Knowing the more accurate values of p_2, T_2 and μ_{av2}, the density in the second approximation can be found by the equation of state. This iteration process is continued until the required accuracy is achieved.

An oblique shock can also be studied on the basis of known parameters of undisturbed flow (including Mach number M_1) and the angle β_c. As a first approximation the angle of shock θ_c for an undissociated gas is obtained [(see (4.3.25)] and then the necessary corresponding quantities $\Delta\overline{V}_n$, p_2 and i_2 can be calculated by formulas (4.2.19), (4.2.15) and (4.2.16). Using these values the temperature T_2 and average molecular weight μ_{av2} are calculated from tables [18] and graphs [7, 17]. Further, with the help of formulas (4.2.23) and (4.2.24) the value of $\Delta\overline{V}_n$ can be improved and from the expression (4.2.19) $\tan\theta_c$ and angle θ_c are rendered more

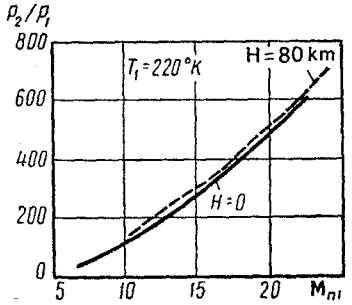

Fig. 4.7.3. Ratio of air pressures behind and ahead of shock taking into account dissociation and ionization.

accurate. The remaining parameters are corrected by the respective formulas.

The calculations of gas parameters behind normal shock are similarly performed with the use of tables and graphs of thermodynamic functions at high temperatures. For this we must consider $\theta_c=\pi/2$ and $\beta_c=0$ and then relations (4.2.27) through (4.2.35) should be applied.

In the presence of dissociation and ionization the relative values of gas parameters behind a shock wave depend not only on temperature, which is the characteristic of variable heat coefficients, but also on pressure. These relations are graphically shown in Figs. 4.7.1 through 4.7.3.

The calculations of temperature ratio and pressure ratio were carried out for the average values of temperature $T_1=220$ and 350°K, which are the probable minimum and maximum values chosen according to the change in temperature with altitude in the case of low and high yearly mean values.

The data obtained show that dissociation and ionization indicate significant variations in equilibrium temperature and density in comparison with the case of constant specific heats ($k=1.4=$const). So far as pressure is concerned it depends very slightly on physico-chemical changes in the air. The ratio p_2/p_1 differs negligibly from its maximum value $p_2/p_1=1+k_1\,\mathbf{M}_{n1}^2$ which is determined only by the conditions of undisturbed flow and not by the change in the structure and physico-chemical properties of air behind a shock wave.

The calculations also show that at one and the same angle in a real heated gas medium the inclination of flow (angle β_c) is more than in a perfect gas ($k=$const). This leads up to the fact that in a heated gas a detached shock appears later than in a cold gas. Specifically the wedge angle at which detachment of shock begins is greater in a heated gas than in a cold gas.

Calculations of parameters at the point of complete stagnation: The theory of normal shock has important practical applications in the determination of gas parameters at the point of complete stagnation. This is realized in the following way. Entropy S_2 is found from the values of i_2, p_2 obtained with allowance for dissociation and ionization from the i–S diagram or tables of the thermodynamic functions of air. Assum-

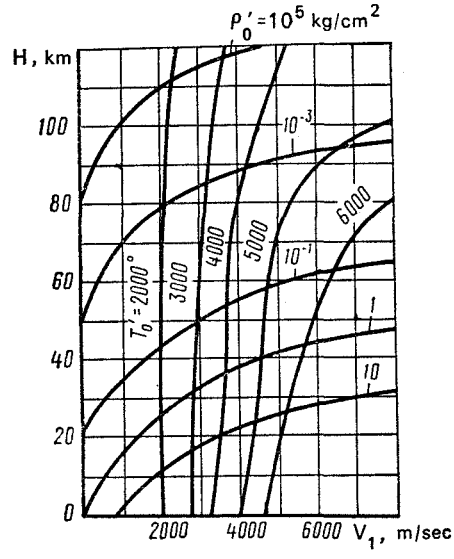

Fig. 4.7.4. Stagnation pressure and temperature at point of complete stagnation.

ing that the flow behind the shock is isentropic entropy S_0' at the stagnation point can be taken as equal to the value S_2 behind the shock wave. Also at this point the enthalpy $i_0'=i_1+0.5V_1^2$ can be found. Now, knowing S_0' and i_0', the remaining parameters, namely: p_0', T_0', ρ_0', etc. can be obtained from the same i–S diagram or thermodynamic tables.

The results of calculations will correspond to the given flight altitude. With a change in altitude the conditions of flow-interaction and hence the parameters at the stagnation point will also change. This relation is graphically reproduced in Fig. 4.7.4. The curves allow us to determine temperature T_0' and pressure p_0' as a function of velocity V_1 and flight altitude H.

The results of calculations of density with allowance for dissociation and ionization at the stagnation point for air as well as pure oxygen and nitrogen are set out in Fig. 4.7.5 [52]. The following conclusions can be derived from the analysis of these results: At $M_\infty=18$, when oxygen is already considerably dissociated, the value of ρ_0'/ρ_∞ reaches its maximum value. With an increase in M_∞ the gas becomes completely dissociated and the density decreases. Then, with further rise in M_∞, ionization of oxygen sets in, leading to a rise in specific heats and hence to some increase in density.

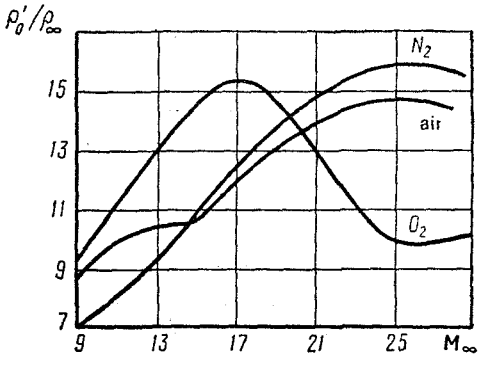

Fig. 4.7.5. Density at point of complete stagnation for nitrogen, oxygen and air ($p_\infty=0.01$ atm, $T_\infty=290°K$).

The effect of variation of specific heats on the change in density of nitrogen is observed only at very high Mach numbers M_∞ when dissociation and ionization take place. These processes occur not one after the other as in the case of oxygen but practically simultaneously. This is confirmed by the small difference of energies for the dissociation and ionization of nitrogen. Due to this the curve of ρ_0'/ρ_∞ for nitrogen is more monotonous than for oxygen.

At Mach numbers $M_\infty<13$ basic dissociation of oxygen takes place and the curve of density of air is close to the corresponding curve for O_2. At $M_\infty>13$, when dissociation of nitrogen begins to play a part, the ratio of ρ_0'/ρ_∞ for air will be similar to that for nitrogen because it then becomes the active component in air.

Calculations of gas parameters behind a shock with allowance for variations in specific heats are discussed in more detail in book [10].

8. Shock Wave in Pure Dissociating Diatomic Gas

The parameters behind a shock can be calculated in a comparatively simple way using the general system of equations of an oblique shock, relations for determining the thermodynamic functions and the degree of dissociation of a heated diatomic pure gas.

For this an equation of energy (4.2.6) can be used. Together with relation (1.5.13′) for enthalpy it can be written in the following form:

$$a_1+\frac{4+a_1}{1+a_1}\cdot\frac{\bar{p}_1}{\bar{\rho}_1}+\frac{\bar{V}_{n1}^2}{2}=a_2+\frac{4+a_2}{1+a_2}\cdot\frac{\bar{p}_2}{\bar{\rho}_2}+\frac{\bar{V}_{n2}^2}{2}. \tag{4.8.1}$$

Here the pressure and density are related to the characteristic parameters p_d and ρ_d respectively and the velocity is related to the characteristic quantity V_d. Assume that the degree of dissociation up to the shock is low and that the shock is very strong (pressure, density and temperature behind the shock considerably exceed their values before the shock). In this case, neglecting the first two terms on the left side of the equation (4.8.1), we get

$$\frac{\bar{V}_{n1}^2}{2}=a_2+\frac{4+a_2}{1+a_2}\cdot\frac{\bar{p}_2}{\bar{\rho}_2}+\frac{\bar{V}_{n2}^2}{2} \tag{4.8.2}$$

or

$$\frac{\bar{V}_{n1}^2}{2}\Delta\bar{V}_n(2-\Delta\bar{V}_n)=a_2+\frac{4+a_2}{1+a_2}\cdot\frac{\bar{p}_2}{\bar{\rho}_2}. \tag{4.8.2′}$$

Now we use the equation of momentum (4.2.4″). For very high velocities at which $p_1 \ll p_2$ it is written as

$$\rho_1 V_{n1}^2 \approx p_2+\rho_2 V_{n2}^2. \tag{4.8.3}$$

Dividing this equation by $\rho_1 V_{n1}=\rho_2 V_{n2}$, we get

$$V_{n1}=(p_2/\rho_2 V_{n2})+V_{n2},$$

from which we obtain

$$p_2/\rho_2=V_{n1}^2\,\Delta\bar{V}_n(1-\Delta\bar{V}_n). \tag{4.8.4}$$

Introduction of the characteristic parameters p_d, ρ_d and V_d in this equation results in

$$\bar{p}_2/\bar{\rho}_2=\bar{V}_{n1}^2\,\Delta\bar{V}_n\,(1-\Delta\bar{V}_n). \tag{4.8.4′}$$

Substituting the given value in (4.8.2′), we write the following quadratic equation of the unknown variable $\Delta\bar{V}_n$:

$$\Delta\bar{V}_n^2-\Delta\bar{V}_n\frac{6}{7+a_2}-\frac{2\,(1+a_2)\,a_2}{(7+a_2)\,\bar{V}_{n1}^2}=0.$$

Solution of this equation gives

$$\Delta\bar{V}_n=\frac{3}{7+\alpha_2}\left(1+\sqrt{1+\frac{D}{\bar{V}_{n1}^2}}\right), \tag{4.8.5}$$

where

$$D=\frac{2}{9}(7+\alpha_2)\,(1+\alpha_2)\,\alpha_2. \tag{4.8.6}$$

Equation (4.8.5) is solved simultaneously with equation (1.5.14), which can be rewritten in the form

$$\bar{T}_2=(\bar{i}_2-\alpha_2)/(4+\alpha_2). \tag{4.8.7}$$

Further, (4.8.5) can be solved simultaneously with the equation of enthalpy (4.2.16), which under the condition of $i_1 \ll i_2$ takes the form

$$\bar{i}_2=(\bar{V}_{n1}^2/2)\,\Delta\bar{V}_n(2-\Delta\bar{V}_n). \tag{4.8.8}$$

Here $\bar{i}_2$ represents an enthalpy with respect to the characteristic energy of dissociation u_d and $\bar{V}_{n1}$ is the velocity in terms of characteristic speed V_d. The calculations are carried out by successive iterations. Strictly speaking this method of calculation for shock in relation to a dissociating diatomic gas can be applied to the calculation of the parameters of air behind the shock within a given approximation. For this the characteristic parameters of dissociation must be found for air as a model gas consisting of a mixture of nitrogen and oxygen in proportion to their mass content. As shown by the calculations, the parameters of air for real air differ from those obtained by the method devised for the diatomic model. Thus, for speed $V_{n1}=1.5V_d=$ 8.1 km/sec the density of real air behind the shock is $\rho_2=14.7\rho_1$, which is higher by about 5% than the diatomic model.

9. Relaxation Phenomena

In the previous section we examined the methods of calculating gas parameters behind a shock with allowance for physico-chemical changes and the condition of equilibrium of thermodynamic processes taking place in a gas. However, in the most general case these processes are characterized by their unbalanced nature, which seems to have some effect on the gas flow behind the shock.

9.1 Concept of nonequilibrium flows

As is known from any course in thermodynamics, the assumption of thermodynamic equilibrium is related to the parameters characterizing the state of a gas in accordance with the mode of internal degrees of freedom. For example, at not very high temperatures comparatively (not at high velocities) an equilibrium between temperature and vibrational degree of

freedom is established which corresponds to the equilibrium between temperature and specific heat. At high temperatures (at high speeds), i.e. when gas dissociates, the equilibrium state is reached in the following way: With the development of dissociation the probability of triple collisions rises because the number of gas particles increases. This leads to recombination and a low rate of dissociation. There exists a moment of time at some temperature when the rates of direct and reverse reactions are equal and the gas enters a state of equilibrium which is characterized by a constant composition relation between the degree of dissociation from one side and temperature and pressure from the other. Finally, at still higher temperatures (at very high speeds) one can talk about the equilibrium processes of existing electronic states and ionization.

In an equilibrium flow the internal degrees of freedom are abruptly established with an instantaneous variation of temperature, whereby the dissociation and ionization can be considered as the appearance of new degrees of freedom. In these cases there is no delay in establishing degrees of freedom, i.e. the time to achieve equilibrium is equal to zero.

In practice the equilibrium flow is observed at supersonic speeds of flow over a body at Mach number $M_\infty = 4$ to 5 in conditions corresponding to altitudes of 10 to 15 km and less. This is explained by the fact that at maximum temperatures of the order of 1,000–1,500°K arising under these conditions the main part of the internal energy comes from the translational and rotational degrees of freedom which, during sudden changes in temperature, are established almost instantaneously. This is because it is enough to have only a few molecular collisions to achieve equilibrium. For this reason the translational and rotational modes of freedom are usually known as "active" modes. With a rise in speed and hence in temperature the significant part of the internal energy goes to vibrations and then to dissociation, excitation of electronic levels of energy and ionization.

Practically speaking these processes are such that the energy modes are set more slowly than the translational and rotational modes because they need a fairly high number of collisions. Therefore the vibrational and dissociating modes are sometimes called the "inert" modes. Thus, inert modes are characterized by a delay in achieving equilibrium, known as relaxation. The time when equilibrium is reached in the flow, i.e. when the correlation is established between temperature and energy level, represents in itself the relaxation time.

According to this discussion, the relaxation time serves as a criterion of the rate of diminution of the deviation of a gas from its equilibrium position, which is represented in a general case in the form of variation of energy distribution by different modes of freedom.

The following example is an intuitive representation of the relaxation process and relaxation time: Let us assume that two thermodynamically

closed, balanced gas systems are brought into contact with heat. As a result their equilibrium is disturbed. However, after heat exchange over a period of time both systems reach another thermodynamic equilibrium state. The process of transfer to the equilibrium state is known as the relaxation and the time required to establish equilibrium is called the relaxation time.

The relaxation processes are determined according to which mode of freedom comes to excitation. If a sudden change in temperature results in vibrations the corresponding disequilibrium process is called the vibrational relaxation. It is characterized by sluggishness in the variation of specific heats with change in temperature. If the temperature rises the specific heat increases as a result of vibrations of atoms in molecules. The time during which the vibrational motion returns to equilibrium is known as the vibrational time of relaxation.

In an unbalanced dissociating gas, for any instantaneous variation in temperature there results a sluggishness in the change of degree of dissociation. This phenomenon is known as dissociational relaxation. In connection with the difference in rates of formation of atoms and loss of atoms (rate of dissociation higher than recombination) a gradual rise in degrees of dissociation occurs. A balanced state of degree of dissociation is reached when the rates of direct and reverse reactions are the same. The time required to achieve a balanced degree of dissociation is called the dissociational time of relaxation.

At temperatures up to roughly 10,000°K the vibrational and dissociational relaxation processes happen to be the basic processes. The relaxation phenomena connected with the excitation of electronic levels of molecules and atoms and also ionization can be neglected because only a small part of the internal energy goes to these modes at these temperatures.

An unbalanced state seems to have a considerable effect on different processes associated with gas flows at high speeds. In particular, the vibrational and dissociational relaxations change the gas parameters during transition through shock waves and during the flow-interaction of bodies. In its turn this affects the process of friction, heat transfer and redistribution of pressure.

9.2 Equation of rate of chemical reactions

Study of an unbalanced flow must include investigation of the motion of the medium and chemical processes which occur at finite rates. Formally speaking, this is characterized by addition of the equation for rates of chemical reactions to the usual system of gas dynamic equations.

To simplify the investigation we use the equation describing a simple binary reaction of dissociation and recombination of pure dissociating diatomic gas which is represented by the general relation (1.5.1). In this relation the rates of dissociation and recombination are not equal and hence the chemical reaction is characterized by some difference in these reaction rates.

Equilibrium is reached when the rate of formation of new molecules as a result of recombination of atoms is equal to the rate of loss of molecules dissociating into atoms. Thus the real rate of reaction of dissociation will be

$$da/dt = r_D - r_R, \tag{4.9.1}$$

where a is the instantaneous value of degree of dissociation.

To find the general expressions for rates of dissociation and recombination it is necessary to use the relations of chemical kinetics. The recombination of two atoms A in molecule A_2 during collision with a third particle B is expressed by the formula $A + A + B \underset{k_R}{\rightarrow} A_2 + B$, where B is a particle carrying away the energy of recombination; k_R is the constant of rate of recombination. According to this formula the rate of change of concentration of atoms during recombination is

$$\left\{\frac{d[A]}{dt}\right\}_R = 2k_R [A]^2 [B]. \tag{4.9.2}$$

The square brackets indicate concentration in units of mol/cm^3; k_R has the dimension of cm^6/mol^2 · sec.

For a binary mixture of molecules and atoms the sum of concentrations $c_M + c_A = 1$; consequently

$$\left.\begin{aligned} [A] = \frac{\rho c_A}{m_A}, \quad [A_2] = \frac{\rho c_M}{m_M} = \frac{\rho(1-c_A)}{2m_A}; \\ [B] = [A] + [A_2] = \frac{\rho(1+c_A)}{2m_A}, \end{aligned}\right\} \tag{4.9.3}$$

where m_M, m_A are the molecular weight of diatomic molecules and atomic gas ($m_M = 2m_A$); concentrations c_A and c_M are related to the degree of dissociation by formulas $c_A = a$, $c_M = 1 - a$. For concentration and density we also have the relations

$$c_A = a = \frac{[A]}{[A] + 2[A_2]};$$

$$\rho = m_M\left([A_2] + \frac{[A]}{2}\right) = \frac{m_M [A]}{2a} = \frac{m_A [A]}{a}.$$

Introducing relations (4.9.3) in (4.9.2), we get the relation for rate of recombination:

$$r_R = (da/dt)_R = k_R (\rho/m_A)^2 a^2 (1+a). \tag{4.9.4}$$

Let us examine the simple scheme of reaction of dissociation $A_2 + B \underset{k_D}{\rightarrow} A + A + B$, which represents the process of disintegration of molecules as a result

of mutual collisions. According to this scheme of reactions, the rate of dissociation will be

$$\left\{\frac{d[A]}{dt}\right\}_D = 2k_D [A_2] [B]. \tag{4.9.2'}$$

Here k_D is the constant for rate of dissociation, B is the second particle participating in a collision with the molecules and providing it with the energy of dissociation.

Introducing values of $[A_2]$ and [B] from (4.9.3) in (4.9.2'), we get

$$r_D = (da/dt)_D = \frac{1}{2} k_D (\rho/m_A) (1-a^2). \tag{4.9.5}$$

Substitution of relations (4.9.4) and (4.9.5) in equation (4.9.1) gives

$$\frac{da}{dt} = 0.5\, k_R (\rho/m_A) (1+a) [K_p (1-a) - 2 (\rho/m_A) a^2], \tag{4.9.6}$$

where $K_p = k_D/k_R$; for balanced processes this quantity is defined as a constant of thermodynamic equilibrium. Under certain conditions this constant is valid even for unbalanced reactions. Keeping this in view and assuming $da/dt = 0$ in equation (4.9.6), we get the value of $K_p = 2\frac{\rho}{m_A} a_e^2/(1-a_e)$ in a balanced condition, where a_e is the degree of dissociation in equilibrium condition. Recalling equation (1.5.2), we will get

$$K_p = \frac{2\rho a_e^2}{(1-a_e)\, m_A} = \frac{2\rho_d \rho}{\rho\, m_A} e^{-D/kT} = \frac{2\rho}{\bar{\rho}\, m_A} e^{-1/\bar{T}}.$$

Substituting this expression in (4.9.6), we have

$$da/dt = C\bar{\rho}\rho_d [(1-a)\, e^{-1/\bar{T}} - \bar{\rho} a^2], \tag{4.9.7}$$

where

$$C = (k_R/m_A^2) (1+a)\, \rho_d. \tag{4.9.8}$$

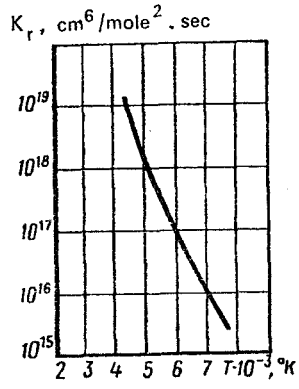

Fig. 4.9.1. Variation in coefficient of rate of recombination in air with temperature.

As can be seen from the expression (4.9.7), it is important to know the constants of the rate of recombination for investigation of unbalanced flows. This is enough to determine the rate of dissociation because it is possible to use this as a constant of thermodynamic equilibrium.

The mean empirical values of the constant for recombination in air obtained at a pressure of about one atmosphere are shown in Fig. 4.9.1. It is assumed that these values correspond to the lower limit of the rate of recombination.

During the experiments with oxygen and nitrogen the measured values of constants of rates of recombination were of the order of 10^{15}–10^{16} $cm^6/mol^2 \cdot sec$.

Weightwise the rate of formation of atoms $(W_{chem})_i = (W_{chem})_A$ occurring in the equation of diffusion (3.2.5) is connected with (4.9.7) by the obvious relation

$$(W_{chem})_A = (d\,[A]/dt)m_A = (da/dt)\rho. \tag{4.9.7'}$$

9.3 Time of relaxation

Equation (4.9.7) can be modified to some extent. For this purpose we use the concept of the constant of equilibrium which is useful under the conditions of unbalanced and balanced flows. Then the ratio $e^{-1/\bar{T}}/\bar{\rho}$ can be replaced by the quantity $a_e^2/(1-a_e)$ which, after substitution of (4.9.7), gives

$$\frac{da}{dt} = C\bar{\rho}^2 \rho_d \left(a + \frac{a_e}{1-a_e}\right)(a_e - a). \tag{4.9.9}$$

Introducing the notation

$$t_D = \left[C\bar{\rho}^2 \rho_d \left(a + \frac{a_e}{1-a_e}\right)\right]^{-1}, \tag{4.9.10}$$

we get

$$da/dt = (a_e - a)/t_D. \tag{4.9.10'}$$

Integration of this equation leads to the relation $a\,(t)$, which characterizes the change in degree of dissociation as a function of time t beginning with its value a at time $t=0$ and ending with the value at equilibrium $a=a_e$, which is reached in some time Δt (time of relaxation). To the order of this value the derivative da/dt can be expressed in the form

$$da/dt \approx (a_e - a)/\Delta t.$$

Consequently, according to (4.9.10') we have

$$\Delta t \approx t_D.$$

In this way the parameter t_D (4.9.10) can be approximately defined as the time of relaxation. The most important problem of the physics of relaxation processes is included in the determination of this parameter. Some data on the relaxation time

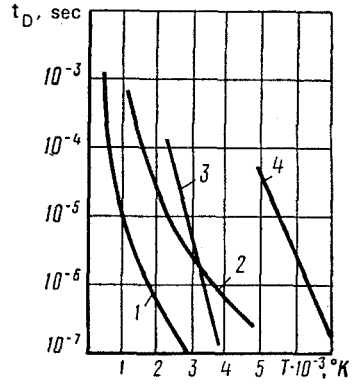

Fig. 4.9.2. Experimental curves (*1, 2*) for time of vibrational relaxation and theoretical curves (*3, 4*) for time of relaxation for dissociation of oxygen and nitrogen respectively at atmospheric pressure.

for oxygen and nitrogen are obtained experimentally in shock tubes (Fig. 4.9.2).

Analysis shows that the time of relaxation for dissociation is less than that for recombination by approximately the first order. Therefore to estimate the effects of relaxation it is desirable to use the time of recombination even though a rough estimate can also be made from the time of direct reaction. The same thing can be said of vibrational relaxation, keeping in mind that in an actual process the time required to excite vibrations up to a given temperature is less than the time taken to damp the vibrations in the opposite process beginning from that temperature.

To estimate the relaxation time of oxygen or nitrogen the following approximate expression can be used:

$$t_D = 7.7 \times 10^{-7} \frac{1}{a(1-0.7a)} \left(\frac{T_K}{T}\right)^{1/2} \left(\frac{\rho_K}{\rho}\right)^2, \qquad (4.9.11)$$

where index "K" indicates final values of parameters.

Formula (4.9.11) shows that reactions take place at a faster rate if the initial density and temperature increase; this reduces the relaxation time. The same formula indicates that time t_D decreases with a rise in pressure, which is confirmed by the graphs in Fig. 4.9.3. It can be seen that an increase in pressure to the third order gives a tenfold reduction in relaxation time (pressure p in graph is related to atmospheric pressure p_3 at sea level). Investigations proved that the relaxation time during dissociation of air is less than that of pure nitrogen or oxygen.

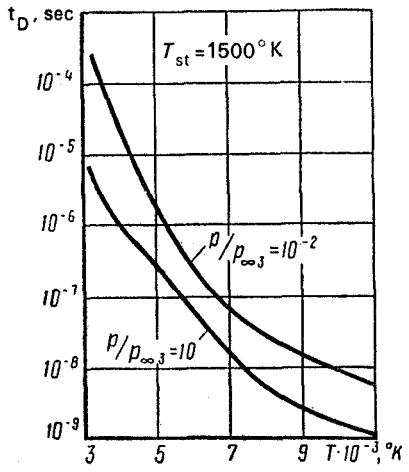

Fig. 4.9.3. Relaxation time for dissociation of oxygen.

Some information from the kinetic theory of gases: In the kinetic theory of gases the relaxation time is defined as the time during which the motion of a molecule undergoing collisions with other molecules having an indefinite character must in general be independent of the previous history of the motion of the molecules. Obviously this time t_r depends on the number of collisions n suffered by a molecule in unit time and hence it may be assumed that t_r is inversely proportional to n, i.e.

$$t_r = a_r/n, \qquad (4.9.12)$$

where coefficient a_r depends on whether the molecule collides with the wall or with another molecule. Besides, its value changes with the nature of the interaction. For example, to change the energy of vibrational motion it may

be necessary to have somewhat bigger collisions than to change the energy of translational motion. If a mixture of gases is considered the coefficient a_r will depend on whether molecules of one kind interact with those of the other kind. This coefficient will depend on the type of process of interactions between molecules, which is determined by the properties of the gas medium and the material of the wall with which the molecules collide.

The average number of collisions suffered by a molecule per unit time depends on the cross section of molecule A, average speed $\bar{c}$ and number of molecules N in unit volume. The proposed number of collisions will be expressed by number of molecules n situated in volume $A\bar{c}$ representing a "corridor" of its own kind formed by a molecule in unit time. Thus $n = NA\bar{c}$. From this it is possible to find the interval between two collisions of one molecule with another, i.e. $t = 1/(NA\bar{c})$. Accordingly the time of relaxation (4.9.12) will be

$$t_r = a_r t = a_r/NA\bar{c}. \tag{4.9.13}$$

The average distance traversed by a molecule during this time indicates the relaxation path

$$l_r = t_r\bar{c} = a_r\bar{c}t = a_r/NA. \tag{4.9.14}$$

For estimation of the order of quantities t_r and l_r the data on the properties of air at normal temperature and pressure can be used: $N = 2.69 \times 10^{19}$ cm^{-3}; $\bar{c} = 4.5 \times 10^4$ cm/sec; $A = 10^{-15}$ cm^2. Introducing these data into (4.9.13) and (4.9.14), we get

$$t_r = a_r\ 10^{-9} \text{ sec}; \quad l_r = 4a_r\ 10^{-5} \text{ cm}.$$

Experiments showed that for active modes of freedom (translational and vibrational) the coefficient a_r will be of the order of unity and for inert modes (vibrational, dissociational and other internal degrees of freedom) the quantity a_r can be high, approaching 10^6.

As can be seen from (4.9.13) the time of relaxation diminishes with an increase in density. Its relation to temperature will be more complicated because not only average molecular speed $\bar{c}$ but also a_r and A depend on temperature.

9.4 Equilibrium processes

Equilibrium flows have been studied in more detail than unbalanced flows from both the quantitative and qualitative points of view. The regions of flow in which equilibrium is established differ due to the unequal times of relaxation for excitation levels. As mentioned earlier, the time to establish an equilibrium in vibrational modes of freedom is a few orders greater than that for translational and rotational modes. Equilibrium of the gas composition mixture during its dissociation and ionization takes still longer.

Accordingly the scheme of an unbalanced process is such that achievement of equilibrium of one degree of freedom may be accompanied by the beginning of the relaxation process of another. In the more general case we encounter overlapping of the regions where equilibrium is established.

An approximate model of the process can be presented on the basis of the principle of "freezing." It is assumed that the region where equilibrium is achieved is related to one or several degrees of freedom at a time when other modes are not excited. The sequence of these regions of equilibrium can be expressed by degrees of freedom with the rise in temperature in the following order: translational, rotational and vibrational modes, dissociation, excitation of electronic levels, ionization. For example, in considering the process of acquiring equilibrium in the vibrational mode the first two degrees of freedom can be assumed as completely excited. This process continues under conditions of "frozen" dissociation and ionization.

Such a scheme is not acceptable for some gases, in particular for nitrogen at high temperatures, as ionization starts before the completion of dissociation. This is explained by the fact that the energies of dissociation and ionization in nitrogen differ between themselves by at least one and one-half times. In this case the regions where equilibrium is achieved overlap. A similar phenomenon is observed in air at comparatively low temperatures. At temperatures above 3,200°K the relaxation time for dissociation of oxygen is less than the time it takes nitrogen to achieve the vibrational mode. Hence equilibrium of dissociation in oxygen will be reached before vibrations start in nitrogen.

Investigation of the flow of an unbalanced gas over a body is simplified if the characteristic time for this process is considerably less than the relaxation time of one of the inert processes and we get the conditions of "freezing" of the flow without the participation of this inert process. In particular, if the time of interaction of some part of the surface is less than the time required for chemical equilibrium but equal to the time of vibrational relaxation then on this part of the surface it is possible to consider the process with "frozen" dissociation and ionization.

9.5 Effects of relaxation in shock waves

During transition of a gas through a shock wave a part of the kinetic energy is converted into the energy of active and inert degrees of freedom where the equilibrium for active degrees of freedom, translational and rotational, is established in a time equal to time of relaxation t_r^A, which is the same as the transition time for gas passing through the thickness of the shock. As this time is very small it may be assumed in practice that the active degrees of freedom are established instantaneously. So just behind the shock the temperature T_2' will be such that the specific heats of the gas remain constant.

According to this scheme the inert degrees of freedom immediately behind the shock are not excited. Since these modes have a finite relaxation time t_r^i significantly higher than t_r^A and the transition time through the thickness of the actual shock the temperature will decrease until the inert modes (first vibrations and then dissociation, excitation of electronized levels and ionization) no longer reach equilibrium.

In Fig. 4.9.4, which schematically illustrates the relaxation process, the time of relaxation t_r^A refers to temperature T_2' calculated on the basis of the beginning of motion on the leading surface of a shock wave where the temperature of the undisturbed gas is T_1. Density ρ_2' corresponding to temperature T_2' is shown in this figure. Temperature $T_2 < T_2'$ corresponds to the equilibrium condition. The unbalanced gas flow process behind the shock is accompanied by a rise in density to its equilibrium value $\rho_2 > \rho_2'$. During this process a small rise in pressure by comparison with the ideal gas flow is observed. Simultaneously the degree of dissociation (and at very high temperatures the degree of ionization) increases from zero to its equilibrium value.

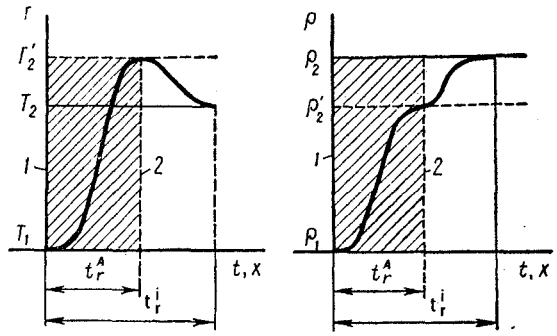

Fig. 4.9.4. Relaxation process in shock wave (hatched region determines thickness of shock wave):

1 and *2*—front and rear surfaces of shock wave respectively.

The study of an unbalanced flow behind a shock consists in determination of the extent of the disequilibrium zone or the length of the relaxation path and the estimation of unbalanced flow parameters. Let us take the disequilibrium motion of a model diatomic gas along a stream line behind a strong normal shock. The system of equations describing this motion includes the equation of momentum (4.8.3) which can be written as

$$\bar{\rho}_1 \bar{V}_1^2 = \bar{p} + \bar{\rho} \bar{V}^2. \tag{4.9.15}$$

The equation of energy (4.8.1) will be

$$a + \frac{4+a}{1+a} \cdot \frac{\bar{p}}{\bar{\rho}} + \frac{\bar{V}^2}{2} = i_0. \tag{4.9.16}$$

The equation of state and the equation for the rate of chemical reactions are given by (1.5.4′) and (4.9.7) respectively.

In these expressions $\overline{p}$, $\overline{\rho}$, $\overline{T}$, $\overline{V}$ represent nondimensional values of pressure, density, temperature and velocity at an arbitrary point on a stream line in the unbalanced zone. These quantities are obtained with respect to the corresponding characteristic parameters. The quantity a determines the unbalanced degree of dissociation at this point. The parameter C, appearing in (4.9.7), is calculated by formula (4.9.8). If the derivative da/dt is expressed in the form

$$\frac{da}{\overline{dt}}=\frac{da}{\overline{dx}}\cdot\frac{dx}{\overline{dt}}=\frac{da}{\overline{dx}}V,$$

equation (4.9.7) can be written in the following way:

$$\frac{da}{\overline{dx}}=\frac{C\overline{\rho}\rho d}{V}\left[(1-a)e^{-1/\overline{T}}-\overline{\rho}a^2\right]. \tag{4.9.17}$$

The determination of unbalanced parameters deals with the solution of this differential equation along with the other equations of the system. During integration the initial conditions are determined by the parameters immediately behind the shock wave which can be found on the assumption that dissociation is absent, i.e. at $x=0$ the quantity $a=0$. At the end of the relaxation path these parameters reach equilibrium values corresponding to degree of dissociation $a=a_e$ at the equilibrium condition. Here for simplification the pressure in the relaxation zone can be taken as constant and equal to its unbalanced value just behind the shock. For this purpose we can apply the equation for rate of chemical reactions.

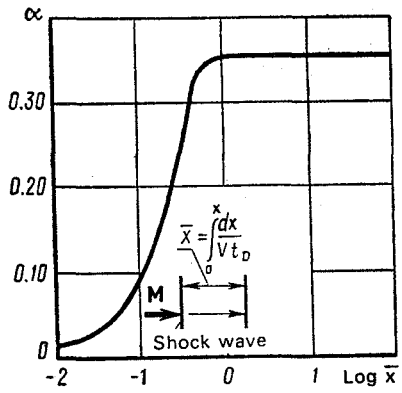

Fig. 4.9.5. Variation in unbalanced degree of dissociation and density of oxygen behind shock wave ($M_1=13$, $T_1=295°K$, $p_1=5.65$ mm mercury column).

$$da/d\overline{x}=a_e-a, \tag{4.9.18}$$

which can be obtained from (4.9.10′) by substituting

$$dt=dx/V=t_D\,d\overline{x}. \tag{4.9.18′}$$

The results of numerical integration of equation (4.9.18) for an unbalanced flow of oxygen behind a normal shock wave are graphically shown in Fig. 4.9.5. The calculations were carried out on the basis of the experimental coefficient of rate of recombination $k_R=8.4\times10^{14}$ cm^6/mol^2·sec. The curve on this figure helps in estimating the unbalanced values of the degree of dissociation in

the zone of relaxation for the case of an equilibrium in the vibrational mode. According to the nature of the variation in the degree of dissociation the density and temperature change from their respective values for a nondissociating gas to the values of balanced dissociation.

For an approximate evaluation of the effect of disequilibrium on an airflow the same equations may be used with the diatomic model of air consisting of the additive mixture of oxygen and nitrogen. Here the parameters C in equation (4.9.17) can be determined for oxygen because the coefficient of the rate of recombination k_R is known more accurately from the experimental data for this gas. All the remaining parameters, particularly the degree of balanced dissociation a_e, characteristic density, pressure, etc. are found for the diatomic model of air.

The unbalanced parameters determined by the above method correspond to the condition under which the gas medium in the initial (undissociated) state has the excited vibrational modes and for such gas $k=c_p/c_v=1.33$.

If the equation of energy in the form $i+V^2/2=i_0$ is applied in place of equation (4.9.16) the initial condition of the heated gas in the first stage can be avoided. Then the above unbalanced parameters in the zone of relaxation can be investigated depending on whether vibrational levels are initially excited or not. The results of such investigations for the air mixture of oxygen and nitrogen are reproduced in Fig. 4.9.6.

The thick curves were obtained on the basis of instantaneous vibrational excitation and the broken curves were obtained in the absence of vibration. From these results it follows that the vibrations have significant value in the immediate vicinity of the shock. For example, without consideration of vibrations the temperature behind the shock is equal to 12,000°K while for the completely excited state it is about 9,800°K, i.e. considerably lower. At the end of the relaxation zone vibrational excitation has practically no significance. Therefore in calculations of balanced dissociation it is possible to assume that the velocity for vibrational excitation is infinitely high and hence that the gas before the beginning of dissociation as fully excited. In Fig. 4.9.6 it can be seen that the extent of the unbalanced zone is comparatively small: it is of the order of 8 to 10 mm.

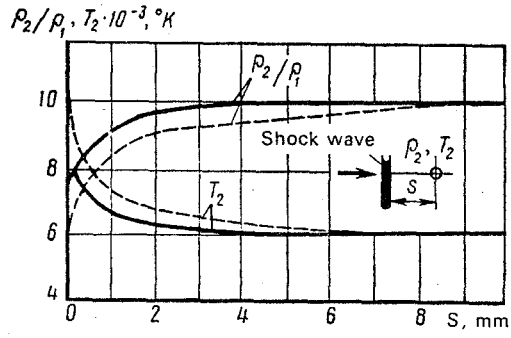

Fig. 4.9.6. Effect of unbalanced dissociation on density and temperature behind shock wave ($M_1=14.2$, $T_1=300$°K, $p_1=1$ mm mercury column).

5

METHOD OF CHARACTERISTICS

1. Equations for Velocity Potential and Stream Function

The method of characteristics plays an important role in aerodynamics. It helps us to analyze the disturbed flow of an ideal (inviscid) fluid. With the application of this method it is possible to determine correctly the contour of nozzles for supersonic wind tunnels and to find the parameters of supersonic flow of wing profiles and cones of a flight vehicle.

The method of characteristics is worked out for various cases as for the solution of a system of equations in steady supersonic two-dimensional (plane or three-dimensional axisymmetric) rotational and irrotational gas flows. Research connected with the application of the method of characteristics in calculations of a three-dimensional flow over bodies has a wide range of applications. The present chapter deals with this method and its utility for the problems of supersonic two-dimensional flows.

The equations of the two-dimensional plane steady motion of an inviscid gas can be obtained from (3.1.20), which under the condition of $\mu=0$, $\partial V_x/\partial t = \partial V_y/\partial t = 0$ takes the following form:

$$\left.\begin{aligned} V_x\frac{\partial V_x}{\partial x}+V_y\frac{\partial V_x}{\partial y}&=-\frac{1}{\rho}\cdot\frac{\partial p}{\partial x};\\ V_x\frac{\partial V_y}{\partial x}+V_y\frac{\partial V_y}{\partial y}&=-\frac{1}{\rho}\cdot\frac{\partial p}{\partial y}. \end{aligned}\right\} \tag{5.1.1}$$

For two-dimensional axisymmetric flows the equations of motion obtained from (3.1.36) under similar conditions ($\nu=0$, $\partial V_x/\partial t=\partial V_r/\partial t=0$) can be written in the form:

$$\left.\begin{aligned} V_x\frac{\partial V_x}{\partial x}+V_r\frac{\partial V_x}{\partial r}&=-\frac{1}{\rho}\cdot\frac{\partial p}{\partial x};\\ V_x\frac{\partial V_r}{\partial x}+V_r\frac{\partial V_r}{\partial r}&=-\frac{1}{\rho}\cdot\frac{\partial p}{\partial r}. \end{aligned}\right\} \tag{5.1.2}$$

The equation of continuity for plane and axisymmetric flows having the form of (2.4.5) and (2.4.32) respectively can be written in the general form:

$$\frac{\partial(\rho V_x y^\varepsilon)}{\partial x}+\frac{\partial(\rho V_y y^\varepsilon)}{\partial y}=0. \tag{5.1.3}$$

At $\varepsilon=0$ this equation coincides with the continuity equation for two-dimensional plane motion in Cartesian coordinates x, y. If $\varepsilon=1$ we get the continuity equation for a two-dimensional axisymmetric flow in cylindrical coordinates $y(r)$, x. Accordingly the equations of motion (5.1.1) for both types of flow can be assumed to have been written in general form.

Taking the partial derivative of the equation of continuity (5.1.3), we get

$$\left(\frac{\partial\rho}{\partial x}V_x+\frac{\partial\rho}{\partial y}V_y\right)y^\varepsilon+\rho y^\varepsilon\left(\frac{\partial V_x}{\partial x}+\frac{\partial V_y}{\partial y}\right)+\rho V_y\,\varepsilon y^{\varepsilon-1}=0. \tag{5.1.4}$$

The partial derivative $\partial\rho/\partial x$ can be replaced by the expression $\partial\rho/\partial x=(d\rho/dp)\,(dp/dx)$, where $dp/d\rho=1/a^2$ and $\partial p/\partial x$ is found from (5.1.1) in the form

$$\frac{\partial p}{\partial x}=-\rho\left(V_x\frac{\partial V_x}{\partial x}+V_y\frac{\partial V_x}{\partial y}\right).$$

Then

$$\frac{\partial\rho}{\partial x}=-\frac{\rho}{a^2}\left(V_x\frac{\partial V_x}{\partial x}+V_y\frac{\partial V_x}{\partial y}\right). \tag{5.1.5}$$

Similarly the expression for derivative $\partial\rho/\partial y$ can be obtained:

$$\frac{\partial\rho}{\partial y}=-\frac{\rho}{a^2}\left(V_x\frac{\partial V_y}{\partial x}+V_y\frac{\partial V_y}{\partial y}\right). \tag{5.1.6}$$

After substitution of the values of these derivatives in (5.1.4) we get

$$(V_x^2-a^2)\frac{\partial V_x}{\partial x}+V_xV_y\left(\frac{\partial V_x}{\partial y}+\frac{\partial V_y}{\partial x}\right)+(V_y^2-a^2)\frac{\partial V_y}{\partial y}-\frac{a^2V_y\varepsilon}{y}=0. \tag{5.1.7}$$

This equation is the basic differential equation of gas dynamics for a two-dimensional (plane or axisymmetric) steady flow, which must be satisfied by the velocity components V_x, V_y. As this equation relates velocities it is known as the basic kinematic equation.

If the flow is potential,

$$V_x=\partial\varphi/\partial x,\quad V_y=\partial\varphi/\partial y,\quad \partial V_x/\partial y=\partial V_y/\partial x=\partial^2\varphi/\partial x\partial y,$$

and hence equation (5.1.7) can be reduced to the form

$$(V_x^2-a^2)\frac{\partial^2\varphi}{\partial x^2}+2V_x\,V_y\frac{\partial^2\varphi}{\partial x\partial y}+(V_y^2-a^2)\frac{\partial^2\varphi}{\partial y^2}-\frac{a^2V_y\varepsilon}{y}=0, \tag{5.1.8}$$

where

$$a^2=\frac{k-1}{2}\left[V_{\max}^2-\left(\frac{\partial\varphi}{\partial x}\right)^2-\left(\frac{\partial\varphi}{\partial y}\right)^2\right].$$

Equation (5.1.8) is the basic differential equation of gas dynamics for a diatomic potential steady flow and is known as the equation for velocity potential. Thus unlike (5.1.7) this equation is applied only in steady irrotational gas flows.

If a two-dimensional gas flow is rotational it is necessary to use the stream function ψ for this flow. The velocity components, expressed through function ψ, have the following form according to equation (2.5.5):

$$V_x=\frac{1}{\rho y^{\epsilon}}\cdot\frac{\partial\psi}{\partial y},\quad V_y=-\frac{1}{\rho y^{\epsilon}}\cdot\frac{\partial\psi}{\partial x}. \tag{5.1.9}$$

Replacing ρ by formula (3.6.31) in which stagnation density ρ_0 along the given stream line has constant value, expressions (5.1.9) can be written in the form:

$$\left.\begin{aligned} V_x&=y^{-\epsilon}(1-\overline{V}^2)^{-1/(k-1)}(\partial\psi/\partial y),\\ V_y&=-y^{-\epsilon}(1-\overline{V}^2)^{-1/(k-1)}(\partial\psi/\partial x),\end{aligned}\right\} \tag{5.1.9'}$$

where $\overline{V}=V/V_{\max}$. The calculation of a rotational gas flow lies in solving the differential equation for stream function ψ. To get this equation differentiate V_x and V_y in (5.1.9') with respect to y and x respectively:

$$\frac{\partial V_x}{\partial y}=-\varepsilon y^{-\epsilon-1}(1-\overline{V}^2)^{-\frac{1}{k-1}}\frac{\partial\psi}{\partial y}+y^{-\epsilon}\frac{1}{k-1}(1-\overline{V}^2)^{-\frac{1}{k-1}-1}\frac{\partial\overline{V}^2}{\partial y}$$
$$\times\frac{\partial\psi}{\partial y}+y^{-\epsilon}(1-\overline{V}^2)^{-\frac{1}{k-1}}\frac{\partial^2\psi}{\partial y^2};$$
$$\frac{\partial V_y}{\partial x}=-y^{-\epsilon}\frac{1}{k-1}(1-\overline{V}^2)^{-\frac{1}{k-1}-1}\frac{\partial\overline{V}^2}{\partial x}\cdot\frac{\partial\psi}{\partial x}$$
$$-y^{-\epsilon}(1-\overline{V}^2)^{-\frac{1}{k-1}}\frac{\partial^2\psi}{\partial x^2}.$$

Considering the expression (3.6.22) for the square of sound velocity and the equations (5.1.9'), the relations obtained for derivatives $\partial V_x/\partial y$ and $\partial V_y/\partial x$ can be written as following:

$$\frac{\partial V_x}{\partial y}=-\frac{\varepsilon}{y}V_x+\frac{V_x}{2a^2}\cdot\frac{\partial V^2}{\partial y}+y^{-\epsilon}(1-\overline{V}^2)^{-1/(k-1)}\frac{\partial^2\psi}{\partial y^2}; \tag{5.1.10}$$

$$\frac{\partial V_y}{\partial x}=\frac{V_y}{2a^2}\cdot\frac{\partial V^2}{\partial x}-y^{-\epsilon}(1-\overline{V}^2)^{-1/(k-1)}\frac{\partial^2\psi}{\partial x^2}. \tag{5.1.11}$$

The derivations $\partial V^2/\partial y$ and $\partial V^2/\partial x$ appearing here could be determined with the help of the relations (5.1.9'). Combining these relations, we get

$$(\partial\psi/\partial x)^2+(\partial\psi/\partial y)^2=V^2y^{2\epsilon}(1-\overline{V}^2)^{2/(k-1)}. \tag{5.1.12}$$

Differentiating (5.1.12) with respect to x and y, the following relations can be obtained:

$$2\frac{\partial\psi}{\partial x}\cdot\frac{\partial^2\psi}{\partial x^2}+2\frac{\partial\psi}{\partial y}\cdot\frac{\partial^2\psi}{\partial x\,\partial y}=\frac{\partial V^2}{\partial x}y^{2\epsilon}(1-\overline{V}^2)^{2/(k-1)}$$

$$-V^2y^{2\epsilon}\frac{2}{k-1}(1-\overline{V}^2)^{\frac{2}{k-1}-1}\frac{\partial\overline{V}^2}{\partial x};$$

$$2\frac{\partial\psi}{\partial x}\cdot\frac{\partial^2\psi}{\partial x\partial y}+2\frac{\partial\psi}{\partial y}\cdot\frac{\partial^2\psi}{\partial y^2}=\frac{\partial V^2}{\partial y}y^{2\epsilon}(1-\overline{V}^2)^{2/(k-1)}$$

$$+2\varepsilon V^2y^{2\epsilon-1}(1-\overline{V}^2)^{2/(k-1)}-V^2y^{2\epsilon}\frac{2}{k-1}(1-\overline{V}^2)^{\frac{2}{k-1}-1}\frac{\partial\overline{V}^2}{\partial y}.$$

Using equation (3.6.22) for the square of the sound velocity and the relations (5.1.9′), we can transform the above relations into the following:

$$-V_y\frac{\partial^2\psi}{\partial x^2}+V_x\frac{\partial^2\psi}{\partial x\,\partial y}=\frac{y^\epsilon}{2}\cdot\frac{\partial V^2}{\partial x}(1-\overline{V}^2)^{1/(k-1)}\left(1-\frac{V^2}{a^2}\right);\qquad(5.1.13)$$

$$-V_y\frac{\partial^2\psi}{\partial x\,\partial y}+V_x\frac{\partial^2\psi}{\partial y^2}=\frac{y^\epsilon}{2}\cdot\frac{\partial V^2}{\partial y}(1-\overline{V}^2)^{1/(k-1)}$$

$$\times\left(1-\frac{V^2}{a^2}\right)+\frac{\varepsilon}{y^{1-\epsilon}}V^2(1-\overline{V}^2)^{1/(k-1)}.\qquad(5.1.14)$$

The derivatives $\partial V^2/\partial y$ and $\partial V^2/\partial x$ can be determined from these relations. Substituting these values in (5.1.10) and (5.1.11) respectively, we get:

$$\frac{y^\epsilon}{2}(1-\overline{V}^2)^{1/(k-1)}\left(1-\frac{V^2}{a^2}\right)\frac{\partial V_x}{\partial y}=-\frac{\varepsilon}{2y^{1-\epsilon}}V_x(1-\overline{V}^2)^{1/(k-1)}$$

$$\times\left(1-\frac{V^2}{a^2}\right)+\frac{V_x}{2a^2}\Big[-V_x\frac{\partial^2\psi}{\partial x\,\partial y}+V_x\frac{\partial^2\psi}{\partial y^2}$$

$$-\frac{\varepsilon}{y^{1-\epsilon}}V^2(1-\overline{V}^2)^{1/(k-1)}\Big]+\frac{1}{2}\left(1-\frac{V^2}{a^2}\right)\frac{\partial^2\psi}{\partial y^2};$$

$$\frac{y^\epsilon}{2}(1-\overline{V}^2)^{1/(k-1)}\left(1-\frac{V^2}{a^2}\right)\frac{\partial V_y}{\partial x}$$

$$=\frac{V_y}{2a^2}\left(-V_y\frac{\partial^2\psi}{\partial x^2}+V_x\frac{\partial^2\psi}{\partial x\partial y}\right)-\frac{1}{2}\left(1-\frac{V^2}{a^2}\right)\frac{\partial^2\psi}{\partial x^2}.$$

Subtracting the first equation from the second, we get the relation for vorticity:

$$\frac{\partial V_y}{\partial x}-\frac{\partial V_x}{\partial y}=\frac{V_y}{a^2-\overline{V}^2}\cdot\frac{1}{y^\epsilon}\left(-V_y\frac{\partial^2\psi}{\partial x^2}+V_x\frac{\partial^2\psi}{\partial x\partial y}\right)(1-\overline{V}^2)^{-1/(k-1)}$$

$$-\frac{1}{y^\epsilon}(1-\overline{V}^2)^{-1/(k-1)}\frac{\partial^2\psi}{\partial x^2}-\frac{V_x}{a^2-\overline{V}^2}\cdot\frac{1}{y^\epsilon}\left(-V_y\frac{\partial^2\psi}{\partial x\partial y}+V_x\frac{\partial^2\psi}{\partial y^2}\right)$$

$$\times(1-\overline{V}^2)^{-1/(k-1)}-\frac{1}{y^\epsilon}(1-\overline{V}^2)^{-1/(k-1)}\frac{\partial^2\psi}{\partial y^2}+\frac{\varepsilon}{y}\cdot\frac{a^2}{a^2-\overline{V}^2}V_x.\qquad(5.1.15)$$

Vorticity can also be determined with the help of equation (3.1.22′), which is obtained for the condition of steady flow of an ideal gas in the form

$$\operatorname{grad}(V^2/2)+\operatorname{rot}\overline{V}\times\overline{V}=-(1/\rho)\operatorname{grad}p. \tag{5.1.16}$$

Taking the gradient of the equation of energy (3.4.14), we get

$$\operatorname{grad}(V^2/2)=-\operatorname{grad}i. \tag{5.1.17}$$

Consequently equation (5.1.16) can be rewritten in the form:

$$\operatorname{rot}\overline{V}\times\overline{V}=\operatorname{grad}i-(1/\rho)\operatorname{grad}p. \tag{5.1.18}$$

Rotational supersonic flows of a gas can be thermodynamically characterized by the variation in entropy from one stream line to the other. Therefore it is convenient to introduce a parameter into the calculation that can reflect the given variation in entropy as the peculiarity of rotational flows.

From the second law of thermodynamics we have

$$TdS=di-(dp/\rho),$$

or in the vector form

$$T\operatorname{grad}S=\operatorname{grad}i-(1/\rho)\operatorname{grad}p. \tag{5.1.19}$$

Combining (5.1.18) and (5.1.19), we get

$$\operatorname{rot}\overline{V}\times\overline{V}=T\operatorname{grad}S. \tag{5.1.20}$$

Let us find the vector product $\operatorname{rot}\overline{V}\times\overline{V}$, keeping in mind that according to (2.2.12) the vector

$$\operatorname{rot}\overline{V}=\left(\frac{\partial V_y}{\partial x}-\frac{\partial V_x}{\partial y}\right)i_3,$$

and hence the component $(\operatorname{rot}\overline{V})_x=(\operatorname{rot}\overline{V})_y=0$. Using the determinant of the third order, we get

$$\operatorname{rot}\overline{V}\times\overline{V}=\begin{vmatrix} i_1, & i_2 & i_3 \\ 0 & 0 & (\operatorname{rot}\overline{V})_3 \\ V_x & V_y & 0 \end{vmatrix},$$

in which the component

$$(\operatorname{rot}\overline{V})_3=\frac{\partial V_y}{\partial x}-\frac{\partial V_x}{\partial y}.$$

This gives

$$\operatorname{rot}\overline{V}\times\overline{V}=-V_y\left(\frac{\partial V_y}{\partial x}-\frac{\partial V_x}{\partial y}\right)i_1+V_x\left(\frac{\partial V_y}{\partial x}-\frac{\partial V_x}{\partial y}\right)i_2. \tag{5.1.21}$$

Accordingly we get the relation for the projection of vector rot $\overline{V}\times\overline{V}$ along the normal to a given stream line as:

$$(\operatorname{rot}\overline{V}\times\overline{V})_n^2=(\operatorname{rot}\overline{V}\times\overline{V})_x^2+(\operatorname{rot}\overline{V}\times\overline{V})_y^2=V^2\left(\frac{\partial V_y}{\partial x}-\frac{\partial V_x}{\partial y}\right)^2. \quad (5.1.22)$$

From (5.1.20) it follows that this component of the vector can also be expressed in the form

$$(\operatorname{rot}\overline{V}\times\overline{V})_n=T(dS/dn)$$

or, taking into account (5.1.22), it will be

$$V\left(\frac{\partial V_y}{\partial x}-\frac{\partial V_x}{\partial y}\right)=T\frac{dS}{dn}. \quad (5.1.23)$$

As $a^2=kRT$ we obtain from this and (3.6.22) the expression for temperature:

$$T=\frac{a^2}{kR}=\frac{k-1}{2k}\cdot\frac{1}{R}(V_{\max}^2-V^2)=\frac{k-1}{2k}\cdot\frac{V_{\max}^2}{R}(1-\overline{V}^2).$$

Using this expression in (5.1.23), we get

$$\frac{\partial V_y}{\partial x}-\frac{\partial V_x}{\partial y}=\frac{k-1}{2k}\cdot\frac{V_{\max}^2}{RV}(1-\overline{V}^2)\frac{dS}{dn}. \quad (5.1.24)$$

Substituting vortex strength from this in (5.1.15) we get a differential equation for stream function:

$$(V_x^2-a^2)\frac{\partial^2\psi}{\partial x^2}+2V_xV_y\frac{\partial^2\psi}{\partial x\partial y}+(V_y^2-a^2)\frac{\partial^2\psi}{\partial y^2}$$
$$+\frac{\varepsilon}{y^{1-\epsilon}}a^2V_x(1-\overline{V}^2)^{1/(k-1)}$$
$$=\frac{k-1}{2k}\cdot\frac{V_{\max}^2}{RV}(1-\overline{V}^2)^{k/(k-1)}y^{\epsilon}(a^2-V^2)\frac{dS}{dn}. \quad (5.1.25)$$

2. Cauchy's Problem

Equations (5.1.8) and (5.1.25) for velocity potential and stream function respectively are nonlinear differential equations of the second order. Besides terms with second-order partial derivatives these equations also contain free terms without partial derivatives. Therefore they are not homogenous.

The solutions of equations $\varphi=\varphi(x, y)$ and $\psi=\psi(x, y)$ are geometrically represented by integral surfaces in space which can be determined by systems of coordinates x, y, φ or x, y, ψ: In these systems the plane x, y is regarded as

the main plane. It is known as the physical plane or plane of independent variables.

The process of finding solutions satisfying given additional conditions on a curve in the neighborhood of some given (initial) curve $y=y(x)$ forms the content of Cauchy's problem. The values of the functions $\varphi(x, y)$ or $\psi(x, y)$ being investigated and their first derivatives $\varphi_x(\psi_x)$ or $\varphi_y(\psi_y)$, known as Cauchy's initial conditions, are examples of such additional conditions. It should be noted here that a given function that is itself on the initial curve, for example $\varphi[x, y(x)]$, and one of its first derivatives $\varphi_y=\partial\varphi/\partial y$ automatically determine the other derivative $\varphi_x=\partial\varphi/\partial x$. This follows from the relation

$$\frac{d\varphi[x, y(x)]}{dx}=\frac{\partial\varphi[x, y(x)]}{\partial x}+\frac{\partial\varphi[x, y(x)]}{\partial y}\cdot\frac{dy}{dx},$$

which is obtained from the formula for total derivatives of the complicated function of two variables x and y on the assumption that the initial curve is given and hence the relation between y and x is known.

From the geometrical point of view Cauchy's problem consists of finding an integral surface in the space x, y, φ (or x, y, ψ) passing through some given curve in space. The projection of this curve on the x, y plane also represents an initial curve $y=y(x)$ on this plane. The solution of Cauchy's problem is applicable to the study of supersonic gas flows and the credit for developing the corresponding method of characteristics belongs to the Soviet scientist Prof. F. Frankl'.

To study Cauchy's problem we express equations (5.1.8) and (5.1.25) in a general form:

$$Au+2Bs+Ct+H=0, \tag{5.2.1}$$

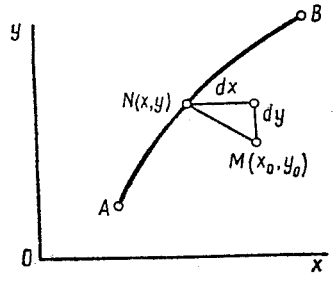

Fig. 5.2.1. Initial curve AB on which desired function and its first derivatives with respect to x and y are known.

where $u=\varphi_{xx}$ (or ψ_{xx}) $s=\varphi_{xy}$ (or ψ_{xy}), $t=\varphi_{yy}$ (or ψ_{yy}) are the second-order partial derivatives; the values of A, B and C are equal to the coefficients for the corresponding second-order partial derivatives; the quantity H is determined from the free terms in equations (5.1.8), (5.1.25).

Let us find the solution of equation (5.2.1) in the neighborhood of the initial curve AB (Fig. 5.2.1), which is in the form of a series. At some point $M(x_0, y_0)$ the function being investigated will be

$$\varphi(x_0, y_0)=\varphi(x, y)+\sum_{n=1}^{\infty}\frac{1}{n!}\left[(\Delta x)^n\frac{\partial^n\varphi}{\partial x^n}+\frac{n}{1}(\Delta x)^{n-1}\Delta y\frac{\partial^{n-1}\varphi}{\partial x^{n-1}\partial y}\right.$$

$$+\frac{n(n-1)}{1\cdot 2}(\Delta x)^{n-2}(\Delta y)^2\frac{\partial^{n-2}\varphi}{\partial x^{n-2}\partial y^2}+\ldots+(\Delta y)^n\frac{\partial^n\varphi}{\partial y^n}\Big], \qquad (5.2.2)$$

where $\varphi(x, y)$ is the value of this function at a given point $N(x, y)$ on the initial curve; $\Delta x=x_0-x$, $\Delta y=y_0-y$. In place of φ in (5.2.2) the function ψ can be used.

The series (5.2.2) gives the function we are looking for if the values of function φ (or ψ) and its partial derivatives of any order $\partial^n\varphi/\partial x^n$, $\partial^{n-1}\varphi/\partial x^{n-1}$, etc. exist and are known on the given curve. Since on this curve the first derivatives [denoted by $p=\varphi_x$ (or ψ_x) and $q=\varphi_y$ (or ψ_y)] are given it is necessary to find second derivatives and the derivatives of higher order on this curve. In this way the solution of Cauchy's problem is connected with the investigation of conditions in which it is possible to determine actual derivatives on a given curve.

Here we confine ourselves to the determination of second-order derivatives. As there are three such derivatives (u, s and t) only three independent equations can be formulated. The first of them will be equation (5.2.2), which is satisfied on the initial curve AB. The remaining two equations can be obtained from the following known relations for the complete differentials of the functions of two independent variables existing on this curve:

$$dp=(\partial p/\partial x)\,dx+(\partial p/\partial y)\,dy=u\,dx+s\,dy;$$
$$dq=(\partial q/\partial x)\,dx+(\partial q/\partial y)\,dy=s\,dx+t\,dy.$$

Hence the system of equations for determining second derivatives will be written in the form:

$$\left.\begin{aligned} &Au+2Bs+Ct+H=0;\\ &dx\cdot u+dy\cdot s+0\cdot t-dp=0;\\ &0\cdot u+dx\cdot s+dy\cdot t-dq=0. \end{aligned}\right\} \qquad (5.2.3)$$

This system of equations is solved for the unknowns u, s, t with the help of determinants. If the main and the partial determinants are expressed by the notations Δ and Δ_u, Δ_s and Δ_t, respectively,

$$u=\Delta_u/\Delta, \quad s=\Delta_s/\Delta, \quad t=\Delta_t/\Delta. \qquad (5.2.4)$$

From these relations it follows that if the main determinant is not equal to zero on the initial curve AB the second-order derivatives u, s and t can have unique values.

Let us consider a case where the curve is selected in such a way that the main determinant lying on it is equal to zero, i.e.

$$\Delta=\begin{vmatrix} A & 2B & C\\ dx & dy & 0\\ 0 & dx & dy \end{vmatrix}=0.$$

This gives

$$A\,(dy/dx)^2-2B\,(dy/dx)+C=0. \tag{5.2.5}$$

From the course in mathematics we know that under the condition when main determinant Δ of the system of equations (5.2.3) is zero, i.e. on the curve expressed by the equation (5.2.5), the second-order derivatives u, s, t (5.2.4) are either multi-valued or in general cannot be determined in terms of φ, p and q.

Let us take quadratic equation (5.2.5). Solving it for derivative dy/dx, we get

$$(dy/dx)_{1,2}=y'_{1,2}=(1/A)\,(B\pm\sqrt{B^2-AC}). \tag{5.2.6}$$

These equalities determine the inclination of the tangent at every point of the initial curve on which the main determinant $\Delta=0$. It can easily be seen that the equations (5.2.6) are the differential equations of two families of real curves if $B^2-AC>0$. These curves, at each point of which the main determinant of system (5.2.3) is equal to zero, are known as the characteristics and equation (5.2.6) is called the characteristic equation.

From the above discussion we get the condition under which it is possible to find a unique solution for second-order derivatives on the initial curve: An elemental arc of this curve must not coincide with the characteristics. Similarly while determining higher-order derivatives uniquely the same conditions $\Delta\neq0$ is to be satisfied. Hence if $\Delta\neq0$, all the coefficients of series (5.2.2) can be determined uniquely from the data on the initial curves.

In this way the condition $\Delta\neq0$ is the necessary and sufficient condition for solving Cauchy's problem. The problem is very important in the mathematical theory of partial differential equations and formula (5.2.2), generally speaking, can be used for calculation of a gas flow. However, from the point of view of physical principles and in particular the calculation of supersonic gas flows the problem of determination of a solution from the data on characteristics, i.e. the method of characteristics, is very important. This method can be obtained from the analysis of Cauchy's problem and may be described as follows: Let us assume that the initial curve AB coincides with one of the characteristics and that not only the main determinant of system (5.2.3) but also the auxiliary determinants are zero, i.e. $\Delta_u=\Delta_s=\Delta_t=0$ along it. If, for example, determinants Δ and Δ_t are equal to zero the remaining determinants will be automatically zero. To prove this let us find the auxiliary determinants:

$$\Delta_u=\begin{vmatrix} -H & 2B & C \\ dp & dy & 0 \\ dq & dx & dy \end{vmatrix}=(dx)^2\,[-Hy'^2-2By'p'+C\,(p'-y'q')]; \tag{5.2.7}$$

$$\Delta_s=\begin{vmatrix} A & -H & C \\ dx & dp & 0 \\ 0 & dq & dy \end{vmatrix}=(dx)^2\,(Ay'p'+Hy'+Cq'); \tag{5.2.8}$$

$$\Delta_t=\begin{vmatrix} A & 2B & -H \\ dx & dy & dp \\ 0 & dx & dq \end{vmatrix}=(dx)^2\,[A\,(y'q'-p')-2Bq'-H], \qquad (5.2.9)$$

where $p'=dp/dx$, $q'=dq/dx$.

As $dx\neq 0$ the condition $\Delta_t=0$ leads to the equality

$$A\,(y'q'-p')-2Bq'-H=0. \qquad (5.2.10)$$

From the condition of $\Delta=0$ we get equation (5.2.5). Multiplying this equation by $(p'-y'q')$ and equation (5.2.10) by y'^2 and then adding, we have

$$-Hy'^2-2By'p'+C(p'-y'q')=0.$$

Comparing this expression with (5.2.7) it can be seen that $\Delta_u=0$. Now if equation (5.2.5) is multiplied by q' and equation (5.2.10) by y' then, after subtracting the products, we get

$$Ay'p'+Hy'+Cq'=0$$

which, according to (5.2.8), corresponds to Δ_s.

The condition of zero values of all the determinants, as shown in the theory of the system of algebraic equations, signifies that solutions of system (5.2.3), although not single-valued, do exist. Here if one of the solutions, for example of u, is the final solution then the solutions for s and t will also be final.

3. Characteristics

3.1 Conditions of existence

Equations (5.2.5) and (5.2.10) determining the conditions under which solutions for u, s and t exist, even if multi-valued, are known as the conditions of existence. Geometrically speaking the first of these equations represents two families of curves of characteristics in the physical plane x, y; the second expresses two families of curves of characteristics in the plane p, q. The characteristics of different families in these planes are known as conjugate families.

The solution of a problem concerning a supersonic flow of gas found from the solution of characteristic equations (or of conditions of coexistence) also happens to be the solution of a basic equation of gas dynamics, (5.1.8) or (5.1.25). Its proof follows from the so-called theorem of equivalence according to which the characteristic equations (5.2.5) and (5.2.10) are equivalent to the basic equation (5.1.8) or (5.1.25) (the proof of this theorem is given in [21]).

From the geometrical point of view the proven equivalence indicates that the solution of equations of characteristics also means transformation of some plane x, y to the plane p, q. That is, the points on the curves determined

by differential equation (5.1.8) correspond to the points on the curves determined by differential equation (5.1.25).

In this way at each point on the characteristic in plane x, y there exists a point on the characteristic in plane p, q. Obviously the given correspondence can be established by various methods depending on the given graphical conditions. As will be seen further on, this relation particularly facilitates the use of characteristics in calculations of gas flows.

From the above discussion it follows that the distinct property of characteristics lies in the fact that the initial conditions cannot be given arbitrarily along characteristics but can be given along a curve that is different from the characteristics.

3.2 Existence of characteristics

Type of characteristics: From (5.2.6) it follows that the roots of quadratic characteristic equations (5.2.5) can be real (equal or unequal values) and also complex conjugate roots. The difference in roots is determined by the expression $B^2-AC=\delta$. In a case where $\delta>0$, the equation (5.2.6) gives two different families of real characteristics. The quantity $\delta=0$ determines two equal roots which correspond to two coinciding characteristics, i.e. factually to only one characteristic. Finally, if $\delta<0$, the roots of the equation represent a pair of imaginary characteristics.

As the roots of characteristic equations depend on coefficients A, B, C of differential equation (5.2.1) it is the convention to classify these equations according to the type of characteristics. If $\delta>0$ equation (5.2.1) will be of the hyperbolic type, if $\delta=0$ it will be of the parabolic type and for $\delta<0$ it will be of the elliptic type.

In equations (5.1.8) and (5.1.25) for velocity potential and stream function respectively the coefficients A, B and C are determined identically, namely,

$$A=V_x^2-a^2,\ B=V_x V_y,\ C=V_y^2-a^2. \tag{5.3.1}$$

Hence

$$\delta=B^2-AC=a^2(V^2-a^2), \tag{5.3.2}$$

where the total velocity $V=\sqrt{V_x^2+V_y^2}$.

Thus for regions of gas flow with supersonic speeds ($V>a$) the equations will be of the hyperbolic type and for regions of flow with subsonic speeds ($V<a$) they will be of the elliptic type. At the boundary of these regions the speed is sonic ($V=a$) and the equations will be of the parabolic type.

Characteristics in physical plane: The characteristics in plane x, y are determined from the solution of differential equation (5.2.6) in which the plus sign corresponds to the characteristics of the first family and the minus sign to the characteristics of the second.

The quantity $\lambda_1=dy/dx$ which can be directly calculated from the expres-

sion (5.2.6) and the plus sign in this expression determines the angular coefficient of the characteristic of the first family, while $\lambda_2=dy/dx$ with the minus sign determines the angular coefficient of the characteristic of the second family. Recalling expressions (5.3.1) and (5.3.2) we get the equation for characteristics in the x, y plane:

$$\lambda_{1,2}=\frac{dy}{dx}=\frac{1}{V_x^2-a^2}(V_x V_y \pm a\sqrt{V^2-a^2}). \tag{5.3.3}$$

The characteristics in a physical plane have a particular physical meaning which can be established if angle μ between the velocity vector $\overline{V}$ at some point in the flow (Fig. 5.3.1) and the direction of characteristics at that point is determined. This angle is determined with the help of equation (5.3.3) if it is transformed to the local system of coordinates x_1, y_1 with origin at point A and axis x_1 coinciding with the direction of velocity vector $\overline{V}$. With this choice of axes of coordinates $V_x=V$, $V_y=0$ and consequently,

$$\lambda_{1,2}=\tan\mu_{1,2}=\pm(\mathbf{M}^2-1)^{-1/2}.$$

From this it can be seen that μ represents by itself the Mach angle. Thus a very important property of characteristics is established. It indicates that at every point on the characteristic the angle between the tangent to it and the velocity vector at this point is equal to the Mach angle. Consequently the characteristic by itself represents a line of weak disturbances (or Mach line) having the form of a curve in the general case.

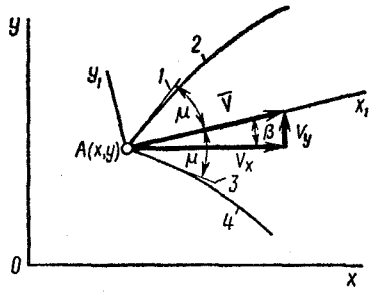

Fig. 5.3.1. Scheme representing physical meaning of characteristic:

1—direction of characteristic of first family at point A; *2*—characteristic of first family with angular coefficients λ_1; *3*—direction of characteristic of second family at point A; *4*—characteristic of second family with angular coefficient λ_2.

Determination of characteristic as the Mach line is directly related to the two-dimensional plane supersonic flow. If a two-dimensional space (axisymmetric) supersonic flow is considered the Mach lines (characteristics) may be regarded as the generators of a rotating surface which is the slant Mach cone with its apex at the points of disturbance (on characteristics). The surface enveloping the region of disturbance is known as the wave surface or the space Mach wave.

The compression waves arising in a gas where supersonic motion is characterized by a rise in pressure were discussed in Chapter 4. However, such motion can be accompanied by a decrease in pressure, i.e. the supersonic flow will be accompanied by expansion and the Mach lines will characterize expansion waves. The characteristics, which are generally curved lines (for a

plane flow) or surfaces formed by the rotation of these lines (for an axisymmetric flow), coincide with the corresponding Mach lines. If there are Mach lines (characteristics) in a flow in the form of straight lines they correspond to the plane expansion waves having the same direction of velocity of propagation. The Mach lines corresponding to expansion waves will be further known as lines of weak disturbances, using the accepted terminology for weak compression waves. Here it is necessary to bear in mind that in an expanding supersonic flow there cannot be any other than weak expansion waves because otherwise the possibility could arise of formation of strong expansion waves (expansion shocks), which cannot occur in real flows.

If the flow velocity and speed of sound are known at a given point in the physical plane the above property of characteristics helps us to determine the direction of characteristic at that point by calculating the Mach angle from the formula $\mu = \pm \sin^{-1}(1/\mathbf{M})$. The angular coefficients of characteristics in relation to the coordinates x, y (see Fig. 5.3.1) will be obtained from the equation

$$\lambda_{1,2} = dy/dx = \tan(\beta \pm \mu), \tag{5.3.4}$$

where β is the angle of inclination of the velocity vector from the x axis; the plus and minus signs refer to the characteristics of the first and second family respectively. Equation (5.3.4) is the differential equation for the characteristics in the physical plane.

Characteristics in plane p, q: If the quantity y' in equation (5.2.10) is replaced by first root ($y' = \lambda_1$) of the characteristic equation (5.2.5) the equation so obtained:

$$A(\lambda_1 q' - p') - 2Bq' - H = 0 \tag{5.3.5}$$

will represent the first family of characteristics in plane p, q. Similar substitution of y' by second root $y' = \lambda_2$ gives the equation of the second family of characteristics in the same plane:

$$A(\lambda_2 q' - p') - 2Bq' - H = 0. \tag{5.3.6}$$

The equations of characteristics (5.3.5) and (5.3.6) can be transformed by the use of the property of the roots of quadratic equation (5.2.5), according to which

$$\lambda_1 + \lambda_2 = 2B/A. \tag{5.3.7}$$

Taking the first family of characteristics and introducing the relation $A\lambda_1 - 2B = -\lambda_2 A$ from (5.3.7) into (5.3.5), we write the equation

$$A(\lambda_2 q' + p') + H = 0. \tag{5.3.8}$$

Similarly, for the characteristic of the second family we find

$$A(\lambda_1 q' + p') + H = 0. \tag{5.3.9}$$

Taking into account expression (5.3.4), equations (5.3.8) and (5.3.9) can be rewritten in the form

$$\frac{dp}{dx}+\tan(\beta\mp\mu)\frac{dq}{dx}+\frac{H}{A}=0, \tag{5.3.10}$$

where the plus and minus signs correspond to the characteristics of first and second families respectively.

3.3 Property of orthogonal conjugate characteristics

If the differentials in the equation for characteristics are replaced by finite differences the equations obtained will be the equations of straight lines in the corresponding planes x, y and p, q.

Let us study the equations for conjugate characteristics, in particular for the characteristics of the first family in the x, y plane and of the second family in the p, q plane. From (5.3.4) it follows that for the element of a characteristic that is a straight segment in the x, y plane the equation has the form

$$y-y_0=(x-x_0)\,\lambda_1, \tag{5.3.4'}$$

where x_0, y_0 are coordinates of some fixed point; λ_1 is the angular coefficient calculated on the basis of gas parameters at this point; x, y are variable coordinates.

According to (5.3.9) the equation of the element of a characteristic of the second family in the p, q plane can be written in the following way:

$$A\lambda_1(q-q_0)+A(p-p_0)+H(x-x_0)=0, \tag{5.3.9'}$$

where p_0, q_0 are values of functions p and q at point x_0, y_0 in the physical plane; the angular coefficient λ_1 and the values of A, H are worked out from the gas parameters at this point; p and q are variable coordinates.

From these equations it can be seen that the inclination of a straight line in the y, x plane is determined by the angular coefficient λ_1 and in the p, q plane by the angular coefficient $1/\lambda_1$. Similarly it can be shown that the element of a characteristic of the second family in the x, y plane has angular coefficient λ_2 and the element of a conjugate characteristic in the p, q plane has angular coefficient $1/\lambda_2$. From this it can be said that the conjugate characteristics in the two planes are mutually perpendicular.

The above property facilitates the determination of the direction of characteristics in the p, q plane if the direction of the conjugate characteristics in the physical plane is known. Let us assume that the velocity components V_{x0}, V_{y0} and the values of functions p_0, q_0 are known at some point $P(x_0, y_0)$ in the x, y plane. The directions of Mach lines at this point (Fig. 5.3.2) can be determined by equation (5.3.4'). The element of a characteristic of the second family in the form of a straight line in the p, q plane given by equation (5.3.9') corresponds to the element of characteristic PN of the first family in

the x, y plane. This straight line is perpendicular to line PN but does not pass through point P' with coordinates p_0, q_0 due to the independent term in equation (5.3.9′). Therefore to construct the element of a characteristic it is necessary to determine distance δ_1 from point P' to the element using the rules of analytic geometry. Similarly the conjugate characteristic of the first family in the p, q plane which is perpendicular to line PM at distance δ_2 from point P' can be constructed (see Fig. 5.3.2).

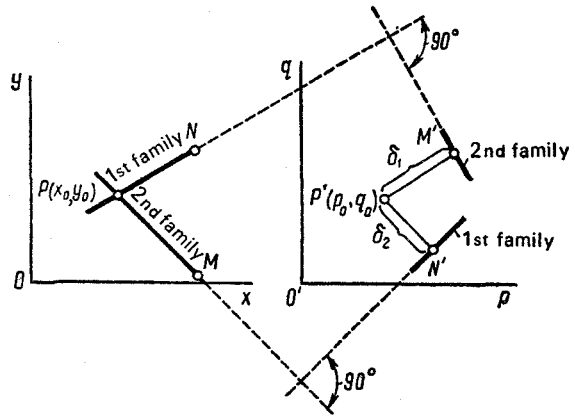

Fig. 5.3.2. Orthogonal property of conjugate characteristics.

The property of orthogonality of conjugate characteristics exists in the case of a potential flow for planes y, x and V_y, V_x (hodograph plane), and also in the case of rotational flow for which plane p, q is replaced by the same hodograph plane V_y, V_x.

3.4 Transformation of equations of characteristics in hodograph plane of velocity

Let us transform equation (5.3.10) into a form such that it can determine the characteristics in the hodograph plane where the velocity components are the coordinates or independent variables. To do this, differentiate (5.1.9′) with respect to x and calculate derivatives dp/dx and dq/dx:

$$\frac{dp}{dx}=\frac{d}{dx}\left(\frac{\partial\psi}{\partial x}\right)=-V_y\,\varepsilon y^{\epsilon-1}\frac{dy}{dx}\,(1-\overline{V}^2)^{1/(k-1)}$$

$$-y^{\epsilon}\frac{dV_y}{dx}\,(1-\overline{V}^2)^{1/(k-1)}+\frac{2y^{\epsilon}}{k-1}\,V_y\,(1-\overline{V}^2)^{\frac{1}{k-1}-1}\,\overline{V}\,\frac{d\overline{V}}{dy}\,; \qquad (5.3.11)$$

$$\frac{dq}{dx}=\frac{d}{dx}\left(\frac{\partial\psi}{\partial y}\right)=V_x\,\varepsilon y^{\epsilon-1}\frac{dy}{dx}\,(1-\overline{V}^2)^{1/(k-1)}$$

$$+y^{\epsilon}\frac{dV_x}{dx}\,(1-\overline{V}^2)^{1/(k-1)}-\frac{2y^{\epsilon}}{k-1}\,V_x\,(1-\overline{V}^2)^{\frac{1}{k-1}-1}\,\overline{V}\,\frac{d\overline{V}}{dx}. \qquad (5.3.12)$$

From equation (5.1.25) it can be seen that

$$\left.\begin{aligned} H=\varepsilon y^{\epsilon-1}\, a^2 V_x\,(1-\overline{V}^2)^{1/(k-1)}-\frac{k-1}{2k}\cdot\frac{V_{\max}^2}{RV}\,(1-\overline{V}^2)^{k/(k-1)} \\ \times y^{\epsilon}\,(a^2-V^2)\frac{dS}{dn}; \\ A=V_x^2-a^2. \end{aligned}\right\} \tag{5.3.13}$$

After substituting (5.3.11) through (5.3.13) in (5.3.10) and replacing the values of dy/dx by angular coefficients of characteristics $\lambda_{1,2}$ and the functions $\tan(\beta\mp\mu)$ by the corresponding values of $\lambda_{2,1}$ we get

$$\begin{aligned} &\varepsilon y^{\epsilon-1}\,\lambda_{1,2}\,(1-\overline{V}^2)^{1/(k-1)}\,(V_x\,\lambda_{2,1}-V_y)+y^{\epsilon}\,(1-\overline{V}^2)^{1/(k-1)} \\ &\times\left(\frac{dV_x}{dx}\,\lambda_{2,1}-\frac{dV_y}{dx}\right)+\frac{2y^{\epsilon}}{k-1}\,(1-\overline{V}^2)^{\frac{1}{k-1}-1}\,\overline{V}\,\frac{d\overline{V}}{dx}\,(V_y-V_x\lambda_{2,1}) \\ &\quad+\frac{1}{V_x^2-a^2}\left[\varepsilon y^{\epsilon-1}\,a^2V_x\,(1-\overline{V}^2)^{1/(k-1)}-\frac{k-1}{2k}\right. \\ &\quad\left.\times\frac{V_{\max}^2}{RV}\,(1-\overline{V}^2)^{k/(k-1)}\,y^{\epsilon}\,(a^2-V^2)\,\frac{dS}{dn}\right]=0. \end{aligned}$$

Effecting the necessary simplifications and introducing nondimensional quantities

$$\overline{V}_x=V_x/V_{\max},\ \overline{V}_y=V_y/V_{\max},\ \overline{V}=V/V_{\max},\ V/a=\mathbf{M},$$

this equation can be rewritten in the following way:

$$\begin{aligned} &\frac{\varepsilon}{y}\,\lambda_{1,2}\,(\overline{V}_x\lambda_{2,1}-\overline{V}_y)+\left(\frac{d\overline{V}_x}{dx}\,\lambda_{2,1}-\frac{d\overline{V}_y}{dx}\right)+\frac{2\overline{V}}{k-1}\cdot\frac{\overline{V}_y-\overline{V}_x\,\lambda_{2,1}}{1-\overline{V}^2} \\ &\times\frac{d\overline{V}}{dx}-\frac{\varepsilon}{y}\cdot\frac{\overline{V}_x}{1-V_x^2/a^2}-\frac{k-1}{2k}\cdot\frac{1}{R\overline{V}}\,(1-\overline{V}^2)\,\frac{\mathbf{M}^2-1}{1-V_x^2/a^2}\cdot\frac{dS}{dn}=0. \end{aligned} \tag{5.3.14}$$

Recalling polar angle β, the following expressions can be written for the projection of the velocity vector:

$$\overline{V}_x=\overline{V}\cos\beta,\ \overline{V}_y=\overline{V}\sin\beta. \tag{5.3.15}$$

Differentiating these expressions with respect to x:

$$\left.\begin{aligned} \frac{d\overline{V}_x}{dx}&=\frac{d\overline{V}}{dx}\cos\beta-\overline{V}\sin\beta\,\frac{d\beta}{dx}; \\ \frac{d\overline{V}_y}{dx}&=\frac{d\overline{V}}{dx}\sin\beta+\overline{V}\cos\beta\,\frac{d\beta}{dx}. \end{aligned}\right\} \tag{5.3.16}$$

Inserting (5.3.15) and (5.3.16) in (5.1.14) and recalling that $\tan^2\mu=(\mathbf{M}^2-1)^{-1}$, $\sin^2\mu=\mathbf{M}^{-2}$, we get

$$\frac{d\bar{V}}{dx}\left(\frac{2\bar{V}^2}{k-1}\cdot\frac{\sin\beta-\lambda_{2,1}\cos\beta}{1-\bar{V}^2}+\lambda_{2,1}\cos\beta-\sin\beta\right)-\bar{V}\frac{d\beta}{dx}(\lambda_{2,1}\sin\beta$$
$$+\cos\beta)+\frac{\varepsilon}{y}\bar{V}\left[\lambda_{1,2}(\lambda_{2,1}\cos\beta-\sin\beta)-\frac{\cos\beta}{1-(\cos^2\beta/\sin^2\mu)}\right]$$
$$-\frac{k-1}{2k}\cdot\frac{1}{R\bar{V}}(1-\bar{V}^2)\frac{\cot^2\mu}{1-(\cos^2\beta/\sin^2\mu)}\cdot\frac{dS}{dn}=0.$$

Taking into account that $[(k-1)/2]\ (1-V^2/V^2_{\max})=a^2/V^2_{\max}=\bar{V}^2\sin^2\mu$, we get

$$\frac{dV}{\bar{V}}+d\beta\frac{(\lambda_{2,1}\sin\beta+\cos\beta)\tan^2\mu}{\lambda_{2,1}\cos\beta-\sin\beta}-\varepsilon\frac{dx}{y}$$
$$\times\left[\lambda_{1,2}-\frac{\sin^2\mu\cos\beta}{(\lambda_{2,1}\cos\beta-\sin\beta)(\sin^2\mu-\cos^2\beta)}\right]\tan^2\mu+\frac{dx}{kR}$$
$$\times\frac{\sin^4\mu}{(\sin^2\mu-\cos^2\beta)(\lambda_{2,1}\cos\beta-\sin\beta)}\cdot\frac{dS}{dn}=0. \qquad (5.3.17)$$

Taking into account

$$\lambda_{2,1}=\tan(\beta\mp\mu)\text{ and }\lambda_{1,2}=\tan(\beta\pm\mu)$$

the separate expressions appearing in (5.3.17) can be transformed into the following form:

$$\frac{\lambda_{2,1}\sin\beta+\cos\beta}{\lambda_{2,1}\cos\beta-\sin\beta}=\frac{\tan(\beta\mp\mu)\sin\beta+\cos\beta}{\tan(\beta\mp\mu)\cos\beta-\sin\beta}=\frac{1}{\mp\tan\mu}; \qquad (5.3.18)$$

$$\lambda_{1,2}-\frac{\sin^2\mu\cos\beta}{(\lambda_{2,1}\cos\beta-\sin\beta)(\sin^2\mu-\cos^2\beta)}=\frac{\sin(\beta\pm\mu)}{\cos(\beta\pm\mu)}$$
$$+\frac{\sin^2\mu\cos\beta}{[\tan(\beta\mp\mu)\cos\beta-\sin\beta]\cos(\beta+\mu)\cos(\beta-\mu)}=\frac{\sin(\beta\pm\mu)}{\cos(\beta\pm\mu)}$$
$$\mp\frac{\sin^2\mu\cos\beta\cos(\beta\mp\mu)}{\sin\mu\cos(\beta+\mu)\cos(\beta-\mu)}=\frac{\sin(\beta\pm\mu)}{\cos(\beta\pm\mu)}\mp\frac{\sin\mu\cos\beta}{\cos(\beta\pm\mu)}=\frac{\sin\beta\cos\mu}{\cos(\beta\pm\mu)}; \qquad (5.3.19)$$

$$\frac{\sin^4\mu}{(\sin^2\mu-\cos^2\beta)(\lambda_{2,1}\cos\beta-\sin\beta)}$$
$$=\frac{\sin^4\mu}{\cos(\beta+\mu)\cos(\beta-\mu)[\sin\beta-\tan(\beta\mp\mu)\cos\beta]}$$
$$=\frac{\pm\sin^4\mu\cos(\beta\mp\mu)}{\cos(\beta+\mu)\cos(\beta-\mu)\sin\mu}=\pm\frac{\sin^3\mu}{\cos(\beta\pm\mu)}. \qquad (5.3.20)$$

Taking into account the expressions (5.3.18) through (5.3.20), the equations (5.3.17) for the characteristics of the first and second family respectively take the form:

$$\frac{dV}{V}-\tan\mu d\beta-\varepsilon\frac{dx}{y}\cdot\frac{\sin\mu\sin\beta\tan\mu}{\cos(\beta+\mu)}+\frac{dx}{kR}\cdot\frac{\sin^3\mu}{\cos(\beta+\mu)}\cdot\frac{dS}{dn}=0; \quad (5.3.21)$$

$$\frac{dV}{V}+\tan\mu d\beta-\varepsilon\frac{dx}{y}\cdot\frac{\sin\mu\sin\beta\tan\mu}{\cos(\beta-\mu)}-\frac{dx}{kR}\cdot\frac{\sin^3\mu}{\cos(\beta-\mu)}\cdot\frac{dS}{dn}=0. \quad (5.3.22)$$

The gradient of stagnation pressure dp_0'/dn can be used in the place of the gradient of entropy dS/dn. For this purpose we will use relations (4.3.6) and (4.3.20), which give the formula for the difference in entropy:

$$S_2-S_1=-c_v(k-1)\ln(p_0'/p_0). \quad (5.3.23)$$

Since $c_v(k-1)=R$, the calculation of derivative with respect to n with the notation of $dS_2/dn=dS/dn$, results in

$$\frac{1}{R}\cdot\frac{dS}{dn}=-\frac{1}{p_0'}\cdot\frac{dp_0'}{dn}. \quad (5.3.24)$$

In this way the equations of characteristics in the hodograph plane can be written as follows:

$$\cot\mu\frac{dV}{V}-d\beta-\varepsilon\frac{dx}{y}\cdot\frac{\sin\beta\sin\mu}{\cos(\beta+\mu)}-\frac{dx}{kp_0'}\cdot\frac{\sin^2\mu\cos\mu}{\cos(\beta+\mu)}\cdot\frac{dp_0'}{dn}=0; \quad (5.3.25)$$

$$\cot\mu\frac{dV}{V}+d\beta-\varepsilon\frac{dx}{y}\cdot\frac{\sin\beta\sin\mu}{\cos(\beta-\mu)}+\frac{dx}{kp_0'}\cdot\frac{\sin^2\mu\cos\mu}{\cos(\beta-\mu)}\cdot\frac{dp_0'}{dn}=0. \quad (5.3.26)$$

Let us introduce the new variable

$$\omega=\int_{a^*}^{V}\cot\mu\frac{dV}{V}, \quad (5.3.27)$$

which indicates some angle. The ratio dV/V may be expressed in the form $d\lambda/\lambda\left(\lambda=\frac{V}{a^*}\right)$ and with the help of (3.6.23) $\cot\mu$ may be represented by

$$\cot\mu=\sqrt{M^2-1}=\sqrt{\frac{\lambda^2-1}{1-\frac{k-1}{k+1}\lambda^2}}. \quad (5.3.28)$$

Consequently

$$\omega=\int_1^{\lambda}\sqrt{\frac{\lambda^2-1}{1-\frac{k-1}{k+1}\lambda^2}}\frac{d\lambda}{\lambda}. \quad (5.3.27')$$

This integral can be divided into elementary integrals. For this purpose we use the substitution

$$\Lambda=\sqrt{(\lambda^2-1)\Big/\left(1-\frac{k-1}{k+1}\lambda^2\right)}. \tag{5.3.29}$$

Then

$$\omega=\frac{2}{k+1}\int_0^{\Lambda}\frac{\Lambda^2 d\Lambda}{(1+\Lambda^2)\left(1+\frac{k-1}{k+1}\Lambda^2\right)},$$

or

$$\omega=\int_0^{\Lambda}\frac{d\Lambda}{1+\frac{k-1}{k+1}\Lambda^2}-\int_0^{\Lambda}\frac{d\Lambda}{1+\Lambda^2}.$$

Integration on the right side leads to

$$\omega=\sqrt{\frac{k+1}{k-1}}\tan^{-1}\sqrt{\frac{k-1}{k+1}\cdot\frac{\lambda^2-1}{1-\frac{k-1}{k+1}\lambda^2}}-\tan^{-1}\sqrt{\frac{\lambda^2-1}{1-\frac{k-1}{k+1}\lambda^2}}. \tag{5.3.30}$$

Keeping in view that

$$\lambda_{\max}=\frac{V_{\max}}{a^*}=\sqrt{\frac{k+1}{k-1}},$$

we get

$$\omega=\sqrt{\frac{k+1}{k-1}}\tan^{-1}\sqrt{\frac{\lambda^2-1}{\lambda_{\max}^2-\lambda^2}}-\tan^{-1}\sqrt{\frac{k+1}{k-1}\cdot\frac{\lambda^2-1}{\lambda_{\max}^2-\lambda^2}}. \tag{5.3.30'}$$

Replacing λ in (5.3.30) by M from (5.3.28), we can write

$$\omega=\sqrt{\frac{k+1}{k-1}}\tan^{-1}\sqrt{\frac{k-1}{k+1}(\mathbf{M}^2-1)}-\tan^{-1}\sqrt{\mathbf{M}^2-1}. \tag{5.3.31}$$

From equations (5.3.30') and (5.3.31) it can be seen that the angle ω happens to be the function of λ (or **M**) only and hence it can be calculated in advance. This simplifies the calculation of supersonic gas flows by the method of characteristics.

The values of ω for different Mach numbers **M** at $k=1.4$ are given in Table 5.3.1. In the same table the angles of inclination of the line of disturbances obtained from the formula $\mu=\sin^{-1}(1/\mathbf{M})$ are set out. Using angle ω in (5.3.21) and (5.3.22), we get the equations for characteristics:

$$d(\omega\mp\beta)-\varepsilon\frac{dx}{y}\cdot\frac{\sin\beta\sin\mu}{\cos(\beta\pm\mu)}\pm\frac{dx}{kR}\cdot\frac{\sin^2\mu\cos\mu}{\cos(\beta\pm\mu)}\cdot\frac{dS}{dn}=0. \tag{5.3.32}$$

TABLE 5.3.1

M	ω°	μ°	M	ω°	μ°
1.0	0.000	90.000	5.6	82.032	10.287
1.1	1.336	65.380	5.7	82.796	10.104
1.2	3.558	56.443	5.8	83.537	9.928
1.3	6.170	50.285	5.9	84.256	9.758
1.4	8.987	45.585	6.0	84.955	9.594
1.5	11.905	41.810	6.1	85.635	9.435
1.6	14.861	38.682	6.2	86.296	9.282
1.7	17.810	36.032	6.3	86.937	9.133
1.8	20.725	33.749	6.4	87.561	8.989
1.9	23.586	31.757	6.5	88.168	8.850
2.0	26.380	30.000	6.6	88.759	8.715
2.1	29.097	28.437	6.7	89.335	8.584
2.2	31.732	27.036	6.8	89.895	8.457
2.3	34.283	25.771	6.9	90.441	8.333
2.4	36.746	24.624	7.0	90.973	8.213
2.5	39.124	23.578	7.1	91.491	8.097
2.6	41.415	22.620	7.2	91.997	7.984
2.7	43.621	21.738	7.3	92.490	7.873
2.8	45.746	20.925	7.4	92.970	7.776
2.9	47.790	20.171	7.5	93.440	7.662
3.0	49.757	19.471	7.6	93.898	7.561
3.1	51.650	18.819	7.7	94.345	7.462
3.2	53.470	18.210	7.8	94.781	7.366
3.3	55.222	17.640	7.9	95.208	7.272
3.4	56.907	17.105	8.0	95.625	7.181
3.5	58.530	16.602	8.2	96.430	7.005
3.6	60.091	16.128	8.4	97.200	6.837
3.7	61.595	15.680	8.6	97.936	6.677
3.8	63.044	15.258	8.8	98.642	6.525
3.9	64.440	14.857	9.0	99.318	6.379
4.0	65.785	14.478	9.2	99.967	6.240
4.1	67.082	14.117	9.4	100.589	6.107
4.2	68.333	13.774	9.6	101.188	5.979
4.3	69.541	13.448	9.8	101.763	5.857
4.4	70.706	13.137	10.0	102.316	5.739
4.5	71.832	12.814	10.2	102.849	5.626
4.6	72.919	12.556	10.4	103.362	5.518
4.7	73.970	12.284	10.6	103.857	5.413
4.8	74.986	12.025	10.8	104.335	5.313
4.9	75.969	11.776	11.0	104.796	5.216
5.0	76.920	11.537	11.2	105.241	5.123
5.1	77.841	11.308	11.4	105.671	5.032
5.2	78.732	11.087	11.6	106.087	4.945
5.3	79.596	10.876	11.8	106.489	4.861
5.4	80.433	10.672	12.0	106.879	4.780
5.5	81.245	10.476			

The corresponding substitution in (5.3.25) and (5.3.26) gives:

$$d(\omega \mp \beta) - \varepsilon \frac{dx}{y} \cdot \frac{\sin\beta \sin\mu}{\cos(\beta \pm \mu)} \mp \frac{dx}{kp_0'} \cdot \frac{\sin^2\mu \cos\mu}{\cos(\beta \pm \mu)} \cdot \frac{dp_0'}{dn} = 0. \quad (5.3.33)$$

Equations (5.3.32) and (5.3.33) correspond to the most general case of a supersonic two-dimensional (plane or axisymmetric) rotational (nonisentropic) gas flow.

3.5 Equations of characteristics in the hodograph plane for particular cases of gas motion

The form of the equation of characteristics (5.2.5) in the physical plane is unique for all the cases of gas flow if this flow is supersonic and two-dimensional. But in the hodograph plane the equations for characteristics will be different depending on the type of flows.

If the two-dimensional flow is irrotational then, by (5.1.23), the entropy at all points in space will be constant ($dS/dn=0$) and hence the equations of characteristics assume their most simple form:

$$d(\omega \mp \beta) - \varepsilon \frac{dx}{y} \cdot \frac{\sin\beta \sin\mu}{\cos(\beta \pm \mu)} = 0. \quad (5.3.34)$$

For a plane nonisentropic flow ($\varepsilon=0$)

$$d(\omega \mp \beta) \pm \frac{dx}{kR} \frac{\sin^2\mu \cos\mu}{\cos(\beta \pm \mu)} \cdot \frac{dS}{dn} = 0. \quad (5.3.35)$$

In the most simple case of a plane irrotational flow ($dS/dn=0$) we have

$$d(\omega \mp \beta) = 0. \quad (5.3.36)$$

Integrating (5.3.36), we get $\beta = \pm\omega + \text{const}$. Inserting some fixed values of angles β_1 and β_2 in place of the constant, the first of which corresponds to the plus sign and the second to the minus sign, we find equations of characteristics in the form

$$\beta = \pm\omega + \beta_{1,2}. \quad (5.3.37)$$

Introducing the relation (5.3.30′) in place of ω, we have

$$\beta = \pm\left(\sqrt{\frac{k+1}{k-1}} \tan^{-1}\sqrt{\frac{\lambda^2-1}{\lambda_{\max}^2-\lambda^2}} - \tan^{-1}\sqrt{\frac{k+1}{k-1} \cdot \frac{\lambda^2-1}{\lambda_{\max}^2-\lambda^2}}\right) + \beta_{1,2}. \quad (5.3.38)$$

Thus, unlike equation (5.2.5) for the characteristics in the physical plane and equations (5.3.32), (5.3.34) or (5.3.35) for the characteristics in the hodograph plane having differential form, the corresponding equations (5.3.38) of the characteristics of a plane isentropic flow have a simple form. Geometrically these equations determine two families of curves—characteristics lying in a

circular ring with an internal radius of $\lambda=1$ and an external radius of $\lambda=[(k+1)/(k-1)]^{1/2}$ (Fig. 5.3.3). The constant of integration β_1 and the plus sign before functions $\omega(\lambda)$ refer to the characteristic of the first family while the constant β_2 and minus sign before $\omega(\lambda)$ correspond to the characteristic of the second family. These curves are epicycloids which can be obtained by following the motion of the points on the circle of radius 1/2 ($\lambda_{max}-1$) (see Fig. 5.3.3). The polar coordinates of the points of the epicycloid happen to be angle of inclination β of the velocity vector and the relative velocity λ.

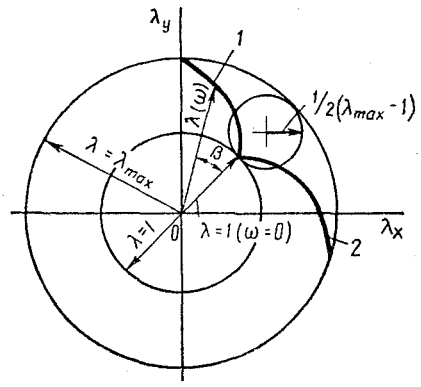

Fig. 5.3.3. Epicycloids—characteristics of plane supersonic flow:

1—characteristic of first family; *2*—characteristic of second family.

Analyzing the graph on which the network of epicycloids is represented, it can be said that the increase in velocity based on the expansion of flow corresponds to the higher values of angle β, i.e. to the considerably larger deviation of flow from the original direction. At low velocities the deviation of flow direction will be small.

The angle of inclination of the velocity vector is directly determined by angle ω whose physical significance can be established from (5.3.37). Let us assume that the constants of integration $\beta_{1,2}=0$. This indicates that expansion of flow begins from the conditions of $\beta=0$ and $\mathbf{M}=1$. Accordingly the quantity $\beta=\pm\omega$ (**M**) will represent the angle of flow deviation during its isentropic expansion from the point where $\mathbf{M}=1$ up to the state characterized by some arbitrary Mach number $\mathbf{M}>1$ which is the upper limit of integration (5.3.27′).

From the above discussion the difference between the angle of inclination of flow at $\mathbf{M}>1$ from some original direction and the angle $\beta=\pm\omega$ is obvious. Here β determines the total turning of flow during its expansion from the condition of Mach number $\mathbf{M}=1$.

The angle of deviation of flow at some arbitrary section can be determined in the following way: Let us assume that the initial Mach number $\mathbf{M}_1>1$ is known. This may have increased during expansion of the flow to the value $\mathbf{M}_2>\mathbf{M}_1$. The Mach numbers $\mathbf{M}_1$ and $\mathbf{M}_2$ correspond to the angles of flow inclination ω_1 and ω_2 from the flow direction at the point where Mach number $\mathbf{M}=1$. These angles could be obtained graphically with the help of one of the epicycloids of the expressions (5.3.31) or Table 5.3.1. From the values of ω_1 and ω_2 the angles of inclination of velocity vectors can be found.

Examining, in particular, the characteristic of the first family, we get

$$\beta_1=\omega_1(\mathbf{M}_1),\ \beta_2=\omega_2(\mathbf{M}_2).$$

Consequently the angle of inclination from the original direction will be

$$\Delta\beta=\beta_2-\beta_1=\omega_2(\mathbf{M}_2)-\omega_1(\mathbf{M}_1). \tag{5.3.39}$$

The calculations may be carried out in reverse order, i.e. by determining the corresponding local Mach number $\mathbf{M}_2$ from the known angle of flow inclination $\Delta\beta$ and the initial Mach number $\mathbf{M}_1$. So we calculate from (5.3.39) (in the example given it is also desired to know the characteristic of the first family):

$$\omega_2(\mathbf{M}_2)=\Delta\beta+\omega_1(\mathbf{M}_1). \tag{5.3.40}$$

From the graph or Table 5.3.1 we find the values of λ_2 or $\mathbf{M}_2$ corresponding to the value of ω_2.

It is useful to calculate the critical angle of flow deviation. This is needed to obtain the maximum velocity $V_{\max}$. Let us assume that the flow begins to turn from the initial value of Mach number $\mathbf{M}=1$. In this case the critical value of the angle of flow deviation could be found from formula (5.3.31), in which it is required to take the value of $\mathbf{M}$ for the value of $V_{\max}$ equal to infinity:

$$\omega_{\max}=\sqrt{\frac{k+1}{k-1}}\frac{\pi}{2}-\frac{\pi}{2}=\frac{\pi}{2}\left(\sqrt{\frac{k+1}{k-1}}-1\right),$$

or for $k=1.4$

$$\omega_{\max}=0.726\pi=130^\circ\ 46'.$$

Thus a supersonic flow cannot turn by an angle exceeding $\omega_{\max}$ and theoretically it can be said that a portion of space remains empty of gas.

If the initial Mach number $\mathbf{M}$ at which the flow deviation starts is more than unity the angle of this deviation from the flow direction at $\mathbf{M}=1$ will be $\omega(\mathbf{M})$ and the critical angle of flow deviation corresponding to this Mach number will be

$$\beta_{\max}=\omega_{\max}-\omega(\mathbf{M})=\frac{\pi}{2}\left(\sqrt{\frac{k+1}{k-1}}-1\right)-\omega(\mathbf{M}),$$

or at $k=1.4$

$$\beta_{\max}=130^\circ\ 46'-\omega(\mathbf{M}).$$

At hypersonic flows the calculation of function ω and the respective angle of flow deviation becomes simple. Actually at $\mathbf{M}\gg 1$ the terms appearing in (5.3.31) can be represented in the following form with an accuracy of higher order:

$$\sqrt{\frac{k+1}{k-1}}\tan^{-1}\sqrt{\frac{k-1}{k+1}(\mathbf{M}^2-1)}\approx\sqrt{\frac{k+1}{k-1}}\left(\frac{\pi}{2}-\frac{1}{\mathbf{M}}\sqrt{\frac{k+1}{k-1}}\right);$$

$$\tan^{-1}\sqrt{\mathbf{M}^2-1}\approx\frac{\pi}{2}-\frac{1}{\mathbf{M}}.$$

Then

$$\omega=\frac{\pi}{2}\left(\sqrt{\frac{k+1}{k-1}}-1\right)-\frac{2}{k-1}\cdot\frac{1}{\mathbf{M}}. \tag{5.3.41}$$

All the above relations are obtained for a perfect gas. However, at very low pressure the properties of a perfect gas are not observed. Therefore these calculated angles of flow deviation are not realized in practice and have only theoretical importance. The formula corresponding to (5.3.39) takes the form

$$\Delta\beta=\beta_2-\beta_1=-\frac{2}{k-1}\left(\frac{1}{\mathbf{M}_2}-\frac{1}{\mathbf{M}_1}\right). \tag{5.3.39'}$$

4. Scheme of Solving Gas Dynamic Problems by Method of Characteristics

Determination of the parameters of a disturbed supersonic gas flow is related to the solution of a system of equations for an conjugate characteristics in the physical and hodograph planes if the initial conditions are in some respects given in the form of Cauchy's conditions. In the general case of a two-dimensional nonisentropic flow this system takes the following forms:

for characteristics of the first family

$$dy=dx\tan(\beta+\mu); \tag{5.4.1}$$

$$d(\omega-\beta)-\varepsilon\frac{dx}{y}l+\frac{dx}{kR}c\frac{dS}{dn}=0; \tag{5.4.2}$$

for characteristics of the second family

$$dy=dx\tan(\beta-\mu); \tag{5.4.3}$$

$$d(\omega+\beta)-\varepsilon\frac{dx}{y}m-\frac{dx}{kR}t\frac{dS}{dn}=0, \tag{5.4.4}$$

where l, c, m, t are coefficients:

$$l=\frac{\sin\beta\sin\mu}{\cos(\beta+\mu)},\quad c=\frac{\sin^2\mu\cos\mu}{\cos(\beta+\mu)}; \tag{5.4.5}$$

$$m=\frac{\sin\beta\sin\mu}{\cos(\beta-\mu)},\quad t=\frac{\sin^2\mu\cos\mu}{\cos(\beta-\mu)}; \tag{5.4.6}$$

for a two-dimensional isentropic flow

$$\frac{dS}{dn}=0. \tag{5.4.7}$$

Therefore the system of equations is simplified as follows:

for characteristics of the first family

$$\left.\begin{aligned} dy&=dx\tan(\beta+\mu);\\ d(\omega-\beta)&-\varepsilon(dx/y)\,l=0; \end{aligned}\right\} \tag{5.4.8}$$

for characteristics of the second family

$$\left.\begin{aligned} dy&=dx\tan(\beta-\mu);\\ d(\omega+\beta)&-\varepsilon(dx/y)m=0. \end{aligned}\right\} \tag{5.4.9}$$

For a plane flow $\varepsilon=0$ in the above equations and for an axisymmetric flow $-\varepsilon=1$ and y is replaced by r.

The solution of any problem of flow-interaction over a body by the method of characteristics consists of three basic problems:

First problem: This deals with the determination of velocity and other parameters at a point of intersection of the characteristics of different families originating from two closely situated points.

Suppose we have to determine the flow parameters (velocity V_C, Mach number $\mathbf{M}_C$, angle of flow deviation β_C, entropy S_C, etc.) at a point C lying at the intersection of the elements of the characteristics from points A and B of the first and second families (Fig. 5.4.1, a). The velocities V_A, V_B and other parameters including S_A and S_B are known at these two points lying on two different stream lines of flow.

All calculations are based on the use of equations of characteristics (5.4.1) through (5.4.4), which can be written in terms of finite differences:

for the first family

$$\Delta y_B=\tan(\beta_B+\mu_B)\Delta x_B; \tag{5.4.10}$$

$$\Delta\omega_B-\Delta\beta_B-\varepsilon\frac{\Delta x_B}{y_B}l_B+\frac{\Delta x_B}{kR}\cdot\frac{\Delta S}{\Delta n}c_B=0; \tag{5.4.11}$$

and for the second family

$$\Delta y_A=\tan(\beta_A-\mu_A)\Delta x_A; \tag{5.4.12}$$

$$\Delta\omega_A+\Delta\beta_A-\varepsilon\frac{\Delta x_A}{y_A}m_A-\frac{\Delta x_A}{kR}\cdot\frac{\Delta S}{\Delta n}t_A=0, \tag{5.4.13}$$

where

$$\left.\begin{aligned} &\Delta y_B=y_C-y_B,\ \Delta x_B=x_C-x_B,\ \Delta\omega_B=\omega_C-\omega_B,\ \Delta\beta_B=\beta_C-\beta_B;\\ &\Delta y_A=y_C-y_A,\ \Delta x_A=x_C-x_A,\ \Delta\omega_A=\omega_C-\omega_A,\ \Delta\beta_A=\beta_C-\beta_A; \end{aligned}\right\} \tag{5.4.14}$$

$$\left.\begin{aligned} l_B &= \frac{\sin\beta_B \sin\mu_B}{\cos(\beta_B+\mu_B)}, \quad c_B = \frac{\sin^2\mu_B \cos\mu_B}{\cos(\beta_B+\mu_B)}; \\ m_A &= \frac{\sin\beta_A \sin\mu_A}{\cos(\beta_A-\mu_A)}, \quad t_A = \frac{\sin^2\mu_A \cos\mu_A}{\cos(\beta_A-\mu_A)}. \end{aligned}\right\} \tag{5.4.15}$$

Equations (5.4.10) through (5.4.13) are written on the assumption that the coefficients l, m, c and t remain constant along the elements of characteristics BC and AC and are equal to their values at the initial points B and A.

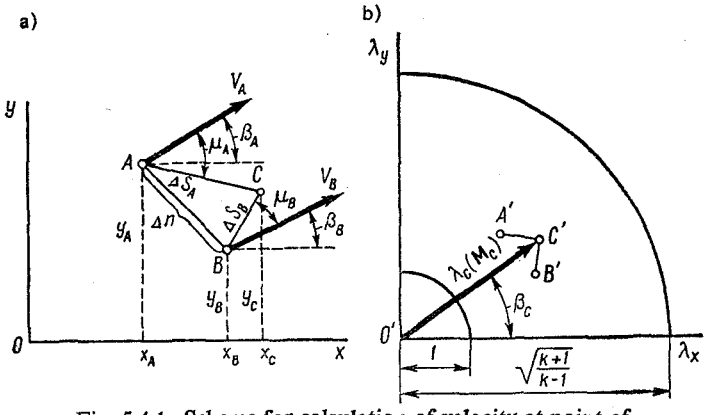

Fig. 5.4.1. Scheme for calculation of velocity at point of intersection of two characteristics of different families:

a—physical plane; *b*—hodograph plane.

The variation over unit length of normal $\Delta S/\Delta n$ is calculated in the following way: From Fig. 5.4.1, a it can be seen that the distance from point B to point A is

$$\Delta n \approx (AC)\sin\mu_A + (BC)\sin\mu_B,$$

where

$$AC = \frac{x_C - x_A}{\cos(\beta_A-\mu_A)}, \quad BC = \frac{x_C - x_B}{\cos(\beta_B+\mu_B)}.$$

Introducing the notation

$$e = (x_C - x_A)\sin\mu_A \cos(\beta_B+\mu_B),$$
$$f = (x_C - x_B)\sin\mu_B \cos(\beta_A-\mu_A),$$

we get

$$\frac{\Delta S}{\Delta n} = \frac{(S_A - S_B)\cos(\beta_B+\mu_B)\cos(\beta_A-\mu_A)}{f+e}. \tag{5.4.16}$$

Entropy at point C is determined from the relation

$$S_C=\Delta S_B+S_B=\frac{\Delta S}{\Delta n}(BC)\sin\mu_B+S_B=\frac{(S_A-S_B)f}{f+e}+S_B. \quad (5.4.17)$$

The entropy gradient can be replaced by the gradient of stagnation pressure using equation (5.3.24):

$$\frac{1}{R}\cdot\frac{\Delta S}{\Delta n}=-\frac{1}{p_0'}\cdot\frac{\Delta p_0'}{\Delta n}=-\frac{(p_{0A}'-p_{0B}')\cos(\beta_B+\mu_B)\cos(\beta_A-\mu_A)}{(f+e)\,p_{0B}'}. \quad (5.4.18)$$

The stagnation pressure at point C will be

$$p_{0C}'=\frac{(p_{0A}'-p_{0B}')f}{f+e}+p_{0B}'. \quad (5.4.19)$$

To determine the coordinate x_C, y_C of point C it is necessary to solve the system of equations (5.4.10), (5.4.12) for the elements of characteristics in the physical plane:

$$y_C-y_B=(x_C-x_B)\tan(\beta_B+\mu_B);$$
$$y_C-y_A=(x_C-x_A)\tan(\beta_A-\mu_A).$$

The graphical solution of these equations is shown in Fig. 5.4.1, a. From the value of x_C obtained the differences $\Delta x_B=x_C-x_B$, $\Delta x_A=x_C-x_A$ appearing in equations (5.4.11), (5.4.13) are determined. The increments $\Delta\omega_B$, $\Delta\omega_A$, $\Delta\beta_B$ and $\Delta\beta_A$ happen to be the unknowns in these equations. The number of unknowns should be reduced to two according to the number of equations in the system. For this purpose let us write the obvious relations:

$$\left.\begin{aligned}\Delta\omega_A&=\omega_C-\omega_A=\Delta\omega_B+\omega_B-\omega_A;\\ \Delta\beta_A&=\beta_C-\beta_A=\Delta\beta_B+\beta_B-\beta_A.\end{aligned}\right\} \quad (5.4.20)$$

Equation (5.4.13) will be transformed with help of these equations into:

$$\Delta\omega_B+\omega_B-\omega_A+\Delta\beta_B+\beta_B-\beta_A-\varepsilon\frac{\Delta x_A}{y_A}m_A-\frac{\Delta x_A}{kR}\cdot\frac{\Delta S}{\Delta n}t_A=0. \quad (5.4.21)$$

Solving this equation together with (5.4.11) to find the variable $\Delta\beta_B$, we get

$$\Delta\beta_B=\frac{1}{2}\left[\frac{1}{kR}\cdot\frac{\Delta S}{\Delta n}(\Delta x_A t_A+\Delta x_B c_B)+\varepsilon\left(\frac{\Delta x_A}{y_A}m_A-\frac{\Delta x_B}{y_B}l_B\right)\right.$$
$$\left.-(\omega_B-\omega_A)-(\beta_B-\beta_A)\right]. \quad (5.4.22)$$

From the value of $\Delta\beta_B$ so obtained we calculate the increase in function from equation (5.4.11):

$$\Delta\omega_B=\Delta\beta_B+\varepsilon\frac{\Delta x_B}{y_B}l_B-\frac{\Delta x_B}{kR}\cdot\frac{\Delta S}{\Delta n}c_B. \quad (5.4.23)$$

Now it is possible to find the angles for the point C:

$$\left.\begin{aligned}\beta_C&=\Delta\beta_B+\beta_B;\\ \omega_C&=\Delta\omega_B+\omega_B.\end{aligned}\right\} \quad (5.4.24)$$

Now from the value of ω_C so obtained the Mach number $\mathbf{M}_C$ and Mach angle μ_C at a point C can be determined from Table 5.3.1.

The scheme of the graphic solution of the system of characteristic equations in the hodograph plane determining angle β_C and Mach number λ_C ($\mathbf{M}_C$) is shown in Fig. 5.4.1, b where $B'C'$ and $A'C'$ are the elements of characteristics of first and second families corresponding to the elements of conjugate characteristics BC and AC in the physical plane. From the value of Mach number $\mathbf{M}_C$ (or λ_C) obtained the parameters like pressure, density, temperature, etc. can be worked out if necessary.

The accuracy of the calculated parameters can be increased if the values of angles β and μ between points A and C and points B and C are used in equations (5.4.10) through (5.4.13) in place of l_B, m_A, c_B, t_A as a first approximation, i.e. if they are replaced by the respective values of:

$$\left.\begin{aligned} \mu_A^{(2)}=(\mu_A+\mu_C)/2,\ \mu_B^{(2)}=(\mu_B+\mu_C)/2;\\ \beta_A^{(2)}=(\beta_A+\beta_C)/2,\ \beta_B^{(2)}=(\beta_B+\beta_C)/2. \end{aligned}\right\} \tag{5.4.25}$$

The more accurate coordinates x_C, y_C of point C will be obtained from the equations:

$$\left.\begin{aligned} \Delta y_B=\tan(\beta_B^{(2)}+\mu_B^{(2)})\,\Delta x_B;\\ \Delta y_A=\tan(\beta_A^{(2)}-\mu_A^{(2)})\,\Delta x_A. \end{aligned}\right\} \tag{5.4.26}$$

Second problem: This concerns the calculation of velocity at a point of intersection of the solid wall and the characteristic. Let point B be situated at the intersection of the wall and the straight element DB of characteristics of the second family drawn from point D and situated near the wall (Fig. 5.4.2). The magnitude and direction of velocity, entropy and coordinates of this point are known.

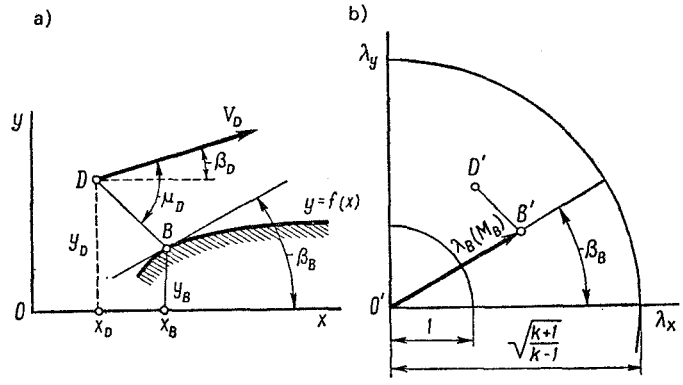

Fig. 5.4.2. Scheme for calculation of velocity at point of intersection of characteristic with wall:

a—physical plane; *b*—hodograph plane.

The determination of velocity at point B is done directly with the help of the equation (5.4.4) for the characteristics of the second family. If this equation is taken with the conditions along the element of characteristic DB and expressed in terms of finite difference,

$$\Delta\omega_D = -\Delta\beta_D + \varepsilon \frac{\Delta x_D}{y_D} m_D - \frac{\Delta x_D}{kR} \cdot \frac{\Delta S}{\Delta n} t_D, \tag{5.4.27}$$

where

$$\left.\begin{aligned} &\Delta\omega_D = \omega_B - \omega_D,\ \Delta\beta_D = \beta_B - \beta_D;\ \Delta x_D = x_B - x_D; \\ &m_D = \frac{\sin\beta_D \sin\mu_D}{\cos(\beta_D - \mu_D)},\ t_D = \frac{\sin^2\mu_D \cos\mu_D}{\cos(\beta_D - \mu_D)}; \end{aligned}\right\} \tag{5.4.28}$$

$$\left.\begin{aligned} &\frac{\Delta S}{\Delta n} = \frac{(S_B - S_D)\cos(\beta_D - \mu_D)}{(x_D - x_B)\sin\mu_D}, \\ \text{or}\quad &\frac{\Delta S}{\Delta n} = -\frac{R}{p'_{0D}} \cdot \frac{\Delta p'_0}{\Delta n} = -\frac{R}{p'_{0D}} \cdot \frac{(p'_{0B} - p'_{0D})\cos(\beta_D - \mu_D)}{(x_D - x_B)\sin\mu_D}. \end{aligned}\right\} \tag{5.4.29}$$

The coordinates x_B, y_B of point B are determined from the simultaneous solution of the equation of characteristics of the second family and the equation of wall contour:

$$\left.\begin{aligned} &y_B - y_D = (x_B - x_D)\tan(\beta_D - \mu_D); \\ &y_B = f(x_B). \end{aligned}\right\} \tag{5.4.30}$$

A graphic solution of these equations is shown in Fig. 5.4.2, a.

Angle β_B can be calculated from equation

$$\tan\beta_B = (dy/dx)_B \tag{5.4.31}$$

using the derived coordinates x_B, y_B. Entropy S_B (or stagnation pressure p'_{0B}) at a point B is supposed to be known: it is equal to its value on the stream line coinciding with the contour of the network on which the entropy is supposed to be constant.

After finding the increment $\Delta\omega_D$ by equation (5.4.27) it is possible to calculate an angle $\omega_B = \Delta\omega_D + \omega_D$ and then Mach number M_B can be determined from Table 5.3.1. The scheme of graphic determination of velocity at a point B is shown in Fig. 5.4.2, b where the element $D'B'$ of the characteristic of the second family in the hodograph corresponds to the element of characteristic of the same family in the physical plane.

Third problem: This consists of the calculation of velocity at the intersection of characteristics with a shock wave and the determination of the deviation of shock at this point. As the characteristic happens to be the line of weak disturbances the above intersection physically refers to the intersection of a weak wave with shock. Let the adjacent expansion waves corresponding

to the characteristics of the first family pass through points S and H on shock MN of given form $y=f(x)$ (Fig. 5.4.3, a). As a result the intensity of shock and hence the inclination of shock diminish. Since points S and H happen to be the sources of disturbances there arise reflected expansion waves and the characteristics of the second family can be drawn through these points. One such characteristic passing through point S intersects the neighboring conjugate characteristic at point F, called the nodal point of characteristics.

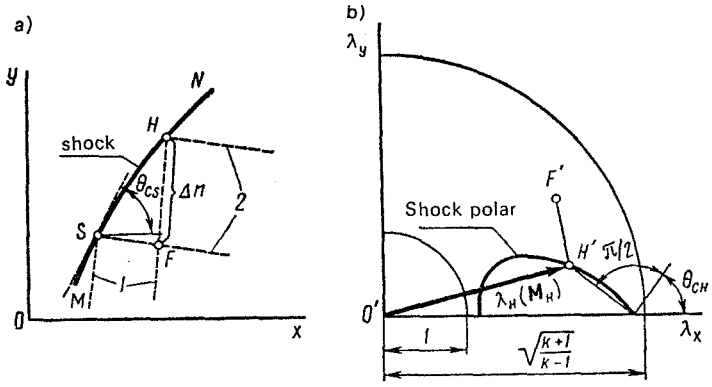

Fig. 5.4.3. Scheme for calculation of velocity at intersection of characteristics with compression shock:

a—physical plane; *b*—hodograph plane; *1*—characteristics of first family; *2*—characteristics of second family.

The properties of characteristics SF and FH passing through nodal point F and the relations for calculation of the shock wave are used to determine the variation in shock deviation and in the velocity behind the shock. As the length SH of the shock is small it can be assumed that this segment is a straight line. The angle of deviation of the shock on this segment and the corresponding gas parameters are approximately equal to their values at point of intersection H of the element FH of the characteristics of the first family with the shock.

One of the unknown parameters is the angle of deviation of velocity vector β_H at this point, which can be represented as $\beta_H=\Delta\beta_F+\beta_F$, where $\Delta\beta_F=\beta_H-\beta_F$ and β_F is the known angle of deviation of the velocity vector at point F. The second unknown, i.e. the Mach number $\mathbf{M}_H$ at the same point, can be determined by the formula

$$\mathbf{M}_H=\mathbf{M}_S+(d\mathbf{M}/d\beta)_S\,\Delta\beta_{SH}, \tag{5.4.32}$$

where $(d\mathbf{M}/d\beta)_S$ is the derivative which can be obtained from the theory of shock for known conditions at point S. Quantity $\Delta\beta_{SH}$, which can be determined from the variation in angle β along an element of shock, is equal to the difference $\beta_H-\beta_S$. This quantity can be taken as approximately equal to

the change in angle β along element FH of the characteristic of the first family $\Delta\beta_{FH}=\beta_H-\beta_F$.

The derivative $d\mathbf{M}/d\beta$ is calculated from the differentiation of (4.3.19′):

$$\frac{d\mathbf{M}}{d\beta}=\frac{d\mathbf{M}_2}{d\beta_C}=-\mathbf{M}_2\left[\cot(\theta_C-\beta_C)\left(\frac{d\theta_C}{d\beta_C}-1\right)\right.$$
$$\left.+\frac{\mathbf{M}_2^2}{2(1-\delta)}\sin^2(\theta_C-\beta_C)\frac{d}{d\beta_C}\left(\frac{\rho_2}{\rho_1}\right)\right]. \tag{5.4.33}$$

The derivative $d(\rho_2/\rho_1)/d\beta_C$ appearing on the right side can be obtained from the differentiation of (4.3.13):

$$\frac{d}{d\beta_C}\left(\frac{\rho_2}{\rho_1}\right)=2\cot\theta_C\left(1-\delta\frac{\rho_2}{\rho_1}\right)\frac{\rho_2}{\rho_1}\cdot\frac{d\theta_C}{d\beta_C}. \tag{5.4.34}$$

The derivative $d\theta_C/d\beta_C$ can be determined as follows: Let us differentiate (4.3.24) first:

$$\frac{d}{d\beta_C}\left(\frac{\rho_2}{\rho_1}\right)=\frac{\rho_2}{\rho_1}\left\{\frac{d\theta_C}{d\beta_C}\left[\frac{1}{\sin\theta_C\cos\theta_C}-\frac{1}{\sin(\theta_C-\beta_C)\cos(\theta_C-\beta_C)}\right]\right.$$
$$\left.+\frac{1}{\sin(\theta_C-\beta_C)\cos(\theta_C-\beta_C)}\right\}.$$

This relation can be slightly modified with the help of (4.3.24):

$$\frac{d}{d\beta_C}\left(\frac{\rho_2}{\rho_1}\right)=\frac{\rho_2}{\rho_1}\frac{1}{\tan\theta_C\cos^2(\theta_C-\beta_C)}$$
$$\times\left\{\frac{d\theta_C}{d\beta_C}\left[\frac{\cos^2(\theta_C-\beta_C)}{\cos^2\theta_C}-\frac{\rho_2}{\rho_1}\right]+\frac{\rho_2}{\rho_1}\right\}. \tag{5.4.35}$$

Equating the right sides of (5.4.34) and (5.4.35) and solving the equation so obtained for the derivative $d\theta_C/d\beta_C$, we find

$$\frac{d\theta_C}{d\beta_C}=\frac{\rho_2}{\rho_1}\left[2\cos^2(\theta_C-\beta_C)\left(1-\delta\frac{\rho_2}{\rho_1}\right)\right.$$
$$\left.-\frac{\cos^2(\theta_C-\beta_C)}{\cos^2\theta_C}+\frac{\rho_2}{\rho_1}\right]^{-1}. \tag{5.4.36}$$

Further, let us write the relation for variation in Mach number $\mathbf{M}$ during transition along the characteristic from point F to point H, i.e. for the quantity $\Delta\mathbf{M}_F=\mathbf{M}_H-\mathbf{M}_F$. For this purpose the expression (5.4.32) can be used here in place of $\mathbf{M}_H$:

$$\Delta\mathbf{M}_F=\mathbf{M}_S+(d\mathbf{M}/d\beta)_S\,\Delta\beta_F-\mathbf{M}_F. \tag{5.4.37}$$

It is possible to replace Mach number $\mathbf{M}$ with function ω obtained from the relation (5.3.31):

$$\Delta\omega_F=\omega_S+(d\omega/d\beta)_S\,\Delta\beta_F-\omega_F, \tag{5.4.38}$$

where

$$\left(\frac{d\omega}{d\beta}\right)_S=\left(\frac{d\mathbf{M}}{d\beta}\right)_S\left(\frac{d\omega}{d\mathbf{M}}\right)_S. \tag{5.4.39}$$

Derivative $d\omega/d\mathbf{M}$ is determined as a result of differentiation (5.3.31):

$$\frac{d\omega}{d\mathbf{M}}=\sqrt{\mathbf{M}^2-1}\left[\mathbf{M}\left(1+\frac{k-1}{2}\mathbf{M}^2\right)\right]^{-1}. \tag{5.4.40}$$

Using the equation (5.4.11) for the characteristics of the first family to the element FH we find

$$\Delta\omega_F-\Delta\beta_F-\varepsilon\frac{\Delta x_F}{y_F}l_F+\frac{\Delta x_F}{kR}\cdot\frac{\Delta S}{\Delta n}c_F=0, \tag{5.4.41}$$

where

$$\Delta\omega_F=\omega_H-\omega_F,\ \Delta\beta_F=\beta_H-\beta_F,\ \Delta x_F=x_H-x_F;$$
$$l_F=\frac{\sin\beta_F\sin\mu_F}{\cos(\beta_F+\mu_F)},\quad C_F=\frac{\sin^2\mu_F\cos\mu_F}{\cos(\beta_F+\mu_F)}. \tag{5.4.42}$$

The distance between points F and H along the normal to the stream line

$$\Delta n=(FH)\sin\mu_F=\frac{x_H-x_F}{\cos(\beta_F+\mu_F)}\sin\mu_F. \tag{5.4.43}$$

Consequently the entropy gradient in equation (5.4.41) will be

$$\frac{\Delta S}{\Delta n}=\frac{(S_H-S_F)\cos(\beta_F+\mu_F)}{(x_H-x_F)\sin\mu_F} \tag{5.4.44}$$

or

$$\frac{\Delta S}{\Delta n}=-\frac{R}{p'_{0F}}\cdot\frac{(p'_{0H}-p'_{0F})\cos(\beta_F+\mu_F)}{(x_H-x_F)\sin\mu_F}, \tag{5.4.45}$$

where p'_{0H} is found from the theory of the shock wave using Mach number $\mathbf{M}_H$.

The entropy S_F or stagnation pressure p'_{0F} at a point F can be approximately taken on the basis of corresponding values at point S on the shock, i.e. $S_F\approx S_S$ and $p'_{0F}\approx p'_{0S}$.

Solving equations (5.4.38), (5.4.41) for $\Delta\beta_F$, we get

$$\Delta\beta_F=\left[\left(\frac{d\omega}{d\beta}\right)_S-1\right]^{-1}\left(\omega_F-\omega_S+\varepsilon\frac{\Delta x_F}{y_F}l_F-\frac{\Delta x_F}{kR}\cdot\frac{\Delta S}{\Delta n}c_F\right). \tag{5.4.46}$$

Substituting the value of $\Delta\beta_F$ in (5.4.38), $\Delta\omega_F$ can be found, the angle $\omega_H=\Delta\omega_H+\omega_F$ can be calculated and Mach number $\mathbf{M}_H$ can be improved. After calculating the angle $\beta_H=\Delta\beta_F+\beta_F$ the new angle of inclination θ_{CH} of the shock at a point H can be found from the value of this angle and the

given Mach number $\mathbf{M}_\infty$. In this way its form on the segment SH is modified. If need be the calculations can be carried out taking values of parameters between points S and H in place of those at point S as a second approximation. In particular the values of 0.5 $(\omega_S+\omega_H)$ and 0.5 $(\beta_S+\beta_H)$ may be taken in place of ω_S, β_S respectively.

The scheme of graphic solution is shown in Fig. 5.4.3, b. The point H' in the hodograph plane corresponding to the point H in the physical plane is determined as a result of the intersection of element $F'H'$ of the characteristic of the first family with the shock polar constructed for a given Mach number $\mathbf{M}_1$ of an undisturbed flow. The vector $O'H'$ determines the velocity λ_H at a point H.

5. Application of Method of Characteristics to Solution of the Problem of Contour Design of Nozzle of a Supersonic Aerodynamic Wind Tunnel

The method of characteristics helps us to solve one of the important problems of gas dynamics regarding the shape of the nozzle of an aerodynamic wind tunnel to obtain a two-dimensional supersonic flow with a given speed. The nozzle providing this flow represents a type of tube with the front and rear walls plane, and the upper and lower walls in the form of a curvilinear specially profiled contour (Fig. 5.5.1).

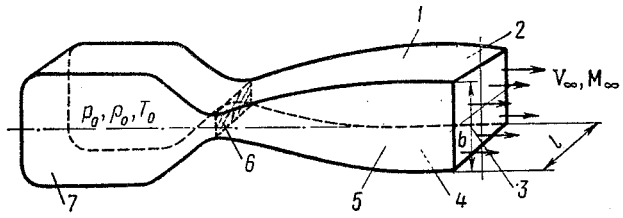

Fig. 5.5.1. Nozzle of supersonic wind tunnel:

1—upper wall; *2*—rear wall; *3*—exit section; *4*—lower wall; *5*—front wall; *6*—critical section; *7*—reservoir.

Along with the determination of the form of the curvilinear contour the calculation of gas parameters at the reservoir (parameters of complete stagnation) and at the critical section of area S^* is included in calculations of the nozzle. The gas parameters at the nozzle exit such as Mach number $\mathbf{M}_\infty$, pressure p_∞, area of exit cross section S and temperature T_0 are usually given quantities. The area of critical nozzle section is found from the equation of flow rate (3.6.44), which may be expressed in the form $\rho_\infty V_\infty S = \rho^* a^* S^*$. From this

$$S^* = (\rho_\infty V_\infty / \rho^* a^*)\, S = \bar{q} S.$$

From (3.6.46′) it follows that the parameter $\bar{q}$ is determined by the given Mach number M_∞ at the nozzle exit. From this value of M_∞ and pressure p_∞ at the nozzle exit the pressure required at reservoir p_0 to achieve the given Mach number M_∞ at exit can be found by the application of formula (3.6.29).

In addition the angle 2γ of a non-profiled nozzle is given (Fig. 5.5.2). As shown by experimental research, this angle is usually selected in the range of 30–35°. Smaller values lead to an excessively long nozzle in which a thick boundary layer is formed on the wall, reducing the effective nozzle cross section. With higher values of the angle of the diffuser flow separation may take place, rendering the application of the nozzle meaningless in experimental research.

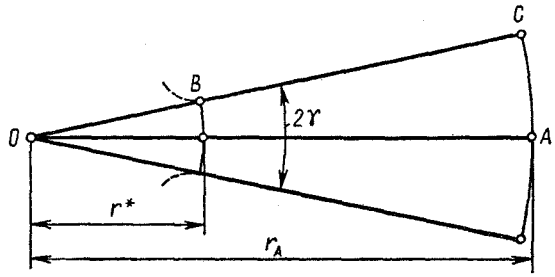

Fig. 5.5.2. Non-profiled plane supersonic nozzle with radial flow.

If the entrance section of the nozzle is smooth enough the motion in the region of the subcritical section can be regarded as an expanding radial flow from the source situated at point O. Such a flow has the property that its direction coincides with the direction of radial lines originating in point O. The variation in the magnitude of gas parameters along all these lines will have the same character. The length of the subsonic zone of a nozzle of unit width is determined by the quantity $r^*=S^*\ [360/(2\pi\times 2\gamma\times 1)]$ and the distance to the exit section $r_A=S[360/(2\pi\times 2\gamma\times 1)]$.

In the part of the nozzle restricted by the arcs of two circles with radii r^* and r_A, i.e. in the limit of the critical section, the gas flow will be supersonic. The profiled nozzle has a straight wall BC in this part so that it provides gradual transition from radial flow to uniform rectilinear flow with a given velocity at the exit. For this purpose we draw a series of closely distributed lines from point O and determine velocity (Mach number M) on these lines at the points of intersection $A_1, A_2, \ldots, A_n$ of the characteristic of one of the families AA_n (this will be considered as the characteristic of the second family), starting from point A on the arc of radius r_A (Fig. 5.5.3). Then point A_1 lies at the intersection of the ray $r_1=OA_1$ with the element of characteristic

AA_1 drawn at an angle of $\mu_\infty = -\sin^{-1}(1/\mathbf{M}_\infty)$, where $\mathbf{M}_\infty$ is the given Mach number at the nozzle exit.

Mach number $\mathbf{M}_1$ at point A_1 can be found with the help of the expression $\bar{q}_1 = S^*/S_1$. As $S_1 = 2\pi r_1 \times 1(2\gamma/360)$, $S^* = 2\pi r^* \times 1(2\gamma/360)$, we have $\bar{q}_1 = r^*/r_1$. Then λ_1 and the corresponding Mach number $\mathbf{M}_1$ can be found from (3.6.46).

Similarly we can determine the coordinates of point of intersection A_2 of neighboring ray $r_2 = OA_2$ with an element of the characteristic A_1A_2 with an inclination of angle $\mu_1 = \sin^{-1}(1/\mathbf{M}_1)$ to the line OA_1. The value of Mach number $\mathbf{M}_2$ and other quantities can be obtained as for the first case. As a result the characteristic of the second family in the form of segments of line $AA_1, A_1A_2, \ldots A_{n-1}A_n$, intersecting the network of straight lines BA_n at point A_n, can be constructed. As at other points A_{n-2}, A_{n-1}, A_n, etc. of intersection of characteristics with the straight lines from the source O, the corresponding Mach numbers and angles $\mu = \sin^{-1}(1/\mathbf{M})$ can be calculated at this point.

The region of flow OAA_n with the known velocity field bounded by the characteristic AA_n and the straight walls of the nozzle is known as the triangle of information. The type of flow is maintained even if the nozzle contour behind point A_n downstream is changed because the disturbances this produces cannot propagate upstream beyond the limit of Mach line AA_n. Here a change of contour can be executed so that the radial flow on the Mach line is gradually transformed to a rectilinear flow of given Mach number $\mathbf{M}_\infty$ at the nozzle exit.

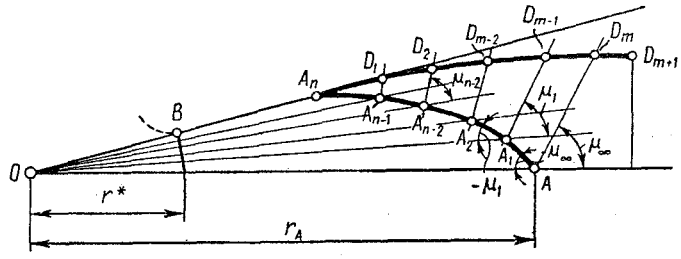

Fig. 5.5.3. Construction of profiled supersonic plane nozzle.

Taking this condition into account, the characteristic of the first family emerging from point A in the form of a straight line can be constructed. Now if the velocity field is determined between the characteristics AA_n and AD_m the corresponding stream lines can be determined. The stream line that passes through point A_n will coincide with the profiled contour of the nozzle.

The condition that in the plane flow we are considering all the characteristics of the first family originating in points A_{n-2}, A_{n-1}, etc. and the characteristic AD_m will be straight lines (see Fig. 5.5.3) is used to determine the velocity field. The inclination of each characteristic to the radial line is determined by the corresponding Mach angle $\mu_1 = \sin^{-1}(1/\mathbf{M}_1)$, $\mu_2 = \sin^{-1}(1/\mathbf{M}_2)$,... etc. The

velocity along the characteristic is determined by the value of velocity at the starting points A_1, A_2,... etc.

Let us consider the stream line emerging from point A_n. The initial part of this line coincides with the direction of velocity at point A_n and represents by itself the line which is an extension of contour BA_n until it intersects with the characteristic of the first family $A_{n-1}A_n$ at a point D_1. Behind point D_1 the element of stream line coincides with the direction of velocity at point D_1, which is equal to the velocity at a point A_{n-1}. Drawing a straight line from point D_1 parallel to ray OA_{n-1} up to the point of intersection D_2 with characteristic $A_{n-2}D_2$, we get the following part of the stream line. Behind point D_2 the stream line on the segment D_2D_{m-2} (the point D_{m-2} lies on the characteristic A_2D_{m-2} of the first family) will be parallel to the line OA_{n-2}. The construction of the remaining segments of stream line can be done the same way. The segment of stream line behind point D_m, lying on the characteristic AD_m, is parallel to the nozzle axis. The contour of the nozzle, coinciding with the stream line A_nD_{m+1} and drawn in the form of a smooth curve, gives a uniform supersonic flow with a given Mach number $\mathbf{M}_\infty$ at the nozzle exit.

This method of profiling does not take care of the effect of the boundary layer on the form of the contour of a nozzle which distorts the character of the flow and changes the form of the stream line from the calculated one. The effect of the boundary layer can be accounted for approximately if the contour at the exit is inclined from the nozzle axis by an angle equal to 10–20′.

Using the equations of characteristics for a two-dimensional flow, the construction of the contour of a circular nozzle can be carried out analogically to give an axisymmetric supersonic flow with a given velocity at the nozzle exit.

6

AN AIRFOIL AND A FINITE WING IN AN INCOMPRESSIBLE FLUID FLOW

In this chapter problems connected with the formulation of aerodynamic theory for the calculation of flow around a wing profile in an incompressible fluid flow will be examined. The formation of a plane disturbed flow around an airfoil is the characteristic feature of this flow-interaction. Aerodynamic equations that are simpler than those for three-dimensional flows are used in this investigation.

Strictly speaking the flow around an airfoil that is supposed to be a plane flow is an idealized situation. In reality the flow around a real wing of finite span will be three-dimensional. Therefore the aerodynamic characteristics of an airfoil cannot be used directly for a finite wing. However, these characteristics can be one of the basic parameters used in calculation of similar characteristics of real wings. Besides this, the solution of the problem of an airfoil has its own importance because the flow over certain parts of a wing is practically a plane flow.

In the present chapter we will confine ourselves to the study of the interaction between an airfoil and plane incompressible fluid flow. At the same time the problem of a finite wing in the same type of flow will be examined. The results so obtained have their own significance and can be used (see Chapters 7 and 8) for aerodynamic study of high-speed motion.

1. Thin Airfoil in Incompressible Flow

Let us consider how to calculate the flow interaction of a steady incompressible fluid flow and a small, thin cambered airfoil at a small angle of attack (Fig. 6.1.1). The results to be obtained from this calculation for the aerodynamic characteristics of an airfoil can be directly used for cases of motion at low subsonic speeds ($M_\infty < 0.3-0.4$) when the gas can be considered as an incompressible medium. These results can also be used as the initial data for aerodynamic calculations of airfoils of given form in a subsonic compressible flow.

As the airfoil is thin and the angle of attack is small the flow velocity near the airfoil will differ insignificantly from the undisturbed flow velocity. This kind of flow is said to be one with small disturbances.

For the velocity of a small perturbation flow the following condition can be written:

$$V_x = V_\infty + u \ (u \ll V_\infty), \ V_y = v \ (v \ll V_\infty), \tag{6.1.1}$$

where u and v are the small perturbation components.

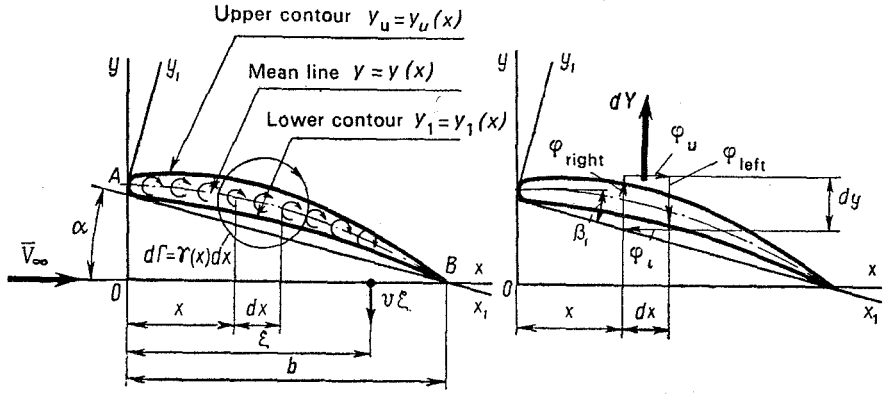

Fig. 6.1.1. Thin profile in incompressible flow.

According to this condition we have

$$V^2 = V_x^2 + V_y^2 = (V_\infty + u)^2 + v^2 \approx V_\infty^2 + 2 V_\infty u. \tag{6.1.2}$$

Now let us determine the pressure in a flow with small disturbances. From Bernoulli's equation in which C_2 is assumed to be equal to $(p_\infty/\rho_\infty) + (V^2_\infty/2)$ and $\rho = \text{const}$ we get the change in pressure

$$p - p_\infty = \rho_\infty \left(\frac{V_\infty^2}{2} - \frac{V^2}{2} \right) = -\rho_\infty V_\infty u. \tag{6.1.3}$$

Determining u here in terms of velocity potential $u = \partial\varphi/\partial x$, we find

$$p - p_\infty = -\rho_\infty V_\infty (\partial\varphi/\partial x). \tag{6.1.4}$$

The corresponding coefficient of pressure will be

$$\bar{p} = \frac{p - p_\infty}{q_\infty} = -\frac{2u}{V_\infty} = -\frac{2}{V_\infty} \cdot \frac{\partial\varphi}{\partial x}. \tag{6.1.5}$$

According to (6.1.4) the pressure difference on the lower side of the airfoil will be $p_l - \rho_\infty = -(\partial\varphi_l/\partial x) V_\infty \rho_\infty$ and on the upper surface

$$p_u - p_\infty = -(\partial\varphi_u/\partial x) V_\infty \rho_\infty,$$

where φ_l, φ_u are the velocity potentials on the lower and upper sides of the airfoil respectively. Consequently the lift force due to pressure acting on an element is

$$dY=(p_l-p_u)\,dx=-V_\infty\,\rho_\infty\left(\frac{\partial\varphi_l}{\partial x}-\frac{\partial\varphi_u}{\partial x}\right)dx,$$

and the lift force of a complete airfoil of chord b is

$$Y=-V_\infty\,\rho_\infty\int_0^b\left(\frac{\partial\varphi_l}{\partial x}-\frac{\partial\varphi_u}{\partial x}\right)dx.$$

The corresponding coefficient of lift force

$$c_y=\frac{Y}{q_\infty\,b}=-\frac{2}{V_\infty\,b}\int_0^b\left(\frac{\partial\varphi_l}{\partial x}-\frac{\partial\varphi_u}{\partial x}\right)dx. \tag{6.1.6}$$

Let us consider the circulation of velocity along a contour having rectangular form with sides dx, dy surrounding an element of the profile. Then from Fig. 6.1.1 the circulation will be

$$d\Gamma=\left(V_\infty+\frac{\partial\varphi_u}{\partial x}\right)dx-\left(V_\infty+\frac{\partial\varphi_l}{\partial x}\right)dx+\left(\frac{\partial\varphi_L}{\partial y}-\frac{\partial\varphi_R}{\partial y}\right)dy.$$

Introducing the concept of intensity of circulation (vortex) determined by the derivative $d\Gamma/dx=\gamma\,(x)$, we get

$$\gamma\,(x)=(\partial\varphi_u/\partial x)-\frac{\partial\varphi_l}{\partial x}+\frac{dy}{dx}\left(\frac{\partial\varphi_L}{\partial y}-\frac{\partial\varphi_R}{\partial y}\right).$$

As the slope dy/dx for a thin airfoil is small the product of this coefficient with the difference in the vertical components of velocity will be a small quantity of second order and hence

$$\gamma\,(x)=(\partial\varphi_u/\partial x)-(\partial\varphi_l/\partial x). \tag{6.1.7}$$

In this way equation (6.1.6) can be written as

$$c_y=(2/V_\infty\,b)\int_0^b\gamma\,(x)\,dx. \tag{6.1.8}$$

Similarly the coefficient of moment is calculated by

$$m_z=(2/V_\infty\,b^2)\int_0^b\gamma\,(x)x\,dx. \tag{6.1.9}$$

From formulas (6.1.8) and (6.1.9) it can be seen that the coefficients of lift and moment due to pressure depend on the distribution of intensity of cir-

culation over the profile. This shows that the flow past an airfoil can be replaced by a system of continuously distributed vortices.

The vertical component of velocity induced at a point with abscissa ξ (see Fig. 6.1.1) by the element of distributed vortex of circulation $d\Gamma=\gamma(x)dx$ may be given by the Biot-Savart formula (2.7.12):

$$dv=d\Gamma/[2\pi\,(x-\xi)]=\gamma\,(x)\,dx/[2\pi\,(x-\xi)].$$

Then the velocity induced at this point by all the vortices will be

$$v=\frac{1}{2\pi}\int_0^b\frac{\gamma\,(x)\,dx}{x-\xi}. \tag{6.1.10}$$

From the boundary condition over the airfoil surface we have $v/(V_\infty+\partial\varphi/\partial x)=dy/dx$. Assuming that the airfoil is thin, $V_\infty=\partial\varphi/\partial x\approx V_\infty$ may be accepted and the derivative may be calculated from the given equation of mean line

$$y=y\,(x)=0.5\,(y_u+y_l), \tag{6.1.11}$$

where $y_u=y_u\,(x)$, $y_l=y_l\,(x)$ are equations of the upper and lower contours of profile respectively.

In this way the distribution of vortices $\gamma\,(x)$ is determined by the integral equation

$$\frac{1}{2\pi V_\infty}\int_0^b\frac{\gamma\,(x)\,dx}{x-\xi}=\left(\frac{dy}{dx}\right)_\xi. \tag{6.1.12}$$

Let us introduce a new independent variable θ in place of x which is determined by the relation

$$x=(b/2)\,(1-\cos\theta). \tag{6.1.13}$$

We will find the solution of equation (6.1.12) in the form of Fourier's trigonometrical series

$$\gamma\,(\theta_0)=2\,V_\infty\left[A_0\cot\frac{\theta_0}{2}+\sum_{n=1}^{\infty}A_n\sin\,(n\theta_0)\right], \tag{6.1.14}$$

in which the variable θ_0, according to (6.1.13), is connected with the coordinate $x=\xi$ by the equation

$$\xi=(b/2)\,(1-\cos\theta_0). \tag{6.1.15}$$

Let us carry out the change of variables in (6.1.12). Differentiating (6.1.13), we get

$$dx=(b/2)\sin\theta\,d\theta. \tag{6.1.16}$$

Substitution of (6.1.14) through (6.1.16) in (6.1.12) results in

$$\frac{A_0}{\pi}\int_0^{\pi}\frac{\cot\frac{\theta}{2}\sin\theta\,d\theta}{\cos\theta_0-\cos\theta}+\frac{1}{\pi}\sum_{n=1}^{\infty}A_n\int_0^{\pi}\frac{\sin(n\theta)\sin\theta\,d\theta}{\cos\theta_0-\cos\theta}=\beta(\theta_0), \tag{6.1.17}$$

where $\beta(\theta_0)=(dy/dx)_{\xi}$.

Since $\cot(\theta/2)=(1+\cos\theta)/\sin\theta$, we have

$$\int_0^{\pi}\frac{\cot\frac{\theta}{2}\sin\theta\,d\theta}{\cos\theta_0-\cos\theta}=\int_0^{\pi}\frac{d\theta}{\cos\theta_0-\cos\theta}+\int_0^{\pi}\frac{\cos\theta\,d\theta}{\cos\theta_0-\cos\theta}.$$

Similarly the second integral in (6.1.17) will be

$$\int_0^{\pi}\frac{\sin(n\theta)\sin\theta\,d\theta}{\cos\theta_0-\cos\theta}=\frac{1}{2}\int_0^{\pi}\frac{\cos[(n-1)\theta]\,d\theta}{\cos\theta_0-\cos\theta}-\frac{1}{2}\int_0^{\pi}\frac{\cos[(n+1)\theta]\,d\theta}{\cos\theta_0-\cos\theta}.$$

It can also be noted [1] that*

$$\int_0^{\pi}\frac{d\theta}{\cos\theta_0-\cos\theta}=0;\quad\int_0^{\pi}\frac{\cos\theta\,d\theta}{\cos\theta_0-\cos\theta}=-\pi.$$

In the same work [1] it is shown that for the integer values* of m there is a formula

$$\int_0^{\pi}\frac{\cos(m\theta)\,d\theta}{\cos\theta_0-\cos\theta}=-\pi\frac{\sin(m\theta_0)}{\sin\theta_0}.$$

Consequently

$$\int_0^{\pi}\frac{\sin(n\theta)\sin\theta\,d\theta}{\cos\theta_0-\cos\theta}=-\frac{\pi}{2}\left\{\frac{\sin[(n-1)\theta_0]}{\sin\theta_0}-\frac{\sin[(n+1)\theta_0]}{\sin\theta_0}\right\}.$$

After substituting the values of the integrals in (6.1.17) we get

$$-A_0+\sum_{n=1}^{\infty}A_n\cos(n\theta_0)=\beta(\theta_0). \tag{6.1.18}$$

Integrating both parts of equation (6.1.18) in the range of 0 to π, we get the relation for coefficient A_0 in the Fourier series:

*These integrals are popularly known as Glauert's integral in the British and American literature—Translator.

$$A_0 = -\frac{1}{\pi}\int_0^{\pi} \beta(\theta)\, d\theta. \tag{6.1.19}$$

Multiplying by $\cos\theta$ and then by $\cos 2\theta$, we find the expressions for the Fourier coefficients A_1 and A_2 respectively. Thus in general

$$A_n = \frac{2}{\pi}\int_0^{\pi} \beta(\theta)\cos(n\theta)\, d\theta. \tag{6.1.20}$$

Let us consider the relation (6.1.8) for the coefficient of lift. Using the variable θ therein and substituting (6.1.16), we get

$$c_y = \frac{1}{V_\infty}\int_0^{\pi} \gamma(\theta)\sin\theta\, d\theta. \tag{6.1.21}$$

Taking into account (6.1.14), this becomes

$$c_y = 2A_0\int_0^{\pi} \cot\frac{\theta}{2}\sin\theta\, d\theta + 2\sum_{n=1}^{\infty} A_n\int_0^{\pi} \sin(n\theta)\sin\theta\, d\theta.$$

Integration of this gives

$$c_y = 2\pi\,[A_0 + (A_1/2)]. \tag{6.1.22}$$

In this way the coefficient of lift depends on the first two coefficients of the series. Substituting expression (6.1.19) and formula (6.1.20) in (6.1.22) with $n=1$, we find

$$c_y = -2\int_0^{\pi} \beta(\theta)(1-\cos\theta)\, d\theta. \tag{6.1.23}$$

Similarly transferring the variable x to θ in (6.1.9), for the coefficient of moment we get

$$m_z = \frac{1}{2V_\infty}\int_0^{\pi} \gamma(\theta)(1-\cos\theta)\sin\theta\, d\theta. \tag{6.1.24}$$

Using the expression (6.1.14) for $\gamma(\theta)$, the coefficient of moment is reduced to

$$m_z = A_0\int_0^{\pi} (1-\cos\theta)^2\, d\theta + \sum_{n=1}^{\infty} A_n\int_0^{\pi} \sin(n\theta)(1-\cos\theta)\sin\theta\, d\theta.$$

Integration of this results in

$$m_z = \frac{\pi}{2}\left(A_0 + A_1 - \frac{A_2}{2}\right). \tag{6.1.25}$$

Taking (6.1.22) into account,

$$m_z=\frac{\pi}{4}(A_1-A_2)+\frac{1}{4}c_y. \tag{6.1.26}$$

Determining the values of A_1 and A_2 from (6.1.20) and substituting in (6.1.26), we get

$$m_z=\frac{1}{2}\int_0^{\pi}\beta(\theta)(\cos\theta-\cos 2\theta)\,d\theta+\frac{1}{4}c_y. \tag{6.1.27}$$

Let us consider the coordinates x_1, y_1 related to an airfoil, in which case the equation of mean line will be $y_1=y_1(x_1)$ and the angle of inclination of tangent will be given by the derivative dy_1/dx_1. This angle (Fig. 6.1.2) is $\beta_1=\beta+a$, where $\beta\approx dy/dx$. Finding the angle $\beta=\beta_1-a$ from this and inserting its value in (6.1.23) and (6.1.27), we get:

$$c_y=2\pi(a+\varepsilon_0); \tag{6.1.28}$$

$$m_z=2\left(\frac{\pi}{4}\varepsilon_0-\mu_0\right)+\frac{1}{4}c_y, \tag{6.1.29}$$

where

$$\left.\begin{aligned}\varepsilon_0&=-\frac{1}{\pi}\int_0^{\pi}\beta_1(1-\cos\theta)\,d\theta;\\ \mu_0&=-\frac{1}{4}\int_0^{\pi}\beta_1(1-\cos 2\theta)\,d\theta.\end{aligned}\right\} \tag{6.1.30}$$

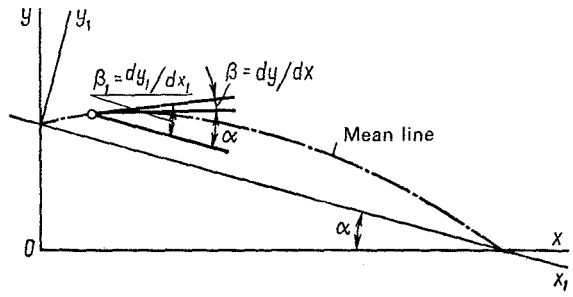

Fig. 6.1.2. Mean line of profile.

From (6.1.28) it follows that the coefficient of lift is equal to zero at $a=-\varepsilon_0$. The angle $a=-\varepsilon_0$ is called the zero lift angle. The coefficients ε_0 and μ_0 are calculated from a given equation of mean line of profile under the condition that the variable $\bar{x}_1$ in the expression for function $\beta_1(\bar{x}_1)$ is replaced in accordance with (6.1.13) by the relation $\bar{x}_1=(1/2)(1-\cos\theta)$.

2. Cross Flow Over Thin Plate

Let us study an incompressible fluid flow over the simplest profile in the form of a thin plate, oriented perpendicularly to the direction of undisturbed velocity of flow. The solution of this problem may serve as an example of the application of the method of conformal transformation for investigating fluid motion. The results are used in real cases to determine the aerodynamic characteristics of finite wings (see Section 4).

Let the plate be placed in the plane of a complex variable $\sigma=z+iy$ along real axis z (Fig. 6.2.1, b). The velocity vector of undisturbed flow $\overline{V}$ will coincide with the direction of imaginary axis y. In this case the flow-interaction of such a plate may be studied by means of conformal transformation from the flow-interaction of a circular cylinder in plane $\zeta=\xi+i\eta$ (Fig. 6.2.1, a). If we know the function $W=f(\zeta)$, representing the complex potential for flow about a circular cylinder, and the analytic function $\zeta=F(\sigma)$ of complex variable $\sigma=z+iy$ (the so-called conformed function), transforming the circular contour in place ζ to the segment of a straight line placed in the flow in plane σ in transverse direction, then the function $W=f[F(\sigma)]$ will represent the complex potential for flow around a flat plate.

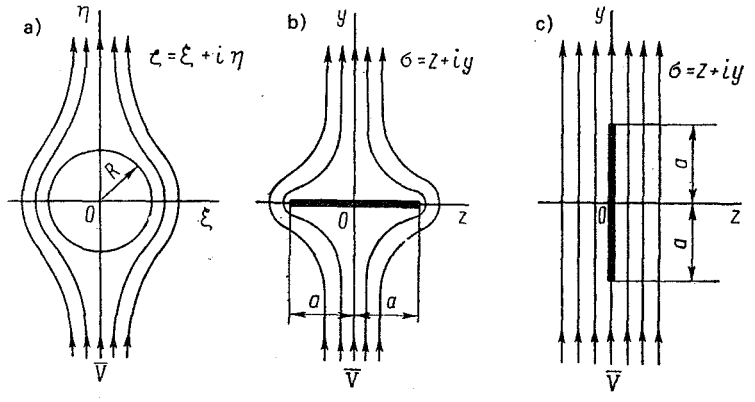

Fig. 6.2.1. Conformal transformation of flow over circular cylinder (*a*) into flow over flat plate oriented vertically to velocity vector of undisturbed flow (*b*) over flat plate oriented along flow (*c*).

We will show that the formula

$$\sigma=\zeta+(R^2/\zeta) \tag{6.2.1}$$

gives this conformal transformation of a circle of radius R in plane ζ to the segment of a line of length $2a=4R$ in plane σ. The equation (6.2.1) can be rewritten in the following way:

$$z+iy=\xi+i\eta+\frac{R^2}{\xi+i\eta},$$

or $$z+iy=\xi+i\eta+\frac{R^2(\xi-i\eta)}{\xi^2+\eta^2}.$$

As $R^2=\xi^2+\eta^2$, after separating the real and imaginary components we get: $z=2\xi$, $y=0$. Thus, the points on a horizontal line of length $2a=4R$ in plane σ correspond to the points on the circle of radius R in plane ξ.

Now we determine the complex potential for the flow around a circular cylinder. The method of conformal transformation, using the known function of complex potential for a flow around a flat plate oriented along the flow, is again used for this purpose. This function has the form

$$W=\varphi+i\psi=-iV(z+iy)=-iV\sigma. \tag{6.2.2}$$

It can easily be shown that the conformal function

$$\sigma=\zeta-(R^2/\zeta) \tag{6.2.3}$$

transforms the segment of straight line in plane σ placed along the flow into the circle in plane ζ (see Fig. 6.2.1, a and c). Practically speaking, it follows from (6.2.3) that since for the points situated on the line $\sigma=iy$ ($-2R\leqslant y\leqslant 2R$, $z=0$), we have

$$\zeta=\xi+i\eta=\frac{iy}{2}\pm\sqrt{R^2-\frac{y^2}{4}}.$$

Separating the real and imaginary parts of this equation, we get:

$$\eta=y/2,\ \xi=\pm\sqrt{R^2-(y^2/4)},$$

whence $\xi^2+\eta^2=R^2$. Thus the points lying on the circle in plane σ correspond to the points lying on the vertical segment of line in plane ζ. Replacement of σ in (6.2.2) by the value from (6.2.3) leads to the complex potential of flow around a circular cylinder of radius R in a rectilinear plane flow with velocity V:

$$W=-iV\left(\zeta-\frac{R^2}{\zeta}\right). \tag{6.2.4}$$

To obtain the complex potential for the flow past a flat plate placed across the flow (see Fig. 6.2.1, b) the following value of ζ obtained from the formula (6.2.1) is to be used in (6.2.4):

$$\zeta=\frac{\sigma}{2}\pm\sqrt{\frac{\sigma^2}{4}-R^2}. \tag{6.2.5}$$

Then

$$W=-iV\left(\frac{\sigma}{2}\pm\sqrt{\frac{\sigma^2}{4}-R^2}-\frac{R^2}{\frac{\sigma}{2}\pm\sqrt{\frac{\sigma^2}{4}-R^2}}\right). \tag{6.2.6}$$

As $\sigma=z$ for the points lying on the plate where $-a\leqslant z\leqslant a$ ($a=2R$) the complex potential will be

$$W=-iV\left(\frac{z}{2}\pm i\sqrt{R^2-\frac{z^2}{4}}-\frac{R^2}{\frac{z}{2}\pm i\sqrt{R^2-\frac{z^2}{4}}}\right).$$

From this the potential function will be

$$\varphi=\pm V\sqrt{4R^2-z^2}=\pm V\sqrt{a^2-z^2}, \tag{6.2.7}$$

where the plus sign refers to the upper surface and the minus sign to the lower surface.

Calculating the derivative $\partial\varphi/\partial z$, the velocity past the plate and the pressure can be found. From the details obtained it follows that the pressure on the upper and lower surfaces of the plate is the same. Consequently in the case of an unseparated flow over a flat plate across the flow of an ideal (inviscid) fluid the plate has no drag force. This interesting aerodynamic effect will be studied in the example of the flow-interaction of a flat plate placed in a flow at some finite angle of attack in Section 3.

The flow characterized by the potential function (6.2.7) is shown in Fig. 6.2.1, b. This flow can be represented as an irrotational flow around the plate which can be obtained by superposition of the flow from the dipole with potential

$$W_\infty=-iV\zeta \tag{6.2.8}$$

to the undisturbed flow with potential

$$W_{\text{dip}}=\pm iV\,(R^2/\zeta), \tag{6.2.9}$$

where ζ is determined by the function (6.2.5).

3. Thin Plate at An Angle of Attack

Let us find the potential function for a disturbed flow of incompressible fluid past a thin plate oriented at an angle of attack a using the method of conformal transformation as in the previous problem (see Section 2). Let us place the plate in the plane of complex variable $\sigma=x+iy$ along real axis x.

If it is assumed that the flow we are considering is irrotational its complex potential can be represented as the sum of potentials $W_1=V_\infty\sigma$ and W_2 respectively for longitudinal and cross flows over the plate with an undisturbed velocity $V=aV_\infty$ (Fig. 6.3.1). The total complex potential will be

$$W=W_1+W_2=V_\infty\sigma-ia\,V_\infty\left[\frac{\sigma}{2}\pm\sqrt{\frac{\sigma^2}{4}-R^2}\right.$$

$$\left.-R^2\left(\frac{\sigma}{2}\pm\sqrt{\frac{\sigma^2}{4}-R^2}\right)^{-1}\right]=V_\infty\sigma\pm iaV_\infty\sqrt{\sigma^2-4R^2}. \tag{6.3.1}$$

Taking into account (6.2.7) in which z is replaced by x, the total velocity potential past the flat plate will be

$$\varphi = V_\infty x \pm aV_\infty \sqrt{a^2 - x^2}. \tag{6.3.2}$$

From this value of velocity potential we find the component of velocity

$$V_x = V_\infty \pm (aV_\infty x / \sqrt{a^2 - x^2}). \tag{6.3.3}$$

The second component of velocity $V_y = 0$ at the plate.

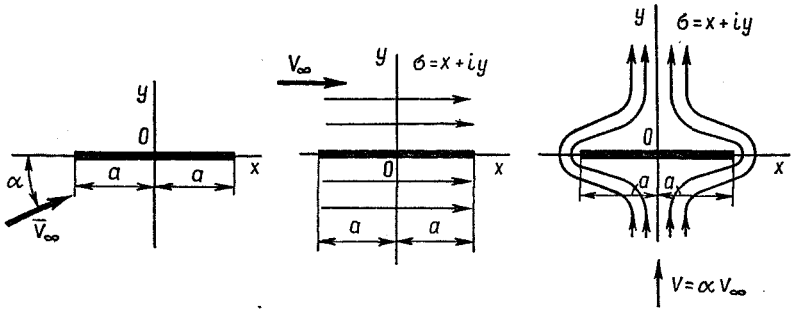

Fig. 6.3.1. System of flow-interaction of flat plate at given angle of attack.

From (6.3.3) it follows that at leading edge ($x = -a$) and trailing edge ($x = a$) the velocity V_x is infinite. Physically, this flow picture is not to be found. The limitation of velocity at one of the edges, for example at the trailing edge, can be found by superposing circulatory flow over the flow we are considering. The potential of rotating flow in plane ζ is determined, in accordance with (2.9.22), by the expression

$$W_3 = -(\Gamma i / 2\pi) \ln \zeta. \tag{6.3.4}$$

Substituting here the value of ζ from (6.2.5), we get

$$W_3 = -\frac{\Gamma i}{2\pi} \ln \left(\frac{\sigma}{2} \pm \sqrt{\frac{\sigma^2}{2} - R^2} \right). \tag{6.3.5}$$

Adding (6.3.1) and (6.3.5), we find the complex potential of rotational-rectilinear flow over an inclined flat plate:

$$W = W_1 + W_2 + W_3 = V_\infty \sigma \pm iaV_\infty \sqrt{\sigma^2 - 4R^2} - \frac{\Gamma i}{2\pi} \ln \left(\frac{\sigma}{2} \pm \sqrt{\frac{\sigma^2}{4} - R^2} \right). \tag{6.3.6}$$

The circulation Γ can be determined from the Zhukovskii-Chaplygin* hypothesis according to which the velocity at the trailing edge of a flat plate has a finite value. The value of this velocity can be obtained with the help of the theory of conformal transformation in the form of the derivative $d\overline{W}/d\sigma$

*In the American literature this is known as the Kutta-Zhukovskii condition at the trailing edge—Translator.

of complex potential $\overline{W}$ for a cylinder. This potential, in turn, helps us to find the complex velocity at the corresponding point on the cylinder in terms of the derivative $d\overline{W}/d\zeta$. By the rules of differentiation of a complex function this is equal to

$$\frac{d\overline{W}}{d\zeta}=\frac{dW}{d\sigma}\cdot\frac{d\sigma}{d\zeta}, \tag{6.3.7}$$

where $\overline{W}$ and W are the complex potentials for the cylinder and flat plate respectively. By the Zhukovskii-Chaplygin hypothesis the quantity $dW/d\sigma$ is limited in its absolute value. As the derivative $d\sigma/d\zeta$, which can be determined from (6.2.1) by the formula

$$\frac{d\sigma}{d\zeta}=1-\frac{R^2}{\zeta^2},$$

is equal to zero on the cylinder at a point $\zeta=R$ the derivative $d\overline{W}/d\zeta=0$ at the corresponding point on the trailing edge of the plate.

The complex potential for the cylinder will be

$$\overline{W}=\overline{W}_1+\overline{W}_2+\overline{W}_3.$$

The potential $\overline{W}_1$ characterizes the flow in the direction of the axis that corresponds to the flow over the flat plate in the same direction with a velocity V_∞. It is obtained by replacing the quantity σ from (6.2.1) in formula $W_1=V_\infty\sigma$:

$$\overline{W}_1=V_\infty[\zeta+(R^2/\zeta)].$$

The complex potentials $\overline{W}_2$ and $\overline{W}_3$ are determined by the equations (6.2.4) and (6.3.4) respectively. Replacing V by aV_∞ in the first, we find the total complex potential

$$\overline{W}=V_\infty\left(\zeta+\frac{R^2}{\zeta}\right)-iaV_\infty\left(\zeta-\frac{R^2}{\zeta}\right)-\frac{i\Gamma}{2\pi}\ln\zeta. \tag{6.3.8}$$

Then the derivative

$$\frac{d\overline{W}}{d\zeta}=V_\infty\left(1-\frac{R^2}{\zeta^2}\right)-iaV_\infty\left(1+\frac{R^2}{\zeta^2}\right)-\frac{i\Gamma}{2\pi\zeta}. \tag{6.3.8'}$$

For the point $\zeta=R$ corresponding to the point on the trailing edge of the plate the derivative $d\overline{W}/d\zeta$ is equal to zero, i.e.

$$-2iaV_\infty-(i\Gamma/2\pi R)=0.$$

Hence

$$\Gamma=-4\pi aRV_\infty, \tag{6.3.9}$$

or, since $2R=a$,

$$\Gamma=-2\pi aaV_\infty. \tag{6.3.9'}$$

On substituting this result in (6.3.6) and differentiating with respect to σ, the complex velocity will be given by

$$\frac{dW}{d\sigma}=V_x-iV_y=V_\infty\pm\frac{iaV_\infty\sigma}{\sqrt{\sigma^2-4R^2}}$$

$$+\frac{2\pi iaaV_\infty}{2\pi}\cdot\frac{2}{\sigma\pm\sqrt{\sigma^2-4R^2}}\left(\frac{1}{2}\pm\frac{\sigma}{\sqrt{\sigma^2-4R^2}}\right).$$

After simple transformations and the substitution $2R=a$ we get

$$\frac{dW}{d\sigma}=V_x-iV_y=V_\infty\left(1\mp ia\sqrt{\frac{\sigma-a}{\sigma+a}}\right). \tag{6.3.10}$$

On the surface of the plate ($\sigma=x$):

$$\frac{dW}{d\sigma}=V_x-iV_y=V_\infty\left(1\mp ia\sqrt{\frac{x-a}{x+a}}\right). \tag{6.3.11}$$

As $|x|\leqslant a$, we have

$$\frac{dW}{d\sigma}=V_x-iV_y=V_\infty\left(1\pm a\sqrt{\frac{a-x}{a+x}}\right), \tag{6.3.11'}$$

from which it follows that the total velocity past the flat plate is

$$V=V_x=V_\infty\left(1\pm a\sqrt{\frac{a-x}{a+x}}\right), \tag{6.3.12}$$

where the plus sign corresponds to the upper surface and the minus sign to the lower. The velocity at the trailing edge ($x=a=2R$) is equal to V_∞ and at the leading edge ($x=-a$) it is infinitely high. In actual cases the thickness of the leading edge is not equal to zero. Specifically, the edge of the airfoil, though not large, has a finite radius of curvature. For this reason the velocity at this edge has large but finite values.

The general expressions for the main vector of forces due to hydrodynamic pressures acting on a steady cylindrical body of arbitrary shape in a steady incompressible fluid flow can be used to determine the forces acting on the plate. Let us introduce the concept of complex force $\bar{F}=X-iY$ by analogy with complex velocity, defining this force as the mirror image of the main vector $\bar{F}$ in the real axis.

The vector $\bar{F}$ we are considering is determined by the formulas (1.3.2) and (1.3.3) in which the coefficient c_{fx} is taken to be zero. Then

$$\bar{F}=X-iY=-\oint_C p\,[\cos(\widehat{nx})-i\cos(\widehat{ny})]\,ds$$

$$=-\oint_C p\,(\sin\theta+i\cos\theta)\,ds=-i\oint_C p\,e^{-i\theta}\,ds, \tag{6.3.13}$$

where n is the direction of the external normal to the contour C of the body in the flow; θ is the angle between the element of contour ds and the x axis (Fig. 6.3.2).

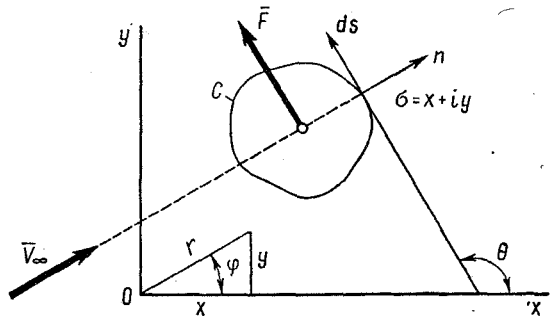

Fig. 6.3.2. Contour in incompressible fluid flow.

Since

$$\left.\begin{aligned} d\sigma &= dx+idy=ds\,(\cos\theta+i\sin\theta)=e^{i\theta}\,ds;\\ d\bar{\sigma} &= dx-idy=ds\,(\cos\theta-i\sin\theta)=e^{-i\theta}\,ds,\end{aligned}\right\} \tag{6.3.14}$$

and the pressure is determined by the Bernoulli equation:

$$p=p_\infty+\frac{\rho V_\infty^2}{2}-\frac{\rho V^2}{2}=C_2-\frac{\rho V^2}{2}, \tag{6.3.15}$$

it follows that

$$\bar{F}=-iC_2\oint_C d\bar{\sigma}+\frac{i\rho}{2}\oint_C V^2\,d\bar{\sigma}=\frac{i\rho}{2}\oint_C V^2\,d\bar{\sigma}\,.$$

Taking into account that $d\bar{\sigma}=e^{-2i\theta}d\sigma$ on the basis of (6.3.14) and keeping in view that the complex velocity at the given point of contour by the condition of unseparated flow

$$\bar{V}=V_x-iV_y=V\cos\theta-iV\sin\theta=Ve^{-i\theta}, \tag{6.3.16}$$

we find

$$\bar{F}=X-iY=\frac{i\rho}{2}\oint_C \bar{V}^2\,d\sigma. \tag{6.3.17}$$

Since the complex velocity for potential flow is $\bar{V}=dW/d\sigma$ the force

$$\bar{F}=X-iY=\frac{i\rho}{2}\oint_C\left(\frac{dW}{d\sigma}\right)^2 d\sigma. \tag{6.3.18}$$

This expression (6.3.18) is known as the Zhukovskii-Chaplygin formula.

The integration in (6.3.18) can be carried out over other contours surrounding the given contour C. As an example of such a contour the circular contour K may be selected, so that the complex velocity in plane σ can be expressed in the form

$$\frac{dW}{d\sigma}=\overline{V}_\infty-\frac{i\Gamma}{2\pi\sigma}+\frac{A}{\sigma^2}, \tag{6.3.19}$$

where $\overline{V}_\infty=V_{x\infty}-iV_{y\infty}$ and the coefficient A can be determined from (6.3.8′). The square of the complex velocity will be

$$\left(\frac{dW}{d\sigma}\right)^2=\overline{V}_\infty^2-\frac{i\Gamma\overline{V}_\infty}{\pi\sigma}+\frac{2A\overline{V}_\infty-(\Gamma^2/4\pi^2)}{\sigma^2}+\cdots.$$

Substituting this value in (6.3.18), we get

$$\overline{F}=X-iY=\frac{i\rho}{2}\left[\overline{V}_\infty^2\oint_K d\sigma-\frac{i\Gamma\overline{V}_\infty}{\pi}\oint_K\frac{d\sigma}{\sigma}\right.$$
$$\left.+\left(2A\overline{V}_\infty-\frac{\Gamma^2}{4\pi^2}\right)\oint_K\frac{d\sigma}{\sigma}+\cdots\right].$$

Here the first and third terms are zero. The integral $\oint_K d\sigma/\sigma$ is calculated taking into account the formula $\sigma=x+iy=re^{i\varphi}$ (see Fig. 6.3.2) and is equal to

$$\oint_K\frac{d\sigma}{\sigma}=\ln\sigma|_K=\ln(re^{i\varphi})|_K=2\pi i.$$

In this way the force

$$\overline{F}=X-iY=i\rho\Gamma\overline{V}_\infty. \tag{6.3.20}$$

Coming back to the conjugate value of this force, we have

$$F=X+iY=i\rho\Gamma V_\infty, \tag{6.3.21}$$

where $V_\infty=V_{x\infty}+iV_{y\infty}$. According to the expression for the force acting on a contour it is equal to the product of the density, velocity of undisturbed flow and circulation of velocity:

$$|F|=\rho|V_\infty||\Gamma|. \tag{6.3.22}$$

This expression is known as the Zhukovskii formula.

From (6.3.21) it follows that the acting force represents the vector that is perpendicular to the velocity vector of an undisturbed flow. Hence it is a lift force. Its direction coincides with the direction of the vector obtained by

turning the velocity vector $\bar{V}_\infty$ through an angle of $\pi/2$ against the direction of the circulation. This force is called the Zhukovskii force.

Let us apply formula (6.3.22) for calculation of the lift force on a flat plate. Keeping in mind the value of circulation from (6.3.9′), we get

$$Y=\rho|\Gamma||V_\infty|=2\pi a a\rho V_\infty^2. \tag{6.3.23}$$

The normal and axial components N and R of the Zhukovskii force are respectively determined as follows (Fig. 6.3.3):

$$N=Y\cos a\approx Y=2\pi a a\rho V_\infty^2; \tag{6.3.24}$$

$$R=-Y\sin a\approx -Ya=-2\pi a^2 a\rho V_\infty^2. \tag{6.3.25}$$

The presence of axial force R acting along the flat plate against the flow seems to offer a paradox because all the elemental forces due to pressure are directed along the normal to a surface. This component of the Zhukovskii force is known as the suction drag. The physical nature of its existence is explained like this: Let us assume that the leading edge is slightly rounded. Then the velocities in the neighborhood of the leading edge would be high but not infinitely high as happens in the case of a flat edge. According to Bernoulli's equation the difference between the pressures at the leading edge and at infinity will be negative. Separation also results in the suction drag. The value of the suction drag is given by the expression (6.3.25).

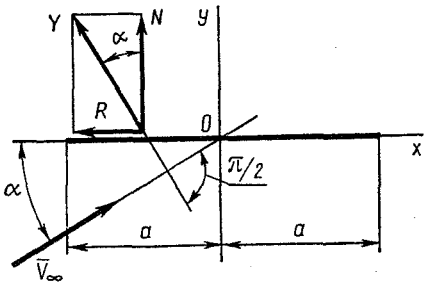

Fig. 6.3.3. System of forces acting on flat plate (R—suction force).

The expression (6.3.25) for suction drag refers to the case of flow past a flat plate where the velocity near its leading edge is determined by the formula (6.3.12). The axial component of perturbation velocity about a given plate, determined by this formula, will be

$$U=\pm aV_\infty\sqrt{\frac{a-x}{a+x}}. \tag{6.3.26}$$

The expression for suction drag can be generalized for the case of an arbitrary given velocity near the leading edge. For this purpose we write (6.3.25) in the form

$$T=-R=\pi\rho C^2, \tag{6.3.27}$$

where

$$C^2=2aa^2V_\infty^2. \tag{6.3.28}$$

Quantity C^2 can be represented in the form of the expression

$$C^2 = \lim_{x \to x_{L.E}} [V'^2_x (x - x_{L.E}), \qquad (6.3.28')$$

where $x_{L.E}$ is the abscissa of leading edge ($x_{L.E} = -a$); x is the varying abscissa of the points on the flat plate; V'_x is the axial component of perturbation velocity on the upper side of the wing.

It can be shown that formula (6.3.28′) is valid in practice. To do this we introduce expression (6.3.26) in (6.3.28′):

$$C^2 = \lim_{x \to -a} \left[V^2_\infty a^2 \left(\frac{a-x}{a+x} \right) (x+a) \right] = 2aa^2 V^2_\infty .$$

Substituting this quantity in (6.3.27), we get the formula (6.3.25) obtained earlier.

The results obtained for an incompressible irrotational uniform flow over an airfoil in the form of a thin plate are useful in studying the aerodynamic characteristics of airfoils of actual shapes and also for finite wings in incompressible fluid flows as well as in a compressible gaseous medium.

4. Finite Wing in Incompressible Fluid

So far we have been examining the flow-interaction of an airfoil and an incompressible fluid flow. It can be assumed that this profile corresponds to an elemental part of the lifting surface of a wing of infinite span in a rectilinear uniform flow. Hence the theory of this flow-interaction also happens to be the foundation of the aerodynamics of wings of infinite span.

According to formula (6.3.22) the lift force on the part of a wing of unit span $Y^{(1)} = \rho_\infty V_\infty \Gamma$ (Fig. 6.4.1, a). Consequently there is a rotational flow with circulation Γ around the profile. If the circulation is in a clockwise direction the velocities will be higher on the upper side of the profile (the circulatory flow is superposed on the oncoming flow in the same direction) and lower on the under side of the profile (circulatory flow is in the opposite direction to the undisturbed flow). Therefore, by Bernoulli's equation the pressure will be less on the upper side than on the lower side and the lift force will be directed

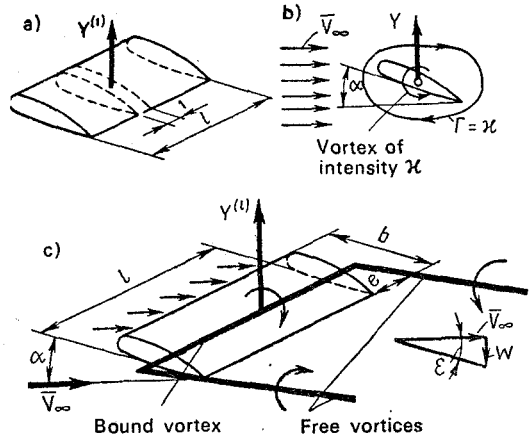

Fig. 6.4.1. System of equivalent vortices for wing of rectangular plan.

upward as shown in Fig. 6.4.1, b.

Since the circulation, according to (2.7.8) and (2.7.8′), is equal to the intensity of vortex κ the element of wing can be replaced by the equivalent vortex with a given intensity of vortex along the span. Zhukovskii called this vortex the bound vortex. In a hydrodynamic sense a wing of infinite span is equivalent to a bound vortex.

Let us now consider an approximate scheme of flow-interaction of a finite wing with a rectangular wing plan. The bound vortex, as established by S.A. Chaplygin, turns near the wingtips in the form of a pair of vortices and moves away behind the wing in the direction of the undisturbed flow. The distance e (see Fig. 6.4.1, c) from the point where the vortex turns to the wingtip depends on the geometry of the wing. Hence the hydrodynamic effect of a finite wing can be obtained by replacing it with a bound vortex and a pair of free vortices resembling the form of the letter Π. This scheme of wing is known as Chaplygin's Π-shaped scheme.

The equivalent vortex system of a finite wing induces additional velocities in flow and results in the downwash that is the characteristic of flow past a finite wing. The following theorems of Helmohltz form the basis for calculation of the induced velocities and downwash angle due to free vortices:

1. The intensity of a vortex does not change in magnitude and consequently a vortex cannot suddenly cut off or terminate in a fluid;
2. The intensity of a vortex is independent of time;
3. A vortex in an ideal fluid is not subject to extinction.

In the system of a rectangular wing that we are considering the circulation along the span is taken to be constant on the assumption that the lift force of each elemental segment of the wing is equal. In reality the lift force of this rectangular wing plan varies along its span. This variation is small in the middle part of the wing but quite significant near the wingtips. For a wing of arbitrary plane the variation in circulation has an absolutely clear form which is based on the unequal sizes of segments and hence is characterized by different values of lifting force. The vortex system of flow over a wing not of rectangular plan can be obtained if the wing is replaced not by a single Π-shaped vortex* but by a system of Π-shaped vortices forming a vortex sheet (Fig. 6.4.2). The circulation will be constant along each vortex but will change from one vortex to another. For the middle cross section of the wing (root section) the lift force is maximum and therefore the intensity of vortex and circulation will be maximum at that section.

Experiments show that this vortex sheet behind the wing is unsteady and at a comparatively small distance from the wing it twists around in two parallel vortex threads (see Fig. 6.4.2).

*In the English and American literature it is known as a horseshoe vortex system—Translator.

Let us study the relations required for calculation of induced velocities and downwash angle. First we have to determine the distance l_0 between the free (curling) vortices. Here we will assume that the vortex system for a wing of span l can be replaced by one horseshoe vortex with constant circulation Γ_0. It is assumed that the fixed vortex, known as the lifting part of a horseshoe vortex, passes through the aerodynamic center of a wing with a coordinate $x_{a.c}$.

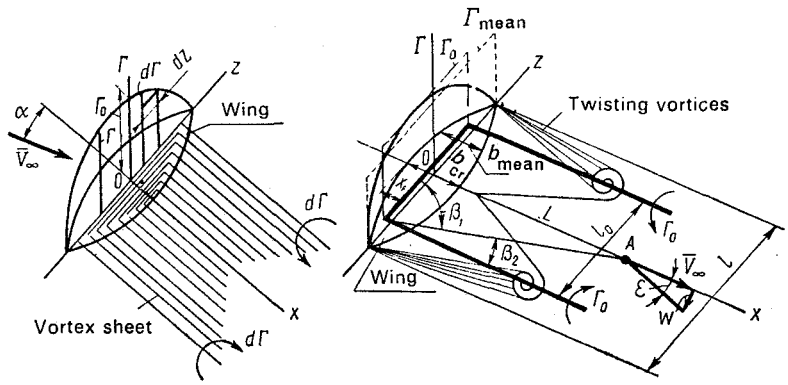

Fig. 6.4.2. Vortex sheet behind wing.

The distance l_0 between the free (curling) vortices is determined in the following way: The area under the curve $\Gamma(z)$ is equal to $\Gamma_{av}l$ and the average circulation Γ_{av} along the span is determined from the known lift force Y on the wing with the help of Zhukovskii's formula $Y=\rho_\infty V_\infty \Gamma_{av} l$. In accordance with this formula, taking into account that $Y=c_y q_\infty b_{av} l$, average circulation will be

$$\Gamma_{av}=0.5c_y b_{av} V_\infty. \tag{6.4.1}$$

Therefore for circulation it may be written:

$$\Gamma_0=0.5c_{y0} b_r V_\infty, \tag{6.4.2}$$

where c_{y0} is the coefficient of lift for root section;

b_r is the root chord.

Equations (6.4.1) and (6.4.2) establishing the relation between circulation of velocity and the corresponding values of the coefficient of lift and wing chord are known as the equations of correlation. From these equations we have

$$\frac{\Gamma_{av}}{\Gamma_0}=\frac{c_y b_{av}}{c_{y0} b_r} \tag{6.4.3}$$

The elemental value of the lift force, by equation (6.3.23), will be $dY=\rho_\infty V_\infty \Gamma dz$ and the lift acting on the wing will be

$$Y=2\rho_\infty V_\infty \int_0^{l/2} \Gamma dz. \tag{6.4.4}$$

The concepts of vortex systems Γ_{av} and Γ_0 on our assumption correspond to one and the same lift force Y and therefore

$$2\int_0^{l/2} \Gamma dz=\Gamma_{av} l=\Gamma_0 l_0. \tag{6.4.5}$$

So equations (6.4.5) and (6.4.3) lead to

$$l_0/l=c_y b_{av}/c_{y0} b_r. \tag{6.4.6}$$

Let us determine the downwash angle ε induced by the system of a horseshoe vortex of intensity Γ_0 at a given point A lying in the plane of vortices (see Fig. 6.4.2) at equal distances from the free vortices and at a distance L from the wing. We first find the downwash angle due to the bound vortex of length l_0

$$\varepsilon_1=-w_1/V_\infty, \tag{6.4.7}$$

where w_1 is the velocity at a point A induced by the bound vortex. According to (2.7.11)

$$w_1=(-\Gamma_0/4\pi L)[\cos\beta_1-\cos(\pi-\beta_1)]=(-\Gamma_0/2\pi L)\cos\beta_1.$$

Therefore

$$\varepsilon_1=\Gamma_0\cos\beta_1/2\pi V_\infty L=\Gamma_0\cos^2\beta_1/\pi V_\infty \sin\beta_1 l_0. \tag{6.4.8}$$

The induced velocity w_2^1 at the same point A due to one of the free vortices is calculated by formula (2.7.11). It is necessary to make the following substitutions: $\Gamma=\Gamma_0$, $h=l_0/2$, $\alpha_1=0$, $\alpha_2=\pi-\beta_2$. As a result

$$w_2^1=\{-\Gamma_0/[4\pi(l_0/2)]\}(1+\cos\beta_2)=(-\Gamma_0/2\pi l_0)(1+\sin\beta_1). \tag{6.4.9}$$

The velocity created by a pair of free vortices will be twice w_2^1:

$$w_2=2w_2^1=(-\Gamma_0/\pi l_0)(1+\sin\beta_1). \tag{6.4.10}$$

The corresponding downwash angle is

$$\varepsilon_2=-w_2/V_\infty=(\Gamma_0/\pi V_\infty l_0)(1+\sin\beta_1). \tag{6.4.11}$$

The total value of the downwash angle due to the system of horseshoe vortices is

$$\varepsilon=\varepsilon_1+\varepsilon_2=\frac{\Gamma_0}{\pi V_\infty l_0}\left(\frac{\cos^2\beta_1}{\sin\beta_1}+1+\sin\beta_1\right)=\frac{\Gamma_0(1+\sin\beta_1)}{\pi V_\infty l_0\sin\beta_1}. \tag{6.4.12}$$

Replacing Γ_0 here with the value from (6.4.2) and determining

$$\sin \beta_1 = L/\sqrt{L^2+(l_0/2)^2},$$

we get

$$\varepsilon = (c_{y0} b_r/2\pi l_0)[1+\sqrt{1+(l_0/2L)^2}]. \tag{6.4.13}$$

According to (6.4.6)

$$\frac{c_{y_0} b_r}{l_0} = \frac{c_y b_{av}}{l} \cdot \frac{l^2}{l_0^2} \cdot \tag{6.4.14}$$

Introducing the notations

$$k = l/l_0, \quad \lambda = l/b_{av}$$

and taking into account (6.4.14), equation (6.4.13) can be transformed into the form

$$\varepsilon = \frac{c_y}{2\pi\lambda} k^2 \left[1+\sqrt{1+\left(\frac{l}{2L}\right)^2 \frac{1}{k^2}}\right]. \tag{6.4.13'}$$

According to formula (6.4.13') the downwash angles behind the wing in a subsonic flow are proportional to the coefficient of lift and are inversely proportional to the aspect ratio λ.

Let us introduce the new quantity

$$\tau = \frac{k^2}{2}\left[1+\sqrt{1+\left(\frac{l}{2L}\right)^2 \frac{1}{k^2}}\right]-1; \tag{6.4.15}$$

then

$$\varepsilon = (c_y/\pi\lambda)(1+\tau). \tag{6.4.13''}$$

Research has shown that the quantity τ is less than unity and therefore the downwash angle can be regarded as a function basically determined by the coefficient of lift and the aspect ratio of the wing. Now let us see what types of changes are brought about by downwash in the flow-interaction of a wing at an angle of attack α (also known as the goemetrical angle of attack) in a flow with velocity $\overline{V}_\infty$. The appearance of downwash at angle ε behind the wing results in the flow-interaction being characterized by values of velocity $\overline{V}'_\infty$ and angle of attack α_u differing from the values of $\overline{V}_\infty$ and α that determine the flow around a wing of infinite span. The effective angle of attack α_e of a finite wing will be less than the geometrical angle of attack by the value of downwash angle ε (Fig. 6.4.3), i.e.

$$\alpha_e = \alpha - \varepsilon. \tag{6.4.16}$$

The presence of downwash leads to a change in the force-interaction of the medium and the body in the flow. If the downwash were absent the vector of an aerodynamic force, according to formula (6.3.21), would have been normal to the direction of undisturbed velocity $\overline{V}_\infty$. In the presence of

downwash velocity the resultant aerodynamic force vector will be oriented along the normal to the direction of real velocity $\overline{V}'_\infty$ (see Fig. 6.4.3). As a result of inclination of the resultant force by angle ε there appears component X_i in the direction of undisturbed flow. This complementary force X_i, appearing as a result of downwash induced by the vortices, is known as the induced drag. From the physical point of view the presence of induced drag is associated with loss of part of the kinetic energy of a moving wing, spent in the formation of vortices shed from its trailing edge. The value of this drag is determined from Fig. 6.4.3 by the expression

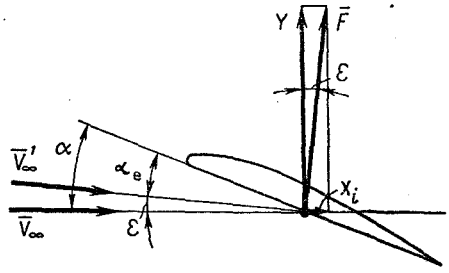

Fig. 6.4.3. Downwash near wing and occurrence of induced drag.

$$X_i = Y\varepsilon. \tag{6.4.17}$$

Here lift force Y is found in the same way as for the wing of infinite span on the assumption that the downwash is small. If the force X_i is divided by the quantity $(\rho_\infty V_\infty^2/2)S_w$ we get the coefficient of induced drag

$$c_{xi} = 2X_i/(\rho_\infty V_\infty^2 S_w) = c_y\varepsilon. \tag{6.4.18}$$

If we assume the values of $k \approx 1$, $(l/2L)^2/k^2 \approx 1$ in expression (6.4.13′) for ε and introduce notation $\lambda = \lambda_w$ then, after substitution in (6.4.18), we get

$$c_{xi} = c_y^2/(\pi\lambda_w). \tag{6.4.19}$$

7

WING PROFILE IN A COMPRESSIBLE GAS FLOW

1. Subsonic Compressible Flow Over Thin Airfoil

1.1 Linearization of equation of velocity potential

The study of the flow-interaction between an airfoil and a subsonic flow is related to the solution of the equation of velocity potential for a plane two-dimensional flow that is obtained from (5.1.8) at $\varepsilon=0$. This has the form

$$(V_x^2-a^2)\frac{\partial^2\varphi}{\partial x^2}+2V_x V_y\frac{\partial^2\varphi}{\partial x\,\partial y}+(V_y^2-a^2)\frac{\partial^2\varphi}{\partial y^2}=0. \tag{7.1.1}$$

This partial differential equation of second order happens to be the nonlinear equation with respect to the unknown function φ. It describes the flow past fairly thick profiles creating large disturbances in the gas such that velocity of flow V and speed of sound a differ considerably from the corresponding parameters of an undisturbed flow.

If an airfoil is thin and the perturbations it creates are small, the equation (7.1.1) can be simplified to the linear differential equation with constant coefficients and second-order partial derivatives. This simplification is known as linearization and the equation so obtained and the small perturbation flow described by it are known as the linearized equation and linearized flow respectively.

The velocity conditions (6.1.1) and the actual equality (6.1.2) are fulfilled for a linearized flow. Within an accuracy of the order of perturbation velocities u and v (6.1.1) the equation for the speed of sound can be formulated from (3.6.20), which takes the form

$$a^2=a_\infty^2+[(k-1)/2]\,(V_\infty^2-V^2). \tag{7.1.2}$$

Using the expression (6.1.2) here in place of V^2, we get

$$a^2=a_\infty^2-(k-1)\,V_\infty u. \tag{7.1.2'}$$

Substituting the quantity (7.1.2') in (7.1.1) and recalling that

$$V_x=V_\infty+u,\ V_y=v,\ V_x^2=V_\infty^2+2V_\infty u,\ V_y^2\approx v^2,$$

and further assuming that the total velocity potential of a linearized flow can be expressed by $\varphi=\varphi_\infty+\varphi'$, where φ_∞ is the velocity potential of an undisturbed flow and the perturbation velocity will be $\varphi'\ll\varphi_\infty$ according to the condition (6.1.1), we get

$$[V_\infty^2-a_\infty^2+(k+1)\,V_\infty u]\frac{\partial^2\varphi'}{\partial x^2}+2\,(V_\infty+u)\,v\,\frac{\partial^2\varphi'}{\partial x\,\partial y}$$

$$+[v^2-a_\infty^2+(k-1)\,V_\infty u]\frac{\partial^2\varphi'}{\partial y^2}=0. \tag{7.1.3}$$

The second-order partial derivatives of the potential φ' with respect to the coordinates x, y are small quantities of first order:

$$\frac{\partial^2\varphi'}{\partial x^2}=\frac{\partial u}{\partial x},\quad \frac{\partial^2\varphi'}{\partial x\,\partial y}=\frac{\partial u}{\partial y}=\frac{\partial v}{\partial x},\quad \frac{\partial^2\varphi'}{\partial y^2}=\frac{\partial v}{\partial y}.$$

Taking this in (7.1.3), the group of small terms of second and third order can be determined and, neglecting them, we get the linearized equation in the following form:

$$(V_\infty^2-a_\infty^2)\frac{\partial^2\varphi'}{\partial x^2}-a_\infty^2\frac{\partial^2\varphi'}{\partial y^2}=0 \tag{7.1.4}$$

or

$$(\mathbf{M}_\infty^2-1)\frac{\partial^2\varphi'}{\partial x^2}-\frac{\partial^2\varphi'}{\partial y^2}=0, \tag{7.1.4'}$$

where $\mathbf{M}_\infty=V_\infty/a_\infty$.

Let us study the expression for pressure in a linearized flow. For this purpose we use the formula (3.6.26), which will be rewritten as

$$\frac{p}{p_\infty}=\left(1-\frac{V^2}{V_{\max}^2}\right)^{k/(k-1)}\left(1-\frac{V_\infty^2}{V_{\max}^2}\right)^{-k/(k-1)}.$$

Substituting here the value of V^2 from (6.1.2), we get

$$\frac{p}{p_\infty}=\left(1-\frac{2V_\infty u}{V_{\max}^2-V_\infty^2}\right)^{k/(k-1)}.$$

Keeping in view that by formula (3.6.22)

$$V_{\max}^2-V_\infty^2=\frac{2}{k-1}\,a_\infty^2=\frac{2k}{k-1}\cdot\frac{p_\infty}{\rho_\infty},$$

we find

$$\frac{p}{p_\infty}=\left(1-\frac{k-1}{k}\cdot\frac{\rho_\infty V_\infty u}{p_\infty}\right)^{k/(k-1)}. \tag{7.1.4''}$$

Expanding the right side of this expression in series and maintaining the second term therein, we get

$$p/p_\infty = 1-(\rho_\infty V_\infty u/p_\infty).$$

From this the pressure difference will be $p-p_\infty = -\rho_\infty V_\infty u$ and the coefficient of pressure will be $\overline{p} = -2u/V_\infty$, i.e. we get the same relations (6.1.3), (6.1.5) as in the case of an incompressible fluid flow. However, in applying these relations in the case of high subsonic speeds it is necessary to take into account that the perturbation velocity $u=\partial\varphi'/\partial x$ should be determined taking into account compressibility.

1.2 Relationship between compressible gas flow and incompressible fluid flow over thin airfoil

The flow-interaction of a thin airfoil in a compressible subsonic flow at a small angle of attack is studied with the help of equation (7.1.4′) in which $\mathbf{M}_\infty < 1$. Let us now perform the replacement of variables in accordance with the relations

$$x_0 = x, \quad y_0 = y\sqrt{1-\mathbf{M}_\infty^2}, \quad \varphi_0' = \varphi'\gamma(V_{\infty 0}/V_\infty), \tag{7.1.5}$$

where γ is some arbitrary parameter, $V_{\infty 0}$ is the velocity of a fictitious flow (fictitious velocity) which differs in general from the velocity V_∞ of a given flow. The substitution of (7.1.5) in equation (7.1.4′) gives the Laplace equation for determination of velocity potential φ_0' for an incompressible flow in plane x_0, y_0:

$$\frac{\partial^2\varphi_0'}{\partial x_0^2}+\frac{\partial^2\varphi_0'}{\partial y_0^2}=0. \tag{7.1.6}$$

In this way the problem of flow-interaction between a given profile and a compressible fluid flow can be solved using the results of the solution of the problem of an incompressible fluid flow with a fictitious velocity $V_{\infty 0}$ over some transformed airfoil. Let us find out the relation between the corresponding parameters of flow past an airfoil and their geometrical characteristics. The relation between perturbation velocities u_0 and u in incompressible and compressible flows respectively is established, in accordance with (7.1.5), in the following way:

$$u_0 = \frac{\partial\varphi_0'}{\partial x_0} = \frac{\partial\varphi'}{\partial x}\gamma\frac{V_{\infty 0}}{V_\infty} = u\gamma\frac{V_{\infty 0}}{V_\infty}. \tag{7.1.7}$$

Substituting (6.1.5) in this equation, the coefficients of pressure in incompressible and compressible flows $\overline{p}_{\text{in}} = -2u_0/V_{\infty 0}$ and $\overline{p} = -2u/V_\infty$ respectively can be found. Consequently from (7.1.7) we get

$$\overline{p}_{\text{in}} = \gamma\overline{p}. \tag{7.1.8}$$

From the formulas

$$c_{y\,\text{in}} = \oint \overline{p}_{\text{in}}\, d\overline{x}_0, \quad m_{z\,\text{in}} = \oint \overline{p}_{\text{in}}\,\overline{x}_0\, d\overline{x}_0$$

along with the expression (7.1.8) we find the relation between the corresponding coefficients of lift and moment:

$$\left.\begin{aligned} c_{y\ \text{in}} &= \gamma \oint \bar{p}\, d\bar{x}\,; \\ m_{z\ \text{in}} &= \gamma \oint \bar{p}\bar{x}\, d\bar{x} = \gamma m_z\,. \end{aligned}\right\} \tag{7.1.9}$$

Let us establish the relation between the forms of the airfoils and the angles of attack. For this purpose we first determine the relation between the vertical components of velocity. According to (7.1.5) we have:

$$v_0 = \frac{\partial \varphi_0'}{\partial y_0} = \frac{\partial \varphi'}{\partial y} \cdot \frac{1}{\sqrt{1-\mathbf{M}_\infty^2}} \frac{V_{\infty 0}}{V_\infty} = v \frac{\gamma}{\sqrt{1-\mathbf{M}_\infty^2}} \cdot \frac{V_{\infty 0}}{V_\infty}\,. \tag{7.1.10}$$

For an incompressible fluid the condition of unseparated flow (3.3.17'), by which $F=F_0=y_0-f_0\ (x_0)$ and $y_0=f_0\ (x_0)$ as the equation of airfoil contour, results in

$$v_0/(V_{\infty 0}+u_0)=dy_0/dx_0$$

or, recalling that $u_0 \ll V_{\infty 0}$, it will be

$$v_0/V_{\infty 0}=dy_0/dx_0.$$

Similarly for a compressible gas flow it will be

$$v/V_\infty = dy/dx.$$

Consequently

$$(v_0/v)\ (V_\infty/V_{\infty 0})=(dy_0/dy)\ (dx/dx_0).$$

Keeping in view equations (7.1.5) and (7.1.10), we get

$$dy_0/dy=\gamma/\sqrt{1-\mathbf{M}_\infty^2}.$$

Under the condition that at $y=0$ the quantity $y_0=0$; integration of this relation gives the equation connecting the vertical coordinates of fictitious and given profiles:

$$y_0=y(\gamma/\sqrt{1-\mathbf{M}_\infty^2}). \tag{7.1.11}$$

At the same time it follows from (7.1.5) that the horizontal coordinates of these profiles do not change. Considering this, the angles of attack in the above two cases can be expressed in the form

$$a_{\text{in}}=y_0/(b-x) \quad \text{and} \quad a=y/(b-x),$$

where b is the distance to the trailing edge of the profile, x is the horizontal coordinate of a point (Fig. 7.1.1). Thus according to (7.1.11) we have

$$a_{\text{in}}=a(\gamma/\sqrt{1-\mathbf{M}_\infty^2}). \tag{7.1.12}$$

Let us assume that the arbitrary parameter $\gamma=1$. Then

$$\left.\begin{gathered}\bar{p}=\bar{p}_{\text{in}},\ y=y_0\sqrt{1-\mathbf{M}_\infty^2},\ a=a_{\text{in}}\sqrt{1-\mathbf{M}_\infty^2};\\ c_y=c_{y\,\text{in}},\ m_z=m_{z\,\text{in}}.\end{gathered}\right\} \tag{7.1.13}$$

In this way, if the pressure coefficients at the corresponding points of the profiles in the compressible and incompressible flows are identical the profile in the compressible flow must be thinner than that in the incompressible flow by $\sqrt{1-\mathbf{M}_\infty^2}$ times. The angle of attack will be reduced in the same proportion.

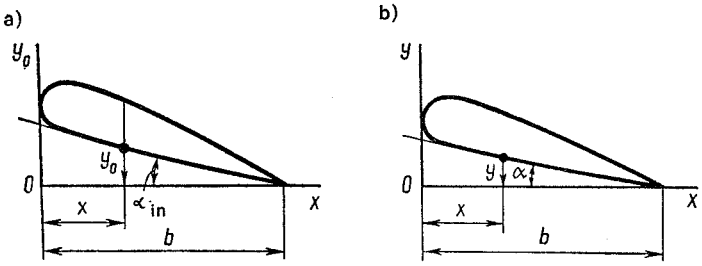

Fig. 7.1.1. Profiles in small-perturbation incompressible (*a*) and compressible (*b*) flows.

Let us consider the case when $\gamma=\sqrt{1-\mathbf{M}_\infty^2}$ and hence

$$\left.\begin{gathered}\bar{p}=\bar{p}_{\text{in}}/\sqrt{1-\mathbf{M}_\infty^2},\ y=y_0,\ a=a_{\text{in}};\\ c_y=c_{y\,\text{in}}/\sqrt{1-\mathbf{M}_\infty^2},\ m_z=m_{z\,\text{in}}/\sqrt{1-\mathbf{M}_\infty^2}.\end{gathered}\right\} \tag{7.1.14}$$

From the results obtained it can be seen that for the two profiles under the same angle of attack the pressure coefficients at the corresponding points of the profile and their total lift coefficient and moment coefficient in the compressible flow will be $1/\sqrt{1-\mathbf{M}_\infty^2}$ times greater than those in the incompressible flow. From this it can be concluded that the compressibility effect leads to a rise in pressure and lift. The factor $1/\sqrt{1-\mathbf{M}_\infty^2}$ is called the Prandtl-Glauert correction factor for compressibility effect.

2. Academician S.A. Khristianovich's Method

2.1 Description of method

If the airfoil or other body under flow-interaction induces finite disturbances in a flow the linearized equations are not applicable. In studying this kind of flow it is necessary to use the nonlinear equations of gas dynamics.

Many problems of supersonic flows of gas can be solved by the application of the method of characteristics. The number of problems in supersonic aero-

dynamics that can be solved is further increased by the numerical methods of integrating equations of motion. The analysis of a subsonic gas flow is quite difficult. Mathematically this can be explained by the different types of equations: hyperbolic for supersonic flows and elliptical for subsonic flows. The application of imaginary characteristics for elliptical equations does not yield any particular simplification. The greater difficulty in the investigation of subsonic flows can be physically explained by the fact that the disturbances in such flows propagate all over in the region of motion. On the other hand, in the case of supersonic flows the disturbances are confined by the surface of a cone with its apex at the point of disturbance and they propagate only downstream. Here the investigation of small-perturbation subsonic flows, due to the linearized character of the equations, is somewhat simpler than for subsonic flows with large perturbations during the flow-interactions of thick profiles.

Academician S.A. Chaplygin's book on gas jets is devoted to the investigation of the method of studying such flows. In it the equations forming the mathematical basis of the theory of potential subsonic flows are set out. These equations are known as Chaplygin's equations in gas dynamics. Their specialty is that they determine the motion of a gas not in the x, y plane but in the plane of special coordinates τ and β ($\tau = V^2$ is the square of total velocity at a given point in flows; β is the polar angle which can be determined from $V = V_x \cos \beta$). Unlike the usual equations they are linear because the coefficients in these equations represent by themselves the functions of independent variables τ, β. These equations were solved by S.A. Chaplygin for a series of cases of gas motion at high subsonic speeds.

Chaplygin's equations turned out to be the basis for many other methods in the field of high-speed aerodynamics. Using these equations, Academician Khristianovich worked out a method that helps us to characterize the effect of compressibility for a subsonic flow past airfoils of arbitrary shapes. The theoretical concepts of this method are to be found in detail in work [25]. Let us study the basic concept of this method and its application to the solution

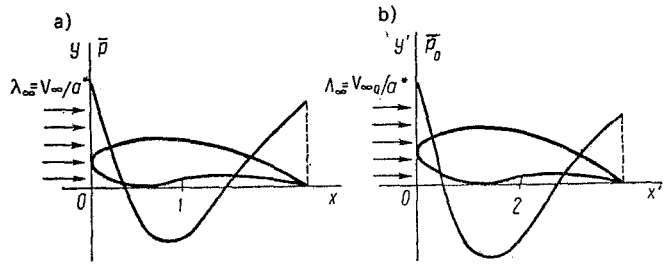

Fig. 7.2.1. Calculation of pressure over profile in compressible flow: *a*—real flow; *b*—fictitious flow; *1*—given profile; *2*—fictitious profile.

of various problems of flow-interactions of profiles in a compressible subsonic flow.

Examining a compressible flow past an airfoil of given form, S.A. Khristianovich showed that the equations of this flow-interaction can be assimilated to the equations of an incompressible fluid flow past an airfoil of some different form (Fig. 7.2.1). So, with the help of S.A. Khristianovich's method a relatively simple problem of a fictitious incompressible flow past some fictitious profile is solved to start with and then the parameters obtained are worked out for the conditions of the compressible flow past a given profile.

The above analysis is based on the use of the functional relation between the real relative velocity $\lambda = V/a^*$ in the compressible flow and the value of the fictitious nondimensional velocity $\Lambda = V_0/a^*$ at the corresponding points on the actual and fictitious profiles respectively (Table 7.2.1). Here the method we are considering makes it possible to transform the given profile into the fictitious profile.

TABLE 7.2.1

λ	0	0.05	0.10	0.15	0.20	0.25	0.30	0.35
Λ	0	0.0500	0.0998	0.1493	0.1983	0.2467	0.2943	0.3410
λ	0.400	0.450	0.500	0.550	0.600	0.625	0.650	
Λ	0.3862	0.4307	0.4734	0.5144	0.5535	0.5722	0.5904	
λ	0.675	0.7000	0.725	0.750	0.775	0.800	0.825	0.850
Λ	0.6080	0.6251	0.6413	0.6568	0.6717	0.6857	0.6988	0.7110
λ	0.875	0.900	0.925	0.950	0.975	1.000		
Λ	0.7223	0.7324	0.7413	0.7483	0.7546	0.7577		

As shown by S.A. Khristianovich, the difference in the forms of the actual and fictitious profiles can be neglected in the case of thin airfoils. S.A. Khristianovich's method allows us to recalculate the flow parameters over the airfoil (pressure, velocity) fairly easily for any Mach number $\mathbf{M}_\infty > 0$, i.e. accounting for the compressibility, if the distribution of these parameters around the same airfoil in a low subsonic flow without compressibility effect ($\mathbf{M}_\infty \approx 0$) is known. In addition, this method helps us to extend the calculation of parameters for one Mach number $\mathbf{M}_{\infty 1} > 0$ to the other Mach number $\mathbf{M}_{\infty 2} > 0$ ($\mathbf{M}_{\infty 2} \neq \mathbf{M}_{\infty 1}$).

In performing calculations by S.A. Khristianovich's method it is necessary to bear in mind that it is valid under the condition of subsonic flow velocity all over the profile. This condition is observed when the Mach number of the undisturbed flow is less than its critical value $\mathbf{M}_{\infty cr}$. Therefore before embarking on the calculation it is necessary to find this critical value and to

establish that $M_\infty < M_{\infty cr}$. The critical Mach number $M_{\infty cr}$ can also be determined by S.A. Khristianovich's method.

2.2 Conversion of pressure coefficient from incompressible fluid flow to Mach number $M_\infty > 0$

Let the distribution of the pressure coefficient over an airfoil in an incompressible flow be known, i.e. the nature of function $\bar{p}_0 = \bar{p}_0(x)$ be known (Fig. 7.2.2). The transformation of this function for the new Mach number $M_{\infty cr} > M_\infty > 0$ will be carried out in the following order:

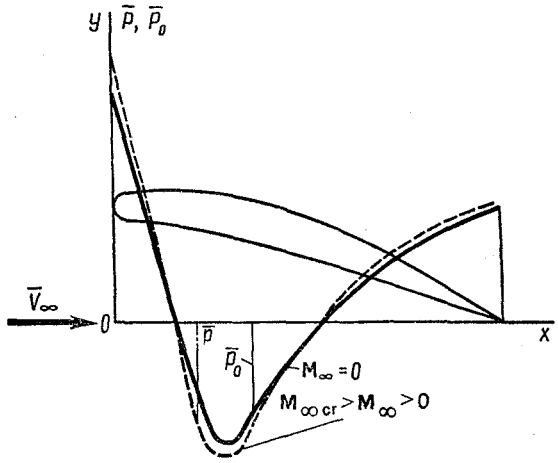

Fig. 7.2.2. Type of pressure distribution on one side of profile at different values of M_∞.

For a given Mach number $M_\infty > 1$ the relative velocity is determined by

$$\lambda_\infty = \left[\frac{k+1}{2} M_\infty^2 \left(1 + \frac{k-1}{2} M_\infty^2\right)^{-1}\right]^{1/2}. \tag{7.2.1}$$

The fictitious speed Λ_∞ of an incompressible flow corresponding to the value of λ_∞ can be found from Table 7.2.1. For a selected value of $\bar{p}_0$, from Bernoulli's equation

$$\bar{p}_0 = 1 - (\Lambda/\Lambda_\infty)^2 \tag{7.2.2}$$

we determine the fictitious velocity in the form

$$\Lambda = \Lambda_\infty \sqrt{1 - \bar{p}_0}. \tag{7.2.2'}$$

Knowing Λ, the actual local velocity λ for a compressible flow can be obtained from Table 7.2.1 and the pressure p can be calculated by the formula (3.6.26) in which it is assumed that $V^2/V^2_{max} = [(k-1)/(k+1)]\,\lambda^2$. The pressure coefficient is then determined by the formula $\bar{p} = 2[(p/p_\infty) - 1]/kM_\infty^2$. The

nature of curve $\bar{p}=\bar{p}(x)$ recalculated for a given Mach number $\mathbf{M}_\infty$ is shown in Fig. 7.2.2.

2.3 Conversion of pressure coefficient from Mach number $\mathbf{M}_{\infty 1}>0$ to Mach number $\mathbf{M}_{\infty 2}>0$ ($\mathbf{M}_{\infty 1}\neq\mathbf{M}_{\infty 2}$)

Let us assume that the distribution of pressure coefficient $\bar{p}_1=\bar{p}_1(x)$ is known in the compressible fluid flow at some Mach number $\mathbf{M}_{\infty 1}$ ($\mathbf{M}_{\infty cr}>\mathbf{M}_{\infty 1}>0$). To calculate the corresponding distribution of the pressure coefficient at the new Mach number $\mathbf{M}_{\infty 2}>0$ it is necessary first to find the relative velocities $\lambda_{\infty 1}$ and $\lambda_{\infty 2}$ by using formula (7.2.1) for the Mach numbers $\mathbf{M}_{\infty 1}$ and $\mathbf{M}_{\infty 2}$ respectively. Then the relative velocities $\Lambda_{\infty 1}$ and $\Lambda_{\infty 2}$ of a fictitious incompressible flow can be determined from Table 7.2.1.

By inserting some value of coefficient of pressure $\bar{p}_1$ the absolute pressure

$$p_1=p_{\infty 1}\left(\bar{p}_1\frac{k\mathbf{M}_{\infty 1}^2}{2}+1\right) \tag{7.2.3}$$

can be found from the formula $\bar{p}_1=2(p_1-p_{\infty 1})/(k\mathbf{M}_{\infty 1}p_{\infty 1})$ and the local relative velocity of the actual flow can be obtained:

$$\lambda_1=\left\{\frac{k+1}{k-1}\left[1-\left(\frac{p_1}{p_0}\right)^{(k-1)/k}\right]\right\}^{1/2}. \tag{7.2.4}$$

For the value of λ_1 Table 7.2.1 gives the local velocity in the fictitious incompressible flow. The corresponding coefficient of pressure can be calculated by Bernoulli's equation (7.2.2)

$$\bar{p}_0=1-(\Lambda_1/\Lambda_{\infty 1})^2.$$

Calculation of coefficient of pressure $\bar{p}_2$ from this value of $\bar{p}_0$ for Mach number $\mathbf{M}_{\infty 2}$ is carried out in the same way as the conversion of the pressure coefficient of the incompressible flow to the Mach number $\mathbf{M}_\infty>0$ already discussed.

2.4 Determination of critical Mach number M

According to S.A. Khristianovich's hypothesis, in an incompressible flow past an airfoil the local sonic speed corresponding to the critical Mach number of an undisturbed flow $\mathbf{M}_{\infty cr}$ arises at the point where the highest suction occurs. Khristianovich established the relation between the minimum pressure coefficient $\bar{p}_{0\min}$ for the highest suction and the critical Mach number $\mathbf{M}_{\infty cr}$.

So it is clear that the value of the highest suction $\bar{p}_{0\min}$ should be determined first by some means, for example with the help of a low-speed wind tunnel, before attempting to find the critical Mach number. If the pressure distribution, taking into account compressibility, for $\mathbf{M}_{\infty cr}>\mathbf{M}_\infty>0$ is obtained from the wind tunnel test the quantity $\bar{p}_{0\min}$ can be determined by the

reverse conversion of highest suction $\bar{p}_{0\min}$ to the Mach number $M_\infty = 0$.

Let us assume that the value of highest suction $\bar{p}_{0\min}$ is known. As the relative velocity $\lambda = 1$ at the point of appearance of sonic speed, the value of the local velocity of the fictitious incompressible flow $A = 0.7577$ from Table 7.2.1 for the value of $\lambda = 1$. Now from Bernoulli's equation

$$\bar{p}_{0\min} = 1 - (A/A_\infty)^2$$

the relative speed of the fictitious undisturbed flow will be

$$A_\infty = A/\sqrt{1-\bar{p}_{0\min}} = 0.7577/\sqrt{1-\bar{p}_{0\min}}, \tag{7.2.5}$$

and Table 7.2.1 and the value of A_∞ give the critical velocity $\lambda_{\infty cr}$ in the compressible flow. The corresponding critical Mach number will be

$$M_{\infty cr} = \lambda_{\infty cr}\left(\frac{k+1}{2} - \frac{k-1}{2}\lambda^2_{\infty cr}\right)^{-1/2}. \tag{7.2.6}$$

The graph of critical Mach number versus $\bar{p}_{0\min}$ developed on the basis of the results of the above calculation is shown in Fig. 7.2.3.

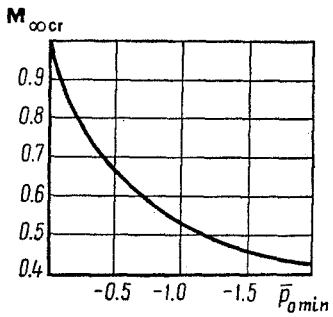

Fig. 7.2.3. Curve for determination of critical Mach number M by S.A. Khristianovich.

3. Wing Profile in Flow Having Supercritical Velocity ($M_\infty > M_{\infty cr}$)

A subsonic flow past an airfoil may be characterized by the following two cases. In the first case the local flow velocity on the surface does not go beyond sonic velocity anywhere on the airfoil. This is a case of pure subsonic flow interaction. It is known that at this velocity shock waves cannot arise at any point on the airfoil. The lift and drag forces will be determined with the compressibility effect. In general they depend on the forces due to normal pressure and friction. This kind of drag consisting of drag due to normal pressure and frictional drag is known as profile drag.

In the second case, known as the supercritical flow interaction, the Mach number M of an undisturbed flow is higher than critical, i.e. $M_\infty > M_{\infty cr}$. The local velocity at some points around the profile becomes higher than sonic velocity and a zone of local supersonic speeds comes into the picture. Now the flow-interaction of the profile is characterized by the fact that the local velocity is less than sonic velocity ahead of the leading edge as well as behind the airfoil. Therefore during transition from supersonic to subsonic speeds local shocks arise near the wing (Fig. 7.3.1). These shocks, resembling in form the letter λ (λ shocks), consist of two shocks each: the front curvilinear (oblique) shock DE and the rear almost linear shock CB (see Fig. 7.3.1, b).

Local shocks, which may appear on the upper as well as the lower surface of the wing profile, significantly alter the pressure distribution and set up additional drag known as wave drag X_w. Thus the total drag of profile X will consist of profile drag X_{pr} and wave drag X_w, i.e.

$$X = X_{pr} + X_w$$

or

$$c_x = c_{xpr} + c_{xw},$$

where c_x is the coefficient of resultant drag of an airfoil; c_{xpr} and c_{xw} are the coefficients of profile and wave drag respectively.

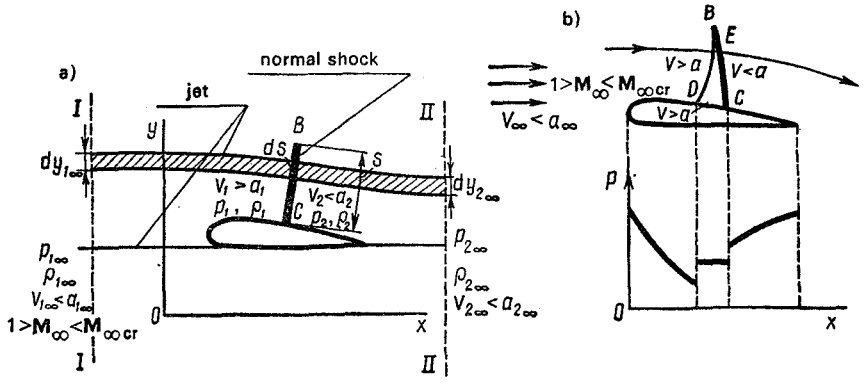

Fig. 7.3.1. Profile in subsonic flow with supercritical speed:

a—scheme of calculation of flow-interaction in presence of local normal shock;
b—pressure distribution over profile with formation of local λ shock.

Let us examine the simple method of calculation of wave drag suggested by Prof. G.F. Burago (see the book [1]). Assume that a local supersonic zone is formed on the upper side of the profile which takes the approximate form of the nearly straight shock BC (see Fig. 7.3.1, a). Let us separate out a flow-jet passing through this shock. The gas parameters in this jet will be V_1, p_1, ρ_1, M_1 just before the shock and V_2, p_2, ρ_2, M_2 behind the shock. Take two control surfaces I–I, II–II to the left and right side at a fair distance from the profile. Denote the gas parameters on the left plane by $V_{1\infty}$, $p_{1\infty}$, $\rho_{1\infty}$ and those on the right plane by $V_{2\infty}$, $p_{2\infty}$, $\rho_{2\infty}$.

Applying the theorem according to which the rate of change of mass momentum of a gas flowing through the control surfaces is equal to the resultant force acting on the left and right surfaces and the wave drag force X_w acting on the profile, we get

$$\int_{-\infty}^{\infty} V_{2\infty}\, dm_{2\infty} - \int_{-\infty}^{\infty} V_{1\infty}\, dm_{1\infty} = \int_{-\infty}^{\infty} (p_{1\infty} - p_{2\infty})\, dy - X_w, \qquad (7.3.1)$$

where $dm_{1\infty}$, $dm_{2\infty}$ are the mass flow rates per second of gas along the jet:

$$dm_{1\infty}=\rho_{1\infty}V_{1\infty}dy_{1\infty};$$
$$dm_{2\infty}=\rho_{2\infty}V_{2\infty}dy_{2\infty}.$$

These are equal from the condition of constant flow rate, i.e.

$$\rho_{1\infty}V_{1\infty}\,dy_{1\infty}=\rho_{2\infty}V_{2\infty}\,dy_{2\infty}. \tag{7.3.2}$$

As postulated by G.F. Burago, we assume that equality of velocity is reestablished at a considerable distance behind the wing, i.e. $V_{2\infty}\to V_{1\infty}$. Accordingly, using (7.3.2) we get

$$\int_{-\infty}^{\infty}V_{2\infty}\,dm_{2\infty}-\int_{-\infty}^{\infty}V_{1\infty}\,dm_{1\infty}=\int_{-\infty}^{\infty}\rho_{1\infty}V_{1\infty}(V_{2\infty}-V_{1\infty})\,dy_{1\infty}=0.$$

Consequently

$$X_w=\int_{-\infty}^{\infty}(p_{1\infty}-p_{2\infty})\,dy\,. \tag{7.3.3}$$

It can be assumed that $p_{2\infty}=p_{1\infty}$ for jets not intersecting with the shock, i.e. the pressure at a considerable distance behind the profile settles down to the value of pressure in the undisturbed flow. For jets passing across the shock we have $p_{2\infty}<p_{1\infty}$.

In reality, since

$$\left.\begin{aligned}p_{1\infty}&=p_0\left(1-\frac{V_{1\infty}^2}{V_{\max}^2}\right)^{k/(k-1)};\\ p_{2\infty}=p_0'\left(1-\frac{V_{2\infty}^2}{V_{\max}^2}\right)^{k/(k-1)}&=p_0'\left(1-\frac{V_{1\infty}^2}{V_{\max}^2}\right)^{k/(k-1)},\end{aligned}\right\} \tag{7.3.4}$$

where $p_0'<p_0$; we have

$$p_{2\infty}/p_{1\infty}=p_0'/p_0=\nu_0<1. \tag{7.3.5}$$

Taking into account (7.3.5), equation (7.3.3) can be transformed with the help of the equation of mass flow rate

$$\rho_{1\infty}V_{1\infty}dy_{1\infty}=\rho_1V_1ds,$$

so that

$$dy_{1\infty}=dy=(\rho_1V_1/\rho_{1\infty}V_{1\infty})ds.$$

As a result the wave drag will be

$$X_w=p_{1\infty}\int_0^s\frac{\rho_1V_1}{\rho_{1\infty}V_{1\infty}}(1-\nu_0)\,ds, \tag{7.3.6}$$

and the coefficient of wave drag will be

$$c_{xw}=\frac{X_w}{q_\infty b}=\frac{2X_w}{kp_\infty \mathbf{M}_\infty^2 b}=\frac{2}{k\mathbf{M}_\infty^2 b}\int_0^s \frac{\rho_1 V_1}{\rho_{1\infty} V_{1\infty}}(1-\nu_0)\,ds, \qquad (7.3.6')$$

where s is the length of the shock.

The function ν_0 (4.3.20) may be expressed in the form of a series with $n=\mathbf{M}_1-1$:

$$\nu_0(n)=\nu_0(0)+\left(\frac{d\nu_0}{dn}\right)_{n=0} n+\frac{1}{2}\left(\frac{d^2\nu_0}{dn^2}\right)_{n=0} n^2 + \frac{1}{6}\left(\frac{d^3\nu_0}{dn^3}\right)_{n=0} n^3+\cdots. \qquad (7.3.7)$$

In the expression (7.3.7) the value of $\nu_0(0)=1$ because at $\mathbf{M}_1=1$ ($n=0$) the shock changes to a wave of infinitesimally small intensity and the pressure $p_0'=p_0$.

Using (4.3.20), (4.3.13) and (4.3.15) it can also be shown that

$$\left(\frac{d\nu_0}{dn}\right)_{n=0}=\left(\frac{d\nu_0}{d\mathbf{M}_1}\right)_{\mathbf{M}_1=1}=0 \quad \text{and} \quad \left(\frac{d^2\nu_0}{dn^2}\right)_{n=0}=\left(\frac{d^2\nu_0}{d\mathbf{M}_1^2}\right)_{\mathbf{M}_1=1}=0.$$

Keeping in view that for thin airfoils at small angles of attack the difference $(\mathbf{M}_1-1)$ is small and in the series expansion (7.3.7) it can be truncated to the fourth term, we have

$$\nu_0(n)=1+\frac{1}{6}\left(\frac{d^3\nu_0}{d\mathbf{M}_1^3}\right)_{\mathbf{M}_1=1}(\mathbf{M}_1-1)^3\,. \qquad (7.3.7')$$

As shown by experiment, up to the given approximation it can be assumed that the quantity $(\mathbf{M}_1-1)$ for a given airfoil is proportional to the difference $(\mathbf{M}_\infty-\mathbf{M}_{\infty cr})$. Denoting the corresponding coefficient of proportionality by A_1 and including it in the general coefficient A, which can be determined in the form

$$A=-\frac{A_1}{3k\mathbf{M}_\infty^2 b}\left(\frac{d^3\nu_0}{d\mathbf{M}_1^3}\right)_{\mathbf{M}_1=1}\int_0^s \frac{\rho_1 V_1}{\rho_{1\infty} V_{1\infty}}\,ds, \qquad (7.3.8)$$

we get the following expression for the coefficient of wave drag using (7.3.6') and (7.3.7'):

$$c_{xw}=A(\mathbf{M}_\infty-\mathbf{M}_{\infty cr})^3. \qquad (7.3.9)$$

The coefficient A, in the general case, depends on the form of the profile, angle of attack and Mach number $\mathbf{M}_\infty$. However, aerodynamic experiments in wind tunnels on modern airfoils at low angles of attack showed that coefficient $A\approx 11$. In such cases satisfactory results are obtained from formula (7.3.9) if the difference $\mathbf{M}_\infty-\mathbf{M}_{\infty cr}$ does not exceed 0.15.

From formula (7.3.9) it follows that the coefficient of wave drag increases with the rise in M_∞. This happens because the shocks appearing at the profile become more intensive and elongated with the rise in flight speed. To reduce c_{x_w} at a given M_∞ it is necessary to raise the critical Mach number $M_{\infty cr}$, which is basically achieved by reducing the thickness of the profile. A similar effect can be achieved by reducing the angle of attack.

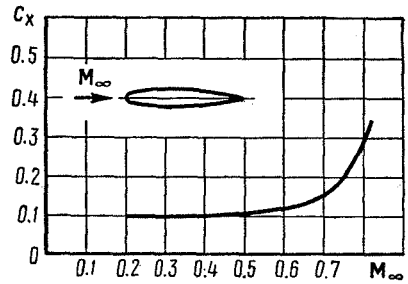

Fig. 7.3.2. Profile drag in transonic zone of flow-interaction.

Figure 7.3.2 shows the empirical curve characterizing variation in coefficient of drag $c_x = c_{x_{pr}} + c_{x_w}$ in the transonic regime of flow-interaction. For values of $M_\infty < 0.45$–0.5 there is only profile drag. The higher values of M_∞ correspond to supercritical velocities of flow ($M_\infty > 0.5$–0.55) where wave drag comes into the picture due to the formation of local shocks.

4. Flat Plate in Supersonic Flow of Gas Having Constant Heat Coefficients

Let us study the simplest wing profile in the form of a flat plate placed in a supersonic flow at an angle of attack α. The scheme of flow-interaction of this plate is shown in Fig. 7.4.1. Near the leading edge the supersonic flow is split into two parts: upper (above flat plate) and lower (below it)—parts which do not affect each other. Therefore the supersonic flow-interaction on each side of the plate can be studied independently.

Let us examine the upper side of the plate. The flow over this side represents in itself a plane supersonic flow over a surface which makes an angle of more than 180° with the direction of the undisturbed flow. This kind of flow, shown in Fig. 7.4.2 with the plane OC corresponding to the upper surface of the plate, was first investigated by Prandtl and Meyer and is called the Prandtl-Meyer flow.

According to the system of flow in Fig. 7.4.2 the flow parallel to the plane OB gradually turns, undergoes expansion and takes a new direction parallel to the plane OC. The angle of inclination of this plane β_{OC} to the vector $\overline{V}_\infty$ corresponds to the angle of attack α of the flat plate in Fig. 7.4.1. The disturbed part of the flow with expansion is limited from the left side by the Mach line OD which is inclined to the velocity vector of undisturbed flow $\overline{V}_\infty$ at an angle $\mu_\infty = \sin^{-1}(1/M_\infty)$, where M_∞ is the Mach number in the undisturbed flow. The process of expansion ends on the Mach line OE inclined to the velocity vector of disturbed flow $\overline{V}_{OC}$ by an angle $\mu_{OC} = \sin^{-1}(1/M_{OC})$, which can be determined from the Mach number of the disturbed flow over plane OC. The change in the direction of flow between the Mach

lines OD and OE can be expressed as the successive summation of inclinations of stream lines by small angles $\Delta\beta$. To each such inclination indicating the appearance of additional disturbance there corresponds a straight Mach line passing through point O.

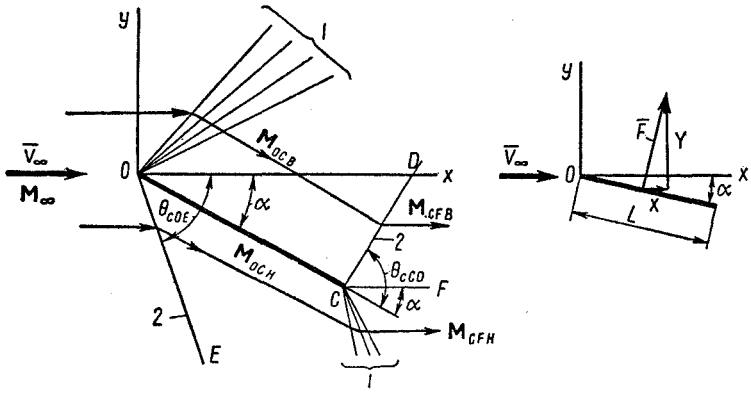

Fig. 7.4.1. System of supersonic flow-interaction of flat plate:

1—expansion fan; *2*—compression shock.

In this way the region of turning will be filled up by an infinite number of Mach lines forming a "fan" of lines of disturbance which characterizes the centralized expansion wave. This centralized wave, known as Prandtl-Meyer's expansion fan, is determined by the straight Mach lines. The flow parameters are constant along each of these lines and therefore each line corresponds to a series of plain expansion waves.

The problem of the motion of a gas about an obtuse angle, which is related to the formation of a centralized expansion wave, can be solved by the characteristics method. The point of intersection F of the stream line in a steady uniform flow (angle of inclination of the stream line at this point $\beta=0$) with the characteristics OD in a fixed plane corresponds to point F' on the epicycloidal characteristic in the hodograph plane of the same family. To be more precise, each of these characteristics can be referred, for example, to the characteristics of the first family. The equation of characteristics of this family in the hodograph plane will be $\beta=\omega+\beta_1$. Since $\beta=0$ by the above condition we have $\beta_1=-\omega_\infty(M_\infty)$, where the angle ω_∞ is found from (5.3.31) for a given Mach number M_∞. Hence the equation of characteristics will be $\beta=\omega-\omega_\infty$, from which

$$\omega=\beta+\omega_\infty. \tag{7.4.1}$$

For a given small inclination of stream line $\beta=\Delta\beta$ the corresponding angle can be taken as $\omega=\Delta\beta+\omega_\infty$ and the Mach number M can be found out on the neighboring Mach line inclined to the new direction of the stream line

at an angle $\mu=\sin^{-1}(1/\mathbf{M})$. The Mach number on the plate OC having angle of inclination $\beta=\beta_{OC}=\alpha$, i.e. on the upper surface, is determined by

$$\omega_{OC}=\beta_{OC}+\omega_{\infty}. \tag{7.4.2}$$

The value of local Mach number $\mathbf{M}_{OC}$ obtained helps in determining the Mach angle $\mu_{OC}=\sin^{-1}(1/\mathbf{M}_{OC})$. A graphic solution of the Prandtl-Meyer flow is shown in Fig. 7.4.2, b. The coordinate of the point G' of the intersection of the epicycloid with the line $O'G'$ parallel to the plane OC determines the relative velocity λ_{OC} of a disturbed flow near plane OC. In a physical plane the point G of the intersection of the stream line with the characteristic OE corresponds to point G'.

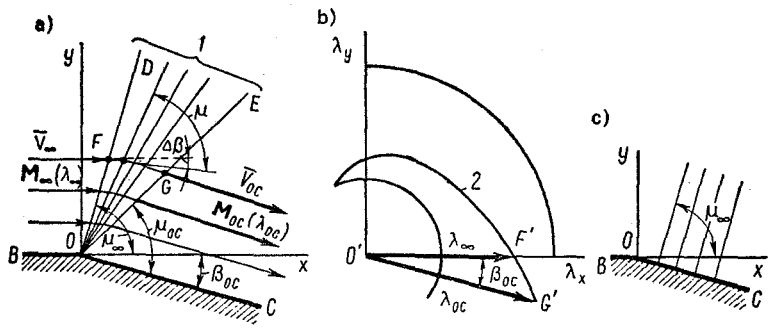

Fig. 7.4.2. System of flow-interaction of obtuse angle (Prandtl-Meyer flow):
a—physical plane; *b*—hodograph plane; *c*—system of small-perturbation flow; *1*—expansion wave; *2*—epicycloid.

From the known Mach number $\mathbf{M}_{OC}$ (λ_{OC}) the pressure on the upper side of the plate can be found out by applying formula (3.6.30)

$$p_u=p_{OC\,u}=p_{\infty}\left(\frac{1+\frac{k-1}{2}\mathbf{M}_{\infty}^2}{1+\frac{k-1}{2}\mathbf{M}_{OC}^2}\right)^{k/(k-1)}. \tag{7.4.3}$$

The corresponding value of the coefficient of pressure will be

$$\bar{p}_u=\bar{p}_{OC\,u}=2\,(p_{OC\,u}-p_{\infty})/k\mathbf{M}_{\infty}^2 p_{\infty}.$$

At hypersonic speeds $(\mathbf{M}_{\infty}\gg 1)$ the analysis of the Prandtl-Meyer flow is simplified because in determining the function ω we can use (5.3.41), which helps to determine local Mach number $\mathbf{M}$ directly. Replacing angles ω_{OC} and ω_{∞} in (7.4.2) by their values from (5.3.41), we get

$$\mathbf{M}_u=\mathbf{M}_{OC}=\left(\frac{1}{\mathbf{M}_{\infty}}-\frac{k-1}{2}\beta_{OC}\right)^{-1}. \tag{7.4.4}$$

The corresponding pressure can be determined by formula (3.6.39).

Let us study the Prandtl-Meyer flow arising at hypersonic speeds in the case of small angles of flow inclination $\beta_{OC}=a$. At very high Mach numbers $\mathbf{M}_\infty$ the bundle of Mach lines emerging from point O will be very narrow. With fair accuracy it can be assumed that these Mach lines condense to one line across which the flow turns suddenly and an expansion of flow takes place. Hence this line can apparently be regarded as the 'expansion shock' behind which speed (Mach number) increases and pressure decreases. The angle μ'_{OC} of inclination of this line to the vector $\overrightarrow{V}_\infty$ is obtained if the analogy of a compression shock is followed and the calculation of this angle is carried out by formula (4.6.9) under the condition that the angle $\beta_c=\beta_{OC}=a$ in this formula is negative. Assuming that $\theta_c=\mu'_{OC}$, we find

$$\frac{\mu'_{OC}}{|\beta_{OC}|}=-\frac{1}{2(1-\delta)}+\sqrt{\frac{1}{4(1-\delta)^2}+\frac{4}{\mathbf{K}^2}}, \tag{7.4.5}$$

where $|\beta_{OC}|=|a|$ is the absolute value of the angle of turn of flow (angle of attack) and the quantity $\mathbf{K}^2=(\mathbf{M}_\infty\beta_{OC})^2$. Applying the formula (4.6.11′) for calculation of the coefficient of pressure, and taking into account the sign of angle $\beta_{OC}=a$, we get

$$\frac{\bar{p}_u}{a^2}=\frac{\bar{p}_{OC\,u}}{a^2}=\frac{1}{1-\delta}-\sqrt{\frac{1}{(1-\delta)^2}+\frac{4}{\mathbf{K}^2}}\,. \tag{7.4.6}$$

At low Mach number $\mathbf{M}_\infty$ and small angles of attack $\beta_{OC}=a$ Prandtl-Meyer's small perturbation flow comes into the picture near the inclined surface. The expression for sonic speed is valid for such a flow. Now if the formula for the local Mach number is found from (7.1.2):

$$\mathbf{M}^2=\frac{V^2}{a^2}=\frac{2}{k-1}\left(\frac{a_\infty^2}{a^2}-1\right)+\frac{V_\infty^2}{a^2}$$

and if the value of a^2 in this formula is introduced from (7.1.2′), we get

$$\frac{V^2}{a^2}=\mathbf{M}^2=\mathbf{M}_\infty^2\left(1+\frac{2u}{V_\infty}\right)\left[1-(k-1)\,\frac{uV_\infty}{a_\infty^2}\right]^{-1}. \tag{7.4.7}$$

In accordance with this expression we can assume as a first approximation that $\mathbf{M}\approx\mathbf{M}_\infty$ in a small perturbation flow and hence the characteristic equation in the physical plane will be $dy/dx=\tan(\beta\pm\mu_\infty)$. As the angle of flow inclination β is small and $\beta\ll\mu_\infty$ we get $dy/dx\approx\pm\tan\mu_\infty$. Consequently the characteristics themselves represent the Mach lines inclined to the x axis by the angles $\pm\mu_\infty$. For a Prandtl-Meyer flow we have the family of characteristics in the form of parallel lines inclined to the horizontal axis by an angle μ_∞ (see Fig. 7.4.2, c).

The equations of characteristics for a plane supersonic flow in the hodograph plane can be obtained from (5.3.21) and (5.3.22) in terms of finite

differences:

$$(\Delta V/V) \mp \tan \mu \Delta\beta = 0. \tag{7.4.8}$$

For a small perturbation flow we may take

$$\Delta V = u, \quad V = V_\infty, \quad \Delta\beta = \beta, \quad \tan \mu = \tan \mu_\infty = (\mathbf{M}_\infty^2 - 1)^{-1/2}.$$

Hence

$$u/V_\infty = \pm \beta/\sqrt{\mathbf{M}_\infty^2 - 1}. \tag{7.4.8'}$$

Substituting the value of u in (6.1.5) from (7.4.8'), we get the coefficient of pressure,

$$\bar{p} = \mp 2\beta/\sqrt{\mathbf{M}_\infty^2 - 1}. \tag{7.4.9}$$

Since a suction flow is assumed for which $\bar{p} < 0$ and it is assumed that angle β is an absolute quantity the minus sign should be taken in formula (7.4.9).

Accordingly the coefficient of pressure on the upper surface of the plate inclined at a small angle of attack $\beta = \alpha$ will be

$$\bar{p}_u = \bar{p}_{OC\,u} = -2\alpha/\sqrt{\mathbf{M}_\infty^2 - 1}. \tag{7.4.10}$$

Let us examine the lower side of the flat plate. The flow-interaction of this side (see Fig. 7.4.1) is accompanied by the formation of shock OE emerging from a point on the leading edge and hence by the compression of flow. It is necessary to use the formula (4.3.25) to determine the angle of inclination of shock θ_{cOE}, where $\mathbf{M}_1 = \mathbf{M}_\infty$ and $\beta_c = \alpha$. From the value of θ_{cOE} obtained the Mach number $\mathbf{M}_2 = \mathbf{M}_{OCl}$ on the lower side can be found from (4.3.19) or (4.3.19').

In determining the flow character in the region behind point C on the trailing edge the following conclusions can be drawn: On the upper side of the plate the Mach number $\mathbf{M}_{OCu}$ before the shock CD is higher than the Mach number $\mathbf{M}_\infty$ before the shock OE appearing at the lower side of the leading edge. If we assume that the flow behind a point C does not deviate from the undisturbed flow direction (stream line CF is parallel to the velocity vector $\bar{V}_\infty$) it is obvious that the losses in the shock on the upper side will be heavier and therefore $\mathbf{M}_{CFu} < \mathbf{M}_{CFl}$. Then the pressure from the top of line CF seems to be more than that from below.

Discontinuity in pressure on the boundary surface cannot be maintained in a gas flow although the velocities can remain different. Therefore in actual conditions the direction of the stream line CF differs from the direction of an undisturbed velocity, i.e. downwash is formed behind the plate. From the physical conditions it must be clear that the line CF inclines toward the lower side. Meantime the flow behind shock CD turns by a small angle, which leads to reductions in pressure.

Experiments show that the downwash angle is small and therefore it can be said with fair accuracy that the flow direction coincides with the direction of an undisturbed flow at a point C. Accordingly the shock angle θ_{cCD} on the upper side is determined by the formula (4.3.25) where $\mathbf{M}_1=\mathbf{M}_{OCu}$, $\beta_c=a$. The corresponding Mach number behind the shock $\mathbf{M}_2=\mathbf{M}_{CFu}$ is determined from (4.3.19) or (4.3.19′) for the given values of $\theta_c=\theta_{cCD}$, $\mathbf{M}_1=\mathbf{M}_{OCu}$ and $\beta_c=a$.

The Prandtl-Meyer flow with Mach number $\mathbf{M}_{CFl}$, which can be determined with the help of formula $\omega_{CFl}=\omega_{OCl}+a$, takes place below the line CF in the region behind the trailing edge.

The pressure $p_u=p_{OCu}$ on the upper side of the plate is determined by formula (7.4.3) and the corresponding pressure on the lower side $p_l=p_{OCl}$ is obtained from the relation (4.3.15), where $p_2=p_l$, $p_1=p_\infty$, $\theta_c=\theta_{cOE}$ and $p_l<p_u<p_\infty$.

If the length of the plate is L and its width is equal to unity the force due to normal pressure acting on the plate is given by $F=L\ (p_l-p_u)$. Hence the lift force is $Y=F\cos a$ and the drag force is $X=F\sin a$. The corresponding values of the lift and drag coefficients will be $c_y=Y/q_\infty L$ and $c_x=X/q_\infty L$ respectively. Introducing the coefficients of pressure on the upper and lower sides in the form $\bar{p}_u=(p_u-p_\infty)/q_\infty$ and $\bar{p}_l=(p_l-p_\infty)/q_\infty$ respectively, we get the following expressions for the aerodynamic coefficients:

$$\left.\begin{aligned} c_y&=(\bar{p}_l-\bar{p}_u)\cos a;\\ c_x&=(\bar{p}_l-\bar{p}_u)\sin a.\end{aligned}\right\} \tag{7.4.11}$$

The force X arising during the supersonic flow-interaction of the plate and induced by the formation of shock waves and plain waves of disturbances is known as wave drag and the corresponding quantity c_x is called the coefficient of wave drag. This drag is not zero even in the case of an ideal (inviscid) fluid.

The aerodynamic efficiency factor of plate $\mathbf{K}=c_y/c_x=\cot a$ is obviously the function solely of the angle of attack. As a consequence of the uniform pressure distribution over the plate surface the center of pressure is situated at the middle. Hence the moment of pressure forces about an axis at the leading edge will be $\mathbf{M}_z=F\cdot L/2$ and the corresponding coefficient of moment will be

$$m_z=\mathbf{M}_z/(q_\infty L^2)=\frac{1}{2}(\bar{p}_l-\bar{p}_u). \tag{7.4.12}$$

At hypersonic speeds the coefficient of pressure on the upper surface of the plate is approximately obtained from formula (7.4.6) and on the lower surface from formula (4.6.12). Taking this into account and assuming $\beta_c=a$ in (4.6.12), we get the following expression for the difference in pressure coefficients $(\bar{p}_l-\bar{p}_u)$, which is also known as the coefficient of pressure drop:

$$\frac{\bar{p}_l-\bar{p}_u}{a^2}=4\sqrt{\frac{1}{4(1-\delta)^2}+\frac{1}{\mathbf{K}^2}}. \tag{7.4.13}$$

Hence

$$\frac{c_y}{a^2}=4\sqrt{\frac{1}{4(1-\delta)^2}+\frac{1}{\mathbf{K}^2}}; \tag{7.4.14}$$

$$\frac{c_x}{a^3}=4\sqrt{\frac{1}{4(1-\delta)^2}+\frac{1}{\mathbf{K}^2}}; \tag{7.4.15}$$

$$\frac{m_z}{a^2}=2\sqrt{\frac{1}{4(1-\delta)^2}+\frac{1}{\mathbf{K}^2}}. \tag{7.4.16}$$

Formulas (7.4.13) through (7.4.16) indicate the law of hypersonic similarity applicable to the flow-interaction of a thin plate. The basic content of this law is that the corresponding values of $\bar{p}/a^2$, c_y/a^2 c_x/a^3 and m_z/a^2 for a flat plate will be one and the same for equal values of $\mathbf{K}=\mathbf{M}_\infty a$ but independent of the quantities $\mathbf{M}_\infty$ and a. The parameter $\mathbf{K}=\mathbf{M}_\infty a$ is known as the criterion of hypersonic similarity. From formulas (7.4.13) through (7.4.16) it follows that the relations for the coefficients of pressure, lift and moment are quadratic. For the coefficient of drag it is the cubic function of the angle of attack a. In the limiting case at $\mathbf{K}\to\infty$:

$$(\bar{p}_l-\bar{p}_u)/a^2=c_y/a^2=c_x/a^3=2/(1-\delta); \tag{7.4.17}$$

$$m_z/a^2=1/(1-\delta). \tag{7.4.18}$$

For a flat plate situated in a small-perturbation (linearized) flow the pressure coefficients are calculated by formula (7.4.9) in which $\beta=a$ is considered. The minus sign in this formula determines the pressure coefficient on the upper side and the plus sign that on the lower side. Hence the difference between the pressure coefficients with respect to angle of attack is

$$(\bar{p}_l-\bar{p}_u)/a=4/\sqrt{\mathbf{M}_\infty^2-1}. \tag{7.4.19}$$

Substituting in formulas (7.4.11) and (7.4.12), we get

$$c_y/a=4/\sqrt{\mathbf{M}_\infty^2-1}; \tag{7.4.20}$$

$$c_x/a^2=4/\sqrt{\mathbf{M}_\infty^2-1}; \tag{7.4.21}$$

$$m_z/a=2/\sqrt{\mathbf{M}_\infty^2-1}. \tag{7.4.22}$$

In the given case the criterion of similarity happens to be the Mach number $\mathbf{M}_\infty$. The corresponding values of $\bar{p}/a$, c_y/a, c_x/a^2 and m_z/a will be identical independent of the value of the angle of attack but keeping the value of $\mathbf{M}_\infty$ constant. If the case of a small-perturbation flow at very high values of Mach numbers $\mathbf{M}_\infty>1$ is taken formulas (7.4.19) and (7.4.22) can be expressed in the following way:

$$(\bar{p}_l-\bar{p}_u)/a^2=c_y/a^2=c_x/a^3=4/\mathbf{K}; \tag{7.4.23}$$

$$m_z/a^2=2/\mathbf{K}. \tag{7.4.24}$$

In this way the criterion of hypersonic similarity $\mathbf{K}=\mathbf{M}_\infty a$ is valid even for a small-perturbation (linearized) flow with high Mach numbers. It is obvious that this kind of flow can occur only at very small angles of attack.

5. Supersonic Flow Past Airfoil of Arbitrary Form

5.1 Application of method of characteristics

Let us study a supersonic flow past a sharp airfoil of arbitrary form (Fig. 7.5.1). The upper and lower contours of the profile are given by the equations $y_u=f_u(x)$ and $y_l=f_l(x)$ respectively. Let us assume that the angle of attack is more than the angle β_{Ou} formed by the tangent to a profile contour on the upper side at a point O at the leading edge. The Prandtl-Meyer flow comes into the picture at this point. The flow assumes the form of an expansion fan emerging from point O as from the source of disturbances and follows the direction of the tangent to the contour at this point. Beyond point O the flow continues to expand along the contour. Consequently the flow past the airfoil can be considered as the successive summation of Prandtl-Meyer flows. As the flow turns at the points on the contour by an infinitesimally small angle separate Mach lines will emerge from these points in place of the fans of expansion lines (see Fig. 7.5.1).

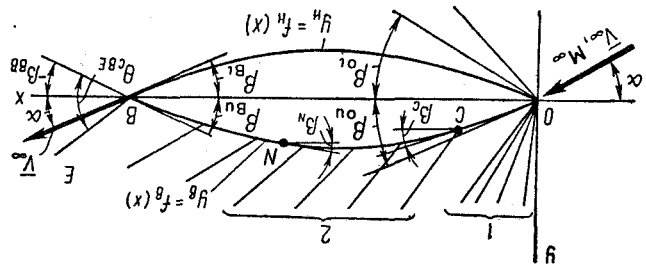

Fig. 7.5.1. Sharp-nosed profile in supersonic flow:
1—expansion fan; *2*—Mach line.

The velocity at a point O is found with the help of formula (7.4.2), which can be written in the form

$$\omega_O=\omega_\infty+(a-\beta_{Ou}), \tag{7.5.1}$$

where $\beta_{Ou}=\tan^{-1}(dy_u/dx)_O$. The corresponding Mach number $\mathbf{M}_O$ is obtained from Table 5.3.1 for the given value of ω_O.

At a neighboring point C situated at a small distance from the edge the

velocity of the gas is calculated as for a Prandtl-Meyer flow with the help of the formula

$$\omega_C=\omega_O+(\beta_{Ou}-\beta_C). \tag{7.5.2}$$

Adding the left and right sides of equations (7.5.1) and (7.5.2), we get the relation

$$\omega_C=\omega_\infty+(\alpha-\beta_C), \tag{7.5.3}$$

where $\beta_C=\tan^{-1}(dy_u/dx)_C$. Hence, in accordance with (7.5.3) we have for any arbitrary point N on the contour

$$\omega_N=\omega_\infty+(\alpha-\beta_N), \tag{7.5.4}$$

where angle $\beta_N=\tan^{-1}(dy_u/dx)_N$ is calculated taking into account its sign. For the front part of the contour the signs of angles will be positive and for the rear part negative.

We assume that the flow at a point B, as in the case of the flow-interaction of a flat plate, approximately maintains the direction of an undisturbed flow. Moving now at a speed corresponding to $\mathbf{M}_{Bu}$ near the contour, the flow turns at point B and shock BE emerges therefrom. The angle of inclination θ_{cBE} of the shock and the parameters behind it are worked out with the help of the corresponding formulas of the theory of shocks for the known values of angle of attack α, Mach number $\mathbf{M}_{Bu}$ and the contour angle at point B on the upper side. The parameters on the upper surface of an airfoil (pressure, velocity, etc.) are determined by the relations for an isentropic gas flow from the known value of the local Mach number.

If the angle of attack is equal to the angle β_{Ou} we have the limiting case of the Prandtl-Meyer flow at a point O for which the Mach number at this point $\mathbf{M}_{Ol}=\mathbf{M}_\infty$. The formula (7.5.4) can be rewritten in the form

$$\omega_N=\omega_\infty+(\beta_{Ol}-\beta_N). \tag{7.5.4'}$$

Calculation of flow-interaction on the lower side of the profile (Fig. 7.5.2) begins with the determination of gas parameters at point O immediately behind the shock. For this purpose the angle of inclination of shock θ_{cO} is calculated on the basis of the values $\mathbf{M}_1=\mathbf{M}_\infty$ and $\beta_C=\alpha+\beta_{Ol}$. The Mach number $\mathbf{M}_{Ol}=\mathbf{M}_2$ at a point O is found from (4.3.19) or (4.3.19'). This Mach number will be assumed to be constant in the infinitesimally small region around point O on the segment of the contour in the form of a straight element OD. The straight element OJ of the oblique shock corresponds to this segment OD. Its length is determined as the distance from point O to point J, which lies at the intersection of the shock and the characteristic of the first family emerging from point D.

The flow behind the rectilinear shock will be irrotational. Therefore the part of the contour behind point D is in the isentropic flow. To determine the

velocity of this kind of flow at a point F we use equation (7.4.1) from which we find $\omega_F=\omega_D-(\beta_D-\beta_F)$, where ω_D is the value of angle ω worked out by formula (5.3.31) for a value of **M** on the segment OD of a contour. The values of angles β_D and β_F are determined taking into account the sign (in the present case the angles β_D and β_F on the front part of the contour are negative).

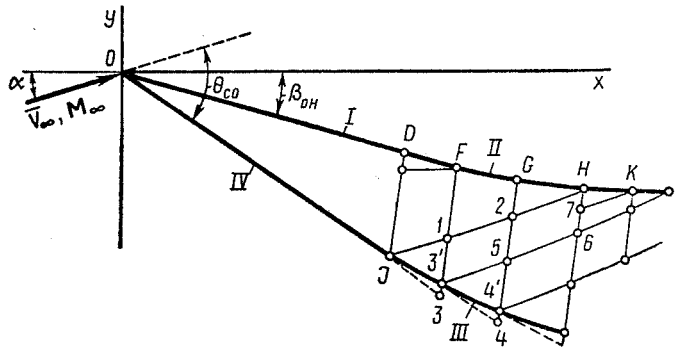

Fig. 7.5.2. Supersonic flow-interaction on lower surface of profile with formation of compression shock:

I—straight portion of contour of body; *II*—curved portion of contour of body; *III*—curvilinear part of compression shock; *IV*—linear part of compression shock.

The flow around the contour segment DF can be considered as a Prandtl-Meyer flow. Therefore the line of disturbance *F–1–3* emerges from point F as from the source of disturbance. It crosses the extension of a straight shock at point *3* and bends it. As a result the actual direction of the shock will be determined by the point of intersection *3'* of the shock and the characteristic.

The bending of the shock downstream will be governed by the interaction between it and the characteristics emerging from the points *G*, *H*, *K*, etc. The flow becomes rotational due to the shock bending. To calculate this it is necessary to apply the relations of a non-isentropic plane flow to the characteristics.

The characteristic JH of the second family happens to be the boundary of this rotational flow. This characteristic will be gradually built up in the form of a broken line from the known values of Mach number **M** and angle β along the rectilinear characteristics of the second family emerging from points *F*, *G*, etc. on the contour. The velocity at point H on a contour lying at the same time on the characteristic JH is obtained from the expression $\omega_H=\omega_D-(\beta_D-\beta_H)$. At point K, in the neighborhood of point H, the flow parameters are worked out from the equations of characteristics which take into account the rotational character of the flow behind a shock. To determine the velocity at this point it is enough here to know the speed and its direction (angle β) at point *7*, which is situated near point K on the

element *7–K* of the characteristic of the second family. To determine this velocity we have to work out the curvature of the shock behind point *J* on the segment *J–3′* and find out the parameters on the shock at point 3′. The following data can be used for this purpose: Mach number $\mathbf{M}=\mathbf{M}_1=\mathbf{M}_F$ and angle $\beta=\beta_F$ for the direction of flow at point *1* and the parameters $\mathbf{M}_2=\mathbf{M}_J$, $\beta_c=\beta_{cJ}$ on the segment at point *J*. Applying the formula (5.4.46) and assuming that $\varepsilon=0$, we get the following expressions for the change in angle β along the characteristic *1–3*:

$$\Delta\beta_1=\left[\left(\frac{d\omega}{d\beta}\right)_J-1\right]^{-1}\left(\omega_1-\omega_J-\frac{\Delta x_1}{kR}\cdot\frac{\Delta S}{\Delta n}c_1\right), \tag{7.5.5}$$

where

$$\Delta\beta_1=\beta_3-\beta_1,\quad \Delta x_1=x_3-x_1;$$

$$\frac{\Delta S}{\Delta n}=\frac{(S_3-S_1)\cos(\beta_1+\mu_1)}{(x_3-x_1)\sin\mu_1},\quad c_1=\frac{\sin^2\mu_1\cos\mu_1}{\cos(\beta_1+\mu_1)}.$$

The derivative $(d\omega/d\beta)_J$ is calculated from (5.4.39) for the values of the corresponding parameters at point *1*; the angles ω_1 and ω_J are obtained from (5.3.31) for the Mach numbers $\mathbf{M}$ at points *1* and *J* respectively.

Point *3* in Fig. 7.5.2 lies at the point of intersection of a rectilinear shock and the characteristic *1–3*. Consequently its coordinates are found from the simultaneous solution of the equations:

$$\left.\begin{aligned} y_3-y_1&=(x_3-x_1)\tan(\beta_1+\mu_1);\\ y_3&=x_3\tan(\theta_{c0}-\alpha).\end{aligned}\right\} \tag{7.5.6}$$

The intersection of the characteristic and the shock will be different (at point *3′*) because of the shock bending. The new angle of inclination $\theta_{cJ3'}$ of the shock on the segment *J–3′* is determined from the angle of flow inclination behind the shock $\beta_c=\beta_3'=\Delta\beta_1+\beta_1$ and the Mach number $\mathbf{M}_3'$. This $\mathbf{M}_3'$ is calculated with the help of an expression $\omega_3'=\Delta\omega_1+\omega_1$ in which $\Delta\omega_1$ is found from (5.4.38):

$$\Delta\omega_1=\omega_J+(d\omega/d\beta)_J\,\Delta\beta_1-\omega_1. \tag{7.5.7}$$

Hence the equation of the element *J–3′* of a shock will be $y_{3'}-y_J=(x_{3'}-x_J)\tan(\theta_{cJ3'}-\alpha)$. As a result of the flow turning at point *3′* the characteristic changes its direction on the segment *1–3′*. The equation of characteristics on this segment will take the form $y_{3'}-y_1=(x_{3'}-x_1)\tan(\beta_{3'}+\mu_{3'})$. Solving these two equations simultaneously, we get the coordinates $x_{3'}$, $y_{3'}$ for point 3′.

Let us examine a point *5* situated at the intersection of the elements of characteristics *2–5* and *3′–5* of the first and second family respectively. The coordinates of this point y_5 and x_5 can be determined from the solution of the equations for the elements of the corresponding characteristics:

$$\left.\begin{aligned} y_5-y_2&=(x_5-x_2)\tan(\beta_2+\mu_2);\\ y_5-y_{3'}&=(x_5-x_{3'})\tan(\beta_{3'}-\mu_{3'}).\end{aligned}\right\} \tag{7.5.8}$$

The change in the flow-direction during transition from point *2* to point *5* along the element *2–5* of the characteristic can be obtained from equation (5.4.22) with $\varepsilon=0$:

$$\Delta\beta_2=\frac{1}{2}\left[\frac{1}{kR}\cdot\frac{\Delta S}{\Delta n}(\Delta x_{3'}\, t_{3'}+\Delta x_2\, c_2)-(\omega_2-\omega_{3'})-(\beta_2-\beta_{3'})\right], \tag{7.5.9}$$

where $\Delta\beta_2=\beta_5-\beta_2$; $\Delta x_{3'}=x_5=x_{3'}$;

$\dfrac{\Delta S}{\Delta n}=\dfrac{(S_{3'}-S_2)\cos(\beta_2+\mu_2)\cos(\beta_{3'}-\mu_{3'})}{f+e}$ is the entropy gradient in which

$$f=(x_5-x_2)\sin\mu_{3'}\cos(\beta_2+\mu_2);$$
$$e=(x_5-x_{3'})\sin\mu_2\cos(\beta_{3'}-\mu_{3'}).$$

The values of c_2 and t_3' are determined by (5.4.15). The Mach number **M** at a point *5* is found from (5.4.23) for the given $\Delta\beta_2$. Similarly the velocity at a point *6*, lying at the intersection of the elements of characteristics *H–6* and *5–6* of the first and second family respectively, is determined for the known values of the gas parameters at point *5* and point *H* on the wall. Here the coordinates x_H, y_H of point *H* are obtained from the solution of the contour equation $y_H=f_H(x_H)$ and the equation $y_H-y_2=(x_H-x_2)\times\tan(\beta_2-\mu_2)$ for the element *2–6* of a characteristic.

Let us take an arbitrary point *7* with coordinates y_7, x_7 on the element *H–6* of a characteristic. The flow parameters at this point are determined by the interpolation process. For example, angle $\beta_7=\beta_6-(\beta_6-\beta_H)(6-7)/(6-H)$. Similarly the Mach number $\mathbf{M}_7$ and the corresponding Mach angle μ_7 can be found. Point *7* has been selected in such a way that the element *7–K* of a characteristic drawn from this point at an angle $\beta_7-\mu_7$ intersects the contour at point *K* lying at a small distance from point *H*. The coordinates of this point y_K, x_K are obtained from the solution of the equations $y_K-y_7=(x_K-x_7)\times\tan(\beta_7-\mu_7)$ and $y_K=f_H(x_K)$ for the element of a characteristic and for a contour respectively. As the flow at point *K* is rotational the calculation of velocity at this point should be carried out with the help of (5.4.27). Assuming $\varepsilon=0$ in this equation, we get

$$\Delta\omega_7=-\Delta\beta_7-\frac{\Delta x_7}{kR}\cdot\frac{\Delta S}{\Delta n}\,t_7, \tag{7.5.10}$$

where $\Delta\omega_7=\omega_K-\omega_7$; $\Delta\beta_7=\beta_K-\beta_7$ and the angle $\beta_K=\tan^{-1}(dy_H/dx)_K$. The parameter t_7 is determined from (5.4.28) for the given values of μ_7 and β_7 and the entropy gradient is calculated by formula (5.4.29):

$$\frac{\Delta S}{\Delta n}=\frac{(S_7-S_K)\cos(\beta_7-\mu_7)}{(x_K-x_7)\sin\mu_7}.$$

The entropy S_K at point K is found by calculation of its value at a point O immediately behind the shock. The entropy S_7 at a point *7* is calculated by interpolation from its values at points H and *6*.

Similarly the velocity field in the region between the characteristic DJ, the contour of profile and the curved shock J–*3′*–*4′* is determined by means of successive solution of each of the three problems examined in Chapter 5 Section 4. The form of this shock is determined step by step as a broken line and the given region of flow is filled up with a network of characteristics. At the nodal points of the net of characteristics pressure can be determined by using formula (3.6.28) for a given Mach number. In this formula stagnation pressure $p_0=p_0'$ is calculated by interpolation from formula (5.4.19). The pressure at the points on a contour is found for the corresponding Mach numbers and the stagnation pressure $p_0=p_0'$ calculated from (4.3.22) for angle θ_{cO} and a given Mach number M_∞. Similarly we can determine the velocity, density and pressure at points on the lower side of a contour including point B at the leading edge.

The flow calculation on the lower side of the airfoil is simplified in that case when the characteristic of a second family from point J does not intersect the contour, so that the flow can be considered isentropic (Fig. 7.5.3). For calculation of the Mach number at an arbitrary point L on a contour we use equation (7.5.1):

$$\omega_L=\omega_D-(\beta_D-\beta_L). \tag{7.5.11}$$

Here angle β_L is determined by the formula $\beta_L=\tan^{-1}(dy_H/dx)_L$, taking the sign into account: it will be negative over the front part of a contour and positive near the leading edge; the angle β_D will be negative. The form of a shock is determined by the angle θ_c of its inclination at points *3′* and *4′*. These points are situated at the intersection of the shock and the rectilinear characteristics from points F, G. The shock angle θ_c at point *3′* is approximately determined from (4.3.25) for given values of $\beta_3'=\beta_F$ and M_∞. Similarly we can find the angle of inclination of the shock at a point *4′*.

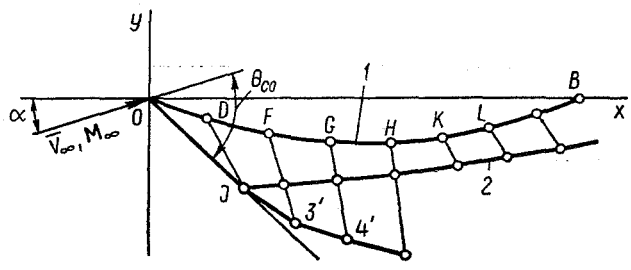

Fig. 7.5.3. Supersonic isentropic flow-interaction of curvilinear sharp profile:

1—contour of body in flow; *2*—characteristic of second family.

The calculation of flow-interaction at the angles of attack $a \geqslant \beta_{Ol}$ has been examined for the case where there exists a suction flow all over the upper side of an airfoil. If this condition is not satisfied ($a < \beta_{Ol}$) the gas flow will be compressed over the upper contour near the leading edge and the shock will be formed there. Hence the calculation of this kind of flow-interaction should be carried out in the same way as on the lower surface.

5.2 Hypersonic flow over thin profile

If a thin profile with sharp edges (see Fig. 7.5.1) is placed in a hypersonic flow at such small angles of attack that the local Mach numbers at all points of its upper and lower surfaces considerably exceed unity and if in addition the conditions of isentropic flow are maintained on the lower contour (see Fig. 7.5.3) the simplified relations of characteristics can be applied for the calculation of perturbation velocity.

If angle of attack $a \geqslant \beta_{Ou}$, then to calculate Mach number $\mathbf{M}$ at any arbitrary point N on the upper contour it is necessary to use, in accordance with (7.4.4), the formula

$$\mathbf{M}_N = \left[\frac{1}{\mathbf{M}_\infty} - \frac{k-1}{2} (a - \beta_N) \right]^{-1}. \tag{7.5.12}$$

As there exists a suction flow all over the upper contour the Mach number $\mathbf{M}_N > \mathbf{M}_\infty$.

The flow-interaction on the lower surface is accompanied by the formation of a shock and hence by the compression of the gas flow. The coefficient of pressure at a point O immediately behind the shock is calculated with the help of formula (4.6.12) in the following way:

$$\frac{\bar{p}_l}{(a - \beta_{Ol})^2} = \frac{1}{1-\delta} + \sqrt{\frac{1}{(1-\delta)^2} + \frac{4}{\mathbf{K}^2}}, \tag{7.5.13}$$

where $\mathbf{K} = \mathbf{M}_\infty (a - \beta_{Ol})$ and the angle β_{Ol} is taken with the minus sign. From the formula $\bar{p}_l = 2\theta_{cO} (a - \beta_{Ol})$ it is possible to calculate the angle of shock inclination θ_{cO} and then the Mach number at point O can be found for the given value of $\mathbf{K}_c = \mathbf{M}_\infty \theta_{cO}$ by using formula (4.6.16):

$$\frac{\mathbf{M}_{Ol}^2}{\mathbf{M}_\infty^2} = \frac{\mathbf{K}_c^2}{[(1+\delta)\mathbf{K}_c^2 - \delta](1 - \delta + \delta\mathbf{K}_c^2)}. \tag{7.5.14}$$

The flow behind point O will be a suction flow, so to determine the velocity at an arbitrary point L we can use the relation

$$\mathbf{M}_L = \left[\frac{1}{\mathbf{M}_{Ol}} + \frac{k-1}{2} (\beta_{Ol} - \beta_L) \right]^{-1}. \tag{7.5.15}$$

An approximate calculation of the hypersonic flow-interaction of a thin profile can be carried out with the help of the method of a local plate. According to this method the flow at any arbitrary point on a contour is worked

out from the corresponding formulas for a flat plate with the assumption that a plate is placed in a flow with a Mach number $\mathbf{M}_\infty$ at an angle of attack equal to the angle between the velocity vector $\overline{V}_\infty$ and the tangent to a contour at the point in question. In this way the coefficient of pressure at some point N on the upper side of the contour will be, according to (7.4.6):

$$\frac{\bar{p}_N}{(a-\beta_N)^2}=\frac{1}{1-\delta}-\sqrt{\frac{1}{(1-\delta)^2}+\frac{4}{\mathbf{K}_N^2}}, \tag{7.5.16}$$

where $\mathbf{K}_N=\mathbf{M}_\infty\,(a-\beta_N)$.

Using (7.5.13) we get the relation

$$\frac{\bar{p}_L}{(a-\beta_L)^2}=\frac{1}{1-\delta}+\sqrt{\frac{1}{(1-\delta)^2}+\frac{4}{\mathbf{K}_L^2}} \tag{7.5.17}$$

for the arbitrary point L on the lower surface of the airfoil. Here

$$\mathbf{K}_L=\mathbf{M}_\infty(a-\beta_L).$$

In formula (7.5.16) the angle β_N has a plus sign for the front part of the contour and a minus sign near the trailing edge. In formula (7.5.17) the angle β_L has a minus sign near the leading edge and a plus sign near the trailing edge.

In the limit of $\mathbf{K}\to\infty$:

$$\bar{p}_N=0; \tag{7.5.18}$$

$$\bar{p}_L=2(a-\beta_L)^2/(1-\delta). \tag{7.5.19}$$

At zero angle of attack formulas (7.5.16), (7.5.17) and (7.5.19) take the following form:

$$\frac{\bar{p}_N}{\beta_N^2}=\frac{1}{1-\delta}-\sqrt{\frac{1}{(1-\delta)^2}+\frac{4}{\mathbf{K}_L^2}}; \tag{7.5.16'}$$

$$\frac{\bar{p}_L}{\beta_L^2}=\frac{1}{1-\delta}+\sqrt{\frac{1}{(1-\delta)^2}+\frac{4}{\mathbf{K}_L^2}}; \tag{7.5.17'}$$

$$\bar{p}_L=2\beta_L^2/(1-\delta). \tag{7.5.19'}$$

In formulas (7.5.16') and (7.5.17') the quantities $\mathbf{K}_N=\mathbf{M}_\infty\beta_N$, $\mathbf{K}_L=\mathbf{M}_\infty\beta_L$.

5.3 Thin profile in small perturbation flow

In this case we are considering the flow-interaction of a thin airfoil at small angles of attack. This kind of flow-interaction is characterized by the property that shocks of finite strength are absent and the characteristics on the upper and lower sides are straight lines with an angle of inclination $\mu_\infty=\sin^{-1}(1/\mathbf{M}_\infty)$.

We use equation (7.4.9) to determine the pressure coefficient on this profile. If an angle of attack $a>\beta_{Ou}$ the pressure coefficient at any arbitrary

point N on the upper side according to (7.4.9), will be

$$\bar{p}_N = -2(\alpha - \beta_N)/\sqrt{M_\infty^2 - 1}, \tag{7.5.20}$$

and at some point L on the lower side it will be

$$\bar{p}_L = 2(\alpha - \beta_L)/\sqrt{M_\infty^2 - 1}. \tag{7.5.21}$$

For zero angle of attack we have

$$\bar{p}_N = 2\beta_N/\sqrt{M_\infty^2 - 1}; \tag{7.5.20'}$$

$$\bar{p}_L = -2\beta_L/\sqrt{M_\infty^2 - 1}. \tag{7.5.21'}$$

5.4 Aerodynamic coefficients

Formulas (1.3.2) and (1.3.3) can be used to determine aerodynamic pressure forces by transferring them to the fixed axes x, y (see Fig. 7.5.1). Formula (1.3.2) gives the axial force R for the airfoil and formula (1.3.3) the normal force N:

$$R = q_\infty S_0 \int_{(S)} \bar{p} \cos(\widehat{\bar{P}_n x}) \frac{dS}{S_0};$$

$$N = q_\infty S_0 \int_{(S)} \bar{p} \cos(\widehat{\bar{P}_n y}) \frac{dS}{S_0}.$$

Taking $S_0 = b \cdot 1$ as a characteristic area and recalling that $dS = dl \cdot 1$ (b is the chord of the profile, dl is the element of a contour), we get the following expressions for aerodynamic coefficients:

$$c_R = R/q_\infty S_0 = \oint \bar{p} \cos(\widehat{\bar{P}_n x})\, d\bar{l};$$

$$c_N = N/q_\infty S_0 = \oint \bar{p} \cos(\widehat{\bar{P}_n y})\, d\bar{l},$$

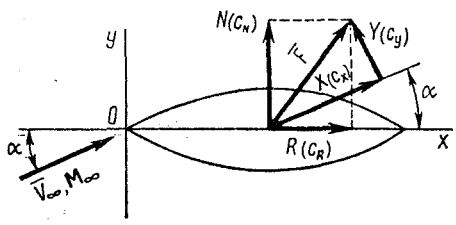

Fig. 7.5.4. Aerodynamic forces for profile in fixed and velocity systems of coordinates.

where $d\bar{l} = dl/b$ and the integrals are worked out along the contour of an airfoil.

Let us introduce the substitution

$$d\bar{l} = d\bar{x}/\sin(\widehat{\bar{P}_n x}),\ d\bar{l}\cos(\widehat{\bar{P}_n y}) = d\bar{x},$$

where $d\bar{x} = dx/b$. Now, coming to the usual integrals from the curvilinear integrals, we get:

$$c_R = -\int_0^1 \bar{p}_l \left(\frac{dy}{dx}\right)_l d\bar{x} + \int_0^1 \bar{p}_u \left(\frac{dy}{dx}\right)_u d\bar{x}; \tag{7.5.22}$$

$$c_N=\int_0^1 (\bar{p}_l-\bar{p}_u)\,d\bar{x}, \tag{7.5.23}$$

where $\bar{p}_l$ and $\bar{p}_u$ are the pressure coefficients on the upper and lower sides of the profile respectively.

Applying the formula for transformation [see formula (1.2.3) and Table 1.2.1], we get aerodynamic coefficients in the velocity system of coordinates (Fig. 7.5.4):

$$\left.\begin{aligned} c_x&=c_R\cos\alpha+c_N\sin\alpha;\\ c_y&=c_N\cos\alpha-c_R\sin\alpha. \end{aligned}\right\} \tag{7.5.24}$$

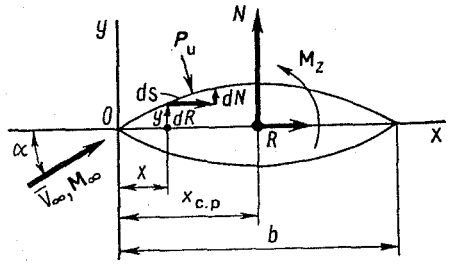

Fig. 7.5.5. Scheme for determination of moment of forces for profile.

By analogy with (1.3.6) we get the formula for the coefficient of moment past the leading edge of the profile due to pressure forces (Fig. 7.5.5):

$$m_z=\frac{\mathbf{M}_z}{q_\infty S_0 b}=\frac{1}{q_\infty S_0 b}\left(\int x\,dN-\int y\,dR\right)$$

$$=\frac{1}{b}\int_{(S)}\bar{p}\,x\cos(\widehat{\bar{P}_n y})\frac{dS}{S_0}-\frac{1}{b}\int_{(S)}\bar{p}\,y\cos(\widehat{\bar{P}_n x})\frac{dS}{S_0},$$

or

$$m_z=\frac{\mathbf{M}_z}{q_\infty b^2}=\int_0^1 (\bar{p}_l-\bar{p}_u)\,\bar{x}\,d\bar{x}$$

$$+\int_0^1\left[\bar{p}_l\bar{y}_l\left(\frac{dy}{d\bar{x}}\right)_l-\bar{p}_u\bar{y}_u\left(\frac{dy}{d\bar{x}}\right)_u\right]d\bar{x}, \tag{7.5.25}$$

where $\bar{y}=y/b$.

We will determine the pressure coefficient of the profile under the condition that the center of pressure lies on the profile chord. If its coordinate is $x_{c.p}$,

$$c_{c.p}=\frac{x_{c.p}}{b}=\frac{\int_0^1(\bar{p}_l-\bar{p}_u)\,\bar{x}d\bar{x}+\int_0^1\left[\bar{p}_l\bar{y}_l\left(\frac{dy}{d\bar{x}}\right)_l-\bar{p}_u\bar{y}_u\left(\frac{dy}{d\bar{x}}\right)_u\right]d\bar{x}}{\int_0^1(\bar{p}_l-\bar{p}_u)\,d\bar{x}}. \tag{7.5.26}$$

As an example let us find the relations of the aerodynamic coefficients for a wedge-shaped airfoil (Fig. 7.5.6). Recalling that $(dy/dx)_l=\tan\beta_l$ for the

lower contour and $(dy/dx)_u=\tan\beta_u$ for the upper contour and assuming that the pressure coefficients $\bar{p}_l$ and $\bar{p}_u$ are constant, we get from (7.5.22) and (7.5.23):

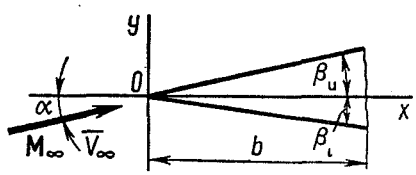

Fig. 7.5.6. Wedge-shaped profile.

$$c_R=-\bar{p}_l\tan\beta_l+\bar{p}_u\tan\beta_u; \quad (7.5.27)$$

$$c_N=\bar{p}_l-\bar{p}_u. \quad (7.5.28)$$

Here angle β_l in formula (7.5.27) should be considered as negative.

The coefficient of moment can be found from (7.5.25):

$$m_z=0.5\,(\bar{p}_l-\bar{p}_u)+0.5\,(\bar{p}_l\tan^2\beta_l-\bar{p}_u\tan^2\beta_u). \quad (7.5.29)$$

At zero angle of attack the coefficients c_R and c_N determine respectively the coefficient of drag $c_x=c_R$ and the coefficient of lift $c_y=c_N$. Two possible cases must be taken into account in calculating these coefficients. In the first case the angle of attack $\alpha>\beta_u$ and so there arises a Prandtl-Meyer expansion flow on the upper side: hence $\bar{p}_u<0$. On the lower side of the airfoil we find the compression of flow ($\bar{p}_l>0$), which is analyzed by the theory of shock waves for angle of inclination $\beta_c=\alpha+|\beta_l|$.

The relations for calculation of the aerodynamic coefficients can be written in the form:

$$c_R=\bar{p}_l|\tan\beta_l|-|\bar{p}_u|\tan\beta_u; \quad (7.5.30)$$

$$c_N=\bar{p}_l+|\bar{p}_u|; \quad (7.5.31)$$

$$m_z=\frac{1}{2}(\bar{p}_l+|\bar{p}_u|)+\frac{1}{2}(\bar{p}_l\tan^2\beta_l+|\bar{p}_u|\tan^2\beta_u). \quad (7.5.32)$$

For a symmetrical wedge we have $\tan\beta_u=|\tan\beta_l|$ in these formulas. If the angle of attack $\alpha=\beta_u$, $\bar{p}_u=0$.

For small wedge angles $\tan\beta\approx\beta$; then

$$c_R=\bar{p}_l|\beta_l|-|\bar{p}_u|\beta_u; \quad (7.5.30')$$

$$m_z=0.5\,(\bar{p}_l+|\bar{p}_u|)+0.5\,(\bar{p}_l\beta_l^2+|\bar{p}_u|\beta_u^2). \quad (7.5.32')$$

For a hypersonic flow over a thin wedge formulas (7.4.6) and (4.6.12) can be used to calculate the pressure coefficients. The pressure coefficient on the lower side, using (4.6.12), will be

$$\bar{p}_l=(\alpha+|\beta_l|)^2\left[\frac{1}{1-\delta}+\sqrt{\frac{1}{(1-\delta)^2}+\frac{4}{\mathbf{K}_l^2}}\right], \quad (7.5.33)$$

and on the upper side its absolute value can be found with the help of (7.4.6):

$$|\bar{p}_u|=(\alpha-\beta_u)^2\left[-\frac{1}{1-\delta}+\sqrt{\frac{1}{(1-\delta)^2}+\frac{4}{\mathbf{K}_u^2}}\right], \quad (7.5.34)$$

where

$$\mathbf{K}_l=\mathbf{M}_\infty(a+|\beta_l|);\ \mathbf{K}_u=\mathbf{M}_\infty(a-\beta_u).$$

Substituting the values of $\bar{p}_l$ and $|\bar{p}_u|$ from (7.5.33) and (7.5.34) in (7.5.30'), (7.5.31) and (7.5.32'), we get the coefficient of axial and normal pressure forces and also the coefficient of moment due to pressure forces.

If a thin wedge is placed in a flow not having high velocity the pressure coefficient is determined by formula (7.4.9), according to which

$$\bar{p}_l=2(a+|\beta_l|)/\sqrt{\mathbf{M}_\infty^2-1}; \tag{7.5.35}$$

$$|\bar{p}_u|=2(a-\beta_u)/\sqrt{\mathbf{M}_\infty^2-1}. \tag{7.5.36}$$

Substituting the values of $\bar{p}_l$ and $\bar{p}_u$ from (7.5.35) and (7.5.36) in (7.5.30'), (7.5.31) and (7.5.32'), we get the coefficients of axial and normal forces and also the coefficient of moment due to pressure forces.

Let us examine the second case of flow-interaction with $a<\beta_u$. Now the compression of flow will be observed on the lower as well as on the upper side of the airfoil; consequently $\bar{p}_l>0$ and $\bar{p}_u>0$. To determine the coefficients c_R, c_N and m_z we have to apply formulas (7.5.27) through (7.5.29). For the arbitrary values of β_l and β_u the pressure coefficients $\bar{p}_l$ and $\bar{p}_u$ will be obtained from the theory of shocks for angles of inclination $\beta_c=a+|\beta_l|$ and $\beta_c=\beta_u-a$ respectively.

At hypersonic speeds the pressure coefficient on the lower side is calculated by the formula (7.5.33). On the upper side it will be found from the similar relation

$$\bar{p}_u=(\beta_u-a)^2\left[\frac{1}{1-\delta}+\sqrt{\frac{1}{(1-\delta)^2}+\frac{4}{\mathbf{K}_u^2}}\right], \tag{7.5.37}$$

where $\mathbf{K}_u=\mathbf{M}_\infty(\beta_u-a)$.

At low supersonic speeds formula (7.5.35) can be used. In place of (7.5.36) we can apply the relation

$$\bar{p}_u=2(\beta_u-a)/\sqrt{\mathbf{M}_\infty^2-1}. \tag{7.5.38}$$

For a symmetrical airfoil ($|\beta_l|=\beta_u$) and at zero angle of attack these formulas are simplified. At hypersonic speeds this case gives

$$\bar{p}_l=\bar{p}_u=\beta^2\left[\frac{1}{1-\delta}+\sqrt{\frac{1}{(1-\delta)^2}+\frac{4}{\mathbf{K}^2}}\right], \tag{7.5.39}$$

where $\beta=|\beta_l|=\beta_u$, $\mathbf{K}=\mathbf{M}_\infty\beta$.

According to the relations (7.5.27) through (7.5.29),

$$c_R=c_x=2\beta^3\left[\frac{1}{1-\delta}+\sqrt{\frac{1}{(1-\delta)^2}+\frac{4}{\mathbf{K}^2}}\right]; \tag{7.5.40}$$

$$c_N=0,\quad m_z=0. \tag{7.5.41}$$

For low supersonic speeds

$$\bar{p}_l=\bar{p}_u=2\beta/\sqrt{M_\infty^2-1}, \tag{7.5.42}$$

and hence

$$\left.\begin{aligned} c_R=c_x=4\beta^2/\sqrt{M_\infty^2-1};\\ c_N=m_z=0. \end{aligned}\right\} \tag{7.5.43}$$

Zhukovskii's formula: We have seen from Chapter 6 Section 3 that the lift force acting on a profile in an incompressible flow is determined by Zhukovskii's formula (6.3.22). Experiments showed that this formula could be extended to the case of the flow-interaction of thin airfoils in a low-perturbation (linearized) gas flow with high speed. Let us examine this for the case of a flat plate at a low angle of attack in a supersonic flow. If the velocity of a disturbed flow over the upper side of a plate is equal to $V_\infty+u$ and on the lower side $V_\infty-u$ the circulation about the contour surrounding this plate will be

$$\Gamma=(V_\infty+u)\,b-(V_\infty-u)\,b=2ub.$$

According to (6.1.5) the additional velocity

$$u=|V_\infty\bar{p}/2|,$$

and hence

$$\Gamma=2b|V_\infty\bar{p}/2|.$$

Using formula (7.5.31) in which it is assumed that

$$\bar{p}_l+|\bar{p}_u|=2\bar{p},\quad c_N\approx c_y,$$

we get the expression

$$Y=c_y\frac{\rho_\infty V_\infty^2}{2}b=2\bar{p}\,\frac{\rho_\infty V_\infty^2}{2}b=\frac{2\Gamma}{V_\infty b}\cdot\frac{\rho_\infty V_\infty^2}{2}b=\rho_\infty V_\infty\Gamma, \tag{7.5.44}$$

which represents by itself Zhukovskii's well-known formula.

6. Swept Wing of Infinite Span

As an example of the application of aerodynamic characteristics of an airfoil we will take up the analysis of the flow-interaction of a swept wing of infinite span in an inviscid gas flow. The scheme of this system is shown in Fig. 7.6.1. If κ is an angle of sweep this flow-interaction is characterized by the velocity component $V_{n\infty}=V_\infty\cos\kappa$ normal to the leading edge. Here it is assumed that the other velocity component $V_{\tau\infty}=V_\infty\sin\kappa$, parallel to this edge, does not call for any change in pressure distribution. Consequently the velocity field in each plane perpendicular to the leading edge will remain one

and the same. This indicates that the coefficients of pressure, lift and drag acting on a swept wing of infinite span could be determined from the values of these coefficients corresponding to the wing section (airfoil) in the plane perpendicular to its leading edge. The velocity and Mach number on the basis of which these coefficients are calculated will be $V_{n\infty}=V_\infty \cos \kappa$ and $\mathbf{M}_{n\infty}=\mathbf{M}_\infty \cos \kappa$ respectively.

Let us assume that in an undisturbed flow with supersonic speed ($V_\infty > a_\infty$, $\mathbf{M}_\infty > 1$) the sweep angle satisfies an inequality $\kappa > \pi/2 - \mu_\infty$, according to which $\cos \kappa < \sin \mu_\infty$ and hence $V_{n\infty} < a_\infty = V_\infty \sin \mu_\infty$, i.e. the velocity component normal to the leading edge will be subsonic. So the flow-interaction of the section of a swept wing in its very nature will be subsonic. In this case the swept edge is known as a subsonic edge.

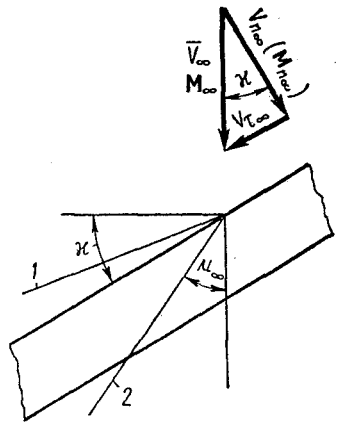

Fig. 7.6.1. Swept wing of infinite span in supersonic flow:

1—Mach line for subsonic edge;
2—Mach line for supersonic edge.

At increased velocities the normal component may exceed sonic speed ($V_{n\infty} > a_\infty = V_\infty \sin \mu_\infty$) so that we have $\kappa < \pi/2 - \mu_\infty$ and $\cos \kappa > \sin \mu_\infty$. In that case the flow-interaction of the swept wing profile will be supersonic. Then the leading edge will be called a supersonic edge.

Let us study the calculation of the supersonic flow-interaction of a swept wing for both these cases.

Supersonic leading edge: The flow-interaction of this wing can be worked out by the formulas derived for a flat plate of infinite span under the condition that the undisturbed flow velocity is $V_{n\infty}=V_\infty \cos \kappa > a_\infty$ and the corresponding Mach number is $\mathbf{M}_{n\infty}=\mathbf{M}_\infty \cos \kappa > 1$. The angle of attack of a flat plate a_l is connected with the given angle of attack of a swept wing by the obvious relation $\sin a_l = \sin a/\cos \kappa$. At small angles of attack it will be $a_l = a/\cos \kappa$.

Using formula (7.4.9) and replacing β and $\mathbf{M}_\infty$ in it by $a_l = a/\cos \kappa$ and $\mathbf{M}_{n\infty}=\mathbf{M}_\infty \cos \kappa$ respectively, we get a relation for the pressure coefficient on a swept wing:

$$\overline{p}_n = \pm 2\, a/(\cos \kappa \sqrt{\mathbf{M}_\infty^2 \cos^2 \kappa - 1}).$$

In this formula pressure coefficient $\overline{p}_n$ is taken with respect to the velocity head $q_n=(1/2)\, k p_\infty \mathbf{M}_{n\infty}^2$. To obtain the value of pressure coefficient $\overline{p}$ with respect to the velocity head of an undisturbed flow $q_\infty=(1/2)\, k p_\infty \mathbf{M}_\infty^2$ we have to use the formula $\overline{p}=\overline{p}_n \cos^2 \kappa$, according to which

$$\overline{p} = \pm 2a \cos \kappa / \sqrt{\mathbf{M}_\infty^2 \cos^2 \kappa - 1}. \qquad (7.6.1)$$

In (7.6.1) the plus sign determines the pressure coefficient on the lower side of the wing and the minus sign that on the upper side.

The coefficients of lift and wave drag can be found from the expressions (7.4.11). Considering small angles of attack, we get

$$c_y = 4a \cos \kappa / \sqrt{\mathbf{M}_\infty^2 \cos^2 \kappa - 1}, \tag{7.6.2}$$

$$c_x = 4a^2 \cos \kappa / \sqrt{\mathbf{M}_\infty^2 \cos^2 \kappa - 1}. \tag{7.6.3}$$

By substituting the value of $\kappa = 0$ for unswept wings in (7.6.2) and (7.6.3) it can be seen that the sweep increases wave drag coefficient c_x. At the same time the lift coefficient c_y also increases. They are connected by the relation $c_y = c_x/a$. It will be shown in Chapter 8 that the results relating to an infinite aspect-ratio wing with sweep can be used for calculation of the flow-interaction of the parts of finite swept wings having supersonic leading edges.

Subsonic leading edge: In this case the flow-interaction of the wing sections, corresponding to the motion of a rectangular wing with Mach number $\mathbf{M}_{n\infty} < 1$, must be examined with the help of the subsonic or transonic theory of profile. The drag will be determined by the laws of subsonic flows and the wave drag may arise only during supercritical flow past the wing ($\mathbf{M}_{n\infty} > \mathbf{M}_{\infty cr}$), in which case shocks appear on the wing surface. If $\mathbf{M}_{n\infty} < \mathbf{M}_{\infty cr}$ shocks and wave drag do not arise. This discussion is related to a wing of infinite span. Wave losses are always present for finite wings because the velocity component $V_\infty \sin \kappa$ has an effect on the wingtips. As a result the supersonic properties of a flow come into the picture and wave drag appears. For the study of this drag it is necessary to apply the three-dimensional theory of supersonic flow-interaction.

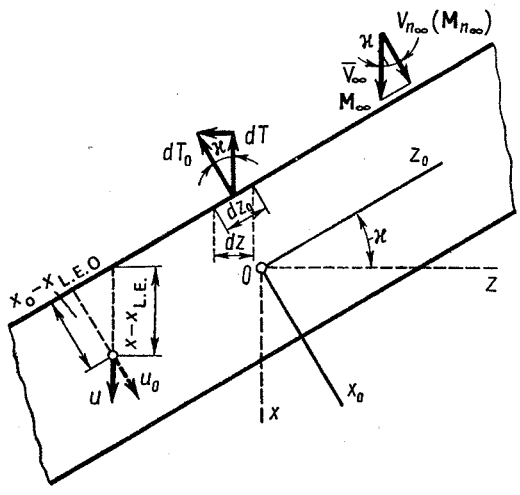

Fig. 7.6.2. Suction force of swept wing.

Suction force: As shown in Chapter 6 Section 3, a suction force arises at the leading edge of an airfoil in an incompressible fluid flow. A similar effect appears in the case of a subsonic flow of compressible gas over an airfoil. Here the sweep of the wing's leading edge will have an effect on the value of this suction force.

For calculation of this force we apply the expression (6.3.25) which can be

extended, with the help of the appropriate transformations, to the more general case of the flow-interaction of a wing with a swept leading edge (Fig. 7.6.2). Let us study this transformation. The velocity component of an undisturbed inviscid flow, tangential to the leading edge of a swept wing, does not change the field of perturbation velocities. It remains the same as for a rectangular wing in a fluid flow with velocity $V_{n\infty}=V_\infty\cos\kappa$. The forces acting on the wing also remain unchanged.

As a result of this a suction force

$$dT_0=\pi\rho c_0^2 dz_0 \tag{7.6.4}$$

will act on an element dz_0 of the wing with a straight leading edge (in the system of coordinates z_0, x_0) where, in accordance with (6.3.28′),

$$c_0^2=\lim_{x_0\to x_{\text{L.E.0}}}[u_0^2(x_0-x_{\text{L.E.0}})].$$

From Fig. (7.6.2) it follows that

$$dT_0=dT/\cos\kappa,\quad dz_0=dz/\cos\kappa,\quad u_0=u/\cos\kappa;$$
$$x_0-x_{\text{L.E.0}}=(x-x_{\text{L.E}})\cos\kappa.$$

Substituting these values in (7.6.4), we get

$$dT/dz=\pi\rho c^2\sqrt{1+\tan^2\kappa}, \tag{7.6.5}$$

where

$$c^2=\lim_{x\to x_{\text{L.E}}}[u^2(x-x_{\text{L.E}})]. \tag{7.6.6}$$

Expressions (7.6.5) and (7.6.6) can be generalized for the case of compressible flows. For this purpose see Chapter 8 Section 2 and use the relation (8.2.4) connecting the geometrical characteristics of wings in compressible and incompressible flows. From these relations it follows that all linear dimensions along the x axis for a wing in a compressible flow are reduced by $\sqrt{1-\mathbf{M}_\infty^2}$ times compared to those in an incompressible flow; at the same time the wing thickness and the spanwise dimensions remain unchanged. Therefore

$$\left.\begin{aligned} x=x_{\text{in}}\sqrt{1-\mathbf{M}_\infty^2},\quad bdz=b_{\text{in}}\,dz_{\text{in}}\sqrt{1-\mathbf{M}_\infty^2};\\ \tan\kappa=\tan\kappa_{\text{in}}\sqrt{1-\mathbf{M}_\infty^2}, \end{aligned}\right\} \tag{7.6.7}$$

where index "in" shows the dimensions of a wing in an incompressible flow.

From (8.2.4) it follows that

$$\frac{\partial\varphi'}{\partial x}=\frac{\partial\varphi'_{\text{in}}}{\partial x_{\text{in}}}\cdot\frac{1}{\sqrt{1-\mathbf{M}_\infty^2}},$$

i.e.

$$u=u_{\text{in}}/\sqrt{1-\mathbf{M}_\infty^2}, \tag{7.6.8}$$

and therefore the pressure coefficients in compressible and incompressible flows are related by

$$\bar{p}=\bar{p}_{\text{in}}/\sqrt{1-\mathbf{M}_\infty^2}. \tag{7.6.9}$$

Suction force T, by its physical nature, happens to be a force dependent on the action of normal pressure. It is determined from the condition $T\approx aY$ at small angles of attack. The corresponding coefficient of suction drag will be given by $c_{xT}=T/(q_\infty S_0)=ac_y$. As the wing dimensions along the y axis do not change as between compressible and incompressible flows the angles of attack for the two kinds of flow also remain unchanged, i.e. $a=a_{\text{in}}$. Hence

$$c_{xT}/c_{xT\text{ in}}=c_y/c_{y\text{ in}}$$

or, according to (7.1.14),

$$c_{xT}=c_{xT\text{ in}}/\sqrt{1-\mathbf{M}_\infty^2}. \tag{7.6.10}$$

Keeping in view the relations obtained, the following expressions can be written for the airfoil of a swept wing:

$$c_{xT}\frac{\rho_\infty V_\infty^2}{2}\,bdz=\frac{C_xT_{\text{in}}}{\sqrt{1-\mathbf{M}_\infty^2}}\cdot\frac{\rho_\infty V_\infty^2}{2}\,b_{\text{in}}\sqrt{1-\mathbf{M}_\infty^2}\,dz_{\text{in}}$$

or

$$dT=dT_{\text{in}}.$$

But since $dz=dz_{\text{in}}$ we have

$$dT/dz=dT_{\text{in}}/dz_{\text{in}}. \tag{7.6.11}$$

The right side of equation (7.6.11), dealing with an incompressible flow, is determined by formulas (7.6.5) and (7.6.6):

$$dT_{\text{in}}/dz_{\text{in}}=\pi\rho_\infty c_{\text{in}}^2\sqrt{1+\tan^2\kappa_{\text{in}}},$$

where

$$c_{\text{in}}^2=\lim_{x_{\text{in}}\to x_{\text{L.E.in}}}[u_{\text{in}}^2(x_{\text{in}}-x_{\text{L.E.in}})].$$

The changes based on the relations (7.6.11), (7.6.7) and (7.6.8) result in

$$c_{\text{in}}^2=\lim_{x\to x_{\text{L.E}}}[u^2(x-x_{\text{L.E}})]\sqrt{1-\mathbf{M}_\infty^2};$$

$$\sqrt{1+\tan^2\kappa_{\text{in}}}=\sqrt{1+\frac{\tan^2\kappa}{1-\mathbf{M}_\infty^2}}.$$

Hence

$$dT/dz=\pi\rho_\infty c^2\sqrt{1+\tan^2\kappa-\mathbf{M}_\infty^2}, \tag{7.6.12}$$

where

$$c^2 = \lim_{x \to x_{L.E}} [u^2 (x - x_{L.E})]. \tag{7.6.13}$$

7. Airfoil in Supersonic Gas Flow with Variable Heat Coefficients

Let us consider the analysis of a flow-interaction process for a wing profile in a high-temperature supersonic flow of gas in which the variation of specific heats can be defined by balanced dissociation. We assume that the flow is potential about the curvilinear surface of the profile and that it represents by itself a suction flow described by equation (5.3.27) for the calculation of an angle ω of turn of flow from the initial value of Mach number $\mathbf{M}$ equal to unity. The integral on the right side of this equation can be determined beforehand by giving a series of values of enthalpy $i_1 < i_0$ for selected fixed values of stagnation enthalpy i_0 and entropy S.

The calculations are carried out in the following way: The corresponding values of velocity should be worked out from the formula $V_i = \sqrt{2(i_0 - i_1)}$ and the sonic speed a_i could be worked out for the given values of i_i and S from the table or graph of thermodynamic functions. Now from the values of a_i and V_i obtained above it is possible to calculate $\mu_i = \sin^{-1}(a_i/V_i)$ and $\cot \mu_i = \sqrt{\mathbf{M}_i^2 - 1}$. Among the values of V_i and a_i we find certain values that happen to be the critical ones ($V_i = a_i = a^*$). The value of a^* so obtained is the lower limit of the integral (5.3.27). The upper limit is any arbitrary quantity selected from the condition of $V_i > a^*$. From the results of the numerical solution of this integral tables are composed [13] containing the data for the values of entropy S from 10^4 to 1.9×10^4 m^2/sec^2·degree at an interval of $\Delta S = 10^3$ m^2/sec^2·degree and the maximum values of stagnation enthalpy i_0 to 4×10^7 m^2/sec^2 at an interval of $\Delta i_0 = 10^6$ m^2/sec^2. These are selected as the fixed parameters. The corresponding values of velocity V in m/sec, sonic speed a in m/sec, Mach number $\mathbf{M}$ and turning angle ω° are given in the tables for each pair of values of i_0 and S depending on the selected values of enthalpy i with an interval of $\Delta i = 10^5$ m^2/sec^2.

With the help of these tables the problem of a dissociating gas flow around a sharp-edged airfoil of curvilinear form under given conditions of undisturbed flow (V_∞, i_∞, S_∞, a) is solved in the following way:

To determine the velocity on the upper side of the airfoil (see Fig. 7.5.1) with suction flow all over we must use formula (7.5.4). The value of ω_∞ in (7.5.4) is found from the table [13] for the given values of enthalpy $i_0 = i_\infty + 0.5V_\infty^2$ and entropy $S_\infty = S(p_\infty, T_\infty)$. After selecting an arbitrary point N at which the inclination of the surface to the vector $\overline{V}_\infty$ is determined by an angle $(\alpha - \beta)$, the angle ω_N can be determined by (7.5.4) and then velocity V_N and the corresponding Mach number $\mathbf{M}_N$ can be found from the same tables [13] for given i_0 and S.

The calculation of flow-interaction with formation of shock on the lower side can be carried out in the following way: First we work out the parameters of a dissociating gas behind the shock near the leading edge point O (velocity V_{Ol}, pressure p_{Ol}, temperature T_{Ol}, enthalpy i_{Ol}, entropy S_l). Then $i_0=i_{Ol}+0.5\,V^2_{Ol}$ is found from the values of i_{Ol} and V_{Ol} and the angle ω_{Ol} is determined from the tables [13] for given values of i_0 and S.

The flow behind the shock will be rotational (non-isentropic) and the calculation of its parameters should, strictly speaking, be performed taking this peculiarity into account. But this of course makes the analysis complicated. However, the simpler method based on the application of formula (7.5.4) for an isentropic flow appears to be useful for evaluation of these parameters. For a given point L on the contour this formula will be written in the form

$$\omega_L=\omega_{Ol}-(\beta_{Ol}-\beta_L),$$

where β_{Ol}, β_L are the angles of inclination of tangents at point O on the leading edge and point L respectively. The velocity V_L and Mach number $\mathbf{M}_L$ are found on the basis of the value of ω_L obtained from tables [13] for given values of i_0 and S. The pressure, density and temperature at point L are determined from the i–S diagram or from the appropriate tables in the form of the functions $p(i_L, S)$, $\rho(i_L, S)$, $T(i_L, S)$ for $i_L=i_0-0.5V^2_L$.

It is obvious that the calculation of the parameters of a dissociating gas over a flat plate is simplified. Let us consider the upper side of it. From the known values of V_∞, p_∞, T_∞ we determine $i_\infty(p_\infty, T_\infty)$ and $S(p_\infty, T_\infty)$ and also the stagnation enthalpy $i_0=i_\infty+0.5V^2_\infty$. Next we find ω_∞ from tables [13] for given values of i_0 and S and then work out $\omega_{0c}=\omega_\infty+a$. The remaining parameters will be determined from the same table for this value of ω_{0c}. The calculation of flow-interaction on the lower side is related to the calculation of the dissociating gas parameters behind an oblique shock for a given angle of inclination of the plate and the known parameters of an undisturbed flow (see Chapter 4 Sections 7 and 8). Here it is assumed that the parameters obtained for the conditions immediately behind the shock will be the flow parameters on the lower side of the plate.

8

A WING IN A SUPERSONIC FLOW

1. Linearized Theory of Finite Wing in Supersonic Flow

1.1 Linearization of equation for a potential function

Let us consider a thin, small cambered wing of arbitrary plan and finite span in a supersonic flow at a small angle of attack. The disturbances created in the flow by such a wing will be small. The linearized theory used to study a small-perturbation flow around a thin airfoil (see Chapter 6 Section 2) can be applied to the flow-interaction problem of this kind of wing. The velocity conditions for such flows were given in the form of (6.1.1). If a linearized three-dimensional gas flow is considered these conditions must be completed by adding the terms for the velocity component along the z axis. Accordingly the following relations will be valid for a linearized three-dimensional flow with small disturbances:

$$V_x = V_\infty + u,\ V_y = v,\ V_z = w, \tag{8.1.1}$$

where u, v, w are components of the perturbation velocity along the x, y, z axes respectively. By virtue of the property of a linearized flow we have

$$u \ll V_\infty,\quad v \ll V_\infty,\quad w \ll V_\infty. \tag{8.1.2}$$

These conditions help to linearize the equation of motion and equation of continuity and simplify the solution of the flow-interaction problem of a thin wing in a steady inviscid fluid flow. The equations of motion of this kind of flow in their general form are obtained from the system (3.1.17), where $\mu=0$, $\partial V_x/\partial t = \partial V_y/\partial t = \partial V_z/\partial t = 0$:

$$\left.\begin{aligned} V_x\frac{\partial V_x}{\partial x}+V_y\frac{\partial V_x}{\partial y}+V_z\frac{\partial V_x}{\partial z} &= -\frac{1}{\rho}\cdot\frac{\partial p}{\partial x};\\ V_x\frac{\partial V_y}{\partial x}+V_y\frac{\partial V_y}{\partial y}+V_z\frac{\partial V_y}{\partial z} &= -\frac{1}{\rho}\cdot\frac{\partial p}{\partial y};\\ V_x\frac{\partial V_z}{\partial x}+V_y\frac{\partial V_z}{\partial y}+V_z\frac{\partial V_z}{\partial z} &= -\frac{1}{\rho}\cdot\frac{\partial p}{\partial z}. \end{aligned}\right\} \tag{8.1.3}$$

The continuity equation is assumed in the form of (2.4.4). Expanding the partial derivatives, we get

$$\rho\left(\frac{\partial V_x}{\partial x}+\frac{\partial V_y}{\partial y}+\frac{\partial V_z}{\partial z}\right)+V_x\frac{\partial \rho}{\partial x}+V_y\frac{\partial \rho}{\partial y}+V_z\frac{\partial \rho}{\partial z}=0. \tag{8.1.4}$$

As shown in Chapter 5 Section 1, the equation of motion and the continuity equation can be combined into one equation relating the velocity components. Performing the transformations as in Chapter 5 Section 1, we get this equation in the following form:

$$\begin{aligned}(V_x^2-a^2)\frac{\partial V_x}{\partial x}+(V_y^2-a^2)\frac{\partial V_y}{\partial y}+(V_z^2-a^2)\frac{\partial V_z}{\partial z}\\ +V_xV_y\left(\frac{\partial V_x}{\partial y}+\frac{\partial V_y}{\partial x}\right)+V_xV_z\left(\frac{\partial V_x}{\partial z}+\frac{\partial V_z}{\partial x}\right)\\ +V_yV_z\left(\frac{\partial V_y}{\partial z}+\frac{\partial V_z}{\partial y}\right)=0.\end{aligned} \tag{8.1.5}$$

Keeping in view the relation (2.3.2) for the potential function and the equality condition of partial cross derivatives ($\partial^2\varphi/\partial x\partial y=\partial^2\varphi/\partial y\partial x$, etc.), the equation of velocity potential from (8.1.5) will be as follows:

$$\begin{aligned}(V_x^2-a^2)\frac{\partial^2\varphi}{\partial x^2}+(V_y^2-a^2)\frac{\partial^2\varphi}{\partial y^2}+(V_z^2-a^2)\frac{\partial^2\varphi}{\partial z^2}\\ +2V_xV_y\frac{\partial^2\varphi}{\partial x\,\partial y}+2V_xV_z\frac{\partial^2\varphi}{\partial x\,\partial z}+2V_yV_z\frac{\partial^2\varphi}{\partial y\,\partial z}=0.\end{aligned} \tag{8.1.6}$$

These equations (8.1.5) and (8.1.6) are the basic differential equations of gas dynamics for three-dimensional steady gas flows. The first corresponds to the more general case of rotational (not potential) gas motion and the second is used only for the study of irrotational (potential) flows.

As the flow around thin wings at small angles of attack is potential the equation of velocity potential (8.1.6) can be applied to the study of this flow-interaction. To linearize equation (8.1.6), which is a nonlinear differential equation, we introduce into it the expression for sonic velocity (7.1.2′) and the quantities

$$\begin{gathered}V_x=V_\infty+u,\ V_y=v,\ V_z=w;\\ V_x^2=V_\infty^2+2V_\infty u,\ V_y^2=v^2,\ V_z^2=w^2;\\ \varphi=\varphi_\infty+\varphi'.\end{gathered}$$

Analyzing the equation so obtained from the viewpoint of the order of smallness of the terms, as we did in Chapter 6 Section 2 for a small-perturbation plane gas flow, we get the linearized equation for the velocity potential of three-dimensional perturbation components in the following way:

$$(\mathbf{M}_\infty^2-1)\frac{\partial^2\varphi'}{\partial x^2}-\frac{\partial^2\varphi'}{\partial y^2}-\frac{\partial^2\varphi'}{\partial z^2}=0. \tag{8.1.7}$$

1.2 Boundary conditions

Study of the flow-interaction of a thin wing of finite aspect ratio leads to the solution of the linearized equation (8.1.7) in terms of second-order partial derivatives of the velocity potential φ' for given boundary conditions. Let us examine these boundary conditions.

1. The wing in a linearized flow (Fig. 8.1.1) induces disturbances which are concentrated in the region of waves. This region is bounded by the surface representing the Mach cones with their apexes at the points on the leading edge with the angle $\mu_\infty=\sin^{-1}(1/\mathbf{M}_\infty)$. The boundary condition to be satisfied by the solution of equation (8.1.7) for function φ' can be written as

$$[\varphi'(x, y, z)]_\Sigma=0. \tag{8.1.8}$$

By this condition the perturbation velocities are equal to zero on the surface of the wave (denoted by Σ) or outside this surface.

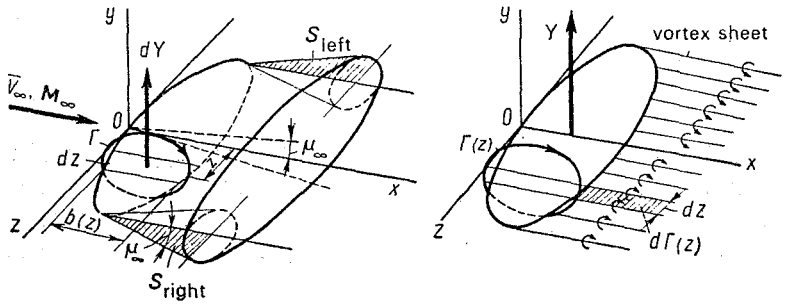

Fig. 8.1.1. Thin wing in linearized flow.

2. The solution for an additional potential φ' must satisfy the boundary condition of an unseparated flow over wing surface S so that the normal component of velocity at every point on the wing is equal to zero, i.e.

$$(V_n)_s=\left(\frac{\partial\varphi}{\partial n}\right)_s=\frac{\partial\varphi}{\partial x}\cos\widehat{(nx)}+\frac{\partial\varphi}{\partial y}\cos\widehat{(ny)}+\frac{\partial\varphi}{\partial z}\cos\widehat{(nz)}=0. \tag{8.1.9}$$

Here

$$\frac{\partial\varphi}{\partial x}=V_\infty+u=V_\infty+\frac{\partial\varphi'}{\partial x},\quad \frac{\partial\varphi}{\partial y}=v=\frac{\partial\varphi'}{\partial y},\quad \frac{\partial\varphi}{\partial z}=w=\frac{\partial\varphi'}{\partial z}.$$

The directional cosines of the external normal to the surface are found from the formulas of analytical geometry:

$$\left.\begin{aligned} \cos\widehat{(nx)} &= -A\,(\partial f/\partial x),\ \cos\widehat{(ny)} = A,\\ \cos\widehat{)nz)} &= -A\,(\partial f/\partial z), \end{aligned}\right\} \tag{8.1.10}$$

where

$$A=[1+(\partial f/\partial x)^2+(\partial f/\partial z)^2]^{-1/2}, \tag{8.1.11}$$

and the function f is determined by the nature of the wing surface [function $y=f_u(x, z)$ for an upper surface, function $y=f_l(x, z)$ for a lower surface].

The linearized (small-perturbation) character of the flow is realized under the condition that the wing is thin and hence $\partial f/\partial x \ll 1$, $\partial f/\partial z \ll 1$. Accordingly $\cos\widehat{(nx)} = -\partial f/\partial x$, $\cos\widehat{(ny)} = 1$, $\cos\widehat{(nz)} = -\partial f/\partial z$. During the flow-interaction of a thin wing the following conditions are also fulfilled:

$$(\partial\varphi'/\partial x)(\partial f/\partial x) \ll 1 \text{ and } (\partial\varphi'/\partial z)(\partial f/\partial z) \ll 1.$$

Taking this into account, equation (8.1.9) can be written in the form

$$-V_\infty(\partial f/\partial x)+(\partial\varphi'/\partial y)=0,$$

from which the boundary condition will be

$$(\partial\varphi'/\partial y)=V_\infty(\partial f/\partial x). \tag{8.1.12}$$

3. The flow-interaction may be accompanied by the appearance of a lift force whose resultant value is obtained by integrating the values of the elemental lift force [for wing elements having width dz and lengths equal to the chords $b(z)$ (see Fig. 8.1.1)]. According to the expression (6.1.8) the coefficient of lift for an elemental surface, assuming circulation $\Gamma(z)$ at the section z equal to

$$\Gamma(z)=\int_0^b \gamma(x)\,dx,$$

will be

$$c'_y=(2/V_\infty b)\,\Gamma(z).$$

Hence the circulation at a given section is

$$\Gamma(z)=0.5c'_yV_\infty b. \tag{8.1.13}$$

From the correlating equation (8.1.13) (see Chapter 6 Section 4) it is clear that the circulation changes as we move to a neighboring section with a different lift coefficient. This variation is given by

$$d\Gamma(z)=(d\Gamma/dz)\,dz=0.5V_\infty(d/dz)(c'_yb)\,dz. \tag{8.1.14}$$

According to the vortex model of a wing discussed in Chapter 6 Section 4 the elementary bound vortex of the section in question must pass through the contour surrounding the neighboring section. This vortex undergoes a turn and leaves the trailing edges in the form of a pair of elementary free vortices forming a vortex sheet behind the wing (see Fig. 8.1.1). In the case of a thin wing at a low angle of attack the width of this sheet may be taken as the wingspan and the free vortices may be directed along the direction of the undisturbed flow.

The following boundary conditions on a vortex sheet may be established from the physical considerations. The normal velocity component of a particle $v_n=\partial\varphi'/\partial n$ must remain continuous on it. Since the direction of the normal over the vortex sheet differs negligibly from the direction of axis Oy the derivative $\partial\varphi'/\partial n$ can be replaced by the quantity $\partial\varphi'/\partial y$. Consequently the condition may be written as

$$(\partial\varphi'/\partial y)_{y=+0}=(\partial\varphi'/\partial y)_{y=-0}, \tag{8.1.15}$$

where the left side corresponds to velocity V_n immediately above the vortex sheet ($y=+0$) and the right side to that below it ($y=-0$). The condition (8.1.15) represents continuity of the function $\partial\varphi'/\partial y$ across the vortex sheet.

In addition the dynamic condition of continuity of pressure must be satisfied on the vortex sheet. From (6.1.5) we get the relation

$$(\partial\varphi'/\partial x)_{y=+0}=(\partial\varphi'/\partial x)_{y=-0}, \tag{8.1.16}$$

indicating the continuity of the derivative $\partial\varphi'/\partial x$ during transition through the vortex sheet.

Let us examine the flow-interaction of a wing of symmetrical profile ($y_u=-y_l$) at zero angle of attack. In this case there is no lift force and hence no vortex sheet. The vertical components of velocity on the upper and lower sides are equal in magnitude and opposite in sign due to the symmetry of the wing, i.e. $v(x, +y, z)=-v(x, -y, z)$. The component $v=0$ in the plane xOz outside the wing. Hence

$$\partial\varphi'/\partial y=0. \tag{8.1.17}$$

Next let us assume that a wing of zero thickness and the same plan given by the surface equation $y=f(x, z)$ is placed in the flow at a small angle of attack. It follows from (8.1.12) that the vertical components of velocity $V_n=\partial\varphi'/\partial y$ on the upper and lower sides of the wing at the corresponding points are equal. In view of the rather small angle of attack the above condition can be used for the plane $y=0$. At the same time this condition can be extended to the vortex sheet behind the wing, which is treated as an extension of the vortices in the plane $y=0$. Therefore the components of velocity V_n at the points situated symmetrically about this plane are equal, i.e.

$$\partial\varphi'(x, -y, z)/\partial y=\partial\varphi'/(x, +y, z)/\partial y.$$

Consequently the additional potential φ' is an odd function of coordinate y, i.e.

$$\varphi'(x, -y, z) = -\varphi'(x, +y, z). \tag{8.1.18}$$

Therefore, the derivative $\partial\varphi'/\partial x$ on the lower side of the vortex sheet is equal to the value of $-\partial\varphi'/\partial x$ on the upper side. However, the equality of the derivatives $\partial\varphi'/\partial x$ was established from the condition of continuity of pressure. The above equalities may be simultaneously fulfilled if and only if

$$\partial\varphi'/\partial x = 0 \tag{8.1.19}$$

on the vortex sheet.

4. To establish the last boundary condition we take the disturbed regions S_{right}, S_{left} (see Fig. 8.1.1) representing the parts of the plane $y=0$ divided by the Mach wave surface situated outside the wing and vortex sheet. The flow is continuous over these parts of the plane $y=0$ in the limits of the Mach wave zone. Therefore the potential φ' also turns out to be a continuous function. At the same time, taking into account that function φ' is an odd function according to (8.1.18), it is necessary to take

$$\varphi'(x, 0, z) = 0 \tag{8.1.20}$$

for the plane $y=0$.

1.3 Components of resultant velocity potential and aerodynamic coefficients

The above boundary conditions must be satisfied by the solution of equation (8.1.7) of an additional potential φ'. This solution for a wing of a given plan can be obtained by adding the potential φ_1' for an ideal plane wing *1* (Fig. 8.1.2) of the same plan as the given wing but with a symmetrical profile at an angle of attack $a=0$, and the potential φ_2' for another idealized wing *2* with camber and zero thickness at the given angle of attack a.

The surface of the idealized wing with a symmetrical airfoil may be given by the equation

$$y = \pm 0.5\,(f_u - f_l) \tag{8.1.21}$$

and that of a wing of zero thickness by an equation of mean lines of the airfoil

$$y = 0.5\,(f_u + f_l). \tag{8.1.22}$$

In this way the resultant potential for a given wing will be

$$\varphi' = \varphi_1' + \varphi_2'. \tag{8.1.23}$$

The flow about wing *2* at $a \neq 0$ can be represented as the flow about a wing *3* at zero angle of attack with the surface equation $y=0.5\,(f_u+f_l)$ and an addi-

tional flow superposed on this taking place about a wing *4* in the form of a flat plate with the same chord as the original wing placed at an angle α (see Fig. 8.1.2).

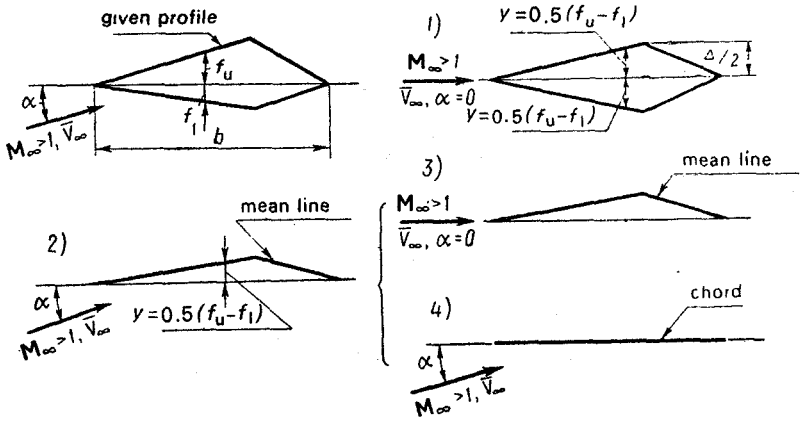

Fig. 8.1.2. System of linearized supersonic flow-interaction of wing of finite thickness at a given angle of attack:

1—wing at $\alpha=0$ with symmetrical profile and given thickness distribution; *2*—wing at $\alpha\neq0$ with zero thickness (wing profile coincides with mean line); *3*—wing at $\alpha=0$ with zero thickness (wing profile coincides with mean line); *4*—wing at $\alpha\neq0$ with zero thickness (wing profile in form of flat plate of same chord).

According to this system of dividing the flow about a wing into two additional components of flow the resultant potential for a given wing will be

$$\varphi' = \varphi_1' + \varphi_3' + \varphi_4'. \tag{8.1.24}$$

By analogy with this value of the velocity potential the distribution of pressure coefficient may be given by

$$\bar{p} = \bar{p}_1 + \bar{p}_3 + \bar{p}_4, \tag{8.1.25}$$

and then the drag force and lift can be found. From (8.1.24) and (8.1.25) it can be seen that the resultant drag force of a given wing can be obtained from the forces for wings *1*, *3* and *4*, i.e.

$$X = X_1 + X_3 + X_4. \tag{8.1.26}$$

Introducing the notation for the sum of two components X_3 and X_4 in the form $X_i = X_3 + X_4$ and writing the above equation of drag force in terms of aerodynamic drag coefficient, we have

$$\frac{X}{q_\infty S_w} = \frac{X_1}{q_\infty S_w} + \frac{X_3 + X_4}{q_\infty S_w} = \frac{X_1}{q_\infty S_w} + \frac{X_i}{q_\infty S_w}$$

or

$$c_x = c_{x0} + c_{x3} + c_{x4} = c_{x0} + c_{xi}. \tag{8.1.27}$$

From (8.1.27) it follows that the coefficient of drag of a wing consists of the coefficient of drag c_{x0} of a symmetrical wing at $c_y = 0$ and the additional drag coefficient c_{xi} related to the lift force calculated for a wing of zero thickness at $c_y \neq 0$. This coefficient c_{xi} is further composed of the coefficient of induced wave drag calculated for a case where induced vortices are absent and the complementary coefficient of induced vortex drag due to the finite span and the consequent formation of a vortex sheet behind the trailing edge of the wing.

By analogy with the expression (8.1.26) for drag we can write, in a general form, the relation determining the resultant lift force on a wing $Y = Y_1 + Y_3 + Y_4$. It can be seen from Fig. 8.1.2 that wing *1* having a symmetrical profile creates no lift force at zero angle of attack, i.e. $Y_1 = 0$. Hence the resultant lift force on a wing is

$$Y = Y_3 + Y_4 \tag{8.1.28}$$

and the corresponding coefficient of this force is

$$c_y = c_{y3} + c_{y4}. \tag{8.1.29}$$

In this way, according to the approximate linearized theory of flow-interaction, the wing thickness will have no effect on lift force. Wing *3* gives constant lift force independent of the angle of attack and represents the value of this force at zero angle of attack for a given camber of wing. The lift force related to the angle of attack is provided by wing *4* and hence depends on the wing plan.

The main problem of the aerodynamics of finite wings in a small-perturbation supersonic flow lies in finding the pressure distribution resulting in forces and the corresponding aerodynamic coefficients in terms of their individual components from formulas (8.1.27), (8.1.29). This problem also forms part of the basic material of the present chapter.

1.4 Characteristics of supersonic flow-interaction of wings

When determining the aerodynamic characteristics of wings it is necessary to take into account the peculiarities of supersonic flow-interactions. The peculiarities are based on the specific property of supersonic flows whereby the disturbances spread only downstream and within the boundaries of the cone of disturbances (Mach cone) with the angle $\mu_\infty = \sin^{-1}(1/M_\infty)$ at the apex.

Let us examine the flow-interaction of a thin wing of arbitrary plan in a supersonic flow (Fig. 8.1.3). Point O at the leading edge happens to be the source of disturbances spreading downstream in the limits of the Mach cone. Here the Mach lines OF and OG can be taken in front of the leading edge

(Fig. 8.1.3, a) as well as behind it (Fig. 8.1.3, b). The position of Mach lines for a given form of wing depends on the Mach number $\mathbf{M}_\infty$. In the first case the Mach number $\mathbf{M}_\infty$ is less than that in the second case and the angle of disturbance $\mu_\infty > (\pi/2) - \kappa$ (κ—angle of sweep back). The component of velocity normal to the leading edge is $V_{n\infty} = V_\infty \cos \kappa$. As $\cos \kappa < \sin \mu_\infty = 1/\mathbf{M}_\infty$ and $V_\infty = a_\infty \mathbf{M}_\infty$ it is obvious that the normal component $V_{n\infty}$ is less than the speed of sound. The motion of a gas in the region near the leading edge of a swept wing for this case was studied in Chapter 7 Section 6. This motion is similar to the subsonic flow-interaction of an airfoil which is characterized by interaction between the upper and lower surfaces occurring through the leading edge. This kind of edge is called a subsonic leading edge (see Fig. 8.1.3, a).

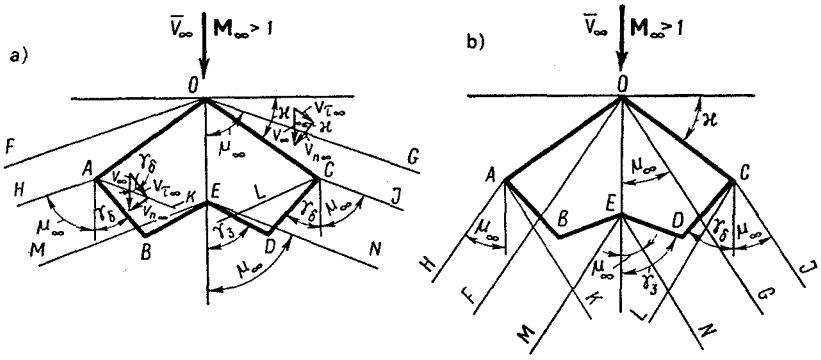

Fig. 8.1.3. Scheme of supersonic flow-interaction of wing:
a—wing with subsonic edges; *b*—wing with supersonic edges.

With an increase in speed the zone of propagation of disturbances diminishes and the Mach lines remain behind the leading edges. In this case, as shown in Fig. 8.1.3, b, the normal velocity component becomes higher than sonic velocity. In reality, it can be seen from Fig. 8.1.3, b that the angle of disturbances $\mu_\infty < \frac{\pi}{2} - \kappa$. Hence $\sin \mu_\infty = 1/\mathbf{M}_\infty < \cos \kappa$ and therefore $V_{n\infty} = V_\infty \cos \kappa > a_\infty$. This kind of leading edge is called a supersonic leading edge. The flow-interaction of a wing in the region of this leading edge is supersonic in nature. The peculiarity of this flow is the absence of interaction between the upper and lower surfaces.

If the Mach line coincides with the leading edge ($\kappa = \pi/2 - \mu_\infty$) the edge will be a sonic one. It is obvious that the velocity component normal to the leading edge in this case is equal to the speed of sound.

Let us introduce the parameter of sweep $n = \tan \kappa / \cot \mu_\infty$. For a supersonic leading edge $\cot \mu_\infty > \tan \kappa$ and therefore $n < 1$. With subsonic and sonic leading edges we have $n > 1$ and $n = 1$ respectively because in the first case $\cot \mu_\infty < \tan \kappa$ and in the second $\cot \mu_\infty = \tan \kappa$.

By analogy with the leading edge the concept of subsonic, sonic and supersonic wing tips and trailing edges can be introduced. Wing tip CD, having an angle of inclination γ_δ to the direction of undisturbed flow velocity less than the angle of disturbances (see Fig. 8.1.3, a), is called a subsonic tip. The component of velocity normal to the tip and equal to $V_{n\infty}=V_\infty \sin \gamma_\delta$ in the given case will be less than sonic velocity. In reality, since $a_\infty = V_\infty \sin \mu_\infty$ and $\mu_\infty > \gamma_\delta$ we have $V_{n\infty} < a_\infty$. It is obvious that the parameter of sweep will be $n>1$. The part of the wing surface with the subsonic tip lies in the region bounded by the cones of disturbance emerging from the points of discontinuity A and C of the contour. A cross-flow of air across the wing tips will be observed due to the pressure of the subsonic normal component of velocity determining the flow-interaction over this part of the wing. This will result in a change in pressure distribution. These effects of wing tips on the flow-interaction of a wing are not found in general if the wing tips are supersonic, which will happen when $\gamma_\delta > \mu_\infty$ (see Fig. 8.1.3, b). In this case the normal velocity component $V_{n\infty}=V_\infty \sin \gamma_\delta$ is higher than the sonic velocity $a_\infty = V_\infty \sin \mu_\infty$.

Similar conclusions may be derived for the trailing edge of a wing. A subsonic trailing edge ($\gamma_3 < \mu_\infty$; $V_n < a_\infty$) and a supersonic trailing edge ($\gamma_3 > \mu_\infty$; $V_{n\infty} > a_\infty$) are shown in Figs. 8.1.3, a and 8.1.3, b respectively.

From the above analysis a qualitative difference between the supersonic and subsonic flow-interactions of a wing can be explained. This difference enters the picture due to the different types of effects of wing tips and trailing edges on the flow-interaction over the wing surface. Whereas the wing tips and trailing edges in a supersonic flow do not affect the flow near the wing at all (see Fig. 8.1.3, b), or this effect is restricted to the part of the wing surface in the vicinity of these edges (see Fig. 8.1.3, a) the effect of wing tips and trailing edges in a subsonic flow will be felt all over the surface due to the possibility of propagation of disturbances downward as well as upward.

2. Method of Sources

The method of sources is used to solve the problem of the determination of the aerodynamic characteristics ($\bar{p}_1$, c_{x0}) of a thin wing of arbitrary plan and symmetrical profile in a small-perturbation flow at zero angle of attack ($c_y=0$).

The sources in an incompressible flow were discussed in Chapter 2 Section 9. The velocity potential of flow due to an incompressible point source situated at the origin of the coordinate system x_n, y_n, z_n according to (2.9.14) will be

$$\varphi_n = -q_n/4\pi \sqrt{x_n^2+y_n^2+z_n^2}, \tag{8.2.1}$$

where q_n is volume flow from the source per unit time.

In the method of sources we are not dealing with isolated point sources

but with sources continuously distributed over some part of a plane—usually the coordinate plane xOz.

Let dq_n be an elementary volume flow rate of fluid created by sources on a small area $d\sigma_n = d\xi_n d\zeta_n$ in plane xOz. Then the derivative $dq_n/d\sigma_n = Q_n$, known as the intensity of distribution of sources, defines the strength of sources per unit area.

If $\pm v$ is the vertical component of velocity on an elemental area (the plus sign indicates that the fluid emerges from sources on the area and the minus sign shows downward source flow) it is obvious that the elemental volume flow rate $dq_n = 2v d\sigma_n$ and hence

$$Q_n = 2v. \tag{8.2.2}$$

For this elementary source the corresponding velocity potential will be

$$d\varphi'_n = -Q_n \, d\sigma_n / 4\pi \sqrt{x_n^2 + y_n^2 + z_n^2}. \tag{8.2.3}$$

Using this expression we can find the relation for the elementary potential of a source in a subsonic compressible flow. Let us examine equation (8.1.7) for this purpose and introduce new variables

$$x_n = x/\sqrt{1-\mathbf{M}_\infty^2}, \quad y_n = y, \quad z_n = z. \tag{8.2.4}$$

With the help of these variables equation (8.1.7) will be transformed into

$$\frac{\partial^2 \varphi'}{\partial x_n^2} + \frac{\partial^2 \varphi'}{\partial y_n^2} + \frac{\partial^2 \varphi'}{\partial z_n^2} = 0, \tag{8.2.5}$$

which coincides with the continuity equation (2.4.8′) for an incompressible flow. Hence the problem of a compressible perturbation flow in coordinates x, y, z can be reduced to the problem of an incompressible perturbation flow in coordinates x_n, y_n, z_n. Here both systems of coordinates are related to equations (8.2.4).

So it is possible to go from the potential (8.2.3) for an incompressible elementary source to the corresponding potential for a compressible subsonic source. Let us find the relation between the small area $d\sigma_n$ in plane $x_n O z_n$ for an incompressible flow and the area $d\sigma$ in the comparable plane for a compressible flow. Using equation (8.2.4) (by replacing x_n with ξ and z_n with ζ) and the expression $d\sigma_n = d\xi_n d\zeta_n$ we find $d\sigma_n = (d\xi d\zeta)\ (1/\sqrt{1-\mathbf{M}_\infty^2})$, from which, recalling that $d\xi d\zeta = d\sigma$, we get the relation

$$d\sigma_n = d\sigma/\sqrt{1-\mathbf{M}_\infty^2}. \tag{8.2.6}$$

Further we transform the expression for Q_n appearing in (8.2.3). The component $v_n = \partial\varphi'/\partial y_n$ or, according to (8.2.4), $v_n = \partial\varphi'/\partial y$. It follows from this that the component of velocity v in a compressible flow is equal to the component of velocity v_n in an incompressible flow. That is, the densities of distribution of sources in compressible and incompressible flows are identical:

$$Q_n = Q = 2v_n = 2v. \tag{8.2.7}$$

Taking the relations obtained above into account, equation (8.2.3) can be transformed into the following form for a compressible flow:

$$d\varphi' = -Qd\sigma/4\pi\sqrt{x^2+(1-\mathbf{M}_\infty^2)(y^2+z^2)}. \tag{8.2.8}$$

Direct substitution of this indicates that the function φ' is an integral of equation (8.2.5). Here it is immaterial whether the speeds are subsonic ($\mathbf{M}_\infty < 1$) or supersonic ($\mathbf{M}_\infty > 1$). In the latter case the expression for an elementary potential may conveniently be written in the form

$$d\varphi' = -Qd\sigma/4\pi\sqrt{x^2-a'^2(y^2+z^2)}, \tag{8.2.9}$$

where $a'^2 = \mathbf{M}_\infty^2 - 1$. It can be seen from the expression (8.2.9) that at $\mathbf{M}_\infty > 1$ it has real values in the part of space where $x^2 \geqslant a'^2(y^2+z^2)$. This indicates that the region of influence of sources, i.e. the region of perturbed flow witnessing interaction of these sources, lies inside the conical surface represented by the equation $x^2 = a'^2(y^2+z^2)$. If a point is situated outside this surface, the sources will have no effect on that point. Here perturbation flow due to the given source is absent.

Equation $x^2 = a'^2(y^2+z^2)$ formally determines the surfaces of two coaxial cones (Fig. 8.2.1) with their apexes at the origin of coordinates. Hence the strength of a source $Qd\sigma$ is used in creating perturbation flows inside these cones. In an actual case the supersonic disturbances propagate only downstream, i.e. only in one of the cones (right-hand cone in Fig. 8.2.1). The perturbation flow in such a cone is determined by the potential having twice the value of that in (8.2.9) because the whole strength of the source, not just half its value, is felt in the flow enclosed in the cone of disturbance. According to this

$$d\varphi' = -\frac{Qd\sigma}{2\pi\sqrt{x^2-a'^2(y^2+z^2)}}. \tag{8.2.10}$$

In the previous case the elementary area $d\sigma = d\xi d\zeta$ with sources was placed at the origin of coordinates. If it is moved from the origin of coordinates to the point with coordinates $x=\xi$, $z=\zeta$, equation (8.2.10) will be written as

$$d\varphi' = -\frac{Qd\sigma}{2\pi\sqrt{(x-\xi)^2-a'^2[y^2+(z-\zeta)^2]}}. \tag{8.2.11}$$

During the study of the flow-interaction of a wing its surface is replaced by a system of distributed sources. To find the potential due to these sources at a point $A(x, y, z)$ (Fig. 8.2.2) it is necessary to integrate (8.2.11) over the region σ in which at least part of the sources are situated. Each of these sources will have an effect at a point $A(x, y, z)$ if this point lies inside the

cone of disturbances with its apex at the source. Thus the zone of action of sources (region of integration) is assumed to be in the region of intersection of the wing surface and the "inverted cone of disturbances" having its apex at a point $A\ (x, y, z)$.

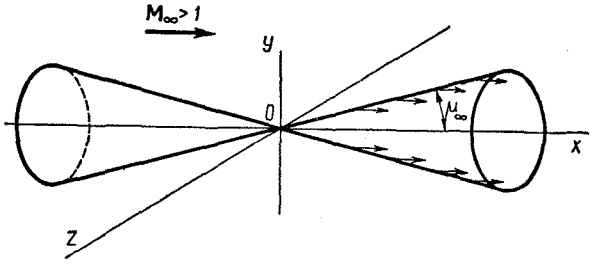

Fig. 8.2.1. Regions of disturbed flow due to supersonic source; right—cone of disturbances (Mach cone) in real supersonic flow.

In the simpler case the point A and the source are placed, as shown in Fig. 8.2.2, in the same plane $y=0$. In this case the zone of action coincides with the region of intersection of the wing and the lines of disturbances emerging from a point $M\ (x, z)$. The region of integration lies on the wing and represents the intersection of the wing with the "inverted plane Mach wave" with its apex at the point $A\ (x, z)$.

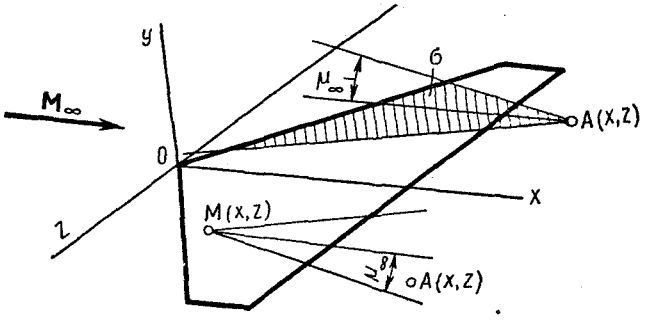

Fig. 8.2.2. Region of effect of supersonic sources.

After determining the region of integration σ it is possible to find the resultant potential at a point $A\ (x, y, z)$:

$$\varphi'(x, y, z)=\frac{-1}{2\pi}\iint\limits_{\sigma}\frac{Q(\xi, \zeta)\,d\xi d\zeta}{\sqrt{(x-\xi)^2-a'^2[y^2+(z-\zeta)^2]}}. \qquad (8.2.12)$$

The additional axial component of velocity can be found by taking the partial derivative of φ' in (8.2.12):

$$\frac{\partial\varphi'}{\partial x}=u=\frac{1}{2\pi}\iint\limits_{\sigma}\frac{Q(\xi, \zeta)(x-\xi)\,d\xi\,d\zeta}{\sqrt{\{(x-\xi)^2-a'^2[y^2+(z-\zeta)^2]\}^3}}. \qquad (8.2.13)$$

The pressure coefficient at the corresponding point $\bar{p}=-2\,(u/V_\infty)$ can be obtained from this expression.

Let us introduce the new coordinates

$$x_1=\frac{x}{a'},\ y_1=y,\ z_1=z. \tag{8.2.14}$$

In terms of these coordinates expression (8.2.12) will be

$$\varphi'(x_1, y_1, z_1)=-\frac{1}{2\pi}\iint\limits_\sigma \frac{Q(\xi,\zeta)\,d\xi d\zeta}{\sqrt{(x_1-\xi)^2-y_1^2-(z_1-\zeta)^2}}. \tag{8.2.15}$$

In the particular case of a point lying on the wing ($y_1=0$) the additional potential

$$\varphi'(x_1, 0, z_1)=-\frac{1}{2\pi}\iint\limits_\sigma \frac{Q(\xi,\zeta)\,d\xi d\zeta}{\sqrt{(x_1-\xi)^2-(z_1-\zeta)^2}}, \tag{8.2.16}$$

where

$$Q=2v_{y_1=0}=2\,(\partial\varphi'/\partial y_1)_{y_1=0} \tag{8.2.17}$$

according to (8.2.7).

The expressions obtained for the potential function help us to find the distribution of velocity and pressure over the surface of a thin wing for a given plan, shape of wing profile and Mach number **M** of undisturbed flow.

3. Delta Wing with Symmetrical Profile ($\alpha=0$, $c_y=0$)

3.1 Semi-wing with subsonic leading edge

Let us study the flow-interaction of a semi-wing with symmetrical airfoil in a supersonic flow at zero angle of attack. This semi-wing represents a triangular surface with one of its sides lying on the x axis and the trailing edge

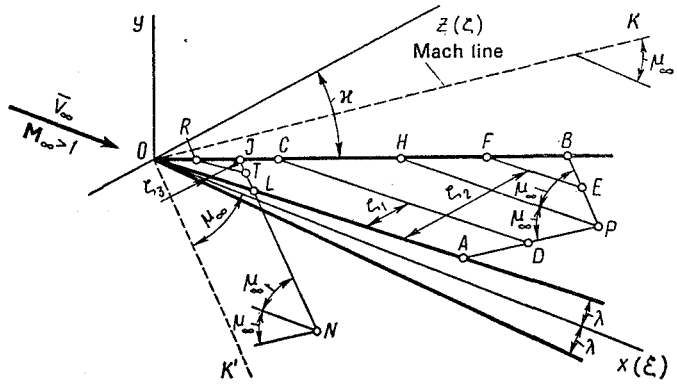

Fig. 8.3.1. Triangular panel of wing with subsonic leading edge.

at infinity (this kind of semi-wing is also known as a delta semi-wing of infinite length) (Fig. 8.3.1). If this surface has a subsonic leading edge the Mach line emerging from apex O will be situated ahead of this edge.

The parameters of flow-interaction at small angles of attack can be determined by replacing the lifting surface with a system of sources distributed in the plane $y=0$. Consider an arbitrary point P on the surface and calculate the velocity potential at this point by adding the effects of sources lying in the region $OAPB$ bounded by the leading edge and side edges OA and OB and the Mach lines AP and BP.

The intensity of sources $Q(\xi, \zeta)$ is determined by formula (8.2.7) in which $v=\lambda V_\infty$ from the condition of unseparated flow, where $\lambda=dy/dx$ is the slope of the wing surface. In this way

$$Q(\xi, \zeta)=2\lambda V_\infty.$$

The velocity potential at point P is obtained from formula (8.2.12). Substituting Q by $2\lambda V_\infty$ and taking $y=0$, we get

$$\varphi'=-\frac{\lambda V_\infty}{\pi}\iint\limits_{\sigma}\frac{d\xi d\zeta}{\sqrt{(x_P-\xi)^2-a'^2(z_P-\zeta)^2}}, \tag{8.3.1}$$

where x_P, z_P are coordinates of point P. This integral takes into account the effect of sources lying on the area σ at point P. This area σ is equal to the region $OAPB$ which can be represented in the form of the sum of the two segments $OAPH$ and HPB. Accordingly the integral φ' in (8.3.1) can be written in the form of the sum of two integrals:

$$\varphi'=-\frac{\lambda V_\infty}{\pi}\left[\iint\limits_{OAPH} f(\xi, \zeta)\, d\xi d\zeta+\iint\limits_{HPB} f(\xi, \zeta)\, d\xi d\zeta\right], \tag{8.3.2}$$

where

$$f(\xi, \zeta)=[(x_P-\xi)^2-a'^2(z_P-\zeta)^2]^{-1/2}. \tag{8.3.3}$$

The integration in the section $OAPH$ with respect to ζ for each of the value of $\zeta=\zeta_1$ can be taken from $\xi=\xi_C=\zeta\tan\kappa$ up to $\xi=\xi_D=x_P-(z_P-\zeta)a'$ and the integration with respect to ζ can be taken from 0 to z_P. On the section HPB it is necessary to carry out integration with respect to ξ for values of $\zeta=\zeta_2$ from $\xi=\xi_F=\zeta\tan\kappa$ up to $\xi=\xi_E=x_P-(\zeta-z_P)a'$. Integration with respect to ζ should be carried out from z_P up to $z_B=(x_P+a'z_P)/(a'+\tan\kappa)$. Thus

$$\varphi'=-\frac{\lambda V_\infty}{\pi}\left[\int\limits_0^{z_P} d\zeta\int\limits_{\zeta\tan\kappa}^{x_P-a'(z_P-\zeta)} f(\xi, \zeta)\, d\xi+\int\limits_{z_P}^{z_B} d\zeta\int\limits_{\zeta\tan\kappa}^{x_P-a'(z_P-\zeta)} f(\xi, \zeta)\, d\xi\right]. \tag{8.3.4}$$

The integral to be determined (up to the accuracy of the constant) will be

$$\int f(\xi, \zeta)\, d\xi = \int \frac{d\xi}{\sqrt{(x_P-\xi)^2 - a'^2 (z_P-\zeta)^2}} = \cosh^{-1}\left\{\frac{x_P-\xi}{a'(z_P-\zeta)}\right\}. \quad (8.3.5)$$

Using this expression and applying the main value of the integral, we get the following formula for potential function:

$$\varphi' = \frac{\lambda V_\infty}{\pi} \int_0^{z_B} \cosh^{-1} \frac{x_P - \zeta \tan \kappa}{a' \mid z_P - \zeta \mid}\, d\zeta, \quad (8.3.6)$$

where the function $|z_P-\zeta|$ is taken with its absolute value.

Calculating the partial derivative $\partial\varphi'/\partial x$, we get the component of additional velocity at a point P along the x axis:

$$u = \frac{\partial \varphi'}{\partial x} = \frac{\lambda V_\infty}{\pi} \int_0^{z_B} \frac{d\zeta}{\sqrt{(x_P - \zeta \tan \kappa)^2 - a'^2 (z_P-\zeta)^2}} \quad (8.3.7)$$

or

$$u = \frac{\partial \varphi'}{\partial x} = \frac{\lambda V_\infty}{\pi} \int_0^{z_B} \frac{d\zeta}{\sqrt{\zeta^2 (\tan^2 \kappa - a'^2) - 2\zeta (x_P \tan \kappa - a'^2 z_P) + x_P^2 - a'^2 z_P^2}}.$$

Noting that $\tan \kappa > a'$, we get after integration

$$u = \frac{\lambda V_\infty}{\pi \sqrt{\tan^2 \kappa - a'^2}} \left(\ln \left\{ 2 \sqrt{(\tan^2 \kappa - a'^2)\, [z_B^2 (\tan^2 \kappa - a'^2)} \rightarrow \cdots \right.\right.$$

$$\cdots \rightarrow \overline{-2 z_B (x_P \tan \kappa - a'^2 z_P) + x_P^2 + a'^2 z_P^2}] + 2 z_B (\tan^2 \kappa - a'^2)$$

$$\left. + 2 (a'^2 z_P - x_P \tan \kappa) \right\} - \ln \left[2 \sqrt{(\tan^2 \kappa - a'^2)(x_P^2 - a'^2 z_P^2)} \right.$$

$$\left.\left. + 2 (a'^2 z_P - x_P \tan \kappa) \right] \right).$$

Substituting here the value of $z_B = (x_P + a' z_P)/(a' + \tan \kappa)$, we get after simplification:

$$u = \frac{\lambda V_\infty}{\pi \sqrt{\tan^2 \kappa - a'^2}} \ln \frac{a' (z_P \tan \kappa - x_P)}{a'^2 z_P - x_P \tan \kappa + \sqrt{(\tan^2 \kappa - a'^2)(x_P^2 - a'^2 z_P^2)}}.$$

The expression under the square root sign in the denominator can be brought to the following form:

$$(\tan^2 \kappa - a'^2)(x_P^2 - a'^2 z_P^2) = (x_P \tan \kappa - a'^2 z_P)^2 - a'^2 (x_P - z_P \tan \kappa)^2.$$

Consequently

$$u = \frac{\lambda V_\infty}{\pi \sqrt{\tan^2 \kappa - a'^2}} \ln \left\{ \frac{x_P \tan \kappa - a'^2 z_P}{a'(x_P - z_P \tan \kappa)} + \sqrt{\left[\frac{x_P \tan \kappa - a'^2 z_P}{a'(x_P - z_P \tan \kappa)}\right]^2 - 1} \right\}^{-1}$$

or

$$u=-\frac{\lambda V_\infty}{\pi\sqrt{\tan^2\kappa-a'^2}}\cosh^{-1}\left\{\frac{x_P\tan\kappa-a'^2 z_P}{a'(x_P-z_P\tan\kappa)}\right\}. \tag{8.3.8}$$

For convenience of calculation we introduce angle θ determined by the condition $\tan\theta=z_P/x_P$ and the angle of sharpness of the leading edge $\gamma=\pi/2-\kappa$ (Fig. 8.3.2). We also introduce the notations

$$n=\tan\kappa/a'=\tan\mu_\infty/\tan\gamma,$$
$$\sigma=z_P\tan\kappa/x_P=\tan\theta/\tan\gamma.$$

Then

$$u=-\frac{\lambda V_\infty}{\pi a'\sqrt{n^2-1}}\cosh^{-1}\frac{n^2-\sigma}{n(1-\sigma)}. \tag{8.3.9}$$

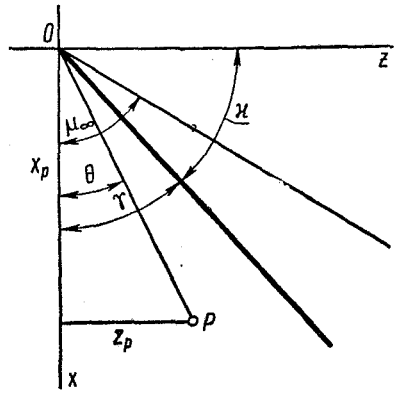

Fig. 8.3.2. Angular parameters for triangular panel of wing.

Using the formula $\cosh^{-1}a=\ln(a+\sqrt{a-1})$ we have

$$u=-\frac{\lambda V_\infty}{\pi a'\sqrt{n^2-1}}\ln\frac{n^2-\sigma+\sqrt{(n^2-1)(n^2-\sigma^2)}}{n(1-\sigma)}. \tag{8.3.9'}$$

The pressure coefficient at the point in question will be

$$\bar{p}=-\frac{2u}{V_\infty}=\frac{2\lambda}{\pi a'\sqrt{n^2-1}}\cosh^{-1}\left\{\frac{n^2-\sigma}{n(1-\sigma)}\right\}. \tag{8.3.10}$$

Let us now consider point N lying on a wing in the region between the Mach line OK' and the x axis (see Fig. 8.3.1) and calculate the velocity at this point induced by the sources distributed over the wing surface. Formula (8.3.1) for determining velocity potential can be used for this purpose. Taking into account that the effect of the source at a point N is restricted to the region $\sigma=OLJ$, we get the expression

$$\varphi'=-\frac{\lambda V_\infty}{\pi}\iint\limits_{OLJ}f(\xi,\zeta)\,d\xi d\zeta, \tag{8.3.11}$$

where the function $f(\xi,\zeta)$ is determined by the relation (8.3.3). The integration with respect to ξ for each value of $\zeta=\zeta_3$ should be carried out from $\xi=\xi_R=\zeta\tan\kappa$ to $\xi=\xi_T=x_N+a'(z_N-\zeta)$ and the integration with respect to ζ should be done from 0 to z_J. Thus

$$\varphi'=-\frac{\lambda V_\infty}{\pi}\int_0^{z_J}d\zeta\int_{\zeta\tan\kappa}^{x_N+a'(z_N-\zeta)}f(\xi,\zeta)\,d\xi, \tag{8.3.12}$$

where $z_J=(x_N+a'z_N)/(\tan\kappa+a')$. On integrating and then using the main value of the integral we get

$$\varphi'=\frac{\lambda V_\infty}{\pi}\int_0^{z_J}\cosh^{-1}\frac{x_N-\zeta\tan\kappa}{a'|z_N-\zeta|}d\zeta.$$

This expression is similar to (8.3.6) with the difference that the upper limit of integration here is taken as the coordinate of a point z_J. After finding the derivative $\partial\varphi'/\partial x$ and carrying out the integration we get the relation (8.3.9′) for an additional velocity component where it is necessary to take $\sigma<0$ because the coordinate z_N happens to be of negative value. It is possible to take the coordinate z_N as positive in calculations and then $\sigma>0$. If an absolute value of $\tan\kappa$ is taken in this process it is possible to use equation (8.3.9) for determination of the induced velocity. In (8.3.9) the sign before σ should be changed for this case. The relation will then have the following form:

$$u=-\frac{\lambda V_\infty}{\pi a'\sqrt{n^2-1}}\cosh^{-1}\frac{n^2+\sigma}{n(1+\sigma)} \tag{8.3.13}$$

or

$$u=-\frac{\lambda V_\infty}{\pi a'\sqrt{n^2-1}}\ln\frac{n^2+\sigma+\sqrt{(n^2-1)(n^2-\sigma^2)}}{n(1+\sigma)}. \tag{8.3.13′}$$

The pressure coefficient will be

$$\bar{p}=-\frac{2u}{V_\infty}=\frac{2\lambda}{\pi a'\sqrt{(n^2-1)}}\cosh^{-1}\frac{n^2+\sigma}{n(1+\sigma)}. \tag{8.3.14}$$

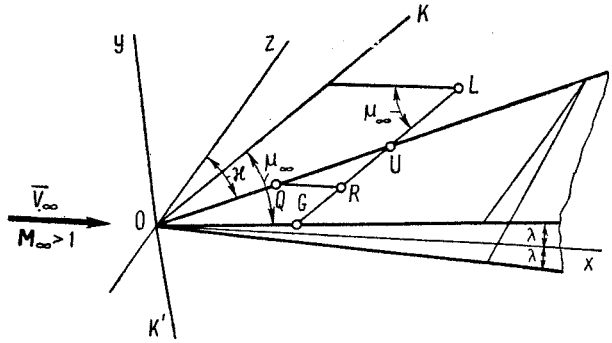

Fig. 8.3.3. Effect of sources on velocity beyond wing.

The sources distributed over a wing also induce velocity in the region between the Mach line OK and the leading subsonic edge (Fig. 8.3.3). The value of this velocity at any point L is determined by the sources distributed

in the region OUG. The corresponding potential function can be obtained from the expression (8.3.12) in which z_J and $x_N+a'(z_N-\zeta)$ should be replaced by z_U and $x_L-a'(z_L-\zeta)$ respectively where the last-named is the coordinate of a point R (see Fig. 8.3.3). Thus

$$\varphi' = -\frac{\lambda V_\infty}{\pi} \int_0^{z_U} d\zeta \int_{\zeta \tan \kappa}^{x_L - a'(z_L-\zeta)} f(\xi, \zeta)\, d\xi, \tag{8.3.15}$$

where $z_U = (x_L - a' z_L)/(\tan \kappa - a')$. Integration on this gives

$$\varphi' = \frac{\lambda V_\infty}{\pi} \int_0^{z_U} \cosh^{-1}\left\{\frac{x_L - \zeta \tan \kappa}{a'|z_L - \zeta|}\right\} d\zeta.$$

After finding the derivative $\partial\varphi'/\partial x$ and then integrating under the condition that $\sigma = z_L \tan \kappa / x_P > 1$ we get, as for (8.3.9), the following formula for additional velocity component:

$$u = -\frac{\lambda V_\infty}{\pi a' \sqrt{n^2-1}} \cosh^{-1} \frac{n^2-\sigma}{n(\sigma-1)} \tag{8.3.16}$$

or

$$u = -\frac{\lambda V_\infty}{\pi a' \sqrt{n^2-1}} \ln \frac{n^2-\sigma+\sqrt{(n^2-1)(n^2-\sigma^2)}}{n(\sigma-1)}, \tag{8.3.16'}$$

where $n > \sigma$.

The coefficient of pressure in the region in question will be

$$\bar{p} = -\frac{2u}{V_\infty} = \frac{2\lambda}{\pi a' \sqrt{n^2-1}} \cosh^{-1} \frac{n^2-\sigma}{n(\sigma-1)}. \tag{8.3.17}$$

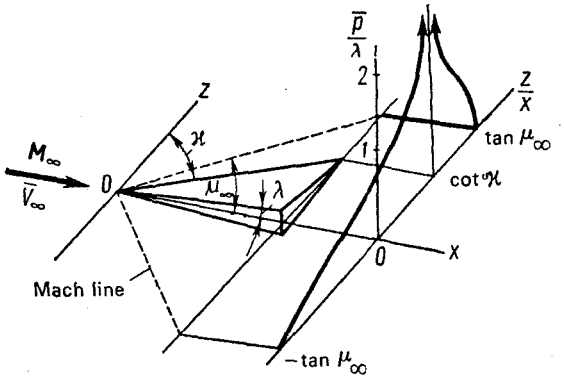

Fig. 8.3.4. Pressure field for triangular panel of wing with subsonic leading edge.

The pressure field for a semi-wing of triangular plan with a subsonic leading edge is shown in Fig. 8.3.4. The coefficient of pressure along the Mach lines is equal to zero. The theoretical value of the pressure coefficient

on the leading edge is equal to infinity. The pressure realized can be considered as physically a significant pressure in magnitude which corresponds to the stagnation pressure at subsonic speed with its direction coinciding with the normal to the leading edge.

3.2 Delta wing symmetrical about x axis with subsonic leading edge

The velocity at a point P on a delta wing symmetrical about the x axis with subsonic leading edges (Fig. 8.3.5) is obtained by superposition of the effect of sources in the region $OBPA'$ bounded by the leading edges OA' and OB and the Mach lines PA' and PB. The velocity induced by the sources lying in the region $OAPB$ is determined by formula (8.3.9). The sources distributed in the region OAA' are responsible for the velocity at point P, which is calculated from the expression (8.3.13). The resultant value of the velocity is

$$u=-\frac{\lambda V_\infty}{\pi a'\sqrt{n^2-1}}\left[\cosh^{-1}\frac{n^2-\sigma}{n(1-\sigma)}+\cosh^{-1}\frac{n^2+\sigma}{n(1+\sigma)}\right]. \tag{8.3.18}$$

This expression can be simplified. Taking summation and using the property of logarithm, we get

$$u=-\frac{\lambda V_\infty}{\pi a'\sqrt{n^2-1}}\ln\frac{[n^2+\sqrt{(n^2-1)(n^2-\sigma^2)}]^2-\sigma^2}{n^2(1-\sigma^2)}$$

or

$$u=-\frac{\lambda V_\infty}{\pi a'\sqrt{n^2-1}}\ln\left[\frac{n^2-\sigma^2}{1-\sigma^2}+2\sqrt{\frac{(n^2-\sigma^2)(n^2-1)}{(1-\sigma^2)^2}}+\frac{n^2-1}{1-\sigma^2}\right],$$

which gives

$$u=-\frac{2\lambda V_\infty}{\pi a'\sqrt{n^2-1}}\ln\left(\sqrt{\frac{n^2-\sigma^2}{1-\sigma^2}}+\sqrt{\frac{n^2-1}{1-\sigma^2}}\right). \tag{8.3.19}$$

The second term under the square root sign can be expressed in the form

$$\sqrt{\frac{n^2-1}{1-\sigma^2}}=\sqrt{\frac{n^2-\sigma^2}{1-\sigma^2}-1}.$$

Thus

$$u=-\frac{2\lambda V_\infty}{\pi a'\sqrt{n^2-1}}\cosh^{-1}\sqrt{\frac{n^2-\sigma^2}{1-\sigma^2}}. \tag{8.3.20}$$

Expressions (8.3.18) through (8.3.20) are valid under the condition that $n>1>\sigma$.

The coefficient of pressure can be determined with the help of (6.1.5) for the given value of the additional velocity component:

$$\bar{p}=-\frac{2u}{V_\infty}=\frac{4\lambda}{\pi a'\sqrt{n^2-1}}\cosh^{-1}\sqrt{\frac{n^2-\sigma^2}{1-\sigma^2}}. \tag{8.3.21}$$

The sources distributed on the part of the wing OUG' have an effect on the point L situated between the leading edge and the Mach wave (see Fig. 8.3.5). The velocity induced by these sources can be calculated as a sum of the velocities induced by the sources lying in the region OUG [formula (8.3.16)] and by sources distributed in the triangle OGG' [formula (8.3.13)].

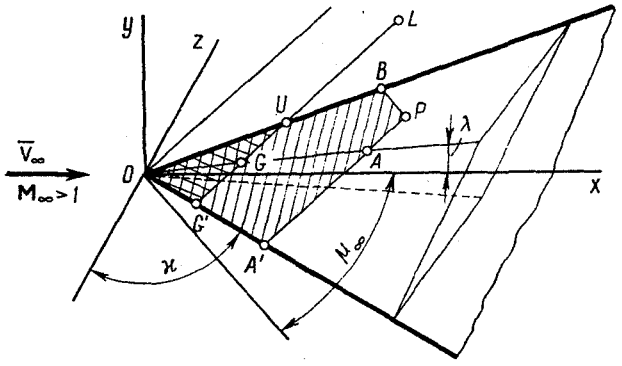

Fig. 8.3.5. Delta wing, symmetrical about x axis, with subsonic leading edge.

Consequently

$$u=-\frac{\lambda V_\infty}{\pi a'\sqrt{n^2-1}}\left[\cosh^{-1}\frac{n^2-\sigma}{n(\sigma-1)}+\cosh^{-1}\frac{n^2+\sigma}{n(1+\sigma)}\right], \qquad (8.3.22)$$

where $n>\sigma>1$.

Formula (8.3.22) can be expressed in the form

$$u=-\frac{\lambda V_\infty}{\pi a'\sqrt{n^2-1}}\ln\frac{[n^2+\sqrt{(n^2-1)(n^2-\sigma^2)}]^2-\sigma^2}{n^2(\sigma^2-1)},$$

which gives the expression

$$u=-\frac{2\lambda V_\infty}{\pi a'\sqrt{n^2-1}}\ln\left(\sqrt{\frac{n^2-\sigma^2}{\sigma^2-1}}+\sqrt{\frac{n^2-1}{\sigma^2-1}}\right). \qquad (8.3.23)$$

The first term under the square root sign may be represented by

$$\sqrt{\frac{n^2-\sigma^2}{\sigma^2-1}}=\sqrt{\frac{n^2-1}{\sigma^2-1}-1}.$$

Then the additional velocity component will be

$$u=-\frac{2\lambda V_\infty}{\pi a'\sqrt{n^2-1}}\cosh^{-1}\sqrt{\frac{n^2-1}{\sigma^2-1}}. \qquad (8.3.24)$$

The pressure coefficient at a given point L, determined by the formula $\bar{p}=-2\,(u/V_\infty)$, will be

$$\bar{p}=\frac{4\lambda}{\pi a'\sqrt{n^2-1}}\cosh^{-1}\sqrt{\frac{n^2-1}{\sigma^2-1}}. \tag{8.3.25}$$

3.3 Infinite semi-wing with supersonic edge

For this kind of wing (Fig. 8.3.6) the Mach line OK emerging from the apex lies on its surface. Consequently

$$(\pi/2)-\kappa>\mu_\infty,\ \tan\kappa<a',\ n=\tan\kappa/a'<1\ (a'=\cot\mu_\infty=\sqrt{\mathbf{M}_\infty^2-1}).$$

Let us consider the velocity at a point L on the wing between the leading edge and the Mach line OK. As the side edge of the wing, coinciding with the x axis, lies behind the Mach line drawn from point L this edge has no effect on the flow at this point. This flow will be the same as that on a flat plate interacting with the supersonic flow $V_{n\infty}=V_\infty\sin\kappa>a_\infty$ in the direction normal to the leading edge. The additional velocity component by the expression (7.6.1) and the formula $\bar{p}=-2u/V_\infty$ will be

$$u=-\lambda V_\infty\cos\kappa/\sqrt{\mathbf{M}_\infty^2\cos^2\kappa-1}.$$

As

$$\mathbf{M}_\infty^2=a'^2+1\ \text{ and }\ 1-1/\cos^2\kappa=-\tan^2\kappa,$$

we have

$$u=-\lambda V_\infty/\sqrt{a'^2-\tan^2\kappa},$$

from which

$$u=-\lambda V_\infty/a'\sqrt{1-n^2}, \tag{8.3.26}$$

where $n=\tan\kappa/a'<1$.

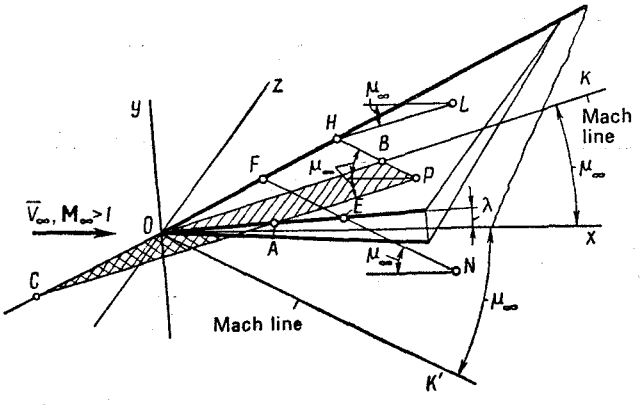

Fig. 8.3.6. Triangular wing panel with supersonic edge.

The corresponding value of the pressure coefficient will be

$$\bar{p}=-2u/V_\infty=2\lambda/a'\sqrt{1-n^2}. \tag{8.3.27}$$

Formulas (8.3.26) and (8.3.27) are applicable in cases when $n<1$ and $1>\sigma>n$.

Let us find the velocity and pressure at point P lying between the Mach line OK and a side edge. If we assumed that this point lies on a wing whose apex is situated at a point C (see Fig. 8.3.6) the velocity could be obtained taking into account only the effect of the leading edge, that is, of sources distributed in the region PCH. By formula (8.3.26) this velocity becomes

$$u_{PCH}=-\lambda V_\infty/a'\sqrt{1-n^2}. \tag{8.3.28}$$

To determine the actual velocity at point P on the given wing with apex at a point O it is necessary to calculate the velocity induced by the sources distributed over a triangle ACO from formula (8.3.28) but with the opposite sign for the intensity of vortices. The value of this actual velocity is obtained from formula (8.3.7). Replacing the upper limit of integration by $z_C=(x_P-a'z_P)/(\tan\kappa-a')$ in this formula, we get

$$u_{AOC}=\frac{\lambda V_\infty}{\pi}\int_0^{z_C}\frac{d\zeta}{\sqrt{\zeta^2(\tan^2\kappa-a'^2)-2\zeta(x_P\tan\kappa-a'^2z_P)+x_P^2-a'^2z_P^2}}, \tag{8.3.29}$$

where $\tan\kappa<a'$ $(\gamma>\mu_\infty)$.

Recalling that at $n=\tan\kappa/a'<1$, $\sigma=z_P\tan\kappa/x_P<1$ and $\sigma<n$

$$\tan^2\kappa-a'^2=a'^2(n^2-1)<0,$$

$$4(\tan^2\kappa-a'^2)(x_P^2-a'^2z_P^2)-4(x_P\tan\kappa-a'^2z_P)$$

$$=4a'^2x_P^2\left[(n^2-1)\left(1-\frac{\sigma^2}{n^2}\right)-n^2\left(1-\frac{\sigma}{n^2}\right)^2\right]<0,$$

we get, after integration,

$$u_{AOC}=-\frac{\lambda V_\infty}{\pi\sqrt{a'^2-\tan^2\kappa}}$$

$$\times\left[\sin^{-1}\frac{2(\tan^2\kappa-a'^2)z_C-2(x_P\tan\kappa-a'^2z_P)}{\sqrt{4(x_P\tan\kappa-a'^2z_P)^2-4(\tan^2\kappa-a'^2)(x_P^2-a'^2z_P^2)}}\right.$$

$$\left.-\sin^{-1}\frac{-2(x_P\tan\kappa-a'^2z_P)}{\sqrt{4(x_P\tan\kappa-a'^2z_P)^2-4(\tan^2\kappa-a'^2)(x_P^2-a'^2z_P^2)}}\right]. \tag{8.3.30}$$

Inserting the value of $z_C=(x_P-a'z_P)/(\tan\kappa-a'^2)$, we find that

$$\frac{2(\tan^2\kappa-a'^2)(x_P-a'z_P)}{\tan\kappa-a'}-2(x_P\tan\kappa-a'^2z_P)=2a'(x_P-z_P\tan\kappa).$$

The quantity under the square root sign in equation (8.3.30) can be simplified to

$$4(x_P\tan\kappa-a'^2z_P)^2-4(\tan^2\kappa-a'^2)(x_P^2-a'^2z_P^2)$$
$$=4a'^2(x_P-z_P\tan\kappa)^2. \tag{8.3.31}$$

Hence

$$u_{AOC}=-\frac{\lambda V_\infty}{\pi\sqrt{a'^2-\tan^2\kappa}}\left[\frac{\pi}{2}-\sin^{-1}\frac{a'^2z_P-x_P\tan\kappa}{a'(x_P-z_P\tan\kappa)}\right]$$

or

$$u_{AOC}=-\frac{\lambda V_\infty}{\pi\sqrt{a'^2-\tan^2\kappa)}}\cos^{-1}\frac{a'^2z_P-x_P\tan\kappa}{a'(x_P-z_P\tan\kappa)}.$$

Taking into account that $n=\tan\kappa/a'$, $\sigma=z_P\tan\kappa/x_P$, we get

$$u_{AOC}=-\frac{\lambda V_\infty}{\pi a'\sqrt{1-n^2}}\cos^{-1}\frac{\sigma-n^2}{n(1-\sigma)}. \tag{8.3.32}$$

The resultant velocity at point P will be

$$u=u_{PCH}-u_{AOC}=-\frac{\lambda V_\infty}{a'\sqrt{1-n^2}}\left[1-\frac{1}{\pi}\cos^{-1}\frac{\sigma-n^2}{n(1-\sigma)}\right]. \tag{8.3.33}$$

The coefficient of pressure at point P will be

$$\bar{p}=-\frac{2u}{V_\infty}=\frac{2\lambda}{a'\sqrt{1-n^2}}\left[1-\frac{1}{\pi}\cos^{-1}\frac{\sigma-n^2}{n(1-\sigma)}\right], \tag{8.3.34}$$

where $\sigma<n<1$.

The induced velocity at a point N, lying between the Mach wave OK' and the side edge, is obtained by superposition of effects of sources distributed in the region of a surface OEF bounded by the leading edge OF, side edge OE and Mach line EF emerging from point N.

Formula (8.3.29) is used to calculate the velocity where the upper limit of integration is to be replaced by the quantity $z_F=(x_N+a'z_N)/(\tan\kappa+a')$ and the coordinates x_P, z_P are to be changed to the corresponding quantities x_N, z_N:

$$u_{OEF}=\frac{\lambda V_\infty}{\pi}\int_0^{z_F}\frac{d\zeta}{\sqrt{\zeta^2(\tan^2\kappa-a'^2)-2\zeta(x_N\tan\kappa-a'^2z_N)+x_N^2-a'^2z_N^2}}. \tag{8.3.35}$$

After integration we get

$$u_{OEF} = -\frac{\lambda V_\infty}{\pi\sqrt{a'^2-\tan^2\kappa}}$$

$$\times\left[\sin^{-1}\frac{2(\tan^2\kappa-a'^2)z_F-2(x_N\tan\kappa-a'^2 z_N)}{\sqrt{4(x_N\tan\kappa-a'^2 z_N)^2-4(\tan^2\kappa-a'^2)(x_N^2-a'^2 z_N^2)}}\right.$$

$$\left.-\sin^{-1}\frac{-2(x_N\tan\kappa-a'^2 z_N)}{\sqrt{4(x_N\tan\kappa-a'^2 z_N)^2-4(\tan^2\kappa-a'^2)(x_N^2-a'^2 z_N^2)}}\right].$$

Inserting the value of $z_F=(x_N+a'z_N)/(\tan\kappa+a'^2)$, the numerator of the first term in the square bracket will be

$$\frac{2(\tan^2\kappa-a'^2)(x_N+a'z_N)}{\tan\kappa+a'}-2(x_N\tan\kappa-a'^2 z_N)=2a'(z_N\tan\kappa-x_N).$$

For convenience in further simplifications we express the quantity (8.3.31) for point N in the form $4a'^2(z_N\tan\kappa-x_N)^2$. Taking these values, we get

$$u_{OEF}=-\frac{\lambda V_\infty}{\pi\sqrt{a'^2-\tan^2\kappa}}\left[\frac{\pi}{2}-\sin^{-1}\frac{-(x_N\tan\kappa-a'^2 z_N)}{a'(z_N\tan\kappa-x_N)}\right]$$

or

$$u_{OEF}=-\frac{\lambda V_\infty}{\pi\sqrt{a'^2-\tan^2\kappa}}\cos^{-1}\frac{x_N\tan\kappa-a'^2 z_N}{a'(x_N-z_N\tan\kappa)}.$$

Introducing the notations of σ and n, this reduces to

$$u_{OEF}=-\frac{\lambda V_\infty}{\pi a'\sqrt{1-n^2}}\cos^{-1}\frac{n^2-\sigma}{n(1-\sigma)},$$

where $\sigma<0$, $n<1$, $|\sigma|<n$.

If the positive values of $z_N>0$ and $\sigma=z_N\tan\kappa/x_N>0$ are assumed and if the absolute values of n are taken,

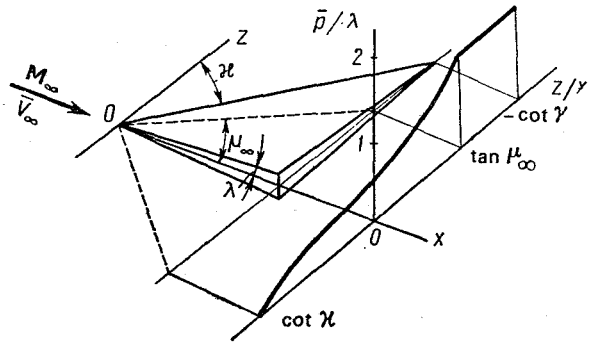

Fig. 8.3.7. Pressure field for triangular panel of wing with supersonic leading edge.

$$u=-\frac{\lambda V_\infty}{\pi a'\sqrt{1-n^2}}\cos^{-1}\frac{n^2+\sigma}{n(1+\sigma)} \tag{8.3.36}$$

the coefficient of pressure at point N will be

$$\bar{p}=-\frac{2u}{V_\infty}=\frac{2\lambda}{\pi a'\sqrt{1-n^2}}\cos^{-1}\frac{n^2+\sigma}{n(1+\sigma)}. \tag{8.3.37}$$

The pressure field for an infinite delta semi-wing with a supersonic leading edge is shown in Fig. 8.3.7. The pressure is constant between the leading edge and the inner Mach line. It decreases further and reaches the value of the pressure of undisturbed flow at the external Mach line ($\bar{p}=0$).

3.4 Delta wing symmetrical about x axis with supersonic leading edge

The velocity and pressure coefficient at a point L (Fig. 8.3.8) lying between the Mach line OK and the leading edge are determined by formulas (8.3.26) and (8.3.27) respectively because the leading edge OR affects the flow only in this region. These formulas are applicable under the conditions of $n<1$; $1>\sigma>n$.

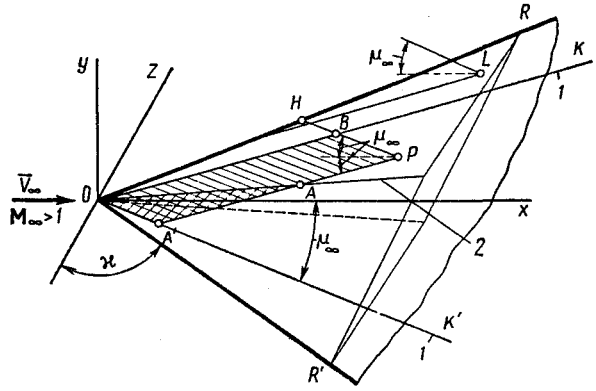

Fig. 8.3.8. Delta wing, symmetrical about x axis, with supersonic leading edge:

1—Mach line; *2*—line of maximum thickness.

If point P situated within the Mach angle is taken, not only the leading edge but also the side and trailing edge have an effect on the flow at that point. The velocity, governed by the effect of the leading edge and a section of the line of maximum thickness OA (see Fig. 8.3.8), is determined by formula (8.3.33). The velocity induced by the sources distributed in the region $OA'A$ is calculated from the expression (8.3.36). Superposing all these components, we get the resultant velocity at point P on a symmetrical wing:

$$u=-\frac{\lambda V_\infty}{a'\sqrt{1-n^2}}\left[1-\frac{1}{\pi}\cos^{-1}\frac{\sigma-n^2}{n(1-\sigma)}+\frac{1}{\pi}\cos^{-1}\frac{n^2+\sigma}{n(1+\sigma)}\right]. \tag{8.3.38}$$

Let us simplify this expression using the formula

$$\cos^{-1} x-\cos^{-1} y=\cos^{-1}[xy+\sqrt{(1-x^2)(1-y^2)}].$$

Then

$$u=-\frac{\lambda V_\infty}{a'\sqrt{1-n^2}}\left[1-\frac{1}{\pi}\cos^{-1}\left(1-2\frac{n^2-\sigma^2}{1-\sigma^2}\right)\right].$$

Considering that

$$\cos^{-1}\left(1-2\frac{n^2-\sigma^2}{1-\sigma^2}\right)=2\sin^{-1}\sqrt{\frac{n^2-\sigma^2}{1-\sigma^2}},$$

we get the final form for the velocity at P:

$$u=-\frac{\lambda V_\infty}{a'\sqrt{1-n^2}}\left(1-\frac{2}{\pi}\sin^{-1}\sqrt{\frac{n^2-\sigma^2}{1-\sigma^2}}\right). \tag{8.3.39}$$

The corresponding value of the pressure coefficient will be

$$\bar{p}=-\frac{2u}{V_\infty}=\frac{2\lambda}{a'\sqrt{1-n^2}}\left(1-\frac{2}{\pi}\sin^{-1}\sqrt{\frac{n^2-\sigma^2}{1-\sigma^2}}\right). \tag{8.3.40}$$

4. Flow-interaction of Swept Wing with Four Corners Having Symmetrical Profile and Subsonic Edges at Zero Angle of Attack

Using the formulas for determination of velocity and pressure on the surface of a delta wing it is possible to analyze the flow-interaction of wings with symmetrical profiles and arbitrary plan at zero angle of attack. Let us take a swept wing with four corners as shown in Fig. 8.4.1. Here and in some other figures the left system of coordinates is used for the convenience of three-dimensional representation of the wing system, the sections in question and the necessary notations. We assume that for this kind of wing the leading edge, trailing edge and line of maximum thickness CBC' will be subsonic. Accordingly the angles of sweep κ_1 and κ_3 of the leading edge and trailing edge and the angle κ_2 of the line of maximum thickness will be more than $(\pi/2)-\mu_\infty$.

The distribution of velocity and pressure over a profile depends on the position of the profile along the wing span, i.e. on the coordinate z of the wing section.

Profile FL $(z=z_1)$: It is necessary to examine the four regions of flow interaction on the profile: FG, GH, HJ and JL. Region FG is bounded by point F on the leading edge and point G lying at the intersection of a Mach line and the coordinate plane $z=z_1$. Here point G is assumed to be situated in the zOx plane and hence it is determined as the point of intersection of a Mach line from point B', which is a projection of point B in the zOx plane,

and the line $z=z_1$ (see Fig. 8.4.1). The velocity and the pressure coefficient in region FG situated behind Mach line OK_O on the wing surface are determined with the help of the distribution of sources in a triangle OCC' using formulas (8.3.20) and (8.3.21) respectively.

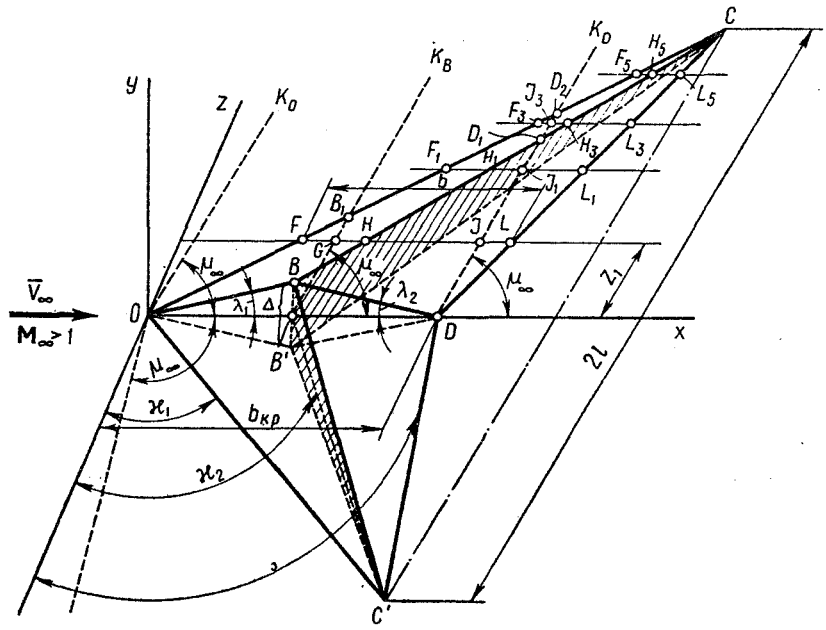

Fig. 8.4.1. Wing having four corners and symmetrical profile with subsonic edges.

As the inclination of a surface is equal to λ_1 the pressure coefficient will be obtained from (8.3.21) as

$$\bar{p}_{FG}=\frac{4\lambda_1}{\pi a'\sqrt{n^2-1}}\cosh^{-1}\sqrt{\frac{n_1^2-\sigma_1^2}{1-\sigma_1^2}}, \tag{8.4.1}$$

where $n_1=\tan\varkappa_1/a'$, $\sigma_1=z_1\tan\varkappa_1/x_1$, x_1 is the variable coordinate of a point.

The drag coefficient of an airfoil corresponding to region FG will be

$$c_{xFG}=\frac{\lambda_1}{b}\int_{x_F}^{x_G}(\bar{p}_u+\bar{p}_l)\,dx_1, \tag{8.4.2}$$

where b is the local chord of an airfoil.

Since

$$\bar{p}_u+\bar{p}_l=2\bar{p}_{FG},$$

$$\sigma_1=\frac{z_1\tan\kappa_1}{x_1},\quad d\sigma_1=-\frac{z_1\tan\kappa_1}{x_1^2}dx_1=-\frac{dx_1}{z_1\tan\kappa_1}\sigma_1^2,$$

we have

$$c_{xFG}=\frac{-8\,z_1\lambda_1^2\tan\kappa_1}{b\pi a'\sqrt{n^2-1}}\int\limits_{\sigma_{1F}}^{\sigma_{1G}}\cosh^{-1}\sqrt{\frac{n_1^2-\sigma_1^2}{1-\sigma_1^2}}\cdot\frac{d\sigma_1}{\sigma_1^2},\tag{8.4.3}$$

where

$$\sigma_{1F}=-\frac{z_1\tan\kappa_1}{x_F}=1,\quad \sigma_{1G}=\frac{z_1\tan\kappa_1}{x_G}.$$

The distribution of sources in $\triangle OCC'$ with intensity of $Q=2\lambda_1V_\infty$ has an effect in region GH and in the triangular surface BCC' where the strength of sources $Q=2(\lambda_2-\lambda_1)V_\infty$ (the sign of angle λ_2 is opposite to that of λ_1).

As the section GH stretches behind the Mach line OK_O within the limits of the wing the calculation of the pressure coefficient, based on the action of distributed sources in the region OCC', should be done with the help of formula (8.3.21). The effect of distribution of sources in triangle BCC' on the pressure coefficient could be obtained with the help of the relation (8.3.25) because section GH is situated behind the boundaries of triangle BCC' between Mach wave $B'K_B$ and edge BC. So

$$\bar{p}_{GH}=\frac{4\lambda_1}{\pi a'\sqrt{n^2-1}}\cosh^{-1}\sqrt{\frac{n_1^2-\sigma_1^2}{1-\sigma_1^2}}+\frac{4(\lambda_2-\lambda_1)}{\pi a'\sqrt{n_1^2-1}}\cosh^{-1}\sqrt{\frac{n_2^2-1}{\sigma_2^2-1}},\tag{8.4.4}$$

where $n_2=\tan\kappa_2/a'$, $\sigma_2=z_1\tan\kappa_2/x_2$, x_2 is the coordinate taken from a point B and equal to $x_2=x_1-x_B$.

Using formulas (8.4.2) and (8.4.4) the coefficient of drag for section GH will be obtained:

$$\begin{aligned}c_{xGH}=&-\frac{8\lambda_1^2 z_1\tan\kappa_1}{b\pi a'\sqrt{n_1^2-1}}\int\limits_{\sigma_{1G}}^{\sigma_{1H}}\cosh^{-1}\sqrt{\frac{n_1^2-\sigma_1^2}{1-\sigma_1^2}}\cdot\frac{d\sigma_1}{\sigma_1^2}\\&-\frac{8(\lambda_2-\lambda_1)\lambda_1 z_1\tan\kappa_2}{b\pi a'\sqrt{n_2^2-1}}\int\limits_{\sigma_{2G}}^{\sigma_{2H}}\cosh^{-1}\sqrt{\frac{n_2^2-1}{\sigma_2^2-1}}\cdot\frac{d\sigma_2}{\sigma_2^2},\end{aligned}\tag{8.4.5}$$

where σ_{2H} and σ_{2G} are taken with respect to point B.

Summing (8.4.3) and (8.4.5) and taking into account that

$$\sigma_{1F}=\frac{z_1\tan\kappa_1}{x_F},\quad \sigma_{1H}=\frac{z_1\tan\kappa_1}{x_H}=\frac{z_1\tan\kappa_1}{x_B+z_1\tan\kappa_2},$$

$$\sigma_{2G}=\frac{z_1\tan\kappa_2}{x_G}=\tan\mu_\infty\tan\kappa_2=\frac{\tan\kappa_2}{a'}=n_2,\quad \sigma_{2H}=\frac{z_1\tan\kappa_2}{x_H}=1,$$

we get

$$c_{xFH}=c_{xFG}+c_{xGH}=-\frac{8\lambda_1^2 z_1\tan\kappa_1}{b\pi a'\sqrt{n_1^2-1}}\int\limits_{\sigma_1=1}^{\sigma_1=\frac{z_1\tan\kappa_1}{x_B+z_1\tan\kappa_2}}\cosh^{-1}\sqrt{\frac{n_1^2-\sigma_1^2}{1-\sigma_1^2}}\cdot\frac{d\sigma_1}{\sigma_1^2}$$

$$-\frac{8(\lambda_2-\lambda_1)\lambda_1 z_1\tan\kappa_2}{b\pi a'\sqrt{n_2^2-1}}\int\limits_{\sigma_2=n_2}^{\sigma_2=1}\cosh^{-1}\sqrt{\frac{n_2^2-1}{\sigma_2^2-1}}\cdot\frac{d\sigma_2}{\sigma_2^2}. \tag{8.4.6}$$

Let us assume that the part of chord HL (considering that point H is located on line BC) is equal to $\bar{r}b$, where $\bar{r}$ is some nondimensional coefficient of proportionality determined from the condition $\bar{r}=B'D/b_r$ (b_r is the root chord). Then for the surface OBC the part of chord FH will be $(1-\bar{r})\,b$.

As part $B'D$ of a root chord is equal to $\bar{r}\cdot b_r$ the remaining part OB' will be equal to $(1-\bar{r})b_r$. The angles λ_1 and λ_2 can be expressed in the following way:

$$\lambda_1=\bar{\Delta}/2(1-\bar{r}),\ \lambda_2=-\bar{\Delta}/2\bar{r}, \tag{8.4.7}$$

where $\bar{\Delta}=\Delta/b_r$ is the relative thickness of the profile.

Taking into account the values of λ_1 and λ_2, formula (8.4.6) could be represented in the form

$$c_{xFH}=-\frac{2\bar{\Delta}^2 z_1}{b(1-\bar{r})\pi a'}\left[\frac{\tan\kappa_1}{\sqrt{n_1^2-1}}\int\limits_{\sigma_{1F}=1}^{\sigma_{1H}=\frac{z_1\tan\kappa_1}{(1-\bar{r})b_r+z_1\tan\kappa_2}}\cosh^{-1}\sqrt{\frac{n_1^2-\sigma_1^2}{1-\sigma_1^2}}\cdot\frac{d\sigma_1}{\sigma_1^2}\right.$$

$$\left.+\frac{\tan\kappa_2}{\bar{r}\sqrt{n_2^2-1}}\int\limits_{\sigma_{2H}=1}^{\sigma_{2F}=n_2}\cosh^{-1}\sqrt{\frac{n_2^2-1}{\sigma_2^2-1}}\cdot\frac{d\sigma_2}{\sigma_2^2}\right]. \tag{8.4.8}$$

The velocity on a line HJ is induced by the sources of intensity $Q=2\lambda_1 V_\infty$ distributed in triangle OCC' and by the sources of intensity $Q=2(\lambda_2-\lambda_1)V_\infty$ distributed in section BCC'. The first distribution of sources establishes the pressure coefficient which is determined by formula (8.3.21) with the substitution of $\lambda=\lambda_1$, $n=n_1$ and $\sigma=\sigma_1$. The pressure coefficient due to the second distribution of sources is also determined by (8.3.21). Here we must take $\lambda=\lambda_2-\lambda_1$, $n=n_2$ and $\sigma=\sigma_2$. Adding these pressure coefficients, we get

$$\bar{p}_{HJ}=\frac{4\lambda_1}{\pi a'\sqrt{n_1^2-1}}\cosh^{-1}\sqrt{\frac{n_1^2-\sigma_1^2}{1-\sigma_1^2}}$$

$$+\frac{4(\lambda_2-\lambda_1)}{\pi a'\sqrt{n_2^2-1}}\cosh^{-1}\sqrt{\frac{n_2^2-\sigma_2^2}{1-\sigma_2^2}}. \tag{8.4.9}$$

Applying formula (8.4.5) with the replacement of λ_1 by λ_2 and noting that in it

$$\lambda_1=\bar{\Delta}/2(1-\bar{r}),\ \lambda_2-\lambda_1=-\bar{\Delta}^2/2\bar{r}(1-\bar{r}),\ \lambda_2=-\bar{\Delta}/2\bar{r},$$

$$n_1=\tan\kappa_1/a',\ n_2=\tan\kappa_2/a',\ \sigma_1=z_1\tan\kappa_1/x_1,$$

$$\sigma_2=z_2\tan\kappa_2/x_2',\ x_H\leqslant x_1\leqslant x_J,\ x_2'=x_1-x_H,$$

we get

$$c_{xHJ}=\frac{-2\bar{\Delta}^2 z_1}{b\bar{r}(1-\bar{r})\pi a'}\left[\frac{\tan\kappa_1}{\sqrt{n_1^2-1}}\int_{\sigma_{1H}}^{\sigma_{1J}}\cosh^{-1}\sqrt{\frac{n_1^2-\sigma_1^2}{1-\sigma_1^2}}\cdot\frac{d\sigma_1}{\sigma_1^2}\right.$$

$$\left.-\frac{\tan\kappa_2}{\sqrt{n_2^2-1}}\int_{\sigma_{2H}}^{\sigma_{2J}}\cosh^{-1}\sqrt{\frac{n_2^2-\sigma_2^2}{1-\sigma_2^2}}\cdot\frac{d\sigma_2}{\sigma_2^2}\right], \tag{8.4.10}$$

where σ_2 is taken with respect to point B.

For section JL the effect of a threefold distribution of sources, namely in triangular surfaces OCC', BCC' and DCC', should be taken into account. The first two distributions of sources control the pressure coefficient determined with the help of formula (8.4.9) in which σ_1 and σ_2 are taken with respect to the points O and D respectively. The additional coefficient of pressure given by the induced effects of the sources distributed in region DCC' having intensity $-\lambda_2$ could be found from formula (8.3.25), in which it is necessary to assume $\lambda=\lambda_2$, $n=n_3$, $\sigma=\sigma_3$.

Superposing the coefficients of pressure due to all three distributions of sources, we get

$$\bar{p}_{JL}=\frac{4\lambda_1}{\pi a'\sqrt{n_1^2-1}}\cosh^{-1}\sqrt{\frac{n_1^2-\sigma_1^2}{1-\sigma_1^2}}+\frac{4(\lambda_2-\lambda_1)}{\pi a'\sqrt{n_2^2-1}}$$

$$\times\cosh^{-1}\sqrt{\frac{n_2^2-\sigma_2^2}{1-\sigma_2^2}}-\frac{4\lambda_2}{\pi a'\sqrt{n_3^2-1}}\cosh^{-1}\sqrt{\frac{n_3^2-1}{\sigma_3^2-1}}, \tag{8.4.11}$$

where σ_1, σ_2 and σ_3 are taken with respect to points O, B and D. Inserting the value of $\bar{p}_{JL}$ in formula (8.4.2) and replacing λ_1 by λ_2, we get

$$c_{xJL}=-\frac{2\bar{\Delta}^2 z_1}{b\bar{r}\pi a'}\left[\frac{\tan\kappa_1}{(1-\bar{r})\sqrt{n_1^2-1}}\int_{\sigma_{1J}}^{\sigma_{1L}}\cosh^{-1}\sqrt{\frac{n_1^2-\sigma_1^2}{1-\sigma_1^2}}\cdot\frac{d\sigma_1}{\sigma_1^2}\right.$$

$$-\frac{\tan\kappa_2}{\bar{r}(1-\bar{r})\sqrt{n_2^2-1}}\int_{\sigma_{2J}}^{\sigma_{2L}}\cosh^{-1}\sqrt{\frac{n_2^2-\sigma_2^2}{1-\sigma_2^2}}\cdot\frac{d\sigma_2}{\sigma_2^2}$$

$$\left.+\frac{\tan\kappa_3}{\bar{r}\sqrt{n_3^2-1}}\int_{\sigma_{3J}}^{\sigma_{3L}}\cosh^{-1}\sqrt{\frac{n_3^2-1}{\sigma_3^2-1}}\cdot\frac{d\sigma_3}{\sigma_3^2}\right]. \tag{8.4.12}$$

Adding (8.4.10) and (8.4.12), we will have

$$c_{xHL}=-\frac{2\bar{\Delta}^2 z_1}{b\bar{r}\pi a'}\left[\frac{\tan\kappa_1}{(1-\bar{r})\sqrt{n_1^2-1}}\int_{\sigma_{1H}}^{\sigma_{1L}}\cosh^{-1}\sqrt{\frac{n_1^2-\sigma_1^2}{1-\sigma_1^2}}\cdot\frac{d\sigma_1}{\sigma_1^2}\right.$$

$$-\frac{\tan\kappa_2}{\bar{r}(1-\bar{r})\sqrt{n_2^2-1}}\int_{\sigma_{2H}}^{\sigma_{2L}}\cosh^{-1}\sqrt{\frac{n_2^2-\sigma_2^2}{1-\sigma_2^2}}\cdot\frac{d\sigma_2}{\sigma_2^2}$$

$$\left.+\frac{\tan\kappa_3}{\bar{r}\sqrt{n_3^2-1}}\int_{\sigma_{3J}}^{\sigma_{3L}}\cosh^{-1}\sqrt{\frac{n_3^2-1}{\sigma_3^2-1}}\cdot\frac{d\sigma_3}{\sigma_3^2}\right]. \tag{8.4.13}$$

In this expression

$$\left.\begin{aligned}\sigma_{1H}&=\frac{z_1\tan\kappa_1}{(1-\bar{r})\,b_r+z_1\tan\kappa_2},\quad \sigma_{1L}=\frac{z_1\tan\kappa_1}{b_r+z_1\tan\kappa_3},\\ \sigma_{2H}&=1,\ \sigma_{2L}=\frac{z_1\tan\kappa_2}{\bar{r}\,b_r+z_1\tan\kappa_3},\\ \sigma_{3J}&=\frac{z_1\tan\kappa_3}{x_J'}=n_3,\ \sigma_{3L}=\frac{z_1\tan\kappa_3}{x_L'}=1,\end{aligned}\right\} \tag{8.4.13'}$$

where

$$x_J'=z_1\cot\mu_\infty=z_1 a',\ x_L'=z_1\tan\kappa_3.$$

The integrals appearing in (8.4.8) and (8.4.13) can be solved by parts using the formula $\cosh^{-1}a=\ln(a+\sqrt{a^2-1})$. Then

$$\int \cosh^{-1}\sqrt{\frac{n^2-\sigma^2}{1-\sigma^2}}\cdot\frac{d\sigma}{\sigma^2}=-\frac{1+\sigma}{\sigma}\ln\frac{\sqrt{n^2-1}+\sqrt{n^2-\sigma^2}}{\sqrt{\sigma+1}}$$

$$+\frac{1-\sigma}{2\sigma}\ln[\pm(1-\sigma)]\pm\ln 2\,[n^2-\sigma+\sqrt{(n^2-1)(n^2-\sigma^2)}]. \quad (8.4.14)$$

The plus sign is taken for $x=2$, $n>1>\sigma$ and the minus sign for $x=0$, $1<\sigma<n$. Let us introduce the notations:

$$\frac{1}{\sigma}\int \cosh^{-1}\sqrt{\frac{n^2-\sigma^x}{1-\sigma^2}}\cdot\frac{d\sigma}{\sigma^2}\left|\begin{array}{l}=N \text{ for } x=2,\ n>1>\sigma\\ [\text{“plus” sign in (8.4.14)}]\\ =Q \text{ for } x=0,\ 1<\sigma<n\\ [\text{“minus” sign in (8.4.14)}].\end{array}\right\} \quad (8.4.15)$$

Substituting $\sigma=1$ in expression (8.4.14) with the plus sign, we get $N=\ln 2$. Assuming $\sigma=n$ in the same expression (8.4.14) with the minus sign, we get $Q=(\ln 2n)/n$. Noting this, the resultant coefficient of profile drag is obtained as a result of summation of (8.4.8) and (8.4.13):

$$c_{xFL}=-\frac{2z_1\bar{\Delta}^2}{\pi b\bar{r}^2(1-\bar{r})^2}\left\{\frac{n_1}{\sqrt{n_1^2-1}}[N_1\bar{r}-\bar{r}(1-\bar{r})N_2-\bar{r}^2\ln 2]\right.$$

$$\left.+\frac{n_2}{\sqrt{n_2^2-1}}[(1-\bar{r})N_3+\bar{r}\ln(2n_2)-\ln 2]+\frac{n_3}{\sqrt{n_3^2-1}}(1-\bar{r})^2\ln n_3\right\}, \quad (8.4.16)$$

where N_1, N_2 and N_3 are obtained by formulas (8.4.14), (8.4.15) for the conditions $n>1>\sigma$, $x=2$ (plus sign) according to the values

$$\left.\begin{array}{c}\sigma_{1H}=\dfrac{z_1\tan\kappa_1}{(1-\bar{r})b_r+z_1\tan\kappa_2},\quad \sigma_{1L}=\dfrac{z_1\tan\kappa_1}{b_r+z_1\tan\kappa_3},\\ \sigma_{2L}=\dfrac{z_1\tan\kappa_2}{b_r\bar{r}+z_1\tan\kappa_3}\end{array}\right\} \quad (8.4.17)$$

respectively.

Formula (8.4.17) is valid (see Fig. 8.4.1) at

$$0<z<z_{B1}<z_{D1}, \quad (8.4.18)$$

where

$$z_{B1}=(1-\bar{r})b_r/(\tan\kappa_1-a'),\ z_{D1}=\bar{r}b_r/(\tan\kappa_2-a'), \quad (8.4.19)$$

or (Fig. 8.4.2) at

$$0<z<z_{D1}<z_{B1}. \quad (8.4.20)$$

The drag coefficient of a profile, determined by formula (8.4.16), is with respect to the local chord b. The value of drag coefficient c_{xo} with respect to the root chord b_r is obtained from the formula $c_{xO}=c_x(b/b_r)$.

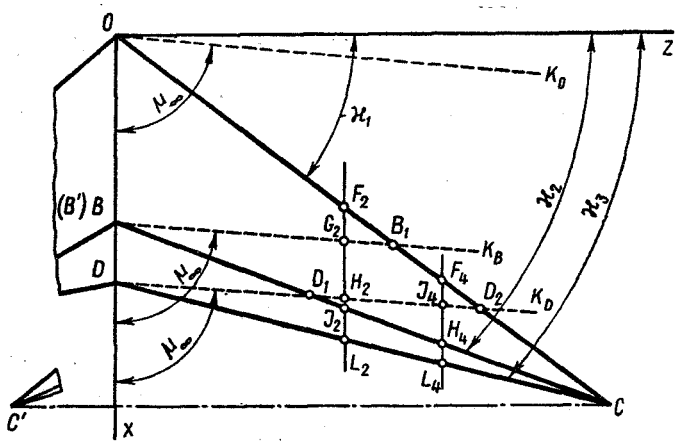

Fig. 8.4.2. Scheme of interaction of wing with Mach lines.

Profile at wing root section ($z=0$): The values of aerodynamic coefficients for this profile are determined in the following way: The velocity in section OB of length $(1-\bar{r})\,b_r$ of this airfoil (see Fig. 8.4.1) is induced by the sources of intensity $Q=2\lambda_1 V_\infty$ distributed over the triangle OCC'. According to this the coefficient of pressure can be calculated from the formula (8.3.21). Assuming $\sigma=z_1 \tan \varkappa_1/x_1=0$, we get

$$\bar{p}_{OB}=\frac{4\lambda_1}{\pi a'\sqrt{n_1^2-1}}\cosh^{-1} n_1. \tag{8.4.21}$$

The sources with intensity $Q=2\lambda_1 V_\infty$ distributed over region OCC' and with intensity $Q=2(\lambda_2-\lambda_1)V_\infty$ distributed over a triangle BCC' act on region DB of length $\bar{r}b_r$ of the profile. The coefficients of pressure are determined accordingly. Applying formula (8.3.21) with $\sigma=0$, we get

$$\bar{p}_{BD}=\frac{4\lambda_1}{\pi a'\sqrt{n_1^2-1}}\cosh^{-1} n_1+\frac{4(\lambda_2-\lambda_1)}{\pi a'\sqrt{n_2^2-1}}\cosh^{-1} n_2. \tag{8.4.22}$$

The coefficient of drag of a profile, taking both upper and lower surfaces, with respect to the root chord b_r will be:

$$c_x=\frac{2}{b_r}\int_0^{(1-\bar{r})\,b_r}\bar{p}_{OB}\,\lambda_1\,dx+\frac{2}{b_r}\int_0^{\bar{r}\,b_r}\bar{p}_{BD}\,\lambda_2\,dx. \tag{8.4.23}$$

Using the values of $\bar{p}_{OB}$ from (8.4.21) and of $\bar{p}_{BD}$ from (8.4.22) and keeping in view that

$$\lambda_2=-\bar{\Delta}/(2\bar{r}),\ \lambda_2-\lambda_1=-\bar{\Delta}/[2\bar{r}\,(1-\bar{r})],$$
$$(1-\bar{r})\,b_r\,\lambda_1=\bar{\Delta}/2 \text{ and } \bar{r}\,b_r\lambda_2=-\bar{\Delta}/2,$$

we get

$$c_x = \frac{2\bar{\Delta}^2}{\pi a' \bar{r}(1-\bar{r})\sqrt{n_2^2-1}} \cosh^{-1} n_2, \tag{8.4.24}$$

where

$$\cosh^{-1} n_2 = \ln(n_2 + \sqrt{n_2^2-1}).$$

Profile F_1L_1: Let us find the coefficient of drag of a profile (see Fig. 8.4.1) that has the coordinate z_1 satisfying the inequality $z_{B1} < z_1 < z_{D1}$. The sources of intensity $Q = 2\lambda_1 V_\infty$ distributed over the region $OCDC'$ and those with intensity $Q = 2(\lambda_2 - \lambda_1) V_\infty$ distributed over BCC' act on section F_1H_1 of this profile. Therefore it is possible to use formula (8.4.4) to calculate the pressure coefficient and the relation (8.4.5) to determine the drag coefficient. This relation (8.4.5) for the section F_1H_1 of this profile can be written in the form

$$c_{xF_1H_1} = -\frac{8\lambda_1^2 z_1 \tan \kappa_1}{b\pi a' \sqrt{n_1^2-1}} \int_{\sigma_{1F_1}}^{\sigma_{1H_1}} \cosh^{-1} \sqrt{\frac{n_1^2-\sigma_1^2}{1-\sigma_1^2}} \cdot \frac{d\sigma_1}{\sigma_1^2}$$

$$-\frac{8(\lambda_2-\lambda_1) z_1 \tan \kappa_2 \lambda_1}{b\pi a' \sqrt{n_2^2-1}} \int_{\sigma_{2F_1}}^{\sigma_{2H_1}} \cosh^{-1} \sqrt{\frac{n_2^2-1}{\sigma_2^2-1}} \cdot \frac{d\sigma_2}{\sigma_2^2}, \tag{8.4.25}$$

where σ_1 and σ_2 are taken with respect to O and B respectively.

The pressure in region H_1L_1 of the profile is determined in the same way as for region HL using formulas (8.4.9) and (8.4.11). The corresponding pressure coefficient $c_{xH_1L_1}$ is found from the expression (8.4.13) in which the limits σ_{1H} and σ_{1L} are replaced by the quantities σ_{1H_1} and σ_{1L_1}, the limits σ_{2H} and σ_{2L} by σ_{2H_1} and σ_{2L_1}, and the limits σ_{3J} and σ_{3L} by σ_{3J_1} and σ_{3L_1}, which could be determined from formula (8.4.13′). The total drag coefficient of profile F_1L_1 with respect to root chord b_r is equal to

$$c_{xF_1L_1} = c_{xF_1H_1} + c_{xH_1L_1} = \frac{2z_1\bar{\Delta}^2}{b_r \pi \bar{r}^2(1-\bar{r})^2} \left\{ [N_1 \bar{r} - N_2 \bar{r}(1-\bar{r}) \right.$$

$$-\bar{r}^2 \ln 2] \frac{n_1}{\sqrt{n_1^2-1}} + \frac{n_2}{\sqrt{n_2^2-1}} [(1-\bar{r}) N_3 + \bar{r} Q_1 - \ln 2]$$

$$\left. + \frac{n_3}{\sqrt{n_3^2-1}} (1-\bar{r})^2 \ln n_3 \right\}, \tag{8.4.26}$$

where N_1, N_2, N_3 are obtained from the expressions (8.4.14), (8.4.15) for the corresponding values of σ_{1H_1} σ_{1L_1} and σ_{2L_1} which are calculated for points

H_1 and L_1 by formula (8.4.17). The quantity Q_1 is determined from the relations (8.4.14) and (8.4.15) for $x=0$ at

$$\sigma=z_1 \tan \kappa_2/[z_1 \tan \kappa_1-(1-\bar{r})\, b_r]. \tag{8.4.27}$$

Profile F_2L_2: Let us take the profile situated between points D_1 and B_1 (see Fig. 8.4.2) with the coordinate z_1 which satisfies the inequality $z_{D1}< z_1< z_{B_1}$. The flow-interaction of this profile is fairly complicated in nature. The velocity in region F_2G_2 is induced by sources with intensity $Q=2\lambda_1 V_\infty$ distributed over the triangle OCC'. Hence the coefficient of pressure in this region is determined with the help of formula (8.4.1) and the corresponding drag coefficient $c_{xF_2G_2}$ is given by expression (8.4.3) in which the integration is taken in the range from σ_{1F_2} to σ_{1G_2}.

The pressure in region G_2H_2 depends on the influence of sources with intensity $Q=2\lambda_1 V_\infty$ distributed over region OCC' and also of sources with intensity $Q=2\,(\lambda_2-\lambda_1)\, V_\infty$ situated in region BCC'. Consequently the pressure coefficient is calculated by formula (8.4.4) and the drag coefficient $c_{xG_2H_2}$ is given by expression (8.4.5) in which the first integral is carried out in the range from σ_{1G_2} to σ_{1H_2} and the second integral in the range from σ_{2G_2} to σ_{2H_2}.

The sources distributed in region OCC' $(Q=2\lambda_1 V_\infty)$ and those over triangle BCC' $[Q=2\,(\lambda_2-\lambda_1)\, V_\infty]$ and surface BCC' $(Q=-2\lambda_2 V_\infty)$ have their effect in section H_2J_2 of this profile. The first distribution establishes the pressure coefficient obtained from formula (8.3.21) and the remaining two distributions give the coefficient determined by expression (8.3.25). The total value of the pressure coefficient on this section of profile will be

$$\bar{p}_{H_2J_2}=\frac{4\lambda_1}{\pi a'\sqrt{n_1^2-1}}\cosh^{-1}\sqrt{\frac{n_1^2-\sigma_1^2}{1-\sigma_1^2}}+\frac{4\,(\lambda_2-\lambda_1)}{\pi a'\sqrt{n_1^2-1}}$$
$$\times\cosh^{-1}\sqrt{\frac{n_2^2-1}{\sigma_2^2-1}}-\frac{4\lambda_2}{\pi a'\sqrt{n_3^2-1}}\cosh^{-1}\sqrt{\frac{n_3^2-1}{\sigma_3^2-1}}, \tag{8.4.28}$$

where σ_1, σ_2 and σ_3 are taken with respect to O, B and D respectively.

Applying the formula

$$c_{xH_2J_2}=\frac{2}{b_r}\int_{x_{H_2}}^{x_{J_2}}\bar{p}_{H_2J_2}\,\lambda_2\,dx, \tag{8.4.29}$$

it is possible to calculate the drag coefficient of the section of profile in question with respect to root chord b_r.

The flow-interaction of the last section J_2L_2 of this profile is governed by the influence of the sources distributed over the same regions of the wing as those for section H_2J_2 of this profile. Here we must take into account the

fact that the velocity induced by the sources over region BCC' is determined by formula (8.3.20) where λ is replaced by the angular coefficient $(\lambda_2-\lambda_1)$. Therefore the pressure coefficient should be calculated by formula (8.4.11) and the drag coefficient $c_{xJ_2L_2}$ should be obtained from expression (8.4.12) in which the integrals are evaluated in the range from σ_{nJ_2} to σ_{nL_2} $(n=1, 2, 3)$.

The resultant drag coefficient is obtained by superposition of coefficients for all four sections of the profile:

$$c_{xF_2L_2}=c_{xF_2G_2}+c_{xG_2H_2}+c_{xH_2J_2}+c_{xJ_2L_2}\,. \tag{8.4.30}$$

As a result of substitution of the corresponding values of c_x we get

$$\begin{aligned} c_{xF_2L_2}=\frac{2\bar{\Delta}^2 z_1}{\pi b_r \bar{r}^2(1-\bar{r})^2}\Bigg\{&[N_1\ \bar{r}-\bar{r}\ (1-\bar{r})\ N_2-\bar{r}^2\ln 2]\ \frac{n_1}{\sqrt{n_1^2-1}}\\ &+\frac{n_2}{\sqrt{n_2^2-1}}\ [N_3\ (1-\bar{r})-\ln 2+\bar{r}\ \ln 2n_2]\\ &+\frac{n_3}{\sqrt{n_3^2-1}}\ [(1-\bar{r})\ Q_2-\bar{r}\ (1-\bar{r})\ \ln 2n_3-(1-\bar{r})^2\ln 2]\Bigg\}, \end{aligned} \tag{8.4.31}$$

where Q_2 is determined by (8.4.14) and (8.4.15) for $x=0$ at

$$\sigma=z_1\tan\kappa_3/(z_1\tan\kappa_2-\bar{r}\ b_r),$$

provided the value of z_1 satisfies the inequality

$$\frac{\bar{r}\ b_r}{\tan\kappa_1-a'}<z_1<\frac{(1-\bar{r})\ b_r}{\tan\kappa_1-a'}\,.$$

Profile F_3L_3: Let us consider section F_3L_3 (see Fig. 8.4.1) with the coordinate z_1 satisfying the inequality:

$$z_{D_1}<z_1<z_{D2}\,, \tag{8.4.32}$$

where

$$z_{D_2}=b_r/(\tan\kappa_1-a'). \tag{8.4.33}$$

The pressure on section F_3J_3 of the profile is established by the action of the sources distributed over the triangular surfaces OCC' $(Q=2\lambda_1 V_\infty)$ and BCC' $[Q=2\ (\lambda_2-\lambda_1)\ V_\infty]$. Therefore the coefficient of pressure can be calculated from expression (8.4.4) and the drag coefficient can be obtained from formula (8.4.5) in which the limits σ_{nG} and σ_{nH} are replaced by the quantities σ_{nF_3} and σ_{nJ_3} $(n=1, 2)$.

Besides the above distributions of sources OCC' and BCC' the sources of intensity $Q=-2\lambda_2 V_\infty$ distributed over triangle DCC' also act on section J_3H_3 of the profile. The coefficient of pressure is equal to the value calculated from formula (8.4.4) and the additional value obtained from formula (8.3.25) in which $\lambda=-\lambda_2$.

The flow-interaction of section H_3L_3 is characterized by the induced effect of the sources distributed in three regions of the wing: OCC', BCC' and DCC'. Accordingly the calculation of the pressure coefficient on this section of wing should be carried out with the help of formula (8.4.11).

Calculating the corresponding components of the coefficient of drag for all three sections and summing them, we get the resultant coefficient of drag:

$$c_{xF_3L_3}=\frac{2\bar{\Delta}^2 z_1}{\pi b_r \bar{r}^2(1-\bar{r})^2}\left\{[N_1\bar{r}-\bar{r}(1-\bar{r})\,N_2-\bar{r}^2\ln 2]\,\frac{n_1}{\sqrt{n_1^2-1}}\right.$$

$$+\frac{n_2}{\sqrt{n_2^2-1}}\,[N_2(1-\bar{r})+\bar{r}Q_1-\ln 2]$$

$$\left.+\frac{n_3}{\sqrt{n_3^2-1}}\,[(1-\bar{r})\,Q_2-\bar{r}(1-\bar{r})\ln(2n_3)-(1-\bar{r})^2\ln 2]\right\}. \qquad (8.4.34)$$

It is easy to see that expression (8.4.34) is convenient for calculation of the drag coefficient of the profile situated between points D_1 and D_2 (see Fig. 8.4.2) and having coordinate z_1 which satisfies the inequality:

$$\frac{\bar{r}\,b_r}{\tan\kappa_2-a'}<z_1<\frac{b_r}{\tan\kappa_1-a'}. \qquad (8.4.35)$$

Profile F_5L_5: Let us consider section F_5L_5 (see Fig. 8.4.1) with the coordinates

$$z_1>z_{D2}, \qquad (8.4.36)$$

where

$$z_{D2}=b_r/(\tan\kappa_1-a'). \qquad (8.4.37)$$

Three distributions of sources, namely OCC' ($Q=2\lambda_1 V_\infty$), BCC' [$Q=2(\lambda_2-\lambda_1)V_\infty$] and DCC' ($Q=-2\lambda_2 V_\infty$), act simultaneously on this section. Section F_5H_5 of the profile is situated behind Mach line OK_O within the boundary of a wing. So we must use formula (8.3.21) with $\lambda=\lambda_1$ for calculation of pressure due to the distribution of source OCC'. The second distribution of sources BCC' acts on section F_5H_5, which is situated between the Mach line and edge BC within the limit of the wing surface. Here it is necessary to apply formula (8.3.25), substituting λ by $\lambda_2-\lambda_1$, for calculation of additional pressure caused by the effects of distribution of sources BCC'. The second section H_5L_5 of the profile lies on the Mach lines OK_O and $B'K_B$, i.e. on one side of the Mach line and the corresponding edges OC and BC. Formula (8.3.21), having the distribution OCC' corresponding to the quantity $\lambda=\lambda_1$ and the distribution BCC' corresponding to the quantity $\lambda=\lambda_2-\lambda_1$, is applied to determine the coefficient of pressure from the distributed sources OCC' and BCC'.

Section H_5L_5 lies on different sides with respect to Mach line DK_D and railing edge DC, i.e. behind the triangular surface DCC' where the intensity of sources $Q=-2\lambda_2 V_\infty$. So we must apply formula (8.3.25), changing λ to $-\lambda_2$, to calculate the coefficient of pressure due to these sources.

Using the value of the coefficient of pressure obtained it is possible to determine the corresponding coefficient of drag of profile F_5L_5:

$$c_x F_5L_5=\frac{2\bar{\Delta}^2 z_1}{\pi b_r \bar{r}^2(1-\bar{r})^2}\left\{[N_1\bar{r}-\bar{r}(1-\bar{r})N_2-\bar{r}^2\ln 2]\frac{n_1}{\sqrt{n_1^2-1}}\right.$$

$$+\frac{n_2}{\sqrt{n_2^2-1}}[(1-\bar{r})N_3+Q_1\bar{r}-\ln 2]$$

$$\left.+\frac{n_3}{\sqrt{n_3^2-1}}[(1-\bar{r})Q_2-\bar{r}(1-\bar{r})Q_3-(1-\bar{r})^2\ln 2]\right\}, \qquad (8.4.38)$$

where Q_3 is determined from (8.4.14) and (8.4.15) for $x=0$ at

$$\sigma=z_1\tan\kappa_3/(z_1\tan\kappa_1-b_r). \qquad (8.4.39)$$

The results of calculation of the distribution of the function for drag coefficient $c_x/\bar{\Delta}^2$ ($\bar{\Delta}=\Delta/b$) along the span of a swept wing having constant chord b ($\kappa_1=\kappa_2=\kappa_3=60°$) and symmetrical rhombus airfoil ($\bar{r}=1/2$) at $M_\infty=1.8$ and 1.9 are shown in Fig. 8.4.3. From the graph it is seen that as we move away from the root chord the drag coefficient reduces. The value of the function $c_x/\bar{\Delta}^2$ for the profile of a rectangular wing is shown in the figure for comparison. To determine the resultant drag coefficient of a wing it is necessary to integrate along the span the distribution of drag coefficients c_{xk} of the profile using the formula

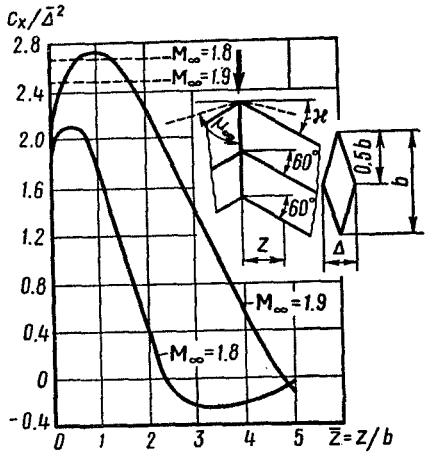

Fig. 8.4.3. Distribution of coefficient of drag along span of swept wing with constant chord and subsonic edges (dotted lines—for unswept wing).

$$c_x=\frac{1}{l}\int_0^l c_{xk}\,dz. \qquad (8.4.40)$$

Effect of side edges (tips): If the wing has a side edge (Fig. 8.4.4) it is necessary to take into account its effect on the pressure distribution and coefficient of drag. Calculation of the flow-interaction of this kind of wing having

six corners will be done in the following way: First the velocities and pressures in region $OO'D'D$ due to the distribution of sources in triangular section OCD are calculated. The calculation will be carried out as in the previous case (see Fig. 8.4.1), in which a wing plan with four corners without side edges was examined. But it is necessary to improve the calculated velocities and pressures to account for the effect of side edges $O'C''$, which is equivalent to the action of sources distributed over a triangle $O'CD'$. The intensity of these sources will have a sign opposite to that of the sources corresponding to a wing with an area $O'CD'$. The section of sources distributed over a triangle $O'CD'$ spreads over the wing within the boundaries of section $O'T''D'$ surrounded by Mach line $O'K'$, trailing edge and side edges. For example, for the profile F_2L_2 the effect of sources is restricted to the region $F_2'L_2$ (point F_2' lies at the intersection of the chord F_2L_2 and Mach line $O'K'$).

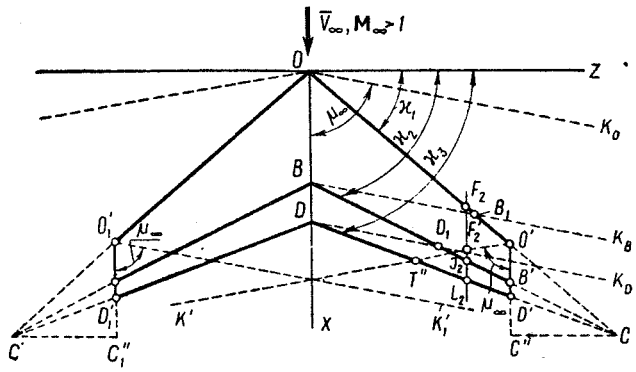

Fig. 8.4.4. Wing with side edges.

Let us examine how the pressure on section J_2L_2 of this profile is calculated. Considering only the distribution of sources in the region OCC', the coefficient of pressure can be determined by formula (8.4.11). The correction $\Delta\bar{p}$ on the influence of sources with the opposite sign in a triangle $O'CD'$ can be carried out so that

$$\bar{p}_{J_2L_2}=\bar{p}_{JL}-\Delta\bar{p}. \tag{8.4.41}$$

In determining the correction $\Delta\bar{p}$ the position of section J_2L_2 of the profile with respect to Mach line $O_1'K_1'$ passing through a point O_1' which lies on the opposite side edge should be taken into account (see Fig. 8.4.4). If this line does not intersect section J_2L_2 the distribution of vortices in the region $O'CD'$ of one side of the wing will affect only this section. At the same time the effect of the sources $O_1'C'D_1'$ is excluded. The induced velocity is calculated by formula (8.3.13) and the corresponding additional value of the pressure coefficient $\Delta\bar{p}=-2u/V_\infty$. This additional quantity can be represented in the form of the summation

$$\Delta\bar{p}=\Delta\bar{p}_1+\Delta\bar{p}_2+\Delta\bar{p}_3, \tag{8.4.42}$$

where $\Delta\bar{p}_1$ depends on the distribution of the sources $O'CC'$ ($Q=2\lambda_1 V_\infty$) and $\Delta\bar{p}_2$ and $\Delta\bar{p}_3$ are due to the distributions of sources $B'CC''$ [$Q=2(\lambda_2-\lambda_1)V_\infty$] and $D'CC''$ ($Q=-2\lambda_2 V_\infty$) respectively.

Applying formula (8.3.14), we get

$$\Delta\bar{p}=\frac{2\lambda_1}{\pi a'\sqrt{n_1^2-1}}\cosh^{-1}\frac{n_1^2+\sigma_1}{n_1(1+\sigma_1)}+\frac{2(\lambda_2-\lambda_1)}{\pi a'\sqrt{n_2^2-1}}$$
$$\times\cosh^{-1}\frac{n_2^2+\sigma_2}{n_2(1+\sigma_2)}-\frac{2\lambda_2}{\pi a'\sqrt{n_3^2-1}}\cosh^{-1}\frac{n_3^2+\sigma_3}{n_3(1+\sigma_3)}, \tag{8.4.43}$$

where σ_1, σ_2 and σ_3 are taken with respect to points O', B' and D'.

If Mach line $O_1'K_1'$ intersects chord F_2L_2 then, along with the effect of the sources $O'CC''$, we have to take into account the effect of the sources distributed in triangle $O_1'C'C_1''$ on the opposite side of the wing. The same formula (8.3.13) is used for the calculation of induced velocity.

5. Flow-interaction of Wing with Four Corners, Symmetrical Airfoil and Edges of Different Types (Subsonic and Supersonic)

5.1 Leading edge and middle edge subsonic, trailing edge supersonic

Disturbances from the supersonic trailing edges of a wing (Fig. 8.5.1, a) propagate downstream within the boundaries of the Mach cone with generator DK_D. As such they have no effect on the flow-interaction of a wing surface. The velocity and pressure depend on the effect of the leading edge and middle edge.

Let us consider the profile FL with a coordinate $z_1<z_{B1}$. The coefficient of pressure at section FG, due to interaction of the sources with intensity $Q=2\lambda_1 V_\infty$ distributed over a triangle OCC', is determined by formula (8.4.1) and the corresponding drag coefficient c_{xFG} by expression (8.4.3). The coefficient of pressure at the next section GH affected by distributed sources in the triangles OCC' ($Q=2\lambda_1 V_\infty$) and BCC' [$Q=2(\lambda_2-\lambda_1)V_\infty$] can be calculated by formula (8.4.4). The corresponding value of coefficient of drag c_{xGH} for this section can be determined from expression (8.4.5).

We find the interaction of the same distribution of sources on section HL as on section GH. However, considering that section HL lies on the wing surface below Mach line BK_B the calculation of pressure coefficient $\bar{p}_{HL}$ should be carried out with the help of formula (8.4.9) and that of drag coefficient c_{xHL} from expression (8.4.10). The resultant drag coefficient of this profile will be

$$c_{xFL}=c_{xFG}+c_{xGH}+c_{xHL}. \tag{8.5.1}$$

In examining section F_1L_1 having a coordinate $z_1 > z_{B1}$ the effect of the distribution of sources OCC' and BCC' should be taken into account simultaneously. Drag coefficient $c_{xF_1H_1}$ for section F_1H_1 can be determined by formula (8.4.25) and drag coefficient $c_{xH_1L_1}$ for section H_1L_1 can be found from expression (8.4.13) in which the third term in the square brackets is taken as zero and the limits σ_{nH} and σ_{nL} are replaced by the quantities σ_{nH_1} and σ_{nL_1} $(n=1, 2)$ respectively. The total drag coefficient of airfoil F_1L_1 will be

$$c_{xF_1L_1} = c_{xF_1H_1} + c_{xH_1L_1}. \tag{8.5.2}$$

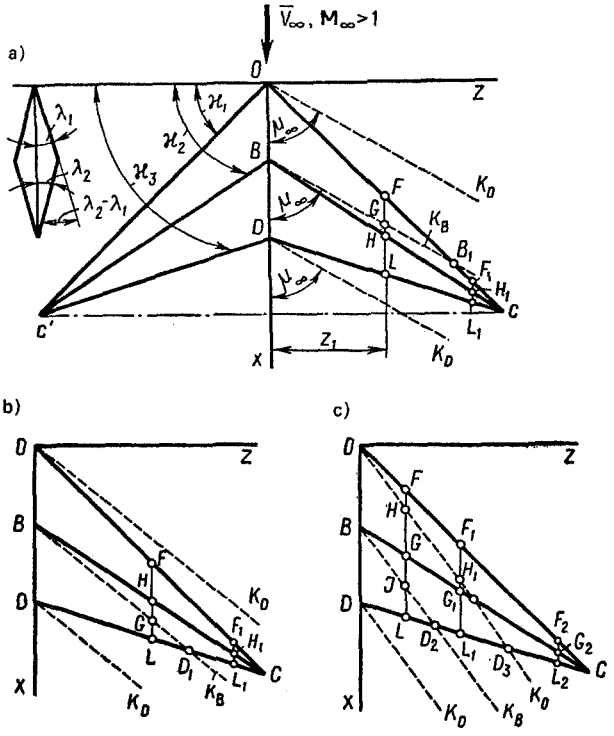

Fig. 8.5.1. Wing with four corners in supersonic flow:

a—leading edge and side edge subsonic, trailing edge supersonic;
b—leading edge subsonic, side edge and trailing edge supersonic.
c—all edges supersonic.

5.2 Leading edge subsonic, middle edge and trailing edge supersonic

The main feature of the flow interaction of the wing shown in (Fig. 8.5.1, b) in that the sources distributed over the region BDD_1 have no effect on the distribution of velocities and pressures in the remaining part of the wing situated above Mach line BK_B.

Let us take the airfoil FL with coordinates $z_1 < z_{D_1}$. The sources distributed in triangle OCC' (see Fig. 8.5.1, a) interact on the section FH of this profile. Hence the pressure distribution can be found with the help of formula (8.4.1) and the corresponding drag coefficient c_{xFH} can be obtained from expression (8.4.3) in which the upper limit σ_{1G} should be changed to σ_{1H}. The second section HG undergoes the effect of the subsonic leading edge OC (and hence of the distribution of sources OCC') and of the supersonic middle edge BC. The corresponding pressure coefficient is determined in the form of the sum of two coefficients. The first of these coefficients is calculated from expression (8.4.1) and the second from formula (8.3.27), where it is necessary to take $\lambda = \lambda_2 - \lambda_1$ and $n = n_2$. Thus

$$\bar{p}_{HG} = \frac{4\lambda_1}{\pi a' \sqrt{n_1^2 - 1}} \cosh^{-1} \sqrt{\frac{n_1^2 - \sigma_1^2}{1 - \sigma_1^2}} + \frac{2(\lambda_2 - \lambda_1)}{a' \sqrt{1 - n_2^2}}. \tag{8.5.3}$$

The velocity on section GL is induced by sources distributed over triangles OCC' and BCC' (see Fig. 8.5.1, a). Applying formulas (8.5.3) and (8.3.40), we get the following relation for the coefficient of pressure:

$$\bar{p}_{GL} = \frac{4\lambda_1}{\pi a' \sqrt{n_1^2 - 1}} \cosh^{-1} \sqrt{\frac{n_1^2 - \sigma_1^2}{1 - \sigma_1^2}}$$

$$+ \frac{2(\lambda_2 - \lambda_1)}{a' \sqrt{1 - n_2^2}} \left(1 - \frac{2}{\pi} \sin^{-1} \sqrt{\frac{n_2^2 - \sigma_2^2}{1 - \sigma_2^2}}\right). \tag{8.5.4}$$

The drag coefficient of this airfoil will be

$$c_{xFL} = \frac{2}{b} \left(\int_{x_F}^{x_H} \bar{p}_{FH} \lambda_1 \, dx + \int_{x_H}^{x_G} \bar{p}_{HG} \lambda_2 \, dx + \int_{x_G}^{x_L} \bar{p}_{GL} \lambda_2 \, dx \right). \tag{8.5.5}$$

The airfoil F_1L_1 is situated below Mach line OK_O and therefore the distribution of sources with intensity $Q = 2\lambda_1 V_\infty$ in triangle OCC' will affect it. Besides that, the distribution of sources with intensity $Q = 2(\lambda_2 - \lambda_1) V_\infty$ over a triangle BCC' will act on section H_1L_1 and cause additional pressure which can be calculated by using formula (8.3.27), replacing λ by $(\lambda_2 - \lambda_1)$. Accordingly, the coefficient of pressure $\bar{p}_{F_1H_1}$ at section F_1H_1 is calculated from expression (8.3.21) and the coefficient of pressure $\bar{p}_{H_1L_1}$ at section H_1L_1 from formula (8.5.3). The coefficient of drag of the profile will be

$$c_{xF_1L_1} = \frac{2}{b} \left(\int_{x_{F_1}}^{x_{H_1}} \bar{p}_{F_1H_1} \lambda_1 \, dx + \int_{x_{H_1}}^{x_{L_1}} \bar{p}_{H_1L_1} \lambda_2 \, dx \right). \tag{8.5.6}$$

5.3 All edges of wing supersonic

For this kind of wing (Fig. 8.5.1, c) the Mach lines OK_O, BK_B and DK_D drawn from the points O, B and D are located below the corresponding edges OC, BC and DC. Therefore the pressure coefficient should be calculated using formulas (8.3.27) and (8.3.40).

Let us study airfoil FL with a coordinate $0<z_1<z_{D_2}$. The section FH lies between the leading edge OC and the Mach line OK_O. Therefore, the other edge OC' (see Fig. 8.5.1, a) will not affect the flow in this region which is considered to be a plane supersonic flow. Considering that the sources in a triangle OCC' with intensity $Q=2\lambda_1 V_\infty$ interact on the section FH the pressure coefficient $\bar{p}_{FH}$ can be determined from formula (8.3.27) in which λ and n are changed to λ_1 and n_1 respectively. The additional pressure on the section HG is established from the effect of the edge OC'. The pressure coefficient $\bar{p}_{HG}$ on this section is found from expression (8.3.40) with $n=n_1$ and $\sigma=\sigma_1$.

Besides the interaction of distribution of sources OCC' on section GJ the distribution of sources BCC' with intensity $Q=2(\lambda_2-\lambda_1)\,V_\infty$ gives induced effects in this section. Applying formulas (8.3.40) and (8.3.27), we get the expression for the pressure coefficient:

$$\bar{p}_{GJ}=\frac{2\lambda_1}{a'\sqrt{1-n_1^2}}\left(1-\frac{2}{\pi}\sin^{-1}\sqrt{\frac{n_1^2-\sigma_1^2}{1-\sigma_1^2}}\right)+\frac{2(\lambda_2-\lambda_1)}{a'\sqrt{1-n_2^2}}. \tag{8.5.7}$$

The last section JL of the profile undergoes the additional effect of the opposite edge BC'. Accordingly the coefficient of pressure on section JL, where sources with intensity $Q=2(\lambda_2-\lambda_1)\,V_\infty$ interact, will be

$$\begin{aligned}p_{JL}=&\frac{2\lambda_1}{a'\sqrt{1-n_1^2}}\left(1-\frac{2}{\pi}\sin^{-1}\sqrt{\frac{n_1^2-\sigma_1^2}{1-\sigma_1^2}}\right)\\&+\frac{2(\lambda_2-\lambda_1)}{a'\sqrt{1-n_2^2}}\left(1-\frac{2}{\pi}\sin^{-1}\sqrt{\frac{n_2^2-\sigma_2^2}{1-\sigma_2^2}}\right).\end{aligned} \tag{8.5.8}$$

The drag coefficient of the profile FL will be

$$c_{xFL}=\frac{2}{b}\left(\int_{x_F}^{x_H}\bar{p}_{FH}\,\lambda_1 dx+\int_{x_H}^{x_G}\bar{p}_{HG}\,\lambda_1 dx+\int_{x_G}^{x_J}\bar{p}_{GJ}\,\lambda_2 dx+\int_{x_J}^{x_L}\bar{p}_{JL}\,\lambda_2 dx\right). \tag{8.5.9}$$

The coefficient of pressure $\bar{p}_{F_1H_1}$ on section F_1H_1 of profile F_1L_1 with the coordinate $z_{D_2}<z_1<z_{D_3}$ is determined by formula (8.3.27) in which $\lambda=\lambda_1$ and $n=n_1$. At the neighboring section H_1G_1 formula (8.3.40) with $\lambda=\lambda_1$, $n=n_1$ and $\sigma=\sigma_1$ should be applied to determine the pressure coefficient $\bar{p}_{H_1G_1}$. The pressure on the last section G_1L_1 is obtained from interaction of the distribution of sources OCC' ($Q=2\lambda_1 V_\infty$) and BCC' [$Q=2(\lambda_2-\lambda_1)\,V_\infty$]. Therefore

formula (8.5.7) can be used to calculate pressure coefficient $\bar{p}_{G_1L_1}$. The drag coefficient of profile F_1L_1 will then be given by

$$c_{xF_1L_1}=\frac{2}{b}\left(\int_{x_{F_1}}^{x_{H_1}}\bar{p}_{F_1H_1}\lambda_1\,dx+\int_{x_{H_1}}^{x_{G_1}}\bar{p}_{H_1G_1}\lambda_1\,dx+\int_{x_{G_1}}^{x_{L_1}}\bar{p}_{G_1L_1}\lambda_2 dx\right). \tag{8.5.10}$$

The flow around the airfoil F_2L_2 at a section $z_{D_3}<z_1$ happens to be the plane supersonic flow. Therefore the pressure coefficient on it is determined by formula (8.3.27). The sources distributed over triangle OCC' with intensity $Q=2\lambda_1V_\infty$ act on the section F_2G_2. Hence the coefficient of pressure $\bar{p}_{F_2G_2}$ is found from formula (8.3.27) in which $\lambda=\lambda_1$ and $n=n_1$. The sources with intensity $Q=2(\lambda_2-\lambda_1)V_\infty$ distributed over triangle BCC', have an additional effect on section G_2L_2. Therefore the pressure coefficient on this section will be

$$\bar{p}_{G_2L_2}=\frac{2\lambda_1}{a'\sqrt{1-n_1^2}}+\frac{2(\lambda_2-\lambda_1)}{a'\sqrt{1-n_2^2}}. \tag{8.5.11}$$

The coefficient of drag for profile F_2L_2 will be

$$c_{xF_2L_2}=\frac{2}{b}\left(\int_{x_{F_2}}^{x_{G_2}}\bar{p}_{F_2G_2}\lambda_1\,dx+\int_{x_{G_2}}^{x_{L_2}}\bar{p}_{G_2L_2}\lambda_2 dx\right). \tag{8.5.12}$$

5.4 Delta wing

From the relations obtained for a swept wing with a plan having four corners it is possible to get the relations for the aerodynamic characteristics of

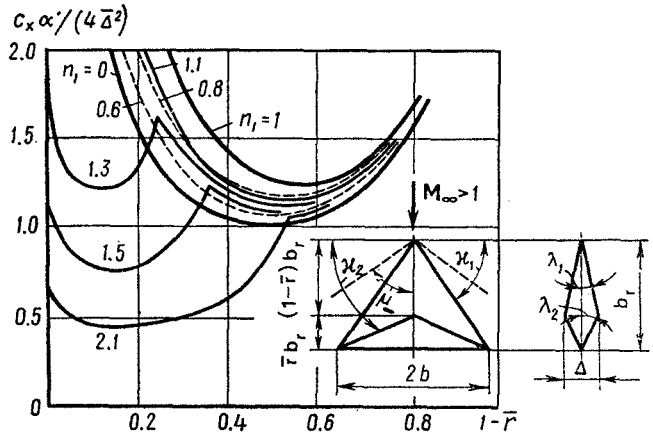

Fig. 8.5.2. Drag of delta wings with symmetrical rhombic profile in supersonic flow:

$\bar{\Delta}=\Delta/b_r$, $n_1=\tan\varkappa/a'$ $(a'=\sqrt{M_\infty^2-1})$.

a delta wing (Fig. 8.5.2). For this kind of wing the trailing edge is supersonic. The leading edge and the line of maximum thickness (middle edge) can be either subsonic or supersonic. Accordingly the local velocities and pressures and also the resultant drag coefficient c_x are determined.

The results of the calculation of a function $c_x a'/4\bar{\Delta}^2$ for delta wings with subsonic ($n_1 > 1$) and supersonic ($n_1 < 1$) leading edges with respect to $(1-\bar{r})$ at various values of n_1 (angle of sweep κ_1) are shown in Fig. 8.5.2. The values of $c_x a'/4\bar{\Delta}^2$ at $n_1 = 0$ correspond to a rectangular wing with symmetrical profile.

The coefficient of drag of this kind of wing can be determined with the help of formula (7.5.22). The coefficients of pressure $\bar{p}_l$ and $\bar{p}_u$ entering into it are calculated from expression (8.3.27). As the airfoil is symmetrical $\bar{p}_l = |\bar{p}_u| = \bar{p}$ and $|dy/dx|_l = (dy/dx)_u = \lambda$. Therefore

$$c_x = 2\int_0^{1-\bar{r}} \bar{p}_1 \lambda_1 \, d\bar{x} + 2\int_{1-\bar{r}}^{1} \bar{p}_2 \lambda_2 \, d\bar{x},$$

where $\bar{x} = x/b_r$ and the coefficient $\bar{p}_1$ and $\bar{p}_2$ are determined from (8.3.27) at $n_1 = 0$ for λ_1 and λ_2 respectively. Inserting the values of $\bar{p}_1$ and $\bar{p}_2$, we get

$$c_x = \frac{4}{a'}\left[(1-\bar{r})\,\lambda_1^2 + \bar{r}\,\lambda_2^2\right]. \tag{8.5.13}$$

Using the values of λ_1 and λ_2 from (8.4.7), we have

$$c_x = \bar{\Delta}^2/a'\bar{r}\,(1-\bar{r}). \tag{8.5.14}$$

The effect on drag of the location of the maximum thickness of an airfoil can be obtained from Fig. 8.5.2. A value of $\bar{r}$ can be obtained that corresponds to the minimum drag coefficient. The points where the curves turn refer to the values of $\bar{r}$ at which the line of maximum thickness becomes sonic ($n_2 = n_1\,\bar{r} = 1$).

6. Zone of Application of Method of Sources

The method of sources was used in Sections 3 and 5 to study flow-interaction and determine the drag force of a wing with a symmetrical airfoil at zero angle of attack, i.e. in the absence of lift force. Experiments show that the limits of application of this method in aerodynamic studies can be extended. Let us consider cases where a small-perturbation flow around a thin wing at zero angle of attack can be determined with the help of this method of sources and the lift force and drag calculated.

Let us take two wings with different leading edges. One of them (Fig.

8.6.1) has a curvilinear edge with a finite supersonic region and the other wing a completely subsonic leading edge (Fig. 8.6.2).

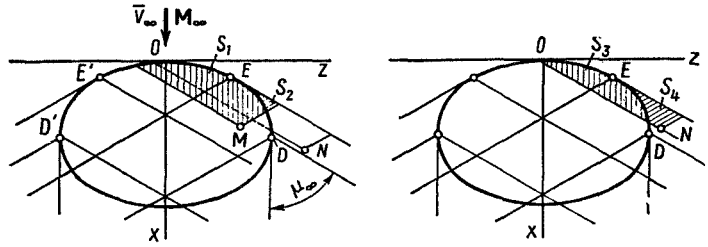

Fig. 8.6.1. Wing with limited part of leading edge supersonic.

In Fig. 8.6.1 points E, E' at which the tangent to the contour coincides with the generators of the cones of disturbances happen to be the boundaries of a supersonic region. Consider the velocity potential at some point M situated in the region bounded by the side edge ED and the lines of disturbance emerging from points E, D, D' and E' in plane xOz.

According to formula (8.2.16), in which the zone of integration σ is equal to $\sigma = S_1 + S_2$, the velocity potential at a given point will be

$$\varphi' = -\frac{1}{2\pi}\iint\limits_{S_1}\frac{Q_1(\xi,\zeta)\,d\xi d\zeta}{\sqrt{(x_1-\xi)^2-(z_1-\zeta)^2}} - \frac{1}{2\pi}\iint\limits_{S_2}\frac{Q_2(\xi,\zeta)\,d\xi d\zeta}{\sqrt{(x_1-\xi)^2-(z_1-\zeta)^2}}. \quad (8.6.1)$$

In this expression the function $Q_1(x, z) = 2(\partial\varphi'/\partial y)_{y=0}$, which follows from (8.2.17). This function is determined from the condition of smooth flow over the wing surface (8.1.12). As the equation of this surface is given the function $Q_1(x, z)$ will be known. In the particular case of a wing in the form of a flat plate at an angle of attack α the function $Q_1 = 2V_\infty \alpha$. So determination of φ' from formula (8.6.1) is connected with determination of the unknown function Q_2, which governs the intensity of distribution of sources over the region of area S_2.

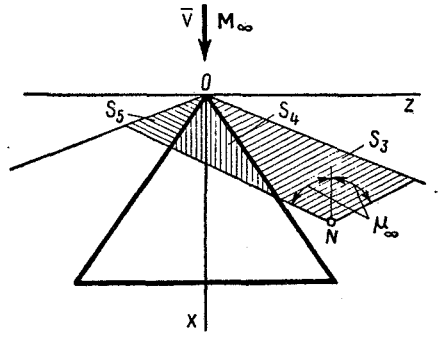

Fig. 8.6.2. Wing with subsonic leading edge.

To find this function Q_2 we take an arbitrary point $N(x, O, z)$ lying in the region between the Mach lines drawn from points E and D. According to (8.1.20) the velocity potential at this point is equal to zero. Therefore the following expression can be obtained according to the notations indicated in Fig. 8.6.1:

$$0=-\frac{1}{2\pi}\iint\limits_{S_3}\frac{Q_1(\xi,\zeta)\,d\xi d\zeta}{\sqrt{(x_1-\xi)^2-(z_1-\zeta)^2}}+\frac{1}{2\pi}\iint\limits_{S_4}\frac{Q_2(\xi,\zeta)\,d\xi d\zeta}{\sqrt{(x_1-\xi)^2-(z_1-\zeta)^2}}\cdot \quad (8.6.2)$$

The first term on the right side of this integral equation is a known function because the intensity Q_1 on the area S_3 is determined from the boundary conditions. Therefore the unknown function Q_2 representing the intensity of sources in the region S_4 can be obtained from this equation.

So if the leading edge of a wing with a symmetrical airfoil is completely or partially supersonic the method of sources is applicable in the study of the flow-interaction of the wing at a given angle of attack. The same conclusion can be drawn for a wing with similar edges and cambered airfoil placed in a flow at an angle of attack $\alpha\neq 0$ or at zero angle of attack.

Now let us take a wing with subsonic leading edges. For the similar point N the following relation can be written as (see Fig. 8.6.2):

$$0=-\frac{1}{2\pi}\iint\limits_{S_5}\frac{Q_3(\xi,\zeta)\,d\xi d\zeta}{\sqrt{(x_1-\xi)^2-(z_1-\zeta)^2}}-\frac{1}{2\pi}\iint\limits_{S_3}\frac{Q_1(\xi,\zeta)\,d\xi d\zeta}{\sqrt{(x_1-\xi)^2-(z_1-\zeta)^2}}$$

$$-\frac{1}{2\pi}\iint\limits_{S_4}\frac{Q_2(\xi,\zeta)\,d\xi d\zeta}{\sqrt{(x_1-\xi)^2-(z_1-\zeta)^2}}\cdot \quad (8.6.3)$$

It can be seen that we get one equation with two unknown functions Q_3 and Q_2. By analogy with Q_2 the function Q_3 represents the intensity of sources on the area S_5 in the region between the left leading edge and the Mach line drawn from the apex of the wing. So if the wing has a subsonic leading edge it is not possible, by the method of sources, to work out the flow-interaction of a thin wing with symmetrical profile at any angle of attack or of a wing with a subsonic edge and cambered profile at zero angle of attack or $\alpha\neq 0$.

7. Method of Dipoles

The application of the method of sources to the study of the supersonic flow-interaction, as shown above, is limited to wings with completely or partially supersonic leading edges. In other cases connected with the study of the supersonic aerodynamic characteristics of wings with subsonic leading edges at a given angle of attack (or for similar wings with cambered airfoil at $\alpha=0$) it is necessary to use the method of dipoles.

Let us study a dipole in a supersonic flow. To do this we determine the velocity potential of the flow formed due to an elementary source and an elementary sink of the same strength Q having the coordinates $x=\xi, z=\zeta, y=\varepsilon$ and $x=\xi, z=\zeta, y=-\varepsilon$ respectively. The selected source is located above the plane $y=0$ at a small distance ε from it and the sink is situated under this

plane at the small distance $-\varepsilon$. Writing (8.2.11) in terms of finite differences, the potential due to the source and sink pair can be expressed in the form

$$\Delta\varphi=\frac{Q\Delta\sigma}{2\pi}\left\{\frac{-1}{\sqrt{(x-\xi)^2-a'^2\,[(y-\varepsilon)^2+(z-\zeta)^2]}}\right.$$
$$\left.+\frac{1}{\sqrt{(x-\xi)^2-a'^2\,[(y+\varepsilon)^2+(z-\zeta)^2]}}\right\}.$$

Introducing the notation $\rho=\sqrt{(x-\xi)^2-a'^2\,[y^2+(z-\zeta)^2]}$ and neglecting the quantity $a'^2\,\varepsilon^2$ in square brackets, we get

$$\Delta\varphi=\frac{Q\Delta\sigma}{2\pi\rho}\left(\frac{-1}{\sqrt{1+\dfrac{2a'^2\,y\varepsilon}{\rho^2}}}+\frac{1}{\sqrt{1-\dfrac{2a'^2\,y\varepsilon}{\rho^2}}}\right).$$

Using series expansion of the square root and omitting the quantities of second and higher orders of smallness in these expansions, we have

$$\Delta\varphi=\frac{a'^2\,Qy\varepsilon\Delta\sigma}{\pi\rho^3}=\frac{a'^2\,Qy\varepsilon d\sigma}{\pi\,\{(x-\xi)^2-a'^2\,[y^2+(z-\zeta)^2]\}^{3/2}}.$$

After finding the limit of $\Delta\varphi$ as $\varepsilon\to 0$ and assuming the constant value of $M=Q\cdot\varepsilon$ known as the momentum (or strength) of a dipole we get the expression for a differential of the potential function of a dipole

$$d\varphi_{\text{dip}}=\frac{My d\sigma}{\pi\,\{(x-\xi)^2-a'^2\,[y^2+(z-\zeta)^2]\}^{3/2}}.$$

This expression can be written in the form

$$d\varphi_{\text{dip}}=\frac{Md\sigma}{\pi}\cdot\frac{\partial}{\partial y}\left\{\frac{1}{\sqrt{(x-\xi)^2-a'^2\,[y^2+(z-\zeta)^2]}}\right\}.$$

Integration of this over the region σ, in which the effect of the dipole is felt, gives the expression for a potential function

$$\varphi_{\text{dip}}=\frac{\partial}{\partial y}\iint_{\sigma}\frac{M(\xi,\zeta)\,d\xi d\zeta}{\sqrt{(x-\xi)^2-a'^2\,[y^2+(z-\zeta)^2]}},\qquad(8.7.1)$$

where π is included in the function of distribution of dipoles.

It can be shown that the function (8.7.1) satisfies equation (8.1.7). To do this let us differentiate (8.1.7) with respect to y:

$$(\mathbf{M}_\infty^2-1)\frac{\partial}{\partial y}\left(\frac{\partial^2\varphi'}{\partial x^2}\right)-\frac{\partial}{\partial y}\left(\frac{\partial^2\varphi'}{\partial y^2}\right)-\frac{\partial}{\partial y}\left(\frac{\partial^2\varphi'}{\partial z^2}\right)=0.$$

This equation can be rewritten in the form

$$(\mathbf{M}_\infty^2-1)\frac{\partial^2}{\partial x^2}\left(\frac{\partial\varphi'}{\partial y}\right)-\frac{\partial^2}{\partial y^2}\left(\frac{\partial\varphi'}{\partial y}\right)-\frac{\partial^2}{\partial z^2}\left(\frac{\partial\varphi'}{\partial y}\right)=0.\qquad(8.7.2)$$

Let us now examine expression (8.7.1) for the potential of a dipole. If the quantity $-1/2\pi$ is included in the expression for this potential then by (8.2.12) the double integral can be considered as a potential of sources whose distribution over an area σ is given by some function M. Consequently

$$\varphi_{\text{dip}}=\partial\varphi'/\partial y. \tag{8.7.3}$$

From the comparison of (8.7.2) and (8.7.3) it can be seen that the function φ_{dip} actually satisfies equation (8.1.7) for the velocity potential.

Knowing the form of a wing surface, velocity of an undisturbed flow and angle of attack it is possible to find the distribution of dipoles M and hence the potential φ_{dip} of dipoles. The derivative of the function φ_{dip} with respect to x gives an additional axial component of the disturbed velocity $u=\partial\varphi_{\text{dip}}/\partial x$. Then the coefficient of pressure $\bar{p}=-2u/V_\infty$ on the lifting surface and the lift force created by it can be culculated.

8. Flow-interaction of Delta Wing with Subsonic Leading Edge

A wing in the form of a flat plate having a triangular plan and subsonic leading edges is supposed to fall within the Mach cone (Fig. 8.8.1). The method of distributed dipoles and the corresponding relation (8.7.1) for a velocity potential of dipoles can be used to find the lift force of this kind of wing.

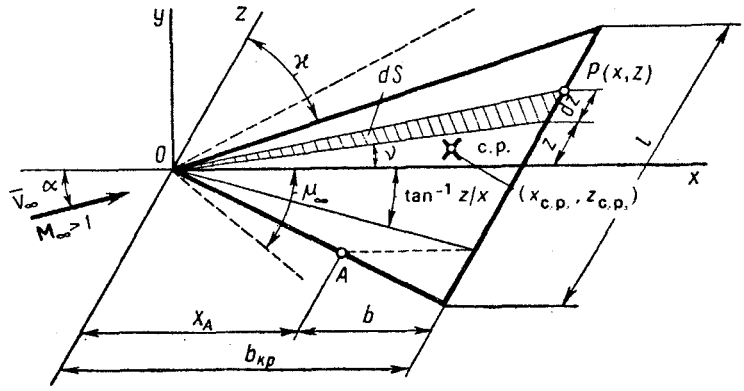

Fig. 8.8.1. Plane delta wing with subsonic edges.

In Section 3 it was shown that the additional velocity u induced by the sources distributed over an inclined triangular surface with subsonic edges depends only on the function $\sigma=za'/x$ [see, for example, formula (8.3.20)]. This means that the velocity will be constant along the ray emerging from the point of discontinuity of a leading edge at an angle $\gamma=\tan^{-1}(z/x)$. This ray can be treated as the generator of a cone whose apex coincides with the point of discontinuity of a leading edge.

A flow having the property of maintaining constant the velocity and hence the other parameters along the generators of this conical surface is called a conical flow. For this kind of flow in the plane $y=0$ it can be said that additional velocity is the function of ratio z/x, i.e. $u=f(z/x)$. From this it follows that the potential due to sources for a conical flow also depends on this ratio.

Considering the flow about a triangular surface created by the dipoles as a conical flow, the potential at a point P lying in the plane $y=0$ (see Fig. 8.8.1) can be expressed in the form

$$\varphi_{\text{dip}}=xF_{\text{dip}}(z/x), \tag{8.8.1}$$

where $F_{\text{dip}}(z/x)$ is a function depending only on the angle of conical surface $\gamma=\tan^{-1}(z/x)$. The potential of a conical flow at a point with the coordinates x, y, z can be written in a more general form:

$$\varphi_{\text{dip}}=xF_{\text{dip}}(z/x,\ y/x). \tag{8.8.2}$$

According to equation (8.8.1) the relation characterizing distribution of dipoles in the plane $y=0$ (on the surface of a wing) is such that

$$M(\xi, \zeta)=\xi m(h), \tag{8.8.3}$$

where $h=\zeta/\xi$; $m(h)$ is some function of the argument h.

Let us transform equation (8.7.1). The elementary area occupied by a dipole can be expressed in the form $d\sigma=d\xi d\zeta=\xi dh d\xi$ because $d\zeta=\xi dh$. Therefore

$$\varphi_{\text{dip}}=\int_{h_A=-\cot\varkappa}^{h_B=\cot\varkappa} m(h)\,dh\,\frac{\partial}{\partial y}\int_0^{\xi_1}\frac{\xi^2 d\xi}{\sqrt{(x-\xi)^2-a'^2\,[y^2+(z-h\xi)^2]}}, \tag{8.8.4}$$

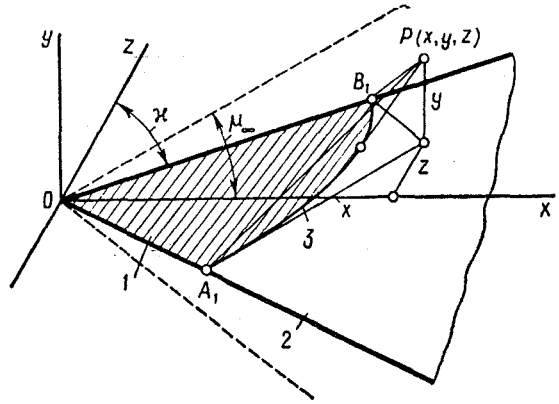

Fig. 8.8.2. Region of effect of dipoles on flow-interaction of wing with subsonic leading edges:
1—region of effect of dipoles; *2*—delta wing; *3*—parabolic curve.

where ξ_1 represents the coordinate of a dipole which may have an effect on the flow at a point $P(x, y, z)$. This dipole is situated on the curve bounding the region of influence of dipoles (Fig. 8.8.2) and is obtained as a result of the intersection of the plane $y=0$ and the Mach cone drawn along the flow from a point P. This curve represents the parabola A_1B_1 satisfying the equation

$$(x-\xi_1)^2-a'^2\,[y^2+(z-\zeta_1)^2]=0 \tag{8.8.5}$$

in terms of the coordinates ξ_1, ζ_1.

The expression under the square root sign (8.7.1) can be written in the following way:

$$(x-\xi)^2-a'^2\,[y^2+(z-h\xi)^2] = a\xi^2+b\xi+c, \tag{8.8.6}$$

where

$$\left.\begin{aligned} a=1-a'^2\,h^2,\ b=2x\left(a'^2\,h\,\frac{z}{x}-1\right),\\ c=x^2\left[1-a'^2\left(\frac{y^2}{x^2}+\frac{z^2}{x^2}\right)\right]. \end{aligned}\right\} \tag{8.8.7}$$

The integral in (8.8.4) will then be

$$\int_0^{\xi_1}\frac{\xi^2 d\xi}{\sqrt{a\xi^2+b\xi+c}}=\left(\frac{\xi}{2a}-\frac{3b}{4a^2}\right)\sqrt{a\xi^2+b\xi+c}\,\Big|_0^{\xi_1}$$

$$+\frac{3b^2-4ac}{8a^2}\int_0^{\xi_1}\frac{d\xi}{\sqrt{a\xi^2+b\xi+c}}\,. \tag{8.8.8}$$

Noting that $a=1-a'^2$, $h^2>0$, we find the integral on the right side of (8.8.8):

$$\int_0^{\xi_1}\frac{d\xi}{\sqrt{d\xi^2+b\xi+c}}=\frac{1}{\sqrt{a}}\ln\left[2\sqrt{a\,(a\xi^2+b\xi^2+c)}+2a\xi+b\right]\Big|_0^{\xi_1}. \tag{8.8.9}$$

According to (8.8.5) the quantity $a\xi_1^2+b\xi_1+c=0$. Hence

$$\int_0^{\xi_1}\frac{\xi^2 d\xi}{\sqrt{a\xi^2+b\xi+c}}=\frac{3b}{4a^2}\sqrt{c}+\frac{3b^2-4ac}{8a^2\sqrt{a}}\left[\ln(2a\xi_1+b)\right.$$

$$\left.-\ln(2\sqrt{ac}+b)\right]. \tag{8.8.10}$$

Solving expression (8.8.5) written in the form

$$a\xi_1^2+b\xi_1+c=0, \tag{8.8.11}$$

we get

$$\xi_1=\frac{-b+\sqrt{b^2-4ac}}{2a}. \tag{8.8.12}$$

Then

$$\ln(2a\xi_1+b)=\ln\sqrt{b^2-4ac}. \tag{8.8.13}$$

The difference between the logarithmic terms in (8.8.10), taking (8.8.13) into account, will be

$$\ln(2a\xi_1+b)-\ln(2\sqrt{ac}+b)=\ln\frac{\sqrt{b^2-4ac}}{2\sqrt{ac}+b}=\frac{1}{2}\ln\frac{b^2-4ac}{(2\sqrt{ac}+b)^2}$$

$$=\frac{1}{2}\ln\frac{b-2\sqrt{ac}}{b+2\sqrt{ac}}=-\operatorname{cot h}^{-1}\frac{b}{2\sqrt{ac}}. \tag{8.8.14}$$

Thus

$$\int_0^{\xi_1}\frac{\xi^2 d\xi}{\sqrt{a\xi^2+b\xi+c}}=\frac{3b\sqrt{c}}{4a^2}-\frac{3b^2-4ac}{8a^2\sqrt{a}}\operatorname{cot h}^{-1}\frac{b}{2\sqrt{ac}}. \tag{8.8.15}$$

The derivative of (8.8.15) with respect to y will be:

$$\frac{\partial}{\partial y}\int_0^{\xi_1}\frac{\xi^2 d\xi}{\sqrt{a\xi^2+b\xi+c}}=N=\frac{1}{2a\sqrt{a}}$$

$$\times\frac{\partial c}{\partial y}\left(\frac{b}{4\sqrt{ac}}\cdot\frac{8ac}{4ac-b^2}+\operatorname{cot h}^{-1}\frac{b}{2\sqrt{ac}}\right).$$

Introducing the notation

$$\nu=b/2\sqrt{ac} \tag{8.8.16}$$

and keeping in view that $\partial c/\partial y=-2ya'^2$ [see formula (8.8.7)], we can write

$$N=\frac{-ya'^2}{a\sqrt{a}}\left(\frac{\nu}{1-\nu^2}+\operatorname{cot h}^{-1}\nu\right). \tag{8.8.17}$$

Inserting this expression in (8.8.4):

$$\varphi_{\text{dip}}=\int_{-\cot\kappa}^{\cot\kappa}Nm(h)\,dh. \tag{8.8.18}$$

To determine the form of function $m(h)$ for the distribution of dipoles we use the condition of smooth flow over a wing, which states that

$$(v)_{y=0}=V_\infty\alpha=(\partial\varphi_{\text{dip}}/\partial y)_{y=0}. \tag{8.8.19}$$

The partial derivative $(\partial\varphi_{\text{dip}}/\partial y)_{y=0}$ is determined by (8.8.18) in the form

$$(\partial\varphi_{\text{dip}}/\partial y)_{y=0} = \int\limits_{-\cot\kappa}^{\cot\kappa} (\partial N/\partial y)_{y=0}\, m\,(h)\, dh.$$

Inserting this expression in (8.8.19), we get

$$V_\infty a = \int\limits_{-\cot\kappa}^{\cot\kappa} (\partial N/\partial y)_{y=0}\, m\,(h)\, dh. \tag{8.8.20}$$

Differentiation of (8.8.17) with respect to y gives

$$\left(\frac{\partial N}{\partial y}\right)_{y=0} = -\frac{a'^2}{a\sqrt{a}}\left(\frac{\nu}{1-\nu^2}+\coth^{-1}\nu\right)_{y=0}. \tag{8.8.21}$$

Let us calculate the partial derivative of (8.8.20) with respect to (z/x) taking into account (8.8.21):

$$0 = \int\limits_{-\cot\kappa}^{\cot\kappa} \frac{2}{a\sqrt{a}\,(1-\nu^2)^2}\cdot\frac{\partial v}{\partial\,(z/x)}\bigg|_{y=0} m\,(h)\, dh. \tag{8.8.22}$$

From (8.8.16) it follows that the derivative

$$\frac{\partial\nu}{\partial\left(\frac{z}{x}\right)}\bigg|_{y=0} = \frac{a'^2}{\sqrt{a}}\cdot\frac{h\left[1-a'^2\left(\frac{y^2}{x^2}+\frac{z^2}{x^2}\right)\right]+\frac{z}{x}\left(a'^2 h\frac{z}{x}-1\right)}{\left[1-a'^2\left(\frac{y^2}{x^2}+\frac{z^2}{x^2}\right)\right]^{3/2}}\bigg|_{y=0}$$

$$= \frac{h-\frac{z}{x}}{\left(1-a'^2\frac{z^2}{x^2}\right)^{3/2}}\cdot\frac{a'^2}{(1-a'^2 h^2)^{1/2}}. \tag{8.8.23}$$

From (8.8.7) and (8.8.16) we arrive at the relation

$$\frac{2}{a\sqrt{a}\,(1-\nu^2)^2}\bigg|_{y=0} = \frac{2}{(1-a'^2 h^2)^{3/2}}$$

$$\times\frac{(1-a'^2h^2)^2\left[1-a'^2\left(\frac{y^2}{x^2}+\frac{z^2}{x^2}\right)\right]^2}{\left\{(1-a'^2h^2)\left[1-a'^2\left(\frac{y^2}{x^2}+\frac{z^2}{x^2}\right)\right]-\left(a'^2 h\frac{z}{x}-1\right)^2\right\}^2}\bigg|_{y=0}$$

$$= \frac{\left(1-a'^2\frac{z^2}{x^2}\right)^2}{\left(h-\frac{z}{x}\right)^4}\cdot\frac{2\,(1-a'^2 h^2)^{1/2}}{a'^4}. \tag{8.8.24}$$

Using (8.8.23) and (8.8.24) in equation (8.8.22) we have

$$\int_{-\cot\kappa}^{\cot\kappa} \frac{m(h)\,dh}{\left(h-\frac{z}{x}\right)^3}=0. \tag{8.8.25}$$

It will be shown that this equation has the same form as the equation obtained by using the method of dipoles in solving the problem of the flat plate of infinite length oriented perpendicularly to the direction of an incompressible undisturbed flow. The velocity potential for the flat plate, representing part of a wing at a section AB of coordinates $z_A=-c$, $z_B=c$ in an incompressible flow of velocity $v=V_\infty\alpha$ in a direction perpendicular to the wing (Fig. 8.8.3), can be determined with the help of equation (2.9.16), which can be rewritten in the system of coordinates shown in Fig. 8.8.3 in the form

$$\varphi_{\text{dip}}=y/[(z-\eta)^2+y^2]. \tag{8.8.26}$$

This expression determines the potential at a point $P\,(y, z)$ due to a plane point dipole of unit strength ($M=1$). If the strength of the dipole differs from unity and the distribution of dipoles along the span of the flat plate is given by the function $M\,(\eta)$ the velocity potential induced by dipoles on the section of the wing $d\eta$ will be

$$d\varphi_{\text{dip}}=M\,(\eta)\,y\,d\eta/[(z-\eta)^2+y^2]. \tag{8.8.27}$$

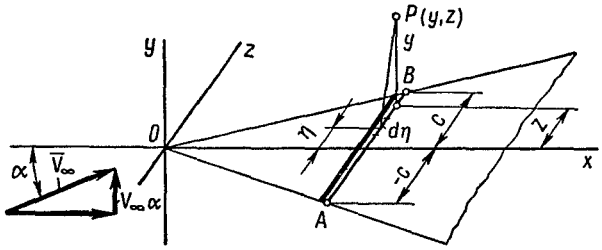

Fig. 8.8.3. Incompressible two-dimensional flow past flat plate AB from delta wing in cross flow of velocity $V_\infty\alpha$.

The velocity potential at a point P induced by the effect of dipoles distributed along the span of a flat plate at the section from $z_A=-c$ to $z_B=c$ can be written in the form

$$\varphi_{\text{dip}}=\int_{-c}^{c}\frac{M\,(\eta)\,y\,d\eta}{(z-\eta)^2+y^2}. \tag{8.8.28}$$

The vertical component of velocity $v=\partial\varphi_{\text{dip}}/\partial y$ on the surface of a wing ($y=0$) will be

$$v_{y=0}=\left(\frac{\partial \varphi_{\text{dip}}}{\partial y}\right)_{y=0}=\left[\frac{\partial}{\partial y}\int_{-c}^{c}\frac{M(\eta)\,y d\eta}{(z-\eta)^2+y^2}\right]_{y=0}=\int_{-c}^{c}\frac{M(\eta)\,d\eta}{(z-\eta)^2}. \quad (8.8.29)$$

Since the component $v_{y=0}$ remains constant along the span we have

$$\left(\frac{\partial v}{\partial z}\right)_{y=0}=\frac{\partial}{\partial z}\int_{-c}^{c}\frac{M(\eta)\,d\eta}{(z-\eta)^2}=0.$$

Differentiation of this results in

$$\int_{-c}^{c}\frac{M(\eta)\,d\eta}{(z-\eta)^3}=0. \quad (8.8.30)$$

Comparing equations (8.8.25) and (8.8.30), we find that they are of the same type. Therefore the possible function of distribution of dipoles $m(h)$ in a supersonic linearized flow can be chosen so that it has the same external form as the corresponding function $M(\eta)$ in an incompressible flow.

To determine the form of a function $M(\eta)$ we can use the solution of the problem of determination of potential function for a flat plate in an incompressible fluid flow in a perpendicular direction (see Chapter 6 Section 2). By this method the velocity potential over the plate is obtained from formula (6.2.7). Hence the difference of potentials over the two sides of the plate will be $\Delta\varphi=2V\sqrt{a^2-z^2}$. Now we recall that an incompressible fluid flow about a flat plate is taken as the resultant of superposition of the flow due to dipoles over the undisturbed flow [see formula (6.3.6)]. Consequently the distribution of dipoles for the flat plate in an irrotational incompressible fluid flow is equivalent to the difference of potentials $\Delta\varphi$ obtained above. Keeping in view that the function $m(h)$ for distribution of dipoles in a compressible flow has the same form as that for an incompressible flow, the expression for this function can be assumed to have the form

$$m(h)=L\sqrt{H^2-h^2}, \quad (8.8.31)$$

where $H^2=\cot^2\kappa$; L is some coefficient of proportionality. Equation (8.8.20) can be used to determine the coefficient L. Inserting (8.8.21) and (8.8.31), we get

$$aV_\infty=-a'^2\,L\int_{-\cot\kappa}^{\cot\kappa}\frac{1}{a\sqrt{a}}\left(\frac{\nu}{1-\nu^2}+\cot h^{-1}\nu\right)_{y=0}\sqrt{\cot^2\kappa-h^2}\,dh. \quad (8.8.32)$$

According to (8.8.7) and (8.8.16) the quantity

$$\nu_{y=0}=\left(\frac{b}{2\sqrt{ac}}\right)_{y=0}=\frac{a'^2 h\dfrac{z}{x}-1}{\sqrt{(1-a'^2 h^2)\left(1-a'^2\dfrac{z^2}{x^2}\right)}}. \tag{8.8.33}$$

Taking into account (8.8.7), the quantity

$$1/a\sqrt{a}=1/(1-a'^2 h^2)^{3/2}. \tag{8.8.34}$$

To simplify the calculation of coefficient L from (8.8.32) the integration may be carried out along the axial coordinate on the wing. Keeping in mind that $z=0$, $y=0$, for the axial line we have

$$aV_\infty=-La'^2\int_{-\cot\kappa}^{\cot\kappa}\frac{\sqrt{\cot^2\kappa-h^2}}{(1-a'^2 h^2)^{3/2}}\left(\frac{\sqrt{1-a'^2 h^2}}{a'^2 h^2}+\cot h^{-1}\frac{-1}{\sqrt{1-a'^2 h^2}}\right)dh. \tag{8.8.35}$$

Integration of this leads to

$$aV_\infty=\pi L\int_0^{\pi/2}\sqrt{1-(1-a'^2\cot^2\kappa)\sin^2\varphi}\,d\varphi. \tag{8.8.36}$$

The integral

$$\int_0^{\pi/2}\sqrt{1-(1-a'^2\cot^2\kappa)\sin^2\varphi}\,d\varphi=E(k) \tag{8.8.37}$$

represents the complete elliptic integral of the second kind with the parameter

$$k=\sqrt{1-a'^2\cot^2\kappa}. \tag{8.8.38}$$

The values of the integral (8.8.37) are obtained from the tables for different values of the parameter k.

The distribution of dipoles can be represented by function (8.8.3) provided we replace $m(h)$ by (8.8.31) and use the value of L obtained from (8.8.36). As a result we get

$$M(\xi,\zeta)=\xi\sqrt{\cot^2\kappa-h^2}\,\frac{aV_\infty}{\pi E(k)}. \tag{8.8.39}$$

Let us find the component of an induced velocity due to the dipoles over the wing surface $y=0$. From (8.7.3) it follows that

$$(\varphi_{\text{dip}})_{y=0}=(\partial\varphi'/\partial y)_{y=0}=(v_{y=0})_{\text{dip}}, \tag{8.8.40}$$

i.e. the potential due to dipoles over the wing is determined by the value of the vertical component of velocity induced by the sources. Comparing (8.2.12) and (8.7.1), it can be shown that $M(\xi, \zeta)$ may be considered as a function like the function $Q(\xi, \zeta)$ determining the distribution of sources over a wing surface of given form at a given angle of attack. If the quantity π is then included in $M(\xi, \zeta)$ in (8.7.1) the following equation can be written according to (8.2.7), (8.8.39) and (8.8.40):

$$(\varphi_{\text{dip}})_{y=0} = \pi M(\xi, \zeta) = \frac{aV_\infty \xi \sqrt{\cot^2 \kappa - h^2}}{E(k)}, \tag{8.8.41}$$

where $h = \zeta/\xi$ or $h = z/x$.

The component of induced velocity due to the dipoles will be

$$u = \left(\frac{\partial \varphi_{\text{dip}}}{\partial x}\right)_{y=0} = \frac{aV_\infty}{E(k)} \cdot \frac{\partial}{\partial x}\left(x\sqrt{\cot^2 \kappa - \frac{z^2}{x^2}}\right)$$

$$= \frac{aV_\infty \cot^2 \kappa}{E(k)\sqrt{\cot^2 \kappa - h^2}}. \tag{8.8.42}$$

The corresponding value of pressure coefficient, taking into account the possible signs before the square root term, will be

$$\bar{p} = \frac{2(p - p_\infty)}{\rho_\infty V_\infty^2} = -\frac{2u}{V_\infty} = \frac{\pm 2a \cot^2 \kappa}{E(k)\sqrt{\cot^2 \kappa - h^2}}, \tag{8.8.43}$$

where the plus sign refers to the pressure on the lower side and the minus sign to that on the upper side of the wing. The pressure field happens to be conical about the leading edge of a wing, i.e. the coefficient of pressure $\bar{p}$ = constant for all the values of z/x = constant.

The lift force acting on a delta wing consists of the pressure force on the lower surface and the suction force arising from suction on the upper surface. The elementary value of a lift force acting on the area $dS = 0.5x dz$ (see Fig. 8.8.1) will be

$$dY = 2(p - p_\infty)\, dS = (p - p_\infty)\, x dz.$$

The total lift is obtained by integrating this over the whole wing surface $S_w = x^2 \cot \kappa$:

$$Y = \int_{S_w} 2(p - p_\infty)\, dS.$$

The coefficient of lift will be

$$c_y = \frac{2Y}{\rho_\infty V_\infty^2 S_w} = \frac{1}{\cot \kappa} \int_{-\cot \kappa}^{\cot \kappa} |\bar{p}|\, dh = \frac{2a \cot \kappa}{E(k)} \int_{-\cot \kappa}^{\cot \kappa} \frac{dh}{\sqrt{\cot^2 \kappa - h^2}}.$$

Integration of this gives

$$c_y = 2a\pi \cot \kappa / E(k). \tag{8.8.44}$$

For a conical flow the center of pressure of each of the triangular elements starting from the leading edge is situated at a distance of two-thirds of the depth from the leading edge. Therefore the center of pressure of the whole wing will be located on the root chord at a point lying at a distance two-thirds of a chord from the leading edge.

Let us find the position of the center of pressure of a semi-wing. For this we calculate the coefficient of lift of the section

$$c_y' = \frac{2}{b} \int_{x_A}^{b_r} |\bar{p}| \, dx,$$

where $x_A = b_r - b$; b is the local chord (see Fig. 8.8.1). Using the value of $\bar{p}$ from (8.8.43) and integrating, we get

$$bc_y' = (bc_y')_r (1 - \tan^2 \nu \tan^2 \kappa)^{1/2}, \tag{8.8.45}$$

where $\tan \nu = z/b_r$ (see Fig. 8.8.1). The quantity bc_y' is called the spanwise wing loading.

The load at the root section $(bc_y')_r$ is determined from the condition at $x_A = 0$, $z = 0$. It is then given by

$$(bc_y')_r = 4ab_r \cot \kappa / E(k). \tag{8.8.46}$$

The distribution of spanwise wing loading, as seen from (8.8.45), happens to be elliptic.

The position of the center of pressure of the semi-wing (coordinate $z_{c.p}$, see Fig. 8.8.1) is determined from the equation of moment of forces about the x axis:

$$M_x = q_\infty \int_0^{l/2} c_y' bz \, dz = c_y z_{c.p} \left(\frac{1}{2} b_r \right) \frac{l}{2} q_\infty,$$

whence

$$z_{c.p} = \frac{4}{b_r l c_y} \int_0^{l/2} c_y' bz \, dz.$$

Substituting the value of c_y' in this expression, taking the value of c_y from (8.8.44) and integrating, the following value of the coordinate of the center of pressure can be obtained:

$$z_{c.p} = \frac{4}{3\pi} \left(\frac{l}{2} \right). \tag{8.8.47}$$

For a delta wing of low-aspect ratio ($\kappa \to \pi/2$) the quantity $a' \cot \kappa \ll 1$ and the value of the elliptical integral may be taken as $E(k) \approx 1$. Hence for this wing

$$c_y = 2a\pi \cot \kappa. \tag{8.8.48}$$

Expressing $\cot \kappa$ in terms of the aspect ratio of the wing $\lambda_w = 4 \cot \kappa$, we get

$$c_y = a\pi\lambda_w/2. \tag{8.8.48'}$$

If the angle of sweep κ is chosen so that $\kappa = \pi/2 - \mu_\infty$ consequently the Mach line coincides with the leading edge,

$$\cot \kappa = \tan \mu_\infty \text{ and } a' \cot \kappa = \cot \mu_\infty \cot \kappa = 1.$$

In this case the elliptic integral $E(k) = \pi/2$. Therefore for a delta wing with a subsonic leading edge

$$c_y = 4a \cot \kappa. \tag{8.8.49}$$

Since

$$\cot \kappa = \tan \mu_\infty = 1/\sqrt{M_\infty^2 - 1},$$

we have

$$c_y = 4\, a/\sqrt{M_\infty^2 - 1}. \tag{8.8.50}$$

This value of lift coefficient coincides with that of a thin profile with sharp edge in a linearized supersonic flow.

It will be shown that the coefficient of lift of a delta wing with a supersonic leading edge can be described by the same expression (8.8.50). According to (8.3.40) the pressure coefficient over a wing in the region between the Mach cones will be

$$\bar{p} = \frac{\pm 2a}{a'\sqrt{1-n^2}} \left(1 - \frac{2}{\pi} \sin^{-1} \sqrt{\frac{n^2-\sigma^2}{1-\sigma^2}}\right), \tag{8.8.51}$$

and on the section between the leading edge and the Mach cone [see formula (8.3.27)]:

$$\bar{p} = \pm 2\, a/a'\sqrt{1-n^2}, \tag{8.8.52}$$

where $n = \tan \kappa/a'$, $\sigma = z \tan \kappa/x = h \tan \kappa$.

Let us determine the coefficient of pressure difference:

$$\Delta \bar{p} = \bar{p}_l - \bar{p}_u.$$

According to (8.8.51) and (8.8.52) we get the value of this coefficient for the section between the Mach lines

$$\Delta\bar{p} = \frac{4a}{a'\sqrt{1-n^2}} \left(1 - \frac{2}{\pi} \sin^{-1} \sqrt{\frac{n^2-\sigma^2}{1-\sigma^2}}\right); \tag{8.8.51'}$$

and on the section between the leading edge and the Mach line it will be

$$\Delta \bar{p}=4a/\alpha' \sqrt{1-n^2}. \tag{8.8.52'}$$

The spanwise distribution of lift will be

$$bc_y'=\int_{x_A}^{b_r} \Delta\bar{p}\, dx.$$

Inserting the value of $\Delta\bar{p}$ from (8.8.51') and integrating, we get the following relation for the section between the Mach lines:

$$bc_y'=\frac{4ab_r}{\alpha' \sqrt{1-n^2}}\left[1+\frac{1}{\pi}(1-\sigma')\sin^{-1}\frac{\sigma'-n^2}{n(1-\sigma')}\right.$$
$$\left.-\frac{1}{\pi}(1+\sigma')\sin^{-1}\frac{\sigma'+n^2}{n(1+\sigma')}\right], \tag{8.8.53}$$

where

$$\sigma'=z\tan\kappa/b_r,\ 0\leqslant\sigma'\leqslant n.$$

Substituting the value of $\Delta\bar{p}$ from (8.8.52') and integrating, we get the relation for the section between the Mach lines and the leading edge

$$bc_y'=\frac{4ab_r(1-\sigma')}{\alpha' \sqrt{1-n^2}}, \tag{8.8.54}$$

where $n\leqslant\sigma'\leqslant 1$.

The distribution of spanwise wing loading does not remain elliptical in this case as in the case of the wing with a subsonic leading edge. It varies linearly over the section between the Mach lines and the leading edge and it has a curvilinear variation over the region between the Mach lines (Fig. 8.8.4). The distribution of pressure in conical form is shown in the same figure. As long as the pressure field remains conical the center of pressure lies at a distance of two-thirds of the root chord from the leading edge.

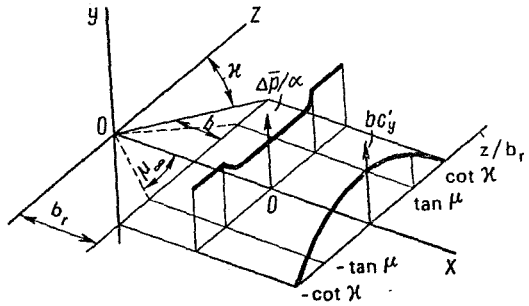

Fig. 8.8.4. Distribution of coefficient of pressure difference and load along span of wing with supersonic leading edge.

The coefficient of lift of the wing will be

$$c_y=\frac{1}{\cot\kappa}\int_{-\cot\kappa}^{\cot\kappa}|\bar{p}|\,dh=\frac{2}{\cot\kappa}\int_{0}^{\cot\kappa}|\bar{p}|\,dh=2\int_0^1\frac{2ad\sigma}{a'\sqrt{1-n^2}}$$

$$-\frac{4}{\pi}\int_0^n\frac{2a}{a'\sqrt{1-n^2}}\sin^{-1}\sqrt{\frac{n^2-\sigma^2}{1-\sigma^2}}\,d\sigma.$$

This integration leads to the expression $c_y=4a/a'$, which coincides with (8.8.50).

9. Wing with Six Corners having Subsonic Leading Edges and Supersonic Trailing Edges

Let us find the aerodynamic characteristics in the more general case of a flow-interaction at a small angle of attack with a wing in the form of a flat plate with six corners in plan with subsonic leading edges and supersonic trailing edges (Fig. 8.9.1). This form of trailing edge eliminates the vortex sheet effect behind a wing during flow-interaction.

The results of the solution of the problem of the flow-interaction of a delta wing with subsonic leading edges can be used to determine the velocity

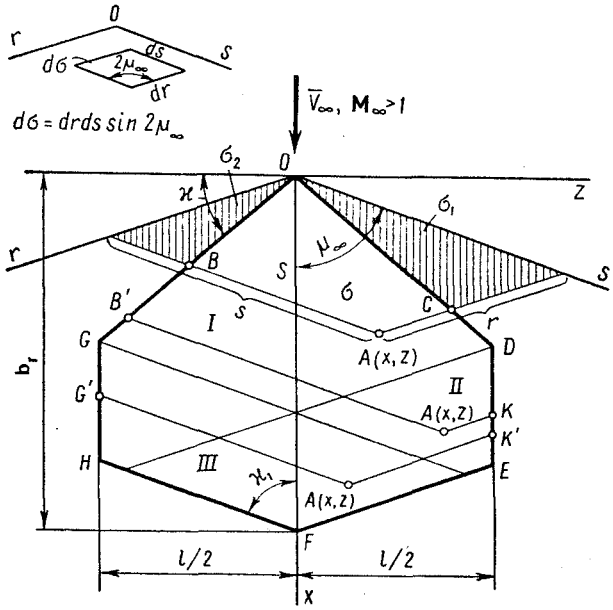

Fig. 8.9.1. Wing with six corners having subsonic leading edges and supersonic trailing edges.

potential. Let us consider a point A with coordinates x, z situated in the region I which is bounded by the leading edges and the Mach lines drawn from the points G and D. The velocity potential at this point can be expressed, by analogy with (8.6.1), by the following formula:

$$\varphi_I' = -\frac{1}{2\pi}\iint_{\sigma}\frac{Q_1(\xi,\zeta)\,d\xi d\zeta}{\sqrt{(x-\xi)^2-a'^2(z-\zeta)^2}} + \Delta\varphi_2+\Delta\varphi_3, \tag{8.9.1}$$

where σ is the region of integration on the wing surface; the quantities $\Delta\varphi_2$ and $\Delta\varphi_3$, representing additional potentials, are determined by expressions similar to the second and third terms on the right side of (8.6.3) for the regions of integration σ_1 and σ_2 (shaded regions in Fig. 8.9.1).

Keeping in mind that $Q_1=2\lambda V_\infty=2aV_\infty$, equation (8.9.1) can be rewritten in the following way:

$$\varphi_I' = -\frac{aV_\infty\Omega}{\pi}\iint_{\sigma}\frac{d\xi d\zeta}{\sqrt{(x-\xi)^2-a'^2(z-\zeta)^2}}, \tag{8.9.2}$$

where

$$\Omega = 1-(\Delta\varphi_2+\Delta\varphi_3)\left[\frac{aV_\infty}{\pi}\iint_{\sigma}\frac{d\xi d\zeta}{\sqrt{(x-\xi)^2-a'^2(z-\zeta)^2}}\right]^{-1}, \tag{8.9.3}$$

which is obtained from (8.9.1).

Let us introduce a characteristic system of coordinates for further transformations. In this system the axes r and s coincide with the directions of the Mach lines drawn from the leading edge of the wing (see Fig. 8.9.1):

$$r=(\mathbf{M}_\infty/2a')(x-a'z), \quad s=(\mathbf{M}_\infty/2a')(x+a'z). \tag{8.9.4}$$

The characteristic coordinates of a point $A(x_A, z_A)$ will be:

$$r_A=(\mathbf{M}_\infty/2a')(x_A-a'z_A), \quad s_A=(\mathbf{M}_\infty/2a')(x_A+a'z_A). \tag{8.9.4'}$$

Let us apply these characteristic coordinates r and s to equation (8.9.2). From (8.9.4) we have:

$$r+s=(\mathbf{M}_\infty/a')x, \quad r-s=-\mathbf{M}_\infty z. \tag{8.9.4''}$$

Hence

$$\left.\begin{aligned} x-\xi=x_A-x&=(a'/\mathbf{M}_\infty)[(r_A+s_A)-(r+s)];\\ a'(z-\zeta)=a'(z_A-z)&=-(a'/\mathbf{M}_\infty)[(r_A-s_A)-(r-s)].\end{aligned}\right\} \tag{8.9.5}$$

Using these expressions in (8.9.2) and remembering that the elementary area in terms of the coordinates r and s will be $d\sigma=dr\cdot ds\sin(2\mu_\infty)$ (see Fig. 8.9.1) and the limits of integration will be s_B and s_A, r_C and r_A, we get the equation for a potential function:

$$\varphi_I' = -\frac{V_\infty a \Omega}{\pi \mathbf{M}_\infty} \int_{r_C}^{r_A} \frac{dr}{\sqrt{r_A - r}} \int_{s_B}^{s_A} \frac{ds}{\sqrt{s_A - s}}. \tag{8.9.6}$$

The coordinates of s_B and r_C can be expressed in terms of the coordinates of points r_A and s_A respectively. Since the equations of leading edges in the coordinates z and x will be $z = \pm x \tan \kappa$ then, according to (8.9.4''), these equations in the coordinates r and s are transformed into the form:

$$\left.\begin{array}{c} r = sm \text{ (for right side leading edge} \\ z = +x \cot \kappa); \\ r = s/m \text{ (for left side leading edge} \\ z = -x \cot \kappa), \end{array}\right\} \tag{8.9.7}$$

where $m = (n-1)/(n+1)$, $n = \tan \kappa / a'$. Therefore the coordinates r_C and s_B can be expressed in the following way:

$$r_C = s_C m = s_A m \quad \text{and} \quad s_B = r_B m = r_A m. \tag{8.9.8}$$

Replacing r_C and s_B in (8.9.6) by $s_A m$ and $r_A m$ respectively and carrying out integration, we get

$$\varphi_I' = -\frac{4aV_\infty \Omega}{\pi \mathbf{M}_\infty} \sqrt{(r_A - ms_A)(s_A - mr_A)}. \tag{8.9.9}$$

Substitution of the values of r_A and s_A from (8.9.4') and the quantity

$$m = (n-1)/(n+1), \tag{8.9.10}$$

gives

$$\varphi_I' = -\frac{4aV_\infty n x_A \Omega}{\pi (n+1)} \sqrt{\cot^2 \kappa - h^2}, \tag{8.9.11}$$

where $h = z_A/x_A$ or $h = \zeta/\xi$.

Comparing equation (8.9.11) with the exact relation (8.8.41) for the potential function at a given point it will be seen that for equality of results the quantity Ω in (8.9.11) should be equal to

$$\Omega = -\frac{\pi}{4} \cdot \frac{n+1}{nE(k)}. \tag{8.9.12}$$

Then at point A lying on a wing in region I the velocity potential will be

$$\varphi_I' = \frac{aV_\infty x_A}{E(k)} \sqrt{\cot^2 \kappa - h^2}. \tag{8.9.13}$$

Accordingly the equation that should be used to determine the potential function on the wing will have the general form:

$$\varphi_I' = \frac{aV_\infty (n+1)}{4n\mathbf{M}_\infty E(k)} \iint\limits_{\sigma} \frac{dr}{\sqrt{r-r_A}} \cdot \frac{ds}{\sqrt{s_A-s}}. \tag{8.9.14}$$

Let us use equation (8.9.14) to determine the potential function at point A situated in region II which is bounded by the Mach lines from the points D and G, the side edges and part of the trailing edge. Equation (8.9.14) may be written in the following way:

$$\varphi_{II}' = \frac{aV_\infty (n+1)}{4n\mathbf{M}_\infty E(k)} \int\limits_{r_K}^{r_A} \frac{dr}{\sqrt{r_A-r}} \int\limits_{s_B'}^{s_A} \frac{ds}{\sqrt{s_A-s}}. \tag{8.9.15}$$

By analogy with (8.9.8)

$$s_{B'} = r_{B'}\, m = r_A m. \tag{8.9.16}$$

Point K is situated on the side edge satisfying the equation $z=l/2$. In terms of coordinates r and s the equation of the side edge, in accordance with (8.9.4''), will be

$$r-s = -\mathbf{M}_\infty (l/2). \tag{8.9.17}$$

Then the coordinate for point K will be

$$r_K = s_K - (\mathbf{M}_\infty\, l/2) = s_A - (\mathbf{M}_\infty\, l/2). \tag{8.9.18}$$

Considering also that $s_{B'} = r_A\, m$, after integration of (8.9.15) we obtain

$$\varphi_{II}' = \frac{aV_\infty (n+1)}{n\,\mathbf{M}_\infty E(k)} \sqrt{\left[r_A - \left(s_A - \frac{\mathbf{M}_\infty\, l}{2}\right)\right](s_A - r_A m)}\,. \tag{8.9.19}$$

Replacement of r_A, s_A and m by the corresponding values from (8.9.4') and (8.9.10) gives

$$\varphi_{II}' = \frac{aV_\infty}{nE(k)} \sqrt{\frac{n+1}{2}(l-2z_A)\left(\frac{x_A}{a'} + nz_A\right)}. \tag{8.9.20}$$

The velocity potential at a point A lying in region III will be

$$\varphi_{III}' = \frac{aV_\infty (n+1)}{4n\,\mathbf{M}_\infty E(k)} \int\limits_{r_{K'}}^{r_A} \frac{dr}{\sqrt{r_A-r}} \int\limits_{s_{G'}}^{s_A} \frac{ds}{\sqrt{s_A-s}}. \tag{8.9.21}$$

Points K' and G' are situated on the side edges and satisfy the equations $z = \pm\, l/2$ (the plus sign for the right edge and the minus sign for the left edge). In terms of the coordinates r and s the equations of these edges, according to (8.9.4), will be

$$\left.\begin{aligned} r-s &= -\mathbf{M}_\infty\, l/2 \text{ (for right edge);} \\ r-s &= \mathbf{M}_\infty\, l/2 \text{ (for left edge).} \end{aligned}\right\} \tag{8.9.22}$$

Therefore we can write for points K' and G':

$$\left.\begin{aligned} r_{K'} &= s_{K'} - (\mathbf{M}_\infty l/2) = s_A - (\mathbf{M}_\infty l/2); \\ s_{G'} &= r_{G'} - (\mathbf{M}_\infty l/2) = r_A - (\mathbf{M}_\infty l/2). \end{aligned}\right\} \tag{8.9.23}$$

Integration of (8.9.21), taking into account the limits shown in (8.9.23), gives

$$\varphi'_{III} = \frac{aV_\infty (n+1)}{n\mathbf{M}_\infty E(k)} \sqrt{\left(r_A - s_A + \frac{\mathbf{M}_\infty l}{2}\right)\left(s_A - r_A + \frac{\mathbf{M}_\infty l}{2}\right)}. \tag{8.9.24}$$

Using the values of s_A and r_A from (8.9.4') we have

$$\varphi'_{III} = \frac{aV_\infty (n+1)}{2nE(k)} \sqrt{l^2 - 4z_A^2}. \tag{8.9.25}$$

Calculating the partial derivative with respect to x_A, we get the components of perturbation velocity $u = \partial\varphi'_n/\partial x_A$ $(n = I, II, III)$. Then the coefficients of pressure in the respective regions on the lower and upper sides of the wing will be:

$$\left.\begin{aligned} \bar{p}_I &= \mp\frac{2}{V_\infty} \cdot \frac{\partial\varphi'_I}{\partial x_A} = \pm\frac{2a\cot^2\kappa}{E(k)} \cdot \frac{x_A}{\sqrt{x_A^2\cot^2\kappa - z_A^2}}; \\ \bar{p}_{II} &= \mp\frac{2}{V_\infty} \cdot \frac{\partial\varphi'_{II}}{\partial x_A} = \pm\frac{a}{nE(k)} \sqrt{\frac{(n+1)(l-2z_A)}{2a'(x_A + z_A\tan\kappa)}}; \\ \bar{p}_{III} &= \mp\frac{2}{V_\infty} \cdot \frac{\partial\varphi'_{III}}{\partial x_A} = 0. \end{aligned}\right\} \tag{8.9.26}$$

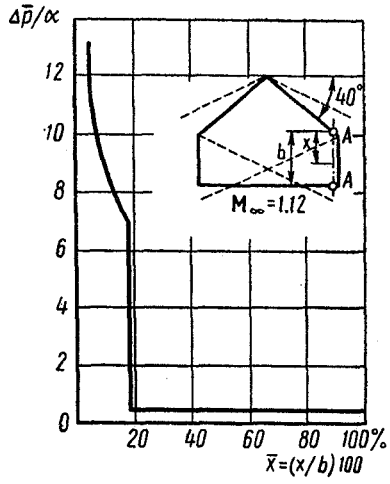

Fig. 8.9.2. Distribution of coefficient $\Delta\bar{p}/a = (\bar{p}_l - \bar{p}_u)/a$ near side edge of five-cornered wing (section AA).

Here the plus sign on the right side of the equality corresponds to the lower side of a wing and the minus sign to the upper side.

The variation in the coefficient $\Delta\bar{p}/a = (\bar{p}_l - \bar{p}_u)/a$ near the side edge as a function of the distance from the leading edge (as a percentage of the chord) calculated with the above formulas for a wing with five corners at $\mathbf{M}_\infty = 1.12$ is shown in Fig. 8.9.2. The discontinuity in pressure due to the action of the corner point of a wing is observed on the surface of a Mach cone at the tip. The pressure remains constant at the section between the side edge and the Mach cone at the tip.

The coefficients of lift and moment are determined from the known pressure

distribution:

$$c_y = \frac{Y}{q_\infty S_w} = \frac{1}{S_w} \iint\limits_{(S)} (\bar{p}_l - \bar{p}_u)\, dxdz; \tag{8.9.27}$$

$$m_z = \frac{M_z}{q_\infty S_w b_r} = \frac{1}{S_w b_r} \iint\limits_{(S)} (\bar{p}_l - \bar{p}_u)\, xdxdz, \tag{8.9.28}$$

where S_w and b_r are the plan area and the root chord of the wing; $\bar{p}_l$ and $\bar{p}_u$ are the coefficients of pressure on lower and upper sides determined by formula (8.9.26). From these formulas it can be seen that the pressure coefficients $\bar{p}_l$ and $\bar{p}_u$ will be different in sign but the same in absolute value.

Introducing the notation $\bar{p}_l = |\bar{p}_u| = \bar{p}$, we get

$$c_y = \frac{2}{S_w} \iint\limits_{(S)} \bar{p}\, dxdz; \tag{8.9.29}$$

$$m_z = \frac{2}{S_w b_r} \iint\limits_{(S)} \bar{p}\, xdxdz. \tag{8.9.30}$$

This integration should be carried out over the complete wing plan area.

10. Wing with Six Corners having Supersonic Leading and Trailing Edges

The flow-interaction of a six-cornered wing with supersonic leading and trailing edges (Fig. 8.10.1, a) can be studied with the help of equation (8.3.1) and the velocity potential due to sources and sinks can be obtained. This equation in new coordinates r and s [see (8.9.4)] is transformed into the form

$$\varphi' = \frac{-aV_\infty}{\pi \mathbf{M}_\infty} \iint\limits_{o} \frac{drds}{\sqrt{(r_A - r)(s_A - s)}}, \tag{8.10.1}$$

where r_A, s_A are coordinates of the point A in question lying on the surface of a six-cornered wing.

The coordinate lines r and s are directed along the Mach lines. These Mach lines, like the lines of weak disturbances emerging from points G and D and from points G' and D' lying at the intersection of coordinate lines r and s (Mach lines) with the side edges, divide the wing surface into eight regions. The velocity potential in each of these regions is calculated with the help of equation (8.10.1).

The potential function at point A with coordinates x_A, z_A situated in region I (see Fig. 8.10.1, a) will be

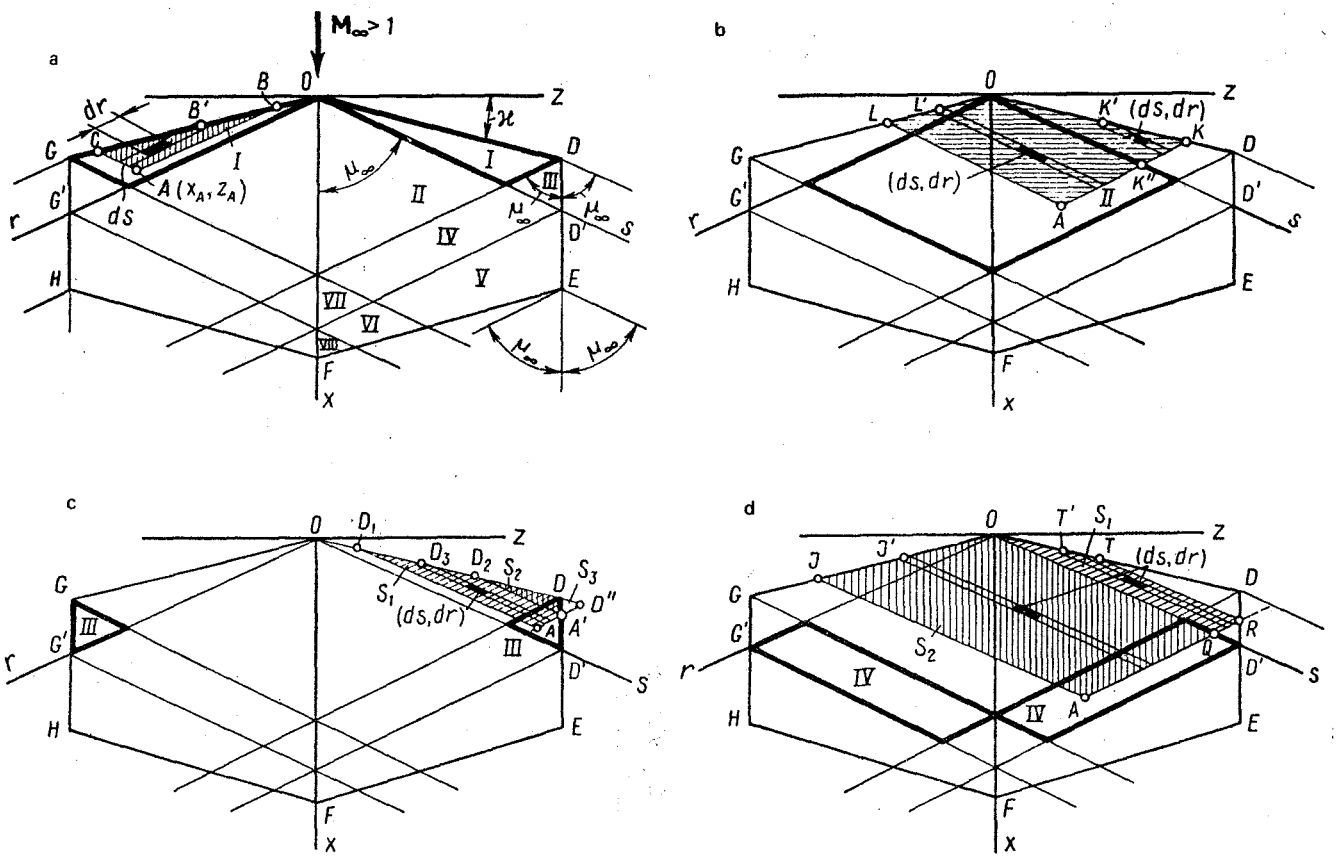
a
$M_\infty > 1$
B
O
Z
dr
B'
G
C
G'
A (x_A, z_A)
I
dS
r
H
F
X
μ_∞
II
IV
V
VII
VI
VIII
III
D
D'
E
S
b
L
L'
K'
(dS, dr)
K
K''
A
c
D_1
D_3
D_2
S_2
S_3
S_1
D''
d
T'
S_1
T
J
J'
R
Q
S_2
IV

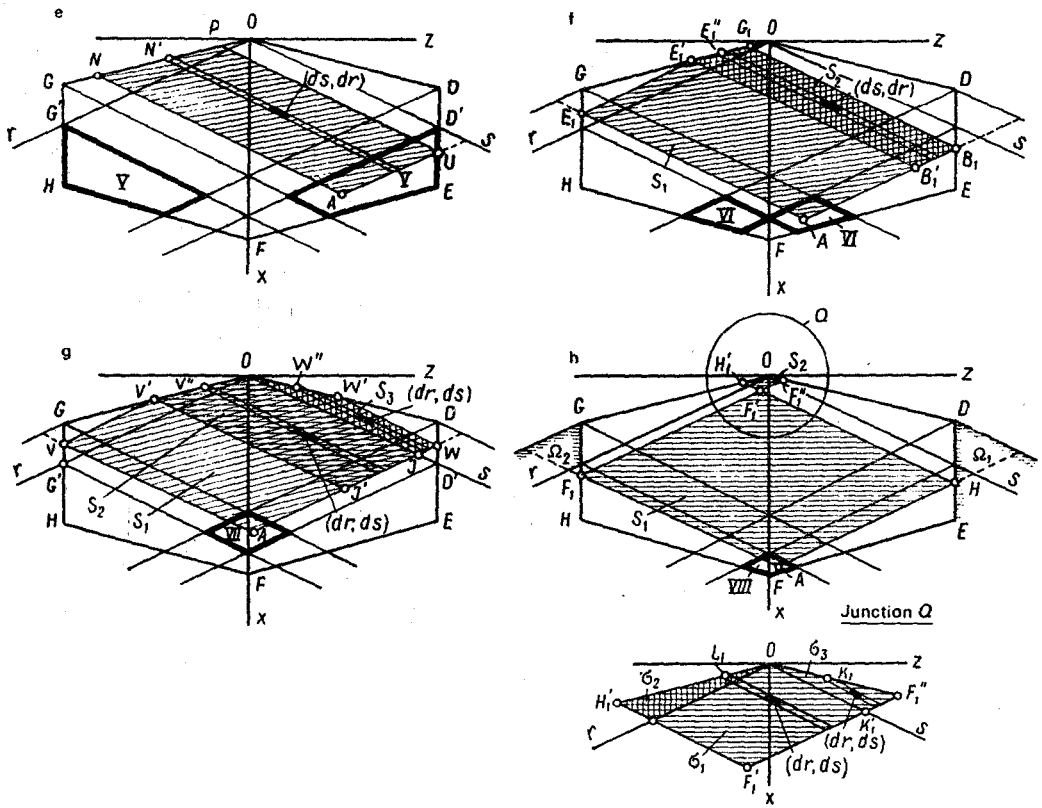

Fig. 8.10.1. Six-cornered wing with supersonic leading and trailing edges.

$$\varphi_I' = \frac{-aV_\infty}{\pi \mathbf{M}_\infty} \int_{s_C}^{s_A} \frac{ds}{\sqrt{s_A - s}} \int_{r_{B'}}^{r_A} \frac{dr}{\sqrt{r_A - r}}. \tag{8.10.2}$$

From (8.9.8) it follows that the coordinate of a point C lying on the leading edge will be

$$s_C = r_C m = r_A m, \tag{8.10.3}$$

where $m = (n-1)/(n+1)$, $n = \tan \kappa / a'$. The variable coordinate $r_{B'}$ of point B' situated on this edge will be

$$r_{B'} = s_{B'}/m = s/m. \tag{8.10.4}$$

The derivative of a line integration in (8.10.2), taking into account the values of the limits in (8.10.3) and (8.10.4), will be

$$\varphi_I' = \frac{2aV_\infty}{\pi \mathbf{M}_\infty} \int_{r_A m}^{s_A} \sqrt{\frac{mr_A - s}{m(s_A - s)}}\, ds.$$

In a given case $n = \tan \kappa / a' < 1$. Taking this, we can write:

$$\varphi_I' = \frac{2aV_\infty}{\pi \mathbf{M}_\infty \sqrt{\overline{m}}} \int_{r_A m}^{s_A} \sqrt{\frac{s - mr_A}{s_A - s}}\, ds,$$

where $\overline{m} = (1-n)/(1+n)$. Let us carry out the integration

$$\varphi_I' = \frac{2aV_\infty}{\pi \mathbf{M}_\infty \sqrt{\overline{m}}} \left| -\sqrt{(s_A - s)(s - mr_A)} \right.$$

$$\left. + (s_A - mr_A) \tan^{-1} \sqrt{\frac{s_A - s}{s - mr_A}} \right|_{r_A m}^{s_A}.$$

After substituting the values of the limits it results in

$$\varphi_I' = \frac{-2aV_\infty}{\pi \mathbf{M}_\infty \sqrt{\overline{m}}} \cdot \frac{\pi}{2} (s_A - mr_A).$$

Substituting here the values of s_A and r_A from (8.9.4'), we get

$$\varphi_I' = \frac{-aV_\infty (x_A + z_A \tan \kappa)}{a' \sqrt{1 - n^2}} \tag{8.10.5}$$

Calculating the derivative $\partial \varphi_I' / \partial x_A$ and determining the pressure coefficient $\bar{p}_I = -2 (\partial \varphi_I' / \partial x_A) V_\infty$ on the lower and upper sides of a wing, we find

$$\bar{p}_I = \pm 2a / (a' \sqrt{1 - n^2}). \tag{8.10.6}$$

This expression coincides with formula (8.3.27) obtained for a wing with symmetrical airfoil at zero angle of attack.

Let us consider region *II*. At a point A lying in this region (Fig. 8.10.1, b) the velocity potential is established by the sources distributed over an area $OLAK$ bounded by the cone of disturbances with its apex at point A and the leading edges. The area $OLAK$ can be divided into two regions $OLAK''$ and $OK''K$ and the velocity potential at point A can be taken as the sum of the potentials due to sources distributed over these regions. Accordingly expression (8.10.1) can be written in the following form:

$$\varphi_{II}=\frac{-aV_\infty}{\pi\mathbf{M}_\infty}\left[\iint\limits_{OLAK''}\frac{drds}{\sqrt{(r_A-r)\,(s_A-s)}}+\iint\limits_{OK''K}\frac{drds}{\sqrt{(r_A-r)\,(s_A-s)}}\right]$$

$$=\frac{-aV_\infty}{\pi\mathbf{M}_\infty}\left(\int\limits_0^{r_A}\frac{dr}{\sqrt{r_A-r}}\int\limits_{s_{L'}}^{s_A}\frac{ds}{\sqrt{s_A-s}}\right.$$

$$\left.+\int\limits_{r_K}^{0}\frac{dr}{\sqrt{r_A-r}}\int\limits_{s_{K'}}^{s_A}\frac{ds}{\sqrt{s_A-s}}\right). \tag{8.10.7}$$

The values of the limits of integration (see Fig. 8.10.1) are determined from expression (8.9.8).

For points L', K and K' situated on the left and right edges respectively we have

$$s_{L'}=m.r,\ s_{K'}=r/m,\ r_K=s_Km=s_Am. \tag{8.10.8}$$

Let us carry out the line integration in (8.10.7):

$$\int\limits_{s_{L'}}^{s_A}\frac{ds}{\sqrt{s_A-s}}=\int\limits_{mr}^{s_A}\frac{ds}{\sqrt{s_A-s}}=-2\sqrt{s_A-s}\Big|_{mr}^{s_A}$$

$$=2\sqrt{s_A-mr}=2\sqrt{\bar{m}}\sqrt{r-\frac{s_A}{m}}; \tag{8.10.9}$$

$$\int\limits_{s_{K'}}^{s_A}\frac{ds}{\sqrt{s_A-s}}=\int\limits_{r/m}^{s_A}\frac{ds}{\sqrt{s_A-s}}=-2\sqrt{s_A-s}\Big|_{r/m}^{s_A}=\frac{2}{\sqrt{\bar{m}}}\sqrt{r-s_Am}, \tag{8.10.10}$$

where

$$m=(n-1)/(n+1);\ \bar{m}=-m.$$

Taking these values into account, we get

$$\varphi'_{II}=\frac{-2aV_\infty\sqrt{\overline{m}}}{\pi M_\infty}\int_0^{r_A}\sqrt{\frac{r-s_A/m}{r_A-r}}\,dr-\frac{2aV_\infty}{\pi M_\infty\sqrt{\overline{m}}}\int_{r_K}^{0}\sqrt{\frac{r-s_A m}{r_A-r}}\,dr.$$

Taking into account the value of r_K from (8.10.8) and integrating, we get

$$\varphi'_{II}=\frac{-2aV_\infty}{\pi M_\infty\sqrt{\overline{m}}}\left[\frac{\pi}{2}(r_A-s_A\,m)-(r_A m-s_A)\tan^{-1}\sqrt{\frac{r_A\overline{m}}{s_A}}\right.$$
$$\left.-(r_A-s_A\,m)\tan^{-1}\sqrt{\frac{r_A}{s_A m}}\right]. \qquad (8.10.11)$$

Using the values of r_A and s_A from (8.9.4′) we get:

$$\varphi'_{II}=\frac{-2aV_\infty}{\pi a'\sqrt{1-n^2}}\left[\frac{\pi}{2}(x_A-a'\,z_A)+(x_A+a'\,z_A)\tan^{-1}\sqrt{\frac{\overline{m}\,(x_A-a'z_A)}{x_A+a'\,z_A}}\right.$$
$$\left.-(x_A-a'\,z_A)\tan^{-1}\sqrt{\frac{x_A-a'\,z_A}{\overline{m}\,(x_A+a'\,z_A)}}\right]. \qquad (8.10.11')$$

Then the coefficient of pressure will be

$$\bar{p}_{II}=\mp\frac{2}{V_\infty}\cdot\frac{\partial\varphi'_{II}}{\partial x_A}=\frac{\pm 4a}{\pi a'\sqrt{1-n^2}}\left[\frac{\pi}{2}+\tan^{-1}\sqrt{\frac{(1-n)\,(x_A-a'\,z_A)}{(1+n)\,(x_A+a'\,z_A)}}\right.$$
$$\left.-\tan^{-1}\sqrt{\frac{(1+n)\,(x_A-a'\,z_A)}{(1-n)\,(x_A+a'\,z_A)}}\right], \qquad (8.10.12)$$

where the plus sign refers to the lower side of the wing and the minus sign to the upper.

Using the formula

$$\tan^{-1}x-\tan^{-1}y=\tan^{-1}\frac{x-y}{1+xy},$$

we have

$$\bar{p}_{II}=\pm\frac{4a}{a'\pi\sqrt{1-n^2}}\left(\frac{\pi}{2}-\tan^{-1}\sqrt{\frac{n^2-\sigma^2}{1-n^2}}\right), \qquad (8.10.12')$$

where

$$n=\tan\kappa/a',\quad \sigma=z_A\tan\kappa/x_A.$$

Keeping in mind that

$$\tan^{-1}\sqrt{\frac{n^2-\sigma^2}{1-n^2}}=\sin^{-1}\sqrt{\frac{n^2-\sigma^2}{1-\sigma^2}},$$

equation (8.10.12′) will be

$$\bar{p}_{II} = \pm \frac{4a}{a'\pi\sqrt{1-n^2}}\left(\frac{\pi}{2} - \sin^{-1}\sqrt{\frac{n^2-\sigma^2}{1-\sigma^2}}\right). \qquad (8.10.12'')$$

This formula coincides with expression (8.3.40) for a delta wing with symmetrical airfoil and supersonic leading edges at zero angle of attack.

Let us consider an arbitrary point A situated in region *III* (Fig. 8.10.1, c). In determining the velocity potential in this region it is necessary to consider the sources over the surface of the wing (over the region $S_1 = AD_1D_2A'$ and $S_2 = A'D_2D$) as well as those beyond the surface (region $S_3 = A'DD''$).

Using (8.2.12) the expression for φ'_{III} at a point A (x, O, z) can be written in the following form:

$$\varphi'_{III} = -\frac{1}{2\pi}\iint\limits_{S_1+S_2+S_3} \frac{Q(\xi,\zeta)\,d\xi d\zeta}{\sqrt{(x-\xi)^2 - a'^2(z-\zeta)^2}}. \qquad (8.10.13)$$

The strength of the sources over regions $S_1 + S_2$ of the wing is known and is equal to $Q = 2v = 2aV_\infty$. Therefore

$$\varphi'_{III} = \frac{-aV_\infty}{\pi}\iint\limits_{S_1}\frac{d\xi d\zeta}{\sqrt{(x-\xi)^2 - a'^2(z-\zeta)^2}}$$

$$-\frac{aV_\infty}{\pi}\iint\limits_{S_2}\frac{d\xi d\zeta}{\sqrt{(x-\xi)^2 - a'^2(z-\zeta)^2}} - \frac{1}{2\pi}\iint\limits_{S_3}\frac{Q(\xi,\zeta)\,d\xi d\zeta}{\sqrt{(x-\xi)^2 - a'^2(x-\zeta)^2}}, \qquad (8.10.13')$$

where $Q(\xi, \zeta)$ is the function determining the distribution of sources in the region S_3 beyond the wing. If this function is known the integration can be carried out. To determine it we can use the boundary condition (8.1.20), indicating the potential function on the plane xOz in the region between the side edge and the Mach line from a point D equal to zero. For a point A' in this region the condition of the zero value of a potential function, by analogy with (8.6.2), can be written in the following way:

$$0 = \frac{-aV_\infty}{\pi}\iint\limits_{S_2}\frac{d\xi d\zeta}{\sqrt{(x-\xi)^2 - a'^2(z-\zeta)^2}} - \frac{1}{2\pi}\iint\limits_{S_3}\frac{Q(\xi,\zeta)\,d\xi d\zeta}{\sqrt{(x-\xi)^2 - a'^2(z-\zeta)^2}}.$$

From comparison of this equation with (8.10.13') it follows that it is sufficient to carry out integration over region S_1 in the basic formula (8.10.13) for calculation of the velocity potential at the point A (x, O, z), i.e.

$$\varphi'_{III} = \frac{-aV_\infty}{\pi}\iint\limits_{S_1}\frac{d\xi d\zeta}{\sqrt{(x-\xi)^2 - a'^2(z-\zeta)^2}}. \qquad (8.10.14)$$

The resultant interaction at point A in the region of sources *III* lying over

the region S_2 of the wing surface and over the region S_3 beyond the wing is equal to zero by this formula [9].

Using expression (8.10.14), transformed into the form of (8.10.1) in terms of the coordinates r, s, we get

$$\varphi'_{III}=\frac{-aV_\infty}{\pi \mathbf{M}_\infty}\int_{r_{A'}}^{r_A}\frac{dr}{\sqrt{r_A-r}}\int_{s_{D_3}}^{s_A}\frac{ds}{\sqrt{s_A-s}}, \tag{8.10.15}$$

where the coordinate of the point D_3 on the right-side edge

$$s_{D_3}=r_{D_3}/m=r/m, \tag{8.10.16}$$

as indicated by (8.9.8).

The lower limit of the integral $r_{A'}$ can be found from the equation of the side edge $z=l/2$. This equation, in terms of the coordinate r and s, has the form of (8.9.17). Hence the coordinate

$$r_{A'}=s_{A'}-\frac{\mathbf{M}_\infty l}{2}=s_A-\frac{\mathbf{M}_\infty l}{2}. \tag{8.10.17}$$

Taking (8.10.16) into account, the integral

$$\int_{r/m}^{s_A}\frac{ds}{\sqrt{s_A-s}}=2\sqrt{s_A-\frac{r}{m}}=\frac{2}{\sqrt{\bar{m}}}\sqrt{r-s_A m},$$

where $m=(n-1)/(n+1)$; $\bar{m}=(1-n)/(n+1)$. Therefore,

$$\varphi'_{III}=\frac{-2aV_\infty}{\pi \mathbf{M}_\infty\sqrt{\bar{m}}}\int_{r_{A'}}^{r_A}\sqrt{\frac{r-s_A m}{r_A-r}}\,dr.$$

Let us integrate this expression:

$$\varphi'_{III}=\frac{-2aV_\infty}{\pi \mathbf{M}_\infty\sqrt{\bar{m}}}\left[-\sqrt{(r_A-r)(r-s_A m)}\right.$$
$$\left.-(r_A-s_A m)\tan^{-1}\sqrt{\frac{r_A-r}{r-s_A m}}\right]_{r_{A'}}^{r_A}$$
$$=\frac{-2aV_\infty}{\pi \mathbf{M}_\infty\sqrt{\bar{m}}}\left[\sqrt{(r_A-r_{A'})(r_{A'}-s_A m)}\right.$$
$$\left.+(r_A-s_A m)\tan^{-1}\sqrt{\frac{r_A-r_{A'}}{r_{A'}-s_A m}}\right].$$

Using the value of $r_{A'}$ from (8.10.17) we get

$$\varphi'_{III}=\frac{-2aV_\infty}{\pi \mathbf{M}_\infty \sqrt{m}}\left[\sqrt{\left(r_A-s_A+\frac{\mathbf{M}_\infty l}{2}\right)\left(s_A-s_A m-\frac{\mathbf{M}_\infty l}{2}\right)}\right.$$

$$\left.+(r_A-s_A m)\tan^{-1}\sqrt{\frac{r_A-s_A+\mathbf{M}_\infty l/2}{s_A-s_A m-\mathbf{M}_\infty l/2}}\right].$$

Noting expressions (8.9.4′) for r_A and s_A and the values of $m=(n-1)/(n+1)$ $=-\bar{m}$, the velocity potential

$$\varphi'_{III}=\frac{-aV_\infty}{\pi\sqrt{1-n^2}}\left[\sqrt{(l-2z_A)\left[(x_A+a'z_A)-a'l(n+1)\right]\frac{n+1}{a'}}\right.$$

$$\left.+\frac{2(x_A-z_A\tan\kappa)}{a'}\tan^{-1}\sqrt{\frac{a'(n+1)(l-2z_A)}{2(x_A+a'z_A)-l(n+1)a'}}\right]. \quad (8.10.18)$$

Determination of the derivative $\partial\varphi'_{III}/\partial x_A$ gives the coefficient of pressure

$$\bar{p}_{III}=\mp\frac{2}{V_\infty}\left(\frac{\partial\varphi'_{III}}{\partial x_A}\right)$$

$$=\frac{\pm 4a}{\pi a'\sqrt{1-n^2}}\tan^{-1}\sqrt{\frac{a'(n+1)(l-2z_A)}{2(x_A+a'z_A)-l(n+1)a'}}. \quad (8.10.19)$$

The velocity potential at a point A in region IV (Fig. 8.10.1, d) is determined from the effect of the sources distributed over the area $AJOTR$. Let us divide this plane into two parts $S_1=OTRQ$ and $S_2=OQAJ$ and determine the potential at a given point as the sum of the two potentials induced by the sources over the regions S_1 and S_2. Application of formula (8.10.1) gives

$$\varphi'_{IV}=\frac{-aV_\infty}{\pi\mathbf{M}_\infty}\iint\limits_{S_1+S_2}\frac{dr\,ds}{\sqrt{(r_A-r)(s_A-s)}}=\frac{-aV_\infty}{\pi\mathbf{M}_\infty}\int\limits_{r_R}^{0}\frac{dr}{\sqrt{r_A-r}}$$

$$\times\int\limits_{s_{T'}}^{s_A}\frac{ds}{\sqrt{s_A-s}}-\frac{aV_\infty}{\pi\mathbf{M}_\infty}\int\limits_{0}^{r_A}\frac{dr}{\sqrt{r_A-r}}\int\limits_{s_{J'}}^{s_A}\frac{ds}{\sqrt{s_A-s}}. \quad (8.10.20)$$

The limits $s_{T'}$ and $s_{J'}$ of integration are determined with the help of (8.9.8). As the points T' and J' are on the right side edge and left side edge respectively we have

$$s_{T'}=r_{T'}/m=r/m,\quad s_{J'}=r_{J'}m=rm. \quad (8.10.21)$$

Then the integrals will be reduced to the following values:

$$\int\limits_{s_{T'}}^{s_A}\frac{ds}{\sqrt{s_A-s}}=-2\sqrt{s_A-s}\Big|_{r/m}^{s_A}=2\sqrt{s_A-\frac{r}{m}}=\frac{2}{\sqrt{m}}\sqrt{r-s_A m};$$

$$\int_{s_{J'}}^{s_A} \frac{ds}{\sqrt{s_A-s}} = -2\sqrt{s_A-s}\Big|_{rm}^{s_A} = 2\sqrt{s_A-rm} = 2\sqrt{\overline{m}}\sqrt{r-\frac{s_A}{m}}\,.$$

According to this the potential will be

$$\varphi'_{IV} = \frac{-2aV_\infty}{\pi \mathbf{M}_\infty \sqrt{\overline{m}}} \int_{r_R}^{0} \sqrt{\frac{r-s_A m}{r_A-r}}\, dr - \frac{2aV_\infty \sqrt{\overline{m}}}{\pi \mathbf{M}_\infty} \int_{0}^{r_A} \sqrt{\frac{r-s_A/m}{r_A-r}}\, dr,$$

where r_R is determined by formula (8.9.23) in the form

$$r_R = s_R - (\mathbf{M}_\infty l/2) = s_A - (\mathbf{M}_\infty l/2).$$

Let us carry out the integration:

$$\varphi'_{IV} = \frac{-2aV_\infty}{\pi \mathbf{M}_\infty \sqrt{\overline{m}}} \Bigg[-\sqrt{(r_A-r)(r-s_A m)} - (r_A - s_A m)\tan^{-1}\sqrt{\frac{r_A-r}{r-s_A m}}\Bigg]_{s_A-\frac{\mathbf{M}_\infty l}{2}}^{0}$$

$$+ \frac{2aV_\infty \sqrt{\overline{m}}}{\pi \mathbf{M}_\infty} \Bigg[-\sqrt{(r_A-r)(r-s_A/m)} - \frac{r_A m - s_A}{m}\tan^{-1}\sqrt{\frac{r_A-r}{r-s_A/m}}\Bigg]_0^{r_A}$$

$$= \frac{-2aV_\infty}{\pi \mathbf{M}_\infty \sqrt{\overline{m}}} \Bigg[-\sqrt{r_A s_A \overline{m}} - (r_A - s_A m)\tan^{-1}\sqrt{\frac{r_A}{s_A \overline{m}}}$$

$$+ \sqrt{\left(r_A - s_A + \frac{\mathbf{M}_\infty l}{2}\right)\left(s_A - s_A m - \frac{\mathbf{M}_\infty l}{2}\right)}$$

$$+ (r_A - s_A m)\tan^{-1}\sqrt{\frac{r_A - s_A + \mathbf{M}_\infty l/2}{s_A - s_A m - \mathbf{M}_\infty l/2}}\Bigg]$$

$$+ \frac{2aV_\infty \sqrt{\overline{m}}}{\pi \mathbf{M}_\infty}\left(\sqrt{\frac{r_A s_A}{\overline{m}}} + \frac{r_A m - s_A}{m}\tan^{-1}\sqrt{\frac{r_A \overline{m}}{s_A}}\right).$$

After substituting the values of s_A and r_A from (8.9.4′) and taking $m = -\overline{m} = (n-1)/(n+1)$, we get

$$\varphi'_{IV} = \frac{-2aV_\infty}{a'\pi\sqrt{1-n^2}} \Bigg\{ (x_A - z_A\tan\kappa)\Bigg[-\tan^{-1}\sqrt{\frac{(n+1)(x_A - a'z_A)}{(1-n)(x_A + a'z_A)}}$$

$$+ \tan^{-1}\sqrt{\frac{a'(n+1)(l-2z_A)}{2(x_A + a'z_A) - a'l(n+1)}}\Bigg] + \frac{1}{2}\sqrt{(l-2z_A)\,[2(x_A + a'z_A)}} \to \cdots$$

$$\cdots \to \overline{-a'l(n+1)](n+1)a'} + (x_A + z_A\tan\kappa)\tan^{-1}\sqrt{\frac{(1-n)(x_A - a'z_A)}{(n+1)(x_A + a'z_A)}}\Bigg\}. \tag{8.10.22}$$

Then the coefficient of pressure will be

$$\bar{p}_{IV}=\mp\frac{2}{V_\infty}\cdot\frac{\partial\varphi'_{IV}}{\partial x_A}=\frac{\pm 4a}{a'\pi\sqrt{1-n^2}}\left[\tan^{-1}\sqrt{\frac{a'(n+1)(l-2z_A)}{2(x_A+a'z_A)-a'l(n+1)}}\right.$$

$$\left.+\tan^{-1}\sqrt{\frac{(1-n)(x_A-a'z_A)}{(n+1)(x_A+a'z_A)}}-\tan^{-1}\sqrt{\frac{(n+1)(x_A-a'z_A)}{(1-n)(x_A+a'z_A)}}\right]. \quad (8.10.23)$$

Using the formula $\tan^{-1}x-\tan^{-1}y=\tan^{-1}[(x-y)/(1+xy)]$ for the last two terms in the above expression we get the relation

$$\bar{p}_{IV}=\frac{\pm 4a}{a'\pi\sqrt{1-n^2}}\left[\tan^{-1}\sqrt{\frac{a'(n+1)(l-2z_A)}{2(x_A+a'z_A)-a'l(n+1)}}-\tan^{-1}\sqrt{\frac{n^2-\sigma^2}{1-n^2}}\right]. \quad (8.10.23')$$

Let us now consider region V. The velocity potential at point A situated in this region (see Fig. 8.10.1, d) will be

$$\varphi'_V=\frac{-aV_\infty}{\pi\mathbf{M}_\infty}\int_{r_U}^{r_A}\frac{dr}{\sqrt{r_A-r}}\int_{s_{N'}}^{s_A}\frac{ds}{\sqrt{s_A-s}}. \quad (8.10.24)$$

According to this formula the velocity at point A will be induced by the sources distributed over the wing area $ANPU$. The inner integral in (8.10.24) with the lower limit of $s_{N'}=rm$ will be

$$\int_{s_{N'}}^{s_A}\frac{ds}{\sqrt{s_A-s}}=2\sqrt{\bar{m}}\sqrt{r-\frac{s_A}{m}}.$$

So

$$\varphi'_V=\frac{-2a\,V_\infty\sqrt{\bar{m}}}{\pi\mathbf{M}_\infty}\int_{r_U}^{r_A}\sqrt{\frac{r-(s_A/m)}{r_A-r}}\,dr.$$

Keeping in mind that

$$r_U=s_A-(\mathbf{M}_\infty l/2),$$

the above expression, after integration, results in

$$\varphi'_V=\frac{2aV_\infty\sqrt{\bar{m}}}{\pi\mathbf{M}_\infty}\left[\sqrt{\left(r_A-s_A+\frac{\mathbf{M}_\infty l}{2}\right)\left(s_A-\frac{\mathbf{M}_\infty l}{2}-\frac{s_A}{m}\right)}\right.$$

$$\left.+\frac{r_A m-s_A}{m}\tan^{-1}\sqrt{\frac{r_A-s_A+(\mathbf{M}_\infty l/2)}{s_A-(\mathbf{M}_\infty l/2)-s_A/m}}\right]. \quad (8.10.25)$$

Going back to the usual coordinates x and y and taking into account the values of $m=(n-1)/(n+1)$, $\bar{m}=-m$, we have

$$\varphi'_V=\frac{2aV_\infty\sqrt{1-n}}{\mathbf{M}_\infty\pi\sqrt{n+1}}\left\{\mathbf{M}_\infty\sqrt{\left(z_A-\frac{l}{2}\right)\left[(x_A+a'z_A)\frac{1}{a'(n-1)}+\frac{l}{2}\right]}\right.$$

$$\left.-\frac{\mathbf{M}_\infty(x_A+z_A\tan\kappa)}{a'(n-1)}\tan^{-1}\sqrt{\frac{z_A-\frac{l}{2}}{\frac{x_A+a'z_A}{a'(n-1)}+\frac{l}{2}}}\right\}. \qquad (8.10.25')$$

Differentiating with respect to x_A and using the definition of pressure coefficient, we get

$$\bar{p}_V=\mp\frac{2}{V_\infty}\cdot\frac{\partial\varphi'_V}{\partial x_A}=\frac{\pm 4a}{\pi a'\sqrt{1-n^2}}\tan^{-1}\sqrt{\frac{a'\left(z_A-\frac{l}{2}\right)(n-1)}{x_A+a'z_A+\frac{l}{2}(n-1)a'}}\cdot \qquad (8.10.26)$$

The velocity potential in region VI can be determined in the following way (Fig. 8.10.1, e):

$$\varphi'_{VI}=\frac{-aV_\infty}{\pi\mathbf{M}_\infty}\iint\limits_{S_1+S_2}\frac{drds}{\sqrt{(r_A-r)(s_A-s)}}=\frac{-aV_\infty}{\pi\mathbf{M}_\infty}\int\limits_{r_{B'_1}}^{r_A}\frac{dr}{\sqrt{r_A-r}}$$

$$\times\int\limits_{s_{E_1}}^{s_A}\frac{ds}{\sqrt{s_A-s}}-\frac{aV_\infty}{\pi\mathbf{M}_\infty}\int\limits_{r_{B_1}}^{r_{B'_1}}\frac{dr}{\sqrt{r_A-r}}\int\limits_{s_{E''_1}}^{s_A}\frac{ds}{\sqrt{s_A-s}}. \qquad (8.10.27)$$

According to (8.9.4) and (8.9.7) the limits of the integrals in expression (8.10.27) will be

$$\left.\begin{aligned}&s_{E''_1}=mr,\ s_{E_1}=r_{E_1}-\frac{\mathbf{M}_\infty l}{2}=r_A-\frac{\mathbf{M}_\infty l}{2};\\&r_{B'_1}=r_{E'_1}=\frac{s_{E'_1}}{m}=\frac{s_{E_1}}{m}=\frac{1}{m}\left(r_A-\frac{\mathbf{M}_\infty l}{2}\right);\\&r_{B_1}=s_A-\frac{\mathbf{M}_\infty l}{2}.\end{aligned}\right\} \qquad (8.10.28)$$

Integration of (8.10.27) will then give the relation for φ_{VI} in terms of the variables r_A, s_A. Knowing their relation with x_A and z_A, this velocity potential can be obtained as a function of these coordinates. Calculation of the derivative $\partial\varphi'_{VI}/\partial x_A$ and its substitution in the formula $\bar{p}^*_{VI}=\mp 2\,(\partial\varphi'_{VI}/\partial x_A)/V_\infty$

*$\bar{p}_{VI}$ was printed as $\bar{p}$ in Russian text. This has been corrected here—Translator.

give the following expression for the coefficient of pressure in the region we are considering:

$$\bar{p}_{VI}=\frac{\pm 4a}{\pi a'\sqrt{1-n^2}}\left[\tan^{-1}\sqrt{\frac{a'(n-1)\left(z_A-\frac{l}{2}\right)}{x_A+a'z_A+\frac{l}{2}(n-1)a'}}\right.$$
$$\left.-\tan^{-1}\sqrt{\frac{(x_A-a'z_A)-\frac{l}{2}a'(n+1)}{a'(l/2+z_A)(n+1)}}\right]. \tag{8.10.29}$$

Similarly, for point A situated in region VII (Fig. 8.10.1, f) we have

$$\varphi'_{VII}=\frac{-aV_\infty}{\pi\mathbf{M}_\infty}\iint\limits_{s_1+s_2+s_3}\frac{drds}{\sqrt{(r_A-r)(s_A-s)}}$$
$$=\frac{-aV_\infty}{\pi\mathbf{M}_\infty}\int\limits_{r_{J'}}^{r_A}\frac{dr}{\sqrt{r_A-r}}\int\limits_{s_V}^{s_A}\frac{ds}{\sqrt{s_A-s}}$$
$$-\frac{aV_\infty}{\pi\mathbf{M}_\infty}\int\limits_{0}^{r_{J'}}\frac{dr}{\sqrt{r_A-r}}\int\limits_{s_{V''}}^{s_A}\frac{ds}{\sqrt{s_A-s}}$$
$$-\frac{aV_\infty}{\pi\mathbf{M}_\infty}\int\limits_{r_W}^{0}\frac{dr}{\sqrt{r_A-r}}\int\limits_{s_{W''}}^{s_A}\frac{ds}{\sqrt{s_A-s}}, \tag{8.10.30}$$

where

$$\left.\begin{aligned}&s_V=r_A-\frac{\mathbf{M}_\infty l}{2},\ r_{J'}=\frac{1}{m}\left(r_A-\frac{\mathbf{M}_\infty l}{2}\right);\\&s_{V''}=mr,\ s_{W''}=\frac{r}{m},\ r_W=s_A-\frac{\mathbf{M}_\infty l}{2}.\end{aligned}\right\} \tag{8.10.31}$$

The pressure coefficient corresponds to the potential (8.10.30) calculated according to the limits of integration in (8.10.31):

$$\bar{p}_{VII}=\frac{\pm 4a}{\pi a'\sqrt{1-n^2}}\left[\tan^{-1}\sqrt{\frac{1+n}{1-n}}\sqrt{\frac{x_A-a'z_A}{x_A+a'z_A}}\right.$$
$$-\tan^{-1}\sqrt{\frac{a'(l/2-z_A)(n+1)}{x_A+a'z_A-(l/2)a'(n+1)}}+\tan^{-1}\sqrt{\frac{(x_A+a'z_A)-(l/2)a'(n+1)}{a'(l/2+z_A)(n+1)}}$$
$$\left.-\tan^{-1}\sqrt{\frac{1-n}{n+1}}\sqrt{\frac{x_A-a'z_A}{x_A+a'z_A}}\right]. \tag{8.10.32}$$

Finally, let us consider region *VIII* (Fig. 8.10.1, g). For the points in this region the range of integration intersects with the regions Ω_1 and Ω_2 simultaneously: In these regions there appear disturbances arising due to flow-interaction of both side edges *DE* and *GH*. To find the velocity potential at a given point *A* in region *VIII* it is sufficient to extend the integration in the formula (8.10.1) to the region $S=S_1+S_2$, shown shaded in Fig. 8.10.1, g. Here, the integral calculated over the region S_2 in formula (8.10.1) should be taken with the opposite sign, i.e. with the plus sign. Then

$$\varphi'_{VIII}=\frac{-aV_\infty}{\pi \mathbf{M}_\infty}\iint\limits_{S_1}\frac{drds}{\sqrt{(r_A-r)(s_A-s)}}+\frac{aV_\infty}{\pi \mathbf{M}_\infty}\iint\limits_{S_2}\frac{drds}{\sqrt{(r_A-r)(s_A-s)}}\cdot \tag{8.10.33}$$

Here

$$\iint\limits_{S_1}\frac{drds}{\sqrt{(r_A-r)(s_A-s)}}=\int\limits_{r_{H_1}}^{r_A}\frac{dr}{\sqrt{r_A-r}}\int\limits_{s_{F_1}}^{s_A}\frac{ds}{\sqrt{s_A-s}}; \tag{8.10.34}$$

$$\iint\limits_{S_2}\frac{drds}{\sqrt{(r_A-r)(s_A-s)}}=\iint\limits_{\sigma_1}\frac{drds}{\sqrt{(r_A-r)(s_A-s)}}+\iint\limits_{\sigma_2}\frac{drds}{\sqrt{(r_A-r)(s_A-s)}}$$

$$+\iint\limits_{\sigma_3}\frac{drds}{\sqrt{(r_A-r)(s_A-s)}}=\int\limits_{0}^{r_{F_1}'}\frac{dr}{\sqrt{(r_A-r)}}\int\limits_{s_{L_1}}^{s_{F_1}'}\frac{ds}{\sqrt{s_A-s}}$$

$$+\int\limits_{r_{F_1}''}^{0}\frac{dr}{\sqrt{r_A-r}}\int\limits_{s_{K_1}}^{s_{F_1}'}\frac{ds}{\sqrt{s_A-s}}\cdot \tag{8.10.35}$$

The limits of the above integrals have the following values:

$$\left.\begin{gathered} r_{F_1}'=r_{H_1}=s_A-\frac{\mathbf{M}_\infty l}{2},\quad s_{L_1}=mr; \\ s_{F_1}'=s_{F_1}=r_A-\frac{\mathbf{M}_\infty l}{2},\quad r_{F_1}''=ms_{F_1}''=ms_{F_1}=m\left(r_A-\frac{\mathbf{M}_\infty l}{2}\right); \\ s_{K_1}=r/m, \end{gathered}\right\} \tag{8.10.36}$$

under the condition that

$$s_{F_1}=r_A-\frac{\mathbf{M}_\infty l}{2},\quad r_{H_1}=s_A-\frac{\mathbf{M}_\infty l}{2}\cdot \tag{8.10.36'}$$

The integrals in (8.10.34) and (8.10.35) are calculated taking into account the above values of the limits of integration and then the velocity potential

(8.10.33) can be found. The coefficient of pressure corresponding to this potential will be:

$$\bar{p}_{VIII}=\frac{\mp 4a}{a'\pi\sqrt{1-n^2}}\left[\tan^{-1}\sqrt{\frac{1+n}{1-n}}\sqrt{\frac{(x_A-a'z_A)+(l/2)\,a'\,(n-1)}{a'\,(l/2+z_A)\,(n+1)}}\right.$$
$$-\tan^{-1}\sqrt{\frac{1+n}{1-n}}\sqrt{\frac{x_A-a'z_A}{x_A+a'z_A}}+\tan^{-1}\sqrt{\frac{1-n}{1+n}}\sqrt{\frac{x_A-a'z_A}{x_A+a'z_A}}$$
$$\left.-\tan^{-1}\sqrt{\frac{1-n}{1+n}}\sqrt{\frac{a'\,(l/2-z_A)\,(n+1)}{x_A+a'z_A+(l/2)\,a'\,(n-1)}}\right]. \qquad (8.10.37)$$

A typical distribution of the quantity $\Delta\bar{p}/a=(\bar{p}_l-\bar{p}_u)/a$, near the side edge, as a function of the distance from the leading edge (as a percentage of the chord) calculated from the formulas for a six-cornered wing (see Section 9) with straight trailing edge (i.e. for a wing with a five-cornered plan) at $M_\infty=1.61$ is shown in Fig. 8.10.2. The coefficient $\Delta\bar{p}/a$ is constant in the region between the leading edge and the Mach cones starting from the apex and the wing tips over the section bounded by the side edge, the trailing edge and the Mach wave reflected from the side edge. We find a discontinuity in the curve characterizing the variation in the coefficient of pressure ratio on the Mach lines. This results from the discontinuity in the contour of the edge of the wing.

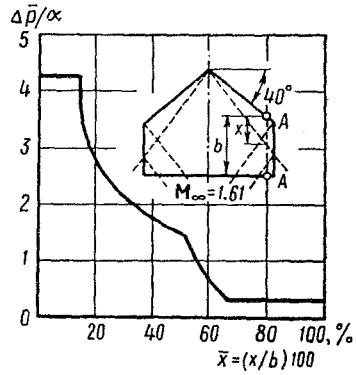

Fig. 8.10.2. Distribution of quantity $\Delta\bar{p}/a=(\bar{p}_l-\bar{p}_u)/a$ near side edge of five-cornered wing (section AA).

The coefficients of lift and moment can be found from the distribution of pressure obtained together with formulas (8.9.29), (8.9.30).

Effect of vortex sheet behind wing: If the wing has a subsonic trailing edge the vortex sheet behind it will have an effect on the flow-interaction of the part of the wing surface lying within the limits of the Mach lines emerging from points E and H (Fig. 8.10.3).

Let us take a point $M(x, O, z)$ on this part of the wing surface and study the solution of the problem of determining a potential function therein in a general form. Using the relation (8.2.16) this function can be represented in the following way:

$$\varphi'(x_A, O, z_A)=-\frac{1}{2\pi}\iint\limits_{S_1}\frac{Q_1(\xi,\zeta)\,d\xi d\zeta}{\sqrt{(x_A-\xi)^2-(z_A-\zeta)^2}}$$
$$-\frac{1}{2\pi}\iint\limits_{S_2}\frac{Q_1(\xi,\zeta)\,d\xi d\zeta}{\sqrt{(x_A-\xi)^2-(z_A-\zeta)^2}}-\frac{1}{2\pi}\iint\limits_{S3}\frac{Q_2(\xi,\zeta)\,d\xi d\zeta}{\sqrt{(x_A-\xi)^2-(z_A-\zeta)^2}}, \qquad (8.10.38)$$

where, according to Fig. 8.10.3,

$$S_1 = S_{ABCEP},\ S_2 = S_{LCT},\ S_3 = S_{PEJ}.$$

The strength of the sources Q_1 is determined by (8.2.17) and is equal to $Q_1 = 2aV_\infty$. The function Q_2, determining the strength of the sources over region PEJ, should be determined taking into account the effect of the vortex sheet. Let us derive the integral equation for determination of this function. To do this we take a point $N(x, O, z)$ and express the velocity potential at this point, by analogy with (8.10.38), in the following way:

$$\varphi' = -\frac{1}{2\pi}\iint\limits_{\Omega_1} \frac{Q_1(\xi, \zeta)\, d\xi d\zeta}{\sqrt{(x_N-\xi)^2-(z_N-\zeta)^2}} - \frac{1}{2\pi}\iint\limits_{\Omega_2} \frac{Q_2(\xi, \zeta)\, d\xi d\zeta}{\sqrt{(x_N-\xi)^2-(z_N-\zeta)^2}}. \quad (8.10.39)$$

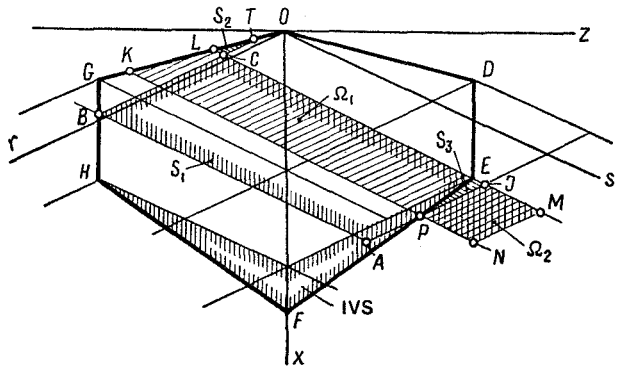

Fig. 8.10.3. Six-cornered wing with subsonic trailing edge.

Differentiate this expression with respect to x_N, i.e. in a direction parallel to the direction of an undisturbed flow. The velocity potential φ' beyond the wing in plane xOz, according to the boundary condition (8.1.19), remains constant along the given direction. Hence the quantity (8.10.39), if differentiated with respect to x_N, becomes zero:

$$0 = \frac{\partial}{\partial x_N}\iint\limits_{\Omega_1} \frac{Q_1(\xi, \zeta)\, d\xi d\zeta}{\sqrt{(x_N-\xi)^2-(z_N-\zeta)^2}} + \frac{\partial}{\partial x_N}\iint\limits_{\Omega_2} \frac{Q_2(\xi, \zeta)\, d\xi\, d\zeta}{\sqrt{(x_N-\xi)^2-(z_N-\zeta)^2}}. \quad (8.10.40)$$

Determining function Q_2 from this equation and using (8.10.39), it is possible to find the potential function for the points in the section of the wing surface situated in the zone of influence of a vortex sheet IVS. A detailed study of this problem has been made by Prof. E.A. Krasilshikova in the work [9].

11. Drag of Wings with Subsonic Leading Edges

Let us consider the calculation of the drag of swept wings with subsonic leading edges in a supersonic flow at a given angle of attack. As we said

above, a disturbed flow about such wings is subsonic by nature in the direction of the normal to the leading edge. This flow-interaction is accompanied by a gas flow from the region of higher pressure to the region of low pressure (from the lower side of a wing to the upper side or vice versa) and this results in a corresponding force-interaction on the wing. The results of analysis of the disturbed flow of an incompressible fluid around an airfoil in the form of a flat plate placed in a flow at some angle of attack (see Chapter 6 Section 3) can be used to determine this force-interaction.

11.1 Suction force

The coefficient of drag of a thin wing with subsonic leading edges in a supersonic flow is determined by the formula

$$c_x = ac_y - c_{xT}, \tag{8.11.1}$$

in which c_{xT} is the coefficient of suction force of a wing, which depends on the angle of the leading sweep κ and the Mach number $\mathbf{M}_\infty$; and

$$c_{xT} = T/q_\infty S_w, \tag{8.11.2}$$

where T is the suction force of the finite swept wing in question; $q_\infty = \rho_\infty V_\infty^2/2$ is the velocity head; S_w is the wing plan area:

$$S_w = (1/2)\, hl = (1/4) l^2 \tan \kappa.$$

The relations obtained in Chapter 7 Section 6 for a wing of finite aspect ratio can be used to determine force T. This follows from the fact that the suction force, according to (7.6.12) and (7.6.13), is determined by the variation in the axial component of velocity in the neighborhood of the leading edge of a given airfoil (wing section) and the local angle of sweep but does not depend on the condition of this velocity away from the leading edge.

Using (7.6.12) we can write

$$T = 2\pi\rho_\infty \sqrt{1+\tan^2\kappa - \mathbf{M}_\infty^2} \int_0^{l/2} c^2\, dz, \tag{8.11.3}$$

where coefficient c is determined from (7.6.13).

Let us find, as an example, the drag of a delta wing. To do this we use expression (8.8.42) for a perturbation velocity. Assuming the value of $\cot \kappa = z/x_{\text{L.E}}$ in this expression, we can write

$$u = \frac{a V_\infty (z/x_{\text{L.E}})}{E(k) \sqrt{1-(x_{\text{L.E}}/x)^2}},$$

where $x_{\text{L.E}}$ is the distance from the leading edge; z, x are coordinates of a point on the wing (Fig. 8.11.1). Inserting the value of u^2 in (7.6.13) and recalling that $\lim_{x \to x_{\text{L.E}}} x/x_{\text{E.L}} = 1$, we get

$$c^2=\left[\frac{aV_\infty}{E(k)}\right]^2\lim_{x\to x_{L.E}}\frac{z^2(x/x_{L.E})^2(x-x_{L.E})}{(x-x_{L.E})(x+x_{L.E})}=\frac{1}{2}\left[\frac{aV_\infty}{E(k)}\right]^2$$

$$\times\frac{z^2}{x_{L.E}}=\frac{1}{2}\left[\frac{aV_\infty}{E(k)}\right]^2 z\cot\kappa.$$

Substituting this expression in (7.6.12) and integrating, we have

$$T=\frac{\pi\rho_\infty\cot\kappa}{2}\left[\frac{aV_\infty}{E(k)}\right]^2 2\sqrt{1+\tan^2\kappa-\mathbf{M}_\infty^2}\int_0^{l/2}zdz$$

$$=\frac{\pi\rho_\infty\cot\kappa}{2}\left[\frac{aV_\infty}{E(k)}\right]^2\frac{l^2}{4}\sqrt{1+\tan^2\kappa-\mathbf{M}_\infty^2}.$$

The coefficient of suction force, according to (8.11.2), will then be

$$c_{xT}=\left[\frac{a\cot\kappa}{E(k)}\right]^2\pi\sqrt{1+\tan^2\kappa-\mathbf{M}_\infty^2}. \qquad (8.11.4)$$

Taking expression (8.8.44) for a c_y into consideration, we get

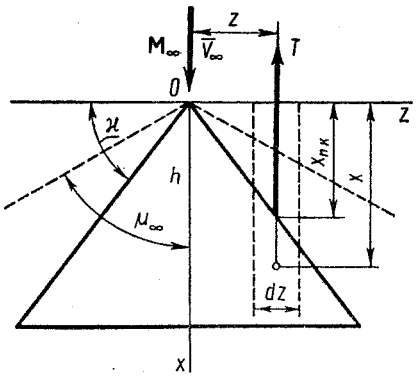

Fig. 8.11.1. Suction force of delta wing with subsonic leading edges.

$$c_{xT}=\frac{c_y^2}{4\pi}\sqrt{1+\tan^2\kappa-\mathbf{M}_\infty^2}. \qquad (8.11.4')$$

For a supersonic leading edge ($\mathbf{M}_\infty\cos\kappa>1$) and also in a case where the leading edge is sonic ($\tan\kappa=\cot\mu_\infty=\sqrt{\mathbf{M}_\infty^2-1}$) the coefficient of a suction force is equal to zero. But in the case of a subsonic edge ($\mathbf{M}_\infty\cos\kappa<1$) the quantity $c_{xT}\neq0$: its actual value, shown by experiment, is less than the calculated one. This is quite significant at high angles of attack or large sweep, at which local separation takes place around the leading edge and no further growth of suction is observed.

11.2 Induced drag

Let us consider the total drag of a wing. According to (8.11.1), (8.1.4') and (8.8.44) this can be represented in the following form:

$$c_x=ac_y-c_{xT}=\frac{E(k)}{2\pi\cot\kappa}c_y^2-\frac{c_y^2}{4\pi}\sqrt{1+\tan^2\kappa-\mathbf{M}_\infty^2}$$

$$=\frac{c_y^2}{4\pi\cot\kappa}\left[2E(k)-\sqrt{1-\cot^2\kappa(\mathbf{M}_\infty^2-1)}\right].$$

Keeping in mind that the aspect ratio of the wing

$$\lambda_w = l^2/S_w = 4 \cot \kappa, \tag{8.11.5}$$

we have

$$c_x = \frac{c_y^2}{\pi \lambda_w}\left[2E \text{ thin } (k) - \sqrt{1-\cot^2 \kappa\,(\mathbf{M}_\infty^2 - 1)}\right]. \tag{8.11.6}$$

Let us consider the case of a sonic velocity of flow-interaction. If $\mathbf{M}_\infty \to 1$, $E(k) \to 1$ and hence the drag coefficient is

$$c_x = c_y^2/\pi\lambda_w. \tag{8.11.7}$$

It follows from this expression that the drag of the wing decreases with an increase in λ_w while maintaining the condition of subsonic flow-interaction of the leading edge. In the limit where $\lambda_w \to \infty$ the drag tends to zero. This brings us to the well-known Euler-d'Alembert paradox to the effect that there is no drag for an infinite-aspect ratio wing in an ideal gas flow. From this it follows that the appearance of drag depends on the wing having a finite span.

Expression (8.11.7) coincides with formula (6.4.19) for the coefficient of induced vortex drag of a finite-span wing (see Chapter 6 Section 4). So the physical nature of the drag force appearing during the flow-interaction of a delta wing with subsonic leading edges is based on the induced effects of vortices felt behind this wing. Accordingly the quantity determined by (8.11.6) is known as the coefficient of induced drag.

If the leading edge is sonic ($\tan \kappa = \sqrt{\mathbf{M}_\infty^2 - 1}$) the second term in the square brackets of (8.11.6) is equal to unity and $E(k) = E(0) = \pi/2$. Hence the coefficient of induced drag will be

$$c_x = c_{xi} = c_y^2/\lambda_w. \tag{8.11.8}$$

For a very narrow wing ($\kappa \to \pi/2$) we may assume $\cot \kappa \approx 0$ and $E(k) \approx E(1) = 1$. In this case expression (8.11.6) coincides with (8.11.7).

12. Aerodynamic Characteristics of a Wing of Rectangular Plan

The supersonic flow-interaction of a thin wing of finite aspect ratio and rectangular plan at a small angle of attack is characterized by the effect of a leading supersonic edge and side subsonic edge on the disturbed flow about the surface. Here the simultaneous effects of the leading edge and one of the side edges operate within the limit of the Mach cones with their apexes at the corners O and O' of the wing (Fig 8.12.1, a) if the generators of these cones intersect each other beyond the wing. If the intersection of these generators takes place on the wing surface (Fig. 8.12.1, b) there then arises zone *III* where both side edges influence the disturbed flow simultaneously. This is apart from regions *II* and *II'* where the effect of one side edge is experienced.

The disturbed flow on the wing in region *I*, situated between the leading edge and the Mach cones, is set up solely by the leading edge. Here the pressure coefficient is determined by the formula for a flat plate

$$\bar{p}_I = \pm 2\alpha/\sqrt{\mathbf{M}_\infty^2 - 1}. \tag{8.12.1}$$

The method of sources can be used to analyze the disturbed flow in region *II* (see Fig. 8.12.1, a). The velocity at a point *A* lying in this region is induced by the sources distributed over wing section *ACOE*. Meantime the resultant influence of sources *BCO* and *OBD* at point *A* is equal to zero and hence it is necessary to carry out integration in (8.10.1) over the region *ABDE*. Accordingly the velocity potential at point *A* will be

$$\varphi_{II} = \frac{-aV_\infty}{\pi \mathbf{M}_\infty} \iint\limits_{ABDE} \frac{dr\,ds}{\sqrt{(r_A - r)(s_A - s)}} = \frac{-aV_\infty}{\pi \mathbf{M}_\infty} \int_{s_B}^{s_A} \frac{ds}{\sqrt{s_A - s}} \int_{r_F}^{r_A} \frac{dr}{\sqrt{r_A - r}}. \tag{8.12.2}$$

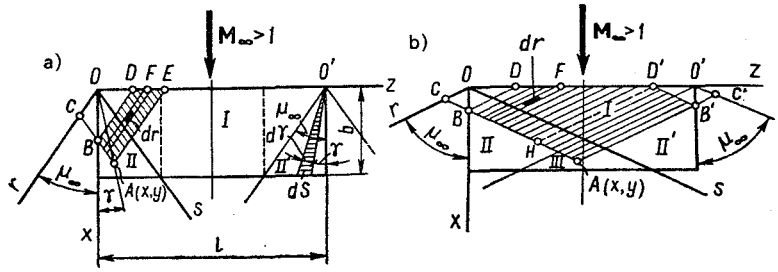

Fig. 8.12.1. Rectangular wing in linearized supersonic flow.

Point *F* lies on the leading edge, satisfying the equation $x=0$. Therefore according to (8.9.4″) we have for this edge

$$r = -(\mathbf{M}_\infty/2)\, z, \quad s = (\mathbf{M}_\infty/2)\, z. \tag{8.12.3}$$

Hence the equation of the leading edge in terms of the coordinates r, s will be

$$r = -s. \tag{8.12.4}$$

Therefore the coordinate of point *F* is

$$r_F = r = -s.$$

Point *B* lies on the side edge and satisfies the equation $z=0$. Therefore according to (8.9.4″), for this edge

$$r = (\mathbf{M}_\infty/2a')\, x, \quad s = (\mathbf{M}_\infty/2a')\, x. \tag{8.12.5}$$

Hence the equation of side edge in terms of the coordinates r, s will be

$$r=s. \tag{8.12.6}$$

The coordinate of point B will be

$$s_B=r_B=r_A.$$

Carrying out integration in (8.12.2), taking into account the values of the limits $r_F=-s$ and $s_B=r_A$, we get

$$\varphi'_{II}=\frac{-2aV_\infty}{\pi M_\infty}\left|-\sqrt{(r_A+s)(s_A-s)}-(s_A+r_A)\tan^{-1}\sqrt{\frac{s_A-s}{r_A+s}}\right|_{r_A}^{s_A}$$

$$=\frac{-2aV_\infty}{\pi M_\infty}\left[\sqrt{2r_A(s_A-r_A)}+(s_A+r_A)\tan^{-1}\sqrt{\frac{s_A-r_A}{2r_A}}\right]. \tag{8.12.7}$$

Inserting the values of r_A and s_A from (8.9.4') in this equation, we have

$$\varphi'_{II}=\frac{-2aV_\infty}{\pi}\left[\sqrt{\frac{z_A}{a'}(x_A-a'z_A)}+\frac{x_A}{a'}\tan^{-1}\sqrt{\frac{a'z_A}{x_A-a'z_A}}\right]. \tag{8.12.7'}$$

Let us find the pressure coefficient by applying the formula $\bar{p}=-(2/V_\infty)\,\partial\varphi'_{II}/\partial x_A$:

$$\bar{p}_{II}=\frac{\pm 4a}{\pi a'}\tan^{-1}\sqrt{\frac{a'z_A}{x_A-a'z_A}}. \tag{8.12.8}$$

On the boundary of two regions I and II separated by the Mach line the coefficient of pressure determined by formula (8.12.8) must be equal to the value of (8.12.1). In practice, since the equation of this boundary

$$z_A=x_A\tan\mu_\infty=x_A/a',$$

we have from (8.12.8)

$$\bar{p}_{II}=\frac{\pm 4a}{\pi a'}\cdot\frac{\pi}{2}=\bar{p}_I.$$

It follows from (8.12.8) that at the wing tips the pressure along the line $z/x=\text{const}$ remains unchanged. These lines can be taken as the generators of the conical surfaces and hence the flow on this region of the wing is treated as a conical flow.

Let us calculate the aerodynamic coefficients of the wing. The lift force, acting on an element dS of the end section of the wing, is equal to

$$dY=(\bar{p}_l-\bar{p}_u)(\rho_\infty V_\infty^2/2)\,dS. \tag{8.12.9}$$

It can be seen from Fig. 8.12.1, a that

$$dS=\frac{1}{2}\cdot\frac{b^2}{\cos^2\gamma}d\gamma, \tag{8.12.10}$$

where γ is the angle considered from the side edge.

Inserting the values of $\bar{p}_l$ and $-\bar{p}_u$ from (8.12.8) and the quantity dS from (8.12.10) in (8.12.9) and replacing z_A/x_A by $\tan\gamma$, we will have

$$dY=\frac{4ab^2}{\pi a'}\cdot\frac{\rho_\infty V_\infty^2}{2}\tan^{-1}\sqrt{\frac{a'\tan\gamma}{1-a'\tan\gamma}}\cdot\frac{d\gamma}{\cos^2\gamma}.$$

Dividing this expression by the product of the wing area $S_{II}=b^2/2a'$ enclosed in the Mach cone and the velocity head $q_\infty=\rho_\infty V_\infty^2/2$ and carrying out the integration, we get the coefficient of lift of the wing tips:

$$c_y''=\frac{Y}{S_{II}\,q_\infty}=\frac{8a}{\pi}\int_0^{\mu_\infty}\tan^{-1}\sqrt{\frac{a'\tan\gamma}{1-a'\tan\gamma}}\cdot\frac{d\gamma}{\cos^2\gamma}.$$

Integrating by parts, we get

$$c_y''=2a/a'=2a/\sqrt{\mathbf{M}_\infty^2-1}. \tag{8.12.11}$$

Let us find the lift coefficient c_{yII} of the end-sections of the wing with respect to the total wing area $S_w=lb$:

$$c_{yII}=c_y''\frac{S_{II}+S_{II}'}{S_w}=c_y''\frac{b^2}{lba'}=c_y''\frac{1}{\lambda_w a'}, \tag{8.12.11'}$$

where $\lambda_w=l/b$.

The coefficient of lift of section I of the wing taken with respect to the area S_I of this section will be

$$c_y'=4a/a'=4a/\sqrt{\mathbf{M}_\infty^2-1}. \tag{8.12.12}$$

Then the coefficient of lift of this section with respect to the total wing surface area is

$$c_{yI}=c_y'\frac{S_I}{S_w}=c_y'\frac{S_w-(S_{II}+S_{II}')}{S_w}=c_y'\left(1-\frac{1}{\lambda_w a'}\right). \tag{8.12.13}$$

The resultant coefficient of lift will then be given by

$$c_y=c_{yII}+c_{yI}=\frac{4a}{\sqrt{\mathbf{M}_\infty^2-1}}\left(1-\frac{1}{2\lambda_w\sqrt{\mathbf{M}_\infty^2-1}}\right). \tag{8.12.14}$$

The coefficient of wave drag

$$c_{xu}=ac_y=\frac{4a^2}{\sqrt{\mathbf{M}_\infty^2-1}}\left(1-\frac{1}{2\lambda_w\sqrt{\mathbf{M}_\infty^2-1}}\right). \tag{8.12.15}$$

The coefficient of moment about the z axis can be calculated from the available data on the distribution of pressure and the lift coefficients of various sections of the wing:

$$m_z=M_z/q_\infty S_w b. \tag{8.12.16}$$

Moment M_z due to the pressure forces distributed over the wing surface can be found as the sum of moments of the lift forces about the z axis that are acting on the different sections of the wing (Fig. 8.12.2). Since the point of exertion of lift force on the triangular sections of the wing coincides with the center of gravity of the area of the section, the value of M_z will be (sign of the moment is taken as positive for rotation of the wing from the x axis to the y axis):

$$M_z=\frac{b}{3}2Y_I^{(1)}+\frac{b}{2}Y_I^{(2)}+\frac{2b}{3}2Y_{II}, \tag{8.12.17}$$

where $Y_I^{(1)}$, $Y_I^{(2)}$ and Y_{II} are values of lift forces calculated for the areas of sections CDB (HFE), $EFCB$ and ADB (GHE) respectively. According to (8.12.11) and (8.12.12):

$$\left.\begin{aligned} Y_I^{(1)}&=c_y'\frac{\rho_\infty V_\infty^2}{2}S_{II}=\frac{4a}{a'}\cdot\frac{\rho_\infty V_\infty^2}{2}S_{II};\\ Y_I^{(2)}&=c_y'\frac{\rho_\infty V_\infty^2}{2}S_{EFCB}=\frac{4a}{a'}\cdot\frac{\rho_\infty V_\infty^2}{2}(S_w-4S_{II});\\ Y_{II}&=c_y''\frac{\rho_\infty V_\infty^2}{2}S_{II}=\frac{2a}{a'}\cdot\frac{\rho_\infty V_\infty^2}{2}S_{II}. \end{aligned}\right\} \tag{8.12.18}$$

Inserting (8.12.17) and (8.12.18) in (8.12.16) and keeping in mind the value of $S_{II}/S_w=1/(2\lambda_w a')$, we get

$$m_z=\frac{2a}{\sqrt{\mathbf{M}_\infty^2-1}}\left(1-\frac{2}{3\lambda_w\sqrt{\mathbf{M}_\infty^2-1}}\right). \tag{8.12.19}$$

The coefficient of the center of pressure

$$c_{c.p}=\frac{x_{c.p}}{b}=\frac{M_z}{b\bar{Y}}=\frac{m_z}{c_y}=\frac{(3\lambda_w\sqrt{\mathbf{M}_\infty^2-1}-2)}{3(2\lambda_w\sqrt{\mathbf{M}_\infty^2-1}-1)}. \tag{8.12.20}$$

If the number $\mathbf{M}_\infty$ of the flow over the wing shown in Fig. 8.12.1, a is reduced then at some value of this Mach number the tip Mach cones intersect on the wing. There then arises region *III* (see Fig. 8.12.1, b) in which the leading supersonic edge and both the side subsonic edges have an effect on the disturbed flow. The nature of the flow in regions *I* and *II* (*II'*) will be the same as in the corresponding regions *I* and *II* (*II'*) of the wing whose scheme is shown in Fig. 8.12.1, a.

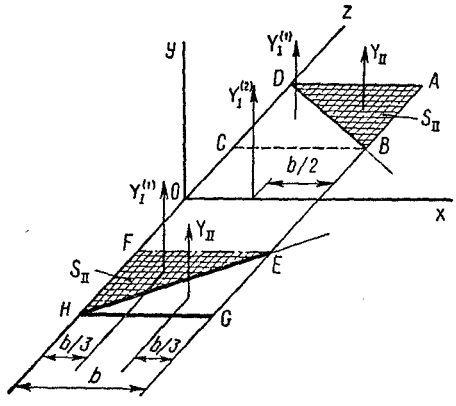

Fig. 8.12.2. Determination of aerodynamic moment of rectangular wing.

Let us consider the flow at a point A in region *III* (see Fig. 8.12.1, b). The region of effect of the sources on this flow coincides with the section of wing $ABDD'B'$. This section can be represented as the sum of areas $HBDD'$ and $AHD'B'$. Then the velocity potential at point A, according to (8.10.1), will be

$$\varphi'_{III}=\frac{-aV_\infty}{\pi \mathbf{M}_\infty}\left[\iint\limits_{HBDD'}\frac{drds}{\sqrt{(r_A-r)\,(s_A-s)}}+\iint\limits_{AHD'B'}\frac{drds}{\sqrt{(r_A-r)\,(r_A-s)}}\right].$$

The limits of integration can be determined directly from Fig. 8.12.1, b and the above potential can be written as:

$$\varphi'_{III}=\frac{-aV_\infty}{\pi \mathbf{M}_\infty}\left[\int\limits_{s_B}^{s_H}\frac{ds}{\sqrt{s_A-s}}\int\limits_{r_F}^{r_A}\frac{dr}{\sqrt{r_A-r}}+\int\limits_{s_H}^{s_A}\frac{ds}{\sqrt{s_A-s}}\int\limits_{r_{B'}}^{r_A}\frac{dr}{\sqrt{r_A-r}}\right].$$

The first two integrals are calculated in the same way as (8.12.7); the remaining two integrals are determined independent of each other because the region of integration represents a parallelogram (see Fig. 8.12.1, b). Taking this into account, we get

$$\varphi'_{III}=\frac{-2aV_\infty}{\pi \mathbf{M}_\infty}\left\{\left|-\sqrt{(r_A+s)\,(s_A-s)}-(s_A+r_A)\tan^{-1}\sqrt{\frac{s_A-s}{r_A+s}}\right|_{r_A}^{s_H}\right.$$

$$\left.+2\sqrt{(s_A-s_H)\,(r_A-r_B')}\right\}=\frac{-2aV_\infty}{\pi \mathbf{M}_\infty}\left\{-\sqrt{(r_A+s_H)\,(s_A-s_H)}\right.$$

$$+\sqrt{2r_A\,(s_A-r_A)}-(s_A+r_A)\left(\tan^{-1}\sqrt{\frac{s_A-s_H}{r_A+s_H}}\right.$$

$$\left.\left.-\tan^{-1}\sqrt{\frac{s_A-r_A}{2r_A}}\right)+2\sqrt{(s_A-r_H)\,(r_A-r_B')}\right\}. \qquad (8.12.21)$$

It can be seen from Fig. 8.12.1, b that the coordinate $s_H=s_D'$ and according to (8.12.4) the value of $s_D'=-r_D'$. Therefore $s_H=-r_D'=-r_B'$.

Point B' lies on the right side edge, satisfying the equation $z=l$. From (8.9.4′) it is possible to find the equation of this edge in terms of the coordinates r, s:

$$r-s=-\mathbf{M}_\infty l. \qquad (8.12.22)$$

Then for point B'

$$r_B'=s_B'-\mathbf{M}_\infty l=s_A-\mathbf{M}_\infty l. \qquad (8.12.23)$$

Accordingly the coordinate

$$s_H=-r_B'=-s_A+\mathbf{M}_\infty l. \qquad (8.12.24)$$

Substituting the coordinate r_A and s_A from (8.9.4′) and r_B' and s_H from (8.12.23) and (8.12.24) in (8.12.21), we get

$$\varphi'_{III}=\frac{-2aV_\infty}{\pi a'}\left\{\sqrt{[(x_A-a'z_A)-a'l]\,(l-z_A)\,a'}+\sqrt{a'z_A\,(x_A-a'z_A)}\right.$$
$$\left.-x_A\left[\tan^{-1}\sqrt{\frac{(x_A+a'z_A)-a'l}{(l-z_A)\,a'}}-\tan^{-1}\sqrt{\frac{a'z_A}{x_A-a'z_A}}\right]\right\}. \quad (8.12.25)$$

Applying the formula $\bar{p}=\mp(2/V_\infty)\,\partial\varphi'_{III}/\partial x_A$, we find the coefficient of pressure in the form

$$\bar{p}_{III}=\frac{\pm 4a}{\pi a'}\left[\tan^{-1}\sqrt{\frac{a'z_A}{x_A-a'z_A}}-\tan^{-1}\sqrt{\frac{(x_A+a'z_A)-a'l}{(l-z_A)\,a'}}\right]. \quad (8.12.26)$$

Let us express the second term in the square brackets in the form

$$\tan^{-1}\sqrt{\frac{(x_A+a'z_A)-a'l}{(l-z_A)\,a'}}=\frac{\pi}{2}-\tan^{-1}\sqrt{\frac{(l-z_A)\,a'}{(x_A+a'z_A)-a'l}}.$$

Then

$$\bar{p}_{III}=\frac{\pm 4a}{\pi a'}\tan^{-1}\sqrt{\frac{a'z_A}{x_A-a'z_A}}\pm\frac{4a}{\pi a'}\tan^{-1}\sqrt{\frac{(l-z_A)\,a'}{(x_A+a'z_A)-a'l}}\mp\frac{2a}{a'}. \quad (8.12.27)$$

The first and second terms in this expression represent the coefficients of pressure $\bar{p}_{II}$ and $\bar{p}_{II'}$ for the end sections of the wing respectively. The third term indicates the pressure coefficient $\bar{p}_I$ in region I where the effect of the side edges is not felt. So the pressure coefficient in region III can be expressed in the form

$$\bar{p}_{III}=\bar{p}_{II}+\bar{p}_{II'}-\bar{p}_I. \quad (8.12.28)$$

Expression (8.12.28) can be obtained from the following physical considerations: The coefficient of pressure at point A in region III changes under the influence of the left side edge with respect to coefficients $\bar{p}_I$ by the quantity $\Delta\bar{p}_{II}=\bar{p}_I-\bar{p}_{II}$. Similarly, under the influence of the right side edge it changes by the quantity $\Delta\bar{p}_{II'}=\bar{p}_I-\bar{p}_{II'}$. As a consequence of the simultaneous effects of both side edges the coefficient of pressure at a given point changes by the quantity $\Delta\bar{p}_{III}=\Delta\bar{p}_{II}+\Delta\bar{p}_{II'}$. Substituting the values of $\Delta\bar{p}_{II}$ and $\Delta\bar{p}_{II'}$ obtained and using the relation $\Delta\bar{p}_{III}=\bar{p}_I-\bar{p}_{III}$, we arrive at relation (8.12.28).

The coefficients of lift and moment are worked out from the known distribution of pressure with the help of formulas (8.9.29) and (8.9.30). The coefficient of drag of the wing in question is then worked out from the expression $c_x=ac_y$.

13. Method of Reversal

Let us consider one of the methods of aerodynamic investigation—the

method of reversal of flows. This method establishes the relations between the aerodynamic characteristics of two thin wings of the same plan placed in opposite postures.

It is assumed that one of these wings is placed in a flow to the right at an angle of attack a_1 and the other in a flow in the opposite direction at an angle a_2 (Fig. 8.13.1). According to the theory of linearized flow-interaction the pressure difference at any point on the surface is $p-p_\infty=-\rho_\infty V_\infty u$ and the resultant pressure between the lower and upper surfaces is

$$\Delta p=p_l-p_u=\rho_\infty V_\infty(u_u-u_l)=\rho_\infty V_\infty \Delta u. \tag{8.13.1}$$

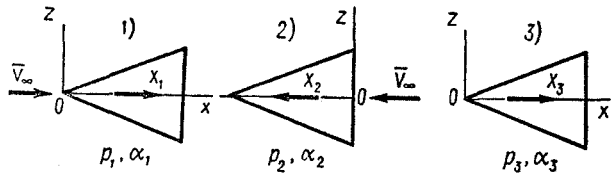

Fig. 8.13.1. System to define method of reversal:
1—normal flow; *2*—reverse flow; *3*—mixed flow.

The elementary value of the drag force due to pressure will be

$$dX=\Delta p a dS.$$

According to this expression the total drag force for wing *1* placed in a flow to the right will be

$$X_1=\iint\limits_{(S)}\Delta p_1 a_1 dS, \tag{8.13.2}$$

and for wing *2* placed in a flow to the left it will be

$$X_2=\iint\limits_{(S)}\Delta p_2 a_2 dS. \tag{8.13.3}$$

The values of the pressure difference Δp_1, Δp_2 and the local angles of attack a_1, a_2 are measured at one and the same point.

We will not consider suction force, which may arise at the subsonic leading edge but does not alter the results of the above calculations. As the flows around these wings are small-perturbation flows the superposition of one upon the other yields some new flow with parameters satisfying the linearized equation for velocity potential. Let us carry out superposition of the flows in such a way that the undisturbed flows cancel each other. Then the new wing *3* (see Fig. 8.13.1) will coincide with the picture of wings *1* and *2* with superposed flows but the camber of the surface will be different.

This camber is determined by local angle of attack α_3 which is equal to the sum of the angles of attack:

$$\alpha_3 = v_3/V_\infty = (v_1/V_\infty) + (v_2/V_\infty) = \alpha_1 + \alpha_2. \tag{8.13.4}$$

According to (8.13.4) the vertical components at the corresponding points of the surface are added. The horizontal components of velocity will be cancelled out by superposition so that for wing *3* we get

$$\Delta u_3 = \Delta u_1 - \Delta u_2.$$

Then the differential pressure between the lower and upper sides of this wing will be

$$\Delta p_3 = \rho_\infty V_\infty \Delta u_3 = \rho_\infty V_\infty (\Delta u_1 - \Delta u_2)$$

or according to (8.13.1)

$$\Delta p_3 = \Delta p_1 - \Delta p_2. \tag{8.13.5}$$

The drag force of wing *3* will be

$$X_3 = \iint_{(S)} (\Delta p_1 - \Delta p_2)(\alpha_1 + \alpha_2)\, dS. \tag{8.13.6}$$

The existence of a drag force for the wing in question is related to the appearance of a perturbation flow behind it representing an infinitely long vortex sheet moving away from the trailing edge. From the physical considerations it must be clear that there is a close relation between the disturbed condition of flow behind the wing and the drag force. Specifically force X_1 and the disturbed flow condition behind wing *1* and force X_2 and the disturbed flow condition behind wing *2* stand in a direct relation.

If we take wing *3* the flow past it obtained as a result of superposition of the flows past wings *1* and *2* will have the property that ahead of it the disturbances will be the same as for wing *2* and behind it the same as for wing *1*. In other words the drag force of wing *3* is equal to the difference between the drag forces of wings *1* and *2*, i.e.

$$X_3 = X_1 - X_2 = \iint_{(S)} (\Delta p_1 \alpha_1 - \Delta p_2 \alpha_2)\, dS. \tag{8.13.7}$$

Equating the right sides of (8.13.6) and (8.13.7), we get

$$\iint_{(S)} \Delta p_1 \alpha_2 dS = \iint_{(S)} \Delta p_2 \alpha_1 dS. \tag{8.13.8}$$

This relation represents the basic equation of the method of reversal of flows.

Coming to the coefficients of pressure in (8.13.8), we can write this relation in the form

$$\iint_{(S)} \Delta\bar{p}_1 a_2 dS = \iint_{(S)} \Delta\bar{p}_2 a_1 dS, \tag{8.13.8'}$$

where the coefficients of pressure differential are

$$\Delta\bar{p}_1 = \bar{p}_{1l} - \bar{p}_{1u};$$
$$\Delta\bar{p}_2 = \bar{p}_{2l} - \bar{p}_{2u}.$$

Using the right of arbitrary choice of angles of attack we take the values a_1 and a_2 as constant for all points of the surface of the wings and assume that they are identical, i.e. we will consider that $a_1 = a_2 = a$. Then from (8.13.8') we find that

$$\iint_{(S)} \Delta\bar{p}_1 \, dS = \iint_{(S)} \Delta\bar{p}_2 \, dS$$

or

$$Y_1 = Y_2.$$

So the method of reversal of flows says that the lift force of a flat plate in a flow to the right (Y_1) and the reverse flow (Y_2) will be identical during flow-interaction if the angles of attack and the velocities of undisturbed flow are the same.

Experiments show that the basic relation (8.13.8) of the method of reversal can be used for study of the aerodynamic characteristics not only of isolated wings but also of flight vehicles which in themselves represent "thin" combinations of wing with other structural elements like fuselage (body of revolution), tail and control surfaces (see Chapter 11).

9

CONE IN A SUPERSONIC FLOW

1. System of Equations of Axisymmetrical Flow-Interaction of Sharp-Nosed Cone

The problem of the flow-interaction of a sharp-nosed cone is very important for aerodynamics. The solution is of great practical value in that it helps in working out the aerodynamic characteristics of flight vehicles and their elements of conical shape. Besides this it can be used for study of a supersonic flow past sharp-nosed rotating bodies. For example, it gives the initial point on a curve for distribution of the parameters of the flow-interaction of a sharp-nosed curvilinear body. In addition, the results of the symmetrical flow-interaction of cones are applied in the approximate calculation of the distribution of flow parameters over the peripheral surface of rotating bodies (method of "local cones"). The same results are used for comparison in the investigation of the aerodynamic properties of blunt-nosed cones.

Along with the exact solutions a series of approximate solutions facilitating a simplified analysis of the flow-interaction of a cone is worked out in theoretical aerodynamics. Some of these solutions deal with slender cones interacting with a linearized flow or with a flow at a very large Mach number **M**. The exact solution may, in general, be applicable to cones of arbitrary thickness and the flows interacting with them may have any velocity. The basic condition to be satisfied is connected with observing the conical flow past the body in the flow. This kind of flow has parameters that remain constant along the lines emerging from the apex of the body in an inviscid flow. However, the results so obtained are also applied in studying viscous flow-interactions. "Inviscid" parameters like pressure, velocity, density are regarded as the parameters at the external limit of the boundary layer formed over the cone and hence they are the factors that determine frictional stress and heat flows from the gas to the wall.

Let us take a cone with semi-angle β_K at its apex in an axisymmetrical supersonic flow. The main problem is to work out the gas flow between this

cone and the shock appearing in front of it, which also takes the form of a conical surface. Here it is necessary to determine the angle of inclination θ_c of the linear generator of a conical shock (Fig. 9.1.1). For this purpose we examine the system of equations in the spherical coordinates θ and r applicable to the case of flow-interaction where the gas behind a shock undergoes physico-chemical changes under the effect of high temperatures. We will assume here that thermodynamic equilibrium is established in the disturbed region of flow.

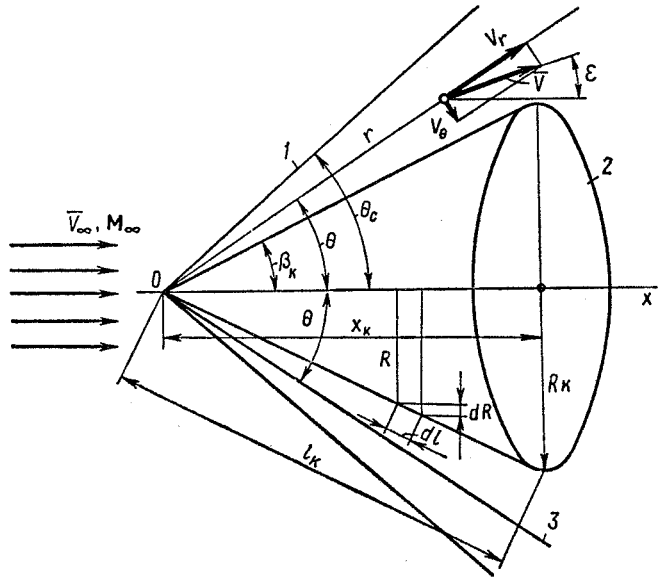

Fig. 9.1.1. Velocity components on conical surface:
1—compression shock; *2*—cone in flow: *3*—conical surface.

The solution to be obtained for a cone must correspond to the axisymmetrical conical field of a disturbed flow in which the gas parameters are constant along the lines emerging from the nose that constitute the generators of the interspace conical surfaces including the conical surfaces with angles $\theta=\theta_c$ and $\theta=\beta_K$.

On the basis of this property of the solution sought, any partial derivative of the gas parameters with respect to the spherical coordinate r (see Fig. 9.1.1) is equal to zero. Then the equation of continuity (2.4.37), in which the partial derivatives with respect to the spherical coordinate r and also those with respect to ψ (two-dimensional flow) should be equal to zero, will have the form

$$2\rho V_r + V_\theta \frac{d\rho}{d\theta} + \rho \frac{dV_\theta}{d\theta} + \rho V_\theta \cot\theta = 0. \qquad (9.1.1)$$

The equations of axisymmetrical motion about a cone obtained from the system (3.1.45), with viscous terms and partial derivatives with respect to t and r assumed to be zero, are written:

$$dV_r/d\theta = V_\theta; \tag{9.1.2}$$

$$\rho V_\theta \frac{dV_\theta}{d\theta} + \rho V_r V_\theta + \frac{dp}{d\theta} = 0. \tag{9.1.3}$$

According to the number of parameters to be obtained it is necessary to add the following equation to these equations:

$$\frac{p}{p_c} = \frac{(\mu_{av})_c}{\mu_{av}} \cdot \frac{\rho}{\rho_c} \cdot \frac{T}{T_c}, \tag{9.1.4}$$

which is obtained from the equation of state (1.4.8) for a gas at an arbitrary point in the flow and from the equation of state $p_c = \rho_c T_c R_0/(\mu_{av})_0$ related to the conditions immediately behind the shock wave (index "c"). The energy equation (3.4.14) and the general relations of the type (4.2.8) through (4.2.11) for the calculation of enthalpy, entropy, average molecular weight and sound velocity

$$i + (V^2/2) = i_c + (V_c^2/2); \tag{9.1.5}$$

$$i = f_1(p, T); \tag{9.1.6}$$

$$S = f_2(p, T); \tag{9.1.7}$$

$$\mu_{av} = f_3(p, T); \tag{9.1.8}$$

$$a = f_4(p, T) \tag{9.1.9}$$

must be included in the system in question. In this form the system can be used to study the flow-interaction of a cone in a dissociating gas. The system is simplified in the absence of dissociation. If it is assumed that the specific heats and average molecular weight of a gas in a disturbed region between the shock and the surface of the cone remain the same as those in an undisturbed part of the flow, the sound velocity and enthalpy will then depend only on temperature. Then instead of equations (9.1.6) through (9.1.9) we will have to use the relations (4.3.1) through (4.3.4). These can be represented in the following form:

$$i = c_p T = \frac{c_p p}{R\rho} = \frac{k}{k-1} \cdot \frac{p}{\rho}; \tag{9.1.10}$$

$$S = c_v \ln \frac{T}{\rho^{k-1}} + C_1 = c_v \ln \frac{p}{\rho^k} + C_2; \tag{9.1.11}$$

$$\mu_{av} = \text{const}; \tag{9.1.12}$$

$$a^2 = kRT = kp/\rho. \tag{9.1.13}$$

Equations (9.1.1) through (9.1.3) remain unchanged.

2. Flow-Interaction of Cone at Constant Specific Heats

The results obtained for the flow-interaction of a cone at constant heat coefficients have great practical value. They can be used for an approximate evaluation of some flow parameters (for example, pressure) when the flow-interaction is accompanied by a considerable amount of heat productive of physico-chemical changes and consequent changes in specific heats.

Equations (9.1.1) through (9.1.3) and (9.1.10) through (9.1.13) can be used for the solution of this problem. Equation (9.1.3) will come in handy if some changes are made in it. For this purpose we use the expression of the speed of sound $a^2=dp/d\rho$, written in the form

$$\frac{dp}{d\theta}=a^2\frac{d\rho}{d\theta}. \tag{9.2.1}$$

Substitution of the value of $dp/d\theta$ from (9.2.1) in equation (9.1.3) leads to

$$\rho V_\theta\frac{dV_\theta}{d\theta}+\rho V_r V_\theta+a^2\frac{d\rho}{d\theta}=0.$$

Inserting here the value of the derivative $d\rho/d\theta$ obtained from the equation (9.1.1) and rearranging terms, we get

$$\frac{dV_\theta}{d\theta}=\left[-V_\theta\cot\theta+V_r\left(\frac{V_\theta^2}{a^2}-2\right)\right]\left(1-\frac{V_\theta^2}{a^2}\right)^{-2}. \tag{9.2.2}$$

The square of sound velocity in this equation, according to (3.6.21), is equal to

$$a^2=\frac{k+1}{2}a^{*2}-\frac{k-1}{2}(V_r^2+V_\theta^2). \tag{9.2.3}$$

Examining the system of equations (9.1.2), (9.2.2), (9.2.3), we find that the problem of the flow-interaction of a cone is reduced to the kinematic problem connected with determination of the velocity field in a disturbed flow around a cone, i.e. with the determination of functions $V_r(\theta)$ and $V_\theta(\theta)$ as the components of velocity or function $V(\theta)=\sqrt{V_r^2+V_\theta^2}$ for the total velocity. From the calculated total velocity it is possible to determine pressure, density, temperature, enthalpy and entropy of the gas with the help of (9.1.4), (9.1.5), (9.1.10), (9.1.11). The relations (3.6.26), (3.6.31), (3.6.33) can be used to find pressure, density and temperature respectively in place of the above formulas.

The boundary conditions on the basis of which we integrate differential equations (9.1.2.) and (9.2.2) are determined from the conditions of gas flow past a cone and from the conditions characterizing the gas parameters immediately behind the shock.

The boundary condition of the flow-interaction of a cone emerges from the fact that the normal component of velocity over its surface is equal to zero, i.e.

$$V_\theta = 0 \quad \text{at} \quad \theta = \beta_K. \tag{9.2.4}$$

We have two conditions for shock. The first is obtained from the equality of tangential components ahead of and behind the shock, i.e. $V_{cr\infty} = V_{cr}$ (Fig. 9.2.1). Accordingly

$$V_{cr} = V_\infty \cos \theta_c. \tag{9.2.5}$$

Using this expression it is possible to get the second condition. For this purpose we write the expression for the horizontal component of velocity U_c of a gas at the shock (see Fig. 9.2.1):

$$U_c = V_{cr} \cos \theta_c - V_{c\theta} \sin \theta_c.$$

Multiplying both parts of this expression by V_{cr} and recalling (9.2.5), we get

$$U_c V_\infty = V_{cr}(V_{cr} - V_{c\theta} \tan \theta_c), \tag{9.2.6}$$

where V_{cr} and $V_{c\theta}$ are the tangential and normal components of velocity at the shock respectively.

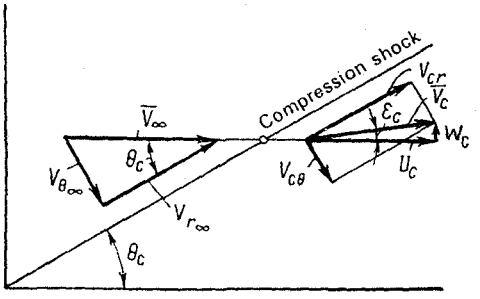

Fig. 9.2.1. System of velocity triangles in front of and immediately behind compression shock for cone in supersonic flow.

Now we use equation (4.4.4) for a shock polar and write it in the form

$$\frac{W_c^2}{(V_\infty - U_c)^2} = \frac{(V_\infty U_c - a^{*2})(k+1)}{2V_\infty^2 + (k+1)(a^{*2} - V_\infty U_c)},$$

where W_c is the vertical component of velocity on the shock.

Taking into account (4.4.3), this can also be written as

$$-\tan^2 \theta_c = \frac{2}{k+1} \cdot \frac{V_\infty^2}{a^{*2} - V_\infty U_c} + 1.$$

Recalling that $\tan^2 \theta_c = \cos^{-2} \theta_c - 1$ and that the quantity $V_\infty U_c$ is determined from (9.2.6), we find

$$-\frac{1}{\cos^2 \theta_c} = \frac{2}{k+1} \cdot \frac{V_\infty^2}{a^{*2} - V_{cr}^2 + V_{c\theta} V_{cr} \tan \theta}.$$

Keeping in mind (9.2.5), we finally get the boundary condition at the shock:

$$\tan\theta_c=\frac{1}{V_{cr}V_{c\theta}}\left(\frac{k-1}{k+1}V_{cr}^2-a^{*2}\right). \tag{9.2.7}$$

Integration of the system of equations (9.1.2), (9.2.2) and (9.2.3) can be carried out by a numerical method. Here the angle of shock θ_c and velocity of undisturbed flow V_∞ are taken as known. The velocity field is determined in the course of solution of these equations and the corresponding cone angle β_K and velocity $V_r=V_K$ are found.

Let us see how a problem is solved. The radial component of velocity can be determined from (9.2.5) using given values of θ_c and V_∞:

$$V_{cr\infty}=V_{cr}=V_\infty\cos\theta_c. \tag{9.2.8}$$

The velocity is identical for the conditions ahead of the shock and immediately behind it. It is denoted by $V_{r1}=V_\infty\cos\theta_1$, where $\theta_1=\theta_c$. The normal component of velocity $V_{c\theta}=V_{\theta 1}$ behind the shock is obtained from (9.2.7) on the basis of this value of $V_{cr}=V_{r1}$:

$$V_{\theta 1}=\frac{1}{V_\infty\sin\theta_1}\left(\frac{k-1}{k+1}V_{r1}^2-a^{*2}\right). \tag{9.2.9}$$

Let us take an intermediate conical surface, near the shock, with inclination of the generator $\theta_1-\Delta\theta_1$, where $\Delta\theta_1$ is a small rise in angle θ (Fig. 9.2.2).

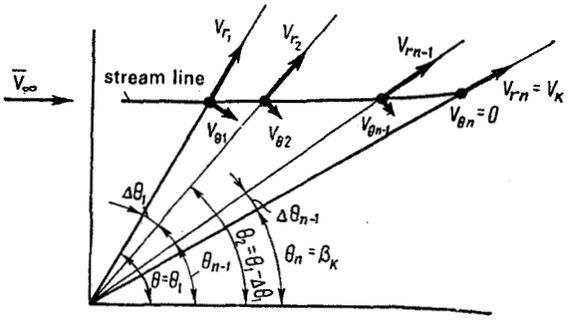

Fig. 9.2.2. Scheme for analysis of flow-interaction of cone.

The radial component of velocity V_{r2} past this surface can be calculated from equation (9.1.2), written in terms of finite differences:

$$V_r-V_{r1}=V_{\theta 1}\Delta\theta. \tag{9.2.10}$$

Assuming here that $V_r=V_{r2}$ and $\Delta\theta=\Delta\theta_1=\theta_1-\theta_2$, we get

$$V_{r2}=V_{r1}+V_{\theta 1}\Delta\theta_1. \tag{9.2.10'}$$

The normal component $V_{\theta 2}$ can be obtained from equation (9.2.2) written in terms of finite differences:

$$V_\theta - V_{\theta 1} = \left(\frac{dV_\theta}{d\theta}\right)_1 \Delta\theta. \tag{9.2.11}$$

Assuming $V_\theta = V_{\theta 2}$ and $\Delta\theta = \Delta\theta_1$, we find

$$V_{\theta 2} = V_{\theta 1} + \left(\frac{dV_\theta}{d\theta}\right)_1 \Delta\theta_1, \tag{9.2.11'}$$

where the derivative $(dV_\theta/d\theta)_1$ is calculated from equation (9.2.2) using the parameters on the shock:

$$\left(\frac{dV_\theta}{d\theta}\right)_1 = \left[-V_{\theta 1}\cot\theta_1 + V_{r1}\left(\frac{V_{\theta 1}^2}{a_1^2} - 2\right)\right]\left(1 - \frac{V_{\theta 1}^2}{a_1^2}\right)^{-1}, \tag{9.2.12}$$

where, according to (9.2.3),

$$a_1^2 = a_c^2 = \frac{k+1}{2}a^{*2} - \frac{k-1}{2}(V_{r1}^2 + V_{\theta 1}^2). \tag{9.2.13}$$

Assuming the values obtained for V_{r2}, $V_{\theta 2}$ and also a_2^2, which is determined by (9.2.3) in the form

$$a_2^2 = \frac{k+1}{2}a^{*2} - \frac{k-1}{2}(V_{r2}^2 + V_{\theta 2}^2),$$

as the initial data, it is possible to find V_{r3}, $V_{\theta 3}$, a_3 on the next intermediate surface with an angle of inclination of generator

$$\theta_3 = \theta_2 - \Delta\theta_2 = \theta_1 - \sum_1^{i=2} \Delta\theta_i.$$

For an arbitrary conical surface with an angle of inclination of generator

$$\theta_m = \theta_1 - \sum_1^{i=m-1} \Delta\theta_i \tag{9.2.14}$$

the velocity components are calculated from the formulas:

$$V_{rm} = V_{rm-1} + V_{\theta m-1}\,\Delta\theta_{m-1}; \tag{9.2.15}$$

$$V_{\theta m} = V_{\theta m-1} + \left(\frac{dV_\theta}{d\theta}\right)_{m-1}\Delta\theta_{m-1}, \tag{9.2.16}$$

where the derivative $(dV_\theta/d\theta)_{m-1}$ is obtained from (9.2.2) using the parameters $V_{\theta m-1}$, V_{rm-1}, a_{m-1} and $\theta_{m-1} = \theta_{m-2} - \Delta\theta_{m-2}$. The calculations are complete when, for some value of angle of intermediate cone (see Fig. 9.2.2),

$$\theta_n = \theta_{n-1} - \Delta\theta_{n-1} = \theta_1 - \sum_1^{i=n-1} \Delta\theta_i, \tag{9.2.17}$$

the normal component of velocity $V_{\theta n}$ does not become zero, i.e.

$$V_{\theta n}=V_{\theta n-1}+\left(\frac{dV_\theta}{d\theta}\right)_{n-1}\Delta\theta_{n-1}=0. \tag{9.2.18}$$

Here the derivative $(dV_\theta/d\theta)_{n-1}$ is found from (9.2.2) using the values of $V_{\theta n-1}$, V_{rn-1}, a_{n-1} on the neighboring intermediate conical surface with an angle of inclination of generator

$$\theta_{n-1}=\theta_1-\sum_1^{i=n-2}\Delta\theta_i. \tag{9.2.19}$$

In calculating it is not usually possible to select such a small angle $\Delta\theta_{n-1}$ as a first approximation that the equality $V_{\theta n}=0$ is satisfied. Usually for the selected value of $\Delta\theta_{n-1}$ there exists a calculated value of $V_{\theta n}$ which changes its sign to the opposite of that of $V_{\theta n}$ on the surrounding surface with an angle of inclination of generator θ_{n-1}. This indicates that the value $V_{\theta n}=0$ corresponds to an increase in angle $\Delta\theta_{n-1}$ less than the one selected. To determine this increase in angle it is necessary to carry out the operation of interpolation using the equality

$$\Delta\theta_{n-1}=-V_{\theta n-1}\left(\frac{dV_\theta}{d\theta}\right)_{n-1}^{-1}. \tag{9.2.18'}$$

The calculation of velocity and angle on the cone are based on this value of $\Delta\theta_{n-1}$:

$$V_{r\mathrm{K}}=V_{\mathrm{K}}=V_{rn-1}+V_{\theta n-1}\cdot\Delta\theta_{n-1} \tag{9.2.20}$$

and

$$\theta_n=\beta_{\mathrm{K}}=\theta_1-\sum_1^{i=n-1}\Delta\theta_i. \tag{9.2.21}$$

Similar calculations can be carried out in reverse order, imposing conditions on the cone. In this case we have to know the angle β_{K} and the velocity V_{K} on the cone. Numerical integration is supposed to be complete when the boundary conditions (9.2.5) and (9.2.7) are satisfied. On the basis of the gas parameters in the perturbed region the angle of inclination of shock ahead of the given cone and the velocity (Mach number) of undisturbed flow are found.

Each operation of the numerical integration for given values of θ_{c}, V_∞ (or β_{K}, V_{K}) provides a possibility of determining the velocity field, i.e. of finding the nature of function $V=V(\theta)$, where $V=\sqrt{V_r^2+V_\theta^2}$, and of establishing the relation between the given angle of cone β_{K} and the velocity on it V_{K}, or between the angle of shock θ_{c} and the velocity V_∞ from the other point of view.

Repeating the calculations for different given angles θ_{c} and a fixed value

of velocity V_∞, it is possible to find relations of the type $\beta_K = \beta_K(\theta_c)$, $V_K = V_K(\beta_K)$ or $V_K = V_K(\theta_c)$. The results so obtained can be represented graphically in a hodograph plane W, U in the form of a so-called "apple-shaped" curve (Fig. 9.2.3, a). This curve is the geometrical location of the ends of velocity vectors $\bar{V}_K$ for a perturbation flow right on the cone in a flow.

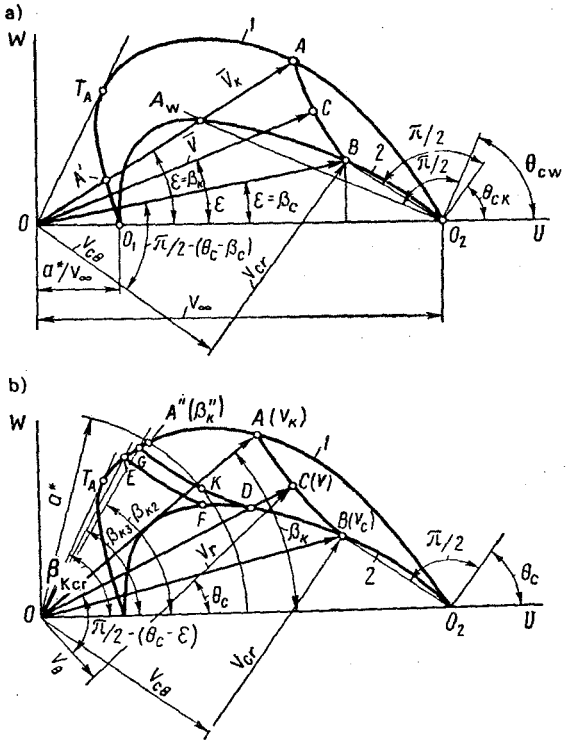

Fig. 9.2.3. "Apple-shaped" curve (*1*) and shock polar (*2*).

Point A situated on the "apple-shaped" curve and lying at the end of a velocity vector, corresponds to the cone with a given semi-angle β_K. The point B located on the shock polar coincides with the end of velocity $\bar{V}_{cr}$ on the corresponding shock with angle of inclination θ_c.

The curve AB happens to be the hodograph of velocity, i.e. it is the geometrical location of the ends of velocity vectors in the region of disturbed flow between the cone and the shock. A hodograph should be developed in the following way: The velocity components for the intermediate conical surface can be determined from Fig. 9.1.1 with the help of a velocity triangle behind the shock:

$$\left.\begin{aligned} V_r &= V\cos(\theta-\varepsilon);\\ V_\theta &= -V\sin(\theta-\varepsilon). \end{aligned}\right\} \qquad (9.2.22)$$

In the process of numerical integration using values of V_r and V_θ obtained for given angles the ratio

$$V_r/V_\theta = -\cot(\theta - \varepsilon), \tag{9.2.23}$$

is determined, from which the angle of inclination ε to the cone axis of a velocity vector $\overline{V}$ can be worked out. The polar coordinates V and ε determine the positions of points on the hodograph of velocity (see point C in Fig. 9.2.3, a).

The graphic method of solving the problem of supersonic flow over a circular cone is developed by Prof. A. Bussman.

The physical picture of a supersonic flow of gas over a cone can be clearly presented with the help of the apple-type curve and the family of hodographs of velocity. A phased isentropic compression of gas takes place in the region between the shock and the cone along the stream line. In Fig. 9.2.3, a the interchange from point B on a shock polar along the hodograph of velocity to point A on the apple-type curve corresponds to this. As can be seen from Fig. 9.2.2, the stream line gradually bends and approaches the cone surface following the direction of the generator of a cone.

Let us draw an arc of radius a^* with point O as the center (see Fig. 9.2.3, b). If the hodograph of velocity AB for a given angle β_{K1} of a cone lies on the right side of the arc the isentropic compression behind the shock wave takes place at supersonic speeds. For the angle of cone $\beta_{K2} > \beta_{K1}$ the part of the hodograph GK can be on the left side of the arc and the part KD on the right side. The disturbed flow will be a mixed one. The flow will be supersonic in the region around the shock and subsonic near the surface of the cone. For a still higher angle of cone $\beta_{K3} > \beta_{K2}$ the hodograph of velocity EF lies to the left of the arc a^* and hence the disturbed flow will be completely subsonic.

Analysis of the apple-type curve shows that for each angle of cone β_K theoretically there exist two solutions (see points of intersection A and A' of apple-type curve AO in Fig. 9.2.3, a). One solution gives a low velocity and a high angle of shock inclination and the other a high velocity and a low angle of shock inclination. As shown by experimental research, the second solution, representing steady flow behind the shock, corresponds to reality.

It can be shown that the ray from the origin of coordinates passing through point T_A is tangential to the apple-type curve. This point T_A theoretically corresponds to the unique solution and determines the critical angle of cone $\beta_{K\cdot cr}$. If the actual angle of the cone is more than the critical one it is not possible to investigate the flow-interaction of the cone formally with the help of this curve. Under real conditions this flow-interaction is characterized by the fact that the shock becomes detached from the sharp nose and gets bent. This kind of flow over a cone is called supercritical.

It can easily be seen that the critical angle happens to be the function only of undisturbed velocity (corresponding to Mach number $\mathbf{M}_\infty = V_\infty/a_\infty$ or the relative velocity $\lambda_\infty = V_\infty/a^*$).

When the cone angle is near the critical angle ($\beta_K \leqslant \beta_{K.cr}$) the nature of the flow, as shown by experiment, diverges from the theoretical one. According to the apple-type curve the attached straight shock and conical field of velocity (pure subsonic or mixed) corresponds to the so-called transcritical regime of flow-interaction (points E, G in Fig. 9.2.3, b).

However, observation of flows over cones with cylindrical tail sections in wind tunnels shows that in reality the shock remains straight near the nose and gets bent only at some distance from it. For the same cone the point where the shock begins to bend moves nearer the nose with a reduction in Mach number $\mathbf{M}_\infty$. This bending of the shock indicates that the flow does not remain conical. This is well seen in Fig. 9.2.5, a, where the flow pattern for a conical body with angle $\beta_K = 25°$ at $\mathbf{M}_\infty = 1.4$ is shown.

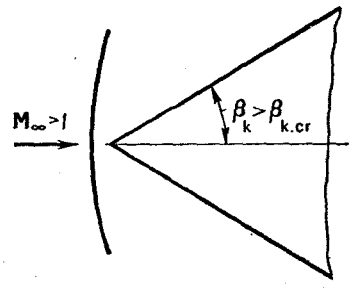

Fig. 9.2.4. Cone in supersonic flow.

The bending of a "sonic" line indicates divergence from a conical flow. It may be noted that near a sharp nose this line, though it does not fully coincide with the theoretical line obtained from the hodograph of velocity, remains straight, which indicates that the conical nature of the flow is maintained. At some distance from the nose the "sonic" line gets bent, indicating that the conical velocity distribution is disturbed.

With a reduction in Mach number $\mathbf{M}_\infty$ to 1.27 the subsonic region increases and the "sonic" line, as seen from Fig. 9.2.5, b, moving away from the apex of the cone, approaches the shock, which is already somewhat bent near the nose. A conical flow is no longer possible all over the space between the shock and the body. With further reduction in $\mathbf{M}_\infty$ we get the conditions for complete detachment of the bent shock from the nose of the cone.

Experimental data show that the shock moves away from the apex at angles β_K somewhat greater than those determined by accurate theoretical flow-interaction calculations for a cone. For example, for Mach number $\mathbf{M}_\infty = 2.45$ it is found by experiment that detachment of shock takes place at angle $\beta_K = 46°$, whereas the calculated value of this angle in theory is 45° 46′.

Experimental research shows that a conical flow corresponding to constant velocity past the cone is observed until the velocity over its surface reaches the speed of sound. The corresponding angle of cone β''_K can be determined by the point A'' of the intersection of the arc of radius a^* and the apple-type curve (see Fig. 9.2.3, b). So in practical cases it is possible to use the apple-type curve for calculation of the flow-interaction of a complete

conical surface for angle $\beta_K \leqslant \beta_K''$. As far as the apex of the conical surface is concerned the velocity past it obtained by conical theory (with the help of the apple-type curve), tallies well with the experimental data for all values of angles $\beta_K \leqslant \beta_{K\cdot cr}$, i.e. for those conditions of flow-interaction under which the shock remains attached.

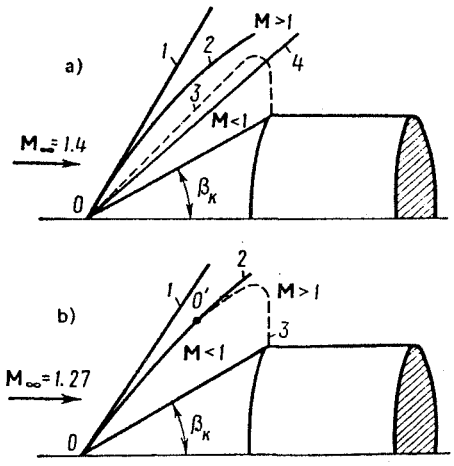

Fig. 9.2.5. Position of compression shock and "sonic" line near cone attached to cylinder:

a—at $M_\infty = 1.4$, *b*—at $M_\infty = 1.27$; *1*—linear shock (theory); *2*—curved shock (experiment); *3*—"sonic" line (experiment); *4*—"sonic" line (theory).

The apple-type curve gives the relation for velocity V_K past a cone and angle of inclination of shock θ_c as a function of cone angle β_K at a given velocity of undisturbed flow V_∞ (at given Mach numbers M_∞ or λ_∞). To get the appropriate relation at other values of velocity V_∞ (M_∞ or λ_∞) it is necessary to carry out the numerical calculation of the flow-interaction of the cone and construct the corresponding apple-type curve for the new conditions. The family of such curves represents the relation of velocity on a cone and the angle of inclination of shock as functions of cone angle β_K and velocity V_∞ (M_∞ or λ_∞). Fig. 9.2.6 shows a family of apple-type curves drawn for different values of the relative velocity $\lambda_\infty = V_\infty/a^*$. The corresponding shock polars are shown in the same figure to facilitate comparison of the flow-interaction of a wedge with bodies of similar semi-angle β_K, e.g. a cone.

It can be seen from Fig. 9.2.6 that the velocity past a cone is higher than that past a wedge ($\overline{OA}_K > \overline{OA}_w$). For a wedge the flow turns through an angle $\beta_c = \beta_w$ at an oblique shock. At the same time the flow is turning by an angle less than the cone angle, $\beta_c < \beta_K$. Consequently the angle of inclination of the main shock wave ahead of the wedge $\theta_{c\cdot w}$ is more than the angle $\theta_{c\cdot K}$ ahead of the cone. Further $\beta_{K\cdot cr} > \beta_{w\cdot cr}$.

The same result can be obtained directly from Fig. 9.2.3, a. Let us join points A_w and B with a point O_2 and draw perpendiculars from this point to the straight lines so obtained. Then the angles between the perpendiculars and horizontal axis U determine the inclination of the generators of shocks ahead of wedge $\theta_{c\cdot w}$ and ahead of cone $\theta_{c\cdot K}$. It can be directly seen from the figure that $\theta_{c\cdot w} > \theta_{c\cdot K}$.

The important factor of calculation of the flow-interaction of a cone happens to be the determination of pressure, density and temperature from

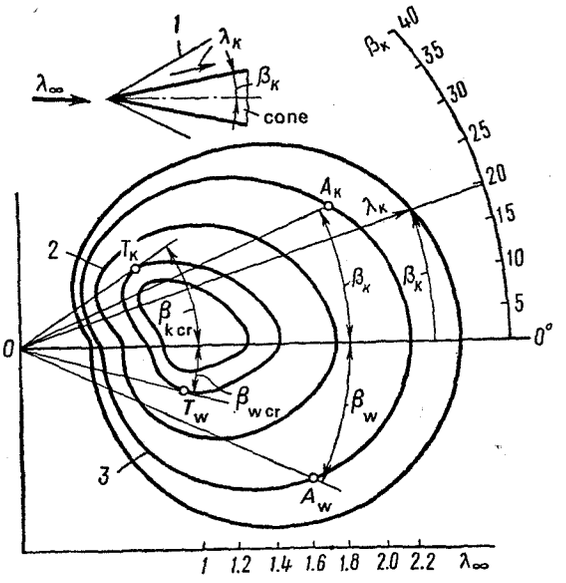

Fig. 9.2.6. Family of apple-type curves and shock polars:

1—compression shock; *2*—family of apple-type curves; *3*—family of shock polars.

the values of V_K and θ_c obtained. Keeping in view the isentropic character of the gas flow behind the shock, the corresponding relations (3.6.26) through (3.6.33) can be used. Assuming that the temperature T_0 in formula (3.6.33) does not change behind the shock and is determined by (3.6.35), we get the following formula for temperature on a cone:

$$\frac{T_K}{T_\infty}=(1-\bar{V}_K^2)\left(1+\frac{k-1}{2}\,\mathbf{M}_\infty^2\right), \tag{9.2.24}$$

where $\bar{V}_K=V_K/V_{max}$.

The stagnation pressure in formula (3.6.26) should be calculated taking into account the loss across the shock. Denoting this pressure by p_0' and introducing the parameter $\nu=p_0'/p_0$ calculated on the basis of stagnation pressure p_0 before the shock from formula (3.6.29), we get the pressure over a cone as

$$\frac{p_K}{p_\infty}=\nu_0\left[(1-\bar{V}_K^2)\left(1+\frac{k-1}{2}\,\mathbf{M}_\infty^2\right)\right]^{k/(k-1)}. \tag{9.2.25}$$

The parameter $\nu_0=p_0'/p_0$ depends on Mach number $\mathbf{M}_\infty$ and angle of inclination of shock θ_c ahead of the cone and is determined with the help of (4.3.21) and (4.3.22) in the following form:

$$\nu_0=[(1+\delta)\mathbf{M}_\infty^2\sin^2\theta_c-\delta]^{\frac{\delta-1}{2\delta}}$$

$$\times\left[\frac{\mathbf{M}_\infty^2\sin^2\theta_c}{(1-\delta)\left(1+\frac{\delta}{1-\delta}\mathbf{M}_\infty^2\sin^2\theta_c\right)}\right]^{\frac{1+\delta}{2\delta}}. \tag{9.2.26}$$

The density ratio is obtained from the equation of state

$$\rho_K/\rho_\infty=(p_K/p_\infty)\,(T_\infty/T_K). \tag{9.2.27}$$

The pressure coefficient on a cone will be

$$\bar{p}_K=(p_K-p_\infty)/q_\infty=2\,(p_K-p_\infty)/k\,\mathbf{M}_\infty^2\,p_\infty. \tag{9.2.28}$$

The drag force based on the action of pressure (wave drag) is determined with the help of the relation (1.3.2). Taking $\bar{p}=\bar{p}_K$, $c_{fx}=0$, $S=S_{max}=\pi R_K^2$, $dS=2\pi R dl$, $\cos(\widehat{\bar{P}_n x})=\sin\beta_K$ (all notations are given in Fig. 9.1.1), we have

$$X_w=q_\infty S_{max}\int_0^{l_K}\bar{p}_K\sin\beta_K\frac{2\pi R dl}{\pi R_K^2}.$$

Recalling that $dl\sin\beta_K=dR$, we get the following expression for drag coefficient:

$$c_{xw}=\frac{X_w}{q_\infty S_{max}}=2\int_0^1\bar{p}_K\bar{R}d\bar{R}, \tag{9.2.29}$$

where $\bar{R}=R/R_K$.

As the pressure coefficient $\bar{p}_K$ on a cone in a supersonic flow is a constant quantity we get the following relation for the wave drag coefficient of a cone:

$$c_{xw}=\bar{p}_K. \tag{9.2.30}$$

So the coefficient of wave drag during a supersonic axisymmetrical flow-interaction is equal to the pressure coefficient on its surface.

3. Effect of Balanced Dissociation and Ionization of Gas on Flow-Interaction of Cone

A system of differential equations (9.1.2), (9.2.2), equation of state (9.1.4), energy equation (9.1.5) and the general relations (9.1.6) through (9.1.9) determining enthalpy, entropy, average molecular weight and the speed in a

dissociating and ionizing gas is used for the solution of the problem of the flow-interaction of a cone taking into account the effect of balanced dissociation and ionization. Here we use the general method of numerical integration of differential equations, as in the case of a gas flow with constant specific heats.

The first step in the calculation is the determination of the gas parameters behind the oblique shock for a given angle θ_c. The radial component of velocity V_{cr} is determined by (9.2.8). The normal component of velocity $V_{c\theta}$ is determined from the theory of shocks, taking into account the effect of dissociation and ionization (see Chapter 4 Section 2). As a first approximation let us take the value from (4.2.12):

$$\Delta\bar{V}_n^{(1)}=\frac{V_{n1}-V_{n2}}{V_{n1}}=\frac{V_{\theta\infty}-V_{c\theta}}{V_{\theta\infty}} \tag{9.3.1}$$

is equal to unity, i.e. we assume the condition of complete stagnation behind the shock so that $V_{c\theta}\approx 0$. The pressure corresponding to this condition can be found from formula (4.2.15). Assuming $\Delta\bar{V}_n=1$ and recalling that $\mathbf{M}_{n1}=\mathbf{M}_\infty \sin\theta_c$, we get

$$p_c^{(1)}=(1+k_1\mathbf{M}_\infty^2 \sin^2\theta_c)\, p_\infty. \tag{9.3.2}$$

Enthalpy is calculated from the expression (4.2.16) in which it is assumed that $\Delta\bar{V}_n=1$ and $V_{n1}=V_\infty \sin\theta_c$:

$$i_c^{(1)}=i_\infty+\frac{V_\infty^2 \sin\theta^2{}_c}{2}. \tag{9.3.3}$$

It is possible to find density $\rho_c^{(1)}$ from the values of $p_c^{(1)}$ and $i_c^{(1)}$ using the curves of thermodynamic functions of air [7, 17] and then, as a second approximation, the variation in relative velocity can be determined from (4.2.21)

$$\Delta\bar{V}_n^{(2)}=1-(\rho_\infty/\rho_c^{(1)}). \tag{9.3.4}$$

From this rise in velocity the improved value of pressure will be

$$p_c^{(2)}=p_\infty\,(1+k_1\,\mathbf{M}_\infty^2 \sin^2\theta_c\,\Delta\bar{V}_n^{(2)}) \tag{9.3.5}$$

and that of enthalpy

$$i_c^{(2)}=i_\infty\left[1+\frac{V_\infty^2 \sin^2\theta_c}{2}\cdot\frac{\Delta\bar{V}_n^2}{i_1}(2-\Delta\bar{V}_n^{(2)})\right]. \tag{9.3.6}$$

Density $\rho_c^{(2)}$ can be obtained from the graphs of thermodynamic functions and the value of $\Delta\bar{V}_n$ is corrected:

$$\Delta\bar{V}_n^{(3)}=1-(\rho_\infty/\rho_c^{(2)}). \tag{9.3.7}$$

If the value of $\Delta\bar{V}_n^{(3)}$ differs by a fairly small quantity from $\Delta\bar{V}_n^{(2)}$ the

approximation procedure can be considered to be complete and the normal component of velocity behind the shock is determined

$$V_{c\theta} = V_{\theta 1} = V_{\theta\infty}\,(1-\Delta\bar{V}_n^{(3)}) = V_\infty \sin\theta_c\,(1-\Delta\bar{V}_n^{(3)}). \tag{9.3.8}$$

The tables given in the work [18] can also be used for these calculations. The temperature $T_c^{(1)}$ and average molecular weight of air $(\mu_{av})_c^{(1)}$ can be determined from these tables for given values of $p_c^{(1)}$ and $i_c^{(1)}$ (enthalpy is here denoted by h, m^2/sec^2). Next, the corresponding value of density can be calculated from formula (4.2.17):

$$\rho_c^{(1)} = \frac{p_c^{(1)}}{p_\infty}\cdot\frac{(\mu_{av})_c^{(1)}}{(\mu_{av})_\infty}\cdot\frac{T_\infty}{T_c^{(1)}}\,\rho_\infty, \tag{9.3.9}$$

where $(\mu_{av})_\infty = 29$ gm/gm·mol may be taken for undissociated air.

Then $p_c^{(2)}$, $i_c^{(2)}$ can be calculated from formulas (9.3.4) through (9.3.6), $T_c^{(2)}$, $(\mu_{av})_c^{(2)}$ can be found from the tables and using the expression (9.3.9) the quantity

$$\rho_c^{(2)} = \frac{p_c^{(2)}}{p_\infty}\cdot\frac{(\mu_{av})_c^{(2)}}{(\mu_{av})_\infty}\cdot\frac{T_\infty}{T_c^{(2)}}\,\rho_\infty \tag{9.3.9'}$$

can be determined.

The quantity $\Delta\bar{V}_n^{(3)}$ is found from this value of $\rho_c^{(2)}$ and formula (9.3.7). Then $V_{c\theta} = V_{\theta 1}$ is obtained from the expression (9.3.8).

The values of V_{r2} and $V_{\theta 2}$ on a neighboring conical surface can be calculated by (9.2.10′) and (9.2.11′) respectively for a given step of integration $\Delta\theta_1$. Here the derivative $(dV_\theta/d\theta)_1$ in formula (9.2.11′) is determined by (9.2.12), in which the speed of sound a_1 can be found from the tables or the graphs of thermodynamic functions for known values of $p_c^{(2)}$ and $i_c^{(2)}$ (or from $p_c^{(2)}$ and $T_c^{(2)}$).

Enthalpy on the selected conical surface is determined by equation (9.1.5):

$$i_2 = i_c^{(3)} + \tfrac{1}{2}\,[(V_{r1}^2 + V_{\theta 1}^2) - (V_{r2}^2 + V_{\theta 2}^2)]. \tag{9.3.10}$$

For further calculations it is necessary to use the value of entropy of gas, assuming that the disturbed flow behind the shock is isentropic all over the region and hence that entropy will be everywhere the same as that in the flow immediately behind the shock. This entropy $S = S_c = \text{const}$ is determined from the tables of thermodynamic functions for the values of $p_c^{(2)}$, $i_c^{(2)}$ (or $p_c^{(2)}$, $T_c^{(2)}$).

The speed of sound a_2 can be found from the tables or graphs for given values of enthalpy i_2 and entropy S. The corresponding velocity components V_{r3} and $V_{\theta 3}$ on a conical surface with angle $\theta = \theta_c - \sum_{i=1}^{2}\Delta\theta_i$ can be calculated by formulas (9.2.10′) and (9.2.11′). Similar calculations can be carried out for the surrounding conical surface, etc. The calculations are complete when the

velocity component $V_{\theta n}$ on one of these surfaces is equal to zero. The corresponding angle (9.2.21) will be the angle of cone under flow-interaction and the corresponding velocity will be the velocity V_K (9.2.20) over this cone. The corresponding enthalpy will be

$$i_K = i_c + (V_c^2 - V_K^2)/2,$$

where

$$V_c^2 = V_{\theta 1}^2 + V_{r1}^2; \quad i_c = i_c^{(2)}.$$

The temperature T_K, pressure p_K and density ρ_K on the cone can be determined from the tables, graphs or corresponding formulas for enthalpy i_K and entropy $S = S_c$.

All the flow parameters over a cone in a flow of given Mach number M_∞ depend not only on temperature T_∞ as characterized in the case of variable specific heats but also on pressure p_∞ of the undisturbed flow which governs the degree of dissociation and ionization. For given values of parameters β_K, M_∞ and T_∞ the flight altitude H may be selected in place of p_∞ as an example of a function determining variation of gas parameters over a conical surface. For given values of T_∞ and M_∞ the flow parameters over a cone are functions of angle β_K and flight altitude.

Some results of calculations of these parameters are shown in Figs. 9.3.1 through 9.3.3. The nature of the variation in pressure p_K, temperature T_K and density ρ_K over a cone in the presence of dissociation and ionization is the same as that immediately behind the shock. Here the pressure, as behind the shock, varies only slightly during dissociation and ionization. Its value

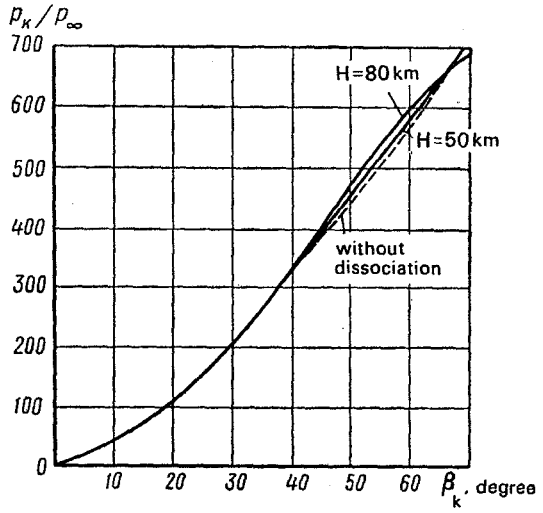

Fig. 9.3.1. Pressure on cone with adjustment for dissociation of gas $T_\infty = 220°K$; $M_\infty = 23.5$).

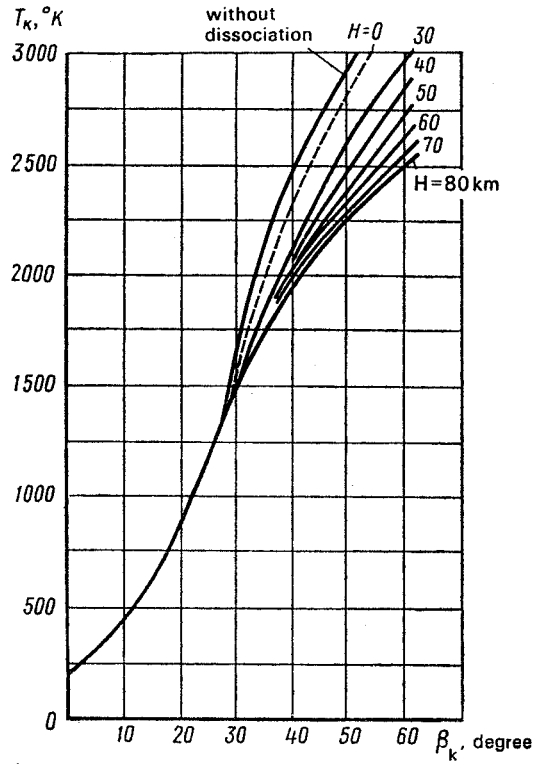

Fig. 9.3.2. Temperature on cone with adjustment for dissociation of gas (T_∞=220°K; M_∞=10).

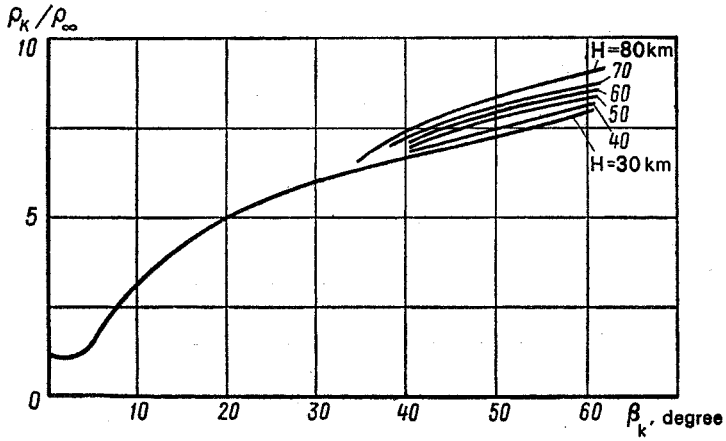

Fig. 9.3.3. Density of air on cone in dissociating flow (T_∞=220°K, M_∞=10).

basically depends on the condition of undisturbed flow, whereby the maximum change in pressure on a cone cannot exceed some limited value of this pressure (p_2-p_1), which is obtained from (4.2.14) under the condition of $V_{n2}=0$, $V_{n1}=V_1=V_\infty$ (normal shock) and is equal to $p_2-p_1=\rho_\infty V_\infty^2$. The temperature and density vary considerably at the same time and this variation is higher with thicker cones.

If the cone angles are not high these parameters on the cone are affected only very slightly by physico-chemical transformations even at quite high velocities of oncoming flow. For example, calculations show that at $M_\infty=24$ density hardly changes with altitude up to angle $\beta_K=15°$. At $M_\infty=10$ (see Fig. 9.3.3) it does not change up to angle $\beta_K=35°$. Thus the interval of angles β_K that corresponds to a comparatively low temperature and a negligibly low degree of dissociation increases with reduction in speed. A similar phenomenon is observed with reduction in flight altitude.

An increase in the thickness of the cone brings about more intensive heating and as a consequence results in dissociation and ionization which may considerably affect the flow parameters. The effect of change of shock inclination θ_c in front of a cone of angle $\beta_K=40°$ is shown in Fig. 9.3.4. The angle θ_c diminishes in comparison with that observed at constant specific heats ($k=1.4$). This results in a decrease in the strength of the shock and increase in velocity behind it, which means the velocity over the cone increases.

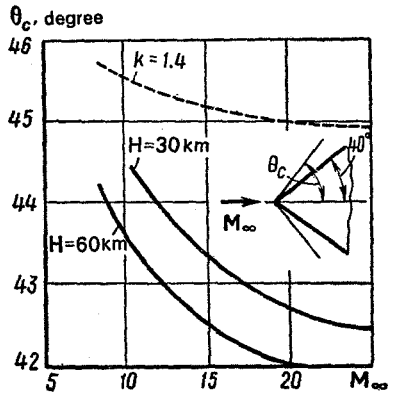

Fig. 9.3.4. Variation of angle inclination of shock ahead of cone placed in supersonic flow (*solid line*—real gas; *broken line*—perfect gas).

The rise in flow velocity and reduction in sonic velocity lead to an increase in Mach number M_K over a conical surface placed in a dissociating gas flow. Gas parameters on a cone in a flow (conditions of flow-interactions: $\beta_K=45°$, $V_\infty=6200$ m/sec, $T_\infty=5800°K$, $p_\infty=0.0602$ kg/cm^2) calculated with and without allowance for dissociation are compared in Table 9.3.1.

4. Blunt Cone

4.1 Form of blunt noses

The nose section of many flight vehicles has a blunt form. These blunt forms are, first of all, used for very high speeds. Here the main requirement of the nose section is its capacity to withstand the high temperatures of the gas flow over it. However, flight vehicles (or their individual components)

operating at low velocities often have a blunt form which may be required by peculiarities of construction, the type of apparatus, etc. Almost always we have to deal with blunt bodies because it is practically impossible to find absolutely sharp nose sections.

This section deals with the conical bodies with different blunt nose profiles that are in most common use. A conical body with a blunt nose of spherical form is shown in Fig. 9.4.1. The equation of the linear part of the generator of this kind of body, tangential to its spherical part, will be

TABLE 9.3.1

Conditions of calculations	V_K, m/sec	a_K, m/sec	T_K, °K	$M_K = V_K/a_K$	i_K, m²/sec²	p_K, kg/cm²	ρ_K, $\frac{\text{kg.sec}^2}{\text{m}^4}$	θ_c
With dissociation	3980	2058	7211	1.934	32.2×10^6	0.545	1.533×10^{-3}	50°
Without dissociation	3275	2580	16560	1.27	6×10^6	0.577	0.812×10^{-3}	56° 6′

$$r - r_T = (x - x_T)\tan\beta_K, \tag{9.4.1}$$

where r_T, x_T are the coordinates of a point at the junction of the spherical part and the generator of the cone, which can be determined through the radius of sphere R_T and cone angle β_K in the form:

$$\left.\begin{aligned} r_T &= R_T\cos\beta_K; \\ x_T &= R_T\cot\beta_K\cos\beta_K. \end{aligned}\right\} \tag{9.4.2}$$

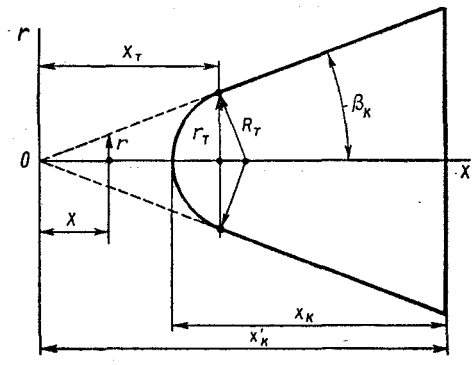

Fig. 9.4.1. Cone with blunt tangential spherical nose.

The equation of the generator of a spherical nose in the system of coordinates with its origin at the apex will have the nondimensional form:

$$\bar{r}^2 = 1 - (\bar{x} - 1)^2, \tag{9.4.3}$$

where $\bar{r} = r/R_T$, $\bar{x} = x/R_T$. The angle of inclination β of the tangent to the axis at a point on this part will be given by

$$\tan\beta = dr/dx = (1 - \bar{x})/\bar{r}. \tag{9.4.4}$$

The nose section of a cone can be made in such a way that the generator will not be tangential to the spherical surface but will intersect

it (Fig. 9.4.2). The radius of this surface drawn for the point with coordinates r_T, x_T will be $R_{TC} > R_T$, where R_T is the radius of a tangential nose related to the coordinates r_T and x_T by the relations (9.4.2).

A cone with a blunt nose in the form of a plane surface (plane section) which can be taken as a sphere of infinite radius is shown in Fig. 9.4.2. The spherical nose and the flat nose can be regarded as particular cases of elliptical surface. A cone with a blunt nose in the form of such a surface is shown in Fig. 9.4.3.

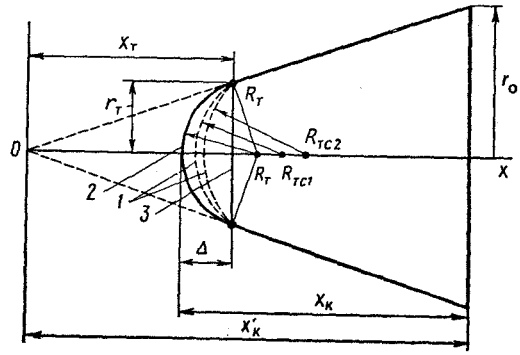

Fig. 9.4.2. Cone with blunt intersecting spherical nose:

1—intersecting spherical nose; *2*—tangential spherical nose; *3*—plane section blunt nose.

The major and minor axes $2a$ and $2b$ of an elliptical nose are its geometrical characteristics where their orientation may be different. A particular case when the major axis is perpendicular to the axis of the cone is shown in Fig. 9.4.3. If the two axes are equal an elliptical nose becomes a spherical one. When one of the axes, coinciding with axis of the cone, is equal to zero the elliptical surface becomes plane. An elliptical nose, like a spherical one, can be tangential or intersect the generator. Besides those considered here, conical bodies with other forms of surface can be used for the nose section. We will not go into the details of these types.

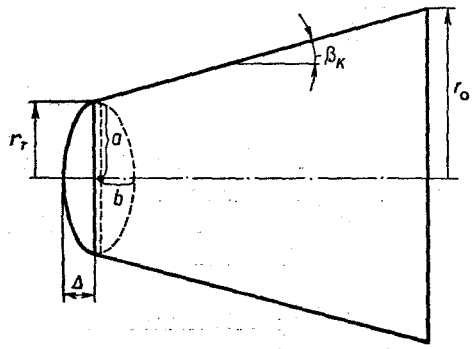

Fig. 9.4.3. Cone with elliptical blunt nose.

The spherical tangential nose and plane section happen to be the most characteristic forms of blunt noses. These may be considered as the limiting cases expressing other possible forms in their own way. Both of these characteristic forms are relevant to the process of aerodynamic research on blunt bodies with some intermediate form of nose because they allow us to work out the limiting values of the various aerodynamic parameters associated with them.

The aerodynamic characteristics of blunt bodies largely depend on the degree of bluntness for a given type of nose. The degree of bluntness

is the ratio of the radius of the base of nose r_T to the radius of the maximum cross section of body r_m. Moreover the value of the geometrical parameter of the blunt nose itself is very important. For a spherical nose this parameter is the ratio R_T/R_{TC}, where R_T and R_{TC} are the radii of tangential and intersecting spheres respectively (see Fig. 9.4.2). This parameter varies from unity (for a spherical tangential nose) to zero (for a plane section). For an elliptical nose the ratio of semi-axes $\bar{b}=b/a$, which varies in the interval $0\leqslant\bar{b}\leqslant 1$ for a conical blunt body, may be taken as such a parameter.

For a given form of spherical or elliptical nose the ratio $\bar{\Delta}=\Delta/r_T$, where Δ is the height of the nose (see Figs. 9.4.2 and 9.4.3), may be chosen as a nondimensional geometrical parameter. If the nose has an elliptical form with the major axis oriented along the normal to the cone axis the value of parameter $\bar{\Delta}$ will vary in the interval $0\leqslant\bar{\Delta}\leqslant d$. Quantity $\bar{\Delta}=d=0$ corresponds to a plane section and the quantity $\bar{\Delta}=d=(1-\sin\beta_K)/\cos\beta_K$ corresponds to a tangential spherical nose.

4.2 Special features of supersonic flow

An important aerodynamic property of blunt bodies from the practical point of view is that they heat up less and suffer less damage moving through the atmosphere at very high speeds by comparison with sharp-nosed bodies.

Let us find out which gas dynamic phenomena are responsible for this property of blunt bodies. A system of flow about a blunt conical body is shown in Fig. 9.4.4. The detached shock of varying intensity at different points of the surface is formed in front of the body. At a distance from the nose the shock wave changes to the usual wave of disturbances of infinitely small strength and an angle of inclination $\theta_c=\mu_\infty=\sin^{-1}(1/M_\infty)$. The maximum strength will be at the apex of the wave (point B in Fig. 9.4.4), where $\theta_c=\pi/2$. As the angle θ_c hardly differs from $\pi/2$ in the neighborhood of the nose the corresponding section of wave will be quite strong, almost with the strength of a normal shock.

The transition of gas particles through such a strong shock will be accompanied by a considerable loss of total head and rise in entropy. As a result the surface of the body is covered by a layer of some thickness in which the gas has high entropy. This high entropy layer is bounded partly by the shock wave and the surface created by rotation of the "sonic" stream line, i.e. the stream line passing through the "sonic" point on the wave (point S having coordinates r_{ST} in Fig. 9.4.4).

Due to differing degrees of stagnation at different points on the shock wave the flow in the high entropy layer will be characterized by some velocity gradient along normal n as shown in Fig. 9.4.4 and hence by a variable value of local Mach number M across thickness Δ. If the boundary layer is appreciably thinner than the high entropy layer the velocity gradient in it, by comparison with that in the high entropy layer, can be neglected. This

simplifies the analysis. It is assumed that the velocity at different points of the section in the high entropy layer is equal. It can be taken as approximately equal to the mean velocity between the values on the "sonic" and "zero" stream lines passing through the apex of the wave. This velocity is obviously less than the velocity past a sharp cone. The flow region in the neighborhood of the surface of the cone, occupied by the high entropy layer and characterized by low velocities (and hence by a low Mach number and a low Reynolds number), seems to be the deciding factor in the formulation of processes in a boundary layer.

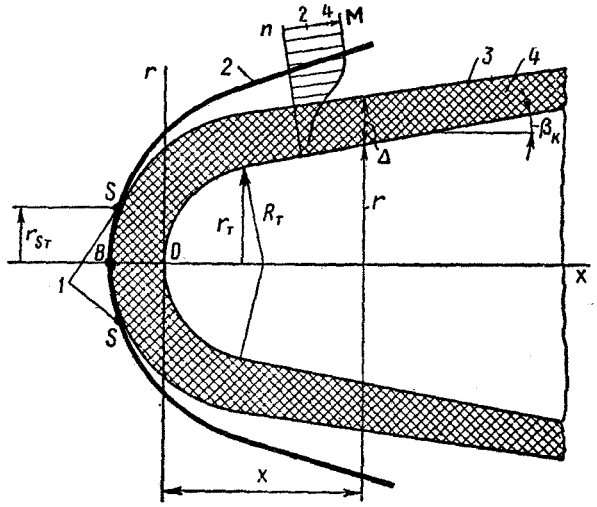

Fig. 9.4.4. Blunt cone in supersonic flow:

1—"sonic" points; *2*—shock wave; *3*—"sonic" stream line; *4*—high entropy layer.

The main peculiarity of the flow-interaction is that the flow regime in the boundary layer changes under the effect of the blunt nose. Due to a reduction in the local Reynolds numbers calculated on the basis of velocity in the high entropy layer the laminar boundary layer changes to a turbulent layer somewhat downstream and so the extent of the laminar boundary layer increases. This helps to reduce friction and heat flows to the wall.

Reduction in heat flows based on the enhanced entropy of gas during transition through a shock is known as entropy effect. Here it should be borne in mind that entropy effect not only leads to a reduction in velocity at the external surface of the boundary layer but also to a reduction in the density of the gas, i.e. to a reduction in the Reynolds number. At the same time a rise in entropy also results in an increase (compared to a sharp-nosed body) in the temperature at the external limit of the boundary layer. This brings about the anti-effect of the high entropy layer whereby there

is some rise in the heat flow from the boundary layer to the wall. However, the resultant entropy effect for an appropriate choice of wall and form of nose leads to a reduction in heat flows, as is shown by calculations and experimental research.

The wave drag of a blunt body as a rule increases in comparison to that of a sharp-nosed body. However, drag decreases for thin conical bodies with a low degree of bluntness. This is explained by the fact that although pressure rises near the nose it decreases over a considerable part of the surface of the body in comparison with a sharp cone. This phenomenon of reduction in pressure behind the nose is illustrated in Fig. 9.4.5, showing empirical results obtained in aerodynamic wind tunnel tests of thin cones with a blunt nose in the form of a plane section in a supersonic flow of $M_\infty = 6.85$. The minimum pressure is achieved at a distance of about 10 times the diameter of the nose section. At double this distance from the nose pressure builds up to its value for a sharp cone. If such a cone is of small length and hence has a small surface having low pressure the reduction in drag for this section will not be enough to compensate for its increase due to the drag increase of the plane section nose. For a long enough cone the reduction in drag of the peripheral section can be quite appreciable and can result in a reduction in the total drag of a blunt-nosed conical surface compared to that of a sharp-nosed conical surface.

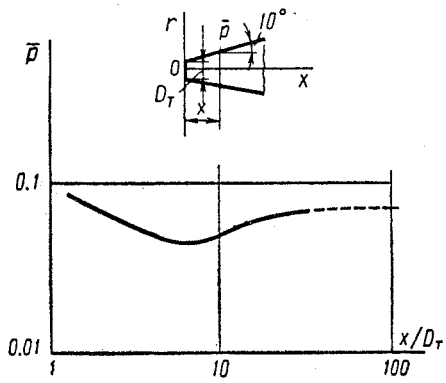

Fig. 9.4.5. Pressure coefficient on surface of cone with plane section blunt nose at $M_\infty = 6.85$:

——by experiment; - - - - calculated by conical theory for sharp-nosed body.

The main point of using a blunt nose is not the reduction in drag, which for a low degree of bluntness seems to be comparatively small, but the appreciable reduction in heat transfer to the wall. This advantage, as shown by experiment, arises mainly in the regime of hypersonic velocities.

Other cases of the use of blunt surfaces can be found that are connected with the necessity not so much of reduction in heat transfer as of increase in drag. Space craft have just this form of surface because it is important to have high c_x providing most intensive braking in the atmosphere.

The great practical relevance of aerodynamic research on blunt bodies is clear from the above discussion.

4.3 Flow-interaction of cone with spherical blunt nose

Study of the aerodynamics of a whole blunt body is related to the

investigation of the flow-interaction of the front part in the form of a blunt nose of some shape. The results of these investigations happen to be the basis of calculations of flow parameters over the remaining part of the body. On the other hand these results have their own value as they facilitate determination of the aerodynamic characteristics of a blunt nose. The resultant aerodynamic characteristics of the body can be determined by adding the components for the nose and the remaining part.

We must note here that whereas the flow-interaction of a peripheral part of the body depends on its bluntness the flow condition about the nose is determined only by its form or, correctly speaking, by the form of the nose section up to the "sonic" point on its surface. It is obvious that if this "sonic" point lies on the peripheral surface (downstream behind the line joining nose and body) the disturbances appearing in the region of peripheral surface of the body propagate upstream toward the nose and its flow-interaction should not be examined without consideration of the flow over this region.

Let us take the problem of the flow-interaction of the spherical nose of a blunt conical surface. Let us consider this problem as independent, i.e. assume that the peripheral surface of the body has no effect on the flow past the nose. We will study an inviscid flow keeping in mind that the solution sought, irrespective of this limitation, has a great practical significance: it gives the basic conditions of flow outside the boundary layer, the friction and heat transfer governing the processes occurring in the boundary layer itself.

First we will study the flow around the point of complete stagnation which is one of the most characteristic points on a spherical surface. Study of this flow is interesting mainly because it is connected with such practical problems as the determination of heat flows, which may reach the highest values. In addition the solution of the problem of flow near the point of complete stagnation helps us to determine the distance from the shock wave to the nose and the distribution of gas dynamic parameters in this small region. Here the solution may be obtained, in general, taking into account the physico-chemical transformations of the gas.

The equation of motion can be used to solve the problem thus formulated. This equation, according to (3.1.21) for an "inviscid" ($\nu=0$) and "weightless" gas ($\overline{W}=0$), has the following vector form:

$$d\overline{V}/dt=-(1/\rho)\ \text{grad}\ p. \tag{9.4.5}$$

Let us write equation (9.4.5) in the system of curvilinear orthogonal coordinates. The origin of coordinates of this system coincides with point of complete stagnation O on a spherical surface. The x coordinate will be taken along the surface and y coordinate along the normal to it (Fig. 9.4.6). Keeping in mind (3.1.22) and taking a steady flow ($\partial\overline{V}/\partial t=0$), equation (9.4.5) may be given by

$$\text{grad}\,(V^2/2)+\text{rot}\,\bar{V}\times\bar{V}=-(1/\rho)\,\text{grad}\,p. \tag{9.4.6}$$

Taking the components of vectors along coordinate lines q_1 and q_2 of the curvilinear system [see (2.4.11)] we get equations of motion:

$$\left.\begin{aligned}&[\text{grad}\,(V^2/2)]_1+(\text{rot}\,\bar{V}\times\bar{V})_1=-(1/\rho)\,(\text{grad}\,p)_1;\\&[\text{grad}\,(V^2/2)]_2+(\text{rot}\,\bar{V}\times\bar{V})_2=-(1/\rho)\,(\text{grad}\,p)_2.\end{aligned}\right\} \tag{9.4.7}$$

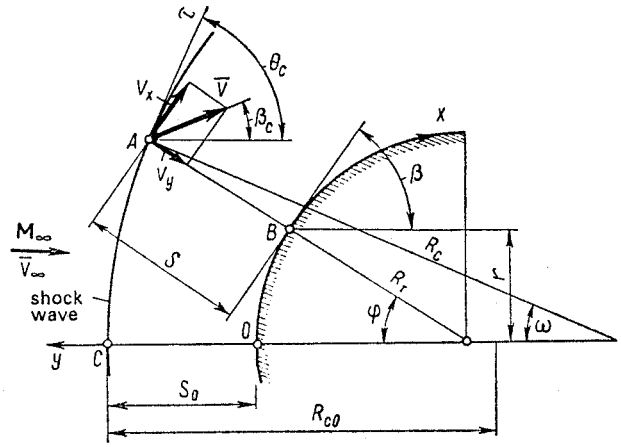

Fig. 9.4.6. Blunt spherical nose in a supersonic flow.

Quantities $[\text{grad}\,(V^2/2)]_1$ and $[\text{grad}\,(V^2/2)]_2$ can be determined with the help of relation (3.1.24). Replacing p by $V^2/2$, we have

$$\text{grad}\,\frac{V^2}{2}=\frac{1}{h_1}\cdot\frac{\partial(V^2/2)}{\partial q_1}i_1+\frac{1}{h_2}\cdot\frac{\partial(V^2/2)}{\partial q_2}i_2+\frac{1}{h_3}\cdot\frac{\partial(V^2/2)}{\partial q_3}i_3, \tag{9.4.8}$$

where q_1, q_2 and q_3 are determined by the values of (2.4.40).

Since the case of an axisymmetrical flow is being considered we can write

$$\partial(V^2/2)/\partial q_3=\partial(V^2/2)/\partial\gamma=0.$$

Keeping in view the value of (2.4.42) for Lame's parameters h_1 and h_2, equation (9.4.8) can be written in the form:

$$\left(\text{grad}\,\frac{V^2}{2}\right)_1 i_1+\left(\text{grad}\,\frac{V^2}{2}\right)_2 i_2=\left(1+\frac{y}{R_T}\right)^{-1}\times\frac{\partial(V^2/2)}{\partial x}i_1+\frac{\partial(V^2/2)}{\partial y}i_2,$$

from which

$$\left.\begin{aligned}\left(\operatorname{grad}\frac{V^2}{2}\right)_1&=\left(1+\frac{y}{R_T}\right)^{-1}\frac{\partial(V^2/2)}{\partial x};\\ \left(\operatorname{grad}\frac{V^2}{2}\right)_2&=\frac{\partial(V^2/2)}{\partial y}.\end{aligned}\right\} \tag{9.4.9}$$

Let us consider the vector product

$$\operatorname{rot}\bar{V}\times\bar{V}=[(\operatorname{rot}\bar{V})_1\,i_1+(\operatorname{rot}\bar{V})_2\,i_2+(\operatorname{rot}\bar{V})_3\,i_3]\times(V_1i_1+V_2i_2+V_3i_3).$$

From this the components:

$$\begin{aligned}(\operatorname{rot}\bar{V}\times\bar{V})_1&=(\operatorname{rot}\bar{V})_2\,V_3-(\operatorname{rot}\bar{V})_3V_2;\\ (\operatorname{rot}\bar{V}\times\bar{V})_2&=-(\operatorname{rot}\bar{V})_1\,V_3+(\operatorname{rot}\bar{V})_3V_1.\end{aligned}$$

Since an axisymmetrical flow is being investigated it is necessary to take $\bar{V}_3=0$ in these expressions. The component of vector $(\operatorname{rot}\bar{V})_3$, by (3.1.28), will be

$$(\operatorname{rot}\bar{V})_3=\frac{1}{h_1h_2}\left[\frac{\partial(h_2V_2)}{\partial q_1}-\frac{\partial(h_1V_1)}{\partial q_2}\right]$$

or, taking into account (2.4.40) and (2.4.42), it will be given by

$$(\operatorname{rot}\bar{V})_3=\left(1+\frac{y}{R_T}\right)^{-1}\left\{\frac{\partial V_y}{\partial x}-\frac{\partial\left[\left(1+\frac{y}{R_T}\right)V_x\right]}{\partial y}\right\}. \tag{9.4.10}$$

Therefore

$$\left.\begin{aligned}(\operatorname{rot}\bar{V}\times\bar{V})_1&=-(\operatorname{rot}\bar{V})_3\,V_2\\ &=-\left(1+\frac{y}{R_T}\right)^{-1}V_y\left\{\frac{\partial V_y}{\partial x}-\frac{\partial\left[\left(1+\frac{y}{R_T}\right)V_x\right]}{\partial y}\right\};\\ (\operatorname{rot}\bar{V}\times\bar{V})_2&=(\operatorname{rot}\bar{V})_3\,V_1\\ &=\left(1+\frac{y}{R_T}\right)^{-1}V_x\left\{\frac{\partial V_y}{\partial x}-\frac{\partial\left[\left(1+\frac{y}{R_T}\right)V_x\right]}{\partial y}\right\}.\end{aligned}\right\} \tag{9.4.11}$$

From (3.1.24) it follows that

$$(\operatorname{grad}p)_1=\frac{1}{h_1}\cdot\frac{\partial p}{\partial q_1},\quad(\operatorname{grad}p)_2=\frac{1}{h_2}\cdot\frac{\partial p}{\partial q_2}$$

or, recalling (2.4.40) and (2.4.42),

$$(\operatorname{grad} p)_1=\left(1+\frac{y}{R_T}\right)^{-1}\frac{\partial p}{\partial x},\quad (\operatorname{grad} p)_2=\frac{\partial p}{\partial y}. \tag{9.4.12}$$

Inserting (9.4.9), (9.4.11), (9.4.12) in (9.4.7), we get

$$\left(1+\frac{y}{R_T}\right)^{-1}\frac{\partial(V^2/2)}{\partial x}-\left(1+\frac{y}{R_T}\right)^{-1}V_y\left\{\frac{\partial V_y}{\partial x}-\frac{\partial[(1+y/R_T)V_x]}{\partial y}\right\}=-\frac{(1+y/R_T)^{-1}}{\rho}\cdot\frac{\partial p}{\partial x};$$

$$\frac{\partial(V^2/2)}{\partial y}+\left(1+\frac{y}{R_T}\right)^{-1}V_x\left\{\frac{\partial V_y}{\partial x}-\frac{\partial[(1+y/R_T)V_x]}{\partial y}\right\}=-\frac{1}{\rho}\cdot\frac{\partial p}{\partial y}.$$

After simplifying these relations we get the following equations of motion:

$$\frac{V_x}{1+y/R_T}\cdot\frac{\partial V_x}{\partial x}+V_y\frac{\partial V_x}{\partial y}+\frac{V_xV_y}{y+R_T}=-\frac{1}{\rho(1+y/R_T)}\cdot\frac{\partial p}{\partial x}; \tag{9.4.13}$$

$$\frac{V_x}{1+y/R_T}\cdot\frac{\partial V_y}{\partial x}+V_y\frac{\partial V_y}{\partial y}-\frac{V_x^2}{y+R_T}=-\frac{1}{\rho}\cdot\frac{\partial p}{\partial y}. \tag{9.4.14}$$

It is necessary to combine the equation of continuity with the equations of motion. For a steady flow ($\partial\rho/\partial t=0$), according to (2.4.46), this is written in the form

$$\frac{\partial(\rho r\,V_x)}{\partial x}+\frac{\partial[\rho r\,(1+y/R_T)\,V_y]}{\partial y}=0. \tag{9.4.15}$$

If the region in the neighborhood of the critical point is considered and the oncoming flow has very high supersonic speed the basic equations (9.4.13) through (9.4.15) can be simplified. Actually the flow behind the shock wave under these conditions is incompressible by nature because the Mach number $\mathbf{M}_2$ hardly differs from the value $[(k-1)/2k]^{1/2}$ corresponding to the case of a limiting flow (as $\mathbf{M}_\infty\to\infty$, $k=\text{const}$) behind a normal shock. Consequently density in the region in question can be assumed constant and equal to ρ_{c0}, the density behind the shock wave at the point of complete stagnation. Thus the variable density ρ in the equations of motion and continuity can be replaced by a constant quantity ρ_{c0}.

As very high speeds are being considered the shock wave in this case will move nearer to the surface of the body. Here the region of disturbed flow is assumed to be a thin layer of some thickness s which is very small compared to the radius of curvature R_T of the surface.

In this way, if $s/R_T\ll 1$ is assumed it is obvious that $y/R_T\ll 1$ as $0\leqslant y\leqslant s$. Hence the quantity y/R_T in comparison of unity can be neglected in equations of motion (9.4.13), (9.4.14) and equation of continuity (9.4.15). Taking into account the above simplifications and noting that the quantity r in (9.4.15)

can be assumed to be equal to $r \approx x$ under the conditions near the points of stagnation, equations (9.4.13) through (9.4.15) will be written in the form:

$$V_x \frac{\partial V_x}{\partial x} + V_y \frac{\partial V_x}{\partial y} + \frac{V_x V_y}{R_T} = -\frac{\bar{\rho}}{\rho_\infty} \cdot \frac{\partial p}{\partial x}; \tag{9.4.16}$$

$$V_x \frac{\partial V_y}{\partial x} + V_y \frac{\partial V_y}{\partial y} - \frac{V_x^2}{R_T} = -\frac{\bar{\rho}}{\rho_\infty} \cdot \frac{\partial p}{\partial y}; \tag{9.4.17}$$

$$\frac{\partial (xV_x)}{\partial x} + \frac{\partial (xV_y)}{\partial y} = 0. \tag{9.4.18}$$

In equations (9.4.16) and (9.4.17) nondimensional density

$$\bar{\rho} = \rho_\infty / \rho \approx \rho_\infty / \rho_{c0} = \text{const}$$

is introduced.

Let us show equations (9.4.16) and (9.4.17) can be further simplified. For this purpose we consider the order of magnitude of the terms appearing in these equations. Physically the order of value of V_y will be $V_y \sim V_{c0}$, where V_{c0} is the velocity behind the straight part of a shock wave. The order of magnitude of the coordinate x and y in the immediate vicinity of the stagnation point is determined by the quantities $x \sim s_0$, $y \sim s_0$ (s_0 is the distance from the straight part of a shock wave to the surface of the nose).

From equation (9.4.18) it follows that the order of magnitude

$$xV_x \sim \int_0^{s_0} \frac{\partial (xV_y)}{\partial y}\, dx$$

or

$$s_0 V_x \sim \int_0^{s_0} \frac{s_0 V_{c0}}{s_0}\, dx,$$

whence $V_x \sim V_{c0}$. So the order of magnitude of the velocity component V_x will be the same as V_y. It can easily be seen that the order of magnitude of the third terms on the left side of the equation will be V_{c0}^2/R_T and that of the remaining terms V_{c0}^2/s_0. Since $s_0 \ll R_T$ the third terms are of lower order and can be neglected.

In this way equation (9.4.16) and (9.4.17) may be replaced by

$$V_x \frac{\partial V_x}{\partial x} + V_y \frac{\partial V_x}{\partial y} = -\frac{\bar{\rho}}{\rho_\infty} \cdot \frac{\partial p}{\partial x}; \tag{9.4.16'}$$

$$V_x \frac{\partial V_y}{\partial x} + V_y \frac{\partial V_y}{\partial y} = -\frac{\bar{\rho}}{\rho_\infty} \cdot \frac{\partial p}{\partial y}. \tag{9.4.17'}$$

The solution of the system of equations (9.4.16'), (9.4.17'), (9.4.18) must satisfy the boundary conditions at any point of the surface of the body at

$y=0$ the normal velocity component $V_y=0$ and then at the point of complete stagnation, i.e. at $y=x=0$, the corresponding velocity components $V_x=V_y=0$. The boundary conditions immediately behind the shock should also be satisfied by the solution. These conditions, for the velocity components at a point A situated at a distance S from the surface of the nose, will have the form (see Fig. 9.4.6):

$$V_x=V_c\cos(\beta-\beta_c); \tag{9.4.19}$$

$$V_y=-V_c\sin(\beta-\beta_c), \tag{9.4.20}$$

where β is the angle of inclination of a tangent surface at a point B on the same normal on which point A is situated.

The total velocity V_c immediately behind the shock is determined with the help of formula (4.3.18). Taking $V_2=V_c$, $V_1=V_\infty$ and $\rho_1/\rho_2\approx\rho_\infty/\rho_{c0}=\bar{\rho}$ in this formula, we have

$$V_c/V_\infty=(\cos^2\theta_c+\bar{\rho}^2\sin^2\theta_c)^{1/2}. \tag{9.4.21}$$

The solution of the problem of flow-interaction in the neighborhood of complete stagnation may lead to the solution of the velocity field. Thus the problem being considered will be a purely kinematic problem. To solve it we have to exclude density and pressure from the equations of motion. For this purpose we differentiate (9.4.16′) and (9.4.17′) with respect to y and x:

$$\frac{\partial V_x}{\partial y}\cdot\frac{\partial V_x}{\partial x}+V_x\frac{\partial^2 V_x}{\partial x\partial y}+\frac{\partial V_y}{\partial y}\cdot\frac{\partial V_x}{\partial y}+V_y\frac{\partial^2 V_x}{\partial y^2}=-\frac{\bar{\rho}}{\rho_\infty}\cdot\frac{\partial^2 p}{\partial x\,\partial y}; \tag{9.4.22}$$

$$\frac{\partial V_x}{\partial x}\cdot\frac{\partial V_y}{\partial x}+V_x\frac{\partial^2 V_y}{\partial x^2}+\frac{\partial V_y}{\partial x}\cdot\frac{\partial V_y}{\partial y}+V_y\frac{\partial^2 V_y}{\partial y\partial x}=-\frac{\bar{\rho}}{\rho_\infty}\cdot\frac{\partial^2 p}{\partial y\partial x}. \tag{9.4.23}$$

Next we introduce the function determining double the value of the vortex component [component of rotation of velocity $(\mathrm{rot}\,\bar{V})_z=2\omega_z$; see (2.2.3)]:

$$2\omega_z=\Omega_z=\frac{\partial V_x}{\partial y}-\frac{\partial V_y}{\partial x}. \tag{9.4.24}$$

Using the function (9.4.24) and equation of continuity (9.4.18), equations (9.4.22) and (9.4.23) can be transformed. Since the right sides of these equations are identical we get

$$\frac{\partial V_x}{\partial y}\cdot\frac{\partial V_x}{\partial x}+V_x\frac{\partial^2 V_x}{\partial x\,\partial y}+\frac{\partial V_y}{\partial y}\cdot\frac{\partial V_x}{\partial y}+V_y\frac{\partial^2 V_x}{\partial y^2}$$
$$-\frac{\partial V_x}{\partial x}\cdot\frac{\partial V_y}{\partial x}-V_x\frac{\partial^2 V_y}{\partial x^2}-\frac{\partial V_y}{\partial x}\cdot\frac{\partial V_y}{\partial y}-V_y\frac{\partial^2 V_y}{\partial y\,\partial x}=0;$$

$$\left(\frac{\partial V_x}{\partial y}-\frac{\partial V_y}{\partial x}\right)\left(\frac{\partial V_x}{\partial x}+\frac{\partial V_y}{\partial y}\right)+V_x\left(\frac{\partial^2 V_x}{\partial x\,\partial y}-\frac{\partial^2 V_y}{\partial x^2}\right)$$
$$+V_y\left(\frac{\partial^2 V_x}{\partial y^2}-\frac{\partial^2 V_x}{\partial y\,\partial x}\right)=0. \qquad (9.4.25)$$

From (9.4.24) it follows that

$$\frac{\partial^2 V_x}{\partial x\,\partial y}-\frac{\partial^2 V_y}{\partial x^2}=\frac{\partial \Omega_z}{\partial x},\quad \frac{\partial^2 V_x}{\partial y^2}-\frac{\partial^2 V_y}{\partial y\,\partial x}=\frac{\partial \Omega_z}{\partial y}.$$

Now equation of continuity (9.4.18) gives

$$\frac{\partial V_x}{\partial x}+\frac{\partial V_y}{\partial y}=-\frac{V_x}{x}.$$

Therefore equation (9.4.25), in which $(\partial V_x/\partial y)-(\partial V_y/\partial x)=\Omega_z$, can be written in the form

$$\frac{\Omega_z V_x}{x}=V_x\frac{\partial \Omega_z}{\partial x}+V_y\frac{\partial \Omega_z}{\partial y}. \qquad (9.4.25')$$

Thus the problem lies in finding the solutions of equations (9.4.18) and (9.4.25') satisfying the above boundary conditions.

We will find the solution for V_x in the neighborhood of a point of complete stagnation with coordinates $x=0$, $y=0$ in series form:

$$V_x=a_0(y)+a_1(y)\,x+a_2(y)\,x^2+a_3(y)x^3+\ldots, \qquad (9.4.26)$$

in which x is a small parameter and the coefficients a_n are some functions of coordinate y.

The structure of the series (9.4.26) can be somewhat simplified. In fact the function $V_x(x)$ will be odd due to symmetry of flow, i.e. the values of velocity components will be equal in magnitude but opposite in sign for the corresponding values of x which are equal in magnitude but opposite in sign. Therefore only the terms with odd powers of x in the series expansion (9.4.26) are maintained, i.e.

$$V_x=a_1(y)\,x+a_3(y)\,x^3+\ldots. \qquad (9.4.27)$$

Taking into account that a region in the immediate vicinity of the complete stagnation point is being examined, the terms containing the third or higher power of x can be neglected. In this way, we arrive at the expression

$$V_x=a_1(y)x. \qquad (9.4.28)$$

Let us introduce the function

$$F(y)=\int_0^y a_1(y)dy, \qquad (9.4.29)$$

so that

$$dF/dy=F'(y)=a_1(y) \text{ and } F(0)=0. \tag{9.4.30}$$

Then

$$V_x=xF'(y). \tag{9.4.31}$$

Substituting the expression for V_x from (9.4.31) in the equation of continuity (9.4.18), we get:

$$xF'(y)+xF''(y)+x\frac{\partial V_y}{\partial y}=0.$$

From this we find the expression for the other velocity component:

$$V_y=-2\int F'(y)dy+f(x)=-2F(y)+f(x),$$

where $f(x)$ is some arbitrary function of x. From the condition of smooth flow over a body $V_y(x, 0)=0$ and hence,

$$f(x)=-2F(0).$$

But according to (9.4.30) function $F(0)=0$, so $f(x)=0$ and

$$V_y=-2F(y). \tag{9.4.32}$$

To determine the nature of function $F(y)$ we insert (9.4.31) and (9.4.32) in (9.4.25'):

$$[xF''(y)/x]V_x=V_xF''(y)-2F(y)F'''(y).$$

According to (9.4.32) the function $F(y)\neq 0$, so

$$F'''(y)=0. \tag{9.4.33}$$

The general solution of this equation is

$$F(y)=-V_y/2=c_0+c_1y+c_2y^2. \tag{9.4.34}$$

As $V_y=0$ at $y=0$ the constant $c_0=0$. The other two coefficients can be determined if the conditions on the shock wave near the critical point as $x\to 0$ are applied. In particular, it follows from the condition (9.4.21) that the velocity immediately behind the "straight" part of the shock wave ($\theta_c=\pi/2$) at a point C (see Fig. 9.4.6) will be equal to

$$V_y=V_c=-\bar{\rho}V_\infty.$$

Since the coordinate of this point $y=s_0$ we get

$$V_y=V_c=-2(c_1s_0+c_2s_0^2).$$

Therefore the first condition for determination of the coefficients c_1 and c_2 will be

$$\bar{\rho}V_\infty = 2(c_1 s_0 + c_2 s_0^2). \tag{9.4.35}$$

To find the second equation we differentiate (9.4.34) with respect to y:

$$F'(y) = c_1 + 2c_2 y.$$

According to this result and equation (9.4.31) the velocity component will be

$$V_x = x(c_1 + 2c_2 y). \tag{9.4.36}$$

Let us take point A on the shock wave at a distance $y = s$ from the surface of the nose section. Equating the velocity V_x obtained from (9.4.36)

$$V_{xA} = x(c_1 + 2c_2 s)$$

and its value from (9.4.19) on the shock wave

$$V_{xA} = V_c \cos(\beta - \beta_c),$$

we get

$$x(c_1 + 2c_2 s) = V_c \cos(\beta - \beta_c).$$

Taking the limit as $x \to 0$ and assuming $s = s_0$, $V_c = \bar{\rho} \cdot V_\infty$, we get the relation corresponding to the point C on the straight part of the shock wave:

$$\lim_{x \to 0} \frac{\cos(\beta - \beta_c)}{x} = \frac{c_1 + 2c_2 s_0}{\bar{\rho} V_\infty}. \tag{9.4.37}$$

The limit on the left side can be calculated in the following way: It can be seen from Fig. 9.4.6 that the angle $(\beta - \beta_c)$ at a point A on the shock wave is

$$\beta - \beta_c = (\pi/2) - (\varphi + \beta_c).$$

Consequently $\cos(\beta - \beta_c) = \sin(\varphi + \beta_c)$. Around the point of complete stagnation the angles φ and β_c are small and it may be assumed that $\cos(\beta - \beta_c) \approx \varphi + \beta_c$.
Accordingly

$$\lim_{x \to 0} \frac{\cos(\beta - \beta_c)}{x} = \lim_{x \to 0} \frac{\varphi}{x} + \lim_{x \to 0} \frac{\beta_c}{x}.$$

It is obvious that $\lim_{x \to 0} (\varphi/x) = 1/R_T$ and the second limit can be represented as

$$\lim_{x \to 0} \frac{\beta_c}{x} = \lim_{x \to 0} \left(\frac{\beta_c}{\omega} \cdot \frac{\omega}{x} \right) = \left(\frac{\beta_c}{\omega} \right)_{x=0} \cdot \frac{1}{R_{c0}}, \tag{9.4.38}$$

where

$$\lim_{x \to 0} \frac{\beta_c}{\omega} = \left(\frac{\beta_c}{\omega} \right)_{x=0}, \quad \lim_{x \to 0} \frac{\omega}{x} = \frac{1}{R_{c0}}.$$

Quantity R_{c0} is the radius of curvature of the shock wave at its apex (if R_c is the variable value of the radius of curvature of the shock wave, $R_{c0}=\lim_{x\to 0} R_c$). The angle ω, as can be seen from Fig. 9.4.6, is connected with the angle of inclination of shock wave θ_c by the formula

$$\omega=(\pi/2)-\theta_c. \tag{9.4.39}$$

To determine $(\beta_c/\omega)_{x=0}$ we use formula (4.2.19), which can be rewritten with the help of (4.2.21) and (9.4.39) as

$$\rho_\infty/\rho_c=[\tan(\theta_c-\beta_c)]/\tan\theta_c=\tan\omega/\tan(\omega+\beta_c).$$

For small values of ω and β_c

$$\rho_\infty/\rho_c=\omega/(\omega+\beta_c).$$

Hence

$$\lim_{x\to 0}\frac{\beta_c}{\omega}=\lim_{x\to 0}\left(\frac{\rho_c}{\rho_\infty}-1\right)$$

or

$$\left(\frac{\beta_c}{\omega}\right)_{x=0}=\frac{\rho_{c0}}{\rho_\infty}-1=\frac{1}{\bar{\rho}}-1.$$

In this way

$$\lim_{x\to 0}\frac{\cos(\beta-\beta_c)}{x}=\frac{1}{R_T}+\left(\frac{1}{\bar{\rho}}-1\right)\frac{1}{R_{c0}}.$$

Inserting this expression in (9.4.37), we have:

$$\frac{1}{R_T}+\left(\frac{1}{\bar{\rho}}-1\right)\frac{1}{R_{c0}}=\frac{c_1+2c_2s_0}{\bar{\rho}V_\infty}$$

or

$$\frac{R_{c0}}{R_T}+\frac{1}{\bar{\rho}}-1=\frac{R_{c0}(c_1+2c_2s_0)}{\bar{\rho}V_\infty}.$$

At high speed we can assume that $R_{c0}/R_T\approx 1$, so

$$c_1+2c_2s_0=V_\infty/R_{c0}. \tag{9.4.40}$$

Along with c_1, c_2 a third unknown has appeared, the distance s_0 from the shock wave to the nose, in equations (9.4.35) and (9.4.40). Therefore we must add one more independent equation to the system of (9.4.35) and (9.4.40). This additional equation arises from the expression for vortex

$$\Omega_z=\frac{\partial V_x}{\partial y}-\frac{\partial V_y}{\partial x}=\frac{\partial}{\partial y}\left[x(c_1+2c_2y)\right]$$
$$-\frac{\partial}{\partial x}\left[-2(c_1y+c_2y^2)\right]=2c_2x. \tag{9.4.41}$$

The relation (9.4.41) can be used to determine the vortex on the surface of the nose as well as immediately behind the shock wave in the flow region around the point of complete stagnation. The vortex in the flow behind the shock wave can also be found from the expression (9.4.6) which, according to the relation $i+(V^2/2)=\text{const}$, is transformed into:

$$\text{rot}\,\bar{V}\times\bar{V}=\text{grad}\,i-(1/\rho)\,\text{grad}\,p. \tag{9.4.42}$$

Now we use the known thermodynamic relation for entropy

$$TdS=di-(dp/\rho). \tag{9.4.43}$$

The vector relation can be written from this equation:

$$T\,\text{grad}\,S=\text{grad}\,i-(1/\rho)\,\text{grad}\,p. \tag{9.4.44}$$

From this equation (9.4.42) can be given in the form

$$\text{rot}\,\bar{V}\times\bar{V}=T\,\text{grad}\,S. \tag{9.4.45}$$

This equation can be reduced to the conditions on the shock wave. Let us take an arbitrary point A on it (see Fig. 9.4.6). Taking the projections of vectors appearing in (9.4.5) along tangent τ, we get the relation

$$(\text{rot}\,\bar{V}\times\bar{V})_\tau=T_2(dS_2/d\tau), \tag{9.4.46}$$

where T_2 is the temperature at a point A immediately behind the shock. The component $(\text{rot}\,\bar{V}\times\bar{V})_\tau$ of the vector product is determined in the following way: The vector rot $\bar{V}$ at a point A with mode Ω_z is oriented along the normal to a vertical plane of symmetry (Fig. 9.4.7, a). Quantity $\bar{V}$ represents the velocity vector behind shock wave $\bar{V}=\bar{V}_c$ lying in this plane of symmetry. Due to the orthogonality of vectors rot $\bar{V}$ and $\bar{V}$ their vector product in absolute value will be

$$|\text{rot}\,\bar{V}\times\bar{V}|=|\text{rot}\,\bar{V}||\bar{V}|\sin\pi/2=\Omega_z V_c.$$

The vector equal to the vector product rot $\bar{V}\times\bar{V}$, perpendicular to the plane of vectors rot $\bar{V}$ and $\bar{V}$, is obviously situated in the plane of symmetry like vector $\bar{V}=\bar{V}_c$ (see Fig. 9.4.7, a). As can be seen from Fig. 9.4.7 the component of vector product rot $\bar{V}\times\bar{V}$ along the tangent is equal to

$$(\text{rot}\,\bar{V}\times\bar{V})_\tau=\Omega_z V_c\sin(\theta_c-\beta_c). \tag{9.4.47}$$

Equation (9.4.43) can be used to determine the right side of (9.4.46) by applying it to the same point immediately behind the shock wave:

$$T_2dS_2=di_2-(dp_2/\rho_2). \tag{9.4.43'}$$

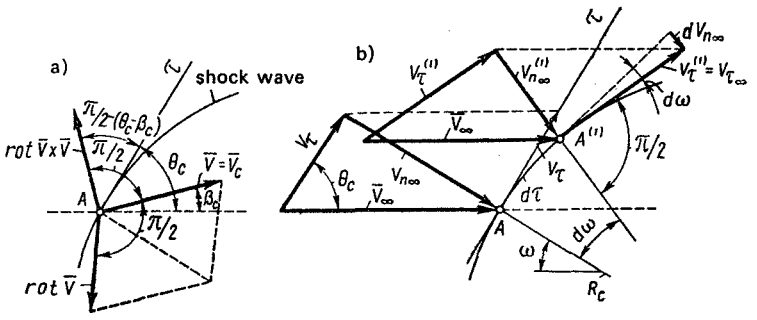

Fig. 9.4.7. Determination of vortex strength on shock wave.

We take the equations of enthalpy i_2 and pressure p_2 in the form of (4.2.6) and (4.2.4) respectively. Since high-speed flows are being considered at which $i_1 \ll i_2$ and $p_1 \ll p_2$ these equations can be written as:

$$i_2 = V(_{n1}^2/2) - (V_{n2}^2/2); \tag{9.4.48}$$

$$p_2 = \rho_1 V_{n1}^2 - \rho_2 V_{n2}^2; \tag{9.4.49}$$

or, taking into account (4.2.3), as

$$i_2 = [V_{n\infty}^2(1-\bar{\rho}^2)]/2; \tag{9.4.48'}$$

$$p_2 = \rho_1 V_{n\infty}^2(1-\bar{\rho}), \tag{9.4.49'}$$

where it is assumed that $V_{n1} = V_{n\infty}$, $\bar{\rho} = \rho_1/\rho_2 = \rho_\infty/\rho$.
Differentiating, we get

$$di_2 = (1-\bar{\rho}^2)V_{n\infty}\, dV_{n\infty} - V_{n\infty}^2 \bar{\rho} d\bar{\rho};$$
$$dp_2 = 2(1-\bar{\rho})\rho_1 V_{n\infty}\, dV_{n\infty} - \rho_1 V_{n\infty}^2 d\bar{\rho}.$$

Substituting these expressions in (9.4.43'), we get

$$T_2 dS_2 = (1-\bar{\rho})^2 V_{n\infty} dV_{n\infty}. \tag{9.4.50}$$

From Fig. 9.4.7, b it follows that the increment in the normal component of velocity $dV_{n\infty} = V_\tau^{(1)} d\omega$. Here, since velocity $V_\tau^{(1)}$ at a point $A^{(1)}$ lying at a small distance from a given point A differs from velocity V_τ at a point A by infinitesimally small quantity, the differential

$$dV_{n\infty} = V_\tau d\omega = V_\tau\, (d\tau/R_c), \tag{9.4.51}$$

where $R_c = d\tau/d\omega$ is the radius of curvature of the wave at a point A (see Fig. 9.4.7, b).

According to (9.4.51) equation (9.4.50) will be rewritten as

$$T_2 dS_2 = (1-\bar{\rho})^2 V_{n\infty}\, V_\tau\, (d\tau/R_c). \tag{9.4.52}$$

Inserting (9.4.47) and (9.4.52) in (9.4.46), we find

$$\Omega_z V_c \sin(\theta_c-\beta_c)=\frac{(1-\bar{\rho})^2 V_{n\infty} V_\tau}{R_c}.$$

Use of formula (9.4.21) for V_c and the expressions

$$\left.\begin{aligned} V_{n\infty}&=V_\infty \sin\theta_c;\\ V_\tau&=V_\infty\cos\theta_c, \end{aligned}\right\} \tag{9.4.53}$$

which are obtained from the velocity triangle in Fig. 9.4.7, b gives the expression for the vortex

$$\Omega_z=\frac{V_\infty(1-\bar{\rho})^2\sin\theta_c\cos\theta_c}{(\bar{\rho}^2\sin^2\theta_c+\cos^2\theta_c)^{1/2}R_c}. \tag{9.4.54}$$

Replacing θ_c by $\pi/2-\omega$ here, we get

$$\Omega_z=\frac{V_\infty(1-\bar{\rho})^2\cos\omega\sin\omega}{(\bar{\rho}^2\cos^2\omega+\sin^2\omega)^{1/2}R_c}. \tag{9.4.54'}$$

In the neighborhood of the point of complete stagnation where ω are small and $R_c\to R_{c0}$ the above expression reduces to

$$\Omega_z=\frac{V_\infty(1-\bar{\rho})^2\omega}{\bar{\rho}R_{c0}}. \tag{9.4.54''}$$

Equating the right side of (9.4.41) and (9.4.54'') and taking into account that $\omega/x=1/R_{c0}$, we find the coefficient

$$c_2=\frac{V_\infty(1-\bar{\rho})^2}{2\bar{\rho}R_{c0}^2}. \tag{9.4.55}$$

Substituting this value of c_2 in equation (9.4.35), (9.4.40) and solving them simultaneously, we get the relation for the second coefficient c_1:

$$c_1=(\pm V_\infty/R_{c0})\sqrt{2\bar{\rho}-\bar{\rho}^2}. \tag{9.4.56}$$

Velocity on the surface of the nose is determined from (9.4.36) under the condition that $y=0$:

$$V_x=xc_1=\pm(xV_\infty/R_{c0})\sqrt{2\bar{\rho}-\bar{\rho}^2}. \tag{9.4.57}$$

From the properties of odd function V_x it follows that at $x>0$ or $x<0$ we must get $V_x>0$ or $V_x<0$ respectively. This means that in formula (9.4.57) and hence in equation (9.4.56) for c_1 we must take the plus sign.

Shift and form of main shock wave: Along with the coefficient c_1 the solution of the system of equations (9.4.35), (9.4.40) gives the relation for shift s_0 of a shock wave from the nose of a body:

$$s_0=\left(\frac{V_\infty}{R_{c0}}-c_1\right)\frac{1}{2c_2}.$$

Using the respective values of c_2 and c_1 from (9.4.55) and (9.4.56) with the plus sign here we have:

$$s_0=\frac{\bar{\rho}R_{c0}}{(1-\bar{\rho})^2}\left[1-\left(2\bar{\rho}-\bar{\rho}^2\right)^{1/2}\right]. \tag{9.4.58}$$

The radius of curvature R_{c0} of the wave about the axis of the body makes its appearance in this formula. This radius is supposed to be a function of the radius of spherical part R_T for given conditions of undistributed flow. If the wave is assumed to be concentric with the sphere, $R_{c0}=R_T+s_0$. Introducing new notations:

$$\bar{R}_{c0}=R_{c0}/R_T,\ \tilde{s}_0=s_0/R_{c0},$$

we can write

$$\bar{R}_{c0}=1/(1-\tilde{s}_0). \tag{9.4.59}$$

In reality the spherical nose and shock wave are not found to be concentric. The corresponding deviation from the relation (9.4.59) will increase with a rise in Mach number M_∞. To calculate the deviation from the concentric of the shock wave with a spherical nose we use the relation obtained from experimental data:

$$\bar{R}_{c0}=R_{c0}/R_T=1/(1-\tilde{s}_0)^{2.5}\ . \tag{9.4.60}$$

Accordingly the shift in terms of the radius of the spherical nose will be

$$\bar{s}_0=\frac{s_0}{R_T}=\frac{s_0}{R_{c0}}\cdot\frac{R_{c0}}{R_T}=\tilde{s}_0(1-\tilde{s}_0)^{-2.5}\ , \tag{9.4.61}$$

where $\tilde{s}_0$ is taken in accordance with (9.4.58) in the form

$$\tilde{s}_0=\frac{\bar{\rho}}{(1-\bar{\rho})^2}\left[1-(2\bar{\rho}-\bar{\rho}^2)^{1/2}\right]. \tag{9.4.62}$$

Quantity $\bar{s}_0$ calculated by formulas (9.4.61), (9.4.62) is shown as a function of $\bar{\rho}=\rho_\infty/\rho_c$ in Fig. 9.4.8, a. In the range up to $\bar{\rho}<0.4$ the curve shown in Fig. 9.4.8, a characterizing variation of shift for a shock wave about a spherical nose can be extrapolated by the simple relation [52]

$$\bar{s}_0=0.52[\bar{\rho}/(1-\bar{\rho})]^{0.86}. \tag{9.4.63}$$

In the relations obtained above the nondimensional density $\bar{\rho}=\rho_\infty/\rho_c$ happens to be the similarity parameter for the relative shift $\bar{s}_0=s_0/R_T$. It is determined from the conditions of equilibrium of dissociation immediately behind the straight part of a shock wave.

The results of calculation for the relative shift of a shock wave obtained in the work [52] are of special interest. These results are reproduced in graphic form in Fig. 9.4.8, b. They indicate the variation in the $\bar{s}_0=s_0/R_T$ as a func-

tion of M_∞ for a sphere in flows of air, oxygen and nitrogen. It can be seen that for the values of Mach number $M_\infty = 9$ to 13, when the variation of specific heat of air is mainly based on dissociation of oxygen, the curve $\bar{s}_0$ (M_∞) for air occupies a place nearer to the corresponding curve for oxygen. With an increase in M_∞ the dissociation of nitrogen plays an ever higher role. The curve characterizing the variation of relative shift of a shock wave for air comes closer to the corresponding curve for nitrogen because this component happens to account for a large proportion of air.

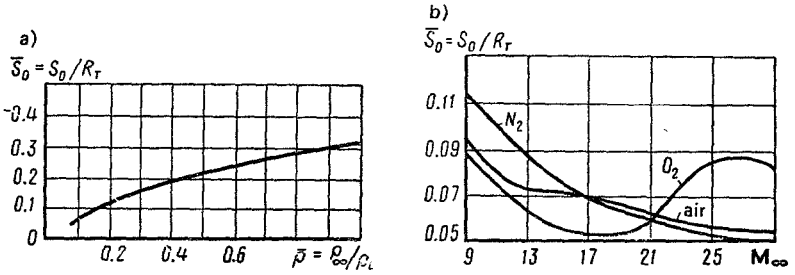

Fig. 9.4.8. Relative shift of shock wave in front of spherical nose in supersonic flow:

a—for air (with parameter $\bar{\rho}$); *b*—for oxygen, nitrogen and air (with parameter M_∞; $p_\infty = 0.01$ atm; $T_\infty = 290°K$).

The nature of the effect of dissociation and ionization on the shift of a shock wave is quite clear in the example of pure gases such as oxygen and nitrogen. At $M_\infty = 18$ oxygen is already considerably dissociated, density reaches maximum value as indicated by calculations and the distance $\bar{s}_0$ (see Fig. 9.4.8, b) will be minimum. With an increase in M_∞ oxygen becomes completely dissociated, compression is reduced and accordingly the value of the shift of shock wave increases. With a further increase in M_∞ the preliminary ionization of gas begins, its specific heat increases and consequently the compression of gas increases, which leads to a reduction of $\bar{s}_0$. The change in the specific heat of nitrogen appears at considerably higher Mach numbers M_∞ than for oxygen. Besides, the processes of dissociation and ionization in nitrogen do not take place one after another as in the case of oxygen but occur practically simultaneously. Therefore the non-monotonous nature of the variation of quantity $\bar{s}_0$ for nitrogen is less clearly expressed than for oxygen.

The character of the curve $\bar{s}_0$ for air, which is a volumetric mixture (about 26% oxygen and 74% nitrogen), will naturally be more monotonous than for pure oxygen, as can be seen from Fig. 9.4.8, b.

The form of the generator of the main shock wave can be determined by calculation based on the solution of the system of corresponding gas dynamic equations for a supersonic flow over blunt bodies. It can also be determined

by experiment. The interesting results of determination of the flow parameters in this problem and, in particular, the form of the shock wave are given in the work [52].

As indicated by calculations and experimental research for a supersonic flow over a cone with a spherical nose the generator of a shock wave can be represented with fair accuracy in the form of a hyperbola:

$$\frac{(x+a)^2}{a^2}-\frac{r^2}{b^2}=1, \tag{9.4.64}$$

which is shown in Fig. 9.4.9. The quantities a and b in equation (9.4.64) represent semiaxes of the hyperbola which may be determined in the following way: We know from analytical geometry that the radius of curvature at any point on the curve given by equation $r=r(x)$ will be

$$R=-(1+r'^2)^{3/2}/r'', \tag{9.4.65}$$

where $r'=dr/dx$, $r''=d^2r/dx^2$.

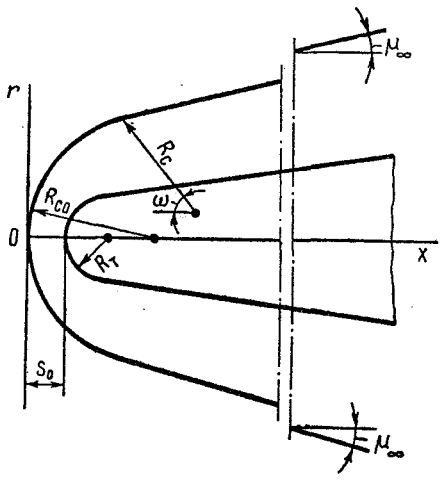

Fig. 9.4.9. Shock wave in front of cone with blunt spherical nose in supersonic flow.

According to (9.4.64)

$$r'=\frac{x+a}{r}\cdot\frac{b^2}{a^2};$$

$$r''=\frac{1}{r}\cdot\frac{b^2}{a^2}\left[1-\frac{(x+a)^2}{r^2}\cdot\frac{b^2}{a^2}\right],$$

or

$$r'=\left(1+\frac{r^2}{b^2}\right)^{1/2}\frac{b^2}{ra};$$

$$r''=-b^4/(r^3a^2).$$

Inserting the values of these derivatives in (9.4.65), we get

$$R=\frac{b^2}{a}\left[1+\frac{r^2}{b^2}\left(1+\frac{a^2}{b^2}\right)\right]^{3/2}. \tag{9.4.66}$$

Assuming $r=0$, we find the radius of curvature R_{c0} about the axis of the cone

$$R_{c0}=b^2/a. \tag{9.4.67}$$

According to this equation (9.4.66) can be rewritten in the form

$$R=R_{c0}\left[1+\frac{r^2}{b^2}\left(1+\frac{a^2}{b^2}\right)\right]^{3/2}. \tag{9.4.66'}$$

The shock wave traveling away from the body downstream must change to a

weak wave of disturbance whose angle of inclination with undisturbed velocity vector is determined by

$$\theta_c=\mu_\infty=\sin^{-1}(1/\mathbf{M}_\infty)=\tan^{-1}(1/\sqrt{\mathbf{M}_\infty^2-1}).$$

From the equation of hyperbola (9.4.64) it follows that the tangent of the angle of inclination for the generator of a shock wave at any arbitrary point will be

$$\tan\theta_c=r'=\left(1+\frac{r^2}{b^2}\right)^{1/2}\frac{b^2}{ra}\,.$$

Taking the limit as $r\to\infty$, we get

$$\lim_{r\to\infty}\tan\theta_c=\tan\mu_\infty=b/a=1/\sqrt{\mathbf{M}_\infty^2-1}\,. \tag{9.4.68}$$

Let us solve equations (9.4.67) and (9.4.68) simultaneously to find a and b:

$$\left.\begin{aligned} b&=R_{c0}\sqrt{\mathbf{M}_\infty^2-1};\\ a&=R_{c0}(\mathbf{M}_\infty^2-1).\end{aligned}\right\} \tag{9.4.69}$$

Now we can calculate the coordinates of the shock wave from (9.4.66′).

Initial gradient and distribution of velocity: According to (9.4.57) the velocity gradient at the point of complete stagnation (initial gradient) will be

$$\left(\frac{\partial V_x}{\partial x}\right)_{\substack{x=0\\y=0}}=\tilde{\lambda}=\frac{V_\infty}{R_{c0}}\sqrt{2\bar{\rho}-\bar{\rho}^2}. \tag{9.4.70}$$

Experimental verification indicated that if we assume

$$R_{c0}=R_T\,(1-\tilde{s}_0)^{-1/2}, \tag{9.4.71}$$

in formula (9.4.70), i.e. if it is based on the expression corresponding to the assumption of lowest shift of the concentric form of shock wave near the spherical surface of the nose, as follows from (9.4.60), then the results obtained for the initial velocity gradient will be applicable for very high as well as low supersonic speeds. The calculated relation will have the form

$$\tilde{\lambda}=(V_\infty/R_T)\sqrt{(2\bar{\rho}-\bar{\rho}^2\,(1-\tilde{s}_0)}\,. \tag{9.4.72}$$

Quantity $\tilde{s}_0$ can be expressed through the relative shift $\bar{s}_0$ with the help of the expression

$$\bar{s}_0=\frac{s_0}{R_T}=\frac{s_0}{R_{c0}}\cdot\frac{R_{c0}}{R_T}=\frac{\tilde{s}_0}{\sqrt{1-\tilde{s}_0}},$$

from which we find

$$\tilde{s}_0 = -\frac{\bar{s}_0^2}{2}\left(1-\sqrt{1+\frac{4}{\bar{s}_0^2}}\right). \tag{9.4.73}$$

In this formula the relative shift $\bar{s}_0$ can be determined from (9.4.63). The relation (9.4.72) is valid under the condition of application of expression (9.4.73) for the values $\bar{\rho} \leqslant 0.4$.

The distribution of velocity on the spherical surface of a nose in the vicinity of the point of complete stagnation can be expressed, in accordance with (9.4.70), through an initial gradient of velocity $\tilde{\lambda}$:

$$V_x = \tilde{\lambda} x. \tag{9.4.74}$$

Here x determines the length of the arc of a circle which can be calculated from the known central angle φ as $x = \varphi R_T$.
Taking this,

$$V_x = \tilde{\lambda} R_T \varphi. \tag{9.4.74'}$$

Experimental research showed that the relation (9.4.74'), corresponding, strictly speaking, to the conditions of flow-interaction of the small section of a sphere near the point of complete stagnation at a very high speed of undisturbed flow, can be applied for calculation of the velocity on a fairly large section of a curvilinear surface and also at comparatively low values of M_∞. Experiments in wind tunnels at Mach numbers M_∞ from 1.2 to 4.9 confirmed the linear relation (9.4.74') of velocity with angle $\varphi = 0$ to $\varphi = 50°$ and helped to establish that there is scope for small deviation from this relation in the range of $50° < \varphi < 90°$.

In practical calculation it is possible to use formula (9.4.74') with reasonably good accuracy for all values of φ from 0 to 90°.

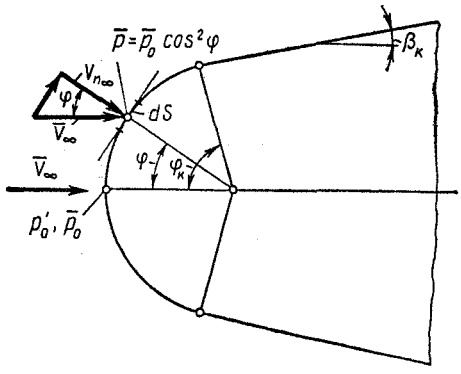

Fig. 9.4.10. Determination of pressure by Newton's method for supersonic flow past blunt-nosed body.

Application of Newton's method for calculation of flow-interaction of a blunt conical body: This method is based on Newton's corpuscular theory (known as the theory of Newtonian stagnation) according to which gas particles undergo disturbances only during bombardment against a solid wall and thereby completely lose the component of momentum normal to the wall. If V_n is a normal component of velocity of undisturbed flow, dS is an elementary area of surface in flow (Fig. 9.4.10), the loss of momentum in unit time for the point in question will be:

$$\rho_\infty V_{n\infty}(V_{n\infty}-0)\,dS=\rho_\infty V_{n\infty}^2 dS.$$

The value of an impulse force due to pressure difference $(p-p_\infty)\,dS$ during the same time, by the theorem of impulse of force, is determined by the loss of momentum. Hence at a given point the pressure difference will be

$$p-p_\infty=\rho_\infty V_{n\infty}^2.$$

Form Fig. 9.4.10 it can be seen that $V_{n\infty}=V_\infty\cos\varphi$, so

$$p-p_\infty=\rho_\infty V_\infty^2\cos^2\varphi.$$

Dividing the left and right sides of this equation by velocity head $\rho_\infty V_\infty^2/2$, we get the formula for coefficient of pressure

$$\bar{p}=\frac{2(p-p_\infty)}{\rho_\infty V_\infty^2}=2\cos^2\varphi, \tag{9.4.75}$$

which is known as Newton's formula. This formula corresponds to the model of flow interaction discussed above, i.e. to the model of Newton's in which the system of elastic reflection of gas particles during interaction with a surface is represented. This model has a defect: it does not give the correct answer, in principle, to the question of the way the gas particles behave after impact. In reality their velocity after impact will not be equal to the component of undisturbed flow velocity tangent to the surface. The velocities of these particles after local bombardment are not determined at all by this model. So in practice Newton's model is not considered as the process of flow-interaction of a body.

Euler's model is free from this defect. It deals with the study of a fluid flow about a surface, i.e. with the determination of velocity and other parameters at every point and, as a result, with the calculation of fluid and body interaction (see Chapter 2 Section 1).

However, in view of the simplicity and convenience of calculation using Newton's theory some attempts have been made to improve it to achieve better results for the calculation of aerodynamic parameters. Let us study one such modification. As can be seen from formula (9.4.75) the coefficient of pressure $\bar{p}_0=2$ at the point of complete stagnation for which the central angle $\varphi=0$. So equation (9.4.75) can be written in the form:

$$\bar{p}=\bar{p}_0\cos^2\varphi. \tag{9.4.75'}$$

Experimental research shows that if the value of $\bar{p}_0$ in (9.4.75') is taken either from experiment or from accurate theoretical calculations instead of $\bar{p}_0=2$, which is not found in real flows, formula (9.4.75') gives results very close to the actual ones over a considerable part of the spherical surface. Unlike (9.4.75), formula (9.4.75') is known as the modified or improved formula of Newton.

According to this formula the pressure difference will be

$$p-p_\infty=(p_0'-p_\infty)\cos^2\varphi,$$

whence the ratio of pressure p at a given point to pressure p_0' at the point of complete stagnation

$$p/p_0'=\cos^2\varphi+(p_\infty/p_0')\sin^2\varphi. \tag{9.4.76}$$

In the neighborhood of the point of complete stagnation the flow may be treated as incompressible within a certain approximation. To calculate it we can apply Bernoulli's equation

$$(V_x^2/2)+(p/\rho)=p_0'/\rho, \tag{9.4.77}$$

where ρ is the density, which is assumed to be constant in the neighborhood of the point of complete stagnation, and is equal to density ρ_0' at this point. After substitution of (9.4.77) in (9.4.76) under the condition that $\rho=\rho_0'$, we get

$$\frac{V_x^2}{2}=\frac{p_0'}{\rho_0'}-\frac{p}{\rho_0'}=\frac{p_0'}{\rho_0'}\left[1-\left(\cos^2\varphi+\frac{p_\infty}{p_0'}\sin^3\varphi\right)\right].$$

Let us calculate the derivative of V_x with respect to x:

$$V_x\frac{dV_x}{dx}=2\cos\varphi\sin\varphi\frac{d\varphi}{dx}\cdot\frac{p_0'}{\rho_0'}\left(1-\frac{p_\infty}{p_0'}\right).$$

Taking the limit with $\varphi\to0$, $x\to0$ and recalling that $(\cos\varphi)_{x\to0}=1$, $(\sin\varphi)_{x\to0}=\varphi=x/R_T$, $(V_x/x)_{x\to0}=(dV_x/dx)_{x\to0}=\tilde{\lambda}$, $(d\varphi/dx)_{x\to0}=1/R_T$, we find the relation for initial velocity gradient:

$$\left(\frac{dV_x}{dx}\right)_{x\to0}=\tilde{\lambda}=\frac{1}{R_T}\sqrt{\frac{2(p_0'-p_\infty)}{\rho_0'}}. \tag{9.4.78}$$

In accordance with this relation, to determine the initial velocity gradient it is necessary to know pressure p_0' and density ρ_0' at the point of complete stagnation.

According to the linear law expressed by the relation (9.4.74') the velocity distribution can be represented by the relation

$$V_x=\varphi\sqrt{[2(p_0'-p_\infty)]/\rho_0'}. \tag{9.4.78'}$$

Along with this formula for calculation of velocity it is possible to use the relation obtained from equation (3.6.26) for pressure in an isentropic flow. We take pressure p_0 in this equation equal to pressure p_0' at the point of complete stagnation, velocity V equal to velocity V_x at an arbitrary point on the surface and finally quantity k equal to the adiabatic index $\overline{k}$ calculated for the point of complete stagnation with the effect of temperature T_0' and pressure p_0' at this point. Solving this equation for velocity V_x, we get

$$V_x=V_{\max}[1-(p/p_0')^{(\overline{k}-1)/\overline{k}}]^{1/2}.$$

We get the expression for maximum velocity from (3.6.22):

$$V_{\max}^2=\frac{2}{k_\infty-1}a_\infty^2+V_\infty^2,$$

where flow parameters with index "∞" correspond to an undisturbed flow up to a shock wave. Dividing both parts of the equality by V_∞^2 and keeping in mind that $\mathbf{M}_\infty^2=V_\infty^2/a_\infty^2$, we get

$$\frac{V_{\max}^2}{V_\infty^2}=\frac{2}{k_\infty-1}\cdot\frac{1}{\mathbf{M}_\infty^2}+1.$$

According to this relation the expression for calculating velocity will have the form:

$$\frac{V_x}{V_\infty}=\left(\frac{2}{k_\infty-1}\cdot\frac{1}{\mathbf{M}_\infty^2}+1\right)^{1/2}\left[1-\left(\frac{p}{p_0'}\right)^{(\bar{k}-1)\bar{k}}\right]^{1/2}, \tag{9.4.79}$$

where the ratio p/p_0' is determined by Newton's formula (9.4.76).

The calculations of velocity and other gas parameters can be further simplified with the help of the tables of gas dynamic functions (see Chapter 3 Section 6). Knowing the law of variation of function $\pi(\lambda)=p/p_0'$ (9.4.76), it is possible to determine the values of gas dynamic functions $\lambda=V_x/a^*$, $\varepsilon=\rho/\rho_0'$ and $\tau=T/T_0'$ from the tables [53] for the corresponding value of $\bar{k}$. Assuming the critical speed of sound a^* and the flow parameters ρ_0', p_0', T_0' for the stagnation point here we find the following quantities for a given point on a blunt nose surface:

$$V_x=\lambda a^*,\ \rho=\varepsilon\rho_0',\ p=\pi p_0',\ T=\tau T_0'.$$

The gas parameters on the peripheral conical surface connected with the spherical nose can be taken within a certain approximation as those on the connecting line, i.e. at the end of the nose. In particular, the velocity on the cone can be found by formula (9.4.78′), assuming $\varphi=\pi/2-\beta_K$:

$$V_x=V_K=(\pi/2-\beta_K)\sqrt{[2(p_0'-p_\infty)]/\rho_0'}. \tag{9.4.80}$$

The second relation for velocity on the cone is obtained from the expression (9.4.79) if we consider, according to (9.4.76),

$$\frac{p}{p_0'}=\frac{p_K}{p_0'}=\sin^2\beta_K+\frac{p_\infty}{p_0'}\cos^2\beta_K \tag{9.4.81}$$

in this expression, where cone angle $\beta_K=\pi/2-\varphi_K$ [φ_K is the central angle for a semisphere (see Fig. 9.4.10)].

The velocity obtained in this way is supposed to be constant over the whole surface of the cone. Experiments show that the real velocity differs somewhat from this velocity and the velocity distribution has the specific character shown in Fig. 9.4.11. It increases with an increase in distance

from the point of complete stagnation and reaches maximum value at some distance from the junction of the nose and the cone. It then decreases downstream, reaching approximately the value corresponding to the velocity on a sharp cone in distant peripheral regions.

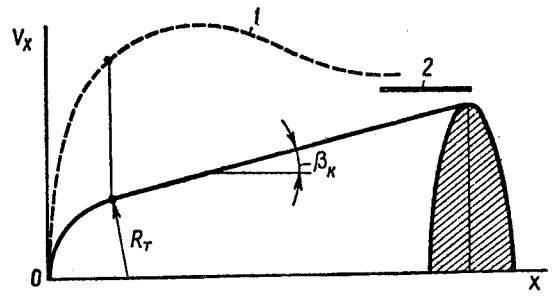

Fig. 9.4.11. Velocity distribution on blunt cone in supersonic flow:
1—empirical curve; *2*—velocity past sharp-nosed cone (theory).

The drag due to pressure (wave drag) of a blunt cone can be obtained from the pressure distribution by calculating this drag as the sum of the drags of a spherical nose section (index "sp") and the conical part of the surface (index "K"):

$$X = X_{sp} + X_K.$$

Assuming the coefficient of drag c_{fx} equal to zero in (1.3.2) and taking the maximum area of cross section of the cone as the characteristic area $S = S_0 = \pi r_0^2$, we get

$$X_{sp} = q_\infty S_0 \int_{S_{sp}} \bar{p} \cos(\widehat{\bar{P}_n x}) \frac{dS}{S_0},$$

whence the coefficient of wave drag

$$(c_{xw})_{sp} = \frac{X_{sp}}{q_\infty S_0} = \int_{S_{sp}} \bar{p} \cos(\widehat{\bar{P}_n x}) \frac{dS}{S_0}.$$

It can be seen from Fig. 9.4.12 that $\cos(\widehat{\bar{P}_n x}) = \cos\varphi$ and $dS = 2\pi r dl = 2\pi r dr/\cos\varphi$. But since $r = R_T \sin\varphi$ and $dr = R_T \cos\varphi\, d\varphi$, we get

$$dS = 2\pi R_T^2 \sin\varphi\, d\varphi.$$

Taking into account the above expressions and formula (9.4.75′) for $\bar{p}$, the wave drag coefficient for the nose section will be

$$(c_{xw})_{sp} = \frac{X_{sp}}{q_\infty S_0} = \int_0^{\varphi_K} \bar{p}_0 \cos^2\varphi \cos\varphi \frac{2\pi R_T^2 \sin\varphi}{\pi r_0^2} d\varphi$$

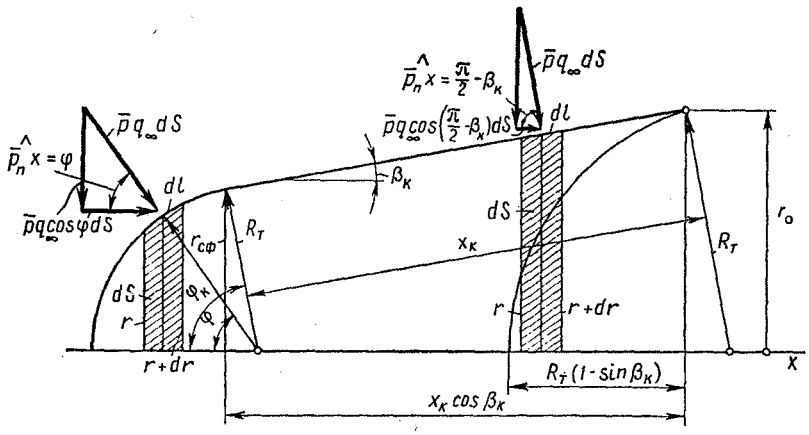

Fig. 9.4.12. Estimation of aerodynamic drag of blunt cone.

$$=-\frac{\bar{p}_0 R_T^2}{r_0^2}\int_1^{\cos^2\varphi_K}\cos^2\varphi\, d\cos^2\varphi=\frac{\bar{p}_0 R_T^2}{2r_0^2}(1-\cos^4\varphi_K)$$

$$=\frac{\bar{p}_0 R_T^2}{r_0^2}\sin^2\varphi_K\left(1-\frac{\sin^2\varphi_K}{2}\right)=\frac{\bar{p}_0 R_T^2}{r_0^2}\cos^2\beta_K\left(1-\frac{\cos^2\beta_K}{2}\right). \quad (9.4.82)$$

If $r_0=r_{sp}$ is assumed in this formula we get the coefficient of wave drag of a blunt nose section calculated for the base area $S=\pi r_{sp}^2$. Recalling that $r_{sp}=R_T\sin\varphi_K$, we find

$$(c_{xw})_{sp}=\bar{p}_0\,[1-(\sin^2\varphi_K)/2]. \quad (9.4.83)$$

The drag of a conical part having a side surface area S_s will be

$$X_K=q_\infty S_0\int_{S_s}\bar{p}\cos(\widehat{\bar{P}_n x})\,(dS/S_0).$$

From Fig. 9.4.12 it can be seen that

$$\cos(\widehat{\bar{P}_n x})=\cos[(\pi/2)-\beta_K]=\sin\beta_K;$$
$$dS=2\pi r dl=2\pi r dr/\sin\beta_K.$$

Next, taking into account that

$$\bar{p}=\bar{p}_0\cos^2\varphi_K=\bar{p}_0\cos^2[(\pi/2)-\beta_K]=\bar{p}_0\sin^2\beta_K;$$
$$S_0=\pi r_0^2,$$

the coefficient of wave drag of a conical part will be given by

$$(c_{xw})_K = \frac{X_K}{q_\infty S_0} = \int_{r_{sp}}^{r_0} \bar{p}_0 \sin^2 \beta_K \sin \beta_K \frac{2\pi r dr}{\pi r_0^2 \sin \beta_K}$$

$$= \frac{\bar{p}_0 \sin^2 \beta_K}{r_0^2} (r_0^2 - r_{sp}^2).$$

According to Fig. 9.4.12 the expression in brackets will be

$$r_0^2 - r_{sp}^2 = (r_0 - r_{sp})\,[2r_0 - (r_0 - r_{sp})] = x_K \sin \beta_K\,(2r_0 - x_K \sin \beta_K).$$

Accordingly

$$(c_{xw})_K = \bar{p}_0 \sin^3 \beta_K \frac{x_K}{r_0^2} (2r_0 - x_K \sin \beta_K). \tag{9.4.84}$$

Adding (9.4.82) and (9.4.84), we get the resultant drag coefficient with respect to the characteristic area $S_0 = \pi r_0^2$:

$$c_{xw} = \frac{X_K + X_{sp}^*}{q_\infty S_0} = (c_{xw})_{sp} + (c_{xw})_K = \bar{p}_0 \left[\frac{R_T^2}{r_0^2} \cos^2 \beta_K \left(1 - \frac{\cos^2 \beta_K}{2}\right) + \frac{x_K}{r_0^2} \sin^3 \beta_K (2r_0 - x_K \sin \beta_K) \right]. \tag{9.4.85}$$

In a particular case (when $R_T = 0$) we get the drag coefficient of a sharp-nosed cone. The value of this coefficient is found from the condition that $\bar{p}_0 = 2$, $x_K \sin \beta_K = r_0$:

$$c_{xw} = (c_{xw})_K = 2 \sin^2 \beta_K. \tag{9.4.86}$$

If $x_K = 0$ the surface under flow-interaction becomes a spherical segment of height $R_T (1 - \sin \beta_K)$ (see Fig. 9.4.12).

Taking $x_K = 0$ in (9.4.85), we arrive at formula (9.4.83) for the coefficient of wave drag of this spherical surface. In this formula $\varphi_K = (\pi/2) - \beta_K$.

5. Special Cases of Flow-Interaction

5.1 Unbalanced gas flows

The flow-interaction of bodies placed in a balanced fluid flow of gas was studied in Sections 2–4. However, the most real case is characterized by an unbalanced flow-interaction. The solution of such problems is complicated because the equations of rate of chemical reactions (equations of relaxation) are added to the system of the usual equations of gas dynamics. The number and type of such equations depend on the nature of the chemical

*In place of $X_K + X_{sp}$ the Russian text gives only X_K, which has been corrected here—Translator.

reactions occurring in the unbalanced gas flow, which are related to each other in a certain way.

In the work [52] it is accepted, specifically, that the following six reactions of dissociation take place simultaneously in unbalanced dissociated air:

$$O_2+M \rightleftarrows 2O+M,\ N_2+M \rightleftarrows 2N+M,\ NO+M \rightleftarrows N+O+M;$$

$$N+O_2 \rightleftarrows NO+O,\ N_2+O \rightleftarrows NO+N,\ N_2+O_2 \rightleftarrows 2NO,$$

where **M** is any one of the components of air. According to the types of these reactions the system of equations of relaxation can be written.

Applying the method of integral relations, calculations of the flow-interactions of spherical noses of different radii in an unbalanced condition of air in a wide range of M_∞ and p_∞ were carried out. These calculations showed that the unbalanced condition of air has a very strong effect on the distributions of temperature and concentrations of gas components. It has little effect on the values of velocity. For the axisymmetrical case the disequilibrium temperature is higher than for a balanced condition of gas, due to a delay in the dissociation process. At the same time this temperature is lower, like the condition on the surface of the body. This is due to a delay in the process of recombination. With an increase in the radius of sphere R_T under given conditions of undisturbed flow the flow in a shock layer approaches the equilibrium gas condition. During this process some fall in temperature and rise in density will be observed. This provides the possibility of high compression of gas in a shock layer and, as a result, reduces the shift of the shock wave away from the body. Similar correlation is also observed during increase in pressure p_∞ in an undisturbed flow.

Similarities of flow behind the shock wave are considered under the condition that complete equilibrium of flow, corresponding to simultaneous zero values of rates of reactions in question, is achieved at the point of complete stagnation. The beginning of the process of dissociation coincides with the shock wave front. The intensity of this dissociation is equal to zero immediately behind the wave front and the flow is supposed to be completely unbalanced.

If it is assumed that the completely unbalanced gas condition is maintained over the whole region between the shock wave and the surface in a flow (this kind of flow, characterized by the absence of chemical reactions, is known as "frozen") it is obvious that the shift of a shock wave will be the highest in comparison with a partially unbalanced gas flow condition or balanced dissociating gas flow condition. This is explained by the fact that the temperature in the shock layer will be highest and the density will be lowest in the absence of chemical reactions (dissociation). A lower compression of gas and hence a thicker shock layer may result from this factor.

In the above flow analysis it is assumed that the vibrational degrees of freedom are excited uniformly and do not affect the rate of chemical

reactions. However, as shown by theoretical and experimental research, the times of vibrational and dissociational relaxations become commensurable with one another with a substantial increase in gas temperature. Therefore we must also bear in mind the vibrational relaxation when analyzing disequilibrium flows. The relaxational equations describing the simultaneous existence of vibrational and dissociational relaxations are used for this purpose. The effect of vibrational relaxation on the rate of dissociation and the effect of dissociational relaxation on change in vibrational energy are taken into account. The equations for a pure diatomic gas are applied in the work [52]. These were used in working out the flow-interaction of blunt bodies in the presence of vibrational dissociational relaxation within a given accuracy.

The results of calculations for oxygen indicate that the shock wave is situated somewhat farther from the body in comparison with the case of unbalanced dissociation and uniform vibrations. This is connected with the fact that the temperature of a gas will be still higher and density will be still lower during nonuniform vibrational excitation. Therefore the possibility of compression of the gas in a shock layer will be reduced and its thickness will be increased. Here it must be clear that the shock wave lies nearer to the body in the presence of vibrational-dissociational relaxation than in the case of a completely "frozen" flow.

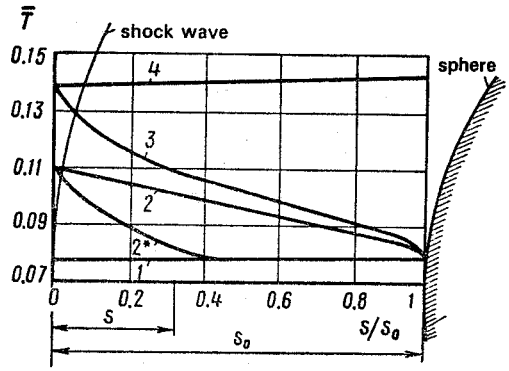

Fig. 9.5.1. Distribution of temperature during supersonic flow-interaction of sphere with flow oxygen ($M_\infty=10$; $p_\infty=0.01$ atm; $T_\infty=290°K$).

The distribution of temperature $\bar{T}$ (s/s_0) in the shock layer of an axisymmetrical flow over a sphere of radius $R_T=1$ cm is reproduced on Fig. 9.5.1. Here $\bar{T}=T/(\mu_{av\infty}V^2_{max}/R_0)$; s is the distance from the shock wave to the given point on the axis of symmetry of the flow. For a completely balanced flow (curve *1*) and steady flow (curve *4*, $k=1.4$) the temperature practically does not change in the direction from the wave to the body. But the change is considerable for unbalanced gas flows. Here the highest change in tempera-

ture takes place near the body for a flow with unbalanced dissociation and balanced vibrations (curve *2*). For a flow with unbalanced dissociation and vibrational relaxation (curve *3*) there exist two regions of sudden fall of temperature: near the shock wave and near the surface. The first region is established by the vibrational relaxation and the second by the unbalanced dissociation. The curve *2** in Fig. 9.5.1 corresponds to the case of balanced vibrations and unbalanced dissociation for a sphere with an increased radius $R_T = 10$ cm.

As shown by calculations, the basic change in the temperature may take place near the shock wave for an increase in sphere radius R_T, Mach number M_∞ and pressure p_∞ in an undisturbed flow. On the other hand, for a reduction in these quantities the main variation in temperature may occur near the surface in a flow.

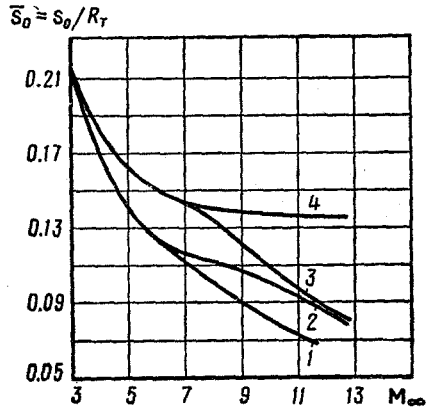

Fig. 9.5.2. Relative shift of shock wave from sphere of radius $R_T = 0.4$ cm in flow of oxygen at $p_\infty = 0.0263$ atm, $T_\infty = 293°K$:

1—flow with total equilibrium; *2*—unbalanced dissociating flow with balanced excitation of vibrations; *3*—unbalanced dissociation and unbalanced excitation of vibrations; *4*—completely "frozen" flow ($k = 1.4$).

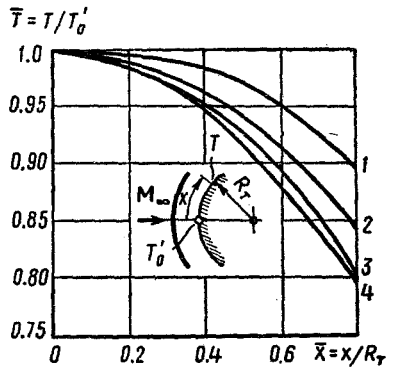

Fig. 9.5.3. Distribution of temperature on surface of sphere of radius $R_T = 1$ cm in flow of oxygen at $M_\infty = 10$, $p_\infty = 0.01$ atm, $T_\infty = 290°K$:

1—flow with total equilibrium; *2*—unbalanced dissociating flow with balanced vibrations; *3*—unbalanced dissociation and unbalanced vibrational excitation; *4*—completely "frozen" flow ($k = 1.4$).

The calculated values of relative shift of shock wave from the sphere are shown in Fig. 9.5.2 allowing for different relaxation processes. It should be noted that the highest shift of wave corresponds to the case of a completely "frozen" flow and the lowest shift to a completely "balanced" flow. At high enough Mach numbers M_∞ the effect of vibrational relaxation on the shift of the shock wave is practically negligible.

Figure 9.5.3 gives the picture of the effect of vibrational relaxation on the

distribution of temperature over the surface of a sphere. As can be seen from the data presented, the reduction in temperature taking into account vibrational-dissociational relaxation can exceed its reduction by about 10% for a balanced flow and by about 5% for a flow with dissociational relaxation. An intensive expansion of gas in a supersonic region, corresponding to a fall of temperature over the surface of the body, causes the distribution of temperature to approach the corresponding value for a "frozen" flow in the case of vibrational-dissociational relaxation. This is not found in calculating unbalanced dissociation.

5.2 Flows with radiation

At very high speeds of flow-interaction ($M_\infty > 10$) the gas behind the shock wave heats up to very high temperatures at which the processes of energy transfer in the form of radiation may have a considerable effect on its motion. Radiation is based on the atomic-molecular processes, as a result of which part of the internal energy of a substance changes into ray energy. This ray energy in its turn is absorbed by the other atoms and molecules, becoming the energy of a heat flow. This process of radiation and absorption of energy calls for a change in the parameters of hypersonic flows.

The corresponding system of equations in the case of an inviscid, nonconducting, thermodynamically balanced gas flow consists of the equations of motion, continuity and state which maintain the same form as for flows without radiation. The equation of energy has an additional term taking into account the heat flow to gas due to radiation. It is equal to the difference between the radiated and absorbed quantity of heat. The equation of transfer of ray energy is the new equation. The system of equations and its solution in its application to the problem of the flow-interaction of blunt bodies are shown in complete form in the work [52].

The results of this solution lead to the following conclusion: Radiation gives a considerable reduction in temperature and hence an increase in density in the shock layer and over the surface of a body in the flow. The change in temperature and density are particularly noticeable near the point of complete stagnation. Moving farther away from this point over the surface, there is a reduction in the effect of radiation distributions of temperature and density.

The pressure in a shock layer and on the surface of a body practically does not change due to radiation. A noticeable variation in velocity is observed on the surface only around the point of complete stagnation, where its value decreases. The shift of shock wave is reduced as a result of the effect of radiation, which is clearly felt in the region around the point of complete stagnation.

10

SHARP-NOSED BODY OF REVOLUTION IN A SUPERSONIC FLOW

1. Application of Method of Characteristics

A flying machine (for example, a rocket or missile) or some of its structural elements may have a sharp-nosed body of revolution. Let us study the supersonic flow-interaction of a sharp-nosed body of revolution placed in a gas flow at zero angle of attack. The form of bodies of revolution (Fig. 10.1.1) is given by the equation of generator $r=f(x)$. Also the parameters of an undisturbed flow (Mach number M_∞, pressure p_∞, density ρ_∞ and temperature T_∞) are known. If the thickness of the body of revolution is such that it creates large disturbances in the flow the calculation of this flow-interaction may be done by the method of characteristics.

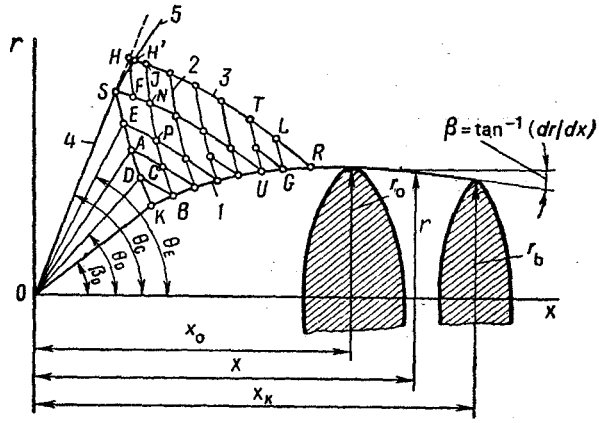

Fig. 10.1.1. Scheme of calculation of supersonic flow-interaction of body of revolution by method of characteristics:

1—generator of body of revolution; *2*—characteristic of first family; *3*—characteristic of second family; *4*—linear shock; *5*—curved shock.

This calculation usually starts with the determination of the conical flow past the nose which can be replaced by a cone in its close vicinity (its limit in

Fig. 10.1.1 is point K). As a result, on the generators OD, OA, etc. of the intermediate conical surfaces (including the generator of cone OK and shock OS) the velocities and the angles ω, μ and β can be found. Here the angles of inclination θ of the generators of intermediate cones are chosen arbitrarily in such a way that the interval $\Delta\theta$ is quite small and provides the desired accuracy of the parameters sought.

It is worthwhile performing calculations by graphic construction of a network of characteristics as shown in Fig. 10.1.1. First the element KD of the characteristic of the first family is constructed by drawing a straight line through point K at an angle $\mu_K+\beta_K$ (where $\beta_K=\beta_O$) to the cone axis to point D where it intersects with the neighboring intermediate conical surface having angle θ_D. As a result the coordinates x_D, r_D of point D are determined graphically.

Greater accuracy is achieved by analytical determination of these coordinates. For this purpose we write the equation for an element of characteristics of the first family

$$r_K-r_D=(x_K-x_D)\tan(\mu_K+\beta_K) \tag{10.1.1}$$

and the equation of the generator

$$r_D=x_D\tan\theta_D. \tag{10.1.2}$$

Solution of these equations gives unknown x_D and r_D. Similarly the coordinates of the remaining points of characteristic KS of the first family in the form of a discontinuous line are calculated. They happen to be the limit of the conical flow. Here the coordinates x_S, r_S of point S lying at the intersection of the element of characteristics of the first family ES and the generator OS of a conical shock are found from the simultaneous solution of equations

$$r_E-r_S=(x_E-x_S)\tan(\mu_E+\beta_E); \tag{10.1.3}$$

$$r_S=x_S\tan\theta_S. \tag{10.1.4}$$

The coordinates of a point on the characteristic KS obtained by the above method correspond to the angles μ and β, which are supposed to be constant along each of the elements of characteristics in question and are equal to the values of these angles at the beginning of the element.

The calculation of coordinates from the average values of μ and β between the end points of an element of characteristic may be carried out to achieve more accurate data. Then, specifically, we may write the following equations in place of equations (10.1.1) and (10.1.3):

$$r_K-r_D=(x_K-x_D)\tan[1/2(\mu_K+\mu_D+\beta_K+\beta_D)], \tag{10.1.1'}$$

$$r_E-r_S=(x_E-x_S)\tan[1/2(\mu_E+\mu_S+\beta_E+\beta_S)]. \tag{10.1.3'}$$

In these equations r_D, x_D and r_S, x_S are the modified coordinates of points D and S respectively.

After determining the form of curve of characteristic KS, velocities, Mach number **M** and angles μ and β at the points of this characteristic the further solution of the problem leads to the determination of the velocity field (Mach number **M**) in the region between this characteristic and the generator of the body under flow-interaction. For this purpose the corresponding correlations for the characteristics in a physical plane (plane of flow) and in a hodograph plane are used.

In selecting the correlations for the characteristics in a hodograph plane it is necessary to take into account that the flow in the region bounded by a linear generator of shock OS, characteristic of second family SU (which is constructed step by step in the process of solving this problem) and the generator of body OU will be irrotational (isentropic). In the neighboring region surrounded by the same characteristic SU, segments of a curvilinear part of shock SH and the generator of a body UR the flow will be rotational (unisentropic).

To find the velocity field in the isentropic region of flow we draw the elements of characteristics of the second family through each point of characteristic KS. One of them passing through point D intersects the wall at a point B where we wish to find the velocity. The coordinates of this point are determined from the simultaneous solution of the equation of the element of characteristics of the second family:

$$r_D - r_B = (x_D - x_B) \tan (\beta_D - \mu_D) \tag{10.1.5}$$

and the equation of the generator of the body:

$$r_B = f(x_B). \tag{10.1.6}$$

Solving these equations (10.1.5) and (10.1.6), we find the coordinates of point B (r_B; x_B). The angle β_B of inclination of a tangent to the generator at point B coincides with the angle of inclination of the velocity vector at this point by virtue of unseparated flow-interaction and is determined from the equation

$$(dr/dx)_B = \tan \beta_B = [df(x)/dx]_{x=x_B}. \tag{10.1.7}$$

Equation (5.4.9) can be used to find the velocity at point B. This equation, written in terms of finite differences at $y=r$, $\varepsilon=1$ (axisymmetrical flow) has the form

$$\Delta\omega_D + \Delta\beta_D - \frac{x_B - x_D}{r_D} m_D = 0. \tag{10.1.8}$$

In this equation the increase $\Delta\beta_D = \beta_B - \beta_D$, i.e. it represents the difference between the angles of inclination of velocity vectors at points B and D. Here, according to (10.1.7), we have

$$\beta_B=\tan^{-1}[(dr/dx)_B]. \qquad (10.1.7')$$

Taking into account that $\Delta\omega_D=\omega_B-\omega_D$, we find from (10.1.8) the angle

$$\omega_B=\omega_D-(\beta_B-\beta_D)+\frac{x_B-x_D}{r_D}m_D, \qquad (10.1.9)$$

where

$$m_D=\sin\beta_D\sin\mu_D/\cos(\beta_D-\mu_D) \qquad (10.1.10)$$

in accordance with (5.4.5).

The angle ω_D appearing in (10.1.9) is found from Table 5.3.1 from the value of Mach number $\mathbf{M}_D$ at point D. After calculating ω_B from (10.1.9) the corresponding values of ω_B, Mach number $\mathbf{M}_B$ and angle $\mu_B=\sin^{-1}(1/\mathbf{M}_B)$ at point B are determined with the help of the same Table 5.3.1. Then the pressure can be found on the basis of the values obtained for Mach numbers $\mathbf{M}$.

Let us first find the pressure p_K at a point K corresponding to Mach number $\mathbf{M}_K$:

$$p_K=p_0\left(1+\frac{k-1}{2}\mathbf{M}_K^2\right)^{-k/(k-1)}=p_0'\pi(\mathbf{M}_K), \qquad (10.1.11)$$

where the stagnation pressure behind a conical shock

$$p_0'=p_0\nu_0 \qquad (10.1.12)$$

is determined from the stagnation pressure p_0 (3.6.29) ahead of the shock and the value of function ν_0, which is determined from (9.2.26) for a given angle of inclination of shock θ_c and Mach number $\mathbf{M}_\infty$. The pressure at point B will be

$$p_B=p_0'\left(1+\frac{k-1}{2}\mathbf{M}_B^2\right)^{-k/(k-1)}=p_0'\pi(\mathbf{M}_B). \qquad (10.1.13)$$

The functions $\pi(\mathbf{M}_K)$ and $\pi(\mathbf{M}_B)$ in (10.1.11) and (10.1.13) are determined on the basis of the values of Mach numbers M_K and M_B respectively from the tables presented in the work [53].

The pressure coefficients are determined by the formulas:

$$\bar{p}_K=2(p_K-p_\infty)/(k\mathbf{M}_\infty^2 p_\infty) \text{ and } \bar{p}_B=2(p_B-p_\infty)/(k\mathbf{M}_\infty^2 p_\infty). \qquad (10.1.14)$$

The velocity, temperature and density are determined respectively from the relations:

$$\frac{V_{K(B)}}{V_{\max}}=\left\{1-\left[\frac{p_{K(B)}}{p_0'}\right]^{(k-1)/k}\right\}^{1/2}; \qquad (10.1.15)$$

$$\frac{T_{K(B)}}{T_0}=\left[1+\frac{k-1}{2}\mathbf{M}_{K(B)}^2\right]^{-1}; \qquad (10.1.16)$$

$$\frac{\rho_{K(B)}}{\rho_0}=\left[\frac{T_{K(B)}}{T_0}\right]^{1/(k-1)}\nu_0, \tag{10.1.17}$$

where ρ_0 and T_0 are found from the parameters of undisturbed flow by formulas (3.6.34), (3.6.35) respectively and the maximum velocity

$$V_{\max}=\left(V_\infty^2+\frac{2}{k-1}a_\infty^2\right)^{1/2} \tag{10.1.18}$$

according to (3.6.22).

After calculating the parameter at point B we draw the element of characteristics of the first family through this point to point of intersection C with the linear part of characteristics of the second family which emerges from point A (see Fig. 10.1.1). The coordinates of point C are determined from the solution of equations for the elements AC and BC of the characteristics. The equations of these elements of characteristics AC and BC have the form

$$r_A-r_C=(x_A-x_C)\tan(\beta_A-\mu_A) \tag{10.1.19}$$

and

$$r_B-r_C=(x_B-x_C)\tan(\beta_B+\mu_B) \tag{10.1.20}$$

respectively. Solving these equations simultaneously, we get the coordinates of point C (x_C, r_C). To find the angles β_C and ω_C at this point we must use equations for characteristics (5.4.8) and (5.4.9). Writing these equations in terms of finite differences and assuming $\varepsilon=1$, we get:

$$\Delta\omega_B-\Delta\beta_B-\frac{x_C-x_B}{r_B}l_B=0; \tag{10.1.21}$$

$$\Delta\omega_A+\Delta\beta_A-\frac{x_C-x_A}{r_A}m_A=0, \tag{10.1.22}$$

where

$$\left.\begin{aligned} l_B&=\sin\beta_B\sin\mu_B/\cos(\beta_B+\mu_B);\\ m_A&=\sin\beta_A\sin\mu_A/\cos(\beta_A-\mu_A);\end{aligned}\right\} \tag{10.1.23}$$

in accordance with (5.4.5) and (5.4.6).

As against the four unkowns $\Delta\omega_B$, $\Delta\omega_A$, $\Delta\beta_B$ and $\Delta\beta_A$, in equations (10.1.21), (10.1.22) only two unknown quantities: $\Delta\omega_B$ and $\Delta\beta_B$ (or $\Delta\omega_A$ and $\Delta\beta_A$) may be considered according to (5.4.20).

Taking equation (5.4.20) into account, equation (10.1.22) will be reduced to the form:

$$\Delta\omega_B+\omega_B-\omega_A+\Delta\beta_B+\beta_B-\beta_A-\frac{x_C-x_A}{r_A}m_A=0. \tag{10.1.24}$$

Solving this equation together with (10.1.21) for the variable $\Delta\beta_B$, we get

$$\Delta\beta_B=\frac{1}{2}\left[\frac{x_C-x_A}{r_A}m_A-\frac{x_C-x_B}{r_B}l_B-(\omega_B-\omega_A)-(\beta_B-\beta_A)\right]. \quad (10.1.25)$$

Then the increase in angle can be obtained from (10.1.21) for the value of $\Delta\beta_B$ obtained:

$$\Delta\omega_B=\Delta\beta_B+\frac{x_C-x_B}{r_B}l_B. \quad (10.1.21')$$

The absolute values of angles at point C will be the following:

$$\beta_C=\Delta\beta_B+\beta_B,\ \omega_C=\Delta\omega_B+\omega_B. \quad (10.1.26)$$

For the value of ω_C we find the Mach number M_C from Table 5.3.1 and hence the angle of disturbance $\mu_C=\sin^{-1}(1/M_C)$. If needed, the other parameters, pressure, density, temperature and velocity, can be obtained from the value of Mach number M_C.

The parameters so obtained represent a first approximation because the coefficients l and m along the elements of characteristics and the radial coordinates take constant values which are equal to their corresponding values at points A and B. These parameters can be improved if the quantities calculated as the average of values at points A and B obtained at point C as a first approximation replace l_B, m_A, r_B, r_A in equations (10.1.21) and (10.1.22). For these average quantities we have the following relations:

$$l'_B=\sin\beta'_B\sin\mu'_B/\cos(\beta'_B+\mu'_B),$$
$$m'_A=\sin\beta'_A\sin\mu'_A/\cos(\beta'_A-\mu'_A), \quad (10.1.23')$$

$$r'_B=(r_B+r_C)/2,\ r'_A=(r_A+r_C)/2, \quad (10.1.27)$$

where

$$\left.\begin{aligned}\beta'_B&=(\beta_B+\beta_C)/2;\ \ \mu'_B=(\mu_B+\mu_C)/2;\\ \beta'_A&=(\beta_A+\beta_C)/2,\ \ \mu'_A=(\mu_A-\mu_C)/2.\end{aligned}\right\} \quad (10.1.28)$$

Continuing this procedure, we can determine the parameters at all points of the second series, including point N lying at the intersection of elements PN of the characteristics of the first family and SN of the characteristics of the second family drawn from the end of the linear conical shock.

Further calculation involves finding the parameters at the point of intersection of the element of the characteristics of the first family drawn from point N and the extension of shock behind point S. In practice, the characteristic is not drawn through point N but through point F lying between the points N and S (see Fig. 10.1.1) so that a closer approximation is achieved. The coordinates x_F, r_F of point F are selected in such a way that the element FH of the characteristic, adjacent to the shock, is small enough to be taken

in the form of a linear segment. The parameters at point $F(\omega, \mathbf{M}, \mu, \beta)$ are calculated from their known values at points S and N by linear interpolation. For example,

$$\omega_F=\omega_S+(\omega_N-\omega_S)\frac{x_F-x_S}{x_N-x_S}. \tag{10.1.29}$$

The equation of element FH of the characteristics of the first family will be

$$r_F-r_H=(x_F-x_H)\tan(\beta_F+\mu_F). \tag{10.1.30}$$

Solving this equation together with the equation of the linear generator of the shock $r_H=x_H\tan\theta_C$, we determine the coordinates x_H, r_H and get the position of point H on the shock as a first approximation. These coordinates must be modified because the real shock behind point S will be curved. In reality, the characteristics of the first family (ES, FH, etc.) are expansion waves by nature. In encountering the shock these waves reduce its strength and hence its angle of inclination. As a result the shock is bent.

The flow behind this shock will be rotational (nonisentropic). In determining velocity at a point H it is necessary to use equation (5.4.41) of element FH of the characteristics of the first family, which takes into account the variation in entropy behind a curved shock. Assuming $y_F=r_F$, $\varepsilon=1$ (axisymmetrical flow) in this equation and solving it together with (5.4.38) to obtain $\Delta\beta_F$, we get the relation (5.4.46) in which $\varepsilon=1$ and $y_F=r_F$:

$$\Delta\beta_F=\left[\left(\frac{d\omega}{d\beta}\right)_S-1\right]^{-1}\left(\omega_F-\omega_S+\frac{x_H-x_F}{r_F}l_F-\frac{x_H-x_F}{kR}\cdot\frac{\Delta S}{\Delta n}c_F\right), \tag{10.1.31}$$

where the derivative $(d\omega/d\beta)_S$ is found from (5.4.39) and the coefficients l_F, c_F are calculated from the corresponding formula (5.4.42).

The quantity ΔS, determining the change in entropy during transition from point H to point F, appears in formula (10.1.31). For the first approximation the calculations assume that point H lies on the extension of the linear generator of the shock. Therefore the change in entropy may be taken as zero, i.e. $\Delta S=0$. However, this assumption lowers the accuracy of the calculations because point H, in practice, lies on the curved part of the shock (H'). Better results are obtained if it is assumed that entropy (or stagnation pressure) at point H is not equal to its value at point F.

Calculation of stagnation pressure p_{0H} at point H to a first approximation will be carried out in the following way: Suppose that the angle of inclination of flow $\beta_{H'}$ behind the shock at point H is equal to the angle of inclination of velocity vector β_F at point F. On the basis of the value of angle $\beta_{H'}=\beta_F$ it is possible to determine the corresponding angle of shock θ'_{cH}. For this purpose we use formula (4.3.25), which may be written in the form

$$\frac{\tan\theta'_{cH}}{\tan(\theta'_{cH}-\beta'_H)}=\frac{\mathbf{M}_\infty^2\sin^2\theta'_{cH}}{1-\delta+\delta\mathbf{M}_\infty^2\sin^2\theta'_{cH}}. \tag{10.1.32}$$

For given values of β'_H, $\mathbf{M}_\infty$ and $\delta=(k-1)/(k+1)$ this transcendental equation is solved for θ'_{cH} by the method of successive iterations. Using formula (10.1.12) the stagnation pressure p'_{0H} at point H can be determined for a known value of θ'_{cH}. Assuming that the stagnation pressure p'_{0F} at point F is equal to the stagnation pressure p'_{0S} at point S calculated for the angel of shock θ_{cS} from formula (4.3.22), it is possible to get the relation

$$(p'_{0H}-p'_{0F})/p'_{0F} = (p'_{0H}-p'_{0S})/p'_{0S}.$$

Inserting this relation in (5.4.45), the entropy gradient $\Delta S/\Delta n$ appearing in formula (10.1.31) will be determined. After determining the quantity $\Delta\beta_F$ by this formula we find the increase in angle $\Delta\omega_F$ with the help of (5.4.41) at $y_F=r_F$ and $\varepsilon=1$:

$$\Delta\omega_F=\Delta\beta_F+\frac{x_H-x_F}{r_F}l_F-\frac{x_H-x_F}{kR}\cdot\frac{\Delta S}{\Delta n}c_F. \tag{10.1.33}$$

From $\Delta\beta_F$ and $\Delta\omega_F$ we determine the following angles at a point H:

$$\beta_H=\beta_{H'}=\Delta\beta_F+\beta_F, \quad \omega_H=\omega_{H'}=\Delta\omega_F+\omega_F. \tag{10.1.34}$$

The values of $\mathbf{M}_{H'}$ and $\mu_{H'}$ can be obtained from Table 5.3.1 for a given value of angle $\omega_{H'}$. The angle of inclination of shock at point H can be modified by formula (10.1.32) for the value of $\beta_{H'}$ obtained and the coordinates $x_{H'}$, $r_{H'}$ of the new point H' can be found as a second approximation. To do this we write an equation for a section of shock behind point S:

$$r_S-r_{H'}=(x_S-x_H)\tan\theta_{cH'} \tag{10.1.35}$$

and the equation of the element of the characteristics of the first family:

$$r_F-r_{H'}=(x_F-x_{H'})\tan(\beta'_F+\mu'_F), \tag{10.1.36}$$

in which the angles β'_F and μ'_F are selected as average values:

$$\beta'_F=\frac{\beta_F+\beta_{H'}}{2}, \quad \mu'_F=\frac{\mu_F+\mu_{H'}}{2}.$$

Simultaneous solution of equations (10.1.35) and (10.1.36) gives the improved coordinates $x_{H'}$, $r_{H'}$. If needed, the parameters at point $H'(\omega_{H'}$, $\mathbf{M}_{H'}$, $\mu_{H'}$ and $\beta_{H'})$ can be worked out as a third approximation.

The data obtained for the parameters at points H' and N help us to calculate the parameters at a point J (see Fig. 10.1.1). This calculation is similar to the solution of the first problem (see Chapter 5 Section 4) connected with the determination of velocity at the point of intersection of the characteristics of different families emerging from two neighboring points.

The coordinates x_J, r_J of point J are determined as a result of solution of equations (5.4.10), (5.4.12) written for the elements NJ and $H'J$ of the characteristics of the first and second families respectively:

$$r_N - r_J = (x_N - x_J) \tan(\beta_N + \mu_N); \tag{10.1.37}$$

$$r_{H'} - r_J = (x_{H'} - x_J) \tan(\beta_{H'} - \mu_{H'}). \tag{10.1.38}$$

The relations for characteristics in the hodograph plane of velocity allowing for variations in entropy should be used for the calculation of parameters at point J situated in the rotational part of the flow. These equations, written in terms of finite differences, have the form of (5.4.11) and (5.4.13). Equation (5.4.11), written for $\varepsilon = 1$ and $y = r$ in terms of notations used for the element NJ of the characteristic of the first family, will have the following form:

$$\Delta\omega_N - \Delta\beta_N - \frac{x_J - x_N}{r_N} l_N + \frac{x_J - x_N}{kR} \cdot \frac{\Delta S}{\Delta n} c_N = 0. \tag{10.1.39}$$

For element $H'J$ of the characteristics of the second family we use equation (5.4.13):

$$\Delta\omega_{H'} + \Delta\beta_{H'} - \frac{x_J - x_{H'}}{r_{H'}} m_{H'} - \frac{x_J - x_{H'}}{kR} \cdot \frac{\Delta S}{\Delta n} t_{H'} = 0, \tag{10.1.40}$$

where

$$\left.\begin{aligned} \Delta\omega_N = \omega_J - \omega_N, \quad & \Delta\beta_N = \beta_J - \beta_N; \\ \Delta\omega_{H'} = \omega_J - \omega_{H'}, \quad & \Delta\beta_{H'} = \beta_J - \beta_{H'}. \end{aligned}\right\} \tag{10.1.41}$$

Formulas (5.4.15) should be used to determine the coefficients l_N, c_N, $m_{H'}$, $t_{H'}$ in which the parameters with indices "B" and "A" are replaced by those with indices "N" and "H'" respectively. The entropy gradient $\Delta S/\Delta n$ is calculated with the help of (5.4.16) or (5.4.18) in which the indices "B" and "A" should be replaced by "N" and "H'" respectively. Here the stagnation pressures $p'_{0H'}$ at point H' and p'_{0N} at point N are determined by formula (4.3.22) from the corresponding values of angles of shock $\theta_{cH'}$ and θ_{cS} ($\theta_{cH'} < \theta_{cS}$).

The system of equations (10.1.39) and (10.1.40) comprises four unknown quantities: $\Delta\omega_N$, $\Delta\beta_N$, $\Delta\omega_{H'}$, $\Delta\beta_{H'}$. The number of unknowns can be reduced to two if equation (5.4.20) is applied. Then,

$$\left.\begin{aligned} \Delta\omega_{H'} &= \Delta\omega_N + \omega_N - \omega_{H'}; \\ \Delta\beta_{H'} &= \Delta\beta_N + \beta_N - \beta_{H'}. \end{aligned}\right\} \tag{10.1.42}$$

Carrying out the corresponding changes in (10.1.40), we get

$$\Delta\omega_N + \omega_N - \omega_{H'} + \Delta\beta_N + \beta_N - \beta_{H'} - \frac{x_J - x_H}{r_{H'}} m_{H'} - \frac{x_J - x_{H'}}{kR} \cdot \frac{\Delta S}{\Delta n} t_{H'} = 0. \tag{10.1.40'}$$

Solving this equation together with (10.1.39) to obtain $\Delta\beta_N$, we get

$$\Delta\beta_N=\frac{1}{2}\left\{\frac{1}{kR}\cdot\frac{\Delta S}{\Delta n}[(x_J-x_{H'})\,t_{H'}+(x_J-x_N)c_N]\right.$$

$$\left.+\frac{x_J-x_{H'}}{r_{H'}}\,m_{H'}-\frac{x_J-x_N}{r_N}\,l_N-(\omega_N-\omega_{H'})-(\beta_N-\beta_{H'})\right\}. \quad (10.1.43)$$

Angular increment can be worked out from (10.1.39) for the value of $\Delta\beta_N$ obtained:

$$\Delta\omega_N=\Delta\beta_N+\frac{x_J-x_N}{r_N}\,l_N-\frac{x_J-x_N}{kR}\cdot\frac{\Delta S}{\Delta n}\,c_N. \quad (10.1.44)$$

The absolute values of angles at point J will then be calculated from $\Delta\omega_N$ and $\Delta\beta_N$:

$$\omega_J=\Delta\omega_N+\omega_N;$$
$$\beta_J=\Delta\beta_N+\beta_N.$$

Mach number $\mathbf{M}_J$ and angle of disturbance μ_J will be found from Table 5.3.1 for the above value of ω_J. The stagnation pressure p'_{0J} (entropy S_J) at point J can be found by interpolation for the values of $p'_{0H'}$ and p'_{0N} at points H' and N respectively.

The parameters calculated above can be improved if the quantities obtained for the average values of angles β and μ according to formula (5.4.25) are used in place of l_N, $m_{H'}$, c_N, $t_{H'}$ in equations (10.1.39), (10.1.40).

In this way the coordinates of points H' J,..., L of the characteristics of the second family are determined step by step. Gas dynamic parameters at these points are worked out in the same way. Using the parameters obtained at point L the velocity and other parameters at a point R lying on the surface of the body in the flow-interaction can be determined. The coordinates of point R are worked out as a result of solution of the equation for element LR of the characteristics of the second family:

$$r_L-r_R=(x_L-x_R)\tan(\beta_L-\mu_L) \quad (10.1.45)$$

and the equation of the generator of the body, $r_R=f(x_R)$. Solution of these equations gives values of x_R, r_R.

Point R is situated in a rotational part of the flow at the intersection of element LR of the characteristics of the second family and the generator of the body. Therefore equation (5.4.27) should be used to calculate velocity at this point. Assuming $\varepsilon=1$ and replacing y by r and index "D" by "L", we have

$$\Delta\omega_L=-\Delta\beta_L+\frac{x_R-x_L}{r_L}\,m_L-\frac{x_R-x_L}{kR}\cdot\frac{\Delta S}{\Delta n}\,t_L, \quad (10.1.46)$$

where

$$\left.\begin{aligned}\Delta\omega_L&=\omega_R-\omega_L;\\ \Delta\beta_L&=\beta_R-\beta_L.\end{aligned}\right\} \quad (10.1.47)$$

The coefficients m_L and t_L are obtained from formulas (5.4.28) in which the index "D" is replaced by "L". The entropy gradient $\Delta S/\Delta n$ is worked out by one of the formulas (5.4.29), replacing index "D" by "L" and "B" by "R". Here stagnation pressure p_{0R} at point R is known and is the same as that at points K, B, ..., U, G, lying on one line of the body adjacent to its surface. The quantity p_{0R} is calculated by formula (4.3.22) for a given value of the angle of inclination of shock θ_{cS}. Stagnation pressure p'_{0L} at point L is determined by interpolation of the values of p'_{0T} and $p'_{0G} = p_{0R}$ at points T and G respectively.

The angle of inclination of the tangent to the generator of the body at point R is known from the equation of generator $r=f(x)$ and is equal to $\beta_R=\tan^{-1}[(dr/dx)_R]$. Therefore the difference $\Delta\beta_L=\beta_R-\beta_L$ will be known and the angular increment $\Delta\omega_L$ can be directly calculated by equation (10.1.46). The angle $\omega_R=\Delta\omega_L+\omega_L$ is worked out from this angular increment and Mach number $\mathbf{M}_R$ is determined. Then pressure and other parameters at point R can be worked out taking into account the effect of a rotational flow.

As shown by calculations and experimental research, the effect of rotational motion behind a curvilinear shock is observed only at high speeds. For example, for a parabolic nose section and the aspect ratio $\lambda_0=x_0/2r_0$ (length of nose section x_0 is five times greater than the diameter of the largest cross section $2r_0$) at the value of parameter $\mathbf{K}_1=\mathbf{M}_\infty/\lambda_0=1$ corresponding to Mach number $\mathbf{M}_\infty=5$ wave drag increased by 5% due to rotational effect in comparison to its value in a potential flow. At the same time, at $\mathbf{K}_1=4$ ($\mathbf{M}_\infty=20$) it increased by more than 25%. This effect of increase in drag can be explained physically by the fact that more of the kinetic energy of the flow is spent in the formation of vortices.

The pressure distribution found by the method of characteristics is shown in Fig. 10.1.2 for two bodies with parabolic nose sections whose generator satisfies the equation

$$\bar{r}=\bar{x}\,(2-\bar{x}) \tag{10.1.48}$$

with $\bar{r}=r/r_0$, $\bar{x}=x/x_0$ (x_0 – distance from nose to the location of the highest cross section of the body of revolution of radius r_0). For a body of revolution having such a generator (Fig. 10.1.3) the tangent of the angle of inclination of a tangent line at an arbitrary point is

$$\tan\beta=\frac{dr}{dx}=\frac{2r_0}{x_0}(1-\bar{x})=\frac{1}{\lambda_0}(1-\bar{x}) \tag{10.1.49}$$

and for a sharp-pointed nose for which $\bar{x}=0$ it will be

$$\tan\beta_0=1/\lambda_0, \tag{10.1.50}$$

where $\lambda_0=x_0/(2r_0)$ is the aspect ratio of the nose section.

The pressure distribution for the value of parameter $\mathbf{K}_1=\mathbf{M}_\infty\tan\beta_0$

$=M_\infty/\lambda_0=2$ is shown in Fig. 10.1.2. Compared to a potential flow the increase in pressure is clearly seen in the rotational flow. This increase in pressure should be considered in practical cases starting from values of $K_1=1.2$ to 1.5 and above. The effect of vortices can be neglected for lower values.

The curve in Fig. 10.1.2 confirms the validity of the law of similarity for parameter K_1 at high speeds not only for cones but also for affinely similar bodies of revolution with curvilinear generator-like bodies of parabolic form (affine similarity is treated in detail in Section 3). This similarity is extended even over the cylindrical part of the bodies. It can be seen that the flow-interaction of two bodies differing in size can be characterized by one curve for function of pressure $(p/p_\infty)-1$ to the extent that the parameter K is one and the same for the two cases.

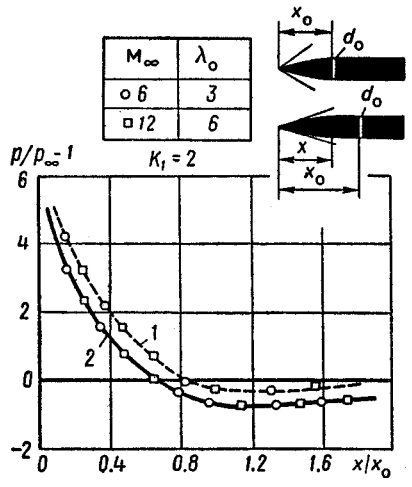

Fig. 10.1.2. Distribution of pressure over body of revolution with parabolic nose section:

1—with adjustment for vortex motion behind shock; *2*—for potential flow behind shock.

The law of similarity for parameter K_1 has great practical significance. In practice it is possible to carry out experiments with one body instead of different models and obtain data about pressure distribution for a series of values of parameter K_1. By the law of similarity these data can be extended to all the infinitely many affinely transformed bodies with concrete geometrical parameters. For example, if the results shown in Fig. 10.1.2 are obtained at $M_\infty=6$ for a body with an aspect ratio of nose section $\lambda_0=3$ so that $K_1=2$ it is obvious that the curve obtained is also valid (see graph) for other bodies of aspect ratio $\lambda_0=6$ in a flow with $M_\infty=12$, i.e. provided we maintain the same value of $K_1=2$. Using the law of similarity the results obtained can also be applied, for example, for a body with $\lambda_0=5$ and $M_\infty=10$, etc. So in this case the applicability of the law of similarity is limited to one and the same value of the parameter $K_1=2$. To expand these limitations experiments or calculations should be carried out for different values of K_1.

One more important implication of the law of similarity should be borne in mind. If facilities are lacking for conducting experiments at high speeds the necessary results can be obtained at lower values of Mach numbers M_∞. For this purpose it is necessary to carry out experiments with the affinely similar model of lower aspect ratio maintaining the given value of parameter K_1. In

liscussing the effect of a rotational flow it was found that an increase in light velocity requires allowance for the effect of factors in the calculation of an inviscid flow-interaction that may be neglected at high speeds.

Experiment and theory show that factors like the boundary layer and various effects observed therein (dissociation, ionization, heat transfer between wall and gas) have a known effect on the flow interaction at high Mach numbers $\mathbf{M}_\infty$. The vibrational excitation, dissociation and ionization of air, which may take place at very high speeds due to the considerable rise in temperature in the inviscid flow region between the shock and the surface of the body, also have a certain effect on the flow-interaction. It may be noted that the effect of high temperature of the gas on the variation in pressure distribution is appreciably less than on the distribution of velocity, temperature and density.

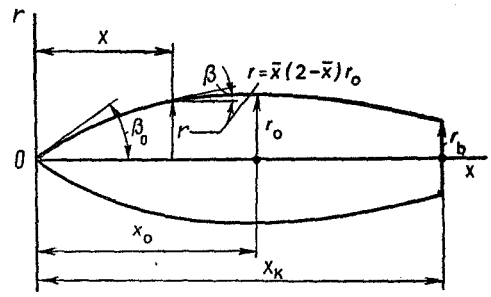

Fig. 10.1.3. Body of revolution with parabolic generator.

Calculation of the parameter of an inviscid flow-interaction, where the gas undergoes physico-chemical changes due to the effect of high temperatures, can be performed by a range of methods including the method of characteristics. This method may be studied in the relevant literature [41, 42, 44].

Knowledge of the distribution of pressure coefficient $\bar{p}=(p-p_\infty)/q_\infty$ ($q_\infty = k\mathbf{M}_\infty^2 p_\infty/2$) helps us to calculate the drag force and coefficient of wave drag for a body of revolution in a supersonic flow at zero angle of attack. To calculate the coefficient of wave drag we use formula (1.3.2) as we used the conclusion of formula (9.2.29). Here we take into account:

$$S_0=\pi r_0^2;\ dS=2\pi r dl;\ dl=dx/\cos\beta;$$

$$\cos(\widehat{\bar{P}_n x})=\sin\beta;\ \sin\beta/\cos\beta=dr/dx.$$

As a result we get

$$c_{xw}=\frac{X_w}{q_\infty S_0}=\frac{2}{r_0}\int_0^{x_K}\bar{p}\bar{r}\left(\frac{dr}{dx}\right)dx \qquad (10.1.51)$$

or

$$c_{xw}=4\lambda_0\int_0^{\bar{x}_K}\bar{p}\bar{r}\tan\beta\, d\bar{x}, \qquad (10.1.51')$$

where x_K is the length of the body of revolution;

$$\bar{x}=x/x_0;\ \bar{x}_K=x_K/x_0;$$
$$\bar{r}=r/r_0;\ \tan\beta=dr/dx;\ \lambda_0=x_0/2r_0.$$

(see Fig. 10.1.3)

2. Linearization of Equations of Flow-Interaction for Thin Bodies of Revolution

Individual models of flying vehicles are made in the form of thin sharp-nosed bodies of rotation (some types of rockets, missiles, etc.) or have one of the structural elements of the fuselage in the form of such a body. That is why we investigate the aerodynamic characteristics of thin sharp-nosed bodies of revolution.

Let us examine the problem of thin bodies at small angles of attack in a steady flow. The disturbed flow about such bodies differs negligibly from an undisturbed flow. This kind of flow, referred to as a linearized flow earlier, can be studied with the help of the corresponding linearized equations of aerodynamics. Let us consider these linearized equations. They are obtained from the general equations of motion (3.1.35), (3.1.35′) in cylindrical coordinates, convenient for study of the flow-interaction of bodies of revolution having the following form for a steady inviscid flow ($\partial\bar{V}/\partial t=0$, $\nu=0$):

$$\left.\begin{aligned}
&V_x\frac{\partial V_x}{\partial x}+V_r\frac{\partial V_x}{\partial r}+\frac{V_\gamma}{r}\cdot\frac{\partial V_x}{\partial\gamma}=-\frac{1}{\rho}\cdot\frac{\partial p}{\partial x};\\
&V_x\frac{\partial V_r}{\partial x}+V_r\frac{\partial V_r}{\partial r}+\frac{V_\gamma}{r}\cdot\frac{\partial V_r}{\partial\gamma}-\frac{V_\gamma^2}{r}=-\frac{1}{\rho}\cdot\frac{\partial p}{\partial r};\\
&V_x\frac{\partial V_\gamma}{\partial x}+V_r\frac{\partial V_\gamma}{\partial r}+\frac{V_\gamma}{r}\cdot\frac{\partial V_\gamma}{\partial\gamma}+\frac{V_r V_\gamma}{r}=-\frac{1}{\rho r}\cdot\frac{\partial p}{\partial\gamma}
\end{aligned}\right\}\qquad(10.2.1)$$

and also the equation of continuity (2.4.31) in these coordinates. Differentiating this question, we get

$$r\left(\frac{\partial\rho}{\partial x}V_x+\frac{\partial\rho}{\partial r}V_r+\frac{1}{r}\cdot\frac{\partial\rho}{\partial\gamma}V_\gamma\right)$$
$$+\rho r\left(\frac{\partial V_x}{\partial x}+\frac{\partial V_r}{\partial r}+\frac{1}{r}\cdot\frac{\partial V_\gamma}{\partial\gamma}\right)+\rho V_r=0.\qquad(10.2.2)$$

As the partial derivative

$$\frac{\partial\rho}{\partial x}=\frac{d\rho}{dp}\cdot\frac{\partial p}{\partial x}=\frac{1}{a^2}\cdot\frac{\partial p}{\partial x},$$

replacing $\partial p/\partial x$ here by the expression from (10.2.1), we have

$$\frac{\partial \rho}{\partial x}=-\frac{\rho}{a^2}\left(V_x\frac{\partial V_x}{\partial x}+V_r\frac{\partial V_x}{\partial r}+\frac{V_\gamma}{r}\cdot\frac{\partial V_x}{\partial \gamma}\right). \tag{10.2.3}$$

Similarly, from the second and third equation of (10.2.1) we get:

$$\frac{\partial \rho}{\partial r}=-\frac{\rho}{a^2}\left(V_x\frac{\partial V_r}{\partial x}+V_r\frac{\partial V_r}{\partial r}+\frac{V_\gamma}{r}\cdot\frac{\partial V_r}{\partial \gamma}-\frac{V_\gamma^2}{r}\right); \tag{10.2.4}$$

$$\frac{1}{r}\cdot\frac{\partial \rho}{\partial \gamma}=-\frac{\rho}{a^2}\left(V_x\frac{\partial V_\gamma}{\partial x}+V_r\frac{\partial V_\gamma}{\partial r}+\frac{V_\gamma}{r}\cdot\frac{\partial V_\gamma}{\partial \gamma}+\frac{V_rV_\gamma}{r}\right). \tag{10.2.5}$$

Inserting values of the partial derivatives from (10.2.3) through (10.2.5) in the continuity equation (10.2.2), we get:

$$\begin{aligned}&(V_x^2-a^2)\frac{\partial V_x}{\partial x}+(V_r^2-a^2)\frac{\partial V_r}{\partial r}+\frac{1}{r}(V_\gamma^2-a^2)\frac{\partial V_\gamma}{\partial \gamma}\\&+V_xV_r\left(\frac{\partial V_x}{\partial r}+\frac{\partial V_r}{\partial x}\right)+V_xV_\gamma\left(\frac{1}{r}\cdot\frac{\partial V_x}{\partial \gamma}+\frac{\partial V_\gamma}{\partial x}\right)\\&+V_rV_\gamma\left(\frac{1}{r}\cdot\frac{\partial V_r}{\partial \gamma}+\frac{\partial V_\gamma}{\partial r}\right)-\frac{V_ra^2}{r}=0.\end{aligned} \tag{10.2.6}$$

Keeping in view the relation (2.4.25′) and recalling that

$$\frac{\partial V_\gamma}{\partial r}=\frac{\partial}{\partial r}\left(\frac{1}{r}\cdot\frac{\partial \varphi}{\partial \gamma}\right)=\frac{1}{r}\cdot\frac{\partial^2\varphi}{\partial r\partial \gamma}-\frac{1}{r^2}\cdot\frac{\partial \varphi}{\partial \gamma},$$

we get an equation for potential function from (10.2.6) in the following form:

$$\begin{aligned}&(V_x^2-a^2)\frac{\partial^2\varphi}{\partial x^2}+(V_r^2-a^2)\frac{\partial^2\varphi}{\partial r^2}+\frac{1}{r^2}(V_\gamma^2-a^2)\frac{\partial^2\varphi}{\partial \gamma^2}\\&+2V_xV_r\frac{\partial^2\varphi}{\partial x\partial r}+\frac{2}{r}V_xV_\gamma\frac{\partial^2\varphi}{\partial x\,\partial \gamma}+\frac{2}{r}V_rV_\gamma\frac{\partial^2\varphi}{\partial r\partial \gamma}-\frac{V_r(a^2+V_\gamma^2)}{r}=0.\end{aligned} \tag{10.2.7}$$

Usually one equation (10.2.7) for velocity potential is obtained in place of the system of the equations of motion (10.2.1) and continuity (10.2.2). According to the property of a linearized perturbation flow

$$V_x=V_\infty+V_x',\quad V_r=V_r',\quad V_\gamma=V_\gamma, \tag{10.2.8}$$

where additional perturbation velocity components

$$V_x'\ll V_\infty,\ V_r'\ll V_\infty,\ V_\gamma'\ll V_\infty.$$

Therefore equation (7.1.2′) for the speed of sound, in which it is assumed that $u=V_x'$, is valid. Using this relation in equation (10.2.7) along with the value of equation (10.2.8) and the quantities

$$V_x^2=V_\infty+2V_\infty V_x',\ V_r^2=V_r'^2,$$
$$V_\gamma^2=V_\gamma'^2,\ \varphi=\varphi_\infty+\varphi',$$

we get

$$[V_\infty^2-a_\infty^2+(k-1)\,V_\infty\,V_x']\frac{\partial^2\varphi'}{\partial x^2}+[V_r'^2-a_\infty^2+(k-1)V_\infty V_x']\frac{\partial^2\varphi'}{\partial r^2}$$
$$+\frac{1}{r^2}[V_\gamma'^2-a_\infty^2+(k-1)V_\infty V_x']\frac{\partial^2\varphi'}{\partial\gamma^2}+2(V_\infty+V_x')V_r'\frac{\partial^2\varphi'}{\partial x\partial r}$$
$$+\frac{2}{r}(V_\infty+V_x')V_\gamma'\frac{\partial^2\varphi'}{\partial x\partial\gamma}+\frac{2}{r}V_r'V_\gamma'\frac{\partial^2\varphi'}{\partial r\partial\gamma}$$
$$-\frac{V_r'}{r}[a_\infty^2-(k-1)V_\infty V_x'+V_\gamma'^2]=0. \qquad (10.2.9)$$

Considering that the second derivatives of φ' are quantities of the first order of smallness, terms incorporating the product of these derivatives and perturbation components of velocity V_x', V_r' or V_γ' in equation (10.2.9) can be neglected. Then we find the linear differential equation for the additional values of potential function φ'

$$(V_\infty^2-a_\infty^2)\frac{\partial^2\varphi'}{\partial x^2}-a_\infty^2\frac{\partial^2\varphi'}{\partial r^2}-\frac{a_\infty^2}{r^2}\cdot\frac{\partial^2\varphi'}{\partial\gamma^2}-\frac{a_\infty^2}{r}\cdot\frac{\partial\varphi'}{\partial r}=0. \qquad (10.2.10)$$

Dividing all the terms of this equation by $-a_\infty^2$, we get:

$$(1-\mathbf{M}_\infty^2)\frac{\partial^2\varphi'}{\partial x^2}+\frac{\partial^2\varphi'}{\partial r^2}+\frac{1}{r^2}\cdot\frac{\partial^2\varphi'}{\partial\gamma^2}+\frac{1}{r}\cdot\frac{\partial\varphi'}{\partial r}=0. \qquad (10.2.10')$$

Equation (10.2.10') is used for study of a flow near thin bodies of revolution at small angle of attack, i.e, a nonaxisymmetrical small-perturbation flow. For an axisymmetrical flow-interaction (angle of attack equal to zero) this equation is simplified because the velocity component $V_\gamma'=(1/r)(\partial\varphi'/\partial\gamma)=0$ and hence

$$(1-\mathbf{M}_\infty^2)\frac{\partial^2\varphi'}{\partial x^2}+\frac{\partial^2\varphi'}{\partial r^2}+\frac{1}{r}\cdot\frac{\partial\varphi'}{\partial r}=0. \qquad (10.2.11)$$

Equations (10.2.10') and (10.2.11) serve as the theoretical basis for the aerodynamics of steady linearized flows past thin bodies of revolution. The solutions of these equations determine the perturbation potential φ'. The solution of equation of potential φ' will be carried out under the following boundary conditions: Potential φ' should be equal to zero at the boundary (at infinity) of the disturbed region. In the present case the surface of the weak shock arising in front of the thin sharp-nosed body and in practice representing small disturbances (plane compression wave) or a Mach line with the angle of inclination of its generator to velocity vector $\overline{V}_\infty$ equal to $\mu_\infty=\sin^{-1}(1/\mathbf{M}_\infty)$ happens to be just this boundary. This potential φ' must satisfy the condition of unseparated flow (3.3.19) on the surface of a body in the flow. Here the function describing the surface of revolution in (3.3.19)

can be expressed in the form $F=f(x)-r$. Then

$$\varphi_r/\varphi_x=dr/dx, \tag{10.2.12}$$

where

$$\left.\begin{aligned}\varphi_r&=\frac{\partial\varphi}{\partial r}=\frac{\partial(\varphi_\infty+\varphi')}{\partial r}=\frac{\partial\varphi_\infty}{\partial r}+\frac{\partial\varphi'}{\partial r}=\varphi_{\infty r}+\varphi'_r;\\ \varphi_x&=\frac{\partial\varphi}{\partial x}=\frac{\partial(\varphi_\infty+\varphi')}{\partial x}=\frac{\partial\varphi_\infty}{\partial x}+\frac{\partial\varphi'}{\partial x}=\varphi_{\infty x}+\varphi'_x.\end{aligned}\right\} \tag{10.2.13}$$

The components of undisturbed velocity in the cylindrical coordinates can be determined from the scheme in Fig. 10.2.1:

$$\left.\begin{aligned}V_{x\infty}&=\partial\varphi_\infty/\partial x=\varphi_{x\infty}=V_\infty\cos\alpha;\\ V_{r\infty}&=\partial\varphi_\infty/\partial r=\varphi_{r\infty}=V_\infty\sin\alpha\cos\gamma.\end{aligned}\right\} \tag{10.2.14}$$

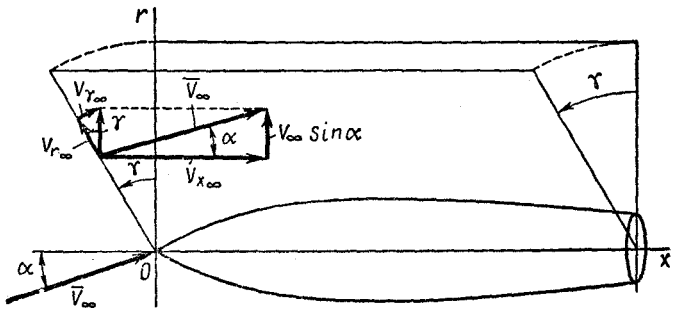

Fig. 10.2.1. Velocity components of undisturbed flow in cylindrical coordinates.

The third component of velocity can be found from this scheme of flow:

$$V_{\gamma\infty}=\frac{1}{r}\cdot\frac{\partial\varphi_\infty}{\partial\gamma}=\frac{1}{r}\varphi_{\gamma\infty}=-V_\infty\sin\alpha\sin\gamma. \tag{10.2.15}$$

According to relations (10.2.14) and (10.2.15) the velocity potential of the undisturbed flow will be

$$\varphi_\infty=xV_\infty\cos\alpha+rV_\infty\sin\alpha\cos\gamma. \tag{10.2.16}$$

For a linearized flow we have $\cos\alpha\approx1-\alpha^2/2$ and $\sin\alpha\approx\alpha$. Therefore

$$\varphi_\infty=xV_\infty[1-(\alpha^2/2)]+rV_\infty\alpha\cos\gamma. \tag{10.2.16'}$$

Consequently the resultant velocity potential will be

$$\begin{aligned}\varphi=\varphi_\infty+\varphi'(x,r,\gamma)&=xV_\infty[1-(\alpha^2/2)]\\ &+rV_\infty\alpha\cos\gamma+\varphi'(x,r,\gamma).\end{aligned} \tag{10.2.17}$$

Calculating the derivatives φ_r and φ_x, inserting them in (10.2.12) and neglect-

ing the quantity $0.5a^2$ in comparison to unity, we get

$$(V_\infty a\cos\gamma+\varphi_r')/(V_\infty+\varphi_x')=dr/dx. \tag{10.2.18}$$

If the flow is axisymmetrical the condition of unseparated flow (10.2.18) will be simplified to:

$$\varphi_r'/(V_\infty+\varphi_x')=dr/dx. \tag{10.2.19}$$

The velocity potential of a linearized flow φ for a body of revolution at a low angle of attack (Fig. 10.2.2) can be expressed as the sum of three components: potential due to undisturbed flow φ_∞, additional potential due to axially disturbed (axisymmetrical) flow $\varphi_1'(x, r)$ and second additional potential $\varphi_2'(x, r, \gamma)$ arising out of cross flow:

$$\varphi=\varphi_\infty+\varphi_1'(x, r)+\varphi_2'(x, r, \gamma). \tag{10.2.20}$$

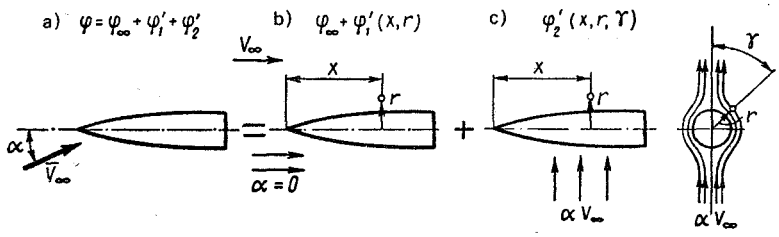

Fig. 10.2.2. Thin body of revolution in linearized flow at small angle of attack:
a—non-axisymmetrical flow-interaction; *b*—axisymmetrical flow-interaction; *c*—additional cross flow past body.

In the theory of linearized flows φ_1' and φ_2' are taken as functions which, appearing as the solutions of equations of motion, determine the flows independent of each other. Therefore the boundary conditions can be separately imposed on each such function. Specifically the solution for φ_1' obtained from equation (10.2.11)

$$(1-\mathbf{M}_\infty^2)\,\varphi_{1xx}'+\varphi_{1rr}'+(\varphi_{1r}'/r)=0 \tag{10.2.11'}$$

(where $\varphi_{1xx}'=\partial^2\varphi_1'/\partial x^2$, $\varphi_{1rr}'=\partial^2\varphi_1'/\partial r^2$, $\varphi_{1r}'=\partial\varphi_1'/\partial r$) should satisfy the condition (10.2.19) of axisymmetrical flow

$$\varphi_{1r}'/(V_\infty+\varphi_{1x}')=dr/dx. \tag{10.2.19'}$$

The boundary condition for function φ_2' satisfying the equation (10.2.10')

$$(1-\mathbf{M}_\infty^2)\,\varphi_{2xx}'+\varphi_{2rr}'+(\varphi_{2\gamma\gamma}'/r^2)+(\varphi_{2r}'/r)=0 \tag{10.2.10''}$$

is obtained from the expression (10.2.18) which may be written in the form

$$aV_\infty\cos\gamma+\varphi_{1r}'+\varphi_{2r}'=\frac{dr}{dx}(V_\infty+\varphi_{1x}'+\varphi_{2x}'). \tag{10.2.21}$$

In these expressions $\varphi'_{1x}=\partial\varphi'_1/\partial x$, $\varphi'_{2x}=\partial\varphi'_2/\partial x$, etc.

Keeping equation (10.2.19′) in view and omitting the term of lower order $(dr/dx)\,\varphi'_{2x}$ in (10.2.21), we get the boundary condition from (10.2.21):

$$\varphi'_{2r}=-aV_\infty\cos\gamma. \tag{10.2.22}$$

According to the condition (10.2.22) the additional potential due to cross flow should be such that the radial component of velocity of an undisturbed flow $V_{r\infty}=aV_\infty\cos\gamma$ vanishes at the surface of the body. This component of velocity may as well be supersonic as subsonic. The assumption $V_{r\infty}<a_\infty$ has no meaning because the additional cross flow in question represents part of the resultant flow and happens to be the mathematical consequence of the model of such a flow.

After determining the resultant velocity potential (10.2.20), taking into account the boundary conditions, it is possible to calculate velocity and then pressure with the help of Bernoulli's equation:

$$\frac{k}{k-1}\cdot\frac{p}{\rho}+\frac{V^2}{2}=\frac{k}{k-1}\cdot\frac{p_\infty}{\rho_\infty}+\frac{V_\infty^2}{2}.$$

Using here the value of $\rho=\rho_\infty\,(p/p_\infty)^{1/k}$, since the flow can be considered isentropic, we find

$$\frac{k}{k-1}\left(\frac{p}{p_\infty}\right)^{(k-1)/k}\frac{p_\infty}{\rho_\infty}+\frac{V^2}{2}=\frac{k}{k-1}\cdot\frac{p_\infty}{\rho_\infty}+\frac{V_\infty^2}{2}.$$

Noting that $kp_\infty/\rho_\infty=a_\infty^2$ and $\mathbf{M}_\infty^2=V_\infty^2/a_\infty^2$, we get

$$\frac{p}{p_\infty}=\left[1+\frac{k-1}{2}\mathbf{M}_\infty^2\left(1-\frac{V^2}{V_\infty^2}\right)\right]^{k/(k-1)}.$$

As the square of total velocity is

$$V^2=(V_\infty\cos a+V'_x)^2+V'^2_r+V'^2_y,$$

pressure will be given by

$$\frac{p}{\rho_\infty}=\left[1-(k-1)\mathbf{M}_\infty^2\left(\frac{V'_x}{V_\infty}\cos a+\frac{V'^2_r}{2V_\infty^2}+\frac{V'^2_y}{2V_\infty^2}+\frac{V'^2_x}{2V_\infty^2}-\frac{\sin^2 a}{2}\right)\right]^{k/(k-1)}. \tag{10.2.23}$$

Here the second term in square brackets is less than unity and hence the complete expression can be given in terms of the binomial series. Maintaining only the first two terms in the series expansion, taking into account the order of smallness of quantity $V'^2_x/2V_\infty^2$ in comparison with the first term in the circular bracket, and assuming that $\cos a\approx 1$, $\sin^2 a\approx a^2$ at small angles of attack, we get

$$\frac{p}{p_\infty}=1-k\mathbf{M}_\infty^2\left(\frac{V_x}{V_\infty}+\frac{V_r'^2}{2V_\infty^2}+\frac{V_y'^2}{2V_\infty^2}-\frac{a^2}{2}\right). \tag{10.2.24}$$

Then the coefficient of pressure will be

$$\bar{p}=\frac{2(p-p_\infty)}{k\mathbf{M}_\infty^2 p_\infty}=-2\left(\frac{V_x'}{V_\infty}+\frac{V_r'^2}{2V_\infty^2}+\frac{V_y'^2}{2V_\infty^2}-\frac{a^2}{2}\right). \tag{10.2.25}$$

According to the condition (10.2.12) in which $\varphi_x\approx\varphi_{x\infty}=V_\infty$ the component V_r' can be replaced by the quantity

$$V_r'=\varphi_r'=V_\infty\,(dr/dx), \tag{10.2.19''}$$

and V_x' and V_y' can be replaced by expressions in terms of additional potentials

$$V_x'=\varphi_x',\ V_y'=\frac{1}{r}\varphi_{y\infty}'+\frac{1}{r}\varphi_{2y}',$$

where the quantity

$$\varphi_{y\infty}'/r=-a\,V_\infty\sin\gamma,$$

according to (10.2.15).
As a result we get

$$\bar{p}=\frac{-2}{V_\infty^2}\left[V_\infty\varphi_x'+\frac{V_\infty^2}{2}\left(\frac{dr}{dx}\right)^2+\frac{1}{2}\left(\frac{\varphi_{2y}'}{r}-a\,V_\infty\sin\gamma\right)^2-\frac{a^2V_\infty^2}{2}\right]. \tag{10.2.26}$$

This value of pressure coefficient can be represented as a sum of two components, i.e. $\bar{p}=\bar{p}_1+\bar{p}_2$. One of the components $\bar{p}_1$ is determined by the conditions of an axisymmetrical flow:

$$\bar{p}_1=\frac{-2}{V_\infty^2}\left[V_\infty\varphi_{1x}'+\frac{V_\infty^2}{2}\left(\frac{dr}{dx}\right)^2\right], \tag{10.2.27}$$

and the other component $\bar{p}_2$ is obtained from the cross flow condition depending on the angle of attack:

$$\bar{p}_2=\frac{-2}{V_\infty^2}\left[V_\infty\varphi_{2x}'+\frac{1}{2}\left(\frac{\varphi_{2y}'}{r}-aV_\infty\sin\gamma\right)^2-\frac{a^2V_\infty^2}{2}\right]. \tag{10.2.28}$$

3. Axisymmetrical Flow-Interaction

One problem of the linearized axisymmetrical flow-interaction of a thin body of revolution will be solved if an additional velocity potential φ_1',

satisfying the linearized equation (10.2.11), is worked out. Direct substitution indicates that the expression

$$\varphi_1' = \int_0^{x-\alpha' r} \frac{f(\varepsilon)\, d\varepsilon}{\sqrt{(x-\varepsilon)^2 - \alpha'^2 r^2}}, \tag{10.3.1}$$

where $\alpha' = \sqrt{M_\infty^2 - 1}$, actually satisfies equation (10.2.11). The meaning of solution (10.3.1) can be established if the variable determined by the equality $\alpha' r\sqrt{-1} = p$ is introduced. Then equation (10.2.11) leads to a form coinciding with the equation of velocity potential for an incompressible flow, namely

$$\varphi_{1xx} + \varphi_{1pp}' + (\varphi_{1p}'/p) = 0, \tag{10.3.2}$$

where indices "x" and "p" denote the corresponding partial derivatives of φ_1' with respect to x and p.

Suppose a source of fluid with flow rate (strength) q lies at some point $x=\varepsilon$ on the axis of a body. The velocity potential due to this source at a point with coordinates x, p situated on a spherical surface of radius

$$\rho = \sqrt{(x-\varepsilon)^2 + p^2}$$

will be determined by formula (2.9.14) in the form

$$\varphi_1' = -q/[4\pi\sqrt{(x-\varepsilon)^2 + p^2}].$$

Now if it is assumed that a system of sources with variable strength $q = -4\pi f(\varepsilon)$ per unit length is situated along the axis of a body over the section $\varepsilon = 0$ to $\varepsilon = x - \alpha' r$ the resultant potential due to the action of all sources at a point x, r here being considered will be expressed by the formula

$$\varphi_1' = \int_0^{x-\alpha' r} f(\varepsilon)\, d\varepsilon / \sqrt{(x-\varepsilon)^2 + p^2}. \tag{10.3.3}$$

It may be shown by direct substitution that the integral (10.3.3) satisfies the differential equation (10.3.2). Consequently the solution (10.3.3) represents the potential function of sources continuously distributed along the axis of the body. Comparing (10.3.3) and (10.3.1), we see that these expressions are identical under the condition $p = \alpha' r\sqrt{-1}$. So with the help of similarity we find that the meaning of solution (10.3.1), as in the case of an incompressible fluid, is that the function φ_1' happens to be the potential of sources continuously distributed along the axis of the body. The solution (10.3.1) obtained reflects the method of sources according to which the body in the flow-interaction is replaced by a system of continuously distributed sources or sinks along its axis.

The law of distribution of sources (sinks), i.e. the form of function $f(\varepsilon)$,

must be such that one of the stream lines of the flow as a result of superposition of the undisturbed flow over the flow due to these sources coincides with the generator of the body of revolution. In other words, the potential function φ_1' must satisfy the condition (10.2.19′) of unseparated flow.

The formal analogy between the incompressible (or compressible subsonic) flow and the compressible supersonic flow due to sources or sinks should be supplemented by the peculiarities of a supersonic flow. Whereas the source in a subsonic flow has its effect on all points in space situated both upstream and downstream disturbances due to sources in a supersonic flow propagate only within the Mach cones with apexes at the sources. If the system of sources continuously distributed along the axis of the body (Fig. 10.3.1) is considered the velocity and pressure at any point $A(x, r)$ will be determined by the disturbances that emerge from the sources lying upstream starting from point $\varepsilon = x - \alpha' r$ and ending at a point $\varepsilon = x = 0$, coinciding with the apex of the body. At a point $\varepsilon = x = 0$ the strength of the source is zero because it is assumed that disturbances are absent at $\varepsilon \leqslant 0$. From the above discussion the limits of the integral in formula (10.3.1) are determined.

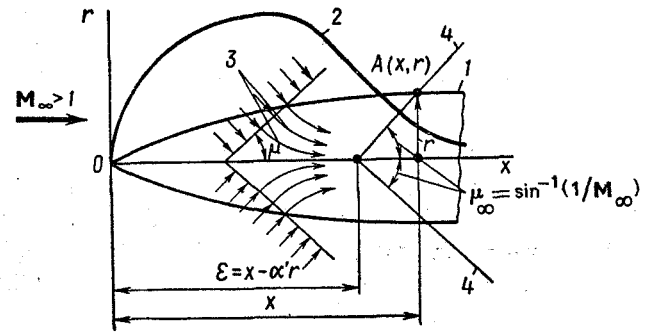

Fig. 10.3.1. Distribution of sources along axis of body and their effect on flow-interaction at supersonic speeds:

1—generator of body of revolution; *2*—curve $f(x)$ characterizing distribution of sources; *3*—flow lines from sources; *4*—cone of disturbances (Mach cone).

The form of a curve $f(\varepsilon)$ [or $f(x)$] representing the law of distribution of sources (sinks) for a thin body with an arbitrary generator is shown in Fig. 10.3.1. This curve determines the continuous nature of small disturbances induced by sources (sinks) and corresponding to a linearized flow-interaction. In a case where large disturbances arise, for example during the flow-interaction of a body with a blunt nose or sharp-nosed bodies with large inclination of generators to the undisturbed velocity vector, the linear theory is not valid.

To find the general relations for velocity and pressure we transform (10.3.1), introducing a new variable of integration:

$$z=\cosh^{-1}[(x-\varepsilon)/(a'r)]. \tag{10.3.4}$$

Taking into account that

$$\cosh z=(x-\varepsilon)/(a'r),\ \varepsilon=x-a'r\cosh z,$$
$$d\varepsilon=-a'r\sinh z\,dz$$

according to (10.3.4), the expression (10.3.1) can be transformed into the form

$$\varphi_1'=\int_0^{\cosh^{-1}(x/a'r)} f(x-a'r\cosh z)\,dz. \tag{10.3.5}$$

The upper limit of $z=\cosh^{-1}(x/a'r)$ and the lower limit $z=0$ of the integral in formula (10.3.5) correspond to the lower limit $\varepsilon=0$ and upper limit $\varepsilon=x-a'r$ of the integral in (10.3.1).

Differentiating φ_1' with respect to x, we find the additional axial component of velocity

$$V_{x1}'=\varphi_{1x}'=\frac{\partial}{\partial x}\int_0^{\cosh^{-1}(x/a'r)} f(x-a'r\cosh z)\,dz$$
$$=\int_0^{\cosh^{-1}(x/a'r)} \dot{f}(x-a'r\cosh z)\,dz+f(x-a'r\cosh z)\Big|_{z=\cosh^{-1}(x/a'r)}$$
$$\times\frac{\partial}{\partial x}\left(\cosh^{-1}\frac{x}{a'r}\right), \tag{10.3.6}$$

where $\dot{f}$ represents the total derivative of function f with respect to $x-a'r\cosh z$. Since the strength of the source near the apex of the body $f(\varepsilon)=f(0)=0$, we have

$$V_{x1}'=\varphi_{1x}'=\int_0^{\cosh^{-1}(x/a'r)} \dot{f}(x-a'r\cosh z)\,dz. \tag{10.3.7}$$

As with (10.3.6), we find the radial component of velocity in the form

$$V_{r1}'=\varphi_{1r}'=-a'\int_0^{\cosh^{-1}(x/a'r)} \dot{f}(x-a'r\cosh z)\cosh z\,dz. \tag{10.3.8}$$

Let us change expression (10.3.8) in terms of the variable determined by the equation $\varepsilon=x-a'r\cosh z$ according to (10.3.4). Since

$$dz=\frac{-d\varepsilon}{\sqrt{[(x-\varepsilon)/(a'r)]^2-1}}\cdot\frac{1}{a'r}=\frac{-d\varepsilon}{\sqrt{(x-\varepsilon)^2-a'^2r^2}};$$

$$\cosh z=\frac{x-\varepsilon}{a'r},$$

the expression under the integration sign will be

$$\dot{f}(x-a'r\cosh z)\cosh z\,dz=\frac{\dot{f}(\varepsilon)\,(x-\varepsilon)\,d\varepsilon}{a'r\sqrt{(x-\varepsilon)^2-a'^2r^2}}.$$

The lower limit $z=0$ corresponds to the value of $1=(x-\varepsilon)/(a'r)$, from which the new limit $\varepsilon=x-a'r$; and the limit ε corresponds to the upper limit $z=\cosh^{-1}(x/a'r)$ obtained from the condition

$$\cosh\,[\cosh^{-1}(x/a'r)]=(x-\varepsilon)/(a'r),$$

according to which $\varepsilon=0$. Thus

$$V'_{r1}=\frac{1}{r}\int\limits_{x-a'r}^{0}\frac{\dot{f}(\varepsilon)\,(x-\varepsilon)\,d\varepsilon}{\sqrt{(x-\varepsilon)^2-a'^2r^2}} \tag{10.3.9}$$

or

$$V'_{r1}=\frac{1}{r}\int\limits_{x-a'r}^{0}\dot{f}(\varepsilon)\left[1-\left(\frac{a'r}{x-\varepsilon}\right)^2\right]^{-1/2}d\varepsilon. \tag{10.3.9'}$$

As $a'r<(x-\varepsilon)$ the expression $[1-(a'r)^2/(x-\varepsilon)^2]^{-1/2}$ can be expanded in the series:

$$V'_{r1}=\frac{1}{r}\int\limits_{x-a'r}^{0}\dot{f}(\varepsilon)\left[1+\frac{1}{2}\left(\frac{a'r}{x-\varepsilon}\right)^2-\ldots\right]d\varepsilon.$$

As $r\to 0$ the term in the square brackets tends to unity and the lower limit of integration tends to the value $\varepsilon=x$. According to this the limiting value for a radial component of velocity at $r\to 0$ will be

$$V'_{r1}=\frac{1}{r}\int\limits_{x}^{0}\dot{f}(\varepsilon)\,d\varepsilon,$$

whence

$$V'_{r1}=[f(0)-f(x)]/r.$$

But near the apex of the body $f(0)=0$ and therefore

$$V'_{r1}=-f(x)/r. \tag{10.3.10}$$

Using the condition (10.2.19) for an unseparated flow interaction, in which the second terms of φ'_{1x} in the numerator can be neglected for a thin body,

we get the relation for determination of the function $f(x)$:

$$f(x)=-r\,(dr/dx)\,V_\infty. \tag{10.3.11}$$

This equation can be written in the form

$$f(x)=-\frac{1}{2\pi}\cdot\frac{dS(x)}{dx}V_\infty=-\frac{V_\infty}{2\pi}\,S'(x), \tag{10.3.12}$$

where $S(x)=\pi r^2$ is the variable value of the area of the cross section of a thin body.

The expression (10.3.12) for a function $f(x)$ determining the law of distribution of sources along the axis in the limiting case at $r\to 0$ can be used for calculation of the component of velocity (10.3.7) which is necessary in calculation of pressure by formula (10.2.27) on the surface of thin real bodies of revolution. For this purpose we replace x in (10.3.12) by $\varepsilon=x-a'r\cosh z$ and substitute the derivative

$$f'(\varepsilon)=\frac{df}{d\varepsilon}=-\frac{V_\infty}{2\pi}\cdot\frac{d^2S(\varepsilon)}{d\varepsilon^2}=-\frac{V_\infty}{2\pi}\,S''(x-a'r\cosh z) \tag{10.3.13}$$

in equation (10.3.7).
As a result we have

$$V'_{x1}=\varphi'_{1x}=\frac{-V_\infty}{2\pi}\int_0^{\cosh^{-1}(x/a'r)} S''(x-a'r\cosh z)\,dz. \tag{10.3.14}$$

So it is necessary to know the form of a body of revolution and the distribution of area along its axis, i.e. the form of function $S(x)$, for the calculation of velocity by formula (10.3.14).

Let us take, for example, a body of revolution with a parabolic generator (see Fig. 10.1.3), whose equation is given in the form of (10.1.48). According to this equation the area of cross section

$$S(x)=\pi r^2=\frac{\pi x^2}{4\lambda_0^2}\left(2-\frac{x}{x_0}\right)^2. \tag{10.3.15}$$

From this the second derivative with respect to x will be

$$S''(x)=\frac{d^2S(x)}{dx^2}=\frac{\pi}{\lambda_0^2}\left(2-\frac{6x}{x_0}+\frac{3x^2}{x_0^2}\right). \tag{10.3.16}$$

Replacing x by $\varepsilon=x-a'r\cosh z$, we get

$$S''(x-a'r\cosh z)=\frac{\pi}{\lambda_0^2}\left[2-\frac{6}{x_0}(x-a'r\cosh z)+\frac{3}{x_0^2}(x-a'r\cosh z)^2\right]. \tag{10.3.16'}$$

Substitution of this in (10.3.14) leads to

$$V'_{x1}=\frac{-V_\infty}{2\lambda_0^2}\int_0^{\cosh^{-1}u}\left[2-\frac{6\bar{x}}{u}(u-\cosh z)+\frac{3\bar{x}^2}{u^2}(u-\cosh z)^2\right]dz, \quad (10.3.17)$$

where $\bar{x}=x/x_0$ and

$$u=x/(a'r). \quad (10.3.18)$$

Let us introduce the notations

$$\left.\begin{aligned} i_x^0&=I_0;\\ i_x^1&=uI_0-I_1;\\ i_x^2&=u^2I_0-2uI_1+I_2, \end{aligned}\right\} \quad (10.3.19)$$

where the quantities I_n are determined in the form of integrals

$$I_n=\int_0^{\cosh^{-1}u}(\cosh z)^n\,dz \quad (n=0,\ 1,\ 2). \quad (10.3.20)$$

In accordance with the notations (10.3.19) we have

$$V'_{x1}=\frac{-V_\infty}{2\lambda_0^2}\left(2i_x^0-\frac{6\bar{x}i_x^1}{u}+\frac{3\bar{x}^2i_x^2}{u^2}\right). \quad (10.3.21)$$

In the case of a more general form of function $S''(x)$ in the form of series

$$S''(x)=\sum_{n=0}^{k}a_n x^n \quad (10.3.22)$$

the expression, like (10.3.21), can be given in the following form:

$$V'_{x1}=-\sum_{n=0}^{k}b_n i_x^n. \quad (10.3.23)$$

The coefficients a_n depend on the form of the generator of the body of revolution and b_n also depends on velocity V_∞. The values of function i_x^n for $n=0,\ 1,\ 2$, given in the form (10.3.19), correspond to the given generator of the body as an equation of a parabola of second order.

For a body of revolution with an equation of generator of higher order it is necessary to calculate the quantities i_x^n for $n=3,\ 4$, etc. In particular, if the equation of generator is such that the derivative $S''(x)$ in (10.3.22) is determined by the equation

$$S''(x)=\sum_{n=0}^{3}a_n x^n, \quad (10.3.22')$$

then according to (10.3.23) the component of velocity will be

$$V'_{x1} = -\sum_{n=0}^{3} b_n i_x^n, \tag{10.3.23'}$$

where i_x^n is calculated for values of $n=0$, 1, 2 by formulas (10.3.19) and for $n=3$ from the expression

$$i_x^3 = u^3 I_0 - 3u^2 I_1 + 3u I_2 - I_3. \tag{10.3.24}$$

The function i_x^n calculated for the values of parameter u from 1 to 8.8 are presented in Table 10.3.1.

In a particular case, it is possible to obtain the expression for a component of velocity over a thin cone using the relation (10.3.21). To do this it is necessary to replace $1/\lambda_0$ by $\beta_0=\beta_K$ (angle of sharpness of a parabolic body of revolution near the nose section of the cone) and to take $\bar{x}=0$. Then we have

$$V'_{x1K} = -V_\infty (i_x^0)_K \beta_K^2. \tag{10.3.25}$$

Keeping in view that according to (10.3.19) and (10.3.20):

$$i_{xK}^0 = I_{0K} = \cosh^{-1} u_K$$

for a cone, where

$$u_K = (x/a'r)_K = 1/a'\beta_K,$$

the velocity component will be

$$V'_{x1K} = -V_\infty \beta_K^2 \cosh^{-1} u_K = -V_\infty \beta_K^2 \ln (u_K + \sqrt{u_K^2 - 1}). \tag{10.3.25'}$$

The coefficient of pressure on the surface of a body of revolution at a corresponding point can be found from formula (10.2.27) for the values of V'_{x1} obtained. In particular, on a conical surface where an additional component of velocity is determined by (10.3.25') the pressure coefficient will be given by

$$\bar{p}_{1K} = \beta_K^2 [2 \ln (u_K + \sqrt{u_K^2 - 1}) - 1]. \tag{10.3.26}$$

In accordance with (9.2.30) the relation (10.3.26) determines the coefficient of wave drag of a thin cone, i.e.

$$c_{xw.K} = \bar{p}_{1K} = \beta_K^2 [2 \ln (u_K + \sqrt{u_K^2 - 1}) - 1]. \tag{10.3.26'}$$

For a thin body of revolution of arbitrary shape calculation of the coefficient of wave drag should be carried out by formula (10.1.51) in which the pressure coefficient, according to (10.3.14) and (10.2.27), will be

$$\bar{p}_1 = \frac{1}{\pi} \int_0^{\cosh^{-1} u} S''(x - a'r \cosh z)\, dz - \left(\frac{dr}{dx}\right)^2. \tag{10.3.27}$$

TABLE 10.3.1

u	i_x^0	i_x^1	i_x^2	i_x^3	i_r^0	i_r^1	i_r^2	i_r^3
1.0	0	0	0	0	0	0	0	0
1.1	0.4435	0.0298	0.0019	0.0001	0.4582	0.0303	0.0026	0.0004
1.2	0.6223	0.0838	0.0149	0.0071	0.6633	0.0856	0.0109	0.0015
1.3	0.7567	0.1527	0.0392	0.0095	0.8312	0.1256	0.0383	0.0096
1.4	0.8673	0.2342	0.0753	0.0254	0.9804	0.2526	0.0794	0.0281
1.6	1.047	0.4265	0.2068	0.2412	1.249	0.4756	0.2230	0.1124
1.8	1.177	0.6690	0.4875	0.4631	1.450	0.7166	0.4137	0.2949
2.0	1.317	0.9024	0.7314	0.6332	1.732	1.073	0.8296	0.6950
2.4	1.522	1.472	1.675	2.030	2.182	1.857	1.990	2.326
2.8	1.690	2.116	3.107	4.854	2.615	2.816	3.846	5.946
3.2	1.831	2.820	5.076	9.701	3.040	3.948	6.543	11.90
3.6	1.954	3.578	7.634	17.28	3.458	5.247	10.21	21.84
4.0	2.064	4.382	10.81	28.28	3.873	6.714	14.98	36.84
4.4	2.162	5.227	14.65	43.46	4.286	8.348	21.00	58.31
4.8	2.251	6.111	19.19	63.76	4.694	10.14	28.37	87.74
5.2	2.333	7.028	24.44	89.85	5.103	12.10	37.26	127.0
5.6	2.408	7.976	30.44	122.7	5.510	14.22	47.78	177.9
6.0	2.478	8.953	37.21	163.2	5.916	16.51	60.07	242.4
6.4	2.544	9.958	44.77	212.3	6.322	18.96	74.25	322.8
6.8	2.605	10.99	53.17	271.1	6.726	21.56	90.44	421.4
7.2	2.663	12.04	62.37	340.2	7.130	24.34	108.8	540.7
7.6	2.717	13.12	72.43	421.0	7.534	27.27	129.4	683.4
8.0	2.769	14.22	83.37	514.5	7.937	30.36	152.5	852.2
8.4	2.818	15.33	95.18	621.4	8.341	33.62	178.1	1050.4
8.8	2.865	16.47	107.9	743.3	8.743	37.04	206.3	1280.6

Assuming $dr/dx = \tan\beta \approx \beta$, we find the formula for the coefficient of wave drag:

$$c_{xw}=2\int_0^{\tilde{x}_K}\left[\frac{1}{\pi}\int_0^{\cosh^{-1}u} S''(x-a'r\cosh z)\,dz-\beta^2\right]\bar{r}\beta d\tilde{x}, \qquad (10.3.28)$$

where $\tilde{x} = x/r_0$.

For a parabolic generator satisfying the equation $r=(r_0/x_0)x\,(2-x/x_0)$ the derivative

$$\frac{dr}{dx}=\frac{2r_0}{x_0}(1-\bar{x}) = \frac{1}{\lambda_0}(1-\bar{x}) = \beta_0(1-\bar{x}), \qquad (10.3.29)$$

where $\bar{x} = x/x_0$.

In accordance with (10.3.16′) the integral in (10.3.27) can be expressed in the form

$$\int_0^{\cosh^{-1} u} S''(x-a'r\cosh z)dz=\beta_0^2 N_1(u, \bar{x}). \tag{10.3.30}$$

Here N_1 is some function of nondimensional coordinate $\bar{x}$ and parameter u that is determined from the condition

$$u=\frac{x}{a'r}=\frac{x_0}{a'r_0}\cdot\frac{1}{2-(x/x_0)}=\frac{u_0}{2-\bar{x}}, \tag{10.3.31}$$

where $u_0=1/(a'\beta_0)$. Keeping the equations (10.3.29) through (10.3.31) in view, the relation (10.3.27) can be represented in the following form:

$$\bar{p}_1=\beta_0^2 N(u_0, \bar{x}), \tag{10.3.32}$$

where N is some function of parameter u_0 and nondimensional coordinate $\bar{x}$.

Taking equation (10.3.32) into account, the coefficient of wave drag in (10.3.28) will be

$$c_{xw}=\beta_0^2 D(u_0), \tag{10.3.33}$$

where D is some function of parameter u_0 only.

The following conclusion concerning the aerodynamic similarity of flows over parabolic bodies of revolution may be derived from the general formulas (10.3.32) and (10.3.33). If these flows are characterized by one and the same value of parameter u_0 the ratios $\bar{p}_1/\beta_0^2$ will be the same at the corresponding points with the same nondimensional coordinates $\bar{x}$. In the case of aerodynamically similar flows the bodies of revolution undergo axial forces such that the ratio of c_{xw}/β_0^2 will be identical for them. So in this case the similarity criterion happens to be the parameter

$$u_0=\frac{1}{a'\beta_0}=\frac{1}{\beta_0\sqrt{\mathbf{M}_\infty^2-1}}=\frac{\lambda_0}{\sqrt{\mathbf{M}_\infty^2-1}}. \tag{10.3.34}$$

For Mach numbers $\mathbf{M}_\infty \gg 1$ the parameter u_0 can be expressed in the form

$$u_0=1/K_1, \tag{10.3.34'}$$

where

$$K_1=\beta_0\mathbf{M}_\infty=\mathbf{M}_\infty/\lambda_0.$$

Multiplying both sides of (10.3.32) by $\mathbf{M}_\infty^2$ and taking the relation (10.3.34') into account, we find

$$(p_1/p_\infty)-1=N_2(K_1, \bar{x}), \tag{10.3.35}$$

where N_2 is a function of variables K_1 and $\bar{x}$. According to the expression (10.3.35) the pressure function $(p_1/p_\infty)-1$ at a given point $\bar{x}$ depends only on parameter K_1. The law of similarity for this parameter is also confirmed by the results of calculation by the method of characteristics.

Research shows that in using linearized methods of calculation of flow-

interaction satisfactory coincidence of results for the pressure function is obtained only for values of parameters of similarity K_1 less than unity. The law of similarity for this parameter seems to be doubtful for some combinations of Mach numbers $\mathbf{M}_\infty$ and aspect ratios λ_0. This directly follows from the analysis of the limitations of applicability of linearized theory. These limitations may be established, for example, from formula (10.3.26) determining the pressure coefficient over a cone. It is obvious that at $u_K = u_0 < 1$ this formula loses its meaning because the quantity $\sqrt{u_0^2 - 1}$ will be imaginary. When u_0, though still exceeding unity, approaches formula (10.3.26) gives an unreal negative value for the pressure coefficient over a thin cone. Consequently calculation by linearized theory gives satisfactory results at least under the condition that u_0 is appreciably higher than unity. From this it follows that the application of the law of similarity will obviously be doubtful in the case where u_0 differs negligibly from unity. Here the quantity u_0 is determined according to the combination of two parameters, namely: the aspect ratio of a parabolic nose section and Mach number $\mathbf{M}_\infty$.

Physically the regions of doubtful similarity of flows correspond to the deviation of the real flow from a linearized flow. In fact, if the aspect ratio, diminishes, i.e. if the body becomes thicker (less sharp) or for the same aspect ratio Mach number $\mathbf{M}_\infty$ increases, the flow correspondingly diverges from a linearized flow. To maintain the linearized character of a flow it is necessary to increase the aspect ratio, i.e. to increase the sharpness of the body at higher values of Mach number $\mathbf{M}_\infty$. At the same time the inequality $\lambda_0 > \mathbf{M}_\infty$ should be observed. Accordingly the similarity parameter $K_1 = \mathbf{M}_\infty/\lambda_0$ must be less than unity.

From the expression $u_0 = (a'\beta_0)^{-1}$ it follows that if the body of revolution is thin, i.e. its aspect ratio is high, it is necessary to fulfill the condition $\mathbf{M}_\infty > 1$ to satisfy the inequality $u_0 > 1$. If the Mach number $\mathbf{M}_\infty \to 1$, according to formula (10.3.25′) the perturbation velocity in its absolute value will reach an infinitely large value, which is physically impossible. So the theory of linearized flows and their laws of similarity are valid only if two inequalities are satisfied simultaneously:

$$\lambda_0 > (\mathbf{M}_\infty^2 - 1)^{1/2} \quad \text{and} \quad \mathbf{M}_\infty > 1. \tag{10.3.36}$$

Comparison with empirical data indicates that calculations by linearized theory and application of similarity criteria are possible only for aspect ratios $\lambda_0 \geqslant 2$ and Mach numbers $\mathbf{M}_\infty$ not less than 1.4 to 1.5.

The similarity based on the parameter $K_1 = \mathbf{M}_\infty\beta_0$ for pressure also determines the similarity for the function of wave drag. Here the application of this law of similarity must be connected with the requirement of maintaining a linearized flow.

Multiplying both sides of formula (10.3.33) by $\mathbf{M}_\infty^2$, we get the general expression for drag function

$$\mathbf{M}_\infty^2 c_{xw} = \beta_0^2 H(K_1), \tag{10.3.37}$$

where $H(K_1)$ is a function depending on the parameter K_1. This expression shows that if the flow-interaction of two or more bodies of revolution with different aspect ratios is characterized by one and the same value of the parameter K_1 the bodies will have the same value of function $\mathbf{M}_\infty^2 c_{xw}$.

The above criteria of similarity were obtained as example of bodies of revolution with a parabolic generator. These bodies of revolution have this property by virtue of equation (10.1.48). It indicates that all of them are characterized by the same distribution of relative thicknesses along the length:

$\bar{x}=x/x_0$	0	0.2	0.4	0.6	0.8	1.0	1.2	1.4	1.6	1.8	2.0
$\bar{r}=r/r_0$	0	0.36	0.64	0.84	0.96	1.0	0.96	0.84	0.64	0.36	0

Among this group there may be geometrically similar bodies differing in their linear dimensions by some constant proportion. As such they obviously have the same aspect ratio and can be grouped together by uniform deformation, i.e. the same deformation in all directions. To fulfill aerodynamic similarity it is necessary to have the same Mach number $\mathbf{M}_\infty$ for a geometrically similar model as for the prototype body of revolution.

However, the class of parabolic bodies includes forms that can be grouped at least by virtue of uneven deformation. Let us consider two bodies with different aspect ratios. If the same linear scale is used for radial and axial coordinates the deformation of the bodies in the longitudinal and axial directions does not give complete coincidence. Concidence, known as affine grouping, may be attained if the scales for radial and axial coordinates are different. According to this, bodies with a parabolic generator are called affinely similar bodies. Conical bodies with generators given by the equation in nondimensional form $\bar{\mu}=\bar{x}$ belong to this class of affinely similar bodies. Conical bodies are consequently characterized by an identical distribution of relative thicknesses.

Unlike parabolic and conical bodies, an ogival nose with an equation of generator in the form of the arc of a circle of radius R (Fig. 10.3.2) has

$$\bar{r} = 2\bar{R}\left\{\left[1-\frac{\lambda_0^2}{\bar{R}^2}(\bar{x}-1)^2\right]^{1/2}-1\right\}+1, \tag{10.3.38}$$

where

$$\bar{r}=r/r_0,\ \lambda_0=x_0/(2r_0),\ \bar{R}=R/(2r_0).$$

With a change in λ_0 the distribution of relative thickness $\bar{r}$ along the length also changes. As a result one ogive-shaped nose cannot be affinely transformed into another. That is, bodies of ogive form cannot be affinely similar. However, when the linearized flow-interaction of thin bodies is being investigated the above similarity criteria can be used. In practice, for thin bodies

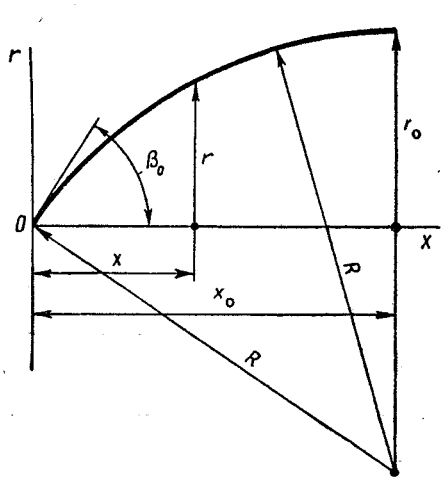

Fig. 10.3.2. Form and geometrical parameters of an ogival body of revolution.

with aspect ratios $\lambda_0 > 3$ it is possible to take a nondimensional radius determined from the equation (see Fig. 10.3.2)

$$\overline{R} = \lambda_0^2 + 0.25,$$

within an accuracy of 2 to 3% of $\overline{R} \approx \lambda_0^2$. It follows from (10.3.38) that the equation of generator (10.1.48) corresponds to this value of radius. In this way the ogive-shaped nose differs little from a parabolic nose for given aspect ratios. Therefore the variation in distribution of relative thicknesses along the length during transition from one body to another can be neglected and thin ogive-shaped noses can be considered affinely similar, for which the above similarity criteria (Section 1) are applicable.

4. Nonaxisymmetrical Flow-Interaction

The problem of a nonaxisymmetrical flow-interaction leads to the determination of an additional potential φ_2' based on the cross flow of gas near a thin body of revolution and satisfying the condition (10.2.10′). We will show that the solution for φ_2' may be obtained with the help of the solution of φ_1' for an axisymmetrical flow-interaction, i.e. we will show that there is a correlation between φ_2' and φ_1'. To do this we differentiate equation (10.2.11′) for an axisymmetrical perturbed flow respect to r:

$$(1-\mathbf{M}_\infty^2)\frac{\partial^2}{\partial x^2}\left(\frac{\partial \varphi_1'}{\partial r}\right)+\frac{\partial^2}{\partial r^2}\left(\frac{\partial \varphi_1'}{\partial r}\right)-\frac{1}{r^2}\cdot\frac{\partial \varphi_1'}{\partial r}+\frac{1}{r}\cdot\frac{\partial^2 \varphi_1'}{\partial r^2}=0. \quad (10.4.1)$$

Now if the expression

$$\varphi_2' = -(\partial \varphi_1'/\partial r)\cos\gamma \quad (10.4.2)$$

for an additional potential φ_2' is considered we arrive at (10.4.1) after substituting this in the basic equation (10.2.10″). Hence the equality (10.4.2) actually exists and the complete potential for disturbances in the case of a nonaxisymmetrical flow-interaction can be taken in the form

$$\varphi' = \varphi_1' + \varphi_2' = \varphi_1' - (\partial \varphi_1'/\partial r)\cos\gamma. \quad (10.4.3)$$

The method of analogy may be used to explain the physical meaning of integral φ_2'. This method was applied in studying the axisymmetrical flow-

interaction. It says that in a compressible flow as well as in an incompressible flow a body can be replaced by a system of sources and sinks.

In the case of the nonaxisymmetrical flow-interaction of a body the method of analogy will be as follows: If φ_1' is the potential function of sources (sinks) in an incompressible fluid flow continuously distributed along the body axis the derivative $\partial\varphi_1'/\partial r$, according to the expression (2.9.21'), should be taken as a function determining the flow due to dipoles distributed along the same axis. Accordingly, in investigating the flow-interaction of a body with a nonaxisymmetrical incompressible flow it can be replaced by the system of continuously distributed dipoles along its axis. Extending this analogy for an axisymmetrical flow over a body with disturbed axial symmetry, it will be assumed that the body in a supersonic linearized flow may be replaced by the system distributed supersonic dipoles along its axis. Now φ_2' happens to be the potential of these dipoles.

According to (10.3.5) the expression for φ_2' can take the form

$$\varphi_2' = -\cos\gamma \frac{\partial}{\partial r} \int_0^{\cosh^{-1}(x/\alpha' r)} f(x-\alpha' r\cosh z)\cosh z\, dz$$

$$= \alpha'\cos\gamma \int_0^{\cosh^{-1}(x/\alpha' r)} f'(x-\alpha' r\cosh z)\cosh z\, dz. \quad (10.4.4)$$

Replacing function $f'(\varepsilon)$ by $m(\varepsilon)$ here and using the notation $x/(\alpha' r)=u$, we get

$$\varphi_2' = \alpha'\cos\gamma \int_0^{\cosh^{-1}u} m(x-\alpha' r\cosh z)\cosh z\, dz. \quad (10.4.4')$$

The function $m(\varepsilon)$ in expression (10.4.4') describes the law of distribution of dipoles, i.e. the nature of variation in their strengths along the axis of a body of revolution. Replacing the body by the distribution of dipoles along its axis, it is necessary to consider the peculiarity of the propagation of disturbances in a supersonic flow. Here the disturbances due to dipoles, like those due to sources, propagate only downstream in the limits of the cone of disturbances.

In this way, using the above method of analogy, we will replace the body by a system of dipoles in order to investigate a nonaxisymmetrical flow or oblique flow over this body of revolution. This device means that an additional disturbance introduced into the flow by a body during a nonaxisymmetrical flow-interaction is equivalent to a disturbance due to dipoles placed over its axis in a certain way depending on the form and conditions of the undisturbed flow.

The solution of the problem of a nonaxisymmetrical flow-interaction, which leads to calculation of parameters of the flow perpendicular to the axis

of the body, will be achieved if the function $m(\varepsilon)$ is selected in such a way that the potential φ_2' satisfies the additional boundary condition on the surface of the body during the nonaxisymmetrical flow-interaction. This condition, on the basis of (10.2.22) and (10.4.4'), can be written in the following form:

$$a' \cos\gamma \frac{\partial}{\partial r} \int_0^{\cosh^{-1} u} m(x - a' r \cosh z) \cosh z \, dz = -aV_\infty \cos\gamma .$$

Taking differentiation of this, we get

$$a'^2 \int_0^{\cosh^{-1} u} \dot{m}(x - a' r \cosh z) \cosh^2 z \, dz = -aV_\infty, \tag{10.4.5}$$

where $\dot{m}$ is a derivative of function m with respect to $x - a' r \cosh z$.

Solving the integral equation (10.4.5), it is possible to determine the function for distribution of dipoles m for a given form of body and velocity of undisturbed flow. Solution of this equation can be simplified if a very thin body of revolution is considered. For this purpose we transform (10.4.5) with the help of the variable $\varepsilon = x - a' r \cosh z$:

$$\frac{1}{r^2} \int_0^{x - a' r} \frac{\dot{m}(\varepsilon)(x-\varepsilon)^2 d\varepsilon}{\sqrt{(x-\varepsilon)^2 - a'^2 r^2}} = aV_\infty. \tag{10.4.6}$$

For a very thin body with small r the integral in (10.4.6) may be taken equal to its value as $r \to 0$ as a first approximation. Then,

$$aV_\infty r^2 = \int_0^x \dot{m}(\varepsilon)(x-\varepsilon)\, d\varepsilon$$

or

$$aV_\infty r^2 = \int_0^x (x-\varepsilon)\, dm.$$

Integrating by parts and assuming $u = x - \varepsilon$, $dv = dm$, we get

$$aV_\infty r^2 = (x-\varepsilon) m(\varepsilon) \Big|_0^x + \int_0^x m(\varepsilon)\, d\varepsilon.$$

As $m(\varepsilon) = m(0) = 0$ near a sharp nose and the value of $\varepsilon \approx x$ as a consequence of $r \ll x$, we have

$$aV_\infty r^2 = \int_0^x m(x)\, dx.$$

After differentiation with respect to x we wet

$$m(x)=2aV_\infty r(dr/dx). \tag{10.4.7}$$

The expression (10.4.7) for function $m(x)$, which determines the law of distribution of dipoles in the limiting case of $r\to 0$, can be used for the calculation of the nonaxisymmetrical flow-interaction of a body. This flow differs from that over a thin body by the analogy given in Section 3 in connection with the function f in equation (10.3.11) for distribution of sources for investigation of an axisymmetrical flow-interaction. For this purpose it is necessary to change variable x to $\varepsilon=x-a'r\cosh z$ and to write

$$m(x-a'r\cosh z)=aV_\infty\frac{dr^2}{d\varepsilon}=\frac{aV_\infty}{\pi}S'(x-a'r\cosh z), \tag{10.4.8}$$

whence the derivative

$$\dot{m}(x-a'r\cosh z)=\frac{aV_\infty}{\pi}S''(x-a'r\cosh z). \tag{10.4.9}$$

After calculating the derivative φ'_{2x} from an additional potential (10.4.4') we get the relation for an axial component of velocity

$$V'_{x2}=\varphi'_{2x}=a'\cos\gamma\int_0^{\cosh^{-1}u}\dot{m}(x-a'r\cosh z)\cosh z\,dz. \tag{10.4.10}$$

Inserting the value of $\dot{m}$ from (10.4.9) in this equation, we have

$$V'_{x2}=\frac{a'aV_\infty\cos\gamma}{\pi}\int_0^{\cosh^{-1}u}S''(x-a'r\cosh z)\cosh z\,dz. \tag{10.4.11}$$

For the particular case of a parabolic generator with equation (10.1.48) the second derivative of function $S(x)$ is determined by formula (10.3.16). Consequently

$$V'_{x2}=\frac{a'aV_\infty\cos\gamma}{\lambda_0^2}\int_0^{\cosh^{-1}u}\left[2-\frac{6\bar{x}}{u}(u-\cosh z)+\frac{3\bar{x}^2}{u^2}(u-\cosh z)^2\right]\cosh z\,dz, \tag{10.4.12}$$

where $\bar{x}=x/x_0$, $u=x/(a'r)$.
Let us introduce the notations:

$$\left.\begin{aligned} i_r^0&=I_1;\\ i_r^1&=uI_1-I_2;\\ i_r^2&=u^2I_1-2uI_2+I_3,\end{aligned}\right\} \tag{10.4.13}$$

where the quantities I_n ($n=1, 2, 3$) are determined in the form of integrals (10.3.20).

Using these notations we have

$$V'_{x2}=\frac{a'a\ V_\infty \cos\gamma}{\lambda_0^2}\left(2i_r^0-\frac{6\bar{x}}{u}i_r^1+\frac{3\bar{x}^2}{u^2}i_r^2\right). \tag{10.4.14}$$

In the case of the more general given function $S''(x)$ in (10.3.22) the expression, on the lines of (10.4.12), can be given in the form

$$V'_{x2}=\sum_{n=0}^{l} g_n\, i_r^n. \tag{10.4.15}$$

The coefficients g_n depend on the shape of the generator of the body of revolution and on the conditions of undisturbed flow (angle of attack α, velocity V_∞). The value of function i_r^n are calculated for $n=0$, 1, 2 from formulas (10.4.13) and for $n=3$ from the expression

$$i_r^3=u^3I_1-3u^2I_2+3uI_3-I_4. \tag{10.4.16}$$

These functions i_r^n calculated for the values of parameter u from 1 to 8.8 are reproduced in Table (10.3.1).

For a thin cone in a flow at a low angle of attack we get

$$V'_{x2K}=2a'a\ V_\infty\, i_{rK}^0\, \beta_K^2 \cos\gamma \tag{10.4.17}$$

from (10.4.14), assuming that $\bar{x}=0$ and $\lambda_0^2=1/\beta_K^2$.

According to (10.3.20)

$$i_{rK}^0=\int_0^{\cosh^{-1}u_K}\cosh z\, dz=\sqrt{u_K^2-1}. \tag{10.4.18}$$

Keeping in view that $u_K=1/(a'\beta_K)$, we get

$$V'_{x2K}=2a\beta_K V_\infty \cos\gamma\sqrt{1-(a'\beta_K)^2}. \tag{10.4.19}$$

Using formula (10.2.28) the pressure coefficient at the point desired on the body of revolution can be determined. The derivative $\varphi'_{2\gamma}$ entering into this formula, in accordance with (10.4.4') and (10.4.8), is equal to

$$\varphi'_{2\gamma}=\frac{\partial\varphi'_2}{\partial\gamma}=a'\sin\gamma\int_0^{\cosh^{-1}u} m\,(x-a'r\cosh z)\cosh z\, dz$$

$$=\frac{a'a\ V_\infty\sin\gamma}{\pi}\int_0^{\cosh^{-1}u} S'\,(x-a'r\cosh z)\cosh z\, dz. \tag{10.4.20}$$

The simplified relation for $\varphi'_{2\gamma}$, which can be obtained from potential φ'_2

established on the basis of (10.3.10) and (10.4.2) in the form

$$\varphi_2' = -(\partial\varphi_1'/\partial r)\cos\gamma = [f(x)/r]\cos\gamma, \tag{10.4.21}$$

can be used in place of (10.4.20).

Differentiating with respect to γ, we get

$$\partial\varphi_2'/\partial\gamma = \varphi_{2\gamma}' = -[f(x)/r]\sin\gamma. \tag{10.4.22}$$

Calculating the derivative with respect to r, we find an additional radial component of velocity for the condition of $r\to 0$:

$$V_{2r}' = \varphi_{2r}' = \partial\varphi_2'/\partial r = -[f(x)/r^2]\cos\gamma. \tag{10.4.23}$$

According to the condition (10.2.22) of unseparated flow this velocity component will be

$$V_{2r}' = -[f(x)/r^2]\cos\gamma = -aV_\infty\cos\gamma.$$

Whence the value of function

$$f(x) = aV_\infty r^2. \tag{10.4.24}$$

Consequently

$$\varphi_{2\gamma}' = -aV_\infty r\sin\gamma. \tag{10.4.25}$$

Inserting this expression in (10.2.28), we get

$$\bar{p}_2 = \frac{-2}{V_\infty^2}\left[V_\infty\varphi_{2x}' + \frac{a^2V_\infty^2}{2}(4\sin^2\gamma - 1)\right], \tag{10.4.26}$$

where φ_{2x}' is calculated with the help of (10.4.14) or (10.4.15), and for the particular case of flow over a cone it is obtained from (10.4.19).

Taking into account (10.2.27), the total pressure coefficient will be

$$\bar{p} = \bar{p}_1 + \bar{p}_2 = \frac{-2}{V_\infty^2}\left[V_\infty\varphi_{1x}' + \frac{V_\infty^2}{2}\left(\frac{dr}{dx}\right)^2 + V_\infty\varphi_{2x}' + \frac{a^2V_\infty^2}{2}(4\sin^2\gamma - 1)\right]. \tag{10.4.27}$$

5. Calculation of Aerodynamic Coefficients

The aerodynamic forces and moments and their aerodynamic coefficients can be determined from the distribution of pressure obtained about a body of revolution in a flow at a given angle of attack, i.e. under the condition where axial symmetry is disturbed. The scheme of the action of forces and moments is shown in Fig. 10.5.1.

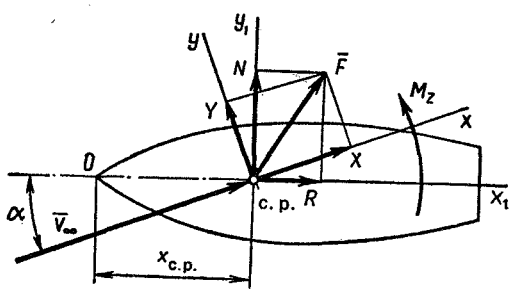

Fig. 10.5.1. System of aerodynamic force and moment acting on body of revolution: $\bar{F}$—main vector of aerodynamic forces; X, Y—drag and lift force respectively (flow system of coordinates x, y); R, N—axial and normal components of force respectively (fixed system of coordinates x_1, y_1); M_z—pitching moment.

First we will obtain general expressions for the calculation of forces, moments and coefficients under the condition that the geometrical form of the body in the flow is known and the pressure distribution over the side surface of the body is found for a given angle of attack a, pressure p_∞ and Mach number M_∞ in an undisturbed flow.

Coefficient of axial force: To calculate the axial force R and coefficient of this force $c_{Rp}=R/(q_\infty S_0)$ we take the system of a body of revolution (Fig. 10.5.2) with an arbitrary generator determined by the equation $r=f(x)$. Let us separate out an element of the surface of width dx situated at a distance x from the nose. The force due to differential pressure, equal to $(p-p_\infty)\,dS$, acts on the section of this element having area $dS=rd\gamma dl$.

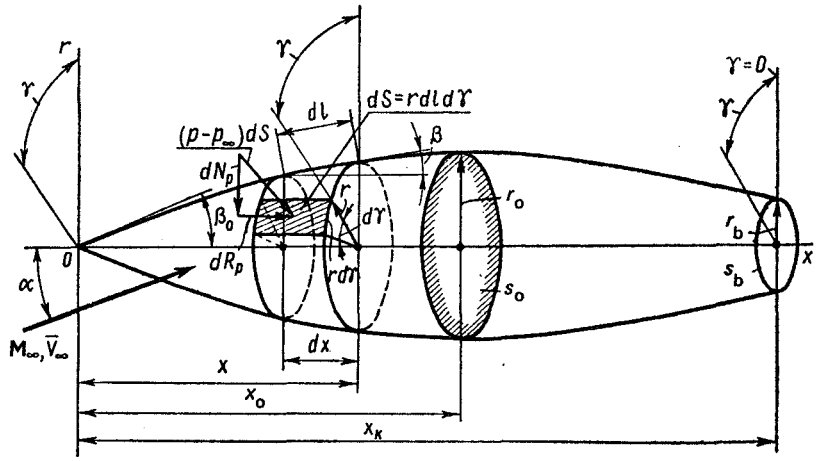

Fig. 10.5.2. Determination of aerodynamic coefficients from known distribution of pressure on surface of body of revolution.

Taking these data and formula (1.3.1) with $\tau=0$, the elementary value of axial force acting on this section of surface will be

$$(p-p_\infty)\cos(\widehat{\bar{P}_n x})\,dS=dR_p=(p-p_\infty)\,rd\gamma dl\sin\beta. \qquad (10.5.1)$$

Taking the pressure coefficient $\bar{p}=(p-p_\infty)/q_\infty$ and noting that $dl=dx/\cos\beta$, we find

$$\bar{p}\, q_\infty \cos(\widehat{\bar{P}_n x})\, dS = dR_p = \bar{p}\, q_\infty\, r \tan\beta\, dy dx.$$

Using this expression in formula (1.3.2), assuming that $X=R_p$ and $c_{fx}=0$ and assuming the symmetrical nature of pressure distribution over both sides of the vertical plane of symmetry, coinciding with the plane of the angle of attack in which the velocity vector $\bar{V}_\infty$ lies (this plane is known as the zero meridian plane), we get the following expression of axial force:

$$R_p = 2q_\infty \int_0^{x_K} r \tan\beta\, dx \int_0^{\pi} \bar{p}\, dy, \tag{10.5.2}$$

where x_K is the distance to the given section.

The same force can be expressed through coefficient c_{Rp} by the formula

$$R_p = c_{Rp}\, q_\infty S_0.$$

From (10.5.2) the coefficient of axial force will be

$$c_{Rp} = \frac{R}{q_\infty S_0} = \frac{4\lambda_0}{\pi} \int_0^{\bar{x}_K} \bar{r} \tan\beta\, d\bar{x} \int_0^{\pi} \bar{p}\, dy, \tag{10.5.3}$$

where $\bar{r}=r/r_0$, $\bar{x}=x/x_0$, $\bar{x}_K=x_K/x_0$;

$\bar{p}=(p-p_\infty)/q_\infty$ is the coefficient of pressure distribution which is supposed to be the known function $r(x)$, γ.

Coefficient of normal force: From Fig. 10.5.2 it can be seen that the elementary value of normal force

$$dN_p = -(p-p_\infty)\, r d\gamma dl \cos\gamma \cos\beta, \tag{10.5.4}$$

which, by analogy expression (1.3.1) with $\tau=0$, is equal to the quantity $(p-p_\infty)\cos(\widehat{\bar{P}_n x})\, dS$. Introducing the pressure coefficient $\bar{p}$ and taking into account that $dl\cos\beta=dx$, we get

$$\bar{p}\, q_\infty \cos(\widehat{\bar{P}_n x})\, dS = -\bar{p}\, q_\infty\, r\, dy\, dx \cos\gamma.$$

Inserting this expression in formula (1.3.3), assuming $y=r$, $Y=N_p$, $c_{fx}=0$, the value of the total normal force will be

$$N_p = -2q_\infty \int_0^{x_K} r dx \int_0^{\pi} \bar{p} \cos\gamma\, dy. \tag{10.5.5}$$

The coefficient of normal force can be obtained from this quantity:

$$c_{Np}=\frac{N_p}{q_\infty S_0}=\frac{-4\lambda_0}{\pi}\int_0^{\bar{x}_K}\bar{r}\,d\bar{x}\int_0^{\pi}\bar{p}\cos\gamma\,d\gamma. \tag{10.5.6}$$

During axisymmetrical flow-interaction $c_{Np}=0$ more because the pressure distribution in this case corresponds to circular symmetry and hence it is independent of angle γ.

Coefficient of moment: The elementary value of the moment of force due to pressure (pitching moment) calculated about the nose of the body, as follows from Fig. 10.5.2, is

$$dM_{zp}=xdN_p-r\cos\gamma\,dR_p.$$

The moment is negative in sign so the first term has the plus sign on account of the negative sign of dN_p in formula (10.5.4). Keeping this formula and the expression (10.5.1) in view, we get

$$\begin{aligned}dM_{zp}=&-x(p-p_\infty)rd\gamma dl\cos\gamma\cos\beta\\&-r\cos\gamma\,(p-p_\infty)\,rd\gamma dl\sin\beta.\end{aligned} \tag{10.5.7}$$

Taking into account the symmetry of pressure distribution, the total moment will be

$$\begin{aligned}M_{zp}=&-2\int_0^{x_K}xrdx\int_0^{\pi}(p-p_\infty)\cos\gamma\,d\gamma\\&-2\int_0^{x_K}r^2\tan\beta\,dx\int_0^{\pi}(p-p_\infty)\cos\gamma\,d\gamma,\end{aligned} \tag{10.5.8}$$

whence the coefficient of moment is

$$\begin{aligned}c_{mzp}=\frac{M_{zp}}{q_\infty S_0 x_K}=&\frac{-4\lambda_0}{\pi\bar{x}_K}\int_0^{\bar{x}_K}\bar{x}\,\bar{r}\,d\bar{x}\int_0^{\pi}\bar{p}\cos\gamma\,d\gamma\\&-\frac{2}{\lambda\bar{x}_K}\int_0^{\bar{x}_K}\bar{r}^2\tan\beta\,d\bar{x}\int_0^{\pi}\bar{p}\cos\gamma\,d\gamma.\end{aligned} \tag{10.5.9}$$

During axisymmetrical flow-interaction the pressure distribution is independent of angle γ. Therefore the integral

$$\int_0^{\pi}\bar{p}\cos\gamma\,d\gamma=\bar{p}\int_0^{\pi}\cos\gamma\,d\gamma=0$$

and hence, $$c_{mzp}=0.$$

Aerodynamic coefficients in a linearized flow: Let us find the values of aerodynamic coefficients for thin bodies of revolution in a linearized flow at a given angle of attack. For this purpose we use the relation (10.4.27) for the pressure coefficient in which φ'_{2x}, according to (10.4.2), will be expressed in the form

$$\varphi'_{2x}=-(\partial^2\varphi'_1/\partial r\partial x)\cos\gamma=-\varphi'_{1rx}\cos\gamma. \tag{10.5.10}$$

Let us separate out from (10.4.27) the terms independent of γ, the terms determining the asymmetrical character of pressure distribution and those that are functions of angle γ:

$$\bar{p}=P_0(x,r)+P_\gamma(x,r,\gamma), \tag{10.5.11}$$

where

$$P_0(x,r)=\frac{-2}{V_\infty^2}\left[V_\infty\varphi'_{1x}+\frac{V_\infty^2}{2}\left(\frac{dr}{dx}\right)^2-\frac{a^2V_\infty^2}{2}\right]; \tag{10.5.12}$$

$$P_\gamma(x,r,\gamma)=\frac{-2}{V_\infty^2}\left(-V_\infty\varphi'_{1rx}\cos\gamma+2a^2V_\infty^2\sin^2\gamma\right). \tag{10.5.13}$$

To determine the coefficient of axial force by formula (10.5.3) it is necessary to calculate the integral

$$\int_0^\pi\bar{p}d\gamma=\int_0^\pi[P_0(x,r)+P_\gamma(x,r,\gamma)]\,d\gamma=\frac{-2}{V_\infty^2}\int_0^\pi\left[V_\infty\varphi'_{1x}+\frac{V_\infty^2}{2}\left(\frac{dr}{dx}\right)^2-\frac{a^2V_\infty^2}{2}\right]d\gamma-\frac{2}{V_\infty^2}\int_0^\pi(-V_\infty\varphi'_{1rx}\cos\gamma+2a^2V_\infty^2\sin^2\gamma)\,d\gamma.$$

Noting that the terms in square brackets and also the quantity φ'_{1rx} are independent of γ, we get as a result of integration

$$\int_0^\pi\bar{p}\,d\gamma=\frac{-2\pi}{V_\infty^2}\left[V_\infty\varphi'_{1x}+\frac{V_\infty^2}{2}\left(\frac{dr}{dx}\right)^2-\frac{a^2V_\infty^2}{2}\right]-2a^2\pi$$

$$=\frac{-2\pi}{V_\infty^2}\left[V_\infty\varphi'_{1x}+\frac{V_\infty^2}{2}\left(\frac{dr}{dx}\right)^2+a^2V_\infty^2/2\right].$$

Inserting this expression in (10.5.3), recalling that $dr/dx\approx\beta$ for thin bodies and using φ'_{1x} from (10.3.14), we have

$$c_{Rp}=\frac{4\lambda_0}{\pi}\int_0^{\bar{x}_K}\bar{r}\beta d\bar{x}\int_0^{\cosh^{-1}u}S''(x-a'r\cosh z)\,dz$$

$$-4\lambda_0\int_0^{\bar{x}_K}\bar{r}\beta^3d\bar{x}-4\lambda_0a^2\int_0^{\bar{x}_K}\bar{r}\beta d\bar{x}. \tag{10.5.14}$$

Comparing the value of c_{R_p} from (10.5.14) with that of the coefficient of axial force at zero angle of attack (coefficient of wave drag), determined from (10.3.28), we find that the effect of breaking the symmetry of flow on the coefficient c_{R_p} is taken into account by the third term in (10.5.14) depending on the square of the angle of attack.

The corresponding expression for a cone is obtained if the following substitutions are effected in (10.5.14):

$$\left.\begin{aligned} &\beta=\beta_K,\ S''=(d^2/dx^2)\,(\pi r^2)=2\pi\beta_K^2;\\ &\bar{x}=\bar{r},\ \bar{x}_K=1,\ \lambda_0=1/(2\beta_K)=a'u_K/2;\end{aligned}\right\} \tag{10.5.15}$$

and then

$$c_{Rp} = \beta_K^2\,[2\ln(u_K+\sqrt{u_K^2-1})-1]-a^2. \tag{10.5.16}$$

For very small angles of attack the terms with a^2 in (10.5.14) and (10.5.16) can be neglected and then the expressions obtained for coefficients of axial force will coincide with the corresponding relations (10.3.28) and (10.3.26′) for the case of axisymmetrical flow-interaction.

To determine the coefficient of normal force it is necessary to find the integral taking into account (10.5.6):

$$\int_0^\pi \bar{p}\cos\gamma\,d\gamma=\int_0^\pi [P_0(x,r)+P_\gamma(x,r,\gamma)]\cos\gamma\,d\gamma$$

$$=\frac{-2}{V_\infty^2}\int_0^\pi\left[V_\infty\varphi'_{1x}+\frac{V_\infty^2}{2}\left(\frac{dr}{dx}\right)^2-\frac{a^2V_\infty^2}{2}\right]\cos\gamma\,d\gamma$$

$$-\frac{2}{V_\infty^2}\int_0^\pi(-V_\infty\varphi'_{1rx}\cos\gamma+2a^2V_\infty^2\sin^2\gamma)\cos\gamma\,d\gamma.$$

The first term on the right side of this expression is equal to zero because the quantities in square brackets are independent of angle γ and the integral $\int_0^\pi \cos\gamma\,d\gamma=0$. Taking into account that the integral appearing in the second term $\int_0^\pi \sin^2\gamma\cos\gamma\,d\gamma=0$ and the integral $\int_0^\pi \cos^2\gamma\,d\gamma=\pi/2$, we get

$$\int_0^\pi \bar{p}\cos\gamma\,d\gamma=\frac{\pi}{V_\infty}\varphi'_{1rx}. \tag{10.5.17}$$

Inserting this expression in (10.5.6), we write

$$c_{Np}=\frac{-4\lambda_0}{V_\infty}\int_0^{\bar{x}_K}\varphi'_{1rx}\,\bar{r}\,d\bar{x}. \tag{10.5.18}$$

According to (10.5.10) and (10.4.11)

$$\varphi'_{1rx} = -\frac{\varphi'_{2x}}{\cos\gamma} = -\frac{a'aV_\infty}{\pi}\int_0^{\cosh^{-1}u} S''(x-a'r\cosh z)\cosh z\,dz\,. \qquad (10.5.19)$$

Consequently

$$c_{Np} = \frac{4\lambda_0 a'a}{\pi}\int_0^{\bar{x}_K} \bar{r}\,d\bar{x}\int_0^{\cosh^{-1}u} S''(x-a'r\cosh z)\cosh z\,dz. \qquad (10.5.20)$$

According to (10.5.15) and taking into account the value of integral

$$\int_0^{\cosh^{-1}u_K} \cosh z\,dz = \sqrt{u_K^2-1},$$

the coefficient of the normal force for a thin cone will be

$$c_{Np} = 2a'a\beta_K\sqrt{u_K^2-1}\,. \qquad (10.5.21)$$

The following relation is obtained for the coefficient of moment (10.5.9), keeping in view the equations (10.5.17) and (10.5.19) and the equality $\tan\beta \approx \beta$:

$$c_{mzp} = \frac{4\lambda_0 a'a}{\pi\bar{x}_K}\int_0^{\bar{x}_K} \bar{x}\bar{r}\,d\bar{x}\int_0^{\cosh^{-1}u} S''(x-a'r\cosh z)\cosh z\,dz$$
$$+\frac{2a'a}{\pi\bar{x}_K}\int_0^{\bar{x}_K} \bar{r}^2\beta\,d\bar{x}\int_0^{\cosh^{-1}u} S''(x-a'r\cosh z)\cosh z\,dz. \qquad (10.5.22)$$

For a thin cone it will be reduced to

$$c_{mzp} = (4/3)a'a\beta_K(1+\beta_K^2)\sqrt{u_K^2-1}\,. \qquad (10.5.23)$$

For very thin conical bodies the quantity β_K^2 can be neglected in comparison of unity. It is obvious that for all very thin bodies of revolution with an arbitrary generator the second terms in (10.5.9) and correspondingly in (10.5.22) can be ignored.

The coordinate of the center of pressure (see Fig. 10.5.1) measured from the nose

$$x_{c.p} = M_{zp}/N_p. \qquad (10.5.24)$$

The corresponding value of the coefficient of center of pressure

$$\bar{c}_{c.p} = x_{c.p}/x_K = c_{mzp}/c_{Np}. \qquad (10.5.24')$$

Inserting here the values of c_{mzp} and c_{N_p} from (10.5.22) and (10.5.21) respectively, the coefficient of the center of pressure for a thin body of revolution with an arbitrary generator in a linearized flow can be calculated. The value of this coefficient for a cone can be obtained without imposing the limitation of linearized flow conditions. The flow about cones inclined to the flow has the property that coefficient of pressure $\bar{p}$ is independent of coordinates x, r: it is solely the function of the meridian angle. Therefore equation (10.5.24), taking into account (10.5.6) and (10.5.9), can be written in the form

$$\bar{c}_{c.p} = \frac{2\lambda_0 \int_0^{\bar{x}_K} \bar{x}\bar{r}d\bar{x} + \int_0^{\bar{x}_K} \bar{r}^2 \tan \beta_K d\bar{x}}{2\lambda_0 \bar{x}_K \int_0^{\bar{x}_K} \bar{r}\, d\bar{x}}.$$

Taking $\bar{x} = \bar{r}$, $\bar{x}_K = 1$, $\lambda_0 = 1/(2 \tan \beta_K)$ for a cone we get, after integration, the value of the center of pressure:

$$\bar{c}_{c.p} = (2/3)(1 + \tan^2 \beta_K). \qquad (10.5.24'')$$

For thin cones we can assume $\tan^2 \beta_K \approx \beta_K^2$ in this expression. Then we get the relation $\bar{c}_{c.p} = (2/3)(1 + \beta_K^2)$ which evidently can be directly determined from the formulas for the coefficients of moment (10.5.23) and of normal force (10.5.21).

Aerodynamic coefficients in the flow coordinates: The coefficients of normal force c_{N_p} and of axial force c_{R_p} in the fixed system of coordinates can be used to obtain the coefficients of aerodynamic forces in the flow system of coordinates. From Fig. 10.5.1 it can be seen that the drag force X_p and the lift force Y_p determined in the flow system of coordinates can be expressed through the forces R_p and N_p, which are calculated in the fixed system of coordinates, in the following way (see Chapter 1 Section 2):

$$\left.\begin{aligned} X_p &= R_p \cos \alpha + N_p \sin \alpha, \\ Y_p &= N_p \cos \alpha - R_p \sin \alpha. \end{aligned}\right\} \qquad (10.5.25)$$

The corresponding values of coefficients of drag c_{xp} and lift force c_{yp}, determined from the expressions (1.3.5), will be represented in terms of c_{N_p} and c_{Rp} in the following way:

$$c_{xp} = c_{Rp} \cos \alpha + c_{Np} \sin \alpha; \qquad (10.5.26)$$

$$c_{yp} = c_{Np} \cos \alpha - c_{Rp} \sin \alpha. \qquad (10.5.27)$$

Introducing here the values of c_{Rp} and c_{Np} expressed through (10.5.14) and (10.5.20) respectively, it is possible to determine the coefficients of drag force c_{xp} and of lift force c_{yp} for the linearized flow-interaction of a thin body of

evolution. The corresponding values of these coefficients for a thin cone are obtained by using the relations (10.5.16) and (10.5.21) for c_{Rp} and c_{Np} respectively. Carrying out the above changes and assuming $\cos\alpha \approx 1$, $\sin\alpha \approx \alpha$ in (10.5.26) and (10.5.27), we get:

$$c_{xp}=\beta_K^2\,[2\ln(u_K+\sqrt{u_K^2-1})-1]+\alpha^2\,(2\alpha'\beta_K\sqrt{u_K^2-1}-1); \quad (10.5.28)$$

$$c_{yp}=\alpha\beta_K\{2\alpha'\sqrt{u_K^2-1}-\beta_K\,[2\ln(u_K+\sqrt{u_K^2-1})-1]\}+\alpha^3. \quad (10.5.29)$$

Law of similarity: The expression (10.4.26) for pressure coefficient $\bar{p}_2$ can be written in the form

$$\bar{p}_2=(-2/V_\infty)\;V'_{x2}-\alpha^2(4\sin^2\gamma-1). \quad (10.5.30)$$

This may be used to establish the law of similarity during the linearized flow over a body of revolution in a linearized flow. For a parabolic form of body the additional velocity component V'_{x2} at a given point on the surface is determined from (10.4.14) as a function of parameter u. This parameter is obtained on the basis of the quantity $u_0=1/(\alpha'\beta_0)$ by formula (10.3.31). Taking this into account and keeping in mind the equality $\lambda_0=1/\beta_0$, the relation (10.5.30) can be written in the general form

$$\bar{p}_2=-2\alpha\beta_0 G\,(u_0,\bar{x})\cos\gamma-\alpha^2(4\sin^2\gamma-1), \quad (10.5.31)$$

where G is some function depending on the quantity u_0 for a given point on the surface.

Let us consider the case where the Mach number $\mathbf{M}_\infty$ of undisturbed flow over a body of revolution is not high and we can assume $\alpha'\approx\mathbf{M}_\infty$. Multiplying both sides of equation (10.5.31) by $\mathbf{M}_\infty^2$, we have

$$(p_2/p_1)-1 = -k(\alpha/\beta_0)\mathbf{K}_1^2\,G_1(\mathbf{K}_1\bar{x})-(k/2)\,(\alpha/\beta_0)^2\mathbf{K}_1^2(4\sin^2\gamma-1), \quad (10.5.32)$$

where G_1 is a function determined by the parameter $\mathbf{K}_1 = \mathbf{M}_\infty\beta_0 = \mathbf{M}_\infty/\lambda_0$ at a given point.

Let us introduce the parameter of similarity

$$\mathbf{K}_2 = \alpha/\beta_0 = \alpha\lambda_0 \quad (10.5.33)$$

and rewrite (10.5.32) in a more general form

$$(p_2/p_1)-1 = B(\mathbf{K}_1, \mathbf{K}_2, \bar{x}, \gamma), \quad (10.5.34)$$

where B is some function. From this relation, which is the expression of the law of similarity for the flow-interaction of thin affinely similar bodies, it follows that the function of pressure at a given point on the surface with the coordinates $\bar{x}$, γ will be the same for any two bodies if they have identical values of $\mathbf{K}_1$ and $\mathbf{K}_2$. These quantities $\mathbf{K}_1$ and $\mathbf{K}_2$ are known as the parameters of similarity of flows over thin bodies of revolution at a given angle of attack. According to formulas (10.5.20) and (10.5.22) the functions

depending on these parameters determine the relations for coefficients of normal force and of moment:

$$\left.\begin{aligned} \mathbf{M}_\infty^2 c_{Np} &= E(\mathbf{K}_1 \mathbf{K}_2); \\ \mathbf{M}_\infty^2 c_{mzp} &= F(\mathbf{K}_1, \mathbf{K}_2), \end{aligned}\right\} \tag{10.5.35}$$

where E and F are the functions of parameters of similarity $\mathbf{K}_1$ and $\mathbf{K}_2$. The law of similarity is here expressed by the condition that the quantities $\mathbf{M}_\infty^2 c_{Np}$ (or $\mathbf{M}_\infty^2 c_{mzp}$) will be identical during the flow-interaction of two affinely similar bodies of revolution of different aspect ratios in flows of different Mach numbers $\mathbf{M}_\infty$ at different angles of attack if the similarity parameters $\mathbf{K}_1$ and $\mathbf{K}_2$ are identical.

11

AERODYNAMIC INTERFERENCE

1. Nature of Aerodynamic Interference

1.1 Interference of wing-body combination

A body of revolution, commonly serving as an element of the structure of a flight vehicle, may carry wings, tail and control unit. An airplane, for example, represents in itself a combination of such structural elements in a fuselage having the form of a body of revolution or something of that type and wings, tail unit and control surfaces. A rocket without control unit may consist of a main body (body of revolution) and tail unit (stabilizer). A rocket with control systems is fairly close to an airplane because it has lifting surfaces, tail unit and control systems.

In studying the aerodynamics of flight vehicles as the combinations of bodies of revolutions, wings, tail surfaces and control systems we encounter the complicated and still incompletely resolved problems of allowance for aerodynamic interference between the individual elements of these combinations. As a result of this interference the sum of aerodynamic forces and moments taken separately (isolated) for wing and main body; tail unit and main body; main body, wing and tail unit or main body, wing, tail unit and control surfaces is not equal to the total force or moment of the combination of corresponding elements representing the whole unit (Fig. 11.1.1). The individual elements like main body, wings, tail unit, control surfaces that we hitherto considered independently lose their individual aerodynamic characteristics and acquire new characteristics as a result of interference when assembled in a single structure.

We know from the results of calculations and experimental research that the lift force of a wing at a given angle of attack increases in the presence of a fuselage by comparison with an isolated wing. The same phenomenon is observed in the case of the lift force of a fuselage in the presence of a wing by comparison with an isolated fuselage.

Let us study the physical picture of the mutual interaction between the body of revolution and the wing that brings about an increase in their lift

force, assuming that the wing is situated on the cylindrical part of the fuselage away from the nose in a mid-wing layout. We also assume that both fuselage and wing are thin and that the flow-interaction takes place at a low angle of attack (Fig. 11.1.2).

As we saw in Chapter 10 Section 2, the perturbation flow about a thin body of revolution can be obtained by superposing the velocity field of additional perturbation flow due to cross flow over this body with velocity $V_{y\infty}=V_\infty \sin \alpha \approx V_\infty \alpha$ on the velocity field arising due to the axisymmetrical flow-interaction of a body with undisturbed flow with velocity $V_{x\infty} = V_\infty \cos \alpha \approx V_\infty$.

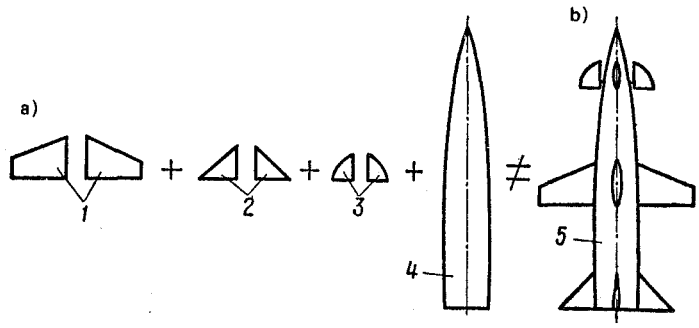

Fig. 11.1.1. Scheme illustrating concept of interference between body of revolution and wing, tail and control surfaces:

a—isolated elements; *b*—elements assembled (combined) in flight vehicle; *1*—wings; *2*—tail unit; *3*—control surfaces; *4*—body of revolution; *5*—flight vehicle.

At low angles of attack the cross flow is usually subsonic and for the approximate calculation of the velocity field we may use the theory of potential flow over a circular cylinder. The complex potential for this flow-interaction is determined by the expression (6.2.4). Taking $V=a\cdot V_\infty$, replacing ζ by σ and then calculating the derivative $dW/d\sigma$, the expression for complex velocity will be written in the form

$$dW/d\sigma=V_z-V_y i=-aV_\infty i[1+(R^2/\sigma^2)], \tag{11.1.1}$$

where $\sigma=z+iy$.

On the line $z-z$ ($y=0$) we have

$$V_z-V_y\, i = -aV_\infty i[1+(R/z^2)], \tag{11.1.2}$$

whence it follows that $V_z = 0$ and

$$V_y = a\,V_\infty[1+(R^2/z^2)]. \tag{11.1.3}$$

According to this formula the velocity V_y of cross flow in plane $y=0$ changes from $V_y=2a\cdot V_\infty$ on the surface of a cylinder ($z=R$) up to $V_y=V_{y\infty}=a\cdot V_\infty$

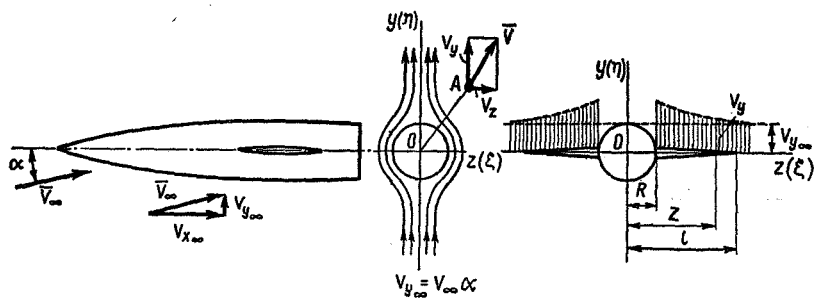

Fig. 11.1.2. Variation of normal component of velocity along wing span due to effect of body of revolution.

away from it as $z \to \infty$ (see Fig. 11.1.2). If a wing is attached to the cylindrical body then at a given angle of attack a it will be in the part of the flow that can be obtained by superposition of induced flow due to the fuselage on the undisturbed flow. This effect of the main body on the wing surface leads to the following cross flow velocity component

$$V_\infty a + V_\infty a R^2/z^2 ,$$

i.e. there arises the additional cross flow velocity component

$$V_y' = V_y - a V_\infty = a V_\infty R^2/z^2. \tag{11.1.4}$$

In the presence of this additional component of velocity the upward cross flow (upwash) takes a value induced by the fuselage. The upwash angle is given by

$$\varepsilon_{iT} = V_y'/V_\infty = aR^2/z^2. \tag{11.1.5}$$

This upwash leads to an increase in local angles of attack at various sections of the wing. These local (effective) angles of attack are determined from the expression

$$a_e = a + \varepsilon_{iT} = a\,[1 + (R^2/z^2)]. \tag{11.1.6}$$

From this formula it can be seen that the effective angle of attack reaches its highest values at the root section with $z = R$, where $a_e = 2a$, and gradually diminishes as we move away from the main body. At the wing tip where $z = l$ the effective angle of attack

$$a_{e\cdot t} = a\,[1 + (R^2/l^2)]\,. \tag{11.1.6'}$$

The lift force of a wing surface will be more than that for an isolated wing because of the increase in local angles of attack in the presence of the main body. The wing in its own way affects the flow-interaction of the fuselage because the rise in pressure appearing on the lower surface and the suction

on the upper surface of the wing spread over the fuselage. As a result redistribution of pressure takes place and we get additional lift force on the fuselage due to wing effect.

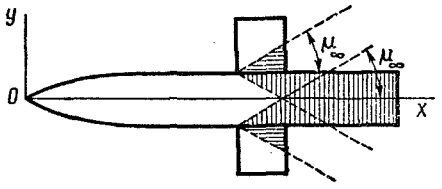

Fig. 11.1.3. Zones of mutual interaction of wing and fuselage.

The size of the zone of mutual interaction of wing and body is established by the law indicating that the disturbances in a supersonic flow propagate only downstream within the limits of a Mach cone. This zone of mutual actions, shown in Fig. 11.1.3, is limited by Mach cones with their generators (dotted lines) drawn at an angle of disturbance $\mu_\infty = \sin^{-1}(1/M_\infty)$ from the origin of the root chord of a wing panel. On the plane wing this zone of effect will take the form of a triangular surface; on the main body it will have a cylindrical form bounded by a curved line representing the intersection of the surface of the cylindrical main body and a Mach cone with its apex at the leading point of a wing root section.

1.2 Interference between wing and tail

For flight vehicles representing a combination of body of revolution and tail unit it is necessary to consider interference not only between the main body and the wing but also between the main body and the tail unit. The latter is similar to the interference effect just now considered. In addition, the effect on the tail plane of cross flow behind the wing (where the wing is located on the fuselage ahead of the tail) or the effect of flow behind the tail on the wing (where the tail is located ahead of the wing in the so-called canard-type layout) should be taken into account.

In a supersonic flow the wing can affect the tail unit if the tail is situated within the Mach cone (wave surface) drawn for the wing, i.e. if it lies in the region of wing wake (Fig. 11.1.4). The wake depends on the wing plan and the position of the point where flow parameters and upwash angle are to be determined.

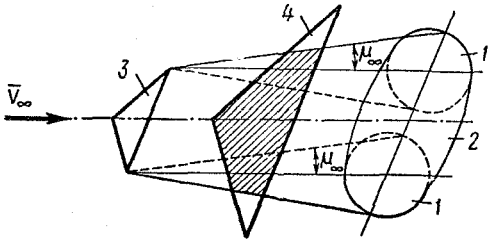

Fig. 11.1.4. Zone of interaction of wing with tail in supersonic linearized flow (hatched region):

1—mach cone; *2*—wave surface drawn for wing (curved Mach cones); *3*—wing; *4*—tail unit.

As an example, let us take a rectangular wing (Fig. 11.1.5). The region of disturbed flow in which the effect of the wing tip is felt on the flow-interaction of the wing is limited by

a Mach cone with its apex at the leading-edge corner of the tip. The cross flow of air from the region of high pressure below the wing to the region of lower pressure on the upper side of the wing takes place within the Mach cone. As a result the flow curls into a vortex which also calls for a cross flow behind the wing. This cross flow is directed downward (downwash) within the region of a Mach cone surrounding the wing. It is directed in the opposite direction (upwash) in the wave region beyond the wing. Accordingly the cross flow on the side edge tip is equal to zero (see Fig. 11.1.5). If the wing is attached to the body of revolution the cross flow behind it will be different from that for an isolated wing. The difference in pressures above and below the wing is enhanced and the cross flow of air from the high-pressure region to the low-pressure region will be more intensive. That means the cross flow will increase in the external region where it is directed upward as well as in the internal region where it is directed downward.

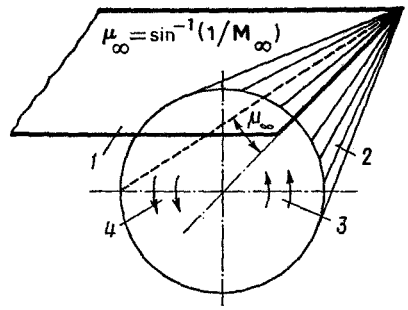

Fig. 11.1.5. Downwash behind rectangular wing:

1—wing; *2*—cone of disturbance (Mach cone); *3*—upwash; *4*—downwash.

If the tail span is less than that of the wing in front of it the tail will be situated in the region of downwash and the effective angle of attack of the tail surface will be reduced. If for a given wing section the downwash angle is ε_{iw} and the initial angle of tail (angle between the chord of the tail and the axis of the fuselage) is α_t the effective angle of attack of the tail (Fig. 11.1.6) will be

$$\alpha_{e.t} = \alpha + \alpha_t - \varepsilon_{iw}. \tag{11.1.7}$$

The reduction of effective angle of attack leads to a reduction in lift force and hence to a reduction in stabilizing tail moment.

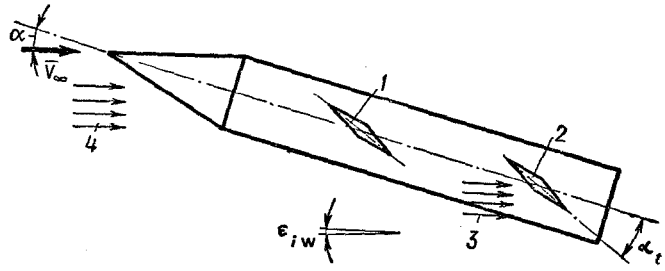

Fig. 11.1.6. Interference between wing and tail:

1—wing; *2*—tail unit; *3*—skewed flow; *4*—free flow.

In the tail region the velocity of flow is reduced due to wing effect and as a result the velocity head will be less than that of an undisturbed flow. This has to be considered when determining the aerodynamic characteristics of a tail. If the tail span is more than that of the wing part of its surface lies in the region of upwash and this compensates the negative effect of downwash, which gives reduced lift.

2. Lift for Combination of Fuselage and Plane Wing

2.1 Concept of coefficients of interference

The lift force acting on the flight vehicle at a low angle of attack with zero bank, represented by a combination of the thin body of revolution and a wing in two parts in the form of a thin flat plate (known as plain combination, Fig. 11.2.1), can be determined as the sum of lift forces for fuselage and wing taken separately and the additional forces conceived as interference corrections. One of these corrections is based on the effect of the fuselage on the flow-interaction of a wing. The second correction concerns the effect of the wing on the flow-interaction of the fuselage. Accordingly the resultant lift force will be given by

$$Y_{f,w}=Y_f+Y_w+\Delta Y_{f(w)}+\delta Y_{w(f)}, \tag{11.2.1}$$

where Y_f is the lift force of an isolated fuselage (body of revolution);

Y_w is the lift force of an isolated wing;

$\Delta Y_{f(w)}$ is the additional lift on the fuselage due to the effect of the wing;

$\delta Y_{w(f)}$ is the additional lift on the wing due to the effect of the fuselage.

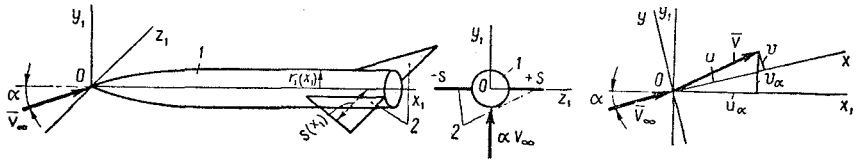

Fig. 11.2.1. Fuselage-plane wing comb nation (plain combination) at small angle of attack and zero banking angle:

1—fuselage (body of revolution); *2*—panels of plane wing.

The expression (11.2.1) can also be written in the form

$$Y_{f,w}=Y_f+\Delta Y_{f(w)}+\Delta Y_{w(f)}, \tag{11.2.2}$$

where

$$\Delta Y_{w(f)}=Y_w+\delta Y_{w(f)} \tag{11.2.3}$$

represents the lift force on the wing in the presence of the fuselage.

The last two components in (11.2.2) may be written in more convenient

form for calculations:

$$\Delta Y_{f(w)} = K_f Y_w; \tag{11.2.4}$$

$$\Delta Y_{w(f)} = K_w Y_w, \tag{11.2.5}$$

where

K_f, K_w are coefficients of interference.

According to (11.2.4), (11.2.5) the additional lift force on a fuselage in the presence of a wing and the lift force on a wing taking into account the interference of the fuselage are expressed as the product of the corresponding coefficients of interference and lift force on the wing.

An isolated wing here is understood as one consisting of two panels joined together. According to (11.2.4) and (11.2.5) the lift force of this plain combination of fuselage and wing will be

$$Y_{f,w} = Y_f + (K_f + K_w)\ Y_w. \tag{11.2.6}$$

If the lift force on the fuselage is given in the form

$$Y_f = K_{f\cdot i}\ Y_w, \tag{11.2.7}$$

where

$K_{f\cdot i}$ is a coefficient connecting the lift forces of isolated fuselage and wing, then

$$Y_{f,w} = (K_{f\cdot i} + K_f + K_w)\ Y_w\,. \tag{11.2.8}$$

The appropriate total lift coefficient of this combination will be

$$c_{yf,w} = Y_{f,w}/(q_\infty S_w) = (K_{f\cdot i} + K_f + K_w)\ c_{yw}, \tag{11.2.9}$$

where $q_\infty = \rho_\infty V_\infty^2/2$ is the velocity head of the undisturbed flow; S_w is the area of isolated panels of the wing.

For a linearized flow there exists a linear relation between lift force and angle of attack, i.e. $c_y = ac_y^\alpha$ ($c_y^\alpha = \partial c_y/\partial\alpha$).

Consequently

$$c_{yf,w}^\alpha = (K_{f\cdot i} + K_f + K_w)\ c_{yw}^\alpha. \tag{11.2.10}$$

The coefficient $K_{f\cdot i}$, K_f, K_w appearing in (11.2.9) and (11.2.10) may be taken in the form of ratios of the corresponding coefficients of lift force:

$$\left.\begin{aligned} &K_{f\cdot i} = c_{yf}/c_{yw}, \quad K_f = \Delta c_{yf(w)}/c_{yw}, \\ &K_w = \Delta c_{yw(f)}/c_{yw}, \end{aligned}\right\} \tag{11.2.11}$$

or in the form of ratios derived from the corresponding coefficients of lift force with the angle of attack:

$$\left.\begin{aligned} &K_{f\cdot i} = c_{yf}^\alpha/c_{yw}^\alpha; \quad K_f = \Delta c_{yf(w)}^\alpha/c_{yw}^\alpha; \\ &K_w = \Delta c_{yw(f)}^\alpha/c_{yw}^\alpha. \end{aligned}\right\} \tag{11.2.12}$$

2.2 Determination of velocity potential

Now we will study aerodynamic interference for flight vehicles representing various combinations of these bodies (fuselage, wing, tail unit) that induce small disturbances in an undisturbed flow. In modern aerodynamics most of the problems of this type are fully solved and the application of the solutions to flight vehicles gives good enough results in practice.

The potential φ' for perturbation velocity during a linearized flow over thin bodies satisfies the equation of type (7.1.4′) for a three-dimensional flow. Let us introduce the nondimensional coordinates

$$\bar{x}=x/L,\ \bar{y}=y/l,\ \bar{z}=z/l, \tag{11.2.13}$$

where L and l are characteristic lengths along axes x and y (for example, L is the length of the whole combination, l is the span of a wing panel). Equation (7.1.4′), expressed in terms of variables (11.2.13), will have the form

$$(\mathbf{M}_\infty^2-1)\frac{l^2}{L^2}\cdot\frac{\partial^2\varphi'}{\partial\bar{x}^2}-\frac{\partial^2\varphi'}{\partial\bar{y}^2}-\frac{\partial^2\varphi'}{\partial\bar{z}^2}=0. \tag{11.2.14}$$

Let us consider a combination of fuselage and wing panels having small span. For such combinations elongated along x axis the ratio $l^2/L^2\ll 1$. Therefore the first terms in equation (11.2.14) can be neglected. Then the differential equation to determine the potential of perturbation velocity during interference between fuselage and plane wing will be

$$(\partial^2\varphi'/\partial\bar{y}^2)+(\partial^2\varphi'/\partial\bar{z}^2)=0,$$

or after substitution of the values of $\bar{y}$ and $\bar{z}$ from (11.2.13):

$$(\partial^2\varphi'/\partial y^2)+(\partial^2\varphi'/\partial z^2)=0. \tag{11.2.15}$$

The equation corresponds to the disturbed flow of an incompressible fluid in the yOz plane. To find the velocity field of flow induced by interference it is necessary to solve differential equation (11.2.15) for function φ' which represents the potential of perturbation velocity during a plane incompressible cross flow of velocity $\alpha\cdot V_\infty$ over this combination of bodies (see Fig. 11.2.1). The velocity field of an incompressible flow about the fuselage and the wing joined to it in plane yOz can be determined with the help of the method based on the theory of conformal transformation (hereinafter we will use the fixed system of coordinates x_1, y_1, z_1, dropping the index "1" for convenience).

The plane in which the flow is being determined happens to be the physical plane of complex variable $\sigma=z+iy$ and the plane for which the flow is known as the flow about a transformed circle will be known as the transformed plane of complex variables $\zeta=\xi+i\eta$ in Fig. 11.2.2.

Let us write the following equation relating the variables σ and ζ:

$$\sigma+(r^2/\sigma)=\zeta+(r_0^2/\zeta), \tag{11.2.16}$$

where

$$r_0 = 0.5\,[s + (r^2/s)]; \tag{11.2.16'}$$

s is the varying value of a semi-span of the wing (span of wing panel).

Equation (11.2.16) happens to be that relation with the help of which the conformal transformation of a circle of radius r_0 in plane $\zeta = \xi + i\eta$ is carried out to the contour that can be obtained as a result of intersection of the plane yOz of the fuselage and the thin wing attached to it. Obviously this contour in the plane $\sigma = z + iy$ has the form of a circle of radius r and a pair of segments of lines of lengths $s - r_0$ each lying on the z axis (see Fig. 11.2.2). To establish the correctness of selection of the formula (11.2.16), which fulfills the given conformal transformation, transformations similar to those used in Chapter 6 Section 2 for the case of conformal transformation of a circle into a flat plate should be performed with the help of this formula [see formula (6.2.1)].

Solving the quadratic equation (11.2.16), we get

$$\zeta = \frac{1}{2}\left\{\left(\sigma + \frac{r^2}{\sigma}\right) + \left[\left(\sigma + \frac{r^2}{\sigma}\right)^2 - 4r_0^2\right]^{1/2}\right\}. \tag{11.2.17}$$

The plus sign before the square brackets indicates the relation between the complex variables ζ and σ for the upper semi-plane. The minus sign should be taken when carrying out transformation for the lower semi-plane.

The complex potential for the flow over a circular cylinder of radius r_0 in ζ plane (see Fig. 11.2.2, b) can be determined from formula (6.2.4) by replacing R by r_0 therein:

$$W = -ia V_\infty [\zeta - (r_0^2/\zeta)]. \tag{11.2.18}$$

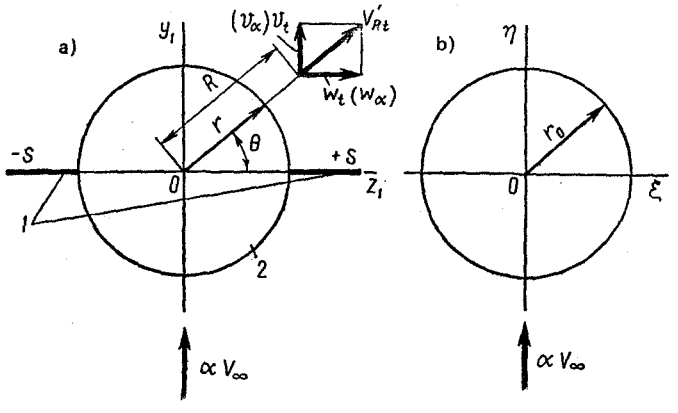

Fig. 11.2.2. System of conformal transformation for fuselage-plain wing combination:

a—physical plane σ (*1*—wing; *2*—fuselage); *b*—plane of transformation ζ.

This complex potential can be transformed into the potential for a cross flow about a plain wing-body combination in the $\sigma=z+iy$ plane by replacing the complex variable $\zeta=\xi+i\eta$ in (11.2.18) with the value from equation of transformation (11.2.17):

$$W=-iaV_\infty\left[\left(\sigma+\frac{r^2}{\sigma}\right)^2-4r_0^2\right]^{1/2}. \tag{11.2.19}$$

To find the resultant value of complex potential W_α the potential function of the flow parallel to the y axis and equal to $iaV_\infty\sigma$ should be added to (11.2.19). This leads to

$$W_\alpha=-iaV_\infty\left\{\left[\left(\sigma+\frac{r^2}{\sigma}\right)^2-4r_0^2\right]^{1/2}-\sigma\right\};$$

or keeping in view the value of r_0 from (11.2.16′), it will be given by

$$W_\alpha=-iaV_\infty\left\{\left[\left(\sigma+\frac{r^2}{\sigma}\right)^2-\left(s+\frac{r^2}{s}\right)^2\right]^{1/2}-\sigma\right\}. \tag{11.2.20}$$

The complex potential W_α can be expressed through a velocity potential φ_α and stream function ψ_α in the form of $W_\alpha=\varphi_\alpha+i\psi_\alpha$. Taking this into account and noting that $\sigma=z+iy$, we can write (11.2.20) as:

$$\varphi_\alpha+i\psi_\alpha=-iaV_\infty\left\{\left[\left(z+iy+\frac{r^2}{z+iy}\right)^2-\left(s+\frac{r^2}{s}\right)^2\right]^{1/2}-(z+iy)\right\}. \tag{11.2.20′}$$

2.3 Velocity and pressure on fuselage with wing

Let us calculate partial derivatives with respect to x on the left and right sides of (11.2.20′):

$$\frac{\partial\varphi_\alpha}{\partial x}+i\frac{\partial\psi_\alpha}{\partial x}=-iaV_\infty\frac{2\left(z+iy+\frac{r^2}{z+iy}\right)\frac{dr}{dx}\cdot\frac{r}{z+iy}}{\left[\left(z+iy+\frac{r^2}{z+iy}\right)^2-\left(s+\frac{r^2}{s}\right)^2\right]^{1/2}}\rightarrow$$

$$\rightarrow\frac{-\left(s+\frac{r^2}{s}\right)\left(\frac{ds}{dx}+\frac{2r\frac{dr}{dx}s-r^2\frac{ds}{dx}}{s^2}\right)}{\left[\left(s+\frac{r^2}{s}\right)^2-\left(s+\frac{r^2}{s}\right)^2\right]^{1/2}}. \tag{11.2.21}$$

Considering the fuselage surface for which $\sigma=z+iy=re^{i\theta}$ and taking into account the following known formulas

$$e^{-i\theta}=\cos\theta-i\sin\theta,\ e^{i\theta}+e^{-i\theta}=2\cos\theta,$$

we get

$$\frac{\partial \varphi_\alpha}{\partial x} + i\frac{\partial \psi_\alpha}{\partial x}$$
$$= -iaV_\infty \frac{4\cos\theta(\cos\theta - i\sin\theta)\, r\frac{dr}{dx} - \left(s+\frac{r^2}{s}\right)\left[2\frac{r}{s}\cdot\frac{dr}{dx} + \frac{ds}{dx}\left(1-\frac{r^2}{s^2}\right)\right]}{\left[4r^2\cos^2\theta - \left(s+\frac{r^2}{s}\right)^2\right]^{1/2}}.$$

Separating out the real part from the right side, we get an expression for the additional axial component of perturbation velocity:

$$\frac{\partial \varphi_\alpha}{\partial x} = u_\alpha = a V_\infty$$
$$\times \frac{4r\frac{dr}{dx}\cos^2\theta - \left(s+\frac{r^2}{s}\right)\left[2\frac{r}{s}\cdot\frac{dr}{dx} + \frac{ds}{dx}\left(1-\frac{r^2}{s^2}\right)\right]}{\left[\left(s+\frac{r^2}{s}\right)^2 - 4r^2\cos^2\theta\right]^{1/2}}. \quad (11.2.22)$$

To obtain the vertical and side components of perturbation velocity v_α and w_α (see Fig. 11.2.2, a) we calculate the derivative of complex potential (11.2.20) with respect to σ:

$$\frac{dW_\alpha}{d\sigma} = w_\alpha - v_\alpha i = -iaV_\infty \left\{ \frac{\left(\sigma+\frac{r^2}{\sigma}\right)\left(1-\frac{r^2}{\sigma^2}\right)}{\left[\left(\sigma+\frac{r^2}{\sigma}\right)^2 - \left(s+\frac{r^2}{s}\right)^2\right]^{1/2}} - 1 \right\}. \quad (11.2.23)$$

The conditions over the fuselage surface require substitution of $\sigma = re^{i\theta}$. Then

$$w_\alpha - v_\alpha i = -iaV_\infty \left\{ \frac{2r\cos\theta(1 + i\sin 2\theta - \cos 2\theta)}{\left[4r^2\cos^2\theta - \left(s+\frac{r^2}{s}\right)^2\right]^{1/2}} - 1 \right\}.$$

Separating the real and imaginary quantities on the right side, we find

$$w_\alpha = \frac{4arV_\infty \cos\theta \sin^2\theta}{\left[\left(s+\frac{r^2}{s}\right)^2 - 4r^2\cos^2\theta\right]^{1/2}}; \quad (11.2.24)$$

$$v_\alpha = -aV_\infty \left\{ \frac{2r\cos\theta\sin 2\theta}{\left[\left(s+\frac{r^2}{s}\right)^2 - 4r^2\cos^2\theta\right]^{1/2}} + 1 \right\}. \quad (11.2.25)$$

It follows from physical considerations that formulas (11.2.22), (11.2.24) and (11.2.25) give the values of velocities on the lower surface of the fuselage, i.e.

$$u_{\alpha l} = u_\alpha,\ w_{\alpha l} = w_\alpha,\ v_{\alpha l} = v_\alpha. \quad (11.2.26)$$

The following correlations for velocity components on the upper surface of the fuselage follow from the property of symmetry of flow:

$$u_{\alpha u}=-u_{\alpha l},\ w_{\alpha u}=-w_{\alpha l},\ v_{\alpha u}=v_{\alpha l}. \tag{11.2.27}$$

Let us now consider how to find the pressure coefficient from the values of perturbation velocities obtained. In Chapter 6 Section 1 the formula (6.1.5) was obtained for this coefficient in the case of a plane small perturbation flow. However, as shown by experiment, this formula requires modification for a three-dimensional linearized flow.

The square of total velocity at a point in space for such a flow will be

$$V^2=V_x^2+V_y^2+V_z^2=(V_\infty+u)^2+v^2+w^2=V_\infty^2+2uV_\infty+u^2+v^2+w^2.$$

Then formula (7.1.4″) for the ratio of pressures p/p_∞ will be rewritten in the following way:

$$\frac{p}{p_\infty}=\left\{1-\frac{k-1}{k}\cdot\frac{\rho_\infty}{p_\infty}\left[uV_\infty+\frac{1}{2}(u^2+v^2+w^2)\right]\right\}^{k/(k-1)}.$$

As a consequence of the smaller values of additional velocity components in comparison with V_∞ the ratio p/p_∞ differs negligibly from unity and hence the expression for p/p_∞ written above can be expanded in the binomial series. Maintaining the square term, we will have

$$\frac{p}{p_\infty}=1-\frac{\rho_\infty}{p_\infty}\left[uV_\infty+\frac{1}{2}(u^2+v^2+w^2)\right]$$
$$+\left(\frac{k-1}{k}\right)^2\frac{k}{k-1}\left(\frac{k}{k-1}-1\right)\frac{\rho_\infty^2}{2p_\infty^2}\left[uV_\infty+\frac{1}{2}(u^2+v^2+w^2)\right]^2.$$

The corresponding relation for the pressure coefficient will be

$$\bar{p}=\frac{2(p-p_\infty)}{\rho_\infty V_\infty^2}=-\frac{2u}{V_\infty}-\frac{u^2+v^2+w^2}{V_\infty^2}$$
$$+\frac{\rho_\infty V_\infty^2}{kp_\infty}\left[\frac{u}{V_\infty}+\frac{1}{2V_\infty^2}(u^2+v^2+w^2)\right]^2.$$

Maintaining the terms of the second order of smallness in comparison with u/V_∞ and recalling that $kp_\infty/\rho_\infty=a_\infty^2$ and $V_\infty^2/a_\infty^2=\mathbf{M}_\infty^2$, we have

$$\bar{p}=-(2u/V_\infty)+[u^2(\mathbf{M}_\infty^2-1)-v^2-w^2]/V_\infty^2.$$

Finally, neglecting the term $u^2(\mathbf{M}_\infty^2-1)$, we get

$$\bar{p}=-(2u/V_\infty)-(v^2+w^2)/V_\infty^2. \tag{11.2.28}$$

Even though the flow has small perturbations the square terms appearing during the flow-interaction of thin bodies of revolution are preserved here.

The velocity components u, v, w in the flow system of coordinates, which

appear in formula (11.2.28), can be expressed through the components u_α, v_α, w_α in the fixed system of coordinates. As the wing has no bank and the axes of fixed coordinates are turned through angle a from the Oz axis of the flow system it is obvious that the component $w=w_\alpha$. From Fig. 11.2.1 it can be seen that the following relations are valid for other velocity components:

$$u=u_\alpha+av_\alpha,\ v=v_\alpha-au_\alpha.$$

Using the relations for w, u, v obtained in equation (11.2.28) and neglecting the terms $av_\alpha u_\alpha/V_\infty^2$, a^2u_α/V_∞^2, which happen to be the terms of a higher order of smallness, we get

$$\bar{p}=-(2/V_\infty)(u_\alpha+av_\alpha)-(v_\alpha^2+w_\alpha^2)/V_\infty^2. \tag{11.2.28'}$$

On the lower surface of the fuselage it will be

$$\bar{p}_{f(w)l}=-2\left(\frac{u_{\alpha l}+av_{\alpha l}}{V_\infty}+\frac{w_{\alpha l}^2}{2V_\infty^2}+\frac{v_{\alpha l}^2}{2V_\infty^2}\right). \tag{11.2.29}$$

Taking into account the property of symmetry of flow (11.2.27), the pressure coefficient on the upper surface of the fuselage will be

$$\bar{p}_{f(w)u}=-2\left(\frac{-u_{\alpha l}+av_{\alpha l}}{V_\infty}+\frac{w_{\alpha l}^2}{2V_\infty^2}+\frac{v_{\alpha l}^2}{2V_\infty^2}\right). \tag{11.2.30}$$

Then the coefficient of pressure difference between the lower and upper surface will be

$$\Delta\bar{p}_{f(w)}=\bar{p}_{f(w)l}-\bar{p}_{f(w)u}=-4u_{\alpha l}/V_\infty. \tag{11.2.31}$$

It can be seen that the coefficient of pressure difference depends solely on the axial velocity component.

Taking into account (11.2.22), we can write

$$\Delta\bar{p}_{f(w)}=\frac{-4a\left\{4r\frac{dr}{dx}\cos^2\theta-\left(s+\frac{r^2}{s}\right)\left[2\frac{r}{s}\cdot\frac{dr}{dx}+\frac{ds}{dx}\left(1-\frac{r^2}{s}\right)\right]\right\}}{\left[\left(s+\frac{r^2}{s}\right)^2-4r^2\cos^2\theta\right]^{1/2}}. \tag{11.2.32}$$

As the coordinate $z=r\cos\theta$ for a point on the fuselage (see Fig. 11.2.2), we have

$$\Delta\bar{p}_{f(w)}=\frac{4a\left[\left(1-\frac{r^4}{s^4}\right)\frac{ds}{dx}+2\frac{r}{s}\cdot\frac{dr}{dx}\left(1+\frac{r^2}{s^2}-2\frac{z^2}{r^2}\right)\right]}{\left[\left(1+\frac{r^2}{s^2}\right)^2-4\frac{z^2}{s^2}\right]^{1/2}}. \tag{11.2.33}$$

2.4 Velocity and pressure on wing in presence of fuselage

Assuming $y=0$ in formula (11.2.21) and noting that the right side of this

formula is a real quantity, we get the following expression for an axial velocity component:

$$\frac{\partial \varphi_\alpha}{\partial x}=u_\alpha=aV_\infty \frac{2\frac{r}{z}\cdot\frac{dr}{dx}\left(z+\frac{r^2}{z}\right)-\left(s+\frac{r^2}{s}\right)\left[\frac{ds}{dx}\left(1-\frac{r^2}{s^2}\right)+2\frac{r}{s}\cdot\frac{dr}{dx}\right]}{\left[\left(s+\frac{r^2}{s}\right)^2-\left(z+\frac{r^2}{z}\right)^2\right]^{1/2}}. \quad (11.2.34)$$

Taking $\sigma=z$ in (11.2.23) and resolving the right side into real and imaginary quantities, we get the relations for side and vertical components w_α and v_α of velocity:

$$w_\alpha=\frac{aV_\infty\left(z+\frac{r^2}{z}\right)\left(1-\frac{r^2}{z^2}\right)}{\left[\left(s+\frac{r^2}{s}\right)^2-\left(z+\frac{r^2}{z}\right)^2\right]^{1/2}}; \quad (11.2.35)$$

$$v_\alpha=-aV_\infty. \quad (11.2.36)$$

Formulas (11.2.34) through (11.2.36) give the values of the corresponding velocities on the lower surface of the wing panels. Here the form of these quantities is similar to that of (11.2.26). From symmetry of flow it follows that the velocity components on the upper surface will be determined by expressions similar to (11.2.27).

The velocity and hence pressure on the fuselage do not change during axial flow-interaction (zero angle of attack) in the presence of a lifting wing surface of "zero" thickness. However, the wing-panels will register the effect of the velocity field and pressure field around the fuselage during this flow-interaction. The resultant flow about the wing-panels will consist of the velocity field induced by the fuselage during the axial flow-interaction plus the velocity field arising during cross flow over it at a given angle of attack.

Let us study the velocity field about the fuselage in a flow at zero angle of attack, which is established by using the aerodynamic theory of a thin body (see Chapter 10 Section 3). According to this theory the additional radial component of velocity during axial flow-interaction (let us denote it by $V'_{Rt}=V'_{r1}$, see Fig. 11.2.2) will be obtained by replacing r by any radial coordinate of point R in formula (10.3.10):

$$V'_{Rt}=-f(x)/R. \quad (11.2.37)$$

From the condition of unseparated flow (10.2.19) represented in the form

$$\varphi'_r=V'_{Rt}=V_\infty(dr/dx), \quad (11.2.38)$$

with φ'_x small compared to V_∞, we get an expression for the function

$$f(x)=-V_\infty r(dr/dx). \quad (11.2.39)$$

Consequently equation (11.2.37) can be written in the form

$$V'_{Rt}=\frac{V_\infty r}{R}\cdot\frac{dr}{dx}. \tag{11.2.40}$$

From Fig. 11.2.2 it can be seen that the side and vertical velocity components w_t and v_t of a disturbed flow during the axial flow interaction of the fuselage will be respectively equal to:

$$w_t=V'_{Rt}\cos\theta=\frac{V_\infty r}{R}\cdot\frac{dr}{dx}\cos\theta; \tag{11.2.41}$$

$$v_t=V'_{Rt}\sin\theta=\frac{V_\infty r}{R}\cdot\frac{dr}{dx}\sin\theta. \tag{11.2.42}$$

For the conditions on the surface of a wing-panel $\theta=0$, $R=z$ and hence

$$w_t=\frac{V_\infty r}{z}\cdot\frac{dr}{dx}; \tag{11.2.43}$$

$$v_t=0. \tag{11.2.44}$$

If the expression (11.2.43) for w_t determines the value of velocity on the lower surface ($w_{tl}=w_t$) it follows from symmetry of flow that

$$w_{tu}=w_{tl} \tag{11.2.45}$$

on the upper surface. For axial additional velocity u_t, which will not be clearly shown here, the equality $u_{tu}=u_{tl}$, obtained by symmetry, is valid.

Values of the components of perturbation velocity on the wing-panel are obtained by summation of the corresponding components of velocity during axial and cross flow-interaction, i.e.

$$u=u_\alpha+u_t,\ w=w_\alpha+w_t,\ v=v_\alpha+v_t=v_\alpha. \tag{11.2.46}$$

Inserting these quantities in the formula for the pressure coefficient rewritten by analogy with (11.2.28) in the form

$$\bar{p}=-2\left(\frac{u+av}{V_\infty}+\frac{v^2}{2V_\infty^2}+\frac{w^2}{2V_\infty^2}\right), \tag{11.2.47}$$

we get

$$\bar{p}_{w(f)}=-2\left[\frac{u_\alpha+u_t+av}{V_\infty}+\frac{v_\alpha^2}{2V_\infty^2}+\frac{(w_\alpha+w_t)^2}{2V_\infty^2}\right]. \tag{11.2.48}$$

For the lower surface of the wing panel we have

$$\bar{p}_{w(f)l}=-2\left(\frac{u_{\alpha l}+u_{tl}+av_{\alpha l}}{V_\infty}+\frac{v_{\alpha l}^2}{2V_\infty^2}+\frac{w_{\alpha l}^2+w_{tl}^2}{2V_\infty^2}+\frac{w_{\alpha l}w_{tl}}{V_\infty^2}\right).$$

Using the property of symmetry [see (11.2.27) and (11.2.45); $u_{tu}=u_{tl}$] the pressure coefficient on the upper surface of a wing-panel will be

$$\bar{p}_{w(f)u}=-2\left(\frac{-u_{\alpha l}+u_{tl}+\alpha v_{\alpha l}}{V_\infty}+\frac{v_{\alpha l}^2}{2V_\infty^2}+\frac{w_{\alpha l}^2+w_{tl}^2}{2V_\infty^2}-\frac{w_{\alpha l}w_{tl}}{V_\infty^2}\right).$$

Then the coefficient of pressure difference between the lower and upper surfaces will be

$$\Delta\bar{p}_{w(f)}=\bar{p}_{w(f)l}-\bar{p}_{w(f)u}=-4\,(u_{\alpha l}/V_\infty)-(4w_{\alpha l}\,w_{tl}/V_\infty^2)\cdot \qquad (11.2.49)$$

Formula (11.2.49) for the coefficient of pressure difference on a wing-panel has a quadratic form, unlike the corresponding formula (11.2.31) for the fuselage. In place of $u_{\alpha l}$, $w_{\alpha l}$, w_{tl} in (11.2.49) the use of corresponding values from (11.2.34), (11.2.35), (11.2.43) gives the coefficient of pressure difference on wing-panels in the presence of a fuselage as:

$$\Delta\bar{p}_{w(f)}=\frac{-4a}{\left[\left(s+\frac{r^2}{s}\right)^2-\left(z+\frac{r^2}{z}\right)^2\right]^{1/2}}\left\{2\,\frac{r}{z}\cdot\frac{dr}{dx}\left(z+\frac{r^2}{z}\right)\right.$$
$$\left.-\left(s+\frac{r^2}{s}\right)\left[\frac{ds}{dx}\left(1-\frac{r^2}{s^2}\right)+2\frac{r}{s}\cdot\frac{dr}{dx}\right]+\frac{r}{z}\cdot\frac{dr}{dx}\left(z+\frac{r^2}{z}\right)\left(1-\frac{r^2}{z^2}\right)\right\}$$

or

$$\Delta\bar{p}_{w(f)}=\frac{4a}{\left[\left(s+\frac{r^2}{s}\right)^2-\left(z+\frac{r^2}{z}\right)^2\right]^{1/2}}\left\{s\,\frac{ds}{dx}\left(1-\frac{r^4}{s^4}\right)\right.$$
$$\left.+r\,\frac{dr}{dx}\left[2\left(\frac{r^2}{s^2}-1\right)+\left(1-\frac{r^2}{z^2}\right)^2\right]\right\}\cdot \qquad (11.2.50)$$

If the fuselage is a circular cylinder $dr/dx=0$ and the relations (11.2.33), (11.2.50) will have the respective form:

$$\Delta\bar{p}_{f(w)}=4a\,\frac{ds}{dx}\left(1-\frac{r^4}{s^4}\right)\left[\left(1+\frac{r^2}{s^2}\right)^2-4\,\frac{z^2}{s^2}\right]^{-1/2}; \qquad (11.2.51)$$

$$\Delta\bar{p}_{w(f)}=4a\,\frac{ds}{dx}\left(1-\frac{r^4}{s^4}\right)\left[\left(1+\frac{r^4}{s^4}\right)-\frac{z^2}{s^2}\left(1+\frac{r^4}{z^4}\right)\right]^{-1/2} \qquad (11.2.52)$$
$$(r\leqslant z\leqslant s).$$

The expressions (11.2.51) and (11.2.52) are convenient for approximate calculation of pressure distribution over the surface in the flow in the case of a larger fuselage and wing assembly where $dr/dx\neq 0$. This is confirmed by calculations indicating that the effect of having a larger fuselage on the nature of pressure distribution is not great.

2.5 Determination of interference coefficients

Let us study the relations for the lift force of a wing and a fuselage taking into account their mutual interaction and determine the corresponding coefficients of interference. Let us assume that the wing panels situated on

the cylindrical fuselage ($dr/dx=0$) have a triangular form for which $ds/dx=\tan\varepsilon$ (Fig. 11.2.3).

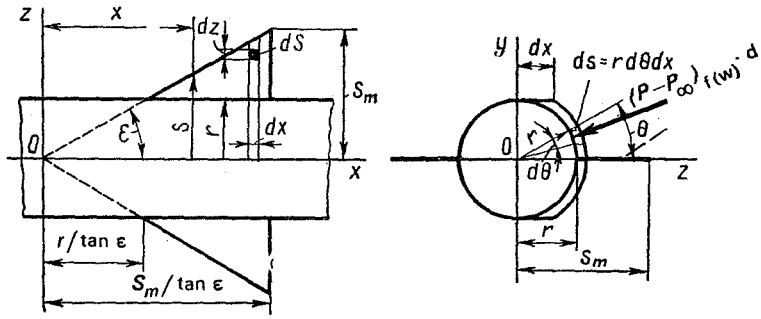

Fig. 11.2.3. Combination of cylindrical fuselage and wing in form of triangular panels.

We know that inclining a thin isolated cylindrical body does not produce lift force. Therefore the quantity $\Delta Y_{f(w)}$ in (11.2.4) can be regarded as the lift force $Y_{f(w)}$ on the fuselage in the presence of a wing. This force can be calculated with the help of formula (10.5.5) for a normal force because these forces, given low angles of attack and linearized flow-interaction, may be assumed to be near enough identical. Assuming $\cos\beta\approx 1$ and $\cos\gamma=\sin\theta$ in (10.5.4), we get the following expression for an elemental lift force acting on an area $dS=rd\theta dx$ (see Fig. 11.2.3):

$$d(\Delta Y_{f(w)})=-dY_{f(w)}=-(p-p_\infty)_{f(w)}\,rd\theta dx\sin\theta.$$

The life force on the part of the fuselage situated below the wing is

$$\Delta Y_{f(w)}=-\int_{r/\tan\epsilon}^{s_m/\tan\epsilon}\int_0^{2\pi}(p-p_\infty)_{f(w)}\,rd\theta dx\sin\theta.$$

The corresponding coefficient of lift obtained with respect to the area of cross section of fuselage $S=\pi r^2$ will be

$$\Delta c'_{yf(w)}=\frac{\Delta Y_{f(w)}}{q_\infty\pi r^2}=-\frac{1}{\pi r}\int_{r/\tan\epsilon}^{s_m/\tan\epsilon}dx\int_0^{2\pi}\bar{p}_{f(w)}\sin\theta\,d\theta.$$

Remembering the symmetry of pressure distribution over both sides of the zero meridian plane and the condition that at the points on the surface determined by angular coordinates θ (upper surface) and $-\theta$ (lower surface), the pressure coefficients are $\bar{p}$ and $-\bar{p}$ respectively, we get the relation

$$\Delta c'_{yf(w)}=-\frac{2}{\pi r}\int_{r/\tan\epsilon}^{s_m/\tan\epsilon}dx\int_0^{\pi/2}\Delta\bar{p}_{f(w)}\sin\theta\,d\theta.$$

Using here the expression (11.2.51) in place of $\Delta\bar{p}_{f(w)}$ and keeping in view the equality $z=r\cos\theta$, we find (in absolute value)

$$\Delta c'_{yf(w)}=\frac{8a\tan\varepsilon}{\pi r^2}\int\limits_{r/\tan\epsilon}^{s_m/\tan\epsilon}dx\int\limits_0^r\left(1-\frac{r^4}{s^4}\right)\left[\left(1+\frac{r^2}{s^2}\right)^2-4\frac{z^2}{s^2}\right]^{-1/2}dz.$$

The first integration leads to

$$\Delta c'_{yf(w)}=\frac{8a\tan\varepsilon}{2\pi r^2}\int\limits_{r/\tan\epsilon}^{s_m/\tan\epsilon}s\left(1-\frac{r^4}{s^4}\right)\sin^{-1}\frac{2r/s}{1+(r^2/s^2)}\,dx,$$

or since $x=s/\tan\varepsilon$ and $dx=ds/\tan\varepsilon$,

$$\Delta c'_{yf(w)}=\frac{4a}{\pi}\int\limits_1^{s_m/r}\left(1-\frac{r^4}{s^4}\right)\sin^{-1}\frac{2r/s}{1+(r^2/s^2)}\cdot\frac{s}{r}\,d\left(\frac{s}{r}\right).$$

This expression can be written in the form

$$\Delta c'_{yf(w)}=\frac{4a}{\pi}\int\limits_1^{\bar{s}_m}\frac{\bar{s}^4-1}{\bar{s}^3}\sin^{-1}\frac{2\bar{s}}{\bar{s}^2+1}\,d\bar{s}, \tag{11.2.53}$$

where $\bar{s}=s/r$, $\bar{s}_m=s_m/r$.

Introducing the variables

$$u=\sin^{-1}\frac{2\bar{s}}{\bar{s}^2+1}\text{ and }v=\frac{1}{2}\left(\bar{s}^2+\frac{1}{\bar{s}^2}\right)$$

and integrating by parts, we get

$$\Delta c'_{yf(w)}=\frac{4a}{\pi}\left[\frac{1}{2}\left(\bar{s}^2+\frac{1}{\bar{s}^2}\right)\sin^{-1}\frac{2\bar{s}}{\bar{s}^2+1}\right|_1^{\bar{s}_m}$$

$$+\int\limits_1^{\bar{s}_m}\left(\bar{s}^2+\frac{1}{\bar{s}^2}\right)(\bar{s}^2+1)^{-1}\,d\bar{s}\Bigg]=\frac{4a}{\pi}\left[\frac{1}{2}\left(\bar{s}_m^2+\frac{1}{\bar{s}_m^2}\right)\sin^{-1}\frac{2\bar{s}_m}{\bar{s}_m^2+1}\right.$$

$$\left.+\frac{\bar{s}_m^2-1}{\bar{s}_m}-2\tan^{-1}\bar{s}_m\right]. \tag{11.2.53'}$$

The corresponding coefficient of lift force for fuselage $\Delta c_{yf(w)}$, calculated on the basis of the area of isolated wing-panels,

$$S_w=(s_m-r)^2/\tan\varepsilon, \tag{11.2.54}$$

will be equal to

$$\Delta c_{yf(w)}=\Delta c'_{yf(w)}\frac{\pi r^2}{S_w}=\frac{\pi\tan\varepsilon r^2}{(s_m-r^2)}\Delta c'_{yf(w)} \tag{11.2.55}$$

Taking into account expression (8.8.48) for the lift coefficient c_{yw} of an isolated wing, if $\cot\kappa=\tan\varepsilon$ is assumed the coefficient of interference

$$K_f=\frac{\Delta c_{yf(w)}}{c_{yw}}=\frac{\Delta c'_{yf(w)}}{2(\bar{s}_m-1)^2a}. \tag{11.2.56}$$

Substituting (11.2.53'), we get

$$K_f=\frac{2}{\pi(\bar{s}_m-1)^2}\left[\frac{1}{2}\left(\bar{s}_m^2+\frac{1}{\bar{s}_m^2}\right)\sin^{-1}\frac{2\bar{s}_m}{\bar{s}_m^2+1}+\frac{\bar{s}_m^2-1}{\bar{s}_m}-2\tan^{-1}\bar{s}_m\right].$$

As

$$2\tan^{-1}\bar{s}_m=\pi-\tan^{-1}\frac{2\bar{s}_m}{\bar{s}_m^2-1}=\pi-\sin^{-1}\frac{2\bar{s}_m}{\bar{s}_m^2+1},$$

we have

$$K_f=\frac{2}{\pi(\bar{s}_m-1)^2}\left[\frac{\bar{s}_m^2-1}{\bar{s}_m}+\frac{\pi}{2}\left(\bar{s}_m^2+\frac{1}{\bar{s}_m^2}\right)-\frac{(\bar{s}_m^2+1)^2}{\bar{s}_m^2}\tan^{-1}\bar{s}_m\right]. \tag{11.2.57}$$

Let us find the relation for coefficient of interference K_w of the wing with the fuselage. The elementary value of lift force acting on an elementary wing area $dS_w=dx\cdot dz$ is

$$d(\Delta Y_{w(f)})=\Delta\bar{p}_{w(f)}\,dxdzq_\infty.$$

The force $\Delta Y_{w(f)}$ of two wing panels, taking into account the expression (11.2.52) for $\Delta\bar{p}_{w(f)}$, will be

$$\Delta Y_{w(f)}=8a\tan\varepsilon q_\infty\int_{r/\tan\epsilon}^{s_m/\tan\epsilon}\left(1-\frac{r^4}{s^4}\right)dx$$

$$\times\int_r^s\left[\left(1+\frac{r^4}{s^4}\right)-\frac{z^2}{s^2}\left(1+\frac{r^4}{z^4}\right)\right]^{-1/2}dz. \tag{11.2.52'}$$

The corresponding coefficient of lift force

$$\Delta c_{yw(f)}=\frac{\Delta Y_{w(f)}}{q_\infty S_w}=\frac{8a\tan^2\varepsilon}{(s_m-r)^2}\int_{r/\tan\epsilon}^{s_m/\tan\epsilon}\left(1-\frac{r^4}{s^4}\right)dx$$

$$\times\int_r^s\left[\left(1+\frac{r^4}{s^4}\right)-\frac{z^2}{s^2}\left(1+\frac{r^4}{z^4}\right)\right]^{-1/2}dz.$$

Integrating once, we get

$$\Delta c_{yw(f)} = \frac{4a\tan^2\varepsilon}{(s_m - r)^2} \int_{r/\tan\epsilon}^{s_m/\tan\epsilon} s\left(1-\frac{r^4}{s^4}\right)\left[\frac{\pi}{2}+\sin^{-1}\frac{1-(r^2/s^2)}{1+(r^2/s^2)}\right]dx,$$

or

$$\Delta c_{yw(f)} = \frac{4a\tan\varepsilon}{(\bar{s}_m-1)^2}\int_1^{\bar{s}_m}\frac{\bar{s}^4-1}{\bar{s}^3}\left(\frac{\pi}{2}+\sin^{-1}\frac{\bar{s}^2-1}{\bar{s}^2+1}\right)d\bar{s}.$$

This may be simplified to

$$\Delta c_{yw(f)} = \frac{4a\tan\varepsilon}{(\bar{s}_m-1)^2}\left[\frac{\pi}{4}\frac{(\bar{s}_m^2-1)^2}{\bar{s}_m^2}+\int_1^{\bar{s}_m}\frac{\bar{s}^4-1}{\bar{s}^3}\sin^{-1}\frac{\bar{s}^2-1}{\bar{s}^2+1}\,d\bar{s}\right].$$

Introducing the variables

$$u=\sin^{-1}[(\bar{s}^2-1)/(\bar{s}^2+1)],\quad v=0.5[\bar{s}^2+(1/\bar{s}^2)]$$

and carrying out integration by parts, we have

$$\Delta c_{yw(f)} = \frac{4a\tan\varepsilon}{(\bar{s}_m-1)^2}\left[\frac{\pi}{4}\cdot\frac{(\bar{s}_m^2-1)^2}{\bar{s}_m^2}-\frac{\bar{s}_m^2-1}{\bar{s}_m}\right.$$
$$\left.+2\left(\tan^{-1}\bar{s}_m-\frac{\pi}{4}\right)+\frac{1}{2}\left(\bar{s}_m^2+\frac{1}{\bar{s}_m^2}\right)\sin^{-1}\frac{\bar{s}_m^2-1}{\bar{s}_m^2+1}\right].$$

Considering that

$$2\left(\tan^{-1}\bar{s}_m-\frac{\pi}{4}\right)=2\tan^{-1}\frac{\bar{s}_m-1}{\bar{s}_m+1}=\tan^{-1}\frac{\bar{s}_m^2-1}{2\bar{s}_m}=\sin^{-1}\frac{\bar{s}_m^2-1}{\bar{s}_m^2+1},\tag{11.2.58}$$

we get

$$\Delta c_{yw(f)} = \frac{4a\tan\varepsilon}{(\bar{s}_m-1)^2}\left[\frac{\pi}{4}\cdot\frac{(\bar{s}_m^2-1)^2}{\bar{s}_m^2}-\frac{\bar{s}_m^2-1}{\bar{s}_m}\right.$$
$$\left.+\frac{(\bar{s}_m^2+1)^2}{2\bar{s}_m^2}\cdot\sin^{-1}\frac{\bar{s}_m^2-1}{\bar{s}_m^2+1}\right].\tag{11.2.59}$$

Then the coefficient of interference, taking into account (8.8.48) for c_{yw}, will be

$$K_w=\frac{\Delta c_{yw(f)}}{c_{yw}}=\frac{2}{\pi(\bar{s}_m-1)^2}\left[\frac{\pi}{4}\cdot\frac{(\bar{s}_m^2-1)^2}{\bar{s}_m^2}-\frac{\bar{s}_m^2-1}{\bar{s}_m}+\frac{(\bar{s}_m^2+1)^2}{2\bar{s}_m^2}\sin^{-1}\frac{\bar{s}_m^2-1}{\bar{s}_m^2+1}\right].\tag{11.2.60}$$

Let us compare this quantity with the coefficient of interference K_f in (11.2.57),

which with the help of

$$\tan^{-1}\bar{s}_m=\frac{1}{2}\left(\sin^{-1}\frac{\bar{s}_m^2-1}{\bar{s}_m^2+1}+\frac{\pi}{2}\right),$$

obtained from (11.2.58), can be simplified as:

$$K_f=\frac{2}{\pi(\bar{s}_m-1)^2}\left[\frac{\pi}{4}\cdot\frac{(\bar{s}_m^2-1)^2}{\bar{s}_m^2}+\frac{\bar{s}_m^2-1}{\bar{s}_m}-\frac{(\bar{s}_m^2+1)^2}{2\bar{s}_m^2}\times\sin^{-1}\frac{\bar{s}_m^2-1}{\bar{s}_m^2+1}\right]. \qquad (11.2.57')$$

Adding (11.2.60) and (11.2.57'), we get

$$K_w+K_f=(\bar{s}_m+1)^2/\bar{s}_m^2. \qquad (11.2.61)$$

From the expressions (11.2.60) and (11.2.57') it follows that the coefficients of interference are the functions of ratio r/s_m only. Thus this parameter represents by itself a basic criterion for evaluation of the mutual interaction of fuselage and wing in terms of lift force. The quantities K_w and K_f are reproduced in Fig. 11.2.4 and in Table 11.2.1 as a function of parameter $1/\bar{s}_m=r/s_m$.

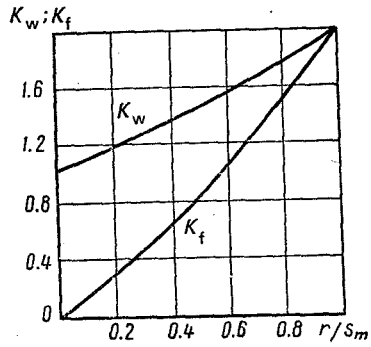

Fig. 11.2.4. Coefficients of interference for plain combination of "fuselage-wing" with no bank.

TABLE 11.2.1

r/s_m	K_w	K_f	$(c_{c\cdot p})_{\alpha w(f)}$	$(c_{c\cdot p})_{\alpha f(w)}$	$(\bar{z}_{c\cdot p})_{\alpha w(f)}$
0	1.000	0	0.667 (2/3)	0.500	0.424 (4/3π)
0.1	1.077	0.133	0.657	0.521	0.421
0.2	1.162	0.278	0.650	0.542	0.419
0.3	1.253	0.437	0.647	0.563	0.418
0.4	1.349	0.611	0.646	0.581	0.417
0.5	1.450	0.800	0.647	0.598	0.417
0.6	1.555	1.005	0.650	0.613	0.416
0.7	1.663	1.227	0.654	0.628	0.418
0.8	1.774	1.467	0.658	0.641	0.420
0.9	1.887	1.725	0.662	0.654	0.422
1.0	2.000	2.000	0.667 (2/3)	0.667 (2/3)	0.424 (4/3π)

If the parameter $r/s_m=0$ (fuselage absent) it is obvious that $K_w=1$ and $K_f=0$. Let us assume that the radius of the fuselage is now greater and the lifting wing-panels smaller, i.e. the parameter r/s_m increases. From (11.1.6') it follows that the effective angle of attack of the wing-panels increases. At

$(R/l)\to 1[(r/s_m)\to 1]$ the fuselage induces local angle of attack $a_{e.t}\to 2a$ along the surface of its sides. Therefore in the presence of the fuselage the wing-panels create a lift force double the value for an isolated wing and hence $K_w=2$.

With decreasing size of wing-panels an ever larger part of the wing's lift force is transferred to the fuselage. When the value of parameter $r/s_m\to 1$, the highest value of lift force is induced on the fuselage and $K_f=2$. Calculations, which we omit here, show that the values of K_f and K_w are independent of the wing plan and therefore the coefficients of interference obtained for triangular wing-panels are applicable to other types of wings.

2.6 Center of pressure

The coordinates of the center of pressure due to lift force induced by the fuselage on the wing are given by

$$(x_{c.p})_{\alpha w(f)}=\Delta M_{zw(f)}/\Delta Y_{w(f)}, \tag{11.2.62}$$

where $\Delta M_{zw(f)}$ is pitching moment about the leading edge of the root section of the wing due to forces established by the effect of the fuselage on the wing:

$$\Delta M_{zw(f)}=\int_0^{(s_m-r)/\tan\epsilon}\int_r^s \Delta\bar{p}_{w(f)}\,q_\infty\,x\,dx\,dz. \tag{11.2.63}$$

The coordinates x and $(x_{c.p})\,a_{w(f)}$ are measured from the leading edge of the wing's root section (Fig. 11.2.5). Taking into account the value of $\Delta Y_{w(f)}$, the coordinate

$$(x_{c.p})_{\alpha w(f)}=\frac{\displaystyle\int_0^{(s_m-r)/\tan\epsilon}\int_r^s \Delta\bar{p}_{w(f)}\,q_\infty\,x\,dx\,dz}{\displaystyle\int_0^{(s_m-r)/\tan\epsilon}\int_r^s \Delta\bar{p}_{w(f)}\,q_\infty\,dx\,dz}. \tag{11.2.64}$$

The coordinate of the center of pressure due to lift force induced by the wing on the fuselage

$$(x_{c.p})_{\alpha f(w)}=\Delta M_{zf(w)}/\Delta Y_{f(w)}, \tag{11.2.65}$$

where $\Delta Y_{f(w)}$ is lift on the part of the fuselage situated below the wing that is the effect of the wing; $\Delta M_{zf(w)}$ is pitching moment about the leading edge of the wing's root section that is also the effect of the wing (see Fig. 11.2.5):

$$\Delta M_{zf(w)}=\int_0^{(s_m-r)/\tan\epsilon}\int_0^r \Delta\bar{p}_{f(w)}\,q_\infty\,x\,dx\,dz. \tag{11.2.66}$$

Taking the value of $\Delta Y_{f(w)}$, the coordinate

$$(x_{c.p})_{\alpha f(w)} = \frac{\int_0^{(s_m-r)/\tan\epsilon}\int_0^{r} \Delta\bar{p}_{f(w)}\, q_\infty\, x\,dx\,dz}{\int_0^{(s_m-r)/\tan\epsilon}\int_0^{r} \Delta\bar{p}_{f(w)}\, q_\infty\, dx\,dz}. \tag{11.2.67}$$

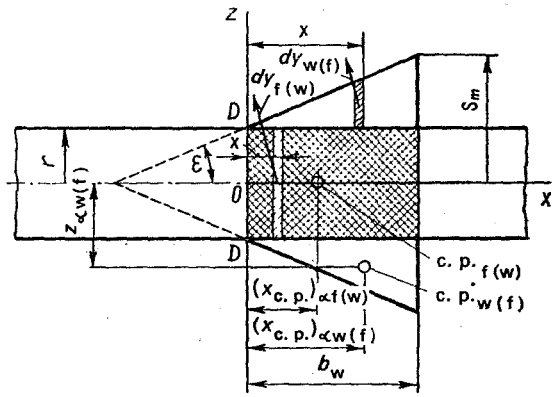

Fig. 11.2.5. Determination of position of center of pressure of fuselage and wing with allowance for interference effect (area to which lift force of wings is transferred is hatched).

The respective coefficients of centers of pressure can be determined from (11.2.64) and (11.2.67):

$$\left.\begin{aligned}(c_{c.p})_{\alpha w(f)} &= (x_{c.p})_{\alpha w(f)}/b_r;\\ (c_{c.p})_{\alpha f(w)} &= (x_{c.p})_{\alpha f(w)}/b_r,\end{aligned}\right\} \tag{11.2.68}$$

where b_r is the root chord of the wing (see Fig. 11.2.5).

The side coordinate of the center of pressure due to lift force $\Delta Y_{w(f)}$ for the wing-panels with fuselage effect (see Fig. 11.2.5) will be

$$(z_{c.p})_{\alpha w(f)} = \Delta M_{xw(f)}/\Delta Y_{w(f)}, \tag{11.2.69}$$

where $\Delta M_{xw(f)}$ is rolling moment about longitudinal axis x induced by the action of lift force $\Delta Y_{w(f)}$:

$$\Delta M_{xw(f)} = \int_0^{(s_m-r)/\tan\epsilon}\int_r^{s} \Delta\bar{p}_{w(f)}\, q_\infty\, z\,dx\,dz. \tag{11.2.70}$$

Taking the value of $\Delta Y_{w(f)}$, the coordinate of the center of pressure will be given as

$$(z_{c.p})_{\alpha w(f)}=\frac{\int\limits_0^{(s_m-r)/\tan\epsilon}\int\limits_r^s \Delta\bar{p}_{w(f)}\, q_\infty\, z\,dx\,dz}{\int\limits_0^{(s_m-r)/\tan\epsilon}\int\limits_r^s \Delta\bar{p}_{w(f)}\, q_\infty\,dx\,dz}. \tag{11.2.71}$$

From this expression the coordinate of the center of pressure along the wing span, measured from the wing root chord and nondimensionalized with respect to the width of the wing-panel (s_m-r), can be found:

$$(\bar{z}_{c.p})_{\alpha w(f)}=\frac{(z_{c.p})_{\alpha w(f)}-r}{s_m-r}.$$

This quantity and the values of the coefficients of the center of pressure (11.2.68) calculated for triangular wing panels [in formulas (11.2.51) and (11.2.52) for $\Delta\bar{p}_{f(w)}$ and $\Delta\bar{p}_{w(f)}$ respectively the derivative ds/dx is taken as $\tan\varepsilon$] are shown in Table 11.2.1 as the functions of a parameter $r/s_m=1/\bar{s}_m$.

From the above data it follows that coefficients of center of pressure $(c_{c.p})_{\alpha w(f)}$ hardly differ from 2/3, which corresponds to the isolated delta wing. The ratio $(\bar{z}_{c.p})_{\alpha w(f)}$ is nearer to the value $4/(3\pi)$, which holds for an elliptical lift distribution along the span of an isolated wing. Both these results indicate that the mutual interference of wing and fuselage has no appreciable effect on the position of the center of pressure of lifting wing-panels either spanwise or chordwise. Therefore in practice when aerodynamic calculations make use of the aerodynamic theory of a thin body the effect of interference on the position of the center of pressure of the wing can be neglected. Here we must keep in mind one basic point, that the value of $(\bar{z}_{c.p})_{\alpha w(f)}$, according to the aerodynamic theory of a thin body, is independent of wing plan. At the same time the position of the center of pressure of the wing along the longitudinal axis depends on wing plan. In particular, calculations by the aerodynamic theory of a thin body indicate that the center of pressure of a rectangular wing moves toward the leading edge.

The effect of interference on the position of the center of pressure of the fuselage, as can be seen from Table 11.2.1, is quite considerable. At $r/s_m=0$, indicating absence of a fuselage (to be more specific, the fuselage is reduced to an infinitesimally thin cylinder coinciding with the root chord of a wing-panel), we get the obvious result for $(c_{c.p})_{\alpha f(w)}=1/2$. For very small sizes of wing-panels compared to the radius of the fuselage, i.e. for the values of $r/s_m\to 1$ practically the whole of the lift force of the wing is transferred to the fuselage (coefficient of interference $K_f\to 2$). Accordingly the coefficient of the center of pressure is nearer to its position for an isolated wing, i.e. $(c_{c.p})_{\alpha f(w)}\to 2/3$.

2.7 Lift force of wing-fuselage combination

Formula (11.2.6) may be used to determine the total lift force $Y_{f,w}$. The lift force Y_f of an isolated thin fuselage appearing in this formula can be determined in the following way: Let us consider a thin fuselage in the form of a cone of very small semi-vertex angle β_K. As may be seen from (10.5.29), the coefficient of lift for a thin fuselage at small angles of attack (when the term a^3 is negligibly small) may be taken as $c_y=2a$ (index "p" is dropped). Extending this formula for a thin body of revolution of arbitrary shape, its lift force will be

$$Y_f=2a\pi r^2 q_\infty , \tag{11.2.72}$$

where r is the radius of maximum cross section of fuselage. According to this formula the lift force of a thin body of revolution is independent of the form of the generator and for a given angle of attack is determined solely by the diameter of the largest cross section.

The lift force of an isolated wing is given by

$$Y_w=c_{yw} S_w q_\infty,$$

where $c_{yw}=2a\pi \tan \varepsilon$, as shown by formula (8.8.48) in which it is assumed that $\cot \kappa=\tan \varepsilon$. As S_w can be found from (11.2.54) we have

$$Y_w=2a\pi (s_m-r)^2 q_\infty . \tag{11.2.73}$$

Keeping in view that the sum of the coefficients of interference K_f+K_w is determined by formula (11.2.61) and taking the values of Y_f and Y_w obtained, the total lift force will be

$$Y_{f,w}=2a\pi s_m^2 (1-1/\bar{s}_m^2+1/\bar{s}_m^4) q_\infty, \tag{11.2.74}$$

where $\bar{s}_m=s_m/r$. The total lift force is independent of the shape of the wing-panels and that part of the fuselage that lies ahead of the section of maximum semi-span s_m. From formula (11.2.74) it also follows that if there exists some area of wing behind this section it will have no effect on the lifting property of the wing-fuselage combination.

3. Effect of Angle of Banking on Interference Between Fuselage and Plane Wing

3.1 General relation for coefficient of pressure

A plain combination of fuselage-wing inclined through a bank angle φ is shown in Fig. 11.3.1. The flow-interaction of this combination and hence the interference between fuselage and wing-panels depend on angle φ as well as angle α_c between the logitudinal axis and the direction of undisturbed flow. This angle (see Fig. 11.3.1) is determined in the $x'Oy'$ plane formed by the fixed axes Ox' and Oy' drawn for the unbanked posture. The flow in question

is equivalent to the flow arising in the presence of angle of attack a and angle of yaw β. The angle of attack is measured in a vertical plane y_1Ox_1 in a fixed system of coordinates Oy_1 and Ox_1 drawn for a banked body and is determined as an angle between the projection V'_∞ of velocity vector $\overline{V}_\infty$ on this plane and the Ox_1 axis.

According to Fig. 11.3.1 the small angle a is equal to the ratio of vertical and horizontal components of undisturbed velocity $V_{y_1\infty}$ and $V_{x_1\infty}$ respectively, i.e.

$$a=V_{y_1\infty}/V_{x_1\infty}\,. \tag{11.3.1}$$

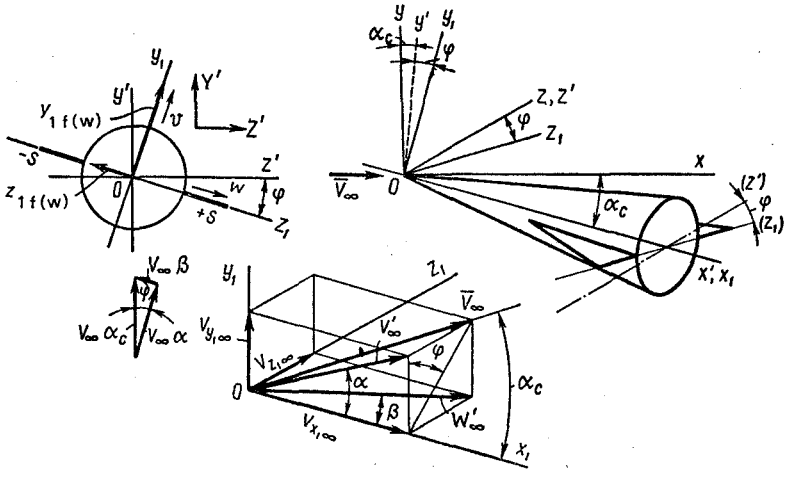

Fig. 11.3.1. Combination of "fuselage-plain wing" at angle of bank.

The angle of yaw β lies in a cross plane z_1Ox_1 of the same fixed system of coordinates as an angle between the projection W'_∞ of vector $\overline{V}_\infty$ on this plane and the longitudinal axis Ox_1. From Fig. 11.3.1 it may be seen that

$$\beta=V_{z_1\infty}/V_{x_1\infty}\,, \tag{11.3.2}$$

where $V_{z1\infty}$ is the side component of undisturbed flow.

From Fig. 11.3.1 it can be seen that

$$\left.\begin{aligned} V_{x_1\infty} &= V_\infty\cos a_c\,, \quad V_{y_1\infty} = V_\infty\sin a_c\cos\varphi;\\ V_{z_1\infty} &= V_\infty\sin a_c\sin\varphi. \end{aligned}\right\} \tag{11.3.3}$$

For small values of a_c

$$V_{x_1\infty}=V_\infty,\ V_{y_1\infty}=V_\infty a_c\cos\varphi,\ V_{z_1\infty}=V_\infty a_c\sin\varphi. \tag{11.3.3'}$$

Accordingly

$$a=a_c\cos\varphi; \tag{11.3.1'}$$

$$\beta = a_c \sin \varphi. \tag{11.3.2'}$$

Taking the linearized property of the flow-interaction, the total potential function can be determined as a sum of three components:

$$\varphi' = \varphi_t' + \varphi_\alpha' + \varphi_\beta', \tag{11.3.4}$$

where φ_t' is the potential function of axisymmetrical flow-interaction with velocity $V_{x_1\infty} = \infty$; φ_α' and φ_β' are additional potentials for the flow in direction a with velocity $V_{y_1\infty} = V_\infty a = V_\infty a_c \cos \varphi$ and in direction β with velocity $V_{z_1\infty} = V_\infty \beta = V_\infty a_c \sin \varphi$.
According to (11.3.4) the velocity components are:

$$\left.\begin{aligned} u_1 &= u_t + u_\alpha + u_\beta; \\ v_1 &= v_t + v_\alpha + v_\beta; \\ w_1 &= w_t + w_\alpha + w_\beta. \end{aligned}\right\} \tag{11.3.5}$$

The general expression for the pressure coefficient over the fuselage allowing for interference can be obtained with the help of formula (11.2.28') in which the perturbation velocity components u, v, w in the flow system of coordinates x, y, z are replaced by the corresponding values of u_1, v_1, w_1 in the fixed system of coordinates x_1, y_1, z_1. Performing the above change, the fixed axes are obtained by turning the flow axis by angle a_c about the Oz axis first and then by angle φ in a clockwise direction about the new position of the Ox_1 axis. The directional cosines between the x, y, z axes and x_1, y_1, z_1 axes are shown in Table 11.3.1.

TABLE 11.3.1

Coordinates	x	y	z
x_1	$\cos a_c$	$-\sin a_c$	0
y_1	$\sin a_c \cos \varphi$	$\cos a_c \cos \varphi$	$\sin \varphi$
z_1	$-\sin a_c \sin \varphi$	$-\cos a_c \sin \varphi$	$\cos \varphi$

According to the data in Table 11.3.1 and taking a low angle for the components of perturbation velocity in the flow system of coordinates, we will write the expressions:

$$\left.\begin{aligned} u &= u_1 + v_1 a_c \cos \varphi - w_1 a_c \sin \varphi; \\ v &= -u_1 a_c + v_1 \cos \varphi - w_1 \sin \varphi; \\ w &= v_1 \sin \varphi + w_1 \cos \varphi. \end{aligned}\right\} \tag{11.3.6}$$

Substituting these expressions for velocity components in (11.2.28') and neglecting the small quantities $u_1^2 a_c^2$, $u_1 v_1 a_c \sin \varphi$, $u_1 v_1 a_c \cos \varphi$, we get

$$\bar{p} = -(2/V_\infty)(u_1 + v_1 a_c \cos \varphi - w_1 a_c \sin \varphi) - (v_1^2 + w_1^2)/V_\infty^2. \tag{11.3.7}$$

Taking into account the relations (11.3.1′) and (11.3.2′), the pressure coefficient may be reduced to

$$\bar{p}=-(2/V_\infty)\,(u_1+v_1\alpha-w_1\beta)-(v_1^2+w_1^2)/V_\infty^2. \tag{11.3.7′}$$

3.2 Pressure over fuselage

Using (11.3.5) the coefficient of pressure over the lower part of the fuselage will be

$$\begin{aligned}\bar{p}_{f(w)l}=&-(2/V_\infty)\,[u_{tl}+u_{\alpha l}+u_{\beta l}+\alpha(v_{tl}+v_{\alpha l}+v_{\beta l})\\&-\beta\,(w_{tl}+w_{\alpha l}+w_{\beta l})]-(1/V_\infty^2)\,[(v_{tl}+v_{\alpha l}+v_{\beta l})^2\\&+(w_{tl}+w_{\alpha l}+w_{\beta l})^2].\end{aligned} \tag{11.3.8}$$

The expression for the pressure coefficient over the upper surface will be similar. This expression can be represented in somewhat different form if the property of symmetry for velocity components over the fuselage is used. The relations (11.2.27) written earlier follow from the symmetry of the flow-interaction of the fuselage in the direction of α. Similarly the expressions following the symmetry of flow in the direction of β can be expressed as follows:

$$u_{\beta u}=u_{\beta l},\quad v_{\beta u}=-v_{\beta l},\quad w_{\beta u}=w_{\beta l}. \tag{11.3.9}$$

Taking the property of symmetry expressed by the relations (11.2.27) and (11.3.9) and also by the expressions

$$u_{tl}=u_{tu},\quad v_{tl}=-v_{tu},\quad w_{tl}=w_{tu}, \tag{11.3.9′}$$

the coefficient of pressure on the upper surface of the fuselage can be written in the form:

$$\begin{aligned}\bar{p}_{f(w)u}=&-(2/V_\infty)\,[u_{tl}-u_{\alpha l}+u_{\beta l}+\alpha(-v_{tl}+v_{\alpha l}-v_{\beta l})\\&-\beta(w_{tl}-w_{\alpha l}+w_{\beta l})]-(1/V_\infty^2)\,[(-v_{tl}+v_{\alpha l}-v_{\beta l})^2\\&+(w_{tl}-w_{\alpha l}+w_{\beta l})^2].\end{aligned} \tag{11.3.10}$$

The coefficient of pressure difference is obtained as the difference between the values of (11.3.8) and (11.3.10), i.e.

$$\begin{aligned}\Delta\bar{p}_{f(w)}=\bar{p}_{f(w)l}-\bar{p}_{f(w)u}=&-(4/V_\infty)\,u_{\alpha l}\\&-(4\alpha/V_\infty)\,(v_{tl}+v_{\beta l})+(4\beta/V_\infty)\,w_{\alpha l}-(4/V_\infty^2)\,(v_{tl}v_{\alpha l}+v_{\alpha l}v_{\beta l})\\&-(4/V_\infty^2)\,(w_{tl}w_{\alpha l}+w_{\alpha l}w_{\beta l}).\end{aligned} \tag{11.3.11}$$

Let us consider any arbitrary point on the lower surface of the fuselage. The perturbation velocity vector at this point in a side plane, derived for the axial flow-interaction of a fuselage of finite thickness, will be $\bar{V}_{tl}=w_{tl}i+v_{tl}j$. For the same point the perturbation velocity vector induced in the presence

of some angle of attack is represented in the form $\overline{V}_{\alpha l}=w_{\alpha l}i+(v_{\alpha l}+aV_\infty)j$. According to (11.2.42) the vector $\overline{V}_{tl}$ coincides with the radial direction and is situated in a meridian plane. By the condition of unseparated flow-interaction the second vector $\overline{V}_{\alpha l}$ coincides with the direction of the tangent to the contour at the point in question. Hence the vectors $\overline{V}_{tl}$ and $\overline{V}_{\alpha l}$ are perpendicular to each other and their scalar product is equal to zero, i.e.

$$\begin{aligned}&(w_{tl}i+v_{tl}j)\,[w_{\alpha l}i+(v_{\alpha l}+aV_\infty)\,j\,]\\&=w_{tl}w_{\alpha l}+v_{tl}\,(v_{\alpha l}+aV_\infty)=0.\end{aligned}\tag{11.3.12}$$

Taking this into account, the expression (11.3.11) takes the form

$$\begin{aligned}\Delta\overline{p}_{f(w)}=&-(4/V_\infty)\,u_{\alpha l}-(4/V_\infty)\,(v_{\beta l}\alpha-w_{\alpha l}\beta)\\&-(4/V_\infty^2)\,(v_{\alpha l}v_{\beta l}+w_{\alpha l}w_{\beta l}).\end{aligned}\tag{11.3.13}$$

By contrast with (11.2.31) terms appear in (11.3.13) characterizing the effect of the angle of bank. These are known as the terms of interaction:

$$v_{\beta l}\alpha,\ w_{\alpha l}\beta,\ v_{\alpha l}v_{\beta l},\ w_{\alpha l}w_{\beta l}\ .$$

The corresponding velocities $u_{\alpha l}$, $w_{\alpha l}$ and $v_{\alpha l}$ are given by the expressions (11.2.22), (11.2.24) and (11.2.25) respectively. The components $w_{\beta l}$ and $v_{\beta l}$ can be obtained with the help of the formula for a complex potential of cross flow over the fuselage in the opposite direction to the Oz axis with the velocity of undisturbed flow βV_∞. By analogy with (11.2.18) this potential will be

$$W=-\beta V_\infty[\sigma+(r^2/\sigma)].\tag{11.3.14}$$

The field of perturbation velocities is obtained if a parallel flow in the direction of the positive Oz axis with velocity βV_∞ and the corresponding potential $\beta V_\infty\sigma$ are superposed on the flow with potential (11.3.14). As a result the complex potential for perturbation velocities will be

$$W_\beta=-\beta V_\infty\,(r^2/\sigma).\tag{11.3.15}$$

Hence the complex velocity of disturbances becomes

$$dW_\beta/d\sigma=w_\beta-v_\beta i=\beta V_\infty(r^2/\sigma^2).\tag{11.3.16}$$

Consequently the complex velocity for the conditions on the fuselage surface $\sigma=re^{i\theta}$ will be

$$w_\beta-v_\beta i=\beta V_\infty\,e^{-2i\theta}=\beta V_\infty(\cos 2\theta-i\sin 2\theta).\tag{11.3.17}$$

Using this expression for the lower surface we get the following relations for velocity components:

$$\left.\begin{aligned}w_{\beta l}&=\beta V_\infty\cos 2\theta;\\v_{\beta l}&=\beta V_\infty\sin 2\theta.\end{aligned}\right\}\tag{11.3.18}$$

Inserting (11.2.22), (11.2.24), (11.2.25) and (11.3.18) in (11.3.13), we find the

relation for the coefficient of pressure difference over the fuselage:

$$\bar{\Delta p}_{f(w)} = \frac{-4a\left\{4r\frac{dr}{dx}\cos^2\theta - \left(s+\frac{r^2}{s}\right)\left[2\frac{r}{s}\cdot\frac{dr}{dx}+\frac{ds}{dx}\left(1-\frac{r^2}{s^2}\right)\right]\right\}}{\left[\left(s+\frac{r^2}{s}\right)^2 - 4r^2\cos^2\theta\right]^{1/2}} + \frac{32a\beta r\cos\theta\sin^2\theta}{\left[\left(s+\frac{r^2}{s}\right)^2 - 4r^2\cos^2\theta\right]^{1/2}} \tag{11.3.19}$$

or

$$\bar{\Delta p}_{f(w)} = \frac{4a\left[\left(1-\frac{r^4}{s^4}\right)\frac{ds}{dx}+2\frac{r}{s}\cdot\frac{dr}{dx}\left(1+\frac{r^2}{s^2}-2\frac{z^2}{r^2}\right)\right]}{\left[\left(1+\frac{r^2}{s^2}\right)^2-4\frac{z^2}{s^2}\right]^{1/2}} + \frac{32a\beta(r/s)\cos\theta\sin^2\theta}{\left[\left(1+\frac{r^2}{s^2}\right)^2-4\frac{z^2}{s^2}\right]^{1/2}}. \tag{11.3.19'}$$

The second term with the multiplier $a\beta$ characterizing the interaction of wing and fuselage based on the angle of yaw is zero in the absence of some banking angle, i.e. in the absence of banking we arrive at the relation (11.2.33) for a plain combination of fuselage and wing without yaw.

The first term in (11.3.19') consists of the derivatives ds/dx and dr/dx, which indicate the relation of interference with variation in the semi-span of the wing and the diameter of the fuselage in the absence of banking. At the same time these derivatives are absent in the second term and hence do not affect the wing-fuselage interaction in the presence of yawing motion.

3.3 Pressure over wing

The expression for the pressure coefficient over the lower surface of a wing-panel including interference effects could be written from formula (11.3.8) and relations (11.3.5):

$$\begin{aligned}\bar{p}_{w(f)l} = &-(2/V_\infty)\,[u_{tl}+u_{\alpha l}+u_{\beta l}+a(v_{tl}+v_{\alpha l}+v_{\beta l})\\ &-\beta(w_{tl}+w_{\alpha l}+w_{\beta l})] - (1/V_\infty^2)\,[(v_{tl}+v_{\alpha l}+v_{\beta l})^2\\ &+(w_{tl}+w_{\alpha l}+w_{\beta l})^2].\end{aligned} \tag{11.3.20}$$

The pressure coefficient for an upper surface can be given by formula (11.3.20) with replacement of index "l" by "u", indicating the relations between the velocity components on the upper and lower surfaces emerging from consideration of symmetry. These relations for the conditions of the upper and lower surfaces take the following form:

$$\left.\begin{array}{lll} u_{tl}=u_{tu}, & w_{tl}=w_{tu}, & v_{tl}=-v_{tu};\\ u_{\alpha l}=-u_{\alpha u}, & w_{\alpha l}=-w_{\alpha u}, & v_{\alpha l}=v_{\alpha u};\\ u_{\beta l}=u_{\beta u}, & w_{\beta l}=w_{\beta u}, & v_{\beta l}=-v_{\beta u}. \end{array}\right\} \tag{11.3.21}$$

Writing (11.3.20) for the conditions over the upper surface and replacing terms with the index "u" by the corresponding values given in (11.3.21), we have

$$\bar{p}_{w(f)u} = -(2/V_\infty)\,[u_{tl} - u_{\alpha l} + u_{\beta l} + \alpha(-v_{tl} + v_{\alpha 1} - v_{\beta l}) - \beta(w_{tl} - w_{\alpha l} + w_{\beta l})] - (1/V_\infty^2)\,[(-v_{tl} + v_{\alpha l} - v_{\beta l})^2 + (w_{tl} - w_{\alpha l} + w_{\beta l})^2]. \tag{11.3.22}$$

Then the coefficient of pressure difference will be

$$\Delta\bar{p}_{w(f)} = \bar{p}_{w(f)l} - \bar{p}_{w(f)u} = -(4/V_\infty)u_{\alpha l} - (4/V_\infty) \times [(v_{tl} + v_{\beta l})\alpha - w_{\alpha l}\beta] - (4/V_\infty^2)\,(v_{tl}v_{\alpha l} + v_{\alpha l}v_{\beta l} + w_{tl}w_{\alpha l} + w_{\alpha l}w_{\beta l}).$$

As $v_t = 0$ from (11.2.44) and $v_\beta = 0$ from the condition of unseparated cross flow over the wing, the coefficient of pressure difference will be

$$\Delta\bar{p}_{w(f)} = -(4/V_\infty)u_{\alpha l} + (4/V_\infty)w_{\alpha l}\beta - (4/V_\infty^2)\,(w_{tl}w_{\alpha l} + w_{\alpha l}w_{\beta l}). \tag{11.3.23}$$

The velocity components $u_{\alpha l}$, $w_{\alpha l}$, w_{tl} were determined by the expressions (11.2.34), (11.2.35) and (11.2.43). Inserting $\sigma = z$ in equation (11.3.16), the component $w_{\beta l}$ can be found:

$$w_{\beta l} = \beta V_\infty\,(r^2/z^2)\,. \tag{11.3.24}$$

After corresponding substitutions in (11.3.23) we get

$$\Delta\bar{p}_{w(f)} = -4\alpha\,\frac{2\frac{r}{z}\cdot\frac{dr}{dx}\left(z+\frac{r^2}{z}\right) - \left(s+\frac{r^2}{s}\right)\left[\frac{ds}{dx}\left(1-\frac{r^2}{s^2}\right) + 2\frac{r}{s}\cdot\frac{dr}{dx}\right]}{\left[\left(s+\frac{r^2}{s}\right)^2 - \left(z+\frac{r^2}{z}\right)^2\right]^{1/2}} - 4\alpha\,\frac{\left(z+\frac{r^2}{z}\right)\left(1-\frac{r^2}{z^2}\right)}{\left[\left(s+\frac{r^2}{s}\right)^2 - \left(z+\frac{r^2}{z}\right)^2\right]^{1/2}}\left[\frac{r}{z}\cdot\frac{dr}{dx} + \beta\left(\frac{r^2}{z^2}-1\right)\right],$$

or after simplifications it will be given by

$$\Delta\bar{p}_{w(f)} = \frac{4\alpha\left\{\frac{r}{s}\cdot\frac{dr}{dx}\left[\left(1-\frac{r^2}{z^2}\right)^2 + 2\left(\frac{r^2}{s^2}-1\right)\right] + \frac{ds}{dx}\left(1-\frac{r^4}{s^4}\right)\right\}}{\left[\left(1+\frac{r^2}{s^2}\right)^2 - \frac{z^2}{s^2}\left(1+\frac{r^2}{z^2}\right)^2\right]^{1/2}} + \frac{4\alpha\beta\,\frac{z}{s}\left(1+\frac{r^2}{z^2}\right)\left(1-\frac{r^2}{z^2}\right)^2}{\left[\left(1+\frac{r^2}{s^2}\right)^2 - \frac{z^2}{s^2}\left(1+\frac{r^2}{z^2}\right)^2\right]^{1/2}}. \tag{11.3.25}$$

In expression (11.3.25) the term with the multiplier $\alpha\beta$ characterizes

interaction of wing and fuselage as a function of banking. This term is asymmetrical for the left and right wing-panels because the angle β will be negative for the left wing and positive for the right wing.

3.4 Lift force and center of pressure

The interaction between wing and fuselage at an angle of yaw results in an increase in the lift force on the right wing with the increase in angle of bank φ and a decrease in the lift force on the left wing by the same amount. Therefore the lift force resulting from this combination does not change: it remains the same in magnitude as in the absence of yaw.

According to (11.2.74) the lift force along axis y_1 (see Fig. 11.3.1) is equal to

$$Y_{\mathrm{lf,w}}=2a_{\mathrm{c}}\cos\varphi\pi\bar{s}_m^2\left(1-\frac{1}{\bar{s}_m^2}+\frac{1}{\bar{s}_m^4}\right)q_\infty. \tag{11.3.26}$$

The side force along the z_1 axis is created only by the fuselage as a result of side slip with velocity $-\beta V_\infty$ and does not depend on the wing of zero thickness, which has no effect on this flow-interaction. According to (11.2.72) the side force

$$Z_{\mathrm{lf,w}}=Z_{\mathrm{lf}}=-2\beta\pi r^2q_\infty=-2a_{\mathrm{c}}\,\pi r^2\sin\varphi\,q_\infty. \tag{11.3.27}$$

The lift force along the y' axis (see Fig. 11.3.1; the system of fixed axes $x'Oy'$ is turned through angle of attack a_{c} about the Oz axis: angle φ for this system is equal to zero) will be

$$Y=Y_{\mathrm{lf,w}}\cos\varphi-Z_{\mathrm{lf}}\sin\varphi=2a_{\mathrm{c}}\pi\bar{s}_m^2\left[\left(1-\frac{1}{\bar{s}^2}\right)^2\cos^2\varphi+\frac{1}{\bar{s}_m^2}\right]q_\infty. \tag{11.3.28}$$

The side force along z' axis will be

$$Z=Y_{\mathrm{lf,w}}\sin\varphi+Z_{\mathrm{lf}}\cos\varphi=2a_{\mathrm{c}}\,\pi\bar{s}_m^2\sin\varphi\cos\varphi[1-(1/\bar{s}_m^2)]q_\infty. \tag{11.3.29}$$

Let us consider the lift force and center of pressure of a wing-panel lifting in the process of banking. For the right side triangular wing-panel the value of this lift force, determined by the second term in (11.3.25) in the form $[\Delta\bar{p}_{\mathrm{w(f)}}]_\varphi$, is equal to

$$\Delta Y_{\mathrm{w(f)}}=q_\infty\int\limits_{(S_{\mathrm{w}})}\int[\Delta\bar{p}_{\mathrm{w(f)}}]_\varphi\,dS_{\mathrm{w}}. \tag{11.3.30}$$

From Fig. 11.2.3 it can be seen that the elementary area of wing-panel

$$dS_{\mathrm{w}}=dzdx=dzds/\tan\varepsilon.$$

Taking into account this value and the quantity in (11.3.25) for the second term, we write

$$\Delta Y_{w(f)}=\frac{q_\infty}{\tan\varepsilon}\int_r^{s_m} dz \int_z^{s_m} [\Delta\bar{p}_{w(f)}]_\varphi\, ds$$

$$=\frac{4a\beta q_\infty}{\tan\varepsilon}\int_r^{s_m} z\left(1+\frac{r^2}{z^2}\right)\left(1-\frac{r^2}{z^2}\right)^2 dz \int_z^{s_m} \frac{ds}{s\left[\left(1+\frac{r^2}{s^2}\right)^2-\frac{z^2}{s^2}\left(1+\frac{r^2}{z^2}\right)^2\right]^{1/2}}.$$

Carrying out calculation of the second integral, we get

$$\Delta Y_{w(f)}=\frac{2a\beta q_\infty}{\tan\varepsilon}\int_r^{s_m} z\left(1+\frac{r^2}{z^2}\right)\left(1-\frac{r^2}{z^2}\right)^2 \cos^{-1}\frac{2s_m^2-\left(z^2+\frac{r^4}{z^2}\right)}{z^2-\frac{r^4}{z^2}}\,dz. \quad (11.3.30')$$

Further integration is carried out numerically. Let us introduce the coefficient of interference calculated in the form

$$K_\varphi=\Delta Y_{w(f)}\tan\varepsilon/Y_w\beta, \quad (11.3.31)$$

where Y_w is the lift force of one triangular isolated wing-panel; according to (11.2.73)

$$Y_w=a\pi\,(s_m-r)^2 q_\infty. \quad (11.3.32)$$

Taking into account the expressions (11.3.30') and (11.3.32), the coefficient

$$K_\varphi=\frac{2}{\pi(s_m-r)^2}\int_r^{s_m} z\left(1+\frac{r^2}{z^2}\right)\left(1-\frac{r^2}{z^2}\right)^2 \cosh^{-1}\frac{2s_m^2-\left(z^2+\frac{r^4}{z^2}\right)}{z^2-\frac{r^4}{z^2}}\,dz. \quad (11.3.33)$$

The values of K_φ obtained by numerical integration are reproduced in Table 11.3.2 and in Fig. 11.3.2 as a function of the ratio r/s_m. The force characterized by the coefficient K_φ depends, as is evident from (11.3.23), on the resultant integration of velocities w_α and w_β, induced by the presence of an angle of attack and an angle of yaw.

The longitudinal coordinate of the center of pressure of the wing-panel, measured from the leading edge of the root chord (see Fig. 11.2.25), is determined from the condition

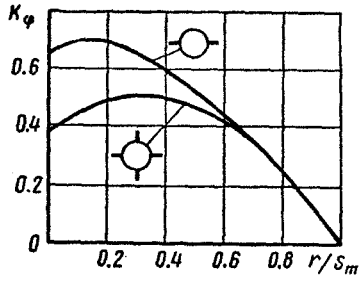

Fig. 11.3.2. Coefficients of interference for plain and cruciform combinations with bank.

$$(x_{c\cdot p})_{\varphi w(f)} = \Delta M_{zw(f)}/\Delta Y_{w(f)}, \tag{11.3.34}$$

where additional pitching moment depending on the banking angle is

$$\Delta M_{zw(f)} = \frac{q_\infty}{\tan^2 \varepsilon} \int_r^{s_m} dz \int_z^{s_m} [\Delta \bar{p}_{w(f)}]_\varphi \, sds. \tag{11.3.35}$$

TABLE 11.3.2

$\frac{r}{s_m}$	Plain combination			Cruciform combination		
	$K\varphi$	$(c_{c\cdot p})_{\varphi w(t)}$	$(\bar{z}_{c\cdot p})_{\varphi w(t)}$	K_φ	$(c_{c\cdot p})_{\varphi w(t)}$	$(\bar{z}_{c\cdot p})_{\varphi w(t)}$
0	0.637 $(2/\pi)$	0.667 (2/3)	0.524 $(\pi/6)$	0.382	0.667 (2/3)	0.556
0.1	0.687	0.667	0.518	0.447	0.654	0.532
0.2	0.681	0.667	0.531	0.490	0.660	0.530
0.3	0.649	0.688	0.546	0.508	0.673	0.540
0.4	0.597	0.699	0.560	0.502	0.687	0.554
0.5	0.529	0.709	0.575	0.471	0.700	0.569
0.6	0.447	0.719	0.588	0.417	0.714	0.585
0.7	0.352	0.729	0.601	0.342	0.725	0.598
0.8	0.246	0.736	0.614	0.244	0.734	0.612
0.9	0.128	0.744	0.616	0.127	0.743	0.625
1.0	0	0.750 (3/4)	0.637 $(2/\pi)$	0	0.750 (3/4)	0.637 $(2/\pi)$

The distance from the axis of symmetry of the fuselage to the center of pressure in a lateral direction is calculated from the expression

$$(z_{c\cdot p})_{\varphi w(f)} = \Delta M_{xw(f)}/\Delta Y_{w(f)}, \tag{11.3.36}$$

where the additional value of the rolling moment during yawing is

$$\Delta M_{xw(f)} = \frac{q_\infty}{\tan \varepsilon} \int_r^{s_m} z dz \int_z^{s_m} [\Delta \bar{p}_{w(f)}]_\varphi \, ds. \tag{11.3.37}$$

The coefficients of the center of pressure are worked out for the values of both coordinates of the center of pressure found by numerical integration:

$$\left.\begin{aligned} (c_{c\cdot p})_{\varphi w(f)} &= [(x_{c\cdot p})_{\varphi w(f)}]/b_r; \\ (\bar{z}_{c\cdot p})_{\varphi w(f)} &= [(z_{c\cdot p})_{\varphi w(f)} - r]/(s_m - r). \end{aligned}\right\} \tag{11.3.38}$$

These coefficients are shown in Table 11.3.2. They may be used to determine the rolling moment and bending moment at the wing root section as a function of the banking angle. Here the loads acting on the fuselage while banking are not considered. These loads, having an asymmetrical nature like the wing, have hardly any effect on lift force and moment and hence on the position of the center of pressure of this combination.

3.5 General relations of forces and moments for plain combination with banking

Let us consider the coefficients of forces and moments acting on the right side wing-panel while rolling (Fig. 11.3.3).

The coefficient of lift among the y_1 axis will be

$$(c_{y_1})_s = K_w\left(\frac{1}{2}\cdot\frac{dc_y}{d\alpha}\right)_w \alpha + \frac{K_\varphi}{\tan\varepsilon}\left(\frac{1}{2}\cdot\frac{dc_y}{d\alpha}\right)_w \alpha\beta, \qquad (11.3.39)$$

where $\alpha = \alpha_c \cos\varphi$, $\beta = \alpha_c \sin\varphi$.

The coefficient of longitudinal moment about the axis passing through the apex of the wing-panel (point D in Fig. 11.2.5), will be

$$m_{1\cdot s} = -K_w\left(\frac{1}{2}\cdot\frac{dc_y}{d\alpha}\right)_w \frac{(x_{c\cdot p})_{\alpha w(f)}}{x_K}\alpha - \frac{K_\varphi}{\tan\varepsilon}\left(\frac{1}{2}\cdot\frac{dc_y}{d\alpha}\right)_w \frac{(x_{c\cdot p})_{\varphi w(f)}}{x_K}\alpha\beta, \qquad (11.3.40)$$

where x_K is the characteristic length (length of fuselage, length of whole combination, etc.).

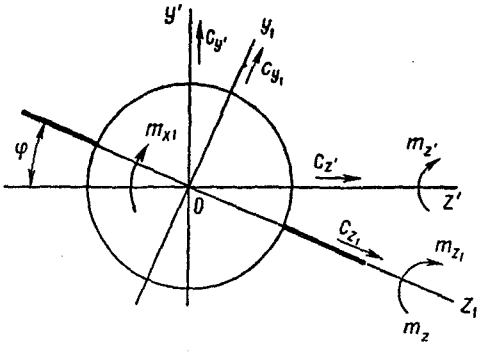

Fig. 11.3.3. Coefficients of forces and moments acting on plain combination during banking.

The coefficient of rolling moment due to the wing-panel will be

$$(m_{x_1})_s = -K_w\left(\frac{1}{2}\cdot\frac{dc_y}{d\alpha}\right)_w \frac{(z_{c\cdot p})_{\alpha w(f)}}{x_K}\alpha - \frac{K_\varphi}{\tan\varepsilon}\left(\frac{1}{2}\cdot\frac{dc_y}{d\alpha}\right)_w \frac{(z_{c\cdot p})_{\varphi w(f)}}{x_K}\alpha\beta. \qquad (11.3.41)$$

Let us find the relations for the aerodynamic coefficients of forces and moments induced by the wing on the fuselage.

The coefficient of lift force acting along the y' axis (see Fig. 11.3.3) is

$$(c_{y'})_{f(w)} = K_f(dc_y/d\alpha)_w\, \alpha \cos\varphi. \qquad (11.3.42)$$

The coefficient of side force along the z' axis is

$$(c_{z'})_{f(w)} = K_f(dc_y/d\alpha)_w\, \beta \cos\varphi. \qquad (11.3.43)$$

The coefficient of pitching moment due to forces induced by the wing on the body about the axis passing through the apex of the wing (point D in Fig. 11.2.5) will be

$$(m_{z'})_{f(w)} = -K_f\left(\frac{dc_y}{d\alpha}\right)_w \frac{(x_{c\cdot p})_{\alpha f(w)}}{x_K}\alpha\cos\varphi. \qquad (11.3.44)$$

The coefficient of rolling moment due to forces induced by the wing on the fuselage $(m_{x'})_{f(w)}$ is taken to be equal to zero.

We will now write the formulas for the resultant coefficients of forces and moments of the combination as a whole.

The coefficient of lift is

$$(c_{y'})_{f,w}=(c_{y'})_f+(dc_y/d\alpha)_w(K_f+K_w)\,\alpha\cos\varphi. \tag{11.3.45}$$

The coefficient of side force is

$$(c_{z'})_{f,w}=(c_{z'})_f+(K_f+K_w)\,(dc_y/d\alpha)_w\,\beta\cos\varphi. \tag{11.3.46}$$

The coefficient of pitching moment of the combination as a whole about the axis passing through the apex of the wing-panel will be

$$(m_{z'})_{f,w}=(m_{z'})_f-[K_f(x_{c\cdot p})_{\alpha f(w)}+K_w(x_{c\cdot p})_{\alpha w(f)}]\times\frac{\alpha\cos\varphi}{x_K}\left(\frac{dc_y}{d\alpha}\right)_w. \tag{11.3.47}$$

The coefficient of rolling moment will be

$$(m_{x'})_{f,w}=-K_w\left(\frac{dc_y}{d\alpha}\right)_w\frac{(z_{c\cdot p})_{\alpha w(f)}}{x_K}\,\alpha. \tag{11.3.48}$$

In using formulas (11.3.39) through (11.3.48) it should be borne in mind that all the aerodynamic coefficients are worked out either on the basis of the area of one wing-panel $[(c_{y_1})_s, m_{1,s}, (m_{x_1})_s]$ or on the basis of the total wing plan area S_w of two panels joined together (aerodynamic coefficients for the fuselage and the combination taken as a whole). Besides, any arbitrary linear dimension may be taken as a characteristic length in calculating moments. The coefficients of forces $(c_{y'})_f$, $(c_{z'})_f$ and of moment $(m_{z'})_f$ induced by the nose section of the main body are calculated by linearized theory for an isolated fuselage.

4. Cruciform Combination

4.1 Pressure and lift force

Let us study the aerodynamic coefficients of a cruciform combination in the form of a circular cylinder and plane wing-panels of zero thickness in a low perturbation (linearized) supersonic flow (Fig. 11.4.1). We assume that vertical wing-panels have the same plan and semi-span as horizontal wing-panels. We assume that the presence of vertical wing-panels has no effect on the flow pattern of this combination in the symmetrical plane x_1Oy_1 when placed at an angle of attack $\alpha=\alpha_c\cos\varphi$. In the same way, the presence of horizontal wing-panels has no effect on the aerodynamic flow-interaction during a change in banking angle $\beta=\alpha_c\sin\varphi$.

In this way the problem we are considering involves the solution of two concurrent problems, one of which concerns determination of the velocity field of plain combination of fuselage and vertical wing at an angle of attack

a and the other the determination of the velocity field of a plain combination of fuselage and horizontal wing at an angle β. By superposing these fields we get the resultant flow about a cruciform combination placed at a pitching angle α_c and banking angle φ.

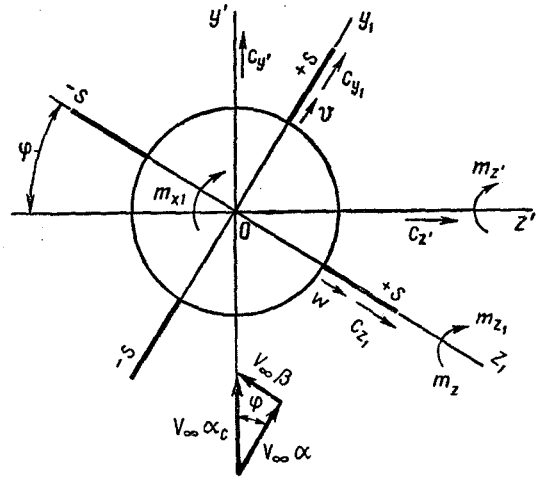

Fig. 11.4.1. Cruciform combination.

According to this procedure the resultant perturbation velocities are determined by formulas (11.3.5) and the pressure coefficient is determined by relation (11.3.7'). The coefficient of pressure difference on the fuselage is found from the expression (11.3.13) in which the components $u_{\alpha l}$, $w_{\alpha l}$, $v_{\alpha l}$ are determined from formulas (11.2.22), (11.2.24) and (11.2.25) respectively, which are obtained for a plain combination under the condition of $\alpha = \alpha_c \cos\varphi$.

The expression for the complex potential of a plain combination in a lateral flow with velocity βV_∞ can be used to determine the components w_β and v_β. This expression will be obtained in the following way: By analogy with (11.2.18) the formula for the complex potential of a circular cylinder of radius r_0 in plane $\zeta = \xi + i\eta$ will be:

$$W = -\beta V_\infty [\zeta - (r_0^2/\zeta)]. \tag{11.4.1}$$

Next, by analogy with (11.2.16) we write the equation

$$\sigma - (r^2/\sigma) = \zeta - (r_0^2/\zeta), \tag{11.4.2}$$

where $$r_0 = 0.5\,[s + (r^2/s)].$$

It can be shown that this equation give conformal transformation of a circle of radius r_0 to a contour consisting of a circle of radius r and a pair of vertical wing panels with span $\pm s$. As a result the combination of wing-body in plane yOz can be obtained.

Solving the quadratic equation (11.4.2) for ζ, we get

$$\zeta=\frac{1}{2}\left[\left(\sigma-\frac{r^2}{\sigma}\right)+\sqrt{\left(\sigma-\frac{r^2}{\sigma}\right)^2+4r_0^2}\right]. \tag{11.4.3}$$

Substitution of this quantity in (11.4.1) gives complex potential

$$W=-\beta V_\infty\left[\left(\sigma-\frac{r^2}{\sigma}\right)^2+4r_0^2\right]^{1/2}. \tag{11.4.4}$$

To find the resultant complex potential it is necessary to add the potential function of flow parallel to the z axis and equal to $\beta V_\infty \sigma$ to (11.4.4). Then the resultant complex potential will be

$$W_\beta=-\beta V_\infty\left\{\left[\left(\sigma-\frac{r^2}{\sigma}\right)^2+4r_0^2\right]^{1/2}-\sigma\right\}. \tag{11.4.5}$$

Differentiating this expression with respect to σ, we get

$$\frac{dW_\beta}{d\sigma}=w_\beta-v_\beta i=-\beta V_\infty\left\{\frac{\left(\sigma-\frac{r^2}{\sigma}\right)\left(1+\frac{r^2}{\sigma^2}\right)}{\left[\left(\sigma-\frac{r^2}{\sigma}\right)^2+4r_0^2\right]^{1/2}}-1\right\}. \tag{11.4.6}$$

For boundary condition on the fuselage we have $\sigma=re^{i\theta}$ and therefore

$$w_\beta-v_\beta i=-\beta V_\infty\left[\frac{2r\sin\theta\,(1+\cos 2\theta-i\sin 2\theta)i}{(4r_0^2-4r^2\sin^2\theta)^{1/2}}-1\right]. \tag{11.4.7}$$

From this we get

$$w_\beta=-\beta V_\infty\left\{\frac{2r\sin\theta\sin 2\theta}{\left[\left(s+\frac{r^2}{s}\right)^2-4r^2\sin^2\theta\right]^{1/2}}-1\right\}; \tag{11.4.8}$$

$$v_\beta=\frac{2\beta r V_\infty\sin\theta\,(1+\cos 2\theta)}{\left[\left(s+\frac{r^2}{s}\right)^2-4r^2\sin^2\theta\right]^{1/2}}. \tag{11.4.9}$$

Substituting the expressions (11.4.8), (11.4.9) and the relations (11.2.22), (11.2.24), (11.2.25) to the formula (11.3.13) for the coefficient of pressure difference on a cone, we get

$$\bar{\Delta p}_{f(w)}=-4\alpha\,\frac{4r\frac{dr}{dx}\cos^2\theta-\left(s+\frac{r^2}{s}\right)\left[2\frac{r}{s}\cdot\frac{dr}{dx}+\frac{ds}{dx}\left(1-\frac{r^2}{s^2}\right)\right]}{\left[\left(s+\frac{r^2}{s}\right)^2-4r^2\cos^2\theta\right]^{1/2}}$$
$$+\frac{16\alpha\beta r^2\sin^2 2\theta}{\left[\left(s+\frac{r^2}{s}\right)^2-4r^2\cos^2\theta\right]^{1/2}\left[\left(s+\frac{r^2}{s}\right)^2-4r^2\sin^2\theta\right]^{1/2}}. \tag{11.4.10}$$

Keeping in mind that $r\cos\theta = z$, we find that

$$\Delta\bar{p}_{f(w)} = -4a\frac{4\frac{z^2}{r^2}\frac{dr}{dx}\frac{r}{s} - \left(1+\frac{r^2}{s^2}\right)\left[2\frac{r}{s}\frac{dr}{dx} + \frac{ds}{dx}\left(1-\frac{r^2}{s^2}\right)\right]}{\left[\left(1+\frac{r^2}{s^2}\right)^2 - 4\left(\frac{z^2}{s^2}\right)\right]^{1/2}} + \frac{64a\beta\frac{z^2}{s^2}\left(1-\frac{z^2}{r^2}\right)}{\left[\left(1+\frac{r^2}{s^2}\right)^2 - 4\frac{z^2}{s^2}\right]^{1/2}\left[\left(1-\frac{r^2}{s^2}\right)^2 + 4\frac{z^2}{s^2}\right]^{1/2}}. \quad (11.4.10')$$

The first term on the right side of this equation consists of terms proportional to derivatives dr/dx and ds/dx characterizing the effect of a change in the radius of the fuselage and in the semi-span of the wing-panels respectively. However, neither of these derivatives has any effect on the second term, which is based on banking and pitching motions. This term of interaction, being proportional to the product $a\beta$, determines the increase in the coefficient of pressure difference on the right half of the fuselage. The value of this coefficient decreases by the same amount on the left half of the fuselage. This follows from formula (11.3.13) in which the component $v_{\beta l}$ should be taken with the opposite sign for the left half of the fuselage. This leads to the negative sign before the second term in (11.4.10').

To determine the coefficient of pressure difference on the right horizontal wing-panel we use formula (11.3.23) in which the velocity components $u_{\alpha l}$, $w_{\alpha l}$ and w_{tl} are found from the expressions (11.2.34), (11.2.35) and (11.2.43) respectively. The component $w_{\beta l}$ can be found from the relation (11.4.6) by taking $\sigma = z$:

$$w_\beta = -\beta V_\infty\left\{\frac{z\left(1-\frac{r^4}{z^4}\right)}{\left[\left(z-\frac{r^2}{z}\right)^2 + \left(s+\frac{r^2}{s}\right)^2\right]^{1/2}} - 1\right\}. \quad (11.4.11)$$

As a result of corresponding substitutions we get

$$\Delta\bar{p}_{w(f)} = -4a\frac{2\frac{r}{z}\frac{dr}{dx}\left(z+\frac{r^2}{z}\right) - \left(s+\frac{r^2}{s}\right)\left[\frac{ds}{dx}\left(1-\frac{r^2}{s^2}\right) + 2\frac{r}{s}\frac{dr}{dx}\right]}{\left[\left(s+\frac{r^2}{s}\right)^2 - \left(z+\frac{r^2}{z^2}\right)^2\right]^{1/2}} \rightarrow$$

$$\rightarrow + \frac{\frac{r}{z}\frac{dr}{dx}\left(z+\frac{r^2}{z}\right)\left(1-\frac{r^2}{z^2}\right)}{\left[\left(s+\frac{r^2}{s}\right)^2 - \left(z+\frac{r^2}{z^2}\right)^2\right]^{1/2}}$$

$$+ \frac{4a\beta z\left(z+\frac{r^2}{z}\right)\left(1-\frac{r^2}{z^2}\right)\left(1-\frac{r^4}{z^4}\right)}{\left[\left(s+\frac{r^2}{s}\right)^2 - \left(z+\frac{r^2}{z}\right)^2\right]^{1/2}\left[\left(z-\frac{r^2}{z}\right)^2 + \left(s+\frac{r^2}{s}\right)^2\right]^{1/2}},$$

which after simplification will be

$$\Delta\bar{p}_{w(f)}=4a\frac{\frac{r}{s}\frac{dr}{dx}\left[\left(1-\frac{r^2}{z^2}\right)^2+2\left(\frac{r^2}{s^2}-1\right)\right]+\frac{ds}{dx}\left(1-\frac{r^4}{s^4}\right)}{\left[1+\frac{r^4}{s^4}-\frac{z^2}{s^2}\left(1+\frac{r^4}{z^4}\right)\right]^{1/2}}$$
$$+\frac{4\frac{z^2}{s^2}a\beta\left(1-\frac{r^4}{z^4}\right)^2}{\left[\left(1+\frac{r^4}{s^4}\right)^2-\frac{z^4}{s^4}\left(1+\frac{r^4}{z^4}\right)^2\right]^{1/2}}. \qquad (11.4.12)$$

According to this formula the pressure differences between the lower and upper surfaces of the right side wing-panel increases during its motion downward (angles φ and β positive) while on the left side wing-panel it decreases (angle β negative), i.e. when the second term in (11.4.12) characterizing mutual interaction is asymmetrical.

The coefficient of pressure difference for the upper and lower wing panels can be determined from the conditions of symmetry using relation (11.4.12), in which z should be replaced by y and a and β should be interchanged. Then for the lower wing-panel

$$\Delta\bar{p}_{w(f)}=4\beta\frac{\frac{r}{s}\frac{dr}{dx}\left[\left(1-\frac{r^2}{y^2}\right)^2+2\left(\frac{r^2}{s^2}-1\right)\right]+\frac{ds}{dx}\left(1-\frac{r^4}{s^4}\right)}{\left[1+\frac{r^4}{s^4}-\frac{y^2}{s^2}\left(1+\frac{r^4}{s^4}\right)\right]^{1/2}}$$
$$+\frac{4\frac{y^2}{s^2}a\beta\left(1-\frac{r^4}{y^4}\right)^2}{\left[\left(1+\frac{r^4}{s^4}\right)^2-\frac{y^4}{s^4}\left(1+\frac{r^4}{y^4}\right)^2\right]^{1/2}}. \qquad (11.4.13)$$

The angles a and β are assumed to be positive. The pressure on the upper wing-panel will be determined by the same formula (11.4.13) with the same difference that the angle β is taken as positive and a as negative. The second term with $a\beta$ (term of mutual interaction) is asymmetrical for lower and upper wing-panels. The presence of an asymmetrical term in (11.4.12) and (11.4.13) leads to a situation where despite the lift force on the panels additional lift force is not created due to the asymmetrical nature of the loads.

Keeping in mind that the resultant forces on the wing-panels are independent of the terms of interaction, the resultant lift force acting on the fuselage-cruciform wing in banking can be obtained by summing the forces acting on two plane versions of the fuselage-wing combination placed in a flow at the corresponding angles $a=a_c\cos\varphi$ and $\beta=a_c\sin\varphi$.

By analogy with (11.3.26) the lift force along the y_1 axis acting on the combination of fuselage-horizontal wings will be

$$Y_{1f,w} = 2a\pi s_m^2[1-(1/\bar{s}_m^2)+(1/\bar{s}_m^4)]q_\infty. \tag{11.4.14}$$

The lift (side force acting on the combination of fuselage and verticle stabilizer along the negative direction of the z_1 axis) will be

$$Z_{1f,w} = -2\beta\pi s_m^2[1-(1/\bar{s}_m^2)+(1/\bar{s}_m^4)]q_\infty. \tag{11.4.15}$$

The lift force along the y' axis (see Fig. 11.3.1) will be

$$\begin{aligned} Y = Y_{1f,w}\cos\varphi - Z_{1f,w}\sin\varphi = 2a_c\pi s_m^2 q_\infty[1-(1/\bar{s}_m^2)+(1/\bar{s}_m^4)] \\ \times\cos^2\varphi + 2a_c\pi s_m^2\, q_\infty[1-(1/\bar{s}_m^2)+(1/\bar{s}_m^4)]\sin^2\varphi = 2a_c\pi s_m^2 \\ \times[1-(1/\bar{s}_m^2)+(1/\bar{s}_m^4)]q_\infty. \end{aligned} \tag{11.4.16}$$

Lift (side force) along the z' axis is equal to zero. In reality

$$\begin{aligned} Z = Y_{1f,w}\sin\varphi + Z_{1f,w}\cos\varphi = \Bigg[2a_c\pi s_m^2\, q_\infty\left(1-\frac{1}{\bar{s}_m^2}+\frac{1}{\bar{s}_m^4}\right) \\ -2a_c\pi s_m^2 q_\infty\left(1-\frac{1}{\bar{s}_m^2}+\frac{1}{\bar{s}_m^4}\right)\Bigg]\sin\varphi\cos\varphi = 0. \end{aligned} \tag{11.4.17}$$

The results so obtained give one important property of the cruciform combination during turning of the flight vehicle, i.e. in banking the lift force in a vertical plane parallel to the undisturbed flow and passing through the longitudinal axis of the flight vehicle remains unchanged.

4.2 Coefficients of interference and center of pressure

Let us find the lift force and center of pressure of the wing-panels in banking. According to the expression (11.3.30) in which $[\Delta\bar{p}_{w(f)}]_\varphi$ is determined by the second term on the right side of (11.4.12), we have

$$\begin{aligned} \Delta Y_{w(f)} = \frac{q_\infty}{\tan\varepsilon}\int_r^{s_m} dz \int_z^{s_m}[\Delta\bar{p}_{w(f)}]_\varphi\, ds = \frac{4a_c^2\sin\varphi\cos\varphi\, q_\infty}{\tan\varepsilon} \\ \times\int_r^{s_m} z^2\left(1-\frac{r^4}{z^4}\right)^2 dz \int_z^{s_m}\frac{ds}{s^2\left[\left(1+\frac{r^4}{s^4}\right)^2-\frac{z^4}{s^4}\left(1+\frac{r^4}{z^4}\right)^2\right]^{1/2}}. \end{aligned}$$

Let us introduce the notations

$$\bar{s} = s^2/r^2,\ \bar{z} = z^2/r^2. \tag{11.4.18}$$

Then the above expression will be given by

$$\Delta Y_{w(f)}=\frac{a_c^2 r^2 q_\infty \sin\varphi\cos\varphi}{\tan\varepsilon}\int_1^{\bar z_m}\frac{(\bar z^2-1)^2\,d\bar z}{\bar z^{5/2}}\int_{\bar s}^{\bar s_m}\frac{\bar s^{1/2}\,d\bar s}{\sqrt{(\bar s^2-\bar z^2)(\bar z^2\bar s^2-1)}},\tag{11.4.19}$$

where

$$\bar z_m=\bar s_m=s_m^2/r^2.$$

Integrating with respect to $\bar s$ leads (11.4.19) to the expression

$$\int_{\bar s}^{\bar s_m}\frac{\bar s^{1/2}\,d\bar s}{\sqrt{(\bar s^2-\bar z^2)(\bar z^2\bar s^2-1)}}=\frac{1}{\sqrt{2\bar z(\bar z^2-1)}}[F_1(\psi_1,k_1)+F_2(\psi_2,k_2)],\tag{11.4.20}$$

where F_1 and F_2 are elliptical integrals of the second kind:

$$F(\psi,k)=\int_0^{\psi}\frac{d\varphi}{\sqrt{1-k^2\sin^2\varphi}},$$

calculated under the condition that

$$\left.\begin{aligned}\sin\psi_1&=\sqrt{1-\frac{\bar s_m^2(\bar z-1)^2}{(\bar s_m^2-1)^2\bar z}},\quad k_1=\frac{\bar z+1}{\sqrt{2(\bar z^2+1)}};\\ \sin\psi_2&=\sqrt{1-\frac{\bar s_m^2(\bar z+1)^2}{(\bar s_m^2+1)^2\bar z}},\quad k_2=\frac{\bar z-1}{\sqrt{2(\bar z^2+1)}}.\end{aligned}\right\}\tag{11.4.21}$$

From the results so obtained we will get

$$\Delta Y_{w(f)}=\frac{a_c^2 r^2 q_\infty\sin\varphi\cos\varphi}{\sqrt{2}\tan\varepsilon}\int_1^{\bar s_m}\frac{(\bar z^2-1)^{3/2}}{\bar z^3}\times[F_1(\psi_1,k_1)+F_2(\psi_2,k_2)]d\bar z.\tag{11.4.22}$$

It is necessary to perform numerical integration to determine the lift force by this formula. The coefficient of integration can be found from the value of lift force obtained by using relation (11.3.31),

$$K_\varphi=\frac{\Delta Y_{w(f)}\tan\varepsilon}{Y_w\beta}=\frac{1}{\pi\sqrt{2}(\bar s_m-1)^2}\int_1^{\bar s_m}\frac{(\bar z^2-1)^{3/2}}{\bar z^3}\times[F_1(\psi_1,k_1)+F_2(\psi_2,k_2)]d\bar z.\tag{11.4.23}$$

The results of calculation of K_φ are reproduced in Table 11.3.2 and in the graph of Fig. 11.3.2. The difference between the values of K_φ for plain and cruciform combinations of wing-fuselage, characterizing the mutual interference of lifting surfaces, can be found from the table or the graph. The

presence of vertical wing-panels in a cruciform combination reduces the effect of interference in comparison with the plain combination and reduces the coefficient K_φ.

The position of the center of pressure on the wing-panels of a cruciform combination can be determined with the help of formulas (11.3.39) through (11.3.41). The corresponding results are shown in Table 11.3.2. From the comparison of data for the plain and cruciform combinations it may be seen that the centers of pressure in the two cases practically coincide.

Comparison of data with the results obtained for banking (see Table 11.2.1) shows that there is a larger difference in the center of pressure for forces due to banking than for interference forces arising at $\alpha \neq 0$, $\beta = 0$ ($\varphi = 0$).

4.3 General relations for forces and moments

The relations obtained for the coefficients of interference and centers of pressure of a cruciform wing-fuselage combination help us to work out the coefficient of forces and moments acting on the separate elements and on the combination as a whole (Fig. 11.4.1). Here the calculation of coefficients $(c_{y_1})_s$ of the lift force for a right side wing-panel acting along the y_1 axis, the coefficients of lateral moment $m_{1,s}$ and rolling moment $(m_{x_1})_s$ will be carried out with the help of formulas (11.3.39), (11.3.40) and (11.3.41) respectively.

In investigating the effect of banking on interference between the fuselage and the wing it was established that the angle of bank creates additional asymmetrical loading on the right and left halves of the fuselage and consequently does not induce additional lift force. Therefore the flow-interaction of the fuselage can be taken as the result of summation of the flows obtained at angles $\alpha = a_c \cos\varphi$ and $\beta = a_c \sin\varphi$. The forces arising under this condition of flow are also added. The additional force $\Delta Y^{\alpha}_{1f(w)}$ acting on the fuselage in a flow at an angle α happens to be the result of its interaction with the wing:

$$\Delta Y^{\alpha}_{1f(w)} = K_f (dc_y/d\alpha)_w a_c \cos\varphi S_w q_\infty,$$

and that acting in a flow at an angle β will be

$$\Delta Y^{\beta}_{1f(w)} = -K_f (dc_y/d\alpha)_w a_c \sin\varphi S_w q_\infty.$$

The lift force in the direction of the y' axis will be

$$Y'_{f(w)} = \Delta Y^{\alpha}_{1f(w)} \cos\varphi - \Delta Y^{\beta}_{1f(w)} \sin\varphi$$

and the corresponding coefficient

$$(c_{y'})_{f(w)} = Y'_{f(w)}/(q_\infty S_w) = K_f (dc_y/d\alpha)_w a_c. \qquad (11.4.24)$$

The side force along the z' axis will be

$$Z'_{f(w)} = \Delta Y^{\alpha}_{1f(w)} \sin\varphi + \Delta Y^{\beta}_{1f(w)} \cos\varphi = 0;$$

and the coefficient of this force

$$(c_{z'})_{f(w)}=Z'_{f(w)}/(q_\infty S_w)=0. \tag{11.4.25}$$

Let us determine the longitudinal moment (in other words, pitching moment) due to forces induced by the wing acting on the fuselage. The value of this moment taken about the longitudinal axis passing through the apex of the wing-panel is given by

$$(M_{z'})_{f(w)}=-(x_{c.p})_{\alpha f(w)}\,(Y'_{f(w)}+Z'_{f(w)})=-(x_{c.p})_{\alpha f(w)}\,Y'_{f(w)}.$$

The coefficient of pitching moment will then be given as

$$\begin{aligned}(m_{z'})_{f(w)}&=(M_{z'})_{f(w)}/(q_\infty\, S_w\, x_K\\ &=-K_f\,(dc_y/da)_w\,[(x_{c.p})_{\alpha f(w)}/x_K]\,a_c.\end{aligned} \tag{11.4.26}$$

As noted earlier, the asymmetrical loading on the fuselage during banking hardly affects forces and moments. Therefore the coefficient of rolling moment $(m_{x'})_{f(w)}$ will be taken as equal to zero as in the case of the plane combination.

The lift coefficient of the combination as a whole

$$\begin{aligned}(c_{y'})_{f,w}&=(c_{y'})_f+[(c_{y_1})_{s,r}+(c_{y_1})_{s,le}]\cos\varphi\\ &\quad-[(c_{z_1})_{s,u}+(c_{z_1})_{s,l}]\sin\varphi+(c_{y'})_{f(w)}.\end{aligned} \tag{11.4.27}$$

The coefficients of lift c_{y_1} and side force c_{z_1} are calculated with the help of formula (11.3.39) in which for the left (index "le") and upper (index "u") wing-panels the angle β is taken as negative and for the right (index "r") and lower (index "l") wing-panels it is assumed to be positive. Keeping the relation (11.4.24) for $(c_{y'})_{f(w)}$ in mind and assigning a negative value to $c_{z'}$ (force Z' directed in the opposite direction of the z' axis), we get

$$(c_{y'})_{f,w}=(c_{y'})_f+(dc_y/da)_w\,(K_f+K_w)\,a_c. \tag{11.4.28}$$

This relation establishes an important property of the cruciform wing-fuselage combination which indicates that the resultant force is independent of the angle of bank in magnitude and direction and always acts in the plane of angle of attack a_c.

The coefficient of side force of this combination, by analogy with (11.4.27), will be

$$\begin{aligned}(c_{z'})_{f,w}&=(c_{z'})_f+[(c_{y_1})_{s,r}+(c_{y_1})_{s,le}]\sin\varphi\\ &\quad+[(c_{z_1})_{s,u}+(c_{z_1})_{s,l}]\cos\varphi+(c_{y'})_{f(w)}.\end{aligned} \tag{11.4.29}$$

Taking formulas (11.3.39) and (11.4.25) into account, it will be given by

$$(c_{z'})_{f,w}=(c_{z'})_f. \tag{11.4.29'}$$

The lateral force of the whole combination, according to this expression, is created by the nose section of the fuselage.

We may note here that the problems discussed in this chapter are solved within the framework of linearized theory for thin bodies whose aerodynamic characteristics are independent of Mach number $\mathbf{M}_\infty$. Besides, viscosity effects are not taken into account. If "thick" bodies are investigated within the limitations of the above theory or if viscous properties leading to a separation of flow are taken into account then side (lift) force based on the redistribution of normal pressure will come into the picture.

Let us now find the pitching moment of the combination we are considering:

$$M_{z'} = M_{z'f} + \{[(c_{y_1})_{s,r} + (c_{y_1})_{s,le}] \cos \varphi - [(c_{z_1})_{s,u} + (c_{z_1})_{s,l}] \sin \varphi\} (x_{c\cdot p})_{\alpha w(f)} q_\infty S_w + (m_{z'})_{f(w)} q_\infty S_w x_K. \tag{11.4.30}$$

Taking the expressions (11.3.39) and (11.4.26), the coefficient of pitching moment will be

$$(m_{z'})_{f,w} = \frac{(M_{z'})_{f,w}}{q_\infty S_w x_K} = (m_{z'})_f - \frac{(x_{c\cdot p})_{\alpha w(f)} K_w + (x_{c\cdot p})_{\alpha f(w)} K_f}{x_K} \left(\frac{dc_y}{da} \right)_w a_c . \tag{11.4.31}$$

The rolling moment $(M_{x'})_{f,w}$ and the corresponding aerodynamic coefficient of rolling moment $(m_{x'})_{f,w}$ are equal to zero because vertical wing-panels create the same amount of rolling moment as horizontal wing-panels but in the opposite direction.

The forces, moments and corresponding aerodynamic coefficients of the fuselage can be worked out specifically by the linearized aerodynamic theory of a thin isolated body of revolution in a flow.

The coefficients of interference K_w, K_f, which could be used to evaluate the interference effect of a cruciform combination, are independent of the plan of the wing-panels, i.e. the theory can be equally well applied for a delta wing as for a rectangular wing. Unlike these coefficients, the quantity K_φ, strictly speaking, depends on the plan of the wing-panel. However, it can be assumed that this coefficient obtained for a delta wing when we evaluated the term of mutual interaction $a\beta$ can also be applied as a first approximation for other plans, in particular, for a rectangular plan.

The coordinates of centers of pressure $x_{c\cdot p\cdot\alpha}$ and $z_{c\cdot p\cdot\alpha}$ are very close to the corresponding values for an isolated delta wing. This result shows that mutual interference of wing and fuselage does not indicate any appreciable effect on the position of the center of pressure. At the same time the coordinates $z_{c\cdot p\cdot\alpha}$, as shown by research, are independent of the plan of a wing panel. Therefore the values obtained can be used for any wing plan. The values of coordinate $x_{c\cdot p}$ for an isolated wing of the given plan can be used as the coordinate of the center of pressure for a wing-panel of nontriangular form.

The wings or tail can be attached to the fuselage in such a way that some part of the rear end of the fuselage is behind them. In this connection it must be noted that for a thin combination the length of the fuselage behind the wing has no effect on the lift force and the position of the center of pressure of the fuselage. This is explained by the fact that the loading induced by the wing, according to the aerodynamic theory of a thin body, is distributed over the fuselage along the diameter DD (see Fig. 11.2.5) and consequently the area on which lift force is exerted is situated directly under the wing-panels (hatched area in Fig. 11.2.5).

4.4 Calculation of interference of flight vehicles consisting of "thick" bodies and wings

The results of calculation of the coefficients of interference for the combination of a thin body and wing-panels can be taken as the basis for determination of the lift force on flight vehicles consisting of "thick" elements. This method indicates that the aerodynamic coefficient for such configurations is calculated from the coefficients of interference obtained by the theory of a thin body (see Tables 11.2.1 and 11.3.2) and from the aerodynamic coefficient of an isolated wing using linearized theory. For example, the coefficient of lift of a "thick" wing in the presence of a fuselage by this method will be

$$(c_y)_{w(f)} = K_w (c_y)_w, \qquad (11.4.32)$$

where K_w can be found from Table 11.2.1 and $(c_y)_w$ is determined taking into account Mach number M_∞ based on the linearized aerodynamic theory of the wing. Similarly other interferential characteristics can be written.

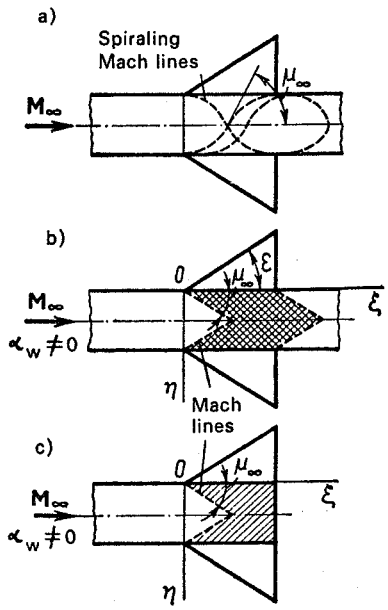

Fig. 11.4.2. Region of effect of wing on fuselage in case of 'thick' configuration in supersonic linearized flow:

a—flow-interaction of 'fuselage-wing' configuration with formation of spiraling Mach lines; *b*—plain model of configuration with tail section and straight Mach lines; *c*—plain model of configuration without tail.

Experimental research confirms the possibility of conducting analysis by this method. It shows that measured and theoretical aerodynamic characteristics for the combination of fuselage and wings tally quite well.

It was noted earlier that the length of the fuselage behind the wing has no appreciable effect on the lift force and center of pressure of the fuselage for a thin wing-fuselage combination. However, for "thick" combinations the presence of the rear section my have a considerable effect on coefficient of interference K_f and on the coordinate of center of pressure of fuselage $(x_{c.p})_{\alpha f(w)}$.

Unlike the thin configuration for which the loading induced by the wing is distributed over the section of fuselage directly below the wing (see Fig. 11.2.5), the disturbances propagating from the wing in the case of a "thick" body envelope the fuselage in spirals intersecting the fuselage generator at a Mach angle $\mu_\infty = \sin^{-1}(1/M_\infty)$ (Fig. 11.4.2, a). A simplified scheme of this phenomenon may be had if the fuselage is assumed to be plain at zero angle of attack. According to this scheme the load induced by the wing is distributed along the fuselage over the region bounded by straight Mach lines emerging from the points of the leading and trailing edges of the wing (Fig. 11.4.2, b). If there is no rear section to the fuselage the lift is determined by integration of loads over the part of the fuselage situated ahead of the trailing edge of the wing (Fig. 11.4.2, c).

The flow about the wing-panel is regarded as the flow about an isolated delta wing of semi-infinite span. According to the formula (8.3.37) the coefficient of differential pressure induced by a wing with a supersonic leading edge over the region between the Mach line from the apex and the root chord (Fig. 11.4.3, shaded region), is equal to

$$\Delta\bar{p} = \bar{p}_l - \bar{p}_u = \frac{4a_w \tan\varepsilon}{\pi\sqrt{a'^2\tan^2\varepsilon - 1}} \cos^{-1}\frac{1+a'^2(\eta/\xi)\tan\varepsilon}{a'[\tan\varepsilon + (\eta/\xi)]}, \quad (11.4.33)$$

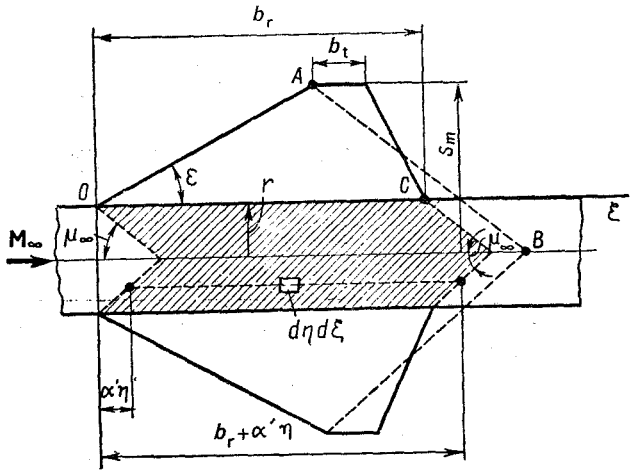

Fig. 11.4.3. Plain model for calculation of lift force with allowance for wing-fuselage interference.

where α_w is the angle of attack of the wing; η, ξ are coordinates shown in Figs. (11.4.2) and (11.4.3).

The coefficient of differential pressure induced by a wing with a subsonic leading edge is set out here without discussion (see [50]):

$$\bar{\Delta p}=\bar{p}_l-\bar{p}_u=\frac{8a_w\,(a'\,\tan\varepsilon)^{3/2}}{\pi a'\,(a'\tan\varepsilon+1)}\sqrt{\frac{1-(a'\eta)/\xi}{a'\,[\tan\varepsilon+(\eta/\xi)]}}\,. \tag{11.4.34}$$

These formulas (11.4.33), (11.4.34) are valid for the condition where the Mach line emerging from point A of the side edge passes behind point C where the trailing edge joins the fuselage, i.e. where the side edge has no effect on the region of interference with lift. These conditions are fulfilled (see Fig. 11.4.3) if

$$\frac{a'(s_m-r)}{b_r}\left(1+\frac{1}{a'\tan\varepsilon}\right)\geqslant 1\,. \tag{11.4.35}$$

For the combination with a tail section the elementary lift force acting on the part of the fuselage under the wing

$$dY=\bar{\Delta p}\,q_\infty d\eta d\xi, \tag{11.4.36}$$

where $d\eta d\xi$ is the elementary area of this section of fuselage (see Fig. 11.4.3).

The coefficient of lift with respect to the area of two isolated wing-panels will be equal to,

for a supersonic swept edge:

$$(c_y)_{f(w)}=\frac{Y}{q_\infty S_w}=\frac{2\iint\limits_{(s)}\bar{\Delta p}\,d\eta d\xi}{(s_m-r)\,(b_r+b_t)}$$

$$=\frac{8a_w\tan\varepsilon}{\pi\sqrt{a'^2\tan^2\varepsilon-1}\,(\bar{s}_m-1)\,[1+(b_t/b_r)]\,rb_r}$$

$$\times\int_0^r d\eta\int_{\alpha'\eta}^{b_r+\alpha'\eta}\cos^{-1}\frac{1+(\eta/\xi)\,a'^2\tan\varepsilon}{a'\,[\tan\varepsilon+(\eta/\xi)]}\,d\xi; \tag{11.4.37}$$

for a subsonic swept edge:

$$(c_y)_{f(w)}=\frac{16(a'\,\tan\varepsilon)^{3/2}\,a_w}{(\bar{s}_m-1)\,[1+(b_t/b_r)]\,(a'\,\tan\varepsilon+1)\pi a'rb_r}$$

$$\times\int_0^r d\eta\int_{\alpha'\eta}^{b_r+\alpha'\eta}\sqrt{\frac{1-a'\,(\eta/\xi)}{a'[\tan\varepsilon+(\eta/\xi)]}}\,d\xi. \tag{11.4.38}$$

The calculation of lift force for the configuration without a tail section of fuselage behind the wing should be carried out with the help of the same for-

mulas (11.4.37), (11.4.38), but with the condition that the upper limit of integration should be taken as b_r in place of $b_r + a'\eta$.

The coefficient of interference K_f for the given plain model is calculated by formula (11.2.11) in which c_{yw} is determined by the linearized theory for an isolated wing (see Chapter 8 Section 1).

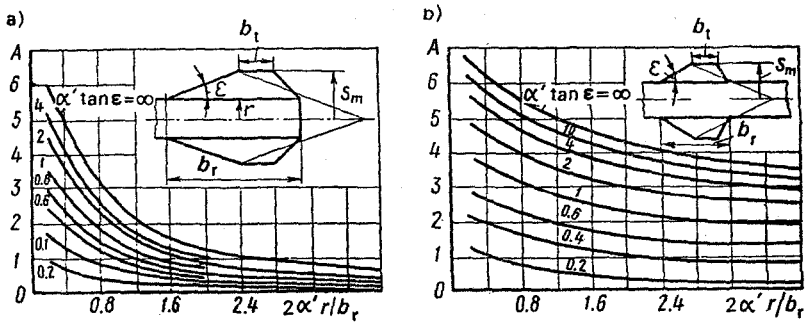

Fig. 11.4.4. Curves characterizing coefficient of interference K_f worked out for plain configuration of 'fuselage-wing' under condition of $[a'(s_m - r)/b_r]\,[1 + (a' \tan \varepsilon)^{-1}] \geqslant 1$:

a—fuselage without tail; *b*—fuselage with tail.

The data for determination of coefficient $c_{yf(w)}$ of the plain model of a wing-fuselage combination with and without a tail section using formulas (11.4.37), (11.4.38) are presented in Fig. 11.4.4. The parameter $A = K_f a' c_{yw}[1 + (b_t/b_r)]\,(\bar{s}_m - 1)$ characterizing interference is shown in the graphs as a function of $a' \tan \varepsilon$ and $2a'r/b_r$. With an increase in $a' \tan \varepsilon$ the coefficient of interference also increases. The reverse effect is observed for an increase in the quantity $2a'r/b_r$. At high values of this quantity the area of interaction of lift situated behind the trailing edge increases, which leads to an increase in K_f.

The effect of the tail section increases with a decrease in Mach number M_∞ because with an increase in the angle of Mach cones a larger area evidently falls within them. The apexes of these cones

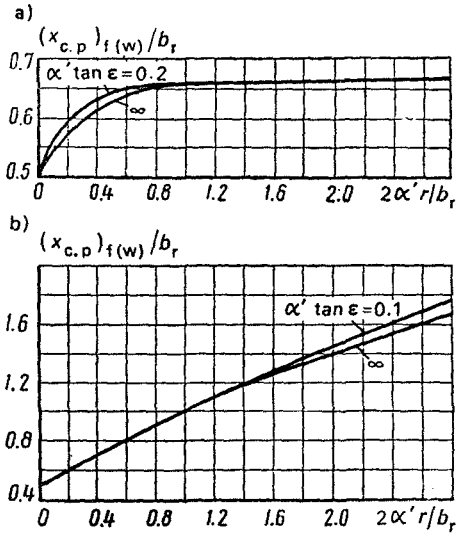

Fig. 11.4.5. Coordinates of center of pressure worked out for plain configuration of 'fuselage-wing' under the condition of $[a'(s_m - r)/b_r]\,[1 + (a' \tan \varepsilon)^{-1}] \geqslant 1$:

a—fuselage without tail; *b*—fuselage with tail.

coincide with the points of intersection of the trailing edge of the tail unit and the generator of the fuselage.

The coordinates of center of pressure $(x_{c\cdot p})_{f(w)}$, measured along the ξ axis starting from the leading edge of a wing behind which the rear part of the fuselage is located, can be determined with the help of the formula:

$$\frac{(x_{c\cdot p})_{f(w)}}{b_r} = \frac{M_{zf(w)}}{Y_{f(w)}b_r} = \frac{\int_0^r d\eta \int_{\alpha'\eta}^{b_r+\alpha'\eta} \xi \Delta\bar{p}\, d\xi}{b_r \int_0^r d\eta \int_{\alpha'\eta}^{b_r+\alpha'\eta} \Delta\bar{p}\, d\xi}. \qquad (11.4.39)$$

If there is no rear part to the fuselage the upper limit in the second integral of (11.4.39) should be replaced by the quantity b_r.

The results of calculation by formula (11.4.39) are shown in Fig. 11.4.5. The presence of the rear part of the fuselage behind the wing results in a shift in the center of pressure to a position farther aft. From Fig. 11.4.5 it is clear that the position of the center of pressure is practically independent of the angle of sweep.

5. Interference between Wing and Tail

5.1 General definitions

If there are no other lifting or control surfaces ahead of the tail joined to the fuselage the calculation of interference for the tail unit and fuselage can be carried out in the same way as for the wing-fuselage combination. In the case where there is a wing on the fuselage ahead of the tail it is necessary to allow for the additional effect of the wing as well as for that of the fuselage when determining the aerodynamic characteristics of the tail unit. This statement will be true even for the case of the canard system with tail unit ahead of the wing.

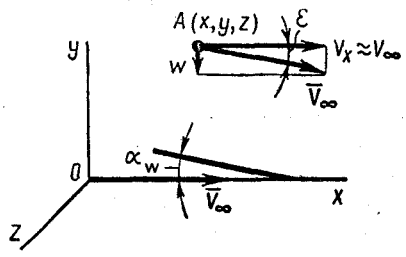

Fig. 11.5.1. Scheme of formation of downwash behind wing.

Let us study the physical nature of the interference between the tail and the wing ahead of it. The vortex sheet moving away from the wing and passing the tail produces downwash, a consequent reduction in the angle of attack and hence a reduction in the lift force of the tail surface.

At any point in space behind the wing the downwash is determined, as we said earlier, in terms of the angle $\varepsilon = -w/V_\infty$ calculated from the vertical velocity component w which is induced by the vortex sheet trailing from the wing (Fig. 11.5.1). It was shown in Chapter 6 that the angle ε for an isolated wing

at a given point in space depends on the geometrical and aerodynamic characteristics of the wing. In determining this angle for the wing-fuselage combination it is necessary to consider the effect of interference. We will assume that if the part of the fuselage behind the wing has constant diameter the vortex sheet lies in the plane of the wing. As shown by experimental research, this assumption may be valid for a very thin combination of fuselage and wing. The flow behind the wing under these conditions will be parallel to the chord of the tail if the wing and tail are located on the fuselage along the same generator at the same initial angles (11.5.2).

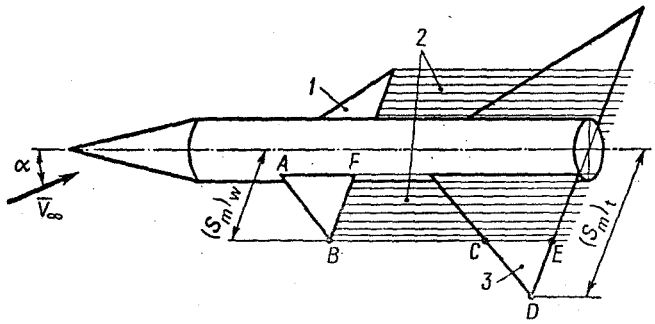

Fig. 11.5.2. Interference between tail and wing for 'thin' combination:
1—wing; *2*—vortex sheet; *3*—tail.

Like that, a section of the tail having a span equal to that of the wing will have no lift force. The remaining part of the tail surfaces with semi-span $(s_m)_t-(s_m)_w$ [$(s_m)_w$ is the semi-span of the wing] should be considered together with the wing panel as a single lifting surface of semi-span $(s_m)_t$ (surfaces *ABF* and *CDE* in Fig. 11.5.2).

According to the above discussion the lift force of the fuselage-wing-tail combination, including the lift force of the nose section of the fuselage, can be represented using formula (11.4.14) as:

$$Y_{f,w,t}=2a\pi\,(s_m^2)_t\,q_\infty\left[1-\frac{1}{(\bar{s}_m^2)_t}+\frac{1}{(\bar{s}_m^4)_t}\right], \qquad (11.5.1)$$

where $(\bar{s}_m)_t=(s_m)_t/r$ and the semi-span of tail $(s_m)_t>(s_m)_w$.

To evaluate the effect of interference on the lift force of the tail unit we introduce the coefficient of effectiveness of tail η_t defined as the ratio of the increase in lift force on a wing-fuselage combination in the presence of a tail unit at the rear to the increase in lift force on an isolated fuselage in the presence of a tail unit:

$$\eta_t=\frac{Y_{f,w,t}-Y_{f,w}}{Y_{f,t}-Y_f}, \qquad (11.5.2)$$

where the lift on the fuselage-wing combination according to (11.4.14) will be

$$Y_{f,w} = 2a\pi\,(\bar{s}_m^2)_w\, q_\infty \left[1 - \frac{1}{(\bar{s}_m^2)_w} + \frac{1}{(\bar{s}_m^4)_w}\right]. \tag{11.5.3}$$

Keeping in view that the lift force of the fuselage-tail combination $Y_{f,t}$ in (11.5.2) is determined in the same way as $Y_{f,w,t}$ by formula (11.5.1) and the quantity $Y_f = 2\pi r^2 \cdot a \cdot q_\infty$, the coefficient of tail effectiveness will be

$$\eta_t = \frac{(\bar{s}_m^2)_t\left[1 + \frac{1}{(\bar{s}_m^4)_t}\right] - (\bar{s}_m^2)_w\left[1 + \frac{1}{(\bar{s}_m^4)_w}\right]}{(\bar{s}_m^2)_t\left[1 - \frac{1}{(\bar{s}_m^2)_t}\right]^2}. \tag{11.5.4}$$

According to this hypothesis the lift force on the tail as a result of interference vanishes when the span of the tail is less than or equal to the wing span and the coefficient of effectiveness is equal to zero.

The coefficient of effectiveness so obtained can be taken as the limiting value corresponding to the most unfavorable case of flow-interaction when the vortex sheet from the trailing edge of the wing happens to be plane and coincides with the plane of the tail surfaces, so that their lift force is at its lowest. However, in practical cases, since the vortex sheet will not be plane but will be curling around in the form of vortex ropes in the vicinity of the tail and since the direction of the vortices is closer to that of the undisturbed flow than to the plane of the chords of the tail surfaces, the vortices as a rule do not lie in this plane: they are located above or below the tail depending on the angle of attack.

5.2 Subsonic speeds

In calculating the interference between wing and tail surfaces the downwash velocity is assumed as an approximation to be constant along the span and equal to its value at a point on the root chord coinciding with the aerodynamic center. Here calculation of the downwash angle is carried out by formula (6.4.13′), which is valid for cases where the tail and wing are located in the same plane.

Downwash behind a wing having the same initial angle as that of the tail surface establishes a reduction in the effective angle of attack of the horizontal tail component which is calculated from the expression

$$a_{e\cdot h\cdot t} = a - \varepsilon. \tag{11.5.5}$$

Accordingly the coefficient of lift of the tail

$$c_{y.h.t} = c^{\alpha}_{y.h.t}\,(a - \varepsilon), \tag{11.5.6}$$

where $c^{\alpha}_{y.h.t} = \partial c_{y.h.t}/\partial a$, derivative of coefficient $c_{y.h.t}$ of an isolated horizontal tail with respect to the angle of attack.

In locating wings and tail on a fuselage it is necessary to take into account the variation in their lift due to the interference of the fuselage. The lift coefficient of wing c_y in (6.4.13′) should be determined from the expression (11.1.6), making allowance for the variation in the effective angle of attack of the sections due to the effect of interference with the fuselage. The concept of an average value of effective angle of attack along the wing span may be used to simplify calculations. This average value of effective angle of attack is determined by the formula

$$\bar{a}_{e.w} = \frac{a}{(l_w/2)-r} \int_r^{l_w/2} \left(1+\frac{r^2}{z^2}\right) dz = a\left(1+\frac{2r}{l_w}\right). \tag{11.5.7}$$

Similarly for the tail surface

$$\bar{a}_{e.t} = a\,[1+(2r/l_t)]. \tag{11.5.7′}$$

Thus the coefficient of tail lift, according to (11.5.7′), will be

$$c_{y.h.t} = c^{\alpha}_{y.h.t}(\bar{a}_{e.t}-\varepsilon), \tag{11.5.6′}$$

where ε is determined from the expression (6.4.13′) in which

$$c_y = c_{yw} = c^{\alpha}_{yw}\,\bar{a}_{e.w}.$$

here $c^{\alpha}_{yw} = \partial c_{yw}/\partial a$ is the derivative of the lift coefficient of an isolated wing with respect to angle of attack.

5.3 Supersonic speeds

In investigating the interference of the tail surface with the wing the simplified vortex model of the fuselage-wing combination (Fig. 11.5.3) may be used. According to this model each of the surface-panels is replaced by a bound vortex of intensity Γ_0 and by a free vortex of the same strength shed by the trailing edge of the panel. As the fuselage has lifting capacity it is also replaced by a section of bound vortex and by a free vortex moving downstream. These vortices with intensity Γ_0 are known as conjugate vortices. The location of conjugate free vortices corresponds to the law of conjugate radii [32] by which

$$r_i = r^2/r_0. \tag{11.5.8}$$

The right side conjugate vortex has a strength equal to the right side free (external) vortex Γ_0 but in the opposite direction. The same applies to the left side vortex. Thus, the vortex model in question for a fuselage-wing combination consists of two pairs of horseshoe vortices of intensity Γ_0.

By the Zhukovskii formula (6.4.4) the lift force of the wing-panels in the presence of a fuselage will be

$$\Delta Y_{w(f)} = 2\rho_\infty V_\infty \Gamma_0 (z_v - r), \tag{11.5.9}$$

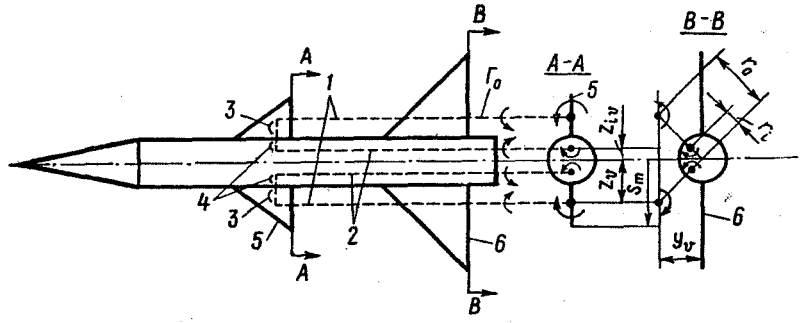

Fig. 11.5.3. Vortex model for 'fuselage-wing' combination:

1—trailing (free) vortices for wing panel; *2*—trailing (conjugate) vortices for fuselage; *3*—bound vortex for wing panel; *4*—bound (conjugate) vortices for fuselage; *5*—wing; *6*—tail.

and the lift force on the fuselage in the presence of the wing will be

$$Y_f + \Delta Y_{f(w)} = 2\rho_\infty V_\infty \Gamma_0 (r - z_{iv}), \tag{11.5.10}$$

where z_v is the lateral coordinate of a free (trailing) vortex coinciding with the center of gravity of the vortex sheet; z_{iv} is the coordinate of a conjugate vortex, which is equal to

$$z_{iv} = r^2/z_v \tag{11.5.11}$$

by formula (11.5.8); the quantity $(z_v - r)$ determines the length of the bound vortex (lifting line) on the panel; $(r - z_{iv})$ represents the length of the section of conjugate bound vortex inside the fuselage.

The lift force of the wing-fuselage combination (without the lift force of the nose section of the fuselage) is

$$Y_{f,w} - Y_f = \Delta Y_{f(w)} + \Delta Y_{w(f)} = 2\rho_\infty V_\infty \Gamma_0 [z_v - (r^2/z_v)]. \tag{11.5.12}$$

This lift force is also determined by (11.5.3) without allowing for the lift of the fuselage $2\pi a r^2 q_\infty$. Consequently

$$2\rho_\infty V_\infty \Gamma_0 \left(z_v - \frac{r^2}{z_v}\right) = 2\pi a (\bar{s}_m^2)_w q_\infty \left[1 - \frac{1}{(\bar{s}_m^2)_w} + \frac{1}{(\bar{s}_m^4)_w}\right]$$

$$- 2\pi a r^2 q_\infty = 2\pi a (\bar{s}_m^2)_w \left[1 - \frac{1}{(\bar{s}_m^2)_w}\right]^2 q_\infty. \tag{11.5.13}$$

Let us examine expression (11.5.2). The value of lift it incorporates can be represented in the following form:

$$Y_{f,w,t} = Y_f + \Delta Y_{f(w)} + \Delta Y_{w(f)} + \Delta Y_{f(t)} + \Delta Y_{t(f)} + \Delta Y_{f(t)v} + \Delta Y_{t(f)v}$$

(the last two components with index "v" are based on the effect of vortices).

It can also be written that

$$Y_{f,w} = Y_f + \Delta Y_{f(w)} + \Delta Y_{w(f)};$$
$$Y_{f,t} = Y_f + \Delta Y_{f(t)} + \Delta Y_{t(f)}.$$

Therefore

$$\eta_t = 1 + (\Delta Y_{f(t)v} + \Delta Y_{t(f)v})/(\Delta Y_{f(t)} + \Delta Y_{t(f)}); \tag{11.5.14}$$

whence

$$\Delta Y_{f(t)v} + \Delta Y_{t(f)v} = \Delta Y_{(f,t)v} = [\Delta Y_{f(t)} + \Delta Y_{t(f)}]\,(\eta_t - 1)$$

or

$$\Delta Y_{(f,t)v} = Y_t\,(K_w + K_f)\,(\eta_t - 1). \tag{11.5.15}$$

The difference $(\eta_t - 1)$ can be obtained from the expression (11.5.4) in the following form:

$$\eta_t - 1 = -\frac{(\bar{s}_m^2)_w}{(\bar{s}_m^2)_t} \cdot \frac{\left[1 - \dfrac{1}{(\bar{s}_m^2)_w}\right]^2}{\left[1 - \dfrac{1}{(\bar{s}_m^2)_t}\right]^2}. \tag{11.5.16}$$

Using (11.5.13) this will be reduced to

$$\eta_t - 1 = -\frac{2\Gamma_0\,[(z_v/r) - (r/z_v)]}{\pi a r V_\infty\,(\bar{s}_m^2)_t \left[1 - \dfrac{1}{(\bar{s}_m^2)_t}\right]^2}. \tag{11.5.17}$$

After substituting (11.5.17) and (11.5.15) and replacing $K_w + K_f$ by the quantity $[(\bar{s}_m)_t + 1]^2/(\bar{s}_m^2)_t$ [see (11.2.61)], we get

$$\Delta Y_{(f,t)v} = -\frac{2\,Y_t \Gamma_0\,[(z_v/r) - (r/z_v)]\,\{[1/(\bar{s}_m)_t] + 1\}^2}{\pi a r V_\infty\,(\bar{s}_m^2)_t\,\{1 - [1/(\bar{s}_m^2)_t]\}^2}$$

or

$$\Delta Y_{(f,t)v} = -\frac{2\Gamma_0\,[z_v - (r^2/z_v)]\,Y_t}{\pi a V_\infty\,[(s_m)_t - r]^2}. \tag{11.5.18}$$

We should keep in mind that this formula is obtained on the assumption that the vortex sheet from the wings and the corresponding free vortices are situated in the plane of the tail surface and the section of this tail surface surrounded by the vortex sheet completely loses its lifting property, i.e. lift force on that part is equal to zero. In reality this assumption, as shown earlier, is not fully justified and hence formula (11.5.18) should be regarded as the relation determining only the order of value $\Delta Y_{(f,t)v}$. To improve the relation (11.5.18) we introduce correction coefficient $\varphi\,(y_v)$, which accounts for the effect of vertical coordinate y_v of the free vortex (see Fig. 11.5.3) on lift force

$\Delta Y_{(f,t)v}$. Taking this coefficient into account, we get

$$\Delta Y_{(f,t)v} = -\frac{4\varphi(y_v)\,[z_v-(r^2/z_v)]}{(s_m)_t-r}\times\frac{\Gamma_0}{2\pi V_\infty\,[(s_m)_t-r]}\cdot\frac{Y_t}{a}.$$

The second multiplier here determines the intensity of the vortex in non-dimensional form and the third component gives the lift force per unit angle of attack for an isolated tail. The first factor consisting of coefficient $\varphi(y_v)$ depends on the position of the vortex and is independent of its intensity. This factor is called the coefficient of interference and is denoted by i_t. Introducing this coefficient and replacing r by the radius of fuselage at tail r_t, we have

$$\Delta Y_{(f,t)v} = i_t\frac{\Gamma_0}{2\pi V_\infty\,[(s_m)_t-r_t]}\cdot\frac{Y_t}{a}. \tag{11.5.19}$$

According to (11.5.9) the circulation

$$\Gamma_0 = \Delta Y_{w(f)}/[2\rho_\infty V_\infty (z_v-r_w)]. \tag{11.5.20}$$

Replacing $\Delta Y_{w(f)}$ here from (11.2.5), we get

$$\Gamma_0 = K_w Y_w/[2\rho_\infty V_\infty (z_v-r_w)].$$

As

$$Y_w = (\partial c_y/\partial a)_w\, a\,(\rho_\infty V_\infty^2/2)S_w,$$

the circulation

$$\Gamma_0 = \frac{K_w(\partial c_y/\partial a)_w\, a\, S_w V_\infty}{4(z_v-r_w)}. \tag{11.5.21}$$

Let us take

$$\Delta Y_{(f,t)v} = (c_y)_{(f,t)v}\, q_\infty S,\quad Y_t = (\partial c_y/\partial a)_t\, a q_\infty S_t \tag{11.5.22}$$

in equation (11.5.19), where S is some characteristic area, S_t is the plan area of an isolated tail surface which is connected with aspect ratio λ_t by the formula

$$\lambda_t = 4\,[(s_m)_t-r_t]^2/S_t. \tag{11.5.23}$$

Taking (11.5.21) through (11.5.23), the relation (11.5.19) is transformed into an expression determining the coefficient of lift force of the tail:

$$(c_y)_{(f,t)v} = i_t\frac{K_w\, a\,(\partial c_y/\partial a)_w\,(\partial c_y/\partial a)_t\,[(s_m)_t-r_t]\,(S_w/S)}{2\pi\,\lambda_t\,(z_v-r_w)}. \tag{11.5.24}$$

To apply formula (11.5.24) it is necessary to know the horizontal coordinate z_v of a free vortex and its vertical coordinate y_v (Fig. 11.5.4). Together these coordinates determine coefficient of interference i_t.

The vortex model of the fuselage-wing combination can be used to deter-

nine the coordinate z_v of a trailing (free) vortex. Let us consider a vortex sheet trailing from the wing-panels and calculate the circulation around an elementary contour in the form of a rectangle $ABCD$ having sides δy and δz near the trailing edge of the wing. From Fig. 11.5.5 we see that

$$\delta\Gamma_{ABCD}=\delta\Gamma_{AB}+\delta\Gamma_{BC}+\delta\Gamma_{CD}+\delta\Gamma_{DA}=v\delta y-w_u\,\delta z$$
$$-v\delta y+w_l\,\delta z=(-w_u+w_l)\,\delta z.$$

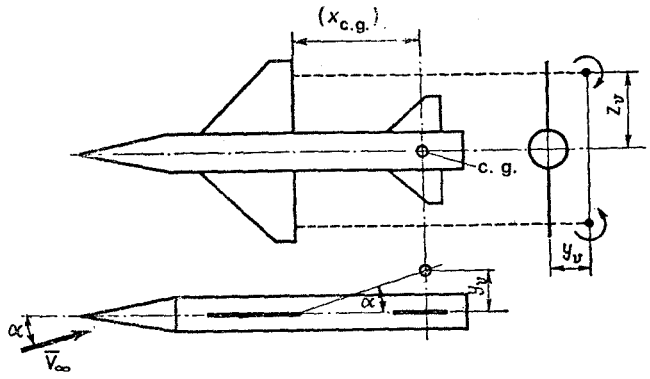

Fig. 11.5.4. Determination of position of trailing free vortex.

This circulation is assumed to be positive for a vortex rotating in an anti-clockwise direction. Let the potentials on the upper and lower sides be φ_u and φ_l respectively. Then

$$\delta\Gamma_{ABCD}=[(\partial\varphi_l/\partial z)-(\partial\varphi_u/\partial z)]\delta z.$$

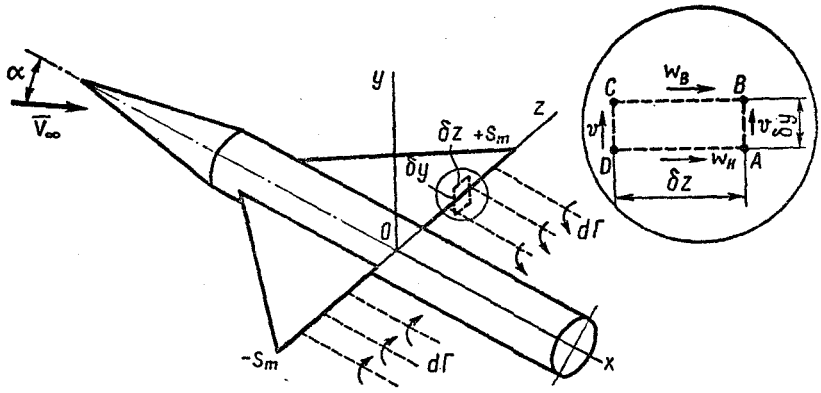

Fig. 11.5.5. Scheme for formation of vortex sheet trailing from wing panel.

Since the potentials φ_l and φ_u near the trailing edge are determined for the condition $y=0$ and hence depend only on z it is possible to use the total derivative and write

$$d\Gamma/dz = d(\varphi_l - \varphi_u)/dz, \tag{11.5.25}$$

when the distribution of circulation

$$\Gamma = \varphi_l - \varphi_u. \tag{11.5.26}$$

Here the index $ABCD$ is left out. So knowing the velocity potential along the trailing edge of the wing-panels it is possible to find the strength of the vortex sheet per unit span, i.e. to find the derivative $d\Gamma/dz$ and also the distribution of circulation. This potential can be determined from the expression (11.2.20′) by taking $y=0$ in it:

$$\varphi_\alpha = \varphi_{u,l} = \pm V_\infty a \left[\left(s_m + \frac{r^2}{s_m}\right)^2 - \left(z + \frac{r^2}{z}\right)^2\right]^{1/2}, \tag{11.5.27}$$

where the plus sign corresponds to the potential φ_u on the upper surface and the minus sign refers to the potential φ_l on the lower surface.

According to (11.5.26)

$$\Gamma = 2aV_\infty \left[\left(s_m + \frac{r^2}{s_m}\right)^2 - \left(z + \frac{r^2}{z}\right)^2\right]^{1/2}. \tag{11.5.28}$$

The circulation at the root section will be obtained when $z=r$:

$$\Gamma_0 = 2aV_\infty \left[\left(s_m + \frac{r^2}{s_m}\right)^2 - 4r^2\right]^{1/2}. \tag{11.5.29}$$

The ratio of these circulations will then be given by

$$\frac{\Gamma}{\Gamma_0} = \frac{[(s_m^2 z^2 - r^4)(s_m^2 - z^2)]^{1/2}}{z(s_m^2 - r^2)}. \tag{11.5.30}$$

If we assume that the vortex sheet is replaced by a vortex of circulation strength Γ_0 at the root section,

$$\int_r^{s_m} \Gamma dz = \Gamma_0 (z_v - r), \tag{11.5.31}$$

where the integral represents an area bounded by a curve of circulation for the panels and $\Gamma_0 (z_v - r)$ gives the quantity equal to this area.

Inserting the value of Γ from (11.5.30) in (11.5.31), we get

$$\int_r^{s_m} \frac{[(s_m^2 z^2 - r^4)(s_m^2 - z^2)]^{1/2}}{z(s_m^2 - r^2)} = z_v - r. \tag{11.5.32}$$

Let us introduce the nondimensional parameter

$$\frac{z_v-r}{s_m-r}=\frac{\int_{r_s}^{1}[(\bar{z}^2-z_s^4)(1-\bar{z}^2)]^{1/2}\bar{z}^{-1}\,d\bar{z}}{(1-r_s)^2(1+r_s)}, \tag{11.5.33}$$

where $\bar{z}=z/s_m$, $r_s=r/s_m$.

The integral on the right side is solved by numerical methods. The results of numerical integration are as follows:

$r_s=r/s_m$	0	0.1	0.2	0.3	0.4	0.5	0.6	0.7	0.8	0.9	1.0
$(z_v-r)/(s_m-r)$	0.786	0.769	0.760	0.757	0.757	0.759	0.763	0.768	0.774	0.780	0.786

From these data the parameter $(z_v-r)/(s_m-r)$ is found as a function of $r_s=r/s_m$. The coordinates z_v obtained determined the lateral position of the vortex on the wing. Experiments show that the similar vortex coordinate for the tail surface differs from the value of z_v obtained on the wing. However, this difference is small because the position of the vortices differs insignificantly in the lateral direction. Therefore the value of z_v for the tail is taken as equal to that for the wing without much loss of accuracy in calculations.

To determine the coordinate y_v of the trailing vortices near the tail we will base our reasoning on the assumption that these vortices coincide with the direction of the flow. Further, if it is assumed that this coordinate is situated above the center of gravity of the tail assembly worked out with allowance for the part obscured by the fuselage then, according to Fig. 11.5.4, we have

$$y_v=a\,(x_{c\cdot g})_t, \tag{11.5.34}$$

where $(x_{c\cdot g})_t$ is the distance of the center of gravity of the tail from the trailing edge of the wing.

5.4 Coefficient of interference

Let us now consider the problem of the coefficient of interference. From (11.5.19) it follows that

$$i_t=\frac{\Delta Y_{(f,t)v}}{Y_t}\,\frac{2\pi a V_\infty[(s_m)_t-r_t]}{\Gamma_0}. \tag{11.5.35}$$

According to this expression the coefficient of interference can be regarded as the ratio of two nondimensional quantities, one of which represents the ratio of lift force $\Delta Y_{(f,t)v}/Y_t$ and the other the nondimensional circulation characterizing the intensity of the trailing vortex. The fact that the coefficient i_t depends on the ratio of lift forces allows us to apply the simplest method for determination of i_t even if this method does not give exact values of the abso-

lute quantities $\Delta Y_{(f,t)v}$ or Y_t but helps us to find their correct ratio. Here we have the known analogy between coefficients of interference K_w, K_f from one side and the coefficient i_t from the other side. As shown earlier, the coefficients K_w, K_f, representing the ratios of corresponding lift forces, are determined with sufficient accuracy by the aerodynamic theory of a thin body, which facilitated calculation of the absolute values of lift force with interference of some combinations.

Keeping the above discussion in view, the deductions of aerodynamic theory of the flow-interaction of thin bodies can be used for determination of the ratio $\Delta Y_{(f,t)v}/Y_t$ and the corresponding coefficient i_t. The data obtained can be used to calculate interference of the tail part corresponding to thick combinations.

The method of reversal of flow, which we studied while investigating the flow-interaction of a thin wing in normal and reverse flows, can be applied to determine lift force $\Delta Y_{(f,t)v}$. In the present case the relation between the aerodynamic characteristics of the fuselage wing-tail in two opposite flows is established with the help of the basic relation of this method obtained in Chapter 8 Section 13.

Let the tail be kept at zero angle of attack with respect to the fuselage and the whole combination be placed in a flow at an angle of attack α_f. The vortices trailing from the wing induce downwash angle near the tail $-\varepsilon=\alpha_i$ so that the effective angle of attack of the tail surfaces will be $\alpha_f+\alpha_i$. The flow about combination A consisting of fuselage and tail (Fig. 11.5.6) can be represented as the complex flow formed as a result of addition of flows about similar combinations B and C following the formula $A=B+C$. In combination B the fuselage and tail surface have the same angle of attack α_f; in combination C the fuselage is not inclined to the flow ($\alpha_f=0$) and the tail surface is in the flow at an angle α_i, which is induced by the vortices.

The lift force of the combination C can be determined by the method of reversal of flow. For the direct flow (see Fig. 11.5.6) we take the following conditions according to the notations of formula (8.13.8′):

$$\left.\begin{aligned} &\alpha_1=\alpha_f=0, \text{ for area } S_f \text{ of fuselage under tail surface;}\\ &\alpha_1=\alpha_i, \quad \text{for area } S_t \text{ of tail surfaces.}\end{aligned}\right\} \tag{11.5.36}$$

For the reversed flow (see Fig. 11.5.6) we assume that fuselage and tail are at unit angle of attack, i.e.

$$\left.\begin{aligned} &\alpha_2=1, \text{ for area } S_f;\\ &\alpha_2=1, \text{ for area } S_t.\end{aligned}\right\} \tag{11.5.37}$$

Applying formula (8.13.8′), we get

$$\iint\limits_{(S_f+S_t)} \Delta\bar{p}_1 \cdot 1 \cdot dS = \iint\limits_{(S_t)} \Delta\bar{p}_2\, \alpha_i\, dS.$$

The integral on the left side determines resultant lift force of the fuselage-tail combination established by the vortex

$$\Delta Y_{(f,t)v} = Y_{f(t)v} + \Delta Y_{t(f)v} = q_\infty \iint\limits_{(S_f+S_t)} \Delta\bar{p}_1 \, dS;$$

therefore

$$\Delta Y_{(f,t)v} = q_\infty \iint\limits_{(S_t)} \Delta\bar{p}_2 \, a_i \, dS. \tag{11.5.38}$$

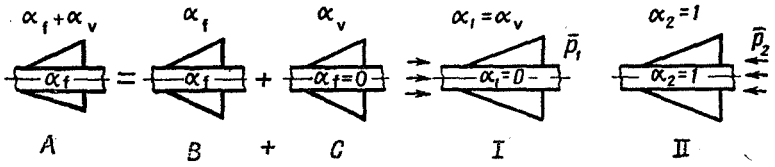

Fig. 11.5.6. Calculation of effectiveness of tail by method of reversal for 'fuselage-tail' combination:

I—combination in direct flow; *II*—combination in reversed flow.

Let us assume that the angle of attack a_i depends solely on lateral coordinate z and remains constant along the chord of the tail. Bearing in mind that $dS = dx \cdot dz$, we get, after integration with respect to x, the relation

$$\Delta Y_{(f,t)v} = 2q_\infty \int\limits_{r}^{(S_m)_t} a_i \, (bc_y') \, dz. \tag{11.5.39}$$

The quantity

$$(bc_y') = \int\limits_{x_l}^{x_t=x_l+b} \Delta\bar{p}_2 \, dx \tag{11.5.40}$$

represents aerodynamic load at a spanwise station of wing, which is determined for unit angle of inclination of fuselage and tail surface to the flow. In expression (11.5.40) x_l, x_t are coordinates of points on the leading and trailing edge respectively, b is the chord of the tail section; c_y' is the coefficient of lift of the tail section.

Let us take formula (11.2.52′) for $\Delta Y_{w(f)}$ to calculate the loading (11.5.40). Introducing the notations $a = a_f$, $\Delta Y_{w(f)} = \Delta Y_{t(f)}$, $s_m = (s_m)_t$ and performing integration with respect to x, we get

$$\Delta Y_{t(f)} = 8a_f q^\infty \int\limits_{r}^{(s_m)_t} \left\{ \left[(s_m)_t + \frac{r^2}{(s_m)_t} \right]^2 - \left(z + \frac{r^2}{z} \right)^2 \right\}^{1/2} dz. \tag{11.5.41}$$

Comparing (11.5.41) and (11.5.39), it can be concluded that the spanwise loading at unit angle of attack for tail surface and fuselage ($a_f=a_t=1$) is determined by the quantity

$$(bc_y')_{t(f)}=4\left\{\left[(s_m)_t+\frac{r^2}{(s_m)_t}\right]^2-\left(z+\frac{r^2}{z}\right)^2\right\}^{1/2}. \qquad (11.5.42)$$

Even though the integration was carried out for a triangular tail surface in a uniform direct flow the distribution of spanwise loading for thin configurations, as can be seen from (11.5.42), does not depend on the plan of the tail surface. Its value at a given point with coordinate z on the tail surface joined to a fuselage of radius r is determined only by semi-span $(s_m)_t$. Therefore formula (11.5.42) is applicable for determination of loading of a delta wing in a reversed flow. The loading appearing in (11.5.39) will be equal to the loading (11.5.42), i.e.

$$b\cdot c_y=(b\cdot c_y')_{t(f)}.$$

Then

$$\Delta Y_{(f,t)v}=8q_\infty\int_r^{(s_m)_t} a_t\left\{\left[(s_m)_t+\frac{r^2}{(s_m)_t}\right]^2-\left(z+\frac{r^2}{z}\right)^2\right\}^{1/2}dz. \qquad (11.5.43)$$

It is required to determine angle of attack $a_t=-\varepsilon$ in this expression; it is equal to the downwash angle near the tail in its absolute value.

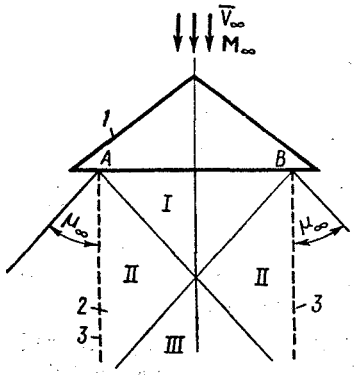

Fig. 11.5.7. Zones of vortex-effect in supersonic flow:
1—wing; *2*—Mach cone; *3*—bound vortex.

In a supersonic flow the downwash angles must be determined making allowance for the boundary of zones of effect of vortices. The zone of effect for the left bound vortex is defined by the Mach cone with apex at point *B* (Fig. 11.5.7). In region *I* situated outside of these cones vortex effect is absent and downwash is equal to zero. In region *II* bounded by the Mach cone with apex at the origin of the bound vortex downwash is determined by the action of the vortex contained by this cone.

Let us consider the tail surface situated in region *III* where the induced velocities due to the right side and left side vortices are superposed. At some distance from the trailing edge of the wing the vertical velocities of the linearized supersonic flow induced by the bound vortex are the same as the downwash velocities created by the infinite vortices in an incompressible fluid. Specifically, for a wind having $a'\lambda_w=2.5$ this distance is equal to twice

the chord, and for $a'\lambda_w = 1$ it is approximately equal to 3/4 of the chord. Considering that the tail surface is situated at a fair distance from the wing, we will determine the downwash velocity with the help of expression (6.4.7) in which the induced velocity is calculated by formula (2.7.12). Assuming $w = w_N$, $\Gamma = \Gamma_0$ and $h = r$ in this formula we can write the following relation for the point N ($y = 0$) lying on the tail surface (Fig. 11.5.8):

$$w_N = \Gamma_0/(2\pi r).$$

The vertical component velocity induced by the right side vortex is:

$$w_{Nr} = -\frac{\Gamma_0}{2\pi r}\sin\nu = -\frac{\Gamma_0}{2\pi r}\cdot\frac{z_v - z}{r} = -\frac{\Gamma_0 (z_v - z)}{2\pi\,[y_v^2 + (z_v - z)^2]}; \quad (11.5.44)$$

and by the left side vortex:

$$w_{Nl} = -\frac{\Gamma_0 (z_v + z)}{2\pi\,[y_v^2 + (z_v + z)^2]}. \quad (11.5.45)$$

The resultant vertical velocity

$$w_N = w_{Nr} + w_{Nl} = -\frac{\Gamma_0}{2\pi}\left[\frac{z_v - z}{y_v^2 + (z_v - z)^2} + \frac{z_v + z}{y_v^2 + (z_v + z)^2}\right]. \quad (11.5.46)$$

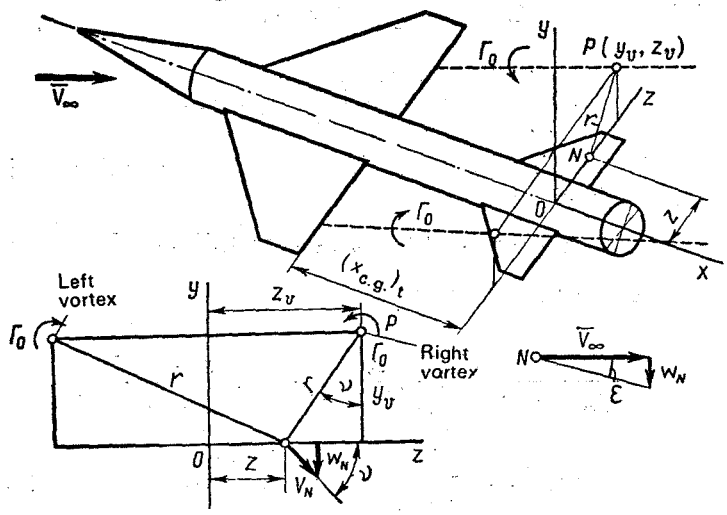

Fig. 11.5.8. Determination of downwash near tail situated behind wing.

The corresponding downwash angle

$$\varepsilon = -\frac{w_N}{V_\infty} = \frac{\Gamma_0}{2\pi V_\infty}\left[\frac{z_v - z}{y_v^2 + (z_v - z)^2} + \frac{z_v + z}{y_v^2 + (z_v + z)^2}\right]. \quad (11.5.47)$$

Inserting the value of $a_i = -\varepsilon$ in (11.5.43), we get

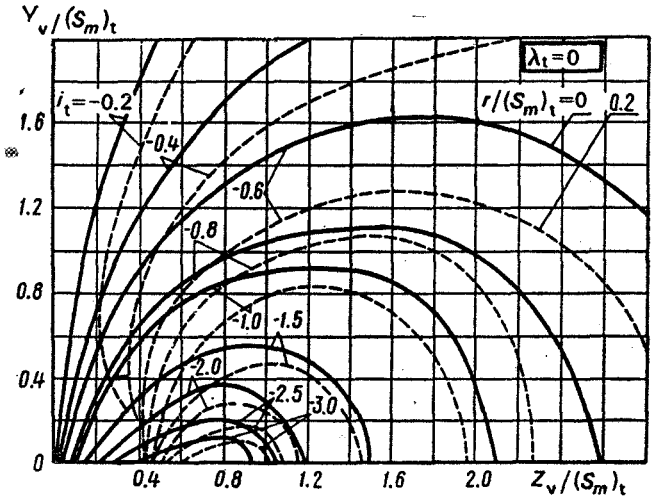

Fig. 11.5.9. Coefficients of interference for triangular tail.

$$\Delta Y_{(f,t)v}=\frac{-4q_\infty \Gamma_0}{\pi V_\infty}\int_r^{(s_m)_t}\left[\frac{z_v-z}{y_v^2+(z_v-z)^2}+\frac{z_v+z}{y_v^2+(z_v+z)^2}\right]$$

$$\times\left\{\left[(s_m)_t+\frac{r^2}{(s_m)_t}\right]^2-\left(z+\frac{r^2}{z}\right)^2\right\}^{1/2}dz\,. \qquad (11.5.48)$$

Substituting (11.5.48) in formula (11.5.35) in which, according to (8.8.48), the value of tail lift will be

$$Y_t=(c_y)_t\, q_\infty\, S_t=2a\pi\cot\kappa\, q_\infty\, S_t=2a\pi\, q_\infty[(s_m)_t-r]^2, \qquad (8.8.48')$$

the coefficient of interference will be

$$i_t=\frac{-4}{[(s_m)_t-r]\,\pi}\int_r^{(s_m)_t}\left[\frac{z_v-z}{y_v^2+(z_v-z^2)}+\frac{z_v+z}{y_v^2+(z_v+z)^2}\right]$$

$$\times\left\{\left[(s_m)_t+\frac{r^2}{(s_m)_t}\right]^2-\left(z+\frac{r^2}{z}\right)^2\right\}^{1/2}dz\,. \qquad (11.5.49)$$

The values of i_t can be worked out by numerical integration. According to (11.5.49) they will be functions of nondimensional parameters $y_v/(s_m)_t$, $z_v/(s_m)_t$ and $r/(s_m)_t$ independent of the plan of the tail surface.

Calculations by another method based on the "strip theory" [51] showed that it also depends on the form determined by the inverse of the taper ratio of the tail surface b_t/b_r. A typical diagram, constructed from the results of

these calculations for a delta wing ($\bar{\lambda}_t = b_t/b_r = 0$), is reproduced in Fig. 11.5.9. In fact, i_t seems to be the function slowly varying with b_t/b_r and $r/(s_m)_t$ for small values of $r/(s_m)_t$.

Let us examine an approximate method of determining i_t using (11.5.49), based on the assumption that the downwash along the span will be constant and equal to its value at the center of pressure of the tail surface. Assuming that point N (see Fig. 11.5.8) coincides with the center of pressure located at the origin of coordinates ($y = z = 0$), we will find the downwash angle from (11.5.47):

$$\varepsilon = \frac{\Gamma_0}{\pi V_\infty} \cdot \frac{z_v}{y_v^2 + z_v^2}. \tag{11.5.50}$$

Hence equation (11.5.48) takes the form

$$\Delta y_{(f,t)v} = \frac{-8 q_\infty \Gamma_0}{\pi V_\infty} \cdot \frac{z_v}{y_v^2 + z_v^2} \times \int_r^{(s_m)_t} \left\{ \left[(s_m)_t + \frac{r^2}{(s_m)_t} \right]^2 - \left(z + \frac{r^2}{z} \right)^2 \right\}^{1/2} dz. \tag{11.5.51}$$

Performing integration and using (8.8.48′), we get the relation

$$\frac{\Delta Y_{(f,t)v}}{Y_t} = \frac{-2\Gamma_0 z_v}{\pi V_\infty a (y_v^2 + z_v^2)} \left\{ \frac{\pi}{2} \left[\frac{(\bar{s}_m^2)_t - 1}{(\bar{s}_m)_t} \right]^2 + \left[\frac{(\bar{s}_m^2)_t + 1}{(\bar{s}_m)_t} \right]^2 \sin^{-1} \left[\frac{(\bar{s}_m^2)_t - 1}{(\bar{s}_m^2)_t + 1} \right] - \frac{2[(\bar{s}_m^2)_t - 1]}{(\bar{s}_m)_t} \right\} \frac{1}{\pi [(\bar{s}_m)_t - 1]^2} \cdot \frac{}{(K_w)_t} \tag{11.5.52}$$

In (11.5.52) the coefficient of interference K_w (11.2.60) for the fuselage-tail combination appears as a factor of one of the terms. Taking this into account and substituting (11.5.52) in (11.5.35), we get

$$i_t = -\frac{4 \bar{z}_v [(\bar{s}_m)_t - 1] (K_w)_t}{(\bar{y}_v^2 + \bar{z}_v^2) (\bar{s}_m)_t}, \tag{11.5.53}$$

where

$$\bar{z}_v = z_v/(s_m)_t, \quad \bar{y}_v = y_v/(s_m)_t, \quad (\bar{s}_m)_t = (s_m)_t/r_t.$$

Let us find the coefficient of effectiveness of the tail from the value of i_t. Taking the area of an isolated wing S_w as a characteristic area, the equation (11.5.14) can be rewritten taking into account (8.8.48′):

$$\eta_t = 1 + \frac{(c_y)_{(f,t)v}}{(c_y)_t (K_w + K_f)_t}. \tag{11.5.54}$$

Inserting here the value of

$$(c_y)_{(f,t)v}/(c_y)_t = \Delta Y_{(f,t)v}/Y_t,$$

obtained from (11.5.35), we get

$$\eta_t = 1 + \frac{i_t \Gamma_0}{2 (K_w + K_f)_t \pi a V_\infty [(s_m)_t - r_t]}. \tag{11.5.55}$$

Substituting the corresponding values (11.2.61) and (11.5.21) for $(K_w + K_f)_t$ and Γ_0, we find

$$\eta_t = 1 + \frac{i_t K_w (\partial c_y/\partial a)_w S_w (s_m^2)_t}{8 [(s_m)_t + r_t]^2 \pi [(s_m)_t - r_t] (z_v - r_w)}. \tag{11.5.56}$$

6. Control Elements

6.1 Basic types of control elements

The trajectory of an uncontrolled flight vehicle experiencing only the interaction forces of resistance and weight is usually known as a natural or ballistic trajectory. This kind of flight vehicle is characterized by the absence of any artificially created aerodynamic or other control force perpendicular to the trajectory.

The trajectory of a controllable flight vehicle, performing a given maneuver, wlll differ from the natural trajectory due to additional control force coinciding in direction with the normal to the flight velocity vector. Devices that create the necessary control force are known as control elements.

The elements of control are used in the flight vehicle's control system, which consists of a group of apparatuses and various mechanisms measuring deviation of the physical motion of the flight vehicle from the given flight conditions, registering appropriate signals and creating a control force.

Depending on the physical nature of the control force the elements of control can be divided into three basic types: aerodynamic, gas dynamic and combined control elements.

The aerodynamic control elements produce a control force by changing the conditions of external flow-interaction and hence the control force is aerodynamic by nature. Control elements of this kind are the means of changing the magnitude and direction of the total vector of aerodynamic forces.

The working of gas dynamic control elements is based on the use of the effect induced by varying the direction of a gas jet emerging from the nozzle of a jet engine. The control force appears as a result of inclination of the thrust vector from the direction of a tangent to the flight trajectory. Special controlling jet engines are used in some designs of gas dynamic control elements. These control elements are applied under conditions where aero-

dynamic control elements are less effective, for example, in rarefied layers of atmosphere or at low speeds of the flight vehicle (in particular, on launching a rocket from the ground).

Combined control elements use the effect of aerodynamic and gas dynamic organs of control simultaneously to produce a control force.

Each type of control element consists of a large number of control mechanisms of fixed types. The choice of type of control elements and fixed types of control mechanism is related to the aerodynamic system, which is determined by the type of flight vehicle and its tactico-technical requirements. The fixed aerodynamic scheme, the type of control element and its detailed construction, fulfilling given tactico-technical requirements, correspond to a given flight vehicle.

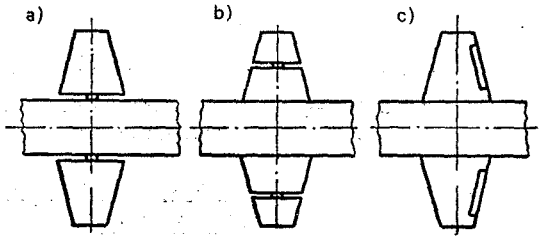

Fig. 11.6.1. Basic types of control surfaces:
a—movable as a whole; *b*—tip movable; *c*—situated along trailing edge.

A detailed discussion of the organs of control and the method of analyzing them is found in the work [10]. Only some types of aerodynamic control elements and methods of analysis will be discussed in this section, including in particular the group of control surfaces widely used in aviational and rocket designs.

The control surfaces, or simply controls, situated at different points on the flight vehicle, can be classified in the following way (Fig. 11.6.1): control elements of the type of the hinged tail; end elements of control; control elements located along the trailing edge of a lifting surface. The end elements of control can, in their own way, be divided into ordinary end controls elements with balancing (Fig. 11.6.2).

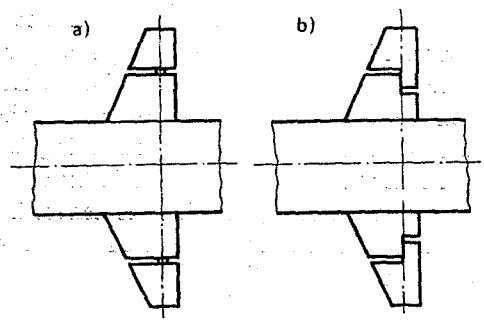

Fig. 11.6.2. Types of tip-movable controls:
a—conventional tip-movable control; *b*—with compensation.

The control elements located along the trailing edge (Fig. 11.6.3) can be used in the form

of part of a control surface with constant or variable chord (control surface with taper). The controls can be placed all along the wing span or may occupy part of the trailing edge (internal or external controls). The control elements of flight vehicles take the form of rudder, elevator, ailerons and elevons.

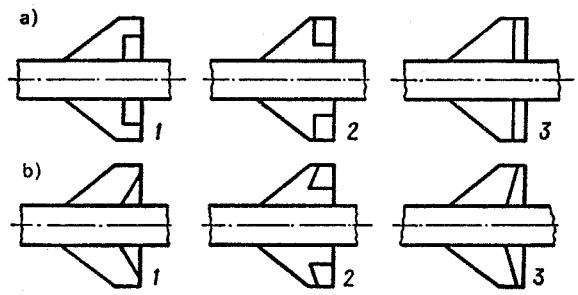

Fig. 11.6.3. Types of control situated near trailing edge:

a—with constant chord; *b*—with reverse taper; *1*—inner control; *2*—outer control; *3*—control extending over whole span.

The rudder controls are usually located in the vertical plane of symmetry in such a way that the chord coincides with the direction of the longitudinal axis of the flight vehicle. The deflection of this control results in turning the vehicle to the left or right side. The elevator controls are situated perpendicular to the plane of the rudder control. Deflection produces a change of flight direction in the vertical plane and hence a change in altitude. The combination of rudder and elevator controls makes it possible to control a flight vehicle in two mutually perpendicular planes simultaneously, i.e. to perform practically any maneuver in space.

The other system of a controlling flight vehicle in the air is also popular. In this elevator and aileron controls, are used. Ailerons, also known as banking controls, consist of two controlling surfaces located on the trailing edges of the two wing-panels. They deflect in opposite directions and cause the flight vehicle to bank. When they are operated the lateral component of force comes into play, causing the vehicle to turn. Obviously simultaneous operation of elevator and ailerons can change the value of this component. Besides, deflection of the elevator while banking facilitates control of the flight altitude and compensates the reduction in lift due to banking.

Unlike ailerons, the ailerons deflect in any direction independent of one another and therefore are used as roll controls as well as elevators when simultaneously applied.

6.2 Aerodynamic analysis of controls

Determination of the aerodynamic characteristics of control elements is an important and at the same time difficult problem. The methods of ana-

lysis of these characteristics are mainly based on experimental research on aerodynamic controls of various types. During the last few years theoretical research on aerodynamic controls has proliferated on the basis of the achievements of mathematics and mechanics which, in particular, made possible techniques of analysis of thin control surfaces located on a fuselage of small thickness. The results of this aerodynamic theory of thin bodies in a series of cases tally well with the experiments and also help us to understand various phenomena connected with the mechanism of the development of control forces.

Let us use this theory to study the methods of calculation of some types of aerodynamic controls.

External control: Let us consider the analysis of the aerodynamic force of the control situated along the trailing edge of the wing and making up part of its surface. For this purpose we use the method of flow reversal, facilitating calculation of the effect of wing and fuselage on this force. Here we will use the relations of the aerodynamic theory of a thin body according to which the plan of a control surface has no effect on the value of the force it creates.

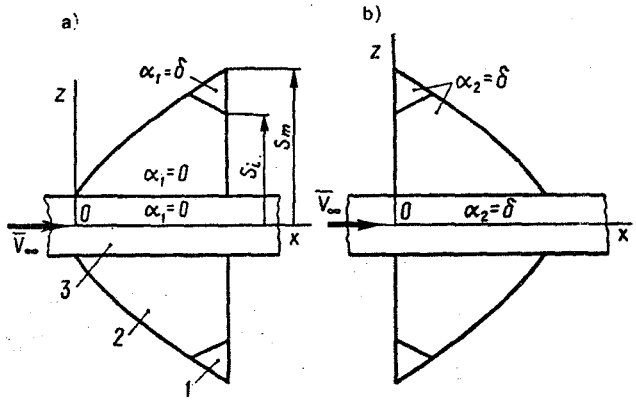

Fig. 11.6.4. Scheme for calculation of aerodynamic characteristics of outer control by method of reversal of flow:

a—direct flow; *b*—reversed flow; *1*—control surface area S_c; *2*—wing area S_w; *3*—area S_t occupied by fuselage under wing.

Let us assume that the control surface occupies part of the wing surface along the trailing edge over length $s_m - s_i$ (Fig. 11.6.4). The lift force induced by this control surface will be calculated on the assumption that the fuselage and wing are located in a direct flow at zero angle of attack ($\alpha_1=0$) and the control surface deflection is δ ($\alpha_1=\delta$). We assume that the fuselage-wing-control surface combination in a reversed flow is placed at a general angle of attack $\alpha_2=\delta$. According to formula (8.13.8′) of the method of reversal, for

the case in question

$$\iint\limits_{(S_c+S_w+S_f)} \Delta\bar{p}_1\delta dS = \iint\limits_{(S_c)} \Delta\bar{p}_2\delta dS$$

or dividing both sides by δ, we have

$$\iint\limits_{(S_c+S_w+S_f)} \Delta\bar{p}_1 dS = \iint\limits_{(S_c)} \Delta\bar{p}_2 dS. \tag{11.6.1}$$

Here the left side determines the unknown lift force of the fuselage-wing-control surface combination arising out of control surface deflection in terms of velocity head $q_\infty = \rho_\infty V_\infty^2/2$, i.e.

$$Y_c = q_\infty \iint\limits_{(S_c)} \Delta\bar{p}_2\, dS. \tag{11.6.2}$$

Taking the elementary area of the control surface $dS = dxdz$, we have

$$Y_c = 2q_\infty \int\limits_{s_l}^{s_m} dz \int\limits_{x_1}^{xt} \Delta\bar{p}_2\, dx. \tag{11.6.3}$$

The quantity

$$\int\limits_{x_1}^{x_t} \Delta\bar{p}_2\, dx = bc_y', \tag{11.6.4}$$

i.e. it is equal to the wing loading at a section of wing determined during inclination of the fuselage and wing-panel by angle δ. According to aerodynamic theory this loading during flow-interaction by reversed flow is independent as the lift of a section concentrated at its leading edge.

The coefficient of differential pressure

$$\Delta\bar{p}_2 = \bar{p}_l - \bar{p}_u = -\frac{2}{V_\infty}\left(\frac{\partial\varphi_l}{\partial x} - \frac{\partial\varphi_u}{\partial x}\right).$$

Therefore the loading at a wing-section, taking into account equation (11.5.40), will be

$$(bc_y') = \int\limits_{x_1}^{x_t} \Delta\bar{p}_2 dx = \frac{-2}{V_\infty} \int\limits_{x_1}^{x_t} \left(\frac{\partial\varphi_l}{\partial x} - \frac{\partial\varphi_u}{\partial x}\right) dx$$

$$= \frac{-2}{V_\infty}(\varphi_l - \varphi_u) = 4\delta\left[\left(s_m + \frac{r^2}{s_m}\right)^2 - \left(z + \frac{r^2}{z}\right)^2\right]^{1/2}. \tag{11.6.5}$$

Inserting this expression in (11.5.39), we get

$$Y_c = 8q_\infty \delta \int_{si}^{s_m} \{[s_m + (r^2/s_m)]^2 - [z + (r^2/z)]^2\}^{1/2}\, dz. \qquad (11.6.6)$$

It can easily be seen that this expression is similar to the relation (11.5.41) obtained earlier. Carrying out integration and using (11.6.6) for the lift of the isolated wing

$$Y_w = 2\delta\pi q_\infty (s_m - s_i)^2, \qquad (11.6.7)$$

produced by two connected end elements of control, we get

$$\frac{Y_c}{Y_w} = \frac{2}{\pi(1-\bar{s}_i)^2}\left[\frac{\pi}{4}(1-r_s^2)^2 - (\bar{s}_i^2 - r_s^4)^{1/2}(1-\bar{s}_i^2)^{1/2} + \frac{1}{2}(1+r_s^4)\sin^{-1}\frac{1-2\bar{s}_i^2+r_s^4}{1-r_s^4} + r_s^2 \sin^{-1}\frac{(1+r_s^4)\bar{s}_i^2 - 2r_s^4}{(1-r_s^4)\bar{s}_i^2}\right], \qquad (11.6.8)$$

where

$$r_s = r/s_m, \quad \bar{s}_i = s_i/s_m.$$

The ratio Y_c/Y_w depends only on the geometrical parameters at the trailing edge. The relation of (Y_c/Y_w) with r/s_m at different values of s_i/s_m is shown in Fig. 11.6.5. The lift force of the combination may considerably exceed the lift Y_w of the isolated wing due to interference between the fuselage and the wing with deflected control surface. For a given value of r/s_m and increased ratio of s_i/r the lift force of the combination increases due to the effect of the control surface. This is explained by the fact that the pressure field created during the flow over the control surface "covers" a considerable area of wing.

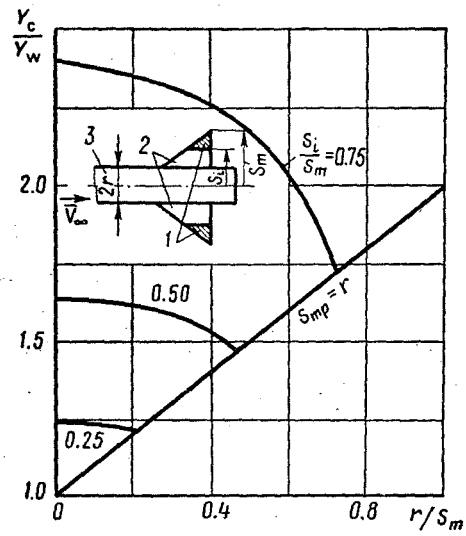

Fig. 11.6.5. Aerodynamic effectiveness of control elements:

1—controls; *2*—wing; *3*—fuselage.

All movable control surfaces: Taking $\bar{s}_i = r_s$ ($s_i = r$) in (11.6.3), we get the general relation for Y_c for all movable control surfaces:

$$Y_c = 2q_\infty \int_r^{s_m} dz \int_{x_1}^{x_t} \Delta\bar{p}_2\, dx. \qquad (11.6.9)$$

Substituting here the value of the second integral from (11.6.5) and dividing the expression so obtained by the lift force of the wing (11.6.7), we arrive at formula (11.6.8), in which $\bar{s}_t$ is replaced by the quantity r_s:

$$\frac{Y_c}{Y_w}=\frac{2}{\pi(1-r_s)^2}\left[\frac{\pi}{4}(1-r_s^2)^2-r_s(1-r_s^2)+\frac{(1+r_s^2)^2}{2}\sin^{-1}\frac{1-r_s^2}{1+r_s^2}\right]. \qquad (11.6.9')$$

This expression coincides with formula (11.2.60) determining coefficient of interference K_w for a wing joined to a fuselage.

In this way an interesting result has been obtained according to which the interference effect as a whole for the combination of fuselage-hinged wing seems to be the same as for a fixed wing with interaction of the fuselage at some angle of attack in a flow.

According to the above discussion

$$Y_c/Y_w=K_w. \qquad (11.6.10)$$

The lift force Y_c can be expressed as a sum:

$$Y_c=Y_{w(f)\delta}+Y_{f(w)\delta}, \qquad (11.6.11)$$

where the first term represents lift force on a wing inclined by an angle δ and undergoing the effect of the fuselage; the second term indicates lift force on the part of the fuselage based on its interference with the wing. Each of these components can be represented in the form:

$$Y_{w(f)\delta}=k_w Y_w; \qquad (11.6.12)$$

$$Y_{f(w)\delta}=k_f Y_w, \qquad (11.6.13)$$

where k_w and k_f, by the analogy with the coefficients K_w and K_f adduced earlier, are the coefficients of interference based on deflection of all moving control surfaces by an angle δ at $\alpha=0$.

According to (11.6.11)

$$Y_c=(k_w+k_f)\,Y_w, \qquad (11.6.14)$$

and taking (11.6.10) into account

$$k_w+k_f=K_w. \qquad (11.6.15)$$

We need one more equation connecting these coefficients among themselves in order to determine k_w and k_f. To get this equation we assume that the wing "transfers" part of its lift to the fuselage whether or not this force is created by the effect of angle of attack α of the combination or by the angle of wing setting δ. This part of the lift, based on the effect of angle of attack α, is determined by the relation

$$\Delta Y_{f(w)\alpha}/\Delta Y_{w(f)\alpha}=K_f/K_w, \qquad (11.6.16)$$

and the ratio

$$\Delta Y_{f(w)\delta}/\Delta Y_{w(f)\delta}=k_f/k_w \tag{11.6.17}$$

determines the part of the lift force imparted to the fuselage at angle of deflection δ. According to this hypothesis these two parts are equal and hence

$$k_f/k_w=K_f/K_w. \tag{11.6.18}$$

This equation can be rewritten in the form

$$(k_f+k_w)/k_w=(K_f+K_w)/K_w. \tag{11.6.18'}$$

Using the values of (11.6.15) and (11.2.61) for k_f+k_w and K_f+K_w respectively we get the following expression for the coefficient of interference:

$$k_w=K_w^2/(1+r_s)^2. \tag{11.6.19}$$

The coefficient k_f, in accordance with (11.6.15), will then be given by

$$k_f=K_w-k_w. \tag{11.6.20}$$

The relations so obtained are also valid for a fuselage-wing-tail combination.

Let us write the relations used for the calculation of the coefficient of lift for the flight vehicle with a given angle of attack for the fuselage and simultaneous deflection of the wing and fuselage by the angles δ_w and δ_t respectively (coefficients are based on the isolated wing area S_w).

1. Coefficient of lift of isolated fuselage

$$(c_y)_f=K_{f,w}\,(c_y^\alpha)_w\,a. \tag{11.6.21}$$

2. Coefficient of lift of wing in the presence of a fuselage

$$(c_y)_{w(f)}=(K_w a+k_w\delta_w)\,(c_y^\alpha)_w. \tag{11.6.22}$$

3. Coefficient of lift of fuselage in the presence of a wing

$$(c_y)_{f(w)}=(K_f a+k_f\delta_w)\,(c_y^\alpha)_w. \tag{11.6.23}$$

4. Coefficient of lift of tail in the presence of fuselage (without the effect of wing vortices)

$$(c_y)_{t(f)}=(K_t a+k_t\delta_t)\,(c_y^\alpha)_t\,(S_t/S_w), \tag{11.6.24}$$

where the coefficients of interference K_t and k_t are found from the parameters for the tail in the same way as the coefficients K_w and k_w were determined from the wing parameters; S_t is the area of isolated tail surface.

5. Coefficient of lift of the fuselage in the presence of a tail (without the effect of wing vortices)

$$(c_y)_{f(t)}=[(K_f)_t a+(k_f)_t\,\delta_t]\,(c_y^\alpha)_t\,(S_t/S_w), \tag{11.6.25}$$

where the coefficients of interference $(K_f)_t$ and $(k_f)_t$ are obtained from the parameters of the tail surface by analogy with the coefficients K_f and k_f calculated from the wing parameters.

6. Coefficient of lift of the tail section due to wing vortices

$$(c_y)_{(f,t)\,v}=i_t\,\frac{(c_y^\alpha)_w\,(c_y^\alpha)_t\,(K_w a+k_w\delta_w)\,[(s_m)_t-r_t]}{2\pi\lambda_t\,(z_v-r_w)}. \qquad (11.6.26)$$

This formula is obtained from the expression (11.5.24) in which the quantity $K_w a$ is replaced by the value of $K_w a+k_w\delta_w$ and the characteristic area S is replaced by S_w.

7. Resultant coefficient of lift for the combination

$$c_y=(c_y)_f+(c_y)_{w(f)}+(c_y)_{f(w)}$$
$$+(c_y)_{t(f)}+(c_y)_{f(t)}+(c_y)_{(f,t)v}. \qquad (11.6.27)$$

The coefficients of interference k_w and k_f obtained from the above relations are, strictly speaking, applicable to thin combinations. However, they can be used in approximate calculations of "thick" wings and fuselages, like the coefficients K_w and K_f, given sizes and forms such that the disturbed flow remains linearized. Calculating Y_w for an isolated wing by linearized theory taking into account its form and the effect of Mach number M_∞ and assuming k_w and k_f as in the theory of a thin body, it is possible to get more accurate results of lift created by control elements provided on "thick" combinations.

Internal control: The effectiveness of internal elements of control located along the trailing edge (Fig. 11.6.6) can be determined by the method of flow reversal using the results obtained for external controls and all moving

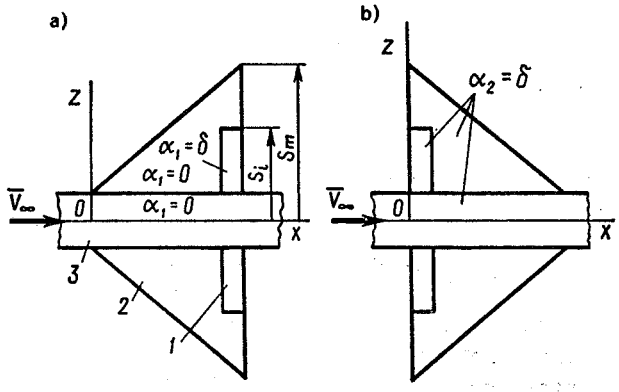

Fig. 11.6.6. Scheme for calculation of aerodynamic characteristics of inner control by method of reversal of flow:

a—direct flow; *b*—reversed flow; *1*—area of control S_c; *2*—wing area S_w; *3*—area S_f occupied by fuselage below wing.

control elements. Let us assume that the control element occupies part of the trailing edge from r to $s_i < s_m$.

In the direct flow the conditions of flow-interaction will be:

$a_1 = 0$ on wing area S_w and fuselage area S_f;

$a_1 = \delta$ on the control surface area S_c.

The condition for reversed flow will be:

$a_2 = \delta$ all over the area $S_c + S_w + S_f$.

The application of the formula for reversed flow (8.13.8′) gives

$$\iint\limits_{(S_c+S_w+S_f)} \Delta\bar{p}_1 \, \delta dS = \iint\limits_{(S_c)} \Delta\bar{p}_2 \, \delta dS.$$

Denoting the left side of this equation by the ratio $Y_{c.e}/q_\infty$ representing the lift force of the fuselage-wing-control surface combination with respect to the velocity head q_∞ and taking $dS = dx \cdot dz$, we find

$$Y_{c.i} = 2q_\infty \int_r^{s_i} dz \int_{x_1}^{x_t} \Delta\bar{p}_2 dx. \tag{11.6.28}$$

This expression can be written in the form

$$Y_{c.i} = \underbrace{2q_\infty \int_r^{s_m} dz \int_{x_1}^{x_t} \Delta\bar{p}_2 dx}_{Y_c = Y_{c.a.m}} - \underbrace{2q_\infty \int_{s_i}^{s_m} dz \int_{x_1}^{x_t} \Delta\bar{p}_2 \, dx}_{Y_c = Y_{c.e}}. \tag{11.6.29}$$

According to (11.6.9) the first term on the right side of (11.6.29) is equal to lift force $Y_c = Y_{c.a.m}$ for a combination fuselage-wing with all moving control surfaces. The second term in (11.6.29), according to (11.6.3), determines lift force $Y_c = Y_{c.e}$ of the combination with external controls deflected.

In this way we get the following relation for the combination with internal control surface:

$$Y_{c.i} = Y_{c.a.m} - Y_{c.e}. \tag{11.6.29′}$$

According to this expression the internal control is regarded as the difference between two external control elements.

If $Y_{c.i}$ is connected with the lift force of the isolated wing

$$Y_{w.i} = 2\pi\delta q_\infty (s_i - r)^2, \tag{11.6.30}$$

representing the combined internal controls, it is possible to determine the effectiveness of control elements:

$$\frac{Y_{c.i}}{Y_{w.i}} = \frac{Y_{c.a.m} - Y_{c.e}}{2\pi\delta q_\infty (s_i - r)^2}. \tag{11.6.31}$$

This ratio, calculated from the theory of a thin body, can be applied to similar "thick" combinations. Then, using the value of $Y_{w.i}$ obtained from the linearized theory, it is possible to determine the lift force for internal control surface taking into account its form and the effect of Mach number M_∞.

12

FRICTION

So far we have been studying problems of aerodynamics relating to the investigation of motion based on the model of an inviscid and nonconducting medium. It is natural that the solutions we arrived at should not have answered the questions concerning the frictional forces and heat transfer that arise during the flow-interaction of bodies. Chapters 12 and 13 of this textbook are devoted to the study of these problems. It should be borne in mind that these two factors, friction and heat transfer, are not just formally related to each other, i.e. by quantitative relations, but also by the existence of general mechanisms of momentum transfer and of heat transfer in a viscous and conducting gas. In a laminar flow, as we learned earlier, this mechanism is based on molecular mixing and in a turbulent flow it can be called molecular exchange. Therefore this class of problems concerning viscous and heat interactions is related to the solution of the system of equations involving the Navier-Stokes equation and the energy equation (see system 3.3.10). These equations, in their general form, are very complicated and difficult to solve. However, they are considerably simplified for thin boundary layers. In practice the equations for the boundary layer form the theoretical basis of investigation of a viscous and conducting gas. Their solution provides data on both frictional force and heat transfer.

However, friction can be considered separately without consideration of heat transfer on certain assumptions. This analysis will be carried out independently using results obtained for viscous interaction. This simplifies investigations even though it may leave us with more approximate results. For this purpose the present chapter is devoted to friction and Chapter 13 to heat transfer.

As we will see later on, study of the boundary layer helps to prepare the ground for use of the data on pressure arising in an inviscid gas during the flow-interaction of bodies for the case of a real viscous gaseous medium.

1. Boundary Layer Equations

Let us consider a steady plane motion of viscous compressible fluid on a

curvilinear surface. The Navier-Stokes differential equations used for the study of this motion take the form of the first two equations in system (3.3.10). Inserting

$$\operatorname{div} \bar{V}=(\partial V_x/\partial x)+(\partial V_y/\partial y),$$
$$\varepsilon_z=0.5\,[(\partial V_x/\partial y)+(\partial Vy/\partial x)]$$

in these equations and assuming the partial derivatives $\partial V_x/\partial t$ and $\partial V_y/\partial t$ are equal to zero, we get:

$$\left.\begin{aligned} V_x\frac{\partial V_x}{\partial x}+V_y\frac{\partial V_x}{\partial y}&=-\frac{1}{\rho}\cdot\frac{\partial p}{\partial x}+\frac{1}{\rho}\cdot\frac{\partial}{\partial x}\left\{\mu\left[2\frac{\partial V_x}{\partial x}-\frac{2}{3}\left(\frac{\partial V_x}{\partial x}\right.\right.\right.\\ &\left.\left.\left.+\frac{\partial V_y}{\partial y}\right)\right]\right\}+\frac{1}{\rho}\cdot\frac{\partial}{\partial y}\left[\mu\left(\frac{\partial V_x}{\partial y}+\frac{\partial V_y}{\partial x}\right)\right];\\ V_x\frac{\partial V_y}{\partial x}+V_y\frac{\partial V_y}{\partial y}&=-\frac{1}{\rho}\cdot\frac{\partial p}{\partial y}+\frac{1}{\rho}\cdot\frac{\partial}{\partial y}\left\{\mu\left[2\frac{\partial V_y}{\partial y}\right.\right.\\ &\left.\left.-\frac{2}{3}\left(\frac{\partial V_x}{\partial x}+\frac{\partial V_y}{\partial y}\right)\right]\right\}+\frac{1}{\rho}\cdot\frac{\partial}{\partial x}\left[\mu\left(\frac{\partial V_x}{\partial y}+\frac{\partial V_y}{\partial x}\right)\right]. \end{aligned}\right\}\quad(12.1.1)$$

Let us examine the flow of a fluid with low viscosity, i.e. with small values of coefficient $\nu=\mu/\rho$. From (12.1.1) it may be seen that if viscosity happens to be a significant property of the flow the co-factors of ν must be quite high so as to compensate the low values of ν. The effect of stagnation due to frictional forces is not high in a free flow. Therefore the changes in velocity in different directions, which are determined by the derivatives $\partial V_x/\partial x$, $\partial V_x/\partial y$, etc., will be small. As a result the co-factors of ν will be small and may be neglected in the equations which account for the effect of frictional forces. This leads to the conclusion that the investigation of a free flow can be carried out on the basis of Euler's equations for an ideal (inviscid) fluid. The effect of viscosity increases as we approach the surface in the flow and this results in considerable changes in velocity in different directions. Therefore the terms containing ν, which characterize the effect of viscosity, cannot be neglected and, strictly speaking, it is necessary to apply the Navier-Stokes equations (12.1.1) in the study of this viscous flow. This is the first condition of the theory of the boundary layer.

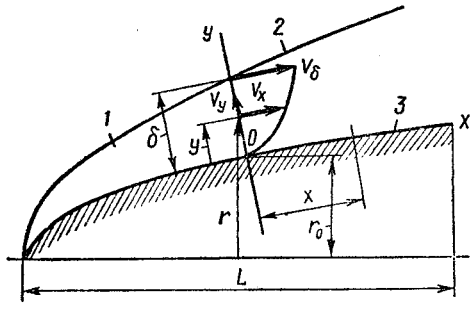

Fig. 12.1.1. Schematic diagram of boundary layer:

1—boundary layer; *2*—limit of boundary layer; *3*—surface in flow.

The second condition of this theory indicates the possibility of simplifying the Navier-Stokes equations

when studying fluid motion in a boundary layer of small thickness δ. Let us study the meaning of these simplified boundary layer equations which are based on determination of the order of terms in (12.1.1) and their successive comparison.

In line with the assumption of small thickness of the boundary layer we assume that $\delta \ll L$, where L is some characteristic linear dimension, for example, the length of the body in the flow (Fig. 12.1.1). Since the inequality $0 \leqslant y \leqslant \delta$ can be written for the coordinate y of a point in the boundary layer the order of value of the coordinate is $y \sim \delta$. The second coordinate x determining the distance along the boundary layer has the order of L ($x \sim L$). If the notation V_δ is introduced for the velocity at the external surface of the boundary layer the order of velocity V_x at any point of the boundary layer with coordinate y will be $V_x \sim V_\delta$.

The equation of continuity (2.4.50') can be used to determine the order of the second component of velocity. Then we have

$$V_y \sim \frac{1}{\rho} \int_0^\delta \frac{\partial(\rho V_x)}{\partial x} dy.$$

Let us take the order of density ρ equal to the value of density ρ_δ at the surface of the boundary layer. To find the order of derivative $\partial(\rho V_x)/\partial x$ we use the condition that the quantity ρV_x can be changed to the quantity of the order $\rho_\delta V_\delta$ (for example, from zero to $\rho_\delta V_\delta$) moving along the surface at a distance of the order of characteristic length L, i.e. in a given case $\Delta(\rho V_x) \sim \rho_\delta V_\delta$. As $\Delta x \sim L$ is assumed, we have

$$\partial(\rho V_x)/\partial x \sim \rho_\delta V_\delta / L. \tag{12.1.2}$$

Therefore for V_y we can write

$$V_y \sim (1/\rho_\delta L)\, \rho_\delta V_\delta\, \delta = V_\delta\, \delta / L. \tag{12.1.3}$$

The order of the derivatives appearing in equation (12.1.1) will be determined by analogy with (12.1.2). For example,

$$\partial V_x/\partial x \sim V_\delta/L,\ \partial V_y/\partial x \sim (V_\delta\, \delta/L)\,(1/L) = V_\delta\, \delta/L^2, \text{ etc.} \tag{12.1.4}$$

In light of these results let us consider the first equation of (12.1.1). The order of terms on the left side of this equation will be as follows:

$$\left.\begin{aligned} V_x\,(\partial V_x/\partial x) &\sim V_\delta\,(V_\delta/L) = V_\delta^2/L; \\ V_y\,(\partial V_x/\partial y) &\sim (V_\delta\,\delta/L)\,(V_\delta/\delta) = V_\delta^2/L. \end{aligned}\right\} \tag{12.1.5}$$

The two terms, as we see from the above, have the same order.

For the terms accounting for the effect of frictional forces on the right side of the equation we get:

$$\left.\begin{aligned} &\underbrace{\frac{1}{\rho}\cdot\frac{\partial}{\partial x}\left(\mu\frac{\partial V_x}{\partial x}\right)\sim\frac{\mu}{\rho}\cdot\frac{V_\delta}{L^2}}_{1},\quad \underbrace{\frac{1}{\rho}\cdot\frac{\partial}{\partial x}\left(\mu\frac{\partial V_y}{\partial y}\right)\sim\frac{\mu}{\rho}\cdot\frac{V_\delta}{L^2}}_{2};\\ &\underbrace{\frac{1}{\rho}\cdot\frac{\partial}{\partial y}\left(\mu\frac{\partial V_x}{\partial y}\right)\sim\frac{\mu}{\rho}\cdot\frac{V_\delta}{\delta^2}}_{3},\quad \underbrace{\frac{1}{\rho}\cdot\frac{\partial}{\partial y}\left(\mu\frac{\partial V_y}{\partial x}\right)\sim\frac{\mu}{\rho}\cdot\frac{V_\delta}{L^2}}_{4}. \end{aligned}\right\} \quad (12.1.6)$$

From (12.1.6) it may be seen that, since $\delta \ll L$, the first, second and fourth terms have a higher order of smallness. They can be neglected in comparison with the third term.

The order of the term $(1/\rho)\,\partial p/\partial x$ is determined from Bernoulli's equation (3.4.11). Dropping potential function U from it (assuming that the weight of the gas has no effect on the motion) and carrying out differentiation, we find $VdV = -dp/\rho$. This equation can also be written in the form $(1/\rho)\,(\partial p/\partial x) = -V(\partial V/\partial x)$ as it deals with the external limit of the boundary layer where friction is negligibly small. Hence it follows that the quantity $(1/\rho)\,(\partial p/\partial x)$ has the order of V_δ^2/L.

If a flow with marked viscosity is considered the order of the last and only term accounting for viscosity $(1/\rho)\,\partial(\mu\partial V_x/\partial y)/\partial y$ should be taken to be the same as the remaining term, i.e.

$$\frac{1}{\rho}\cdot\frac{\partial}{\partial y}\left(\mu\frac{\partial V_x}{\partial y}\right)\sim\frac{V_\delta^2}{L}\cdot \quad (12.1.7)$$

So the first equation of (12.1.1) can be written as:

$$V_x\frac{\partial V_x}{\partial x}+V_y\frac{\partial V_x}{\partial y}=-\frac{1}{\rho}\cdot\frac{\partial p_\delta}{\partial x}+\frac{1}{\rho}\cdot\frac{\partial}{\partial y}\left(\mu\frac{\partial V_x}{\partial y}\right)\cdot \quad (12.1.8)$$

Let us take the second equation of (12.1.1). The order of terms appearing in it is determined in the same way as for the first equation and will be as follows:

$$\begin{aligned} &\underbrace{V_x\frac{\partial V_y}{\partial x}+V_y\frac{\partial V_y}{\partial y}}_{V_\delta^2\,\delta/L^2}=-\frac{1}{\rho}\cdot\frac{\partial p}{\partial y}+\underbrace{\frac{4}{3\rho}\cdot\frac{\partial}{\partial y}\left(\mu\frac{\partial V_y}{\partial y}\right)}_{(\mu/\rho)\,V_\delta/(L\delta)}\\ &\underbrace{-\frac{2}{3\rho}\cdot\frac{\partial}{\partial y}\left(\mu\frac{\partial V_x}{\partial x}\right)}_{(\mu/\rho)\,V_\delta/(L\delta)}+\underbrace{\frac{1}{\rho}\cdot\frac{\partial}{\partial x}\left(\mu\frac{\partial V_x}{\partial y}\right)}_{(\mu/\rho)V_\delta/(L\delta)}+\underbrace{\frac{1}{\rho}\cdot\frac{\partial}{\partial x}\left(\mu\frac{\partial V_y}{\partial x}\right)}_{(\mu/\rho)\,V_\delta\delta/L^3}\cdot \end{aligned} \quad (12.1.9)$$

The last term on the right side can be neglected because it has a higher order of smallness than the other terms accounting for the effect of viscosity. Let us determine the order of quantity $\mu/\rho = \nu$ so as to modify the order of the other terms expressing the viscous effect. The relation (12.1.7) obtained

above can be used for this purpose. The order of the quantity on the left side of this relation is determined by the third expression of (12.1.6). Therefore

$$(\mu/\rho)\, V_\delta/\delta^2 \sim V_\delta^2/L,$$

from which the order of the coefficient of kinematic viscosity will be:

$$\mu/\rho = \nu \sim V_\delta\, \delta^2/L. \tag{12.1.10}$$

As a result of this the order of the remaining terms on the right side of (12.1.9) representing viscous effect will be as follows:

$$(\mu/\rho)\, V_\delta/(L\delta) \sim (V_\delta \delta^2/L)\, V_\delta/(L\delta) = V_\delta^2\, \delta/L^2. \tag{12.1.11}$$

It may be seen that the order of value of the terms in the second equation of (12.1.1) is lower than that in the first equation and hence these terms can be neglected. Then the second equation will be written in the form

$$\partial p/\partial y = 0. \tag{12.1.12}$$

According to this expression the pressure in the boundary layer along the normal to the wall does not change and is equal to pressure p_δ at the external surface of the boundary layer. From this it follows that a thin boundary layer has no effect on the pressure distribution in it. The result so obtained gives the condition of one of the important hypotheses of the theory of the boundary layer, namely, the hypothesis of absence of adverse effect of a boundary layer on free flow. According to this hypothesis the calculation of pressure distribution over the surface of a body in a flow, in the presence of a boundary layer, can be carried out on the basis of Euler's equations for an ideal (inviscid) medium and the shear stresses can be obtained from the simplified equation (12.1.8). This basic equation in the theory of the boundary layer is known as Prandtl's equation.

This kind of analysis can be performed with the help of Euler's and Prandtl's equation as long as the thickness of the boundary layer is small in comparison with the dimensions of the body, that is, while it satisfies the hypothesis of absence of adverse effect of a boundary layer on free flow. At remote regions of the surface where the thickness of the boundary layer is considerable this hypothesis loses its meaning and the analysis of viscous flow-interaction should be performed, strictly speaking, on the basis of the general Navier-Stokes equations.

Examining Prandtl's equation (12.1.8), it will be noticed that the coefficient of dynamic viscosity μ, which in the general case happens to be the function of pressure and temperature, appears in this equation. For a given section of boundary layer characterized by constant pressure p_δ the quantity μ will change across the thickness of the layer as a function of temperature T. The same is also true for density ρ. Hence it is necessary to know the form

of function $T(y)$ when finding the solutions for μ and ρ. To determine this function we have to consider the equation of energy in the form of the last equation of the system of equations (3.3.10).

The equation of energy for the boundary layer is simplified like the Navier-Stokes equation. The corresponding modifications for deductions from the simplified equation of energy will be set out in Chapter 13. The equation in the form of (13.2.5′) that we will use assumes the absence of any type of heat transfer in the boundary layer other than heat conduction. If the Prandtl number in this equation is assumed to be equal to unity ($\mathbf{Pr}=1$) it takes the form of (13.2.6). Obviously one of the possible integrals of equation (13.2.6) will be the equality $i_0=\text{const}$, representing the condition of conservation of total enthalpy of the gas particle, i.e. according to (13.2.2) the equality will be

$$i_0=i+(V_x^2/2)=\text{const}. \tag{12.1.13}$$

It can be shown that this equality refers to the condition of absence of heat transfer near the wall, i.e. to the case of a thermally isolated surface. Actually, assuming $i=c_p\cdot T$ and differentiating (12.1.13) with respect to y, we find

$$c_p(\partial T/\partial y)+V_x(\partial V_x/\partial y)=0.$$

From this it follows that as $y\to 0$ the velocity $V_x\to 0$ and hence $\partial T/\partial y=0$ (no temperature gradient), which proves the absence of heat transfer near the wall. So equation (12.1.13) in a simple form will be used in place of the complicated equation of energy in the form of (13.2.5′). Of course this form of energy equation does not correspond to the real character of the motion of a viscous gas in a boundary layer and gives only approximate values of the parameters, in particular, of frictional stress, that determine this motion. However, the results obtained seem to be valid for practical calculation of friction.

Prandtl's equation and the equations of continuity, state and energy form the system of equations of a compressible boundary layer:

$$\left.\begin{gathered} V_x\frac{\partial V_x}{\partial x}+V_y\frac{\partial V_x}{\partial y}=-\frac{1}{\rho}\cdot\frac{dp_\delta}{dx}+\frac{1}{\rho}\cdot\frac{\partial}{\partial y}\left(\mu\frac{\partial V_x}{\partial y}\right); \\ \partial(V_x\rho)/\partial x+\partial(V_y\rho)/\partial y=0; \\ p_\delta=R\rho T; \\ i+(V_x^2/2)=i_0. \end{gathered}\right\} \tag{12.1.14}$$

Here in the equations of motion and of state pressure p is replaced by the quantity p_δ in accordance with (12.1.12). In the equation of energy the variable value of enthalpy $i=c_p\cdot T$ and the enthalpy at stagnation $i_0=c_p\cdot T_0$.

The system of equations obtained is suitable for the study of a laminar boundary layer. The solution of this system will be carried out under the following boundary conditions:

$$\left.\begin{aligned}&\text{On the wall, at } y=0,\ V_x=V_y=0;\\&\text{A edge of boundary layer, at } y=\delta,\ V_x=V_\delta(x).\end{aligned}\right\} \tag{12.1.15}$$

The density and temperature appearing in (12.1.14) could be expressed through the velocity in a boundary layer.

From (12.1.13) it follows that

$$c_p \cdot T+(V_x^2/2)=c_p \cdot T_0, \tag{12.1.16}$$

and hence

$$T=T_0\,[1-(V_x^2/V_{\max}^2)]. \tag{12.1.17}$$

Using the equation of state $p=\rho RT$, in which pressure p for the boundary layer is taken as equal to its value at the edge of the layer, we get the relation for density:

$$\rho=\frac{p_\delta}{RT}=\left(\frac{p_\delta}{RT_0}\right)\left(1-\frac{V_x^2}{V_{\max}^2}\right)^{-1}. \tag{12.1.18}$$

Since the stagnation temperature

$$T_0=T_\delta\left(1-\frac{V_\delta^2}{V_{\max}^2}\right)^{-1}, \tag{12.1.19}$$

and the density at the external limit of the boundary layer

$$\rho_\delta=p_\delta/(RT_\delta)=\rho_0\left(1-\frac{V_\delta^2}{V_{\max}^2}\right)^{1/(k-1)}, \tag{12.1.20}$$

we get

$$\begin{aligned}\rho&=\rho_\delta\left(1-\frac{V_\delta^2}{V_{\max}^2}\right)\left(1-\frac{V_x^2}{V_{\max}^2}\right)^{-1}\\&=\rho_0\left(1-\frac{V_\delta^2}{V_{\max}^2}\right)^{k/(k-1)}\left(1-\frac{V_x^2}{V_{\max}^2}\right)^{-1}.\end{aligned} \tag{12.1.21}$$

These equations help in working out the parameters of the boundary layer without allowance for the effect of physico-chemical changes which take place at very high speeds of flow-interaction during which the gas in a boundary layer is heated to very high temperatures. Therefore, strictly speaking, these equations are valid at comparatively low velocities when the temperature does not reach high values in the boundary layer. The effect of compressibility and heated gas in a boundary layer diminishes with a decrease in the velocities of flow-interactions.

For an incompressible two-dimensional plane boundary layer the system of equations will be written as:

$$\left.\begin{aligned} V_x\frac{\partial V_x}{\partial x}+V_y\frac{\partial V_x}{\partial y}&=-\frac{1}{\rho}\cdot\frac{dp_\delta}{dx}+\nu\frac{\partial^2 V_x}{\partial y^2};\\ (\partial V_x/\partial x)+(\partial V_y/\partial y)&=0;\\ (V_\delta^2/2)+(p_\delta/\rho_\delta)&=\text{const.}\end{aligned}\right\} \qquad (12.1.22)$$

The integration of these equations will be performed for the boundary conditions given in (12.1.15).

2. Generalized Equation of Boundary Layer

2.1 Generalized equation of boundary layer in differential form

Let us transform the equation of a steady boundary layer into a generalized form convenient for study of laminar as well as turbulent flows making allowance for the effect of physico-chemical changes taking place under the impact of high temperatures.

Let us examine the elementary particle in a boundary layer in the form of a ring with internal radius r, width dx and thickness dy (Fig. 12.2.1). The action of flow around it will be replaced by the forces due to normal pressure and shear stress. Since a thin boundary layer is being considered the pressure at every point of the section passing through a given point A can be taken as constant and equal to its value p_δ on the free boundary of the layer. Therefore the force due to pressure on the left face of the ring in the direction of the x axis will be

$$P=p_\delta\, dS=2\pi r\, p_\delta\, dy. \qquad (12.2.1)$$

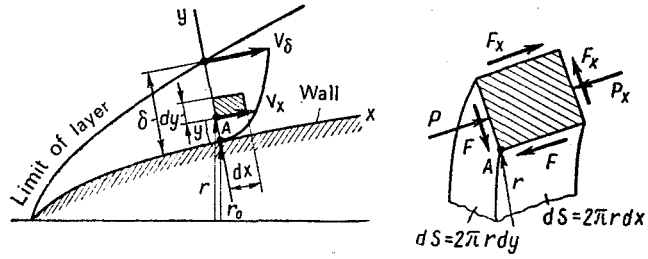

Fig. 12.2.1. Results of general equation of boundary layer.

The force acting on the right side with the same area $dS=2\pi r\cdot dy$ is denoted by P_x. As pressure p_δ is a function of coordinate x, i.e. $p_\delta=p_\delta(x)$, force $P=P(x)$. According to this force $P_x=P(x+dx)$ acts on the right face of the element, or since the coordinate of the section in question is $x=0$ the value of this force will be $P_x=P(dx)$. Expanding this function in Taylor's series and neglecting second- and higher-order terms, we get

$$P_x=P(0)+(\partial P/\partial x)\,dx=2\pi r p_\delta dy$$
$$+(\partial/\partial x)\,(2\pi r p_\delta dy)\,dx=2\pi r\,[p_\delta+(dp_\delta/dx)\,dx]\,dy. \qquad (12.2.2)$$

The differential force acting along the x axis will be

$$P-P_x=-2\pi r\,(dp_\delta/dx)\,dxdy. \tag{12.2.3}$$

The frictional forces imposed on the particle are worked out from the law of conjugate shear stresses (see Fig. 12.2.1). The forces acting on the front and rear areas do not give the force component along the x axis. This component is based on the action of tangential stresses on the internal and external surfaces of the ring and is equal to F_x-F, where

$$F=F(y)=\tau dS=2\pi r\tau dx;$$
$$F_x=F(y+dy)=F(y)+(\partial F/\partial y)dy$$
$$=2\pi r\tau dx+(\partial/\partial y)\,(2\pi r\tau dx)dy;$$

where τ is the frictional stress at the internal surface of a ring.

In this way the differential force of friction acting along the x axis

$$F_x-F=2\pi(\partial/\partial y)\,(r\tau)dxdy. \tag{12.2.4}$$

The product of the mass [density × volume] and acceleration of the particle in question will be

$$-2\pi r\rho\,(dV_x/dt)\,dxdy. \tag{12.2.5}$$

The sum of this quantity and the forces acting on the particle along the x axis is equal to zero, i.e.

$$-2\pi r\rho\,(dV_x/dt)\,dxdy-2\pi r\,(dp_\delta/dx)\,dxdy$$
$$+2\pi\,(\partial/\partial y)\,(r\tau)\,dxdy=0.$$

Assuming that the total acceleration

$$\frac{dV_x}{dt}=V_x\frac{\partial V_x}{\partial x}+V_y\frac{\partial V_x}{\partial y}\,,$$

we find from the above expression the generalized equations

$$\rho r\left(V_x\frac{\partial V_x}{\partial x}+V_y\frac{\partial V_x}{\partial y}\right)=-r\,\frac{dp_\delta}{\partial x}+\frac{\partial}{\partial y}\,(r\tau)\cdot \tag{12.2.6}$$

Equation (12.2.6) is known as the generalized equation of a boundary layer in differential form.

In studying a turbulent boundary layer the values of V_x, V_y, ρ and p_δ should be taken as average values and the frictional stress should be determined from the expression

$$\tau=(\mu+\mu_T)\,(\partial V_x/\partial y), \tag{12.2.7}$$

in which μ_T is the coefficient of turbulent viscosity.

The coefficient μ_T can be regarded as an analog of coefficient of dynamic viscosity μ for the case of a laminar flow of viscous gas. Obviously, for this

flow $\mu_T=0$, frictional stress $\tau=\mu(\partial V_x/\partial y)$ and equation (12.2.6) will be rewritten in the form

$$\rho r\left(V_x\frac{\partial V_x}{\partial x}+V_y\frac{\partial V_x}{\partial y}\right)=-r\frac{dp_\delta}{dx}+\frac{\partial}{\partial y}\left(r\mu\frac{\partial V_x}{\partial y}\right). \tag{12.2.8}$$

In the general case when the gas undergoes physico-chemical changes under the action of high temperatures the coefficient μ changes across the boundary layer. When these changes are absent the value of μ is taken to be constant. In studying the boundary layer near a plain contour it is necessary to omit r from equation (12.2.8).

2.2 Integral relation of boundary layer

Let us change the generalized equation (12.2.6) to a somewhat different form which is widely used for practical calculations of boundary layers. For this purpose the left side of (12.2.6) is written in the form

$$\rho r\left(V_x\frac{\partial V_x}{\partial x}+V_y\frac{\partial V_x}{\partial y}\right)$$
$$=\left[\frac{\partial V_x^2}{\partial x}+\frac{\partial(V_xV_y)}{\partial y}-V_x\frac{\partial V_x}{\partial x}-V_x\frac{\partial V_y}{\partial y}\right]\rho r.$$

Calculating the derivatives in the continuity equation (2.4.48), we get

$$V_x\frac{\partial(\rho r)}{\partial x}+\rho r\frac{\partial V_x}{\partial x}+V_y\frac{\partial(\rho r)}{\partial y}+\rho r\frac{\partial V_y}{\partial y}=0.$$

From this we will have

$$-\rho rV_x\frac{\partial V_x}{\partial x}-\rho r\frac{\partial V_y}{\partial y}=V_x^2\frac{\partial(\rho r)}{\partial x}+V_xV_y\frac{\partial(\rho r)}{\partial y}.$$

According to this

$$\rho r\left(V_x\frac{\partial V_x}{\partial x}+V_y\frac{\partial V_x}{\partial y}\right)=\rho r\frac{\partial V_x^2}{\partial x}+\rho r\frac{\partial(V_xV_y)}{\partial y}$$
$$+V_x^2\frac{\partial(\rho r)}{\partial x}+V_xV_y\frac{\partial(\rho r)}{\partial y}=\frac{\partial(\rho rV_x^2)}{\partial x}+\frac{\partial(\rho rV_xV_y)}{\partial y}. \tag{12.2.9}$$

Using this expression in equation (12.2.6), we get

$$\frac{\partial(\rho rV_x^2)}{\partial x}+\frac{\partial(\rho rV_xV_y)}{\partial y}=-r\frac{dp_\delta}{dx}+\frac{\partial}{\partial y}(r\tau).$$

Combining this with the equation of continuity written in the form

$$V_\delta\frac{\partial(\rho rV_x)}{\partial x}+V_\delta\frac{\partial(\rho rV_y)}{\partial y}=0,$$

we arrive at the relation

$$V_\delta \frac{\partial(\rho r V_x)}{\partial x} + V_\delta \frac{\partial(\rho r V_y)}{\partial y} - \frac{\partial(\rho r V_x^2)}{\partial x} - \frac{\partial(\rho r V_x V_y)}{\partial y} = r \frac{dp_\delta}{dx} - \frac{\partial}{\partial y}(r\tau)$$

or

$$\frac{\partial}{\partial x}[\rho r V_x (V_\delta - V_x)] - \rho r V_x \frac{dV_\delta}{\partial x} + \frac{\partial}{\partial y}[\rho r V_y (V_\delta - V_x)] = r \frac{dp_\delta}{dx} - \frac{\partial}{\partial y}(r\tau).$$

Performing integration with respect to y within the limits of the boundary layer, we get

$$\underbrace{\int_0^\delta \frac{\partial}{\partial x}[\rho r V_x (V_\delta - V_x)]\, dy}_{1} - \underbrace{\int_0^\delta \rho r V_x \frac{dV_\delta}{dx} dy}_{2} + \underbrace{\int_0^\delta \frac{\partial}{\partial y}[\rho r V_y (V_\delta - V_x)] dy}_{3} = \underbrace{\int_0^\delta r \frac{dp_\delta}{dx} dy}_{4} - \underbrace{\int_0^\delta \frac{\partial}{\partial y}(r\tau)\, dy}_{5}. \quad (12.2.10)$$

The terms appearing in equation (12.2.10) will be expressed in the following form:

1. $$\int_0^\delta \frac{\partial}{\partial x}[\rho r V_x (V_\delta - V_x)]\, dy = \frac{d}{dx}\int_0^\delta \rho r V_x (V_\delta - V_x)\, dy$$

$$\underbrace{-[\rho r V_x (V_\delta - V_x)]_{y=\delta} \frac{d\delta}{dx}} = \frac{d}{dx}\int_0^\delta \rho r V_x (V_\delta - V_x)\, dy\,; \quad (12.2.11)$$

the expression above the bracket is equal to zero as $V_x = V_\delta$ at $y = \delta$;

2. $$\int_0^\delta \rho r V_x \frac{dV_\delta}{dx} dy = \frac{dV_\delta}{dx}\int_0^\delta \rho r V_x\, dy$$

$$= \frac{d}{dx}\left(V_\delta \int_0^\delta \rho r V_x\, dy\right) - V_\delta \frac{d}{dx}\int_0^\delta \rho r V_x\, dy\,; \quad (12.2.12)$$

3. $$\int_0^\delta \frac{\partial}{\partial y}[\rho r V_y (V_\delta - V_x)]\, dy = [\rho r V_y (V_\delta - V_x)]_{y=0}^{y=\delta} = 0, \quad (12.2.13)$$

because $V_x = V_\delta$ at $y = \delta$ and $V_y = 0$ at $y = 0$;

4. $$\int_0^{\delta} r\frac{dp_\delta}{dx}\,dy=\frac{dp_\delta}{dx}\int_0^{\delta} r\,dy\,; \tag{12.2.14}$$

5. $$\int_0^{\delta}\frac{\partial}{\partial y}(r\tau)\,dy=[r\tau]_{y=0}^{y=\delta}=-r_0\,\tau_w\cdot \tag{12.2.15}$$

Keeping these results in view, equation (12.2.10) will be written as

$$\frac{d}{dx}\int_0^{\delta}\rho r V_x(V_\delta-V_x)\,dy-\frac{d}{dx}\left(V_\delta\int_0^{\delta}\rho r V_x\,dy\right)$$
$$+V_\delta\frac{d}{dx}\int_0^{\delta}\rho r V_x\,dy=\frac{dp_\delta}{dx}\int_0^{\delta} r\,dy+r_0\tau_w\cdot \tag{12.2.16}$$

Carrying out simplifications here and assuming that for small thicknesses of boundary layer the coordinate r can be approximately replaced by the coordinate r_0 corresponding to the point on the surface under flow-interaction (see Fig. 12.2.1), we can write

$$-\frac{d}{dx}\int_0^{\delta}\rho r_0 V_x^2\,dy+V_\delta\frac{d}{dx}\int_0^{\delta}\rho r_0 V_x\,dy-r_0\delta\frac{dp_\delta}{dx}=r_0\tau_w\cdot \tag{12.2.16'}$$

This generalized equation obtained by Karman is known as the integral equation of a boundary layer. It helps in directly determining the frictional stress τ_w at the wall, which is connected with the solution of the practical problem of determination of frictional drag. To apply the integral relation for this purpose we have to know the distribution of velocity along the thickness of the boundary layer, i.e. the type of function $V_x=V_x(y)$. In Sections 3 and 4 the different forms of this function for a laminar and a turbulent boundary layer will be studied.

The solution of equation (12.2.16') must satisfy the condition on the external limit of the boundary layer, where at $y=\delta$ the velocity $V_x=V_\delta$. If this velocity and pressure p_δ are known the parameters can be worked out by solution of Euler's equation for an ideal (inviscid) flow. The quantities V_x, δ and τ_w happen to be unknown parameters. Thus equation (12.2.16') must be provided with two more additional independent equations involving the above-mentioned unknown parameters. The integral equation (12.2.16') facilitates application of these equations in approximate form. In particular, it is sufficient to represent velocity V_x by a reasonably approximate relation. Even then quite satisfactory results can be obtained because velocity V_x appears under an integral sign and in solving it the magnitude of the error diminishes.

2.3 Characteristic thicknesses of boundary layer

Let us represent the integral equation (12.2.16) in a somewhat different form. For this purpose we transpose the last two terms on the left side with the help of relation (12.2.12) and we express dp_δ/dx, according to (3.6.3), in the form

$$dp_\delta/dx = -\rho_\delta V_\delta (dV_\delta/dx). \tag{12.2.17}$$

As a result we get

$$\frac{d}{dx}\int_0^\delta \rho r V_x (V_\delta - V_x) dy - \frac{dV_\delta}{dx}\int_0^\delta \rho r V_x \, dy = -\int_0^\delta \rho_\delta r V_\delta \frac{dV_\delta}{dx}\, dy + r_0\tau_w$$

or

$$\frac{d}{dx}\int_0^\delta \rho r V_x (V_\delta - V_x)\, dy + \frac{dV_\delta}{dx}\int_0^\delta r (\rho_\delta V_\delta - \rho V_x)\, dy = r_0\, \tau_w. \tag{12.2.18}$$

We will write this equation in the form

$$\frac{d}{dx}\int_0^\delta 2\pi r \rho V_x (V_\delta - V_x)\, dy + \frac{dV_\delta}{dx}\int_0^\delta 2\pi r (\rho_\delta V_\delta - \rho V_x)\, dy = 2\pi r_0\, \tau_w. \tag{12.2.18'}$$

The integral

$$\int_0^\delta 2\pi r \rho V_x (V_\delta - V_x)\, dy \tag{12.2.19}$$

determines the reduction in momentum (impulse) which is transferred through an area $2\pi r\delta$ and conditioned by stagnation of flow in the boundary layer. Let us introduce the concept of momentum thickness δ^{**} based on the thickness of some layer surrounding the surface $2\pi r_0\delta^{**}$ across which the momentum of fluid $2\pi r_0\, \delta^{**}\rho_\delta V_\delta^2$ is transferred in unit time at constant velocity V_δ. This quantity is equal to the above reduction in momentum (12.2.19), i.e.

$$2\pi r_0\, \delta^{**}\, \rho_\delta V_\delta^2 = \int_0^\delta 2\pi r \rho V_x (V_\delta - V_x)\, dy.$$

Assuming $r \approx r_0$ within the integral sign, we have

$$\delta^{**} = \int_0^\delta \frac{\rho}{\rho_\delta} \cdot \frac{V_x}{V_\delta}\left(1 - \frac{V_x}{V_\delta}\right) dy. \tag{12.2.20}$$

The second integral in (12.2.18′),

$$\int_0^{\delta} 2\pi r\,(\rho_\delta V_\delta - \rho V_x)\,dy,$$

determines the difference in the fluid flow rate per second through area $2\pi r\delta$; for an inviscid gas flow we have

$$\int_0^{\delta} 2\pi r \rho_\delta V_\delta\,dy$$

and for a viscous gas flow we have

$$\int_0^{\delta} 2\pi r \rho V_x\,dy.$$

This reduction in flow rate is due to the decrease in velocity of flow in the boundary layer. Let us introduce the concept of displacement thickness δ^* representing a characteristic thickness of layer in an inviscid flow defining the surface $2\pi r_0\delta^*$ across which the mass of fluid flows at constant velocity V_δ at all points of this surface in unit time. This mass of fluid is equal to the above-mentioned reduction in flow rate, i.e.

$$2\pi r_0\,\delta^*\rho_\delta V_\delta = \int_0^{\delta} 2\pi r\,(\rho_\delta V_\delta - \rho V_x)\,dy.$$

Assuming $r \approx r_0$, we find

$$\delta^* = \int_0^{\delta} \left(1 - \frac{\rho}{\rho_\delta}\cdot\frac{V_x}{V_\delta}\right) dy. \tag{12.2.21}$$

It may be noticed that in expression (12.2.20) for δ^{**} and in (12.2.21) for δ^* the quantity r does not appear. Consequently the characteristic thicknesses for a compressible three-dimensional boundary layer can be approximately determined in the same way as a plane boundary layer. In the case of an incompressible flow it is necessary to take $\rho = \rho_\delta = \text{const}$ in the above expressions. Use of such parameters as displacement thickness δ^* and momentum thickness δ^{**}, representing particular physical properties of the boundary layer, helps us in a number of cases to achieve the most effective method of solution of the problem of motion of a viscous fluid. With the help of these parameters it is possible, in particular, to get the differential equation in a form more convenient for analysis of the boundary layer along curvilinear surfaces (see [2], [15], [16]).

Let us take by way of illustration one of the applications of the concept of displacement thickness δ^* used in aerodynamic research. From physical considerations it is clear that the external inviscid flow apparently compresses the boundary layer, displacing its stream lines away from the wall surface. Here thickness δ^* can be taken as the quantity determining some average displacement of these stream lines. The external flow in this way interacts with the surface derived from the real surface of the body by extending it through δ^* along the normal to it at all points of sections. The distribution of velocities and pressures in the external flow should be worked out as if the flow interacted with a new surface belonging to some fictitious thicker body. From the above discussion it may be seen that the use of the concept of displacement thickness helps to account for the adverse effect of the boundary layer on the parameters of external flow.

3. Laminar Boundary Layer over Flat Plate

Let us study the analysis of a boundary layer over a flat plate placed in a compressible flow. The solution of this problem plays an important part in the theory of viscous fluid flow. The parameters of a boundary layer obtained as a result of this analysis are used in practice for approximate estimation of viscous flow parameters not only past surfaces approximating to a flat plate but also past those widely different from it, for example, the viscous flow about bodies of revolution. However, as will be shown later, the formulas so obtained for the calculation of the parameters of an incompressible boundary layer over a flat plate retain their external form for the case of determination of the corresponding parameters of a boundary layer in a compressible medium.

Let us take an integral relation for a flat plate. It is obtained from equation (12.2.18) under the condition that r is eliminated from it and the derivative dV_δ/dx is assumed to be zero as the velocity of free flow along the plate remains unchanged. We find therefore that

$$\frac{d}{dx}\int_0^\delta \rho V_x (V_\delta - V_x)\, dy = \tau_w. \tag{12.3.1}$$

We transform this equation using the new variables ξ and η introduced by Academician A.A. Dorodnitsin [5]:

$$\left.\begin{aligned} \xi &= \int_0^x f(x)\, dx; \\ \eta &= \int_0^y g(x, y)\, dy, \end{aligned}\right\} \tag{12.3.2}$$

where $f(x)$ and $g(x, y)$ are functions selected from the condition that the transformed integral relation of a compressible boundary layer will be closer to the form of the corresponding relation for an incompressible medium. The integration of this relation is a comparatively simple problem.

According to (12.3.2) the derivative

$$\frac{d}{dx}=\frac{\partial}{\partial\xi}\cdot\frac{\partial\xi}{\partial x}+\frac{\partial}{\partial\eta}\cdot\frac{\partial\eta}{\partial x}=f\frac{\partial}{\partial\xi}\int_0^{\eta_\delta}\rho V_x(V_\delta-V_x)\frac{d\eta}{g}$$

$$+\frac{\partial\eta}{\partial x}\cdot\frac{\partial}{\partial\eta}\int_0^{\eta_\delta}\rho V_x(V_\delta-V_x)\frac{d\eta}{g},$$

where η_δ is a value of η corresponding to the external limit of the boundary layer. In this equation

$$\frac{\partial}{\partial\eta}\int_0^{\eta_\delta}\rho V_x(V_\delta-V_x)\frac{d\eta}{g}=\frac{1}{g}\rho V_x(V_\delta-V_x)\Big|_0^{\eta_\delta}=0,$$

because at $\eta=0$ on the wall the velocity component $V_x=0$ and at the edge of the layer with $\eta=\eta_\delta$ its value is $V_x=V_\delta$. Therefore equation (12.3.1) can be rewritten in the form

$$f\frac{d}{d\xi}\int_0^{\eta_\delta}\rho V_x(V_\delta-V_x)\frac{d\eta}{g}=\tau_w. \tag{12.3.3}$$

It is necessary to take $\rho/g=\text{const}$ so that the integral in this relation coincides with the corresponding expression for an incompressible medium. As the function g, according to (12.3.2), happens to be nondimensional it can be taken as constant and equal to the density at stagnation, i.e. $\rho/g=\rho_0$.
Hence

$$\eta=\int_0^{\delta}\frac{\rho}{\rho_0}dy. \tag{12.3.4}$$

In the same way, for (12.3.3) we get

$$\frac{d}{d\xi}\int_0^{\eta_\delta}V_x(V_\delta-V_x)\,d\eta=\tau_w\frac{g_w}{f_w\rho_w}.$$

The right side of this equation will be

$$\frac{\tau_w}{\rho_w}\cdot\frac{g_w}{f_w}=\frac{\tau_w}{\rho_w}\cdot\frac{\rho_w}{\rho_0}\cdot\frac{1}{f_w}.$$

From (12.1.21) it follows that the density at the wall

$$\rho_w=\rho_\delta\left[1-(V_\delta^2/V_{max}^2)\right]=\rho_\delta T_\delta/T_0=p_\delta\rho_0/p_0, \tag{12.3.5}$$

whence

$$\rho_w/\rho_0=p_\delta/p_0. \tag{12.3.5'}$$

Therefore

$$\frac{\tau_w}{\rho_w}\cdot\frac{g_w}{f_w}=\frac{\tau_w}{\rho_w}\cdot\frac{p_\delta}{p_0}\cdot\frac{1}{f_w}.$$

Taking this expression into account, we have

$$\frac{d}{d\xi}\int_0^{\eta_\delta}V_x(V_\delta-V_x)\,d\eta=\frac{\tau_w}{\rho_w}\cdot\frac{p_\delta}{p_0}\cdot\frac{1}{f_w}.$$

Let us here take $p_\delta/p_0=f_w$, i.e. assume that

$$\xi=\int_0^x\frac{p_\delta}{p_0}\,dx=\frac{p_\delta}{p_0}\,x. \tag{12.3.6}$$

Accordingly,

$$\frac{d}{d\xi}\int_0^{\eta_\delta}V_x(V_\delta-V_x)\,d\eta=\frac{\tau_w}{\rho_w}. \tag{12.3.7}$$

Equation (12.3.7) coincides in form with the corresponding boundary layer relation for an incompressible medium in the system of coordinates ξ, η. Consequently the method used in the theory of the boundary layer of an incompressible fluid can be used to solve the integral relation in this form. This method takes into account the distribution of velocity V_x along the section of boundary layer we wish to know about using the integral relation.

Let us consider a laminar boundary layer, for which the integral relation has the form

$$\frac{d}{d\xi}\int_0^{\eta_\delta}V_x(V_\delta-V_x)\,d\eta=\frac{\mu_w}{\rho_w}\left(\frac{\partial V_x}{\partial y}\right)_{y=0}=\frac{\mu_w}{\rho_w}\left(\frac{\partial V_x}{\partial\eta}\right)_{\eta_\delta=0}\left(\frac{\partial\eta}{\partial y}\right)_{y=0}. \tag{12.3.8}$$

The function $V_x(\eta, \xi)$ in the theory of the laminar boundary layer of an incompressible fluid over any arbitrary surface was suggested by Pohlhausen in the form of a polynomial of the third order:

$$V_x=a(\xi)+b(\xi)\,\eta+c(\xi)\,\eta^2+d(\xi)\,\eta^3. \tag{12.3.9}$$

The coefficients of this polynomial $a(\xi)$, $b(\xi)$, $c(\xi)$ and $d(\xi)$ are determined

from the boundary conditions that should be satisfied by this velocity. According to the boundary condition at the wall, i.e. at $\eta=0$, velocity $V_x=0$. Hence the coefficient $a=0$. From equation (12.2.8), which is transformed into the variables ξ, η and reduced to the conditions of a flat plate ($dp_\delta/dx=0$, $r=\text{const}$), it follows that at the wall, where $V_x=V_y=0$, the derivative

$$(\partial^2 V_x/\partial\eta^2)_{\eta=0}=0. \tag{12.3.10}$$

According to (12.3.9) the derivative

$$\partial^2 V_x/\partial\eta^2=2c+6d\eta, \tag{12.3.11}$$

whence it follows that the coefficient $c=0$ by satisfying condition (12.3.10). In this way

$$V_x=b\eta+d\eta^3. \tag{12.3.12}$$

To determine the coefficients b and d we use the boundary conditions at the free surface of the boundary layer. At $\eta=\eta_\delta$ the velocity component $V_x=V_\delta$ and therefore

$$V_\delta=b\eta_\delta+d\eta_\delta^3. \tag{12.3.13}$$

At the free surface of the layer the frictional stress

$$(\tau_w)_{\eta=\eta_\delta}=0.$$

By Newton's formula $\tau=\mu(\partial V_x/\partial y)$ the derivative $(\partial V_x/\partial\eta)_{\eta=\eta_\delta}=0$. Taking this and (12.3.12) into account, we get

$$(\partial V_x/\partial\eta)_{\eta=\eta_\delta}=b+3d\eta_\delta^2=0. \tag{12.3.14}$$

We solve equations (12.3.13) and (12.3.14) simultaneously to find the coefficients b and d. Then

$$b=\frac{3}{2}\cdot\frac{V_\delta}{\eta_\delta},\quad d=-\frac{1}{2}\cdot\frac{V_\delta}{\eta_\delta^3}.$$

So the velocity distribution will be

$$V_x=\left[\frac{3}{2}\cdot\frac{\eta}{\eta_\delta}-\frac{1}{2}\left(\frac{\eta}{\eta_\delta}\right)^3\right]V_\delta. \tag{12.3.15}$$

Substituting this expression in (12.3.8), we get

$$\frac{d}{d\xi}\int_0^{\eta_\delta}\left(\frac{3}{2}V_\delta\frac{\eta}{\eta_\delta}-\frac{1}{2}V_\delta\frac{\eta^3}{\eta_\delta^3}\right)\left(V_\delta-\frac{3}{2}V_\delta\frac{\eta}{\eta_\delta}+\frac{1}{2}V_\delta\frac{\eta^3}{\eta_\delta^3}\right)d\eta$$
$$=\frac{3}{2}\cdot\frac{\nu_w V_\delta}{\eta_\delta}\cdot\frac{\rho_w}{\rho_0}.$$

Solving the integral and performing differentiation, we get the following

equation:

$$\frac{d\eta_\delta^2}{d\xi}=\frac{280}{13}\cdot\frac{\nu_w\rho_w}{V_\delta\rho_0}.$$

Integrating this equation under the assumption that $\nu_w=\text{const}$ and $\rho_w=\text{const}$ past a flat plate, we have

$$\eta_\delta^2=\frac{280}{13}\cdot\frac{\nu_w\rho_w}{V_\delta\rho_0}\xi+C.$$

Assuming that thickness $\eta_\delta=0$ at the initial point of the plate $\xi=0$, we find $C=0$. Therefore

$$\eta_\delta=4.64\sqrt{\frac{\nu_w\rho_w}{V_\delta\rho_0}\xi}. \tag{12.3.16}$$

Keeping in mind formula (12.3.5) for ρ_w/ρ_δ and the expression (12.3.6) for ξ, we find

$$\eta_\delta=4.64\sqrt{\frac{\nu_w x}{V_\delta}\cdot\frac{p_\delta}{p_0}\cdot\frac{\rho_w}{\rho_0}}=4.64\,\frac{p_\delta}{p_0}\sqrt{\frac{\nu_w x}{V_\delta}}. \tag{12.3.16'}$$

The thickness of the boundary layer could be determined from the expression

$$\delta=\int_0^\delta dy=\int_0^{\eta_\delta}\frac{\rho_0}{\rho}\,d\eta.$$

Using (12.1.21) and $V_x=V_\delta(\eta/\eta_\delta)$ the ratio of ρ_0/ρ could be expressed in the form

$$\frac{\rho_0}{\rho}=\frac{\rho_0[1-(V_x^2/V_{\max}^2)]}{\rho_\delta[1-(V_\delta^2/V_{\max}^2)]}=\frac{[1-(V_\delta^2/V_{\max}^2)]^{-1/(k-1)}[1-(V_x^2/V_{\max}^2)]}{1-(V_\delta^2/V_{\max}^2)}$$
$$=\frac{p_0}{p_\delta}\left(1-\frac{V_x^2}{V_{\max}^2}\right)=\frac{p_0}{p_\delta}\left(1-\frac{V_\delta^2}{V_{\max}^2}\cdot\frac{\eta^2}{\eta_\delta^2}\right).$$

According to this we have

$$\delta=\frac{p_0}{p_\delta}\int_0^{\eta_\delta}\left(1-\frac{V_\delta^2}{V_{\max}^2}\cdot\frac{\eta^2}{\eta_\delta^2}\right)d\eta=\frac{p_0}{p_\delta}\left(1-\frac{V_\delta^2}{3V_{\max}^2}\right)\eta_\delta$$
$$=\frac{p_0}{p_\delta}\left[1-\frac{1}{3}+\left(1-\frac{V_\delta^2}{V_{\max}^2}\right)\frac{1}{3}\right]\eta_\delta=\frac{p_0}{p_\delta}\left(\frac{2}{3}+\frac{T_\delta}{3T_0}\right)\eta_\delta.$$

Inserting the value of η_δ from (12.3.16') here, we get

$$\delta=4.64\left(\frac{2}{3}+\frac{T_\delta}{3T_0}\right)\sqrt{\frac{\nu_w x}{V_\delta}}.$$

The coefficient ν_w can be represented in the form

$$\nu_w=\frac{\mu_w}{\rho_w}=\frac{\mu_\delta}{\rho_\delta}\cdot\frac{\mu_w}{\mu_\delta}\cdot\frac{\rho_\delta}{\rho_w}=\nu_\delta\left(\frac{T_w}{T_\delta}\right)^n\frac{\rho_\delta}{\rho_0}\cdot\frac{\rho_0}{\rho_w}$$

$$=\nu_\delta\left(\frac{T_w}{T_\delta}\right)^n\frac{\rho_\delta}{\rho_0}\cdot\frac{p_0}{p_\delta}=\nu_\delta\left(\frac{T_w}{T_\delta}\right)^n\frac{T_0}{T_\delta}. \qquad (12.3.17)$$

Since we are considering the case of a thermally isolated wall over which the temperature of the gas for the assumed value of $\mathbf{Pr}=1$ will be

$$T_w=T_0=T_\delta\left(1-\frac{V_\delta^2}{V_{max}^2}\right)^{-1}=T_\delta\left(1+\frac{k-1}{2}\mathbf{M}_\delta^2\right), \qquad (12.3.18)$$

kinematic viscosity will be

$$\nu_w=\nu_\delta\left(\frac{T_0}{T_\delta}\right)^{1+n}=\nu_\delta\left(1+\frac{k-1}{2}\mathbf{M}_\delta^2\right)^{1+n}. \qquad (12.3.17')$$

According to this the boundary layer thickness

$$\delta=\delta_c=4.64\left[\frac{2}{3}+\frac{1}{3\left(1+\frac{k-1}{2}\mathbf{M}_\delta^2\right)}\right]\sqrt{\frac{\nu_\delta x}{V_\delta}\left(1+\frac{k-1}{2}\mathbf{M}_\delta^2\right)^{1+n}}$$

$$=4.64\left(1+\frac{k-1}{3}\mathbf{M}_\delta^2\right)\left(1+\frac{k-1}{2}\mathbf{M}_\delta^2\right)^{(n-1)/2}\sqrt{\frac{\nu_\delta x}{V_\delta}}. \qquad (12.3.19)$$

Taking $\mathbf{M}_\delta=0$, we find the relation for thickness of the boundary layer in an incompressible medium:

$$\delta_{inc}=4.64\sqrt{\frac{\nu_\delta x}{V_\delta}}; \qquad (12.3.19')$$

or in nondimensional form

$$\bar{\delta}_{inc}=\delta_{inc}/L=4.64\ (\bar{x}^{1/2}/\mathbf{Re}_L^{1/2}), \qquad (12.3.19'')$$

where $\bar{x}=x/L$, $\mathbf{Re}_L=V_\delta L/\nu_\delta$.

The ratio of thicknesses in compressible and incompressible flows will then be given by

$$\frac{\delta_c}{\delta_{inc}}=\left(1+\frac{k-1}{3}\mathbf{M}_\delta^2\right)\left(1+\frac{k-1}{2}\mathbf{M}_\delta^2\right)^{(n-1)/2}. \qquad (12.3.20)$$

It can be seen that the effect of compressibility seems to be to increase the thickness of the boundary layer. This is explained by the fact that the compressible gas is heated up during stagnation. As a consequence of heating the viscosity increases and its effect spreads through the increased thickness of gas.

The shear stress on the wall can be determined by Newton's formula,

taking into account (12.3.15) and (12.3.4):

$$\tau_w=\mu_w\left(\frac{\partial V_x}{\partial y}\right)_{y=0}=\mu_w\left(\frac{\partial V_x}{\partial \eta}\right)_{\eta=0}\left(\frac{\partial \eta}{\partial y}\right)_{y=0}=\mu_w\frac{3V_\delta}{2\eta_\delta}\cdot\frac{\rho_w}{\rho_0}=\nu_w\frac{3V_\delta}{2\eta_\delta}\cdot\frac{\rho_w^2}{\rho_0}.$$

Introducing the value of (12.3.16′) for η_δ here and using $\rho_w/\rho_0=p_\delta/p_0$, we have

$$\tau_w=\frac{3}{2}\cdot\frac{V_\delta\rho_w}{4.64}\sqrt{\frac{\nu_w V_\delta}{x}}. \tag{12.3.21}$$

Inserting the value of ν_w from (12.3.17′) through (12.3.21) and remembering that

$$\rho_w=\rho_\delta\frac{\rho_w}{\rho_0}\cdot\frac{\rho_0}{\rho_\delta}=\rho_\delta\frac{p_\delta}{p_0}\cdot\frac{\rho_0}{\rho_\delta}=\rho_\delta\frac{T_\delta}{T_0}, \tag{12.3.21′}$$

the relation for τ_w will be written in the following way:

$$\tau_w=\frac{3}{2}\cdot\frac{\rho_\delta V_\delta^2}{4.64}\sqrt{\frac{\nu_\delta}{V_\delta x}}\left(\frac{T_0}{T_\delta}\right)^{(1+n)/2}\frac{T_\delta}{T_0}$$

$$=0.323\,\rho_\delta V_\delta^2\sqrt{\frac{\nu_\delta}{V_\delta x}}\left(\frac{T_0}{T_\delta}\right)^{(n-1)/2}; \tag{12.3.22}$$

or using (12.3.18) and denoting the local Reynolds' number by $\mathbf{Re}_x=V_\delta\cdot x/\nu_\delta$, we find

$$\tau_w=(\tau_w)_c=0.323\,\rho_\delta V_\delta^2\sqrt{\frac{1}{\mathbf{Re}_x}}\left(1+\frac{k-1}{2}\mathbf{M}_\delta^2\right)^{(n-1)/2*} \tag{12.3.22′}$$

For an incompressible medium ($\mathbf{M}_\delta=0$)

$$(\tau_w)_{inc}=0.323\rho_\delta V_\delta^2\sqrt{1/\mathbf{Re}_x}. \tag{12.3.23}$$

The ratio of frictional stresses for compressible and incompressible flows will then be given by

$$\frac{(\tau_w)_c}{(\tau_w)_{inc}}=\left(\frac{T_0}{T_\delta}\right)^{(n-1)/2}=\left(1+\frac{k-1}{2}\mathbf{M}_\delta^2\right)^{(n-1)/2}. \tag{12.3.24}$$

From equation (12.3.24) it follows that with an increase in Mach number $\mathbf{M}_\delta$ or a rise in temperature in the boundary layer the frictional stress decreases ($n<1$) in spite of the rise in viscosity. This happens due to the predominant part played by density ρ_w in friction [see formula (12.3.21)] which, as may be seen from (12.3.21′), diminishes with the increase in temperature $T_w=T_0$. Consequently the capacity of the gas to resist motion decreases.

Let us determine the local frictional coefficient:

*There is a printing mistake in this equation in the original Russian text. It has been corrected here—Translator.

$$(c_{fx})_c = \frac{2(\tau_w)_c}{\rho_\delta V_\delta^2} = 0.646\sqrt{\frac{1}{\mathbf{Re}_x}}\left(1+\frac{k-1}{2}\mathbf{M}_\delta^2\right)^{(n-1)/2}. \quad (12.3.25)$$

For an incompressible medium ($\mathbf{M}_\delta = 0$) it will be given by

$$(c_{fx})_{inc} = 2(\tau_w)_{inc}/(\rho_\delta V_\delta^2) = 0.646\sqrt{1/\mathbf{Re}_x}. \quad (12.3.26)$$

It can be seen that the ratio of local coefficients of friction will be the same as the ratio of frictional stresses (12.3.24):

$$\frac{(c_{fx})_c}{(c_{fx})_{inc}} = \frac{(\tau_w)_c}{(\tau_w)_{inc}} = \left(\frac{T_0}{T_\delta}\right)^{(n-1)/2} = \left(1+\frac{k-1}{2}\mathbf{M}_\delta^2\right)^{(n-1)/2}. \quad (12.3.27)$$

Let us calculate the frictional drag of a flat plate. The elementary value of this force acting on the area $dx \cdot 1$ is

$$dX_{fc} = (\tau_w)_c\, dx \cdot 1.$$

The resultant frictional drag of one side of the plate having area $L \cdot 1$ (L—length of plate)

$$X_{fc} = \int_0^L (\tau_w)_c\, dx. \quad (12.3.28)$$

The coefficient of this force will be

$$(c_{xf})_c = \frac{X_{fc}}{(\rho_\delta V_\delta^2/2)L \cdot 1} = \frac{1}{L}\int_0^L \frac{(\tau_w)_c}{\rho_\delta V_\delta^2/2}\, dx = \frac{1}{L}\int_0^L (c_{fx})_c\, dx. \quad (12.3.28')$$

Introducing here the value of $(c_{fx})_c$ from expression (12.3.25), we get

$$(c_{xf})_c = 0.646\left(1+\frac{k-1}{2}\mathbf{M}_\delta^2\right)^{(n-1)/2}\frac{1}{L}\int_0^L \frac{dx}{\sqrt{\mathbf{Re}_x}}$$

$$= 0.646\left(1+\frac{k-1}{2}\mathbf{M}_\delta^2\right)^{(n-1)/2}\frac{1}{L}\int_0^L \sqrt{\frac{\nu_\delta}{V_\delta x}}\, dx.$$

After integration this reduces to

$$(c_{xf})_c = \frac{1.292}{\sqrt{\mathbf{Re}_L}}\left(1+\frac{k-1}{2}\mathbf{M}_\delta^2\right)^{(n-1)/2}, \quad (12.3.29)$$

where the Reynolds number calculated on the basis of length L of plate

$$\mathbf{Re}_L = V_\delta L/\nu_\delta.$$

For an incompressible medium

$$(c_{xf})_{inc} = 1.292/\sqrt{\mathbf{Re}_L}. \quad (12.3.30)$$

4. Turbulent Boundary Layer over Flat Plate

4.1 Application of logarithmic velocity distribution

The integral relation (12.3.7) in terms of the variables (ξ and η), in which this relation has the same form as for an incompressible flow, can be used for solution of the problem of determination of the parameters of a turbulent boundary layer over a flat plate.

Formula (1.1.3) will be used to determine the distribution of velocity V_x in a boundary layer, which we need to know in order to evaluate the integral in relation (12.3.7). Let us rewrite this formula assuming $\overline{V}_x = V_x$:

$$\tau = \rho l^2 (\partial V_x/\partial y)^2, \tag{12.4.1}$$

whence

$$\partial V_x/\partial y = (1/l)\sqrt{\tau/\rho}\,.$$

According to Prandtl's proposition the length of transition path

$$l = ky, \tag{12.4.2}$$

where k is some constant coefficient of proportionality; y is the distance from the wall. Then

$$\partial V_x/\partial y = (1/ky)\sqrt{\tau/\rho}\,,$$

whence

$$V_x = \int \frac{1}{ky}\sqrt{\frac{\tau}{\rho}}\,dy + C_1, \tag{12.4.3}$$

where C_1 is some constant determined from the boundary conditions of the gas flow in the boundary layer. Let us transform this equation using variables η (12.3.4) and ξ (12.3.6). Let us introduce the function

$$\vartheta = (\tau/\rho_0)(1-\overline{V}_\delta^2)^{-k/(k-1)}\,, \tag{12.4.4}$$

for the sake of convenience in transformation, where $\overline{V}_\delta = V_\delta/V_{\max}$. The density in (12.4.3) can be replaced with the help of (12.1.21):

$$\rho = \rho_0(1-\overline{V}_\delta^2)^{k/(k-1)}(1-\overline{V}_x^2)^{-1}, \tag{12.4.5}$$

where $\overline{V}_x = V_x/V_{\max}$. The differential dy in (12.4.3) can be expressed, using (12.3.4) and (12.4.5), in the form

$$dy = (\rho_0/\rho)\,d\eta = (1-\overline{V}_\delta^2)^{-k/(k-1)}(1-\overline{V}_x^2)d\eta. \tag{12.4.6}$$

Finally, let us consider transformation of the length of the mixing path (12.4.2). Academician A.A. Dorodnitsin takes $k=0.3914$, i.e. equal to the value of this coefficient adjacent to the wall for a boundary layer in an incompressible medium. However, $V_x \approx 0$ close to the wall and according to (12.4.6)

$$y \approx (1-\bar{V}_\delta^2)^{-k/(k-1)}\eta. \tag{12.4.7}$$

Using relations (12.4.4) through (12.4.7) in (12.4.3) we have

$$V_x = \int \frac{1}{k(1-\bar{V}_\delta^2)^{-k/(k-1)}\eta}\sqrt{\frac{\vartheta(1-\bar{V}_\delta^2)^{k/(k-1)}(1-\bar{V}_x^2)}{(1-\bar{V}_\delta^2)^{k/(k-1)}}}$$

$$\times(1-\bar{V}_\delta^2)^{-k/(k-1)}(1-\bar{V}_x^2)d\eta + C_2 = \int \frac{(1-\bar{V}_x^2)^{3/2}}{k\eta}\sqrt{\vartheta}\,d\eta + C_2, \tag{12.4.8}$$

where C_2 is some constant determined by the boundary conditions for variable η. The quantity $k\eta/(1-\bar{V}_x^2)^{3/2}$, which will be denoted by $\bar{l}$, corresponds to the length of transition path l in (12.4.1). Since it was accepted that this length is determined from the coefficient k for the condition adjacent to the wall where $\bar{V}_x \ll 1$, it is obvious that

$$\bar{l} \approx k\eta, \tag{12.4.9}$$

which exactly coincides with the accepted law for the length of a transition path in an incompressible flow.

In this way,

$$V_x = \int \frac{\sqrt{\vartheta}}{k\eta}d\eta + C_2.$$

In deriving the above velocity distribution we used the hypothesis that frictional stress is constant over the section of the boundary layer. According to this $\tau = \tau_w = \text{const}$ and hence $\vartheta = \vartheta_w = \text{const}$. Therefore

$$V_x = \int \frac{\sqrt{\vartheta_w}}{k\eta}d\eta + C_2,$$

from which

$$V_x = (\sqrt{\vartheta_w}/k)\ln\eta + C_2. \tag{12.4.10}$$

Using this equation in the conditions over the external limits of the boundary layer where $\eta = \eta_\delta$, $V_x = V_\delta$, we get

$$V_\delta = (\sqrt{\vartheta_w}/k)\ln\eta_\delta + C_2. \tag{12.4.11}$$

Combining this with (12.4.10), we find

$$V_x - V_\delta = (\sqrt{\vartheta_w}/k)\ln(\eta/\eta_\delta). \tag{12.4.12}$$

The equation for V_x in the form given represents the logarithmic law of velocity distribution over a section of the boundary layer. Equations (12.4.10) and (12.4.12) are valid only near the surface under flow-interaction, i.e. in the neighborhood of a laminar sublayer. This layer is formed in the immediate vicinity of the wall and delays mixing (with the turbulent flow). This phenomenon of

delaying turbulent flow near the wall is described by the formula (12.4.2) according to which the transition is shortened at the wall (at $y=0$). Academician A.A. Dorodnitsin, in work [5], introduced a modification wherever the velocity distribution in the turbulent core of a boundary layer can be expressed on the basis of logarithmic law (12.4.10) with the help of equation

$$V_x=(\sqrt{\vartheta_w}/k)\,[\ln\eta+C_2+f(\eta/\eta_\delta)]. \qquad (12.4.10')$$

Here the function $f(\eta/\eta_\delta)$ represents the modification to the logarithmic law introduced by Dorodnitsin. This modification is the universal function independent of the Mach number or velocity V_δ. In other words, Academician A.A. Dorodnitsin assumes that the velocity distribution in terms of coordinates η, ξ is, as in the case of a laminar boundary layer, independent of compressibility.

Taking the variable $\eta=\eta_\delta$ in (12.4.10'), we get the velocity at the external limit of the boundary layer

$$V_\delta=(\sqrt{\vartheta_w}/k)\,[\ln\eta_\delta+C_2+f(1)]. \qquad (12.4.11')$$

From (12.4.10') and (12.4.11') we have

$$V_x-V_\delta=(\sqrt{\vartheta_w}/k)\,F(\eta/\eta_\delta), \qquad (12.4.12')$$

where

$$F(\eta/\eta_\delta)=\ln(\eta/\eta_\delta)-f(1)-f(\eta/\eta_\delta). \qquad (12.4.12'')$$

The analysis of the parameters of a turbulent boundary layer based on application of equation (12.4.12') containing Dorodnitsin's correction is set out in the work [5].

The possibility of applying the usual logarithmic law for simplification of the solution of the problem of determining these parameters can be examined retaining the principal scheme of solution of this problem without introducing the above correction, i.e. by assuming the function $F(\eta/\eta_\delta)=\ln(\eta/\eta_\delta)$.

Calculations show that the numerical coefficients appearing in the relations for boundary layer parameters obtained differ somewhat from the data in the work [5]. However, this difference is quite permissible if the general character of approximate calculations is remembered.

The equation for velocity corresponding to the logarithmic law assumed in its conventional form (12.4.12) can be somewhat modified by expressing thickness η_δ in terms of ϑ_w. For this purpose we consider equation (12.4.12) as applied to the conditions at the boundary of a laminar sublayer, where the velocity on this boundary $V_x=V_l$ at $\eta=\eta_l$:

$$V_l-V_\delta=(\sqrt{\vartheta_w}/k)\ln(\eta_l/\eta_\delta). \qquad (12.4.13)$$

Karman's equation, which is written for variable y in the form

$$\delta_l=a\mu_w/\sqrt{\rho_w\tau_w}, \qquad (12.4.14)$$

where the coefficient a is taken as for an incompressible medium and equals 11.5 from empirical data, can be used to determine the thickness η_l of the laminar sublayer and velocity V_l on its boundary. Let us change equation (12.4.14) to the new parameter η. The quantity

$$\delta_l = \int_0^{\delta_l} dy$$

or, taking into account (12.3.4) and (12.1.21),

$$\delta_l = (1-\overline{V}_\delta^2)^{-k/(k-1)} \int_0^{\eta_l} (1-\overline{V}_x^2)\, d\eta. \tag{12.4.15}$$

In the vicinity of the wall $\overline{V}_x \ll 1$. Hence

$$\delta_l \approx (1-\overline{V}_\delta^2)^{-k/(k-1)} \eta_l. \tag{12.4.16}$$

The expression for τ_w in (12.4.14) is:

$$\tau_w = \vartheta_w \rho_0 (1-\overline{V}_\delta^2)^{k/(k-1)}. \tag{12.4.17}$$

The density on the wall will be obtained from (12.4.5) by taking $V_x = 0$:

$$\rho_w = \rho_0 (1-\overline{V}_\delta^2)^{k/(k-1)}. \tag{12.4.5'}$$

Using (12.4.16), (12.4.17) and (12.4.5') in (12.4.14), we get

$$\eta_l = a\mu_w/(\rho_0 \sqrt{\vartheta_w}). \tag{12.4.18}$$

The quantity ϑ_w in this expression can be determined with the help of Newton's formula $\tau_w = \mu_w (\partial V_x/\partial y)_{y=0}$. Assuming the small thickness of the laminar sublayer, it is possible to consider the linear law of velocity distribution $V_x = V_l(y/\delta_l)$ for it. According to this

$$\tau_w = \mu_w (V_l/\delta_l),$$

whence

$$V_l = (\tau_w/\mu_w)\delta_l\,;$$

or, taking the values of (12.4.16) for δ_l and of (12.4.17) for τ_w, we have

$$V_l = (\rho_0 \vartheta_w/\mu_w)\eta_l. \tag{12.4.19}$$

Introducing here the value of η_l from (12.4.18), we get

$$V_l = a\sqrt{\vartheta_w}. \tag{12.4.19'}$$

Substituting the values of η_l from (12.4.18) and V_l from (12.4.19') in (12.4.13), we arrive at the relation:

$$a\sqrt{\vartheta_w} - V_\delta = \frac{\sqrt{\vartheta_w}}{k} \ln\left(\frac{a\mu_w}{\rho_0\sqrt{\vartheta_w}} \cdot \frac{1}{\eta_\delta}\right),$$

from which

$$\eta_\delta = \frac{a\mu_w}{\rho_0\sqrt{\vartheta_w}} e^{kV_\delta/\sqrt{\vartheta_w}} e^{-k\alpha}. \tag{12.4.20}$$

Let us introduce the parameter

$$z = kV_\delta/\sqrt{\vartheta_w} \tag{12.4.21}$$

and denote the constant quantity

$$ae^{-k\alpha} = A.$$

Then

$$\eta_\delta\sqrt{\vartheta_w} = e^z(A\mu_w/\rho_0). \tag{12.4.22}$$

Now we will use the integral relation (12.3.7) in which we insert the value of

$$\tau_w/\rho_w = \vartheta_w, \tag{12.4.23}$$

obtained from (12.4.17) and (12.4.5′). According to (12.4.12) we next carry out the change

$$V_x = V_\delta + (\sqrt{\vartheta_w}/k) \ln(\eta/\eta_\delta). \tag{12.4.24}$$

As a result

$$-\frac{d}{d\xi}\int_0^{\eta_\delta}\left(V_\delta + \frac{\sqrt{\vartheta_w}}{k}\ln\frac{\eta}{\eta_\delta}\right)\frac{\sqrt{\vartheta_w}}{k}\ln\frac{\eta}{\eta_\delta} = \vartheta_w$$

or

$$\frac{d}{d\xi}\left(\frac{V_\delta\sqrt{\vartheta_w}}{k}\int_0^{\eta_\delta}\ln\frac{\eta}{\eta_\delta}\,d\eta\right) + \frac{d}{d\xi}\left(\frac{\vartheta_w}{k^2}\int_0^{\eta_\delta}\ln^2\frac{\eta}{\eta_\delta}\,d\eta\right) = \vartheta_w. \tag{12.4.25}$$

Here the integrals are worked out in the usual form:

$$\left.\begin{aligned}\int_0^{\eta_\delta}\ln\frac{\eta}{\eta_\delta}\,d\eta &= \eta_\delta\int_0^1\ln\frac{\eta}{\eta_\delta}\,d\left(\frac{\eta}{\eta_\delta}\right) = -\eta_\delta;\\ \int_0^{\eta_\delta}\ln^2\frac{\eta}{\eta_\delta}\,d\eta &= \eta_\delta\int_0^1\ln^2\frac{\eta}{\eta_\delta}\,d\left(\frac{\eta}{\eta_\delta}\right) = 2\eta_\delta.\end{aligned}\right\} \tag{12.4.26}$$

According to this

$$-\frac{d}{d\xi}\left[\eta_\delta\frac{\sqrt{\vartheta_w}}{k}\left(-V_\delta+\frac{2\sqrt{\vartheta_w}}{k}\right)\right]=\vartheta_w.$$

Inserting here the values of $\eta_\delta\sqrt{\vartheta_w}$ from (12.4.22) and of ϑ_w from (12.4.21), we have

$$-\frac{d}{d\xi}\left[e^z\frac{A\mu_w}{k\rho_0}\left(-V_\delta+2\frac{V_\delta}{z}\right)\right]=\frac{k^2V_\delta^2}{z^2}.$$

Dividing both sides of this equation by $A\mu_w/(\rho_0 k)$, it will be

$$\frac{d}{d\xi}\left[e^z\left(1-\frac{2}{z}\right)\right]=\frac{\rho_0k^3}{A\mu_w}\cdot\frac{V_\delta}{z^2}. \tag{12.4.27}$$

Differentiating this, we have

$$e^z\left(1-\frac{2}{z}\right)\frac{dz}{d\xi}+e^z\frac{2}{z^2}\cdot\frac{dz}{d\xi}=\frac{k^3\rho_0V_\delta}{A\mu_w z^2}.$$

Dividing both sides of this equation by

$$e^z\left(1-\frac{2}{z}\right)+e^z\frac{2}{z^2}=e^z\left(1-\frac{2}{z}+\frac{2}{z^2}\right),$$

we get

$$\frac{dz}{d\xi}=\frac{k^3\rho_0V_\delta}{A\mu_w}\cdot\frac{e^{-z}}{z^2\left(1-\frac{2}{z}+\frac{2}{z^2}\right)},$$

or

$$\frac{d(z^2e^z)}{d\xi}=\frac{\rho_0V_\delta k^3}{A\mu_w}\cdot\frac{1+\frac{2}{z}}{1-\frac{2}{z}+\frac{2}{z^2}}. \tag{12.4.28}$$

Experiments with an incompressible medium showed that at high Reynolds numbers the value of z varies within very narrow limits. This can be verified if the empirical formula for the average value of frictional stress along the length of a flat plate,

$$(\tau_w)_{inc}=0.022\rho_\delta V_\delta^2\,\mathbf{Re}_L^{-0.167} \tag{12.4.29}$$

is used. It is valid for values of $\mathbf{Re}_L=V_\delta L/\nu_w$ in the range of 5×10^6 to 10^{10}.

From (12.4.4) and (12.4.21) it follows that for an incompressible medium

$$z_{inc}=kV_\delta\Big/\sqrt{\frac{(\tau_w)_{inc}}{\rho_\delta}}; \tag{12.4.30}$$

and, assuming $k=0.3914$, we find

$$z_{\text{inc}} \approx 2.66\, \mathbf{Re}_L^{0.084}. \tag{12.4.31}$$

Let us take values of Reynolds number $\mathbf{Re}_{L1}$ and $\mathbf{Re}_{L2}=m\mathbf{Re}_{L1}$. The ratio of the corresponding values of z_{inc} is

$$(z_{\text{inc}})_2/(z_{\text{inc}})_1 = m^{0.084}. \tag{12.4.32}$$

From this it may be seen that if $m=2$, for example, the second Reynolds number is raised to twice its value the corresponding value $(z_{\text{inc}})_2$ is increased 1.06 times. This property of low variation in function z can be extended to cases of flow in the boundary layer at high speeds of flow-interaction, i.e. taking into account the medium. This property can then be used to simplify equation (12.4.28). If $z=10$ taken on the right side of this equation [as is easily seen from (12.4.31), this corresponds to the value of $\mathbf{Re}_L \approx 10^8$], then

$$\frac{1+\dfrac{2}{z}}{1-\dfrac{2}{z}+\dfrac{2}{z^2}} \approx \text{const} = 1.38$$

and hence

$$d(z^2e^z) = 1.38\rho_0 V_\delta k^3/A\mu_w.$$

Assuming $k=0.3914$ and $a=11.5$, we have the constant value

$$1.38k^3/A = 1.38k^3e^{k\alpha}/a = 0.656.$$

Thus

$$d(z^2e^z) = (0.656\rho_0 V_\delta/\mu_w)d\xi.$$

Taking $z=0$ at $\xi=0$, we get after integration

$$z^2e^z = (0.656\rho_0 V_\delta/\mu_w)\,\xi.$$

According to (12.3.6)

$$\xi = (p_\delta/p_0)x = (1-\overline{V}_\delta^2)^{k/(k-1)}\,x. \tag{12.4.33}$$

Next, using (12.4.5′) we find

$$z^2e^z = 0.656\rho_w V_\delta x/\mu_w. \tag{12.4.34}$$

Let us replace the ratio ρ_w/μ_w in (12.4.34) from (12.3.17):

$$\frac{\rho_w}{\mu_w} = \frac{1}{\nu_\delta}\left(\frac{T_\delta}{T_w}\right)^n \frac{T_\delta}{T_0} = \frac{1}{\nu_\delta}\left(\frac{T_\delta}{T_0}\right)^{n+1} = \frac{(1-\overline{V}_\delta^2)^{n+1}}{\nu_\delta}. \tag{12.4.35}$$

Introducing the notation for the Reynolds number $\mathbf{Re}_x = V_\delta \cdot x/\nu_\delta$, we get

$$z^2e^z = 0.656\,(1-\overline{V}_\delta^2)^{n+1}\mathbf{Re}_x. \tag{12.4.36}$$

The frictional stress can be determined for the value of z obtained from (12.4.36). Equations (12.4.5′) and (12.4.21) can be used to find the relation between τ_w and z:

$$\tau_w=\frac{k^2V_\delta^2}{z^2}\rho_0(1-\overline{V}_\delta^2)^{k/(k-1)}=\frac{k^2V_\delta^2\rho_\delta}{z^2}(1-\overline{V}_\delta^2)=\frac{k^2\rho_\delta V_\delta^2}{z^2}\cdot\frac{T_\delta}{T_0}. \quad (12.4.37)$$

The coefficient of local friction

$$c_{fx}=\frac{2\tau_w}{\rho_\delta V_\delta^2}=\frac{2k^2}{z^2}(1-\overline{V}_\delta^2)=\frac{2k^2}{z^2}\cdot\frac{T_\delta}{T_0}; \quad (12.4.38)$$

from which

$$z=k\sqrt{2(1-\overline{V}_\delta^2)/c_{fx}}. \quad (12.4.39)$$

Taking the logarithm of both sides of expression (12.4.36), we have

$$2\ln z+z=(n+1)\ln(1-\overline{V}_\delta^2)+\ln \mathbf{Re}_x+\ln 0.656.$$

After substitution of the value of z from (12.4.39) we arrive at the relation

$$2\ln\left[k\sqrt{2(1-\overline{V}_\delta^2)/c_{fx}}\right]+k\sqrt{2(1-\overline{V}_\delta^2)/c_{fx}}$$
$$=(n+1)\ln(1-\overline{V}_\delta^2)+\ln \mathbf{Re}_x+\ln 0.656$$

or

$$k\sqrt{2(1-\overline{V}_\delta^2)/c_{fx}}=\ln(\mathbf{Re}_x c_{fx})+n\ln(1-\overline{V}_\delta^2)+C_3,$$

where

$$C_3=\ln 0.656-2\ln(k\sqrt{2}).$$

Taking $k=0.3914$ and changing to the logarithm to the base 10, we get

$$0.242\sqrt{1-\overline{V}_\delta^2}/\sqrt{c_{fx}}=\log(\mathbf{Re}_x c_{fx})+n\log(1-\overline{V}_\delta^2)+0.33. \quad (12.4.40)$$

Since $1-\overline{V}_\delta^2=\left(1+\frac{k-1}{2}\mathbf{M}_\delta^2\right)^{-1}$ we find, using the notation $c_{fx}=(c_{fx})_c$, the relation

$$\frac{0.242}{\sqrt{(c_{fx})_c}}=\sqrt{1+\frac{k-1}{2}\mathbf{M}_\delta^2}\left\{\log[\mathbf{Re}_x(c_{fx})_c]\right.$$
$$\left.-n\log\left(1+\frac{k-1}{2}\mathbf{M}_\delta^2\right)+0.33\right\}. \quad (12.4.41)$$

Formula (12.4.41) corresponds to the expression obtained in reference [5] on the basis of the rule of logarithm as modified by Dorodnitsin. Here the numerical coefficient on the right side of this expression is equal to 0.15 and not to 0.33. This difference, however, has no significant effect on the value of $(c_{fx})_c$.

From (12.4.41) it follows that the coefficient of local friction of a flat plate diminishes with an increase in Mach number M. It should be noted that this result, valid for a flat plate, may have no meaning in the context of a boundary layer over a curved surface due to the effect of the longitudinal gradient of pressure on the flow in this layer.

The coefficient of friction is calculated from formula (12.4.41) by successive approximations. As a first approximation the coefficient $c_{fx}=(c_{fx})_c^{(1)}$ may be found from (12.4.38) for a given ratio T_δ/T_0 taking z equal to 10–12. Inserting this value of $(c_{fx})_c^{(1)}$ in the right side of (12.4.41) we get the value of $c_{fx}=(c_{fx})_c^{(2)}$ for a second approximation. This result can be improved by taking the value of $c_{fx}=(c_{fx})_c^{(2)}$ in the right side of (12.4.41) and further calculating the value of $c_{fx}=(c_{fx})_c^{(3)}$.

The resultant coefficient of frictional drag for a flat plate with allowance for compressibility is determined from formula (12.3.28) by numerical integration using expression (12.4.41) for $(c_{fx})_c$.

The coefficient of local friction for an incompressible medium can be found from (12.4.41) by putting $\mathbf{M}_\delta=0$:

$$0.242/\sqrt{(c_{fx})_{inc}} = \log [\mathbf{Re}_x (c_{fx})_{inc}] + 0.33. \tag{12.4.42}$$

Equation (12.4.6) can be used to determine the thickness of the boundary layer:

$$\delta=(1-\overline{V}_\delta^2)^{-k/(k-1)} \int_0^{\eta_\delta} (1-\overline{V}_x^2)\, d\eta. \tag{12.4.6'}$$

Introducing here the value of V_x from (12.4.24), we get

$$\delta=(1-\overline{V}_\delta^2)^{-k/(k-1)} \int_0^{\eta_\delta} \left[1-\left(\overline{V}_\delta+\frac{\sqrt{\vartheta_w}}{kV_{max}} \ln\frac{\eta}{\eta_\delta}\right)^2\right] d\eta,$$

or

$$\delta=(1-\overline{V}_\delta^2)^{-k/(k-1)} \int_0^{\eta_\delta} \left(1-\overline{V}_\delta^2-\frac{2\overline{V}_\delta\sqrt{\vartheta_w}}{kV_{max}} \ln\frac{\eta}{\eta_\delta}-\frac{\vartheta_w}{k^2V_{max}^2}\ln^2\frac{\eta}{\eta_\delta}\right) d\eta.$$

Considering the values of the integrals in (12.4.26), this will reduce to

$$\delta=(1-\overline{V}_\delta^2)^{-k/(k-1)}\left[(1-\overline{V}_\delta^2)\eta_\delta+\frac{2\overline{V}_\delta\eta_\delta\sqrt{\vartheta_w}}{kV_{max}}\eta_\delta-\frac{2\eta_\delta\vartheta_w}{k^2V_{max}^2}\right]$$

$$=(1-\overline{V}_\delta^2)^{-k/(k-1)}\eta_\delta\sqrt{\vartheta_w}\left(\frac{1-\overline{V}_\delta^2}{\sqrt{\vartheta_w}}+\frac{2\overline{V}_\delta}{kV_{max}}-\frac{2\sqrt{\vartheta_w}}{k^2V_{max}^2}\right).$$

Let us substitute here the values of $\eta_\delta\sqrt{\vartheta_w}$ and ϑ_w from (12.4.22) and (12.4.21)

respectively. Then

$$\delta=(1-\overline{V}_\delta^2)^{-k/(k-1)}\, e^z \frac{A\mu_w}{\rho_0}\left[\frac{z\,(1-\overline{V}_\delta^2)}{kV_\delta}+\frac{2\overline{V}_\delta}{kV_{max}}-\frac{2V_\delta}{kzV_{max}^2}\right].$$

Keeping in mind the expression (12.4.5′) for ρ_0 and the relation (12.4.35) for ρ_w/μ_w, we find

$$\delta=\frac{ze^zA\nu_\delta}{k\,(1-\overline{V}_\delta^2)^{n+1}V_\delta}\left[1-\overline{V}_\delta^2\left(1-\frac{2}{z}+\frac{2}{z^2}\right)\right].$$

Using the Reynolds number

$$\mathbf{Re}_L=V_\delta L/\nu_\delta$$

and keeping in view the quantities

$$1-\overline{V}_\delta^2=\left(1+\frac{k-1}{2}\mathbf{M}_\delta^2\right)^{-1},\quad \overline{V}_\delta^2=\frac{\frac{k-1}{2}\mathbf{M}_\delta^2}{1+\frac{k-1}{2}\mathbf{M}_\delta^2},\quad \frac{A}{k}=0.322,$$

we can write the following expression for the nondimensional thickness of a boundary layer:

$$\overline{\delta}=\frac{\delta}{L}=\frac{0.322ze^z}{\mathbf{Re}_L}\left(1+\frac{k-1}{2}\mathbf{M}_\delta^2\right)^{n+1}$$
$$\times\left[1-\frac{\frac{k-1}{2}\mathbf{M}_\delta^2}{1+\frac{k-1}{2}\mathbf{M}_\delta^2}\left(1-\frac{2}{z}+\frac{2}{z^2}\right)\right].$$

Replacement of z^2e^z in accordance with (12.4.36) and of z by z_c results in

$$\overline{\delta}=\overline{\delta}_c=\frac{\delta_c}{L}=\frac{0.212\overline{x}}{z_c}\left[1-\frac{\frac{k-1}{2}\mathbf{M}_\delta^2}{1+\frac{k-1}{2}\mathbf{M}_\delta^2}\left(1-\frac{2}{z_c}+\frac{2}{z_c^2}\right)\right], \quad (12.4.43)$$

where $\overline{x}=x/L$. So it is possible to find the thickness of a boundary layer with allowance for compressibility from (12.4.43) by determining $c_{fx}=(c_{fx})_c$ and calculating the corresponding value of z for given values of x and μ_δ.

For an incompressible medium

$$\overline{\delta}_{inc}=\delta_{inc}/L=0.212\,\overline{x}/z_{inc}, \quad (12.4.43')$$

where, according to (12.4.39), the quantity

$$z_{inc}=k\sqrt{2/(c_{fx})_{inc}}. \quad (12.4.39')$$

4.2 Index law for velocity distribution

The analogy of the movement of a viscous incompressible fluid through a circular cylinder (Fig. 12.4.1) can be used to establish the law of velocity distribution along the section of a turbulent boundary layer and to determine the relation for frictional stress on the surface of a flat plate. Let us examine this flow. Let us separate out the mass of fluid bounded by sections 1 and 2 lying at a distance l from each other. We assume that these sections are far enough away from the entrance to the tube for the movement of the fluid through them to be identical, i.e. tangential stresses and velocity distributions are identical. The same value of velocities at these sections indicates that the fluid particles move without undergoing any acceleration. Therefore the forces acting on the separate volume of fluid between sections 1 and 2 are supposed to be in equilibrium, i.e.

$$F=(p_1-p_2)\,(\pi d^2/4)=\tau_w\,\pi l d, \tag{12.4.44}$$

where $d=2r_0$, tube diameter; τ_w is the frictional stress at the wall. From this we have

$$p_1-p_2=4\tau_w\,(l/d). \tag{12.4.45}$$

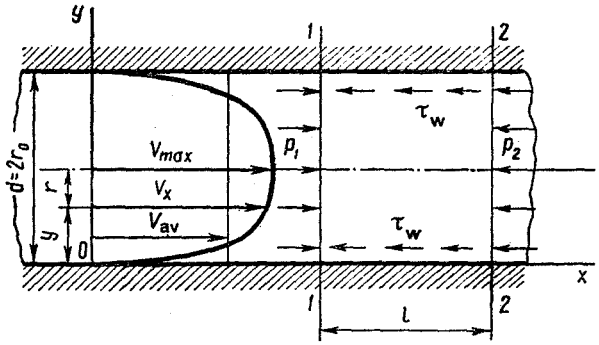

Fig. 12.4.1. Schematic representation of motion of viscous fluid in circular cylinder.

On the other hand force F in (12.4.44) can be expressed with the help of formula (1.3.5) for hydrodynamic drag. Introducing the notations for drag force $X=F$ and for coefficient of hydrodynamic drag $c_x=\lambda$ in this formula and further defining velocity head q on the basis of average velocity V_{av} in the tube (see Fig. 12.4.1), $q=\rho V_{av}^2/2$ and characteristic area of peripheral surface $S=\pi l d$, we write

$$(p_1-p_2)\,(\pi d^2/4)=\lambda\,(\rho V_{av}^2/2)\,\pi l d.$$

In this way we find the formula to determine frictional loss:

$$p_1-p_2=4\lambda\,(\rho V_{av}^2/2)\,(l/d), \tag{12.4.46}$$

where the average velocity is determined from a given flow rate Q through the tube:

$$V_{av}=4Q/\pi d^2. \tag{12.4.47}$$

The coefficient of drag λ can be obtained by experimental research. Experiments were performed by Blasius, who established that the coefficient of drag for smooth tubes in a turbulent flow regime at Reynolds numbers reaching the values

$$2.3\times 10^3 \leqslant \mathbf{Re}_d=\rho V_{av}\, d/\mu \leqslant 10^5, \tag{12.4.48}$$

will be

$$\lambda=0.3164/\mathbf{Re}_d^{1/4}. \tag{12.4.49}$$

Let us use this expression in (12.4.46) and replace (p_1-p_2) in accordance with (12.4.45). As a result

$$\tau_w=0.3164\rho V_{av}^2/(8\mathbf{Re}_d^{1/4})=0.03955\, V_{av}^{7/4}\, \rho^{3/4}\, \mu^{1/4} d^{-1/4}. \tag{12.4.50}$$

To determine average velocity V_{av} we use the results of research on the movement of a fluid through a circular tube that established that the velocity over its section varies by the law of the index of one-seventh root

$$V_x=V_{max}\,(y/r_0)^{1/7}. \tag{12.4.51}$$

This law represents the hypothesis according to which kinematic similarity is observed during motion of a fluid, i.e. the ratio of local velocity V_x to the velocity at the axis of the tube V_{max} will be the same at points with the same value of y/r_0 independent of the absolute values of tube sizes.

The average velocity over the section of tube, in accordance with (12.4.47), will be

$$V_{av}=\frac{Q}{\pi r_0^2}=\frac{\int_0^{r_0} 2\pi r V_x\, dr}{\pi r_0^2}=\frac{V_{max}\int_0^{r_0} 2\pi r\left(\frac{r_0-r}{r_0}\right)^{1/7} dr}{\pi r_0^2}$$
$$=\frac{2V_{max}}{\left(\frac{1}{7}+1\right)\left(\frac{1}{7}+2\right)}=0.816V_{max}. \tag{12.4.52}$$

Substitution of this expression in (12.4.50) results in

$$\tau_w=0.03955\,(0.816\,V_{max})^{7/4}\,\rho^{3/4}\,\mu^{1/4}\,(2r_0)^{-1/4}$$
$$=0.0233\rho V_{max}^2\,(\nu/V_{max}\,r_0)^{1/4}. \tag{12.4.53}$$

Observation of the motion of a viscous turbulent fluid along a circular tube and in a boundary layer established the identity of the velocity profiles over their sections. Here maximum velocity V_{max} at the axis of the tube corres-

ponds to velocity V_δ at the external limit of the boundary layer and radius of tube r_0 corresponds to boundary layer thickness δ.

Research showed that this analogy may be used to obtain the relations of the flow in a turbulent boundary layer. Replacing r_0 by δ and V_{max} by V_δ in (12.4.51), the index law (law of one-seventh root) of velocity distribution over the boundary layer section will be

$$V_x = V_\delta (y/\delta)^{1/7}. \tag{12.4.54}$$

A similar substitution in (12.4.53) helps us to obtain the formula for frictional stress at the wall

$$\tau_w = 0.0233\, \rho V_\delta^2 (\nu/V_\delta\delta)^{1/4}. \tag{12.4.55}$$

To determine frictional stress by (12.4.55) it is necessary to determine the thickness of the boundary layer first. For this purpose we use the integral relation (12.3.1). After substituting the relation (12.4.54) for V_x and the value of τ_w from (12.4.55), we get

$$\rho V_\delta^2 \frac{d}{dx} \int_0^\delta \left(\frac{y}{\delta}\right)^{1/7} \left[1 - \left(\frac{y}{\delta}\right)^{1/7}\right] dy = 0.0233 \rho V_\delta^2 \left(\frac{\nu}{V_\delta \delta}\right)^{1/4}. \tag{12.4.56}$$

Integration of the left side of this expression leads to

$$\frac{d}{dx}\left(\frac{7}{8}\delta - \frac{7}{9}\delta\right) = 0.0233 \left(\frac{\nu}{V_\delta \delta}\right)^{1/4}$$

or

$$\frac{d\delta}{dx} = \frac{0.0233 \times 72}{7} \left(\frac{\nu}{V_\delta \delta}\right)^{1/4}.$$

Rearranging the variables in this differential equation, we get

$$\delta^{1/4}\, d\delta = 0.2395\, (\nu/V_\delta)^{1/4}\, dx.$$

Integration of this gives

$$(4/5)\, \delta^{5/4} = 0.2395\, (\nu/V_\delta)^{1/4} x + C. \tag{12.4.57}$$

The constant of integration C must be determined, strictly speaking, from the condition at a point of transition from a laminar to a turbulent boundary layer according to which the thickness of the layer at this point is $\delta = \delta_{cr}$ at a distance $x = x_{cr}$ from the leading edge. Here the distance x_{cr} is determined from the given critical Reynolds number $\mathbf{Re}_{cr} = V_\delta\, x_{cr}/\nu$ and the thickness δ_{cr} is found for this Reynolds number $\mathbf{Re}_{cr}$ by the formula for a laminar boundary layer. At high Reynolds numbers the length of this laminar region is not large and its effect on the thickness of the turbulent boundary layer can in practice be neglected. In these cases it may be assumed that the turbulent

boundary layer starts from the leading edge, where the thickness of layer $\delta=0$ at $x=0$. According to this the constant $C=0$ in (12.4.57) and consequently the thickness of layer

$$\delta=\delta_{\max}=0.37\,(\nu_\delta/V_\delta\,x)^{1/5}\,x=(0.37/\mathbf{Re}_x^{1/5})\,x, \tag{12.4.58}$$

where $\mathbf{Re}_x=V_\delta\,x/\nu_\delta$; $\nu=\nu_\delta$.

Introducing nondimensional quantities $\bar{\delta}_{\text{inc}}=\delta_{\text{inc}}/L$, $\bar{x}=x/L$ and Reynolds number $\mathbf{Re}_L=V_\delta\,L/\nu_\delta$, equation (12.4.58) will be written in the form

$$\bar{\delta}=\bar{\delta}_{\text{inc}}=\delta_{\text{inc}}/L=0.37\,(\bar{x}^{\,4/5}/\mathbf{Re}_L^{1/5}). \tag{12.4.58'}$$

Comparing relations (12.3.19'') and (12.4.58'), it may be concluded that the thickness of a turbulent boundary layer over a flat plate is greater than the thickness of a laminar boundary layer. This is explained by the intensive intermixing of particles attributed to the turbulent character of the fluid flow.

Formula (12.4.55) can be applied for calculation of the stress τ_w. Taking $\rho=\rho_\delta$, $\nu=\nu_\delta$, we introduce the value of δ in this formula using (12.4.58):

$$\tau_w=(\tau_w)_{\text{inc}}=0.0233\rho_\delta V_\delta^2\left(\frac{\nu_\delta\,V_\delta^{1/5}x^{1/5}}{0.37\,\nu_\delta^{1/5}\,V_\delta x}\right)^{1/4}$$

$$=0.0299\rho_\delta V_\delta^2\left(\frac{\nu_\delta}{V_\delta x}\right)^{1/5}=\frac{0.0299\rho_\delta V_\delta^2}{\mathbf{Re}_x^{1/5}}, \tag{12.4.59}$$

where $\mathbf{Re}_x=V_\delta\cdot x/\nu_\delta$. Introducing the quantities $\mathbf{Re}_L=V_\delta\cdot L/\nu_\delta$ and $\bar{x}=x/L$, equation (12.4.59) will be rewritten in the form

$$(\tau_w)_{\text{inc}}=0.0299\rho_\delta V_\delta^2/(\mathbf{Re}_L^{1/5}\,\bar{x}^{1/5}). \tag{12.4.59'}$$

As may be seen from the relations (12.3.23) and (12.4.59), the frictional stress for a turbulent flow will be considerably more than for laminar flow with one and the same value of Reynolds number $\mathbf{Re}_x$. In this way, the transition to a turbulent boundary layer is accompanied by a sharp rise in tangential stresses. At the same time the frictional stress and other parameters of the boundary layer in a turbulent flow depend much less on the Reynolds number than in a laminar flow. The effect of this Reynolds number, as we already know, is based on the action of molecular forces of viscosity which are most effective in the laminar sublayer. Here, the higher the velocity the higher the Reynolds number, the thinner the sublayer and the weaker the action of the molecular forces of viscosity. Accordingly the less the effect of the Reynolds number on the flow parameters.

The coefficient of local friction can be determined from the value of tangential stress:

$$(c_{fx})_{\text{inc}}=2(\tau_w)_{\text{inc}}/(\rho_\delta V_\delta^2)=0.0598/\mathbf{Re}_x^{1/5} \tag{12.4.60}$$

or

$$(c_{fx})_{\text{inc}}=0.0598/(\mathbf{Re}_L^{1/5}\bar{x}^{1/5}). \tag{12.4.60'}$$

The frictional drag force for one side of the plate is determined with the help of formula and (12.3.28):

$$X_{f\text{inc}}=\int_0^L (\tau_w)_{\text{inc}}\,dx\,. \tag{12.4.61}$$

According to this formula and (12.4.60') the coefficient of frictional drag will be

$$(c_{xf})_{\text{inc}}=\frac{2X_{f\text{inc}}}{\rho_\delta V_\delta^2 L\cdot 1}=\frac{1}{L}\int_0^L \frac{2\,(\tau_w)_{\text{inc}}}{\rho_\delta V_\delta^2}\,dx=\frac{0.0598}{\mathbf{Re}_L^{1/5}}\int_0^1 \frac{d\bar{x}}{\bar{x}^{1/5}}\,,$$

whence

$$(c_{xf})_{\text{inc}}=0.075/\mathbf{Re}_L^{1/5}. \tag{12.4.62}$$

5. Temperature and Enthalpy in Boundary Layer in Presence of Heat Transfer

So far the boundary layer has been studied on the assumption that the effect of compressibility is either non-existent (low velocities of flow) or (if the velocities are high) appears in the form of temperature reactions based on the absence of heat-transfer at the wall. This case, as we know from an earlier discussion, corresponds to Prandtl's number equaling unity.

The real processes in a boundary layer are, in fact, characterized by the presence of heat transfer at the wall that changes the temperature distribution and at the same time has an effect on friction. In this section we will study the possible nature of temperature (enthalpy) distribution due to heat flows in the boundary layer at the surface or in their absence when Prandtl number $\mathbf{Pr}\neq 1$, without dealing directly with the calculation of heat-transfer itself. In Section 6 we will use these data for an approximate method of calculating friction and other parameters of the boundary layer in a high-temperature gas flow over a flat plate. It will be shown that these methods, in a simplified form, facilitate determination of frictional parameters taking into account the dissociation and ionization that are possible in a boundary layer heated to a high temperature.

5.1 Distribution of temperature and enthalpy

At a low speed of flow-interaction heating of gas based on stagnation in the boundary layer is almost absent and the temperature can be considered practically equal to its value in the free flow. Actually it follows from

(12.3.18) that in the absence of heat transfer the temperature of the gas at the wall for $\mathbf{M}_\delta = 0.5$ is equal to stagnation temperature $T_w = T_0 = T_\delta\ (1 + 0.2 \times 0.25) = 1.05 T_\delta$, i.e. it differs from the temperature in the free flow by only 5 %.

At high speeds a considerable rise in temperature and enthalpy takes place in the boundary layer due to retardation of the gas flow. This increase corresponds to the nature of variations in velocity over a section of the boundary layer.

If all other forms of heat transfer are absent except heat conduction, Prandtl number $\mathbf{Pr} = 1$ and heat transfer at the wall is equal to zero the temperature in the boundary layer, according to equation (12.1.16), will be

$$T = T_0 - [V_x^2/2\,(c_p)_{av}], \tag{12.5.1}$$

where $(c_p)_{av}$ is the average specific heat in the interval of temperature $(T_0 - T)$. Temperature T_0, being the measure of total energy, does not change over the thickness of the boundary layer. It is determined by the parameters $T = T_\delta$, $V_x = V_\delta$ at the external limit of the boundary layer from the expression

$$T_0 = T_\delta + [V_\delta^2/2(c_p)_{av}]. \tag{12.5.2}$$

Carrying out the following substitutions here:

$$\left.\begin{aligned} V_\delta^2 &= \mathbf{M}_\delta^2 a_\delta^2 = \mathbf{M}_\delta^2 \bar{k} R T_\delta\,; \\ (c_p)_{av} &= R \frac{(c_p)_{av}}{(c_p)_{av} - (c_v)_{av}} = \frac{R\bar{k}}{\bar{k} - 1}, \end{aligned}\right\} \tag{12.5.3}$$

where $\bar{k} = (c_p)_{av}/(c_v)_{av}$ is the average value of the ratio of specific heats over the interval of temperature $(T_0 - T_\delta)$, we get

$$T_0 = T_\delta \left(1 + \frac{\bar{k} - 1}{2} \mathbf{M}_\delta^2\right). \tag{12.5.4}$$

At constant specific heats we have $(c_p)_{av} = c_p = \text{const}$ and $\bar{k} = k = \text{const}$. In cases where the specific heat considerably varies with temperature as a result of dissociation and ionization and cannot be replaced by the average value it is advisable to use enthalpy i and i_0 in place of T and T_0 respectively. According to (3.4.14) and by analogy with (12.5.1) the enthalpy at a point on the section of a boundary layer is given by

$$i = i_0 - (V_x^2/2). \tag{12.5.5}$$

Substituting here values of $i = i_\delta$ and $V_x = V_\delta$, we find the following relation for stagnation enthalpy:

$$i_0 = i_\delta + (V_\delta^2/2). \tag{12.5.6}$$

At constant specific heats

$$i_\delta = c_p T_\delta = kRT_\delta/(k-1) = a_\delta^2/(k-1); \tag{12.5.7}$$

therefore (since $\mathbf{M}_\delta = V_\delta/a_\delta$)

$$i_0 = i_\delta\left(1+\frac{V_\delta}{2i_\delta}\right) = i_\delta\left(1+\frac{k-1}{2}\mathbf{M}_\delta^2\right). \tag{12.5.8}$$

The assumptions of absence of heat transfer at the wall and Prandtl's number $\mathbf{Pr}=1$ do not correspond to reality. Therefore in actual conditions the temperature and enthalpy on the wall differ from the values of T_0 and i_0 obtained earlier.

Let us consider the case already discussed of an adiabatic (thermally insulated) wall which is characterized by the fact that the heat carried to the wall from the boundary layer is not spent on heating it and the wall surface by itself does not give out heat to the boundary layer. Meantime the exchange of energy in the boundary layer itself takes the following form: The temperature rises from its value at the outer edge of the layer to some value on the wall as a result of stagnation of flow, which is based on the action of viscous forces, and so the temperature gradient rises, i.e. $\partial T/\partial y \neq 0$. In this case according to Fourier's law (3.2.7) there must occur heat transfer by heat conduction to the external layers of gas at lower temperature. This heating process will continue until equilibrium is reached between this heat transfer and the reverse flow of heat from the external layers to the inner layer, which is based on the work done by viscous force. As a consequence of the outflow of heat from the regions of the boundary layer situated at the wall the temperature on the wall surface $T_w = T_r$ will be less than the stagnation temperature T_0. The temperature T_r and the corresponding enthalpy i_r are known as the temperature of recovery and enthalpy of recovery respectively. The fall in temperature at the wall may be characterized by the parameter

$$r = (T_r - T_\delta)/(T_0 - T_\delta), \tag{12.5.9}$$

known as the coefficient of recovery of temperature. It indicates how close the temperature of recovery is to the stagnation temperature. This coefficient characterizes the fraction of kinetic energy of the external flow that is transferred to heat content (enthalpy) during complete stagnation.

From (12.5.9) it is possible to get the following expression for the temperature of recovery:

$$T_r = T_\delta + r(T_0 - T_\delta) = T_\delta\left[1+r\left(\frac{T_0}{T_\delta}-1\right)\right]. \tag{12.5.10}$$

Inserting here the values of difference $(T_0 - T_\delta)$ from (12.5.2) and the ratio T_0/T_δ from (12.5.4), we get

$$T_r = T_\delta + r\frac{V_\delta^2}{2(c_p)_{\text{av}}}; \tag{12.5.11}$$

$$T_r = T_\delta\left(1 + r\,\frac{\bar{k}-1}{2}\,\mathbf{M}_\delta^2\right). \tag{12.5.12}$$

In investigating the motion of viscous dissociating gases it is better to go to other relations. For such gases the considerable increase in specific heat is a characteristic property because the losses of part of the energy for dissociation are added to the heat energy. In similar cases it is convenient to use temperature as the measure of energy. For this purpose it is better to use enthalpy.

In a given case the enthalpy of recovery i_r and the corresponding coefficient of recovery of enthalpy r where

$$r = (i_r - i_\delta)/(i_0 - i_\delta) \tag{12.5.13}$$

should be used to evaluate the effect of heat transfer in the boundary layer.

Like the concept of the coefficient of recovery of temperature r, the introduction of a similar coefficient of recovery of energy is justified in the study of heat transfer under the conditions of high-speed flows in the absence of dissociation for $\mathbf{Pr} \neq 1$. This can take into account the transformation of chemical energy into heat energy.

From (12.5.10) it follows that

$$i_r = i_\delta + r(i_0 - i_\delta) = i_\delta\left[1 + r\left(\frac{i_0}{i_\delta} - 1\right)\right]. \tag{12.5.14}$$

Using formulas (12.5.6) for $(i_0 - i_\delta)$ and (12.5.8) for i_0/i_δ, we get

$$i_r = i_\delta + r\,(V_\delta^2/2); \tag{12.5.15}$$

$$i_r = i_\delta\left(1 + r\frac{k-1}{2}\,\mathbf{M}_\delta^2\right). \tag{12.5.16}$$

The variation of temperature T and enthalpy i over the section of the boundary layer can be explained with the help of coefficient of recovery r. By analogy with (12.5.11) and (12.5.15)

$$T_r = T + r\,[V_x^2/2\,(c_p)_{\text{av}}];$$

$$i_r = i + r\,(V_x^2/2),$$

whence

$$T = T_r - r\,[V_x^2/2\,(c_p)_{\text{av}}]; \tag{12.5.17}$$

$$i = i_r - r\,(V_x^2/2), \tag{12.5.18}$$

where $(c_p)_{\text{av}}$ is the average specific heat for the interval of temperatures $(T_r - T)$.

In Chapter 3 Section 5 it was noted that the relation between the heat flow based on friction and the quantity of heat carried by molecules during their intermixing is determined by Prandtl's number [see (3.5.11)]. Therefore

it is natural to assume that the coefficient of recovery r depends on Prandtl's number which, for the condition at the wall, is given by analogy with (3.5.11):

$$\mathbf{Pr} = \mu_w (c_p)_w / \lambda_w. \tag{12.5.19}$$

From theoretical and experimental research it has been established that the coefficient of recovery can be taken as

$$r_L = \sqrt{\mathbf{Pr}}, \tag{12.5.20}$$

for a laminar flow and

$$r_T = \sqrt[3]{\mathbf{Pr}} \tag{12.5.21}$$

for a turbulent flow.

The Prandtl number for air varies from 0.75 at low temperatures to 0.65 at high temperatures. The average value of the Prandtl number $\mathbf{Pr}=0.7$ can be used for practical purposes. This value corresponds to

$$r_L \approx 0.84 \text{ and } r_T \approx 0.89. \tag{12.5.22}$$

For $\mathbf{Pr}=1$ the coefficient of recovery $r=1$. In this case the temperature of recovery coincides with that at the stagnation condition.

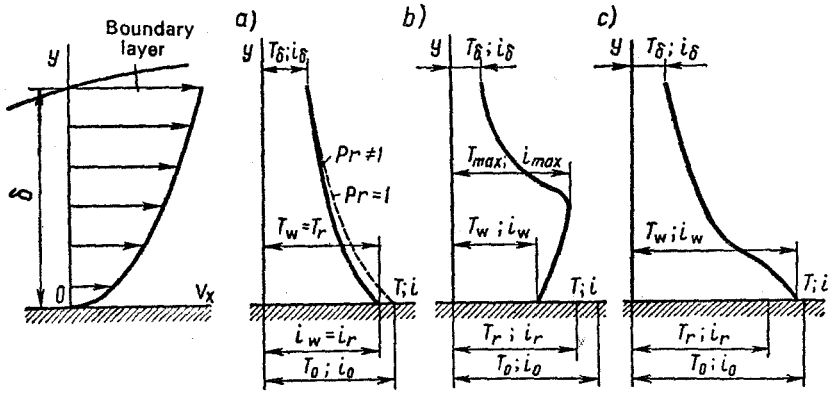

Fig. 12.5.1. Variation in temperature and enthalpy over section of boundary layer: *a*—adiabatic (thermally insulated) wall; *b*—wall with cooling; *c*—wall with heating.

The nature of variation of temperature and enthalpy over the section of a boundary layer under different conditions of flow-interaction is shown in Fig. 12.5.1. Here the curves in Fig. 12.5.1, a characterize the variation of temperature and enthalpy for a thermally insulated wall when $\mathbf{Pr}=1$ and $\mathbf{Pr}\neq 1$. Of course the distribution of temperature and enthalpy changes in the case of a conducting wall, i.e. in the presence of inflow or outflow of heat

(Fig. 12.5.1, b and c). During outflow of heat (wall becoming cooler) the thermally insulated boundary layer giving off heat itself gets cooler and therefore the temperature of gas T_w at the wall is lower than the recovery temperature T_r. Consequently the enthalpy of gas i_w is less than the enthalpy of recovery i_r. Here the temperature of gas T_w may be taken as the temperature of the surface, which will also be known as the wall temperature. If heat flows from some external source and the wall temperature exceeds the maximum temperature in the boundary layer (wall under heating), the boundary layer will also be heated and hence $T_w > T_r$ and $i_w > i_r$ for the gas near the surface.

At very high speeds the wall of a flight vehicle is usually cooled ($i_w < i_r$; $T_w < T_r$), which is explained by radiation of heat from the surface that cannot be compensated by the comparatively low inflow of heat through heat conduction along the material of the wall from the sources of heat situated inside the flight vehicle. Let us denote the temperature of this wall by T_w, i.e. the same as the temperature of the gas at the wall. However, it must be remembered that in the most general case the temperature of the gas does not coincide with the wall temperature and besides that it differs from T_r. The quantity i_w indicated earlier should be regarded as the enthalpy of a hypothetical gas whose temperature could have been equal to wall temperature T_w.

A moving vehicle may heat up ($i_w > i_r$; $T_w > T_r$) if it is losing speed and there is a concomitant reduction in the temperature of recovery and the overheated wall cannot lose heat fast enough.

In aerodynamic wind tunnels where special heating of air is absent and stagnation temperature is closer to the temperature of the surrounding medium the wall of the experimental model may possibly accept heat. This is explained by the fact that the heat flow to the surface of the model may occur through the stand (supposing the model), when radiational flow from the cool wall of the model will be negligibly small.

Temperature of recovery in a dissociating gas: Let us consider the variation of temperature of recovery in a dissociating gas with the help of formula (12.5.15). For this purpose we use the expression (1.5.27) which, for a diatomic dissociating gas, can be represented in the form

$$i = i_A\, a + i_M\,(1-a) = a(i_A - i_M) + i_M,$$

where i_A and i_M are enthalpies of atomized and molecular gases respectively. We know that the partial derivative $\partial i/\partial a$ represents enthalpy of dissociation i_R which is equal to the characteristic energy of dissociation u_d according to (1.5.15). Further, taking into account that $i_M = c_{pM} \cdot T$ (where c_{pM} is the specific heat of a perfect gas, taken as constant), we get

$$i = a u_d + c_{pM}\, T.$$

According to this

$$i_r = a_r u_d + c_{pM} T_r;$$
$$i_\delta = a_\delta u_d + c_{pM} T_\delta,$$

where

$$a_r = f_1 (p_\delta, T_r) \text{ and } a_\delta = f_2 (p_\delta, T_\delta).$$

Consequently

$$i_r - i_\delta = c_{pM} (T_r - T_\delta) + (a_r - a_\delta) u_d.$$

So we can write

$$c_{pM} (T_r - T_\delta) = r (V_\delta^2/2) - (a_r - a_\delta) u_d.$$

The following conclusion can be drawn from this expression. As $T_r > T_\delta$ we have $a_r > a_\delta$ and consequently the temperature of recovery in a dissociating gaseous medium will be less than in the absence of dissociation. This means that part of the internal energy is spent in overcoming and breaking molecular bonds and so cannot be used to heat the gas. The lowest recovery temperature will be in the limiting case which corresponds to absence of dissociation of the gas at the extremity of the boundary layer ($a_\delta = 0$) and complete dissociation at the wall ($a_r = 1$):

$$T_r = T_\delta + (rV_\delta^2/2c_{pM}) - (u_d/c_{pM}).$$

Assuming that the characteristic temperature of dissociation $T_d = u_d/R$ and $c_{pM} = [k/(k-1)]\, R$, we can also write:

$$T_r = T_\delta + (rV_\delta^2/2c_{pM}) - [(k-1)/k]\, T_d,$$

where the quantity $k = c_{pM}/c_{vM}$ refers to undissociated gas.

Going back to the ratios of temperatures and recalling that

$$\frac{V_\delta^2}{a_\delta^2} = \frac{V_\delta^2}{kRT_\delta} = \mathbf{M}_\delta,$$

we find

$$\frac{T_r}{T_\delta} = 1 + \frac{k-1}{2}\left(r\,\mathbf{M}_\delta^2 - \frac{2T_d}{kT_\delta}\right).$$

5.2 Characteristic temperature

The presence of the Mach number in the above relations for determination of the flow parameters of a viscous medium reflects the fact that the density changes as a result of stagnation of flow in the boundary layer and the consequent rise in temperature. Meantime there appears the property of compressibility which affects the gas flow in the boundary layer. The temperature increases with increase in speed, leading to changes in the thermodynamic

parameters and kinetic coefficients of the gas in the boundary layer along with the change in density. At high temperature chemical reactions may also take place.

These phenomena are important for the formulation of the processes of friction and heat exchange in the boundary layer. However, adjustment for these phenomena in the calculation of the boundary layer parameters and particularly the distribution of temperature across the section, which is very complicated in character, is fraught with difficulty. Therefore attempts have been made to find comparatively easy approximate methods of calculation of the boundary layer parameters at very high speeds of flow-interaction. One of the methods pursued is based on the use of relations similar in external form to the relations obtained as a result of study of the boundary layer in an incompressible medium.

This possibility follows from the fact that the flow is very much slowed down (stagnated) in the part of the boundary layer adjacent to the wall and hence the gas is closer to an incompressible medium in its properties. If it is assumed that the flow in this region is mainly responsible for the processes of friction and heat transfer relations of the form used for an incompressible medium can be used to calculate the boundary layer parameters. The difference lies in the fact that parameters that can be determined as functions of temperature enter into these relations. This of course raises the question which particular temperature in the boundary layer these parameters should be calculated on the basis of.

As shown by theoretical and experimental research, satisfactory results are obtained when the calculation is based on the characteristic temperature T^*, which represents an average value over a section of the boundary layer. The gas parameters calculated for the temperature T^* are known as the characteristic parameters (enthalpy i^*, density ρ^*, coefficient of dynamic viscosity μ^*, etc.).

At high speeds where physico-chemical transformations play an important part in the boundary layer the characteristic enthalpy i^* can be taken as the basis of the calculation of parameters as the other characteristic parameters including temperature T^* are calculated from this enthalpy.

The following formula for characteristic enthalpy was obtained by Ackeret by solving the equation of heat transfer for a laminar boundary layer:

$$i^* = 0.5\,(i_w + i_\delta) + 0.22\,(i_r - i_\delta). \qquad (12.5.23)$$

The characteristic enthalpy depends on the structure of the boundary layer and also on Mach number $\mathbf{M}_\infty$. There exists a series of relations facilitating calculation of the quantity i^* independently for laminar and turbulent boundary layers and also for different ranges of Mach number $\mathbf{M}_\infty$. Formula (12.5.23) differs from these relations by its universal nature and can be used with known accuracy for laminar as well as turbulent flows in a fairly wide range

of Mach numbers $\mathbf{M}_\infty$.

As may be seen from (12.5.23) it is necessary to know the enthalpy of gas i_w at the wall temperature in order to calculate i^*. In a particular case when the surface temperature is maintained at the required level with the help of some special cooling device this enthalpy will be a known quantity. If the heating takes place automatically the determination of i_w is connected with the solution of the problem of heat transfer between wall and gas. In a particular case of a thermally insulated wall $i_w = i_r$ the characteristic enthalpy

$$i^* = 0.72 i_r + 0.28\, i_\delta. \tag{12.5.24}$$

Enthalpy i_r, without allowance for heat transfer in the boundary layer and with $\mathbf{Pr}=1$, will be equal to stagnation enthalpy i_0, which is calculated from (12.5.6). According to this

$$i^* = 0.72\left(i_\delta + \frac{V_\delta^2}{2}\right) + 0.28 i_\delta = i_\delta + 0.36 V_\delta^2. \tag{12.5.24'}$$

Enthalpy i_δ at the external limit of the boundary layer can be found by solving the problem of flow-interaction between the given surface and an inviscid gas flow. The recovery enthalpy i_r, appearing in (12.5.23) and (12.5.24), is determined from the expression

$$i_r = i_\delta + r^* (V_\delta^2/2), \tag{12.5.25}$$

where the coefficient of recovery can be worked out as the definitive parameter from formulas (12.5.20), (12.5.21):

$$r_L^* = \sqrt{\mathbf{Pr}^*}; \tag{12.5.26}$$

$$r_T^* = \sqrt[3]{\mathbf{Pr}^*}. \tag{12.5.27}$$

Here Prandtl's number

$$\mathbf{Pr}^* = c_p^* \mu^* / \lambda^* \tag{12.5.28}$$

is found from the definitive values of specific heat and coefficients of dynamic viscosity and heat conductivity.

The relation (12.5.23) is used in the general case of a dissociating gas as well as in the case where the gas in the boundary layer is heated to a point where dissociation does not begin but the specific heat changes. The characteristic temperature T^* in the first case is found as a function of p and i^*. The tables or diagrams of state of air at very high temperatures can be used for the calculations. The relation (12.5.23) can be applied in the second case to find the characteristic temperature. In this relation enthalpy is replaced by temperature in accordance with the expressions

$$\left.\begin{aligned} i^* - i_\delta &= (c_p)_{av}^* (T^* - T_\delta); \\ i_w - i_\delta &= (c_p)_{av}^{(w)} (T_w - T_\delta); \\ i_r - i_\delta &= (c_p)_{av}^{(r)} (T_r - T_\delta). \end{aligned}\right\} \tag{12.5.29}$$

where average values of specific heats $(c_p)^*_{av}$, $(c_p)^{(w)}_{av}$ and $(c_p)^{(r)}_{av}$ are calculated for the interval of temperatures T^*-T_δ, T_w-T_δ and T_r-T_δ respectively.

Substituting the values of enthalpies from (12.5.29) in (12.5.23), we get the relation for characteristic temperature T^*. Here the recovery temperature can be found with the help of formulas (12.5.11), (12.5.12), which can be written in the following form:

$$T_r=T_\delta+r^*\,[V_\delta^2/2\,(c_p)^*_{av}]; \tag{12.5.30}$$

$$T_r=T_\delta\left(1+r^*\,\frac{\bar{k}^*-1}{2}\mathrm{M}_\delta^2\right). \tag{12.5.31}$$

When the specific heats are practically independent of temperature (at $T\approx 700$ to 800°K and below), we have

$$T^*=0.5\,(T_w+T_\delta)+0.22\,(T_r-T_\delta). \tag{12.5.32}$$

For a thermally insulated wall we take $T_w=T_r$ and consequently

$$T^*=0.72T_r+0.28T_\delta. \tag{12.5.33}$$

Thermodynamic functions and kinetic coefficients are calculated according to characteristic temperature using formulas (1.4.1), (1.4.2), (1.4.4) expressed in the form

$$\left.\begin{aligned} c_p^*/c_{p\infty}&=(T^*/T_\infty)^\varphi;\\ \mu^*/\mu_\infty&=(T^*/T_\infty)^n;\\ \lambda^*/\lambda_\infty&=(T^*/T_\infty)^\kappa. \end{aligned}\right\} \tag{12.5.34}$$

6. Application of Characteristic Parameters for Boundary Layer Calculations over Flat Plate at High Speeds of Flow-Interaction

6.1 Laminar boundary layer

The relation between the basic characteristics of a laminar boundary layer for an inviscid fluid and a compressible gas, i.e. at high speeds of flow-interaction, can be obtained by using the concept of characteristic parameters. For this purpose we introduce corresponding parameters for an incompressible boundary layer in the relations obtained earlier (see Sections 3 and 4).

Let us consider the thickness of the boundary layer. Its value for an incompressible medium is determined by the formula (12.3.19′), which will be written in the form

$$\delta_{inc}=4.64\,\sqrt{\mu_\delta x/(V_\delta\rho_\delta)}\;;$$

in which the parameters of a boundary layer in an incompressible medium are given with index δ.

A similar formula will be obtained for a compressible gas if the values of

μ_δ and ρ_δ are replaced by the corresponding characteristic parameters μ^* and ρ^*:

$$\delta_c = 4.64\sqrt{\mu^* x/(V_\delta \rho^*)}. \tag{12.6.1}$$

The thickness ratio

$$\delta_c/\delta_{inc} = \sqrt{(\mu^*/\mu_\delta)(\rho_\delta/\rho^*)}. \tag{12.6.2}$$

A similar comparison may be made for frictional stress.

According to (12.3.23), for an incompressible fluid

$$(\tau_w)_{inc} = 0.323\rho_\delta V_\delta^2 \sqrt{\mu_\delta/V_\delta \rho_\delta x)},$$

and for a compressible gas

$$(\tau_w)_c = 0.323\rho^* V_\delta^2 \sqrt{\mu^*/(V_\delta \rho^* x)}. \tag{12.6.3}$$

The ratio of frictional stresses will then be

$$(\tau_w)_c/(\tau_w)_{inc} = \sqrt{(\rho^*/\rho_\delta)(\mu^*/\mu_\delta)}. \tag{12.6.4}$$

For local frictional coefficients on the basis of velocity head of free flow $q_\delta = \rho_\delta V_\delta^2/2$ we have

$$(c_{fx})_{inc} = 2(\tau_w)_{inc}/(\rho_\delta V_\delta^2) = 0.646\sqrt{\mu_\delta/(V_\delta \rho_\delta x)};$$

$$(c_{fx})_c = 2(\tau_w)_c/(\rho_\delta V_\delta^2) = 0.646\sqrt{\frac{\mu^*}{V_\delta \rho^* x}} \cdot \frac{\rho^*}{\rho_\delta}. \tag{12.6.5}$$

The ratio of these coefficients

$$(c_{fx})_c/(c_{fx})_{inc} = (\tau_w)_c/(\tau_w)_{inc} = \sqrt{(\rho^*/\rho_\delta)(\mu^*/\mu_\delta)}. \tag{12.6.6}$$

According to (12.3.30) the frictional drag coefficient (or average frictional coefficient over the length of the plate) in an incompressible medium

$$(c_{xf})_{inc} = 1.292\sqrt{\mu_\delta/(V_\delta \rho_\delta L)}.$$

The comparable relation for a compressible gas using (12.3.28′) and (12.6.5) will be

$$(c_{xf})_c = \frac{1}{2}\int_0^L (c_{fx})_c\, dx = \frac{0.646}{L}\int_0^L \sqrt{\frac{\mu^*}{V_\delta^* \rho}} \cdot \frac{\rho^*}{\rho_\delta} \cdot \frac{dx}{\sqrt{x}}. \tag{12.6.7}$$

At constant wall temperature the quantities μ^* and ρ^* are independent of coordinate x. Therefore

$$(c_{xf})_c = 1.292\sqrt{\mu^*/(V_\delta \rho^* L)} \cdot (\rho^*/\rho_\delta). \tag{12.6.8}$$

Hence the ratio of frictional coefficients

$$(c_{xf})_c/(c_{xf})_{inc} = (c_{fx})_c/(c_{fx})_{inc} = (\tau_w)_c/(\tau_w)_{inc} = \sqrt{(\mu^*/\mu_\delta)(\rho^*/\rho_\delta)}. \tag{12.6.9}$$

Let us consider the case where dissociation takes place in the boundary layer as a result of high temperature during free flow at constant specific heat. Assuming here that the pressure does not change across the boundary layer section, it is possible to write the relation for the ratio of densities using the equation of state:

$$\rho^*/\rho_\delta=(\mu^*_{av}/\mu_{av\,\delta})\,(T_\delta/T^*), \tag{12.6.10}$$

where μ^*_{av} is the definitive average molecular weight of the gas.

Next, applying the law of index (1.4.2) for the coefficient of dynamic viscosity, we have

$$\mu^*/\mu_\delta=(T^*/T_\delta)^n. \tag{12.6.11}$$

Inserting (12.6.10) and (12.6.11) in (12.6.2) and (12.6.9), we get

$$\delta_c/\delta_{inc}=(T^*/T_\delta)^{(n+1)/2}\left(\frac{\mu_{av\delta}}{\mu^*_{av}}\right)^{1/2}, \tag{12.6.12}$$

$$(c_{xf})_c/(c_{xf})_{inc}=(c_{fx})_c/(c_{fx})_{inc}$$
$$=(\tau_w)_c/(\tau_w)_{inc}=(T^*/T_\delta)^{(n-1)/2}\,(\mu^*_{av}/\mu_{av\delta})^{1/2}. \tag{12.6.13}$$

Formula (12.6.12) shows that the thickness of the laminar boundary layer depends closely on the quantity T^*/T_δ and hence, on Mach number $\mathbf{M}_\delta$ (velocity V_δ) and ratio T_w/T_δ. The boundary layer thickness increases with any increase in these parameters. The dependence of the frictional coefficient on the definitive temperature and consequently on $\mathbf{M}_\delta$ and T_w/T_δ is comparatively loose and is of inverse character. The coefficient of friction decreases with a rise in temperature.

Application of formulas (12.6.12), (12.6.13) is connected with the calculation of T^* and μ^*_{av} for a dissociating gas in a boundary layer. First the characteristic enthalpy i^* is found and then T^* and μ^*_{av} are worked out with the help of tables or graphs of thermodynamic functions for a given pressure p_δ and the above value of i^*. If dissociation is not taken into account T^* can be obtained directly from (12.5.32) and the ratio $\mu^*_{av}/\mu_{av\delta}$ in (12.6.12), (12.6.13) is taken as unity, i.e. in this case

$$\delta_c/\delta_{inc}=(T^*/T_\delta)^{(n+1)/2}; \tag{12.6.14}$$

$$(c_{xf})_c/(c_{xf})_{inc}=(c_{fx})_c/(c_{fx})_{inc}=(\tau_w)_c/(\tau_w)_{inc}=(T^*/T_\delta)^{(n-1)/2}. \tag{12.6.15}$$

Comparing the values obtained from formulas (12.6.12), (12.6.14), (12.6.13) and (12.6.15) respectively, we can draw a conclusion as to the effect of dissociation on the thickness of the boundary layer and frictional force. From direct comparison of the relations (12.6.12) and (12.6.14), in which the ratios T^*/T_δ are assumed to be the same, it follows that dissociation results in reduction of the thickness of the boundary layer as $\mu_{av\delta}/\mu^*_{av}<1$. In fact, if

he ratio T^*/T_δ in the above equations is not equal the reduction in the thickness of the boundary layer will be still larger because the temperature T^* in a dissociating boundary layer [formula (12.6.12)] is less than that without dissociation [formula (12.6.14)].

The frictional stress will be somewhat greater in a dissociating gas due to the lower temperature. This reduction in temperature is responsible for a stronger interaction than the rise in average molecular weight [see formula (12.6.13)]. This change in frictional stress may be physically explained by the fact that the density of the gas increases and its viscosity decreases with an increase in dissociation and the consequent reduction in temperature. The effect of dissociation on frictional force is the opposite: this force increases with an increase in density and decreases with a reduction in viscosity. However, the increase in density is more intensive than the reduction in viscosity and hence frictional force increases. Here it should be noted that the above-mentioned rise in frictional forces will be somewhat higher due to the formation of additional molecules of gas during dissociation (average molecular weight increases) and due to the consequent rise in viscosity.

As can be seen from the above discussion, the simple method of calculation of a boundary layer based on characteristic parameters is quite effective because it helps to account for the effect on the thickness of the boundary layer and frictional force of factors such as compressibility, variation in specific heats, dissociation and heat transfer. The last factor has its own expression in terms of the relation of characteristic temperature T^* on the temperature of recovery T_r and the wall temperature $T_w \neq T_r$ (with inflow or outflow of heat to or from the wall).

6.2 Turbulent boundary layer

The relations for the thickness of the boundary layer, frictional stress and coefficient of friction in the case of a turbulent flow can be obtained with the help of the characteristic parameters in the same way as for a laminar boundary layer. Here we will make use of the relations for the parameters of a turbulent boundary layer in an incompressible medium that were obtained with the help of the index law of velocity distribution over the section of the boundary layer (law of one-seventh power).

The thickness of the boundary layer in an incompressible medium is determined by formula (12.4.58), which will be written in the form

$$\delta_{inc} = 0.37\,(\mu_\delta / V_\delta\,\rho_\delta)^{1/5}\,x^{4/5}.$$

Replacing μ_δ and ρ_δ here by their characteristic values μ^* and ρ^*, we get the relation for boundary layer thickness in a compressible gas flow

$$\delta_c = 0.37\,(\mu^*/V_\delta \rho^*)^{1/5}\,x^{4/5}. \tag{12.6.16}$$

The ratio of thicknesses will be

$$\delta_c/\delta_{inc}=(\mu^*/\mu_\delta)^{1/5}\,(\rho_\delta/\rho^*)^{1/5}. \tag{12.6.17}$$

Let us consider how to find the frictional stress in a turbulent compressible boundary layer. For this purpose we write the expression for τ_w in a turbulent incompressible boundary layer using (12.4.59) as:

$$(\tau_w)_{inc}=0.0299\rho_\delta V_\delta^2\,(\mu_\delta/V_\delta\,\rho_\delta)^{1/5}\,\bar{x}^{1/5}.$$

Introducing the definitive parameters here, we find the corresponding relation for a compressible gas

$$(\tau_w)_c=0.0299\rho^*\,V_\delta^2(\mu^*/V_\delta\,\rho^*)^{1/5}\,\bar{x}^{1/5}. \tag{12.6.18}$$

The ratio of the frictional stresses

$$(\tau_w)_c/(\tau_w)_{inc}=(\mu^*/\mu_\delta)^{1/5}\,(\rho^*/\rho_\delta)^{4/5}. \tag{12.6.19}$$

Similar relations will be obtained for the local frictional coefficient c_{fx} and average frictional coefficient c_{xf}:

$$\begin{aligned}(c_{xf})_c/(c_{xf})_{inc}&=(c_{fx})_c/(c_{fx})_{inc}\\&=(\tau_w)_c/(\tau_w)_{inc}=(\mu^*/\mu_\delta)^{1/5}\,(\rho^*/\rho_\delta)^{4/5},\end{aligned} \tag{12.6.20}$$

where $(c_{fx})_{inc}$ and $(c_{xf})_{inc}$ are determined by formulas (12.4.60) and (12.4.62) respectively.

Taking the general case of a dissociating gas, we will calculate the ratios ρ^*/ρ_δ and μ^*/μ_δ by formulas (12.6.10) and (12.6.11) respectively. Then

$$\delta_c/\delta_{inc}=(T^*/T_\delta)^{(n+1)/5}\,(\mu_{av\delta}/\mu^*_{av})^{1/5}; \tag{12.6.21}$$

$$\begin{aligned}(c_{xf})_c/(c_{xf})_{inc}&=(c_{fx})_c/(c_{fx})_{inc}\\&=(\tau_w)_c/(\tau_w)_{inc}=(T^*/T_\delta)^{(n-4)/5}\,(\mu^*_{av}/\mu_{av\delta})^{4/5}.\end{aligned} \tag{12.6.22}$$

From these formulas it can be seen that the qualitative picture of variation in boundary layer thickness and frictional force in a turbulent flow is the same as for a laminar flow, namely the thickness of the layer increases and frictional force decreases with a rise in characteristic temperature. However, quantitative evaluation of this variation shows that according to (12.6.21) the thickness of a turbulent boundary layer increases more slowly with the rise in characteristic temperature than that of a laminar layer and the coefficient of friction falls more steeply [see (12.6.22)].

The effect of dissociation will be the same as for a laminar boundary layer. It will result in some reduction in the thickness of the boundary layer and an increase in frictional stress.

The boundary layer thickness and coefficients of friction in the presence of dissociation will be determined by formulas (12.6.21) and (12.6.22) respectively using the method of successive iterations. First we find the characteristic enthalpy i^* by formula (12.5.23) for a given wall temperature T_w and

conditions of undisturbed flow ($\mathbf{M}_\delta$, p_δ, ρ_δ, i_δ etc.) taking $r_L^*=0.84$ or $r_T^*=0.89$ as a first approximation. Next we find T^* with the help of graphs or tables of the thermodynamic and kinetic functions of air for given i^* and pressure p_δ. The values of $(c_p)^*$, μ^* and λ^* can be obtained from the tables or graphs for this temperature and pressure p_δ and the Prandtl number $\mathbf{Pr}^*$ can be improved by formula (12.5.28). Coefficient of recovery r^* can be modified by formula (12.5.26) or (12.5.27). The enthalpy i^* will be worked out from this value of r^* as a second approximation. Temperature T^* and the corresponding molecular weight μ_{av}^* will be determined and their values will be substituted in formulas (12.6.21) and (12.6.22).

In the absence of dissociation the ratio of molecular weights $\mu_{av}^*/\mu_{av\delta}=1$, and hence

$$\delta_c/\delta_{inc}=(T^*/T_\delta)^{(n+1)/5}; \tag{12.6.23}$$

$$(c_{xf})_c/(c_{xf})_{inc}=(c_{fx})_c/(c_{fx})_{inc}=(\tau_w)_c/(\tau_w)_{inc}=(T^*/T_\delta)^{(n-4)/5}. \tag{12.6.24}$$

6.3 Friction on cone at supersonic speeds of flow-interaction

Laminar boundary layer: The supersonic flow over a sharp cone has the property that the velocity $V_\delta=V_k$ is constant along the generator of the conical surface and hence the lateral pressure gradient is equal to zero. The same property is observed with a flat plate in an inviscid flow: the boundary layer parameters at the external limit are constant along it. This similarity of flow-interaction helps us to use the results of boundary layer calculations for a flat plate to determine the corresponding parameters for a viscous flow over a conical surface.

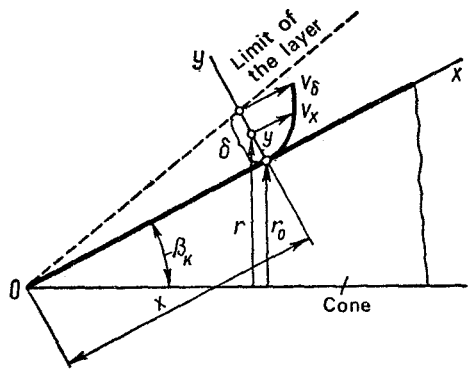

Fig. 12.6.1. Boundary layer on cone.

Let us use the integral relation (12.2.16) for this purpose. Considering that the gas parameters at the external surface of the boundary layer all over the cone are the same ($V_\delta=V_k=$const; $p_\delta=p_k=$const, etc.) and hence the pressure gradient in x direction is equal to zero ($dp_\delta/dx=0$), we can represent this relation in the form

$$\frac{d}{dx}\int_0^\delta \rho r_0 V_x(V_x-V_k)dy=-r_0\tau_w, \tag{12.6.25}$$

where r_0 is the distance from the axis to a point on the surface of the cone with coordinate x (Fig. 12.6.1) and τ_w is frictional stress at this point.

Let us apply relation (12.6.25) for calculation of a laminar boundary layer. At an arbitrary point of the section situated at a distance x from the nose the frictional stress can be obtained by the formula $\tau=\mu(\partial V_x/\partial y)$. The quantity $dy=(\mu/\tau)dV_x$ in equation (12.6.25) can be changed in accordance with this formula. Dividing both sides of this equation by $\rho_k V_k^3 \mu_k$, where ρ_k and μ_k are density ($\rho_k=\rho_\delta$) and coefficient of dynamic viscosity ($\mu_k=\mu_\delta$) respectively at the external limit of the boundary layer over the cone, we get the integral relation

$$\frac{d}{dx}\int_0^1 \frac{\rho V_x}{\rho_k V_k}\cdot\frac{\mu}{\mu_k}\cdot\frac{r_0}{\tau}\left(1-\frac{V_x}{V_k}\right)d\left(\frac{V_x}{V_k}\right)=\frac{r_0\tau_w}{\rho_k V_k^3\mu_k}. \tag{12.6.26}$$

For the present case of a boundary layer without a pressure gradient the ratio of velocities $V_x/V_k=f_1(y/\delta)$ is solely the function of relative coordinate y/δ and does not depend on x. Consequently the ratio of tangential stresses in the boundary layer, according to the formulas $\tau=\mu(\partial V_x/\partial y)$, $\tau_w=\mu_k(dV_x/dy)_k$, will also depend on the same relative coordinate, i.e. $\tau/\tau_w=f_2(y/\delta)$. Let us introduce functions f_1, f_2 in (12.6.26) and use the notation

$$J=\int_0^1 \frac{\rho V_x}{\rho_k V_k}\cdot\frac{\mu}{\mu_k}\cdot\frac{1-f_1}{f_2}df_1. \tag{12.6.27}$$

Keeping in view that with constant temperature all over the surface of the cone the ratio μ/μ_k is independent of x and that the density ratio ρ/ρ_k, being the function of V_x/V_k, does not depend on these coordinates either, we find the relation

$$J\frac{\tilde{r}_0}{\tau_w}\cdot\frac{d}{dx}\left(\frac{r_0}{\tau_w}\right)=\frac{r_0^2}{\rho_k V_k^3\mu_k}. \tag{12.6.28}$$

Replacing r_0 by $x\sin\beta_k$ on the right side of this formula and separating the variables, we get

$$\frac{J}{2}d\left(\frac{r_0}{\tau_w}\right)^2=\frac{\sin^2\beta_k}{\rho_k V_k^3\mu_k}x^2dx. \tag{12.6.29}$$

After integration, this reduces to

$$\frac{J}{2}\cdot\frac{r_0^2}{\tau_w^2}=\frac{1}{3}\cdot\frac{x^3\sin^2\beta_k}{\rho_k V_k^3\mu_k}+\text{const}. \tag{12.6.30}$$

Taking ratio $r_0^2/\tau_w^2=0$ at the beginning point (at $x=0$) and consequently assuming the constant on the right side of (12.6.30) equal to zero and also taking into account the reverse relation $x\sin\beta_k=r_0$ with notation $\tau_w=\tau_{w*k}$ for frictional stress on the cone, we get

$$\tau_{w.k}=\sqrt{3}\left(\frac{J}{2}\cdot\frac{\rho_k V_k^3 \mu_k}{x}\right)^{1/2}. \tag{12.6.31}$$

A similar expression can be obtained for the frictional stress $\tau_w=\tau_{w.p}$ on a flat plate. Here we assume that the flat plate interacts with a hypothetical supersonic flow having the same parameters as the flow over the cone. Then the integration of equation (12.6.28), from which r_0 is dropped, leads to the relation

$$\tau_{w.p}=\left(\frac{J}{2}\cdot\frac{\rho_k V_k^3 \mu_k}{x}\right)^{1/2}. \tag{12.6.32}$$

From formulas (12.6.31) and (12.6.32) we have the important relation

$$\tau_{w.k}=\sqrt{3}\,\tau_{w.p}\approx 1.73\tau_{w.p}, \tag{12.6.33}$$

according to which the frictional stress on the cone is $\sqrt{3}$ times larger than that on a flat plate, worked out on the basis of the parameters on the cone. The local and average values of coefficients of friction are determined by a formula similar to (12.6.33):

$$c_{fxk}=\sqrt{3}\,c_{fxp}; \tag{12.6.34}$$

$$c_{xfk}=\sqrt{3}\,c_{xfp}. \tag{12.6.35}$$

These values are obtained with respect to the velocity head of undisturbed flow $q_k=\rho_k V_k^2/2$. To calculate the coefficient of friction on the basis of the velocity head of undisturbed flow the following relations should be used:

$$c_{fx\infty k}=c_{fxk}(q_k/q_\infty)=\sqrt{3}\,c_{fxp}(\rho_k V_k^2/\rho_\infty V_\infty^2); \tag{12.6.36}$$

$$c_{xf\infty k}=c_{xfk}(q_k/q_\infty)=\sqrt{3}\,c_{xfp}(\rho_k V_k^2/\rho_\infty V_\infty^2). \tag{12.6.37}$$

The frictional drag force can be worked out from the average frictional coefficient $c_{xf\infty k}$ and the side surface area S_k of a cone:

$$X_f=c_{xf\infty k}\,q_\infty S_k=\sqrt{3}\,c_{xfp}(\rho_k V_k^2/2)S_k. \tag{12.6.38}$$

The frictional stress $\tau_{w.p}=(\tau_w)_c$ and the coefficient of friction $c_{xfp}=(c_{xf})_c$, $c_{fxp}=(c_{fx})_c$ can be obtained from the relation (12.6.13) using definitive parameters in a general case of dissociating air.

The approximate relation between the thickness of the boundary layer on a cone and on a flat plate can also be established. Polhausen's method for calculating velocity distribution over the section of the boundary layer in an incompressible medium will be used here. According to this method the velocity is determined by equation (12.3.15). Replacing η by y, η_δ by δ and V_δ by V_k, we get

$$V_x = V_k\left(\frac{3}{2}\cdot\frac{y}{\delta} - \frac{1}{2}\cdot\frac{y^2}{\delta^2}\right). \tag{12.6.39}$$

Using Newton's formula the frictional stress on the surface of the cone will be

$$\tau_{w\cdot k} = \mu_k V_k\left[\frac{\partial}{\partial y}\left(\frac{3}{2}\cdot\frac{y}{\delta} - \frac{1}{2}\cdot\frac{y^2}{\delta^2}\right)\right]_{y=0} = \mu_k V_k \frac{3}{2\delta_k}, \tag{12.6.40}$$

where δ_k is the thickness of the boundary layer over the cone.

Similar expressions can be written for a flat plate:

$$\tau_{w\cdot p} = \mu_k V_k (3/2\delta_p), \tag{12.6.41}$$

where δ_p is the thickness of the boundary layer over the flat plate.

From relations (12.6.40) and (12.6.41) it follows that

$$\delta_p/\delta_k = \tau_{w\cdot k}/\tau_{w\cdot p}, \tag{12.6.42}$$

whence, according to (12.6.33), we have

$$\delta_k = (\tau_{w\cdot p}/\tau_{w\cdot k})\delta_p = \delta_p/\sqrt{3} = 0.578\delta_p. \tag{12.6.43}$$

In this way, formula (12.6.43) shows that the thickness of the laminar boundary layer on a cone is $\sqrt{3}$ times less than that on a flat plate. The thickness $\delta_p = \delta_c$ for the plate in the general case of a dissociating gas may be worked out from the definitive parameters over a conical surface with the help of formula (12.6.12).

Turbulent boundary layer: Use of the same integral relation (12.2.16) gives analogical relations in approximate form for a turbulent boundary layer. Changing to the definitive parameters in (12.6.25) and substituting expression (12.4.55) in place of τ_w, denoting V_δ and δ by V_k and δ_k respectively, we get

$$\frac{d}{dx}\int_0^\delta \rho^* r_0 V_x (V_k - V_x)dy = 0.0233\rho^* V_k^2\left(\frac{\mu^*}{V_k\rho^*}\right)^{1/4}\frac{r_0}{(\delta^*)^{1/4}}.$$

Keeping in mind that the surface temperature is the same everywhere and hence the characteristic parameters are constant, the density ρ^* on the left and right sides can be reduced and after simplifications the following equation can be obtained:

$$\frac{d}{dx}\left[r_0\,\delta_k\int_0^1 \frac{V_x}{V_k}\left(1-\frac{V_x}{V_k}\right)d\left(\frac{y}{\delta_k}\right)\right] = 0.0233\left(\frac{\mu^*}{V_k\rho^*}\right)^{1/4}\frac{r_0^{5/4}}{(r_0\delta_k)^{1/4}}. \tag{12.6.44}$$

If the one-seventh root law of velocity distribution is used the nondimensional velocity $V_x/V_k = (y/\delta_k)^{1/7}$, i.e. it happens to be the function of the relative coordinate. Therefore

$$J_1=\int_0^1 \frac{V_x}{V_k}\left(1-\frac{V_x}{V_k}\right) d\left(\frac{y}{\delta_k}\right)=\text{const.}$$

Accordingly equation (12.6.44) will be rewritten in the form

$$J_1(r_0\delta_k)^{1/4}\, d(r_0\delta_k)=0.0233(\mu^*/V_k\,\rho^*)^{1/4}\, r_0^{5/4}\, dx. \tag{12.6.45}$$

Substituting $r_0=x\sin\beta_k$ on the right side and integrating it with the condition that the quantity $r_0\delta_k=0$ at $x=0$, we have

$$(4J_1/5)\,(r_0\delta_k)^{5/4}=0.0233(\mu^*/V_k\,\rho^*)^{1/4}\sin^{5/4}\beta_k(4x^{9/4}/9).$$

Considering the reverse replacement $(x\sin\beta_k)^{5/4}=r_0^{5/4}$ and the appropriate reduction of this quantity on the right and left sides, we get

$$(\delta_k)^{5/4}=(4/9)J_2x,$$

whence

$$\delta_k=(4/9)^{4/5}\,(J_2x)^{4/5}, \tag{12.6.46}$$

where

$$J_2=(0.0292/J_1)\,(\mu^*/V_k\,\rho^*)^{1/4}. \tag{12.6.47}$$

Substituting δ_k in (12.6.45) by δ_p and dropping r_0, we get similar expressions for boundary layer thickness on a flat plate. After integration we arrive at

$$(4J_1/5)\,(\delta_p)^{5/4}=0.0233\,(\mu^*/V_k\,\rho^*)^{1/4}\,x,$$

from which

$$\delta_p=(J_2x)^{4/5}. \tag{12.6.48}$$

The relation between the thickness of a boundary layer on a cone and on a plate can be obtained from the expressions (12.6.46) and (12.6.48):

$$\delta_k=\left(\frac{4}{9}\right)^{4/5}\delta_p=0.523\delta_p. \tag{12.6.49}$$

The relation for frictional stress can be found from the relation (12.4.55) by introducing the definitive parameters and writing this relation for a cone and for a plate separately:

$$\tau_{w.k}=0.0233\rho^*V_k^2\,(\nu^*/V_k)^{1/4}\,(1/\delta_k^{1/4});$$

$$\tau_{w.p}=0.0233\rho^*V_k^2\,(\nu^*/V_k)^{1/4}\,(1/\delta_p^{1/4}).$$

Assuming that the definitive parameters are identical on a cone and on a flat plate, the last two relations lead to

$$\tau_{w\cdot k}/\tau_{w\cdot p}=(\delta_p/\delta_k)^{1/4}. \tag{12.6.50}$$

Inserting the value of δ_k from (12.6.49) in (12.6.50), we get

$$\tau_{w\cdot k}=(9/4)^{1/5}\,\tau_{w\cdot p}=1.17\tau_{w\cdot p}. \tag{12.6.51}$$

From comparison of formulas (12.6.33) and (12.6.51) it can be concluded that the difference between the frictional stress on a cone and its corresponding value on a plate is less for a turbulent boundary layer than for a laminar boundary layer. This is explained by the intensive effect of mixing of flow on frictional stress in a turbulent boundary layer in comparison to the interaction of the form of surface. So far as thickness is concerned [see (12.6.43) and (12.6.49)] its values on a cone differ by approximately 10% as between a turbulent and a laminar boundary layer. This small difference indicates that the form of the surface of a body has a stronger influence on the thickness of the boundary layer than the mixing of flow.

The local and average coefficients of friction can be determined from the known frictional stress:

$$c_{fx\mathrm{k}}=1.17c_{fx\mathrm{p}}; \tag{12.6.52}$$

$$c_{xf\mathrm{k}}=1.17c_{xf\mathrm{p}}. \tag{12.6.53}$$

These coefficients are worked out on the basis of velocity heat $q_k=\rho_k V_k^2/2$. To recalculate them with respect to the velocity head of an undisturbed flow it is necessary to apply formulas similar to (12.6.36) and (12.6.37).

The frictional drag force in a turbulent boundary layer is determined by an expression similar to (12.6.38):

$$X_f=1.17c_{xf\mathrm{p}}\,(\rho_k V_k^2/2)\,S_k. \tag{12.6.54}$$

The frictional stress $\tau_{w\cdot p}=(\tau_w)_c$ and the coefficients of friction $c_{xfp}=(c_{xf})_c$, $c_{fxp}=(c_{fx})_c$ for a flat plate can be obtained from the relation (12.6.22) and boundary layer thickness $\delta_p=\delta_c$ can be found from (12.6.17) using definitive parameters with allowance for dissociation.

7. Effect of Axial Pressure Gradient on Friction

In the previous section we examined the problem of the boundary layer on a flat plate and on a conical surface in a supersonic flow. For this kind of boundary layer the characteristic feature is that the pressure at all sections is identical ($p_\delta=\text{const}$) and consequently the axial gradient of pressure $dp_\delta/dx=0$. However, during the flow-interaction of a curvilinear surface (for example, a wing profile or body of revolution with curvilinear generator) this gradient differs from zero because the pressure at the external limit of the boundary layer will be a variable quantity depending on the coordinate x. As may be seen from the integral equation (12.2.16), where $dp_\delta/dx\neq 0$, this is followed by variation in the frictional stress and hence in the velocity distribution and thickness of the boundary layer in comparison with the case of the flow-interaction of a flat plate or a cone.

If a wing profile with curved contour in a subsonic flow (Fig. 12.7.1, a) is considered the pressure gradient on the nose section (from point O of complete stagnation to some point B) will be a negative quantity ($dp_\delta/dx < 0$) and on the region from point B to point C on the trailing edge it will be positive ($dp_\delta/dx > 0$). This kind of variation in the pressure gradient is demarcated by critical points of flow-interaction along the profile whereby the velocity on the nose section from point O to point B increases and hence pressure falls, as shown by Bernoulli's equation; conversely, in the region around the trailing edge the velocity decreases and pressure increases.

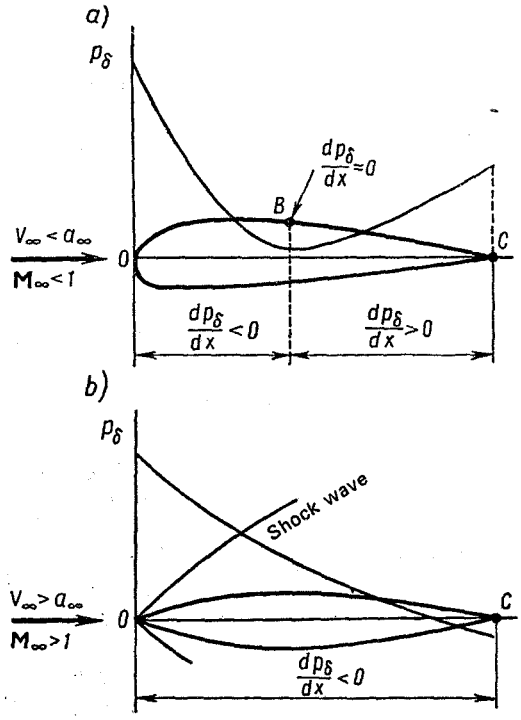

Fig. 12.7.1. Variation of axial pressure gradient over profile:

a—subsonic flow-interaction; *b*—supersonic flow-interaction.

In the case of a supersonic flow-interaction (Fig. 12.7.1, b) velocity V_δ going toward the trailing edge of the profile increases continuously and consequently the pressure p_δ and the derivative dp_δ/dx diminish, i.e. all over the surface the flow in the boundary layer will exhibit a negative pressure gradient.

The integral relation (12.2.16) will be used for qualitative evaluation of the variation in tangential stresses with the given distribution of axial pressure gradient. If the derivative $dp_\delta/dx < 0$ the first term on the left side will be

positive and in the case of $dp_\delta/dx>0$ it will be negative. This indicates that under identical conditions the tangential stresses in the region of negative pressure gradient where the flow speeds up will be higher than those in a uniform flow. On the other hand, on the part of the surface where pressure rises and the flow is slowed down the frictional stress will be reduced. It is possible to find the point on the surface in this region where the frictional stress becomes zero and behind which its value becomes negative.

This kind of variation in frictional stress is closely related to the velocity distribution V_x over the section of the boundary layer. If we take a laminar boundary layer for which $\tau_w=\mu_w(\partial V_x/\partial y)_w$ then, in the region of adverse pressure gradient where $\tau_w>0$, the derivative $(\partial V_x/\partial y)_w>0$. The picture of the corresponding velocity distribution is shown in Fig. 12.7.2, a where the velocity V_x near the wall has the same direction as the velocity of free flow V_δ.

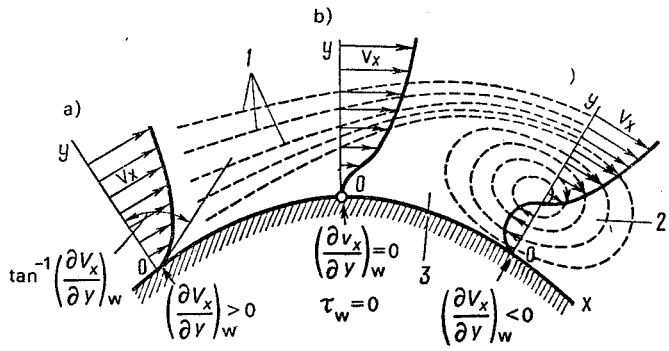

Fig. 12.7.2. Variation of velocity profile over section of boundary layer and formation of vortex in zone of separation:

1—stream line; *2*—vortex; *3*—zone of separation.

At the point of the profile where $\tau_w=0$ and consequently $(\partial V_x/\partial y)_w=0$ the distribution of velocities in the boundary layer tangential to the curve (see Fig. 12.7.2, b) coincides with the normal to the wall. The stress τ_w behind this point is negative and the derivative $(\partial V_x/\partial y)_w<0$. The corresponding flow pattern in the boundary layer is shown in Fig. 12.7.2, c. It is characterized by the fact that the velocities of particles situated near the wall take a direction opposite to that of the free flow. This phenomenon is explained by the effect of viscosity leading to a reduction in the kinetic energy of the particles in a fluid.

In the rear part of the profile this energy may not be enough to overcome the positive pressure gradient. For this reason the fluid in the vicinity of the surface first undergoes complete stagnation and then changes its direction of motion. As a result of the formation of this opposite flow the stream

lines get closer and hence the boundary layer separates from the surface. The point where $\tau_w=0$ is known as the separation point. The separation of the boundary layer from the surface leads to a basic change in the conditions of its flow-interaction and has a definitive effect on the aerodynamic characteristics of a flight vehicle. The determination of frictional stress in the region of separation has no physical meaning because its effect on the motion of the fluid is infinitesimally small in comparison with normal pressure. The stress τ_w in this region in practice may be taken as equal to zero. So far as curved surfaces with unseparated flows are concerned the investigation of frictional stress in these regions can be carried out using the integral relation of the boundary layer along with the relations establishing velocity distribution over the section of the layer and the law of variation of tangential stresses.

Let us see how to calculate the laminar boundary layer over the curved surface of an airfoil in a compressible gas flow, as worked out by Academician A.A. Dorodnitsin [5]. The integral relation of this boundary layer will be obtained from (12.2.16′) by eliminating r_0 and taking $\tau_w=\mu_w(\partial V_x/\partial y)_{y=0}$:

$$-\frac{d}{dx}\int_0^\delta \rho V_x^2\,dy+V_\delta\frac{d}{dx}\int_0^\delta \rho V_x\,dy-\delta\frac{dp_\delta}{dx}=\mu_w\left(\frac{\partial V_x}{\partial y}\right)_{y=0}. \qquad (12.7.1)$$

Let us transform this equation to the variables in (12.3.4) and (12.3.6). We will then find

$$-\left[\frac{d}{d\xi}\left(\int_0^{\eta_\delta}\rho V_x^2\frac{\rho_0}{\rho}\,d\eta\right)\right]\frac{d\xi}{dx}+V_\delta\left[\frac{d}{d\xi}\left(\int_0^{\delta}\rho V_x\frac{\rho_0}{\rho}\,d\eta\right)\right]\frac{d\xi}{dx}$$
$$-\delta\frac{dp_\delta}{d\xi}\cdot\frac{d\xi}{dx}=\mu_w\left(\frac{\partial V_x}{\partial\eta}\right)_{\eta=0}\left(\frac{\partial\eta}{\partial y}\right)_{y=0}. \qquad (12.7.2)$$

Inserting here the value of δ from (12.4.6′) and the values of $d\xi/dx$ and $(\partial\eta/\partial y)_w$ in accordance with (12.3.6), (12.3.4), (12.3.5) and (12.4.5′), we get

$$\left.\begin{aligned} &d\xi/dx=p_\delta/p_0=(1-\bar V_\delta^2)^{k/(k-1)};\\ &(\partial\eta/\partial y)_w=\rho_w/\rho_0=(1-\bar V_\delta^2)^{k/(k-1)},\end{aligned}\right\} \qquad (12.7.3)$$

Keeping in view the equality in (12.2.17), which can be represented in the form

$$dp_\delta/d\xi=-\rho_\delta V_\delta\,(dV_\delta/d\xi), \qquad (12.7.4)$$

we get the integral relation

$$-\rho_w\frac{d}{d\xi}\int_0^{\eta_\delta}V_\delta^2\,d\eta+\rho_wV_\delta\frac{d}{d\xi}\int_0^{\eta_\delta}V_x\,d\eta+\rho_\delta V_\delta\frac{dV_\delta}{d\xi}\int_0^{\eta_\delta}(1-\bar V_x^2)\,d\eta$$

$$=\mu_w\,(1-\overline{V}_\delta^2)^{k/(k-1)}\left(\frac{\partial V_x}{\partial\eta}\right)_{\eta=0}.$$

Dividing both sides of this equality by ρ_w and changing the ratio ρ_δ/ρ_w according to (12.7.3) to the value

$$\frac{\rho_\delta}{\rho_w}=\frac{\rho_\delta}{\rho_0}\cdot\frac{\rho_0}{\rho_w}=(1-\overline{V}_\delta^2)^{1/(k-1)}\,(1-\overline{V}_\delta^2)^{-k/(k-1)}=(1-\overline{V}_\delta^2)^{-1} \qquad (12.7.5)$$

and the quantity μ_w/ρ_w to the value obtained from (12.4.35), we find

$$-\frac{d}{d\xi}\int_0^{\eta_\delta} V_x^2\,d\eta+V_\delta\frac{d}{d\xi}\int_0^{\eta_\delta} V_x\,d\eta+(1-\overline{V}_\delta^2)^{-1}V_\delta\frac{dV_\delta}{d\xi}\int_0^{\eta_\delta}(1-\overline{V}_x^2)\,d\eta$$

$$=\nu_\delta\,(1-\overline{V}_\delta^2)^{\frac{1}{k-1}-n}\left(\frac{\partial V_x}{\partial\eta}\right)_{\eta=0}. \qquad (12.7.6)$$

Now, following A.A. Dorodnitsin, we give the equation approximate velocity distribution V_x at the sections of the boundary layer in the form of a polynomial of the fourth order of η:

$$V_x=a\eta+b\eta^2+c\eta^3+d\eta^4. \qquad (12.7.7)$$

This expression is similar to Pohlausen's polynomial (12.3.9), differing only by the addition of a fourth term which is introduced to allow for peculiarities of flow in the boundary layer in the presence of an axial pressure gradient. The coefficients in equation (12.7.7), which are functions of ξ, are determined by the use of boundary conditions and differential equations of the boundary layer as for solution of the problem of the boundary layer on a flat plate.

On the surface in the flow (at $\eta=0$)

$$V_x=V_y=0. \qquad (12.7.8)$$

At the external limit of the boundary layer (at $\eta=\eta_\delta$)

$$V_x=V_\delta. \qquad (12.7.9)$$

Besides, as frictional stress on this boundary is equal to zero, we will have

$$\partial V_x/\partial\eta=0. \qquad (12.7.10)$$

In addition, we will find the boundary conditions for the derivative $\partial^2V_x/\partial\eta^2$. For this purpose we use the differential equation of motion in a boundary layer (12.1.14) and transform it into the variables in (12.3.4) and (12.3.6):

$$V_x\left(\frac{\partial V_x}{\partial\xi}\cdot\frac{\partial\xi}{\partial x}+\frac{\partial V_x}{\partial\eta}\cdot\frac{\partial\eta}{\partial x}\right)+V_y\frac{\partial V_x}{\partial\eta}\cdot\frac{\partial\eta}{\partial y}$$

$$=-\frac{1}{\rho}\cdot\frac{dp_\delta}{d\xi}\cdot\frac{d\xi}{dx}+\frac{1}{\rho}\cdot\frac{\partial}{\partial\eta}\left[\left(\mu\frac{\partial V_x}{\partial\eta}\cdot\frac{\partial\eta}{\partial y}\right)\right]\frac{\partial\eta}{\partial y}.$$

Inserting the values of the derivatives $\partial\xi/\partial x$ and $\partial\eta/\partial y$ from (12.3.4), (12.3.6) here, replacing the quantity $dp_\delta/d\xi$ taking into account (12.7.4) and carrying out differentiation on the right side, we get

$$V_x\left(\frac{\partial V_x}{\partial\xi}\cdot\frac{p_\delta}{p_0}+\frac{\partial V_x}{\partial\eta}\cdot\frac{\partial\eta}{\partial x}\right)+V_y\frac{\partial V_x}{\partial\eta}\cdot\frac{\rho}{\rho_0}$$
$$=\frac{\rho_\delta V_\delta}{\rho}\cdot\frac{dV_\delta}{d\xi}\cdot\frac{p_\delta}{p_0}+\frac{\mu\rho}{\rho_0^2}\cdot\frac{\partial^2V_x}{\partial\eta^2}+\frac{1}{\rho_0^2}\cdot\frac{\partial V_x}{\partial\eta}\cdot\frac{\partial}{\partial\eta}(\mu\rho), \qquad (12.7.11)$$

where, according to (12.4.5), (1.4.2) and (12.5.1), the quantity

$$\frac{\partial}{\partial\eta}(\mu\rho)=\frac{\partial}{\partial\eta}\left[\mu_0\left(\frac{T}{T_0}\right)^n\rho_0(1-\overline{V}_\delta^2)^{k/(k-1)}(1-\overline{V}_x^2)^{-1}\right]$$
$$=\mu_0\rho_0(1-\overline{V}_\delta^2)^{k/(k-1)}\frac{\partial}{\partial\eta}[(1-\overline{V}_x^2)^{n-1}]$$
$$=-\frac{2\mu_0\rho_0}{V_{\max}^2}(1-\overline{V}_\delta^2)^{k/(k-1)}(n-1)(1-\overline{V}_x^2)^{n-2}V_x\frac{\partial V_x}{\partial\eta}.$$

Assuming $\eta=\eta_\delta$ in equation (12.7.11) and correspondingly $V_x=V_\delta$, $\rho=\rho_\delta$, and keeping in mind that $\partial V_x/\partial\eta=0$ because frictional stress is absent at the free surface, we get the boundary condition

$$(\partial^2V_x/\partial\eta^2)_{\eta=\eta_\delta}=0. \qquad (12.7.12)$$

If $\eta=0$ is assumed the velocities at the wall will be $V_x=V_y=0$, density $\rho=\rho_w$ and coefficient of dynamic viscosity $\mu=\mu_w=\mu_0$. Using these quantities in (12.7.11), we have

$$\frac{\rho_\delta V_\delta}{\rho_w}\cdot\frac{dV_\delta}{d\xi}\cdot\frac{p_\delta}{p_0}=-\frac{\mu_0\rho_w}{\rho_0^2}\left(\frac{\partial^2V_x}{\partial\eta^2}\right)_{\eta=0}.$$

Replacing ρ_w/ρ_0 in this expression by the quantity p_δ/p_0 according to (12.3.5′) and the ratio of densities ρ_δ/ρ_w by the relation

$$\rho_\delta/\rho_w=(1-\overline{V}_\delta^2)^{-1}, \qquad (12.7.13)$$

which is obtained from (12.3.5), and introducing coefficient of kinematic viscosity $\nu_0=\mu_0/\rho_0$, we get the boundary condition for the second derivative at $\eta=0$:

$$\left(\frac{\partial^2V_x}{\partial\eta^2}\right)_{\eta=0}=-\frac{V_\delta}{\nu_0(1-\overline{V}_\delta^2)}\cdot\frac{dV_\delta}{d\xi}. \qquad (12.7.14)$$

In this way we can find all the boundary conditions with whose help we determine the coefficients of the polynomial (12.7.7). Here the boundary condition (12.7.8) on the surface under flow-interaction is taken into account by using the type of polynomial that determined the value of $V_x=0$ at $\eta=0$. The second boundary condition is used on the surface (12.7.14). For this

purpose we should differentiate (12.7.7):

$$\frac{\partial^2 V_x}{\partial \eta^2}=2b+6c\eta+12d\eta^2\cdot \tag{12.7.15}$$

Assuming $\eta=0$ here and comparing the second derivative $(\partial^2 V_x/\partial\eta^2)_{\eta=0}$ with its value in (12.7.14), we get the coefficient of polynomial

$$b=-\frac{V_\delta}{2\nu_0(1-\bar{V}_\delta^2)}\cdot\frac{dV_\delta}{d\xi}\cdot \tag{12.7.16}$$

Let us consider the boundary conditions at the external limit of the boundary layer. According to (12.7.9) the velocity $V_x=V_\delta$ at $\eta=\eta_\delta$. Therefore from (12.7.7) we have

$$V_\delta=a\eta_\delta+b\eta_\delta^2+c\eta_\delta^3+d\eta_\delta^4\cdot \tag{12.7.17}$$

In this equation the coefficient b is already determined in the form of (12.7.16). To calculate it we have to combine two more independent equations to calculate the other three coefficients in equation (12.7.17). For this purpose we differentiate (12.7.7) with respect to η:

$$\frac{\partial V_x}{\partial \eta}=a+2b\eta+3c\eta^2+4d\eta^3\cdot \tag{12.7.18}$$

According to the boundary condition (12.7.10) we have, at $\eta=\eta_\delta$, the derivative

$$(\partial V_x/\partial\eta)_{\eta=\eta_\delta}=0\cdot$$

Hence

$$0=a+2b\eta_\delta+3c\eta_\delta^2+4d\eta_\delta^3\cdot \tag{12.7.19}$$

Recalling the condition (12.7.12) for the second derivative, we get the following equation from (12.7.15):

$$0=b+3c\eta_\delta+6d\eta_\delta^2\cdot \tag{12.7.20}$$

Solving the system of equations (12.7.17), (12.7.19), (12.7.20) for the coefficients a, c, d taking into account the value of b from (12.7.16), we get:

$$a=\frac{V_\delta}{\eta_\delta}\left(2+\frac{\lambda}{6}\right);\quad c=\frac{V_\delta}{\eta_\delta^3}\left(\frac{\lambda}{2}-2\right);\quad d=\frac{V_\delta}{\eta_\delta^4}\left(1-\frac{\lambda}{6}\right), \tag{12.7.21}$$

where

$$\lambda=\frac{\eta_\delta^2}{\nu_0(1-\bar{V}_\delta^2)}\cdot\frac{dV_\delta}{d\xi}\cdot \tag{12.7.22}$$

Using this value of λ the coefficient b in (12.7.16) will be rewritten in the form

$$b=-\frac{1}{2}\cdot\frac{V_\delta}{\eta_\delta^2}\lambda\cdot \tag{12.7.23}$$

With the help of the coefficients obtained the velocity in (12.7.7) can be expressed in the following way:

$$V_x=V_\delta\left(2+\frac{\lambda}{6}\right)\frac{\eta}{\eta_\delta}-\frac{V_\delta}{2}\lambda\left(\frac{\eta}{\eta_\delta}\right)^2+V_\delta\left(\frac{\lambda}{2}-2\right)\left(\frac{\eta}{\eta_\delta}\right)^3 + V_\delta\left(1-\frac{\lambda}{6}\right)\left(\frac{\eta}{\eta_\delta}\right)^4,$$

or

$$V_x=V_\delta\left[(2\bar{\eta}-2\bar{\eta}^3+\bar{\eta}^4)+\frac{\lambda}{6}\bar{\eta}(1-\bar{\eta})^3\right], \tag{12.7.24}$$

where $\bar{\eta}=\eta/\eta_\delta$. As may be seen from (12.7.24) and (12.7.22), the velocity profile at the sections of a boundary layer over a curved surface, unlike over a flat plate, will vary due to the effect of axial gradient of velocity V_δ (or axial gradient of pressure p_δ).

We now use the integral relation (12.7.6) and introduce in it the expression (12.7.24) in place of V_x and the value of:

$$\left(\frac{\partial V_x}{\partial\eta}\right)_{\eta=0}=\frac{V_\delta}{\eta_\delta}\left(2+\frac{\lambda}{6}\right), \tag{12.7.25}$$

for the derivative $(\partial V_x/\partial\eta)_{\eta=0}$. As a result we have the relation

$$-\frac{d}{d\xi}[V_\delta^2\eta_\delta\Phi_1(\lambda)]+V_\delta\frac{d}{d\xi}[V_\delta\eta_\delta\Phi_2(\lambda)] +(1-\bar{V}_\delta^2)^{-1}V_\delta\frac{dV_\delta}{d\xi}\eta_\delta[1-\bar{V}_\delta^2\Phi_1(\lambda)] =\nu_\delta(1-\bar{V}_\delta^2)^{\frac{1}{k-1}-n}\frac{V_\delta}{\eta_\delta}\left(2+\frac{\lambda}{6}\right), \tag{12.7.26}$$

where

$$\Phi_1(\lambda)=\int_0^1\left(\frac{V_x}{V_\delta}\right)^2 d\bar{\eta}=\int_0^1\left[(2\bar{\eta}-2\bar{\eta}^3+\bar{\eta}^4)+\frac{\lambda}{6}\bar{\eta}(1-\bar{\eta})^3\right]^2 d\bar{\eta} =\frac{367}{630}+\frac{71}{7560}\lambda+\frac{1}{9072}\lambda^2; \tag{12.7.27}$$

$$\Phi_2(\lambda)=\int_0^1\frac{V_x}{V_\delta}d\bar{\eta}=\int_0^1\left[(2\bar{\eta}-2\bar{\eta}^3+\bar{\eta}^4) +\frac{\lambda}{6}\bar{\eta}(1-\bar{\eta})^3\right]d\bar{\eta}=\frac{7}{10}+\frac{1}{120}\lambda. \tag{12.7.28}$$

According to (12.7.22) the thickness η_δ appearing in (12.7.26) will be expressed in the form

$$\eta_\delta=\sqrt{\lambda\nu_0/f(\xi)}, \tag{12.7.29}$$

where

$$f(\xi)=\frac{dV_\delta/d\xi}{1-\overline{V}_\delta^2}\cdot \tag{12.7.30}$$

Inserting (12.7.29) and (12.7.30) in (12.7.26), we arrive at the following relation:

$$-\frac{d}{d\xi}\left[V_\delta^2\frac{\sqrt{\lambda}\,\Phi_1(\lambda)}{\sqrt{f(\xi)}}\right]+V_\delta\frac{d}{d\xi}\left[V_\delta\frac{\sqrt{\lambda}\,\Phi_2(\lambda)}{\sqrt{f(\xi)}}\right]$$

$$+V_\delta\sqrt{\lambda f(\xi)}\,[1-\overline{V}_\delta^2\,\Phi_1(\lambda)]=\frac{\nu_\delta}{\nu_0}(1-\overline{V}_\delta^2)^{\frac{1}{k-1}-n}\frac{\sqrt{f(\xi)}}{\sqrt{\lambda}}\left(2+\frac{\lambda}{6}\right)V_\delta,$$

where

$$\frac{\nu_\delta}{\nu_0}(1-\overline{V}_\delta^2)^{\frac{1}{k-1}-n}=\frac{\mu_\delta}{\mu_0}\cdot\frac{\rho_0}{\rho_\delta}(1-\overline{V}_\delta^2)^{\frac{1}{k-1}-n}$$

$$=(1-\overline{V}_\delta^2)^n(1-\overline{V}_\delta^2)^{-\frac{1}{k-1}}(1-\overline{V}_\delta^2)^{\frac{1}{k-1}-n}=1\cdot$$

Taking this into account, we will have the following relation after simplification:

$$\frac{\sqrt{\lambda}}{\sqrt{f(\xi)}}\cdot\frac{d}{d\bar{\xi}}\left[\overline{V}_\delta^2\frac{\sqrt{\lambda}}{\sqrt{f(\xi)}}\,\Phi_1(\lambda)\right]+\frac{\overline{V}_\delta\sqrt{\lambda}}{\sqrt{f(\xi)}}\cdot\frac{d}{d\bar{\xi}}\left[\overline{V}_\delta\frac{\sqrt{\lambda}}{\sqrt{f(\xi)}}\,\Phi_2(\lambda)\right]$$

$$+\overline{V}_\delta\lambda\,[1-\overline{V}_\delta^2\,\Phi_1(\lambda)]=\overline{V}_\delta\left(2+\frac{\lambda}{6}\right),$$

where $\overline{V}_\delta=V_\delta/V_{\max}$; $\bar{\xi}=\xi/L$. After differentiation the equation reduces to the form

$$d\lambda/d\bar{\xi}=M_1(\lambda)\,N_1(\bar{\xi})+M_2(\lambda)\,N_2(\bar{\xi}), \tag{12.7.31}$$

where

$$\left.\begin{aligned}M_1(\lambda)&=\frac{\lambda(213-1.92\lambda-0.2\lambda^2)}{213-57.6\lambda-\lambda^2};\\ M_2(\lambda)&=\frac{7258-1336\lambda+37.92\,\lambda^2+0.8\lambda^3}{213-57.6\,\lambda-\lambda^2};\end{aligned}\right\} \tag{12.7.32}$$

$$\left.\begin{aligned}N_1(\bar{\xi})&=\frac{4\overline{V}_\delta\,\overline{V}'}{1-\overline{V}_\delta^2}+\frac{\overline{V}''_\delta}{\overline{V}'_\delta};\\ N_2(\bar{\xi})&=\frac{\overline{V}_\delta\,\overline{V}'_\delta}{1-\overline{V}_\delta^2}+\frac{\overline{V}'_\delta}{\overline{V}_\delta}\cdot\end{aligned}\right\} \tag{12.7.33}$$

In the expressions (12.7.33) notations for the first and second derivatives of velocity in the form $\overline{V}'_\delta = d\overline{V}_\delta/d\overline{\xi}$ and $\overline{V}''_\delta = d^2\overline{V}_\delta/d\overline{\xi}^2$ have been introduced.

According to the above discussion the analysis of the boundary layer over a curved surface will be conducted in the following way: First the velocity distribution $V_\delta(x)$ at the external limit of the boundary layer is obtained from study of the potential flow-interaction or by experiment. Then the derivatives V'_δ and V''_δ are determined and the functions N_1, N_2 are calculated. Next the quantity λ is determined by numerical integration of equation (12.7.31), which may be carried out on an electronic digital computer. This quantity must satisfy the boundary condition according to which the function λ is equal to some final value λ_0 at the point of branching of the flow that coincides with the point of complete stagnation, i.e. at $\xi=0$ ($x=0$). This quantity can be obtained with the help of equation (12.7.31) in the following way: The derivative $d\lambda/d\overline{\xi}$ at a point of complete stagnation is expressed in the form $d\lambda/d\overline{\xi} = [(\lambda-\lambda_0)/\overline{\xi}]_{\overline{\xi}\to 0}$, where the value of function λ is determined at a small distance from this point. According to this

$$[(\lambda-\lambda_0)/\overline{\xi}]_{\overline{\xi}\to 0} = M_1(\lambda)\, N_1(\overline{\xi}) + M_2(\lambda)\, N_2(\overline{\xi}),$$

or

$$(\lambda-\lambda_0)_{\overline{\xi}\to 0} = \{[M_1(\lambda)\, N_1(\overline{\xi}) + M_2(\lambda)\, N_2(\overline{\xi})]\,\overline{\xi}\}_{\overline{\xi}\to 0}.$$

Here the left side is equal to zero and according to (12.7.32) the term on the right side

$$[M_1(\lambda)\, N_1(\overline{\xi})\,\overline{\xi}]_{\overline{\xi}\to 0} = 0,$$

because

$$[M_1(\lambda)\,\overline{\xi}]_{\overline{\xi}\to 0} = 0.$$

Therefore

$$[M_2(\lambda)\, N_2(\overline{\xi})\,\overline{\xi}]_{\overline{\xi}\to 0} = 0,$$

or

$$M_2(\lambda_0)\,[N_2(\overline{\xi})\,\overline{\xi}]_{\overline{\xi}\to 0} = 0. \tag{12.7.34}$$

We will show that $[N_2(\overline{\xi})\,\overline{\xi}]_{\overline{\xi}\to 0} \neq 0$. For this purpose we use the expression (12.7.33) for $N_2(\overline{\xi})$. The derivative $\overline{V}'_\delta$ appearing in this expression can be expressed in the form $\overline{V}'_\delta = d\overline{V}_\delta/d\overline{\xi} = (\overline{V}_\delta/\overline{\xi})_{\overline{\xi}\to 0}$, where $\overline{V}_\delta$ is the velocity at a point with a small value of coordinate $\overline{\xi}$. According to this

$$[N_2(\overline{\xi})\,\overline{\xi}]_{\overline{\xi}\to 0} = \left[\left(\frac{\overline{V}_\delta \overline{V}'_\delta}{1-\overline{V}_\delta^2} + \frac{\overline{V}_\delta}{\overline{\xi}}\cdot\frac{1}{\overline{V}_\delta}\right)\overline{\xi}\right]_{\overline{\xi}\to 0} = 1.$$

Hence it follows from (12.7.34) that $M_2(\lambda_0)=0$ and

$$7258 - 1336\lambda_0 + 37.92\,\lambda_0^2 + 0.8\lambda_0^3 = 0,$$

whence

$$\lambda_0 = 7.052. \tag{12.7.35}$$

This calculation, being connected with determination of the characteristics of a boundary layer, can be used for the case of subsonic speeds of undisturbed flow and for a supersonic flow over a profile with a blunt leading edge. In the latter case it is necessary to take the values of density ρ_0' and stagnation pressure p_0' worked out for the flow conditions behind the linear part of a curved shock wave detached from the profile in place of ρ_0 and p_0 in formulas (12.3.4) and (12.3.6). For the supersonic flow-interaction of a sharp-nosed airfoil the values of ρ_0' and p_0' must be worked out for Mach number $\mathbf{M}_\infty > 1$ and for angle of inclination θ_c of a shock wave near the leading edge. The initial value of $\lambda = \lambda_0$ (at $\xi = 0$) is determined from the condition that at the sharp leading edge, as on a flat plate, the thickness of the boundary layer is equal to zero. According to (12.7.22) this value of λ_0 is also equal to zero.

The values of λ obtained from equation (12.7.31) help us to determine the parameters of the boundary layer. The frictional stress is worked out on the basis of (12.3.4), (12.3.6) and (12.7.25) with the help of the expression

$$\tau_w = \mu_w \left(\frac{\partial V_x}{\partial \eta}\right)_{\eta=0} \left(\frac{d\eta}{dy}\right)_{y=0} = \mu_w \frac{V_\delta}{\eta_\delta}\left(2+\frac{\lambda}{6}\right)\frac{\rho_w}{\rho_0}.$$

Taking into account that η_δ is determined by the expression (12.7.29) and the ratio ρ_w/ρ_0 by the relation (12.7.3), and assuming $\mu_w = \mu_0$, we find the relation

$$\tau_w = \mu_0 V_\delta \frac{\sqrt{f(\xi)}}{\sqrt{\lambda \nu_0}}\left(2+\frac{\lambda}{6}\right)(1-\overline{V}_\delta^2)^{k/(k-1)}.$$

Here

$$\frac{\mu_0}{\sqrt{\nu_0}} = \sqrt{\mu_0 \rho_0} = \left(\frac{\mu_0}{\mu_\delta}\cdot\frac{\rho_0}{\rho_\delta}\,\mu_\delta\,\rho_\delta\right)^{1/2} = (\mu_\delta\,\rho_\delta)^{1/2}(1-\overline{V}_\delta^2)^{-\frac{1}{2}\left(n+\frac{1}{k-1}\right)}$$

and the function $f(\xi)$ is determined from fromula (12.7.30). Accordingly

$$\tau_w = V_\delta \sqrt{\mu_\delta \rho_\delta V_\delta'}\,(1-\overline{V}_\delta^2)^{-\frac{1}{2}\left(n+\frac{1}{k-1}\right)}\left(2+\frac{\lambda}{6}\right)\frac{1}{\sqrt{\lambda}}. \tag{12.7.36}$$

The local coefficient of friction will then be given by

$$c_{fx} = \frac{2\tau_w}{\rho_\delta V_\delta^2} = \frac{2}{V_\delta}\sqrt{\frac{\mu_\delta V_\delta'}{\rho_\delta}}\,(1-\overline{V}_\delta^2)^{-\frac{1}{2}\left(n+\frac{1}{k-1}\right)}\left(2+\frac{\lambda}{6}\right)\frac{1}{\sqrt{\lambda}}. \tag{12.7.37}$$

To find the thickness of the boundary layer we apply formula (12.4.6′), which will be rewritten in the form

$$\delta = (1-\overline{V}_\delta^2)^{-k/(k-1)}\,\eta_\delta \int_0^1 \left(1-\frac{V_\delta^2}{V_{\max}^2}\cdot\frac{V_x^2}{V_\delta^2}\right) d\left(\frac{\eta}{\eta_\delta}\right)$$

$$=(1-\overline{V}_\delta^2)^{-k/(k-1)}\,\eta_\delta\,[1-\overline{V}_\delta^2\Phi_1(\lambda)], \qquad (12.7.38)$$

where η_δ and $\Phi_1(\lambda)$ are obtained as functions of λ from the expressions (12.7.29) and (12.7.27) respectively. The corresponding values for the boundary layer parameters in an incompressible fluid can be found if $1-\overline{V}_\delta^2=1-V_\delta^2/V_{\max}^2=1$ is introduced in the relations obtained above [this follows from the formula $1-\overline{V}_\delta^2=\{1+[(k-1)/2]\,\mathbf{M}_\delta^2\}^{-1}$, in which the Mach number $\mathbf{M}_\delta=0$ must be taken for an incompressible medium]. From (12.7.37) we will arrive at the relation for the coefficient of friction

$$c_{fx}=\frac{2\tau_w}{\rho_\delta V_\delta^2}=\frac{2}{V_\delta}\sqrt{\frac{\mu_\delta V_\delta'}{\rho_\delta}}\left(2+\frac{\lambda}{6}\right)\frac{1}{\sqrt{\lambda}}. \qquad (12.7.39)$$

The thickness of the boundary layer, according to formula (12.7.38) with $\overline{V}=0$, will be equal to the value of $\delta=\eta_\delta$. This value can be determined with the help of Newton's formula $\tau_w=\mu_w(\partial V_x/\partial\eta)_{\eta=0}$ in the following way: Let us write the above formula taking into account equation (12.7.25) in the form

$$\tau_w=\mu_w\frac{V_\delta}{\eta_\delta}\left(2+\frac{\lambda}{6}\right)=\frac{\mu_\delta V_\delta}{\delta}\left(2+\frac{\lambda}{6}\right).$$

Keeping in mind (12.7.39), we get

$$\delta=\frac{\mu_\delta V_\delta}{\tau_w}\left(2+\frac{\lambda}{6}\right)=\frac{2\mu_\delta}{\rho_\delta V_\delta}\cdot\frac{2+(\lambda/6)}{c_{fx}}, \qquad (12.7.40)$$

or

$$\delta=\sqrt{\lambda\mu_\delta/(\rho_\delta V_\delta')}. \qquad (12.7.41)$$

The quantity λ appearing in (12.7.39) through (12.7.41) is determined by the solution of differential equation (12.7.31), in which

$$N_1(\bar{\xi})=V_\delta''/V_\delta,\ N_2(\bar{\xi})=V_\delta'/V_\delta \qquad (12.7.42)$$

are substituted in place of (12.7.33).

For airfoils with small curvature of contour the method of characteristic parameters will be applied to determine the characteristics of an incompressible boundary layer to their corresponding values taking into account the effects of compressibility and high temperatures.

From the above relations for the boundary layer over a curved surface it is possible to get, as a particular case, the corresponding relations for a flat plate interacting with either a compressible or an incompressible flow if the axial velocity gradient is assumed to be zero in these relations.

Effect of boundary layer separation on aerodynamic characteristics: The part of the boundary layer behind the point of separation is characterized by the presence of two mutually opposite flows: an external flow with the direction of a free flow and an internal flow moving in the opposite direction. The

boundary layer is twisted to form a vortex in the flow (see Fig. 12.7.2). The appearance and shedding of vortices is accompanied by the accumulation of stagnant flow and formation of a region of stagnation.

The vortices produce a higher velocity of particles in the tail section of the body lying in their path than during a flow-interaction without separation and obviously the pressure will be lower (Fig. 12.7.3). Therefore additional drag due to redistribution of pressure, known as form drag or vortex, will appear. The increase in drag may be explained by the fact that an additional part of the kinetic energy of the flow around the body is spent in formation of vortices and separation of flow.

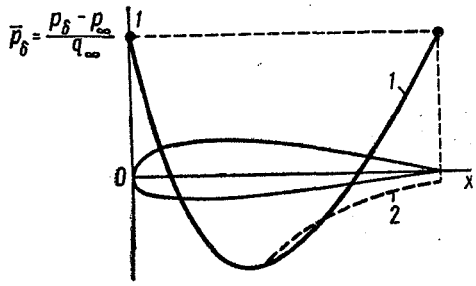

Fig. 12.7.3. Distribution of pressure over profile surface ($M_\infty = 0$):

1—without flow separation; *2*—with flow separation.

The position of the point of separation and hence the size of the region determining the value of additional drag depend on the value of the pressure gradient. For surfaces in a flow in the form of airfoils or elongated bodies of revolution with small curvatures and at small angles of attack the positive pressure gradient is not large, separation scarcely takes place and vortex drag is infinitesimally small. The pressure gradient dp_δ/dx increases with an increase in angle of attack and curvature of surface and separation takes place. Here the higher the derivative dp_δ/dx the closer the point of separation to the nose of the surface in the flow.

All these phenomena are observed in laminar as well as turbulent boundary layers. However, in the case of a turbulent flow some specific peculiarities of the separated flow may be noted. A region of turbulent flow arises when the Reynolds number exceeds its critical value. The velocities are distributed more uniformly over the section of a turbulent boundary layer and therefore the particles near the surface have a high velocity and hence more kinetic energy. For this reason they strongly resist the stagnating action of increasing pressure along the flow. This results in a less abrupt fall in tangential stress. The particles move over the surface to the point of separation where $\tau_w = 0$ farther than in a laminar flow. So crossing of the critical Reynolds number is associated with the movement of the separation point downstream. As a result the width and intensity of the vortex region behind the body is reduced and pressure drag (vortex drag) suddenly diminishes. In spite of some increase in drag based on turbulent friction total drag will be less than that in the case of a laminar boundary layer. This phenomenon of reduction in the total drag of blunt bodies (bodies with intensively separated

flow around them whose drag is mainly based on pressure forces and to a lesser degree on friction are generally known as blunt bodies) upon appearance of a turbulent boundary layer is known as drag crisis. Further increase in the Reynolds number (beyond critical point) leads to some rise in drag because the point of separation shifts upstream on the body.

We must note here that the above effect of "drag crisis" exists only in the case of blunt bodies such as, for example, a cylinder or sphere. For streamlined surfaces, for example, wing profiles or the fuselages of airplanes, the reduction in the zone of separation in the rear section of the body and the reduction in pressure drag are overcompensated by the frictional drag due to formation of a turbulent boundary layer in this part of the body.

Let us examine how compressibility affects the position of the point of separation and drag. It was established earlier that the thickness of the boundary layer for a flat plate increases with an increase in the Mach number and the frictional drag diminishes. These conditions remain valid even for curved surfaces [see (12.7.38) and (12.7.36)]. From this it follows that the point of separation shifts upstream with an increase in M_∞, i.e. it shifts toward the nose of the body. As a result the zone of separation extends and along with it the pressure drag and total drag increase.

From the above discussion it follows that the calculation of flow-interaction and determination of aerodynamic drag are connected with finding the point of separation of the boundary layer from the surface under flow-interaction. An approximate value of the coordinate of the separation point for a laminar boundary layer in a subsonic flow can be determined by the method of Academician A.A. Dorodnitsin discussed in this section. For this purpose we have to use equation (12.7.36). Taking $\tau_w=0$, we find the value of the parameter $\lambda=-12$ on the basis of which the solution of equation (12.7.22) gives the position of the point of separation for a given form of body. The method of calculation of separation for turbulent boundary layer has been discussed in the work [23].

The above methods are based on the solution of the differential equation of the boundary layer. On the lower limit the fluid parameters are determined from the equations of an inviscid unseparated flow-interaction with a given surface, i.e. these methods do not take into account the effects of a separating boundary layer on free flow. The data obtained on separation by these methods will be valid for sufficiently streamlined bodies where the separating free flow and the boundary layer are not very much displaced from the surface so that the flow differs insignificantly from a nonseparating inviscid flow. However, during the rather intensive separation generated by blunt bodies, when the external flow moves appreciably away from the wall, this difference seems to be quite considerable and the flow will have a significant effect on the boundary layer upstream as well as downstream and hence on the position of the separation point.

The scheme of an approximate solution of the problem of the separation of an incompressible boundary layer under the above conditions was proposed in MVTU in the name of N.E. Bauman. It is based on the idea of an ideal model of flow-interaction according to which the existence of an external potential flow and of zones of "silence" (in place of the usually accepted steady vortex zone) is assumed. Here the jets happen to be the boundaries between the potential flow and the steady fluid. The point of separation of the boundary layer is taken as the point of origin of the free jets. Calculation of the point of separation according to the usual model of flow-interaction is carried out by the method of interaction. The coordinate of the point of separation is first worked out using the usual methods of the theory of the boundary layer with the help of the parameters of external ("inviscid") flow-interactions for a given form of body. Then, assuming that the free jets emerge from the separation points, the problem of the form of the jets is solved approximately on the assumption that the jets coincide with stream lines along which the velocities are constant.

After determining the formula for the "semi-body" bounded by the contour of the surface in front (to the point of separation) and by the boundary of the free jets in back it is possible to work out the external potential flow as a second approximation and improve the position of the point of separation for this body. The results of calculations obtained by this scheme tally well with the experimental data. Here the effectiveness of the solution of problems of potential flow-interaction and determination of the boundaries of free jets was improved by use of a special calculating machine, the electro-integrator, which functions on the basis of the analogy between equations describing hydrodynamic and electro-dynamic processes (electro-hydrodynamic analogy).

We have studied the separation of the boundary layer due to a positive pressure gradient that arises as a result of free flow over the rear part of a curved surface. It is not connected with the presence of projections or the roughness of this surface. This phenomenon of separation may be observed in a compressible or an incompressible flow. Specific processes may take place in a compressible flow that establish the same effect of separation as we have already considered. As we know from the earlier discussion, local shock waves appear in a compressible medium at Mach numbers M_∞ higher than the critical Mach numbers. The increased pressure behind such shocks spreads not only downstream but also upstream. On the other hand the thickening of the boundary layer in front of the shock wave calls for compression of the stream lines from the body surface in the supersonic part of the boundary layer and also in the external flow. This leads to the fact that the supersonic flow during interaction with this part undergoes an additional turn which results in the formation of an oblique shock wave (λ-type shock). As a result of this interaction between shock wave and boundary layer a

rise in pressure takes place, leading to separation of the boundary layer. The rise in drag at supercritical Mach numbers is attributed not only to the losses in local shock waves but also to the separation of the boundary layer under the impact of shocks.

As shown by research, all these phenomena take place very intensively in the case of a laminar flow-interaction. Transition to a turbulent flow weakens the interaction between the shock waves and the boundary layer because thickening of the boundary layer is considerably less evident in a turbulent flow than in a laminar flow. Because there is less compression of stream lines in a turbulent flow ahead of the normal shock no additional oblique shock wave arises, as shown by experiment.

8. Mixed Boundary Layer. Critical Reynolds Number

In studying the calculation of the boundary layer over the surface in a flow we have to analyze its character. Observations show that the character of a boundary layer largely depends on the regime of flow-interaction, which can be determined by the Reynolds number. If the surface is assumed to take the form of a flat plate (Fig. 12.8.1) we find the formation of a laminar boundary layer on the front section at comparatively small Reynolds numbers $\mathbf{Re} = V_\delta x \rho_\delta / \mu_\delta$. Then there is a region of transition from laminar to turbulent boundary layer which eventually becomes a completely turbulent flow at the rear. These regions correspond to fairly high Reynolds numbers **Re**. This kind of boundary layer on the surface in a flow is known as a mixed boundary layer.

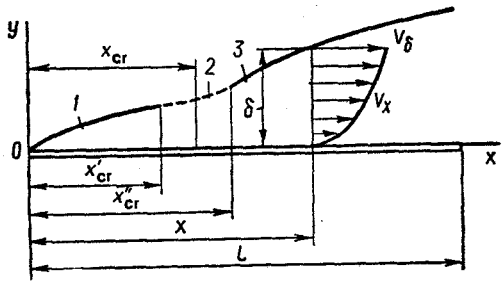

Fig. 12.8.1. Mixed boundary layer on flat plate: *1*—laminar boundary layer; *2*—transition region; *3*—turbulent boundary layer.

It should be noted that a laminar as well as a turbulent boundary layer may exist at any Reynolds number. However, in practice the flow regime in the boundary layer over the surface under flow-interaction is established that is stable under the given conditions. At low Reynolds numbers **Re** the laminar regime is stable. At high values of **Re** laminar boundary layers seem to be unstable. It is possible to achieve a laminar boundary layer even at quite high Reynolds numbers by using some artificial devices, for example, by setting up a smooth flow of fluid to a plate with a smooth surface. However, this regime of fluid is unstable and from any small disturbance it becomes a stable turbulent flow regime. The same thing is also true of the unstable turbulent boundary layer that may arise at the front of the plate (where Reynolds

numbers are small) if some initial disturbance arises. But however intense this disturbance is it dies away near the leading edge if the local Reynolds number $\mathbf{Re} = V_\delta x \rho_\delta / \mu_\delta$ does not exceed its critical value.

This Reynolds number dividing the region of stable laminar flow from the rest of the surface where the transition region and stable turbulent flow obtain is known as the critical Reynolds number. It is denoted by

$$\mathbf{Re}'_{cr} = V_\delta x'_{cr} \rho_\delta / \mu_\delta.$$

Sometimes this number, determined on the basis of distance x'_{cr} to the beginning of the transition region, is known as the first or minimum critical number in contrast to the second critical Reynolds number $\mathbf{Re}''_{cr} = V_\delta x''_{cr} \rho_\delta / \mu_\delta$ which separates the transition region from the zone of fully developed turbulence and is calculated on the basis of coordinate x''_{cr} of the end of this region.

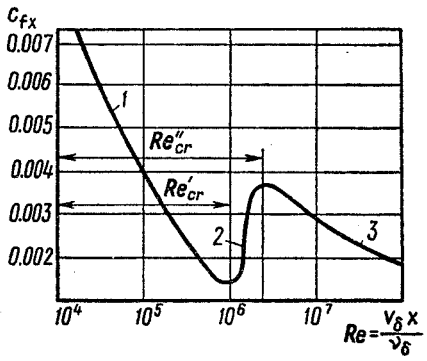

Fig. 12.8.2. Variation in local frictional coefficient on plate and value of critical Reynolds numbers:

1—laminar boundary layer; *2*—transition region; *3*—turbulent boundary layer.

In experimental research the range of Reynolds numbers is usually found that is bounded by the first and second critical values and determines the size of the transition region. The approximate values of these numbers can be found from the graph (Fig. 12.8.2) prepared on the basis of experiments with a flat plate in an incompressible flow.

The first critical Reynolds number is determined by the minimum value of the coefficient of friction corresponding to the end of the region of laminar boundary layer. Usually $\mathbf{Re}'_{cr} \approx 10^6$. Behind the point of minimum c_{fx} there is a sharp, almost abrupt, rise in the local frictional coefficient which reaches its maximum value at the limit of the transition region and corresponds to the second critical Reynolds number $\mathbf{Re}''_{cr} \approx 5 \times 10^6$. On the right side of this limit we will find the turbulent boundary layer.

In approximate calculations it may be assumed that the laminar boundary layer is separated from the turbulent region by a transition zone of infinitesimally small size, i.e. by a point. The coordinate x_{cr} of this transition point P (Fig. 12.8.3) is determined from the critical Reynolds number which in turn is taken as some value between the first and second critical numbers.

In estimating the value of Reynolds number $\mathbf{Re}_{cr}$ it is necessary to rely basically on experimental data. This helps in qualitative evaluation and in quantitative analysis of the phenomenon of a stabilizing laminar boundary layer, its transition into a turbulent boundary layer and the limitations on

formation of flow in this layer. In particular it has been established that the presence of a laminar region and a transition region has no effect on the law of development of the turbulent boundary layer behind the transition point. Consequently for calculation of the boundary layer behind the transition point it is possible to use the usual relations obtained from the assumption that the flow in this region is completely turbulent.

The position of the transition point (or region) on the surface in a flow depends on a series of factors, basically the degree of turbulence in the external flow, the condition of the surface, the wall temperature, Mach number M_δ at the external limit of the boundary layer, the form of the surface and the axial pressure gradient.

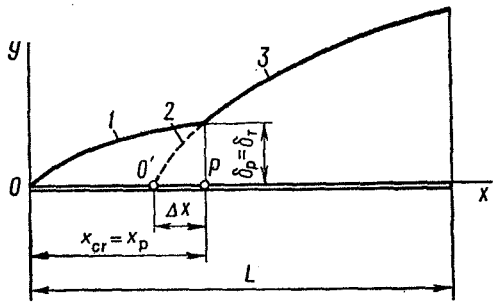

Fig. 12.8.3. Transition of laminar boundary layer to turbulent layer:

1—laminar boundary layer; *2*—fictitious region of turbulent boundary layer; *3*—turbulent boundary layer behind transition point.

The effect of the degree of turbulence of the external incompressible fluid flow on the critical Reynolds number $\mathbf{Re}_{cr}$ is shown in Fig. 12.8.4. The degree of turbulence along the abscissa is measured in percentages and is equal to

$$A = \frac{1}{V}\sqrt{\frac{1}{3}(V_x'^2 + V_y'^2 + V_z'^2)} \cdot 100\%, \qquad (12.8.1)$$

where V_x', V_y', V_z' are the perturbation components of velocity; V is the average flow velocity. An increase in the degree of turbulence of the external flow leads to additional disturbances in the boundary layer, which results in earlier appearance of transition and hence in reduction of the critical Reynolds number.

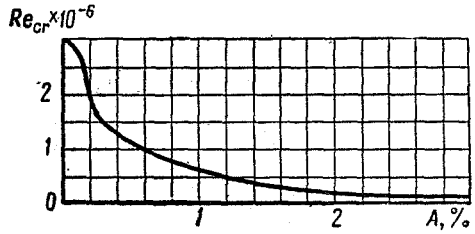

Fig. 12.8.4. Effect of degree of turbulence in incompressible fluid on critical Reynolds number for flat plate in flow.

The same qualitative effect of reduction in the stability of the laminar boundary layer is observed with a rough surface. The roughness is also considered as a source of disturbances. If the surface condition is characterized by the relative roughness $\bar{\Delta} = \Delta/\delta^*$ (Δ is the grade of roughness; δ^* is displacement thickness) the effect of this condition on the

critical Reynolds number for an incompressible fluid can be graphically represented by the curve shown in Fig. 12.8.5.

Let us study the effect of all temperatures on the stability of the laminar boundary layer. It has been established that the cooling of the surface of the wall helps to stabilize the boundary layer and to increase the critical Reynolds number. This is explained by the fact that the temperature of the fluid is reduced due to this cooling and the density of gas increases near the wall, as a result of which the kinetic energy of the flow increases. It is clear that particles with large energy are less susceptible to the effect of disturbing pulsations. It

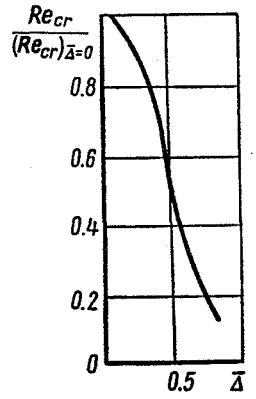

Fig. 12.8.5. Effect of surface roughness of plate on critical Reynolds number.

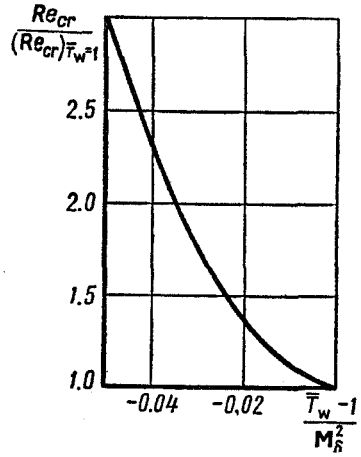

Fig. 12.8.6. Empirical curve characterizing variation in Re_{cr} with temperature factor and Mach number M_δ.

is found that at very high speeds of flow-interaction the Reynolds number has an insignificant role as a stability criterion in comparison with parameters like relative wall temperature T_w/T_δ (T_w/T_∞ or T_w/T_r) and Mach number M_δ. The results of experimental research on the relation of the critical Reynolds number to the temperature of the surface of the plate are shown in Fig. 12.8.6. With the help of these results it is possible to find the relation of the quantity $Re_{cr}/(Re_{cr})_{\bar{T}_w=1}$ [$(Re_{cr})_{\bar{T}_w=1}$ is the critical Reynolds number at $\bar{T}_w = T_w/T_r = 1$] with the parameter $(\bar{T}_w - 1)/M_\delta^2$ involving factor of temperature $\bar{T}_w$ and Mach number M_δ.

In this way the above data help us to establish the effect of Mach number M_δ at the external limit of the layer on the stability of a laminar boundary layer. It can easily be seen that the critical Reynolds number decreases with an increase in Mach number M_δ because the recovery temperature rises with an increase in Mach number M_δ. As a result the density and kinetic energy of the gas near the wall diminish.

It is natural that the effect of disturbances registers more strongly on gas

particles with less kinetic energy. This leads to earlier transition of the boundary layer.

Let us establish the effect of a degree of turbulence of external flow and surface roughness on the stability of a laminar boundary layer at different Mach numbers M_δ. Observations show that this effect diminishes with a rise in M_δ and at $M_\delta > 4$ to 5 the critical Reynolds number is practically independent of the degree of turbulence and surface roughness. The physical nature of this phenomenon is as follows: It is well known that the thickness of the boundary layer increases with a rise in Mach number M_δ and hence a larger part of the fluid mass becomes involved in a viscous flow. This is why a thick laminar boundary layer is less disturbed by turbulence in the external flow and surface roughness. The stabilizing effect of Mach number M_δ does not follow from this. In a given case there may be a reduction in the role of such factors as turbulence and surface roughness in a change in the critical Reynolds number. But the value of this number will be reduced simultaneously with a rise in M_δ.

The critical Reynolds number, worked out on the basis of the local parameters of the boundary layer, depends on the form of the surface in the flow. Let us study this with the example of the flow-interaction of a cone. At one and the same value of Mach number M_δ and wall temperature the thickness of the boundary layer over the cone is less than that on the flat plate at a corresponding point. In this thin layer of viscous fluid the tendency of particles

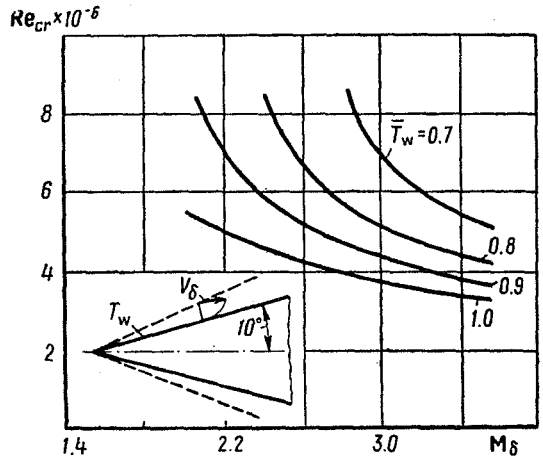

Fig. 12.8.7. Variation in critical Reynolds number for cone.

to intermix becomes less marked and the critical value of the Reynolds number increases. Experimental data on the variation of this number in relation to Mach number M_δ and temperature factor $\bar{T}_w = T_w/T_r$ are reproduced in Fig. 12.8.7. Analysis of these data shows that the qualitative picture of the

effect of Mach number M_δ and surface temperature on the stability of the boundary layer for a cone is the same as that for a flat plate. At the same time the peculiarity of flow-interaction may be noted whereby at Mach number $M_\delta > 4$ to 5 the critical Reynolds numbers for a conical surface remain practically constant for a given value of temperature factor $\overline{T}_w$. Here, as shown by the calculations, the value of the critical Reynolds number is approximately inversely proportional to the relative wall temperature $\overline{T}_w = T_w/T_r$ which can be determined with the help of the expression (12.5.12) for T_r.

In investigating the stability of a laminar boundary layer on a curved surface it is necessary to consider the effect of the axial pressure gradient along with the above factors. If it is positive the gas particle is slowed down and therefore its kinetic energy decreases. This results in less resistance to disturbing interactions, which leads to more intensive intermixing and hence to a reduction in the critical Reynolds number.

The acceleration of particles induced by a negative pressure gradient helps to retard laminar motion up to very high Reynolds numbers. A curve obtained as a result of experimental research in a subsonic flow over a profile is shown in Fig. 12.8.8. This helps us to estimate the effect of the axial pressure gradient on the critical Reynolds number. This curve corresponds to an empirical formula:

$$(\mathbf{Re}_{cr})_\lambda/(\mathbf{Re}_{cr})_0 = 1/(1-0.048\lambda)^2, \qquad (12.8.2)$$

where $\lambda = -18x d\tilde{p}_\delta/dx$ is a parameter worked out on the basis of the value of pressure in boundary layer $\tilde{dp}_\delta/dx$; $\tilde{p}_\delta = 2p_\delta/(\rho_\delta V_\delta^2)$ is a nondimensional value of pressure in a boundary layer; $(\mathbf{Re}_{cr})_\lambda$ and $(\mathbf{Re}_{cr})_0$ are the critical Reynolds numbers corresponding to $\lambda \neq 0$ (pressure gradient different from zero) and $\lambda = 0$ (pressure gradient equal to zero).

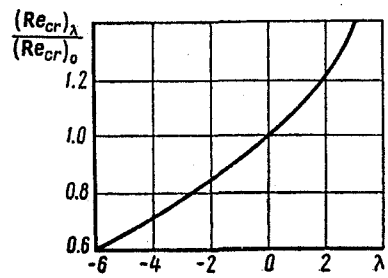

Fig. 12.8.8. Effect of axial pressure gradient on critical Reynolds number of flow over plain curved surface.

After determining the critical Reynolds number with adjustment for the above factors it is possible to calculate the parameters of a mixed boundary layer taking these parameters separately for the regions of laminar and turbulent flows. Let us take as an example the method of calculating this kind of boundary layer on a flat plate (see Fig. 12.8.3). In the region from the leading edge to point P (length of section $x_{cr} = x_P$) on the plate the parameters of viscous flow-interaction (thickness of layer, coefficient of friction) are worked out from the usual relations for a laminar boun-

dary layer. However, for the calculation of turbulent flow beginning from point P the earlier relations for a turbulent boundary layer should not be applied because this layer begins not from zero thickness but from some finite thickness of layer. It has been proved by experiment that these relations can be used with fair accuracy if the coordinate x is taken from the conditional origin of the turbulent boundary layer, which can be determined by the point O' in Fig. 12.8.3.

To determine this point we can use one of the following schemes: According to the first scheme it is assumed that the distance $O'P=\Delta x$, which is equal to the length of imaginary plate with turbulent boundary layer δ_T at the point of transition, K is equal to the thickness of laminar boundary layer δ_L at a distance $x_{cr}=x_P$. If an incompressible fluid is considered this leads to the condition

$$A_1 x_P\,(\mathbf{Re}_{cr})_{x_P}^{-1/2}=A_2\,\Delta x\,(\mathbf{Re}_{\Delta x})^{-1/5}, \tag{12.8.3}$$

where $A_1=4.64$; $A_2=0.37$;

$$(\mathbf{Re}_{cr})_{x_P}=V_\delta\,x_P/\nu_\delta,\quad \mathbf{Re}_{\Delta x}=V_\delta\,\Delta x/\nu_\delta \tag{12.8.4}$$

according to (12.3.19′) and (12.4.58). Here the critical number $(\mathbf{Re}_{cr})_{x_P}$ is taken as a known quantity equal to $(1\text{–}5)\times 10^6$. Knowing this quantity, the value of Δx can be found from (12.8.3).

The characteristic parameters can be used to work out the effect of compressibility and high temperatures. For this purpose the expression for the Reynolds number will be written in the following way:

$$(\mathbf{Re}_{cr})_{x_P}=V_\delta\,x_P/\nu^*,\quad \mathbf{Re}_{\Delta x}=V_\delta\Delta x/\nu^*. \tag{12.8.5}$$

In the case in question the critical Reynolds number $(\mathbf{Re}_{cr})_{x_P}$ should be obtained taking into account the wall temperature and Mach number $\mathbf{M}_\delta$. Inserting the values of (12.8.5) in (12.8.3), the length Δx can be worked out. This will be determined by the effect of high-speed flows.

According to the second scheme it is assumed that the thicknesses of the layers at transition points are not equal but the momentum thicknesses δ^{**} for laminar and turbulent boundary layers are equal, i.e.

$$(\delta_L^{**})_{x_P}=(\delta_p^{**})_{\Delta x}. \tag{12.8.6}$$

For an incompressible fluid the momentum thickness is found from equation (12.2.20) in which $\rho=\rho_\delta$ is assumed:

$$\delta^{**}=\int_0^\delta \frac{V_x}{V_\delta}\left(1-\frac{V_x}{V_\delta}\right)dy.$$

Introducing the notation for integral

$$B=\int_0^1 \frac{V_x}{V_\delta}\left(1-\frac{V_x}{V_\delta}\right) d\left(\frac{y}{\delta}\right)=\text{const}, \tag{12.8.7}$$

we get

$$\delta^{**}=\delta B. \tag{12.8.8}$$

Inserting this value in (12.8.6) and keeping in view the expression (12.8.3) for thickness, we have

$$A_1 B_1 x_P\,(\mathbf{Re}_{cr})_{x_P}^{-1/2}=A_2\,B_2\,\Delta x\,(\mathbf{Re}_{\Delta x})^{-1/5}, \tag{12.8.9}$$

where B_1 is calculated from (12.8.7) with substitution of V_x/V_δ by equation (12.3.15) in which $\eta/\eta_\delta=y/\delta$ is assumed, and B_2 is found from the same expression (12.8.7) with substitution of V_x/V_δ according to (12.4.54). The quantity Δx, obtained from (12.8.9), will be somewhat higher than that from the formula (12.8.3). It may be assumed that a value somewhere between the values of Δx obtained from these formulas will be nearer to the actual value.

The results of calculation of the coordinates of point O' can be used to calculate thicknesses, distribution of local frictional coefficients and the average values of these coefficients in the case of a mixed boundary layer. The average frictional coefficient for a plate of length L will be

$$(c_f)_{inc}=(c_{fL})_{inc}\frac{x_P}{L}+(c'_{fT})_{inc}\frac{x'}{L}-(c''_{fT})_{inc}\frac{\Delta x}{L}, \tag{12.8.10}$$

where $(c_{fL})_{inc}$ is the average coefficient of laminar friction over the region $O'P$ worked out on the basis of the critical Reynolds number; $(c'_{fT})_{inc}$ and $(c''_{fT})_{inc}$ are the average coefficients of turbulent friction corresponding to the regions of length $x'=L-x_P+\Delta x$ and Δx. Here the coefficient $(c'_{fT})_{inc}$ is obtained for the Reynolds number worked out on the basis of length x' and the coefficient $(c''_{fT})_{inc}$ is obtained for the Reynolds number **Re** worked out on the basis of distance Δx.

13

HEAT TRANSFER

1. Aerodynamic Heating

1.1 Equation of heat balance

During flight through the atmosphere there is a heat flow from the surrounding medium to the flight vehicle when the temperature of the gas coming into contact with the surface is higher than that of the body. Regions of high temperatures arise due to deceleration of the flow across shock waves and in the boundary layer, which increases the static enthalpy of the air.

Calculation of heat transfer includes determination of the specific heat flow, which is the quantity of heat flowing to unit surface per unit time (kilo·cal/m^2·sec [MKS] or watt/m^2 [SI]), and aggregate heat flow to the surface under flow-interaction during a given interval of time. The solution of these problems allows us to work out a system of cooling or to select other devices to protect the surface against overheating. It also allows us to determine the regions where excessive thermal stresses occur, leading to possible destruction of the surface, so that precautionary measures can be taken.

Let us consider the equation of heat balance which, in its general form, determines the resultant specific heat flow contributing to heating of the wall. The value of this specific heat flow q_w is equal to the difference between heat inflow q_{in} and heat outflow q_0, i.e.

$$q_w = q_{in} - q_0. \tag{13.1.1}$$

The heat inflow to the wall arises due to conductivity and diffusion in the gas ($q_k = q_c + q_d$), radiation of the gas q_{rad}, solar and terrestrial radiation q_s and q_e and heat transfer from the machine q_m. So

$$q_{in} = q_k + q_{rad} + q_s + q_e + q_m. \tag{13.1.2}$$

The heat outflow consists of the heat q_r radiated by the heated surface, the heat q_{ab} absorbed by the material of the wall and dispersed in the surrounding medium during mass transfer or ablation, the heat q_{ca} carried away by various cooling aids and the heat q_{mo} consumed in heating of the machine.

Hence

$$q_0 = q_r + q_{ab} + q_{ca} + q_{mo}. \tag{13.1.3}$$

In the thermal balance the heat flow q_m from the machine or q_{mo} to it and the heat q_{ca} carried away by cooling have a greater effect. The problems connected with the permissible values of q_m, q_{mo} and the required values of q_{ca} are of a technico-structural character. They are solved for each concrete case taking into account the specific peculiarities of the flight vehicle. Let us consider here only the processes of natural inflow and outflow of heat related to the heating of gas, radiation from the wall and thermal radiation from the sun and the earth.

1.2 Heat inflow from heated gas

Molecular thermal conductivity: During the radiation process the phenomenon of a high-speed flow of gas over a body gives rise to nonuniform heating of the gas, leading to a three-dimensional distribution of temperatures as well as of the constituents of the gas. The temperature gradients arising in this way result in a heat flow which is based on molecular thermal conductivity. This heat flow is determined by Fourier's law:

$$q_T = -\lambda_w (\partial T/\partial y)_w, \tag{13.1.4}$$

where λ_w, $(\partial T/\partial y)_w$ are the coefficient of thermal conductivity and temperature gradient for a heated gas near the wall. The minus sign on the right side reflects the fact that the value of q_T is positive and the temperature gradient $(\partial T/\partial y)_w$ is negative because temperature is low in the direction of heat propagation.

Heat flow due to diffusion: One of the peculiarities of the process of heat transfer in a boundary layer at very high speeds is that the atoms and ions produced by dissociation and ionization take part in the process of heat transfer by diffusing into the regions of low atomic and ionic concentration. The process of diffusion, associated with recombination of atoms and ions, leads to the separation of additional heat (see Chapter 3 Section 2 for a detailed account):

$$q_d = \Sigma Q_{id}\, i_i, \tag{13.1.5}$$

where Q_{id} is a diffusive flow of substance, i_i is an enthalpy of the i-th component of the mixture, these are determined by formulas (3.2.1) and (1.5.28) respectively.

For the model of air representing the reacting atomic-molecular mixture, we have

$$q_d = Q_{Ad} \cdot i_A + Q_{Md} \cdot i_M, \tag{13.1.5'}$$

where $$i_A = \int_0^T c_{pA} dT + i_{chem},\ i_M = \int_0^T c_{pM} dT. \qquad (13.1.6)$$

In addition the transfer of substance in a given direction y can be taken as

$$Q_{Ad} = -Q_{Md} = -\rho D_{AM} (\partial c_A / \partial y),\ D_{AM} = D_{MA} = \bar{D}, \qquad (13.1.7)$$

where $D_{AM(MA)} = \bar{D}$ is the coefficient of diffusion of atomized (molecular) component into molecular (atomized); c_A [kg/kg] is the mass concentration of atoms. Obviously it is possible to come out of the given binary structure of dissociating air with some approximation because the coefficients of transfer which characterize the viscosity, thermal conductivity, diffusion and atomic weights of oxygen and nitrogen are close to one another. We assume that the concentration of nitrogen oxide is low and its effect on the energy transfer can be neglected. It is also possible to take into account the effect of ionization, which begins only at a Mach number $M_\infty > 20$–25.

Inserting (13.1.7) in (13.1.5′) and taking into account the conditions on the wall, we get

$$q_d = -\rho_w \bar{D} (\partial c_A / \partial y)_w (i_A - i_M). \qquad (13.1.8)$$

The enthalpies i_A and i_M of the atomized and molecular components are expressed through the enthalpy i of the mixture:

$$i = i_A c_A + i_M (1 - c_A). \qquad (13.1.9)$$

According to (13.1.6) the difference

$$i_A - i_M = \int_0^T (c_{pA} - c_{pM})\, dT + i_{chem}. \qquad (13.1.10)$$

In actual cases the second term on the right side is considerably higher than the first term and hence we can take $i_A - i_M \approx i_{chem}$, where $i_{chem} = u_d$ [(see 1.5.9)].

Besides the transfer of material based on the varying concentration there occur diffusion flows due to the presence of temperature gradients (thermo-diffusion) and pressure gradients (baro-diffusion). These two components of the diffusion flow are of little significance and therefore are not taken into account in the study of thermal conductivity in a gas flow over a body. The gas components diffusing as a result of the presence of the concentration gradient, transferring enthalpy, are the sources of an energy flow that may overtake the heat flow due to thermal conductivity under certain conditions.

Total specific heat flow: The value of the total specific heat flow is determined by the heat transfer due to the usual molecular heat conductivity and by the separation of energy as a result of recombination of the atoms participating in diffusion. From this the total specific heat flow to the wall, in accordance with (13.1.4) and (13.1.8), will be

$$q_k = q_T + q_d = -\lambda_w (\partial T/\partial y)_w - \rho_w \bar{D} (i_A - i_M) (\partial c_A/\partial y)_w. \quad (13.1.11)$$

The derivative $(\partial T/\partial y)_w$ in this expression can be determined in the following way: Differentiating (13.1.9) with respect to y, we get:

$$\frac{\partial i}{\partial y} = \frac{\partial c_A}{\partial y} (i_A - i_M) + \frac{\partial i_A}{\partial y} c_A + \frac{\partial i_M}{\partial y} (1 - c_A). \quad (13.1.9')$$

Now we use formula (1.5.28) after simplifying it to the following form:

$$di_i = c_{pi}\, dT,$$

keeping in view that $d\,(i_{chem})_i = 0$ here because the enthalpy of its formation $(i_{chem})_i = \text{const}$ for each component. According to the expression for di_i obtained we have

$$di_A = c_{pA}\, dT, \quad di_M = c_{pM} dT.$$

Consequently equation (13.1.9') can be simplified to the form

$$\frac{\partial i}{\partial y} = \frac{\partial c_A}{\partial y} (i_A - i_M) + \frac{\partial T}{\partial y} [c_{pA} c_A + c_{pM} (1 - c_A)],$$

where according to (1.5.25)

$$c_{pA} \cdot c_A + c_{pM} (1 - c_A) = (c_p)_{av}.$$

From the above relation for $\partial i/\partial y$ we find the derivative $\partial T/\partial y$ on the wall

$$\left(\frac{\partial T}{\partial y}\right)_w = \frac{1}{(c_p)_w} \left(\frac{\partial i}{\partial y}\right)_w - \frac{1}{(c_p)_w} \left(\frac{\partial c_A}{\partial y}\right)_w (i_A - i_M)_w,$$

where $[(c_p)_{av}]_w$ is denoted by $(c_p)_w$.

Substituting the expressions obtained for $(\partial T/\partial y)_w$ in (13.1.11), we get

$$q_k = -\frac{\lambda_w}{(c_p)_w} \left[\left(\frac{\partial i}{\partial y}\right)_w - \left(\frac{\partial c_A}{\partial y}\right)_w (i_A - i_M)_w + \frac{\rho_w (c_p)_w \bar{D}}{\lambda_w} \left(\frac{\partial c_A}{\partial y}\right)_w (i_A - i_M)_w \right] \quad (13.1.12)$$

or

$$q_k = -\frac{\lambda_w}{(c_p)_w} \left(\frac{\partial i}{\partial y}\right)_w \left\{ \underbrace{\left[1 - \frac{(\partial c_A/\partial y)_w (i_A - i_M)_w}{(\partial i/\partial y)_w}\right]}_{\text{thermal conductivity (1)}} + \mathbf{Le} \underbrace{\frac{(\partial c_A/\partial y)_w (i_A - i_M)_w}{(\partial i/\partial y)_w}}_{\text{diffusion (2)}} \right\}. \quad (13.1.12')$$

The nondimensional parameter

$$\mathbf{Le} = \rho_w (c_p)_w \bar{D}/\lambda_w, \quad (13.1.13)$$

introduced in equation (13.1.12'), is known as the Lewis-Semyenov number.

This happens to be one of the important criteria of diffusive heat transfer. The physical meaning of this parameter is that it determines the ratio of intensity of heat transfer during mass transfer as a result of diffusion to the intensity of heat exchange by thermal conductivity. In a general case the value of $\mathbf{Le}>1$ and consequently the thermal conductivity is less intensive than the heat transfer by diffusion.

Let us rewrite the Lewis-Semyenov number **Le** (13.1.13) in a different form:

$$\mathbf{Le}=\frac{\mu_w (c_p)_w}{\lambda_w}\cdot\frac{\rho_w \bar{D}}{\mu_w}.$$

The first multiplier on the right side represents the Prandtl number $\mathbf{Pr}=\mu_w (c_p)_w/\lambda_w$ and the second term is a nondimensional quantity which can be taken as the characteristic of the diffusive heat transfer. The parameter inverse to this is introduced in the theory of heat transfer. This is known as Prandtl's number for diffusion or Schmidt's number:

$$\mathbf{Sc}=\mu_w/\rho_w \bar{D}. \tag{13.1.14}$$

The physical meaning of the parameter **Sc** is that it determines the relation between the kinetic energy based on molecular transfer and the energy carried away by diffusion. Like Prandtl's criteria Schmidt's number for gases is $\mathbf{Sc}<1$, where $\mathbf{Sc}<\mathbf{Pr}$. The relation between the Schmidt and Lewis-Semyenov numbers is as follows:

$$\mathbf{Le}=\mathbf{Pr}/\mathbf{Sc}. \tag{13.1.13'}$$

The study of the numerical values of the above parameters is of great practical importance. It has been established theoretically that Schmidt's number varies very little in a wide range of temperatures for a two-component atomic-molecular mixture. For example, if the value of $\mathbf{Sc}=0.495$ at $T=252°\mathrm{K}$ its value will be $\mathbf{Sc}=0.482$ at $T=3360°\mathrm{K}$. The same can also be said of the nature of variation in Prandtl's number, the value of which is $\mathbf{Pr}\approx 0.71$. If Schmidt's number is taken as an average value $\mathbf{Sc}=0.49$ the Lewis-Semyenov parameter will be

$$\mathbf{Le}=\frac{\mathbf{Pr}}{\mathbf{Sc}}=\frac{c_p\mu}{\lambda}\cdot\frac{\rho\bar{D}}{\mu}=\frac{\rho\bar{D}c_p}{\lambda}=\frac{0.71}{0.49}=1.45.$$

From the data available this parameter depends only slightly on temperature up to values of $T\approx 9000°\mathrm{K}$.

Analysis of possible cases of heat transfer: Let us consider equation (13.1.12') and analyze different cases of heat transfer in a boundary layer. From (13.1.12') it follows that if the temperature near the wall is below the limit of dissociation the concentration of atoms is equal to zero and hence $(\partial c_A/\partial y)_w=0$ and the heat flow

$$q_k = q_T = -\frac{\lambda_w}{(c_p)_w}\left(\frac{\partial i}{\partial y}\right)_w. \tag{13.1.15}$$

In the above case of critical thermodynamic equilibrium the heat transfer is characterized by molecular thermal conductivity consisting of transfer of the kinetic energy of uniform motion of molecules and of their vibrational and rotational energies.

The real flow in a dissociating boundary layer is characterized by the presence of a gradient of concentrations of atoms and molecules and by the disequilibrium of chemical reactions. In this case the mode of heat transfer in a boundary layer may be somewhat different from the process of pure molecular thermal conduction. Along with the molecular heat transfer exchange of heat takes place due to chemical energy being separated during recombination. The following critical cases are typical for this process:

In the first critical case when the number $\mathbf{Le}=1$ the heat flow, as can be seen from (13.1.12′), is exactly equal to (13.1.15). In this case the peculiarity of the heat transfer process is that the quantity of heat absorbed during dissociation [first term in (13.1.12′)] is exactly equal to the heat flow due to dissociation [second term in (13.1.12′)]. Obviously, the case in question is characterized by an infinitely high rate of recombination so that thermodynamic equilibrium is established at each point in the boundary layer. According to this the heat transferred by diffusion in a boundary layer is established by the presence of the profile of concentrations of equilibrium.

In practical cases conditions of flow approximating to this hypothetical boundary layer in "equilibrium" will exist when the rate of diffusion is negligibly small in comparison with the rate of dissociation and recombination (and in the case of ionization, in comparison with electronic reactions).

In the second critical case, which comes about at very high speeds of flight when the gas in the boundary layer is highly dissociated, the parameter

$$\frac{(\partial c_A/\partial y)_w\,(i_A - i_M)_w}{(\partial i/\partial y)_w} \approx 1.$$

This can be proved with the help of the expression (13.1.9′). According to this assumption $c_A \to 1$ at very high speeds, and hence

$$\frac{\partial i}{\partial y} \to \frac{\partial c_A}{\partial y}(i_A - i_M) + \frac{\partial i_A}{\partial y}.$$

Here the derivative

$$\frac{\partial i_A}{\partial y} = \frac{\partial}{\partial y}\left[\int_0^T c_{pA}\,dT + (i_{chem})_A\right].$$

Assuming that the heat of formation in actual cases $(i_{chem})_A \gg \int_0^T c_{pA}dT$ and is

a constant quantity we may take $\partial i_A/\partial y \approx 0$. Consequently we have on the wall

$$\left(\frac{\partial i}{\partial y}\right)_w \to \left(\frac{\partial c_A}{\partial y}\right)_w (i_A - i_M)_w.$$

According to this

$$q_k = q_d = -\frac{\lambda_w}{(c_p)_w} \mathbf{Le} \left(\frac{\partial i}{\partial y}\right)_w. \tag{13.1.15'}$$

In this way the whole of the heat in a given critical case is transferred by diffusion. This process of heat-exchange is characterized by very low rates of recombination. As a result diffusion of atoms takes place but the energy in the boundary layer does not get separated. In practice this can happen in a flow where the period of chemical reaction is not high in comparison with the characteristic time of motion of particles. Such flows are known as "frozen" flows.

In a frozen flow the atoms formed during dissociation diffuse in the direction of the cold wall, where they later recombine. The energy liberated depends on the catalytic properties of the wall arising at different values of rates of catalytic reaction of recombination.

It is assumed that all the actual processes of heat transfer take place between these two critical cases.

Newton's formula: The general heat flow from a heated gas to a wall $q_k = q_T + q_d$, determined by equation (13.1.11), can be represented as a convective heat exchange, known as the process of heat transfer, occurring between a solid wall and the gas around it. In practical cases the value of this heat transfer is usually expressed with the help of Newton's formula

$$q_k = a_w (T - T_w), \tag{13.1.16}$$

where T_w is the temperature of the wall; T is some characteristic temperature of the flow past the surface. The coefficient a_w in (13.1.16), having the dimensions kilo·cal/m²·sec· degree in the MKS system or wt/m²·degree in the SI system, is known as the coefficient of heat transfer. Numerically it is equal to the quantity of heat accepted (or given) by a section of surface of unit area in unit time at a temperature difference of one degree between wall and gas.

The temperature T in (13.1.16) is chosen in the following way: We know that if the wall is thermally isolated the temperature of the gas reaches its maximum value near the surface and is equal to the temperature of recovery T_r. This temperature is physically considered as the biggest participating factor determining heat transfer from the heated gas to the surface depending on the condition of the value of the temperature on this wall. Here it may be noted that the quantity T_r, under the given conditions, happens to be a weak function of the flow parameters. It is this characteristic temperature taken as

the temperature T in (13.1.16) that precludes uncertainty in understanding the temperature of the flow past a body. According to the above discussion Newton's formula will be written in the form

$$q_k = a_w (T_r - T_w). \tag{13.1.16'}$$

This representation of the specific heat flow has the important peculiarity that the coefficient of heat transfer a_w seems to be a weak function of the temperature difference and therefore in practical calculations the effect of this difference can be neglected. However, we must bear in mind that the coefficient of heat transfer is a parameter that is dependent on series of other factors such as velocity of the gas flow, form, size and position (angle of attack) of the body in the flow, type of boundary layer (laminar or turbulent), physical parameters of medium (thermal conductivity, viscosity, specific heat), etc.

The equation of heat transfer in the form of (13.1.16') is applicable at speeds where there are no chemical reactions in the boundary layer. Under conditions of very high velocities chemical processes play an active part and it is necessary to take into account the variation of enthalpy during calculation of heat transfer. This may be done according to the formula

$$q_k = [a_w/(c_p)_w] (i_r - i_w), \tag{13.1.17}$$

where $(c_p)_w$ is the average specific heat under the conditions of the gas on the wall; i_r, i_w are the enthalpy of recovery and enthalpy of the gas on the surface of the wall respectively. It should be remembered that it was proposed to take the temperature of the wall and the temperature of the gas (or corresponding enthalpies) on its surface as equal. The results of calculations show that the ratio of $a_w/(c_p)_w$ in (13.1.17) varies little in the case of dissociation (up to 10 to 15%) and it may be taken, as a first approximation, from the solutions for a boundary layer without chemical reaction. The enthalpies i_r, i_w are calculated here with allowance for dissociation. From the calculations by formula (13.1.17) it follows that the heat flows can differ appreciably from the values obtained by (13.1.16') without adjustment for dissociation even though the variation in $a_w/(c_p)_w$ is small.

For the characteristics of heat transfer it is convenient to apply nondimensional criteria in place of the dimensional coefficient of heat transfer. The Stanton number

$$\mathbf{St} = q_k/[\rho_\delta V_\delta (i_r - i_w)] = a_w/[\rho_\delta V_\delta (c_p)_w] \tag{13.1.18}$$

and Nusselt number

$$\mathbf{Nu} = a_w l/\lambda_w, \tag{13.1.19}$$

where l is an arbitrary linear dimension; λ_w is the coefficient of thermal conductivity of gas at the wall, are nondimensional criteria.

The connection between these two numbers is established by the well-

known relation

$$\mathbf{Nu}=\mathbf{St}\cdot\mathbf{Re}\cdot\mathbf{Pr}, \tag{13.1.20}$$

where Reynolds number $\mathbf{Re}=V_\delta\rho_\delta\, l/\mu_\delta$; Prandtl number $\mathbf{Pr}=(c_p)_w\,\mu_\delta/\lambda_w$.

The basic problem of the theory of aerodynamic heat transfer is determination of the coefficient of heat transfer a_w or the nondimensional criteria of heat transfer. For this purpose it must be borne in mind that since the additional terms affecting heat flow are separated in formulas (13.1.18) and (13.1.19) the numbers **St** and **Nu** depend on flow conditions weaker than

$$a_w=\rho_\delta V_\delta\,(c_p)_w\,\mathbf{St} \text{ and } a_w=(\lambda_w/l)\,\mathbf{Nu}.$$

In the general case the values of **St** and **Nu** happen to be the functions of nondimensional criteria which determine the flow conditions: Reynolds number **Re**; Mach number $\mathbf{M}_\delta=V_\delta/a_\delta$; Prandtl number **Pr**; Schmidt's number $\mathbf{Sc}=\mu_\delta/(\rho_\delta\overline{D})$. They also depend on the nature of the boundary layer and the temperature of the wall.

Radiational heat flow: As a result of the intensive rise in temperature behind the shock wave or in a boundary layer the degree of dissociation increases and consequently the amount of atomized oxygen and nitrogen in the air increases. This leads to a more intensive rate of reactions with formation of nitric oxide and to an increase in the concentration of the latter.

The rise in pressure leads to acceleration of recombination following the reaction $A+A\rightleftarrows A_2$ and results in an increase in the concentration of nitric oxide NO formed according to the equation $O_2+N_2\rightleftarrows 2NO$. Nitric oxide, unlike oxygen and nitrogen, is optically opaque, i.e. it has the capacity of absorbing and radiating energy. Air comprising a higher percentage of nitric oxide has this property of opacity. Therefore at very high temperatures air becomes the source of radiational heat flow.

The optical properties of air are characterized by a parameter ε which represents the radiational capacity of unit length of radiating layer of dimension $1/l$. For a radiating layer of thickness s_0 the quantity $\varepsilon\cdot s_0$, known as the effective radiating capacity of gas, will be the nondimensional characteristic radiational capacity.

By the Stephan-Boltzman law the heat radiated by an absolutely black body is $q_{rad}=\sigma\cdot T^4$, where σ is Stephan-Boltzman's constant or the coefficient of radiation of an absolutely black body ($\sigma=5.85\times10^{-9}$ kg·m/m²·sec·degree$^4=1.36\times10^{-11}$ kilo·cal/m²·sec·degree$^4=5.67\times10^{-8}$ t/m²·degree^4); T is the temperature of a radiating gas. The function $f(\varepsilon\cdot s_0)$, depending on the effective radiational capacity that characterizes the degree of blackness of a gas, must be introduced in this formula to take into account transparency. So the relation for determining the radiational heat flow to the wall will have the form

$$q_{rad}=f(\varepsilon s_0)\,\sigma\,T^4. \tag{13.1.21}$$

This formula (13.1.21) deals with the case where the wall does not radiate and its temperature $T_w < 3000°K$.

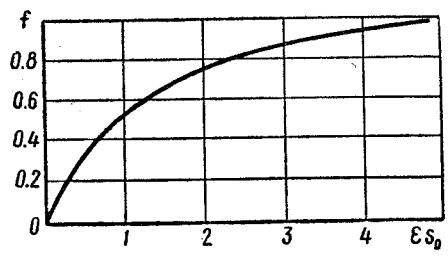

Fig. 13.1.1. Function characterizing degree of blackness of radiating gas.

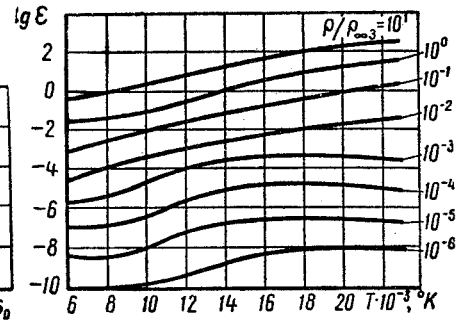

Fig. 13.1.2. Empirical data on radiating capacity of gas (ε, cm).

The curve characterizing variation in function $f(\varepsilon \cdot s_0)$ with the effective radiational capacity of the air is shown in Fig. 13.1.1. This curve may be approximated by the equation

$$f = 1 - e^{-(\varepsilon \cdot s_0)}, \tag{13.1.22}$$

which gives an error of less than 20%.

Figure 13.1.2 represents the results of experimental research. It may be seen that the parameter ε depends on the temperature and the density of the air. In the range of temperature $8000°K \leqslant T \leqslant 16{,}000°K$ the family of curves can be approximately given by the formula

$$\varepsilon = 0.138\,(\rho/\rho_{\infty e})^{1.28}\,(T°K/10^4)^{6.54}\ [cm^{-1}], \tag{13.1.23}$$

where $\rho_{\infty e}$ is the density of atmospheric air near the earth's surface.

1.3 Solar and earth radiation

The radiational heat flow from the sun is given by

$$q_s = \bar{q}\,\beta_s \cos\psi, \tag{13.1.24}$$

where ψ is the angle between the direction of the solar rays and the normal to the surface of the body; $\bar{q}$ is the radiational capacity of the sun, which mainly depends on the flight altitude and meteorological conditions.

For average geographical conditions the values of $\bar{q}$ from the sun at zenith without allowance for absorption of rays by the atmosphere are shown in Fig. 13.1.3.

The data on coefficient β_s taking into account the absorptive capacity of the material are shown in Table 13.1.1.

The radiational capacity $\bar{q}$ during flight at low altitudes ($H \approx 10$–15 km) decreases due to the presence of cloud. For example, the actual value of

$\bar{q}$ for average cloudiness is 0.5–0.7 of the values corresponding to the data in Fig. 13.1.3 and 0.1–0.2 in the case of dense cloud. The radiational capacity under night time conditions is equal to zero.

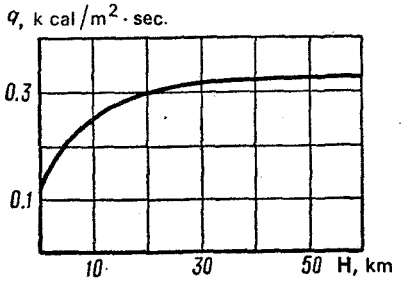

Fig. 13.1.3. Radiational capacity of sun as function of altitude H in atmosphere of earth.

Formula (13.1.24) deals with the part of the surface of the flight vehicle facing the sun. The portions of this surface in shade also receive heat due to scattered solar radiation, about one-third or one-fourth as much.

The specific heat flow from the earth's radiation is very small; it can be considered as the sum of $q_e = q_{e\cdot s} + q_{e\cdot r}$, where $q_{e\cdot s}$ is self-originated radiation from the earth; $q_{e\cdot r}$ is the energy of solar rays reflected from the earth's surface and clouds. Research shows that for flight conditions at an altitude of 500 km,

$$q_{e\cdot s} = 0.007\,(1 + 2\cos\varphi)\,\beta_e, \tag{13.1.25}$$

where φ is the angle between the normal to the surface and a line joining the

TABLE 13.1.1

Materials	Type of radiation	
	From earth (β_e)	From sun (β_s)
Al	0.04–0.10	0.10–0.49
Fe	0.06–0.74	0.45
Ni	0.04–0.39	0.40
Alloys:		
type of duralumin	0.04–0.55	0.53
mild steel	0.12–0.62	0.60
Isolating materials:		
plexiglass	0.89	—
glass	0.85	—
Painted surfaces:		
dark	0.80–0.99	0.97
bright	0.80–0.90	0.14–0.18

Note: The data on the coefficients β_e and β_s are reproduced for the range of wall temperatures 200 to 600°C.

body and earth. From the experimental data available the maximum value of the radiational flow of the earth is

$$q_{e.s\ max} = \bar{q}_e\,\beta_e, \tag{13.1.26}$$

where $\bar{q}_e$ is the radiational capacity of the earth.

The values of $\bar{q}_e$ and β_e are given in Fig. 13.1.4 and in Table 13.1.1 respectively.

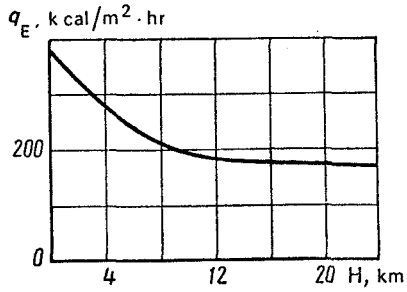

Fig. 13.1.4. Radiational capacity of earth as function of altitude H in atmosphere.

The data on specific heat flow $q_{e\cdot r}$ were also obtained experimentally under the condition that the body was situated at an altitude of 500 km on a line joining the earth and the sun. According to these data

$$q_{e\cdot r}=0.016\,(1+2\cos\varphi)\,\beta_e. \quad (13.1.27)$$

1.4 Radial heat flow from wall surface

The heat radiated by unit wall surface is given by the Stephan-Boltzman law:

$$q_r=\varepsilon\sigma T_{cr}^4, \quad (13.1.28)$$

where ε is the degree of blackness of the surface depending on the material, finish of the surface and its temperature. The scale of blackness shows how much smaller the coefficient of radiation of the given surface is than the coefficient of radiation of an absolutely black body. The value of ε increases with an increase in surface roughness. If the size of the grains of roughness exceeds by a few times the wavelength λ of radiation of maximum intensity the quantity ε_r for a rough surface can be expressed with reference to the degree of blackness of a smooth surface in the following way:

$$\varepsilon_r=\varepsilon\,[1+2.8\,(1-\varepsilon)^2], \quad (13.1.29)$$

in which the wavelength λ in mk depends on the temperature and is equal to

$$\lambda=2898/T. \quad (13.1.30)$$

2. Relation between Friction and Heat Transfer

The problem of aerodynamic heat exchange, as noted earlier, leads to determination of the coefficient of heat transfer α_w appearing in Newton's equation (13.1.16), (13.1.16′) or of the corresponding nondimensional criteria **St** or **Nu**. Determination of the coefficient of heat transfer is related in the general case to the solution of a system of differential equations of the boundary layer consisting of equations of motion, energy, continuity and diffusion. By solving them the relation between the parameters of heat transfer and friction is established. With certain simplifying assumptions this relation takes the form of elementary relations allowing direct determination of α_w, **St** or **Nu** from the coefficient of friction for a given point on the surface.

To obtain these relations we use the equation of a laminar gas flow

(12.1.8) and the equation of energy simplified to the form used in boundary layer theory. First we write it with the help of the general form of energy equation (3.2.14) in such a way that it includes the above numbers **Le, Sc, Pr.** The equation of energy obtained will be more convenient for the analysis of different phenomena and processes of heat transfer. Next this equation is transformed to the conditions of a viscous gas flow in a thin layer near the wall and is obtained in the simplified form of the equation of energy for the boundary layer. Keeping in view the expression (1.5.27) for enthalpy of a mixture, we find that

$$di=\sum_i i_i\, dc_i+\sum_i c_i\, di_i,$$

where $di_i=c_{pi}\cdot dT$ according to (1.5.28). Now, keeping in mind formula (1.5.25) for average heat capacity of a mixture, we get

$$di=\sum_i i_i\, dc_i+(c_p)_{\text{av}}\, dT.$$

The temperature gradient can be written as

$$\operatorname{grad} T=\frac{1}{(c_p)_{\text{av}}}\operatorname{grad} i-\frac{1}{(c_p)_{\text{av}}}\sum_i i_i \operatorname{grad} c_i.$$

Substituting this value in equation (3.2.14) and introducing the notations for local values of Prandtl and Schmidt numbers

$$\mathbf{Pr}=\mu\,(c_p)_{\text{av}}/\lambda,\quad \mathbf{Sc}=\mu/\rho\overline{D},$$

we get the equation of energy

$$\frac{di}{dt}=\frac{1}{\rho}\cdot\frac{dp}{dt}+\nu\left[\left(\frac{\partial V_x}{\partial x}\right)^2+\left(\frac{\partial V_y}{\partial y}\right)^2+\frac{2}{3}(\operatorname{div}\overline{V})^2+4\varepsilon_z^2\right]+\frac{1}{\rho}\operatorname{div}\left[\frac{\lambda}{(c_p)_{\text{av}}}\operatorname{grad} i\right]$$
$$+\sum_i i_i \operatorname{div}\left[\overline{D}\left(1-\frac{\mathbf{Sc}}{\mathbf{Pr}}\right)\operatorname{grad} c_i\right]+\frac{\varepsilon}{\rho},\qquad (13.2.1)$$

where the ratio **Sc/Pr** may be replaced by 1/**Le**, i.e. the quantity that is the inverse of the Lewis-Semyenov number.

The equation of energy written in the form of (13.2.1) and expressed by the enthalpy happens to the basic equation for study of the dynamics of dissociating gases. In the most general case the number **Sc** < **Pr** (**Le** > 1). The physical meaning of this is that the processes of diffusion take place more intensively than those of heat transfer and hence the chemical energy is not completely converted into heat energy. In the particular case where **Pr** = **Sc** equation (13.2.1) takes the form:

$$\frac{di}{dt}=\frac{1}{\rho}\cdot\frac{dp}{dt}+\nu\left[\left(\frac{\partial V_x}{\partial x}\right)^2+\left(\frac{\partial V_y}{\partial y}\right)^2+\frac{2}{3}(\operatorname{div}\overline{V})^2+4\varepsilon_z^2\right]$$
$$+\frac{1}{\rho}\operatorname{div}\left[\frac{\lambda}{(c_p)_{\text{av}}}\operatorname{grad} i\right]+\frac{\varepsilon}{\rho}.\qquad (13.2.1')$$

By its form equation (13.2.1′) represents the equation of energy for flows from which chemical reactions are absent. When **Sc=Pr** the intensity of heat transfer through heat conductivity is the same as that by diffusion. This condition corresponds to the fact that the part of the chemical energy on the external surface of the boundary layer in excess of the chemical energy at the temperature of the wall is completely transformed into heat.

In further discussion we assume that the radiation is not taken into account, i.e. we use the value of $\varepsilon=0$ in equation (13.2.1′). Now to transform this equation to the flow conditions in the boundary layer we determine the order of values of its terms in the same way as for the Navier-Stokes equation in Chapter 12 Section 1 [see the relations (12.1.3), (12.1.4), etc.].

Unlike the equation of motion, terms containing enthalpy i appear in the equation of energy. Therefore it is desirable to examine in addition the problem of the evaluation of the order of these terms. To do this we use the formula for stagnation enthalpy in the form

$$i_0=i+(V_x^2/2). \tag{13.2.2}$$

From the above discussion it is clear that in the particular case where $\mathbf{Pr}=1$ the quantity $i_0=\text{const}$. However, for real flow conditions this enthalpy happens to be a variable quantity due to the presence of thermodynamically irreversible processes created by chemical reactions and dissociation of gas in the boundary layer, i.e. $i_0\neq I_0$ (where I_0 is stagnation enthalpy during an isentropic flow). But the order of these quantities is the same ($i_0\sim I_0=\text{const}$). Taking this into account, we have

$$\frac{\partial i}{\partial x}\sim\frac{\partial V_x^2}{\partial x},\quad \frac{\partial i}{\partial y}\sim\frac{\partial V_x^2}{\partial y},$$

when the order of derivatives will be determined as follows:

$$\frac{\partial i}{\partial x}\sim\frac{V_\delta^2}{L},\quad \frac{\partial i}{\partial y}\sim\frac{V_\delta^2}{\delta}.$$

These data are used to determine the order of the term on the right side of equation (13.2.1′) containing enthalpy i. Evaluating the order of quantities of all the terms on the right side [except the first term $(1/\rho)\,(dp/dt)$] and assuming here that the order of Prandtl number $\mathbf{Pr}=\mu\,(c_p)_{\text{av}}/\lambda\sim 1$, we will write the results of this evaluation directly below each term of the equation in an opened-out form:

$$\frac{di}{dt}=\frac{1}{\rho}\cdot\frac{dp}{dt}+\frac{\mu}{\rho}\underbrace{\left\{\left(\frac{\partial V_x}{\partial x}\right)^2+\left(\frac{\partial V_y}{\partial y}\right)^2\right.}_{(\mu/\rho)\,V_\delta^2/L^2}$$

$$+\frac{2}{3}\underbrace{\left[\left(\frac{\partial V_x}{\partial x}\right)^2+2\frac{\partial V_x}{\partial x}\cdot\frac{\partial V_y}{\partial y}+\left(\frac{\partial V_y}{\partial y}\right)^2\right]}_{(\mu/\rho)\,V_\delta^2/L^2}$$

$$+\underbrace{\left(\frac{\partial V_x}{\partial y}\right)^2}_{(\mu/\rho)\,V_\delta^2/\delta^2}+\underbrace{2\frac{\partial V_x}{\partial y}\cdot\frac{\partial V_y}{\partial x}}_{(\mu/\rho)\,V_\delta^2/L^2}+\underbrace{\left(\frac{\partial V_y}{\partial x}\right)^2}_{(\mu/\rho)\,V_\delta^2\,\delta^2/L^4}\Bigg\}$$

$$+\frac{1}{\rho}\Bigg[\underbrace{\frac{\partial}{\partial x}\left(\frac{\mu}{\mathbf{Pr}}\cdot\frac{\partial i}{\partial x}\right)}_{(\mu/\rho)\,V_\delta^2/L^2}+\underbrace{\frac{\partial}{\partial y}\left(\frac{\mu}{\mathbf{Pr}}\cdot\frac{\partial i}{\partial y}\right)}_{(\mu/\rho)\,V_\delta^2/\delta^2}\Bigg]. \tag{13.2.3}$$

Considering the right side of equation (13.2.3), it can be concluded that the terms

$$\frac{\mu}{\rho}\left(\frac{\partial V_x}{\partial y}\right)^2,\quad \frac{1}{\rho}\cdot\frac{\partial}{\partial y}\left(\frac{\mu}{\mathbf{Pr}}\cdot\frac{\partial i}{\partial y}\right)$$

have a higher order than the remaining terms. Retaining the terms of higher order, we get an energy equation in the following form:

$$\frac{di}{dt}=\frac{1}{\rho}\cdot\frac{dp}{dt}+\frac{\mu}{\rho}\left(\frac{\partial V_x}{\partial y}\right)^2+\frac{1}{\rho}\cdot\frac{\partial}{\partial y}\left(\frac{\mu}{\mathbf{Pr}}\cdot\frac{\partial i}{\partial y}\right). \tag{13.2.4}$$

Replacing the terms in (13.2.4) according to equation (12.1.8), i.e.

$$\frac{dp}{dt}=\frac{dp_\delta}{dt}=V_x\frac{dp_\delta}{dx}=-\rho V_x\left[V_x\frac{\partial V_x}{\partial x}+V_y\frac{\partial V_x}{\partial y}-\frac{1}{\rho}\cdot\frac{\partial}{\partial y}\left(\mu\frac{\partial V_x}{\partial y}\right)\right],$$

we get

$$\frac{di}{dt}=-\frac{V_x}{2}\cdot\frac{\partial V_x^2}{\partial x}-\frac{V_y}{2}\cdot\frac{\partial V_x^2}{\partial y}+\frac{V_x}{\rho}\cdot\frac{\partial}{\partial y}\left(\mu\frac{\partial V_x}{\partial y}\right)+\frac{\mu}{\rho}\left(\frac{\partial V_x}{\partial y}\right)^2+\frac{1}{\rho}\cdot\frac{\partial}{\partial y}\left(\frac{\mu}{\mathbf{Pr}}\cdot\frac{\partial i}{\partial y}\right).$$

The first two terms on the right side of the equation can be expressed in the form

$$-\frac{V_x}{2}\cdot\frac{\partial V_x^2}{\partial x}-\frac{V_y}{2}\cdot\frac{\partial V_x^2}{\partial y}=-\frac{1}{2}\cdot\frac{dV_x^2}{dt},$$

and the summation of the third and fourth terms in the form

$$\frac{V_x}{\rho}\cdot\frac{\partial}{\partial y}\left(\mu\frac{\partial V_x}{\partial y}\right)+\frac{\mu}{\rho}\left(\frac{\partial V_x}{\partial y}\right)^2=\frac{1}{\rho}\cdot\frac{\partial}{\partial y}\left(\frac{\mu}{2}\cdot\frac{\partial V_x^2}{\partial y}\right).$$

Taking these relations into account, we have

$$\rho\frac{d}{dt}\left(i+\frac{V_x^2}{2}\right)=\frac{\partial}{\partial y}\left[\frac{\mu}{\mathbf{Pr}}\left(i+\frac{V_x^2}{2}\right)\right]+\frac{\partial}{\partial y}\left[\frac{\mu}{2}\left(1-\frac{1}{\mathbf{Pr}}\right)\frac{\partial V_x^2}{\partial y}\right]. \tag{13.2.5}$$

Keeping the expression (13.2.2) for enthalpy i_0 in view and expanding the total derivative on the left side of (13.2.5), we get

$$\rho V_x \frac{\partial i_0}{\partial x}+\rho V_y \frac{\partial i_0}{\partial y}=\frac{\partial}{\partial y}\left(\frac{\mu}{\mathbf{Pr}}\cdot\frac{\partial i_0}{\partial y}\right)+\frac{\partial}{\partial y}\left[\frac{\mu}{2}\left(1-\frac{1}{\mathbf{Pr}}\right)\frac{\partial V_x^2}{\partial y}\right]. \quad (13.2.5')$$

Let us study the flow characterizing the quantity $\mathbf{Pr}=1$. For such a flow the equation of energy has the form

$$\rho V_x \frac{\partial i_0}{\partial x}+\rho V_y \frac{\partial i_0}{\partial y}=\frac{\partial}{\partial y}\left(\mu\frac{\partial i_0}{\partial y}\right). \quad (13.2.6)$$

If the flow in question interacts with a flat plate for which $dp_\delta/dx=0$ the equation of motion in a boundary layer according to (12.1.8) will have the following form:

$$\rho V_x \frac{\partial V_x}{\partial x}+\rho V_y \frac{\partial V_x}{\partial y}=\frac{\partial}{\partial y}\left(\mu\frac{\partial V_x}{\partial y}\right). \quad (13.2.7)$$

It may be seen that the equation of energy (13.2.6) and the equation of motion (13.2.7) are similar to one another. If we change over to the variables

$$\theta=(i_0-i_w)/(i_{0\delta}-i_w),\ \bar{V}_x=V_x/V_\delta, \quad (13.2.8)$$

where

$$i_{0\delta}=i_\delta+(V_\delta^2/2), \quad (13.2.9)$$

equations (13.2.6) and (13.2.7) will be identical because θ and $\bar{V}_x$ satisfy one and the same boundary conditions: at the wall θ and $\bar{V}_x$ are equal to zero since $V_x=0$ and $i_0=i_w$; and at the external limit of the boundary layer where $V_x=V_\delta$ and $i_0=i_{0\delta}$, they are equal to unity. Consequently they function $\bar{V}_x$ and θ must coincide by the theorem of uniqueness of solution, i.e.

$$(i_0-i_w)/(i_{0\delta}-i_w)=V_x/V_\delta. \quad (13.2.10)$$

In this way the condition ($\mathbf{Pr}=1$) and other assumptions made above determine the similarity of the velocity and enthalpy profiles in the boundary layer. If the velocity profile is known it is possible to determine the frictional stress

$$\tau_w=\mu_w\left(\frac{\partial V_x}{\partial y}\right)_w=\frac{\mu_w V_\delta}{i_{0\delta}-i_w}\left(\frac{\partial i_0}{\partial y}\right)_w=\frac{\mu_w V_\delta (c_p)_w}{i_{0\delta}-i_w}\left(\frac{\partial T}{\partial y}\right)_w.$$

Multiplying the numerator and denominator of the right side of this equation by λ_w and assuming that $q_w=q_k=\lambda_w(\partial T/\partial y)_w$, we find

$$\tau_w=\frac{\mu_w V_\delta (c_p)_w}{\lambda_w (i_{0\delta}-i_w)}q_k.$$

Substituting the value of q_k from equation (13.1.17) here and replacing $\tau_w=c_{fx}(\rho_\delta V_\delta^2/2)$, we get

$$c_{fx}\frac{\rho_\delta V_\delta^2}{2}=a_w\frac{\mu_w V_\delta}{\lambda_w}\cdot\frac{i_r-i_w}{i_{0\delta}-i_w}.$$

Since the Prandtl number $\mathbf{Pr}=1$ the coefficient of recovery $r=1$ and

$$i_r=i_\delta+r\frac{V_\delta^2}{2}=i_\delta+\frac{V_\delta^2}{2}=i_{0\delta};\quad\frac{i_r-i_w}{i_{0\delta}-i_w}=1.$$

In this way we get the relation between the coefficients of heat transfer and friction in the following form:

$$a_w=a_x=\frac{c_{fx}}{2}\cdot\frac{\rho_\delta V_\delta\lambda_w}{\mu_w}. \tag{13.2.11}$$

From the expression (13.2.11) the formula for the local Nusselt number follows:

$$\mathbf{Nu}_w=\mathbf{Nu}_x=\frac{a_x x}{\lambda_w}=\frac{c_{fx}}{2}\cdot\mathbf{Re}_x, \tag{13.2.12}$$

where the Reynolds number $\mathbf{Re}_x=\rho_\delta V_\delta x/\mu_w$. From (13.1.20), at the value of Prandtl number $\mathbf{Pr}=1$, we have

$$\mathbf{St}_w=\mathbf{St}_x=\mathbf{Nu}_x/\mathbf{Re}_x=c_{fx}/2. \tag{13.2.13}$$

The relation established between the parameters of friction and heat transfer is approximate because the **Pr** and **Sc** numbers differ from unity in practice. The effect of these parameters can be taken into account if the expressions for the Nusselt and Stanton criteria are written in the form:

$$\mathbf{Nu}_x=(c_{fx}/2)\,\mathbf{Re}_x f_1(\mathbf{Pr},\mathbf{Sc}); \tag{13.2.14}$$

$$\mathbf{St}_x=(c_{fx}/2)\,f_2(\mathbf{Pr},\mathbf{Sc}), \tag{13.2.15}$$

where f_1 and f_2 are some functions of **Pr** and **Sc**. The physical meaning of adjustment for values of these numbers different from unity is that the transformation of part of the chemical and kinetic energy into heat is taken into account. The concrete form of the relations f_1, f_2 is determined from the solutions of the boundary layer under the condition that $\mathbf{Pr}\neq1$, $\mathbf{Sc}\neq1$ ($\mathbf{Le}\neq1$).

Research shows that if the condition $\mathbf{Le}=1$ is considered $f_1=\mathbf{Pr}^{1/3}$ and according to (13.1.20) $f_2=\mathbf{Pr}^{-2/3}$. According to this we may write in particular for the local Stanton number,

$$\mathbf{St}_x=(c_{fx}/2)\,\mathbf{Pr}^{-2/3}. \tag{13.2.16}$$

The corresponding expression for the Nusselt number can be found from (13.1.20). From the local criterion of the Nusselt and Stanton numbers it is possible to change to the corresponding average quantities of a flat plate

along its length, dropping the index "x". Here it may be assumed that the local and average Prandtl numbers are equal.

Formula (13.2.16) has great practical importance. It reflects the Reynolds analogy according to which the criterion of heat transfer depends basically on the same parameter as the coefficient of friction, i.e. on the Reynolds number $\mathbf{Re}_x$. According to this the quantity $f_2=\mathbf{Pr}^{-2/3}$ in (13.2.16) is known as the Reynolds analogy factor.

As shown by research, formula (13.2.15) is also convenient for a turbulent boundary layer but with the difference that the frictional coefficient c_{fx} and parameter f_2 must be calculated from the corresponding relations for a turbulent boundary layer. In particular, the quantity f_2 can be determined by the formula

$$f_2=[1+2.135\mathbf{Re}_x^{-0.1}(\mathbf{Pr}-1)]^{-1}. \tag{13.2.17}$$

In calculating the value of the Stanton number of a flat plate of average length the parameter

$$f_2=[1+2.2\mathbf{Re}\,(\mathbf{Pr}-1)]^{-1}, \tag{13.2.18}$$

where $\mathbf{Re}=V_\delta\rho_\delta L/\mu_w$. Here the calculations show that the value of f_2 in the absence of diffusion in a turbulent layer can be taken as equal to $\mathbf{Pr}^{-2/3}$ within a known approximation in the same way as for a laminar boundary layer.

The effect of physico-chemical changes on heat transfer in the boundary layer at high temperatures can be accounted for by using the definitive parameters. In particular, using the Reynolds number we get the following expression for the definitive value of the Stanton number according to (13.2.16):

$$\mathbf{St}_x^*=(c_{fx}^*/2)\,(\mathbf{Pr}^*)^{-2/3}, \tag{13.2.19}$$

where the coefficient $c_{fx}^*=(c_{fx})_c$ for a laminar boundary layer can be found from formula (12.6.15) and for a turbulent boundary layer from the relation (12.6.22); the definitive Prandtl number can be calculated from the definitive parameters $\mathbf{Pr}^*=c_p^*\cdot\mu^*/\lambda^*$.

According to this the heat flow to the wall is

$$q_x^*=(\alpha_x^*/c_p^*)\,(i_r-i_w)=\mathbf{St}_x^*\,\rho_\delta\,V_\delta\,(i_r-i_w), \tag{13.2.20}$$

where the definitive coefficient of heat transfer is

$$\alpha_x^*=c_p^*\,q_x^*/(i_r-i_w)=\mathbf{St}_x^*\,c_p^*\,\rho_\delta\,V_\delta. \tag{13.2.21}$$

From formula (13.2.16) or (13.2.19) it follows that the nondimensional parameter of heat transfer varies along the plate in the same way as the local coefficient of friction. As may be seen from (13.2.20), the specific heat flow will vary correspondingly. Its average value over the length of the plate is obviously determined as the average integral of local heat flows. Performing

the calculation on the basis of the definitive parameters [see (13.2.20)], we get

$$q^*_{\text{av}}=\frac{1}{L}\int_0^L q_x\,dx=\rho_\delta V_\delta\int_0^1 \mathbf{St}^*_x\,(i_r-i_w)\,d\bar{x}, \tag{13.2.22}$$

where $\bar{x}=x/L$. Assuming i_w to be constant along the plate and replacing $\mathbf{St}^*_x$ from formula (13.2.19), we get

$$q^*_{\text{av}}=\frac{1}{2}\rho_\delta V_\delta\,(\mathbf{Pr}^*)^{-2/3}\,(i_r-i_w)\int_0^1 c^*_{fx}\,d\bar{x}.$$

The integral on the right side of the equation determines the average frictional coefficient $c^*_{xf}=(c_{xf})_c$ over the length of the plate, which can be calculated from formula (12.6.15) and expression (12.6.22) for laminar and turbulent boundary layers respectively. Consequently the average heat flow

$$q^*_{\text{av}}=(c^*_{xf}/2)\,(\mathbf{Pr}^*)^{-2/3}\,\rho_\delta V_\delta\,(i_r-i_w). \tag{13.2.23}$$

Introducing the concept of an average value of the Stanton number

$$\mathbf{St}^*_{\text{av}}=(c^*_{xf}/2)\,(\mathbf{Pr}^*)^{-2/3}, \tag{13.2.24}$$

we have

$$q^*_{\text{av}}=\mathbf{St}^*_{\text{av}}\,\rho_\delta V_\delta\,(i_r-i_w). \tag{13.2.25}$$

The parameters of heat transfer for a flat plate could be directly used to calculate the corresponding parameters for a cone in a supersonic flow. The calculation will be carried out with the help of formulas (12.6.34), (12.6.35), (12.6.52) and (12.6.53) connecting the frictional coefficients (local and average) on the plate and on the cone. Multiplying the left and right sides of these formulas by $(\mathbf{Pr}^*)^{-2/3}$, we get:

for local frictional coefficient

$$(c^*_{fxc}/2)\,(\mathbf{Pr}^*)^{-2/3}=\mathrm{A}\,(c^*_{fxp}/2)\,(\mathbf{Pr}^*)^{-2/3};$$

and for the average value of this coefficient

$$(c^*_{xfc}/2)\,(\mathbf{Pr}^*)^{-2/3}=\mathrm{A}\,(c^*_{xfp}/2)\,(\mathbf{Pr}^*)^{-2/3},$$

where $\mathrm{A}=\sqrt{3}$ for a laminar boundary layer and $\mathrm{A}=1.17$ for a turbulent boundary layer.

According to (13.2.19) and (13.2.24) the left sides of these equalities determine the local and average Stanton numbers on a cone and the right sides give the values on a flat plate. Thus

$$\mathbf{St}^*_{xc}=\mathrm{A}\,\mathbf{St}^*_{x.p}; \tag{13.2.26}$$

$$\mathbf{St}^*_{\text{avc}}=\mathrm{A}\,\mathbf{St}^*_{\text{avp}}. \tag{13.2.27}$$

According to formulas (13.2.26) and (13.2.27) the calculation of the Stanton number on the cone will be carried out on the basis of the corresponding value obtained for a plate from the boundary layer parameters on a conical surface. Inserting the values of $\mathbf{St}^*_{x.p}=\mathbf{St}^*_x$, $\mathbf{St}^*_{av.p}=\mathbf{St}^*_{av}$ obtained from (13.2.19) and (13.2.24) respectively in the right sides of these formulas in place of the Stanton numbers, we get

$$\mathbf{St}^*_{xc}=(A\, c^*_{fx.p}/2)\,(\mathbf{Pr}^*)^{-2/3}; \tag{13.2.28}$$

$$\mathbf{St}^*_{av.c}=(A\, c^*_{xf.p}/2)\,(\mathbf{Pr}^*)^{-2/3}. \tag{13.2.29}$$

The resultant quantity of heat transferred by the gas to the wall in unit time for a cone with surface $S_s=\pi r_0 x_c$ (where r_0 and x_c are the radius of the base section and length of the generator of the cone), according to (13.2.25) and (13.2.28), will be

$$Q_k=q^*_{av}\pi r_0 x_c=(A/2)\, c^*_{xf.p}\,(\mathbf{Pr}^*)^{-2/3}\rho_\delta V_\delta (i_r-i_w)\,\pi r_0 x_c. \tag{13.2.30}$$

Formulas for the heat transfer parameters show the direct dependence of heat due to friction on the surface under interaction. The frictional stress and hence the heat transfer will be considerably higher in the case of a turbulent boundary layer. That is why it is necessary to maintain a laminar boundary layer to reduce the heat transfer from the heated gas to the surface, whereby a reduction in losses due to friction can be achieved.

3. Heat Transfer in Laminar Boundary Layer over Curved Surface

3.1 Arbitrary form of surface

Let us examine the analysis of heat transfer to a curved surface in the case of a laminar flow in which balanced dissociation may take place. If we take $\mathbf{Le}=1$ for this flow condition, which is justified to some extent in the case of a hypersonic flow, the above analysis based on the application of formula (13.1.15) leads to the solution of the system of equations for a laminar boundary layer including the equations of continuity (2.4.48′), motion (12.1.8) and energy (13.2.5′):

$$\left.\begin{aligned}
&\frac{\partial(\rho V_x r_0^\varepsilon)}{\partial x}+\frac{\partial(\rho V_y r_0^\varepsilon)}{\partial y}=0;\\
&\rho\left(V_x\frac{\partial V_x}{\partial x}+V_y\frac{\partial V_x}{\partial y}\right)=-\frac{dp_\delta}{dx}+\frac{\partial}{\partial y}\left(\mu\frac{\partial V_x}{\partial y}\right);\\
&\rho\left(V_x\frac{\partial i_0}{\partial x}+V_y\frac{\partial i_0}{\partial y}\right)=\frac{\partial}{\partial y}\left(\frac{\mu}{\mathbf{Pr}}\cdot\frac{\partial i_0}{\partial y}\right)+\frac{\partial}{\partial y}\left[\frac{\mu}{2}\left(1-\frac{1}{\mathbf{Pr}}\right)\frac{\partial V_x^2}{\partial y}\right].
\end{aligned}\right\} \tag{13.3.1}$$

Here the continuity equation differs from (2.4.48′) by the fact that the radial coordinate r of the point in the boundary layer is replaced by the coordinator

r_0 of a point on a contour situated at a corresponding section of the boundary layer. In this equation the value $\varepsilon=0$ corresponds to the wing profile and $\varepsilon=1$ refers to the body of revolution. As shown earlier, the Prandtl number $\mathbf{Pr}=(c_p)_{av}\,\mu/\lambda$ in the above energy equation.

The energy equation appearing in the system (13.3.1) is obtained from the general equation (3.2.14) in which $\mathbf{Sc}=\mathbf{Pr}$ ($\mathbf{Le}=1$) is assumed. However, in making this assumption we may fulfill the condition of grad $c_i\neq 1$. Therefore it seems to be necessary to add the equation of diffusion (3.2.4) to the system (13.3.1). This equation of diffusion relates concentration c_i and rate of formation of each element of the mixture of gases. But during thermodynamic equilibrium the concentration of each element is uniquely determined by the local values of pressure and temperature and the rate of formation of components $(W_{\text{chem}})_i$ is high enough to compensate losses due to convection and diffusion. Therefore the equation of diffusion (3.2.4) in the case of equilibrium of heat transfer will be superfluous.

The system of equations (13.3.1) is solved under the following boundary conditions:

on the wall (at $y=0$)

$$\left.\begin{array}{c} V_x=V_y=0,\ i_0=i_w,\ \rho=\rho_w; \\ i=i_w,\ T=T_w; \end{array}\right\} \tag{13.3.2}$$

at the external limit of the layer (at $y\to\infty$)

$$\left.\begin{array}{c} V_x=V_\delta,\ V_y=0,\ i_0=i_{0\delta}; \\ \rho=\rho_\delta,\ i=i_\delta,\ T=T_\delta. \end{array}\right\} \tag{13.3.3}$$

In addition we have the functional relations

$$\mu=\mu\,(p,\,T),\ \lambda=\lambda\,(p,\,T) \tag{13.3.4}$$

for determination of coefficients μ and λ.

Let us transform equation (13.3.1) by introducing some new independent variables and functions in question here. Following Liz [31], we introduce variables similar in form to Dorodnitsin's [see (12.3.2)]:

$$\left.\begin{array}{l} \eta\,(x,\,y)=\dfrac{V_\delta\, r_0^\varepsilon}{(2\tilde{x})^{1/2}}\displaystyle\int_0^y \rho dy; \\ \tilde{x}\,(x)=\displaystyle\int_0^x \rho_\delta V_\delta \mu_\delta\, r_0^{2\varepsilon}\, dx, \end{array}\right\} \tag{13.3.5}$$

whence

$$\left.\begin{array}{l} \dfrac{\partial\eta}{\partial y}=\dfrac{\rho V_\delta\, r_0^\varepsilon}{(2\tilde{x})^{1/2}}\,; \\ \dfrac{d\tilde{x}}{dx}=\rho_\delta V_\delta\,\mu_\delta\, r_0^{2\varepsilon}. \end{array}\right\} \tag{13.3.6}$$

To change the coordinates x, y to $\tilde{x}$, η we have to use the well-known relations from the course in mathematical analysis:

$$\frac{\partial}{\partial y}=\frac{\partial}{\partial \eta}\cdot\frac{\partial \eta}{\partial y}=\frac{\rho V_\delta r_0^\varepsilon}{(2\tilde{x})^{1/2}}\cdot\frac{\partial}{\partial \eta}; \tag{13.3.7}$$

$$\frac{\partial}{\partial x}=\frac{\partial}{\partial \eta}\cdot\frac{\partial \eta}{\partial x}+\frac{\partial}{\partial \tilde{x}}\cdot\frac{\partial \tilde{x}}{\partial x}=\frac{\partial}{\partial \eta}\cdot\frac{\partial \eta}{\partial x}+\rho_\delta V_\delta \mu_\delta r_0^{2\varepsilon}\frac{\partial}{\partial \tilde{x}}. \tag{13.3.8}$$

For further simplification we use the stream function ψ, which is determined by the relations (2.5.1). Let us replace r by r_0 therein and rewrite it in the form:

$$\left.\begin{aligned}\partial\psi/\partial y&=\rho V_x r_0^\varepsilon;\\ \partial\psi/\partial x&=-\rho V_y r_0^\varepsilon.\end{aligned}\right\} \tag{13.3.9}$$

Substituting these values in the continuity equation of the system (13.3.1), it can be seen that this equation leads to the identity $(\partial^2\psi/\partial x\partial y)-(\partial^2\psi/\partial y\partial x)\equiv 0$. Thus the equation of continuity is automatically satisfied by introduction of the stream function ψ.

Let us see how to simplify two equations of the system (13.3.1) with the help of the stream function. Taking (13.3.7), we can write

$$\frac{\partial\psi}{\partial y}=\frac{\partial\psi}{\partial\eta}\cdot\frac{\partial\eta}{\partial y}=\frac{\partial\psi}{\partial\eta}\cdot\frac{\rho V_\delta r_0^\varepsilon}{(2\tilde{x})^{1/2}},$$

from which the derivative

$$\frac{\partial\psi}{\partial\eta}=(2\tilde{x})^{1/2}\frac{V_x}{V_\delta}, \tag{13.3.10}$$

taking into account the relation (13.3.9).
Integrating this, we get the stream function

$$\psi=\int_0^\eta(2\tilde{x})^{1/2}\frac{V_x}{V_\delta}\,d\eta+\text{const}.$$

According to (13.3.5) the quantity $(2\tilde{x})^{1/2}$ is independent of η. So, dropping the constant, we may write

$$\psi=(2\tilde{x})^{1/2}f(\eta), \tag{13.3.11}$$

where

$$f(\eta)=\int_0^\eta\frac{V_x}{V_\delta}\,d\eta. \tag{13.3.12}$$

According to this expression

$$\frac{V_x}{V_\delta}=\frac{\partial f}{\partial \eta}=f'. \tag{13.3.13}$$

Using the relations (13.3.7), (13.3.8), equations (13.3.9) and (13.3.11) for the stream function and the expressions (13.3.12) and (13.3.13) we transform the operator on the left side of the equations of motion and energy of the system (13.3.1):

$$\rho V_x \frac{\partial}{\partial x}+\rho V_y \frac{\partial}{\partial y}=r_0^{-\epsilon}\left(\frac{\partial \psi}{\partial y}\cdot\frac{\partial}{\partial x}-\frac{\partial \psi}{\partial x}\cdot\frac{\partial}{\partial y}\right)$$

$$=r_0^{-\epsilon}\left[\frac{\partial \psi}{\partial \eta}\cdot\frac{\partial \eta}{\partial y}\left(\frac{\partial}{\partial \eta}\cdot\frac{\partial \eta}{\partial x}+\frac{\partial}{\partial \tilde{x}}\cdot\frac{\partial \tilde{x}}{\partial x}\right)-\left(\frac{\partial \psi}{\partial \eta}\cdot\frac{\partial \eta}{\partial x}\right.\right.$$

$$\left.\left.+\frac{\partial \psi}{\partial \tilde{x}}\cdot\frac{\partial \tilde{x}}{\partial x}\right)\frac{\partial}{\partial \eta}\cdot\frac{\partial \eta}{\partial y}\right]=r_0^{-\epsilon}\left(\frac{\partial \psi}{\partial \eta}\cdot\frac{\partial}{\partial \tilde{x}}-\frac{\partial \psi}{\partial \tilde{x}}\cdot\frac{\partial}{\partial \eta}\right)\frac{\partial \eta}{\partial y}\cdot\frac{\partial \tilde{x}}{\partial x}.$$

Here the derivatives $\partial\psi/\partial\eta$ and $\partial\psi/\partial\tilde{x}$ are determined from the differentiation of (13.3.11):

$$\left.\begin{aligned}\frac{\partial \psi}{\partial \eta}&=(2\tilde{x})^{1/2}\frac{\partial f}{\partial \eta};\\ \frac{\partial \psi}{\partial \tilde{x}}&=(2\tilde{x})^{-1/2}f+(2\tilde{x})^{1/2}\frac{\partial f}{\partial \tilde{x}}.\end{aligned}\right\} \tag{13.3.14}$$

After substitution of these values and replacement of the derivatives $\partial\eta/\partial y$ and $\partial\tilde{x}/\partial x$ by their values from (13.3.6) we get the operator

$$\rho V_x \frac{\partial}{\partial x}+\rho V_y \frac{\partial}{\partial y}=\rho\rho_\delta V_\delta^2 \mu_\delta r_0^{2\epsilon}\left(\frac{\partial f}{\partial \eta}\cdot\frac{\partial}{\partial \tilde{x}}-\frac{f}{2\tilde{x}}\cdot\frac{\partial}{\partial \eta}-\frac{\partial f}{\partial \tilde{x}}\cdot\frac{\partial}{\partial \eta}\right). \tag{13.3.15}$$

The expressions of the type

$$\frac{\partial}{\partial y}\left(h\frac{\partial}{\partial y}\right), \tag{13.3.16}$$

where $h(x, y)$ is a function of coordinates x, y, appear on the right sides of the equations of motion and energy in (13.3.1). The operator (13.3.16) will be written in terms of the new parameters as follows:

$$\frac{\partial}{\partial y}\left(h\frac{\partial}{\partial y}\right)=\frac{\partial}{\partial \eta}\left(h\frac{\partial}{\partial \eta}\cdot\frac{\partial \eta}{\partial y}\right)\frac{\partial \eta}{\partial y}$$

or, taking into account the value of (13.3.6) for the derivative $\partial\eta/\partial y$, it will be

$$\frac{\partial}{\partial y}\left(h\frac{\partial}{\partial y}\right)=\frac{\rho V_\delta^2 r_0^{2\epsilon}}{2\tilde{x}}\cdot\frac{\partial}{\partial\eta}\left(\rho h\frac{\partial}{\partial\eta}\right). \tag{13.3.17}$$

Let us apply the operators (13.3.15) and (13.3.17) to simplify the equation of motion:

$$\rho\rho_\delta V_\delta^2\mu_\delta r_0^{2\epsilon}\left(\frac{\partial f}{\partial\eta}\cdot\frac{\partial V_x}{\partial\tilde{x}}-\frac{f}{2\tilde{x}}\cdot\frac{\partial V_x}{\partial\eta}-\frac{\partial f}{\partial\tilde{x}}\cdot\frac{\partial V_x}{\partial\eta}\right)$$
$$=-\frac{dp_\delta}{dx}+\frac{\rho V_\delta^2 r_0^{2\epsilon}}{2\tilde{x}}\cdot\frac{\partial}{\partial\eta}\left(\rho\mu\frac{\partial V_x}{\partial\eta}\right).$$

Here the derivative dp_δ/dx can be determined from the equation:

$$\frac{dp_\delta}{dx}=-\rho_\delta V_\delta\frac{dV_\delta}{dx}=-\rho_\delta V_\delta\frac{dV_\delta}{d\tilde{x}}\cdot\frac{d\tilde{x}}{dx}$$

or, taking into account the value of (13.3.6) for $d\tilde{x}/dx$, it will be

$$\frac{dp_\delta}{dx}=-\rho_\delta^2 V_\delta^2\mu_\delta r_0^{2\epsilon}\frac{dV_\delta}{d\tilde{x}}. \tag{13.3.18}$$

Keeping this in mind and also the value of V_x from (13.3.13), i.e.

$$V_x=V_\delta(\partial f/\partial\eta), \tag{13.3.13'}$$

we get

$$\frac{\partial f}{\partial\eta}\cdot\frac{\partial}{\partial\tilde{x}}\left(V_\delta\frac{\partial f}{\partial\eta}\right)-\frac{V_\delta f}{2\tilde{x}}\cdot\frac{\partial^2 f}{\partial\eta^2}-V_\delta\frac{\partial f}{\partial\tilde{x}}\cdot\frac{\partial^2 f}{\partial\eta^2}$$
$$=\frac{\rho_\delta}{\rho}\cdot\frac{dV_\delta}{d\tilde{x}}+\frac{V_\delta}{2\tilde{x}\,\rho_\delta\mu_\delta}\cdot\frac{\partial}{\partial\eta}\left(\rho\mu\frac{\partial^2 f}{\partial\eta^2}\right).$$

Considering that the derivative

$$\frac{\partial}{\partial\tilde{x}}\left(V_\delta\frac{\partial f}{\partial\eta}\right)=\frac{dV_\delta}{d\tilde{x}}\cdot\frac{\partial f}{\partial\eta}+V_\delta\frac{\partial^2 f}{\partial\tilde{x}\,\partial\eta},$$

we get the simplified equation of motion in its final form:

$$2\tilde{x}\left(\frac{\partial f}{\partial\eta}\cdot\frac{\partial^2 f}{\partial\tilde{x}\partial\eta}-\frac{\partial f}{\partial\tilde{x}}\cdot\frac{\partial^2 f}{\partial\eta^2}\right)=f\frac{\partial^2 f}{\partial\eta^2}$$
$$+\frac{2\tilde{x}}{V_\delta}\cdot\frac{dV_\delta}{d\tilde{x}}\left[\frac{\rho_\delta}{\rho}-\left(\frac{\partial f}{\partial\eta}\right)^2\right]+\frac{\partial}{\partial\eta}\left(\overline{\rho\mu}\frac{\partial^2 f}{\partial\eta^2}\right), \tag{13.3.19}$$

where

$$\overline{\rho\mu}=\rho\mu/\rho_\delta\mu_\delta. \tag{13.3.20}$$

Now the energy equation may be rewritten with the help of these same operators (13.3.15), (13.3.17) and the expression (13.3.13′):

$$\rho\rho_\delta V_\delta^2\mu_\delta r_0^{2\varepsilon}\left(\frac{\partial f}{\partial\eta}\cdot\frac{\partial i_0}{\partial\tilde{x}}-\frac{f}{2\tilde{x}}\cdot\frac{\partial i_0}{\partial\eta}-\frac{\partial f}{\partial\tilde{x}}\cdot\frac{\partial i_0}{\partial\eta}\right)=\frac{\rho V_\delta^2 r_0^{2\varepsilon}}{2\tilde{x}}\cdot\frac{\partial}{\partial\eta}\left(\frac{\rho\mu}{\mathbf{Pr}}\cdot\frac{\partial i_0}{\partial y}\right)$$
$$+\frac{\rho V_\delta^4 r_0^{2\varepsilon}}{2\tilde{x}}\cdot\frac{\partial}{\partial\eta}\left[\rho\mu\left(1-\frac{1}{\mathbf{Pr}}\right)\frac{\partial f}{\partial\eta}\cdot\frac{\partial^2 f}{\partial\eta^2}\right].$$

For further simplification we introduce the nondimensional dependent variable

$$g(\eta)=i_0/i_{0\delta}, \tag{13.3.21}$$

which determines the ratio of the stagnation enthalpy at a point on the section of a boundary layer $i_0=i_\delta+(V_x^2/2)$ to its value $i_{0\delta}=i_\delta+(V_\delta^2/2)$ at the external limit of the layer. Bearing in mind that

$$\frac{\partial i_0}{\partial\eta}=i_{0\delta}\frac{\partial g}{\partial\eta},\ \frac{\partial i_0}{\partial\tilde{x}}=\frac{\partial}{\partial\tilde{x}}(gi_{0\delta})=i_{0\delta}\frac{\partial g}{\partial\tilde{x}}+g\frac{\partial i_{0\delta}}{\partial\tilde{x}},$$

we get

$$2\tilde{x}\left(\frac{\partial f}{\partial\eta}\cdot\frac{\partial g}{\partial\tilde{x}}-\frac{\partial f}{\partial\tilde{x}}\cdot\frac{\partial g}{\partial\eta}\right)=f\frac{\partial g}{\partial\eta}+\frac{\partial}{\partial\eta}\left(\frac{\overline{\rho\mu}}{\mathbf{Pr}}\cdot\frac{\partial g}{\partial\eta}\right)$$
$$+\frac{V_\delta^2}{i_{0\delta}}\cdot\frac{\partial}{\partial\eta}\left[\overline{\rho\mu}\left(1-\frac{1}{\mathbf{Pr}}\right)\frac{\partial f}{\partial\eta}\cdot\frac{\partial^2 f}{\partial\eta^2}\right]-\frac{2\tilde{x}g}{i_{0\delta}}\cdot\frac{\partial i_{0\delta}}{\partial\tilde{x}}\cdot\frac{\partial f}{\partial\eta}. \tag{13.3.22}$$

The functions $f(\eta)$ and $g(\eta)$ are the solutions of the system of equations (13.3.19), (13.3.22). They must satisfy the following boundary conditions:

On the wall at $\eta=0$ $(y=0)$

$$f(0)=(\partial f/\partial\eta)_{\eta=0}=0,\ g(0)=g_w; \tag{13.3.23}$$

On the external limit of the boundary layer at $\eta\to\infty$ $(y\to\infty)$

$$f(\infty)=0,\ (\partial f/\partial\eta)_{\eta\to\infty}=1,\ g(\infty)=1,\ (\partial g/\partial\eta)_{\eta\to\infty}=0. \tag{13.3.24}$$

The above system of equations (13.3.19), (13.3.22) includes complex nonlinear partial differential equations. Although they are somewhat simpler in this form than the original equations (13.3.1) we encounter great difficulty in solving them. However, the system of equations in the above form is quite convenient due to the fact that it is possible to work out a large group of

problems of practical interest for which this system may be reduced to "similar" conventional differential equations on certain assumptions.

Solutions of this kind, known as "similarity solutions," have the property that the functions f and g to be found will depend solely on one parameter η. This property of the solution helps in simplifying equations (13.3.19), (13.3.22) because their left sides are reduced to zero as a result of the condition: $dg/d\tilde{x}=df/d\tilde{x}=0$. Then the equations take the following form:

$$ff''+\frac{2\tilde{x}}{V_\delta}\cdot\frac{dV_\delta}{d\tilde{x}}\left(\frac{\rho_\delta}{\rho}-f'^2\right)+(\overline{\rho\mu}f'')'=0; \tag{13.3.25}$$

$$fg'+\left(\frac{\overline{\rho\mu}}{\mathbf{Pr}}g'\right)'+\frac{V_\delta^2}{i_{0\delta}}\left[\overline{\rho\mu}\left(1-\frac{1}{\mathbf{Pr}}\right)f'f''\right]'-\frac{2\tilde{x}g}{i_{0\delta}}\cdot\frac{di_{0\delta}}{d\tilde{x}}f'=0, \tag{13.3.26}$$

where strokes indicate differentiation with respect to η. This system has similarity solutions if the following conditions are satisfied:

a) $$\frac{\tilde{x}}{V_\delta}\cdot\frac{dV_\delta}{d\tilde{x}}=\text{const},\quad\frac{\tilde{x}}{i_{0\delta}}\cdot\frac{di_{0\delta}}{d\tilde{x}}=\text{const},\quad\frac{V_\delta^2}{i_{0\delta}}=\text{const};$$

b) the ratio ρ_δ/ρ, Prandtl number **Pr** and the quantity $\overline{\rho\mu}$ are functions of η or are constants;

c) the function g is constant all over the wall, i.e. $g(0)=g_w=\text{const}$, which corresponds to constant wall temperature.

These conditions of similarity solutions are never satisfied at one time even if the condition of constant wall temperature is observed except in some particular cases (uniform external flow around a flat plate, wedge, cone with formation of attached shock wave). The density ratio ρ_δ/ρ, Prandtl number and the quantity $\overline{\rho\mu}=\rho\mu/\rho_\delta\mu_\delta$ happen to be functions not only of the enthalpy ratio i/i_δ but also of the enthalpy i_δ itself and of pressure p_δ so far as they affect the dissociation of gas. Actually we can point to one more particular case of flow-interaction for which the solution will be of the "similarity" type: the flow-interaction of a small section of blunt surface near the point of complete stagnation where enthalpy i_δ and pressure p_δ remain almost constant.

It is natural to raise the question whether it is possible to find a similarity solution which could be extended to a large part of a curved surface. It can be had in the following two cases of practical interest: 1) during small variations in the parameters of the external flow; 2) during marked cooling of the surface in a flow, i.e. when $g_w=i_w/i_{0\delta}\ll 1$.

In the first case the velocity gradient

$$\beta=\frac{2\tilde{x}}{V_\delta}\cdot\frac{dV_\delta}{d\tilde{x}}=\frac{2d\ln V_\delta}{d\ln\tilde{x}} \tag{13.3.27}$$

and the quantity $V_\delta^2/i_{0\delta}$ are assumed to remain constant all over the surface. At the same time $di_{0\delta}/d\tilde{x}=0$ is assumed, which corresponds to the condition of conservation of total energy in the external flow $[i_{0\delta}=i_\delta+(V_\delta^2/2)=\text{const}]$. In addition the quantity $\overline{\rho\mu}$ and Prandtl number **Pr** are assumed constant and the density ratio $\rho_\delta/\rho=T/T_\delta=i/i_\delta$ is considered as the function of η only.

The second case is characterized by the fact that the wall temperature is very low, i.e. $T_w/T_\delta\ll 1$ and hence $\rho_w/\rho_\delta\gg 1$. Here the density near the wall increases with the decrease in the temperature of the wall not only because of heat carried away (with the help of special cooling aids) but also because of the rise in the degree of dissociation at hypersonic speeds.

Since the axial pressure gradient depends on density ρ_δ at the external limit $(dp_\delta/dx=-\rho_\delta V_\delta\, dV_\delta/dx)$ and happens to be constant for a given section of boundary layer the velocity profile near the wall at $\rho_w\gg\rho_\delta$ is much less sensitive to the pressure gradient than in the case of a small difference in pressure across the boundary layer. This is explained by the low conductivity of a highly compressed gas for variations in the character of the flow during the interaction of differential pressure. Therefore it is possible to neglect the term in equation (13.3.25) in which pressure gradient β (13.3.27) participates. This equation will then be written in the form

$$ff''+(\overline{\rho\mu}f'')'=0. \tag{13.3.28}$$

From a comparison of equations (13.3.25) and (13.3.26) it follows that the velocity gradient has a weaker effect on the distribution of stagnation enthalpy. Actually it can be established from (13.3.25) that the function f, which can be determined from this condition, depends (at least to some extent) on the gradient β, which appears in the equation very clearly. At the same time the function $g=i_0/i_{0\delta}$ is found from equation (13.3.26) from which the quantity β is clearly missing. Here the dependence of g on the gradient appears through the insignificant dependence of function f on β. In this way the system of equations (13.3.25) and (13.3.26), simplified according to the condition $\rho_w/\rho_\delta\gg 1$, is better employed for calculation of the parameters of heat transfer, determining the derivative g', than for calculation of friction parameters (function f').

Equation (13.3.26) can be simplified keeping in view that the total enthalpy of a free flow is constant $(di_{0\delta}/dx=0)$. The quantity $V_\delta^2/i_{0\delta}$ over blunt bodies varies from zero at a stagnation point with $V_\delta=0$ to the value of $V_\delta^2/[i_\delta+(V_\delta^2/2)]\approx 2$ (over regions where velocity V_δ is such that $i_\delta\ll V_\delta^2/2$). Taking this into account and recalling that the Prandtl number **Pr**$\approx$0.7–1.0, we arrive at the conclusion that the third term in (13.3.26) is numerically small.

Neglecting the third and fourth terms in this equation, we get

$$fg'+\left(\frac{\overline{\rho\mu}}{\mathbf{Pr}}g'\right)'=0. \tag{13.3.29}$$

The function $\overline{\rho\mu}=\rho\mu/\rho_\delta\mu_\delta$ can be evaluated with the help of the equations of state $p=R_0\rho T/\mu_{av}$ and $p=p_\delta=R_0\rho_\delta T_\delta/(\mu_{av})_\delta$ (where R_0 is the universal gas constant):

$$\overline{\rho\mu}=\frac{\rho\mu}{\rho_\delta\mu_\delta}=\frac{T_\delta}{T}\cdot\frac{\mu_{av}}{(\mu_{av})_\delta}\cdot\left(\frac{T}{T_\delta}\right)^n=\left(\frac{T_\delta}{T}\right)^{1-n}\frac{\mu_{av}}{(\mu_{av})_\delta}.$$

Let us replace T and μ_{av} by their definitive values T^* and μ^*_{av}

$$\overline{\rho\mu}=\left(\frac{T_\delta}{T^*}\right)^{1-n}\frac{\mu^*_{av}}{(\mu_{av})_\delta}. \tag{13.3.30}$$

From (12.5.32) and (12.5.31) it follows that

$$T^*=0.5\,(T_w+T_\delta)+0.11\,(k^*-1)\,r^*\,\mathbf{M}_\delta^2 T_\delta.$$

For the boundary layer in the neighborhood of the point of complete stagnation where $\mathbf{M}_\delta=0$, the definitive temperature $T^*=0.5\,(T_w+T_\delta)$.

For evaluation of T^* at any other section of boundary layer over a blunt surface in a highly heated gas flow we use the quantities $k^*=1.3$, $\mathbf{M}_\delta=2$, $r^*=\sqrt{0.71}\approx0.84$:

$$T^*=0.5\,(T_w+T_\delta)+0.11\,(1.3-1)\,0.84\times4T_\delta=0.5T_w+0.6T_\delta. \tag{13.3.31}$$

In this way the definitive temperature for this layer is approximately the same as that in the vicinity of the point of complete stagnation.

Using the value of T^* from (13.3.31) in (13.3.30), we get

$$\overline{\rho\mu}=\frac{\mu^*_{av}}{(\mu_{av})_\delta}\left[\frac{2}{(T_w/T_\delta)+1.2}\right]^{1-n}.$$

From this expression it follows that the quantity $\overline{\rho\mu}$ is nearly unity at $T_w/T_\delta\ll1$ and $n\approx0.75$–0.8.

Let us now study the relation between the heat flow and the quantity $\overline{\rho\mu}$. Applying Fourier's law and using expression (13.3.6) for the derivative $\partial\eta/\partial y$, we find

$$q_x=\frac{\lambda_w}{(c_p)_w}\left(\frac{\partial i}{\partial y}\right)_w=\frac{\lambda_w}{(c_p)_w}\left(\frac{\partial i_0}{\partial\eta}\right)_w\left(\frac{\partial\eta}{\partial y}\right)_w=\frac{\lambda_w g'(0)\,\rho_w V_\delta r_0^\epsilon i_{0\delta}}{(c_p)_w(2\tilde{x})^{1/2}}, \tag{13.3.32}$$

where according to (13.3.5) we have

$$(2\tilde{x})^{1/2}=\left[2\int_0^x\rho_\delta\mu_\delta V_\delta r_0^{2\epsilon}\,dx\right]^{1/2}=\left[2\int_0^x\frac{\rho_w\mu_w}{(\overline{\rho\mu})_w}V_\delta r_0^{2\epsilon}\,dx\right]^{1/2}. \tag{13.3.33}$$

The quantity $\overline{\rho\mu}=(\overline{\rho\mu})_w$ appears with the square root sign in the expression (13.3.33) which determines the value of specific heat flow. This reduces the general increment resulting from the approximate selection of this quantity. Therefore it is sufficient to take $\overline{\rho\mu}=1$ in our calculations, i.e.

$$\rho\mu\approx\rho_\delta\,\mu_\delta\approx\rho_w\,\mu_w\cdot \tag{13.3.34}$$

In this way we get the system of equations of the boundary layer:

$$f\cdot f''+f'''=0; \tag{13.3.35}$$

$$\mathbf{Pr}\cdot f\cdot g'+g''=0\cdot \tag{13.3.36}$$

These equations reflect local similarity, which should be taken in the sense that in the case where $\mathbf{Pr}=\text{const}$, the nondimensional velocity V_x/V_δ and enthalpy $i_0/i_{0\delta}$ are the same at those points of various flows where the parameter η is identical, happening to be thereby the parameter of similarity.

Integrating the system of ordinary differential equations (13.3.35) and (13.3.36) under the boundary conditions given earlier, it is possible to find similarity solutions for the functions $f(\eta)$ and $g(\eta)$ and, in particular, for the derivative $g'(\eta)$. Integrating (13.3.36) twice, we get

$$g(\eta)-g(0)=g'(0)\int_0^\eta e^{-\int_0^\eta \mathbf{Pr}\,f d\eta}\,d\eta\cdot \tag{13.3.37}$$

Numerical calculation showed that for $\eta\to\infty$ the value of the integral is approximately equal to $(0.5\,\mathbf{Pr}^{1/3})^{-1}$. So keeping in view that $g(\eta)=(i_0/i_{0\delta})\to 1$ for $\eta\to 0$, we have

$$g'(0)=\frac{1}{i_{0\delta}}\left(\frac{\partial i_0}{\partial\eta}\right)_w=\frac{1}{i_{0\delta}}\left(\frac{\partial i}{\partial\eta}\right)_w=0.5\,\mathbf{Pr}^{1/3}\,[1-g(0)], \tag{13.3.38}$$

where $g(0)=g_w=i_w/i_{0\delta}$; Prandtl number $\mathbf{Pr}=(c_p)_w\cdot\mu_w/\lambda_w$. Inserting the value obtained for $g'(0)$ in (13.3.32) and noting that $g(0)=g_w=i_w/i_{0\delta}$, we get

$$q_x=0.5\,\frac{\lambda_w\,\rho_w\,V_\delta\,r_0^\varepsilon\,\mathbf{Pr}^{1/3}}{(c_p)_w\,(2\tilde{x})^{1/2}}(i_{0\delta}-i_w)\cdot$$

Substituting the value of $\lambda_w/(c_p)_w=\mu_w/\mathbf{Pr}$ and replacing $\rho_w\mu_w$ by $\rho_\delta\mu_\delta$ and $i_{0\delta}$ by enthalpy of recovery i_r [keeping in view the use of this enthalpy in equation (13.1.15) for heat flow], we have

$$q_x=0.5\,\mathbf{Pr}^{-2/3}\,\frac{\rho_\delta\,V_\delta\,r_0^\varepsilon}{(2\tilde{x})^{1/2}}\,(i_r-i_w)\cdot \tag{13.3.39}$$

This equation in this form, as shown by research, helps us to determine heat transfer with sufficient accuracy for the case where cooling does not produce a low enough wall temperature.

Using the equation of state in (13.3.39) it is easy to go to the nondimensional parameter

$$\frac{\rho_\delta \mu_\delta}{\rho_0' \mu_0'} = \frac{p_\delta}{p_0'} \cdot \frac{\mu_\delta}{\mu_0'} \cdot \frac{(\mu_{av})_\delta}{(\mu_{av})_0} \cdot \frac{T_0'}{T_\delta}. \tag{13.3.40}$$

Introducing the following notations:

$$\omega_\delta = \frac{\mu_\delta (\mu_{av})_\delta}{T_\delta}, \quad \omega_0' = \frac{\mu_0' (\mu_{av})_0}{T_0'}, \tag{13.3.41}$$

the above nondimensional parameter will be

$$\frac{\rho_\delta \mu_\delta}{\rho_0' \mu_0'} = \frac{p_\delta}{p_0'} \cdot \frac{\omega_\delta}{\omega_0'}. \tag{13.3.42}$$

Here the parameters p_0', ρ_0', μ_0', $(\mu_{av})_0$ [see (13.3.40)] refer to the external limit of the boundary layer at a point of complete stagnation over a blunt surface. Inserting the value of ρ_δ from (13.3.42) in (13.3.39) and taking into account relation (13.3.5), we arrive at

$$q_x = 0.5\, \mathbf{Pr}^{-2/3} \sqrt{\rho_0' \mu_0' V_\delta}\, F(x)\, (i_r - i_w), \tag{13.3.43}$$

where the function

$$F(x) = \frac{\sqrt{2}}{2} \cdot \frac{p_\delta}{p_0'} \cdot \frac{\omega_\delta}{\omega_0'} \cdot \frac{V_\delta}{V_\infty}\, r_0^\epsilon \left(\int_0^x \frac{p_\delta}{p_0'} \cdot \frac{V_\delta}{V_\infty} \cdot \frac{\omega_\delta}{\omega_0'}\, r_0^{2\epsilon}\, dx \right)^{-1/2}. \tag{13.3.44}$$

Let us consider the change in quantity ω_δ/ω_0' according to (13.3.40):

$$\frac{\omega_\delta}{\omega_0'} = \frac{\mu_\delta}{\mu_0'} \cdot \frac{(\mu_{av})_\delta}{(\mu_{av})_0} \cdot \frac{T_0'}{T_\delta}$$

or

$$\frac{\omega_\delta}{\omega_0'} = \left(\frac{T_\delta}{T_0'} \right)^n \frac{(\mu_{av})_\delta}{(\mu_{av})_0} \cdot \frac{T_0'}{T_\delta} = \left(\frac{T_0'}{T_\delta} \right)^{1-n} \frac{(\mu_{av})_\delta}{(\mu_{av})_0}.$$

This ratio varies from unity at a stagnation point (where $T_0' = T_\delta$) to its value at a point on the surface given by

$$\frac{\omega_\delta}{\omega_0'} \approx \left[\frac{T_0' \left(1 + r^* \frac{k^* - 1}{2} \mathbf{M}_\delta^2 \right)}{T_0'} \right]^{1-n} \frac{(\mu_{av})_\delta}{(\mu_{av})_0}.$$

During intensive heating of the gas behind the shock wave the Mach number $\mathbf{M}_\delta$ in the external flow is not high. Consequently the temperature T_δ, as may be seen from expression $T_\delta = T_0' \left(1 + r^* \frac{k^* - 1}{2} \mathbf{M}_\delta^2 \right)^{-1}$, differs insignificantly

from the temperature T_0' at the point of complete stagnation. For example, for $M_\delta=2$

$$T_\delta=T_0'\left(1+r^*\frac{k^*-1}{2}4\right)^{-1}.$$

Taking $r^*=0.84$ and $k^*=1.3$, we get $T_\delta=T_0'/1.5$. According to this

$$\frac{\omega_\delta}{\omega_0'}=(1.5)^{1-n}\frac{(\mu_{av})_\delta}{(\mu_{av})_0}.$$

At $n=0.75$–0.80 this quantity is about 10% higher than unity.

If we assume that the ratio ω_δ/ω_0' appears under the square root sign in the expression (13.3.44) for determination of heat transfer the change due to substitution of $\omega_\delta/\omega_0'=1$ will be of the order of a few per cent. Accordingly the function (13.3.44) will be rewritten in the form

$$F(x)=\frac{\sqrt{2}}{2}\cdot\frac{p_\delta}{p_0'}\cdot\frac{V_\delta}{V_\infty}r_0^\epsilon\left(\int_0^x\frac{p_\delta}{p_0'}\cdot\frac{V_\delta}{V_\infty}r_0^{2\epsilon}\,dx\right)^{-1/2}. \qquad (13.3.44')$$

So it is necessary to know the distribution of velocity and pressure all over the surface between the point of complete stagnation and the point in question in order to determine the specific heat flow at any point on a surface of a given form. In particular, for calculation of heat transfer at the points on the surface near stagnation point we may take

$$p_\delta/p'\approx 1,\ r_0\approx x \qquad (13.3.45)$$

and

$$V_\delta=\tilde{\lambda}x \qquad (13.3.46)$$

according to equation (9.4.74) if we replace V_x by V_δ. Here the velocity gradient $\tilde{\lambda}$ will be found with the help of one of the expressions (9.4.72) or (9.4.78). Taking (13.3.45) and (13.3.46) into account, the function

$$F=\frac{\sqrt{2}}{2}\cdot\frac{\tilde{\lambda}x}{V_\infty}x^\epsilon\left(\int_0^x\frac{\tilde{\lambda}x}{V_\infty}x^{2\epsilon}\,dx\right)^{-1/2}.$$

After integration it will be reduced to

$$F=F_0=\sqrt{(\tilde{\lambda}/V_\infty)(\varepsilon+1)}. \qquad (13.3.47)$$

Inserting this in (13.3.43) and introducing the notation $q_x=q_0$ for the heat flow at a point of complete stagnation and its vicinity, we get

$$q_0=0.5\mathrm{Pr}^{-2/3}\sqrt{\rho_0'\mu_0'\tilde{\lambda}(\varepsilon+1)}\,(i_r-i_w). \qquad (13.3.48)$$

The value of heat transfer q_x at an arbitrary point on the surface can be conveniently worked out with the help of a nondimensional parameter which can be determined from (13.3.43) and (13.3.48) in the form

$$\frac{q_x}{q_0}=\sqrt{\frac{V_\infty}{\tilde{\lambda}\,(\varepsilon+1)}}\,F(x)\cdot \tag{13.3.49}$$

3.2 Hemisphere

Let us consider the application of (13.3.49) as an example for calculation of heat flow over the surface of a hemisphere. Taking

$$\varepsilon=1,\ dx=R_T\,d\varphi,\ r_0=R_T\sin\varphi, \tag{13.3.50}$$

in formula (13.3.44) and noting that

$$V_\delta=\tilde{\lambda}\,R_T\,\varphi, \tag{13.3.51}$$

$$\frac{p_\delta}{p_0'}=\cos^2\varphi+\frac{p_\infty}{p_0'}\sin^2\varphi, \tag{13.3.52}$$

in accordance with (9.4.74′) and (9.4.76) over the larger part of a spherical nose, we get

$$F(\varphi)=\frac{\sqrt{2}}{2}\cdot\frac{\left(\cos^2\varphi+\frac{p_\infty}{p_0'}\sin^2\varphi\right)\tilde{\lambda}\,R_T^2\,\varphi\sin\varphi}{\left[\int\limits_0^\varphi\left(\cos^2\varphi+\frac{p_\infty}{p_0'}\sin^2\varphi\right)\tilde{\lambda}\,R_T^4\,V_\infty\,\varphi\sin^2\varphi\,d\varphi\right]^{1/2}}\cdot$$

Substituting this expression in formula (13.3.49) in which $\varepsilon=1$ is assumed, we get

$$\frac{q_x}{q_0}=\frac{1}{2}\cdot\frac{\varphi\sin\varphi\left(\cos^2\varphi+\frac{p_\infty}{p_0'}\sin^2\varphi\right)}{\left[\int\limits_0^\varphi\left(\cos^2\varphi+\frac{p_\infty}{p_0'}\sin^2\varphi\right)\varphi\sin^2\varphi\,d\varphi\right]^{1/2}}\cdot$$

Introducing the notation

$$D(\varphi)=16\int_0^\varphi\left(\cos^2\varphi+\frac{p_\infty}{p_0'}\sin^2\varphi\right)\varphi\sin^2\varphi\,d\varphi=\left(1-\frac{p_\infty}{p_0'}\right)(4\varphi\cos\varphi-\sin\varphi)\sin^3\varphi$$
$$+\left(3\frac{p_\infty}{p_0'}+1\right)(\varphi^2+\sin^2\varphi-\varphi\sin 2\varphi), \tag{13.3.53}$$

we get

$$\frac{q_x}{q_0}=2\varphi\sin\varphi\left(\cos^2\varphi+\frac{p_\infty}{p_0'}\sin^2\varphi\right)D^{-1/2}(\varphi). \tag{13.3.54}$$

Here we recall that the calculation of distribution of heat flows by formula (13.3.54), like similar relations, should be carried out for high supersonic flow conditions. Under these circumstances the inequality $p_\infty/p_0' < 0.03$ to 0.04 should be satisfied. Approximately similar relations are obtained if the following empirical relation is made use of:

$$\frac{q_x}{q_0} = 1 - 1.32\left(\frac{\varphi}{\pi/2}\right)^2 + 0.5\left(\frac{\varphi}{\pi/2}\right)^5. \qquad (13.3.54')$$

3.3 Blunt cone

Let us study the analysis of the heat flow on the surface of the fruston of a cone with spherical nose (Fig. 13.3.1). We assume that the "inviscid" gas parameters over a conical surface are constant and are equal to the corresponding values at the end of the spherical nose. In particular, the velocity will be given by

$$V_\delta = \tilde{\lambda} R_T \varphi_k = \tilde{\lambda} R_T \left[\left(\frac{\pi}{2}\right) - \beta_k\right], \qquad (13.3.55)$$

where β_k is the angle of inclination of the cone generator. The pressure ratio will be:

$$\frac{p_\delta}{p_0'} = \cos^2 \varphi_k + \frac{p_\infty}{p_0'} \sin^2 \varphi_k = \sin^2 \beta_k + \frac{p_\infty}{p_0'} \cos^2 \beta_k. \qquad (13.3.56)$$

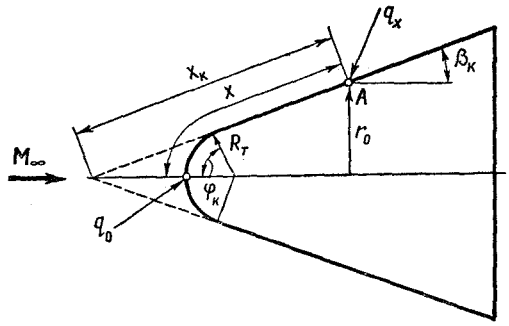

Fig. 13.3.1. Cone with blunt spherical nose.

For one of the geometrical parameters, namely the radial component at an arbitrary point A on the surface of the cone (see Fig. 13.3.1), we can write

$$r_0 = x_k \cos \varphi_k = x_k \sin \beta_k, \qquad (13.3.57)$$

where x_k is the distance along the surface measured from the imaginary apex of a sharp-nosed cone to the given point. This is determined by the relation

$$x_k = x - R_T \varphi_k + R_T \tan \varphi_k \qquad (13.3.58)$$

or, considering that $\varphi_k=(\pi/2)-\beta_k$, it will be

$$x_k=x-R_T\left(\frac{\pi}{2}-\beta_k\right)+R_T\cot\beta_k. \tag{13.3.58'}$$

Let us find the values of function $F(x)$. It is obvious that the integral in (13.3.44'), calculated in the interval from 0 to x (x is a curvilinear coordinate of point A), is obtained as the sum of two integrals: the first integral with limits from 0 to $x=R_T\varphi_k=R_T[(\pi/2)-\beta_k]$ (or for angles from 0 to φ_k) and the second with limits from $\varphi_k R_T$ to x. Obviously the first integral corresponds to the value of the heat flow at the end of the spherical region (at the junction with the conical surface). It is clear that the distribution of heat flow over this region is like that obtained earlier for a hemisphere. Taking this into account, we find the function $F(x)$ (13.3.44') in the following form:

$$F(x)=\frac{\sqrt{2}}{2}\frac{\left(\cos^2\varphi_k+\frac{p_\infty}{p_0'}\sin^2\varphi_k\right)\tilde{\lambda}\,R_T\,\varphi_k\cos\varphi_k\,x_k\,V_\infty^{-1/2}}{\left[\int\limits_0^{\varphi_k}\left(\cos^2\varphi+\frac{p_\infty}{p_0'}\sin^2\varphi\right)\tilde{\lambda}\,R_T^4\cdot\varphi\sin^2\varphi\,d\varphi+\rightarrow\right.}$$

$$\left.\rightarrow+\int\limits_{R_T\varphi_k}^{x}\left(\cos^2\varphi_k+\frac{p_\infty}{p_0'}\sin^2\varphi_k\right)\tilde{\lambda}\,R_T\,\varphi_k\,r_0^2\,dx\right]^{1/2} \tag{13.3.59}$$

The second integral calculated for the region of the linear generator of the cone taking (13.3.58) into account will be written in the form

$$\int\limits_{R_T\varphi_k}^{x}\left(\cos^2\varphi_k+\frac{p_\infty}{p_0'}\sin^2\varphi_k\right)\tilde{\lambda}\,R_T\,\varphi_k\,r_0^2\,dx$$

$$=\left(\cos^2\varphi_k+\frac{p_\infty}{p_0'}\sin^2\varphi_k\right)\tilde{\lambda}\,R_T\,\varphi_k\int\limits_{R_T\tan\varphi_k}^{x_k}x_k^2\cos^2\varphi_k\,dx_k$$

$$=\frac{1}{3}\left(\cos^2\varphi_k+\frac{p_\infty}{p_0'}\sin^2\varphi_k\right)\tilde{\lambda}\,R_T\,\varphi_k\cos^2\varphi_k\,(x_k^3-R_T^3\tan^3\varphi_k). \tag{13.3.60}$$

Let us introduce the notation

$$G(\bar{x}_k)=\frac{16}{3}\left(\cos^2\varphi_k+\frac{p_\infty}{p_0'}\sin^2\varphi_k\right)(\bar{x}_k^3-\tan^3\varphi_k)\,\varphi_k\cos^2\varphi_k, \tag{13.3.61}$$

where $\bar{x}_k=x_k/R_T$. Taking this into account, the substitution of (13.3.59) and (13.3.49) at $\varepsilon=1$ leads to the relation

$$\frac{q_x}{q_0}=\frac{2\left(\cos^2\varphi_k+\frac{p_\infty}{p_0'}\sin^2\varphi_k\right)\varphi_k\cos\varphi_k\,\bar{x}_k}{\sqrt{D(\varphi_k)+G(\bar{x}_k)}}, \tag{13.3.62}$$

where the function $D(\varphi_k)$ is determined from formula (13.3.53) for $\varphi=\varphi_k$.

It should be noted here that equation (13.3.62) is convenient only for a conical surface, i.e. for values of $\bar{x}_k=x_k/R_T \geqslant \tan\varphi_k$. At the joint of the spherical nose and the cone, i.e. at $\bar{x}_k=\tan\varphi_k$ the expression (13.3.62) agrees with equation (13.3.54). For parts of the conical surface situated at a distance from this point ($\bar{x}_k \gg 1$),

$$\frac{q_x}{q_0} \to \frac{2\varphi_k \cos\varphi_k \bar{x}_k}{\sqrt{\frac{16}{3}\varphi_k \cos^2\varphi_k \bar{x}_k^3}} = \frac{\sqrt{3}}{2}\sqrt{\frac{\varphi_k}{\bar{x}_k}}. \tag{13.3.63}$$

From formula (13.3.63) it may be seen that for a very long cone the effect of a blunt nose is small. This cone can be treated as a sharp-nosed cone for which the pressure at nose $p_0' = p_\delta$ and consequently, $p_\delta/p_0' = \cos^2\varphi_k + (p_\infty/p_0')\sin^2\varphi_k \approx 1$. According to this condition the replacement of ρ_0' by $\rho_\delta=\rho_k$, μ_0' by $\mu_\delta=\mu_k$ and assumption of $\varepsilon=1$ change equation (13.3.48) to the form

$$q_0=(\sqrt{2}/2)\,\mathrm{Pr}^{-2/3}\sqrt{\rho_k \mu_k \tilde{\lambda}}\,(i_r-i_w).$$

Therefore the heat flow at distant points on this "equivalent" sharp nosed conical surface will be

$$q_k=0.61\,\mathrm{Pr}^{-2/3}\sqrt{\frac{\rho_k \mu_k \tilde{\lambda}\varphi_k}{\bar{x}_k}}\,(i_r-i_w), \tag{13.3.64}$$

where ρ_k, μ_k are the density and coefficient of dynamic viscosity on a sharp cone.

The distribution of heat flows, calculated from formulas (13.3.54), (13.3.62) and (13.3.63), is shown in Fig. 13.3.2. From this figure it is seen that at β_k angles of between 30 and 40° the distribution of heat flow over

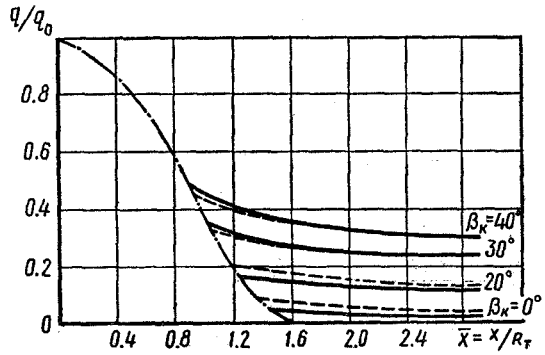

Fig. 13.3.2. Distribution of heat flow over surface of blunt cone in supersonic flow (with laminar boundary layer):

—.— by formula (13.3.54); ——by formula (13.3.62); – – –by formula (13.3.63).

blunt and equivalent cones is practically identical. At the same time the heat flows over the surface of thin blunt bodies are less than those over the surface of "equivalent" cones.

It is possible to switch from the "equivalent" cone to the usual sharp cone if we replace

$$\tilde{\lambda}\,\varphi_k\,R_T=(\partial V_\delta/\partial x)_{x\to 0}\,x=V_\delta$$

by the value of velocity V_k over a conical surface in the formula (13.3.64) in which $\bar{x}_k=x_k/R_T$. According to this we have, for a conventional sharp cone,

$$q_x=0.61\,\mathbf{Pr}^{-2/3}\sqrt{\frac{\rho_k\,\mu_k\,V_k}{x_k}}\,(i_r-i_w). \tag{13.3.65}$$

A similar equation can be obtained directly from the relations (13.3.43) and (13.3.44′) by inserting the following values:

$$p_\delta=p_0',\ V_\delta=V_k=\text{const};$$
$$\rho_0'\,\mu_0'=\rho_k\,\mu_k,\ r_0=x\sin\beta_k.$$

4. Heat Transfer by Diffusion

For quantitative evaluation of heat transfer by diffusion it is necessary, in general, to solve the system of equations of the boundary layer including the equations of motion and energy (13.3.1) and the equation of diffusion (3.2.4).

The equations of motion and energy in terms of the variables η, $\tilde{x}$ (13.3.5) on the assumptions made in the previous section have the form of (13.3.35) and (13.3.36). Let us take the equation of diffusion under the flow conditions of a "frozen" boundary layer. This kind of flow, as noted earlier, is characterized by low rates of recombination which can be neglected in comparison with the rate of diffusion across stream lines. The concentration of atoms in this "frozen" boundary layer is determined by the diffusion of substance to the wall where the recombination also takes place. In this case the concentration is not balanced. It can be determined by local values of temperature and pressure. The distribution of concentrations and temperatures is mutually almost independent.

Assuming $(W_{chem})_i=0$, $r=r_0$, $V_r=V_y$ in equation (3.2.4) and referring this equation to the flow conditions in the boundary layer by replacing the derivative $\partial/\partial r$ by $\partial/\partial y$, we will have

$$\frac{\partial(\rho V_x\,r_0\,c_i)}{\partial x}+\frac{\partial(\rho V_y\,r_0\,c_i)}{\partial y}=-\frac{\partial(Q_i\,r_0)}{\partial y}.$$

Expanding the derivative on the left side and replacing Q_i in accordance with (13.1.7), we get

$$\left[\frac{\partial(\rho V_x\,r_0)}{\partial x}+\frac{\partial(\rho V_y\,r_0)}{\partial y}\right]c_i+\rho r_0\left(V_x\frac{\partial c_i}{\partial x}+V_y\frac{\partial c_i}{\partial y}\right)=\frac{\partial}{\partial y}\left(\rho\overline{D}\,r_0\frac{\partial c_i}{\partial y}\right).$$

According to the continuity equation (2.4.48) the two terms in square brackets are equal to zero. Then, keeping in mind that r_0 for a given section of boundary layer happens to be a constant value, we find

$$\rho\left(V_x\frac{\partial c_i}{\partial x}+V_y\frac{\partial c_i}{\partial y}\right)=\frac{\partial}{\partial y}\left(\rho\bar{D}\frac{\partial c_i}{\partial y}\right). \tag{13.4.1}$$

For the atomic component equation (13.4.1) will have the following form:

$$\rho\left(V_x\frac{\partial c_A}{\partial x}+V_y\frac{\partial c_A}{\partial y}\right)=\frac{\partial}{\partial y}\left(\rho\bar{D}\frac{\partial c_A}{\partial y}\right). \tag{13.4.2}$$

For the molecular component the equation of diffusion will be similar in form with replacement of c_A by c_M, which follows from the condition $c_A=1-c_M$.

Let us transform equation (13.4.2) to the variables η, $\tilde{x}$ keeping in view the values of operators (13.3.15) and (13.3.17):

$$\rho\rho_\delta V_\delta^2\mu_\delta r_0^{2\epsilon}\left(\frac{\partial f}{\partial\eta}\cdot\frac{\partial c_A}{\partial\tilde{x}}-\frac{f}{2\tilde{x}}\cdot\frac{\partial c_A}{\partial\eta}-\frac{\partial f}{\partial\tilde{x}}\cdot\frac{\partial c_A}{\partial\eta}\right)$$
$$=\frac{\rho V_\delta^2 r_0^{2\epsilon}}{2\tilde{x}}\cdot\frac{\partial}{\partial\eta}\left(\rho^2\bar{D}\frac{\partial c_A}{\partial\eta}\right).$$

Assuming that the concentration and the velocity profile are functions of η only (we recall the similarity solution), we get

$$\rho_\delta\mu_\delta f\frac{\partial c_A}{\partial\eta}+\frac{\partial}{\partial\eta}\left(\rho^2\bar{D}\frac{\partial c_A}{\partial\eta}\right)=0.$$

Let us introduce the nondimensional dependent variable

$$z(\eta)=c_A/c_{A\delta}. \tag{13.4.3}$$

Transforming the equation of diffusion to this variable on the assumption that $\rho\mu=\rho_\delta\mu_\delta$ and the Schmidt number $\mathbf{Sc}=\mu/\rho\bar{D}$ is constant and equal to its value at the wall, we can write

$$\mathbf{Sc}\cdot f\cdot z'+z''=0, \tag{13.4.4}$$

where "prime" indicates differentiation with respect to η.

Equation (13.4.4) is similar in form to equation (13.3.36) with the difference that the Prandtl number **Pr** is replaced by the Schmidt number **Sc**. The boundary conditions for the function z to solve equation (13.4.4) will be similar to the boundary conditions for function g [see (13.3.23) and (13.3.24)], i.e. at $\eta=0$ ($y=0$) the quantity $z(0)=z_w=c_{Aw}/c_{A\delta}$ and at $\eta\to\infty$ ($y\to\infty$) the function $z(\infty)\to1$ and the derivative $\partial z/\partial\eta\to0$.

The double integration (13.4.4) leads to an equation similar to (13.3.37):

$$z(\eta)-z(0)=z'(0)\int_0^{\eta} e^{-\int_0^{\eta}\mathrm{Sc}\,f d\eta}\,d\eta. \tag{13.4.5}$$

Taking this analogy into account, the integral at $\eta\to\infty$ will be

$$\int_0^{\eta} e^{-\int_0^{\eta}\mathrm{Sc}\,f d\eta}\,d\eta=(0.5\mathrm{Sc}^{1/3})^{-1}.$$

Keeping in mind that the function $z(\eta)\to 1$ as $\eta\to\infty$, we will have

$$z'(0)=0.5\mathrm{Sc}^{1/3}\,[1-z(0)]. \tag{13.4.6}$$

It is possible to find the derivative $z'(0)=(\partial z/\partial\eta)_w$ simultaneously by using the relation from chemical kinetics to determine the quantity of substance being separated at the wall due to catalytic reactions:

$$Q_w=k_w\,c_{Aw}\,\rho_w, \tag{13.4.7}$$

where k_w is the constant for the rate of catalytic reaction. This quantity of substance is equal to the diffusion flow (in absolute value)

$$Q_w=\rho_w\overline{D}\left(\frac{\partial c_A}{\partial y}\right)_w=\rho_w\overline{D}\left(\frac{\partial z}{\partial y}\right)_w c_{A\delta}.$$

Consequently

$$\left(\frac{\partial z}{\partial y}\right)_w=\frac{k_w}{\overline{D}}\cdot\frac{c_{Aw}}{c_{A\delta}}=\frac{k_w}{\overline{D}}\,z(0)$$

or according to (13.3.5), in terms of variables η, $\tilde{x}$ it will be

$$z'(0)=\left(\frac{\partial z}{\partial\eta}\right)_w=\left(\frac{\partial z}{\partial y}\right)_w\left(\frac{\partial y}{\partial\eta}\right)_w=\frac{(2\tilde{x})^{1/2}}{V_\delta r_0^\epsilon}\cdot\frac{k_w}{\rho_w\overline{D}}\,z(0). \tag{13.4.8}$$

Let us solve the system of equations (13.4.6) and (13.4.8) for $z(0)$ and $z'(0)$:

$$z(0)=z_w=\left[\frac{2\tilde{x}^{1/2}}{V_\delta r_0^\epsilon}\cdot\frac{k_w}{0.5\,\mathrm{Sc}^{1/3}\,\rho_w\overline{D}}+1\right]^{-1}; \tag{13.4.9}$$

$$z'(0)=0.5\,\mathrm{Sc}^{1/3}\left[1+\frac{0.5\,\mathrm{Sc}^{1/3}\,V_\delta r_0^\epsilon\,\rho_w\,\overline{D}}{(2\tilde{x})^{1/2}k_w}\right]^{-1}. \tag{13.4.10}$$

The value of the specific heat flow separated during recombination at the wall can be obtained from formula (13.1.8). After determining the heat flow in its absolute magnitude we can find its running value

$$q_{Dx}=\rho_w\,\overline{D}\,(\partial c_A/\partial\eta)_w\,(\partial\eta/\partial y)_w\,(i_A-i_M)$$

or, keeping in mind that

$$(\partial c_A/\partial\eta)_w = c_{A\delta}\, z'(0)$$

and using (13.3.6) for $(\partial\eta/\partial y)_w$, we get the following relation:

$$q_{Dx} = 0.5\,\mathbf{Sc}^{1/3}\,\bar{D}\,\rho_w^2\,V_\delta\,r_0^\varepsilon\,(\widetilde{2x})^{-1/2} \times\left[1+\frac{0.5\,\mathbf{Sc}^{1/3}\,V_\delta\,r_0^\varepsilon\,\rho_w\,\bar{D}}{(\widetilde{2x})^{1/2}\,k_w}\right]^{-1} c_{A\delta}\,(i_A - i_M). \qquad (13.4.11)$$

From the relations obtained it follows that the value of $z\,(0)=0$ in the limiting case corresponding to an infinitely high rate of recombination (the wall being a catalyst and the coefficient of catalytic reaction $k_w\to\infty$) and hence the concentration at the wall is equal to zero. According to (13.4.11) the heat flow during this infinitely fast catalysis will be

$$q_{Dx} = 0.5\,\mathbf{Sc}^{1/3}\,\rho_w^2\,V_\delta\,\bar{D}\,r_0^\varepsilon\,(\widetilde{2x})^{-1/2}\,c_{A\delta}\,(i_A - i_M). \qquad (13.4.12)$$

So in the limiting case in question the atoms reach the wall even under the condition of zero concentration over the surface. Meantime the maximum amount of heat is separated as a result of the recombination of these atoms into molecules. In the second limiting case of an infinitely low catalytic reaction (wall non-catalytic, $k_w\to 0$) the concentration at the wall remains the same as at the external limit of the boundary layer, i.e. $z\,(0)=1$. In this case the flow of atoms due to diffusion will be zero and consequently additional heat will not be liberated, i.e. $q_{Dx}=0$.

This result follows from (13.4.11) if the coefficient of catalytic reaction $k_w\to 0$.

Let us carry out some simplifications in equation (13.4.11).

Assuming that $\rho_w\mu_w=\rho_\delta\mu_\delta$ and introducing the ratio of $\rho_\delta\mu_\delta/\rho_0'\mu_0'$ according to formula (13.3.42) in which $\omega_\delta/\omega_0'=1$, we will have

$$A=\frac{0.5\,\mathbf{Sc}^{1/3}\,\rho_w^2\bar{D}\,V_\delta\,r_0^\varepsilon}{(\widetilde{2x})^{1/2}}=\frac{0.5\,\mathbf{Sc}^{-2/3}(p_\delta/p_0')\,V_\delta\,r_0^\varepsilon\,\sqrt{\rho_0'\mu_0'}}{\left[2\int\limits_0^x (p_\delta/p_0')\,V_\delta\,r_0^{2\varepsilon}\,dx\right]^{1/2}} \qquad (13.4.13)$$

or according to the formula for function $F(x)$ we will have the expression

$$A = 0.5\,\mathbf{Sc}^{-2/3}\sqrt{\rho_0'\,\mu_0'\,V_\infty}\,F(x), \qquad (13.4.13')$$

in which the Schmidt number $\mathbf{Sc}=\mu_w/\rho_w\,\bar{D}$.

Considering (13.4.13') and keeping in mind that

$$c_{A\delta}\,(i_A - i_M)\approx c_{A\delta}\,i_{chem}, \qquad (13.4.14)$$

and introducing the enthalpy of dissociation

$$i_D = c_{A\delta}\,i_{chem} = c_{A\delta}\,u_d, \qquad (13.4.15)$$

where i_d is the characteristic energy of dissociation [see (1.5.9)], we can write the following relation in place of (13.4.11):

$$q_{Dx}=0.5\,\mathbf{Sc}^{-2/3}\sqrt{\rho_0'\mu_0'V_\infty}\,F(x)\,i_D\,\varphi, \tag{13.4.16}$$

where the catalytic coefficient

$$\varphi=[1+(A/\rho_w k_w)]^{-1} \tag{13.4.17}$$

is introduced.

This coefficient takes care of the effect of a finite rate of recombination because the parameter k_w appears in the expression. Obviously as $k_w\to\infty$ the value of $\varphi\to 1$ (case of infinitely fast catalysis) and as $k_w\to 0$ the value of $\varphi\to 0$ (wall is not catalytic).

For the flow conditions near the point of complete stagnation we get the following expression from (13.4.13′) taking into account (13.3.47):

$$A=A_0=0.5\,\mathbf{Sc}^{-2/3}\sqrt{\rho_0'\mu_0'\tilde{\lambda}(\varepsilon+1)}, \tag{13.4.18}$$

and from the expression (13.4.17), we have

$$\varphi=\varphi_0=\left(1+\frac{0.5\,\mathbf{Sc}^{-2/3}\sqrt{\rho_0'\mu_0'\tilde{\lambda}(\varepsilon+1)}}{\rho_w k_w}\right)^{-1}. \tag{13.4.19}$$

According to this the heat flow in the neighborhood of the point of complete stagnation will be

$$q_{D0}=0.5\,\mathbf{Sc}^{-2/3}\sqrt{\rho_0'\mu_0'\tilde{\lambda}(\varepsilon+1)}\,\varphi_0\,i_D. \tag{13.4.20}$$

In these expressions $\varepsilon=1$ for bodies of revolution and $\varepsilon=0$ for a wing profile.

The total specific heat flow to the wall will be obtained if the heat due to diffusion q_{Dx} is added to the heat due to molecular heat conductivity q_{Tx}. In general, the value of this heat flow is determined by equation (13.1.12), which can be rewritten in the form

$$q_k=q_{Tx}+q_{Dx}=\underbrace{-\frac{\lambda_w}{(c_p)_w}\left(\frac{\partial i}{\partial y}\right)_w\left[1-\frac{(\partial c_A/\partial y)_w(i_A-i_M)}{(\partial i/\partial y)_w}\right]}_{(q_k)_{Le}=1}$$

$$\underbrace{-\rho_w\,\overline{D}\left(\frac{\partial c_A}{\partial y}\right)_w(i_A-i_M)}_{q_k=q_{Dx}}.$$

Taking into account formulas (13.1.8) and (13.1.13), we write

$$q_k=(q_k)_{Le=1}\left[1-\frac{(\partial c_A/\partial y)_w\,(i_A-i_M)}{(\partial i/\partial y)_w}+\frac{q_{Dx}}{(q_k)_{Le=1}}\right], \qquad (13.4.21)$$

where $(q_k)_{Le=1}$ is the specific heat flow corresponding to the value of $\mathbf{Le}=\rho_w \overline{D}\,(c_p)_w/\lambda_w$ equal to unity.

Taking into account (13.3.43) and (13.4.16), it will be

$$q_k=(q_k)_{Le=1}\left[1-\frac{(\partial c_A/\partial y)_w\,(i_A-i_M)}{(\partial i/\partial y)_w}+\left(\frac{\mathbf{Sc}}{\mathbf{Pr}}\right)^{-2/3}\frac{\varphi\, i_D}{i_r-i_w}\right].$$

Let us work out the values of derivatives $(\partial c_A/\partial y)_w$ and $(\partial i/\partial y)_w$, assuming that the concentration $c_{Aw}=0$ on a cold wall:

$$\left(\frac{\partial c_A}{\partial y}\right)_w\sim\frac{c_{A\delta}}{\delta},\left(\frac{\partial i}{\partial y}\right)_w=\left(\frac{\partial i_0}{\partial y}\right)_w\sim\frac{i_{0\delta}-i_w}{\delta}=\frac{i_r-i_w}{\delta},$$

where δ is the boundary layer thickness; $i_{0\delta}=i+(V_x^2/2)$.

Considering this evaluation of derivatives and keeping in mind that $\mathbf{Le}=\mathbf{Pr}/\mathbf{Sc}$ and $c_{A\delta}\,(i_A-i_M)=i_D$, we get

$$q_k=(q_k)_{Le=1}\left[1+(\mathbf{Le}^{2/3}\,\varphi-1)\,\frac{i_D}{i_r-i_w}\right]. \qquad (13.4.22)$$

The heat flow $(q_k)_{Le=1}$ for any arbitrary point on this surface under flow-interaction is obtained from formula (13.3.43) and for the point of complete stagnation it is found from the expression (13.3.48). The coefficients are determined from (13.4.17) and (13.4.19) respectively. The value of i_D is also calculated from the position of a given point on the surface: $i_D=u_d\,[c_{A\delta}-(c_A)_w]$. For a binary mixture we may take $c_{A\delta}=a_\delta$ and $(c_A)_w=a_w$ and consequently

$$i_D=u_d\,(a_\delta-a_w). \qquad (13.4.23)$$

The relations (1.5.21) through (1.5.24) may be used to calculate i_D for dissociating air which is considered as a binary mixture of atoms and molecules.

The number **Le** is determined for the conditions at a point of complete stagnation and is assumed to be constant over the whole surface. The relations corresponding to the two limiting cases of heat transfer follow from formula (13.4.22). In the first of these cases,where the surface in the flow is not catalytic ($k_w\to 0$, $\varphi\to 0$), heat transfer by diffusion is absent and the heat flow to the surface occurs only due to heat conduction:

$$q_{k(k_w\to 0)}=(q_k)_{Le=1}\left(1-\frac{i_D}{i_r-i_w}\right). \qquad (13.4.24)$$

In the second case where the wall is catalytic and recombination on it takes place at an infinitely high rate ($k_w\to\infty$, $\varphi\to 1$), the total heat flow will be

$$q_{k(k_w\to\infty)}=(q_k)_{Le=1}\left[1+(\mathbf{Le}^{2/3}-1)\,\frac{i_D}{i_r-i_w}\right]. \qquad (13.4.25)$$

The ratio of the quantity of heat q_k (13.4.22) separated during a finite process of recombination to the heat flow $q_{k(k_w\to\infty)}$ in the case of an infinitely fast catalysis will be

$$\bar{q}=\frac{q_k}{q_{k(k_w\to\infty)}}=\frac{1+(\mathrm{Le}^{2/3}\varphi-1)\,\tilde{i}_D}{1+(\mathrm{Le}^{2/3}-1)\,\tilde{i}_D}, \tag{13.4.26}$$

where $\tilde{i}_D=i_D/(i_r-i_w)$.

The variation in the ratio of heat flows (13.4.26), calculated for the point of complete stagnation depending on the free stream velocity V_∞ and the constant of catalytic reaction k_w, is graphically shown in Fig. 13.4.1. These results indicate how important it is to consider the finite rate of recombination. They also suggest the possibility of reducing heat transfer by use of a cowling made of non-catalytic materials.

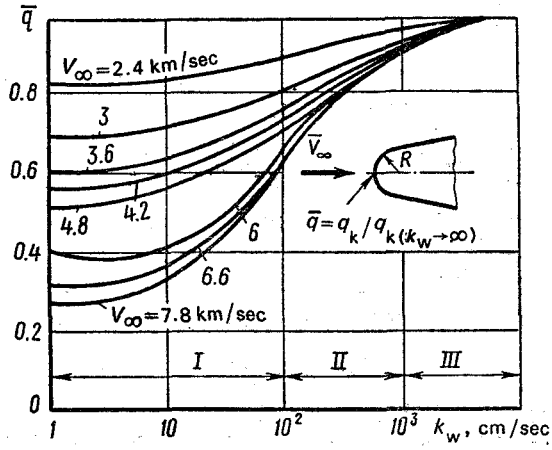

Fig. 13.4.1. Variation in heat transfer as function of flight velocity V_∞ and rate of recombination k_w:

I—non-catalytic wall (glass); *II*—intermediate surface (oxides); *III*—catalysts (metals).

Let us study some data on the constant k_w for the rate of catalytic reaction. Its value can be characterized by a nondimensional parameter

$$\gamma=N_r/N, \tag{13.4.27}$$

where N_r is the proportion of atoms participating in recombination and N is the total number of atoms striking unit surface area in unit time; the parameter γ is known as the criterion of recombination (or catalytic) capability.

According to equation (13.4.7) the number of recombining atoms

$$N_r=Q_w/m_A=k_w\,c_{Aw}\,\rho_w/m_A.$$

The total number of atoms striking the wall is

$$N=p_A/(2\pi m_A k T_w)^{1/2}.$$

Since the partial pressure $p_A=n_A k T_w$ and $c_{Aw}\rho_w=n_A m_A$, we have

$$\gamma=N_r/N=k_w (2\pi m_A/kT_w)^{1/2}. \quad (13.4.28)$$

The empirical values of the criterion of catalytic capability of a glass-based substance (81% SiO_2, 12% B_2O_3, 7% aluminum oxide, nitric oxide and calcium oxide) and of some other materials are shown in Fig. 13.4.2. The variation in γ as a function of T_w at different fixed values of k_w is shown in the same figure.

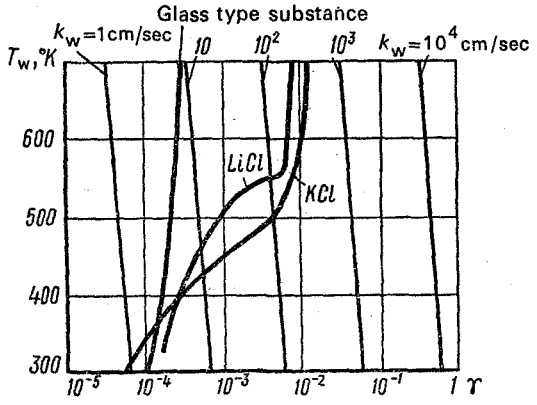

Fig. 13.4.2. Catalytic capability of some materials.

A study of the recombination of oxygen showed that the catalytic capability of glass-based substances is low and is determined by the values $k_w < 10$ cm/sec. The use of these materials as a heat-resistant cowling may appreciably reduce heat transfer. The lowest effect is achieved with the use of chlorides (LiCl, KCl) having high values of k_w in comparison with glass and with the same property that these values increase with a rise in temperature.

The recombination of atomized nitrogen has been studied for different metallic and non-metallic surfaces. It was found that most materials seem to have a strong catalytic reaction on atomized nitrogen. Nonmetallic materials have the opposite property and are characterized by low values of the criterion of catalytic capability. In particular measurements on glass-type materials at a partial pressure of nitrogen equal to 10^{-3} atmosphere showed that the quantity $\gamma=3\times10^{-5}$.

Research on the recombination of pure nitrogen and oxygen has important practical significance because it helps in evaluating cooling catalytic effects during the study of heat transfer from heated air to the surface under flow-interaction. Hence it may be assumed that the recombination of the air mixture is accelerated due to intermediate reactions between oxygen and

nitrogen. The resultant catalytic capability is increased and hence heat transfer is increased.

In this section we have been considering heat transfer in two limiting cases of balanced and "frozen" flows in a boundary layer. However, the mechanism of heat transfer characterized by the condition that the concentration of each chemical component in a boundary layer is determined by a finite rate of chemical reaction $(W_{\text{chem}})_i$ according to equation (3.2.4) happens to be the most general mode of heat transfer. Knowing the data on heat transfer in these limiting cases it is possible to study its mechanism in the more general case where $(W_{\text{chem}})_i \neq 0$. For this purpose it is necessary to use the system of equations (3.2.4), (3.2.14), (12.1.8). Some of the methods and results of solution of this system are presented in the works [21, 31, 35].

About the calculation of heat transfer in a turbulent boundary layer: Earlier we discussed problems connected with the determination of heat transfer in a laminar boundary layer over a curved surface. The solution of these problems was based on the application of a system of boundary layer equations with given velocity profiles and the necessary thermodynamic parameters across the section.

Many problems connected with the calculation of a turbulent boundary layer can be similarly solved. In particular, the equation of motion in the integral form for a boundary layer was used in studying a turbulent boundary layer (see Chapter 12). To study the heat transfer in a turbulent layer this equation should be connected with the equation of energy in an integral form as shown in work [23]. This solution consists of the integral method in the theory of a boundary layer.

The application of integral relations and the equations of a turbulent boundary layer in differential form gives appreciably lower accuracy than in the case of a laminar flow. This is primarily due to the still imperfect relations describing the mechanism for a turbulent heat flow and momentum and the correspondingly approximate nature of the equations of motion and energy. Inaccurate representation of the velocity profile across the boundary layer thickness also leads to low accuracy, which indicates that the gas dynamic properties of the flow at each point across the boundary layer are not properly catered for in using the integral method. However, it has been experimentally established that the universal nature of variation of velocity with a given profile is not fully confirmed and consequently the presence of pressure gradients along the boundary layer leads to additional loss of accuracy.

Modern rocket and aviation technology requires high accuracy in the calculation of friction and heat transfer, which can be achieved only by perfecting the methods of solution of boundary layer equations. In the last few years the method of direct solution of boundary layer equations, as applied to each of the above problems, has gained currency. Here the conditions on the wall and at the free surface of the boundary layer happen to be the boun-

dary conditions and the velocity profiles and thermodynamic characteristics of the gas across the boundary layer section are the result of calculation. The velocity profiles so worked out help to find the frictional stress and specific heat flow to the wall.

Direct integration of the system of boundary layer equations requires the introduction of some assumptions without which calculation with the help of integral methods is impossible. These involve in the first place deviation from given velocity profiles and other thermodynamic parameters, from the use of the Reynolds analogy (see Section 2) and from some empirical formula for heat transfer.

One way to improve the accuracy of investigation of a turbulent boundary layer is based on a more accurate description of the mechanism of turbulent heat transfer and momentum. The quality of the results obtained depends mainly on its correct mathematical formulation. Therefore special attention has been devoted recently to study of the processes of turbulent mixing on the basis of static formulation of the mechanism of small-scale movements of gas. The result of this study is a modification of the concept of intermixing (see Chapter 1 Section 1) which is related to the attempt to make this method universal. It is a purely qualitative and entirely approximate description of oscillatory motion.

The method of direct solution of boundary layer equations has become more attractive for investigators due to the enhanced possibility of performing calculations with the help of numerical mathematics and modern high-speed electronic computers. The technique of complex calculation of the boundary layer is gaining popularity in engineering practice thanks to computers. The results of research on the motion of a viscous gaseous medium with the help of the method of direct solution of the boundary layer are reproduced in the series of scientific articles [55, 56, 41 (1965, No. 4)].

5. Wall Temperature

5.1 Radiational equilibrium temperature

The heat regime over the surface during the steady motion of a flight vehicle is characterized by the equilibrium of heat flows to and from the surface. In this case the equation of heat balance (13.1.1) will have the form $q_{in}-q_0=0$ or, taking the expression (13.1.2) for inflow of heat q_{in} and outflow of heat q_0 (13.1.3), it will be

$$q_k+q_{rad}+q_s+q_e+q_m=q_r+q_{ab}+q_{ca}+q_{mo}. \qquad (13.5.1)$$

The wall temperature determined from the condition of equilibrium of heat flows (13.5.1) and corresponding to a steady flow over the surface is known as equilibrium temperature.

Let us assume that the heat transfer is characterized only by a convective

heat inflow to the wall ($q_{in}=q_k$) and radiational heat outflow from it ($q_0=q_r$). Here equation (13.5.1), taking into account the expression (13.1.17) for q_k and (13.1.28) for q_r, takes the form

$$[a_w/(c_p)_w]\,(i_r-i_w)=\varepsilon\sigma T_w^4. \tag{13.5.2}$$

The wall temperature determined by equation (13.5.2) is known as the radiational equilibrium temperature and is denoted by $T_w=T_e$. This temperature differs from the temperature of recovery T_r which, as we know from earlier discussion, is the temperature of the gas on the wall in the absence of heat transfer, i.e. on a thermally isolated surface.

The temperature T_e represents some upper limit for a radiating surface which is achieved in the case where the heated wall exhaustively radiates all the energy received. This temperature is not real at very high heat flows because it is so high that it cannot be achieved: the covering material would be destroyed (melting, sublimation or burning). However, in some cases the radiational equilibrium temperature may be realized, for example, on the surface of melting flight vehicles. During melting the kinetic energy changes to heat energy gradually and the intensity of the convective heat flow may be comparatively moderate so that there is a possibility of radiating all the energy absorbed at the equilibrium temperature permissible for construction.

The coefficient of radiation σ and the degree of blackness ε in equation (13.5.2) may be assumed to be known and of constant value (see Section 1). The coefficient of heat transfer a_w, sp. heat $(c_p)_w$ and the enthalpies i_r and i_w happen to be functions of the temperature to be determined, $T_w=T_e$, and the given pressure p_δ for a dissociating gas. So the total number of unknown variables will be five and hence equation (13.5.2) must be supplemented by four independent equations to determine a_w, $(c_p)_w$, i_r and i_w.

In the case of a laminar boundary layer the equation for a_w, according to (13.1.17) and (13.4.22), will be written in the form

$$a_w=\frac{(c_p)_w\,q_k}{i_r-i_w}=\frac{(c_p)_w}{i_r-i_w}(q_k)_{Le=1}\left[1+(\mathrm{Le}^{2/3}\varphi-1)\frac{i_D}{i_r-i_w}\right]. \tag{13.5.3}$$

The equation for $(c_p)_w$ and i_w may be expressed in a general form:

$$(c_p)_w=f_1\,(p_\delta, T_w); \tag{13.5.4}$$

$$i_w=f_2\,(p_\delta, T_w), \tag{13.5.5}$$

where f_1 and f_2 are calculated with the help of tables or graphs of the thermodynamic functions of air at high temperatures.

The enthalpy of recovery

$$i_r=i_\delta+r\,(V_\delta^2/2), \tag{13.5.6}$$

where the coefficient of recovery $r=f_3\,(p_\delta, T_w)$ is found as some other function f_3 of pressure p_δ and temperature T_w with the help of formulas (12.5.19) through (12.5.21).

The solution of the system of equilibrium (13.5.2) through (13.5.6) helps us to find the radiational equilibrium temperature of the surface under flow-interaction in the presence of a laminar boundary layer in a dissociating gaseous medium. Using the equation for turbulent heat transfer in place of (13.5.3) it is possible to find the temperature $T_w = T_e$ for a turbulent boundary layer. This equation in particular was obtained above for the conditions of flow-interaction of a flat plate.

The solution of the system of equations (13.5.2) through (13.5.6) will be carried out by the method of successive iterations. Here the flight velocity V_∞ (or Mach number M_∞) and altitude H are the given parameters from which the "inviscid" flow-interaction of the surface (pressure p_δ, density ρ_δ, temperature T_δ, etc.) can be worked out.

Taking $r = r_L = 0.84$ according to (12.5.22) (laminar boundary layer) or $r = r_T = 0.89$ (turbulent boundary layer), the enthalpy i_r (13.5.6) is worked out as a first approximation to find the temperature $T_w = T_e$ at some point on this surface. Then the corresponding value of T_r as a function of i_r and p_δ is found. Next, the temperature $T_w < T_r$ and the corresponding quantities $i_w < i_r$ are given some values. For each of these values of $T_w(i_w)$, a_x and $(c_p)_w$ are worked out as a first approximation and the difference in heat flows is determined:

$$[a_x/(c_p)_w]\,(i_r - i_w) - \varepsilon\sigma T_w^4 = q_w. \tag{13.5.7}$$

From the data so obtained a table can be made or a curve q_w versus T_w can be drawn. Assuming $q_w = 0$, the temperature $T_w = T_e$ is determined with the help of interpolation of tabulated data or a graph. The coefficient r and enthalpy i_r can be modified from this value of the wall temperature and the coefficient of heat transfer a_x and specific heat $(c_p)_w$ can be determined as a next approximation. Then the calculations are repeated using equation (13.5.7) until the value of temperature $T_w = T_e$ is obtained with the required accuracy.

Simpler operations for calculation of temperature $T_w = T_e$ are carried out for a flat plate and a cone, whose flow-interactions are characterized by constant values of the "inviscid" gas parameters on the surface. The calculation of the radiational equilibrium temperature may be carried out by the method of deciding enthalpy (temperature). It can also be calculated starting with a mixed boundary layer on the surface in the flow using the relations for determination of the parameters of friction and heat transfer.

For low speeds of flow-interactions, during which dissociation need not be taken into account and the thermodynamic and kinetic characteristics of air may be considered constant, the calculation of temperature $T_w = T_e$ is further simplified. In this case the corresponding system of equations takes the following form:

$$a_x(T_r - T_w) = \varepsilon\sigma T_w^4; \tag{13.5.8}$$

$$a_x = h(T_w), \tag{13.5.9}$$

where h is some function of temperature T_w that determines the coefficient of heat transfer.

The results of calculation of the radiational equilibrium temperature based on the system of equations (13.5.8), (13.5.9) for a parabolic profile in a supersonic flow are shown in Fig. 13.5.1. This calculation was carried out using the relations for a_x for a flat plate in which the local parameters of an "inviscid" flow over the profile were used. Here the effect of the axial gradient of pressure is not considered and the fixed values of $r_L = 0.84$ and $r_T = 0.89$ corresponding to Prandtl number $\mathbf{Pr} = 0.71$ are taken.

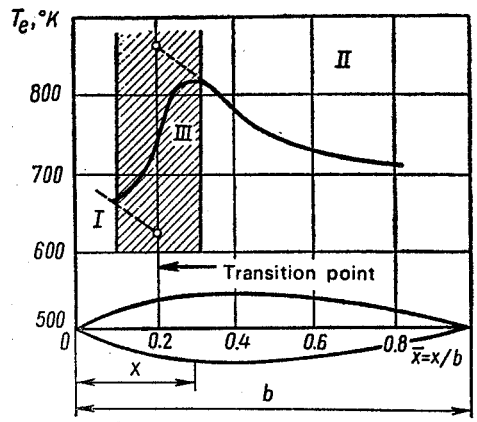

Fig. 13.5.1. Nature of distribution of radiational equilibrium temperature over profile surface in supersonic flow:

I—laminar layer; *II*—turbulent layer; *III*—transition region.

In constructing a graph like that in Fig. 13.5.1 we have to consider the transition region because the heat flows change gradually along some curve in this region. This curve should not have discontinuities because axial heat flows, which smooth out the temperature, occur in actual situations.

The system of equations (13.5.8), (13.5.9) can be used with the required accuracy for calculation of radiational equilibrium temperature at very high speeds when it becomes necessary to account for the effect of compressibility, dissociation or variation in specific heats if we use the definitive parameters in these equations:

$$a_x^*(T_r^* - T_w) = \varepsilon\sigma T_w^4; \tag{13.5.10}$$

$$a_x^* = h^*(T_w), \tag{13.5.11}$$

where T_r^* is determined with adjustment for dissociation from definitive enthalpy (12.5.23); a_x^* is the quantity obtained from expression (13.2.21).

In calculating heat transfer on a flat plate or a cone the Stanton number $\mathbf{St}_x^*$ appearing in the expression for a_x^* found from the corresponding relations (13.2.19) or (13.2.27), which include the parameters of friction and heat transfer.

The analysis called for determination of the radiational equilibrium temperature and the results of calculations lead to the conclusion that the basic way to reduce it is to decrease the ratio a_x/ε. For this purpose it is possible,

first of all, to reduce the coefficient of heat transfer α_x by maintaining a laminar boundary layer. Reduction in α_x is also achieved by taking the flight vehicle to a higher altitude where heating is reduced due to the reduction in the density of the atmosphere. Secondly, it is possible to increase the degree of blackness ε of the surface. A special covering may be used for this purpose to increase ε to 0.7 or 0.8 and thereby enhance the cooling effect due to radiation. An increase in degree of blackness to a value nearer unity has been observed in cases where a metallic wall is thin and is heated to high temperatures.

5.2 Equilibrium temperature in presence of additional sources of input and output of heat

The calculation of equilibrium temperature in the presence of types of heat transfer other than convective and radiational heat flows will be carried out in a similar way to the determination of radiational equilibrium temperature. We have to use equation (13.5.1) for this calculation which, taking the values of $q_k=\alpha_x(T_r-T_w)$ and $q_r=\varepsilon\sigma T_w^4$, will be written in the form

$$\alpha_x(T_r'-T_w)=\varepsilon\sigma T_w^4, \tag{13.5.12}$$

where the modified temperature of recovery

$$T_r'=T_r\left(1+\frac{\Sigma q_i}{\alpha_x T_r}\right). \tag{13.5.13}$$

The sum of specific heat flows is

$$\Sigma q_i=q_{rad}+q_s+q_e+q_m-q_{ab}-q_{ca}-q_{mo}. \tag{13.5.14}$$

Among the many components of (13.5.14) there are the radiational flow q_{rad} to the wall from overheated gas and the heat q_{ab} carried away by ablation of the mass of the cowling as functions of wall temperature. The remaining components may be taken as given quantities.

From (13.5.12) it follows that the problem of determining $T_w=T_e$ is solved in principle in the same way as in the presence of heat outflow by radiation only. The difference lies in the fact that a modified temperature of recovery T'_r is determined in place of temperature of recovery T_r.

The analysis of relations (13.5.12) through (13.5.14) shows that the wall temperature $T_w=T_e$ can be lowered by applying artificial cooling q_{ca} and using ablation of material during which some quantity of heat q_{ab} is carried away along with the destroyed part of the cowling.

At low supersonic speeds of flow-interaction it is not necessary to consider radiational heat flow q_{rad} and heat q_{ab} absorbed during ablation. In this case

$$\Sigma q_i=q_s+q_e+q_m-q_{ca}-q_{mo}, \tag{13.5.15}$$

and the calculation of $T_w = T_e$ becomes simple as the components of heat transfer in (13.5.15) do not depend on the wall temperature and are given in advance.

At high altitudes (100–500 km and above) the aerodynamic heat flow is insignificant in comparison with ray energy. Neglecting dispersion of heat over the surface, it may be assumed that the equation of heat balance during a stationary process will have the form

$$q_s + q_e + q_o = q_r, \tag{13.5.16}$$

where q_o is solar energy reflected from the earth.

At high altitudes the heat radiation from the earth q_e and the energy q_o in practice need not be taken into account and hence

$$q_s = q_r.$$

Inserting the values of q_s and q_r here according to (13.1.24) and (13.1.28), we get

$$\bar{q}\,\beta_c \cos\psi = \varepsilon\sigma T_w^4,$$

whence

$$T_w = \left(\frac{\beta_c}{\varepsilon}\cdot\frac{\bar{q}}{\sigma}\cos\psi\right)^{1/4}. \tag{13.5.17}$$

The maximum temperature will be attained at $\psi \doteq 0$. In practice $\overline{q_s} = 0.332$ kilo·cal/m²·sec as the constant quantity in formula (13.5.17). Then, assuming $\sigma = 1.36 \times 10^{-11}$ kilo·cal/m²·sec·degree⁴, we get the following relation:

$$T_w = 395\,(\beta_c/\varepsilon)^{1/4}\ [^\circ\mathrm{K}]. \tag{13.5.18}$$

14

THERMAL PROTECTION FOR FLIGHT VEHICLES

1. Methods of Thermal Protection

Space vehicles undergo considerable aerodynamic heating on re-entering the dense layers of the atmosphere because they are surrounded by high-temperature gas flows. To avert the destructive effect of aerodynamic heating on the structure of the vehicle to be launched into space various methods of thermal protection are used in rocketry. Here the salient features of the structure of the vehicle and the specific conditions of re-entry determine the particular type of heat protection.

The right selection of the mode of thermal protection provides considerable economy in the weight of a space vehicle, which is an important factor in determining this choice.

The following main methods of protection against aerodynamic heating are used in modern rocket construction: 1) heat absorption by heat sink; 2) forced cooling; 3) radiation and 4) use of a protective shield.

In protection of the vehicle by means of a heat sink the aerodynamic heatflow (q) is absorbed by a thick layer of indestructible material which covers the wall of the flight vehicle (Fig. 14.1.1). Graphite, copper and other materials with high heat conductivity are used for this purpose. A thin layer of material of low heat conductivity may be used on the external surface of the heat-absorbing layer. The presence of a coating of this material appreciably increases radiation from the surface (q_{rad}). However, the heat-absorptive capacity of

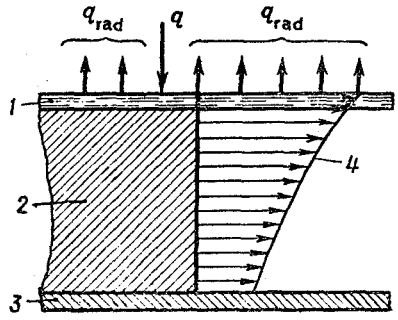

Fig. 14.1.1. Use of heat sink for protection of flight vehicle from heating: *1*—attached shield; *2*—heat-absorbing material; *3*—wall of main body of flight vehicle; *4*—temperature profile; q—heat flow to body surface; q_{rad} is heat flow radiated from surface.

available materials is not that high and therefore the weight of such heat-protection systems is excessive. For example, one kg of copper can absorb only 110 kilo·cal before melting. Therefore the technique of the heat sink may be used for thermal protection of flight vehicles encountering only moderately high heat flows in flight.

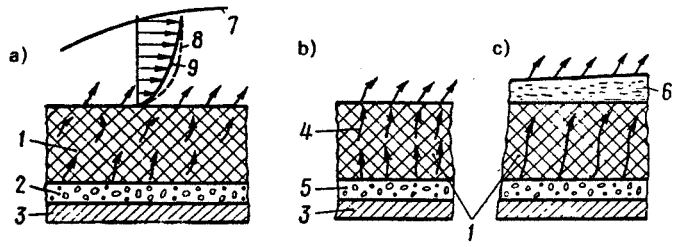

Fig. 14.1.2. Scheme of forced cooling:

a—cooling by gas blast; *b*—cooling by evaporation; *c*—evaporation of film; *1*—porous material; *2*—gas blast; *3*—wall of flight vehicle; *4*—zone of evaporation; *5*—fluid; *6*—fluid film; *7*—boundary layer; *8*—temperature profile without gas blast; *9*—temperature profile with gas blast.

The method of forced cooling (Fig. 14.1.2) works like this: Gas under pressure is blown through a perforated or porous wall of the flight vehicle to the boundary layer, absorbs part of the heat and in the process heats up. It is better to use a light gas of low molecular weight for this purpose, for example helium. Air, nitrogen and other gases can also be used in practice. Other types of forced cooling include evaporation and film cooling in which a fluid is blown through a porous wall and evaporates either in the wall (evaporation cooling) or on its surface (film cooling). The fluid must have a maximum heat

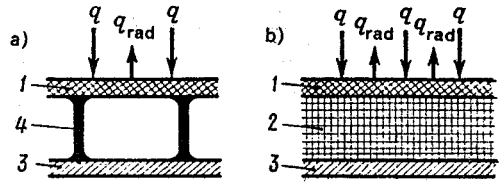

Fig. 14.1.3. Scheme of radiational heat protection of flight vehicle:

1—radiational cover; *2*—heat insulation layer; *3*—wall of flight vehicle; *4*—structural strengthening member; *q*—heat flow to surface; q_{rad}—heat flow radiated from surface.

of evaporation at a comparatively low temperature. Due to the required weight characteristics for a fluid or gas flow this device is very complicated from the point of view of manufacture.

The radiational method of heat protection differs by the marked simplicity

of its construction. The basic element of this device is a radiational screen which is a thin plate of metal (molybdenum, tungsten, etc.) or a film of oxides (for example: ZrO_2, SiO_2). The screen is located either over the structure to be protected (Fig. 14.1.3, a) or directly on it (Fig. 14.1.3, b). In the latter case material of low heat conductivity, for example porous ceramic or glass, is spread between the structure and the screen to reduce heat flow q inside the apparatus. During heating part of the heat q_{rad} is spent on radiation and over-heating of the structure of the vehicle does not take place.

Experiments show that the strength of the heat-resistant materials and oxides known at the present time is not maintained at temperatures exceeding 2600°K. Hence the method of radiational thermal protection can be used only under the impact of heat flows not exceeding about 200 kilo·cal/m^2·sec. Thus the range of application of this method of heat-protection is limited to comparatively low heat flows. However, their endurance is fairly high, 100 seconds or more.

We must also note that films of oxides or ceramic happen to be very fragile and easily peel off during heating and impact loading. Therefore the use of oxide or ceramic isolation is still out of the question in cases where such impact loads are expected, for example, during redistribution or variation of the strength of shock waves depending on the value of the angle of attack.

Heat-protection shield: The use of heat-protection shields is quite effective for vehicles undergoing the action of intense heat flows of short duration (ballistic launching) and for vehicles undergoing the impact of comparatively low heat flows of long duration (launching with aerodynamic effectiveness). The application of this device is quite simple. A layer of material of low heat conductivity is attached, fixed or built up on the surface of the flight vehicle structure. This is heated up or begins to erode under the action of the heat flow. The detached particles are carried away from the surface by gas flow past it, thereby absorbing and dissipating to surrounding space a large part of the heat created by this flow. Thus erosion of the mass of the shield material should be considered as an important mode of thermal protection of a vehicle to be launched. As a result of erosion the thickness of the heat-protection material diminishes. Estimating the appropriate value of this thickness, it is possible to design a structure for the required temperature range.

The materials of thermal-protection shields are subdivided into the following three main groups depending on the type of erosion: sublimating, melting and carbonizing. All these processes of erosion are grouped under the general terminology of ablation or mass transfer which, as follows from the above discussion, plays an important part in solving the problems of thermal protection for flight vehicles. This method, along with high effectiveness, has high reliability. Here the selection of the minimum thickness of heat protection shield depends on the mode of its erosion.

The sublimating materials for thermal shields are the ones that are destroyed by heating and reduced to the gaseous state. The most typical case in this group is floroplast, graphite (heating to temperatures above 3,000°K). The gaseous products formed by erosion flow into the boundary layer, reducing the heat flow (Fig. 14.1.4).

The group of sublimating heat protection coverings include the ones that turn to fluid during heating. Materials based on glass or quartz and also polymers, for example, organic glass, polyethylene, etc., are examples of this group. The fluid film formed as a result of heat flows under the action of the forces of aerodynamic friction and is carried away from the surface, reducing the heating effect. Meanwhile part of this melt evaporates (Fig. 14.1.5). This evaporation increases the effectiveness of such coverings because a considerable part of the heat is dissipated in the form of the latent heat of evaporation which, for example, is 2,400 kilo·cal/kg for quartz.

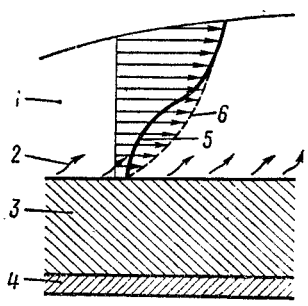

Fig. 14.1.4. Scheme of sublimating heat protection shield:

1—boundary layer; *2*—gaseous product due to destruction; *3*—sublimating material; *4*—strengthening member (wall) of flight vehicle; *5*—temperature profile with allowance for products of destruction; *6*—temperature profile without allowance for products of destruction.

A shield that is eroded by heating in a process similar to the transition to the gaseous state in carbonization is called a carbonizing shield. The materials of this group also form a gaseous product during the process of pyrolysis. Carbonizing (pyrolyzing) shields are composed of filler and bonding material. An example of a carbonizing material is phenyl nylon consisting of nylon cloth soaked in liquid phenyl. The liquid phenyl is hardened as a result of polymerization and layers of plate are formed. Glass, abestos, graphite, polymers and other materials in the form of cloth, separate fibers or grains can be used as a filler material. Epoxides and liquid phenyl and other polymers are used as bonding materials. A picture of erosion of this kind of shield is shown in Fig. 14.1.6. The gaseous products of carbonization (pyrolysis), entering the boundary layer, reduce the heat flow to the structure. The application of carbonizing materials is an effective method of thermal protection.

The above division of heat protection shields is quite provisional because, for example, part of the material that melts, as noted above, evaporates and thereby increases the cooling effect. If in the meantime the heat flows are very high and the forces due to aerodynamic friction are insignificant the whole of the melt will evaporate and the melting material virtually becomes sublimating material by its transfer behavior. On the other hand, given

minor heat flows and high frictional stress a sublimating material may condense and flow like a melting material.

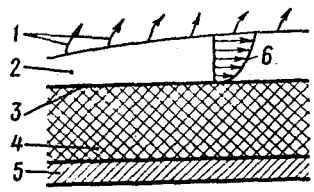

Fig. 14.1.5. Scheme of cooling with melting heat protection shield:

1—vapor of molten mass; *2*—fluid film; *3*—melting surface; *4*—melting heat protection shield; *5*—strengthening member (wall) of flight vehicle; *6*—velocity profile for motion of fluid film.

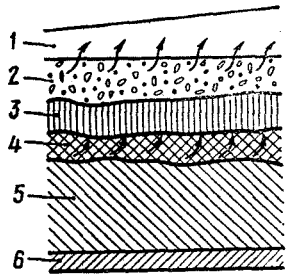

Fig. 14.1.6. Scheme of destruction of carbonizing heat protection shield:

1—boundary layer; *2*—carbonized layer; *3*—zone of melting of filler; *4*—zone of decomposition of tar; *5*—basic heat protection material; *6*—strengthening structure (wall) of flight vehicle.

For practically all heat protection materials in use the process of ablation begins with melting of the structural surface as a result of which a thin film of molten material is formed. This is called the liquid phase of the boundary layer. The second phase is represented by the gas flow surrounding the surface under ablation (Fig. 14.1.7). At this stage the heat flow to the structure is not sufficient to cause evaporation and to affect the gaseous medium. On the other hand, since the viscosity of the melted mass is high the molten layer will have very small tangential velocities in comparison with those of the gas. For example, calculations show that the ratio of local velocities at the external boundary of the liquid phase and the gaseous phase under normal conditions of high flight velocities is $V_{xi}/V_{x\delta} \approx 5 \times 10^{-4}$. Consequently it may be assumed that the flow in the gaseous phase is independent of the presence of the molten layer. In other words, the gaseous phase behaves as a normal boundary layer. The rise in heat flow and increase in temperature lead to evaporation of some part of the molten substance. It is then that the vapor enters the gaseous phase.

While the vapor enters the gaseous phase the interaction between the liquid film of molten substance and the gaseous boundary layer has its own expression which leads to a reduction in aerodynamic heat flow to the surface and as a result to a lower heating effect. If the surface temperature approaches boiling point practically the whole of the molten layer evaporates and the maximum quantity of gas enters the gaseous phase.

This is the simplified physical scheme of the process of ablation in the

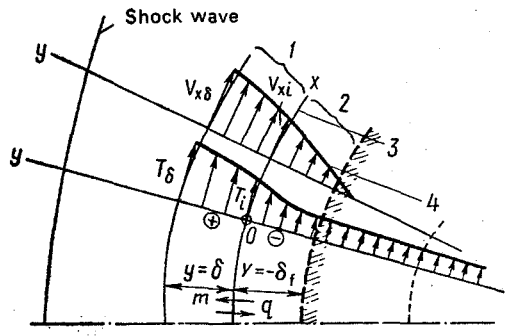

Fig. 14.1.7. Scheme of two-phase boundary layer on melting blunt surface:

1—boundary layer of gas; *2*—fluid layer; *3*—surface of separation; *4*—solid medium; $y=\delta$—thickness of gaseous phase of boundary layer; $y=-\delta_f$—thickness of fluid phase of boundary layer; m—total specific mass transfer of destroyed material; q—aerodynamic heat flow; T_i—surface temperature.

form of a two-phase boundary layer. The ablation process in reality has a very complex nature. Since the basic function of ablation is absorption of heat by mass being carried away it is important to know what this heat ablation is. As we will see, the quantity of substance carried away can be worked out for the value of the heat of ablation.

2. Determination of Heat of Ablation

2.1 Sublimation, complete evaporation or carbonization (pyrolysis)

Complete evaporation of the molten mass and sublimation (for materials that evaporate without passing through the liquid phase) are related to the particular case of ablation characterized by very high viscosity of the heat protection substance. The value of the heat of ablation so obtained will be maximum and independent of viscosity.

The physical processes during sublimation and evaporation are similar to the phenomenon of ablation with carbonization because in both cases there occurs an interaction of the gaseous products of erosion of the shield with the boundary layer. Therefore it should be possible to obtain general relations for calculation of the heat of ablation and mass transfer of heat protection shields.

Let us consider the equation of heat balance during steady ablation to find the general expression for heat ablation. The equation of heat balance characterizing an ablating mass represents the condition that the aerodynamic heat flow q_i to this mass is spent on heating and evaporating it except for the part that is radiated (q_r). Consequently

$$q_i = m_v (c_p T_i + i_v) + q_r, \qquad (14.2.1)$$

where m_v is the specific mass flow of material under erosion in kg/m^2·sec, known as the rate of transfer (ablation); T_i is the temperature of the surface in °K; c_p is the specific heat of the material in kilo·cal/kg·degree. The quantity i_v may be considered as the enthalpy of sublimation. In the case of complete evaporation it will be the enthalpy of evaporation (latent heat of evaporation). In the case of carbonization the quantity i_v represents the enthalpy of the gas.

The aerodynamic heat flow q_i participating in and absorbed during ablation, as we saw above, is less than the quantity of heat q applied to the mass in question in the absence of ablation. The effect of this heat, determining reduction in heat transfer by the quantity

$$\Delta q = q - q_i, \tag{14.2.2}$$

is expressed by this reduced heating based on injection of vapor into the boundary layer. As is shown by experiment, the quantity

$$\Delta q = q\,(1-\psi), \tag{14.2.3}$$

where parameter ψ depends on the type of boundary layer, specific flow of mass m_v, velocity of motion of body (Mach number $\mathbf{M}_\infty$) and molecular weight of vapor $\bar{\mu}_v$.

It has been found by experiment that

$$\psi = 1 - (\beta m_v/q)\,(i_0 - i_w), \tag{14.2.4}$$

where i_0 is the enthalpy of the air during isentropic stagnation; β is the coefficient of heat lost during ablation. Its values for laminar and turbulent boundary layers are determined from the expressions

$$\left.\begin{aligned} \beta_L &= N\,(29/\bar{\mu}_v)^{\bar{\alpha}}; \\ \beta_T &= \beta_L/3, \end{aligned}\right\} \tag{14.2.5}$$

where

$$\left.\begin{aligned} &0.67 \leqslant N \leqslant 0.72; \\ &0.25 \leqslant \bar{\alpha} \leqslant 0.4 \end{aligned}\right\} \tag{14.2.6}$$

according to empirical data depending on the type of shield. In particular, $N=0.68$, $\alpha=0.26$ may be assumed for glass-type materials.

In applying formula (14.2.4) it should be kept in mind that it gives satisfactory results in the interval $0.2 \leqslant \beta \leqslant 4$.

The molecular weight of vapors $\bar{\mu}_v$ of some materials like plastic and glass approximately coincide with the molecular weight of air. If we assume that $\bar{\mu}_v \approx 29$ and $N=0.68$ the coefficients determined by the expressions (14.2.5) will be $\beta_L \approx 0.7$ and $\beta_T = 0.23$ respectively.

In equation (14.2.1) where the temperature T_i can be approximately taken as equal to the temperature of evaporation the term in round brackets represents the heat of ablation. If it is determined by some means and if the quantity q_i is known the mass transfer m_v can obviously be calculated.

It is convenient in practice to use the concept of effective heat of ablation determined by the expression

$$q^* = q/m_v \text{ [kilo·cal/kg]}. \tag{14.2.7}$$

According to this expression the quantity of heat qt applied to unit surface in some time t through a conventional gaseous boundary layer during steady heating is equal to the heat flow $q^* \cdot m_v \cdot t$ absorbed by the mass of material destroyed and carried away from this surface.

Having obtained relation (14.2.4) for ψ it is possible to obtain the formula for the effective heat of ablation with the help of equations (14.2.1) through (14.2.3). For this purpose, keeping (14.2.7) in view, we will write equation (14.2.1) in the form

$$\frac{q_i}{q} = \frac{1}{q^*}(c_p T_i + i_v) + \frac{q_r}{q}. \tag{14.2.8}$$

In addition we will obtain the following relation from (14.2.2) through (14.2.4):

$$\frac{q_i}{q} = \psi = 1 - \frac{\beta}{q^*}(i_0 - i_w). \tag{14.2.9}$$

From the above relations we will have

$$q^* = \frac{c_p T_i + i_v + \beta (i_0 - i_w)}{1 - (q_r/q)}, \tag{14.2.10}$$

where the specific heat flow due to radiation, in accordance with (13.1.28), will be

$$q_r = \varepsilon \sigma T_i^4. \tag{14.2.11}$$

Experimental data facilitating the evaluation of some characteristics and of the heat of ablation have been obtained for a series of materials. Specifically, data have been obtained for such carbonizing polymerized materials as teflon $(C_2F_4)_n$. This polymer results in pyrolysis during thermal interaction as a result of which the solid mass takes on the gaseous form of monomer C_2F_2. The basic physical and thermodynamic parameters for teflon are as follows: temperature of ablation during laminar heating $T_i = 445°K$; enthalpy $i_v = 416$ kilo·cal/kg; molecular weight of vapor $\bar{\mu}_v = 100$; specific heat $c_p = 0.25$ kilo·cal/kg·degree. Substituting these data in formula (14.2.10), we find (assuming $\beta = 0.5$)

$$q^* = \frac{527 + 0.5 (i_0 - i_w)}{1 - (q_r/q)}. \tag{14.2.12}$$

The following formula, similar to (14.2.12), has been found for phenyl nylon which is used as a carbonizing thermal protection shield:

$$q^* = \frac{832 + 0.5 (i_0 - i_w)}{1 - (q_r/q)}. \tag{14.2.13}$$

The peculiarity of this plastic is that the carbon sediment remaining after

evaporation in the form of finely spread solid particles radiates intensively due to overheating.

For some materials the heat flow to the surface of the wall may increase due to combustion of the vapor diffusing in the gas layer in the oxygen of the air. As shown by experiment, this increase in the case of combustion in a laminar boundary layer will be

$$\Delta q_i = 0.21\, i_b\, (q_i/i_0)\ [\text{kilo}\cdot\text{cal/m}^2\cdot\text{sec}], \tag{14.2.14}$$

where i_b, kilo·cal/kg is the heat due to combustion for unit mass of oxygen. According to this the new quantity $q_i+\Delta q_i$ appears in (14.2.1) in place of q_i and the new equation of balance of heat takes the following form:

$$q_i+\Delta q_i = m_v\,(c_pT_i+i_v)+q_r, \tag{14.2.15}$$

or

$$\frac{q_i}{q}\left(1+\frac{\Delta q_i}{q_i}\right)=\frac{1}{q^*}\,(c_pT_i+i_v)+\frac{q_r}{q}.$$

Substituting here the value of q_i/q from (14.2.9), we get

$$q^*=\frac{c_pT_i+i_v+(1+\bar{q}_b)\,(i_0-i_w)\,\beta}{1+\bar{q}_b-(q_r/q)}, \tag{14.2.16}$$

where according to (14.2.14)

$$\bar{q}_b=\Delta q_i/q_i=0.21\,(i_b/i_0). \tag{14.2.14'}$$

Experiments have shown that under ablation teflon has the property of diffusion of vapor which burns in the boundary layer. As a result the monomer C_2F_2 becomes the compound COF_2. Combustion leads to a rise in the heat flow to the wall and consequently to a decrease in the effective heat of ablation. According to experimental data the combustion temperature for teflon is $i_b=5{,}550$ kilo·cal/kg and the corresponding expression for effective heat of ablation (14.2.16) will have the form

$$q^*=\frac{527+0.5\,[1+(1165/i_0)]\,(i_0-i_w)}{1+\,(1165/i_0)-(q_r/q)}. \tag{14.2.17}$$

2.2 Simultaneous melting and sublimation (evaporation)

It is desirable to use a composite fire-resistant material for the thermal protection shield with high effectiveness for heat of ablation and low thermal conductivity. Plastics in combination with glass, having high viscosity and low thermal conductivity, is an example of this kind of material. The special property of such glass-plastics and similar composite materials is that they first act as heat absorbing agents when exposed to a high-temperature interaction. Then the temperature of the surface rises quickly, due to the low coefficient of heat conduction, to the level at which melting and sublimation of different constituents take place simultaneously. Experiments have shown that with fiberglass one of its components, glass, melts and the other component, plastic, sublimates.

The evaporation of part of the molten mass is typical for most materials, including glass-based materials, at surface temperatures exceeding melting point. Evaporation is followed by pyrolysis of the surface layer of molten material, as a result of which an additional quantity of gas diffuses in the gaseous boundary layer. So ablation, in the most general case, is characterized by simultaneous melting and sublimation (evaporation). This peculiarity must be taken into account when determining the effective heat of ablation. If the total specific mass transfer is denoted by m the degree of sublimation (evaporation), known as the coefficient of evaporation, can be determined as the ratio $\overline{m}=m_v/m$. Accordingly the equation of heat balance, similar to (14.2.1), will be rewritten in the form

$$q_i=mc_p T_i+m_v i_v+q_r=m(c_p T_i+\overline{m}\cdot i_v)+q_r. \tag{14.2.18}$$

The effective heat of ablation will be determined by the relation

$$q^*=q/m, \tag{14.2.19}$$

and the coefficient ψ of (14.2.4), taking into account (14.2.19) and $m_v=\overline{m}m$, will be written in the form

$$\psi=1-(\beta\overline{m}m/q)\,(i_0-i_w)=1-(\beta\overline{m}/q^*)\,(i_0-i_w). \tag{14.2.20}$$

Dividing (14.2.18) by q, we get

$$\frac{q_i}{q}=\frac{1}{q^*}(c_p T_i+\overline{m}i_v)+\frac{q_r}{q}. \tag{14.2.21}$$

Combining (14.2.2), (14.2.3) and (14.2.20), we have

$$\frac{q_i}{q}=1-\frac{\beta\overline{m}}{q^*}(i_0-i_w). \tag{14.2.22}$$

From (14.2.21) and (14.2.22) the effective heat of ablation will be

$$q^*=\frac{c_p T_i+\overline{m}\,[i_v+\beta\,(i_0-i_w)]}{1-(q_r/q)}. \tag{14.2.23}$$

Here the temperature of ablation T_i, enthalpy of evaporation i_v and coefficient $\overline{m}$ are the unknowns. The temperature T_i can be taken as equal to the melting point of known constant value, to simplify calculations, with sufficient accuracy. For example, the melting point for glass is about 1,700°K. The enthalpy of evaporation i_v is usually determined experimentally. For approximate calculations of the ablation of glass-based materials it is possible to use, for example, the quantity $i_v=2{,}470$ kilo·cal/kg obtained for silicon. According to experimental data the value of $i_v=3{,}000$ kilo·cal/kg for pure quartz. The value of the coefficient $\overline{m}$ is mainly determined by the elasticity of the vapor and the viscosity of the molten component which depend on the temperature and conditions of flow-interaction.

There are other data available on the nature of variation of $\overline{m}$. For example, the coefficient $\overline{m}$ decreases with a rise in pressure or decrease in stagnation

enthalpy. As a rough estimate this coefficient can be determined as the ratio of the mass of the sublimating component to the total mass of the heat protection material. Considering "pure" sublimation, i.e. assuming $\bar{m} = 1$ we have, from (14.2.23),

$$(q^*)_{\bar{m}=1} = \frac{c_p T_i + \tilde{q}}{1 - (q_r/q)},$$

where $\tilde{q} = i_v + \beta (i_0 - i_w)$.

Accordingly for any arbitrary value $\bar{m} \neq 1$ we have

$$q^* = (q^*)_{\bar{m}=1} + (\bar{m} - 1)\, \tilde{q} \left(1 - \frac{q_r}{q}\right)^{-1}. \qquad (14.2.24)$$

From experimental data for fiberglass consisting of 30% plastic and 70% glass we have

$$\tilde{q} = 0.554\ (7430 + 5.38 \times 10^{-5}\ V_\infty^2)\ \text{kilo·cal/kg}; \qquad (14.2.25)$$

$$(q^*)_{\bar{m}=1} = 0.554\ (8580 + 5.38 \times 10^{-5}\ V_\infty^2)\ \text{kilo·cal/kg}, \qquad (14.2.26)$$

where V_∞ is the velocity in m/sec.

If the value of $\bar{m}$ is not known in advance, the series of possible values of $\bar{m} \leqslant 1$ is assumed in evaluating the process of ablation and the corresponding effective heat of ablation for different points on the trajectory can be determined. For example, the following values of $\bar{m}$ may be assumed: 1; 0.5; 0.25.

It should be borne in mind that the case of sublimation represented by formula (14.2.26) for refractory and similar materials like quartz is not realistic, i.e. it is impossible in practice to create conditions at which the equality $\bar{m} = 1$ could be achieved. The peculiarity of quartz, like other refractory material, is the high surface temperature of about 2,200–2,300°K. Consequently the effcet of radiation on the effective heat of ablation will be considerable. The rate of radiation of heat may be increased by making the material less transparent. For example, quartz becomes almost completely opaque ($\varepsilon \approx 1$) if carbon elements are added to it. Given a considerable amount of radiation of heat from the surface the effective heat of ablation, according to the formula (14.2.24), attains a somewhat higher value and mass transfer is negligibly small. In this case the surface undergoes intensive cooling by radiation and the heat transfer approaches the state of radiational equilibrium. Under these conditions the material behaves as a heat sink.

The phenomenon of complete radiational equilibrium may arise with gradual variation in a small specific heat flow (for example, for a gradually descending satellite) when equilibrium of radiational heat and heat inflow to the body is possible. In this limiting case $q^* \to \infty$ and the mass transfer tends to zero. So under the conditions of radiational equilibrium applicable to a gliding flight vehicle this material takes the role of a heat protection shield.

For the nose section of a rocket, exposed to the interaction of appreciably high heat flows for a short period of time in which the temperature does not achieve its equilibrium value, the use of an ablating material as a thermal protection shield seems to be more appropriate than the usual thermal isolation.

Along with formulas (14.2.24) through (14.2.26) we can use the empirical relation for q^* obtained from research on the ablation of a glass-based substance (containing 30% plastic and 70% glass) in the neighborhood of the point of complete stagnation under laminar flow conditions

$$q^*=\left[125+2.7\frac{i_0}{RT_{\infty g}}+178\left(\frac{\rho_{\infty H}}{\rho_{\infty g}}\right)^{1/(3+n)}\left(\frac{i_0}{RT_{\infty g}}\right)^{3.64/(3+n)}\right]\times\left(1-\frac{q_r}{q}\right)^{-1}\text{[kilo}\cdot\text{cal/kg]},\qquad(14.2.27)$$

where $RT_{\infty g}=18.8$ kilo·cal/kg for atmospheric air near sea level and the value of n for flight conditions at very high speeds may be taken as equal to 10.

2.3 Melting

Melting, like sublimation, is a limiting case of the ablation process. If the material melts but does not evaporate the boundary layer does not undergo the impact of ablating substance during mass transfer. In this case the coefficient of gas formation must be taken as $\overline{m}=0$ when determining the effective heat of ablation (14.2.23); then

$$q^*=\frac{c_p T_i}{1-(q_r/q)},\qquad(14.2.28)$$

where c_p is the specific heat of the molten material.

According to the expression (14.2.28) the heat flow, determined by the difference $q-q_r$, should be completely absorbed by the fluid having specific heat c_p, i.e.

$$q-q_r=q\cdot c_p T_i/q^*=m\cdot c_p\cdot T_i.$$

Comparing expression (14.2.28) with formulas (14.2.10) and (14.2.23), we see that the effective heat of melting is less than that during simultaneous melting and evaporation and more than that during complete evaporation (sublimation). This is supported by experimental research on the ablation of a glass-based substance. The corresponding relation for q^*, which is obtained from the empirical relation (14.2.27), maintaining the last term for the characteristic of ablation by melting, will have the following form:

$$q^*=178\left(\frac{\rho_{\infty H}}{\rho_{\infty g}}\right)^{1/(3=n)}\left(\frac{i_0}{RT_{\infty g}}\right)^{3.64/(3+n)}\times\left(1-\frac{q_r}{q}\right)^{-1}\text{[kilo}\cdot\text{cal/kg]}.\qquad(14.2.29)$$

Metals also act as ablation materials by melting. Experimental data facilitating evaluation of the effective heat of ablation have been obtained for some of them like steel and aluminum (see specialized literature).

3. Mass Transfer and Effectiveness of Thermal Protection Shield

If the effectiveness of the heat of ablation q^* is known the quantity of mass carried away in unit time, as follows from (14.2.19), will be

$$m=q/q^* \text{ [kg/m}^2\cdot\text{sec]}. \tag{14.3.1}$$

Here the specific heat flow q is calculated by the aerodynamic methods set out in Chapter 13 and the effective heat of ablation q^* can be determined from experimental data using formulas (14.2.13), (14.2.17), (14.2.24), (14.2.27), (14.2.29) for various types of local ablation, namely: melting, simultaneous melting and evaporation and sublimation (gasification).

The calculation of the average value of heat flow will be carried out on the basis of the value of q depending on the given form of blunt nose surface:

$$q_{\text{av}}=\frac{1}{\pi R_{\text{T}}^2}\int\limits_{(S)} q\,dS, \tag{14.3.2}$$

where R_T is the maximum diameter of the blunt nose section; S is the area of the surface of this section.

Mass transfer from the surface S during heating time t is

$$Q_{\text{av}}=m_{\text{av}}\cdot t\cdot S \text{ [kg]}, \tag{14.3.3}$$

where $m_{\text{av}}=q_{\text{av}}/q^*$ [kg/m$^2\cdot$sec].

Of course the calculations do not yield identical values of the quantity m_{av} for different materials. As is shown by calculation, the mass transfer for fiberglass and quartz at high speeds is less than that for a glass-based substance or teflon. However, for any final conclusion as to the effectiveness of a shield it is necessary to take into account the thickness of the layer and the corresponding weight of the heat-protection device. This calculation will be carried out by the methods of the theory of heat transfer where the temperature for destruction of the surface and the maximum permissible temperature on the inner side of the shield are taken as given. It can be seen from such calculations that the mass of the substance of a heat protection shield necessary for absorption of heat with minimum mass transfer is greater, due to the high temperature of the surface, than that for a substance exhibiting high ablation. The weight of the heat protection material is correspondingly greater. For this reason heat protection materials like fiberglass and quartz having small mass transfer have been considered in some cases of flow-interaction.

This analysis must be carried out taking into account the time variation in the flow of heat to the surface. If this change takes place fast and the process of ablation is steady the heat flow into a refractory material will be slow in comparison with the rate of ablation due to the low coefficient of

heat conductivity. From this it follows that insulation of the ablative material on the inside may not be necessary. The other case, where the heat flow to the surface takes place over a considerable period and mass transfer plays a less important part, additional refractory material may be used to perform the function of heat insulation.

The mechanical properties of the material also must be kept in view in selecting a thermal protection material. Let us take some relations facilitating, to some extent, correct evaluation for the purpose of selection [58]. The solution of this problem is connected with the determination of the required thickness of insulation to provide the desired difference in temperature between the external and internal walls. For this purpose we may use the formula

$$\delta_i = \sqrt{a\tau/\varphi}, \tag{14.3.4}$$

where δ_i is the thickness of the insulator, $a = \lambda/(c\gamma)$ is the coefficient of temperature flow (λ is the coefficient of heat conductivity, γ is the specific weight, c is the thermal capacity of the resistant material), τ is the time of heating, φ is Fourier's criterion. The weight per m^2 of the protective sheet for the required thermal insulation can be determined from the thickness and specific weight of the resistant material:

$$G_i = \delta_i \gamma = \gamma\sqrt{a\tau/\varphi}. \tag{14.3.5}$$

Since $a = \lambda/(c\gamma)$ the formula for G_i can be expressed in the form

$$G_i = \sqrt{\lambda\gamma/c}\ \sqrt{\tau/\varphi}. \tag{14.3.5'}$$

Here the quantity $\sqrt{\lambda\gamma/c}$, depending on the physical properties of the protective material, can be regarded as the criterion determining the required weight of thermal insulator under given external conditions of flow-interaction and the corresponding value of parameter $\sqrt{\tau/\varphi}$. The values of this criterion for some heat protection materials are given in Table 14.3.1. The limiting temperatures at which the use of a given thermal insulator is permissible are shown in the same table.

Table 14.3.1 lists two groups of materials: laminated plastics and porous insulations. The second group of materials have comparatively low mechanical properties and they are easily destroyed under the impact of quite weak loads. Though this group of materials have the lowest value of weight criterion it is therefore not advisable to use them as heat protection shields. From the table it may be seen that the most promising material for heat protection in the group of laminated plastic is asbestos carton, for which the weight criterion will be the lowest.

The limiting temperature for use of laminated plastics given in Table 14.3.1 corresponds to long periods of action of high temperatures (many hours). For once only short-period work (a few minutes) they can be used at

TABLE 14.3.1

Material	$\lambda \cdot 10^4$, $\frac{\text{k·cal}}{\text{m·sec·degree}}$	γ, $\frac{\text{kg}}{\text{m}^3}$	c, $\frac{\text{k·cal}}{\text{kg·deg}}$	$\sqrt{\frac{\lambda\gamma}{c}}$, $\frac{\text{kg}}{\text{m}^2\cdot\text{sec}^{1/2}}$	Limiting temperature of use, °K
Laminated plastics:					
Textolite	0.7	1,350	0.35	0.52	520
Glass textolite	0.7	1,600	0.24	0.69	570
Asbestos carton	0.44	1,000	0.20	0.47	720
Ftoroplast	0.59	2,200	0.25	0.72	670
Porous insulations:					
Porous asbestos	0.22	100	0.20	0.10	870
Mineral strap	0.18	150	0.22	0.11	870
Fiberglass (mats)	0.26	120	0.20	0.12	720
Foam glass	0.26	200	0.20	0.16	770

very high temperatures of flow of the order of thousands of degrees. The external layer will then be damaged by erosion and sublimation with reduction in the thickness of the plate.

4. Example for Calculation of Thickness of Heat-Protection Shield

Let us perform the approximate calculation of the required thickness of a heat-resistant covering under an unsteady regime of flow over a vehicle to be launched in the form of a sphere of diameter 2 m and weight 1,250 kg intended to re-enter the earth's atmosphere at the second cosmic speed at an angle of 30° [57].

This kind of calculation is connected with determination of some parameters of the external flow during motion along the trajectory of the lofted vehicle. In particular, the stagnation temperature T_0' behind the shock wave and the equilibrium radiational temperature T_e of the air over the external surface will have to be found. The Mach number M_∞ and flight altitude H are the given parameters for these calculations. Here the adiabatic wall temperature T_r achieved along the trajectory is approximately equal to T_0' (excluding the initial layer of atmosphere of high rarefaction). The data for the calculation are illustrated by the curves in Fig. 14.4.1.

According to these data the flight time τ during which the heat flow acts on the lofted vehicle is 26 seconds. The equilibrium wall temperature averaged over this period of time, according to the data from Fig. 14.4.1, is

$$T_{eav} = \sum_{i=1}^{n} T_{ei} \, (\Delta\tau_i/\tau) = 1600°\text{K}.$$

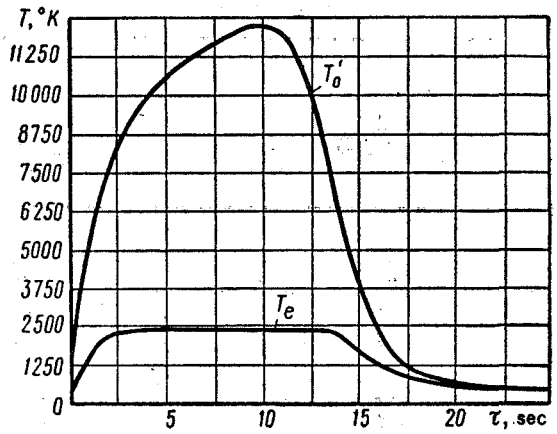

Fig. 14.4.1. Graph of temperature worked out for conditions of entry of flight vehicle in dense layers of atmosphere.

Assuming atmospheric temperature equal to 293°K, the rise in temperature on the surface of the wall will be

$$\Delta T_w = 1600 - 293 = 1307°K.$$

Let us assume that the temperature on the inside surface of a heat protection shield should not exceed 373°K. Then the rise in temperature on this surface

$$\Delta T_p = 373 - 293 = 80°K.$$

From these data we will find the relative temperature gradient across the thickness of the covering

$$\varepsilon_p = 1 - \frac{\Delta T_p}{\Delta T_w} = 1 - \frac{80}{1307} \approx 0.94.$$

Let us take the average adiabatic wall temperature with time (see Fig. 14.4.1):

$$T_{rav} = \sum_{i=1}^{n} T_{ri} \frac{\Delta \tau_i}{\tau} = 5870°K.$$

Now, using formula (13.5.8) we get the average value of the coefficient of heat transfer

$$\alpha_{av} = \frac{\varepsilon \sigma T_{eav}^4}{T_{rav} - T_{eav}} \approx \frac{0.8 \times 13.6 \times 10^{-12} \times 1600^4}{5870 - 1600} = 0.0168 \frac{\text{k.cal}}{\text{m}^2 \cdot \text{sec} \cdot \text{degree}},$$

where the coefficient of radiation of the surface is taken to be equal to $\varepsilon = 0.8$.

Having the values of ε_p and α_{av}, it is now possible to calculate the thickness of the heat-resistant shield. Let us take glass-textolite as the material of the shield (see Table 14.3.1). This problem is solved by the method of

iterations. A value of thickness $\delta_1 = 10$ mm is first assumed and the quantity known as Bio's criterion in the theory of heat conductivity is worked out:

$$\beta = a_{av}\,\delta_1/\lambda = 0.0168 \times 0.01/7 \times 10^{-5} = 2.4.$$

From the curves in Fig. 14.4.2 we have $\beta = 2.4$ and $\varepsilon_p = 0.94$ and Fourier's criterion $\varphi = 0.125$. Then from formula (14.3.4) the thickness will be

$$\delta_1 = \sqrt{2 \times 10^{-7} \times 26/0.125} = 6.45 \text{ mm}.$$

According to Table 14.3.1 the coefficient of temperature flow $a = \lambda/c\gamma \approx 2 \times 10^{-7}$ m^2/sec. After obtaining the value of δ_1 Bio's criterion can be worked out as a second approximation:

$$\beta = 0.0168 \times 0.00645/7 \times 10^{-5} = 1.55.$$

From the values of $\beta = 1.55$ and $\varepsilon_p = 0.94$ Fourier's criterion is improved from the curve in Fig. 14.4.2: $\varphi = 0.127$. According to this value the new thickness of covering

$$\delta_1 = \sqrt{2 \times 10^{-7} \times 26/0.127} = 6.4 \text{ mm}.$$

In final selection of the thickness a margin is usually allowed over the calculated value. Here the excess thickness is given by the coefficient $f \approx 1.3$ to 1.6. Taking $f = 1.5$, we get $\delta_1 = 1.5 \times 6.4 = 9.6$ mm. From the calculation it may be seen that the effect of β on the final result is insignificant. Therefore we are completely justified in determining the value of a_{av} with less accuracy. Accordingly the quantity a_{av} was determined approximately on the basis of an assumed equality between the aerodynamic and radiational heat flows which does not exist in practice. So the above calculation of the thickness of a heat protection shield is based on the assumption that the temperature of the surface is equal to the instantaneous radiational temperature. Actually the temperature of this surface and thickness δ_1 will be higher than their calculated values. However, experiments show that this difference is small—about 5%.

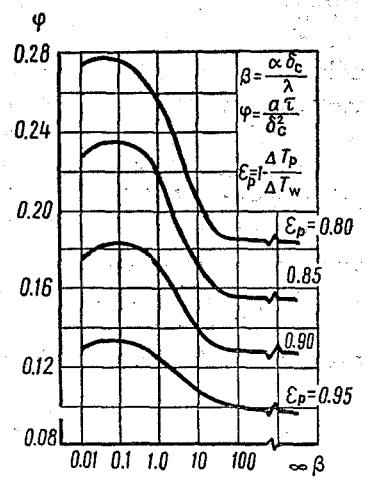

Fig. 14.4.2 Graph for determination of Fourier's criterion.

The thickness of the shield has been calculated without allowance for ablation of the heat protection material and mechanical destruction of the thermal insulating structure. To determine the thickness of the part that will be carried away as a result of the ablation of glass-textolite the following procedure may be adopted: After calculating the heat of ablation q^* from formula (14.2.13) for the actual values of q and q_r the mass of the heat protection substance carried away can be obtained from

(14.3.2). Then its thickness can be determined on the basis of the value of m, (14.3.1). In these calculations q may be replaced by q_{av} specific weight and surface area of the shield.

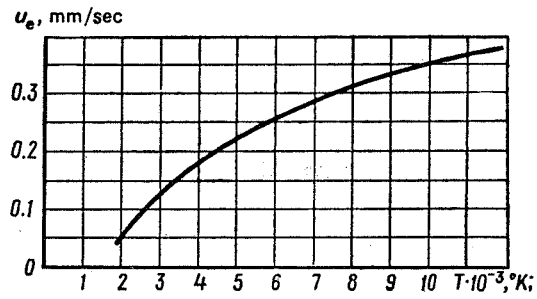

Fig. 14.4.3. Graph of rate of transfer of (carbon monoxide) heat protection material.

The thickness of the shield and its weight can also be determined with the help of the curves in Fig. 14.4.3, which represent the empirical relation between the rate of mass transfer of glass-textolite and the temperature [59]. Using this relation the thickness of the destructible layer of heat protection material at different points of trajectory can be determined. We use the adiabatic temperature of the wall T_r in place of temperature T to determine the rate of erosion u_e. The results for calculation of the thickness of destructible material are presented in Table 14.4.1.

From Table 14.4.1 it may be seen that the erosion of the heat protection shield goes on diminishing during the given flight time (26 sec), which can be understood from the reduction in the speed of the lofted vehicle during motion through the dense layers of atmosphere. As a result the temperature T_r falls to 950°K, at which ablation does not occur.

According to the data in Table 14.4.1 the thickness of ablating shield reaches the following value by the end of the flight:

$$\delta_e = \sum_{n=1}^{11} \delta_{en} = 4.92 \text{ mm}.$$

As shown by experiment, mechanical destruction of the shield takes place along with the ablation. According to experimental data [59] the thickness of the layer lost by mechanical destruction $\delta_{md} \approx 30$ to 40% of the thickness of the material eroded due to ablation δ_e. Taking $\delta_{md} = 0.4\delta_e \approx 2$ mm for the case in question, we get the thickness for the destructible part of the shield $\delta_e + \delta_{md} = 6.92$ mm. Adjusting for the accepted safety factor $f = 1.5$, this thickness will be $\delta_2 = 1.5 \times 6.92 = 10.4$ mm.

Therefore the total thickness of heat protection material will be

$$\delta_c = \delta_1 + \delta_2 = 9.6 \text{ mm} + 10.4 \text{ mm} = 20 \text{ mm}.$$

TABLE 14.4.1

Number of points on trajectory, n	$\Delta\tau$, sec	T_r, °K	u_e, mm/sec	δ_e, mm
1	2	4,370	0.185	0.37
2	2	9,000	0.309	0.61
3	2	10,500	0.340	0.64
4	2	11,500	0.370	0.74
5	2	12,000	0.377	0.75
6	2	11,800	0.370	0.74
7	1	10,000	0.340	0.34
8	1	7,500	0.309	0.31
9	1	5,000	0.220	0.22
10	1	3,100	0.170	0.17
11	1	1,800	0.030	0.03
12	2	950	—	—
13	3	600	—	—
$\sum_{n=1}^{11}$	17	—	—	4.92

Let us assume that protective material of this thickness is used on the leading part of the spherical vehicle, whose surface is $S=(1/2)4\pi r^2=6.28$ m^2. Then the weight of the shield is

$$W_c=\delta_c\,\gamma S=20\times 1.6\times 10^{-6}\times 6.28\times 10^6=201\text{ kg},$$

which is about 16% of the weight of the vehicle.

The calculated results obtained here should be taken as an estimate for approximate determination of the thickness and weight of a heat protection shield. These results could be improved with the help of more accurate calculations and experimental aids.

15

AERODYNAMICS OF RAREFIED MEDIUM

1. Limits of Applicability of Theory of Motion of a Continuous Medium

Experimental data on the flow-interaction of bodies obtained for the conditions of a rarefied medium differ considerably from the values of force and moment characteristics and the parameters of friction and heat transfer calculated from the gas dynamic relations for a continuous medium. This difference is explained by the structure of these relations, which correspond to the hypothesis of a dense medium.

For rarefied atmosphere this hypothesis is not valid and we have to use the kinetic theory, investigating the dynamics of gas with the help of molecular mechanics.

The principal conclusions of this theory are based on the concept of a discrete system of structure according to which the medium consists of molecules moving along fairly long free paths and colliding among themselves. We will not examine the kinetic theory of gases in detail but will discuss the data necessary for an understanding of the physical phenomena and aerodynamic calculations related to flights in a rarefied medium.

1.1 Molecular free path length

First we must consider the question of the limits of applicability of the theoretical relations based on the assumption of a continuous gaseous medium. Here we must note the limits of applicability are conditional because it is not possible to cite the exact altitude in the atmosphere above which only molecular theory can be applied.

To establish these limits it is necessary to determine the length of the molecular free path. From physical observations it is clear that the shorter this length the closer the medium is to the hypothetical continuous one. The flow of such a medium is characterized by a large number of collisions between molecules resulting in a shorter relaxation time in the presence of disturbances, i.e. the time taken to establish an equilibrium of energy level of the colliding molecules.

The methods of statistical physics establish some mean path traveled by a molecule until it collides. This is known as the mean length of free path. This length

$$l=\bar{c}\cdot t, \tag{15.1.1}$$

where $\bar{c}$ is the average velocity of chaotic motion of molecules [see (15.2.4)], t is the time interval between two collisions of a molecule determined by the expression $t=1/n$ in which n is the number of collisions in unit time given by $n=NA\,\bar{c}$ (where N is the number of molecules per unit volume, A is the area of the cross section of a molecule). In this way

$$l=1/NA. \tag{15.1.1'}$$

From example, $N=2.69\times 10^{19}$ cm^{-3}, $A=10^{-15}$ cm^2 for air under normal conditions and consequently free path length $l=4\times 10^{-5}$ cm. From formula (15.1.1') it follows that the mean length of free path increases with a reduction in density. Therefore it increases with an increase in altitude and may be considerably greater than the size of the flight vehicle.

Formula (15.1.1') is not convenient for practical application because the area of the cross section of a molecule cannot be determined by direct measurement. It is better to use the relation for l which can be obtained from formula (1.1.2) for the kinetic theory of gases determining the coefficient of dynamic viscosity. Putting the value from relation (15.2.8') in place of $\bar{c}$, which gives the average velocity through sonic velocity, we get

$$l=1.255\,\nu\sqrt{k/a}, \tag{15.1.2}$$

where k is the adiabatic index; ν is the coefficient of kinematic viscosity.

1.2 Regimes of gas flow

Flow regimes are determined on the basis of the degree of rarefaction of the gas, which is understood as the ratio of mean length of free path of the molecule to some characteristic length of the flow region in question.

The formulation of the above regimes and the parameters used to estimate them can be obtained if the flow between two plates at a small distance δ is studied. The space between these plates is filled with gas and one of them moves parallel to the other at some velocity V. In estimating the degree of rarefaction and the corresponding flow regime it is useful to compare the mean molecular length of free path l and the distance δ between the plates, i.e. to find the ratio

$$\frac{l}{\delta}=1.255\,\frac{\nu\sqrt{k}}{V\delta}\cdot\frac{V}{a}=1.255\sqrt{k}\,\frac{\mathbf{M}}{\mathbf{Re}}, \tag{15.1.3}$$

where $\mathbf{Re}=V\delta/\nu$ is the Reynolds number.

The parameter l/δ is called the Knudsen number. It is denoted by $\mathbf{Kn}=l/\delta$. If $\mathbf{Kn}\leqslant 0.01$ the gas is taken as a continuous medium. In such a medium a disturbance due to collision with the wall is transferred to all the molecules

practically instantaneously as a result of the small mean length of free path. Therefore the assumption of a continuous medium is valid during investigation of such flows. If the mean length of free path is larger than the distance between the walls and the Knudsen number $\mathbf{Kn} \geqslant 10$ the gas has to be considered as highly rarefied and the assumption of a continuous medium seems to be invalid. In such a medium the usual concept of the Reynolds number **Re** as a parameter reflecting the ratio of inertial force to viscous force does not make sense because collisions of particles are rare and hence viscosity does not exist. In line with the above discussion it is necessary to consider the impact reaction of particles on a body together with the flow-interaction of a continuous medium in determining the forces acting and the heat flows. Both of these cases reflect two characteristic flow regimes. The first represents a regime of continuous flow and the second a regime of free molecular flow.

It is accepted that the number of molecules in an elementary volume of free molecular flow is sufficient to determine the macroscopic gas properties in spite of high rarefaction and a negligibly small number of collisions. For example, at an altitude of more than 150 km the molecular length of free path is equal to 3 m, which indicates a highly rarefied condition of air. The number of molecules in a cubic centimeter is even then quite large, about 1.5×10^{12}. For this rarefied medium the pressure and mass density may be worked out as the average values in a given volume. The flow properties of this medium are determined on the basis of Maxwell's law for distribution of velocities of molecules. Hence the forces of interaction of molecules on the surface of a moving body can be obtained by application of this law.

We also have the intermediate regime ($1 \leqslant \mathbf{Kn} \leqslant 10$) and the flow regime with slip ($0.01 \leqslant \mathbf{Kn} \leqslant 1$) between the regimes of continuous and free molecular flows. The intermediate regime is characterized by the condition that there are the same number of collisions of molecules with the wall and with one another. Conditions corresponding to this regime arise during flight at altitudes of about 100 km. Collisions between molecules play an important part in a regime with the gradient found at altitudes a little less than 100 km. But the molecular mean length of path should not be neglected in spite of being small compared to the linear dimension δ.

The difference between the two flow regimes is reflected in the unequal velocity profiles between the two parallel plates. In a continuous flow the

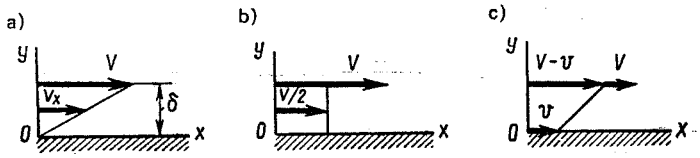

Fig. 15.1.1. Effect of flow regime on nature of variation of gas velocity past wall: *a*—continuous flow; *b*—free molecular flow; *c*—flow with slip.

gas particles attain the speed of plate V and the corresponding momentum after colliding with it (Fig. 15.1.1, a). Here the momentum transferred to the neighboring particles is reduced due to friction, as a result of which their speed is also reduced, becoming zero on the surface of the fixed plate.

In a free molecular flow (Fig. 15.1.1, b) the particles do not change momentum across the thickness after colliding with the wall because they do not collide with other molecules during their movement. As a result the velocity component perpendicular to the plates remains "zero". In the case of the diffusion phenomenon the velocity of a molecule near the upper moving plate is V and that of a molecule near the lower immovable plate is equal to zero. Consequently the average velocity of molecules between the plates is equal to $V/2$.

From the above discussion it is clear that the concept of a boundary layer is lost in a free molecular flow over a body because the flow near the surface has the same velocity as at some distance from it (it is the same as the condition at the external surface of the boundary layer in the usual sense).

The velocity profile with slip (Fig. 15.1.1, c) is found in the intermediate regime. The moving plate transfers momentum to the particles corresponding to the velocity of motion V as in the case of a continuous medium. Here the particles reflected from the plate collide with other particles without reaching the opposite wall and in the process change velocity. This is explained by the condition that the molecular length of free path is of the order of distance δ. The variation in this speed will be continuous between the plates and the velocity profile, in this form, seems to fall between that for a continuous flow and that for a molecular free flow. On the lower plate the molecules kind of crawl around relative to the surface at a speed v and their speed near the upper plate will obviously be equal to the difference $V-v$.

The name of "flow with slip" can be understood from this discussion. For this kind of flow over a body the gas does not "adhere" to the surface and achieves some velocity other than zero but less than that at the external limit of the boundary layer.

Hence there exists discontinuity in velocity between the gas and the wall in the presence of slip near the boundary. The velocity gradient across the layer will be different from zero near the wall. This shows that there still exists a boundary layer in a somewhat rarefied gas moving with slip. For this reason motion near the surface is not given by Maxwell's law and it is possible to use the general equations of a viscous compressible gas with heat conductivity. However, these equations must be modified to account for more general boundary conditions taking into account possible discontinuity in velocity, temperature and pressure on the surface. Here what kind of flow regime we have is determined from the relation between the local values of **M** and **Re** according to eq. (15.1.3). If the distance between the plates is of the order of the thickness of a laminar boundary layer the Reynolds number $\mathbf{Re}=V\delta/\nu$

can be changed to the parameter $\mathbf{Re}_L = \mathbf{Re}\,(L/\delta)$. Replacing the ratio δ/L therein by formula (12.3.19″) in which $\bar{x}=1$ (the trailing edge of a plate, for example) and inserting this in expression (15.1.3), we get the relation for Knudsen's parameter

$$\mathbf{Kn} = l/\delta = 0.264\sqrt{k}\,(\mathbf{M}/\sqrt{\mathbf{Re}_L}). \qquad (15.1.4)$$

This relation is represented graphically in Fig. 15.1.2 for different flow regimes, where the curves are drawn without allowance for the effect of possible physico-chemical changes in the air on the molecular mean length of path. Here it should be borne in mind that dissociation is accompanied by an increase in the number of particles resulting in reduction of their molecular mean length of path.

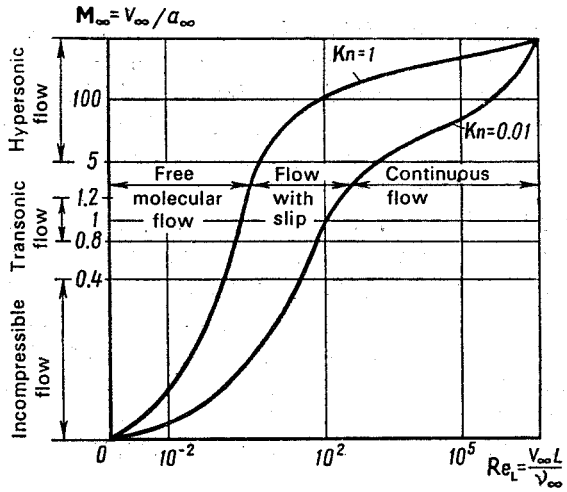

Fig. 15.1.2. Curves characterizing various regimes of gas flow.

The curves in Fig. 15.1.2, strictly speaking, are for flows of undisturbed gas. However, as shown by experiment, they can be used to study the flow past the body under flow-interaction if the local values of M and Re are used. It is found that at a distance from the nose of a body of revolution, where the effect of a shock wave is small, there may exist a flow with slip or free molecular flow even at low altitudes due to expansion of the flow. At the same time the compression near the nose behind the shock wave may result in the formation of a continuous medium even when the flight is at high altitudes. This explains why we must take the Knudsen's number based on local gas parameters when using the formula (15.1.4). In determining this number it is necessary to select the characteristic linear dimension δ. Since the evaluation of an expected flow regime is of approximate nature the quantity δ may be conditionally taken as the boundary layer thickness calculated on the basis of the formulas for a continuous medium.

2. Pressure and Friction in Free Molecular Flow

2.1 Scheme of interaction of molecules with wall

Investigation of the motion of a gas near a surface is connected with the solution of equations of motion under given boundary conditions imposed on this motion. In particular, the condition of unseparated flow, as the form of interaction of this surface and the gas medium, is the boundary condition when we are studying the flow-interaction of a surface and a continuous medium. The flow-interaction is found to be more complicated during free molecular flow. As a result its mechanism is not yet completely understood and it happens to be the subject of intensive research.

A series of hypothetical schemes of interaction between the molecules and the wall are proposed in the theory of free molecular flow. Let us consider the schemes of two critical types of interaction, namely "mirror reflection" and "reflection by diffusion." We will also touch on intermediate schemes, assuming that an interaction representing the combination of the above two limiting types of reflection will be nearer to reality.

Mirror reflection: The scheme of mirror molecular reflection is realized if the surface is very smooth and is inclined at a small angle of attack. According to this scheme the particles arriving at the wall are reflected from it at an angle equal to the angle of attack after collision (Fig. 15.2.1, a). The molecules in this scheme behave like absolutely elastic balls. During mirror reflections the absolute values of velocity components are not changed. Here the component tangential to the surface does not change its sign while the normal component changes its sign. During this ideal interaction of particles with a wall frictional forces in the conventional sense are absent. Experiments have shown that even carefully planed surfaces are not smooth enough for the scheme of mirror reflection to be completely realized. In practice at least a small fraction of the molecules of the order of a few per cent are reflected according to this scheme.

Reflection by diffusion: In reflection by diffusion (Fig. 15.2.1, b) it is assumed

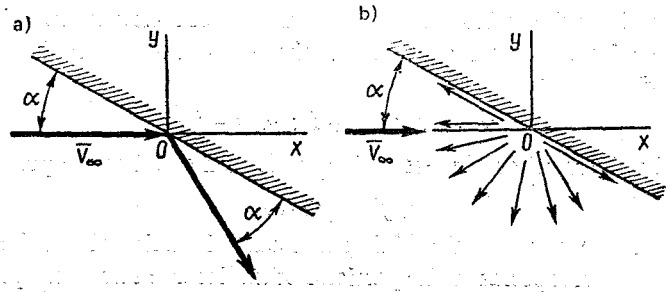

Fig. 15.2.1. Scheme of interaction of molecules with wall:
a—mirror reflection; *b*—diffused reflection.

that the surface is rough and full of cracks. The depth of the rough projections and width of the cracks must be of the same dimensions as the cross section of the molecules. After collision the molecules falling into cracks or between the projections are not in practice completely absorbed by the wall so that their impulse and energy are transferred to the wall. They are reflected from it in some arbitrary direction with some velocity after a lapse of some time interval. Here each direction followed by the particles may have equal probability. If none of the molecules reflected by diffusion attains the direction of motion we have a condition where they do not create tangential stress. Since the real surface always differs from an ideally smooth surface the majority of molecules interact according to the scheme of diffused reflection.

2.2 Mass transfer

Let us study some characteristics of free molecular flow past a body [34]. We will assume that the molecules are reflected by diffusion, where the temperature of the reflected particles is equal to some value T_r, differing in general from the wall temperature T_w and from the gas temperature T_i.

First of all let us take the expression for mass transfer. Let the velocity components of a molecule be

$$u=\bar{u}+U,\ v=\bar{v}+V,\ w=\bar{w}+W.$$

The first terms on the right side of these expressions are the velocity components of $\bar{V}_\infty$ of the mass (uniform) motion of a gas against the wall, which can be determined from the expression

$$\bar{V}_\infty^2=\bar{u}^2+\bar{v}^2+\bar{w}^2.$$

The second terms are the components of velocity c for heat flow (velocity of molecules against uniform motion of gas). The square of this velocity will be

$$c^2=U^2+V^2+W^2. \tag{15.2.1}$$

We assume that the y axis, to which component v corresponds, is directed along the normal to the surface at a given point.

We are interested in the transfer of molecules to the surface of the body, which depends on the number of colliding molecules contained in unit volume. If the molecules are moving with a velocity whose magnitude lies within the intervals of

$$u,\ u+du;\ v,\ v+dv;\ w,\ w+dw,$$

respectively, the number of these molecules is then equal to the product

$$n_i\cdot f\cdot du\cdot dv\cdot dw,$$

in which n_i is the number of colliding molecules in unit volume (hereinafter the index "i" corresponds to the particles of undisturbed flow, the parameters of which are T_∞, p_∞, ρ_∞, etc.); f is the function for the distribution of molecules known as Maxwell's distribution function.

In kinetic theory this distribution function is determined by the exponential relation

$$f=(\pi c_m^2)^{-3/2} e^{-c^2/c_m^2}, \tag{15.2.2}$$

where the quantity c_m is related to the average velocity $\bar{c}$ of chaotic motion by the equation

$$c_m=\bar{c}\sqrt{\pi/4}. \tag{15.2.3}$$

It is known as the maximum possible velocity of a molecule. According to the kinetic theory of gases

$$\bar{c}=2\sqrt{\frac{2RT}{\pi}}. \tag{15.2.4}$$

This value represents the average velocity of the chaotic motion of molecules.

The distribution function f deals only with the disorderly motion of molecules. It depends on the velocity of motion c and, as can be seen from (15.2.3), on the average velocity $\bar{c}$ which determines the internal energy of unit mass gas by the formula $(1/2)\overline{c^2}$. In the general case both $\bar{c}$ and c depend on the coordinates and time. However, if we take the case of uniform distribution of velocities, which is often found in practice, the distribution function f will be independent of time t. Here the number of gas molecules that belong to the elementary velocity space $dudvdw$ in each given element of volume $\tau=dxdydz$ does not change as a result of collisions. This state of a gas is defined as the state of local Maxwell equilibrium.

Let us consider the concept of mean square velocity $\overline{c^2}$ for disorderly motion, determined from the condition

$$\frac{\overline{c^2}}{3}=\overline{U^2}=\overline{V^2}=\overline{W^2}, \tag{15.2.5}$$

where $\overline{U}$, $\overline{V}$, $\overline{W}$ are average values of components of velocity for disorderly motion. According to the kinetic theory of gases the quantity $\overline{c^2}$ is found from the expression

$$\overline{c^2}=3RT. \tag{15.2.6}$$

Hence, using formula (15.2.4) for $\bar{c}$ we obtain

$$\sqrt{\overline{c^2}}=\frac{\bar{c}}{2}\sqrt{\frac{3\pi}{2}}=\sqrt{3RT}=c_m\sqrt{\frac{3}{2}}, \tag{15.2.7}$$

i.e.

$$\sqrt{\overline{c^2}}=1.086\,\bar{c}=1.225\,\bar{c}_m. \tag{15.2.8}$$

The expression governing the relation between $\bar{c}$, $\sqrt{\overline{c^2}}$ and sonic velocity a is given by

$$a=\sqrt{kRT}=\bar{c}\sqrt{\frac{\pi k}{8}}=\sqrt{\overline{c^2}}\sqrt{\frac{k}{3}}. \tag{15.2.8'}$$

From this it follows that average molecular velocities are of the same order as the speed of sound.

The distribution function f can be determined with the help of the graph (Fig. 15.2.2), which shows the relation of the quantity

$$B=f(\pi c_m^2)^{3/2}(c^2/\bar{c}^2)$$

as a function of parameter $c/\sqrt{\bar{c}^2}$. The relative quantities $c_m/\sqrt{\bar{c}^2}$ and $\bar{c}/\sqrt{\bar{c}^2}$ are also shown.

The proportion of the colliding molecules in unit volume that collide with the unit surface in one second is equal to

$$n_i\, v f\, du\, dv\, dw.$$

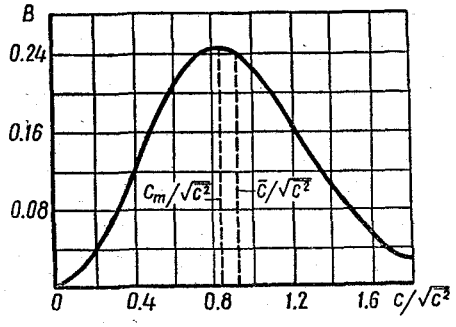

Fig. 15.2.2. Function of Maxwell's distribution.

So in this case we are considering the molecules crossing the surface and lying in the demarcated volume with unit base area and height equal to the vertical component of velocity v. This vertical component of velocity lies in the range of $\infty > v > 0$. The particles with velocity component $v < 0$ will not reach this elemental area. The total number of molecules N_i colliding with the unit surface in one second can be obtained by integrating with respect to all possible velocities $-\infty < u < \infty$, $0 < v < \infty$, $-\infty < w < \infty$, i.e.

$$N_i=\int_{-\infty}^{\infty} du \int_{0}^{\infty} v\,dv \int_{-\infty}^{\infty} n_i f\, dw. \tag{15.2.9}$$

Using the expressions (15.2.2) for f and (15.2.1) for c^2 in the above equation, we get

$$N_i=n_i(\pi c_{mi}^2)^{-\frac{3}{2}} \int_{-\infty}^{\infty} e^{-\frac{1}{2}H_1^2}\, du \int_{0}^{\infty} v e^{-\frac{1}{2}H_2^2}\, dv \int_{-\infty}^{\infty} e^{-\frac{1}{2}H_3^2}\, dw, \tag{15.2.9'}$$

where

$$\left.\begin{aligned} u&=\bar{u}+U=\bar{u}+\frac{c_{mi}}{\sqrt{2}}H_1,\\ v&=\bar{v}+V=\bar{v}+\frac{c_{mi}}{\sqrt{2}}H_2,\\ w&=\bar{w}+W=\bar{w}+\frac{c_{mi}}{\sqrt{2}}H_3;\\ \frac{H_1}{\sqrt{2}}&=\frac{U}{c_{mi}},\ \frac{H_2}{\sqrt{2}}=\frac{V}{c_{mi}},\ \frac{H_3}{\sqrt{2}}=\frac{W}{c_{mi}}. \end{aligned}\right\} \tag{15.2.10}$$

We will write the first integral in (15.2.9′) using (15.2.10) (the third integral will be similar) in the following way:

$$\int_{-\infty}^{\infty} e^{-\frac{1}{2}H_1^2}\,du = c_{mi}\int_{-\infty}^{\infty} e^{-\frac{1}{2}H_1^2}\,d\left(\frac{H_1}{\sqrt{2}}\right).$$

The integral on the right side of this expression is the well-known Eüler-Puasson integral:

$$\int_{-\infty}^{\infty} e^{-\frac{1}{2}H_1^2}\,d\left(\frac{H_1}{\sqrt{2}}\right)=2\int_{0}^{\infty} e^{-\frac{1}{2}H_1^2}\,d\left(\frac{H_1}{\sqrt{2}}\right)=\sqrt{\pi}. \qquad (15.2.11)$$

Consequently

$$\int_{-\infty}^{\infty} e^{-\frac{1}{2}H_1^2}\,du=\int_{-\infty}^{\infty} e^{-\frac{1}{2}H_3^2}\,dw=c_{mi}\sqrt{\pi}\,. \qquad (15.2.11')$$

The second integral in (15.2.9′) can be expressed in the form

$$\int_{0}^{\infty} ve^{-\frac{1}{2}H_2^2}\,dv=\int_{-\bar{v}}^{\infty}(\bar{v}+V)\,e^{-\frac{1}{2}H_2^2}\,dV$$

$$=c_{mi}\int_{-\bar{v}/c_{mi}}^{\infty}\left(\bar{v}+\frac{H_2}{\sqrt{2}}c_{mi}\right)e^{-\frac{1}{2}H_2^2}\,d\left(\frac{H_2}{\sqrt{2}}\right)$$

$$=c_{mi}^2\int_{-\bar{x}}^{\infty}(\bar{x}+y)\,e^{-y^2}\,dy, \qquad (15.2.12)$$

where we substituted

$$\bar{x}=\bar{v}/c_{mi},\ y=H_2/\sqrt{2}. \qquad (15.2.13)$$

Integrating (15.2.12), we find

$$\int_{0}^{\infty} ve^{-\frac{1}{2}H_2^2}\,dv=\frac{c_{mi}^2}{2}\,e^{-\bar{x}^2}+c_{mi}^2\,\bar{x}\int_{-\bar{x}}^{\infty} e^{-y^2}\,dy. \qquad (15.2.12')$$

The integral on the right side of (15.2.12′) will be represented in the form

$$\int_{-\bar{x}}^{\infty} e^{-y^2}\,dy=-\int_{0}^{-\bar{x}} e^{-y^2}\,dy+\int_{0}^{\infty} e^{-y^2}\,dy.$$

According to (15.2.11) the second integral of the last expression will be

$$\int_{0}^{\infty} e^{-y^2}\,dy=\frac{\sqrt{\pi}}{2}. \qquad (15.2.14)$$

Let us introduce the new variable $y=-z$ to determine the first integral of the same expression, so that

$$-\int_0^{-\bar{x}} e^{-y^2}\,dy=\int_0^{\bar{x}} e^{-z^2}\,dz.$$

The integral on the right side of this expression can be calculated with the help of the special function

$$\operatorname{erf}\bar{x}=\frac{2}{\sqrt{\pi}}\int_0^{\bar{x}} e^{-z^2}\,dz, \tag{15.2.15}$$

known as the error function, for which mathematical tables have been drawn up.

Taking into account (15.2.14) and (15.2.15), the relation (15.2.12′) will be written in the form

$$\int_0^{\infty} ve^{-\frac{1}{2}H_2^2}\,dv=\frac{c_{mi}^2}{2}[e^{-\bar{x}^2}+\bar{x}\sqrt{\pi}\,(1+\operatorname{erf}\bar{x})]. \tag{15.2.16}$$

Now keeping (15.2.11′) and (15.2.16) in mind the following relation can be written for the total number of molecules (15.2.9′):

$$N_i=\frac{n_i c_{mi}}{2\sqrt{\pi}}[e^{-\bar{x}^2}+\bar{x}\sqrt{\pi}\,(1+\operatorname{erf}\bar{x})]. \tag{15.2.17}$$

Since

$$c_{mi}=\sqrt{2RT_i}, \tag{15.2.18}$$

according to (15.2.7), we have

$$N_i=n_i\sqrt{\frac{RT_i}{2\pi}}[e^{-\bar{x}^2}+\bar{x}\sqrt{\pi}\,(1+\operatorname{erf}\bar{x})]. \tag{15.2.17′}$$

The product RT_i appearing in formula (15.2.18) is connected with sonic velocity by the relation

$$a_i=\sqrt{kRT_i}. \tag{15.2.19}$$

As may be seen from (15.2.17′), the number of colliding molecules is determined by the value of parameter $\bar{x}$ which corresponds to the given point on the surface. If c_{mi} in this parameter $\bar{x}$ is expressed through sonic velocity we get $\bar{x}=(\bar{v}/a_i)\sqrt{k/2}$. Then, taking β as the angle between the velocity vector $\bar{V}_\infty$ and the tangent to the surface at a given point (Fig. 15.2.3), we get

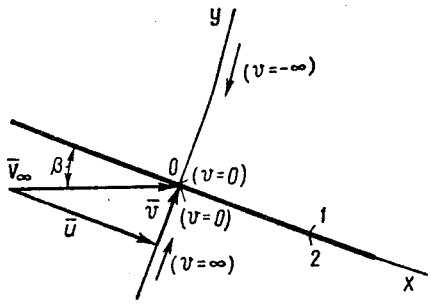

Fig. 15.2.3. Free molecular flow near plane surface:
1—upper surface; *2*—lower surface.

$$\left.\begin{aligned}\bar{x}&=\sin\beta\,\frac{V_\infty}{a_i}\sqrt{\frac{k}{2}}=\bar{x}_\infty\sin\beta,\\ \bar{x}_\infty&=\frac{V_\infty}{a_i}\sqrt{\frac{k}{2}}=\mathrm{M}_\infty\sqrt{\frac{k}{2}}.\end{aligned}\right\} \tag{15.2.20}$$

Formula (15.2.17′) is obtained for the conditions of flow on the lower part of the surface. The limits of variation in the second integral of (15.2.9′), i.e. $0<v<\infty$, correspond to these conditions. If the upper side of the surface is examined the equation of mass transfer will be different because the limits of variation in the given integral will be $-\infty<v<0$ according to Fig. 15.2.3. Keeping this in view, we can write the following expression for the upper surface:

$$N_i=-n_i(\pi c_{mi}^2)^{-\frac{3}{2}}\int_{-\infty}^{\infty}e^{-\frac{1}{2}H_1^2}du\int_{-\infty}^{0}ve^{-\frac{1}{2}H_2^2}dv\int_{-\infty}^{\infty}e^{-\frac{1}{2}H_3^2}dw. \tag{15.2.21}$$

Here the first and third integrals are determined by the value of (15.2.11′). The second integral may be expressed in the following form by analogy with (15.2.12):

$$\int_{-\infty}^{0}ve^{-\frac{1}{2}H_2^2}dv=c_{mi}^2\int_{-\infty}^{-\bar{x}}(\bar{x}+y)\,e^{-y^2}\,dy=-\frac{1}{2}c_{mi}^2\,e^{-\bar{x}^2}+c_{mi}^2\,\bar{x}\int_{-\infty}^{-\bar{x}}e^{-y^2}\,dy.$$

The integral on the right side of this expression will be

$$\int_{-\infty}^{-\bar{x}}e^{-y^2}\,dy=\int_{0}^{-\bar{x}}e^{-y^2}\,dy+\int_{-\infty}^{0}e^{-y^2}\,dy=-\frac{\sqrt{\pi}}{2}\operatorname{erf}\bar{x}+\frac{\sqrt{\pi}}{2}=\frac{\sqrt{\pi}}{2}(1-\operatorname{erf}\bar{x}).$$

In this way

$$\int_{-\infty}^{0}ve^{-\frac{1}{2}H_2^2}dv=-\frac{c_{mi}^2}{2}[e^{-\bar{x}^2}-\bar{x}\sqrt{\pi}(1-\operatorname{erf}\bar{x})].$$

Keeping in view the values of integrals obtained in (15.2.21), we get by analogy with (15.2.17′) the following relation for determination of the number of colliding molecules on the upper surface:

$$N_i=n_i\sqrt{\frac{RT_i}{2\pi}}[e^{-\bar{x}^2}-\bar{x}\sqrt{\pi}(1-\operatorname{erf}\bar{x})]. \tag{15.2.22}$$

If a free molecular flow past a curved surface (Fig. 15.2.4) is studied formula (15.2.17′) is used to calculate the number of colliding molecules on the front side of this surface and formula (15.2.22) is applicable to the back.

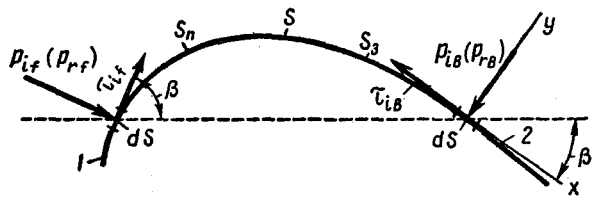

Fig. 15.2.4. Free molecular flow near curved surface:
1—front; *2*—back.

Formulas (15.2.17′) and (15.2.22) can be simplified for high speeds by using the condition that even for $\bar{x} \geqslant 2$ the quantity $e^{-\bar{x}^2}$ is smaller than unity by at least two orders and the integral **erf** $\bar{x}$ differs insignificantly from unity. For example, at $\bar{x}=2$ the quantity $e^{-\bar{x}^2}=0.018$ and erf $\bar{x}=0.995$. For each value of $\bar{x}$ there exists a relation

$$\mathbf{M}_\infty = \frac{\bar{x}}{\sin\beta}\sqrt{\frac{2}{k}}.$$

In particular, for $\bar{x}=2$ and at $\sin\beta=0.2$, $k=1.4$ the Mach number $\mathbf{M}_\infty=12$. At $\beta=90^\circ$ the smallest possible Mach number $\mathbf{M}_\infty$ for $\bar{x}=2$ comes down to 2.4. So the simplified formula (15.2.17′) can be written in the following way:

$$N_{if}=\bar{x}\, n_i \sqrt{2RT_i}=n_i V_\infty \sin\beta. \tag{15.2.23}$$

Here the index "f" shows that the front of a curved surface is in question. If the rear surface is considered (index "b") it can easily be seen that formula (15.2.22) on these assumptions turns into the equality

$$N_{ib}=0 \tag{15.2.24}$$

because the molecules do not reach the rear surface of the body at high flight speeds.

Let us consider the transfer of reflected molecules. The reflection by diffusion is governed by Maxwell distribution, so it is possible to use the relations (15.2.17′) and (15.2.22) by taking $\bar{x}=0$ as the particles lose mass velocity after colliding. Since the reflected particles have different temperature T_r, the number

$$N_r=n_r\sqrt{RT_r/2\pi}, \tag{15.2.25}$$

where n_r is the number of reflected molecules per unit volume. If it is assumed that the total number of colliding particles is equal to the number of reflected particles, i.e. $N_i=N_r$, the relation between the concentration n_r and n_i for the frontal surface under the flow-interaction will be obtained by equating the right sides of expressions (15.2.17′) and (15.2.25):

$$n_{rf}=n_i\sqrt{\frac{T_i}{T_r}}\left[e^{-\bar{x}^2}+\bar{x}\sqrt{\pi}\,(1+\operatorname{erf}\bar{x})\right]. \tag{15.2.26}$$

A similar expression for the back will be obtained by equating the right sides of (15.2.22) and (15.2.25):

$$n_{rb}=n_i\sqrt{\frac{T_i}{T_r}}\left[e^{-\bar{x}^2}-\bar{x}\sqrt{\pi}\,(1-\operatorname{erf}\bar{x})\right]. \tag{15.2.27}$$

2.3 Pressure

Pressure is determined as the loss of momentum on the part of a group of molecules in the direction normal to the surface as a result of collisions with it, i.e. it is equal to the sum of the momentum of these molecules per unit time before colliding. The general expression for determination of pressure

will be obtained in the following way: Numerically the pressure created by a molecule is equal to its momentum mv and the pressure due to a group of molecules colliding with unit area of surface in unit time will be

$$mn_i v^2 f du dv dw.$$

Consequently the pressure created by all the molecules colliding with the frontal surface will be given by

$$p_{if}=\rho_i(\pi c_{mi}^2)^{-\frac{3}{2}}\int_{-\infty}^{\infty} e^{-\frac{1}{2}H_1^2}du\int_0^{\infty} v^2 e^{-\frac{1}{2}H_2^2}dv\int_{-\infty}^{\infty} e^{-\frac{1}{2}H_3^2}dw, \quad (15.2.28)$$

where density $\rho_i=mn_i$. The values of the first and third integrals are determined in (15.2.11′). The second integral will be written in the same way as (15.2.12):

$$\int_0^{\infty} v^2 e^{-\frac{1}{2}H_2^2}dv=c_{mi}^3\int_{-\bar{x}}^{\infty}(\bar{x}+y)^2 e^{-y^2}dy=c_{mi}^3\,\bar{x}^2\int_{-\bar{x}}^{\infty} e^{-y^2}dy$$
$$+2c_{mi}^3\,\bar{x}\int_{-\bar{x}}^{\infty} y\,e^{-y^2}dy+c_{mi}^3\int_{-\bar{x}}^{\infty} y^2 e^{-y^2}dy.$$

We obtained the first and second integrals on the right side earlier. Let us determine the third integral by taking it in parts:

$$\int_{-\bar{x}}^{\infty} y^2 e^{-y^2}dy=\int_{-\bar{x}}^{0} y^2 e^{-y^2}dy+\int_0^{\infty} y^2 e^{-y^2}dy=\frac{1}{2}\Big[-ye^{-y^2}\Big|_{-\bar{x}}^{0}$$
$$+\int_{-\bar{x}}^{0} e^{-y^2}dy-ye^{-y^2}\Big|_0^{\infty}+\int_0^{\infty} e^{-y^2}dy\Big]=\frac{1}{2}\left(-\bar{x}\,e^{-\bar{x}^2}+\frac{\sqrt{\pi}}{2}\operatorname{erf}\bar{x}+\frac{\sqrt{\pi}}{2}\right).$$

In this way

$$\int_0^{\infty} v^2 e^{-\frac{1}{2}H_2^2}dv=c_{mi}^3\,\bar{x}^2\left(\frac{\sqrt{\pi}}{2}\operatorname{erf}\bar{x}+\frac{\sqrt{\pi}}{2}\right)+c_{mi}^3\,\bar{x}\,e^{-\bar{x}^2}$$
$$+\frac{c_{mi}^3}{2}\left(-\bar{x}\,e^{-\bar{x}^2}+\frac{\sqrt{\pi}}{2}\operatorname{erf}\bar{x}+\frac{\sqrt{\pi}}{2}\right)$$
$$=\frac{\sqrt{\pi}}{2}c_{mi}^3\,(1-\operatorname{erf}\bar{x})\left(\bar{x}^2+\frac{1}{2}\right)+\frac{c_{mi}^3}{2}\bar{x}\,e^{-\bar{x}^2}.$$

Keeping in mind this relation and the values of the first and third integrals (15.2.28), each of which is equal to $c_{mi}\sqrt{\pi}$, and noting the expression

$$\bar{x}^2=\sin^2\beta\frac{V_\infty^2}{a_i^2}\cdot\frac{k}{2}=\sin^2\beta\frac{V_\infty^2}{c_{mi}^2},$$

the following formula will be obtained for the nondimensional value of pressure on a frontal surface after appropriate substitutions in (15.2.28):

$$\bar{p}_{if}=\frac{2p_{if}}{\rho_i V_\infty^2}=\sin^2\beta\left[\frac{1}{\bar{x}\sqrt{\pi}}e^{-\bar{x}^2}+\left(1+\frac{1}{2\bar{x}^2}\right)(1+\operatorname{erf}\bar{x})\right]. \quad (15.2.29)$$

To determine the pressure on the rear surface we have to use the same relation (15.2.28) with replacement of the limits of integration by $-\infty<v<0$. According to this

$$p_{ib}=\rho_i(\pi c_{mi}^2)^{-\frac{3}{2}}\int_{-\infty}^{\infty}e^{-\frac{1}{2}H_1^2}du\int_{-\infty}^{0}v^2e^{-\frac{1}{2}H_2^2}dv\int_{-\infty}^{\infty}e^{-\frac{1}{2}H_3^2}dw,$$

where

$$\int_{-\infty}^{0}v^2e^{-\frac{1}{2}H_2^2}dv=c_{mi}^3\int_{-\infty}^{-\bar{x}}(\bar{x}+y)^2e^{-y^2}dy$$

$$=c_{mi}^3\bar{x}^2\int_{-\infty}^{-\bar{x}}e^{-y^2}dy+2c_{mi}^3\bar{x}\int_{-\infty}^{-\bar{x}}ye^{-y^2}dy+c_{mi}^3\int_{-\infty}^{-\bar{x}}y^2e^{-y^2}dy$$

$$=\frac{\sqrt{\pi}}{2}c_{mi}^3(1-\operatorname{erf}\bar{x})\left(\bar{x}^2+\frac{1}{2}\right)-\frac{c_{mi}^3}{2}\bar{x}e^{-\bar{x}^2}. \quad (15.2.30)$$

Taking this value of the integral, we get the following relation for the nondimensional value of pressure on the rear surface:

$$\bar{p}_{ib}=\frac{2p_{ib}}{\rho_i V_\infty^2}=\sin^2\beta\left[\frac{-1}{\bar{x}\sqrt{\pi}}e^{-\bar{x}^2}+\left(1+\frac{1}{2\bar{x}^2}\right)(1-\operatorname{erf}\bar{x})\right]. \quad (15.2.31)$$

It can easily be seen that the relations determining the flow of gas on the rear surface can be obtained from the corresponding expressions for the front by changing $\bar{x}$ to $-\bar{x}$.

The pressure, which is equal to the sum of the momentum of molecules normal to the surface bombarding the wall, is created by the particles being reflected along with the colliding particles. Since the process of reflection of particles is governed by the Maxwell distribution of velocity corresponding to temperature T_r and zero velocity of orderly mass motion (reflection takes place from a relatively fixed surface), it is necessary to use expression (15.2.28) taking $\bar{u}=\bar{v}=\bar{w}=0$, and to change to the parameters with "r". According to this we have for the frontal area

$$p_{rf}=\rho_r(\pi c_{mr}^2)^{-\frac{3}{2}}\int_{-\infty}^{\infty}e^{-\frac{1}{2}H_1^2}dU\int_{0}^{\infty}V^2e^{-\frac{1}{2}H_2^2}dV\int_{-\infty}^{\infty}e^{-\frac{1}{2}H_3^2}dW,$$

which, after solving the integrals, results in

$$p_{rf}=\frac{1}{2}R\rho_r T_r. \quad (15.2.32)$$

Since the density of reflected particles $\rho_r = mn_r$ and their number per unit volume n_r is determined by the condition of steady flow $N_r = N_i$, from formula (15.2.26) we get following equation for the pressure arising due to diffusive reflection:

$$\bar{p}_{rf} = \frac{2p_{rf}}{\rho_i V_\infty^2} = \frac{\sin^2\beta}{2\bar{x}^2}\sqrt{\frac{\overline{T}_r}{\overline{T}_i}}\,[e^{-\bar{x}^2} + \bar{x}\sqrt{\pi}\,(1+\operatorname{erf}\bar{x})]. \qquad (15.2.33)$$

The corresponding formula for the rear surface will be

$$\bar{p}_{rb} = \frac{2p_{rb}}{\rho_i V_\infty^2} = \frac{\sin^2\beta}{2\bar{x}^2}\sqrt{\frac{\overline{T}_r}{\overline{T}_i}}\,[e^{-\bar{x}^2} - \bar{x}\sqrt{\pi}\,(1-\operatorname{erf}\bar{x})]. \qquad (15.2.34)$$

The resultant value of relative pressure is equal to the sum of corresponding values p_i and p_r. For the frontal surface

$$\bar{p}_f = \frac{2\,(p_{if}+p_{rf})}{\rho_i V_\infty^2} = \bar{p}_{if} + \bar{p}_{rf}; \qquad (15.2.35)$$

and for the rear surface

$$\bar{p}_b = \frac{2\,(p_{ib}+p_{rb})}{\rho_i V_\infty^2} = \bar{p}_{ib} + \bar{p}_{rb}, \qquad (15.2.36)$$

where the values of relative pressure $\bar{p}_{if}$ and $\bar{p}_{rf}$ will be found from the expressions (15.2.29) and (15.2.33), and $\bar{p}_{ib}$ and $\bar{p}_{rb}$ will be obtained from (15.2.31) and (15.2.34).

The generalized expression for relative pressure obtained after corresponding summation can be used in place of the relations (15.2.35), (15.2.36):

$$\bar{p} = \frac{2\,(p_i+p_r)}{\rho_i V_\infty^2} = \sin^2\beta\left[\frac{\pm 1}{\bar{x}}\left(\frac{1}{\sqrt{\pi}} \pm \frac{1}{2\bar{x}}\sqrt{\frac{\overline{T}_r}{\overline{T}_i}}\right)e^{-\bar{x}^2}\right.$$
$$\left. + \left(1 + \frac{1}{2\bar{x}^2} \pm \frac{\sqrt{\pi}}{2\bar{x}}\sqrt{\frac{\overline{T}_r}{\overline{T}_i}}\right)(1 \pm \operatorname{erf}\bar{x})\right], \qquad (15.2.37)$$

where the upper sign (plus) refers to the frontal surface and the lower sign (minus) to the rear surface.

From the expression (15.2.37) it follows that the pressure depends on the orientation of the surface with respect to the velocity vector $\overline{V}_\infty$ (i.e. on angle β), the Mach number $\mathbf{M}_\infty$ and the temperature ratio T_r/T_i.

At high speeds corresponding to the condition $\bar{x} \geqslant 2$, the formulas for relative pressure can be simplified. From (15.2.29) and (15.2.31) we get the following approximate relations:

$$\bar{p}_{if} = 2\sin^2\beta\left(1 + \frac{1}{2\bar{x}^2}\right); \qquad (15.2.38)$$

$$\bar{p}_{ib} = 0. \qquad (15.2.39)$$

The corresponding formulas describing the process of reflection can be written according to (15.2.33) and (15.2.34) as:

$$\bar{p}_{rf} = \frac{\sin^2\beta}{\bar{x}}\sqrt{\pi\frac{\overline{T}_r}{\overline{T}_i}}; \qquad (15.2.40)$$

$$\bar{p}_{rb}=0. \tag{15.2.41}$$

Taking these expressions into account, the simplified relations for the resultant value of relative pressure can be written as follows:

$$\bar{p}_f=\bar{p}_{if}+\bar{p}_{rf}=2\sin^2\beta\left(1+\frac{1}{2\bar{x}^2}+\frac{\sqrt{\pi}}{2\bar{x}}\sqrt{\frac{\bar{T}_r}{\bar{T}_i}}\right); \tag{15.2.42}$$

$$\bar{p}_b=0. \tag{15.2.43}$$

2.4 Frictional stress

Frictional stress is the result of total loss of the tangential component of the momentum of molecules in collision. This loss of momentum for one molecule is equal to *mu* and for all the molecules that collide with the unit area of surface in unit time it is equal to

$$n_i m f u v du dv dw.$$

Consequently the frictional stress due to the collisions of all the molecules with the frontal surface will be

$$\tau_i=\rho_i(\pi c_{mi}^2)^{-\frac{3}{2}}\int_{-\infty}^{\infty}ue^{-\frac{1}{2}H_1^2}du\int_0^{\infty}ve^{-\frac{1}{2}H_2^2}dv\int_{-\infty}^{\infty}e^{-\frac{1}{2}H_3^2}dw. \tag{15.2.44}$$

The relation (15.2.44) can be transformed with the help of (15.2.10) to the following form:

$$\tau_i=\rho_i(\pi c_{mi}^2)^{-\frac{3}{2}}c_{mi}^3\underbrace{\int_{-\infty}^{\infty}\left(\bar{u}+\frac{H_1}{\sqrt{2}}c_{mi}\right)e^{-\frac{1}{2}H_1^2}d\left(\frac{H_1}{\sqrt{2}}\right)}_{1}$$

$$\times\underbrace{\int_{-\bar{v}/c_{mi}}^{\infty}\left(\bar{v}+\frac{H_2}{\sqrt{2}}c_{mi}\right)e^{-\frac{1}{2}H_2^2}d\left(\frac{H_2}{\sqrt{2}}\right)}_{2}\underbrace{\int_{-\infty}^{\infty}e^{-\frac{1}{2}H_3^2}d\left(\frac{H_3}{\sqrt{2}}\right)}_{3}. \tag{15.2.44'}$$

The integrals on the right side of the equation have the following values:

$$\left.\begin{aligned}&1)\ \bar{u}\sqrt{\pi};\\&2)\ \frac{1}{2}c_{mi}[e^{-\bar{x}_i^2}+\bar{x}\sqrt{\pi}(1+\operatorname{erf}\bar{x})];\\&3)\ \sqrt{\pi}.\end{aligned}\right\} \tag{15.2.45}$$

The friction on the rear surface will be determined by the same expression (15.2.44') with a change in the limits of the second integral to $-\infty<v<0$. According to this the second integral will be

$$2)\ \frac{1}{2}c_{mi}[e^{-\bar{x}^2}-\bar{x}\sqrt{\pi}(1-\operatorname{erf}\bar{x})]. \tag{15.2.46}$$

Keeping these values of integrals in mind and recalling that

$$\left.\begin{aligned} \bar{u} &= V_\infty \cos\beta; \\ \bar{x} &= (V_\infty/c_{mi}) \sin\beta, \end{aligned}\right\} \tag{15.2.47}$$

equation (15.2.44′) leads to the following relation for the frictional coefficient:

$$c_{fi} = \frac{2\tau_i}{\rho_i V_\infty^2} = \sin\beta\cos\beta\left[\frac{\pm e^{-\bar{x}^2}}{\bar{x}\sqrt{\pi}} + (1 \pm \operatorname{erf}\bar{x})\right], \tag{15.2.48}$$

where the sign "plus" refers to the frontal area as before and the "minus" sign to the back.

Since any directions of motion are equally possible for reflected molecules their resultant interaction does not create frictional stress, i.e. $\tau_r = 0$, and hence

$$c_{fr} = 0. \tag{15.2.49}$$

It can easily be seen that the coefficient of friction for a non-inclined surface ($\beta = 0$) will be

$$c_{fi} = \frac{1}{\bar{x}_\infty\sqrt{\pi}} = \frac{1}{\mathbf{M}_\infty}\sqrt{\frac{2}{k\pi}}. \tag{15.2.50}$$

The relations for the case where $\bar{x} \geqslant 2$ are also simplified. Accordingly the relations for the conditions of the front and rear areas will have the form

$$(c_{fi})_f = \sin 2\beta; \tag{15.2.51}$$

$$(c_{fi})_b = 0. \tag{15.2.52}$$

2.5 Transfer of kinetic energy

As we mentioned earlier, it is necessary to know the ratio of temperature T_r/T_i to determine normal pressure. The calculation of this ratio is connected with determination of the energy of uniform motion of molecules, which is brought to the surface during the collision of molecules and carried away when they are reflected. Each of the molecules transfers the following amount of energy on colliding:

$$(1/2)\, mc^2 = (1/2)\, m\,(U^2 + V^2 + W^2). \tag{15.2.53}$$

The energy brought by all the molecules striking unit area in unit time is determined by the expression

$$(1/2)\, mn_i c^2 f v du dv dw.$$

The resultant quantity of transferable energy E_i during collision can be obtained by integrating this expression within the limits of variation of u and w from $-\infty$ to ∞ and of v from 0 to ∞ for the frontal area (or from $-\infty$ to 0 for v for the back). Taking into account the value of (15.2.2) for f, we have

$$E_i = \frac{1}{2}(mn_i\,(\pi c_{mi}^2)^{-\frac{3}{2}} \int_{-\infty}^{\infty}\int_{t_H}^{t_B}\int_{-\infty}^{\infty} c^2\, e^{-\frac{c^2}{c_{mi}^2}}\, v du dv dw, \tag{15.2.54}$$

where $t_H=0$, $t_B=\infty$ for the frontal area and $t_H=-\infty$ and $t_B=0$ for the back. Keeping in view the expression (15.2.53) for $(1/2)mc^2$, and the relation (15.2.10), further integration leads to

$$E_i=\frac{1}{2}mN_i\left[V_\infty^2+RT_i\left(4+\frac{1}{\varphi+1}\right)\right], \tag{15.2.55}$$

where N_i is determined by formula (15.2.17′) for the frontal area and by (15.2.22) for the back; the function

$$\varphi=e^{-\bar{x}^2}\left[\pm\bar{x}\sqrt{\pi}(1\pm\operatorname{erf}\bar{x})\right]^{-1}. \tag{15.2.56}$$

The reflected particles carry away the elementary energy

$$(1/2)\,mn_rc^2fUdUdVdW$$

from the unit surface area. Integrating this within the limits of U and W from $-\infty$ to ∞ and that of V from $-\infty$ to 0, we get the total value of energy carried away:

$$E_r=\frac{1}{2}mn_r(\pi c_{mr}^2)^{-\frac{3}{2}}\int_{-\infty}^{\infty}\int_{-\infty}^{0}\int_{-\infty}^{\infty}c^2\,e^{-\frac{c^2}{c_{mr}^2}}VdUdVdW. \tag{15.2.57}$$

The solution of this triple integral results in

$$E_r=\rho_r\,(RT_r)^{3/2}\,(2/\pi)^{1/2}. \tag{15.2.58}$$

Let us substitute $\rho_r=mn_r$ and the value of n_r from equation (15.2.25) in this expression. The energy E_r will then be given by

$$E_r=2mN_rRT_r. \tag{15.2.59}$$

Inserting the value of $N_r=N_i$ in view of (15.2.17′) and (15.2.22) and keeping in mind that $m=\rho_i/n_i$, we get

$$E_r=2mN_iRT_r=\sqrt{2/\pi}\;\rho_i\,RT_r\sqrt{RT_i}\,[e^{-\bar{x}^2}\pm\bar{x}\sqrt{\pi}\,(1\pm\operatorname{erf}\bar{x})], \tag{15.2.60}$$

where Boltzman's constant $mR=1.38\times10^{-16}$ erg/degree.

The resultant flow of kinetic energy of molecules is equal to the difference between the energies brought to and carried away from the surface:

$$E=E_i-E_r.$$

At high speeds ($\bar{x}\geqslant2$) it may be assumed that $\varphi_f\approx\varphi_b\approx0$ for front as well as rear surfaces. Keeping in view formulas (15.2.17′), (15.2.22), (15.2.55) and (15.2.56) and carrying out the necessary simplifications, we get

$$E_{if}=\frac{1}{2}\bar{x}\rho_i\sqrt{2RT_i}\,(V_\infty^2+5RT_i); \tag{15.2.61}$$

$$E_{ib}=0. \tag{15.2.62}$$

The corresponding relations for the energy of reflected particles, after simplification of (15.2.60), will be written in the following form:

$$E_{rf}=2\sqrt{2}\,\rho_i\,RT_r\bar{x}\sqrt{RT_i}; \tag{15.2.63}$$

$$E_{rb}=0. \tag{15.2.64}$$

3. Adaptability

3.1 Exchange of momentum

In the previous section we studied the processes of transfer and considered the hypothesis of completely diffused reflection. Here we assume that the molecules fully adapt to the conditions at the wall and the contact arising between the wall and the molecules is sufficient to transfer the momentum of all the molecules to the wall.

Experimental research shows that the real process of interaction between the molecules and the surface differs from the phenomenon of diffused reflection and is characterized by reflection of a more general type. Only part of the colliding molecules transfer the tangential component of impulse to the wall. The contact of the colliding molecules does not last long enough for them to achieve average energy corresponding to wall temperature T_w.

It is assumed that the normal and tangential components of the force created by a reflected flow are determined by the coefficient of adjustability ("adaptation") for the normal component of momentum

$$f_n=\frac{p_i-p_r}{p_i-p_w} \tag{15.3.1}$$

and the coefficient of adjustability for the tangential component of momentum

$$f_\tau=\frac{\tau_i-\tau_r}{\tau_i}, \tag{15.3.2}$$

respectively. This idea forms the basis of the concept of reflection considered here.

According to this concept, only part of the colliding molecules f_n transfer the normal component of momentum to the wall. The fraction of molecules transferring the tangential component of momentum to the wall is determined by the coefficient f_τ. Obviously $f_n=f_\tau=0$ ($p_i=p_r$; $\tau_i=\tau_r$) for perfect mirror reflection of molecules and $f_n=f_\tau=1$ ($p_r=p_w$; $\tau_r=0$) for totally diffused reflection.

Pressure p_w in (15.3.1) can be considered as a normal component of the momentum of molecules reflected following the Maxwell distribution of velocity corresponding to thermodynamic equilibrium at surface temperature T_w in a steady state condition ($V_\infty=0$). According to (15.2.32) we have

$$p_w=(1/2)\,R\rho_w T_w,$$

or, keeping in mind that $\rho_w=mn_w$,

$$p_w=(1/2)\,mRn_w T_w.$$

We use the relation $\rho_i=mn_i$ to go back to the density of undisturbed flow, which gives

$$p_w=(1/2)\,R\rho_i T_w (n_w/n_i).$$

The relation $N_w = N_i$, determining the equality of the number of reflected molecules N_w and colliding molecules, is used to determine the ratio n_w/n_i:

$$n_w \sqrt{RT_w/2\pi} = N_i = (N_i/n_i)\, n_i,$$

where N_i is determined from formulas (15.2.17') and (15.2.22). After calculating the ratio of n_w/n_i we get the formula for pressure

$$\bar{p}_w = \frac{2p_w}{\rho_i V_\infty^2} = \frac{\sin^2\beta}{2\bar{x}^2}\sqrt{\frac{T_w}{T_i}}\,[e^{-\bar{x}^2} \pm \bar{x}\sqrt{\pi}\,(1 \pm \operatorname{erf}\bar{x})], \qquad (15.3.3)$$

where the "plus" sign corresponds to the frontal area and the "minus" sign to the back.

Strictly speaking, the coefficients f_n and f_τ are not identical because they characterize different processes of momentum transfer during reflection. However, Maxwell's hypothesis can be used for approximate calculations, according to which the process of reflection is characterized by the same coefficient of adjustability momentum $f = f_n = f_\tau$. This indicates that fraction f of all molecules is reflected by diffusion and fraction $(1-f)$ is mirror reflected.

From the above discussion pressure p_r during reflection is determined from the expression (15.3.1) in the following way:

$$p_r = p_i(1-f) + fp_w.$$

The total pressure is

$$p = p_i + p_r = (2-f)\, p_i + fp_w. \qquad (15.3.4)$$

Substituting the values of p_i from (15.2.29) and (15.2.31) and the value of p_w from (15.3.3) in this formula, we get

$$\bar{p} = \frac{2(p_i+p_r)}{\rho_i V_\infty^2} = \sin^2\beta\left\{(2-f)\left[\frac{\pm e^{-\bar{x}^2}}{\bar{x}\sqrt{\pi}} + \left(1+\frac{1}{2\bar{x}^2}\right)(1 \pm \operatorname{erf}\bar{x})\right] + \frac{f}{2\bar{x}^2}\sqrt{\frac{T_w}{T_i}}\,[e^{-\bar{x}^2} \pm \bar{x}\sqrt{\pi}\,(1 \pm \operatorname{erf}\bar{x})]\right\}. \qquad (15.3.5)$$

The resultant frictional stress due to the action of colliding and reflecting molecules will be

$$\tau = \tau_i - \tau_r.$$

Inserting here the value of

$$\tau_r = (1-f)\,\tau_i,$$

which can be obtained from (15.3.2), we find

$$\tau = \tau_i - \tau_r = \tau_i f. \qquad (15.3.6)$$

The corresponding coefficient of friction, according to formula (15.2.48), will be

$$c_f = \frac{2\tau}{\rho_i V_\infty^2} = \frac{2\tau_i f}{\rho_i V_\infty^2} = f \sin\beta\cos\beta\left[\frac{\pm e^{-\bar{x}^2}}{\bar{x}\sqrt{\pi}} + (1 \pm \operatorname{erf}\bar{x})\right]. \qquad (15.3.6')$$

For very high velocities ($\bar{x} \geqslant 2$) and a very cold wall ($T_w < T_i$) the relation

(15.3.5) may be simplified. Taking the "plus" sign (the frontal area is in question), we get

$$\bar{p}_f=2(2-f)\sin^2\beta. \tag{15.3.7}$$

For these high speeds the coefficient of friction over the frontal area will be

$$(c_f)_f=f\sin 2\beta. \tag{15.3.8}$$

On the back under these conditions we have

$$\bar{p}_b=0,\ (c_f)_b=0. \tag{15.3.9}$$

The coefficient f in the above expressions is close to unity and can be taken as approximately equal to 0.95–1.0 in calculating. In the limiting case of complete mirror reflection, which is not real, the coefficient $f=0$. In the other limiting case of totally diffused reflection, which is more probable, the coefficient $f=1$.

Experimental research on the interaction of hydrogen, helium and oxygen with a polished surface of silver oxide and of air with brass showed that $f\approx$ 0.99. This confirms the occurrence of almost totally diffused reflection. But other experiments helped to establish that f can be considerably less than unity for some combinations of gas and surface.

3.2 Exchange of energy

The absence of total "adaptability" (adjustability) is not solely the property of the process of momentum transfer but is also typical of the process of exchange of energy between the colliding molecules and the wall. This is shown by experimental research. For this reason it is assumed in formula (15.2.60) for the energy of reflected molecules that their temperature T_r differs from the wall temperature T_w. Due to the brief duration of the collision with the wall the contact of the colliding particles is not sufficient for them to receive the average energy corresponding to wall temperature T_w during reflection. According to (15.2.60) this energy is equal to

$$E_w=2mN_iRT_w=\sqrt{2/\pi}\,\rho_iRT_w\sqrt{RT_i}\,[e^{-\bar{x}2}\pm\bar{x}\sqrt{\pi}\,(1\pm\operatorname{erf}\bar{x})]. \tag{15.3.10}$$

The case of reflection we are considering happens to be the most general. It is characterized by the absence of complete adjustability ("adaptability") between the solid boundary and the molecules during exchange of energy. So in this general case the ratio

$$\eta=\frac{E_i-E_r}{E_i-E_w}, \tag{15.3.11}$$

known as the thermodynamic coefficient of adjustability, differs from unity. The discontinuity in energies arising in this way is the reason for the temperature jump, i.e. difference between T_r and T_w.

The coefficient of adjustability η, as we will see, plays an important part

in the calculation of heat transfer. Therefore it is necessary to know how to evaluate it. At present it is possible to estimate it only by experiment and unfortunately few sufficiently reliable measurements are available. Observations show that the nature of variations in the thermodynamic coefficient of adjustability is very complicated. It is established, specifically, that the value of η increases with an increase in molecular weight and surface temperature. It can be assumed that the coefficient of adjustability will depend on the flight velocity of the body, the angle of incidence of molecules to the surface, the properties of the material and condition of the surface. As shown by experiment, the value of the coefficient of adjustability for air interacting with aluminum and steel with surfaces of different finish is near to unity: it varies from 0.7 to 0.97.

From the information available the value of η may attain about 10^{-2} for clean surfaces and light molecules, particularly of such gases as hydrogen and helium. More detailed information on this question is found in the work [54].

Comparison of the "thermal" and "force" coefficients (η, f) of adjustability shows that f is considerably higher than η. From this it follows that the time for collision of these molecules with the wall is too short for the reflected molecules to attain wall temperature although the colliding molecules undergo a number of collisions with the wall and the process of reflection is near to diffused reflection.

The limiting case in which $\eta=1$ may be examined. This corresponds to the moment when the temperature T_r of the reflected molecules achieves the wall temperature T_w. In this case it looks as if the molecules completely adjust to the wall conditions.

4. Aerodynamic Forces

4.1 General expression for drag forces

Let us consider the determination of aerodynamic drag force as an example for application of the relations obtained in Sections 2 and 3. First we will obtain the expression for force acting on a local area of unit dimension without considering the effect of adjustability, i.e. on the assumption that the coefficient $f=1$. The axial force arising due to normal pressure and friction as a result of collision with this unit area situated on the frontal surface of a body (see Fig. 15.2.4) will be obtained with the help of (15.2.29) and (15.2.48) in the following form:

$$F_{if}=p_{if}\sin\beta+\tau_{if}\cos\beta=\frac{\rho_i V_\infty^2}{2}\sin\beta\left[\frac{e^{-\bar{x}^2}}{\bar{x}\sqrt{\pi}}+\left(1+\frac{\sin^2\beta}{2\bar{x}^2}\right)(1+\operatorname{erf}\bar{x})\right]. \tag{15.4.1}$$

The force acting on the elementary area dS of the front will be

$$dX_{if}=F_{if}\,dS, \tag{15.4.2}$$

and the total axial force will be

$$X_{if}=\int\limits_{(S_f)} F_{if}\,dS, \tag{15.4.3}$$

where S_f is the area of the frontal surface of the body. The corresponding drag coefficient

$$c_{xif}=\frac{2X_{if}}{\rho_i V_\infty^2 S_0}=\int\limits_{(\bar{S}_f)} \sin\beta\left[\frac{e^{-\bar{x}^2}}{\bar{x}\sqrt{\pi}}+\left(1+\frac{\sin^2\beta}{2\bar{x}^2}\right)(1+\operatorname{erf}\bar{x})\right]d\bar{S}, \tag{15.4.4}$$

where

$$\bar{S}=S/S_0;\ \bar{x}=(V_\infty/c_{ml})\sin\beta=\bar{x}_\infty\sin\beta;$$
$$\bar{S}_f=S_f/S_0\ \text{[see (15.2.20)]}.$$

Integration will be carried out for a frontal surface of area S_f. The relations can be obtained for the force and its coefficient for the rear surface.

From Fig. 15.2.4 it can be seen that

$$F_{ib}=p_{ib}\sin\beta+\tau_{ib}\cos\beta.$$

Here the angle β is taken in its absolute value. Recalling formula (15.2.31) for p_{ib} and calculating τ_{ib} from the expression (15.2.48), in which the lower sign "minus" is taken for the rear surface, we get the following relation after appropriate substitutions:

$$\begin{aligned}F_{ib}&=\frac{\rho_i V_\infty^2}{2}\sin^3\beta\left[\frac{-1}{\bar{x}\sqrt{\pi}}e^{-\bar{x}^2}+\left(1+\frac{1}{2\bar{x}^2}\right)(1-\operatorname{erf}\bar{x})\right]\\&+\frac{\rho_i V_\infty^2}{2}\sin\beta\cos^2\beta\left[\frac{-1}{\bar{x}\sqrt{\pi}}e^{-\bar{x}^2}+(1-\operatorname{erf}\bar{x})\right]\\&=\frac{\rho_i V_\infty^2}{2}\sin\beta\left[\frac{-e^{-\bar{x}^2}}{\bar{x}\sqrt{\pi}}+\left(1+\frac{\sin^2\beta}{2\bar{x}^2}\right)(1-\operatorname{erf}\bar{x})\right].\end{aligned} \tag{15.4.5}$$

The drag coefficient will be

$$c_{xib}=\frac{2X_{ib}}{\rho_i V_\infty^2 S_0}=\int\limits_{(\bar{S}_b)} \sin\beta\left[\frac{-e^{-\bar{x}^2}}{\bar{x}\sqrt{\pi}}+\left(1+\frac{\sin^2\beta}{2\bar{x}^2}\right)(1-\operatorname{erf}\bar{x})\right]d\bar{S}. \tag{15.4.6}$$

The solution of the integral is performed for the rear surface of area S_b. The same result can be obtained from expression (15.4.4) by replacing $\bar{x}$ to $-\bar{x}$ in it.

The drag coefficient of the body in such a flow is determined as the difference between the coefficients of forces produced by the molecules colliding with the front and rear surfaces and acting in opposite directions:

$$c_{xi}=c_{xif}-c_{xib}=\frac{2(X_{if}-X_{ib})}{\rho_i V_\infty^2 S_0}. \tag{15.4.7}$$

The reflected particles create additional force. During this process the particles act on the frontal surface, in the process of being reflected from it, with a force given by the following relation according to (15.2.33):

$$F_{rf}=p_{rf}\sin\beta=\frac{\rho_i V_\infty^2}{2}\cdot\frac{\sin^3\beta}{2\bar{x}^2}\sqrt{\frac{\overline{T_r}}{T_i}}\,[e^{-\bar{x}^2}+\bar{x}\sqrt{\pi}\,(1+\operatorname{erf}\bar{x})]. \quad (15.4.8)$$

The coefficient of force acting on the frontal surface S_f will then be given by

$$c_{xrf}=\frac{2X_{rf}}{\rho_i V_\infty^2 S_0}=\frac{1}{2}\int\limits_{(\bar{S}_f)}\frac{\sin^3\beta}{\bar{x}^2}\sqrt{\frac{\overline{T_r}}{T_i}}\,[e^{-\bar{x}^2}+\bar{x}\sqrt{\pi}\,(1+\operatorname{erf}\bar{x})]\,d\bar{S}. \quad (15.4.9)$$

The force experienced per unit area based on the action of reflected molecules on the rear surface will be determined by the relation (15.2.34) for p_{rb} in the form

$$F_{rb}=p_{rb}\sin\beta=\frac{\rho_i V_\infty^2}{2}\cdot\frac{\sin^3\beta}{2\bar{x}^2}\sqrt{\frac{\overline{T_r}}{T_i}}\,[e^{-\bar{x}^2}-\bar{x}\sqrt{\pi}\,(1-\operatorname{erf}\bar{x})]. \quad (15.4.10)$$

The corresponding coefficient of the force X_{rb} acting on the rear surface will be

$$c_{xrb}=\frac{2X_{rb}}{\rho_i V_\infty^2 S_0}=\frac{1}{2}\int\limits_{(\bar{S}_b)}\frac{\sin^3\beta}{\bar{x}^2}\sqrt{\frac{\overline{T_r}}{T_i}}\,[e^{-\bar{x}^2}-\bar{x}\sqrt{\pi}\,(1-\operatorname{erf}\bar{x})]\,d\bar{S}. \quad (15.4.11)$$

The resultant drag coefficient due to reflected molecules will be

$$c_{xr}=c_{xrf}-c_{xrb}=\frac{2(X_{rf}-X_{rb})}{\rho_i V_\infty^2 S_0}. \quad (15.4.12)$$

This drag coefficient is determined as the difference between the corresponding coefficients for the front and rear surfaces. This is established by the nature of the interaction of reflected molecules with the wall. No drag arises on the rear surface: a reactive force opposite to drag is set up. This reactive force by its physical nature comes into the picture during reflection of particles away from the surface.

The resultant drag coefficient for the body in such a flow is obtained by addition of (15.4.7) and (15.4.12):

$$c_x=c_{xi}+c_{xr}. \quad (15.4.13)$$

The above formulas can be simplified for cases where $\bar{x}\geqslant 2$. We have the relations

$$F_{if}=\rho_i V_\infty^2\sin\beta\left(1+\frac{1}{2\bar{x}_\infty^2}\right); \quad (15.4.14)$$

$$c_{xif}=2\left(1+\frac{1}{2\bar{x}_\infty^2}\right)\int\limits_{(\bar{S}_f)}\sin\beta\,d\bar{S}, \quad (15.4.15)$$

in place of the expressions (15.4.1) and (15.4.4) respectively. Similarly

$$F_{ib}=0,\ c_{xib}=0 \tag{15.4.16}$$

replace the expressions (15.4.5) and (15.4.6) respectively. The relations (15.4.8), (15.4.9) are also simplified to the following forms:

$$F_{rf}=\frac{\rho_i V_\infty^2}{2}\cdot\frac{\sin^2\beta}{\bar{x}_\infty}\sqrt{\pi\frac{T_r}{T_i}}; \tag{15.4.17}$$

$$c_{xrf}=\frac{\sqrt{\pi}}{\bar{x}_\infty}\int\limits_{(\bar{S}_f)}\sin^2\beta\sqrt{\frac{T_r}{T_i}}\,d\bar{S}. \tag{15.4.18}$$

The expressions (15.4.10), (15.4.11) will be reduced to

$$F_{rb}=0,\ c_{xrb}=0. \tag{15.4.19}$$

In the case of simultaneous diffused and mirror reflection (coefficient of adjustability of momentum $f<1$) the calculation of forces should be carried out from the formulas:

$$F_{if}=p_{if}\sin\beta+f\tau_{if}\cos\beta; \tag{15.4.20}$$

$$F_{ib}=F_{if}(-\bar{x}); \tag{15.4.21}$$

$$F_{rf}=[p_{if}(1-f)+fp_{wf}]\sin\beta; \tag{15.4.22}$$

$$F_{rb}=F_{rf}(-\bar{x}), \tag{15.4.23}$$

where p_{wf} is determined by formula (15.3.3) using the "plus" sign. The notations in (15.4.21) and (15.4.23) indicate that F_{ib} and F_{rb} are obtained from the expressions for F_{if} and F_{rf} respectively by changing $\bar{x}$ to $-\bar{x}$.

4.2 Cone

As an illustration, let us calculate the aerodynamic drag on a body in the form of a combination of two cones (Fig. 15.4.1, a) in an axisymmetric flow. The relative quantity appearing in the formulas for the drag coefficients

$$d\bar{S}=\frac{2\pi rdl}{\pi r_0^2}=\frac{2\pi rdr}{\pi r_0^2\sin\beta_k}=\frac{d\bar{r}^2}{\sin\beta_k}. \tag{15.4.24}$$

Using this value of $d\bar{S}$ in (15.4.4) and (15.4.6) and recalling the following relation for a cone:

$$\bar{x}_k=\bar{x}_\infty\sin\beta_k=\mathbf{M}_\infty\sqrt{k/2}\sin\beta_k=\text{const}, \tag{15.4.25}$$

we get the drag coefficient in the following form:

$$c_{xif}=\frac{1}{\bar{x}_k\sqrt{\pi}}e^{-\bar{x}_k^2}+\left(1+\frac{1}{2\bar{x}_\infty^2}\right)(1+\operatorname{erf}\bar{x}_k); \tag{15.4.26}$$

$$c_{xib}=\frac{-1}{\bar{x}_k\sqrt{\pi}}e^{-\bar{x}_k^2}+\left(1+\frac{1}{2\bar{x}_\infty^2}\right)(1-\operatorname{erf}\bar{x}_k). \tag{15.4.27}$$

The resultant drag coefficient due to colliding molecules

$$c_{xi}=c_{xif}-c_{xib}=\frac{2}{\bar{x}_k\sqrt{\pi}}e^{-\bar{x}_k^2}+2\left(1+\frac{1}{2\bar{x}_\infty^2}\right)\operatorname{erf}\bar{x}_k. \qquad (15.4.28)$$

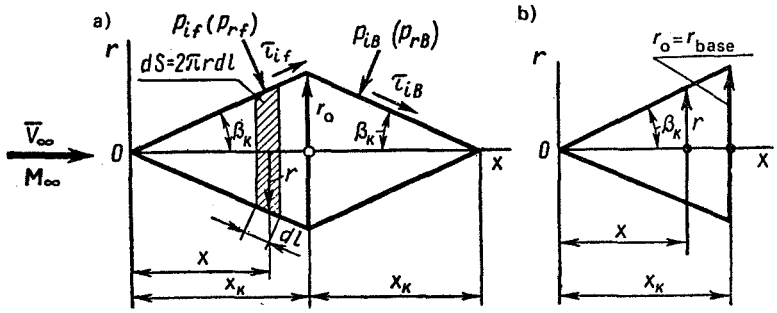

Fig. 15.4.1. Example of calculation of flow-interaction of free molecular flow over conical body:

a—combination from two conical surfaces; *b*—cone with base cross section.

Let us consider the interaction of reflected molecules, assuming that the ratio of T_r/T_i is constant for the conditions of flow over the cone. For these conditions equation (15.4.9) gives

$$c_{xrf}=\frac{1}{2\bar{x}_\infty^2}\sqrt{\frac{T_r}{T_i}}\left[e^{-\bar{x}_k^2}+\bar{x}_k\sqrt{\pi}\,(1+\operatorname{erf}\bar{x}_k)\right], \qquad (15.4.29)$$

and applying formula (15.4.11) we have

$$c_{xrb}=\frac{1}{2\bar{x}_\infty^2}\sqrt{\frac{T_r}{T_i}}\left[e^{-\bar{x}_k^2}-\bar{x}_k\sqrt{\pi}\,(1-\operatorname{erf}\bar{x}_k)\right]. \qquad (15.4.30)$$

Keeping in view that this coefficient characterizes reactive force on the back surface, we determine the resultant drag coefficient due to reflected molecules according to (15.4.12):

$$c_{xr}=c_{xrf}-c_{xrb}=\frac{\sin\beta_k}{\bar{x}_\infty}\sqrt{\pi\frac{T_r}{T_i}}. \qquad (15.4.31)$$

Adding (15.4.28) and (15.4.31), we get the total drag coefficient for a cone:

$$c_x=c_{xi}+c_{xr}=\frac{2}{\bar{x}_k\sqrt{\pi}}e^{-\bar{x}_k^2}+2\left(1+\frac{1}{2\bar{x}_\infty^2}\right)\operatorname{erf}\bar{x}_k+\frac{\sin\beta_k}{\bar{x}_\infty}\sqrt{\pi\frac{T_r}{T_i}}. \qquad (15.4.32)$$

Axisymmetric flow over a cone with flat base: The formulas (15.4.26) for c_{xif} and (15.4.29) for c_{xrf} do not change for this case (Fig. 15.4.1, b). The expressions (15.4.27) for c_{xib} and (15.4.30) for c_{xrb} will be different because $\bar{x}_k=\bar{x}_\infty\sin\beta_k$ should be replaced by $\bar{x}_k=\bar{x}_\infty$, since the base surface is inclined by angle $\beta_k=\pi/2$.

Taking this into account, we get the following relation for the coefficient of force acting on the frontal surface:

$$c_{xf}=c_{xif}+c_{xrf}=\frac{e^{-\bar{x}_k^2}}{\bar{x}_k}\left(\frac{1}{\sqrt{\pi}}+\frac{\sin\beta_k}{2\bar{x}_\infty}\sqrt{\frac{\bar{T}_r}{\bar{T}_i}}\right)$$
$$+(1+\operatorname{erf}\bar{x}_k)\left(1+\frac{1}{2\bar{x}_\infty^2}+\frac{\sin\beta_k}{2\bar{x}_\infty}\sqrt{\pi\frac{\bar{T}_r}{\bar{T}_i}}\right). \tag{15.4.33}$$

The coefficient of force acting on the base surface

$$c_{xb}=c_{xib}+c_{xrb}=\frac{e^{-\bar{x}_\infty^2}}{\bar{x}_\infty}\left(\frac{-1}{\sqrt{\pi}}+\frac{1}{2\bar{x}_\infty}\sqrt{\frac{\bar{T}_r}{\bar{T}_i}}\right)$$
$$+(1-\operatorname{erf}\bar{x}_\infty)\left(1+\frac{1}{2\bar{x}_\infty^2}-\frac{1}{2\bar{x}_\infty}\sqrt{\pi\frac{\bar{T}_r}{\bar{T}_i}}\right). \tag{15.4.34}$$

The force determined by this coefficient acts on the base section in a direction opposite to the undisturbed flow and hence represents a reactive force. According to this the resultant coefficient of drag on the cone will be

$$c_x=c_{xf}-c_{xb}. \tag{15.4.35}$$

At very high flight speeds ($\bar{x}\gg 1$) formulas (15.4.32) and (15.4.35) take the form

$$c_x=2. \tag{15.4.36}$$

Here this result is independent of the form of bodies.

At flight speeds for which the magnitudes of $\bar{x}$ are small the values of c_x increase due to the applicable effect of reflected molecules. This is clear from the graph presented in Fig. 15.4.2, where the values of c_x are given for a cone with spherical surface.

It is worthwhile noting that the value of $c_x=2$ exactly corresponds to the conclusions from Newton's theory of shocks. Actually, drag force according to this theory is determined by the total loss of momentum of particles on the area of maximum cross section of a body. From this we find that the drag force for any body with the area of maximum cross section πr_0^2 (for example, a cone) in a free molecular flow with velocity V_∞ at zero angle of attack will be

$$X=\underbrace{\rho_\infty V_\infty \pi r_0^2 V_\infty}_{\substack{\text{momentum of undisturbed flow before collision}}}-\underbrace{\rho_\infty V_\infty \pi r_0^2\cdot 0}_{\substack{\text{momentum after collision}}}=\rho_\infty V_\infty^2 \pi r_0^2.$$

The coefficient of this force will be

$$c_x=2X/(\rho_\infty V_\infty^2 \pi r_0^2)=2.$$

The same formula can be obtained for any arbitrary angle of attack. Here the force must be worked out as the product of coefficient $c_x=2$, velocity head and the projection of the surface on the plane normal to direction of velocity vector $\bar{V}_\infty$.

It can be seen from the above discussion that the shock theory differs from Newton's scheme of elastic reflection considered earlier (Chapter 9 Section 4). According to Newton's model the particles continue their motion along the wall after collision with the surface, i.e. their path is inclined by the molecules' angle of incidence with the wall. Meantime the normal component of velocity is extinguished and the tangential component remains unchanged. According to the theory of shocks, both of the components are absorbed and consequently tangential stress arises along with normal pressure.

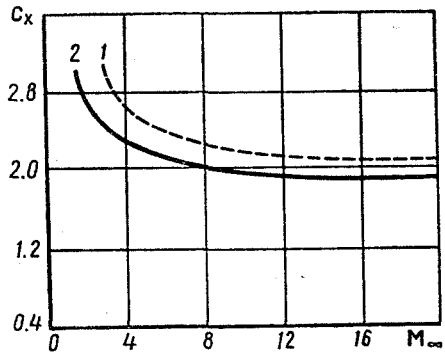

Fig. 15.4.2. Drag coefficient of sphere (*curve 1*) and cone (*curve 2*) in free molecular flow (angle of attack $\alpha=0$; angle of cone $\beta_k=60°$).

From Fig. 15.4.2 it can be seen that the results of accurate calculation for $M_\infty>4$, neglecting some small difference, practically coincide with the value of $c_x=2$ obtained from Newton's theory of shocks. Therefore the aerodynamic forces at comparatively low Mach numbers M_∞ can be worked out from the scheme of diffused reflections. At high Mach numbers M_∞ they may be calculated from Newton's theory of shocks.

Non-axisymmetrical flow-interaction: The expressions for the local coefficients of pressure and friction should be taken as the basis of calculation of coefficients of axial and normal forces and also of moment. The angle β

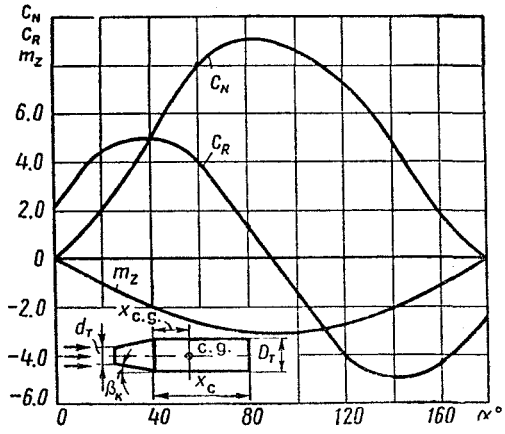

Fig. 15.4.3. Results of calculation of aerodynamic coefficients for body of revolution in free molecular flow ($\beta_k=15°$; $d_T/D_T=0.834$; $x_{c.g}/D_T=1$; $x_c/D_T=3$).

appearing in these expressions should be replaced by the angle θ_k between the velocity vector of molecular flow and the local area.

Knowing the type of distribution of local coefficients of pressure and friction and using general expressions for the calculation of aerodynamic coefficients (see Chapter 1 Section 3), it is possible to calculate their concrete values for a given shape of body.

The results of this kind of calculation for the combination of a cone with a cylinder, obtained under the condition that the ratio of flight velocity to the speed of molecules $\bar{x}_\infty = 7$ and temperature ratio $T_r/T_i = 0.18$, are presented in Fig. 15.4.3. The coefficient of moment, for which data are given in Fig. 15.4.3, is worked out about the axis through the center of gravity situated at a distance of one diameter of the cylinder from the large base of the cone.

4.3 Cylinder

Let us consider the drag of a cylinder during a cross flow of free molecules for the scheme of diffused reflection on the assumption that the coefficient of adjustability $f=1$ (Fig. 15.4.4). We use formulas (15.4.1) through (15.4.13) for this purpose. Keeping in mind that the ratio in (15.4.4)

$$d\bar{S} = dS/S_0 = lR_T\, d\beta/R_T l = d\beta, \tag{15.4.37}$$

and the quantity $\bar{x} = \bar{x}_\infty \sin\beta$, we get

$$c_{xif} = \frac{2X_{if}}{\rho_i V_\infty^2 S_0} = \int_0^{\pi/2} \left[\frac{e^{-\bar{x}^2}}{\bar{x}_\infty \sqrt{\pi}} + \sin\beta \left(1 + \frac{1}{2\bar{x}_\infty^2}\right)(1 + \operatorname{erf}\bar{x}) \right] d\beta. \tag{15.4.38}$$

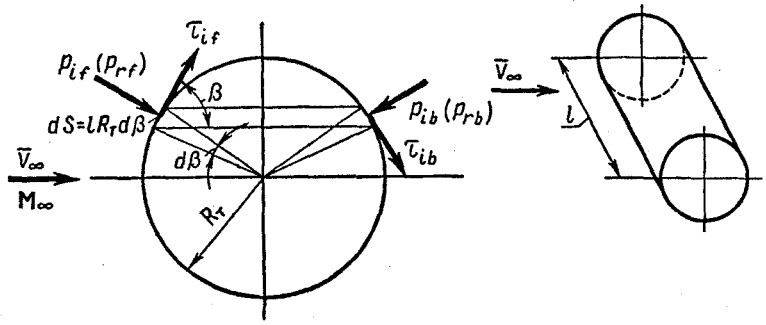

Fig. 15.4.4. Cylinder in free molecular flow.

Applying (15.4.6), we get the relation for coefficient

$$c_{xib} = \frac{2X_{ib}}{\rho_i V_\infty^2 S_0} = \int_0^{\pi/2} \left[\frac{-e^{-\bar{x}^2}}{\bar{x}_\infty \sqrt{\pi}} + \sin\beta \left(1 + \frac{1}{2\bar{x}_\infty^2}\right)(1 - \operatorname{erf}\bar{x}) \right] d\beta. \tag{15.4.39}$$

The drag produced by the reflection of molecules from the frontal surface

is determined by the following coefficient according to (15.4.9):

$$c_{xrf}=\frac{2X_{rf}}{\rho_i V_\infty^2 S_0}=\frac{1}{2}\int_0^{\pi/2}\left[\frac{e^{-\bar{x}^2}}{\bar{x}\sqrt{\pi}}+(1+\operatorname{erf}\bar{x})\right]\bar{x}\sqrt{\pi}\,\frac{\sin\beta}{\bar{x}_\infty^2}\sqrt{\frac{\bar{T}_r}{\bar{T}_i}}\,d\beta. \tag{15.4.40}$$

Reflection of molecules from the rear surface creates a force whose coefficient according to (15.4.11) will be given by

$$c_{xrb}=\frac{2X_{rb}}{\rho_i V_\infty^2 S_0}=\frac{1}{2}\int_0^{\pi/2}\left[\frac{e^{-\bar{x}^2}}{\bar{x}\sqrt{\pi}}-(1-\operatorname{erf}\bar{x})\right]\bar{x}\sqrt{\pi}\,\frac{\sin\beta}{\bar{x}_\infty^2}\sqrt{\frac{\bar{T}_r}{\bar{T}_i}}\,d\beta. \tag{15.4.41}$$

The difference between (15.4.38) and (15.4.39) gives the coefficient of resultant force due to interaction of the colliding molecules

$$c_{xi}=c_{xif}-c_{xib}=2\int_0^{\pi/2}\left[\frac{e^{-\bar{x}^2}}{\bar{x}_\infty\sqrt{\pi}}+\sin\beta\left(1+\frac{1}{2\bar{x}_\infty^2}\right)\operatorname{erf}\bar{x}\right]d\beta$$

$$=\frac{\sqrt{\pi}\,e^{-\frac{1}{2}\bar{x}_\infty^2}}{\bar{x}_\infty}\left\{I_0\left(\frac{\bar{x}_\infty^2}{2}\right)+\left(\bar{x}_\infty^2+\frac{1}{2}\right)\left[I_0\left(\frac{\bar{x}_\infty^2}{2}\right)+I_1\left(\frac{\bar{x}_\infty^2}{2}\right)\right]\right\}, \tag{15.4.42}$$

where $I_0(\bar{x}_\infty^2/2)$ and $I_1(\bar{x}_\infty^2/2)$ represent modified Bassel's functions of "zeroth" and "first" order respectively;

$$\left.\begin{aligned} I_0\left(\frac{\bar{x}_\infty^2}{2}\right)&=\frac{1}{\pi}\int_0^{\pi} e^{\frac{\bar{x}_\infty^2}{2}\cos\varphi}\,d\varphi;\\ I_1\left(\frac{\bar{x}_\infty^2}{2}\right)&=\frac{1}{\pi}\int_0^{\pi}\cos\varphi\, e^{\frac{\bar{x}_\infty^2}{2}\cos\varphi}\,d\varphi. \end{aligned}\right\} \tag{15.4.43}$$

The coefficient of the resultant force of interaction of reflected molecules can be obtained by subtracting (15.4.41) from (15.4.40). Assuming here that $T_r/T_i=$ constant all over the surface, we get

$$c_{xr}=c_{xrf}-c_{xrb}=\frac{1}{\bar{x}_\infty^2}\sqrt{\pi\frac{\bar{T}_r}{\bar{T}_i}}\int_0^{\pi/2}\bar{x}\sin\beta\,d\beta=\frac{\pi^{3/2}}{4\bar{x}_\infty}\sqrt{\frac{\bar{T}_r}{\bar{T}_i}}. \tag{15.4.44}$$

The resultant drag coefficient of the cylinder will be

$$c_x=c_{xi}+c_{xr}=\frac{\sqrt{\pi}\,e^{-\frac{1}{2}\bar{x}_\infty^2}}{\bar{x}_\infty}\left\{I_0\left(\frac{\bar{x}_\infty^2}{2}\right)+\left(\bar{x}_\infty^2+\frac{1}{2}\right)\left[I_0\left(\frac{\bar{x}_\infty^2}{2}\right)+I_1\left(\frac{\bar{x}_\infty^2}{2}\right)\right]\right\}+\frac{\pi^{3/2}}{4\bar{x}_\infty}\sqrt{\frac{\bar{T}_r}{\bar{T}_i}}. \tag{15.4.45}$$

4.4 Flat plate

In the most general case, when the flow-interaction is worked out on the basis of Newton's theory of shocks, the drag force acting on a flat plate of area S_w is determined by the change in the momentum before and after collision:

$$X=(\rho_\infty V_\infty S_w \sin\alpha)\, V_\infty-(\rho_\infty V_\infty S_w \sin\alpha)\cdot 0=\rho_\infty V_\infty^2 S_w \sin\alpha,$$

where α is the angle of attack (Fig. 15.4.5). Consequently the drag coefficient

$$c_x=2X/(\rho_\infty V_\infty^2 S_w)=2\sin\alpha. \tag{15.4.46}$$

Since lift force is absent the aerodynamic efficiency or lift to drag ratio is equal to zero. These conclusions are nearer to reality at very high speeds of free molecular flows. At low speeds the effects of reflection must be taken into account and applied for calculation of the appropriate relations for drag and friction coefficients.

Let us take the case of reflection with the coefficient of adjustability $f<1$. The force on the lower surface of a plate created by the colliding molecules will be

$$X_{if}=F_{if}S_w=(p_{if}\sin\alpha+f\tau_{if}\cos\alpha)\, S_w, \tag{15.4.47}$$

according to (15.4.20), in which β is replaced by α. Then the coefficient of this force will be

$$c_{xif}=\frac{2X_{if}}{\rho_i V_\infty^2 S_w}=\frac{2}{\rho_i V_\infty^2}(p_{if}\sin\alpha+f\tau_{if}\cos\alpha). \tag{15.4.47'}$$

We will substitute τ_{if} here from the expression (15.2.48), retaining the "plus" sign. At the same time we use (15.2.29) for p_{if}. Keeping in view that β is replaced by α in formulas (15.2.48) and (15.2.29), we get the following expression after the above simplifications:

$$c_{xif}=\sin^3\alpha\left[\frac{e^{-\bar{x}^2}}{\bar{x}\sqrt{\pi}}+\left(1+\frac{1}{2\bar{x}^2}\right)(1+\operatorname{erf}\bar{x})\right]$$
$$+f\sin\alpha\cos^2\alpha\left(\frac{e^{-\bar{x}^2}}{\bar{x}\sqrt{\pi}}+1+\operatorname{erf}\bar{x}\right), \tag{15.4.47''}$$

where $\bar{x}=\bar{x}_\infty\sin\alpha$.

Similarly, for the upper surface of the flat plate, we have [see (15.4.21)]:

$$c_{xib}=\frac{2X_{ib}}{\rho_i V_\infty^2 S_w}=\frac{2F_{ib}}{\rho_i V_\infty^2}=\frac{2}{\rho_i V_\infty^2}F_{if}(-\bar{x})=c_{xif}(-\bar{x})$$
$$=\sin^3\alpha\left[\frac{-e^{-\bar{x}^2}}{\bar{x}\sqrt{\pi}}+\left(1+\frac{1}{2\bar{x}^2}\right)(1-\operatorname{erf}\bar{x})\right]+f\sin\alpha\cos^2\alpha\left(\frac{-e^{-\bar{x}^2}}{\bar{x}\sqrt{\pi}}+1-\operatorname{erf}\bar{x}\right). \tag{15.4.48}$$

Let us consider the forces created by the reflection of molecules. From Fig. 15.4.5 it may be seen that the force X_{rf} is acting on the lower surface. This force can be expressed with the help of (15.4.22) in the form

$$X_{rf}=p_{rf}\,S_w\sin\alpha=F_{rf}\,S_w. \tag{15.4.49}$$

The coefficient of this force, according to (15.4.22), will be

$$c_{xrf}=\frac{2X_{rf}}{\rho_i V_\infty^2 S_w}=\frac{2F_{rf}}{\rho_i V_\infty^2}=\frac{2\sin\alpha}{\rho_i V_\infty^2}\,[p_{if}(1-f)+f p_{wf}]. \tag{15.4.50}$$

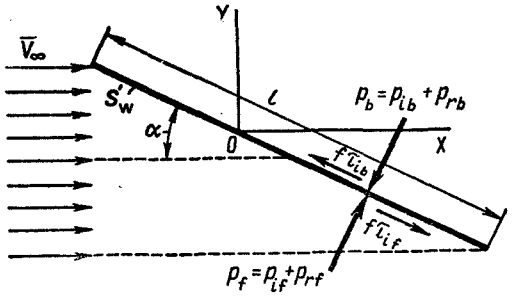

Fig. 15.4.5. Flat plate in free molecular flow.

Substituting the values of p_{if} and p_{wf} from (15.2.29) and (15.3.3) respectively (with the plus sign), we get

$$c_{xrf}=(1-f)\sin^3\alpha\left[\frac{e^{-\bar{x}^2}}{\bar{x}\sqrt{\pi}}+\left(1+\frac{1}{2\bar{x}^2}\right)(1+\operatorname{erf}\bar{x})\right]$$
$$+\frac{f\sin^3\alpha}{2\bar{x}^2}\sqrt{\frac{\overline{T_w}}{T_i}}\,[e^{-\bar{x}^2}+\bar{x}\sqrt{\pi}\,(1+\operatorname{erf}\bar{x})]. \tag{15.4.50'}$$

The molecules reflected from the upper surface create a reactive force [see (15.4.23)]:

$$X_{rb}=F_{rb}\,S_w=p_{rb}\,S_w\sin\alpha. \tag{15.4.51}$$

The coefficient of this force will be

$$c_{xrb}=\frac{2X_{rb}}{\rho_i V_\infty^2 S_w}=\frac{2F_{rb}}{\rho_i V_\infty^2}=\frac{2}{\rho_i V_\infty^2}\,F_{rf}(-\bar{x})=c_{xrf}(-\bar{x}). \tag{15.4.52}$$

According to (15.4.50') we have

$$c_{xrb}=(1-f)\sin^3\alpha\left[-\frac{e^{-\bar{x}^2}}{\bar{x}\sqrt{\pi}}+\left(1+\frac{1}{2\bar{x}^2}\right)(1-\operatorname{erf}\bar{x})\right]$$
$$+\frac{f\sin^3\alpha}{2\bar{x}^2}\sqrt{\frac{\overline{T_w}}{T_i}}\,[e^{-\bar{x}^2}-\bar{x}\sqrt{\pi}\,(1-\operatorname{erf}\bar{x})]. \tag{15.4.53}$$

The difference between (15.4.47'') and (15.4.48) gives

$$c_{xi}=c_{xif}-c_{xib}=2\sin^3\alpha\left[\frac{1}{\bar{x}\sqrt{\pi}}\,e^{-\bar{x}^2}+\left(1+\frac{1}{2\bar{x}^2}\right)\operatorname{erf}\bar{x}\right]$$
$$+2f\sin\alpha\cos^2\alpha\left(\frac{1}{\bar{x}\sqrt{\pi}}\,e^{-\bar{x}^2}+\operatorname{erf}\bar{x}\right). \tag{15.4.54}$$

A similar expression, corresponding to the process of reflection, can be obtained by using (15.4.50′) and (15.4.53),

$$c_{xr}=c_{xrf}-c_{xrb}=2(1-f)\sin^3\alpha\left[\frac{1}{\bar{x}\sqrt{\pi}}e^{-\bar{x}^2}+\left(1+\frac{1}{2\bar{x}^2}\right)\operatorname{erf}\bar{x}\right]+\frac{f\sin^3\alpha}{\bar{x}}\sqrt{\pi\frac{T_w}{T_i}}. \tag{15.4.55}$$

The resultant coefficient of drag force will be

$$c_x=c_{xi}+c_{xr}=2(2-f)\sin^3\alpha\left[\frac{1}{\bar{x}\sqrt{\pi}}e^{-\bar{x}^2}+\left(1+\frac{1}{2\bar{x}^2}\right)\operatorname{erf}\bar{x}\right]$$
$$+f\sin\alpha\left[2\cos^2\alpha\left(\frac{e^{-\bar{x}^2}}{\bar{x}\sqrt{\pi}}+\operatorname{erf}\bar{x}\right)+\frac{\sin^2\alpha}{\bar{x}}\sqrt{\pi\frac{T_w}{T_i}}\right]. \tag{15.4.56}$$

Similarly the lift force Y can be determined and the coefficient of this force will be

$$c_y=\frac{2Y}{\rho_i V_\infty^2 S_w}=\frac{2(Y_i+Y_r)}{\rho_i V_\infty^2 S_w}=c_{yi}+c_{yr}$$
$$=\frac{2}{\rho_i V_\infty^2}[G_{if}-G_{if}(-\bar{x})+G_{rf}-G_{rf}(-\bar{x})], \tag{15.4.57}$$

where

$$\left.\begin{aligned}G_{if}&=p_{if}\cos\alpha-f\tau_{if}\sin\alpha;\\ G_{rf}&=[p_{if}(1-f)+fp_{wf}]\cos\alpha.\end{aligned}\right\} \tag{15.4.58}$$

The coefficients of drag and lift force for the case of totally diffused reflection can be obtained if we take $f=1$ in the corresponding expressions. Similarly $f=0$ describes mirror reflection of molecules from the surface.

5. Heat Transfer

5.1 Temperature of reflected molecules

As we found earlier, the pressure at the wall, which is governed by the reflection of molecules, depends on their temperature T_r. To determine this temperature it is necessary to use the equation of equilibrium of energy between body and medium. Let us consider this equation as applied to the unit area at any arbitrary place on the surface. Energy belonging to impinging molecules E_i is brought to this area. The corresponding energy of reflected molecules can be determined with the help of (15.3.11) and (15.3.10) in the following way:

$$E_r=(1-\eta)E_i+\eta E_w=(1-\eta)E_i+2\eta mN_iRT_w. \tag{15.5.1}$$

If the heat inflow due to external radiation q_{rad} is allowed for, for example solar radiation, the energy input will be equal to the sum E_i+q_{rad}.

Let us assume that along with the heat transfer by reflected molecules loss of energy also occurs by radiation from the external surface and by additional cooling or heating from inside (corresponding "plus" or "minus" q_c).

Then the equation of equilibrium of energy for unit surface area under steady heat transfer conditions will have the form

$$E_i + q_{\text{rad}} = E_r + \varepsilon\sigma T_w^4 \pm q_c, \tag{15.5.2}$$

or using expression (15.5.1) for E_r, it will be

$$\eta E_i + q_{\text{rad}} = \eta E_w + \varepsilon\sigma T_w^4 \pm q_c. \tag{15.5.2'}$$

The relation (15.5.2') and the expressions for E_i (15.2.55) and E_w (15.3.10) appearing here correspond to the motion of a monatomic gas. If the gas consists of multiatomic molecules, in particular, if air is taken as the diatomic model of the medium, each particle will have, besides the energy of advancing motion, internal energy based on rotation and oscillation and the properties of the gas. These particles, colliding with the unit area of surface, transfer their energy to it in unit time. This is equal to

$$E_{i\ \text{int}} = \frac{5-3k}{k-1} \cdot \frac{mRT_i}{2} N_i, \tag{15.5.3}$$

according to the molecular-kinetic theory of gases. The molecules leaving this surface at temperature T_w carry away internal energy

$$E_{w\ \text{int}} = \frac{5-3k}{k-1} \cdot \frac{mRT_w}{2} N_w, \tag{15.5.4}$$

where $N_w = N_i$. According to this the equation of equilibrium of energy (15.5.2') for a diatomic gas will have the following form:

$$\eta \bar{E}_i + q_{\text{rad}} = \eta \bar{E}_w + \varepsilon\sigma T_w^4 \pm q_c, \tag{15.5.5}$$

where

$$\left.\begin{aligned} \bar{E}_i &= E_i + E_{i\ \text{int}}; \\ \bar{E}_w &= E_w + E_{w\ \text{int}}. \end{aligned}\right\} \tag{15.5.6}$$

Inserting the values of E_i (15.2.55) and E_w (15.3.10) in equation (15.5.5) (on the condition that the "plus" sign in these expressions is taken for the frontal surface and the "minus" sign for the back), the wall temperature T_w will be determined for the given values of degree of blackness ε, heat flows q_{rad}, q_c and temperature of air T_i.

Calculation of T_w by equation (15.5.5) for a flat plate as a function of angle of attack α showed that the effect of solar radiation on the wall temperature is more significant at low angles of attack α. This effect also increases with a rise in altitude. From an altitude of 240–250 km and above solar radiation is the basic factor in determining wall temperature. A reduction in temperature T_w can be achieved by using a surface with a low coefficient of adjustability η. It is also desirable for this purpose to have the angle of inclination of the wall as low as possible. This is achieved in flight at low angles of attack. From the temperature T_w obtained it is possible to work out the temperature T_r of reflected molecules. The corresponding relation for calculation can be obtained in the following way: Let us write the formula for the energy of reflected diatomic molecules by analogy with (15.5.1):

$$\bar{E}_r=(1-\eta)\,\bar{E}_i+\eta\bar{E}_w. \tag{15.5.7}$$

Here

$$\bar{E}_r=E_r+E_{r\,\text{int}}=2mN_iRT_r+\frac{5-3k}{k-1}\cdot\frac{mRT_r}{2}N_i=2mN_iRT_r\,k_1; \tag{15.5.8}$$

$$\bar{E}_w=E_w+E_{w\,\text{int}}=2mN_iRT_w\,k_1, \tag{15.5.9}$$

where

$$k_1=1+\frac{5-3k}{4(k-1)}=\frac{k+1}{4(k-1)}. \tag{15.5.10}$$

Besides this, the energy

$$\bar{E}_i=E_i+E_{i\,\text{int}}=E_i\,k_2, \tag{15.5.11}$$

appears in (15.5.7), and its value is determined by the coefficient

$$k_2=1+\frac{E_{i\,\text{int}}}{E_i}=1+\frac{1}{E_i}\cdot\frac{5-3k}{k-1}\cdot\frac{mRT_i}{2}N_i. \tag{15.5.12}$$

Using (15.5.8), (15.5.9) and (15.5.11) in equation (15.5.7) we get the following relation for calculation of the temperature of reflected molecules:

$$\frac{T_r}{T_i}=\frac{T_w}{T_i}\left[\frac{(1-\eta)\,E_i\,k_2}{2mN_iRT_w\,k_1}+\eta\right]. \tag{15.5.13}$$

Here the calculation of temperature T_r will be carried out separately for the front and rear surface which correspond to the values determined for N_i and E_i and therefore also to T_w. If the coefficient of adjustability $\eta=1$, then $T_r=T_w$. The same result is also obtained in the case of a so-called adiabatic wall which is characterized by the absence of any external inflow or outflow of heat other than the energy inflow due to colliding molecules. In this case the wall is heated only as a result of impinging molecules. According to this equation (15.5.5) will be simplified to the form

$$\bar{E}_i=\bar{E}_w,$$

or, using (15.5.11) and (15.5.9), it will reduce to

$$E_i\,k_2=2mN_iRT_w\,k_1=E_w\,k_1. \tag{15.5.14}$$

If this expression is used in (15.5.13) we will find that the temperature of the reflected molecules is equal to the wall temperature. This temperature is determined from (15.5.14) after substituting the value of E_i from (15.2.55) in the following form:

$$\frac{T_w}{T_i}=\frac{T_r}{T_i}=\frac{k_2}{4RT_i\,k_1}\left[V_\infty^2+RT_i\left(4+\frac{1}{\varphi+1}\right)\right]. \tag{15.5.15}$$

The product RT_i in this formula can be replaced with the help of (15.2.19):

$$\frac{T_w}{T_i}=\frac{T_r}{T_i}=\left[1+\frac{k\,\mathbf{M}_\infty^2}{4}+\frac{1}{4(\varphi+1)}\right]\frac{k_2}{k_1}. \tag{15.5.16}$$

It can be seen from this formula that the temperature of an adiabatic wall is a kind of analog of stagnation temperature in the case of continuous flow.

Flight conditions at high altitudes can involve maintaining a constant

wall temperature. In this case the wall temperature is given and the calculations lead to the determination of the temperature of reflected particles by formula (15.5.3). This temperature is then used to calculate pressure.

5.2 Calculation of heat transfer and wall temperature

The resultant specific heat flow to the wall can be determined as the difference in the energies of the colliding and reflected molecules:

$$q=\bar{E}_i-\bar{E}_r. \tag{15.5.17}$$

Combining this equation with (15.5.7), we get

$$q=\eta\,(\bar{E}_i-\bar{E}_w), \tag{15.5.17'}$$

or using expressions (15.5.11) and (15.5.9) for $\bar{E}_i$ and $\bar{E}_w$ it will be

$$q=\eta\,(E_i k_2-2mN_i RT_w k_1). \tag{15.5.17''}$$

Using the value of E_i from (15.2.55) here, we get

$$q=\frac{\eta m N_i}{2}\left\{k_2\left[V_\infty^2+RT_i\left(4+\frac{1}{\varphi+1}\right)\right]-4RT_w k_1\right\}.$$

Recalling that N_i is determined by the expressions (15.2.17') and (15.2.22) for the front and rear surfaces and that the mass of molecules $m=\rho_i/n_i$, we get

$$q=\frac{\eta\rho_i}{2}\sqrt{\frac{RT_i}{2\pi}}\left\{k_2\left[V_\infty^2+RT_i\left(4+\frac{1}{\varphi+1}\right)\right]-4RT_w k_1\right\}e^{-\bar{x}^2}\pm\bar{x}\sqrt{\pi}\,(1\pm\operatorname{erf}\bar{x})], \tag{15.5.18}$$

where φ, k_2 and k_1 are determined by the relations (15.2.56), (15.5.12) and (15.5.10) respectively. With the help of these relations the specific heat flow for the frontal surface will be

$$q=\eta\rho_i\sqrt{\frac{(RT_i)^3}{2\pi}}\left\{[e^{-\bar{x}^2}+\bar{x}\sqrt{\pi}\,(1+\operatorname{erf}\bar{x})]\left[\bar{x}_\infty^2-\frac{k+1}{2(k-1)}\cdot\frac{T_w}{T_i}+\frac{k+1}{2(k-1)}\right]+\frac{1}{2}\,\bar{x}\sqrt{\pi}\,(1+\operatorname{erf}\bar{x})\right\}, \tag{15.5.18'}$$

where

$$\left.\begin{aligned} &RT_i=p_i/\rho_i=a_i^2/k;\\ &\bar{x}=\bar{x}_\infty\sin\beta,\ \bar{x}_\infty=(V_\infty/a_i)\sqrt{k/2}. \end{aligned}\right\} \tag{15.5.19}$$

A similar expression for q can be obtained for the back of the body in this flow by inserting $\bar{x}$ in place of $-\bar{x}$ in (15.5.18').

Assuming the heat flow $q=0$ in the corresponding formulas, the equilibrium temperature of the wall can be determined. In particular, from (15.5.18) we find the following relation under this condition:

$$T_w=T_e=\frac{k_2}{4Rk_1}\left[V_\infty^2+RT_i\left(4+\frac{1}{\varphi+1}\right)\right]. \tag{15.5.20}$$

From (15.5.12) and (15.2.55) it can be seen that at very high speeds ($V_\infty \gg a_i$) the parameter $k_2 \approx 1$. Therefore, keeping in mind formula (15.5.10) for k_1 and neglecting the second term in square brackets in (15.5.20), we get

$$T_w = T_e = \frac{k-1}{k+1} \cdot \frac{V_\infty^2}{R}, \tag{15.5.21}$$

where

$$T_w = T_e = \frac{2T_i(k-1)}{k+1} \bar{x}_\infty^2. \tag{15.5.21'}$$

This relation is obtained from equation (15.5.18') if the quantity $k/(k-1)$ on the right side in square brackets is neglected in comparison with $\bar{x}_\infty^2$ and the remaining sum of two terms is equated to zero.

Let us consider the expression for the Stanton number, which is the nondimensional parameter for heat transfer:

$$\mathrm{St} = \frac{2k}{k+1} \cdot \frac{q}{\eta \rho_i V_\infty c_{pi} (T_e - T_w)}. \tag{15.5.22}$$

In this way this nondimensional parameter is known as the modified local Stanton number. In the case of high speeds ($\bar{x}_\infty \gg 1$, $\bar{x} \gg 1$) the heat flow for the frontal surface can be represented in approximate form, as may be seen from (15.5.18'):

$$q = \frac{1}{2} \eta R \rho_i T_i \sqrt{RT_i} \left(\frac{e^{-\bar{x}^2}}{\bar{x}\sqrt{\pi}} + 1 + \operatorname{erf} \bar{x} \right) \bar{x} \bar{x}_\infty^2.$$

Bearing in mind the relation (15.5.19) for $\bar{x}$ and a_i, we get the following expression after substituting this value of q in formula (15.5.22):

$$\mathrm{St} = \frac{2k}{k+1} \cdot \frac{RT_i \sqrt{RT_i}}{V_\infty c_{pi} (T_e - T_w) \sqrt{2}} \left(\frac{e^{-\bar{x}^2}}{\bar{x}\sqrt{\pi}} + 1 + \operatorname{erf} \bar{x} \right) \bar{x}_\infty^3 \sin \beta.$$

Since $T_w \ll T_e$ we can put T_e in place of $T_e - T_w$, which can be determined from (15.5.21'). Besides this, the substitutions of

$$c_{pi} = R/[1-(c_{vi}/c_{pi})] = kR/(k-1) \text{ and } \bar{x}_\infty = (V_\infty/\sqrt{kRT_i})\sqrt{k/2}$$

lead to

$$\mathrm{St} = \frac{\sin \beta}{2} \left(\frac{e^{-\bar{x}^2}}{\bar{x}\sqrt{\pi}} + 1 + \operatorname{erf} \bar{x} \right). \tag{15.5.23}$$

Let us now consider the coefficient of friction. According to (15.2.48) and (15.3.6') we can write the following expression for this coefficient for the frontal surface:

$$c_{fi} = f \sin \beta \cos \beta \left(\frac{e^{-\bar{x}^2}}{\bar{x}\sqrt{\pi}} + 1 + \operatorname{erf} \bar{x} \right). \tag{15.5.24}$$

Comparing (15.5.23) and (15.5.24), the relation between the Stanton number and the local frictional coefficient can be established:

$$\mathrm{St} = c_{fi}/(2f \cos \beta). \tag{15.5.25}$$

The resultant coefficient of friction can be determined by integrating (15.5.24) over the surface in the flow, working out the corresponding value of the Stanton number with the help of (15.5.25) and finally obtaining total heat flow to the wall using (15.5.22).

Particular attention is devoted to determination of the heat flow at the point of complete stagnation. Experiments showed that the specific heat flow (in kilo·cal/m²·sec) at this point can be obtained by the approximate formula:

$$q=7.35\times 10^7\,\eta\,(\rho_{\infty H}/\rho_{\infty g})\,(V_\infty/V_c)^3, \tag{15.5.26}$$

where V_c is the first cosmic speed and the indices "H" and "g" correspond to the conditions at altitude H and near sea level ($H=0$).

Using formula (15.5.26) and the equation of equilibrium of heat during steady heat transfer the temperature at the point of complete stagnation can be found as:

$$T_w=(q+q_{rad}\pm q_c)^{1/4}\,(\varepsilon\sigma)^{-1/4}. \tag{15.5.27}$$

If heat does not flow to the wall from inside ($q_c=0$) and external radiation is not taken into account ($q_{rad}=0$) the wall temperature (in °K) will be uniform:

$$T_w=4.83\times 10^4\,(\eta/\varepsilon)^{1/4}\,(\rho_{\infty H}/\rho_{\infty g})^{1/4}\,(V_\infty/V_c)^{3/4}. \tag{15.5.28}$$

For example, if we assume that the density ratio $\rho_{\infty H}/\rho_{\infty g}=10^{-8}$ ($H\approx 150$ km) the coefficient of adjustability $\eta=1$, the degree of blackness of surface $\varepsilon=1$ and the body moves at the first cosmic speed ($V_\infty=V_c$), then the equilibrium temperature at the point of complete stagnation $T_w=T_e=483$°K.

In the case of a highly cooled surface the energy of the particles reflected from the wall is very low, i.e. $\bar{E}_w\ll\bar{E}_i$. Therefore we can use the following equation in place of (15.5.17′):

$$q=\eta\bar{E}_i=\eta E_i k_2. \tag{15.5.29}$$

Examining the case of very high speeds at which $k_2\approx 1$ and E_i is determined by formula (15.2.61), we get the following relation for specific heat flow on the frontal surface:

$$q=\frac{\bar{x}\rho_i\eta}{2}\sqrt{2RT_i}\,(V_\infty^2+5RT_i).$$

Expressing RT_i here through the speed of sound a_i according to (15.2.19) and assuming

$$\bar{x}=\sin\beta\frac{V_\infty}{a_i}\sqrt{\frac{k}{2}}=\sin\beta M_\infty\sqrt{\frac{k}{2}},$$

according to (15.2.20), we have

$$q=\frac{1}{2}\rho_i V_\infty^3\eta\sin\beta\left(1+\frac{5}{kM_\infty^2}\right)\left[\frac{\text{kg·m}}{\text{m}^2\cdot\text{sec}}\right] \tag{15.5.30}$$

or

$$q=1.17\times10^{-3}\eta\rho_i V_\infty^3\left(1+\frac{5}{k\mathbf{M}_\infty^2}\right)\sin\beta\left[\frac{\text{kilo}\cdot\text{cal}}{\text{m}^2\cdot\text{sec}}\right]. \qquad (15.5.31)$$

At the point of complete stagnation $\beta=\pi/2$ and consequently

$$q=1.17\times10^{-3}\eta\rho_i V_\infty^3\left(1+\frac{5}{k\mathbf{M}_\infty^2}\right)\left[\frac{\text{kilo}\cdot\text{cal}}{\text{m}^2\cdot\text{sec}}\right]. \qquad (15.5.32)$$

In these expressions density ρ_i is given in $\text{kg}\cdot\text{sec}^2/\text{m}^4$ and velocity V_∞ in m/sec.

We have examined the group of problems connected with the investigation of friction and heat transfer for continuous and free molecular flows of gas. The flow regime with slip occupies an intermediate position. Most modern methods of calculation of friction and heat transfer for this regime are based on the use of equations of the boundary layer whose solution must satisfy the special boundary conditions for discontinuity (slip) in speed. These methods may be studied from different sources, in particular, from the books [21; 28; 38].

Conversion Table for Units of Measurement Used in Aerodynamics, from MKS System to International System (SI), GOST* 9867-61

Name and Designation	Old Unit MKS System	New System (SI)
	Basic Units	
Length [L, l, b, d]	Meter (m)	Meter (m)
Mass [m]	—	Kilogram (kg)
Force [P, X, Y, R, N]	Kilogram (kg)	—
Time [t]	Second (sec)	Second (sec)
Thermodynamic temperature (absolute) [T]	Degree (Kelvin °K)	Degree (Kelvin °K)
	1 kg = 9.81 N (Newton)	
	Derived Units	
Velocity [V, a]	1 m/sec	1 m/sec
Acceleration [w]	1 m/sec^2	1 m/sec^2
Gravitational acceleration [g]	9.81 m/sec^2	9.81 m/sec^2
Density (mass per unit volume) [ρ]	1 kg sec^2/m^4	9.81 kg/m^3
Specific volume (volume per unit mass) [$v = 1/\rho$]	1 m^4/kg sec^2	0.102 m^3/kg
Specific weight (weight per unit volume [γ]	1 kg/m^3	9.81 N/m^3
Weight flow rate [W_{sec}]	1 kg/sec	9.81 N/sec
Pressure [p]	1 kg/cm^2	9.81×10^4 N/m^2
Coefficient of dynamic viscosity [μ]	1 kg sec/m^2	9.81 N sec/m^2
Coefficient of kinetic viscosity [$\nu = \mu/\rho$]	1 m^2/sec	1 m^2/sec
Work, energy [E]	1 kg m	9.81 J (Joule)
Power [N]	1 kg m/sec	9.81 Wt (Watt)
Quantity of heat [Q]	1 kilocal	4.19×10^3 J
Specific heats [c_p, c_v]	1 kilocal/kg degree	4.19×10^3 J/kg degree

Name and Designation	Old Unit MKS System	New System (SI)
Entropy (specific) [S]	1 kilocal/kg degree	4.19×10^3 J/kg degree
Enthalpy (specific) [i]	1 kilocal/kg	4.19×10^3 J/kg
Specific heat flow [q]	1 kilocal/m^2 sec	4.19×10^3 Wt/m^2
Coefficient of heat transfer [a]	1 kilocal/m^2 sec $\times$ degree	4.19×10^3 Wt/m^2 $\times$ degree
Coefficient of heat conductivity [λ]	1 kilocal/m $\times$ sec degree	4.19×10^3 Wt/m degree
Coefficient of radiation of absolutely black body (Stephan-Boltzman constant) [σ]	1.36×10^{-11} kilocal/m^2 $\times$ sec degree^4	5.67×10^{-8} Wt/m^2 degree^4
Boltzman constant [k]	14.1×10^{-25} kg m/degree	1.38×10^{-23} J degree
Gas constant [R]	1 kg m/kg degree	9.81 J/kg degree
Universal gas constant [R_0]	1.99 kilocal/degree kilomole = 847.82 kg m/degree $\times$ kilomole	8.31×10^3 J/degree $\times$ kilomole

*The All-Union State Standard—General Editor.

BIBLIOGRAPHY

1. Arzhanikov, N.S. and B.N. Mal'tsev. Aerodinamika (Aerodynamics). Oborongiz, 1956.
2. Arzhanikov, N.S. and G.S. Sadekova. Aerodinamika bol'shikh skorostei (Aerodynamics of High Speeds). Vysshaya Shkola, 1965.
3. Babenko, K.I. et al. Prostranstvennoe obtekanie gladkikh tel ideal'nym gazom (Three-Dimensional Flow of Ideal Gas over Smooth Bodies). Nauka, 1964.
4. Ginzburg, I.P. Aerodinamika (Aerodynamics). Vysshaya Shkola, 1966.
5. Dorodnitsyn, A.A. Pogranichnyi sloi v szhimaemom gaze (Boundary layer in a compressible gas). *Prikladnaya Matematika i Mekhanika*, Vol. 4, No. 6, 1942.
6. Dorodnitsyn, A.A. Metod integral'nykh sootnoshenii dlya chislennogo resheniya differentsial'nykh uravnenii v chastnykh proizvodnykh (The Method of Integral Correlations for Numerical Solution of Partial Differential Equations). Tr. In-ta Tochnoi Mekhaniki i Vychislitel'noi Tekhniki AN SSSR, 1958.
7. Kibardin, Yu.A. et al. Atlas gazodinamicheskikh funktsii pri bol'shikh skorostyakh i vysokikh temperaturakh vozdushnogo potoka (Atlas of Gas Dynamic Functions at High Speeds and High Temperatures of Air Flow). Gosenergoizdat, 1961.
8. Kochin, N.E. et al. Teoreticheskaya gidrodinamika (Theoretical Hydrodynamics). Parts I & II, Fizmatgiz, 1963.
9. Krasil'shchikova, E.A. Krylo konechnogo razmakha v szimaemom potoke (Finite Wing in a Compressible Flow). Gostekhizdat, 1962.
10. Krasnov, N.F. et al. Aerodinamika raket (Aerodynamics of Rockets). Vysshaya Shkola, 1968.
11. Krasnov, N.F. Aerodinamika tel vrashcheniya (Aerodynamics of Revolving Bodies). Oborongiz, 1958.
12. Krasnov, N.F. Aerodinamika tel vrashcheniya (Aerodynamics of Revolving Bodies). Mashinostroenie, 1964.
13. Kuznetsov, S.I. Diagrammy i tablitsy techeniya dissotsiruyushchego vozdukha okolo klina, konusa i vypukloi poverkhnosti (Diagram and Tables of Dissociating Air Flows about a Wedge, Cone and a Concave Surface). Oborongiz, 1962.

14. Landau, L.D. and E.M. Lifshits. Mekhanika sploshnykh sred (Mechanics of Continuous Media). Gostekhizdat, 1958.
15. Loitsyaniskii, L.G. Mekhanika zhidkosti i gaza (Mechanics of Fluid and Gas). Gostekhizdat, 1950.
16. Loitsyaniskii, L.G. Laminarnyi pogranichnyi sloi (Laminar Boundary Layer). Fizmatgiz, 1962.
17. Predvoditelev, A.S. et al. Termodinamicheskiye funktsii vozdukha dlya temperatur ot 1,000 do 12,000°K i davlenii ot 0.001 do 1,000 atm (grafiki funktsii) [Thermodynamic Functions of Air for Temperatures from 1,000 to 12,000°K and Pressures from 0.001 to 1,000 Atmospheres (Graphs of Functions)]. Izd-vo AN SSSR, 1960.
18. Predvoditelev, A.S. et al. Tablitsy termodinemicheskikh funktsii vozdukha (dlya temperatur ot 6,000 do 12,000°K i davlenii ot 0.001 do 1,000 atm) (Tables of Thermodynamic Functions of Air for Temperatures from 6,000 to 12,000°K and Pressures from 0.001 to 1,000 Atmospheres). Izd-vo AN SSSR, 1967.
19. Martynov, A.K. Eksperimental'naya aerodinamika (Experimental Aerodynamics). Oborongiz, 1951.
20. Povkh, I.L. Tekhnicheskaya gidromekhanika (Technical Hydromechanics). Mashinostroenie, 1964.
21. Rakhmatulin, Kh.A. et al. Gazovaya dinamika (Gas Dynamics). Vysshaya Shkola, 1965.
22. Sedov, L.I. Metody podobiya i razmernosti v mekhanike (Methods of Similarity and Dimensions in Mechanics). Nauka, 1965.
23. Fabrikant, I.Ya. Aerodinamika (Aerodynamics). Nauka, 1964.
24. Frankl', F.I. and E.A. Karpovich. Gazodinamika tonkikh tel (Gas Dynamics of Thin Bodies). Gostekhizdat, 1948.
25. Khristianovich, S.A. Obtekanie tel gazom pri bol'shikh skorostyakh (Gas flow over bodies at high speeds). *Trudy TsAGI*, No. 481, 1940.
26. Chernyi, G.G. Techneiya gaza s bol'shoi sverkhzvukovoi skorost'yu (Gas Flow at High Supersonic Speeds). Fizmatgiz, 1959.
27. Chaplygin, S.A. O gazovykh struyakh (On Gas Jets). GTTI, 1949.
28. *Issledovaniye Giperzvukovykh Techenii* (Studies on Hypersonic Flows). Mir, 1964.
29. Courant, P. and K. Fredrich. Sverkhzvukovoe techenie i udarnye volny (Supersonic Flow and Shock Waves). IL, 1950.
30. Liepmann, G. and A. Rasheko. Elementy gazovoi dinamiki (Elements of Gas Dynamics). IL, 1960.
31. *Nauchnye Problemy Iskusstvennykh Sputnikov Zemli* (Scientific Problems of Artificial Earth Satellites). IL, 1959.
32. Nil'sen, D. Aerodinamika upravlyaemykh snaryadov (Aerodynamics of Guided Missiles). Oborongiz, 1962.
33. *Obshchaya Teoriya Aerodinamiki Bol'shikh Skorostei* (General Theory of

High-Speed Aerodynamics). Ed. I.A. Panichkin, Voenizdat, Ministerstvo Oborony SSSR, 1962.
34. Patterson, G.N. Molekulyarnoe techenie gazov (Molecular Flow of Gases). Fizmatgiz, 1960.
35. *Problemy Dvizheniya Golovnoi Chasti Raket Dal'nego Deistviya* (Problems of Motion of the Nose Part of Long Range Rockets). IL, 1959.
36. *Problemy Poleta s Bol'shimi Skorostyami* (Problems of High-Speed Flights). IL, 1960.
37. Ferri, A. Aerodinamika sverkhzvukovykh techenii (Aerodynamics of Supersonic Flows). Gostekhizdat, 1953.
38. Heiz, U.D. and R.F. Probstein. Teoriya giperzvukovykh techenii (Theory of Hypersonic Flows). IL, 1962.
39. Hilton, U.F. Aerodinamika bol'shikh skorostei (High-Speed Aerodynamics). IL, 1955.
40. Schlichting, G. *Boundary Layer Theory*, 1960.
41. *Izvestiya AN SSSR, Mekhanika i Mashinostroenie, Mekhanika* Zhidkosti i Gaza (Izvestiya AN SSSR. "Mechanics and Machine Building," "Mechanics of Fluid and Gas").
42. *Izvestiya AN SSSR. Prikladnaya Matematika i Mekhanika* (Izvestiya AN SSSR: Applied Mathematics and Mechanics).
43. *Voprosy Raketnoy Tekhniki* (Problems of Rocket Technology). Mir.
44. *Raketnaya Tekhnika i Kosmonavtika* (Rocket Technology and Astronautics). *AJAA Journal.*
45. Jet Propulsion, *ARS Journal.*
46. *Journal of the Aeronautical Sciences* (*Journal of the Aerospace Sciences*).
47. *Journal of the Royal Aeronautical Society.*
48. National Advisory Committee for Aeronautics (NACA).
49. Mekhanika. Sbornik Sokrashchennykh Perevodav i referatov lennostrannoy Periodicheskoy literatury (Mechanics. A Collection of Brief Translations and Abstracts of Foreign Periodic Literature).
50. *Theory of Conical Wings*, NACA Techn. Notes, 1685, 1948.
51. *Lift and Center of Pressure of Wing-Body-Tail Combinations at Subsonic, Transonic and Supersonic Speeds*, NACA Tech. Rept. 1307, 1957.
52. Belotserkovskii, O.M. et al. Obtekanie zatuplennykh tel sverkhzvukovym potokom gaza (Supersonic Flow of Gas over Blunt Bodies). Izd. Vychislitelnogo Tsentra AN SSSR, 1967.
53. Irov, I.D. et al. Gazodinamicheskie funktsii (Gas Dynamic Functions). Mashinostroenie, 1965.
54. Kaminskii, M. Atomnye i ionnye stolknoveniya (Collision of Atoms and Ions). Mir, 1967.
55. Brailovskaya, I.Yu. and L.A. Chudov. Reshenie uravnenii pogranichnogo sloya raznostnym metodom (Solution of boundary layer equations by the method of difference). Sb. *Vychislitel'nye Metody i Pro-*

grammirovanie, Izd-vo MGU, 1963.
56. *Chislitel'nye Metody v Gazovoy Dinamike* (Computation Methods in Gas Dynamics). Izd-vo MGU, 1963.
57. Ostoslavskii, I.V. and I.V. Strazheva. Dinamika poleta. Traektorii letatevnykh apparatoy (Dynamics of Flight. The Trajectory of Flying Machines). Oborongiz, 1963.
58. Drakin, I.I. Aerodinamickeskii i luchistyi nagrev v polete (Aerodynamic and Radiational Heating in Flight). Oborongiz, 1961.
59. *Modern Plastics*, Vol. 36, No. 8.